

**Saturday, 8 August 2020****Weekend Course****Met & Unmet Needs in Musculoskeletal Imaging I - Met & Unmet Needs in Musculoskeletal Imaging I**

Organizers: Riccardo Lattanzi, Jung-Ah Choi, Kimberly Amrami, Miika Nieminen, Hiroshi Yoshioka

Saturday Parallel 1 Live Q&amp;A

Saturday 14:00 - 14:30 UTC

Moderators: Valentina Mazzoli &amp; Xenia Deligianni

[Clinical Experience with Three-Dimensional MRI of the Musculoskeletal System](#)

Richard Kijowski

[New emerging techniques for quantitative musculoskeletal imaging](#)

Azadeh Sharafi

[Clinical Translation of Quantitative Musculoskeletal Imaging](#)

Joon-Yong Jung

[Ultra-High Field Imaging of the Musculoskeletal System](#)

Neal Bangerter

[Clinical MSK Applications of 7 Tesla MRI](#)

Jutta Ellermann

[Rapid Three-Dimensional Musculoskeletal MRI](#)

Ricardo Otazo

**Weekend Course****MRI & Epilepsy: Diagnosis & Treatment of the Epileptogenic Zone - MRI & Epilepsy: Diagnosis & Treatment of the Epileptogenic Zone**

Organizers: Robert Witte, Kader Oguz, Neil Harris

Saturday Parallel 3 Live Q&amp;A

Saturday 14:00 - 14:30 UTC

Moderators:

Quantitative &amp; Treatment: Esin Ozturk-Isik

Imaging in Epilepsy: Clinical &amp; Preclinical: Kader Oguz

[Clinical Review](#)

John Stern

[Animal Model](#)

Terence O'Brien




Epilepsy the most common, serious chronic neurological disease worldwide, affecting 50 million people globally. Current treatment with anti-seizure drugs (ASD) is symptomatic, suppressing seizures, while the medication is being taken at appropriate doses, but having sustained effects, and no effects on the accompanying comorbidities. More than a third of patients with PTE do not have their seizures controlled with currently available ASDs. In-vivo neuroimaging, in particular MRI, is a highly valuable tool in the pre-clinical testing of potential disease modifying treatments for epilepsy, allowing serial assessments of brain structure and function to evaluate the long-term effects of the treatment.

## Resting-State fMRI & Brain Connectivity

Olli Gröhn

Functional connectivity fMRI studies in animal models of epilepsy allow assessment of reorganization of networks already before occurrence of spontaneous seizures. Extreme care has to be taken when planning fMRI experiment especially regarding anesthesia and physiological monitoring. New technological advances such as implantable RF-coils, and radial zero echo time imaging provide solutions to many of the existing problems and make awake fMRI approaches more accessible

---

## MR-Guided Therapy

Robert Watson

---



## MRI Post-Processing & MR Fingerprinting in Epilepsy Pre-Surgical Evaluation

Jianhui Zhong

### OUTLINE:

- Why MRF and how it is used in epilepsy
  - Some technical aspects of MRF
  - Other clinical use of MRF
  - Further tech development
  - Challenges and future of clinical MRF
- 

## MR Spectroscopy

Jullie Pan

---

## PET/MR

Timothy Shepherd

---



## Clinical 7-Tesla MRI for Epilepsy

Kirk Welker

Clinical 7T MRI is a relatively new tool for the evaluation of medically refractory epilepsy. Offering improved signal to noise ratio and spatial resolution over MRI at 1.5 and 3.0 Tesla field strengths, 7T MRI can potentially identify very subtle epileptogenic lesions such as cortical dysplasias in patients that have previously been classified as "MRI negative". Additional epileptogenic pathologies better demonstrated with 7T MRI include mesial temporal sclerosis, tuberous sclerosis, and cavernomas. 7T fMRI may improve mapping of eloquent cortex in preparation for epilepsy surgery. Ongoing challenges with this technique include B1 inhomogeneity artifacts and safety concerns regarding metallic implants.

---

---

## Weekend Course

### MR Physics for Scientists I - MR Physics for Scientists I

Organizers: Jose Marques, Ivana Drobnjak, Hua Guo

Saturday Parallel 4 Live Q&A

Saturday 14:00 - 14:30 UTC

Moderators:

Contrast Mechanisms: Paula Croal & Ferdinand Schweser

MR: From Spins to the Classical Description



Karl Landheer

In this talk the quantum mechanics of a single spin  $1/2$  particle are discussed. The density operator formalism, which is a method to treat an ensemble of spins is then introduced. The effects of free precession and RF pulses are then demonstrated, and it is shown how the density operator relates to the classical Bloch vector model. A brief overview of how to deal with spin  $> 1/2$  particles or coupled spins which are necessary to describe spectroscopy experiments is discussed.

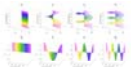
---

#### MRI: What You Need to Make It Happen – A Hardware Overview

Natalia Gudino

The aim of this presentation is to review the main hardware components in the MRI system and provide understanding of specifications based on the MRI physics.

---



#### Bloch Equations: From Steady-State Solutions to Numerical Simulations

Shaihan Malik

This talk is aimed at physicists and engineers who want to understand the different approaches used to simulate MR signals. It will cover steady-state closed form expressions, isochromat simulations, and the extended phase graph method.

---

#### MRS: Beyond Water & Protons, Coupling & Localization

Lijing Xin

MR spectroscopy measures diverse nuclei and molecules beyond water, allowing the measurement of important static/dynamic biochemical information from human or animal organs. This lecture will cover basic knowledge of MRS with a focus on chemical shifts, couplings, spectral modulation, localization methods and polarization transfer.

---

#### Magnetization Transfer & T1 Contrast: Mechanisms, Sensing & Quantifying

Nikolaus Weiskopf

Magnetic resonance imaging (MRI) yields exquisite soft tissue contrast. This lecture focuses on longitudinal relaxation and magnetization transfer (MT) as contrast mechanisms. For both contrast mechanisms the basic theoretical description and definitions are introduced. It is discussed how they are affected by microstructural characteristics, particularly macromolecular content and myelination in the brain. Different acquisition and analysis methods are described for sensing and quantifying the longitudinal relaxation time ( $T_1$ ) and parameters of MT. Examples of the use of  $T_1$  and MT mapping in neuroimaging with a focus on myelin mapping are explored.

---

#### Chemical Exchange Saturation Transfer: Mechanisms, Sensing & Quantifying

Zhongliang Zu

The purpose of the presentation is to 1) provide an overview of the chemical exchange saturation transfer MRI mechanism, signal enhancement principle, sequences, and quantification methods; 2) analyze the dependence of  $MTR_{asym}$ , a commonly used CEST quantification metric, on  $T_1$  and magnetization transfer (MT) whose specificity is under debate; 3) introduce a method using dialyzed tissue homogenates to investigate the contribution from proteins on the CEST imaging of small metabolites. Together with studies on metabolite phantoms under physiological condition, this method can provide a more comprehensive evaluation of CEST signal origin.

---

#### Transverse Relaxation ( $T_2$ & $T_2^*$ ): Mechanisms, Sensing & Quantifying

Cornelia Laule

Relaxation is a fundamental concept in MRI as it plays a key role in determining image contrast for most MR sequences.  $T_2$  and  $T_2^*$  weighted imaging is common in clinical studies; however, some of the many factors which contribute to transverse relaxation-based contrast changes are still poorly understood. By measuring relaxation times accurately it is possible to extract quantitative information about microstructure from MR data. This talk will provide an overview of the processes of transverse relaxation, highlight some common pulse sequences used for quantitative assessment of relaxation and describe what factors influence and  $T_2$  and  $T_2^*$  in vivo.

---

---

## Weekend Course

### Met & Unmet Needs in Musculoskeletal Imaging II - Met & Unmet Needs in Musculoskeletal Imaging II

Organizers: Riccardo Lattanzi, Jung-Ah Choi, Kimberly Amrami, Miika Nieminen, Hiroshi Yoshioka

Saturday Parallel 1 Live Q&A

Saturday 14:30 - 15:00 UTC

Moderators: Yongxian Qian & Xiaojuan Li

[MARS: Pedal to the Metal](#)

Suryanarayanan Kaushik

---

[Clinical Imaging near Orthopedic Implants](#)

Jan Fritz

---

[MRI Techniques for Imaging Peripheral Nerves](#)

Marcelo Bordalo Rodrigues

---

[Clinical MRI of Peripheral Nerves](#)

Benjamin Howe

---

[Technical Development in Ultra-Short TE Sequences](#)

Jiang Du

---

[Clinical Application of Ultra-Short TE Sequences](#)

Christine Chung

---

---

## Weekend Course

### Molecular Imaging - Molecular Imaging

Organizers: Kannie WY Chan, Hai-Ling Cheng

Saturday Parallel 2 Live Q&A

Saturday 14:30 - 15:00 UTC

Moderators:

: Nirbhay Yadav & Iris Zhou

[Imaging Exchangeable Protons: Technique & Applications \(CEST\)](#)

Jiadi Xu

Chemical exchange saturation transfer (CEST) is an MRI technique that is capable of enhancing the MRI sensitivity of low concentration metabolites and proteins in vivo. This course will cover the recent advances of the CEST technique, including the origin of in vivo CEST contrasts, the acquisition modes and the quantification methods. Based on these improvements, applications will be focused on observing several energy metabolites such as creatine, phosphocreatine and glucose in stroke, tumor and neurodegenerative diseases.

---

[Imaging metabolic molecules by MR spectroscopy and fingerprinting](#)

Xin Yu

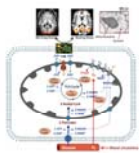
Magnetic resonance spectroscopic imaging (MRSI), especially hetero-nuclear MRSI, allows in vivo assessment of several fundamental metabolic events without the use of ionizing radiation. In particular, phosphorous-31 ( $^{31}\text{P}$ ) MRSI provides a valuable method to evaluate phosphate metabolites and the phosphorylation processes. This lecture will discuss the development of fast, high resolution  $^{31}\text{P}$  MRSI and fingerprinting techniques for quantification of mitochondrial oxidative capacity and metabolic rates in vivo.



### Things You Need to Know for In Vivo Molecular Imaging by MRS- perspectives from neuroradiology

Henry Mak

The first part of the talk gives a brief overview of the key basic concepts of proton MR spectroscopy such as chemical shift, J coupling and spectral editing, and some caveats in interpretation of MR spectroscopy findings. The second part of the talk emphasize its applications in brain tumors, neurodegenerative disease and psychosis. Finally, the future directions in MRS research are discussed.



### What Molecular Properties Can We Image using newly developed X-nuclear MRS methods?

Wei Chen

The advancement of ultrahigh-field (UHF) MRI technology (now reaching 10.5T for human scanner and beyond 16T for preclinical animal) has significantly improved imaging sensitivity, spectral and spatiotemporal resolutions. It accelerates new developments of in vivo MRS imaging technologies enabling quantitative and reliable assessment of various neurochemicals, metabolites, metabolic rates in healthy and diseased brain. This lecture will discuss newly developed X-nuclear MRS imaging methods for quantitatively imaging cerebral metabolic rates of glucose and oxygen, ATP production, TCA cycle and NAD redox ratio; and demonstrate promising applications for studying brain function and neuroenergetics under normal and diseased states at UHF.

### PET/MR

René Botnar

Cardiac PET/MR promises to combine multi-contrast and multi-parametric cardiac MRI that provides information on anatomy, left ventricular function, myocardial tissue viability, perfusion and oxygenation as well as fibrosis (T1), inflammation (T2) and iron (T2\*) with the high sensitivity of PET for radiotracer detection. Thus, it promises to enable simultaneous assessment of molecular and cellular processes related to cardiovascular diseases such as atherosclerosis, post infarct remodelling, cardiomyopathy or heart failure. In this talk we will discuss both the promises but also the challenges related to cardiac PET/MR and show first results from clinical studies.

## Weekend Course

### Neuroinflammation - Neuroinflammation

Organizers: Cornelia Laule, John Port, Pia Maly Sundgren

Saturday Parallel 3 Live Q&A

Saturday 14:30 - 15:00 UTC

Moderators: Manabu Kinoshita

The Influence of Inflammation on CNS Tissue Microstructure

Thomas Tourdias

Neuro-inflammation is characterized by alteration of the BBB which is accompanied by disruption of water homeostasis that can be monitored with diffusion MRI. Contrast agents inform on the status of the BBB in-vivo. Neuro-inflammation is also characterized in several instances by infiltration of immune cells from the blood stream that can be tracked with iron-oxide nanoparticle imaging. In terms of cellular consequences, glial activation is an important hallmark of neuro-inflammation which can induce dendritic/ neuronal alterations, all of them impacting microstructural metrics on MRI. Molecular imaging can also offer more specificities toward modifications of a given cell type.

Neuroinflammation Imaging Approaches: Blood Brain Barrier  
joga chaganti

Neuroinflammation Imaging Approaches: Blood Brain Barrier

---

Neuroinflammation Imaging Approaches: Leptomeninges  
Daniel Harrison

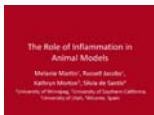
Meningeal inflammation occurs in multiple neurologic disorders, including multiple sclerosis. Recent data suggests that leptomeningeal enhancement (LME) on post-contrast FLAIR MRI may be seen in multiple sclerosis and other neuroinflammatory disorders. In this session, we will review the current data on LME in multiple sclerosis and other disorders.

---

Imaging the Innate Immune Response in MS: PET & MRI  
Susan Gauthier

This talk will discuss imaging methods, including both PET and MRI, used to assess CNS inflammation in MS and highlight the technical challenges and validation studies to provide a comprehensive review. Furthermore, it will be demonstrated how imaging is being utilized to explore the role of the innate immune response on the pathological mechanisms of disease in MS and the impact on clinical disability.

---



The Role of Inflammation in Animal Models  
Melanie Martin

Example of animal models of inflammation will be presented. For many brain diseases, neuroinflammation is emerging as a cause, rather than a consequence of the pathogenesis. Characterizing the neuroinflammation, and understanding the effects of the neuroinflammation are important. The contribution to the field of four studies will be explained.

---

The Role of Inflammation in Pediatric Neurological Disease  
Jan-Mendelt Tillema



DCE-MRI Characterization of Blood-Brain-Barrier Permeability Changes in Neuropsychiatric Systemic Lupus Erythematosus  
Steven Beyea

This educational talk is aimed at MR physicists looking to gain an introductory background to neuropsychiatric systemic lupus erythematosus (NPSLE), the role of neuroinflammation in dysfunction of the blood-brain barrier (BBB) in NPSLE, and specifically the role of Dynamic Contrast Enhanced MRI (DCE-MRI) in evaluating diseases/disorders such as NPSLE.

---

The Role of Inflammation in Neurodegeneration  
Itamar Ronen

---

## Weekend Course

### MR Physics for Scientists II - MR Physics for Scientists II

Organizers: Jose Marques, Hua Guo, Ivana Drobnjak

Saturday Parallel 4 Live Q&A

Saturday 14:30 - 15:00 UTC

Moderators:

MR Physics of Applications: Daniel Gallichan & Rui Pedro Teixeira

Physics of Flow Imaging  
Rui Li

---

## Physics of Diffusion Imaging

Zhe Zhang

Diffusion imaging can non-invasively probe tissue microstructures and has been widely adopted in clinical diagnosis and neuroscience research. In this section, we will briefly review the diffusion imaging contrast mechanisms and discuss the workhorse diffusion imaging sequence, which is single-shot spin-echo EPI. We will also discuss some recent diffusion imaging techniques such as multi-shot diffusion imaging, simultaneous multi-slice imaging, 3D imaging, etc. This section aims to give a comprehensive overview on diffusion imaging physics.

---

## Physics of functional MRI: GE, SE BOLD

Klaus Scheffler

---

## Physics of Perfusion Contrast

Susan Francis

---

## Principles of QSM & Applications

Jongho Lee

This is an educational session for quantitative susceptibility mapping and its applications.

---

## Principles of EPM & Applications

Rosalind Sadleir

This course will present methods of imaging and mapping tissue electrical properties (Electric Properties Mapping, EPM) using MRI. An overview of the characteristics underlying tissue electrical properties will be given followed by a brief summary of methods that have been used to measure them. Finally, the diverse approaches, present applications and emerging areas within EPM using MRI will be presented and described.

---



## Modeling Tissue Interactions with Gradients and RF Fields

Mathias Davids

The time-varying magnetic fields used in MRI induce electric fields (E-fields) in the human body that can have adverse effects. The radio-frequency (RF) coils induce high-frequency (MHz range) E-fields that cause tissue heating and potentially irreversible tissue damage in the conductive tissue (SAR). The gradient coils induce low-frequency (kHz range) E-fields that can stimulate peripheral nerves (PNS), leading to involuntary muscle contraction of touch perception. Understanding SAR and PNS effects is important to allow developing mitigation strategies to overcome their impact on image acquisition, such as reduced excitation fidelity, longer scan times, and reduced spatiotemporal image resolution.

---

---

## Weekend Course

### Common Challenges in Body MRI - Common Challenges in Body MRI

Organizers: Dianna Bardo, Mustafa Shadi Bashir, Vikas Gulani

Saturday Parallel 1 Live Q&A

Saturday 15:00 - 15:30 UTC

Moderators:

The Environment & Physics of Challenges  
in MRI: Verena Obmann

Uncontrollable, Unwilling & Uncooperative  
Patients: Mustafa Shadi Bashir

Coils, Position & Sequences: Optimal Image Acquisition

Shreyas Vasanawala

temp

---

### Artifacts: Signal, Time, Speed & Image Quality

William Masch

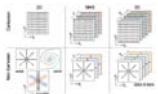
---

### Getting into the Room: The MRI Environment & Implants, Pacemakers, etc.

Scott Reeder

With the increasing number of implanted metallic devices in patients, as well as non-medical implants such as shrapnel or body piercings, MRI safety screening becomes more essential than ever. This presents an increasing challenge to ensure that patients undergoing this potentially lifesaving diagnostic exam can be performed in the safest manner and avoid injury to the patient. It is for this reason that it is essential that institutions develop standardized procedures that can address the existing and increasing number of metallic implants in a systematic way to ensure the safety of our patients.

---



### MRI without Sedation & Anesthesia. Are we there yet?

Suraj Serai

Newer motion robust acquisition methods are now available that have the potential to significantly minimize or remove the need for sedation and anesthesia in abdominal imaging. These new acceleration and motion robust MR techniques allow for free-breathing abdominal MRI and should allow for a decrease in MR scan times and sedation requirements. Familiarity with the advantages and trade-offs of these methods is essential for the radiologist performing the optimal study and for guiding the technologist acquiring the MR images.

---

### Neonates & Children: Uncontrollable & Uncooperative

Sarah Bixby

---

### From Claustrophobia to Obesity: Will Not Cooperate or Fit

Victoria Chernyak

The lecture will discuss common challenges and solutions when patients are uncooperative or who have morbid obesity

---

### Emergency Radiology: Acutely Ill & Unable to Cooperate

David Grand

---

## Weekend Course

### Gliomas - Gliomas

Organizers: Meiyun Wang, Rajan Jain

Saturday Parallel 3 Live Q&A

Saturday 15:00 - 15:30 UTC

Moderators: Meiyun Wang & Harish Poptani

### Preclinical Imaging

Arvind Pathak

---



### Glioma Genomics & Imaging

Sohil Patel



The World Health Organization classifies adult diffuse gliomas by integrating prognostically relevant molecular biomarkers with histopathologic features. Molecular biomarkers integrated in the classification include isocitrate dehydrogenase gene mutation and chromosome 1p/19q codeletion. For high grade gliomas / glioblastomas, *MGMT* promoter hypermethylation confers overall survival benefit and greater sensitivity to alkylating chemotherapy agents. Among pediatric gliomas, histone H3 mutations associate with high grade gliomas, and MAP kinase pathway alterations associate with low grade gliomas. Neuroimaging-based biomarkers can non-invasively predict underlying glioma genomic status and furthermore may add clinical value to the current classification scheme.

---

### MR Imaging for Diagnosis & Surveillance

Pia Maly Sundgren

In this presentation present and future imaging modalities including CEST imaging to grade brain tumor and to evaluate and differentiate between treatment response and tumor recurrence will be presented. The focus will be on MRI but also additional imaging strategies such as PET imaging and the combined value of different imaging strategies will be discussed. Scientific evidence and clinical practical cases will be presented. The advantages and disadvantages of imaging methods will be discussed.

---



### Radiomics in Glioma

Ji Eun Park

This lecture aims at providing insight into radiomics to become a viable tool for glioma patients. Recent radiogenomics studies and methodologic improvements of radiomics as diagnostic, prognostic, and/or predictive biomarkers will be described. A concept of tumor heterogeneity and subregional radiomics will also be introduced.

---

### Presurgical fMRI: Task-Based & Resting-State

Ho-Ling Liu

---

### MR/PET/MRS for Guiding Radiotherapy

Georges El Fakhri

---

### Image Guided Neurosurgery

Wei Chieh Chang

The efficacy and effectiveness of MRgFUS in Taiwanese population, of Asian ethnicity, has not yet been studied extensively. It has been shown that the clinical characteristics of ET and the skull factors might differ in Asians from Caucasians. The main objective of this study is to evaluate outcome of MRgFUS in terms of tremor suppression and adverse events in Taiwanese patients with refractory tremor.

---

### What Is on the Horizon: CEST

Linda Knutsson

A relatively new field of MRI is Chemical Exchange Saturation Transfer (CEST). In this talk basic principles of CEST MRI will be introduced and several examples will be presented to illustrate the potential of using CEST for clinical diagnosis and prognosis in gliomas.

---

## Weekend Course

### Advanced Spectroscopy - Advanced Spectroscopy

Organizers: Malgorzata Marjanska, Wolfgang Bogner

Saturday Parallel 2 Live Q&A

Saturday 15:00 - 15:30 UTC

Moderators: Graham Galloway & Esin

## Single-Voxel Spectroscopy at 7T & Beyond: From Animal to Human

Dinesh Deelchand

This lecture focuses on the pros and cons of utilizing single-voxel proton MR spectroscopy at ultra-high fields (UHF) of 7T and beyond in both human and animal brains. Advantages include higher signal-to-noise ratio, higher spectral dispersion i.e. less overlap between metabolites and these benefits lead to improved quantification of metabolites. However in human brain, going to UHF is associated with  $B_1$  inhomogeneity and increased RF power requirements and these can be mitigated by using dielectric pads or  $B_1$  shimming techniques. In addition, relaxation times of metabolites and water tissue signals change as  $B_0$  field increases.

---

## MRSI Encoding Techniques: Comparison, Advantages & Disadvantages

Anke Henning

---



## Multicenter MRS/MRSI Studies: What to Do & How

Eva-Maria Ratai

Imaging biomarkers may be used to help identify the natural history of disease progression, monitor therapeutic response, and identify side effects.  $^1\text{H}$  MRS offers the unique ability to measure metabolite levels in a non-invasive manner and has been widely used to access metabolisms in the brain, muscle, liver, prostate, breast, kidney, etc. However, MRS has only infrequently used in multi-center clinical trials. Here we discuss the potential and limitations of the techniques and suggest recommendations for the application of MRS to multi-center clinical trials.

---

## Importance of Macromolecules for Quantification of Full Neurochemical Profile & GABA Editing

Lijing Xin

Mobile macromolecules (MM) present as broad resonances underlying sharp metabolite resonances in  $^1\text{H}$  MR spectra at short to moderate TEs. The accurate estimation of MM is an important prerequisite for reliable quantification of metabolites. This lecture covers up-to-date knowledge about MM, how to handle MM for MRS quantification, and also some open questions.

---

## RF Pulse Design: From Adiabatic RF Pulses to Tailored MRS Volumes

Jürgen Finsterbusch

RF pulses are essential for every MR experiment and an important tool to manipulate the magnetization during the experiment. Important parameters of an RF pulse are the complex envelope, the duration, and the peak transmitter voltage that define the pulse's energy, the frequency spectrum, and flip angle. Depending on the purpose of the RF, the desired properties, and the boundary conditions, different RF pulse envelopes may be advantageous. In this presentation, the principles and basic properties of adiabatic, spatial-spectral, and multi-dimensional RF pulses will be covered with the latter being feasible to realize tailored measurement volumes in MRS.

---

## Motion & Instability Correction in MRS/MRSI (Prospective [Acquisition] & Retrospective [Post-Processing])

Ernesta Meintjes

---

### Weekend Course

#### MR Systems Engineering - MR Systems Engineering

Organizers: Ergin Atalar, Christoph Juchem

Saturday Parallel 4 Live Q&A

Saturday 15:00 - 15:30 UTC

Moderators:

: Ergin Atalar & Hiroyuki Fujita

[MR System Overview](#)

Richard Bowtell

---

### B0 Magnet Technology

Andrew Webb

---

### Passive B0 Shimming

Kevin Koch

---

### B0 Field Measurement

Irena Zivkovic

The goal of this talk is to stress out importance of the B0 field measurements and to present different techniques for the B0 field mapping with their advantages and shortcomings. The widely used technique based on NMR probes will be discussed in details.

---

### B0 Shimming with Spherical Harmonic Functions

Hoby Hetherington

Spherical harmonic shimming utilizes an orthogonal basis set of spatial functions to correct for B0inhomogeneity. For 3D mapping of the B0 field, the bandwidth, accuracy and SNR of the acquired maps determine the accuracy of the maps. To achieve optimal results, imperfections in the fields generated by the shim coils need to be considered. Once these issues are addressed, higher order spherical harmonics provide significant advantages (up to 50% more than conventional 1st&2nd order shimming) for both static and dynamic solutions ranging from slices to the entire brain and multi-band shimming.

---

### Gradient Coil Design

William Handler

---

### Current Amplifiers & Electronics

Mike Twieg

---

### Peripheral Nerve Stimulation (PNS)

Valerie Klein

Time-varying MRI gradient fields induce electric fields in the patient that can become strong enough to stimulate peripheral nerves, muscles, and possibly even the heart. These unwanted physiological effects significantly limit the performance of modern MRI gradient systems. This course will discuss the mechanisms underlying gradient field interactions with the human body and will show methods used to investigate and to minimize their occurrence.

---

## Weekend Course

### Liver: Best Practices, Challenges & Emerging Solutions - Liver: Best Practices, Challenges & Emerging Solutions

Organizers: Utaroh Motosugi, Claude Sirlin, Mustafa Shadi Bashir

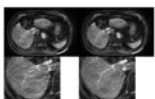
Saturday Parallel 1 Live Q&A

Saturday 15:30 - 16:00 UTC

Moderators:

Liver MRI Acquisition: Michael Ohliger

Liver MRI Interpretation: Hanyu Jiang



### Breathing Artifacts in Liver MRI: Emerging Solutions

Daiki Tamada

Many studies have attempted to reduce motion artifacts in the liver over the years. However, it is still challenging to develop robust and practical methods to address this problem because of the complicated nature of motion artifacts. Recently, the deep learning approach has been used to achieve excellent image processing results. This talk provides an overview of deep learning-based methods to address breathing artifacts in the liver.

---

### Liver DWI: Emerging Solutions

Dimitrios Karampinos

---



### Liver MRI: Which Contrast Agent?

Chang-Hee Lee

Extracellular agents are distributed within the extracellular interstitial space. Gadolinium chelates, which are formed by the chelation of gadolinium to organic ligands such as diethylenetriaminepentaacetic acid, constitute a class of extra-cellular agents. Although several formulations are available with different ligands, their pharmacologic characteristics and imaging considerations are essentially identical. There are multiple indications for the use of extracellular contrast agents in MR imaging of the liver. These include lesion detection, lesion characterization, and liver vasculature assessment. In this lecture, I will talk about “representative pearls and pitfalls” of the GD-EOB-DTPA Liver MRI, comparing ECA enhanced liver MRI.

---

### Liver MRI Acquisition: The Basics

William Masch

---

### Liver MRI Acquisition: Remaining Challenges

Daniel Moses

This educational session looks at some of the remaining challenges in respect to the technical acquisition for liver MRI. It approaches this through examining current quantitative MRI techniques (including T1/T1ρ/T2/T2\* mapping, elastography, diffusion weighted imaging, perfusion weighted imaging, and proton density fat fraction) including explaining their basic principles, their clinical applicability to liver disease, and challenges in implementing these techniques.

---

### How Do I Interpret Treatment Response?

Verena Obmann

---

### Challenges in MRI Liver Interpretation: Emerging Solutions

Koichiro Yasaka

This talk will introduce the emerging solutions for MRI liver interpretations in liver fibrosis staging and liver mass differentiation, especially those based on radiomics strategies and deep learning technique.

---

### How Do I Interpret Diffuse Liver Disease?

Takeshi Yokoo

---

### How Do I Interpret Liver Lesions in Cirrhosis?

JeongHee Yoon

The differential diagnosis of hepatic observations is often challenging. Liver MRI has been increasingly used for characterization of hepatic observations.

---

---

## Weekend Course

### I Did Not Know MRS Can Do That! - I Did Not Know MRS Can Do That!

Organizers: Malgorzata Marjanska, Catherine Hines, Hai-Ling Cheng, Yi-Fen Yen

Saturday Parallel 2 Live Q&A

Saturday 15:30 - 16:00 UTC

Moderators: Malgorzata Marjanska & Ovidiu Andronesi

#### Brain Temperature & Its Applications

Dionyssios Mintzopoulos

---

#### Mitochondrial Dysfunction in Heart Disease

Kerstin Timm

---

#### Cancer Treatment Response

Patrick Bolan

- Understand the strengths and weaknesses of MRS
  - Let the clinical/research question drive the methodology
  - Be rigorous with quantitative methods
- 

#### Insights into Brain Microstructure from DW-MRS

Marco Palombo

This lecture targets researchers and clinicians who are interested in using diffusion-weighted magnetic resonance spectroscopy (DW-MRS) of metabolites for brain microstructure characterisation. The audience will learn the basic mechanisms underpinning in-vivo metabolites DW-MRS, how to extract complex microstructural features characterising the morphology of specific cell-types (i.e. neurons and glia), together with some clinical and preclinical applications. Particular effort will be made to give intuitive insight and exiting perspectives on novel DW-MRS applications for brain microstructure quantification.

---

#### Insights into Neuronal Activation from fMRS

Joao Duarte

---

## Weekend Course

### fMRI Across Spatial & Temporal Scales - fMRI Across Spatial & Temporal Scales

Organizers: Benedikt Poser, Susan Francis, Richard Buxton

Saturday Parallel 3 Live Q&A

Saturday 15:30 - 16:00 UTC

Moderators: Richard Buxton & Susan Francis



#### State-of-the-Art Echo-Planar BOLD Acquisition

Rüdiger Stirnberg

This lecture reviews state-of-the-art 2D and 3D sequences with a focus on gradient echo EPI acceleration with controlled aliasing (CAIPIRINHA). The audience should learn which rapid EPI-based methods for BOLD fMRI are available and what to consider to minimize noise or artifacts due to strong parallel imaging, if needed, for the respective study goal.

---

#### Denosing Techniques

Lars Kasper

Noise is the eminent adversary when studying brain function. First, it incurs sensitivity loss for our small effects of interest by drowning them in un(cor)related fluctuations. Second, noise may correlate with effects, reducing specificity or increasing false positives by conflating them with fluctuations of non-neuronal origin. Here, we revisit how both the scanner and the subject generate noise in fMRI time series through different pathways, namely as thermal noise, encoding noise (magnetic field), and physiological noise of different origin.

We structure different approaches to noise mitigation following the recycling waste hierarchy, which also applies to sustainable science: avoid, reduce, reuse.

---

### Non-BOLD fMRI

Harald Möller

While the BOLD contrast is widely applied to map brain activity, it is also fundamentally limited as it provides only an indirect measure of neural activation that cannot be straightforwardly quantified and is inherently limited in its spatial specificity. Consequently, alternative methods have evolved to address such limitations. Here, we will primarily focus on measurements of CBF and CBV changes as currently popular 'non-BOLD' contrasts in human fMRI studies of the neurovascular coupling or at laminar resolution.

---

### Oxygen Metabolism & Calibrated BOLD

Esther Warnert

---

### fMRI at High Spatial Resolutions: Layers & Columns

Luca Vizioli

The aim of this talk will be to provide a brief overview of some of the main challenges of performing laminar and columnar fMRI, highlighting some of the strategies that can be adopted to tackle such problems.

---

### fMRI across high temporal scales

Burak Akin

With the advent of fast fMRI sequences, whole brain fMRI data can be acquired in few hundreds of milliseconds. Although fast acquisitions are not necessary to sample the low frequency ( $<0.1\text{Hz}$ ) fluctuations associated with most of the BOLD activity. Approaches with increased temporal resolution have some advantages like allowing dynamic connectivity analysis and potential to reveal transient changes of the brain function. This lecture will cover a short overview of available fast fMRI techniques, their advantages over widely used EPI sequence and finally potential applications in brain imaging.

---

### Functional Spectroscopy

Adam Berrington

---

---

## Weekend Course

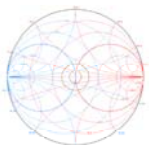
### MRI RF Systems - MRI RF Systems

Organizers: Greig Scott, Ergin Atalar

Saturday Parallel 4 Live Q&A

Saturday 15:30 - 16:00 UTC

Moderators: David Brunner & Manisha Aggarwal



### Basics of Transmission Lines & Power Transfer

Stephen Ogier

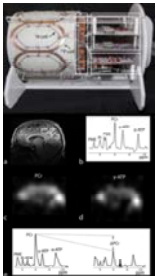
The MRI signal is excited and detected using radiofrequency systems. To those unfamiliar with RF systems the equipment, concepts, and measurements can be intimidating and confusing. Developing an understanding of transmission lines, which form the basis for RF systems, allows one to easily understand most of the RF system at a basic level. The aim of this is to provide an introduction to transmission lines and the parameters/metrics commonly used with them. Additionally, some applications of transmission line theory to MRI will be introduced and discussed.



### Volume & Surface Coils

Özlem Ipek

This talk identifies the coil characterisation parameters as matching, tuning, quality factor, transmit efficiency, specific absorption rate and RF coil losses. Examples using birdcage, TEM, loop and dipole antenna designs are provided using electromagnetic field simulations, measured transmit field maps and bench measurement methods.



### Multi-Nuclear Coils

Ryan Brown

- Dual-tuned coils provide metabolic information (x-nuclei module) and co-registered anatomical images and B0 shim settings (1H module) without repositioning the subject or coil

- X-nuclei signal strength is typically less than 1/1,000<sup>x</sup> that of 1H (1). Therefore it is important to maximize x-nuclei receive sensitivity while simultaneously providing adequate 1H sensitivity

- We will discuss prevalent dual-tuning techniques and considerations for performance characterization and interfacing dual-tuned coils

### Receive Arrays & Circuitry

Gillian Haemer

### Transmit Arrays & Circuits

Sigrun Roat

### Transmit Arrays for UHF Body Imaging

Stephan Orzada

As the main magnetic field strength increases, the corresponding RF wavelength is shortened. This leads to pronounced wave effects in the transmit field, causing inhomogeneous excitation. Multi-channel arrays provide additional degrees of freedom to mitigate such effects and to manipulate (or to tailor) RF transmission. Roughly these can be divided in 3 types, namely local arrays, remote circumferential arrays and travelling wave arrays. Examples of these arrays are presented in this educational talk.

## Weekend Course

### Machine Learning: Everything You Want to Know - Machine Learning: Everything You Want to Know

Organizers: Demian Wassermann, Florian Knoll, Daniel Rueckert

Saturday Parallel 2 Live Q&A

Saturday 16:00 - 16:30 UTC

Moderators: Florian Knoll & Jakob Meineke



### Basic Introduction to Machine Learning

Jo Schlemper

In this talk, we will discuss the basics of machine learning: a supervised learning framework and neural networks. In particular, we will cover the following topics, focussing on the intuition behind them:

- (1) Types of machine learning
- (2) Neural networks, from perceptron, MLP to deep neural networks
- (3) Training, overfitting and regularization
- (4) Practical considerations for applying ML
- (5) Challenges of deep learning.

---

When Does It Work, When Does It Break Down? Analyzing the Theoretical Properties of Machine Learning  
Thomas Pock

---

Which Deep Learning Model Will Work for Me? Practical Considerations & Getting Started  
Matthew Muckley

---

Applications of Machine Learning: Image Processing & Interpretation  
Henkjan Huisman

---

Applications of Machine Learning: Data Acquisition & Image Reconstruction  
Shanshan Wang

Machine learning, especially deep learning, has shown great potential in accelerating MR imaging lately. To accelerate MR imaging with deep learning, the sampling trajectories can be Cartesian or Non-Cartesian subsampling patterns. While the reconstruction methods can be roughly categorized into end-to-end data-driven learning reconstruction methods and model based unrolled iterative learning reconstruction methods. This educational lecture will briefly go through these methods and provide a starting point for researchers interested in this field.

---

Killer Applications: Where Will Machine Learning Make a Substantial Clinical Impact?  
Greg Zaharchuk

---

## Weekend Course

### No Way to Treat a Lady: Breast & Female Reproductive Organ Cancers - No Way to Treat a Lady: Breast & Female Reproductive Organ Cancers

Organizers: Reiko Woodhams, Daniel Margolis

Saturday Parallel 1 Live Q&A

Saturday 16:00 - 16:30 UTC

Moderators:

Breast Cancer: Reiko Woodhams

Female Reproductive Organ Cancers:

Aki Kido

Conventional Breast MRI Techniques & Reporting  
Mami Iima

This course describes the current status of breast MR imaging. The strengths and weaknesses of breast MRI and clinical indications are also discussed. The BI-RADS classification system designed to standardize breast imaging reporting consisting in a lexicon for standardized terminology for mammography, ultrasonography or MRI is introduced, as well as chapters on report organization and guidance chapters for use in daily practice.

---



Breast Cancer Screening in the High-Risk Patient  
Rebecca Rakow-Penner

---

Breast MRI: Future Directions  
Savannah Partridge

---



Endometrial Cancer & Other Uterine Malignancies  
Yumiko Tanaka

Diagnosing local extension of the endometrial carcinoma with MR is crucial as myometrial and cervical stromal invasion are important prognostic factors. However, the utility of T2-weighted, contrast-enhanced, and diffusion-weighted images is controversial. In this lecture, oncologically essential facts and tips of the MR in diagnosing endometrial carcinoma will be presented. Leiomyosarcoma is the most common malignant mesenchymal tumor of the uterus; however, it is still difficult to differentiate it from uterine fibroids. We will provide MR findings of leiomyosarcoma comparing to those of histological variants of uterine fibroid and cutting edge technology in differentiating these two disease entities.

---

Cervical Cancer  
Nandita DeSouza

MRI is the fundamental imaging modality in the management pathway of cervical cancer. Its use is crucial for early diagnosis, for tumor staging, to provide prognostic information, to monitor the effects of treatment and to follow-up patients for detection of disease recurrence.

---

Can We Predict Disease Better?  
Carolyn Mountford

---

Ovarian & Peritoneal Diseases  
TBD

---

## Weekend Course

### Nuts & Bolts of fMRI & Its Clinical Applications - Nuts & Bolts of fMRI & Its Clinical Applications

Organizers: Benedikt Poser, Susan Francis, Richard Buxton

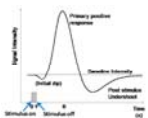
Saturday Parallel 3 Live Q&A

Saturday 16:00 - 16:30 UTC

Moderators:

fMRI Basics: Benedikt Poser

Clinical Applications of fMRI: Susan Francis



Introduction fMRI: Origin of the BOLD Signal  
Karen Mullinger

BOLD fMRI is a popular tool for studying brain function due to its non-invasive nature and the ability to provide high spatial resolution across the brain. However, the BOLD contrast is not a direct measure of neuronal activity and can also be used to interrogate vascular properties of the brain. Here we will explore the physical and physiological mechanisms which generate the BOLD signal. With this knowledge we will briefly explore how a given BOLD signal could have been generated in many different ways; and methods to disentangle this information; highlighting the opportunities and challenges BOLD contrast offers.

---

Introduction fMRI: BOLD Acquisition & Practical Considerations  
Daniel E. Gomez

This course describes the acquisition of functional MRI (fMRI) data and the practical concerns and trade-offs involved when designing imaging protocols. Focus is given to blood oxygenation level dependent (BOLD) acquisitions with a gradient-echo (GRE) 2D echo-planar-imaging (EPI) sequence. Key sequence parameters and common artifacts are discussed.

---

#### Task Design & Analysis: From GLM to MVPA

Anna Blazejewska

This lecture will discuss the motivation, methodology and limitations of different experimental designs and data analysis approaches for task-based fMRI experiments. More specifically, the GLM and MVPA approaches will be discussed and compared.

---

#### Resting State: Analysis Strategies

Sheba Arnold-Anteraper

---

#### Clinical Applications: Pre-Surgical Planning

Yanmei Tie

---

#### Clinical Applications: Real-Time fMRI & Neurofeedback

Susan Whitfield-Gabrieli

---

### Weekend Course

#### Multi-Coil B0 Field Modelling & Systems - Multi-Coil B0 Field Modelling & Systems

Organizers: Ergin Atalar, Christoph Juchem

Saturday Parallel 4 Live Q&A

Saturday 16:00 - 16:30 UTC

Moderators:

: Ergin Atalar & Irena Zivkovic

#### Introduction to the B0 Multi-Coil Technique

Suryanarayana Umesh Rudrapatna

---

#### Combined B0 & RF Arrays

Nicolas Arango

---

#### Multi-Coil B0 Shimming of the Spinal Cord

Ryan Topfer

---

#### Multi-Coil B0 Shimming in the Body

Hui Han

---



#### Multi-Coil B0 Shimming with Irregular Coil Arrays

Jiazheng Zhou

Ultra-high field (UHF) magnetic resonance imaging (MRI) enables functional brain images with sub-millimeter spatial resolution. However, susceptibility induced magnetic field ( $B_0$ ) variations within tissue are the source of various artifacts. Shim coils of different shape and size are applied to reduce these  $B_0$  inhomogeneity. However, most shim coils only have a regular shape and distribute current pattern on a cylinder surface or close-fit helmet. The difference in performance between current multi coil array and irregular shape multi coil array has not been explored. The optimization methods for multi-coil shim arrays are discussed, together with design and construction procedure.

---

## Imaging with B0 Coil Arrays

Koray Ertan

---



## Matrix Gradient Systems

Sebastian Littin

A matrix gradient systems allows to synthesize spatial encoding magnetic fields (SEMs) for new encoding methods. An overview of the implementation and possible applications is given.

---

## Multi-Coil B0 Field Modeling for Accessible MR System

Sebastian Theilenberg

---

**Sunday, 9 August 2020**

### Evening Event

#### ISMRM Opening Reception

Exhibition Hall

Sunday 1:30 - 3:00 UTC

---

### Weekend Course

#### Signal Enhancement: The Power & the Glory - Signal Enhancement: The Power & the Glory

Organizers: Elena Vinogradov, Lucio Frydman

Sunday Parallel 3 Live Q&A

Sunday 14:00 - 14:30 UTC

Moderators: Daniel Gochberg

#### Basics of CEST and Spin Lock

Moritz Zaiss

---

#### Basics of MT

Michael McMahon

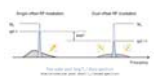
---

#### CEST Applications

Kannie WY Chan

Chemical exchange saturation transfer (CEST) MRI is a robust molecular imaging approach, which has shown many promising clinical applications. For example, to identify radiation necrosis and tumor recurrence. CEST enhances the detectability of many endogenous and exogenous molecules presence at low concentrations in vivo. This course will cover the principles of CEST and its applications mainly in the brain. This is to showcase CEST can detect specific endogenous or exogenous molecules in vivo to facilitate diagnosis and therapy, including brain tumor, cancer treatment and dementia.

---



## ihMT Principles & Applications

Olivier Girard

This lecture will cover the basic principles and applications of the recently developed inhomogeneous Magnetization Transfer (ihMT) MRI technique. IhMT is a promising myelin imaging technique and it offers an exciting opportunity to exploit a new endogenous contrast mechanism in vivo using MRI, by discriminating biological tissues based on their dipolar relaxation time ( $T_{1D}$ ). This presentation will review the basics of the dipolar order concept and associated thermodynamic models. The lecture will also cover typical ihMT experiments and describe up to date MRI sequence optimization. Promising MRI applications will be presented, as well as future research directions.

---

## Basics of Optically Pumped MR

Rosa Tamara Branca

Spin-exchange optical pumping (SEOP) of mixtures of alkali-metal vapors and noble gases can be used to efficiently polarize the nuclei of noble-gas atoms. Liters of noble gases at standard temperature and pressure can now be produced with nuclear spin polarization levels of several tens of percents. In this talk we will review the physics of the SEOP process, and then discuss our understanding on how experimental conditions affect final polarization levels.

---

#### Basics of para-H<sub>2</sub> Enhanced MR

Warren Warren

---

#### Hyperpolarization via Dynamic Nuclear Polarization

Arnaud Comment

In this educational course, basic concepts of dynamic nuclear polarization (DNP) will be outlined. The hyperpolarization methods based on DNP and used for <sup>13</sup>C MRI and MRS applications will be introduced.

---

### Weekend Course

#### Joint MICCAI-ISMRM Session: Synergies Between Our Societies in Data Acquisition, Image Reconstruction & Analysis - Joint MICCAI-ISMRM Session: Synergies Between Our Societies in Data Acquisition, Image Reconstruction & Analysis

Organizers: Florian Knoll, Daniel Rueckert, Zhaolin Chen, Demian Wassermann

Sunday Parallel 3 Live Q&A

Sunday 14:00 - 14:30 UTC

Moderators: Florian Knoll & Daniel  
Rueckert

#### Introduction to MICCAI: Top 5 Current Topics in the Society

Terry Peters

This workshop focuses on the synergies between MICCAI and ISMRM, and this presentation reviews five prominent topics of interest to the ISMRM community, that were presented at the most recent MICCAI meeting, held in Shen Zhen China in October 2019.

---



#### Large Sample Size, Compromises in Data Quality: Challenges & Opportunities in Population Imaging

Tony Stoecker

This lecture briefly introduces the challenges of population imaging by example of the Rhineland Study, a large-scale longitudinal cohort study which investigates aging, in particular of the human brain and related neurological disorders, across the adult lifespan. The emphasis is on quantitative measures, including a one-hour MRI examination of brain structure and function. The talk will present its MRI acquisition and analysis strategies, as well as some preliminary results.

---

#### Small Sample Size, Unprecedented Data Quality: Challenges & Opportunities in High-End Data Acquisition

Jonathan Polimeni

While there is a well-known trend towards large-scale neuroimaging studies, there is also mounting interest in single-subject MRI that enables the investigation of meaningful differences in brain structure and function between individuals. Single-subject MRI opens opportunities for advanced imaging strategies that are infeasible in large-scale studies, such as highly sampling individual brains to boost statistical power, and acquiring multiple averages of high-resolution data to achieve both high sensitivity and specificity. In this lecture I will survey specialized technologies for improving data quality, showcase example high-end datasets, discuss factors that limit data quality, and consider new methods to overcome these limits.

---

#### Lessons from MICCAI Imaging Challenges

Alistair Young

---

## Lessons from Other Imaging Modalities

Andreas Maier

In this presentation, we will look into machine learning-based reconstruction and observations made on other imaging modalities than MR. In particular, we can sub-divide reconstruction methods into purely data-driven, analytically inspired, and optimization-inspired. We find that also from a theoretical point of view, embedding of domain knowledge is beneficial. During the presentation, we will discuss further the benefits and risks of these common approaches. In the end, we will give an outlook on future perspectives and potential enablers in the field.

---

## Learned End-to-End MR Acquisition, Reconstruction & Analysis

Nii Okai Addy

Machine learning techniques provide intriguing possibilities to improve the MR imaging process from acquisition to image analysis. Machine learning techniques provide the possibility to make the acquisition process more efficient by reducing scan time or more consistent with automated control. Learned techniques also provide more options for reconstructing under sampled datasets. Perhaps the most prevalent use of learned techniques at this time is for the analysis of images for tasks ranging from quality control to diagnosis. These topics will be explored and addition to looking forward to see how the application of machine learning to MRI may change over time.

---

---

## Weekend Course

### Perfusion MRI - Perfusion MRI

*Organizers:* Jongho Lee, Fernando Calamante, Seung Hong Choi, Susan Francis

Sunday Parallel 1 Live Q&A

Sunday 14:00 - 14:30 UTC

*Moderators:* Henk Mutsaerts & Kathleen Schmainda

#### ASL: Basics

Maria A. Fernandez-Seara

The objective of this talk is to introduce the methodology of ASL data acquisition and analysis. Upon attendance, the audience should have a basic understanding of the technique and be able to choose the most adequate pulse sequence for a particular clinical application and the most appropriate acquisition parameters.

---

#### ASL: Advanced Topics

Sophie Schmid

---

#### Applications: ASL

Shalini Amukotuwa

---

#### DSC-MRI: Basics

Amit Mehndiratta

Perfusion imaging using dynamic susceptibility contrast MRI is widely used in management of brain ischemia and stroke. It is based on change in  $T2^*$  effect arising from local field inhomogeneity as the contrast flow from the tissue capillary network. Quantitative analysis is completely based on the mathematical understanding of the underlying capillary network model, either a simplified model based approach or a complex model free methods have been used in literature. There are pros and cons of each method, this lecture will discuss few of these important methods and there benefits and limitations.

---

#### DSC-MRI in Neuroimaging: Sources of Errors & Artifacts

Atle Bjørnerud

---



### DCE-MRI: Acquisition

Jaeseok Park

This lecture is to provide fundamental principles of dynamics contrast enhanced (DCE) magnetic resonance imaging (MRI) from the perspective of acquisition. We will talk about T1-weighted dynamic data acquisition for DCE MRI, dynamic T1 (t) quantification with correction of B1 field inhomogeneities, and conversion of T1 maps to concentrations. We move on to delineation of contrast dynamics with time and discuss why we need to have high spatial and temporal resolution for accurate quantification of perfusion and microvascular permeability. Then, I will introduce some of the state-of-the-art, high resolution DCE MRI methods.



### DCE-MRI: Processing

Ka-Loh Li

This educational lecture discusses efforts in making accurate, high-spatial resolution, whole brain coverage microvascular parametric maps and reducing dosage of gadolinium based contrast agents (GBCA), using a newly developed dual-temporal resolution (DTR) DCE-MRI processing technique.



### Applications: Contrast-Based Perfusion MRI

Roh-Eul Yoo

DSC-PWI is dependent on the susceptibility effect caused by paramagnetic gadolinium on T2\*-weighted imaging. Dynamic contrast-enhanced (DCE) MR imaging is based on T1 shortening induced by a gadolinium-based contrast bolus passing through tissue. Various quantitative model-based and semiquantitative model-free pharmacokinetic parameters, that reflect microcirculatory structure and function, can be derived using the technique. This lecture will focus on the clinical applications of the contrast-based perfusion-weighted imaging techniques in neuroimaging (e.g. tumor, stroke, seizure).

## Weekend Course

### Brainstem, Cerebellum & Basal Ganglia/Thalamus: Hodology & Connectivity - Brainstem, Cerebellum & Basal Ganglia/Thalamus: Hodology & Connectivity

Organizers: John Port, Rajan Jain

Sunday Parallel 2 Live Q&A

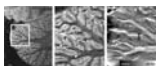
Sunday 14:00 - 14:30 UTC

Moderators: Christopher Hess

Brainstem Anatomy & Hodology: In Vivo imaging

Marta Bianciardi

In this course, we first describe the morphology of major brainstem nuclei involved in wakefulness/sleep, motor, sensory, autonomic and limbic function, as evinced from MRI of *living* humans. We then present recently developed *in-vivo* atlases for brainstem nuclei localization in conventional images of *living* humans. Further, we provide an overview of the opportunities and challenges of *in-vivo* mapping the connectivity pathways of these tiny nuclei using functional and diffusion-based MRI. Finally, we present validation strategies of *in-vivo* brainstem nuclei atlases and connectomes, and their preliminary application to brainstem-related pathologies, such as disorders of consciousness, sleep disorders and neurodegenerative diseases.



### Cerebellum Development, Pathways & Imaging

Wietske van der Zwaag

The cerebellum is an important, but somewhat overlooked brain region. This lecture will discuss the development and connectivity of the cerebellum, as well as discussing the available imaging tools ready to use to best visualise this beautiful brain structure.

Cerebellum and Brainstem Hodology: Clinical Imaging

Rajan Jain

---

### Basal Ganglia Anatomy & Imaging

Erik Middlebrooks

Recent advances in electrophysiological and neuroimaging techniques have refined our understanding of basal ganglia connectivity. These advances stand to improve our understanding of human disease, as well as further refine therapeutic techniques, such as deep brain stimulation. This presentation highlights current understanding of basal ganglia connectivity with an emphasis on common disease processes, as well as exploration of neuroimaging techniques for assessing basal ganglia.

---

### Basal Ganglia & Thalamus Pathology & Imaging: Clinical

Suyash Mohan

---

### HIFU

Dheeraj Gandhi

High Intensity MR Guided Focused Ultrasound of the Brain: Current and Future applications

---

### Brainstem Hodology & Imaging

Michael Hoch

---

---

## Weekend Course

### Data Acquisition & Image Reconstruction I - Data Acquisition & Image Reconstruction I

Organizers: Mariya Doneva, Kawin Setsompop

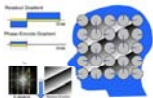
Sunday Parallel 4 Live Q&A

Sunday 14:00 - 14:30 UTC

Moderators:

Spatial Encoding & Contrast Preparation:  
William Grissom

RF Pulses, Preps & Calibrations: Martijn  
Cloos



### MR Basics Recap: Signal Encoding & k-Space

Brian Hargreaves

In MRI, spatial localization is provided by the use of gradients, and augmented by use of RF coil arrays. Gradients impart a linear phase variation of the transverse magnetization of any magnitude and direction. The resulting acquired signal is the Fourier transform of the magnetization for the specific linear phase, known as the k-space location. With sufficient sampling of signal across k-space locations, an inverse Fourier transform can reconstruct the magnetization distribution, or image. The Fourier relationship between image and k-space signals offers tremendous intuition for imaging tradeoffs, including resolution, field-of-view, artifacts, the use of multiple coils, and signal excitation.

---

### Non-Cartesian Sampling: Advantages & Pitfalls

Kathleen Ropella-Panagis

Cartesian sampling is simple to implement, robust, and widely used in clinical applications. However, there are numerous reasons to use non-Cartesian sampling methods. This talk will cover advantages of non-Cartesian sampling; disadvantages of non-Cartesian sampling, including ways to mitigate them; and examples of non-Cartesian sampling methods and their clinical utility.

---

Contrast Prep: GE/SE, TSE, SPACE, GRASE

V. Andrew Stenger

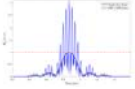
---

### RF Pulse Design

Shaihan Malik

RF pulses are an integral part of every MR sequence, and may take on multiple different functions (excitation, saturation, inversion, refocusing, etc...). The Bloch equation governs the interaction between RF fields and magnetization, and so RF pulse design is essentially the process of inverting the Bloch equation: we ask "What should the RF fields do given the way we want the magnetization to end up?". This talk will cover: the small tip angle approximation (STA); Shinnar Le Roux (SLR) pulse design method; Multidimensional and multiband RF pulses; and Parallel transmission pulse design.

---



### Applications of RF Pulse Designs: Inner Volume Imaging, SMS, B1 Shimming & pTx

Sydney Williams

This talk reviews a few popular RF pulse design applications: inner volume imaging, simultaneous multislice, B1 shimming, and parallel transmission.

---

### Preps & Calibrations: Measuring Non-Imaging Data with the Scanner

Benedikt Poser

---

## Weekend Course

### How to Conduct the "Ideal" In Vivo Preclinical MR Experiment - How to Conduct the "Ideal" In Vivo Preclinical MR Experiment

Organizers: Arvind Pathak

Sunday Parallel 3 Live Q&A

Sunday 14:30 - 15:00 UTC

Moderators: Harish Poptani & Jürgen Schneider

### Considerations When Designing an In Vivo Experiment: Animal Handling, Anesthesia, Physiological Monitoring, Etc.

Olli Gröhn

stress level of the animals influences most of the study designs where preclinical MRI is utilized. Furthermore, anesthesia has profound effect on fMRI, and extreme care has to be taken while choosing the type of anesthesia and for monitoring the anesthesia level and physiological state of the animal in order to obtain reliable and reproducible results. Protocols for scanning awake animals have been around for two decades but only recently have become more popular due to increased awareness on importance of physiological factors for (f)MRI results.

---

### Using Clinical vs. Preclinical Hardware

Michael McMahon

---

### Clinical vs. Preclinical Data Acquisition, Reconstruction & Translation

Jack Miller

Pre-clinical MRI is a powerful and important tool for addressing a variety of basic scientific questions, as well as providing a unique platform for technique development. This course explores its quantitative differences from clinical MR, with a strong emphasis on the statistical analysis of the data it provides, within the context of addressing basic scientific questions.

---

### Data Analysis & Software Considerations

Mark Pagel



This didactic presentation will describe aspects of data analysis and software considerations when performing the "ideal" small animal MRI study. Topics include considerations for 1) incorporating image analysis into the experimental design and financial budget before starting the study; 2) data quality for good analyses; 3) registration and segmentation; 4) repeatability, reproducibility, and rigor of data analyses. Each of these topics will be highlighted with a practical example.

---

#### Multimodality Imaging Techniques Complementary to MRI

Kristine Glunde

---

### Weekend Course

#### Diffusion: Encoding & Acquisition - Diffusion: Encoding & Acquisition

Organizers: Carl-Fredrik Westin, Noam Shemesh

Sunday Parallel 1 Live Q&A

Sunday 14:30 - 15:00 UTC

Moderators: Marco Palombo & Carl-Fredrik Westin

#### Advanced Diffusion Encoding Gradient Waveforms

Markus Nilsson

Most studies using diffusion MRI today rely on a pair of gradient pulses to do the diffusion encoding. However, this approach is fundamentally limited in several ways. This talk will provide examples of these limitations and show how to use advanced gradient waveforms to overcome them. Examples from recent papers will demonstrate how such advanced encodings can radically change the interpretation of diffusion MRI data.

---

#### Diffusion-Relaxation MRI

Jana Hutter

This talk will focus on the recent developments combining diffusion MRI with relaxometry. It will first give details on the parameters and choices available on the acquisition side. Next, possible analysis techniques will be presented and finally recent results detailing possible applications will be discussed.

---

#### The Quest for High-Spatial-Resolution Diffusion MRI

Lucio Frydman

---

#### Spiral Acquisition for Diffusion MRI

Lars Mueller

Spiral readouts for diffusion weighted MRI are gaining more interest. The idea has been around for quite a while, because of the shorter echo time and thus signal to noise ratio achievable compared to EPI. With the advent of field monitoring and/or gradient impulse response function, high quality single shot imaging has become possible. This was achieved by employing an expanded signal model, which incorporates higher order k-space and B<sub>0</sub>-inhomogeneities. We will have a look at the steps necessary to achieve high quality diffusion imaging with spiral readouts.

---

#### SPEN for Diffusion MRI

Eddy Solomon

This talk will discuss a relatively new MRI methodology called SPatio-temporal ENcoding (SPEN). SPEN is a highly robust method overcoming B<sub>0</sub>-inhomogeneities and heterogeneous chemical shift environments, and hence presents advantages in multiple diffusion studies. Attention will be focused on the physical basis employed to quantify diffusion experiments using SPEN and recent substantial advantages will be discussed in terms of both anatomical image qualities and diffusional information vis-à-vis EPI.

---

## Diffusion MRI Outside the Brain

Rita Nunes

Clinical applications of DWI outside the brain have grown significantly over the years, particularly in the detection and characterization of cancer lesions. This lecture will focus on the specific challenges of applying this technique to body imaging, presenting some of the existing strategies for dealing with these issues.

---

---

## Weekend Course

### Cardiovascular MRI: The Heart - Cardiovascular MRI: The Heart

Organizers: Jennifer Keegan, Aleksandra Radjenovic, Peng Hu

Sunday Parallel 2 Live Q&A

Sunday 14:30 - 15:00 UTC

Moderators: Daniel Kim & Yanjie Zhu

#### Evaluation of Cardiac Function: Clinical Applications & Technical Approaches

Yuchi Han

---

#### Myocardial Perfusion: Clinical Applications & Technical Approaches

Michael Jerosch-Herold

Magnetic resonance imaging of myocardial perfusion continues to challenge current limits for fast dynamic imaging to provide sufficient spatial and temporal resolution for accurate detection perfusion defects, and enable almost complete coverage of the left ventricle. The technical capabilities of MR cardiac perfusion imaging impact the clinical use of this technique for the detection of ischemic heart disease, and its relative importance compared to other imaging modalities and tests. Recent studies have shown that cardiac magnetic resonance perfusion imaging provides strong prognostic value for predicting adverse events.

---

#### Scar Imaging: Clinical Applications & Technical Approaches

Wiphada Patricia Bandettini

Late gadolinium enhancement imaging of “scar” and fibrosis is a vital tool in the assessment of a broad spectrum of cardiovascular diseases. In particular, late gadolinium enhancement characterization of myocardial infarction and cardiomyopathy has demonstrated its utility in predicting future adverse cardiovascular events. This presentation reviews the basics of late gadolinium enhancement imaging, touching upon technical challenges and simple solutions that may mitigate image artifact. Additionally, examples of the common clinical applications are discussed.

---

#### Introduction to Relaxometry: Clinical Applications & Technical Approaches

Michael Salerno

---

#### T1 Mapping & ECV

Sebastien Roujol

---

#### T2, T2\* & T1 Rho Mapping Techniques

Ruud van Heeswijk

A presentation on the theory, implementations, clinical applications, and current challenges of T2, T2\*, and T1rho mapping of the heart.

---

---

## Weekend Course

### Data Acquisition & Image Reconstruction II - Data Acquisition & Image Reconstruction II

Sunday Parallel 4 Live Q&A

Sunday 14:30 - 15:00 UTC

Moderators:

Advanced Image Reconstruction  
Techniques : Claudia Prieto

Artifacts & Corrections: Jongho Lee

### Parallel Imaging

Gastao Cruz

The key concepts behind parallel imaging will be discussed through the lens of two of its' most popular approaches: SENSE and GRAPPA. The properties of parallel imaging reconstructions will be discussed, along with their effects on reconstructed images. Finally, iterative parallel imaging reconstructions for non-uniform Cartesian trajectories will be introduced.

---

### Sparsity & Compressed Sensing

Feng Huang

Compressed sensing (CS) is a powerful signal processing technique for reconstructing data from highly undersampled measurements. The introduction of CS to magnetic resonance imaging (MRI) has dramatically reduced scan acquisition time, and has demonstrated great success in diverse applications over the last decade. In this talk, we will cover the basic theory of CS, and then give an overview of the combination of CS with fast imaging approaches, such as parallel imaging and partial Fourier. Furthermore, we will also introduce the advanced CS techniques combined with deep learning.

---

### Low-Rank Reconstruction Approaches

Frank Ong

### Learned Representations: Dictionaries, Subspaces, Manifolds

Lei (Leslie) Ying

### Motion Compensation & Correction

Oliver Speck

Due to the long scan times of seconds or even minutes, MRI is susceptible to subject motion. Such motion can lead to ghosting, blurring and other image artifacts and can result in non diagnostic images or false quantitative results in clinical and scientific studies. Faster imaging is a convenient method to avoid or reduce motion artifacts but has limitations in terms of resolution, and image quality. Motion correction, therefore, is a research field with a long history but only few methods entered clinical routine. A number of approaches have the potential for broader application.

---

### Off-Resonance (Static & Dynamic) Artifacts & Corrections

S. Johanna Vannesjo

### Sensing & Probing for Better Images: MR-Based Markers, Cameras & Other External Devices

Melvyn Ooi

Patient motion can represent a frequent cause of image degradation in MRI examinations. External devices have been employed in both research and clinical settings towards effective motion compensation strategies. Participants will gain an understanding of the basic physics underlying the operation of a range of external devices, and how they can be used to compensate for bulk rigid-body (e.g. head) motion, as well as physiological (e.g. respiration, cardiac cycle) motion. External devices that will be discussed include various MR-based markers, and optical cameras, and some more traditional devices (e.g. respiratory bellows, EKG).

---

---

## Weekend Course

### Multi-Parameter Quantification - Multi-Parameter Quantification

Organizers: Tony Stoecker, Lijun Bao, Krishna Nayak

Sunday Parallel 3 Live Q&A

Sunday 15:00 - 15:30 UTC

Moderators:

Multi-Parameter Quantification: Part 1:  
Christine Preibisch

Multi-Parameter Quantification: Part 2:  
Martijn Cloos



#### Overview & Purpose of Multi-Parameter Quantification

Jing Cai

With the improvement of efficiency and accuracy, multi-parameter quantification has drawn increasingly attention in recent years. Researches has been conducted using multi-parameter quantification in various areas and purposes, including tissues characterization of different anatomical sites, treatment response assessments, multi-center comparison, longitudinal follow-up, radiotherapy applications, imaging biomarkers etc. Most of the researches have shown promising results and indicating the great potential of this technique. In this presentation, we will summarize the development, advantages, clinical applications, challenges and gaps of multi-parameter quantification techniques.

---

#### MR Parameter Quantification: The Basics

Philipp Ehse

This lecture covers the basic principle of MR Parameter Quantification: from experimental design to the final parameter map.

---

#### Simultaneous Mapping of Longitudinal and Transverse Relaxation Times

Rahel Heule

This talk gives a technical overview about acquisition strategies suited to simultaneously map longitudinal and transverse relaxation times. Special focus is on fast joint T1 and T2 quantification based on two main classes: magnetization-prepared (MP) schemes with steady-state free precession (SSFP) readout and multi-contrast imaging in the steady state. Possible acquisition approaches sampling multiple gradient echoes to simultaneously obtain the effective transverse relaxation time T2\* alongside either T1 or T2 are introduced briefly as well.

---

#### Multi-Parameter Mapping of R1, PD, MT & R2\*

Nikolaus Weiskopf

Multi-parameter mapping (MPM) based on multi-echo spoiled gradient echo acquisitions can provide estimates of the longitudinal relaxation rate (R1), effective transverse relaxation rate (R2\*), proton density (PD) and magnetization transfer (MT) saturation. The basic data acquisition scheme is introduced together with the required data analysis and modelling steps. Important implementation aspects, potential pitfalls and limitations are discussed. Different examples are presented of how MPM are used for neuroimaging, including whole-brain and cortical microstructure imaging in aging and trauma of the central nervous system.

---

#### Fingerprinting & Model-Based Reconstruction

Yuchi Liu

MR Fingerprinting (MRF) is a novel approach for simultaneous multi-parameter quantification. This course will introduce MRF basics, including pulse sequence design, data acquisition, dictionary generation and reconstruction. In particular, recent advances in model-based reconstruction such as low rank methods exploiting spatial and temporal sparsity in the acquired data will be reviewed.

---

#### Relaxometry & Diffusion



Daeun Kim

Combining relaxometry and diffusion has been recently interesting for imaging microstructure. In this lecture, an approach to multidimensional correlation spectrum imaging of exponential decays will be introduced. The approach uses multidimensional diffusion-relaxation data and estimate correlation spectrum of diffusion-relaxation, which enables substantially-improved spatial mapping of microstructure. This lecture will provide basic understanding of principles for the approach from theoretical and empirical perspectives.

---

### Multi-Parametric Quantification Plus Motion

Anthony Christodoulou

Quantitative multiparameter mapping is a powerful tool for tissue characterization, but is difficult to perform in moving organs, typically requiring a difficult combination of electrocardiography triggering and breath-holding to control motion. New developments in multidimensional imaging have enabled motion-resolved multiparameter mapping, even without external motion control. This talk will present the foundations and latest developments of these multidimensional approaches, as well as their potential impact on quantitative imaging for neurological, cardiovascular, and oncological applications.

---

### Electric & Magnetic Properties of Tissue

Chunlei Liu

---

## Weekend Course

### Diffusion: Micro & Macro - Diffusion: Micro & Macro

Organizers: Dmitry Novikov, Alexander Leemans

Sunday Parallel 1 Live Q&A

Sunday 15:00 - 15:30 UTC

Moderators: Dmitry Novikov & Andrey Zhyhka

#### More Diffusion, Less Confusion!

Chantal Tax

How can diffusion MRI be sensitive to microstructure if we have mm-sized voxels, and can smaller voxels solve the crossing fibre problem? Why are the estimated parameter maps directly from the scanner different from my offline analysis? Is myelin the main cause of anisotropy? This educational discusses 8 common confusions in diffusion MRI.

---

#### Going Deep Into q-Space

Ileana Jelescu

The overall diffusion weighting, also referred to as the  $b$ -value, is the resulting diffusion attenuation from two different contributions: the spatial dephasing  $q$  imparted by the diffusion gradient pulse and the time  $t$  given to molecules to diffuse before they are rephased. Here, we will focus on increasing the  $q$ -vector for a fixed diffusion time  $t$ . This is what is commonly implied by "increasing the  $b$ -value". Going "deep into  $q$ -space" opens entirely new doors for tissue microstructure mapping and brain tractography. The former are covered in this lecture.

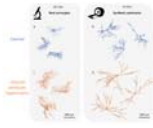
---

#### Once Upon an (Echo) Time

Junzhong Xu

This lecture will cover the basics and recent progress of diffusion time- and echo time-dependent diffusion MRI. We will explore how diffusion time affects diffusion MRI experiments, review some practical approaches to extend the range of achievable diffusion times and provide examples of how varying diffusion times assist better characterizing biological tissue microstructure. Second, we will briefly explore how echo time affects diffusion MRI with the presence of multiple compartments and review how echo time-dependent diffusion MRI provides an additional dimension to disentangle signal contributions from different compartments.

---

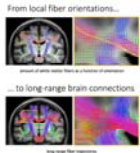


### MRS: A Diffusion Cocktail

Clemence Ligneul

This course aims at introducing diffusion-weighted magnetic resonance spectroscopy (DW MRS) to people with a basic understanding of diffusion MRI. Hopefully, you will be able to seize whether DW MRS techniques can be useful for your research question, and to get an idea of its implementation, from acquisition to analysis.

---



### Tracking Off the Beaten Track

Ben Jeurissen

Fiber tracking is the only tool that can delineate specific fiber bundles within the brain in-vivo, enabling region-specific investigation of MRI parameters and helping neurosurgeons to plan delicate neurosurgery. Fiber tracking has also claimed a central role in the field of 'connectomics', the study of the complex network of connections within the brain. Despite these unique abilities and exciting applications, fiber tracking is not without controversy, in particular when it comes to its interpretation. In light of this controversy, this course will provide an overview of the concepts, technical considerations, algorithms, mistakes and challenges of fiber tracking.

---

### Pathology For Modeling: A Blessing or a Curse?

Pratik Mukherjee

---

## Weekend Course

### Cardiovascular MRI: The Vasculature - Cardiovascular MRI: The Vasculature

Organizers: Tim Leiner, Bernd Wintersperger

Sunday Parallel 2 Live Q&A

Sunday 15:00 - 15:30 UTC

Moderators:

Vascular MRA Principles: M. Eline Kooi  
& Shuo Zhang

### Contrast Agents for Vascular Exams: Practical Use & Safety Aspects

Jeffrey Maki

---

### Contrast-Enhanced MRA Techniques: Basic Techniques & Principles

Giles Roditi

---

### Non-Contrast-Enhanced MRA Techniques: Basic Techniques & Principles

Ioannis Koktzoglou

---

### Thoraco-Abdominal Vessels: Clinical Application & Use

Joanna Escalon

---

### Vessel Wall Imaging: Substrate Visualization Beyond Luminography

Rui Li

---



### Supra-Aortic Vessels: Clinical Application & Use

Hideki Ota

In the clinical settings, conditions in supra-aortic vessels include anatomical variants, steno-occlusive diseases, aneurysms, vasculitis, and shunt diseases. Luminal and vessel-wall morphology, and hemodynamics should be evaluated according to the purpose of imaging exams. TOF MRA is the standard technique. However, in-flow-effect related pitfalls should be recognized. Ultrashort TE MRA is an alternative especially for post-interventional evaluation. Contrast-enhanced MRA allows for improved luminal and vessel-wall contrast as well as hemodynamics. Arterial spin labeling technique can be also used for the evaluation of hemodynamics. This session will introduce MR technique and image findings based on various conditions in supra-aortic vessels.

---

### Cardiovascular Flow imaging: Basic Principles to Advanced Applications

Tino Ebbers

Blood flow is crucial in the development, diagnosis and treatment of many cardiovascular diseases. For many years, two-dimensional (2D), one-directional, time-resolved flow MRI has been the technique of choice. Nowadays, fast 4D flow MRI sequences exist on all modern MR systems and several commercial analysis software solutions are available. The challenge is to selected the most promising and relevant parameters for the research or clinical question at hand, and to obtain these with sufficient quality in a short acquisition and analysis time.

---

### Peripheral Vessels: Clinical Application & Use

Jeremy Collins

---

## Weekend Course

### RF Coils & Demo - RF Coils & Demo

Organizers: Greig Scott, Ergin Atalar

Sunday Parallel 4 Live Q&A

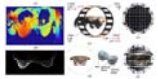
Sunday 15:00 - 15:30 UTC

Moderators: David Brunner & Manisha Aggarwal

### Dielectric Materials & Resonators

Andrew Webb

---



### RF Modelling

Simone Angela Winkler

In recent years, there is increasing interest to move MRI toward higher static field strengths. The motivation for higher field strengths lies in the promise of higher signal-to-noise ratio (SNR), however, higher field (e.g., 7 Tesla [T]) human MRI remains challenging due to several difficulties including the inhomogeneity of the transmitted radio frequency (RF) field, which leads to two phenomena.

1. (1) Non-uniform excitation ( $B_1^+$ ) and therefore non-uniform image intensity;
2. (2) Non-uniform electric fields and therefore locally increased tissue heating.

This talk will focus on RF modeling methods to predict  $B_1^+$  and SAR distributions in the human body.

---

### RF Systems for Implants & Interventions

Yigitcan Eryaman

---

### RF Coil Lab on the Cheap & Construction Demo

Shaoying Huang

---

## Plenary Session

### Plenary Session Sunday - Lauterbur Lecture: Diffusion MRI: Looking Backward, Looking Forward

Sunday Plenary

Sunday 16:00 - 16:45 UTC

---

---

---

---

---

Monday, 10 August 2020

## Plenary Session

### Plenary Session Monday - MR-Guided Radiation Therapy (MRgRT): See What You Treat

Organizers: Peng Hu, Robert Witte, Riccardo Lattanzi

Plenary Monday

Monday 12:00 - 13:30 UTC

Moderators: Peng Hu & Riccardo Lattanzi

[Overview of MRgRT](#)

Bas Raaymakers<sup>1</sup>

<sup>1</sup>Netherlands

---

[Clinical Applications of MR-Based Radiation Treatment Planning](#)

Carri Glide-Hurst<sup>1</sup>

<sup>1</sup>United States

---

[Motion Management in MRgRT](#)

Paul Keall<sup>1</sup>

<sup>1</sup>Australia

---

---

## Weekday Course

### Interventional - Joint MICCAI-ISMRM Session: Computer-Assisted Interventions

Organizers: Daniel Rueckert, Florian Knoll, Demian Wassermann, Zhaolin Chen

Monday Parallel 4 Live Q&A

Monday 13:45 - 14:30 UTC

Moderators: Zhaolin Chen

[Surgical Data Science](#)

Stefanie Speidel<sup>1</sup>

<sup>1</sup>National Center for Tumor Diseases Dresden, Germany

---



[MR Image-Guided Therapy for Oncology](#)

Gary Paul Liney<sup>1</sup>

<sup>1</sup>Ingham Institute, Australia

Real-time MRI guided radiotherapy is now a clinical reality thanks to the introduction of hybrid MRI-Linac systems. This talk describes the differences, challenges and utilisation of the research and commercial systems.

---

[Tracking & Visualization in Image-Guided Interventions](#)

Terry Peters<sup>1</sup>



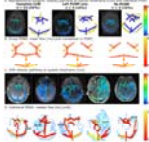
In any Image-guided intervention, it is important not only to know where you are with respect to a pre- or intra-operative image, but equally important to be able to display information to the surgeon in an intuitive manner. This presentation outlines state-of-the-art methods for tracking instruments within the surgical field in relation to the patient and their images, as well as visualization systems that provide an intuitive interface between the surgeon and the patient during a procedure.

---

## Oral

### Young Investigator Awards - Young Investigator Awards

0001



#### Standardized Evaluation of Cerebral Arteriovenous Malformations using Flow Distribution Network Graphs and Dual-venic 4D Flow MRI

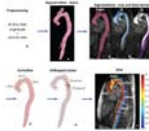
Maria Aristova<sup>1</sup>, Alireza Vali<sup>1</sup>, Sameer A Ansari<sup>1,2,3</sup>, Ali Shaibani<sup>1,2</sup>, Tord D Alden<sup>2,4</sup>, Michael C Hurley<sup>1,2</sup>, Babak S Jahromi<sup>1,2</sup>, Matthew B Potts<sup>1,2</sup>, Michael Markl<sup>1,5</sup>, and Susanne Schnell<sup>6</sup>

<sup>1</sup>Radiology, Northwestern University, Chicago, IL, United States, <sup>2</sup>Department of Neurosurgery, Northwestern University, Chicago, IL, United States, <sup>3</sup>Department of Neurology, Northwestern University, Chicago, IL, United States, <sup>4</sup>Ann & Robert H. Lurie Children's Hospital of Chicago, Chicago, IL, United States, <sup>5</sup>McCormick School of Engineering, Biomedical Engineering, Northwestern University, Chicago, IL, United States, <sup>6</sup>Radiology, University of Greifswald, Chicago, IL, United States

Dual-venic 4D flow MRI with PEAK-GRAPPA acceleration provides time-resolved 3D cerebral hemodynamics and could be applied to cerebral arteriovenous malformations (AVM) with an appropriate standardized protocol. We optimize dual-venic 4D flow imaging for AVM in vitro and in vivo, and apply a Flow Distribution Network Graph paradigm for storing and analyzing complex neurovascular 4D flow data. In vitro and in vivo, 4 voxels across a typical vessel (achievable in vivo with 0.8mm isotropic resolution) will yield flow conservation < 15% and high reproducibility. Venous-arterial ratios of peak velocity and pulsatility index are proposed as potential network-based biomarkers characterizing AVM hemodynamics.

---

0002



#### Parametric Hemodynamic 4D flow MRI maps for the Characterization of Chronic Thoracic Descending Aortic Dissection

Kelly Jarvis<sup>1</sup>, Judith T Pruijssen<sup>2</sup>, Andre Y Son<sup>3</sup>, Bradley D Allen<sup>1</sup>, Gilles Soulat<sup>1</sup>, Alireza Vali<sup>1</sup>, Alex J Barker<sup>4</sup>, Andrew W Hoel<sup>5</sup>, Mark K Eskandari<sup>5</sup>, S. Chris Malaisrie<sup>3</sup>, James C Carr<sup>1</sup>, Jeremy D Collins<sup>6</sup>, and Michael Markl<sup>1</sup>

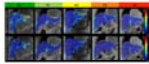
<sup>1</sup>Department of Radiology, Feinberg School of Medicine, Northwestern University, Chicago, IL, United States, <sup>2</sup>Department of Radiology and Nuclear Medicine, Radboud University Medical Centre, Nijmegen, Netherlands, <sup>3</sup>Division of Cardiac Surgery, Feinberg School of Medicine, Northwestern University, Chicago, IL, United States, <sup>4</sup>Department of Radiology, University of Colorado, Denver, CO, United States, <sup>5</sup>Division of Vascular Surgery, Feinberg School of Medicine, Northwestern University, Chicago, IL, United States, <sup>6</sup>Department of Radiology, Mayo Clinic, Rochester, MN, United States

Systematic evaluation of complex flow in descending aortic dissection (DAD) is needed to better understand which patients are predisposed to complications. Our goal was to utilize quantitative maps from 4D flow MRI for monitoring true and false lumen (TL, FL) flow characteristics. 4D flow was acquired in 20 DAD patients (6 medically managed, 14 with surgical repair), and 21 age-matched controls. 4D flow-derived quantitative maps demonstrated global and regional hemodynamic differences between DAD patients and controls. DAD patients with and without repair showed significantly altered TL and FL aortic hemodynamics, indicating this technique's potential to characterize flow dynamics in DAD.

---

0003

MRI Cine-Tagging of Cardiac-Induced Motion for Noninvasive Staging of Liver Fibrosis

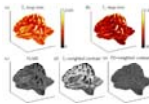


Thierry Lefebvre<sup>1,2,3</sup>, Léonie Petitclerc<sup>1,2,4</sup>, Mélanie Hébert<sup>1,2</sup>, Laurent Bilodeau<sup>1,2</sup>, Giada Sebastiani<sup>5</sup>, Damien Oliivié<sup>1</sup>, Zu-Hua Gao<sup>6</sup>, Marie-Pierre Sylvestre<sup>2,7</sup>, Guy Cloutier<sup>1,8,9</sup>, Bich N Nguyen<sup>10</sup>, Guillaume Gilbert<sup>1,11</sup>, and An Tang<sup>1,2,8</sup>

<sup>1</sup>Radiology, Radio-Oncology and Nuclear Medicine, Université de Montréal, Montreal, QC, Canada, <sup>2</sup>Centre de recherche du Centre hospitalier de l'Université de Montréal (CRCHUM), Montreal, QC, Canada, <sup>3</sup>Medical Physics Unit, McGill University, Montréal, QC, Canada, <sup>4</sup>C.J. Gorter Center for High Field MRI, Department of Radiology, Leiden University Medical Center (LUMC), Leiden, Netherlands, <sup>5</sup>Department of Medicine, Division of Gastroenterology and Hepatology, McGill University Health Centre (MUHC), Montreal, QC, Canada, <sup>6</sup>Department of Pathology, McGill University, Montreal, QC, Canada, <sup>7</sup>Department of Social and Preventive Medicine, École de santé publique de l'Université de Montréal (ESPUM), Montreal, QC, Canada, <sup>8</sup>Institute of Biomedical Engineering, Université de Montréal, Montreal, QC, Canada, <sup>9</sup>Laboratory of Biorheology and Medical Ultrasonics (LBUM), Centre de recherche du Centre hospitalier de l'Université de Montréal (CRCHUM), Montreal, QC, Canada, <sup>10</sup>Service of Pathology, Centre hospitalier de l'Université de Montréal (CHUM), Montreal, QC, Canada, <sup>11</sup>MR Clinical Science, Philips Healthcare Canada, Montreal, QC, Canada

MR elastography techniques for staging liver fibrosis assess the right liver and require additional hardware. MRI cine-tagging evaluates the strain of liver tissue and shows promise for staging liver fibrosis without additional hardware. It can be performed routinely during MRI examinations. Strain showed high correlation with fibrosis stages ( $\rho = -0.68$ ,  $P < 0.0001$ ). AUC was 0.81 to distinguish fibrosis stages F0 vs.  $\geq F1$ , 0.84 for  $\leq F1$  vs.  $\geq F2$ , 0.86 for  $\leq F2$  vs.  $\geq F3$ , and 0.87 for  $\leq F3$  vs. F4. It could be used to assess the left liver lobe as a complement to MR elastography assessing the right lobe.

0004



Multi-pathway multi-echo acquisition and contrast translation to generate a variety of quantitative and qualitative image contrasts

Cheng-Chieh Cheng<sup>1,2</sup>, Frank Preiswerk<sup>1</sup>, and Bruno Madore<sup>1</sup>

<sup>1</sup>Department of Radiology, Brigham and Women's Hospital, Harvard Medical School, Boston, MA, United States, <sup>2</sup>Department of Computer Science and Engineering, National Sun Yat-sen University, Kaohsiung, Taiwan

Ideally, neuro exams would include a variety of contrast types along with basic MRI parametric maps, with full-brain 3D coverage and good spatial resolution. However, tradeoffs exist between the number of contrasts, spatial coverage, spatial resolution, and scan time. We developed a 3D multi-pathway multi-echo (MPME) sequence that rapidly captures vast amounts of information about the object, and a 'contrast translator' to convert this information into desired contrasts. More specifically, a neural network converts 3D full-brain MPME data acquired in about 7 min into MPRAGE, FLAIR, T1W, T2W, T1 and T2 volumes, with the goal of abbreviating neuro exams.

0005



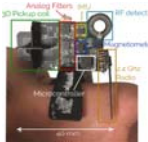
Multiphoton Magnetic Resonance Imaging

Victor Han<sup>1</sup> and Chunlei Liu<sup>1,2</sup>

<sup>1</sup>Electrical Engineering and Computer Sciences, University of California, Berkeley, Berkeley, CA, United States, <sup>2</sup>Helen Wills Neuroscience Institute, University of California, Berkeley, Berkeley, CA, United States

We present a fully geometric view of multiphoton excitation by taking a particular rotating frame transformation. In this rotating frame, we find that multiphoton excitations appear just like single-photon excitations again, and thus, we can readily generalize concepts already explored in standard single-photon excitation. With a homebuilt low-frequency ( $\sim$  kHz) coil, we execute a standard slice-selective pulse sequence with all of its excitations replaced by their equivalent two-photon versions. With a multiphoton interpretation of oscillating gradients, we present a novel way to transform a standard slice-selective adiabatic pulse into a multiband one without modifying the RF pulse shape itself.

0006



Toward “plug and play” prospective motion correction for MRI by combining observations of the time varying gradient and static vector fields.

Adam Marthinus Johannes van Niekerk<sup>1</sup>, Andre van der Kouwe<sup>1,2,3</sup>, and Ernesta Meintjes<sup>1,4,5</sup>

<sup>1</sup>Biomedical Engineering Research Centre, Division of Biomedical Engineering, Department of Human Biology, Faculty of Health Sciences, University of Cape Town, Cape Town, South Africa, <sup>2</sup>Athinoula A. Martinos Center, Massachusetts General Hospital, Charlestown, MA, United States, <sup>3</sup>Radiology, Harvard Medical School, Boston, MA, United States, <sup>4</sup>Cape Universities Body Imaging Centre, Cape Town, South Africa, <sup>5</sup>Neuroscience Institute, Faculty of Health Sciences, University of Cape Town, Cape Town, South Africa

Introducing additional hardware to measure patient motion allows for fast and accurate prospective motion correction that has minimal or no impact on the imaging pulse sequence. This does however entail additional setup that in some cases may be challenging to translate into a dynamic clinical setting. In this work we explore the use of an intelligent marker - a Wireless Radiofrequency-triggered Acquisition Device (WRAD) - for prospective motion correction. This new approach incorporates all additional hardware (besides a wireless receiver) into the marker that is attached to the subject. Initial results show improved image quality without scanner specific calibration.

## Oral

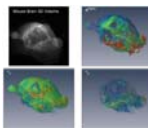
### Perfusion and Permeability - Perfusion & Permeability

Monday Parallel 1 Live Q&A

Monday 13:45 - 14:30 UTC

Moderators: Amit Mehndiratta

0007



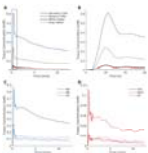
Whole tumor pharmacokinetic model analysis with 3D isotropic high resolution using 3D-UTE-GRASP sequence at 7T

Jin Zhang<sup>1</sup>, Karl Kiser<sup>1</sup>, Chongda Zhang<sup>1</sup>, Ayesha Bharadwaj Das<sup>1</sup>, and Sungheon Gene Kim<sup>1</sup>

<sup>1</sup>New York University School of Medicine, New York, NY, United States

Quantitative pharmacokinetic model parameter maps from dynamic contrast enhanced (DCE)-MRI can provide useful physiologically relevant information about tumor microenvironment, but often in low spatial resolution due to challenges in acquiring high resolution 3D data with high temporal resolution. The purpose of this study is to investigate the feasibility of generating the whole tumor high resolution pharmacokinetic model parameter maps with the 3D-UTE-GRASP<sup>1</sup> sequence for both  $T_1$  mapping and dynamic scan.

0008



Hemodynamics and permeability of the windows of the brain: dynamic contrast-enhanced MRI of the circumventricular organs

Inge Verheggen<sup>1</sup>, Joost de Jong<sup>2</sup>, Martin van Boxtel<sup>1</sup>, Alida Postma<sup>2</sup>, Frans Verhey<sup>1</sup>, Jacobus Jansen<sup>2,3</sup>, and Walter Backes<sup>2</sup>

<sup>1</sup>Department of Psychiatry and Neuropsychology, Maastricht University, Maastricht, Netherlands,

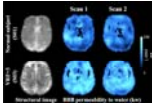
<sup>2</sup>Department of Radiology and Nuclear Medicine, Maastricht University Medical Center, Maastricht,

Netherlands, <sup>3</sup>Department of Electrical Engineering, Eindhoven University of Technology, Eindhoven, Netherlands

Circumventricular organs (CVOs), located around the ventricles without blood-brain barrier, maintain homeostasis between the blood, cerebrospinal fluid, and brain. Secretory CVOs are involved in peptide release and sensory CVOs regulate signal transmission. These organs can be an entrance point for pathogens. For the first time, physiological properties of the CVOs were assessed in vivo with dynamic contrast-enhanced (DCE) MRI.

Assessing pharmacokinetics (leakage rate; blood perfusion; uptake capacity/retention) with DCE MRI in 20 healthy males, demonstrated that only secretory CVOs had noticeable stronger hemodynamics and higher permeability than normal-appearing brain matter.

0009



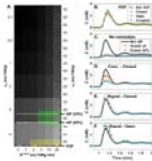
Comparison between blood-brain barrier permeability to water and gadolinium-based contrast agents in an elderly cohort

Xingfeng Shao<sup>1</sup>, Samantha Jenny Ma<sup>1</sup>, and Danny JJ Wang<sup>1,2</sup>

<sup>1</sup>Mark & Mary Stevens Neuroimaging and Informatics Institute, Keck School of Medicine, University of Southern California, Los Angeles, CA, United States, <sup>2</sup>Department of Neurology, University of Southern California, Los Angeles, CA, United States

A diffusion-weighted arterial spin labeling (DW-ASL) technique has been proposed to non-invasively measure water exchange rate (kw) across the BBB. kw was compared with GBCAs permeability (Ktrans) in aged subjects at risk of small vessel disease. A positive correlation was found between kw and Ktrans only in the caudate, suggesting different BBB mechanisms probed by kw and Ktrans. Significant increase of kw was found in subjects with diabetes or high vascular risk while no Ktrans difference was observed. Water permeability could be a sensitive biomarker to study glymphatic function and vascular diseases before detectable BBB disruption occurs.

0010



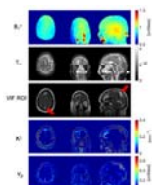
Partial Volume Correction of the Arterial Input Function with Surrounding Tissue Signal for Dynamic Contrast Enhanced MRI in the Brain

Benoît Bourassa-Moreau<sup>1</sup>, Réjean Lebel<sup>1</sup>, Guillaume Gilbert<sup>2</sup>, David Mathieu<sup>3</sup>, and Martin Lepage<sup>1</sup>

<sup>1</sup>Centre d'imagerie moléculaire de Sherbrooke, Département de médecine nucléaire et radiobiologie, Université de Sherbrooke, Sherbrooke, QC, Canada, <sup>2</sup>MR Clinical Science, Philips Healthcare Canada, Markham, ON, Canada, <sup>3</sup>Service de neurochirurgie, Département de chirurgie, Université de Sherbrooke, Sherbrooke, QC, Canada

The arterial input function measured for brain dynamic contrast-enhanced MRI is contaminated by the signal contribution of surrounding tissues. This work corrects these partial volume effects on signal level by using the surrounding gray matter enhancement to discriminate pure arterial signal. The method also accounts for the high contrast agent concentration reached in arteries and veins that leads to signal non-linearity, saturation, and concurrent unwanted  $T_2^*$  effects. This partial volume correction method is compared to concentration scaling on a digital reference object and on eight subjects. Better recovery of the arterial first pass and recirculation are shown.

0011



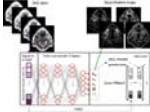
Pseudo Test-Retest Evaluation of Sparse DCE-MRI of Brain Tumor

Yannick Bliesener<sup>1</sup>, Robert Marc Lebel<sup>2,3</sup>, Jay Acharya<sup>4</sup>, Richard Frayne<sup>5</sup>, and Krishna Shrinivas Nayak<sup>1</sup>

<sup>1</sup>Department of Electrical and Computer Engineering, University of Southern California, Los Angeles, CA, United States, <sup>2</sup>Applications and Workflow, GE Healthcare, Calgary, AB, Canada, <sup>3</sup>Department of Radiology, University of Calgary, Calgary, AB, Canada, <sup>4</sup>Department of Clinical Radiology, Keck School of Medicine of University of Southern California, Los Angeles, CA, United States, <sup>5</sup>Departments of Radiology, and Clinical Neurosciences, University of Calgary, Calgary, AB, Canada

Brain DCE MRI suffers from poor spatial coverage, lack of standardization, and insufficient quantitative understanding of the extent of (physical) uncertainty in the measurements. Here, we attempt to overcome these by providing a fully automated high-resolution whole-brain DCE MRI pipeline with no user interaction. Prospective test-retest repeatability evaluation is challenging, therefore we employ a surrogate: multiple post-treatment time points in stable brain tumor patients. The proposed framework is able to yield consistent vascular input functions and tracer kinetic parameter histograms for repeated visits.

0012



### Unsupervised neural networks to improve quantitative DCE modelling

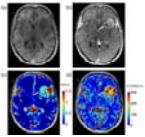
Oliver Gurney-Champion<sup>1</sup>, Matthew Orton<sup>1</sup>, Kevin Harrington<sup>1</sup>, Uwe Oelfke<sup>1</sup>, and Sebastiano Barbieri<sup>2</sup>

<sup>1</sup>The Institute of Cancer Research and Royal Marsden NHS Foundation Trust, London, United Kingdom,

<sup>2</sup>Centre for Big Data Research in Health, University of New South Wales, Sydney, Australia

We introduce a novel approach to fitting parameters from DCE MRI using an unsupervised neural network. The network is trained on in vivo data, with no ground truth, and is able to predict DCE model parameters directly from the obtained MRI images. In simulations, our method outperformed the ordinary least squares fit approach in that it is more accurate and precise. In vivo, it produced substantially less noisy parameter maps than the current practise least-squares fit.

0013



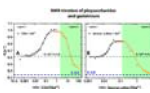
### Quantitative Transport Mapping (QTM): Inverse Solution to a Voxelized Equation of Mass Flux of Contrast Agent in a Porous Tissue Model

Qihao Zhang<sup>1</sup>, Liangdong Zhou<sup>2</sup>, John Morgan<sup>3</sup>, Thanh D Nguyen<sup>4</sup>, Pascal Spincemaille<sup>3</sup>, and Yi Wang<sup>2</sup>

<sup>1</sup>Biomedical Engineering, Cornell University, New York, NY, United States, <sup>2</sup>Weill Cornell Medicine, New York, NY, United States, <sup>3</sup>Radiology, Weill Cornell Medicine, New York, NY, United States, <sup>4</sup>Weill Cornell Medicine College, New York, NY, United States

We propose to calculate a tracer velocity field by solving the inverse problem of a voxelized transport equation for time resolved 3D (4D) dynamic contrast enhanced (DCE) data, which is termed as quantitative transport mapping (QTM). Using a porous medium model, the 4D imaging data is connected to the voxel-averaged transport equation of mass flux. The transport inverse problem is solved to estimate velocity and pseudo tortuosity. QTM provides the advantage of high accuracy in numerical validation and automated procession without manual input for in vivo DCE brain tumor data, compared to the traditional Kety's method of perfusion quantification.

0014



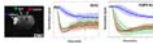
### Gd<sup>3+</sup> Deposition as an Underestimated Hazard? – Potential Masking of Gadolinium Long-Term Deposition in Biological Regimes

Patrick Werner<sup>1,2</sup>, Patrick Schuenke<sup>1</sup>, Antje Ludwig<sup>3</sup>, Daria Dymnikova<sup>4</sup>, Christian Teutloff<sup>4</sup>, Matthias Taupitz<sup>5</sup>, and Leif Schröder<sup>1</sup>

<sup>1</sup>Leibniz-Forschungsinstitut fuer Molekulare Pharmakologie (FMP), Berlin, Germany, <sup>2</sup>BIOphysical Quantitative Imaging Towards Clinical Diagnosis (BIOQIC), Berlin, Germany, <sup>3</sup>Center for Cardiovascular Research (CCR), Charite Berlin, Berlin, Germany, <sup>4</sup>Freie Universität Berlin, Berlin, Germany, <sup>5</sup>Department of Radiology, Charite Berlin, Berlin, Germany

Gd<sup>3+</sup>-ions can be released from GBCAs after in vivo application and polysaccharides like glycosaminoglycans are candidates for binding of released Gd<sup>3+</sup>-ions by acting as competing chelators. We showed that the chelation of Gd<sup>3+</sup>-ions to polysaccharides cause an increase of  $R_1$  due to the high relaxivity of such complexes. However, at high GAG/Gd<sup>3+</sup> ratios and in cell experiments, we observed a decrease of  $R_1$  after the chelation of Gd<sup>3+</sup>. Our results demonstrate the importance of more in vivo-like setups for the investigation of gadolinium transchelation processes to prevent an underestimation of the amount of deposited gadolinium in biological tissues.

0015



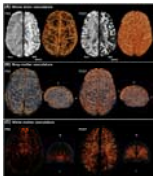
### Distribution of intraperitoneally administered D2O in AQP4-knockout mouse brain after MCA occlusion

Obata Takayuki<sup>1</sup>, Takuya Urushihata<sup>1</sup>, Manami Takahashi<sup>1</sup>, Sayaka Shibata<sup>1</sup>, Nobuhiro Nitta<sup>1</sup>, Jeff Kershaw<sup>1</sup>, Yasuhiko Tachibana<sup>1</sup>, Masato Yasui<sup>2</sup>, Ichio Aoki<sup>1</sup>, Tatsuya Higashi<sup>1</sup>, Makoto Higuchi<sup>1</sup>, and Hiroyuki Takuwa<sup>1</sup>

<sup>1</sup>National Institute of Radiological Sciences, QST, Chiba, Japan, <sup>2</sup>Department of Pharmacology, Keio University School of medicine, Tokyo, Japan

Using dynamic PDWI after intraperitoneal D2O injection, we observed a difference in the D2O distribution between aquaporin-4 knockout (AQP4-ko) and wild type (Wild) mice with MCA occlusion. The results suggest that blood flow changes and cell membrane water permeability have a complex relationship.

0016



### Human cerebral white-matter vasculature imaged using the blood-pool contrast agent Ferumoxytol: bundle-specific vessels and vascular density

Michaël Bernier<sup>1,2</sup>, Olivia Viessmann<sup>1,2</sup>, Ned Ohringer<sup>1</sup>, Jingyuan E. Chen<sup>1,2</sup>, Nina E. Fultz<sup>1,3</sup>, Rebecca Karp Leaf<sup>4</sup>, Lawrence L. Wald<sup>1,2,5</sup>, and Jonathan R. Polimeni<sup>1,2,5</sup>

<sup>1</sup>Athinoula A. Martinos Center for Biomedical Imaging, Massachusetts General Hospital, Charlestown, MA, United States, <sup>2</sup>Radiology, Harvard Medical School, Boston, MA, United States, <sup>3</sup>Engineering, Boston University, Boston, MA, United States, <sup>4</sup>Division of Hematology, Massachusetts General Hospital, Boston, MA, United States, <sup>5</sup>Division of Health Sciences and Technology, Massachusetts Institute of Technology, Cambridge, MA, United States

Ferumoxytol—a safe, superparamagnetic iron oxide nanoparticle that amplifies T2\* dephasing in blood vessels—can be used as a powerful image contrast enhancement agent to aid vascular imaging. Combining this with an innovative vascular segmentation tool, here we evaluate how Ferumoxytol improves vascular detection throughout the brain using a region-based analysis of the gray-matter and a bundle-specific analysis of the white-matter. We report increases in white-matter vasculature specificity and uncover spatial patterns similar to white-matter tracts, therefore this work sheds new light on the possible existence and influence of a concurrent network of vasculature that follows the known fiber bundles.

## Oral

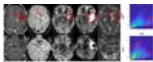
### Perfusion and Permeability - Arterial Spin Labelling Perfusion Imaging

Monday Parallel 1 Live Q&A

Monday 13:45 - 14:30 UTC

Moderators: Thomas Lindner & Vasily Yarnykh

0017



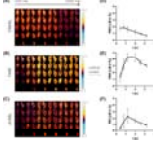
### Differences in quantitative glioma perfusion imaging with ASL and DSC: validation with 15O-H2O PET

Jan Petr<sup>1</sup>, Niels Verburg<sup>2</sup>, Joost P.A. Kuijjer<sup>3</sup>, Thomas Koopman<sup>3</sup>, Vera C. Keil<sup>4</sup>, Esther A.H. Warnert<sup>5</sup>, Frederik Barkhof<sup>3,6</sup>, Jörg van den Hoff<sup>1</sup>, Ronald Boellaard<sup>3</sup>, Philip C. de Witt Hamer<sup>2</sup>, and Henri J.M.M. Mutsaerts<sup>3,7</sup>

<sup>1</sup>Institute of Radiopharmaceutical Cancer Research, Helmholtz-Zentrum Dresden-Rossendorf, Dresden, Germany, <sup>2</sup>Neurosurgical Center Amsterdam, Amsterdam University Medical Center, location VU, Amsterdam, Netherlands, <sup>3</sup>Department of Radiology & Nuclear Medicine, Amsterdam University Medical Center, location VU, Amsterdam, Netherlands, <sup>4</sup>Department of Neuroradiology, Bonn University Hospital, Bonn, Germany, <sup>5</sup>Department of Radiology and Nuclear Medicine, Erasmus MC, Rotterdam, Netherlands, <sup>6</sup>UCL Institutes of Neurology and Healthcare Engineering, London, United Kingdom, <sup>7</sup>Ghent Institute for Functional and Metabolic Imaging (GfMI), Ghent University, Ghent, Belgium

While agreement between ASL, DSC, and PET perfusion is well established in healthy volunteers, an analogous comparison in gliomas is still missing and more challenging. We compared ASL and DSC perfusion measurements with the gold-standard of  $^{15}\text{O}\text{-H}_2\text{O}$ -PET perfusion measurements in eight patients diagnosed with gliomas. We showed the importance of normalization to the contralateral hemisphere, and identified several examples of different regional perfusion as assessed with ASL and DSC and interpreted them using the PET reference.

0018



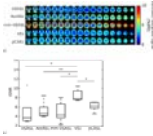
### Exploring label dynamics of velocity selective arterial spin labeling in the kidney

Isabell K. Bones<sup>1</sup>, Suzanne L. Franklin<sup>1,2</sup>, Anita A. Hartevelde<sup>1</sup>, Matthias J.P. van Osch<sup>2</sup>, Sophie Schmid<sup>2</sup>, Jeroen Hendrikse<sup>3</sup>, Chrit Moonen<sup>1</sup>, Marijn van Stralen<sup>1</sup>, and Clemens Bos<sup>1</sup>

<sup>1</sup>Center for Image Sciences, University Medical Center Utrecht, Utrecht, Netherlands, <sup>2</sup>C.J. Gorter Center for High Field MRI, Department of Radiology, Leiden University Medical Center, Leiden, Netherlands, <sup>3</sup>Department of Radiology, University Medical Center Utrecht, Utrecht, Netherlands

VSASL for renal application has constraints on the cut-off velocity, as low  $V_c$  in the presence of respiratory motion causes spurious labeling of moving tissue. With higher  $V_c$ , label could be generated more upstream in the vascular tree, potentially introducing ATT sensitivity. To study label dynamics of renal VSASL using a  $V_c$  compatible with free-breathing ( $V_c$  of 10cm/s), data at multiple time points were acquired. High ASL signal was already observed at early time points, thus supporting that spatially non-selective VSASL in the kidney generates label close to, or even inside the target tissue, also using a free-breathing compatible  $V_c$ .

0019



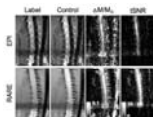
### Multi-organ comparison of flow-based Arterial Spin Labeling techniques: brain and kidney perfusion imaging without transit time artefacts

Suzanne L. Franklin<sup>1,2,3</sup>, Isabell K. Bones<sup>2</sup>, Anita A. Hartevelde<sup>2</sup>, Lydiane Hirschler<sup>1</sup>, Marijn van Stralen<sup>2</sup>, Anneloes de Boer<sup>2</sup>, Hans Hoogduin<sup>2</sup>, Matthias J.P. van Osch<sup>1,3</sup>, Sophie Schmid<sup>1,3</sup>, and Clemens Bos<sup>2</sup>

<sup>1</sup>C.J. Gorter Center for High Field MRI, Department of Radiology, Leiden University Medical Center, Leiden, Netherlands, <sup>2</sup>Center for Image Sciences, University Medical Center Utrecht, Utrecht, Netherlands, <sup>3</sup>Leiden Institute for Brain and Cognition, Leiden University, Leiden, Netherlands

Different flow-based arterial spin labeling (ASL)-techniques were proposed in recent years. In this multi-organ study four flow-based ASL-techniques were compared, with pCASL in brain, and with both pCASL and FAIR in kidney. ASL-techniques were compared based on temporal-SNR, sensitivity to perfusion changes (in brain) and robustness to respiratory motion (in kidney). In brain, Velocity-Selective Inversion showed superior temporal-SNR and sensitivity to perfusion changes. In kidney, flow-based ASL-techniques showed decreased temporal-SNR compared to FAIR, although their settings can be improved to increase robustness to  $B_1$ -inhomogeneity. All ASL-techniques were relatively robust to respiratory motion, showing potential for free-breathing kidney-ASL at 3T.

0020



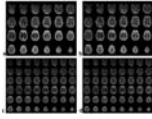
### Preclinical Spinal Cord Perfusion Imaging with Pseudo-Continuous Arterial Spin Labeling

Briana Meyer<sup>1</sup>, Lydiane Hirschler<sup>2,3</sup>, Jan Warnking<sup>2</sup>, Emmanuel Barbier<sup>2</sup>, and Matthew Budde<sup>4</sup>

<sup>1</sup>Biophysics, Medical College of Wisconsin, Wauwatosa, WI, United States, <sup>2</sup>Univ. Grenoble Alpes, Inserm, U1216, Grenoble Institut des Neurosciences, Grenoble, France, <sup>3</sup>C.J. Gorter Center for High Field MRI, Radiology, Leiden University Medical Center, Leiden, Netherlands, <sup>4</sup>Neurosurgery, Medical College of Wisconsin, Milwaukee, WI, United States

Pseudo-continuous arterial spin labeling (pCASL) to monitor spinal cord perfusion and hemodynamics has the potential to inform the clinical care of spinal cord injury and other disorders. This work demonstrates successful implementation and application of pCASL of the rodent cervical spinal cord at high field.

0021

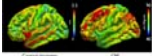


Super-Resolution Multi-band ASL using Slice Dithered Enhanced Resolution (SLIDER) Technique  
Qinyang Shou<sup>1</sup>, Xingfeng Shao<sup>1</sup>, and Danny Wang<sup>1</sup>

<sup>1</sup>University of Southern California, Los Angeles, CA, United States

Arterial Spin Labelling (ASL) is a noninvasive imaging technique that can quantitatively measure Cerebral Blood Flow (CBF). However, existing ASL techniques generally have a low spatial resolution due to a relative low Signal-to-noise ratio (SNR). In this study, we develop a super-resolution ASL method by combining the Slice Dithered Enhanced Resolution (SLIDER) with multi-band ASL with optimized slice-dependent background suppression to enhance both the resolution and SNR. The reconstructed images achieve a resolution of isotropic  $2 \times 2 \times 2$  mm<sup>3</sup>, and show increased spatial and temporal SNR compared to standard high-resolution ASL images.

0022



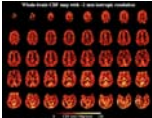
Regional and depth dependence of cortical blood-flow assessed with high-resolution Arterial Spin Labeling

Manuel Taso<sup>1</sup>, Fanny Munsch<sup>1</sup>, Li Zhao<sup>2</sup>, and David C. Alsop<sup>1</sup>

<sup>1</sup>Division of MRI research, Department of Radiology, Beth Israel Deaconess Medical Center, Harvard Medical School, Boston, MA, United States, <sup>2</sup>Diagnostic Imaging and Radiology, Children's National Medical Center, Washington, DC, United States

Imaging cortical blood-flow using ASL is relevant to unravel the basis of brain functional autoregulation or response to stimuli, but challenging because of the usual compromise between brain coverage, SNR and spatial resolution in ASL. We here propose to push the limits of volumetric ASL resolution using sparse variable-density FSE and Compressed-Sensing to study the distribution of cortical flow in healthy volunteers. We show through a group surface-based analysis some regional variations in cortical flow, but also depth-dependence of cortical flow. We also propose a high-resolution average ASL perfusion-weighted template that could have benefits for large-scale group studies.

0023



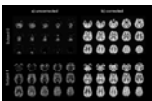
High-resolution whole brain ASL perfusion imaging at 7T with 12-fold acceleration and spatial-temporal regularized reconstruction

Xingfeng Shao<sup>1</sup>, Stefan M Spann<sup>2</sup>, Kai Wang<sup>1</sup>, Lirong Yan<sup>1,3</sup>, Stollberger Rudolf<sup>2</sup>, and Danny JJ Wang<sup>1,3</sup>

<sup>1</sup>Mark & Mary Stevens Neuroimaging and Informatics Institute, Keck School of Medicine, University of Southern California, Los Angeles, CA, United States, <sup>2</sup>Institute of Medical Engineering, Graz University of Technology, Graz, Austria, <sup>3</sup>Department of Neurology, University of Southern California, Los Angeles, CA, United States

Ultra-high field allows ASL to achieve higher spatial resolution due to increased SNR and prolonged T<sub>1</sub> relaxation. We present a single-shot 3D GRASE pCASL technique with 12-fold acceleration using time-dependent 2D CAIPI sampling strategy, and reconstruction of the label/control time series with joint spatial and temporal total-generalized-variation (TGV) regularization. 2D CAIPI under-sampling pattern increases temporal incoherence between measurements which allows joint reconstruction of the highly accelerated ASL time series. Combining the advantages of ultra-high field strength, pTx coils, accelerated acquisition and advanced reconstruction, whole-brain CBF map with 2 mm isotropic resolution was obtained within 5 mins.

0024



Optimization of Pseudo-Continuous Arterial Spin Labeling using Off-resonance Compensation Strategies at 7T

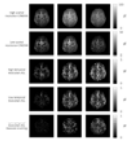
Gael Saib<sup>1</sup>, Alan Koretsky<sup>1</sup>, and S Lalith Talagala<sup>2</sup>

<sup>1</sup>NINDS/LFMI, National Institutes of Health, Bethesda, MD, United States, <sup>2</sup>NINDS/NMRF, National Institutes of Health, Bethesda, MD, United States



Pseudo-continuous arterial spin labeling (PCASL) is very sensitive to off-resonance effects. This is especially a problem at higher fields (>3T). Off-resonance effects can be compensated by using an average or a vessel-specific correction integrated into the PCASL tagging/control pulse. Vessel-specific corrections can be performed using a prescan or a field map. In this study, we compared three off-resonance compensation strategies at 7T. Data showed that a large improvement (> 2 times) of the PCASL signal can be obtained with subject specific off-resonance correction with all 3 methods. The field map based method showed slightly better performance over the others.

0025



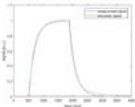
Validation of the estimation of the macrovascular contribution in multi-timepoint arterial spin labeling MRI using a two-component model

Merlijn van der Plas<sup>1</sup>, Sophie Schmid<sup>1</sup>, Martin Craig<sup>2</sup>, Michael Chappell<sup>2,3</sup>, and Matthias van Osch<sup>1</sup>

<sup>1</sup>Radiology, C.J. Gorter Center for High Field MRI, Leiden, Netherlands, <sup>2</sup>Wellcome Centre for Integrative Neuroimaging, FMRIB, Nuffield Department of Clinical Neurosciences, University of Oxford, Oxford, United Kingdom, <sup>3</sup>Institute of Biomedical Engineering, Research Council UK (EP/P012361/1), University of Oxford, Oxford, United Kingdom

A two-component kinetic model allows for the separation of the macrovascular and tissue signal. This model relies on the availability of multi-timepoint data and generates cerebral blood flow, arterial blood volume and arterial transit time maps. The goal of this study was to validate this separation of the macrovascular and tissue signal. A 4D-ASL angiography and densely sampled ASL data were acquired and fitted with different model settings. Fitting the 4D-ASL angiography with a macrovascular component showed the best fit for the model with gamma dispersion included but with limited freedom to change the dispersion parameters.

0026



Towards patient specific dispersion correction for more accurate quantification in pCASL: modeling and experimental findings

Mareike Alicja Buck<sup>1</sup> and Matthias Günther<sup>1,2</sup>

<sup>1</sup>Fraunhofer MEVIS, Bremen, Germany, <sup>2</sup>MR-Imaging and Spectroscopy, Faculty 01 (Physics, Electrical Engineering), University Bremen, Bremen, Germany

This abstract compares quantified perfusion values of the standard model and a new dispersion model based on an AIF using the ASLIF-sequence. For different ATTs, the voxel's signal was simulated using the dispersion model. The simulations show that the standard model overestimates the signal. This may result from lack of dispersion effects especially in the inflow phase of the labeled bolus. Consequently, the determined perfusion values vary for different ATTS. Thus, using an AIF based on an acquired patient specific reference bolus instead could improve the stability and robustness of quantified perfusion values.

## Oral

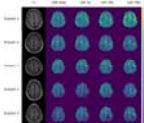
### Perfusion and Permeability - Novel Spin Labelling Methods

Monday Parallel 1 Live Q&A

Monday 13:45 - 14:30 UTC

Moderators: David Thomas

0027



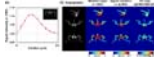
Self-Regulation of Brain Functions using Real-Time Neurofeedback Functional Arterial Spin Labeling

Stefan M Spann<sup>1</sup>, Doris Grössinger<sup>2</sup>, Christoph Stefan Aigner<sup>1,3</sup>, Josef Pfeuffer<sup>4</sup>, Guilherme Wood<sup>2,5</sup>, and Rudolf Stollberger<sup>1,5</sup>

<sup>1</sup>Institute of Medical Engineering, Graz University of Technology, Graz, Austria, <sup>2</sup>Institute of Psychology, University of Graz, Graz, Austria, <sup>3</sup>Physikalisch-Technische Bundesanstalt (PTB), Braunschweig and Berlin, Germany, <sup>4</sup>Application Development, Siemens Healthcare, Erlangen, Germany, <sup>5</sup>BioTechMed-Graz, Graz, Austria

Real-time neurofeedback (RT-NF) fMRI allows the subjects to regulate their own brain activity by providing them a neurofeedback. Functional ASL is perfectly suited for RT-NF studies due to the absolute quantification of activation related changes in the cerebral blood flow (CBF). In this study we implemented a real-time solution for ASL data processing and feedback generation which includes the following steps: data acquisition, image reconstruction, post-processing and neurofeedback presentation. The results of this RT-NF fASL study show that subjects were able to learn to regulate their own brain activation during a finger tapping experiment.

0028



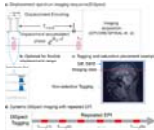
Non-contrast, high-resolution compliance mapping of intracranial vessels

Yang Li<sup>1</sup>, Michael Schär<sup>1</sup>, Dengrong Jiang<sup>1</sup>, and Hanzhang Lu<sup>1</sup>

<sup>1</sup>Johns Hopkins University Department of Radiology, Baltimore, MD, United States

Vascular compliance is an important predictor of cardiovascular disease and stroke. Here we proposed a technique to map vascular compliance along the entire intracranial arterial tree. We applied the ASL MRA to acquire  $k$ -space data in radial fashion. Then the  $k$ -space data was retrospectively grouped by cardiac phases and reconstructed by the GRASP algorithm. A series of cardiac-phase-resolved angiography images were obtained, allowing quantification of vascular compliance.

0029



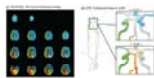
Retrospective Vessel Selective Perfusion Imaging with Displacement Spectrum Imaging (DiSpect) at Multiple Mixing Times

Ekin Karasan<sup>1</sup>, Michael Lustig<sup>1</sup>, and Zhiyong Zhang<sup>1,2</sup>

<sup>1</sup>Department of Electrical Engineering, University of California, Berkeley, CA, United States, <sup>2</sup>Institute for Medical Imaging Technology, School of Biomedical Engineering, Shanghai Jiao Tong University, Shanghai, China

Displacement spectrum imaging (DiSpect) performs multiple scans with increasing displacement (DENSE) encodings. It can resolve the multi-dimensional spectrum of displacements that spins exhibit over the mixing time between tagging and imaging. This work presents two innovations: 1) Imaging dynamic displacement spectra by repeatedly imaging after tagging, each image corresponding to an increased mixing time. 2) Post acquisition, it is possible to retrospectively select source vessels from the displacement maps and display only their contribution to perfusion in the imaging slice. We demonstrate feasibility in flow phantom and in-vivo brain at 3T.

0030



Calibration of patient-specific computational models of cerebral blood flow in cerebrovascular disease using arterial spin labeling

Jonas Schollenberger<sup>1</sup>, Luis Hernandez-Garcia<sup>1,2</sup>, and C. Alberto Figueroa<sup>1,3</sup>

<sup>1</sup>Biomedical Engineering, University of Michigan, Ann Arbor, MI, United States, <sup>2</sup>fMRI Laboratory, University of Michigan, Ann Arbor, MI, United States, <sup>3</sup>Surgery, University of Michigan, Ann Arbor, MI, United States

Collateral flow patterns in the circle of Willis play a major role in maintaining adequate blood supply to the brain in the presence of cerebrovascular occlusive disease. In this work, we present a strategy to quantify collateral flow by calibrating patient-specific computational fluid dynamic models of cerebral blood flow with perfusion data from arterial spin labeling. For a patient with right carotid stenosis, the collateral flow patterns in the circle of Willis obtained with the calibrated computational model show good agreement with territorial perfusion maps acquired with vessel-selective arterial spin labeling.



Improved accuracy of blood-brain barrier (BBB) assessment with water-extraction-with-phase-contrast-arterial-spin-tagging (WEPCAST) MRI

Zixuan Lin<sup>1</sup>, Dengrong Jiang<sup>1</sup>, Yang Li<sup>1</sup>, Pan Su<sup>1</sup>, Jay J. Pillai<sup>1</sup>, and Hanzhang Lu<sup>1</sup>

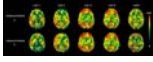
0031



<sup>1</sup>Department of Radiology, Johns Hopkins University, Baltimore, MD, United States

A new scheme of water-extraction-with-phase-contrast-arterial-spin-tagging (WEPCAST) MRI was proposed for non-invasive assessment of blood-brain-barrier (BBB) permeability to water. In this scheme, venous bolus-arrival-time was measured first by Look-Locker WEPCAST and then applied to single-delay long-labeling-duration WEPCAST scan to estimate water extraction fraction. The results showed an improved accuracy for estimation of BBB permeability.

0032



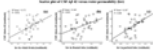
Assessing Repeatability of Blood Brain Barrier Permeability Measure Using Contrast-free MRI

Amnah Mahroo<sup>1</sup>, Nora-Josefin Breutigam<sup>1</sup>, and Matthias Günther<sup>1,2</sup>

<sup>1</sup>MR Physics, Fraunhofer Institute for Digital Medicine MEVIS, Bremen, Germany, <sup>2</sup>MR-Imaging and Spectroscopy, University of Bremen, Bremen, Germany

Disrupted blood brain barrier (BBB) is reported to be one of the causes in various neuropathological diseases<sup>1</sup>. We assessed the quantified permeability of BBB using blood to tissue water exchange dynamics by employing multi-echo ASL sequence in five healthy individuals. A repeated measurement was conducted to assess the robustness and precision of the method. The average gray matter values were  $357 \pm 62$  ms which are in-accordance with the literature reported values.

0033



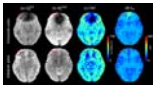
Water exchange across blood-brain barrier is associated with CSF Amyloid- $\beta$  42 and cognition in healthy older adults

Xingfeng Shao<sup>1</sup>, Brian T Gold<sup>2</sup>, and Danny JJ Wang<sup>1,3</sup>

<sup>1</sup>Mark & Mary Stevens Neuroimaging and Informatics Institute, Keck School of Medicine, University of Southern California, Los Angeles, CA, United States, <sup>2</sup>Department of Neuroscience, College of Medicine, University of Kentucky, Lexington, KY, United States, <sup>3</sup>Department of Neurology, University of Southern California, Los Angeles, CA, United States

Abnormally low CSF amyloid- $\beta$  ( $A\beta$ )-42 level is an early biomarker of the Alzheimer's Disease (AD), however lumbar puncture is required to collect CSF samples. A diffusion prepared arterial spin labeling technique was proposed to measure blood-brain barrier (BBB) water permeability ( $k_w$ ) non-invasively. Associations between water permeability and CSF  $A\beta$ 42 levels in the "healthy" aging brains were studied. Significant positive correlations were found between  $k_w$  and CSF  $A\beta$ 42 and digit symbol scores, which suggests  $k_w$  may serve as an early imaging marker of AD.

0034

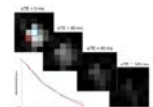


High Resolution Water Exchange Rate Mapping using 3D Diffusion Prepared Arterial Spin Labeled Perfusion MRI

Qihao Zhang<sup>1</sup>, Thanh D Nguyen<sup>2</sup>, Jana Ivanidze<sup>3</sup>, and Yi Wang<sup>3</sup>

<sup>1</sup>Cornell University, Ithaca, NY, NY, United States, <sup>2</sup>Weill Cornell Medicine College, New York, NY, United States, <sup>3</sup>Weill Cornell Medicine, New York, NY, United States

In this work, we propose an optimized acquisition for high resolution water exchange rate ( $k_w$ ) mapping, that uses adiabatic RF pulses, 3D fast spin echo readout, regularized inversion to a direct model of the water exchange rate, and fast T1 mapping. Feasibility and superior performance is shown in a regional based analysis in 6 healthy subjects.



Oxygen Extraction Fraction Mapping using Remote Sensing: Spatially Encoded T2-Relaxation-Under-Spin-Tagging (SE-TRUST)

Caitlin O'Brien<sup>1</sup>, Thomas Okell<sup>1</sup>, Mark Chiew<sup>1</sup>, and Peter Jezzard<sup>1</sup>

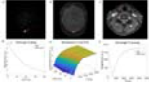
0035



<sup>1</sup>Wellcome Centre for Integrative Neuroimaging (FMRIB), University of Oxford, Oxford, United Kingdom

This work uses remote sensing methods to encode spatial information of venous blood spins in the brain into the longitudinal magnetisation. This information was then decoded remotely from the blood signal in the superior sagittal sinus. A T2-preparation module allowed venous blood T2 and therefore oxygen extraction fraction, to be mapped. An optimum inversion delay (TI) of 2s was found, and the sensitivity of the method to the spatial origins of the blood spins was verified. Low resolution venous T2 maps were obtained in two healthy volunteers. Average values were comparable to global T2 using conventional TRUST.

0036



T1 and T2 relaxometry of arterial and venous blood: reliability of different methods

Koen P.A. Baas<sup>1</sup>, Bram F. Coolen<sup>2</sup>, Gustav J. Strijkers<sup>2</sup>, and Aart J. Nederveen<sup>1</sup>

<sup>1</sup>Radiology and Nuclear Medicine, Amsterdam UMC, Amsterdam, Netherlands, <sup>2</sup>Biomedical Engineering & Physics, Amsterdam UMC, Amsterdam, Netherlands

We investigated the reliability of different T<sub>1</sub> and T<sub>2</sub> relaxometry methods for arterial and venous blood. While TRIR enables measurements of both venous blood T<sub>1</sub> and T<sub>2</sub>, T<sub>2</sub> estimates from TRIR showed poorer repeatability compared to TRUST. Moreover, significantly higher venous blood T<sub>2</sub> values were observed using TRIR. Lastly, arterial blood T<sub>1</sub> measurements showed a better repeatability compared to venous T<sub>1</sub> measurements using TRIR. These findings advocate for the use of the arterial T<sub>1</sub> measurements instead of venous T<sub>1</sub> and the use of TRUST to measure venous blood T<sub>2</sub>.

## Oral

### Multiple Sclerosis & Myelin - Multiple Sclerosis: Brain Lesions & Cord Atrophy

Monday Parallel 2 Live Q&A

Monday 13:45 - 14:30 UTC

Moderators: Michael Barnett & Susie Huang

0037

Section	Topic
Abstract	Abstracts of the presentations
Poster	Posters of the presentations
Oral	Oral presentations
Workshop	Workshop presentations
Panel	Panel presentations
Keynote	Keynote presentations
Special	Special presentations
Other	Other presentations

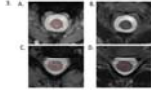
Developing a Universally Useful, Useable and Used Standardized MRI Protocol for Patients with Multiple Sclerosis

David K.B. Li<sup>1</sup>, Frederik Barkhof<sup>2</sup>, Scott Newsome<sup>3</sup>, June Halper<sup>4</sup>, Lori Saslow<sup>4</sup>, Brenda Banwell<sup>5</sup>, Laura Barlow<sup>6</sup>, Kathleen Costello<sup>7</sup>, Peter Damiri<sup>8</sup>, Marilyn Maes<sup>9</sup>, Sarah Morrow<sup>10</sup>, Jiwon Oh<sup>11</sup>, Friedemann Paul<sup>12</sup>, Patrick Quarterman<sup>13</sup>, Daniel Reich<sup>14</sup>, Jason Shewchuk<sup>15</sup>, Russell Shinohara<sup>16</sup>, Wim Van Hecke<sup>17</sup>, Kim van de Ven<sup>18</sup>, Amy Verrinder<sup>9</sup>, Mitchell Wallin<sup>19</sup>, Jerry Wolinsky<sup>20</sup>, and Anthony Traboulsee<sup>21</sup>

<sup>1</sup>Radiology, University of British Columbia, Vancouver, BC, Canada, <sup>2</sup>VU University Medical Center, Amsterdam, Netherlands, <sup>3</sup>Johns Hopkins University, Baltimore, MD, United States, <sup>4</sup>Consortium of MS Centers, Hackensack, NJ, United States, <sup>5</sup>Children's Hospital of Philadelphia, Philadelphia, PA, United States, <sup>6</sup>UBC MRI Research Center, University of British Columbia, Vancouver, BC, Canada, <sup>7</sup>National MS Society, New York, NY, United States, <sup>8</sup>Multiple Sclerosis Association of America, Cherry Hill, NJ, United States, <sup>9</sup>Cortechs Labs, San Diego, CA, United States, <sup>10</sup>London MS Clinic, Western University, London, ON, Canada, <sup>11</sup>University of Toronto, Toronto, ON, Canada, <sup>12</sup>NeuroCure Clinical Research Center, Charité Universitätsmedizin, Berlin, Germany, <sup>13</sup>General Electric Healthcare, Milwaukee, WI, United States, <sup>14</sup>Translational Neuroradiology Section, National Institute of Neurological Disorders and Stroke, NIH, Bethesda, MD, United States, <sup>15</sup>University of British Columbia, Vancouver, BC, Canada, <sup>16</sup>University of Pennsylvania, Philadelphia, PA, United States, <sup>17</sup>icomatrix, Leuven, Belgium, <sup>18</sup>BIU MR, Philips Healthcare, Eindhoven, Netherlands, <sup>19</sup>VA MS Medical Center of Excellence-East, Washington, DC, United States, <sup>20</sup>McGovern Medical School, University of Texas Health Science Center, Houston, TX, United States, <sup>21</sup>Neurology, University of British Columbia, Vancouver, BC, Canada

Standardized MRI protocol and clinical guidelines for the diagnosis and follow-up of multiple sclerosis (MS) have been available for over a decade. These guidelines are useful and useable, but not yet widely used. An expert panel with representatives from CMSC, NAIMS, NMSS, MSA and MRI vendors updated the MRI protocol with the vision of creating international guidelines to be universally adopted as the standard of care for use of MRI in MS. Novel methods of disseminating information to payers, patient groups, MRI Centers and MRI vendors so that the MRI protocol will be used were discussed and will be explored.

0038



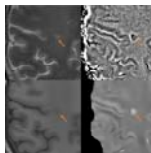
#### Comparison of mFFE & Axial T2-Weighted Fast-Spin-Echo Sequences for Lesion Detection in Low-Disability Multiple Sclerosis Patients

Mereze Visagie<sup>1</sup>, Atlee Witt<sup>1</sup>, Sanjana Satish<sup>1</sup>, Shekinah Malone<sup>2</sup>, Anna Combes<sup>1</sup>, Kristin P O'Grady<sup>1,3</sup>, Dylan Lawless<sup>1,4</sup>, Francesca Bagnato<sup>5</sup>, Colin McKnight<sup>3</sup>, and Seth A Smith<sup>1,3</sup>

<sup>1</sup>Vanderbilt University Institute of Imaging Science, Nashville, TN, United States, <sup>2</sup>Meharry Medical College, Nashville, TN, United States, <sup>3</sup>Radiology & Radiological Sciences, Vanderbilt University Medical Center, Nashville, TN, United States, <sup>4</sup>Biomedical Engineering, Vanderbilt University, Nashville, TN, United States, <sup>5</sup>Clinical Neurology, Vanderbilt University Medical Center, Nashville, TN, United States

In multiple sclerosis (MS), detection of lesions in the spinal cord with MRI is important for diagnosis and monitoring of disease progression. Despite improved clinical MRI sequences, motion and pulsation artifact remain a challenge for small lesion identification. We sought to compare sensitivity for lesion detection between multi-echo gradient echo (mFFE) and T2-weighted fast-spin-echo (T2-FSE) sequences at 3T in 16 relapsing-remitting MS patients with low disability. By comparing lesion fraction and average lesion burden, we demonstrated that mFFE has greater sensitivity for spinal cord lesions than T2-FSE.

0039



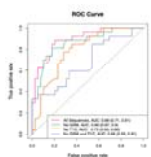
#### A comparison of phase image and quantitative susceptibility mapping in identifying inflammation in chronic multiple sclerosis lesions

Xianfu Luo<sup>1,2</sup>, Ulrike W. Kaunzner<sup>3</sup>, Thanh D. Nguyen<sup>1</sup>, Yeona Kang<sup>4</sup>, Elizabeth Sweeney<sup>5</sup>, Weiyuan Huang<sup>1</sup>, Yi Wang<sup>1</sup>, and Susan Gauthier<sup>3</sup>

<sup>1</sup>Department of Radiology, Weill Medical College of Cornell University, New York, NY, United States, <sup>2</sup>Department of Radiology, Northern Jiangsu People's Hospital, Yangzhou, China, <sup>3</sup>Department of Neurology, Weill Medical College of Cornell University, New York, NY, United States, <sup>4</sup>Department of Radiology/Nuclear Medicine, Weill Medical College of Cornell University, New York, NY, United States, <sup>5</sup>Department of Healthcare Policy and Research, Weill Medical College of Cornell University, New York, NY, United States

Both MR phase imaging and quantitative susceptibility mapping (QSM) are used to assess the presence of chronic active multiple sclerosis lesions. It is important to evaluate which measure can detect ongoing inflammation in chronic active lesions most accurately. This study combined PK11195-PET with QSM versus phase imaging, and demonstrated that QSM can detect higher uptake of PK11195, as compared to phase imaging.

1254

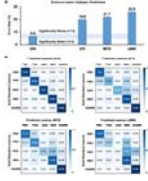


#### Estimation of Multiple Sclerosis Lesion Age without Gadolinium using Quantitative Susceptibility Maps

Elizabeth Margaret Sweeney<sup>1</sup>, Thanh Nygen<sup>1</sup>, Amy Kuceyeski<sup>1</sup>, Sarah Ryan<sup>2</sup>, Shun Zhang<sup>1</sup>, Yi Wang<sup>1</sup>, and Susan Gauthier<sup>1</sup>

<sup>1</sup>Weill Cornell, New York, NY, United States, <sup>2</sup>University of Colorado Denver, Denver, CO, United States

We propose a method to estimate multiple sclerosis (MS) lesion age (less than or greater than a year old) using non-gadolinium magnetic resonance imaging. The method utilizes the less invasive Quantitative Susceptibility Map. Radiomic features are calculated over a lesion and a random forest classification model is used. In a validation set, the model has an AUC of 0.79 (95% CI: [0.63, 0.86]) and an accuracy of 0.73 (95% CI: [0.60, 0.80]). This method can be used to aid in the diagnosis of MS, as part of the diagnostic criteria is to show lesion dissemination in time.

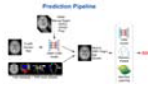


### Diffusion Histology Imaging Classifies Lesions in Multiple Sclerosis

Ze Zhong Ye<sup>1</sup>, Ajit George<sup>1</sup>, Anthony T. Wu<sup>2</sup>, Xuan Niu<sup>1</sup>, Joshua Lin<sup>3</sup>, Gautam Adusumilli<sup>4</sup>, Robert T. Naismith<sup>4</sup>, Anne H. Cross<sup>4</sup>, Peng Sun<sup>1</sup>, and Sheng-Kwei Song<sup>1</sup>

<sup>1</sup>Radiology, Washington University School of Medicine, Saint Louis, MO, United States, <sup>2</sup>Biomedical Engineering, Washington University, Saint Louis, MO, United States, <sup>3</sup>Keck School of Medicine, The University of Southern California, Los Angeles, CA, United States, <sup>4</sup>Neurology, Washington University School of Medicine, Saint Louis, MO, United States

MS lesions have heterogeneous pathology, including inflammation, demyelination, axonal injury, and neuronal loss. Our laboratory has developed a diffusion basis spectrum imaging (DBSI) technique to address the shortcomings of MRI-based MS. Primary DBSI metrics have been demonstrated to be associated with MS pathologies in animal models and human tissue. We propose that profiles of multiple DBSI metrics can identify important patterns within MS lesions and normal appearing white matter. Here we report that Diffusion Histology Imaging (DHI), an improved approach that combines a deep neural network (DNN) algorithm with DBSI-derived diffusion metrics, accurately detected and classified various MS lesion subtypes.

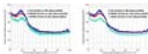


### Breaking the clinico-radiological paradox in multiple sclerosis using machine learning

Arnaud Attyé<sup>1,2</sup>, Stenzel Cackowski<sup>3</sup>, Alan Tucholka<sup>4</sup>, Pauline Roca<sup>4</sup>, Pascal Rubini<sup>4</sup>, Sebastien Vercllytte<sup>5</sup>, Lucie Colas<sup>5</sup>, Juliette Ding<sup>5</sup>, Jean-François Budzik<sup>5</sup>, Felix Renard<sup>6</sup>, Emmanuel L Barbier<sup>3</sup>, Romain Casey<sup>7,8,9,10</sup>, Sandra Vukusic<sup>7,8</sup>, and François Cotton<sup>7,11</sup>

<sup>1</sup>Grenoble alpes university, Grenoble, France, <sup>2</sup>Sydney Imaging Lab, Sydney university, Sydney, Australia, <sup>3</sup>Univ. Grenoble Alpes, Inserm, U1216, Grenoble Institute Neurosciences, Grenoble, France, <sup>4</sup>Pixyl Medical, Grenoble, France, <sup>5</sup>Lille Catholic University, Lille, France, <sup>6</sup>Laboratoire d'informatique de Grenoble, Grenoble, France, <sup>7</sup>Claude Bernard Lyon 1 University, Lyon, France, <sup>8</sup>Lyon University Hospital, Lyon, France, <sup>9</sup>Observatoire Français de la Sclérose en Plaques, INSERM 1028 et CNRS UMR 5292, Lyon, France, <sup>10</sup>EUGENE DEVIC EDMUS Foundation against multiple sclerosis, Lyon, France, <sup>11</sup>CREATIS, CNRS UMR 5220 - INSERM U1206, Lyon, France

MRI is central to the study of white matter lesions in multiple sclerosis (MS). To date, the distribution of MS lesions, as evaluated on FLAIR imaging, has not been linked to patients' disability prediction. Based on an international data challenge with 1500 MS patients and ground truth 2-year Expanded Disability Status Scale (EDSS), we have proposed an adaptive machine learning framework to predict the clinical disability. Here, we report the encouraging finding that our algorithm predicts the 2-year EDSS score with an accuracy estimated to 81%, only based on a single initial FLAIR sequence, added to sex and gender information.



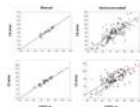
### Cervical- and Thoracic-Cord Atrophy Correlates with Clinical Disability Scores in Various Multiple Sclerosis Phenotypes

Govind Nair<sup>1</sup>, Shila Azodi<sup>1</sup>, Tsemacha Dubuche<sup>1</sup>, Yair Mina<sup>1</sup>, Ikesinachi Osuorah<sup>1</sup>, Joan Ohayon<sup>1</sup>, Tianxia Wu<sup>1</sup>, Daniel S Reich<sup>1</sup>, and Steve Jacobson<sup>1</sup>

<sup>1</sup>National Institutes of Health, Bethesda, MD, United States

We sought to better understand the relationship between atrophy along the entire spinal cord and disease burden in multiple sclerosis using MRI. Towards this, we analyzed spinal cord cross-sectional area in 48 healthy control and 250+ subjects clinically diagnosed with various phenotypes of multiple sclerosis. Our results show cervical cord atrophy early in the onset of the disease, which correlated with clinical measures of disease severity. However, these correlations were reduced as the disease progressed. Such studies may help in better understanding of disease progression and can play a role as an imaging marker in clinical trials.

0043



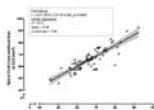
C5 level area can replace whole cervical spinal cord area measurements in multiple sclerosis as a practical biomarker of progression

Burcu Zeydan<sup>1,2</sup>, Selen Ucem<sup>2,3</sup>, Tsemacha Dubuche<sup>4</sup>, Shila Azodi<sup>4</sup>, Govind Bhagavatheeshwaran<sup>4,5</sup>, Jan-Mendelt Tillema<sup>2</sup>, John Port<sup>1</sup>, Daniel Reich<sup>5</sup>, Steven Jacobson<sup>4</sup>, Kejal Kantarci<sup>1</sup>, and Orhun H. Kantarci<sup>2</sup>

<sup>1</sup>Radiology, Mayo Clinic, Rochester, MN, United States, <sup>2</sup>Neurology, Mayo Clinic, Rochester, MN, United States, <sup>3</sup>Marmara University School of Medicine, Istanbul, Turkey, <sup>4</sup>Viral Immunology Section, Neuroimmunology and Neurovirology Division, National Institute of Neurological Disorders and Stroke, Bethesda, MD, United States, <sup>5</sup>Translational Neuroradiology Section, Neuroimmunology and Neurovirology Division, National Institute of Neurological Disorders and Stroke, Bethesda, MD, United States

Subclinical progression reflecting neurodegeneration can be measured and followed through spinal cord volume monitoring in multiple sclerosis (MS). The increased atrophy is reflected more prominently in the caudal cervical spinal cord segment. In this study, we identified the C5 level area measurement which can reflect whole cervical spinal cord area in patients with MS using both semi-automated and manual measurements. We propose that the C5 level area measurement can replace whole cervical spinal cord area measurement in MS as a more practical biomarker of progression.

0044



Accurate cervical spinal cord area measurements can be extracted from brain images

Kamyar Taheri<sup>1</sup>, Irene M. Vavasour<sup>1</sup>, Shawna Abel<sup>1</sup>, Lisa Eunyoung Lee<sup>1</sup>, Poljanka Johnson<sup>1</sup>, Stephen Ristow<sup>1</sup>, Roger Tam<sup>1</sup>, Cornelia Laule<sup>1</sup>, Nathalie Ackermans<sup>1</sup>, Alice J. Schabas<sup>1</sup>, Jillian Chan<sup>1</sup>, Ana-Luiza Sayao<sup>1</sup>, Virginia Devonshire<sup>1</sup>, Robert Carruthers<sup>1</sup>, Anthony Traboulsee<sup>1</sup>, Shannon H. Kolind<sup>1</sup>, and Adam V. Dvorak<sup>1</sup>

<sup>1</sup>University of British Columbia, Vancouver, BC, Canada

**Multiple Sclerosis (MS) is a demyelinating disease of the central nervous system, with MRI routinely performed for brain but often neglected in spinal cord. When cord imaging IS performed, atrophy is usually assessed at the C2/3 segment. We aimed to validate cord cross-sectional-area (CSA) measurements using T1-weighted whole-brain images. In controls, strong correlations were seen between C1 CSA from cord and brain images, and between C1 and C2/3 CSA from cord images.**

**In MS, C1 CSA from brain images and C2/3 CSA from cord images correlated. We showed that metrics obtained from brain images could provide relevant cord atrophy measures.**

## Oral

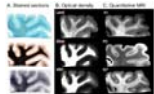
### Multiple Sclerosis & Myelin - Myelin Imaging

Monday Parallel 2 Live Q&A

Monday 13:45 - 14:30 UTC

Moderators: Catherine Lebel

0045



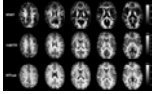
Differences in cortical and white matter myelination: a challenge for MRI myelin biomarkers.

Evgeniya Kirilina<sup>1,2</sup>, Ilona Lipp<sup>1</sup>, Carsten Jäger<sup>1</sup>, Markus Morawski<sup>3</sup>, Merve N. Terzi<sup>4,5</sup>, Hans-Jürgen Bidmon<sup>6</sup>, Markus Axer<sup>4</sup>, Pitter F. Huesgen<sup>5</sup>, and Nikolaus Weiskopf<sup>1,7,8</sup>

<sup>1</sup>Department of Neurophysics, Max Planck Institute for Human Cognitive and Brain Sciences, Leipzig, Germany, <sup>2</sup>Center for Computational Neuroscience, Free University Berlin, Berlin, Germany, <sup>3</sup>Paul Flechsig Institute of Brain Research, University of Leipzig, Leipzig, Germany, <sup>4</sup>Institute of Neuroscience and Medicine, Forschungszentrum Jülich, Juelich, Germany, <sup>5</sup>Zentralinstitut für Engineering, Elektronik und Analytik, Forschungszentrum Jülich, Juelich, Germany, <sup>6</sup>C. und O. Vogt-Institut für Hirnforschung, Heinrich-Heine-Universität Düsseldorf, Duesseldorf, Germany, <sup>7</sup>Felix Bloch Institute for Solid State Physics, Leipzig University, Leipzig, Germany, <sup>8</sup>Wellcome Centre for Human Neuroimaging, University College London, London, United Kingdom

Quantitative MRI parameters in the brain provide unique information on tissue myelination. However, the validation studies performing quantitative comparisons between MRI metrics and tissue myelin content are very limited, mainly due to the lack of methods for histological myelin quantification. Here, we explore lipid imaging using matrix-assisted laser desorption/ionization (MALDI) and multiple histological myelin stains in post-mortem human brain tissue samples for validation of MRI based myelin biomarkers. We show that tissue lipid composition vary across different cortical layers and white matter pathways, potentially reflecting differences in myelin structure and may impact MRI-based myelination metrics.

0046



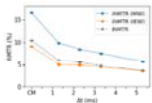
Towards advanced microstructural analyses of white matter: Quantitative regional comparison of different myelin measures

Ronja Berg<sup>1</sup>, Aurore Menegaux<sup>1</sup>, Guillaume Gilbert<sup>2</sup>, Claus Zimmer<sup>1</sup>, Christian Sorg<sup>1</sup>, Irene Vavasour<sup>3</sup>, and Christine Preibisch<sup>1</sup>

<sup>1</sup>School of Medicine, Department of Neuroradiology, Technical University of Munich, Munich, Germany, <sup>2</sup>MR Clinical Science, Philips Healthcare, Markham, ON, Canada, <sup>3</sup>Radiology, University of British Columbia, Vancouver, BC, Canada

Microstructural parameters of the brain such as the myelin concentration or g-ratio (average ratio between axonal and fiber diameter) can provide important information on the pathophysiology of demyelinating diseases. Several myelin sensitive MRI methods exist. However, correlations between different myelin sensitive measures and the best choice for g-ratio mapping is not yet fully explored. Therefore, we compared MWF, ihMTR, and MTsat in white matter and found the highest correlation between MWF and ihMTR. Those measures also varied more strongly across WM regions compared to MTsat, which suggests that they could be more reliable for further analyses such as g-ratio imaging.

0047



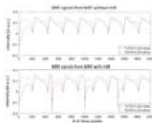
A study on Inhomogeneous Magnetization Transfer in Myelin and Intra-/Extra-cellular Water at 7T

Michelle H Lam<sup>1,2</sup>, Valentin H Prevost<sup>2</sup>, Andrew Yung<sup>2</sup>, and Piotr Kozlowski<sup>1,2,3,4</sup>

<sup>1</sup>Physics, University of British Columbia, Vancouver, BC, Canada, <sup>2</sup>UBC MRI Research Centre, University of British Columbia, Vancouver, BC, Canada, <sup>3</sup>Radiology, University of British Columbia, Vancouver, BC, Canada, <sup>4</sup>International Collaboration on Repair Discoveries, University of British Columbia, Vancouver, BC, Canada

Inhomogeneous magnetization transfer (ihMT) is a novel MR imaging technique that could be used for myelin-specific imaging if the sequence is properly tuned to filter components with short dipolar relaxation time ( $T_{1D}$ ). It is believed that ihMT's dependence on  $T_{1D}$  serves as a method to extract the myelin-related signal, due to its longest dipolar order among the brain structures. Here, we have combined two myelin imaging techniques, ihMT and myelin water imaging (MWI), to study myelin and intra-/extra-cellular water's contribution to the overall ihMT signal.

0048



A Multi-Inversion-Recovery (mIR) Myelin Water Mapping (MWF)-MRF Sequence

Peng Cao<sup>1</sup>, Di Cui<sup>1</sup>, Queenie Chan<sup>2</sup>, and Edward S. Hui<sup>1</sup>

<sup>1</sup>Diagnostic Radiology, The University of Hong Kong, Hong Kong, China, <sup>2</sup>Philips Healthcare, Hong Kong, China

We proposed a new multi-inversion-recovery (mIR) myelin water mapping (MWF)-MRF sequence that allows 24 s/slice scan speed for four-compartment (myelin water, cerebrospinal fluid, gray matter and white matter) brain mapping on clinical 3T MRI.

0049



Quantitative Myelin Mapping in Human Brain Using a Short TR Adiabatic Inversion Recovery Prepared Ultrashort Echo Time (STAIR-UTE) Sequence

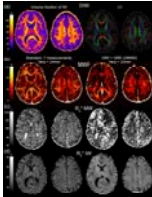


Yajun Ma<sup>1</sup>, Hyungseok Jang<sup>1</sup>, Zhao Wei<sup>1</sup>, Zhenyu Cai<sup>1</sup>, Yanping Xue<sup>1</sup>, Eric Y Chang<sup>2</sup>, Jody Corey-Bloom<sup>1</sup>, and Jiang Du<sup>1</sup>

<sup>1</sup>UC San Diego, San Diego, CA, United States, <sup>2</sup>VA health system, San Diego, CA, United States

To quantitatively image myelin on clinical scanners, we propose a Short TR Adiabatic Inversion Recovery prepared UTE (STAIR-UTE) sequence for in vivo brain imaging. With STAIR technique, long T2 tissues with a broad range of T1s can be sufficiently suppressed. Healthy volunteer has a higher myelin proton density in white matter than that in patient with multiple sclerosis.

0050



### Diffusion informed Myelin Water Imaging

Kwok-Shing Chan<sup>1</sup>, Renaud Hedouin<sup>1</sup>, and José P. Marques<sup>1</sup>

<sup>1</sup>Donders Institute for Brain, Cognition and Behaviour, Radboud University, Nijmegen, Netherlands

In this study, we propose an extension of the formalism of gradient echo based myelin water imaging by incorporating diffusion-weighted imaging data and an analytical white matter fibre model of signal evolution in a hollow cylinder. Voxel-wise analysis illustrated that the proposed model can significantly reduce the noise in the MWF estimation compared to the standard model, providing robust estimation even on high resolution data.

0051



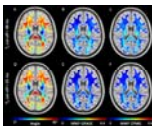
### Exploring generalization capacity of artificial neural network for myelin water imaging

Jieun Lee<sup>1</sup>, Joon Yul Choi<sup>2</sup>, Dongmyung Shin<sup>1</sup>, Se-Hong Oh<sup>3</sup>, and Jongho Lee<sup>1</sup>

<sup>1</sup>Department of Electrical and Computer Engineering, Seoul National University, Seoul, Korea, Republic of, <sup>2</sup>Cleveland Clinic, Epilepsy Center, Neurological Institute, Cleveland, OH, United States, <sup>3</sup>Division of Biomedical Engineering, Hankuk University of Foreign Studies, Gyeonggi-do, Republic of Korea

In this study, the generalization capacity of the artificial neural network for myelin water imaging (ANN-MWI) is explored by testing datasets with different (1) scan protocols (resolution, RF shape, and TE), (2) noise levels, and (3) types of disorders (NMO and edema). The ANN-MWI results show high reliability in generating myelin water fraction maps from the datasets with different resolution and noise levels. However, the increased errors are reported for the datasets with the different RF shape, TEs, and disorder type.

0052



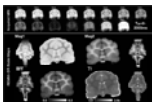
### Myelin water imaging is sensitive to white matter fiber orientation in the human brain

Christoph Birk<sup>1,2</sup>, Jonathan Doucette<sup>1,3</sup>, Eneidino Hernández-Torres<sup>1</sup>, and Alexander Rauscher<sup>1,3,4</sup>

<sup>1</sup>UBC MRI Research Centre, University of British Columbia, Vancouver, BC, Canada, <sup>2</sup>Department of Neurology, Medical University of Graz, Graz, Austria, <sup>3</sup>Department of Physics & Astronomy, University of British Columbia, Vancouver, BC, Canada, <sup>4</sup>Department of Pediatrics (Division of Neurology), University of British Columbia, Vancouver, BC, Canada

We demonstrated that the measurement of MWF is considerably influenced by the angle between the white matter fiber tracts and the main magnetic field. Furthermore, we showed that the traditionally used cut-off between myelin water and intra- and extracellular water of 40 ms overestimates MWF.

0053



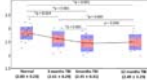
### Quantitative myelin imaging in the ferret brain for traumatic brain injury research

JP Galons<sup>1</sup>, Kevin Harkins<sup>2</sup>, Mark Does<sup>2</sup>, Theodore Trouard<sup>1</sup>, and Elizabeth Hutchinson<sup>1</sup>

<sup>1</sup>University of Arizona, Tucson, AZ, United States, <sup>2</sup>Vanderbilt University, Nashville, TN, United States

MRI tools for mapping myelin content could provide useful markers of injury and repair in neurologic disorders that preferentially affect white matter such as traumatic brain injury (TBI). In this study, we apply two novel myelin water mapping approaches - bound pool fraction (BPF) from selective inversion recovery MRI and myelin water fraction (MWF) from multiple spin echo MRI - in the ex-vivo ferret brain with and without injury in order to develop these myelin mapping markers for pre-clinical TBI research. We demonstrate high quality BPF and MWF maps and describe metric behavior in a region of focal injury.

0054



Longitudinal changes of myelin water fraction during the first year after moderate to severe diffuse traumatic brain injury

Joon Yul Choi<sup>1</sup>, John Whyte<sup>2</sup>, Amanda R Rabinowitz<sup>2</sup>, Vincent L Chow<sup>3</sup>, Se-Hong Oh<sup>4</sup>, Jongho Lee<sup>5</sup>, and Junghoon J Kim<sup>3</sup>

<sup>1</sup>Epilepsy Center / Neurological Institute, Cleveland Clinic, Cleveland, OH, United States, <sup>2</sup>Moss Rehabilitation Research Institute, Elkins Park, PA, United States, <sup>3</sup>Department of Molecular, Cellular, and Biomedical Sciences, CUNY School of Medicine, The City College of New York, New York, NY, United States, <sup>4</sup>Division of Biomedical Engineering, Hankuk University of Foreign Studies, Yongin, Korea, Republic of, <sup>5</sup>Laboratory for Imaging Science and Technology, Department of Electrical and Computer Engineering, Institute of Engineering Research, Seoul National University, Seoul, Korea, Republic of

Reliable MRI biomarkers of white matter degeneration can be useful for monitoring post-traumatic progressive neurodegeneration and identifying potential treatment targets. We report that myelin water signal can be measured reliably during the first year after moderate to severe traumatic axonal injury. We also report that apparent myelin water fraction from the whole brain white matter continued to decrease beyond 3 months post-injury, reflecting progressive axonal degeneration and demyelination.

## Oral - Power Pitch

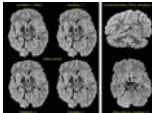
### Multiple Sclerosis & Myelin - Multiple Sclerosis: From Structure to Function

Monday Parallel 2 Live Q&A

Monday 13:45 - 14:30 UTC

Moderators: Cornelia Laule

0055



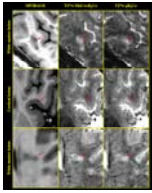
On the Potential of Whole-Brain Postmortem MR Imaging at 3T: New Insights into Multiple Sclerosis with Resolutions Up to 200 $\mu$ m

Matthias Weigel<sup>1,2,3</sup>, Peter Dechent<sup>4</sup>, Riccardo Galbusera<sup>1,2</sup>, Rene Mueller<sup>5</sup>, Govind Nair<sup>6</sup>, Ludwig Kappos<sup>2</sup>, Wolfgang Brück<sup>5</sup>, and Cristina Granziera<sup>1,2</sup>

<sup>1</sup>Translational Imaging in Neurology (ThINk) Basel, Department of Medicine and Biomedical Engineering, University Hospital Basel and University of Basel, Basel, Switzerland, <sup>2</sup>Neurologic Clinic and Policlinic, Departments of Medicine, Clinical Research and Biomedical Engineering, University Hospital Basel and University of Basel, Basel, Switzerland, <sup>3</sup>Radiological Physics, Department of Radiology, University Hospital Basel, Basel, Switzerland, <sup>4</sup>Department of Cognitive Neurology, MR-Research in Neurology and Psychiatry, University Medical Center Göttingen, Göttingen, Germany, <sup>5</sup>Institute of Neuropathology, University Medical Center Göttingen, Göttingen, Germany, <sup>6</sup>Translational Neuroradiology Section, Division of Neuroimmunology and Neurovirology, National Institute of Neurological Disorders and Stroke, National Institutes of Health, Bethesda, MD, United States

MR imaging is an indispensable tool for the depiction of human brain anatomy and pathology. Besides in vivo acquisitions, MRI of the fixated human brain is highly interesting: Very long scan times basically allow unprecedented MRI resolutions on clinical scanners. The present work describes an MRI approach that was developed for standard clinical 3T systems and tests for the viable boundaries: Within scan times between a few hours up to a weekend, acquisitions of high soft tissue contrast with isotropic resolutions up to 200 $\mu$ m can be achieved; revealing fine structure details and allowing an impressive lesion detection and characterization.

0056



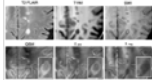
### Improved T<sub>2</sub>\*-weighted MRI of multiple sclerosis through joint motion and B<sub>0</sub> correction

Jiaen Liu<sup>1</sup>, Erin S. Beck<sup>1</sup>, Peter van Gelderen<sup>1</sup>, Pascal Sati<sup>1</sup>, Jacco A. de Zwart<sup>1</sup>, Hadar Kolb<sup>1</sup>, Omar Al-Louzi<sup>1</sup>, Mark Morrison<sup>1</sup>, Daniel S. Reich<sup>1</sup>, and Jeff H. Duyn<sup>1</sup>

<sup>1</sup>National Institute of Neurological Disorders and Stroke, National Institutes of Health, Bethesda, MD, United States

T<sub>2</sub>\*-weighted MRI at high field is a promising tool to detect and characterize multiple sclerosis (MS) lesions. However, its high sensitivity to motion-induced B<sub>0</sub> field changes limits the successful application of this technique in routine clinical use. In this study, we evaluated our recently developed motion and B<sub>0</sub> correction method using a navigator-based 3D GRE acquisition for imaging MS lesions at 7 T.

0057



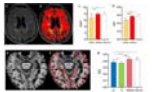
### Closer look at Multiple Sclerosis lesions: an initial result of Positive and Negative Magnetic Susceptibility Separation

Jinhee Jang<sup>1</sup>, Hyeong-geol Shin<sup>2</sup>, Yoonho Nam<sup>1,3</sup>, Jingu Lee<sup>2</sup>, Jongho Lee<sup>2</sup>, and Woojun Kim<sup>4</sup>

<sup>1</sup>Radiology, Seoul St. Mary's Hospital, College of Medicine, The Catholic University of Korea, Seoul, Republic of Korea, <sup>2</sup>Department of Electrical and Computer Engineering, Seoul National University, Seoul, Republic of Korea, <sup>3</sup>Radiology, Eunpyeong St. Mary's Hospital, College of Medicine, The Catholic University of Korea, Seoul, Republic of Korea, <sup>4</sup>Neurology, Seoul St. Mary's Hospital, College of Medicine, The Catholic University of Korea, Seoul, Republic of Korea

While susceptibility contrast gives details for MS lesions, two major changes – iron deposition and demyelination had same contribution on QSM, increasing bulk magnetic susceptibility. In this work, we applied separation of positive and negative sources in clinical MS patients, and had a closer look of in-vivo MS lesions. We demonstrate variable appearances of MS lesions on separation maps as well as conventional imaging and QSM, and complex distribution and dynamic changes of positive (i.e. iron) and negative (i.e. myelin) in MS lesions, in cross-sectional and longitudinal observations.

0058



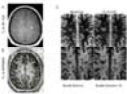
### A quantification of myelin and axonal damage across multiple sclerosis lesions and clinical subtypes with myelin and diffusion MRI

Reza Rahmzadeh<sup>1,2</sup>, Po-Jui Lu<sup>1,2</sup>, Muhamed Barakovic<sup>1,2</sup>, Riccardo Galbusera<sup>1,2</sup>, Matthias Weigel<sup>1,2,3</sup>, Pietro Maggi<sup>4</sup>, Thanh D. Nguyen<sup>5</sup>, Simona Schiavi<sup>6</sup>, Francesco La Rosa<sup>7,8</sup>, Daniel S. Reich<sup>9</sup>, Pascal Sati<sup>9</sup>, Yi Wang<sup>5</sup>, Meritxell Bach-Cuadra<sup>7,8</sup>, Ernst-Wilhelm Radue<sup>1</sup>, Jens Kuhle<sup>2</sup>, Ludwig Kappos<sup>2</sup>, and Cristina Granziera<sup>1,2</sup>

<sup>1</sup>Translational Imaging in Neurology (ThINK) Basel, Department of Medicine and Biomedical Engineering, University Hospital Basel and University of Basel, Basel, Switzerland, <sup>2</sup>Neurologic Clinic and Policlinic, Departments of Medicine, Clinical Research and Biomedical Engineering, University Hospital Basel and University of Basel, Basel, Switzerland, <sup>3</sup>Radiological Physics, Department of Radiology, University Hospital Basel, Basel, Switzerland, <sup>4</sup>Department of Neurology, Lausanne University Hospital, Lausanne, Switzerland, <sup>5</sup>Department of Radiology, Weill Cornell Medical College, New York, NY, United States, <sup>6</sup>Department of Computer Science, University of Verona, Verona, Italy, <sup>7</sup>Signal Processing Laboratory (LTSS), Ecole polytechnique fédérale de Lausanne (EPFL), Lausanne, Switzerland, <sup>8</sup>Radiology Department, Center for Biomedical Imaging, Lausanne University and University Hospital, Lausanne, Switzerland, <sup>9</sup>National Institute of Neurological Disorders and Stroke, Translational Neuroradiology Section, Division of Neuroimmunology and Neurovirology, Bethesda, MD, United States

The interplay between axonal and myelin damage in multiple sclerosis (MS) is poorly understood. This study aimed to evaluate the concomitant presence of axonal and myelin injury in living MS patients by using myelin and multi-shell diffusion MRI. Confirming neuropathological findings, our results show that (i) axonal and myelin damage exists in MS lesions and spreads out from the lesions in a centrifugal way, (ii) the extent of myelin and axonal damage differs among lesion subtypes and according to lesion anatomical locations and (iii) axonal (and not myelin) damage differs between relapsing-remitting and progressive MS patients.

0059



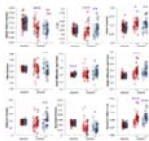
### Mapping temporal changes in myelin properties of newly formed Multiple Sclerosis lesions

Manoj K. Sammi<sup>1</sup>, Elizabeth Silbermann<sup>2</sup>, Greg Zarelli<sup>3</sup>, Dennis Bourdette<sup>2</sup>, Michael Lane<sup>2</sup>, Vijayshree Yadav<sup>2</sup>, Caroline Butler<sup>4</sup>, Katherine Powers<sup>1</sup>, Katherine Powers<sup>1</sup>, Ian Tagge<sup>1</sup>, Susan Goelz<sup>5</sup>, and William D Rooney<sup>1,2,6,7</sup>

<sup>1</sup>Advanced Imaging Research Center, Oregon Health & Science University, Portland, OR, United States, <sup>2</sup>Department of Neurology, Oregon Health & Science University, Portland, OR, United States, <sup>3</sup>Kaiser Sunnyside Medical Center, Clackamas, OR, United States, <sup>4</sup>Oregon Health & Science University, Portland, OR, United States, <sup>5</sup>Myelin Repair Foundation, Saratoga, CA, United States, <sup>6</sup>Department of Behavioral Neuroscience, Oregon Health & Science University, Portland, OR, United States, <sup>7</sup>Knight Cardiovascular Institute, Oregon Health & Science University, Portland, OR, United States

A novel MRI T<sub>1</sub> relaxometry technique is used to monitor myelin water fraction (MWF) in normal appearing white matter and multiple sclerosis lesions in subjects with newly formed white matter lesions at baseline and a follow-up study after six months. MWF was consistently low in new lesions at baseline and recovery over 6 months was highly variable. T<sub>1</sub> relaxometry provides a promising quantitative and non-invasive tool for studying myelin repair in human brain.

0060



### Advanced MRI measures reveal sex differences in the Normal Appearing and Diffusely Abnormal White Matter of Multiple Sclerosis Brain

Irene Margaret Vavasour<sup>1,2</sup>, Carina Graf<sup>2,3</sup>, Shannon H Kolind<sup>1,2,3,4,5</sup>, Peng Sun<sup>6</sup>, Robert Carruthers<sup>4</sup>, Anthony Traboulsee<sup>4,5</sup>, GR Wayne Moore<sup>2,7</sup>, David KB Li<sup>1,4,5</sup>, and Cornelia Laule<sup>1,2,3,7</sup>

<sup>1</sup>Radiology, University of British Columbia, Vancouver, BC, Canada, <sup>2</sup>International Collaboration on Repair Discoveries (ICORD), University of British Columbia, Vancouver, BC, Canada, <sup>3</sup>Physics and Astronomy, University of British Columbia, Vancouver, BC, Canada, <sup>4</sup>Medicine (Neurology), University of British Columbia, Vancouver, BC, Canada, <sup>5</sup>MS/MRI Research Group, University of British Columbia, Vancouver, BC, Canada, <sup>6</sup>Radiology, Washington University, St. Louis, MO, United States, <sup>7</sup>Pathology and Laboratory Medicine, University of British Columbia, Vancouver, BC, Canada

Diffusely abnormal white matter (DAWM) is a non-focal area of mildly increased signal on proton density and T<sub>2</sub>-weighted images. Advanced imaging techniques (T<sub>1</sub> and T<sub>2</sub> relaxation and diffusion basis spectrum imaging) compared measures of myelin, axons, oedema and inflammation between males and females with multiple sclerosis in normal appearing white matter (NAWM) and areas of DAWM. In NAWM, males had higher axial diffusivity indicative of axonal damage. In DAWM, MRI measures suggested demyelination in females whereas axonal damage was suggested in males. Both sexes show increased T<sub>1</sub>, GMT<sub>2</sub> and water content in DAWM likely related to oedema.

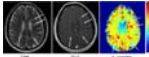
0061

### Lesions to the central and peripheral nervous system in multiple sclerosis are inversely correlated: A Study on magnetic resonance neurography

Johann Malte Enno Jende<sup>1</sup>, Felix Tobias Kurz<sup>1</sup>, Mirjam Korporal-Kuhnke<sup>2</sup>, Markus Weiler<sup>2</sup>, Brigitte Wildemann<sup>2</sup>, Andrea Viehöver<sup>2</sup>, Sabine Heiland<sup>1</sup>, Wolfgang Wick<sup>2</sup>, Martin Bendszus<sup>1</sup>, and Jennifer Kollmer<sup>1</sup>

<sup>1</sup>Neuroradiology, Heidelberg University Hospital, Heidelberg, Germany, <sup>2</sup>Neurology, Heidelberg University Hospital, Heidelberg, Germany

This study investigated the correlation between T2w-hyperintense lesions to the peripheral nervous system (PNS) and the central nervous system (CNS) in multiple sclerosis (MS) by combining 3 Tesla magnetic resonance neurography (MRN) and 3 Tesla CNS MRI. It was found that CNS lesions and PNS lesions were inversely correlated ( $r=-0.432$ ;  $p=0.0002$ ). This finding might help to elucidate the underlying pathomechanism of PNS involvement in MS by indicating that PNS demyelination in MS does not occur secondary to CNS lesions in the sense of Wallerian degeneration.

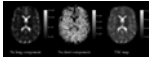


### In vivo proton exchange rate mapping is highly correlated with Gadolinium enhancement for staging Multiple Sclerosis Lesions

Weiwei Chen<sup>1</sup>, Mehran Shaghghi<sup>2</sup>, Haiqi Ye<sup>1</sup>, Qianlan Chen<sup>1</sup>, Yan Zhang<sup>1</sup>, and Kejia Cai<sup>2,3,4</sup>

<sup>1</sup>Radiology, Tongji hospital, Tongji Medical College, Huazhong University of Science and Technology, Wuhan, China, <sup>2</sup>Radiology, University of Illinois at Chicago, Chicago, IL, United States, <sup>3</sup>Center for MR Research, University of Illinois at Chicago, Chicago, IL, United States, <sup>4</sup>Bioengineering, University of Illinois at Chicago, Chicago, IL, United States

In this study, at the first time, we performed in vivo  $k_{ex}$  MRI of MS patients and evaluated its potential value for staging clinical MS lesions. In vivo proton exchange rate mapping was found to be highly correlated with Gadolinium enhancement for determining lesion activity. With further validation,  $k_{ex}$  may be an alternative endogenous MRI contrast for the clinical determination of dissemination in time (DIT) of MS lesions.

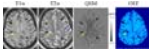


### Short and long sodium concentrations in multiple sclerosis: a multi-echo ultra- high field <sup>23</sup>Na MRI study

Mohamed Mounir El Mendili<sup>1</sup>, Ben Ridley<sup>1</sup>, Bertrand Audoin<sup>1,2</sup>, Soraya Gherib<sup>1</sup>, Lauriane Pini<sup>1</sup>, Françoise Reuter<sup>1,2</sup>, Maxime Guye<sup>1,3</sup>, Armin Nagel<sup>4</sup>, Audrey Rico<sup>2</sup>, Clémence Boutière<sup>2</sup>, Jean Pelletier<sup>1,2</sup>, Jean-Philippe Ranjeva<sup>1</sup>, Adil Maarouf<sup>1,2</sup>, and Wafaa Zaaraoui<sup>1</sup>

<sup>1</sup>Aix-Marseille Université, CNRS, CRMBM, Marseille, France, <sup>2</sup>APHM, Hôpital de la Timone, Pôle de Neurosciences Cliniques, Service de Neurologie, Marseille, France, <sup>3</sup>APHM, Hôpital de la Timone, Pôle d'Imagerie Médicale, CEMEREM, Marseille, France, <sup>4</sup>Institute of Radiology, University Hospital Erlangen, Erlangen, Germany

Alteration of sodium homeostasis was previously evidenced in multiple sclerosis with total sodium concentration (TSC) found to be related to disability. However, the correlations found were moderate, maybe due to the fact that measured sodium accumulation combined intra and extra cellular sodium signal while only intra-cellular sodium concentration is relevant to assess neurodegeneration. One may suppose that developing reliable sequences able to assess only the intra-cellular signal may lead to a better estimation of neurodegeneration in multiple sclerosis and better correlations with irreversible disability. The present study proposes an original multi-TE sequence at 7T to reach this goal.

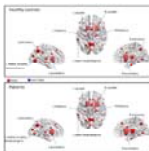


### Regional oxygen extract fraction mapping (rOEF) of multiple sclerosis brains

Junghun Cho<sup>1</sup>, Thanh D. Nguyen<sup>2</sup>, Weiyuan Huang<sup>2</sup>, Shun Zhang<sup>2</sup>, Xianfu Luo<sup>2</sup>, Susan A. Gauthier<sup>3</sup>, Pascal Spincemaille<sup>2</sup>, Ajay Gupta<sup>2</sup>, and Yi Wang<sup>1,2</sup>

<sup>1</sup>Biomedical Engineering, Cornell University, New York, NY, United States, <sup>2</sup>Radiology, Weill Cornell Medical College, New York, NY, United States, <sup>3</sup>Neurology, Weill Cornell Medical College, New York, NY, United States

Impaired energy metabolism is a major contributor to the ongoing inflammation and neurodegeneration in multiple sclerosis (MS) brains, particularly MS lesions. Cerebral regional oxygen extraction fraction mapping (rOEF) obtained from challenge-free multiecho gradient echo data demonstrates that lesions identified on quantitative susceptibility mapping (QSM) without rim (QSM rim-) have heterogenous OEF that is higher than that in other type of lesions. rOEF may offer insight into MS lesion remyelination viability.



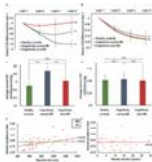
### Virtual hypoxia and structural network alterations in multiple sclerosis: a combined <sup>23</sup>Na and diffusion MRI study

Adil Maarouf<sup>1,2</sup>, Hanna Bou Ali<sup>1</sup>, Pierre Besson<sup>1</sup>, Jan Patrick Stellman<sup>1,3</sup>, Soraya Gherib<sup>1</sup>, Fanelly Pariollaud<sup>1</sup>, Arnaud Le Troter<sup>1</sup>, Maxime Guye<sup>1,3</sup>, Patrick Viout<sup>1</sup>, Jean Pelletier<sup>1,2</sup>, Jean-Philippe Ranjeva<sup>1</sup>, Bertrand Audoin<sup>1,2</sup>, and Wafaa Zaaraoui<sup>1</sup>

<sup>1</sup>Aix-Marseille Université, CNRS, CRMBM, Marseille, France, <sup>2</sup>APHM, Hôpital de la Timone, Pôle de Neurosciences Cliniques, Service de Neurologie, Marseille, France, <sup>3</sup>APHM, Hôpital de la Timone, Pôle d'Imagerie Médicale, CEMEREM, Marseille, France

Virtual hypoxia is a key factor in the induction of pathological processes in multiple sclerosis. <sup>23</sup>Na-MRI is an emerging technique in virtual hypoxia exploration, with previous studies showing relevance of grey matter sodium accumulation in MS. In the present study, we showed that grey matter sodium accumulation is mainly driven by accumulation in the most connected cortical regions (called hubs) and correlate with disability. This study provides an insight in several processes of energy failure and brain reorganization in MS.

0066



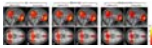
**Reduced arterial compliance-mediated neural-vascular uncoupling underlies cognitive impairment in multiple sclerosis**

Dinesh K Sivakolundu<sup>1</sup>, Kathryn L West<sup>1</sup>, Gayathri B Maruthy<sup>1</sup>, Mark Zuppichini<sup>1</sup>, Monroe P Turner<sup>1</sup>, Dema Abdelkarim<sup>1</sup>, Yuguang Zhao<sup>1</sup>, Jeffrey Spence<sup>1</sup>, Hanzhang Lu<sup>2</sup>, Darin T Okuda<sup>3</sup>, and Bart Rypma<sup>1</sup>

<sup>1</sup>The University of Texas at Dallas, Dallas, TX, United States, <sup>2</sup>Johns Hopkins University, Baltimore, MD, United States, <sup>3</sup>University of Texas Southwestern Medical Center, Dallas, TX, United States

Cognitive impairment occurs in ~70% of multiple sclerosis patients (MSP). The neural mechanism of this slowing is unknown. Vascular compliance reductions along the cerebrovascular tree would result in suboptimal vasodilation upon neural stimulation (i.e., neural-vascular uncoupling) and thus cognitive slowing. We tested arterial and venous cerebrovascular reactivity (CVR) along the cerebrovascular tree in nested cerebral cortical layers. Arterial CVR reduced exponentially along the cortical layers in controls and cognitively-normal MSP, but not in slower MSP. The exponential decay-constant was associated with individual subjects' reaction-time. Such associations implicate neural-vascular uncoupling as a mechanism of cognitive slowing in MS.

0067



**Transcranial direct current stimulation for multiple sclerosis: real time and cumulative effects on functional connectivity**

Marco Muccio<sup>1</sup>, Peidong He<sup>1</sup>, Claire S. Choi<sup>2</sup>, Lillian Walton Masters<sup>2</sup>, Lauren Krupp<sup>2</sup>, Oded Gonen<sup>1</sup>, Leigh Charvet<sup>2</sup>, and Yulin Ge<sup>1</sup>

<sup>1</sup>Department of Radiology, New York University School of Medicine, New York, NY, United States, <sup>2</sup>Department of Neurology, New York University School of Medicine, New York, NY, United States

Transcranial direct current stimulation (tDCS) is an innovative, non-invasive, brain stimulation technique that modulates cortical excitability by applying weak electrical currents. Despite cognitive improvements in multiple sclerosis (MS) subjects have been recently reported, the underlying in-vivo physiological mechanism of tDCS remains largely unclear. The purpose of this study is therefore to firstly address the real time tDCS effect (with simultaneous MRI scans) on the functional connectivity of both controls and MS patients. Secondly, we want to investigate whether such changes are altered in MS subjects following 20 tDCS treatment sessions.

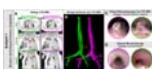
## Oral

### Pediatric Innovations - Pediatric Body & Musculoskeletal

Monday Parallel 3 Live Q&A

Monday 13:45 - 14:30 UTC

Moderators: Corin Willers



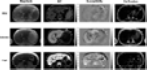
**Virtual bronchoscopy of neonatal dynamic airway collapse with ultrashort echo-time MRI**

Nara S Higano<sup>1,2</sup>, Alister J Bates<sup>1,2,3,4</sup>, Erik B Hysinger<sup>2,4</sup>, Robert J Fleck<sup>3,5,6</sup>, Andrew D Hahn<sup>7</sup>, Sean B Fain<sup>7,8</sup>, Paul S Kingma<sup>4,9</sup>, and Jason C Woods<sup>2,5,6</sup>



<sup>1</sup>Center for Pulmonary Imaging, Cincinnati Children's Hospital, CINCINNATI, OH, United States, <sup>2</sup>Pulmonary Medicine, Cincinnati Children's Hospital, CINCINNATI, OH, United States, <sup>3</sup>Upper Airway Center, Cincinnati Children's Hospital, CINCINNATI, OH, United States, <sup>4</sup>Pediatrics, University of Cincinnati, CINCINNATI, OH, United States, <sup>5</sup>Radiology, Cincinnati Children's Hospital, CINCINNATI, OH, United States, <sup>6</sup>Pediatrics, University of Cincinnati, Cincinnati, OH, United States, <sup>7</sup>Medical Physics, University of Wisconsin - Madison, Madison, WI, United States, <sup>8</sup>Radiology, University of Wisconsin - Madison, Madison, WI, United States, <sup>9</sup>Neonatology and Pulmonary Biology, Cincinnati Children's Hospital, CINCINNATI, OH, United States

Central airway abnormalities in neonates, e.g. dynamic collapse and stenosis, are serious complications often associated with preterm birth and congenital abnormalities, but have not been extensively studied. These conditions are most often assessed through clinical bronchoscopy, which can be unreliable and poses increased risks to patients. Here, we demonstrate novel visualization of static and dynamic neonatal airway abnormalities on virtual bronchoscopy from high-resolution, retrospectively respiratory-gated ultrashort echo-time MRI, which exhibits good agreement with clinical bronchoscopy. This virtual technique allows for assessment of neonatal airway abnormalities that is readily interpretable to clinicians familiar with clinical bronchoscopy.

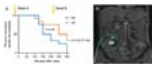


### Quantitative Susceptibility Mapping using a Multi-spectral ARMA Model for Assessment of Hepatic Iron Overload

Aaryani Tipirneni-Sajja<sup>1,2</sup>, Ralf Berthold Loeffler<sup>2,3</sup>, Jane Hankins<sup>4</sup>, and Claudia Maria Hillenbrand<sup>2,3</sup>

<sup>1</sup>Biomedical Engineering, University of Memphis, Memphis, TN, United States, <sup>2</sup>Diagnostic Imaging, St. Jude Children's Research Hospital, Memphis, TN, United States, <sup>3</sup>Research Imaging NSW, University of New South Wales, Sydney, Australia, <sup>4</sup>Hematology, St. Jude Children's Research Hospital, Memphis, TN, United States

Hepatic iron content (HIC) assessment by R2\*-MRI can be confounded by co-existing fibrosis. Instead, quantitative susceptibility mapping (QSM) techniques could be used to assess iron content without being affected by fibrosis. In this study, we demonstrated that the field maps generated from a multi-spectral autoregressive moving average (ARMA) model can be used in conjunction with QSM techniques to measure magnetic susceptibility, as a predictor for HIC.

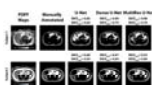


### Digestive disorders in Cystic Fibrosis: Transit, Motility and MRI Signs of Small Intestinal Bacterial Overgrowth

Neele S Dellschaft<sup>1,2</sup>, Christabella Ng<sup>3</sup>, Caroline Hoad<sup>1,2</sup>, Luca Marciani<sup>2,4</sup>, Robin Spiller<sup>2,4</sup>, Penny Gowland<sup>1,2</sup>, Alan Smyth<sup>2,3</sup>, and Giles Major<sup>2,4</sup>

<sup>1</sup>Sir Peter Mansfield Imaging Centre, University of Nottingham, Nottingham, United Kingdom, <sup>2</sup>Nottingham NIHR Biomedical Research Centre, University of Nottingham, Nottingham, United Kingdom, <sup>3</sup>Division of Child Health, Obstetrics and Gynaecology, University of Nottingham, Nottingham, United Kingdom, <sup>4</sup>Nottingham Digestive Diseases Centre, University of Nottingham, Nottingham, United Kingdom

Cystic Fibrosis (CF) is a genetic disease leading to sticky mucus. We used MRI to characterise the effect of CF on gastrointestinal function, comparing people with CF to matched healthy controls. People with CF had slower oro-caecal transit times. No change in gastric emptying rate was apparent but more free water was present in their small bowel with reduced small bowel motility and a reduced gastro-ileal reflex. Some images suggested increased bacterial load in the small bowel. CF colons were larger. These findings are consistent with sticky chyme impeding ileal emptying into the colon, causing obstruction to flow, and constipation.

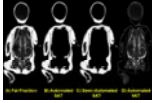


### Fully Convolutional Networks for Adipose Tissue Segmentation Using Free-Breathing Abdominal MRI in Healthy and Overweight Children

Sevgi Gokce Kafali<sup>1,2</sup>, Shu-Fu Shih<sup>1,2</sup>, Xinzhou Li<sup>1,2</sup>, Tess Armstrong<sup>1</sup>, Karrie V. Ly<sup>3</sup>, Shahnaz Ghahremani<sup>1</sup>, Kara L. Calkins<sup>3</sup>, and Holden H. Wu<sup>1,2</sup>

<sup>1</sup>Radiological Sciences, University of California, Los Angeles, Los Angeles, CA, United States, <sup>2</sup>Bioengineering, University of California, Los Angeles, Los Angeles, CA, United States, <sup>3</sup>Pediatrics, University of California, Los Angeles, Los Angeles, CA, United States

The volume and fat content of subcutaneous and visceral adipose tissue (SAT and VAT) have strong associations with metabolic diseases in overweight children. Currently, the gold standard to measure the SAT/VAT content is manual annotation, which is time-consuming. Although several studies showed promising results using machine and deep learning to segment SAT and VAT in adults, there is a lack of research on deep learning-based SAT and VAT segmentation in children. Here, we investigated the performance of 3 deep learning network architectures to segment SAT and VAT in children.

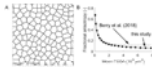


### Semi-Automated Whole Body Neonatal Regional Fat Quantification Using Dixon Chemical Shift (CSI) MRI at 3.0 Tesla

Jonathan P Dyke<sup>1</sup>, Kevin Oh<sup>1</sup>, Amanda Garfinkel<sup>2</sup>, Alan M Groves<sup>3</sup>, and Arzu Kovanlikaya<sup>1</sup>

<sup>1</sup>Radiology, Weill Cornell Medicine, New York, NY, United States, <sup>2</sup>Pediatrics, Weill Cornell Medicine, New York, NY, United States, <sup>3</sup>Pediatrics, Mount Sinai School of Medicine, New York, NY, United States

Whole body fat fraction was previously published by our group in term and preterm infants using Dixon CSI MRI. Advanced semi-automated regional fat quantification was performed yielding: subcutaneous adipose tissue (SAT), visceral adipose tissue (VAT), brown adipose tissue (BAT) volumes and hepatic fat fraction (HFF). Whole body VAT volume (cc) was increased in preterm infants ( $3.4\% \pm 1.5\%$ ) compared to term ( $2.4\% \pm 0.9\%$ ) ( $p=0.079$ ) when normalized to total body volume (cc). HFF and BAT did not differ between term and preterm infants ( $p>0.25$ ). CSI MRI allows quantification of regional fat depots in preterm infants which may potentially help optimize nutritional management and monitor growth.

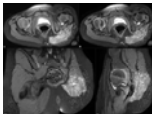


### Using transverse diffusion to measure changes in muscle fibre number and muscle fibre size during childhood growth in humans

Bart Bolsterlee<sup>1,2</sup>, Arkiev D'Souza<sup>1,3</sup>, and Robert D Herbert<sup>1,3</sup>

<sup>1</sup>Neuroscience Research Australia, Randwick, Australia, <sup>2</sup>Graduate School of Biomedical Engineering, University of New South Wales, Randwick, Australia, <sup>3</sup>School of Medical Sciences, University of New South Wales, Randwick, Australia

We used diffusion tensor imaging (DTI) to study macroscopic and microscopic features of skeletal muscles during childhood development (5-17 years). From muscle volume and fibre length measurements, we determined the summed cross-sectional area of all fibres. From measurements of diffusion properties and simulations of restricted diffusion in skeletal muscle, we estimated mean cross-sectional areas of individual fibres. Our findings suggest that human muscles grow both by adding fibres and by increasing fibre cross-sectional areas. DTI-based measurements of skeletal muscle micro- and macrostructure could have important applications in understanding both normal and disordered muscle growth.



### 3D PDWI Accelerated with Compressed SENSE in Pediatric Joint Imaging: Clinical Feasibility Study

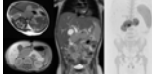
Yupeng Zhu<sup>1</sup>, Di Hu<sup>1</sup>, Yanqiu Lv<sup>1</sup>, Yang Wen<sup>1</sup>, Huiying Kang<sup>1</sup>, Xiaomin Duan<sup>1</sup>, Jiazheng Wang<sup>2</sup>, Queenie Chan<sup>2</sup>, and Yun Peng<sup>1</sup>

<sup>1</sup>Department of Radiology, Beijing Children's Hospital, Capital Medical University, National Center for Children's Health, Beijing, China, <sup>2</sup>Philips Healthcare, Beijing, China



The use of three dimensional (3D) volumetric acquisition in clinical settings has been limited due to long scan time. However, 3D volumetric acquisition could provide higher spatial resolution and decrease partial volume effects. The introduction of compressed sensing in combination of the parallel imaging technique SENSE allows shortening of scan time and provide comparable overall image quality when compared with standard sequences. The purpose of the study is to determine the feasibility of 3D PDWI accelerated with compressed SENSE(CS) for evaluating the pediatric joint image quality and compared with 2D PDWI.

0075



MR imaging and MR guided biopsy in initial diagnosis and staging of pediatric malignancies – a one-stop shop approach

Guenther Schneider<sup>1</sup>, Tobias Woerner<sup>1</sup>, and Arno Buecker<sup>1</sup>

<sup>1</sup>*Diagnostic and Interventional Radiology, Saarland University Medical Center, Homburg, Germany*

Diagnosis and staging in pediatric malignancies today involves different imaging procedures, from conventional x-ray over ultrasound to MR-, CT- and PET-imaging. We evaluated as if MRI can be used as a comprehensive one-stop shop for diagnosis, staging and biopsy in pediatric malignancies. As a result, when comparing the different imaging modalities, differences between MRI and CT were seen regarding the higher number of small lung lesions detected (<3mm) on CT. Comparable results were seen for abdominal tumors, Hodgkin- and Non-Hodgkin Lymphoma. In Ewing sarcoma MRI showed advantages compared with PET imaging regarding detection of skip lesions and bone marrow metastases.

## Oral - Power Pitch

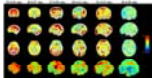
### Pediatric Innovations - Pediatric Head to Toe

Monday Parallel 3 Live Q&A

Monday 13:45 - 14:30 UTC

Moderators: Wilburn Reddick

0076



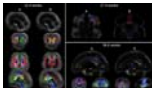
Mapping fetal brain development based on automated brain segmentation and 4D brain atlasing

Haotian Li<sup>1</sup>, Guohui Yan<sup>2</sup>, Wanrong Luo<sup>1</sup>, Tingting Liu<sup>1</sup>, Yan Wang<sup>1</sup>, Yi Zhang<sup>1</sup>, Li Zhao<sup>3</sup>, Catherine Limperopoulos<sup>3</sup>, Yu Zou<sup>2</sup>, and Dan Wu<sup>1</sup>

<sup>1</sup>*Key Laboratory for Biomedical Engineering of Ministry of Education, Department of Biomedical Engineering, College of Biomedical Engineering & Instrument Science, Zhejiang University, Hangzhou, Zhejiang, China,* <sup>2</sup>*Department of Radiology, Women's Hospital, School of Medicine, Zhejiang University, Hangzhou, Zhejiang, China,* <sup>3</sup>*Diagnostic Imaging and Radiology, Children's National Medical Center, Washington, DC, WA, United States*

Fetal brain MRI has become an important tool for in-utero assessment of brain development and disorders. Here we proposed an automated pipeline with fetal brain segmentation, super-resolution reconstruction, and fetal brain atlasing to quantitatively map in-utero fetal brain development in a Chinese population. We designed a U-net CNN implemented for automatic fetal brain segmentation, which showed superior segmentation accuracy compared with conventional methods. We then generated a Chinese fetal brain atlas, using an iterative linear and nonlinear registration method. Based on the 4D spatiotemporal atlas, we characterized the three-dimensional morphological evolution of the fetal brain between 23-36 weeks of gestation.

0077



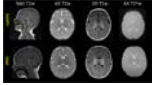
Multi-component atlas of fetal brain development via decomposition of diffusion MRI

Maximilian Pietsch<sup>1,2</sup>, Daan Christiaens<sup>2,3</sup>, Jana Hutter<sup>1,2</sup>, Lucilio Cordero-Grande<sup>1,2</sup>, Anthony N. Price<sup>1,2</sup>, Emer Hughes<sup>2</sup>, David Edwards<sup>2</sup>, Joseph V. Hajnal<sup>1,2</sup>, Serena J. Counsell<sup>2</sup>, and J-Donald Tournier<sup>1,2</sup>

<sup>1</sup>*Biomedical Engineering Department, School of Biomedical Engineering and Imaging Sciences, King's College London, London, United Kingdom,* <sup>2</sup>*Centre for the Developing Brain, School of Biomedical Engineering and Imaging Sciences, King's College London, London, United Kingdom,* <sup>3</sup>*Department of Electrical Engineering (ESAT/PSI), KU Leuven, Leuven, Belgium*

Mapping tissue maturation in the fetal brain with diffusion MRI requires modelling transient processes in early brain development. In this work, we extend a data-driven multi-component framework introduced for modelling neonatal brain development to fetal data of the developing Human Connectome Project (dHCP). To this end, we build weekly templates ranging from 23 to 37 weeks gestational age that consist of one fluid and two orientationally-resolved tissue components. The orientation-resolved components exhibit marked spatial patterns and temporal trajectories, and demonstrate pronounced microstructural changes with gestational age.

0078



Evaluation of brain MRI quality in natural sleep vs anaesthesia in infants within 6 months of life.

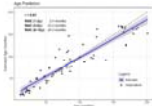
Paolo Bosco<sup>1</sup>, Simona Fiori<sup>2</sup>, Rosa Pasquariello<sup>1</sup>, Elena Scaffei<sup>2,3</sup>, Michela Tosetti<sup>1</sup>, and Laura Biagi<sup>1</sup>

<sup>1</sup>Laboratory of Medical Physics and Magnetic Resonance, IRCCS Stella Maris Foundation, Pisa, Italy,

<sup>2</sup>Department of Developmental Neuroscience, IRCCS Stella Maris Foundation, Pisa, Italy, <sup>3</sup>Department of Clinical and Experimental Medicine, University of Pisa, Pisa, Italy

Natural sleep brain MRI (nsMRI) up to 6 months of life to support early diagnosis in term and preterm infants at high risk for cerebral palsy and other developmental disorders is still far from clinical practice, due to unproven feasibility and quality. We extracted some measures of quality (signal to noise ratio, contrast to noise ratio in a cohort of 23 and 53 infants who underwent sedation or natural sleep brain MR respectively. Most of the quality measures extracted across different MR modalities did not differ between nsMRI and sedation MRI (sMRI) suggesting the feasibility of nsMRI at younger ages.

0079



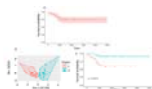
Measuring brain maturation with quantitative MRI

Gian Franco Piredda<sup>1,2,3</sup>, Tom Hilbert<sup>1,2,3</sup>, Baptiste Morel<sup>4,5</sup>, Clovis Tauber<sup>4</sup>, Jean Philippe Cottier<sup>4</sup>, Lars Lauer<sup>6</sup>, Jean-Philippe Thiran<sup>2,3</sup>, Bénédicte Maréchal<sup>1,2,3</sup>, and Tobias Kober<sup>1,2,3</sup>

<sup>1</sup>Advanced Clinical Imaging Technology, Siemens Healthcare AG, Lausanne, Switzerland, <sup>2</sup>Department of Radiology, Lausanne University Hospital and University of Lausanne, Lausanne, Switzerland, <sup>3</sup>LTS5, École Polytechnique Fédérale de Lausanne (EPFL), Lausanne, Switzerland, <sup>4</sup>UMR 1253, iBrain, Université de Tours, Inserm, Tours, France, <sup>5</sup>Pediatric Radiology Department, Clocheville Hospital, CHRU of Tours, Tours, France, <sup>6</sup>SHS DI MR SIP, Siemens Healthcare GmbH, Erlangen, Germany

The sensitivity of  $T_1$  mapping towards brain maturation during the first years of life was shown in previous studies. This work investigates whether this sensitivity is high enough that age of young subjects can be directly estimate from  $T_1$  relaxometry, which in turn enables to determine the developmental stage of the subject's brain. A random forest regression was employed to estimate subjects' age based on median  $T_1$  values of different brain regions. Good correlation ( $r=0.95$ ) was found between actual and predicted ages, and proof-of-concept results in a patient showed the potential of the proposed framework to detect developmental delays.

0080



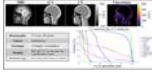
Deriving survival risk features using multi-parametric MRI in paediatric neuro-oncological disease: a multi-centre clinical study.

James Timothy Grist<sup>1</sup>, Stephanie Timothy Withey<sup>1</sup>, Lesley MacPherson<sup>2</sup>, Adam Oates<sup>3</sup>, Stephen Timothy Powell<sup>1</sup>, Jan Novak<sup>4</sup>, Laurence Abernethy<sup>5</sup>, Barry Pizer<sup>6</sup>, Ricahrd Grundy<sup>7</sup>, Simon Bailey<sup>8</sup>, Dipayan Mitra<sup>8</sup>, Theodoros N Arvantis<sup>9</sup>, Dorothee P. Auer<sup>7</sup>, and Andrew C Peet<sup>1</sup>

<sup>1</sup>University of Birmingham, Birmingham, United Kingdom, <sup>2</sup>Birmingham Women's and Children's NHS foundation trust, Birmingham, United Kingdom, <sup>3</sup>Birmingham Women's and Children's NHS foundation trust, Birmingham, United Kingdom, <sup>4</sup>Aston University, Birmingham, United Kingdom, <sup>5</sup>Alder Hey Children's NHS foundation trust, Liverpool, United Kingdom, <sup>6</sup>Institute of Translation Medicine, University of Liverpool, Liverpool, United Kingdom, <sup>7</sup>University of Nottingham, Nottingham, United Kingdom, <sup>8</sup>Royal Victoria Infirmary, Newcastle, United Kingdom, <sup>9</sup>University of Warwick, Warwick, United Kingdom

This study focuses on the combination of diffusion and perfusion imaging with advanced machine learning to predict survival in a cohort of paediatric brain tumours. Results show two novel subgroups with significantly different survival. These results will aid in clinical decision making and therapeutic studies.

0081



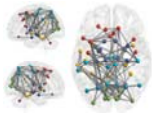
### Deep learning-based sCTs with uncertainty estimation from heterogeneous paediatric brain MRI

Matteo Maspero<sup>1,2</sup>, Laura G Bentvelzen<sup>1,2</sup>, Mark H F Savenije<sup>1,2</sup>, Enrica Seravalli<sup>1</sup>, Geert O R Janssens<sup>1,3</sup>, Cornelis A T van den Berg<sup>1,2</sup>, and Marielle E P Philippens<sup>1</sup>

<sup>1</sup>Radiotherapy, UMC Utrecht, Utrecht, Netherlands, <sup>2</sup>Computational imaging group for MR diagnostic & therapy, UMC Utrecht, Utrecht, Netherlands, <sup>3</sup>Paediatric Oncology, Princess Maxima Center, Utrecht, Netherlands

The feasibility of radiotherapy dose calculations for brain tumours from MRI acquired with a heterogeneous set of acquisition protocols on paediatric patients was investigated using a combination of networks trained on orthogonal planes to estimate the uncertainty of the generated sCT.

0082



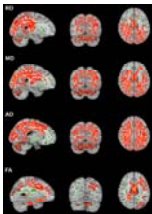
### Disrupted structural connectome in Duchenne's muscular dystrophy: Classifying and subtyping based on Dp140 dystrophin isoform

Apurva Shah<sup>1</sup>, Apoorva Safai<sup>1</sup>, Veeramani Preethish Kumar<sup>2</sup>, Atchayaram Nalini<sup>2</sup>, Jitender Saini<sup>3</sup>, and Madhura Ingalthalikar<sup>1</sup>

<sup>1</sup>Symbiosis Center for Medical Image Analysis, Symbiosis International University, Pune, India, <sup>2</sup>Department of Neurology, National Institute of Mental Health and Neurosciences, Bengaluru, India, <sup>3</sup>Department of Radiology, National Institute of Mental Health and Neurosciences, Bengaluru, India

Duchenne Muscular Dystrophy (DMD) is a genetic neuromuscular disorder, characterized by muscle weakness and cognitive deficits due to mutation in DMD gene. Dp140+ and Dp140- are DMD subtypes derived based on promoter site of isoform Dp140 in DMD gene. Our work investigated the structural connectivity in DMD and its sub-types and demonstrated widespread and global reduction in connectivity across whole brain in DMD compared to controls. Higher dysconnectivity was observed in Dp140- subtype especially in cerebellar and frontal regions compared to Dp140+ implying that the promoter site of Dp140 isoform plays a crucial role in terms of impaired information processing.

0083

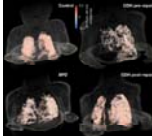


### In vivo evaluation of white matter abnormalities in children with DMD using diffusion MRI

Jitender Saini<sup>1</sup>, Veeramani Preethish Kumar<sup>2</sup>, Apurva Shah<sup>3</sup>, Manoj Kumar<sup>4</sup>, Madhura Ingalthalikar<sup>5</sup>, and Nalini Atchayaram<sup>2</sup>

<sup>1</sup>Neuroimaging and Interventional Radiology, National Institute of Mental Health and, Bangalore, India, <sup>2</sup>Neurology, National Institute of Mental Health and, Bangalore, India, <sup>3</sup>Symbiosis Centre for Medical Image Analysis, Symbiosis International University, Pune, India, <sup>4</sup>Neuroimaging and Interventional Radiology, National Institute of Mental Health and, Bangalore, India, <sup>5</sup>Symbiosis Centre for Medical Image Analysis, Symbiosis International University, Pune, India

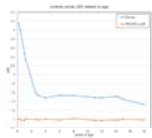
Duchenne muscular dystrophy (DMD), a genetically inherited X-linked neuromuscular disorder characterised by progressive muscle weakness and significant non-motor manifestations like poor IQ, and neuropsychiatric illnesses. In this study, we evaluate white matter (WM) abnormalities in DMD patients using diffusion tensor imaging (DTI). We observed widespread WM changes in DMD patients and the presence of distal mutation was associated with poor clinical and neuropsychological profile with severe and spatially more WM abnormalities.



Alister J Bates<sup>1</sup>, Nara S Higano<sup>1</sup>, Andreas Schuh<sup>2</sup>, Andrew Hahn<sup>3</sup>, Katie J Carey<sup>3</sup>, Sean B Fain<sup>3</sup>, Paul Kingma<sup>4</sup>, and Jason C Woods<sup>1</sup>

<sup>1</sup>Center for Pulmonary Imaging, Cincinnati Children's Hospital Medical Center, Cincinnati, OH, United States, <sup>2</sup>Biomedical Image Analysis Group, Imperial College London, London, United Kingdom, <sup>3</sup>Biomedical Engineering, University of Wisconsin-Madison, Madison, WI, United States, <sup>4</sup>Bronchopulmonary Dysplasia (BPD) Center, Cincinnati Children's Hospital Medical Center, Cincinnati, OH, United States

Neonatal lung disease is often related to premature birth or congenital abnormalities. Structural MRI has been performed in these patients but does not indicate which lung regions perform gas exchange. Registered respiratory gated ultra-short echo-time proton MRI can produce lung ventilation maps in neonates throughout the respiratory cycle. This technique showed clear differences between a control subject and 2 patients with lung disease in terms of ventilation efficiency (inhaled air per milliliter of lung), spatial and temporal ventilation homogeneity. Further differences were shown post-surgical intervention, demonstrating the method and as a potential means to assess treatment efficacy.

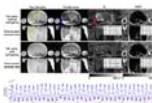


### 3D UTE Cones for assessing lung density in paediatric cases

Konstantinos G. Zeimpekis<sup>1</sup>, Florian Wiesinger<sup>2</sup>, Gaspar Delso<sup>2</sup>, Julia Geiger<sup>3</sup>, and Christian Kellenberger<sup>4</sup>

<sup>1</sup>Nuclear Medicine, University Hospital Zurich, Zurich, Switzerland, <sup>2</sup>GE Healthcare, Chicago, IL, United States, <sup>3</sup>University Children's Hospital Zurich, Zurich, Switzerland, <sup>4</sup>Radiology, University Children's Hospital Zurich, Zurich, Switzerland

3D ultrashort echo-time Cones is tested against PROPELLER for lung density detection in paediatric cases on two cohorts: patients with morphologically normal lungs and patients with Cystic Fibrosis. Cones seems to be able to detect lung density based on lung-to-background signal intensities ratio (LBR) while PROPELLER fails to show any correlation. Cones is able to show the lung anteroposterior gravity gradient as well. There was no difference between Cones LBR of controls and CF while pixel-intensity histogram analysis of Cones slices seem to differentiate pathological from normal lung. Qualitatively, lung contrast decreases with increasing age.



### Free-Breathing Volumetric Liver R<sub>2</sub><sup>\*</sup> Quantification in Pediatric Patients Using 3D Self-Gating Motion-Compensated Stack-of-Radial MRI

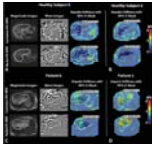
Xiaodong Zhong<sup>1</sup>, Houchun H Hu<sup>2</sup>, Tess Armstrong<sup>3,4</sup>, Marcel D Nickel<sup>5</sup>, Stephan A.R. Kannengiesser<sup>5</sup>, Vibhas Deshpande<sup>6</sup>, Berthold Kiefer<sup>5</sup>, and Holden H Wu<sup>3,4</sup>

<sup>1</sup>MR R&D Collaborations, Siemens Healthcare, Los Angeles, CA, United States, <sup>2</sup>Department of Radiology, Nationwide Children's Hospital, Columbus, OH, United States, <sup>3</sup>Department of Radiological Sciences, University of California Los Angeles, Los Angeles, CA, United States, <sup>4</sup>Department of Physics and Biology in Medicine, University of California Los Angeles, Los Angeles, CA, United States, <sup>5</sup>MR Application Predevelopment, Siemens Healthcare GmbH, Erlangen, Germany, <sup>6</sup>MR R&D Collaborations, Siemens Healthcare, Austin, TX, United States

Liver fat and iron quantification is of growing interest. However, it is challenging and sometimes impossible to perform breath-hold MRI acquisitions in children. Using a breath-hold 3D Cartesian method as reference, a self-gating free-breathing 3D stack-of-radial liver R<sub>2</sub><sup>\*</sup> quantification technique was evaluated. Results showed that the free-breathing stack-of-radial technique accurately quantified fat even without self-gating, while free-breathing R<sub>2</sub><sup>\*</sup> quantification had biases caused by respiratory motion and self-gating was necessary for accurate R<sub>2</sub><sup>\*</sup> quantification in pediatric subjects. This technique has potential for accurate and efficient free-breathing quantification of both liver fat and iron in pediatric patients.

Assessment of Free-Breathing Radial Magnetic Resonance Elastography in Healthy Children and Children with Liver Disease at 3T

0087



Sevji Gokce Kafali<sup>1,2</sup>, Tess Armstrong<sup>1</sup>, Shu-Fu Shih<sup>1,2</sup>, Joseph L Holtrop<sup>3</sup>, Robert S Venick<sup>4</sup>, Shahnaz Ghahremani<sup>1</sup>, Bradley D. Bolster Jr<sup>5</sup>, Claudia M. Hillenbrand<sup>3</sup>, Kara L. Calkins<sup>4</sup>, and Holden H. Wu<sup>1,2</sup>

<sup>1</sup>Radiological Sciences, University of California, Los Angeles, Los Angeles, CA, United States,

<sup>2</sup>Bioengineering, University of California, Los Angeles, Los Angeles, CA, United States, <sup>3</sup>Diagnostic Imaging, St. Jude Children's Research Hospital, Memphis, TN, United States, <sup>4</sup>Pediatrics, University of California, Los Angeles, Los Angeles, CA, United States, <sup>5</sup>Siemens Medical Solutions, Salt Lake City, UT, United States

Hepatic stiffness measured by magnetic resonance elastography (MRE) is a biomarker that correlates with histopathological staging of liver fibrosis. Conventional Cartesian gradient-echo MRE requires breath-holding (BH), which may be inconsistent and challenging for children. Free-breathing (FB) MRE based on radial acquisition is a promising solution to this problem. In this study, we investigated the agreement in hepatic stiffness values from BH-MRE and FB-MRE, as well as repeatability, in healthy children and pediatric patients at 3T. Bland-Altman analysis showed a high level of agreement between BH-MRE and FB-MRE, and repeatability analysis showed similar performance for BH-MRE and FB-MRE.

0088



A first-in-child feasibility study of a new mini-capsule medical device to measure whole gut transit in pediatric constipation using MRI (MAGIC)

Hayfa Sharif<sup>1,2</sup>, Nichola Abreheart<sup>1</sup>, Caroline Hoad<sup>1,3</sup>, Kathryn Murray<sup>1,3</sup>, Alan Perkins<sup>1,4</sup>, Penny Gowland<sup>3</sup>, Robin Spiller<sup>1</sup>, Roy Harris<sup>1</sup>, Sian Kirkham<sup>5</sup>, Sabarinathan Loganathan<sup>5</sup>, Michalis Papadopoulos<sup>5</sup>, Young Persons Advisory Group (YPAG)<sup>6</sup>, David Devadason<sup>5</sup>, and Luca Marciani<sup>1</sup>

<sup>1</sup>Nottingham Digestive Diseases Centre and NIHR Nottingham Biomedical Research Centre, University of Nottingham, Nottingham, United Kingdom, <sup>2</sup>Clinical Radiology, Amiri Hospital, Ministry Of Health, Civil Service Commission, Kuwait, <sup>3</sup>Sir Peter Mansfield Imaging Centre, School of Physics and Astronomy, University of Nottingham, Nottingham, United Kingdom, <sup>4</sup>Medical Physics and Clinical Engineering, Nottingham University Hospitals, Queen's Medical Centre, Nottingham, United Kingdom, <sup>5</sup>Nottingham Children's Hospital, Nottingham University Hospitals NHS Trust, Queen's Medical Centre, Nottingham, United Kingdom, <sup>6</sup>NUH YPAG, Nottingham University Hospitals NHS Trust, Nottingham, United Kingdom

We developed a new MRI mini-capsule marker device to measure whole gut transit (WGTT) in pediatric constipation to overcome image quality and ionizing radiation limitations of current X-ray methods. Thirty five healthy children and 16 patients with constipation were asked to swallow a number of mini-capsules and imaged, following a common X-ray radiopaque marker protocol. The capsules were imaged successfully in the colon. WGTT was calculated from the capsules count and was significantly longer in the patients compared to the controls. The study also showed excellent feasibility and safety of using the new device and methods in children with constipation.

0089



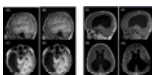
Improved data quality and reduced costs by slice localization integrated MRI monitoring

Yao Sui<sup>1,2</sup>, Onur Afacan<sup>1,2</sup>, Ali Gholipour<sup>1,2</sup>, and Simon Keith Warfield<sup>1,2</sup>

<sup>1</sup>Harvard Medical School, Boston, MA, United States, <sup>2</sup>Boston Children's Hospital, Boston, MA, United States

Motion monitoring has shown helpful in MRI, particularly in long acquisitions such as 2D echo-planar imaging for fMRI. The most widely-used motion monitoring for fMRI relies on volume-to-volume registration (VVR). However, motion happens at the slice level, and VVR is insufficiently sensitive to intra-volume motion. In this work, we present the first slice-by-slice self-navigated motion monitoring system for MRI via a real-time slice-to-volume registration (SVR) algorithm. Extensive experiments demonstrated that our approach provides accurate motion measurements, and allows adaptive acquisition that ensures sufficient amount of data, while not acquiring data in excess, leading to improved data quality and reduced costs.

0090



Fast scan with a wave-CAIPI MPRAGE sequence to minimize motion artifacts in pediatric T1-weighted imaging

Emi Niisato<sup>1</sup>, Yung-Chieh Chen<sup>2</sup>, Shojen Cheng<sup>2</sup>, Yi-Hsin Wang<sup>2</sup>, Wei Liu<sup>3</sup>, Daniel Nicolas Splitthoff<sup>4</sup>, and Cheng-Yu Chen<sup>2</sup>

<sup>1</sup>Siemens Healthcare Limited, Taipei, Taiwan, <sup>2</sup>Department of Medical Imaging, Taipei Medical University Hospital, Taipei, Taiwan, <sup>3</sup>Siemens Shenzhen Magnetic Resonance Ltd, Shenzhen, China, <sup>4</sup>Siemens Healthineers AG, Erlangen, Germany

Pediatric magnetic resonance imaging (MRI) needs extra care since patients cannot remain still for long in the MRI bore. Therefore, scans should be performed as quickly as possible. Our study investigated the role of fast T1 3D Magnetization Prepared Rapid Acquisition Gradient Echo (MPRAGE) scans using wave-controlled aliasing with parallel imaging (wave-CAIPI) in pediatric patients. We presented that scan times were shortened significantly, and images had fewer motion artifacts compared with conventional MPRAGE images. We further evaluated contrast-to-noise ratios (CNRs) in five cerebellar areas and saw no significant differences between the conventional and wave-CAIPI MPRAGE images.

---

---

## Oral

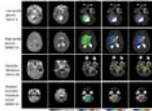
### Pediatric Innovations - Pediatric High-End Potpourri

Monday Parallel 3 Live Q&A

Monday 13:45 - 14:30 UTC

Moderators: Timothy Cain & Dan Wu

0091



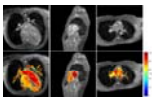
#### Time-dependent Diffusion MRI of Pediatric Brain tumor at 3T

Hongxi Zhang<sup>1</sup>, Hua Li<sup>2</sup>, Zhipeng Shen<sup>1</sup>, Yi Zhang<sup>3</sup>, and Dan Wu<sup>3</sup>

<sup>1</sup>Children's Hospital, Zhejiang University School of Medicine, Hangzhou, China, <sup>2</sup>Nemours Al duPont Hospital for Children, Wilmington, DE, United States, <sup>3</sup>Key Laboratory for Biomedical Engineering of Ministry of Education, Department of Biomedical Engineering, College of Biomedical Engineering & Instrument Science, Zhejiang University, Hangzhou, China

Diffusion-time dependent diffusion MRI has shown potential in probing tumor microstructure. This study investigated the feasibility of time-dependent dMRI to map brain tumor microstructure in a pediatric population at 3T. Oscillating and pulsed gradient dMRI was performed to access a series of diffusion times and b-values, and the data were fitted with the IMPULSED model to estimate cell diameter, intracellular fraction, and diffusivity metrics. In a pilot study of 17 pediatric brain tumor patients, all high-grade tumors showed higher intracellular fraction and cellularity than the low-grade ones, while the cell diameter showed differentiation among different types of high-grade tumors.

0092



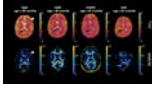
#### Optimized MR blood oximetry using multiple T2 maps: validation with MR-guided catheterization in congenital heart disease

Joshua S. Greer<sup>1,2</sup>, Daniel A. Castellanos<sup>1</sup>, Yousef Arar<sup>1</sup>, Surendranath R. Veeram Reddy<sup>1</sup>, Yin Xi<sup>2</sup>, Gerald F. Greil<sup>1,2,3</sup>, Ananth J. Madhuranthakam<sup>2,3</sup>, and Tarique Hussain<sup>1,2</sup>

<sup>1</sup>Pediatrics, UT Southwestern Medical Center, Dallas, TX, United States, <sup>2</sup>Radiology, UT Southwestern Medical Center, Dallas, TX, United States, <sup>3</sup>Advanced Imaging Research Center, UT Southwestern Medical Center, Dallas, TX, United States

In this study, a recently proposed MRI blood oximetry technique was optimized to improve the accuracy of oxygen saturation measurements. Simulations of the Luz-Meiboom model were performed to optimize the T<sub>2</sub>-prep refocusing intervals and to guide the selection of the blood pool used for nuisance parameter estimation. Blood oxygen saturation measurements were validated against MR-guided cardiac catheterization under the same anesthetic conditions in patients with congenital heart disease, with the proposed O<sub>2</sub> mapping technique demonstrating improved agreement with blood gas analysis. The proposed improvements may allow for future examination of blood pool oxygenation without the need for invasive cardiac catheterization.

0093



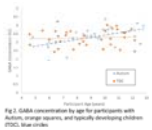
### Myelin water fraction (MWF) mapping using Magnetic Resonance Fingerprinting (MRF) in a cohort of patients from a child neurology unit

Jan W Kurzawski<sup>1,2</sup>, Matteo Cencini<sup>1,3</sup>, Laura Biagi<sup>1,4</sup>, Graziella Donatelli<sup>1,5</sup>, Rosa Pasquariello<sup>4</sup>, Roberta Battini<sup>3,4</sup>, Claudia Dosi<sup>3,4</sup>, Chiara Ticci<sup>3,4</sup>, Alessandra Retico<sup>2</sup>, Guido Buonincontri<sup>1,4</sup>, and Michela Tosetti<sup>1,4</sup>

<sup>1</sup>Imago7, Pisa, Italy, <sup>2</sup>INFN, Pisa, Italy, <sup>3</sup>University of Pisa, Pisa, Italy, <sup>4</sup>IRCCS Stella Maris, Pisa, Italy, <sup>5</sup>Neuroradiology, Azienda Ospedaliero-Universitaria Pisana, Pisa, Italy

New advancements in magnetic resonance fingerprinting (MRF) allow more accurate quantification of tissue characteristics and its components using multi-component dictionaries. Recently, a multi-component method for mapping Myelin-Water fraction (MWF) was suggested and validated in healthy children. Here, we studied a cohort with different disorders including hypo- or de- myelinization, Creatine Deficiency Syndrome and brain malformations. We reconstruct MWF maps using tailored dictionaries and estimate fractional myelin values in the splenium of corpus callosum. We observed that myelinization plateaus at around 30 months from birth, while in patients with white matter disorders the process is distorted.

0094



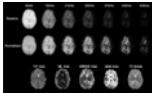
### Parietal GABA in children with Autism Spectrum Disorder and typically developing peers: distinct age-related changes

Marilena M DeMayo<sup>1</sup>, Ashley D Harris<sup>2,3,4</sup>, Ian B Hickie<sup>5</sup>, and Adam J Guastella<sup>1</sup>

<sup>1</sup>Brain and Mind Centre, Children's Hospital Westmead Clinical School, University of Sydney, Camperdown, Australia, <sup>2</sup>Department of Radiology, University of Calgary, Calgary, AB, Canada, <sup>3</sup>Hotchkiss Brain Institute, Calgary, AB, Canada, <sup>4</sup>Alberta Children's Hospital Research Institute, Calgary, AB, Canada, <sup>5</sup>Brain and Mind Centre, University of Sydney, Sydney, Australia

GABA, the mature brain's primary inhibitory neurotransmitter, has been proposed to contribute to the development of Autism Spectrum Disorder (ASD) and the maintenance of ASD symptoms. Investigations have found reductions in GABA in children and adolescents with ASD. In the current study, GABA levels were measured using GABA-edited MEGA-PRESS in the left parietal lobe. The study compared 24 children with ASD and 35 typically developing (TD), aged 4-12 years. Increasing GABA concentration with age was found in the ASD participants but not in the TD cohort, suggesting a distinct pattern of GABA development in ASD within the parietal lobe.

0095



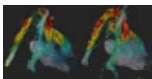
### Fetal and neonatal whole brain T2\* mapping at 3T

Serge Vasylechko<sup>1</sup>, Emer Hughes<sup>2</sup>, Joanna Allsop<sup>2</sup>, Matthew Fox<sup>2</sup>, Daniel Rueckert<sup>1</sup>, and Jo Hajnal<sup>2</sup>

<sup>1</sup>Biomedical Image Analysis Group, Department of Computing, Imperial College London, London, United Kingdom, <sup>2</sup>Centre for the Developing Brain, School of Imaging Sciences and Biomedical Engineering, King's College London, London, United Kingdom

Quantitative T2\* mapping in the developing brain is challenging due to inherent motion of fetal and neonatal subjects. This study uses a motion robust framework for acquisition, reconstruction and segmentation of whole brain T2\* maps. This is achieved by single-shot multi-echo GRE EPI acquisition, multi-level slice-to-volume registration and gestational-age specific brain atlas segmentation. T2\* values are reported for fetal and neonatal subjects at 3T. Findings indicate large variability in T2\* within each subject group, non-linear change in T2\* between fetal and preterm neonatal period, and significantly higher mean T2\* constants than previously reported in adult subjects.

0096



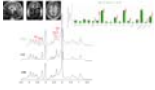
### Fetal whole-heart 4D blood flow MRI with self-calibrated k-t SENSE

Thomas A Roberts<sup>1</sup>, Joshua FP van Amerom<sup>1,2</sup>, Lucilio Cordero-Grande<sup>1</sup>, Alena Uus<sup>1</sup>, Anthony N Price<sup>1</sup>, David FA Lloyd<sup>1,3</sup>, Laurence H Jackson<sup>1</sup>, Milou PM van Poppel<sup>1</sup>, Kuberan Pushparajah<sup>3</sup>, Mary A Rutherford<sup>1</sup>, Reza Rezavi<sup>1,3</sup>, Maria Deprez<sup>1</sup>, and Joseph V Hajnal<sup>1</sup>

<sup>1</sup>*School of Biomedical Engineering & Imaging Sciences, King's College London, London, United Kingdom,* <sup>2</sup>*Division of Pediatric Cardiology, The Hospital for Sick Children, Toronto, ON, Canada,* <sup>3</sup>*Department of Congenital Heart Disease, Evelina Children's Hospital, London, United Kingdom*

Measurement of blood flow in the fetal heart and the great vessels is challenging due to fetal motion and its small size. Previously, we demonstrated use of k-t SENSE real-time 2D imaging combined with slice-to-volume registration to reconstruct 4D velocity cine volumes. This required 50% of the examination to be spent acquiring training data. In this work we combine sliding window reconstruction of the under-sampled target data with some prior knowledge to dispense with training data altogether. We reconstruct 4D blood flow volumes in 5 fetal hearts using both methods and show that they are broadly equivalent.

0097



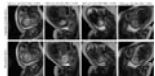
Neurometabolism in children with chronic liver disease or portosystemic shunting: a 1H-MRS/MRI study at 7T

Cristina Cudalbu<sup>1</sup>, Lijing Xin<sup>1</sup>, Bénédicte Maréchal<sup>2,3,4</sup>, Tobias Kober<sup>2,3,4</sup>, Sarah Lachat<sup>5</sup>, Nathalie Valenza<sup>6</sup>, Florence Zangas-Gehri<sup>6</sup>, and Valérie McLin<sup>5</sup>

<sup>1</sup>*Centre d'Imagerie Biomedicale, Ecole Polytechnique Federale de Lausanne, Lausanne, Switzerland,* <sup>2</sup>*Advanced Clinical Imaging Technology, Siemens Healthcare AG, Lausanne, Switzerland,* <sup>3</sup>*Department of Radiology, Lausanne University Hospital and University of Lausanne, Lausanne, Switzerland,* <sup>4</sup>*LTS5, École Polytechnique Fédérale de Lausanne, Lausanne, Switzerland,* <sup>5</sup>*Swiss Pediatric Liver Center, Department of Pediatrics, Gynecology and Obstetrics, University Hospitals Geneva, and University of Geneva Medical School, Geneva, Switzerland,* <sup>6</sup>*Pediatric Neurology Unit, Department of Pediatrics, Gynecology and Obstetrics, University Hospitals Geneva, and University of Geneva Medical School, Geneva, Switzerland*

Children with chronic liver disease (CLD) or congenital portosystemic shunts (CPSS) show neurocognitive deficits that are not entirely reversible following liver transplantation or shunt closure. We measured for the first time the neurometabolic profile, brain volumetry and T1 relaxation times of children with CLD and CPSS at 7T. In patients with compensated CLD, there were no significant neurometabolic alterations as assessed by 1H-MRS, while small changes in amygdala and hippocampus volumes were measured. In CPSS, however, neurometabolic changes were pronounced, together with a marked decrease in all measured brain volumes, and likely related to measurably impaired neurocognitive functioning.

0098



Automatic detection and reacquisition of motion degraded images in fetal HASTE imaging at 3T

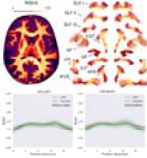
Borjan Gagoski<sup>1,2</sup>, Junshen Xu<sup>3</sup>, Paul Wighton<sup>4</sup>, Dylan Tisdall<sup>5</sup>, Robert Frost<sup>2,4</sup>, Sayeri Lala<sup>6</sup>, Wei-Ching Lo<sup>7</sup>, Polina Golland<sup>8,9</sup>, Andre van der Kouwe<sup>2,4</sup>, Elfar Adalsteinsson<sup>8,10</sup>, and P. Ellen Grant<sup>1,2</sup>

<sup>1</sup>*Fetal Neonatal Neuroimaging and Developmental Science Center, Boston Children's Hospital, Boston, MA, United States,* <sup>2</sup>*Department of Radiology, Harvard Medical School, Boston, MA, United States,* <sup>3</sup>*(co-first author) Electrical Engineering and Computer Science, Massachusetts Institute of Technology, Cambridge, MA, United States,* <sup>4</sup>*Athinoula A. Martinos Center for Biomedical Imaging, Massachusetts General Hospital, Charlestown, MA, United States,* <sup>5</sup>*Department of Radiology, Perelman School of Medicine, University of Pennsylvania, Philadelphia, PA, United States,* <sup>6</sup>*Department of Electrical Engineering, Princeton University, Princeton, NJ, United States,* <sup>7</sup>*Siemens Medical Solutions USA, Inc, Charlestown, MA, United States,* <sup>8</sup>*Electrical Engineering and Computer Science, Massachusetts Institute of Technology, Cambridge, MA, United States,* <sup>9</sup>*Computer Science and Artificial Intelligence Laboratory (CSAIL), Massachusetts Institute of Technology, Cambridge, MA, United States,* <sup>10</sup>*Institute for Medical Engineering and Science, Massachusetts Institute of Technology, Cambridge, MA, United States*



Fetal brain MRI suffers from unpredictable and unconstrained fetal motion that not only causes severe image artifacts even with single-shot FSE readouts, but also results in slice-to-slice variations of the imaging plane and long scanning sessions, as the MR technologist “chases” the fetal head in an attempt to acquire artifact-free orthogonal images. In this work, we have implemented a closed-loop pipeline that automatically detects and reacquires HASTE images that were degraded by fetal motion, without any interaction from the MRI technologist. The presented methods demonstrate the basic infrastructure needed for successful prospective automated fetal brain motion correction.

0099



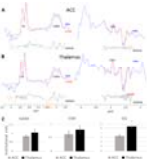
### Highlighting tract-specific microstructural abnormalities in single subjects using autoencoders

Maxime Chamberland<sup>1</sup>, Sila Genc<sup>1</sup>, Erika P Raven<sup>1</sup>, Chantal M.W. Tax<sup>1</sup>, Greg D Parker<sup>1</sup>, Adam Cunningham<sup>2</sup>, Joanne Doherty<sup>1,2</sup>, Marianne van den Bree<sup>2</sup>, and Derek K Jones<sup>1</sup>

<sup>1</sup>CUBRIC, Cardiff University, Cardiff, United Kingdom, <sup>2</sup>MRC Centre for Neuropsychiatric Genetics and Genomics, Cardiff University, Cardiff, United Kingdom

Most clinical diffusion MRI studies rely on the statistical comparison of a group of patients against a group of healthy controls to make inference about disease. This stymies the potential power of microstructural MRI in the clinic, i.e., to identify microstructural abnormalities in a single patient. We present a framework to address this problem on a case-by-case basis, extending the reach of microstructural imaging to rare cases, where group comparisons are otherwise impossible. Our framework operates on the manifold of white matter pathways and uses autoencoders to learn normative microstructural features, and discriminate patients from controls in a paediatric population.

0100



### Characterising thalamic and anterior cingulate GABA, Glx and GSH in the neonatal brain with HERMES

Maria Yanez Lopez<sup>1</sup>, Anthony N Price<sup>1</sup>, Emer Hughes<sup>1</sup>, Nicolaas AJ Puts<sup>2,3</sup>, Richard AE Edden<sup>2,3</sup>, Grainne McAlonan<sup>4</sup>, Tomoki Arichi<sup>1,5</sup>, and Enrico De Vita<sup>6</sup>

<sup>1</sup>Centre for the Developing Brain, School of Biomedical Engineering and Imaging Sciences, King's College London, London, United Kingdom, <sup>2</sup>Russell H. Morgan Department of Radiology and Radiological Science, Johns Hopkins School of Medicine, Baltimore, MD, United States, <sup>3</sup>F.M. Kirby Research Center for Functional Brain Imaging, Kennedy Krieger Institute, Baltimore, MD, United States, <sup>4</sup>Department of Forensic and Neurodevelopmental Sciences, Institute of Psychiatry, Psychology & Neuroscience, King's College London, London, United Kingdom, <sup>5</sup>Department of Bioengineering, South Kensington Campus, Imperial College London, London, United Kingdom, <sup>6</sup>Biomedical Engineering Department, School of Biomedical Engineering and Imaging Sciences, King's College London, London, United Kingdom

We measured GABA, Glx and GSH levels in a population of healthy neonates, using HERMES at 3T. We show that HERMES can be used to measure significant regional differences (in this case between the thalamus and anterior cingulate cortex). Further application of this method to study how these levels and balance are altered by early-life brain injury or genetic risk can provide important new knowledge about the pathophysiology underlying neurodevelopmental disorders.

## Oral

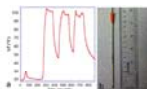
### Interventional - Technology for MRI-Guided Therapy

Monday Parallel 4 Live Q&A

Monday 13:45 - 14:30 UTC

Moderators: Jan Fritz & Henrik Odéen

0101



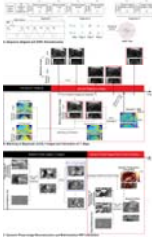
### Investigation of RF heating risk during MRI-guided cryoablation at 1.5T

Aiming Lu<sup>1</sup>, Christopher P Favazza<sup>1</sup>, David A Woodrum<sup>1</sup>, Joel P Felmlee<sup>1</sup>, Jacinta Browne<sup>1</sup>, Brian T Welch<sup>1</sup>, and Krzysztof R Gorny<sup>1</sup>

<sup>1</sup>Radiology, Mayo Clinic, Rochester, MN, United States

Cryoablation with MRI guidance is desirable as a feasible treatment for localized tumors. There is a MRI-conditional cryoablation system and, to the best of our knowledge, no previous report of RF heating/burn incidence. However, since the cryoneedles are metallic and the gas lines have metallic components, potential risks of RF heating/burn exist. In fact, an incidence of skin burn recently occurred in our institution during a MRI-guided liver treatment case. In this work, we demonstrated that RF heating could be significant during MRI-guided cryoablation and showed that several strategies could be potentially used to mitigate the risk.

0102



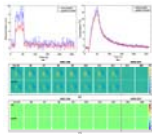
### Dynamic PRF and T<sub>1</sub>-based 3D Thermometry in the Liver using a Variable Flip Angle Stack-of-Radial Technique

Le Zhang<sup>1</sup>, Tess Armstrong<sup>1,2</sup>, and Holden H. Wu<sup>1,2,3</sup>

<sup>1</sup>Radiological Sciences, University of California, Los Angeles, Los Angeles, CA, United States, <sup>2</sup>Physics and Biology in Medicine, University of California, Los Angeles, Los Angeles, CA, United States, <sup>3</sup>Bioengineering, University of California, Los Angeles, Los Angeles, CA, United States

MR thermometry in the liver is challenged by mismatch between baseline and dynamic images caused by motion, leading to temperature errors. To address motion, previous methods had to compromise spatial coverage to increase temporal resolution. We propose a variable-flip-angle (VFA) 3D stack-of-radial technique for combined proton resonance frequency shift (PRF) and T<sub>1</sub>-based MR thermometry with volumetric coverage and high spatiotemporal resolution. Accurate VFA T<sub>1</sub> calculation is achieved by synthesizing B<sub>1+</sub> maps that match the liver position in dynamic images. A multi-baseline approach is used for accurate dynamic PRF measurements. Results from non-heating scans demonstrate reliable liver T<sub>1</sub> and PRF measurements.

0103



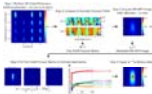
### Simultaneous MR acoustic radiation force imaging and MR thermometry: comparison of coherent echo-shifted and RF spoiled gradient echo sequence

Yangzi Qiao<sup>1</sup>, Chao Zou<sup>1</sup>, Chuanli Cheng<sup>1</sup>, Changjun Tie<sup>1</sup>, Xin Liu<sup>1</sup>, and Hairong Zheng<sup>1</sup>

<sup>1</sup>Shenzhen Institutes of Advanced Technology, Chinese Academy of Sciences, Shenzhen, China

Simultaneous MR acoustic radiation force imaging and MR thermometry (STARFI) based on coherent echo-shifted sequence (cES) was proposed and comprehensively compared to RF spoiled gradient echo (spGRE). The calculated displacement of cES STARFI was always larger than the value of spGRE STARFI through both the simulation and experiments, while the accuracy of the temperature monitoring of cES was maintained. The temperature and displacement map acquired during HIFU heating were in good accordance with each other. The cES STARFI can be an alternative for comprehensively monitoring of HIFU treatment with increased displacement sensitivity and time efficiency compared to spGRE STARFI.

0104



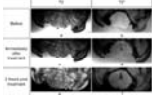
### Rapid autofocusing of MR-guided focused ultrasound acoustic pressure fields using MR-ARFI with spatially coded emissions

Sumeeth Jonathan<sup>1,2</sup>, M Anthony Phipps<sup>2</sup>, Charles F Caskey<sup>2</sup>, and William A Grissom<sup>2</sup>

<sup>1</sup>Biomedical Engineering, Vanderbilt University, Nashville, TN, United States, <sup>2</sup>Vanderbilt University Institute of Imaging Science, Vanderbilt University Medical Center, Nashville, TN, United States

Magnetic resonance-guided focused ultrasound (MRgFUS) has many potential neurological applications, but skull-induced aberrations of the acoustic pressure field limit its specificity and safety. MR-acoustic radiation force imaging (MR-ARFI)-based methods have been proposed to refocus the pressure field *in situ*. However, they take too long for practical *in vivo* use. We propose a multi-voxel MR-ARFI-based autofocusing method for rapid aberration correction of MRgFUS acoustic pressure fields. We compare our proposed method to the canonical single-voxel MR-ARFI-based refocusing method and demonstrate that as few as two MR-ARFI acquisitions can be used to refocus a programmatically aberrated pressure field.

0105



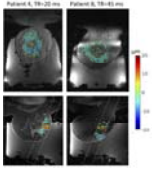
### MRI assessment and monitoring of cavitation-based ultrasound therapy (histotripsy) for transcranial brain treatment in vivo

Dinank Gupta<sup>1</sup>, Ning Lu<sup>1</sup>, Jonathan Sukovich<sup>1</sup>, Krisanne Litnas<sup>2</sup>, Aditya Pandey<sup>3</sup>, Badih Junior Daou<sup>3</sup>, Timothy Hall<sup>1</sup>, Zhen Xu<sup>1</sup>, Scott Peltier<sup>2</sup>, and Douglas Noll<sup>1</sup>

<sup>1</sup>Biomedical Engineering, University of Michigan, Ann Arbor, MI, United States, <sup>2</sup>Functional MRI Laboratory, University of Michigan, Ann Arbor, MI, United States, <sup>3</sup>Department of Neurosurgery, University of Michigan, Ann Arbor, MI, United States

Transcranial MR guided cavitation-based Focused Ultrasound (FUS) treatment (histotripsy) is performed in vivo for the first time on a pig brain. Transcranial histotripsy is delivered by an MRI compatible FUS transducer array inside a 3T MRI scanner. Real-time MRI monitoring with 2 second temporal resolution is carried with an intra-voxel incoherent motion (IVIM) pulse sequence synchronized with the FUS array. IVIM images show the histotripsy ablation effect at the intended treatment location in real-time, and the ablation zone was confirmed by post-treatment images. This is the first study to show successful in vivo transcranial histotripsy guided by MRI.

0106



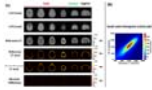
### Three-dimensional magnetic resonance acoustic radiation force imaging in the breast

Allison Payne<sup>1</sup>, Lorne Hofstetter<sup>2</sup>, Henrik Odéen<sup>1</sup>, Erik Dumont<sup>3</sup>, Dennis L Parker<sup>1</sup>, and Jean Palussiere<sup>4</sup>

<sup>1</sup>Radiology and Imaging Sciences, University of Utah, Salt Lake City, UT, United States, <sup>2</sup>Biomedical Engineering, University of Utah, Salt Lake City, UT, United States, <sup>3</sup>Image Guided Therapy, Pessac, France, <sup>4</sup>Institut Bergonie, Bordeaux, France

3D MR acoustic radiation force imaging (MR-ARFI) is a useful treatment planning and monitoring tool for magnetic resonance guided focused ultrasound (MRgFUS) treatments in the breast. MR-ARFI displacement is easily visualized in fat, fibroglandular and tumor tissues, allowing for accurate localization of the ultrasound beam and quantitative tissue assessment. The potential formation of standing shear waves in the breast requires careful optimization of the pulse sequence to ensure clear visualization of the radiation force displacement point. This effect is shown in both human breast and phantom data.

0107



### Deep learning for improved workflow in MRgFUS treatment planning

Pan Su<sup>1,2</sup>, Sijia Guo<sup>1,3</sup>, Florian Maier<sup>4</sup>, Steven Roys<sup>1,3</sup>, Himanshu Bhat<sup>2</sup>, Elias R. Melhem<sup>1</sup>, Dheeraj Gandhi<sup>1</sup>, Rao P. Gullapalli<sup>1,3</sup>, and Jiachen Zhuo<sup>1,3</sup>

<sup>1</sup>Department of Diagnostic Radiology and Nuclear Medicine, University of Maryland School of Medicine, Baltimore, MD, United States, <sup>2</sup>Siemens Medical Solutions USA Inc, Malvern, PA, United States, <sup>3</sup>Center for Metabolic Imaging and Therapeutics (CMIT), University of Maryland Medical Center, Baltimore, MD, United States, <sup>4</sup>Siemens Healthcare GmbH, Erlangen, Germany

Transcranial MRI-guided focused ultrasound (tcMRgFUS) is a promising technique to treat multiple diseases. Here we examined the feasibility of leveraging deep-learning to convert MRI dual echo UTE images directly to synthesized CT skull images. We demonstrated that the derived model is capable of not only segmenting the UTE images to generate synthetic CT skull masks that are highly comparable to true CT skull masks, but is also able to reliably predict the CT skull intensities in Hounsfield units. Furthermore, we demonstrated that synthetic CT skull can be reliably used for skull-density-ratio (SDR) determination and predicting target temperature rise in tcMRgFUS.

0108



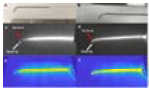
### Real-time estimation of 2D deformation vector fields from highly undersampled, dynamic k-space for MRI-guided radiotherapy using deep learning

Maarten L Terpstra<sup>1,2</sup>, Federico d'Agata<sup>1,2,3</sup>, Bjorn Stemkens<sup>1,2</sup>, Jan JW Lagendijk<sup>1</sup>, Cornelis AT van den Berg<sup>1,2</sup>, and Rob HN Tijssen<sup>1,2</sup>

<sup>1</sup>Department of Radiotherapy, Division of Imaging & Oncology, University Medical Center Utrecht, Utrecht, Netherlands, <sup>2</sup>Computational Imaging Group for MR diagnostics & therapy, Center for Image Sciences, University Medical Center Utrecht, Utrecht, Netherlands, <sup>3</sup>Department of Neurosciences, University of Turin, Turin, Italy

MRI-guided radiotherapy (MRgRT) enables new ways to improve dose delivery to moving tumors and the organs-at-risk (e.g. in abdomen) by steering the radiation beam based on real-time MRI. While state-of-the-art techniques (e.g. compressed sensing) can provide the required acquisition speed, the corresponding reconstruction time is too long for real-time processing. In this work, we investigate the use of multiple deep neural networks for image reconstruction and subsequent motion estimation. We show that a single motion estimation network can estimate high-quality 2D deformation vector fields from aliased images, even for high undersampling factors up to  $R=25$ .

0109



A novel active guidewire design with a curved tip geometry for interventional MRI applications under 0.55T.

Korel Dursun Yildirim<sup>1,2</sup>, Christopher Bruce<sup>1</sup>, Rajiv Ramasawmy<sup>1</sup>, Kendall O'Brien<sup>1</sup>, Adrienne Campbell-Washburn<sup>1</sup>, Daniel Herzka<sup>1</sup>, Robert J. Lederman<sup>1</sup>, and Ozgur Kocaturk<sup>1,2,3</sup>

<sup>1</sup>Cardiovascular Branch, Division of Intramural Research, National Heart Lung and Blood Institute, National Institutes of Health, Bethesda, MD, United States, <sup>2</sup>Institute of Biomedical Engineering, Bogazici University, Istanbul, Turkey, <sup>3</sup>Transmural Systems, Andover, MA, United States

A clinical-grade active MRI 0.035" guidewire design with a curved distal tip geometry and continuous shaft signal ensuring the mechanical and electrical safety, was introduced. Proposed design was tested in-vitro and in-vivo for MRI visibility and mechanical performance, and in-vitro for RF induced heating.

0110



Dynamic control of RF currents in conductive guidewires with an auxiliary PTx system: First in vivo experience in sheep

Felipe Godinez<sup>1</sup>, Raphael Tomi-Tricot<sup>2</sup>, Marylene Delcey<sup>3</sup>, Gunthard Lykowsky<sup>4</sup>, Steven E Williams<sup>1</sup>, Bruno Quesson<sup>3</sup>, Joseph V Hajnal<sup>1</sup>, and Shaihan J Malik<sup>1</sup>

<sup>1</sup>Biomedical Engineering Department, School of Biomedical Engineering and Imaging Sciences, King's College London, London, United Kingdom, <sup>2</sup>Siemens Healthcare Limited, London, United Kingdom, <sup>3</sup>Centre de recherche Cardio-Thoracique de Bordeaux, Bordeaux, France, <sup>4</sup>RAPID Biomedical GmbH, Rimpfing, Germany

This paper presents first in vivo results of a parallel transmit (PTx) system adept at regulating radiofrequency induced guidewire heating, during MRI guided interventions in sheep. The PTx system, which is an add-on to an unmodified conventional 1.5T scanner, regulates heating by operating in modes that couple/decouple the guidewire from the radiofrequency transmit array. With an inserted guidewire decoupling modes allow operation with unrestricted B1+ to safely visualize anatomy, while the coupling mode operated at low radiofrequency power provides safe visualization of the guidewire itself. Temperature measurements at the guidewire tip and in vivo images are shown.

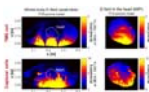
## Oral - Power Pitch

### Interventional - MRI Safety & Intervention

Monday Parallel 4 Live Q&A

Monday 13:45 - 14:30 UTC

Moderators: Laleh Golestani Rad & Joseph Rispoli



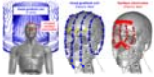
Feasibility of using transcranial magnetic stimulation devices to study magnetically induced cardiac stimulation in pigs

Valerie Klein<sup>1,2</sup>, Mathias Davids<sup>1,2,3</sup>, Christopher Nguyen<sup>2,3,4</sup>, Lothar R. Schad<sup>1</sup>, Lawrence L. Wald<sup>2,3,5</sup>, and Bastien Guérin<sup>2,3</sup>



<sup>1</sup>Computer Assisted Clinical Medicine, Medical Faculty Mannheim, Heidelberg University, Mannheim, Germany, <sup>2</sup>A. A. Martinos Center for Biomedical Imaging, Department of Radiology, Massachusetts General Hospital, Charlestown, MA, United States, <sup>3</sup>Harvard Medical School, Boston, MA, United States, <sup>4</sup>Cardiovascular Research Center, Cardiology Division, Massachusetts General Hospital, Charlestown, MA, United States, <sup>5</sup>Harvard-MIT Division of Health Sciences and Technology, Cambridge, MA, United States

This work evaluates the potential of porcine cardiac stimulation (CS) studies using transcranial magnetic stimulation (TMS) devices with the aim of determining appropriate safety limits for MRI gradients. We investigated the electric fields induced in electromagnetic porcine models and found that typical TMS coils may not generate fields strong enough for CS. Larger coplanar coils, however, may be suitable for CS studies. In addition to these investigations, we created a porcine model from MRI Dixon and cardiac CINE measurements. The use of such custom models of the animal under experimentation will facilitate the comparison between measured and simulated CS thresholds.

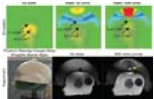


### Mitigating Peripheral Nerve Stimulations for MRI Gradient Coils using Surface Electrodes

Mathias Davids<sup>1,2,3</sup>, Bastien Guerin<sup>1,2</sup>, and Lawrence L Wald<sup>1,2,4</sup>

<sup>1</sup>A.A. Martinos Center for Biomedical Imaging, Massachusetts General Hospital, Dept. of Radiology, Charlestown, MA, United States, <sup>2</sup>Harvard Medical School, Boston, MA, United States, <sup>3</sup>Computer Assisted Clinical Medicine, Medical Faculty Mannheim, Heidelberg University, Mannheim, Germany, <sup>4</sup>Harvard-MIT Health Sciences and Technology, Cambridge, MA, United States

Peripheral Nerve Stimulation is becoming an important limitation for state-of-the-art head gradients, which despite higher PNS thresholds, are also operated at higher slew-rate and have limited degrees-of-freedom for FOV design mitigation strategies. We introduce a new mitigation approach, which uses contact surface electrodes driven simultaneously with the gradient coils to cancel the E-field induced by switching of the coil, thus increasing its PNS thresholds. We simulated the capability of four sets of electrodes placed in different areas of the face and found an up to 56% PNS reduction for the analyzed X-axis of a commercial head gradient coil.

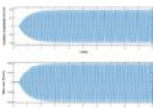


### "Propeller Beanie" Passive Antennas to Alleviate Dark Bands in Transcranial MR-Guided Focused Ultrasound

Xinqiang Yan<sup>1,2</sup>, Steven Allen<sup>3</sup>, and William A. Grissom<sup>1,2,4</sup>

<sup>1</sup>Department of Radiology, Vanderbilt University Medical Center, Nashville, TN, United States, <sup>2</sup>Institute of Imaging Science, Vanderbilt University, Nashville, TN, United States, <sup>3</sup>Department of Biomedical Engineering, University of Virginia, Charlottesville, VA, United States, <sup>4</sup>Department of Biomedical Engineering, Vanderbilt University, Nashville, TN, United States

Transcranial MR-guided focused ultrasound (tcMRgFUS) neurosurgery is a non-invasive treatment for essential tremor and many emerging applications. In the FDA-approved Insightec tcMRgFUS system, however, RF reflections inside the transducer create a curved dark band in brain images that runs through midbrain locations that are targeted for essential tremor, and signal is reduced at least 25% everywhere in the brain, which limits the set of scans that can be performed during treatment. This work proposes a simpler solution that alleviates the problem, which is to place a passive reflecting antenna or resonator above the patient's head, with a "propeller-beanie" crossed-wire shape.



No substantial peripheral nerve stimulation beyond 5000T/m/s when driving a head gradient coil at 20kHz  
Jolanda M Spijkerman<sup>1</sup>, Edwin Versteeg<sup>2</sup>, Dennis WJ Klomp<sup>2</sup>, David G Norris<sup>1,3</sup>, and Jeroen CW Siero<sup>2,4</sup>

<sup>1</sup>Donders Institute for Brain, Cognition and Behavior, Radboud University Nijmegen, Nijmegen, Netherlands, <sup>2</sup>Department of Radiology, University Medical Center Utrecht, Utrecht, Netherlands, <sup>3</sup>Erwin L. Hahn Institute for Magnetic Resonance Imaging, University of Duisburg-Essen, Essen, Germany, <sup>4</sup>Spinoza Center for Neuroimaging Amsterdam, Amsterdam, Netherlands

In this work the PNS threshold of a recently introduced gradient head coil operating at 20kHz was determined in four healthy subjects. The gradient slew rate was increased to 5000T/m/s by varying the amplitude between 7.5–40mT/m, the maximal gradient strength currently available. One subject reported no PNS, two subjects reported mild PNS at the highest gradient amplitudes of 36.25, 37.5 and 40mT/m, and one subject reported mild sensations during 31.25mT/m, but was uncertain whether this was PNS. In conclusion, application of the coil at 20kHz is currently restricted by the available gradient strength, rather than PNS.

0115



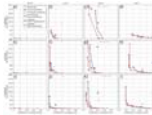
### Prediction of subject-specific local SAR in patients with deep brain stimulation leads using artificial neural networks

Jasmine Vu<sup>1,2</sup>, Bach Nguyen<sup>2</sup>, Justin Baraboo<sup>1,2</sup>, Joshua Rosenow<sup>3</sup>, Julie Pilitsis<sup>4</sup>, and Laleh Golestanirad<sup>1,2</sup>

<sup>1</sup>Biomedical Engineering, Northwestern University, Chicago, IL, United States, <sup>2</sup>Radiology, Northwestern University, Chicago, IL, United States, <sup>3</sup>Northwestern Medicine, Chicago, IL, United States, <sup>4</sup>Neurosurgery, Albany Medical Center, Albany, NY, United States

Patients with deep brain stimulation (DBS) implants can significantly benefit from MRI; however, their access is limited due to safety concerns associated with RF heating of implants. RF heating depends significantly on the trajectory of an implanted lead, but there is a lack of surgical guidelines about positioning the extracranial portion of the leads, resulting in substantial patient-to-patient variation in DBS lead trajectories. Thus, quick and reliable patient-specific assessment of RF heating is highly desirable. Here we present an artificial neural network (ANN) model that demonstrates great potential in predicting local SAR at the tips of the DBS leads.

0116



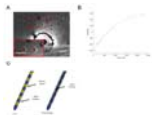
### On the benefit of pTx for implant safety - a multiparameter simulation study

Johannes Petzold<sup>1</sup>, Sebastian Schmitter<sup>1</sup>, Bernd Ittermann<sup>1</sup>, and Frank Seifert<sup>1</sup>

<sup>1</sup>Physikalisch-Technische Bundesanstalt (PTB), Braunschweig and Berlin, Germany

FDTD simulations were used to generate the electromagnetic fields of a human voxel model with a generic implant in a pTx coil.  $B_1^+$  homogeneity and SAR at the implant tip were systematically investigated for 4 field strength, 4 pTx channel counts, 3 implant positions and 6 excitation strategies. Simple and unsurprising conclusions can be drawn for 0.5 T (pTx is not necessary), 7 T (nothing goes without pTx), and on the channel count (the higher, the better). For the clinically most relevant field strength 1.5 T and 3 T, a much more complex pattern emerges.

0117



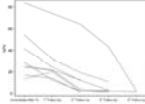
### A Pilot Clinical Study of Quantitative Silicone Oxygen Sensors in Cervical Cancer

Gregory James Ekchian<sup>1</sup>, Junichi Tokuda<sup>2</sup>, Jahanara Freedman<sup>1</sup>, Hannah Harens<sup>1</sup>, Robert Cormack<sup>3</sup>, Larissa Lee<sup>3</sup>, and Michael Cima<sup>1,4</sup>

<sup>1</sup>Koch Institute for Integrative Cancer Research, Massachusetts Institute of Technology, Cambridge, MA, United States, <sup>2</sup>Radiology, Brigham and Women's Hospital, Boston, MA, United States, <sup>3</sup>Radiation Oncology, Brigham and Women's Hospital, Boston, MA, United States, <sup>4</sup>Materials Science and Engineering, Massachusetts Institute of Technology, Cambridge, MA, United States

We report on the first-in-human evaluation of a class of silicone oxygen sensors capable of both high sensitivity and repeated and long-term monitoring of tumor oxygen levels. We are evaluating the use of this sensor in patients receiving high dose rate brachytherapy for cervical cancer. This sensor is a direct and quantitative measurement of tumor oxygen. Low oxygen regions of tumors are more resistant to many common forms of treatment. Understanding tumor oxygen levels can enable personalized radiation and chemotherapy treatments to overcome resistance and improve outcomes for patients.

0118



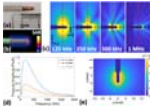
To assess and follow-up the mpMRI and prostate volumetric changes after whole prostate MR-guided transurethral prostate ultrasound ablation.

Afshin Azadikhah<sup>1</sup>, Holden Wu<sup>2</sup>, Melina Hosseiny<sup>2</sup>, and Steven S Raman<sup>2</sup>

<sup>1</sup>Radiology, University of California, Los Angeles, Los Angeles, CA, United States, <sup>2</sup>University of California, Los Angeles, Los Angeles, CA, United States

To evaluate the changes of 3 Tesla (3T) mpMRI and PSA parameters before and during multiple time points after whole gland prostate cancer (PCa) treatment using MRI-guided directional transurethral ultrasound ablation (TULSA). Patients were treated and followed-up for 1, 3, 6 and 12-month in retrospective, cohort, a trial study from October 2017 to February 2019. The mean ADC value, T2W, NPV, PSAD, and prostate volume were significantly decreased after 1 to 12-month follow-up with significant differences. MRI-guided TULSA uses a minimally-invasive transurethral approach, and this appears to be an effective method especially in patients with localized, organ-confined prostate cancer.

0119



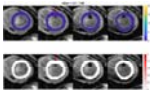
RF Power Deposition and Temperature Rise for Thermo-Acoustic Ultrasound Signal Generation from Lead Tips in MRI

Neerav Dixit<sup>1</sup>, John Pauly<sup>1</sup>, and Greig Scott<sup>1</sup>

<sup>1</sup>Electrical Engineering, Stanford University, Stanford, CA, United States

Using the pressure signals resulting from RF energy absorption, thermo-acoustic ultrasound (TAUS) enables detection of excessive local SAR at the lead tips of implanted devices, which causes RF-induced lead tip heating in MRI. Interleaving TAUS acquisitions with MR sequences may also allow for real-time lead tip temperature tracking during MRI. However, generating TAUS signals requires some RF energy deposition and heating at lead tips. Here, we analyze the amount of RF power at lead tips and the associated lead tip temperature rise needed to generate the TAUS signal.

0120



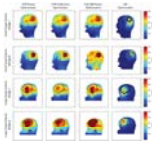
Active tracking based cardiac triggering of MR thermometry in an animal model

Ronald Mooiweer<sup>1</sup>, Rainer Schneider<sup>2</sup>, Radhouene Neji<sup>1,3</sup>, Rahul K Mukherjee<sup>1</sup>, Steven Williams<sup>1</sup>, Li Huang<sup>1</sup>, Valéry Ozenne<sup>4</sup>, Pierre Bour<sup>4</sup>, Jason Stroup<sup>5</sup>, Tom Lloyd<sup>5</sup>, Pierre Jaïs<sup>4</sup>, Bruno Quesson<sup>4</sup>, Mark O'Neill<sup>1</sup>, Tobias Schaeffter<sup>1,6</sup>, Reza Razavi<sup>1</sup>, and Sébastien Roujol<sup>1</sup>

<sup>1</sup>Biomedical Engineering, King's College London, London, United Kingdom, <sup>2</sup>Siemens Healthcare GmbH, Erlangen, Germany, <sup>3</sup>MR Research Collaborations, Siemens Healthcare Limited, Frimley, United Kingdom, <sup>4</sup>IHU-Liryc, Pessac, France, <sup>5</sup>Imricor Medical Systems, Burnsville, MN, United States, <sup>6</sup>Physikalisch-Technische Bundesanstalt, Berlin, Germany

MR thermometry can offer real-time temperature information during RF ablation in the heart. As ECG-triggering can be unreliable in these situations, cardiac triggering based on the position of the ablation catheter could provide an alternative. Active tracking was used to continuously measure the position of microcoils inside the catheter. Cardiac triggers were determined after respiratory motion filtering. Temperature stability over time was below 2.5 °C.

0121



### RF Power Deposition Optimization Algorithms for Thermal MR Targeting Human Brain Tumors

Eva Oberacker<sup>1</sup>, Andre Kuehne<sup>2</sup>, Cecilia Diesch<sup>1</sup>, Thomas Wilhelm Eigentler<sup>1</sup>, Jacek Nadobny<sup>3</sup>, Pirus Ghadjar<sup>3</sup>, Peter Wust<sup>3</sup>, and Thoralf Niendorf<sup>1,2,4</sup>

<sup>1</sup>Berlin Ultrahigh Field Facility (B.U.F.F.), Max Delbrück Center for Molecular Medicine in the Helmholtz Association, Berlin, Germany, <sup>2</sup>MRI.TOOLS GmbH, Berlin, Germany, <sup>3</sup>Clinic for Radiation Oncology, Charité Universitätsmedizin, Berlin, Germany, <sup>4</sup>Experimental and Clinical Research Center (ECRC), joint cooperation between the Charité Medical Faculty and the Max-Delbrück-Center for Molecular Medicine in the Helmholtz Association, Berlin, Germany

Ultrahigh field (UHF) MR employs higher radio frequencies (RF) than conventional MR and has unique potential to provide focal temperature manipulation and high resolution imaging (ThermalMR). The advantage of integrated therapy monitoring allows the consideration of thermal interventions in brain tumor treatments. Optimization algorithms used to confine the RF power deposition to the target volume (TV) are under constant revision. This work compares three in-house developed optimization algorithms with the focus on power delivery to the target volume as well as sparing of the healthy tissue with a more commonly available approach.

0122



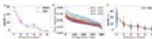
### MR-guided neuromodulation of visual networks in Rhesus Monkey at a 3T system

Xiaojing Long<sup>1</sup>, Yangzi Qiao<sup>1</sup>, Teng Ma<sup>1</sup>, Weibao Qiu<sup>1</sup>, Chao Zou<sup>1</sup>, Jo Lee<sup>1</sup>, Yang Liu<sup>1</sup>, Changjun Tie<sup>1</sup>, Ye Li<sup>1</sup>, Lijuan Zhang<sup>1</sup>, Qiang He<sup>2</sup>, Xin Liu<sup>1</sup>, and Hairong Zheng<sup>1</sup>

<sup>1</sup>Shenzhen Institutes of Advanced Technology, Chinese Academy of Sciences, Shenzhen, China, <sup>2</sup>Shanghai United Imaging Healthcare Co., Ltd., Shanghai, China

In this work, we applied BOLD fMRI in Rhesus monkey on a 3T MR system and investigated the functional effects induced by transcranial ultrasound stimulation (TUS) in both the target spot (the primary visual cortex) and the remote interconnected brain regions. We found that TUS can evoke BOLD reaction not only on the region-specific region but also the interconnected areas in the monkey brain. Additionally, our results demonstrated that the temporal features of BOLD time courses of TUS on the primary visual cortex and those of real visual stimulation have no significant difference in the regions of primary visual pathway.

0123



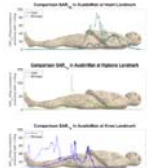
### Required number of tissue compartments for electromagnetic safety simulation of the head: personalized RF safety for 7T pTx

Matthijs H.S. de Buck<sup>1</sup>, Peter Jezzard<sup>1</sup>, and Aaron T. Hess<sup>2</sup>

<sup>1</sup>Wellcome Centre for Integrative Neuroimaging, FMRIB Division, Nuffield Department of Clinical Neurosciences, University of Oxford, Oxford, United Kingdom, <sup>2</sup>Oxford Centre for Clinical Magnetic Resonance Research, Department of Cardiovascular Medicine, University of Oxford, Oxford, United Kingdom

Personalized electromagnetic simulation models can be generated by segmenting MR-images. However, it is unclear how many tissue types are required for accurate 7T head models. Here, a clustering approach is used to determine the error in the simulated pTx SAR for models with different numbers of tissue types (clusters). Models consisting of only four different tissue types plus air were found to consistently generate low errors for human body-models of different ages and genders. Using the proposed method, it should be possible to operate scanners closer to the true SAR limits due to improved estimations of the actual patient-specific SAR.

0124



### Specific Absorption Rate (SAR) Comparison in the Conventional and Open MRI Systems Utilizing an Anatomical Human Computational Model

Kyoko Fujimoto<sup>1</sup>, Tayeb A Zaidi<sup>1</sup>, David Lampman<sup>2</sup>, Joshua W Guag<sup>1</sup>, Hideta Habara<sup>3</sup>, and Sunder S Rajan<sup>1</sup>



<sup>1</sup>Center for Devices and Radiological Health, US Food and Drug Administration, Silver Spring, MD, United States, <sup>2</sup>Hitach Healthcare Americas, Twinsburg, OH, United States, <sup>3</sup>Healthcare Business Unit, Hitachi, Ltd., Tokyo, Japan

There is an increasing use of open-bore vertical Magnetic Resonance (MR) systems which consist of two planar radio-frequency (RF) coils. These planar coils generate different electric field distributions compared to that of the conventional cylindrical coils. A recent study showed that RF-induced heating of a neuromodulation device was much lower in the open-bore system. However, imaging landmarks other than the brain have not been evaluated. In this study, we examined the differences in RF exposure using computational modeling and compared specific absorption rate in an anatomical human model at a 1.2T open-bore system with a 1.5T conventional system.

---

## Oral

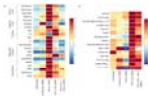
### Cancer Imaging: Pre- & Post-Treatment - Cancer Imaging: Physiology & Metabolism

Monday Parallel 5 Live Q&A

Monday 13:45 - 14:30 UTC

Moderators: Derek Johnson & Harish Poptani

0125



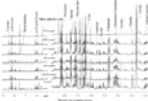
The immune checkpoint PD-L1 alters choline kinase expression and metabolism in triple negative breast cancer cells

Jesus Pacheco-Torres<sup>1</sup>, Marie-France Penet<sup>1,2</sup>, Flonne Wildes<sup>1</sup>, Yelena Mironchik<sup>1</sup>, Balaji Krishnamachary<sup>1</sup>, and Zaver M Bhujwalla<sup>1,2,3</sup>

<sup>1</sup>The Russell H Morgan Department of Radiology and Radiological Science, The Johns Hopkins University, School of Medicine, Baltimore, MD, United States, <sup>2</sup>Sidney Kimmel Comprehensive Cancer Center, The Johns Hopkins University, School of Medicine, Baltimore, MD, United States, <sup>3</sup>Radiation Oncology and Molecular Radiation Sciences, The Johns Hopkins University, School of Medicine, Baltimore, MD, United States

Expression of programmed death-ligand 1 (PD-L1) plays a significant role in creating an immune suppressive tumor microenvironment. We investigated the relationship between the aberrant choline metabolism observed in most cancers and PD-L1 expression in triple negative human MDA-MB-231 breast cancer cells. Using siRNA to downregulate Chk- $\alpha$  or PD-L1 or both, we identified a close inverse interdependence between Chk- $\alpha$  and PD-L1. We identified, for the first time, the role of PD-L1 in cancer cell metabolism. These results have significant implications for therapy and provide new insights into the relationship between metabolism and immune resistance in these breast cancer cells.

0126



Chemotherapeutic drugs profoundly alter the metabolism of triple negative breast cancer cells

Kanchan Sonkar<sup>1</sup>, Caitlin M. Tressler<sup>1</sup>, and Kristine Glunde<sup>1,2</sup>

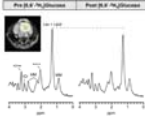
<sup>1</sup>The Russell H. Morgan Department of Radiology and Radiological Science, Johns Hopkins University School of Medicine, Baltimore, MD, United States, <sup>2</sup>The Sidney Kimmel Comprehensive Cancer Center, Johns Hopkins University School of Medicine, Baltimore, MD, United States

Triple negative breast cancer (TNBC) is a highly aggressive form of cancer that poses severe health care problem as no targeted therapeutics are available for its treatment. TNBC is treated with chemotherapeutic agents, including doxorubicin, paclitaxel, vinorelbine, 5-fluorouracil, melphalan and cisplatin, which are either used alone or in various combinations. Studies investigating the metabolic effects of chemotherapy in TNBC are still limited. Here we have used high-resolution <sup>1</sup>H MRS to study the metabolic profiles of TNBC cell lines MDA-MB-231 and SUM159 treated with these chemotherapeutic agents as compared to untreated controls.

---

Detecting glycolytic metabolism in glioblastoma using a new <sup>1</sup>H MRS and [6,6'-<sup>2</sup>H<sub>2</sub>]glucose infusion based approach

0127

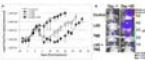


Laurie J Rich<sup>1</sup>, Puneet Bagga<sup>1</sup>, Gabor Mizsei<sup>1</sup>, Mitchell D Schnall<sup>1</sup>, John A Detre<sup>2</sup>, Mohammad Haris<sup>3</sup>, and Ravinder Reddy<sup>1</sup>

<sup>1</sup>Radiology, University of Pennsylvania, Philadelphia, PA, United States, <sup>2</sup>Neurology, University of Pennsylvania, Philadelphia, PA, United States, <sup>3</sup>Research Branch, Qatar University, Doha, Qatar

A key hallmark of malignant tissues is a metabolic shift from oxidative phosphorylation to glycolytic metabolism, leading to increased lactate production. Probing the kinetics of lactate production *in vivo* may play a key role in studying disease mechanisms and developing biomarkers of treatment response. Here, we developed a new approach for studying glycolytic metabolism in glioblastoma by combining <sup>1</sup>H MRS with infusion of deuterated glucose. Infusion of [6,6'-<sup>2</sup>H<sub>2</sub>]glucose leads to downstream deuterium labeling of lactate, resulting in a reduction in the 1.33 ppm lactate peak on <sup>1</sup>H MRS and making it possible to monitor the metabolic turnover of lactate.

0128



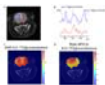
Metabolic modulation towards improved outcome in human glioblastoma model

Kavindra Nath<sup>1</sup>, David Nelson<sup>1</sup>, Jeffrey Roman<sup>1</sup>, Sofya Osharovich<sup>1</sup>, Saad Sheikh<sup>2</sup>, Stepan Orlovskiy<sup>1</sup>, Stephen Pickup<sup>1</sup>, Dennis Leeper<sup>3</sup>, Yancey Gillespie<sup>4</sup>, Corrine Griguer<sup>5</sup>, Jay Dorsey<sup>2</sup>, Mary Putt<sup>6</sup>, and Jerry Glickson<sup>1</sup>

<sup>1</sup>Radiology, University of Pennsylvania, Philadelphia, PA, United States, <sup>2</sup>Radiation Oncology, University of Pennsylvania, Philadelphia, PA, United States, <sup>3</sup>Radiation Oncology, Thomas Jefferson University, Philadelphia, PA, United States, <sup>4</sup>Neurosurgery, University of Alabama, Birmingham, AL, United States, <sup>5</sup>Radiation Oncology, University of Iowa, Iowa City, IA, United States, <sup>6</sup>Biostatistics and Epidemiology, University of Pennsylvania, Philadelphia, PA, United States

Standard of care for glioblastoma multiforme (GBM) patients, the Stupp protocol, involves radiotherapy concurrent with adjuvant temozolomide (TMZ) chemotherapy. Lonidamine (LND), an inhibitor of monocarboxylate transporters, mitochondrial pyruvate carrier and mitochondrial complex I & II, is shown to potentiate TMZ chemotherapy inhibiting the growth of U251 glioblastoma cells orthotopically implanted in mice. LND effects measured *in vivo* by <sup>31</sup>P and <sup>1</sup>H MRS in subcutaneous U251 glioblastoma xenografts showed a sustained and tumor-selective decrease in intracellular pH, decrease in bioenergetics ( $\beta$ NTP/Pi) and an increase in lactate. Selective tumor acidification and deenergization induced by LND potentiated the TMZ response in U251 glioblastoma xenografts.

0129



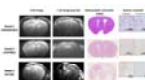
Hyperpolarized  $\delta$ -[1-<sup>13</sup>C]gluconolactone monitors TERT-induced elevation in pentose phosphate pathway flux in brain tumors *in vivo*

Georgios Batsios<sup>1</sup>, Pavithra Viswanath<sup>1</sup>, Celine Taglang<sup>1</sup>, Robert Flavell<sup>1</sup>, Joseph Costello<sup>2</sup>, Russell O Pieper<sup>2</sup>, Peder Larson<sup>1</sup>, and Sabrina Ronen<sup>1</sup>

<sup>1</sup>Radiology and Biomedical Imaging, UCSF, San Francisco, CA, United States, <sup>2</sup>Neurological Surgery, UCSF, San Francisco, CA, United States

Telomerase reverse transcriptase (TERT) expression is essential for tumor proliferation and is also an attractive therapeutic target for gliomas. Imaging TERT can help monitor tumor development and response to therapy. TERT expression has previously been shown to enhance glucose flux via the pentose phosphate pathway in low grade glioma cells expressing TERT. Here, we show that hyperpolarized  $\delta$ -[1-<sup>13</sup>C] gluconolactone metabolism to 6-phospho-[1-<sup>13</sup>C]gluconate is significantly higher in tumor compared to contralateral normal brain in TERT-expressing low-grade oligodendrogliomas, pointing to the utility of hyperpolarized  $\delta$ -[1-<sup>13</sup>C]gluconolactone for non-invasive *in vivo* assessment of this critical tumor hallmark in gliomas.

0130



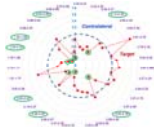
Hyperpolarized <sup>13</sup>C-glucose MRS: a potential biosensor to visualize the infiltrative front in GBM

Mor Mishkovsky<sup>1</sup>, Olga Gusyatiner<sup>2</sup>, Bernard Lanz<sup>1</sup>, Cristina Cudalbu<sup>3</sup>, Irene Vassallo<sup>2</sup>, Marie-France Hamou<sup>2</sup>, Jocelyne Bloch<sup>2</sup>, Arnaud Comment<sup>4</sup>, Rolf Gruetter<sup>1,3,5,6</sup>, and Monika Hegji<sup>2</sup>

<sup>1</sup>Laboratory for Functional and Metabolic Imaging (LIFMET), Ecole Polytechnique Fédérale de Lausanne (EPFL), Lausanne, Switzerland, <sup>2</sup>Department of Clinical Neurosciences, Lausanne University Hospital and University of Lausanne, Lausanne, Switzerland, <sup>3</sup>Centre d'Imagerie Biomédicale (CIBM), Ecole Polytechnique Fédérale de Lausanne (EPFL), Lausanne, Switzerland, <sup>4</sup>General Electric Healthcare, Chalfont St Giles, United Kingdom, <sup>5</sup>Department of Radiology, University of Geneva (UNIGE), Geneva, Switzerland, <sup>6</sup>Department of Radiology, University of Lausanne (UNIL), Lausanne, Switzerland

Glioblastoma (GBM) is the most malignant primary brain tumor in adults. Aberrant glucose metabolism is considered a hallmark of cancer, via the so-called 'Warburg Effect', however recent studies show distinct metabolic profile associated with the invasive phenotype in GBM, indicating active glucose oxidation. Hyperpolarized (HP) endogenous compounds, provides real-time metabolic information which is related to enzymatic activity. The aim of the present study was to apply HP <sup>13</sup>C-glucose MRS in patient-derived GBM models and to investigate glucose metabolism in the infiltrative front of GBM, which potentially would enable to differentiate the invasive front of GBM from normal brain.

0131



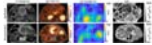
### Metabolomic Characterization of Human Prostate Cancer with Tissue from MRI/US Fusion Biopsy

Leo L Cheng<sup>1</sup>, Lindsey Vandergriff<sup>1</sup>, Andrew Gusev<sup>1</sup>, Shulin Wu<sup>1</sup>, Mukesh Harisinghani<sup>1</sup>, Chin-Lee Wu<sup>1</sup>, and Adam Feldman<sup>1</sup>

<sup>1</sup>MGH/Harvard, Boston, MA, United States

Prostate cancer (PCa) clinic is challenged by heterogeneously distributed and clinically insignificant diseases. Multiparametric (mp)-MRI, with a PI-RADS score, correlated to clinically significant cancer and its morphological variations to establish a biopsy Target, and ultrasound fusion-guided biopsy guided to the targeted area has increased detection of clinically significant cancer. We studied PI-RADS score according to tissue MRS-based metabolomics. Metabolic differences between Target and contralateral cores, regardless if Targets were Ca-positive or not, support the assumption that targeted areas fundamentally and metabolically differ from non-targeted areas.

0132

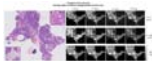


### Differentiation of Murine Pancreatic Tumours at 7 T with Hyperpolarized <sup>13</sup>C-Pyruvate-Lactate MRSI, <sup>18</sup>F-FDG PET, and DWI

Geoffrey J. Topping<sup>1</sup>, Irina Heid<sup>2</sup>, Moritz Mayer<sup>2</sup>, Lukas Kritznern<sup>2</sup>, Florian Englert<sup>2</sup>, Martin Grashei<sup>1</sup>, Christian Hundshammer<sup>1</sup>, Katja Steiger<sup>3</sup>, Katja Peschke<sup>4</sup>, Markus Schwaiger<sup>1</sup>, Maximilian Reichert<sup>4</sup>, Franz Schilling<sup>1</sup>, and Rickmer Braren<sup>2</sup>

<sup>1</sup>Department of Nuclear Medicine, Klinikum rechts der Isar, Technical University of Munich, Munich, Germany, <sup>2</sup>Institute of Radiology, Klinikum rechts der Isar, Technical University of Munich, Munich, Germany, <sup>3</sup>Institute of Pathology, Technical University of Munich, Munich, Germany, <sup>4</sup>Internal Medicine II, Klinikum rechts der Isar, Technical University of Munich, Munich, Germany

Multimodal imaging for characterization of pancreatic tumour cellularity and metabolism has potential to guide treatment. Murine orthotopically transplanted tumours were imaged with DWI, <sup>13</sup>C-pyruvate CSI, and <sup>18</sup>F-FDG PET, and endogenous tumours with DWI and CSI. Transplanted epithelial and mesenchymal tumours had similar cellularity, shown by ADC, but different metabolism, with higher mesenchymal AUC ratios and SUV. Compared with other endogenous tumour growth patterns, classical ductal had lower tumour cellularity (higher ADC), while solid had higher and more-variable AUC ratios. The combination of these methods can characterize tumour metabolism, including correcting for tumour cellularity, better than CSI alone.



### Identification of pancreatic intraepithelial neoplasia in the mouse pancreas with MR Microscopy

Carlos Bilreiro<sup>1</sup>, Rui V. Simões<sup>1</sup>, Francisca F. Fernandes<sup>1</sup>, Mireia Castillo-Martin<sup>1</sup>, Kevin Harkins<sup>2</sup>, Mark Does<sup>2</sup>, Celso Matos<sup>1</sup>, and Noam Shemesh<sup>1</sup>



<sup>1</sup>Champalimaud Research, Champalimaud Centre for the Unknown, Lisbon, Portugal, <sup>2</sup>Department of Biomedical Engineering, Vanderbilt University, Nashville, TN, United States

Survival in pancreatic cancer resides on an early diagnosis, for which current imaging methods are insufficient. Here, we investigated which MRI contrast can reflect pancreatic pre-neoplastic lesions, particularly, pancreatic intraepithelial neoplasia (PanIN). To this end, we developed an ultrafast DWI-MGE pulse sequence and performed MR microscopy on pancreas extracted from transgenic mice with PanIN lesions (along with controls), and validated our findings using histology. PanIN lesions were clearly detected in the transgenic mice and differentiated from inflammatory changes at  $b=1000 \text{ sec/mm}^2$  and long TE. Our findings are encouraging for future detection of PanIN *in vivo*.

## Oral

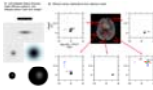
### Cancer Imaging: Pre- & Post-Treatment - Cancer Imaging: Perfusion & Diffusion

Monday Parallel 5 Live Q&A

Monday 13:45 - 14:30 UTC

Moderators: Shu Xing

0134



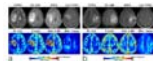
#### Diffusion tensor distribution imaging of brain tumor microstructure and heterogeneity

João de Almeida Martins<sup>1</sup>, Samo Lasic<sup>1</sup>, Yuan Zheng<sup>2</sup>, Qing Wei<sup>2</sup>, Sirui Li<sup>3</sup>, Wenbo Sun<sup>3</sup>, Haibo Xu<sup>3</sup>, Karin Bryske<sup>1</sup>, and Daniel Topgaard<sup>1,4</sup>

<sup>1</sup>Random Walk Imaging, Lund, Sweden, <sup>2</sup>United Imaging Healthcare, Shanghai, China, <sup>3</sup>Zhongnan Hospital of Wuhan University, Wuhan, China, <sup>4</sup>Lund University, Lund, Sweden

For voxels containing multiple cell or tissue types, DTI metrics are challenging to interpret in terms of specific microstructural properties. We address this problem by adapting encoding and inversion strategies from solid-state and low-field NMR to determine diffusion tensor distributions (DTDs) with dimensions corresponding to cell densities, shapes, and orientations. Three patients with glioma, meningioma, or cerebral cyst underwent 5 min DTD imaging giving 15 distinct parameter maps for quantitative analysis and intuitive microstructural interpretation. The DTD-derived metrics showed good agreement with expected tissue properties and structural insights not accessible with DTI.

0135



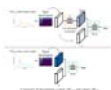
#### Perfusion Measurement in Brain Gliomas Using Velocity-Selective Arterial Spin Labeling: Comparison with PCASL and DSC Perfusion

Yaoming Qu<sup>1</sup>, Zhibo Wen<sup>1</sup>, and Qin Qin<sup>2,3</sup>

<sup>1</sup>Imaging diagnostic department, Zhujiang hospital of southern medical university, Guangzhou, China, <sup>2</sup>The Russell H. Morgan Department of Radiology and Radiological Science, Johns Hopkins University School of Medicine, Baltimore, MD, United States, <sup>3</sup>F.M. Kirby Research Center for Functional Brain Imaging, Kennedy Krieger Institute, Baltimore, MD, United States

Velocity-selective arterial spin labeling (VSASL) employing Fourier-transform based velocity-selective pulse trains is an emerging method for quantifying cerebral blood flow (CBF) with high sensitivity to perfusion signal. Its utility was assessed for glioma patients at 3T by a comparison between pseudo-continuous ASL with DSC-PWI. We demonstrated the existence of various and prolonged arterial transit time (ATT) in high-grade gliomas. Detecting by the dependence of the CBF based on  $T_{max}$ , lesser sensitivity to ATT in VSASL was reported. VSASL showed great promise for accurate quantification of CBF and could potentially improve the diagnostic performance of ASL in preoperative grading of gliomas.

0136



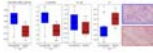
#### Improving the reliability of pharmacokinetic parameters in dynamic contrast-enhanced MRI in gliomas: Deep learning approach

Kyu Sung Choi<sup>1</sup>, Sung-Hye You<sup>2</sup>, Yoseob Han<sup>1</sup>, Jong Chul Ye<sup>1</sup>, Seung Hong Choi<sup>3</sup>, and Bumseok Jeong<sup>1</sup>

<sup>1</sup>Korea Advanced Institute for Science and Technology, Daejeon, Korea, Republic of, <sup>2</sup>Korea University College of Medicine, Seoul, Korea, Republic of, <sup>3</sup>Seoul National University Hospital, Seoul, Korea, Republic of

$AIF_{DCE}$  has been known to be sensitive to noise, because of the relatively weak T1 contrast-enhanced MR signal intensity (SI) compared to the T2\* SI of DSC-MRI, leading to PK parameters –  $K_{trans}$ ,  $V_e$ , and  $v_p$  – with low reliability. In this study, we developed a neural network model generating an AIF similar to the AIF obtained from DSC-MRI –  $AIF_{generated\ DSC}$  – and demonstrated that the accuracy and reliability of  $K_{trans}$  and  $V_e$  derived from  $AIF_{generated\ DSC}$  can be improved compared to those from  $AIF_{DCE}$  without obtaining DSC-MRI, not leading to an additional deposition of gadolinium in the brain.

0137



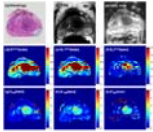
Characterizing the ADC-microstructure relationship in meningiomas through computational modelling.

Giulia Buizza<sup>1</sup>, Chiara Paganelli<sup>1</sup>, Lorenzo Preda<sup>2</sup>, Francesca Valvo<sup>2</sup>, Daniel C. Alexander<sup>3</sup>, Guido Baroni<sup>1,2</sup>, and Marco Palombo<sup>3</sup>

<sup>1</sup>CartCasLab at Department of Electronics, Information and Bioengineering, Politecnico di Milano, Milan, Italy, <sup>2</sup>National Center Of Oncological Hadrontherapy (CNAO), Pavia, Italy, <sup>3</sup>Centre for Medical Image Computing and Dept of Computer Science, University College London, London, United Kingdom

Tumour microstructure can be probed with diffusion-weighted MRI (DW-MRI), but the clinically-adopted apparent diffusion coefficient (ADC) lacks a clear link to microstructure. Aim of this work was to detail the ADC-microstructure relationship using a computational framework. Relying on a sparse representation of simulated DW-MRI data, we estimated diffusivity (D), cell radius (R) and volume fraction (vf) for 27 low and high-grade meningioma patients, which significantly differed in ADC, D and vf. Preliminary results showed the potential of the proposed framework for meningioma grading and proton-therapy response assessment, although extension to richer data and histological validation need to be further addressed.

0138



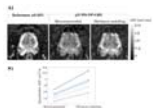
Parametric maps from the two-tissue compartment model for prostate DCE-MRI: compared with the standard Tofts model in diagnosis of cancer

Xiaobing Fan<sup>1</sup>, Xueyan Zhou<sup>2</sup>, Aritrick Chatterjee<sup>1</sup>, Aytekin Oto<sup>1</sup>, and Gregory S. Karczmar<sup>1</sup>

<sup>1</sup>Radiology, The University of Chicago, Chicago, IL, United States, <sup>2</sup>Harbin University, Harbin, China

We compared standard Tofts model with a two-tissue compartment model (2TCM) of dynamic contrast enhanced (DCE) MRI for diagnosis of prostate cancer. The 2TCM has one slow and one fast exchanging compartment. The standard Tofts model parameters ( $K^{trans}$  and  $k_{ep}$ ) were compared with the 2TCM parameters ( $K_i^{trans}$  and  $k_{ep}^i$ ,  $i=1,2$ ). There was a strong correlation between  $K^{trans}$  and  $K_i^{trans}$  for cancer, but weak correlation between  $k_{ep}$  and  $k_{ep}^1$ . This demonstrated that the Tofts model often does not fit contrast agent concentration curves accurately, and the 2TCM can provide new diagnostic information with fewer false positives in diagnosis of prostate cancer.

0139



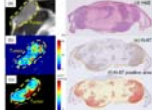
3D multi-shot diffusion imaging of the prostate with inter-shot correction and dictionary-based ADC matching

Elisa Roccia<sup>1</sup>, Radhouene Nejj<sup>1,2</sup>, Thomas Benkert<sup>3</sup>, Berthold Kiefer<sup>3</sup>, Vicky Goh<sup>4</sup>, and Isabel Dregely<sup>1</sup>

<sup>1</sup>Biomedical Engineering Department, School of Biomedical Engineering and Imaging Sciences, King's College London, London, United Kingdom, <sup>2</sup>Siemens Healthcare Limited, Frimley, United Kingdom, <sup>3</sup>Siemens Healthcare GmbH, Erlangen, Germany, <sup>4</sup>Cancer Imaging Department, School of Biomedical Engineering and Imaging Sciences, King's College London, London, United Kingdom

Diffusion imaging is a key contrast in assessing prostate cancer. However, current single-shot EPI-based techniques are often distorted and fundamentally limited in resolution. The aim of this study is to develop multi-shot diffusion-prepared gradient echo imaging to obtain accurate 3D ADC maps in the prostate. We developed a 3D Cartesian centric trajectory with self-navigation, and a shot rejection approach to correct for inter-shot magnitude errors. We used a custom dictionary of acquisition specific signal evolutions to estimate ADC. We have shown in simulations and in vivo that accurate ADC values could be recovered.

0140



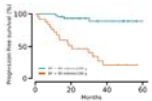
### Investigation of breast cancer microstructure and microvasculature from time-dependent DWI and CEST in correlation with histology

Yuko Someya<sup>1</sup>, Mami Iima<sup>1,2</sup>, Hirohiko Imai<sup>3</sup>, Akihiko Yoshizawa<sup>4</sup>, Yuji Nakamoto<sup>1</sup>, Masako Kataoka<sup>1</sup>, Hiroyoshi Isoda<sup>1</sup>, and Kaori Togashi<sup>1</sup>

<sup>1</sup>Diagnostic Imaging and Nuclear Medicine, Kyoto University Graduate School of Medicine, Kyoto, Japan, <sup>2</sup>Clinical Innovative Medicine, Institute for Advancement of Clinical and Translational Science, Kyoto University Hospital, Kyoto, Japan, <sup>3</sup>Kyoto University Graduate School of Informatics, Kyoto, Japan, <sup>4</sup>Diagnostic Pathology, Kyoto University Graduate School of Medicine, Kyoto, Japan

The association of time-dependent DWI (shifted ADC [sADC], IVIM, and non-Gaussian DWI) at different diffusion times and CEST (MTR<sub>asym</sub>, APT signal intensity) parameters was investigated with histological biomarkers in a breast cancer xenograft model. ADC values decreased with increased diffusion times. sADC values at a diffusion time=5ms had significant negative correlation with Ki-67 ( $r=-0.63$ ,  $P<0.05$ ). MTR<sub>asym</sub> had a significant positive correlation with Ki-67 positive area ( $r=0.73$ ,  $P<0.05$ ). Significant association was found between  $f_{IVIM}$  and microvessel density ( $r=0.80$ ,  $P<0.01$ ). These results indicate their utility for investigating microstructure and microcirculation of breast cancers without using contrast agents.

0141



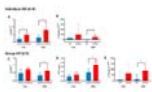
### Perfusion MRI related to survival, treatment response and sex differences in rectal cancer

Kine Mari Bakke<sup>1,2</sup>, Sebastian Meltzer<sup>1</sup>, Endre Grøvik<sup>3</sup>, Anne Negård<sup>4,5</sup>, Stein Harald Holmedal<sup>4</sup>, Kjell-Inge Gjesdal<sup>4</sup>, Atle Bjørnerud<sup>2,3</sup>, Anne Hansen Ree<sup>1,5</sup>, and Kathrine Røe Redalen<sup>6</sup>

<sup>1</sup>Department of Oncology, Akershus University Hospital, Lørenskog, Norway, <sup>2</sup>Department of Physics, University of Oslo, Oslo, Norway, <sup>3</sup>Department of Diagnostic Physics, Division of Radiology and Nuclear Medicine, Oslo University Hospital, Oslo, Norway, <sup>4</sup>Department of Radiology, Akershus University Hospital, Lørenskog, Norway, <sup>5</sup>Institute of Clinical Medicine, University of Oslo, Oslo, Norway, <sup>6</sup>Department of Physics, Norwegian University of Science and Technology, Trondheim, Norway

Three different MRI methods for obtaining perfusion related parameters were compared and evaluated as biomarkers in a study of 94 rectal cancer patients. The methods were dynamic contrast enhanced (DCE) MRI and dynamic susceptibility contrast (DSC) MRI analysed from a multi-echo dynamic EPI sequence, as well as intravoxel incoherent motion (IVIM) MRI analysed from a diffusion weighted sequence with 7 b-values. Tumour blood flow from DSC MRI was correlated to  $D^*$  from IVIM MRI as well as  $K^{trans}$  and  $v_p$  from DCE MRI. Blood flow was also related to progression free survival, overall survival, treatment response and sex differences.

0142



### How the choice of PK model and AIF affect DCE-MRI detection of pancreatic cancer responses to stroma-directed drug?

Jianbo Cao<sup>1</sup>, Stephen Pickup<sup>1</sup>, Peter O'Dwyer<sup>2,3</sup>, Mark Rosen<sup>1,3</sup>, and Rong Zhou<sup>1,3</sup>

<sup>1</sup>Department of Radiology, University of Pennsylvania, Philadelphia, PA, United States, <sup>2</sup>Pancreatic Cancer Research Center, University of Pennsylvania, Philadelphia, PA, United States, <sup>3</sup>Abramson Cancer Center, University of Pennsylvania, Philadelphia, PA, United States

Pancreatic ductal adenocarcinoma (PDA) is characterized by a dense stroma, which poses a substantial barrier to drug penetration and motivates development of stroma-directed interventions. We aim to test the utility of DCE-MRI to predict PDA responses to such treatment. We compared individual versus group-arterial input function approach and metric including  $K^{trans}$ ,  $k_{ep}$  and  $V_p$  derived from three commonly used pharmacokinetic models. Our data provides rationale for choice of PK model and AIF approach which lead to quantitative DCE-MRI marker of optimal sensitivity and specificity for detection of PDA responses to human hyaluronidase that reduces PDA stroma.

## Oral

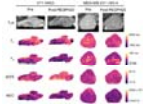
### Cancer Imaging: Pre- & Post-Treatment - Cancer Imaging: Treatment Planning & Response Assessment

Monday Parallel 5 Live Q&A

Monday 13:45 - 14:30 UTC

Moderators: Sola Adeleke & Arvind Pathak

0143



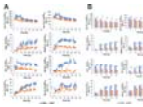
#### Breast tumour response to PEGPH20-induced stromal modulation assessed by multiparametric MRI

Emma L. Reeves<sup>1</sup>, Jin Li<sup>1</sup>, Jessica K. R. Boulton<sup>1</sup>, Barbara Blouw<sup>2</sup>, David Kang<sup>2</sup>, Jeffrey C. Bamber<sup>1</sup>, Yann Jamin<sup>1</sup>, and Simon P. Robinson<sup>1</sup>

<sup>1</sup>Radiotherapy and Imaging, Institute of Cancer Research, London, United Kingdom, <sup>2</sup>Halozyme Therapeutics, San Diego, CA, United States

Degradation of hyaluronan by PEGPH20 can improve stromal-dense tumour response to therapy. Given PEGPH20 treatment is associated with a reduction in tumour water content, we hypothesised that  $T_1$ ,  $T_2$ , MTR and ADC may inform on PEGPH20 response. MRI was performed before and after PEGPH20 treatment in 4T1 HAS3 and MDA-MB-231 LM2-4 orthotopic breast tumours.  $T_1$ ,  $T_2$ , and ADC significantly decreased, and MTR significantly increased following PEGPH20 treatment in 4T1 HAS3 tumours. PEGPH20 significantly decreased ADC but did not change  $T_1$ ,  $T_2$  or MTR in MDA-MB-231 LM2-4 tumours. These data suggest that ADC can detect breast tumour response to PEGPH20.

0144



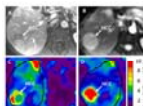
#### The Role of Iron Chelation in the Tumour Microenvironment of Triple-Negative Breast Cancer

Paola Porcari<sup>1</sup>, Ellen Ackerstaff<sup>1</sup>, Dov P Winkleman<sup>1</sup>, Suresh Veeraperumal<sup>1</sup>, Natalia Kruchevsky<sup>1</sup>, H. Carl Lekay<sup>1</sup>, and Jason A. Koutcher<sup>1,2,3,4</sup>

<sup>1</sup>Medical Physics, Memorial Sloan Kettering Cancer Center, New York, NY, United States, <sup>2</sup>Department of Medicine, Memorial Sloan Kettering Cancer Center, New York, NY, United States, <sup>3</sup>Molecular Pharmacology Program, Memorial Sloan Kettering Cancer Center, New York, NY, United States, <sup>4</sup>Weill Cornell Medical College, Cornell University, New York, NY, United States

Intracellular iron, essential for cancer cell proliferation and metabolism, is modified in cancer cells. Triple-negative breast cancers are metastatic cancers associated with a high recurrence rate, poor prognosis and lack of effective targeted therapies. We are investigating the potential of Deferiprone, a clinically approved intracellular iron chelator for non-cancer related diseases, to improve chemotherapeutic treatment response in triple-negative breast cancer by altering iron-dependent proliferation and metabolism. The effectiveness of Deferiprone to impair triple-negative breast cancer cell growth and affect cellular metabolism was evaluated by monitoring live cells, exposed to Deferiprone, in an MR-compatible cell bioreactor using multi-nuclear MRS.

0145



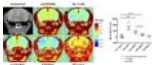
#### Immune Checkpoint Blockade (ICB) Response Evaluation with MRI/MR Elastography (MRE) in Surgical and Non-Surgical Patients with HCC

Aliya Qayyum<sup>1</sup>, Rony Avritscher<sup>2</sup>, Rizwan Aslam<sup>1</sup>, Jingfei Ma<sup>3</sup>, Mark Pagel<sup>4</sup>, Jia Sun<sup>5</sup>, Yehia Ibrahim Mohammed<sup>6</sup>, Manal Hassan<sup>7</sup>, Hesham Amin<sup>8</sup>, Asif Rashid<sup>9</sup>, Sunyoung Lee<sup>6</sup>, Robert A Wolff<sup>6</sup>, James C Yao<sup>6</sup>, Richard L Ehman<sup>10</sup>, Gabriel Daniel Duda<sup>11</sup>, and Ahmed Omar Kaseb<sup>12</sup>

<sup>1</sup>Radiology, MD Anderson, Houston, TX, United States, <sup>2</sup>Interventional Radiology, MD Anderson, Houston, TX, United States, <sup>3</sup>Imaging Physics, MD Anderson, Houston, TX, United States, <sup>4</sup>Cancer Systems Imaging, MD Anderson, Houston, TX, United States, <sup>5</sup>Biostatistics, MD Anderson, Houston, TX, United States, <sup>6</sup>GI Medical Oncology, MD Anderson, Houston, TX, United States, <sup>7</sup>Epidemiology, MD Anderson, Houston, TX, United States, <sup>8</sup>Hemopathology, MD Anderson, Houston, TX, United States, <sup>9</sup>Pathology, MD Anderson, Houston, TX, United States, <sup>10</sup>Radiology, Mayo Clinic, Rochester, MN, United States, <sup>11</sup>Radiation Oncology, Massachusetts General Hospital, Boston, MA, United States, <sup>12</sup>MD Anderson, Houston, TX, United States

Newer systemic treatments for advanced hepatocellular carcinoma (HCC) include immune checkpoint blockade (ICB) which act through increasing cytotoxic T-cell mediated response to tumor. There is a lack of biomarkers of ICB response and treatment outcomes are not correlated with change in tumor size. We evaluated MRI imaging features of HCC and change in tumor stiffness after 6 weeks immunotherapy in surgical and non-surgical patients. An increase in HCC stiffness on MRE after 6 weeks treatment was significantly correlated with treatment response. Longitudinal measurement of tumor stiffness on MRE provides a novel technique for early immunotherapy response assessment.

0146



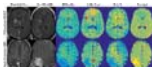
#### Imaging blood-brain barrier disruption caused by CD19 based CAR-T cell immunotherapy

Puneet Bagga<sup>1</sup>, Stephen Pickup<sup>1</sup>, Denis Migliorini<sup>2</sup>, Neil E Wilson<sup>1</sup>, Mohammad Haris<sup>3,4</sup>, Suyash Mohan<sup>1</sup>, Avery D Posey<sup>2</sup>, and Ravinder Reddy<sup>1</sup>

<sup>1</sup>Department of Radiology, University of Pennsylvania, Philadelphia, PA, United States, <sup>2</sup>Center for Cellular Immunotherapies, University of Pennsylvania, Philadelphia, PA, United States, <sup>3</sup>Sidra Medicine, Doha, Qatar, <sup>4</sup>LARC, Qatar University, Doha, Qatar

With the advent of clinically effective CD19 based chimeric antigen receptor (CAR) T cell immunotherapies, there are incidents of associated neurotoxicity. In this study, we report the use of gadolinium enhanced MRI to image BBB disruption caused by CD19 CAR-T cell on target action against brain pericytes of immunodeficient non-tumor bearing NSG mice. Pericytes are mural cells that wrap endothelial cells and are critical for maintaining blood-brain-barrier (BBB) integrity and express CD19. The MRI results were also found to corroborate with the Evans blue dye BBB permeability assay.

0147

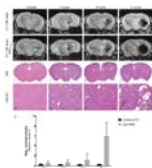


#### Impact of Single Fraction Stereotactic Radiosurgery vs. Hypofractionated Radiation Therapy on CEST and MT Parameters of Brain Metastases

Hatef Mehrabian<sup>1</sup>, Wilfred W Lam<sup>1</sup>, Hany Soliman<sup>1,2,3</sup>, Sten Myrehaug<sup>2,3</sup>, Arjun Sahgal<sup>1,2,3</sup>, and Greg J Stanisz<sup>1,4</sup>

<sup>1</sup>Physical Sciences, Sunnybrook Research Institute, Toronto, ON, Canada, <sup>2</sup>Radiation Oncology, Sunnybrook Health Sciences Centre, Toronto, ON, Canada, <sup>3</sup>Radiation Oncology, University of Toronto, Toronto, ON, Canada, <sup>4</sup>Medical Biophysics, University of Toronto, Toronto, ON, Canada

Brain metastases are treated with single fraction stereotactic radiosurgery (sf-SRS) or hypofractionated radiation therapy (HFTR). CEST was previously shown to identify responders to sf-SRS within one-week post-treatment. This study investigated the differences in CEST and MT properties of brain metastases treated with sf-SRS and 5 fraction HFRT (5f-HFRT) one week after treatment. We observed statistically significantly larger reduction in CEST properties of tumours treated with sf-SRS compared to those treated with 5f-HFRT. However, changes in MT properties of the two cohort were similar. Such differences should be considered when evaluating response of brain metastases to radiotherapy using CEST and MT.



#### Low dose brain irradiation leads to delayed neuro-inflammation

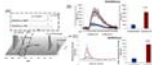
Dina Sikpa<sup>1</sup>, J r mie P. Fouquet<sup>1</sup>, Luc Tremblay<sup>1</sup>, R jean Lebel<sup>1</sup>, Benoit Paquette<sup>1</sup>, and Martin Lepage<sup>1</sup>

<sup>1</sup>Universit  de Sherbrooke, Sherbrooke, QC, Canada





We studied the late radiation effect of a low radiation dose on the healthy mouse brain using MRI and histology. MRI enables the visualisation of early inflammation and late radiation necrosis. Histological analysis confirmed tissue damage and revealed that cellular (astrocytes, microglia) and molecular activation (ICAM-1, VCAM-1) as a result of neuro-inflammation precedes the formation of the necrotic core.

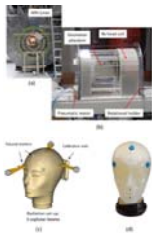


Hyperpolarized [1-<sup>13</sup>C]/[5-<sup>13</sup>C] glutamate as a metabolic imaging marker of IDH1 mutant glioma response to temozolomide therapy

Elavarasan Subramani<sup>1</sup>, Chloe Najac<sup>1</sup>, Georgios Batsios<sup>1</sup>, Marina Radoul<sup>1</sup>, Pavithra Viswanath<sup>1</sup>, Abigail Molloy<sup>1</sup>, Donghyun Hong<sup>1</sup>, Anne Marie Gillespie<sup>1</sup>, Russell O. Pieper<sup>2,3</sup>, Joseph Costello<sup>2</sup>, and Sabrina M Ronen<sup>1,3</sup>

<sup>1</sup>Department of Radiology and Biomedical Imaging, University of California San Francisco, San Francisco, CA, United States, <sup>2</sup>Department of Neurological Surgery, Helen Diller Research Center, University of California San Francisco, San Francisco, CA, United States, <sup>3</sup>Brain Tumor Research Center, University of California San Francisco, San Francisco, CA, United States

Temozolomide (TMZ) is most commonly used for the treatment of primary glioblastoma but is now being considered for the treatment of low-grade glioma that harbor mutations in the cytosolic isocitrate dehydrogenase 1 (IDH1) gene. Though the treatment of IDH1 mutant patients with TMZ improves survival, there is a need for complementary metabolic imaging approaches to help in assessing early response to therapy. Hyperpolarized <sup>13</sup>C magnetic resonance spectroscopy-based metabolic profiling of mutant IDH1 cells treated with TMZ revealed that [1-<sup>13</sup>C]/[5-<sup>13</sup>C] glutamate production from [1-<sup>13</sup>C] α-ketoglutaric acid/[2-<sup>13</sup>C] pyruvate could serve as translatable biomarkers of response to therapy.

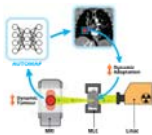


MRI-guided real-time 4D Radiation Dosimetry at an MRI-Linac using Polymer Gel Dosimeters

Yves De Deene<sup>1</sup>, Morgan Wheatley<sup>2</sup>, Gary Liney<sup>3</sup>, David Waddington<sup>4</sup>, Urszula Jelen<sup>3</sup>, and Bin Dong<sup>3</sup>

<sup>1</sup>Engineering, Macquarie University, North Ryde - Sydney, Australia, <sup>2</sup>Macquarie University, North Ryde - Sydney, Australia, <sup>3</sup>Ingham Institute, Liverpool, Australia, <sup>4</sup>The University of Sydney, Sydney, Australia

4D radiation dosimetry using a highly radiation-sensitive polymer gel dosimeter with real-time quantitative MRI readout is presented as a technique to acquire the accumulated radiation dose distribution during image guided radiotherapy (IGRT) in an MRI-Linac. Optimized T<sub>2</sub> weighted TSE scans are converted to quantitative R<sub>2</sub> maps and subsequently to radiation dose maps. A further increase in temporal resolution using a keyhole imaging approach is proposed. The potential use of real-time 4D radiation dosimetry for safeguarding image guided radiotherapy (IGRT) of moving and deforming targets in an MRI-Linac will be discussed.



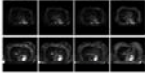
Towards Real-Time Beam Adaptation on an MRI-Linac using AUTOMAP

David Waddington<sup>1,2</sup>, Nicholas Hindley<sup>1</sup>, Neha Koonjoo<sup>2,3</sup>, Tess Reynolds<sup>1</sup>, Bo Zhu<sup>2,3</sup>, Chiara Paganelli<sup>4</sup>, Matthew Rosen<sup>2,3,5</sup>, and Paul Keall<sup>1</sup>

<sup>1</sup>ACRF Image X Institute, Faculty of Medicine and Health, The University of Sydney, Sydney, Australia, <sup>2</sup>A. A. Martinos Center for Biomedical Imaging, Charlestown, MA, United States, <sup>3</sup>Department of Physics, Harvard University, Cambridge, MA, United States, <sup>4</sup>Dipartimento di Elettronica, Informazione e Bioingegneria, Politecnico di Milano, Milan, Italy, <sup>5</sup>Harvard Medical School, Boston, MA, United States

MRI-Linacs are new cancer treatment machines integrating radiotherapy with MRI. Dynamically adapting the radiation beam on the basis of MR-detected anatomical changes (e.g. respiratory and cardiac motion) promises to increase the accuracy of MRI-Linac treatments. A key challenge in real-time beam adaptation is accurately reconstructing images in real time. Historically, reconstruction of data acquired with accelerated techniques, such as compressed sensing, has been very slow. Here, we use AUTOMAP, a machine-learning framework, to quickly and accurately reconstruct radial MRI data simulated from a digital thorax phantom. These results will guide development of real-time adaptation technologies on MRI-Linacs.

0152



### Retrospective Fat Suppression for Lung Radiotherapy Planning with Deep Learning Convolutional Neural Networks

Benjamin C Rowland<sup>1</sup>, Steven Jackson<sup>2</sup>, David Cobben<sup>1,2</sup>, Hanna Maria Hanson<sup>1</sup>, Ahmed Saleem<sup>1</sup>, Kathryn Banfill<sup>2</sup>, Lisa McDaid<sup>2</sup>, Michael Dubec<sup>2</sup>, and Marcel van Herk<sup>1</sup>

<sup>1</sup>University of Manchester, Manchester, United Kingdom, <sup>2</sup>The Christie NHS Trust, Manchester, United Kingdom

We investigated three different Deep Learning techniques for performing retrospective fat suppression in T2 weighted imaging of lung cancer. The methods considered were two U-nets, using an L1 cost function or a conditional GAN, and a CycleGAN. The networks were trained on 900 images and then 16 test images were scored by 3 oncologists and a research radiographer. The L1 U-net and CycleGAN were scored at 73% and 72% respectively, relative to a gold standard of 80% for prospectively fat saturated images, and the scorers indicated they would be happy to use the generated images for radiotherapy target delineation.

## Oral

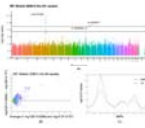
### Quantitative Tissue Properties - Emerging Trends in QSM

Monday Parallel 1 Live Q&A

Monday 14:30 - 15:15 UTC

Moderators: Pascal Spincemaille

0153



### Quantitative susceptibility mapping in UK Biobank brain imaging: pipeline and preliminary results in 2400 subjects

Chaoyue Wang<sup>1</sup>, Stephen M. Smith<sup>1</sup>, Fidel Alfaro-Almagro<sup>1</sup>, Cristiana Fisceone<sup>2</sup>, Richard Bowtell<sup>2</sup>, Lloyd T. Elliott<sup>3</sup>, Karla L. Miller<sup>1</sup>, and Benjamin C. Tandler<sup>1</sup>

<sup>1</sup>Wellcome Centre for Integrative Neuroimaging, FMRIB, Nuffield Department of Clinical Neurosciences, University of Oxford, Oxford, United Kingdom, <sup>2</sup>Sir Peter Mansfield Imaging Centre, School of Physics and Astronomy, University of Nottingham, Nottingham, United Kingdom, <sup>3</sup>Department of Statistics and Actuarial Science, Simon Fraser University, Vancouver, BC, Canada

UK Biobank aims to scan 100,000 participants and its brain protocol acquires susceptibility-weighted MRI (swMRI). To date, only the swMRI magnitude data were processed to produce T2\* maps. The aim of this work is to develop a robust processing pipeline for QSM using the acquired swMRI phase data. We ran this pipeline on 2408 volunteers and report some preliminary results, including age-dependent curves and genetic associations. Significant correlations were found between susceptibility and age in subcortical structures. QSM discovered replicable genetic associations previously identified in T2\*. Our results suggest that there is unique information in susceptibility maps compared to T2\*.

0154



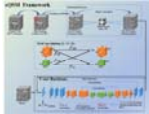
### Eliminating chemical shift and relaxation effects in QSM using SMURF imaging

Beata Bachrata<sup>1,2,3</sup>, Bernhard Strasser<sup>1,2,4</sup>, Wolfgang Bogner<sup>1,2</sup>, Albrecht Ingo Schmid<sup>1,5</sup>, Siegfried Trattnig<sup>1,2,3</sup>, and Simon Daniel Robinson<sup>1,2,6,7</sup>

<sup>1</sup>High Field MR Centre, Medical University of Vienna, Vienna, Austria, <sup>2</sup>Department of Biomedical Imaging and Image-guided Therapy, Medical University of Vienna, Vienna, Austria, <sup>3</sup>Christian Doppler Laboratory for Clinical Molecular MR Imaging, Vienna, Austria, <sup>4</sup>Athinoula A. Martinos Center for Biomedical Imaging, Department of Radiology, Massachusetts General Hospital, Harvard Medical School, Boston, MA, United States, <sup>5</sup>Center for Medical Physics and Biomedical Engineering, Medical University of Vienna, Vienna, Austria, <sup>6</sup>Centre for Advanced Imaging, The University of Queensland, Brisbane, Australia, <sup>7</sup>Department of Neurology, Medical University of Graz, Graz, Austria

The accuracy of Quantitative Susceptibility Mapping in fatty regions is adversely affected by the chemical shift effects and by the relaxation rate differences between fat and water. We propose using a recently developed water-fat separation technique based on multi-band principles, Simultaneous Multiple Resonance Frequency (SMURF) imaging, to correct for these effects. SMURF achieves clean water-fat separation in the head-and-neck, allowing the generation of recombined water-fat images fully corrected for chemical shift and relaxation effects. This makes bias-free Quantitative Susceptibility Mapping possible in body regions containing significant amounts of fat, with the free selection of echo-times, receiver bandwidths and flip angles.

1635



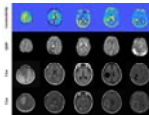
xQSM: a deep learning QSM network using Octave Convolution

Yang Gao<sup>1</sup>, Xuanyu Zhu<sup>1</sup>, Stuart Crozier<sup>1</sup>, Feng Liu<sup>1</sup>, and Hongfu Sun<sup>1</sup>

<sup>1</sup>University of Queensland, Brisbane, Australia

Deep learning frameworks are emerging methods for solving ill-posed inverse problems in medical imaging, including Quantitative Susceptibility Mapping (QSM). Previously, U-net has been successfully trained on susceptibility maps to learn the dipole inversion process; however, susceptibility contrast loss was observed in iron-rich deep grey matter regions. In this study, we propose an enhanced deep learning network “xQSM” using the state-of-the-art Octave Convolution, which shows more accurate susceptibility contrasts than the original U-net in both simulated and *in vivo* datasets.

0155



Morphology Enabled Quantitative Conductivity–Susceptibility Mapping with B1 and B0 Estimation from Complex Multi-echo Gradient Echo Signal

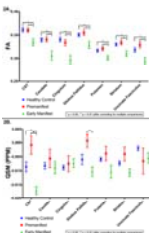
Motofumi Fushimi<sup>1,2</sup>, Thanh Nguyen<sup>2</sup>, and Yi Wang<sup>2,3</sup>

<sup>1</sup>Graduate School of Information Science and Technology, The University of Tokyo, Tokyo, Japan,

<sup>2</sup>Radiology, Weill Cornell Medical College, New York, NY, United States, <sup>3</sup>Biomedical Engineering, Cornell University, Ithaca, NY, United States

We propose a simultaneous conductivity and susceptibility reconstruction method by estimating B1 phase and B0 distributions from a multi-echo gradient echo (mGRE) signal. B1 phase and B0 maps are simultaneously determined by applying nonlinear least squares method on the complex signal equation of the mGRE signal. The poor conditioned inversion of field (B1/B0) to source (conductivity/susceptibility) is regularized using anatomical information. This morphology enabled quantitative conductivity and susceptibility mapping (QCSM) was performed on healthy subjects and patients with brain tumors. Our preliminary in-vivo experiments demonstrated that the proposed QCSM method can reconstruct conductivity and susceptibility from a single mGRE acquisition.

0156



7 Tesla Diffusion Tensor Imaging and Quantitative Susceptibility Mapping of Huntington's Disease

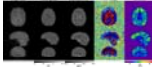
Paul Rowley<sup>1,2</sup>, Melanie Morrison, PhD<sup>1</sup>, Yicheng Chen<sup>1</sup>, Angela Jakary<sup>1</sup>, Michael Geschwind, MD, PhD<sup>3</sup>, Alexandra Nelson, MD, PhD<sup>3</sup>, Duan Xu, PhD<sup>1</sup>, Christopher Hess, MD, PhD<sup>1</sup>, and Janine Lupo, PhD<sup>1</sup>

<sup>1</sup>Radiology & Biomedical Imaging, University of California, San Francisco, San Francisco, CA, United States,

<sup>2</sup>University of Wisconsin School of Medicine and Public Health, Madison, WI, United States, <sup>3</sup>Neurology, University of California, San Francisco, San Francisco, CA, United States

Ultra-high-field 7 Tesla (7T) MRI was acquired to examine and compare white matter microstructure and quantitative susceptibility in patients with premanifest (PM) and early manifest (EM) Huntington's disease (HD) and age-matched healthy control (HC) subjects. Tract-averaged and along-tract fractional anisotropy (FA) and susceptibility (PPM) were calculated to determine the spatial spread of disease along motor tracks originating from the striatum and ending in the cortex. HC and PM patients demonstrated different areas of significantly increased susceptibility compared to EM at the tract-averaged level as well as significant focal along-tract variations in FA and susceptibility which were undetected by tract-averaged analysis.

0157



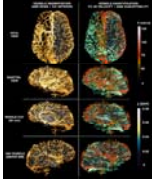
### Simultaneous QSM and MR Elastography of the Brain Using Spiral Staircase

Xi Peng<sup>1</sup> and James G. Pipe<sup>1</sup>

<sup>1</sup>Department of Radiology, Mayo Clinic, Rochester, MN, United States

This work presents a new feasibility to extract tissue susceptibility from gradient-echo MRE data and enables simultaneous QSM and MRE in a single scan. The proposed method builds on a new spiral staircase acquisition which enables high resolution often required by QSM using inherently improved through-plane parallel imaging. In-plane parallel imaging, constrained reconstruction and deblurring method are also integrated to generate high quality spiral images for QSM and MRE processing. In vivo experiment results demonstrate the capability of proposed method in producing high quality tissue susceptibility along with shear stiffness maps from a single 5-minute scan.

0158



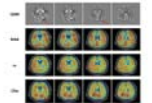
### Multimodal quantitative arterial-venous segmentation of the human brain at 7T: structure, susceptibility and flow

Michaël Bernier<sup>1,2</sup>, Berkin Bilgic<sup>1,2</sup>, Saskia Bollmann<sup>1,2</sup>, Nina E. Fultz<sup>1,3</sup>, and Jonathan R. Polimeni<sup>1,2,4</sup>

<sup>1</sup>Athinoula A. Martinos Center for Biomedical Imaging, Massachusetts General Hospital, Charlestown, MA, United States, <sup>2</sup>Radiology, Harvard Medical School, Boston, MA, United States, <sup>3</sup>Engineering, Boston University, Boston, MA, United States, <sup>4</sup>Division of Health Sciences and Technology, Massachusetts Institute of Technology, Cambridge, MA, United States

Vascular imaging acquisition techniques to extract veins and arteries are not impervious to flaws: venography by susceptibility weighted imaging is prone to blooming effects and false-negatives, and angiography from time-of-flight imaging is affected by veins detection and false-negatives. They also fail to provide quantitative measures of vascular physiology such as flow and susceptibility important for understanding the origin of vascular-based biases. Thus, we aimed to employ multi-orientation quantitative susceptibility mapping, multi-echo time-of-flight and quantitative phase-contrast to more accurately detect and quantify the susceptibility and flow along the vascular tree, paving the way for a joint anatomical/physiological vascular atlas at 7T.

0159



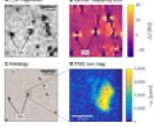
### High-Resolution QSM for Simultaneous QSM/MRSI

Rong Guo<sup>1,2</sup>, Yudu Li<sup>1,2</sup>, Yibo Zhao<sup>1,2</sup>, Tianyao Wang<sup>3</sup>, Yao Li<sup>4,5</sup>, Brad Sutton<sup>1,2,6</sup>, and Zhi-Pei Liang<sup>1,2</sup>

<sup>1</sup>Department of Electrical and Computer Engineering, University of Illinois at Urbana-Champaign, Urbana, IL, United States, <sup>2</sup>Beckman Institute for Advanced Science and Technology, University of Illinois at Urbana-Champaign, Urbana, IL, United States, <sup>3</sup>Radiology Department, The Fifth People's Hospital of Shanghai, Shanghai, China, <sup>4</sup>School of Biomedical Engineering, Shanghai Jiao Tong University, Shanghai, China, <sup>5</sup>Med-X Research Institute, Shanghai Jiao Tong University, Shanghai, China, <sup>6</sup>Department of Bioengineering, University of Illinois at Urbana-Champaign, Urbana, IL, United States

In this work, we present a new method to achieve high-resolution QSM for simultaneous QSM/MRSI experiments. This work extends SPICE with a novel data acquisition scheme that provides larger k-space coverage for the unsuppressed water signals. A union-of-subspaces model incorporating sensitivity encodings (parallel imaging) and pre-determined spatio-spectral features is used to solve the underlying image reconstruction problem. High-resolution capability (on the order of  $1.0 \times 1.0 \times 1.2 \text{ mm}^3$ ) for QSM has been demonstrated in 3D *in vivo* simultaneous QSM/MRSI experiments.

0160



**Magnetic properties of dopaminergic neurons in human substantia nigra quantified with MR microscopy**  
Malte Brammerloh<sup>1,2</sup>, Evgeniya Kirilina<sup>1,3</sup>, Renat Sibgatulin<sup>4</sup>, Karl-Heinz Herrmann<sup>4</sup>, Tilo Reinert<sup>1</sup>, Carsten Jäger<sup>1,5</sup>, Primož Pelicon<sup>6</sup>, Primož Vavpetič<sup>6</sup>, Kerrin J. Pine<sup>1</sup>, Andreas Deistung<sup>7</sup>, Markus Morawski<sup>5</sup>, Jürgen R. Reichenbach<sup>4</sup>, and Nikolaus Weiskopf<sup>1,2</sup>

<sup>1</sup>Department of Neurophysics, Max Planck Institute for Human Cognitive and Brain Sciences, Leipzig, Germany, <sup>2</sup>Faculty of Physics and Earth Sciences, Leipzig University, Leipzig, Germany, <sup>3</sup>Center for Cognitive Neuroscience Berlin, Freie Universität Berlin, Berlin, Germany, <sup>4</sup>Medical Physics Group, University Hospital Jena, Jena, Germany, <sup>5</sup>Paul Flechsig Institute of Brain Research, Leipzig, Germany, <sup>6</sup>Microanalytical Center, Department for Low and Medium Energy Physics, Jožef Stefan Institute, Ljubljana, Slovenia, <sup>7</sup>Department of Radiology, University Hospital Halle, Halle, Germany

MRI-based quantification of dopaminergic neurons (DN) and their neuromelanin (NM) in substantia nigra (SN) has great potential to serve as a specific biomarker for neurodegeneration in movement disorders. We used 22- $\mu\text{m}$ -resolution *post mortem* MR microscopy combined with ion beam microscopy to characterize the magnetic properties of DN. MR microscopy visualized individual DN and provided 3D cellular maps of the entire SN. Static dephasing was determined as main effective transverse relaxation mechanism of DN. We characterized the susceptibility of iron in DN and estimated that the contribution of DN to  $R2^*$  and QSM may also be detected with *in vivo* MRI.

## Oral

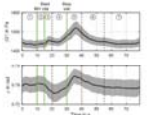
### Quantitative Tissue Properties - Magnetic Resonance Elastography

Monday Parallel 1 Live Q&A

Monday 14:30 - 15:15 UTC

Moderators: Ziyang Yin

0161



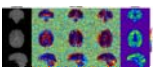
**Real-time MR elastography of the human brain reveals short-term cerebral autoregulation in response to the Valsalva maneuver.**

Helge Herthum<sup>1</sup>, Mehrgan Shahryari<sup>1</sup>, Gergely Bertalan<sup>1</sup>, Carsten Warmuth<sup>1</sup>, Stefan Hetzer<sup>2</sup>, Jürgen Braun<sup>3</sup>, and Ingolf Sack<sup>1</sup>

<sup>1</sup>Department of Radiology, Charité Universitätsmedizin Berlin, Berlin, Germany, <sup>2</sup>Bernstein Center for Computational Neuroscience, Berlin, Germany, <sup>3</sup>Institute of Medical Informatics, Berlin, Germany

Real-time MR elastography (rt-MRE) with 4.9Hz-frame rate was developed for *in-vivo* brain stiffness quantification during short-term tissue mechanical adaptation due to cerebral autoregulation. Six healthy participants performed a 15s-Valsalva maneuver with 50s recovery period following 10s resting period and 5s deep inspiration during continuous rt-MRE. 387 maps of tissue stiffness and fluidity were generated depicting a significant increase of stiffness due to Valsalva and an overshoot of stiffness by 3.4% fading out within 7s after the maneuver. rt-MRE is potentially sensitive to several diseases associated with cerebral autoregulation and reveals new insights into brain viscoelasticity changes on short time scales.

0162

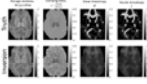


**Fast Whole-Brain MR Elastography Using 3D GRE Multishot Variable Density Spiral Staircase Acquisition**  
Xi Peng<sup>1</sup>, Yi Sui<sup>1</sup>, Sandeep Ganji<sup>2</sup>, Ashley Anderson<sup>2</sup>, John Huston<sup>1</sup>, Richard Ehman<sup>1</sup>, and James Pipe<sup>1</sup>

<sup>1</sup>Department of Radiology, Mayo Clinic, Rochester, MN, United States, <sup>2</sup>Philips Healthcare, Gainesville, FL, United States

This work reports a new method for fast whole-brain MRE using a 3D gradient-echo multishot variable-density spiral staircase acquisition. The proposed method enables high-resolution MRE by exploiting the inherently improved through-plane parallel imaging. The displacement-SNR is further enhanced by exploiting a motion encoding gradient of a 2 wave-period duration. Constrained reconstruction and deblurring method are used to generate high-quality spiral images. By integrating all these features, the proposed technique provides flexible trade-off among SNR, resolution, spatial blurring and scan time. In vivo experiments have demonstrated the capability of the proposed method for high-SNR high-resolution MRE in less than 5 minutes.

0163



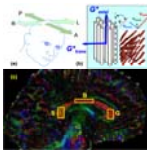
Model-based heterogenous transverse isotropic MR elastography inversion for brain tissue with aligned fiber tracts

Matthew Mcgarry<sup>1</sup>, Elijah Van Houten<sup>2</sup>, Damian Sowinski<sup>1</sup>, Philip Bayly<sup>3</sup>, Daniel Smith<sup>4</sup>, Curtis Johnson<sup>4</sup>, John Weaver<sup>1,5</sup>, and Keith Paulsen<sup>1,5</sup>

<sup>1</sup>Dartmouth College, Hanover, NH, United States, <sup>2</sup>Université de Sherbrooke, Sherbrooke, QC, Canada, <sup>3</sup>Washington University in St Louis, St Louis, MO, United States, <sup>4</sup>University of Delaware, Newark, DE, United States, <sup>5</sup>Dartmouth-Hitchcock Medical Center, Lebanon, NH, United States

An implementation of a transverse isotropic model with fiber directions defined by DTI was added to our finite element model-based nonlinear inversion MRE platform. The algorithm can recover accurate images of complex valued shear modulus, shear anisotropy, and tensile anisotropy from a realistic brain simulation. In vivo application to multi-excitation brain MRE data produced promising results, maintaining high quality images for the base shear modulus and damping ratio, while recovering additional images of anisotropy which may be useful for characterizing diseases affecting white matter tracts or muscle.

0164



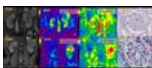
Variation of In Vivo Anisotropic MRE Metrics in Corpus Callosum: Effect of Aging

Nicolas R Gallo<sup>1</sup>, Stacey M Cahoon<sup>1</sup>, Aaron T Anderson<sup>2</sup>, Noel M Naughton<sup>3</sup>, Assimina A Pelegri<sup>4</sup>, and John G Georgiadis<sup>1</sup>

<sup>1</sup>Biomedical Engineering, Illinois Institute of Technology, Chicago, IL, United States, <sup>2</sup>Beckman Institute, Urbana, IL, United States, <sup>3</sup>Department of Mechanical Science and Engineering, University of Illinois at Urbana-Champaign, Urbana, IL, United States, <sup>4</sup>Department of Mechanical and Aerospace Engineering, Rutgers University, New Brunswick, NJ, United States

Healthy aging involves local variations in viscoelastic shear properties of the brain. We employ high-resolution, multi-excitation MRE and a novel anisotropic inversion scheme (iTI) to extract local shear anisotropic moduli in vivo. The ratio of transverse to axial moduli, a new MRE metric, remains greater than 1 along the splenium, body and genu regions of the corpus callosum for both young and old subjects. This metric peaks in the body region and decreases with age throughout the corpus callosum.

0165



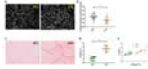
Preliminary application of Three-Dimensional Multifrequency MR Elastography for Chronic Kidney Disease

Shan Pi<sup>1</sup>, Jonathan M. Scott<sup>2</sup>, Yin Li<sup>3</sup>, Hui Peng<sup>3</sup>, Huiquan Wen<sup>1</sup>, Matthew C. Murphy<sup>2</sup>, Jingbiao Chen<sup>1</sup>, Meng Yin<sup>2</sup>, Jun Chen<sup>2</sup>, Kevin J. Glaser<sup>2</sup>, Richard L. Ehman<sup>2</sup>, and Jin Wang<sup>1</sup>

<sup>1</sup>Department of Radiology, the Third Affiliated Hospital, Sun Yat-sen University, Guang Zhou, China, <sup>2</sup>Department of Radiology, Mayo Clinic, Rochester, Micronesia, <sup>3</sup>Department of Nephrology, the Third Affiliated Hospital, Sun Yat-sen University, Guang Zhou, China

Chronic kidney disease (CKD) is increasing in incidence and prevalence worldwide and early detection of CKD is a major challenge. MR elastography (MRE) is a noninvasive technique capable of quantifying the mechanical properties of tissue that has shown potential for assessing kidney diseases. MRE using 60-Hz and 90-Hz vibration frequencies can provide potential quantitative biomarkers for evaluating kidney function and biopsy score in CKD patients.

0166



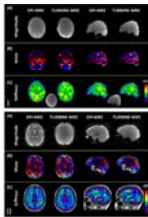
### Evolution of tumour mechanical properties under static preload as potential biomarker of solid stress

Gwenaël Pagé<sup>1</sup>, Laurent Besret<sup>2</sup>, Marion Tardieu<sup>1</sup>, Maïlys Vidal<sup>1</sup>, Bernard Van Beers<sup>1,3</sup>, and Philippe Garteiser<sup>1</sup>

<sup>1</sup>Laboratory of Biomarkers in Imaging, Center of Research on Inflammation, UMR 1149 Inserm-Université de Paris, Paris, France, <sup>2</sup>Sanofi R&D, Vitry-sur-Seine, France, <sup>3</sup>Department of Radiology, Beaujon University Hospital Paris Nord, Clichy, France

The purpose of this study was to assess in two different human liver tumours the correlation between tumour solid stress and changes of mechanical properties under preload. MR elastography acquisitions were performed at different pressure levels by externally compressing the tumour with an inflatable balloon. Reference values for tumour fluid pressure and solid stress were acquired with a catheterized pressure transducer. The results, obtained in two liver tumour types with largely different basal mechanical properties, show that the evolution of tumour elasticity under preload is correlated with the tumour solid stress and could be a potential biomarker of tumour pressure.

0167



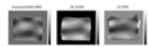
### TURBINE-MRE: A 3D Hybrid Radial-Cartesian EPI Acquisition for MR Elastography

Yi Sui<sup>1</sup>, Arvin Forghanian-Arani<sup>1</sup>, Joshua D. Trzasko<sup>1</sup>, Matthew C. Murphy<sup>1</sup>, Phillip J. Rossman<sup>1</sup>, Kevin J. Glaser<sup>1</sup>, Kiaran P. McGee<sup>1</sup>, Armando Manduca<sup>2</sup>, Richard L. Ehman<sup>1</sup>, Philip A. Arazo<sup>1</sup>, and John III Huston<sup>1</sup>

<sup>1</sup>Radiology, Mayo Clinic, Rochester, MN, United States, <sup>2</sup>Physiology and Biomedical Engineering, Mayo Clinic, Rochester, MN, United States

This study demonstrates the technical feasibility of a 3D radially batched internal navigator echo magnetic resonance elastography (TURBINE-MRE) technique in the brain. The highly efficient TURBINE-MRE approach allows for a true 3D wave displacement field to be acquired over the entire human brain volume in approximately 1.5 minutes.

0168



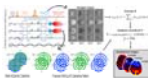
### Ultra-short echo time Magnetic Resonance Elastography

Pilar Sango Solanas<sup>1</sup>, Kevin Tse Ve Koon<sup>1</sup>, Eric Van Reeth<sup>1</sup>, Cyrielle Caussy<sup>2</sup>, and Olivier Beuf<sup>1</sup>

<sup>1</sup>Univ Lyon, INSA-Lyon, Université Claude Bernard Lyon 1, UJM-Saint Etienne, CNRS, Inserm, CREATIS UMR 5220, U1206, F-69616, Lyon, France, Lyon, France, <sup>2</sup>Département d'Endocrinologie, Diabète et Nutrition, Centre Hospitalier Lyon Sud, Hospices Civils de Lyon, CarMeN, INSERM U1060, INRA U1397, Lyon, France, Lyon, France

Magnetic Resonance Elastography (MRE) is a valuable technique to quantitatively characterize mechanical properties of tissues based on the properties of shear waves propagation. In this study, a radial acquisition MRE sequence potentially able to quantify viscoelastic parameters of tissues whose T2 values are very short is proposed. To this end, an optimal control-based RF pulse is applied with a constant gradient during the mechanical excitation to simultaneously perform spatially selective excitation and motion encoding. Acquisition is started right after, enabling a very short TE. Results on phantom experiments demonstrated the feasibility of our ultra-short echo time MRE technique.

0169



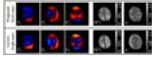
### OSCILLATE: A Low-Rank Approach for Accelerated Magnetic Resonance Elastography

Grace McIlvain<sup>1</sup>, Alex M Cerjanic<sup>2</sup>, Anthony G Christodoulou<sup>3</sup>, Matthew DJ McGarry<sup>4</sup>, and Curtis L Johnson<sup>1</sup>

<sup>1</sup>Biomedical Engineering, University of Delaware, Newark, DE, United States, <sup>2</sup>Bioengineering, University of Illinois, Urbana, IL, United States, <sup>3</sup>Biomedical Imaging Research Institute, Cedars-Sinai Medical Center, Los Angeles, CA, United States, <sup>4</sup>Thayer School of Engineering, Dartmouth College, Hanover, NH, United States

MR elastography (MRE) has emerged as a sensitive measure of brain health, but due to the need for repeated measures of wave motion, it is a fundamentally long scan. We have developed a method for accurate MRE using spatiotemporal undersampling and low rank joint reconstruction across all samples. We demonstrate the ability to collect accurate MRE data in half the time with under 2% stiffness error. This accelerated method will be used to scan challenging populations, such as those with developmental disabilities, as well as improve achievable resolution and feasibility of multi-frequency or multi-excitation methods.

0170



#### Accelerating DENSE MR elastography by including multi-axes motion encoding into the multiphase DENSE-MRE acquisition scheme

Johannes Strasser<sup>1</sup>, Martin Soellradl<sup>1</sup>, Christian Enzinger<sup>1</sup>, and Stefan Ropele<sup>1</sup>

<sup>1</sup>Department of Neurology, Medical University of Graz, Graz, Austria

In MR elastography, the propagation of three-dimensional wave motion is acquired to assess mechanical tissue properties. We here propose an accelerated approach of the multiphase DENSE-MRE acquisition scheme which additionally includes three-dimensional motion encoding besides the multiple phase offsets within one TR. In addition to phantom experiments, this multi-axes encoding concept was also investigated in the human brain *in vivo*. The gathered wave images and shear modulus maps are confirmed by three consecutive single-axes multiphase DENSE-MRE acquisitions for x-, y- and z-motion encoding direction. With this concept, the acquisition can be accelerated up to a factor of 3.

### Oral - Power Pitch

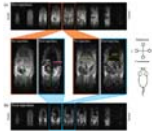
#### Quantitative Tissue Properties - Contrast Mechanisms: Beyond the Usual Suspects

Monday Parallel 1 Live Q&A

Monday 14:30 - 15:15 UTC

Moderators: Janine Lupo & Stefano Mandija

0171



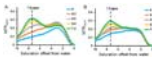
#### High-sensitivity *in vivo* Contrast Agent Imaging at Ultra-low Magnetic Fields with SPIONs

David Waddington<sup>1,2,3</sup>, Thomas Boele<sup>2,4</sup>, Richard Maschmeyer<sup>1</sup>, Zdenka Kuncic<sup>1,5</sup>, and Matthew Rosen<sup>2,6,7</sup>

<sup>1</sup>Institute of Medical Physics, School of Physics, The University of Sydney, Sydney, Australia, <sup>2</sup>A. A. Martinos Center for Biomedical Imaging, Charlestown, MA, United States, <sup>3</sup>ACRF Image X Institute, Faculty of Medicine and Health, The University of Sydney, Sydney, Australia, <sup>4</sup>ARC Centre of Excellence for Engineered Quantum Systems, School of Physics, The University of Sydney, Sydney, Australia, <sup>5</sup>Sydney Nano Institute, The University of Sydney, Sydney, Australia, <sup>6</sup>Department of Physics, Harvard University, Cambridge, MA, United States, <sup>7</sup>Harvard Medical School, Boston, MA, United States

MRI scanners operating at ultra-low fields (ULF) promise to reduce the cost and expand the clinical accessibility of MRI. Here, we use a 6.5 mT MRI scanner and an efficient balanced steady-state free precession MRI protocol to image superparamagnetic iron oxide nanoparticles (SPIONs) *in vivo* by leveraging the extremely high magnetization of SPIONs at ULF. Further, we show how positive contrast imaging of SPIONs can be performed at ULF with susceptibility-based techniques. These advances overcome a key limitation of ULF MRI by enabling high-contrast *in vivo* imaging of clinically safe contrast agents with short acquisition times.

0172



#### Developing imidazoles for performing functional MRI of kidneys

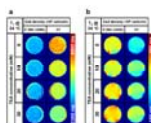
Shaowei Bo<sup>1</sup>, KowsalyaDevi Pavuluri<sup>1</sup>, Yunkou Wu<sup>2</sup>, Farzad Sedaghat<sup>1</sup>, Martin G. Pomper<sup>3</sup>, Max Kates<sup>4</sup>, and Michael T. McMahon<sup>5</sup>



<sup>1</sup>The Russell H. Morgan Department of Radiology and Radiological Science, Division of MR Research, The Johns Hopkins University School of Medicine, Baltimore, MD, United States, <sup>2</sup>Russell H. Morgan Department of Radiology and Radiological Science, The Johns Hopkins University School of Medicine, Baltimore, MD, United States, <sup>3</sup>Russell H. Morgan Department of Radiology and Radiological Science, The Johns Hopkins University School of Medicine, Department of Psychiatry, The Johns Hopkins University School of Medicine, Baltimore, MD, United States, <sup>4</sup>Department of Urology, The James Buchanan Brady Urological Institute, The Johns Hopkins University School of Medicine, Baltimore, MD, United States, <sup>5</sup>The Russell H. Morgan Department of Radiology and Radiological Science, Division of MR Research, The Johns Hopkins University School of Medicine, F.M. Kirby Research Center for Functional Brain Imaging, Kennedy Krieger Institute, Baltimore, MD, United States

Urinary tract obstructions (UTOs) are blockages that inhibit the flow of urine through its normal path, which can lead to kidney injury and infection. Chemical exchange saturation transfer (CEST) MRI is a fast, noninvasive molecular MRI technique which has shown promise for clinical applications. In this study, we designed and tested a series of imidazoles as CEST MRI contrast agents and tested these for performing functional kidney imaging on a UTO mouse model. The results demonstrate that CEST MRI can facilitate early detection of loss in kidney function.

0173



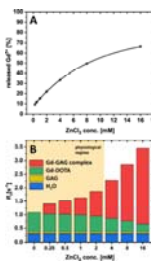
### A Change in Membrane Potential Induces Measurable Changes in Relaxation Times

Kyeongseon Min<sup>1</sup>, Tan Toi Phan<sup>2,3</sup>, Sungkwon Chung<sup>4</sup>, Jongho Lee<sup>1</sup>, Seung-Kyun Lee<sup>2,3</sup>, and Jang-Yeon Park<sup>2,3</sup>

<sup>1</sup>Laboratory for Imaging Science and Technology, Department of Electrical and Computer Engineering, Seoul National University, Seoul, Korea, Republic of, <sup>2</sup>Department of Biomedical Engineering, Sungkyunkwan University, Suwon, Korea, Republic of, <sup>3</sup>Center for Neuroscience Imaging Research, Institute for Basic Science, Suwon, Korea, Republic of, <sup>4</sup>Department of Physiology, Samsung Biomedical Research Institute, Sungkyunkwan University School of Medicine, Suwon, Korea, Republic of

In this study, the effects of membrane potential on  $T_1$  and  $T_2$  were examined using Jurkat T lymphocytes. We applied tetraethylammonium ion (TEA) to depolarize Jurkat cell membrane potential. Significant changes in  $T_1$  and  $T_2$ , which were measured to be  $-10.39$  ms/mM and  $0.920$  ms/mM, respectively, were observed. One potential explanation for the changes of  $T_1$  and  $T_2$  is the depolarization of membrane potential, while the underlying mechanism needs to be explored. Further studies are expected to utilize the membrane potential as a new contrast mechanism for MRI.

0174



### Quantifying the Transchelation of Gd<sup>3+</sup> Ions from Linear and Macrocyclic GBCA to Glycosaminoglycans using MR Relaxometry

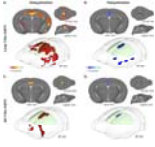
Patrick Schuenke<sup>1</sup>, Patrick Werner<sup>1,2</sup>, Matthias Taupitz<sup>3</sup>, and Leif Schröder<sup>1</sup>

<sup>1</sup>Leibniz-Forschungsinstitut fuer Molekulare Pharmakologie (FMP), Berlin, Germany, <sup>2</sup>BIOQIC, Charité Berlin, Berlin, Germany, <sup>3</sup>Department of Radiology, Charité Berlin, Berlin, Germany

In this study, we quantified the dissociation of GBCAs at different  $ZnCl_2$  concentrations and the subsequent chelation of  $Gd^{3+}$  to glycosaminoglycans (GAGs) like heparin. We showed that the relaxivity of the resulting Gd-GAG complexes is about seven times higher compared to that of GBCAs. Under physiological conditions, we further showed that  $\sim 20\%$  of the  $Gd^{3+}$ -ions transchelated from linear GBCAs to heparin and that these are accountable for more than 50% of the observed relaxation rate. Therefore, Gd-GAG complexes should be considered as the Gd-containing macromolecular substances with high relaxivity that are needed to explain the observed long-term enhancements *in vivo*.

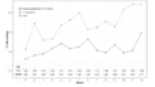
### Multi-T1D weighting ihMT imaging in the Cuprizone mouse model

Andreea Hertanu<sup>1</sup>, Lucas Soustelle<sup>1</sup>, Arnaud Le Troter<sup>1</sup>, Julie Buron<sup>1,2</sup>, Victor Carvalho<sup>1,3</sup>, Myriam Cayre<sup>2</sup>, Pascale Durbec<sup>2</sup>, Gopal Varma<sup>4</sup>, David C. Alsop<sup>4</sup>, Olivier M. Girard<sup>1</sup>, and Guillaume Duhamel<sup>1</sup>



<sup>1</sup>Aix-Marseille Univ, CNRS, CRMBM, Marseille, France, <sup>2</sup>Aix-Marseille Univ, CNRS, IBDM, Marseille, France, <sup>3</sup>Aix-Marseille Univ, CNRS, ICR, Marseille, France, <sup>4</sup>Division of MR Research, Radiology, Beth Israel Deaconess Medical Center, Harvard Medical School, Boston, MA, United States

Inhomogeneous magnetization transfer (ihMT) is a myelin sensitive MRI technique that provides access to multiple contrast regimes by tuning the amount of dipolar relaxation time ( $T_{1D}$ ) weighting of the sequence. This opens new perspectives to characterize the sensitivity and specificity of ihMT for myelin in a pathological context. In this study, multiple  $T_{1D}$ -weighting ihMT imaging was investigated in the cuprizone mouse model. IhMT signals compared to myelin imaging with fluorescence microscopy demonstrate that ihMT techniques that are weighted towards long  $T_{1D}$  values are more specifically related to myelin content during the demyelinating/remyelinating phases of the cuprizone model.

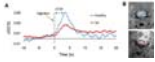


Gadolinium-induced Marrow Signal Changes with Metabolic Correlation: Are Cell Lines Directly Affected?

John J DeBevits<sup>1</sup>, Devin Bageac<sup>1</sup>, Leo Wolansky<sup>1</sup>, Paul Dicamillo<sup>2</sup>, Rong Wu<sup>1</sup>, Chaoran Hu<sup>1</sup>, and David Karimeddini<sup>1</sup>

<sup>1</sup>UConn Health, Farmington, CT, United States, <sup>2</sup>University of Iowa, Iowa City, IA, United States

In the BECOME trial, subjects experienced progressively increased T1W signal changes in deep grey matter nuclei. This retrospective analysis concluded these signal changes also can be seen in the diploic space bone marrow. While increasing trends in hypophosphatemia and leukopenia were also seen in the original study, this analysis has shown that these metabolic abnormalities are not associated with increased marrow signal and that low phosphate and low WBC were not associated with one another. This rejects our hypothesis that gadolinium deposition might interact with a common osteoclast-WBC progenitor cell to result in the metabolic abnormalities.

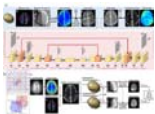


Dynamic Susceptibility Contrast with Undersampled Golden-Angle Radial Imaging in the Rodent Spinal Cord

Briana Meyer<sup>1</sup> and Matthew Budde<sup>2</sup>

<sup>1</sup>Biophysics, Medical College of Wisconsin, Milwaukee, WI, United States, <sup>2</sup>Neurosurgery, Medical College of Wisconsin, Milwaukee, WI, United States

Dynamic susceptibility contrast (DSC) to monitor spinal cord perfusion and hemodynamics has the potential to inform the clinical care of spinal cord injury and other disorders. Acquisition of high spatial and temporal resolution images of the rodent spinal cord for DSC perfusion measurements was achieved using a golden-angle radial gradient-echo acquisition combined with iGRASP iterative undersampled reconstruction.



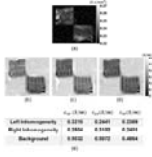
In-vivo Electromagnetic Field Mapping for Transcranial Electrical Stimulation (tES) using Deep Learning

Saurav Zaman Khan Sajib<sup>1</sup>, Munish Chauhan<sup>1</sup>, and Rosalind J Sadleir<sup>1</sup>

<sup>1</sup>School of Biological and Health Systems Engineering, Arizona State University, Tempe, AZ, United States

Magnetic flux densities induced by tES currents can be measured from MR phase and used to reconstruct current density, electric field and conductivity tensor distributions, via diffusion tensor magnetic resonance electrical impedance tomography (DT-MREIT). Determination of tES electric field distributions from DT-MREIT conductivities is challenging, because DT-MREIT requires data from two independent current administrations, increasing acquisition time. We demonstrate a deep-learning model for DT-MREIT reconstruction, showing that conductivity tensors and electric fields can be measured in human subjects *in-vivo* using a single current administration. This strategy can be used to directly monitor tES electric fields and verify treatment precision.

0179



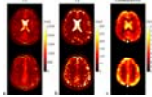
### Experimental Realization of Single Current Diffusion Tensor Magnetic Resonance Electrical Impedance Tomography

Mehdi Sadighi<sup>1</sup>, Mert Şişman<sup>1</sup>, Berk Can Açıkgöz<sup>1</sup>, and B. Murat Eyüboğlu<sup>1</sup>

<sup>1</sup>Electrical and Electronics Engineering Dept., Middle East Technical University (METU), Ankara, Turkey

To obtain low-frequency anisotropic conductivity distribution of biological tissues recently Diffusion Tensor Magnetic Resonance Electrical Impedance Tomography (DT-MREIT), which is combination of the DTI and MREIT techniques, is proposed. There are two *in vivo* applications of DT-MREIT in the literature where two linearly independent current injection patterns are used. Decreasing the number of current injection patterns to one improves the feasibility of DT-MREIT in clinical applications. In this study, DT-MREIT using a single current injection pattern is experimentally realized. The obtained results approve the validity of the proposed single current DT-MREIT method.

0180



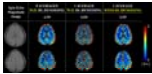
### Configuration-based Electrical Properties Tomography

Santhosh Iyyakkunnel<sup>1,2</sup>, Jessica Schäper<sup>1,2</sup>, and Oliver Bierl<sup>1,2</sup>

<sup>1</sup>Department of Radiology, University Hospital Basel, Basel, Switzerland, <sup>2</sup>Department of Biomedical Engineering, University of Basel, Basel, Switzerland

Only recently, phase imaging with balanced steady-state free precession (bSSFP) has been suggested for electrical properties tomography (EPT). Here we suggest exploring the SSFP configuration space retrieved from multiple phase-cycled bSSFP scans used for relaxometry also for electrical conductivity mapping. Consequently, the conductivity can be estimated in conjunction with standard quantitative tissue properties requiring no additional scan time.

0181



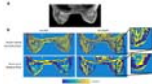
### Improving Phase-based Conductivity Reconstructions by Means of Deep Learning-based Denoising of B1+ Phase Data

Kyu-Jin Jung<sup>1</sup>, Stefano Mandija<sup>2,3</sup>, Jun-Hyeong Kim<sup>1</sup>, Kanghyun Ryu<sup>1</sup>, Soozy Jung<sup>1</sup>, Mina Park<sup>4</sup>, Mohammed A. Al-masni<sup>1</sup>, Cornelis A.T. van den Berg<sup>2</sup>, and Dong-Hyun Kim<sup>1</sup>

<sup>1</sup>Department of Electrical and Electronic Engineering, Yonsei University, Seoul, Korea, Republic of, <sup>2</sup>Department of Radiotherapy, Division of Imaging & Oncology, University Medical Center Utrecht, Utrecht, Netherlands, <sup>3</sup>Computational Imaging Group for MR diagnostics and therapy, Center for Image Sciences, University Medical Center Utrecht, Utrecht, Netherlands, <sup>4</sup>Department of Radiology, Gangnam Severance Hospital, Seoul, Korea, Republic of

Electrical Properties Tomography reconstruction technique is highly sensitive to noise, as it requires Laplacian calculations of phase data. To alleviate the noise amplification, large derivative kernels combined with image filters are used. However, this leads to severe errors at tissue boundaries. In this study, we employ a deep learning-based denoising network allowing for noise robust conductivity reconstructions obtained using smaller derivative kernels sizes. This comes with the intrinsic advantage of reduced boundary errors. The feasibility study was performed using cylindrical numerical simulations. Then, the proposed technique was tested using spin echo *in-vivo* data, and clinical patient data.

0182



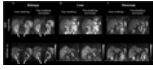
### Protocol Optimization for *in vivo* Electrical Properties Tomography of the Human Breast at 3T

Wyger Brink<sup>1</sup>, Loes Huijnen<sup>1</sup>, Reijer Leijssen<sup>1</sup>, Remco Overdevest<sup>1</sup>, Andrew Webb<sup>1</sup>, and Lucia Bossoni<sup>1</sup>

<sup>1</sup>C.J. Gorter Center for High Field MRI, dept. Radiology, Leiden University Medical Center, Leiden, Netherlands

This work demonstrates a clinically feasible protocol and reconstruction pipeline which is relatively straightforward to implement, and achieves reliable conductivity reconstructions of the human breast. We aim to establish a reliable MR protocol with a scan time of 6 minutes to further develop the clinical potential of this technique.

0183



### Reduction strategies for breathing motion artifacts in abdominal MR elastography

Mehrgan Shahryari<sup>1</sup>, Helge Herthum<sup>1</sup>, Gergely bertalan<sup>1</sup>, Tom Meyer<sup>1</sup>, Heiko Tzschätzsch<sup>1</sup>, Carsten Warmuth<sup>1</sup>, Jürgen Braun<sup>2</sup>, and Ingolf Sack<sup>1</sup>

<sup>1</sup>Department of Radiology, Charité - Universitätsmedizin Berlin, Berlin, Germany, <sup>2</sup>Institute of Medical Informatics, Charité - Universitätsmedizin Berlin, Berlin, Germany

MR elastography can provide high-resolution stiffness maps of abdominal organs. However, MRE – in particular when applied with multiple drive frequencies – requires measure times which significantly exceed single breath holds. Therefore, reduction strategies for motion artifacts are required including breath-holds, navigators and image registration, which all were consistently applied and analyzed in this in-vivo study. Our results show that displacement of organs is smallest during breath-hold MRE while, remarkably, mean stiffness values are not significantly affected by breathing. Overall image quality is comparable between breath-hold and free-breathing MRE when the latter is corrected by 2D-image registration during post processing.

0184



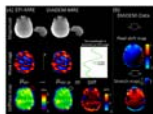
### Microscopic multifrequency MR elastography with 40 micrometer spatial resolution: Application to murine neural tissue specimens

Gergely Bertalan<sup>1</sup>, Bettina Müller<sup>2</sup>, Leif Schröder<sup>3</sup>, Heiko Tzschätzsch<sup>1</sup>, Mehrgan Shahryari<sup>1</sup>, Helge Herthum<sup>1</sup>, Jing Guo<sup>1</sup>, Jürgen Braun<sup>4</sup>, and Ingolf Sack<sup>1</sup>

<sup>1</sup>Department of Radiology, Charite Universitätsmedizin Berlin, Berlin, Germany, <sup>2</sup>Tierhaltung CCM, Charite Universitätsmedizin Berlin, Berlin, Germany, <sup>3</sup>Molecular Imaging, Leibniz Forschungsinstitut für Molekulare Pharmakologie, Berlin, Germany, <sup>4</sup>Department of medical Informatics, Charite Universitätsmedizin Berlin, Berlin, Germany

The purpose of this study was the development of multifrequency MR elastography (MRE) of tissue samples with 40 micrometer pixel edge size for analyzing the mechanical properties of murine neural tissue. The new technique revealed in specimens of cerebellum and cortical brain areas that white matter is significantly stiffer than gray matter. Microscopic multifrequency MRE provides insight into micro mechanical structures of ex-vivo soft tissues and might be used in the future to investigate fresh biopsy samples.

0185



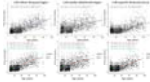
### High-Resolution Distortion-Free Whole-Brain MR Elastography using Multiband DIADEM (DIADEM-MRE)

Yi Sui<sup>1</sup>, MyungHo In<sup>1</sup>, Ziying Yin<sup>1</sup>, Matthew A. Bernstein<sup>1</sup>, Richard L. Ehman<sup>1</sup>, and John III Huston<sup>1</sup>

<sup>1</sup>Radiology, Mayo Clinic, Rochester, MN, United States

The purpose of this study is to implement a distortion-free technique, termed DIADEM (Distortion-free Imaging: A Double Encoding Method) into brain MR Elastography (MRE). The distortion-free whole-brain MRE images with 2-mm isotropic resolution can be achieved using the proposed technique within 6 minutes. The feasibility of DIADEM-MRE was successfully demonstrated on healthy volunteers and patients with brain tumors.

0186



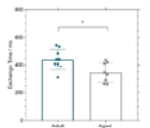
## Perivascular space imaging across the lifespan

Kirsten M Lynch<sup>1</sup>, Giuseppe Barisano<sup>1</sup>, Arthur W Toga<sup>1</sup>, and Farshid Seppehrband<sup>1</sup>

<sup>1</sup>Mark and Mary Stevens Institute for Neuroimaging and Informatics, University of Southern California, Los Angeles, CA, United States

The perivascular space (PVS) is a major component of the glymphatic system and it promotes functional brain clearance. PVS enlargement has been observed in neurological disorders and is considered a biomarker for vascular pathology, however its role in normative development is not well understood. Using a novel technique to segment PVS, we sought to quantify age-related changes in PVS across the lifespan in a large cross-sectional cohort of cognitively normal individuals. We found age was significantly and positively associated with PVS throughout the brain and these results provide a first step towards understanding the typical evolution of brain clearance mechanisms.

0187



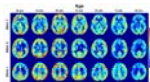
## Increased Blood-Brain Interface Water Permeability in the Ageing Brain detected using non-invasive Multiple Echo Time ASL MRI

Yolanda Ohene<sup>1</sup>, Ian F. Harrison<sup>1</sup>, David L. Thomas<sup>2,3,4</sup>, Mark F. Lythgoe<sup>1</sup>, and Jack A. Wells<sup>1</sup>

<sup>1</sup>Centre for Advanced Biomedical Imaging, UCL, London, United Kingdom, <sup>2</sup>Neuroradiological Academic Unit, UCL Queen Square Institute of Neurology, UCL, London, United Kingdom, <sup>3</sup>Dementia Research Centre, UCL Queen Square Institute of Neurology, UCL, London, United Kingdom, <sup>4</sup>Wellcome Centre for Humans Neuroimaging, UCL Queen Square Institute of Neurology, UCL, London, United Kingdom

Multi-TE ASL technique detects a significant increase (32%) in blood-brain interface (BBI) permeability in the ageing brain. The change in BBI water permeability is associated with a marked increase ( $1.9 \pm 0.4$  fold) in expression of PDGFR $\beta$ , an index of pericyte coverage, and changes to aquaporin water channels and their anchoring proteins in the ageing brain. This technique is a promising non-invasive tool to measure age-related changes to the BBI, that may play a mechanistic role in the pathogenesis of neurodegenerative conditions.

0188



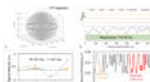
## Association of age and sex with cerebral blood flow measured using pseudo-continuous arterial spin labeling imaging

Joseph Alisch<sup>1</sup>, Nikkita Khattar<sup>1</sup>, Richard Wonjoong Kim<sup>1</sup>, Abinand C. Rejimon<sup>1</sup>, Luis E. Cortina<sup>1</sup>, Wenshu Qian<sup>1</sup>, Mustapha Bouhrara<sup>1</sup>, and Richard G. Spencer<sup>1</sup>

<sup>1</sup>NIA, NIH, Baltimore, MD, United States

Cerebral blood flow (CBF) has been shown to decline with age and differs between men and women. However, limited work has been conducted on cognitively unimpaired subjects. Furthermore, most investigations focus on gray matter (GM), with few results reported for white matter (WM), in which CBF is lower and represents a particularly challenging measurement. We investigate associations of age and sex with CBF in GM and WM regions in a cohort of cognitively unimpaired subjects across a wide age range. We find significant correlations between CBF and age, as well as sexual dimorphism of CBF, in critical brain structures.

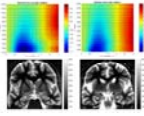
0189

Dynamic sodium (<sup>23</sup>Na) MRI for mapping CSF bulk flow in tissue extracellular space for clearance in human brainsYongxian Qian<sup>1</sup>, Karthik Lakshmanan<sup>1</sup>, Yulin Ge<sup>1</sup>, Yvonne W. Lui<sup>1</sup>, Thomas Wisniewski<sup>2</sup>, and Fernando E. Boada<sup>1</sup>

<sup>1</sup>Radiology, New York University, New York, NY, United States, <sup>2</sup>Neurology, New York University, New York, NY, United States

This study presents preliminary data to demonstrate the potential of dynamic sodium MRI for mapping cerebrospinal fluid (CSF) bulk flow in extracellular space of tissues in whole brain.

0190



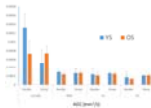
### Age-dependent variation in CEST signal at low B<sub>1</sub> may reflect decline of lipids in older brain tissue

Abigail Cember<sup>1,2</sup>, Puneet Bagga<sup>1</sup>, Hari Hariharan<sup>1</sup>, and Ravinder Reddy<sup>1</sup>

<sup>1</sup>Center for Magnetic Resonance and Optical Imaging, University of Pennsylvania, Philadelphia, PA, United States, <sup>2</sup>Graduate Group in Biochemistry and Biophysics, University of Pennsylvania, Philadelphia, PA, United States

In investigating the problem of CEST correction methods for low saturation B<sub>1</sub>, we observed differences in the behavior of the CEST asymmetry signal as a function of age. We believe this incidental observation to be a manifestation of the low saturation power induced NOE reported in other literature. In this case, we hypothesize that the physiological phenomenon underlying the pattern we observe is a decrease in myelin or other lipids in the aging brain. Our T<sub>1</sub> maps corroborate literature collected at lower field strength that T<sub>1</sub> values increase with age; however, this appears to be an independent, if related, phenomenon.

0191



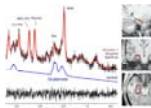
### Altered lactate dynamics with age in human brain during sleep

Manoj K. Sammi<sup>1</sup>, Katherine Powers<sup>1</sup>, Chloe Robinson<sup>1</sup>, Selda Yildiz<sup>1,2</sup>, Miranda Lim<sup>2,3,4,5,6</sup>, Jeffrey J Iliff<sup>7,8,9,10,11</sup>, and William D Rooney<sup>1,2,5,9</sup>

<sup>1</sup>Advanced Imaging Research Center, Oregon Health & Science University, Portland, OR, United States, <sup>2</sup>Department of Neurology, Oregon Health & Science University, Portland, OR, United States, <sup>3</sup>VA Portland Health Care System, Portland, OR, United States, <sup>4</sup>Department of Medicine, Division of Pulmonary and Critical Care Medicine, Oregon Health & Science University, Portland, OR, United States, <sup>5</sup>Department of Behavioral Neuroscience, Oregon Health & Science University, Portland, OR, United States, <sup>6</sup>Oregon Institute of Occupational Health Sciences, Oregon Health & Science University, Portland, OR, United States, <sup>7</sup>Department of Neurology, University of Washington, Seattle, WA, United States, <sup>8</sup>Department of Anesthesiology and Perioperative Medicine, Oregon Health & Science University, Portland, OR, United States, <sup>9</sup>Knight Cardiovascular Institute, Oregon Health & Science University, Portland, OR, United States, <sup>10</sup>VISN 20 Mental Illness Research, Education and Clinical Center (MIRECC), VA Puget Sound Health Care System, Seattle, WA, United States, <sup>11</sup>Department of Psychiatry and Behavioral Sciences, University of Washington, Seattle, WA, United States

Lactate dynamics during sleep-awake cycle in human brain are studied non-invasively using single voxel diffusion weighted magnetic resonance spectroscopy (MRS) technique with simultaneous polysomnography (PSG) recordings to characterize sleep stages. Awake lactate apparent diffusion coefficients (ADC) values are large compared to other brain metabolites and may support active transport - Astrocyte-Neuron Lactate Shuttle (ANLS) mechanism. Lactate ADC are reduced in deep sleep stage in young subjects but are unchanged in older subjects. These results may reflect different interstitial fluid exchange activity or changed metabolic state with aging and require further research.

0192



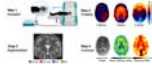
### Age differences in hippocampal glutamate modulation during associative encoding: A proton functional magnetic resonance spectroscopy study

Chaitali Anand<sup>1</sup>, Dalal Khatib<sup>1</sup>, Cheryl Dahle<sup>2</sup>, Naftali Raz<sup>2</sup>, and Jeffrey Stanley<sup>1</sup>

<sup>1</sup>Psychiatry and Behavioral Neuroscience, Wayne State University, Detroit, MI, United States, <sup>2</sup>Psychology, Wayne State University, Institute of Gerontology, Detroit, MI, United States

Memory declines early in normal aging, worsening in dementia. Glutamatergic neurons, abundant in the hippocampus, play a pivotal role in synaptic plasticity underlying formation of associations. We have previously demonstrated with <sup>1</sup>H fMRS, significant modulation of hippocampal glutamate during encoding of object-location associations. We observed that the timing of modulation differentiated proficiency in acquiring the associations. Because age-related hippocampal atrophy may be accompanied by glutamatergic dysfunction, age-differences in task-related levels of hippocampal glutamate may provide a marker of age-related memory deficits. Here, we identified age-differences in hippocampal glutamate modulation during associative memory encoding, which may underlie age-related associative memory deficits.

0193



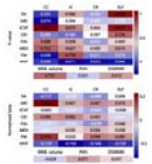
### Reliable High-Resolution MR Elastography Protocol to Assess Hippocampal Subfield Viscoelasticity in Aging

Peyton L Delgorio<sup>1</sup>, Lucy V Hiscox<sup>1</sup>, Ryan T Pohlig<sup>1</sup>, Faria Sanjana<sup>1</sup>, Ana M Daugherty<sup>2</sup>, Hillary Schwarb<sup>3</sup>, Christopher R Martens<sup>1</sup>, Matthew DJ McGarry<sup>4</sup>, and Curtis L Johnson<sup>1</sup>

<sup>1</sup>University of Delaware, Newark, DE, United States, <sup>2</sup>Wayne State University, Detroit, MI, United States, <sup>3</sup>University of Illinois at Urbana-Champaign, Urbana, IL, United States, <sup>4</sup>Dartmouth College, Hanover, NH, United States

The goal of this study is to generate the first high-resolution magnetic resonance elastography (MRE) protocol specifically for characterizing viscoelasticity of the hippocampal subfields (HCsf) and analyzing the effects of age on HCsf properties. We demonstrated that the protocol can sensitively and reliably differentiate between HCsf regions. We find that each HCsf decreases in stiffness and increases in damping ratio with age, and that HCsf exhibit differential relationships with age. This protocol shows promise for investigating the HCsf in health and disease.

0194



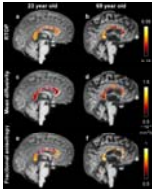
### Effects of Arterial Stiffness on Cerebral White Matter Integrity in the Elderly

Koji Kamagata<sup>1</sup>, Christina Andica<sup>1</sup>, Kazunori Shimada<sup>2</sup>, Hideyoshi Kaga<sup>3</sup>, Yuki Someya<sup>3,4</sup>, Yuya Saito<sup>1,5</sup>, Toshiaki Akashi<sup>1</sup>, Akihiko Wada<sup>1</sup>, Yoshifumi Tamura<sup>3,4</sup>, Ryuzo Kawamori<sup>3,4</sup>, Hirotaka Watada<sup>3</sup>, Hiroyuki Daida<sup>2</sup>, and Shigeki Aoki<sup>1</sup>

<sup>1</sup>Department of Radiology, Juntendo University, Tokyo, Japan, <sup>2</sup>Department of Cardiovascular Medicine, Juntendo University, Tokyo, Japan, <sup>3</sup>Department of Metabolism & Endocrinology, Juntendo University, Tokyo, Japan, <sup>4</sup>Sportology Center, Juntendo University, Tokyo, Japan, <sup>5</sup>Department of Radiological Sciences, Tokyo Metropolitan University, Tokyo, Japan

Arterial stiffness has been shown to be associated with structural and functional abnormalities in the brain; however, white matter pathology related to arterial stiffness is poorly understood. In this study, we used white matter (WM) sensitive techniques (diffusion tensor imaging, neurite orientation dispersion and density imaging, free-water imaging, and magnetization transfer-saturation imaging) to better understand the impact of arterial stiffness on the WM microstructure in healthy elderly individuals. Our results suggest that arterial stiffness largely affects the content of cerebral myelin, as reflected by the myelin volume fraction.

0195



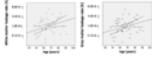
### Return-to-origin probability from single-shell and multi-shell diffusion MRI data correlates with normal aging

Qiyuan Tian<sup>1,2</sup>, Qiuyun Fan<sup>1,2</sup>, Kimberly A. Stephens<sup>1</sup>, Chanon Ngamsombat<sup>1</sup>, Maya Polackal<sup>1</sup>, Brian E. Edlow<sup>1</sup>, Jennifer A. McNab<sup>3</sup>, David Salat<sup>1</sup>, and Susie Y. Huang<sup>1,2</sup>

<sup>1</sup>Martinos Center for Biomedical Imaging, Massachusetts General Hospital, Charlestown, MA, United States, <sup>2</sup>Department of Radiology, Harvard Medical School, Boston, MA, United States, <sup>3</sup>Department of Radiology, Stanford University, Stanford, CA, United States

Return-to-origin probability (RTOP) measures the overall restriction of the microstructural environment and has been used to map microstructural changes related to age and pathology. However, measurement of RTOP requires either specialized acquisition (Cartesian q-space sampling) or processing (q-space gridding or modelling). We show that RTOP from multi-shell data is a weighted summation of the spherical mean signal of each individual shell. We apply our method to a multi-shell dataset of 40 subjects with b-values up to 17,800 s/mm<sup>2</sup> and a dataset of 160 subjects from Lifespan Human Connectome Project in Aging and demonstrate its utility in mapping age-related microstructural change.

0196



#### Increase in blood-brain barrier disruption during normal aging

Inge Verheggen<sup>1</sup>, Joost de Jong<sup>2</sup>, Martin van Boxtel<sup>1</sup>, Frans Verhey<sup>1</sup>, Jacobus Jansen<sup>2,3</sup>, and Walter Backes<sup>2</sup>

<sup>1</sup>Department of Psychiatry and Neuropsychology, Maastricht University, Maastricht, Netherlands,

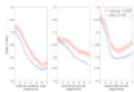
<sup>2</sup>Department of Radiology and Nuclear Medicine, Maastricht University Medical Center, Maastricht,

Netherlands, <sup>3</sup>Department of Electrical Engineering, Eindhoven University of Technology, Eindhoven, Netherlands

Blood-brain barrier (BBB) disruption is assumed to increase with age, but this has not been demonstrated assessing gadolinium leakage using dynamic contrast-enhanced MRI.

We determined BBB leakage rate in healthy middle-aged to elderly individuals (47 - 91 years) combining DCE MRI with pharmacokinetic modeling. Results demonstrated BBB leakage in white and gray matter increased with age. However, this effect was not independent of white matter lesions or cortical thinning, so other physiological changes may influence the age and leakage association. Our study demonstrates that BBB disruption manifests in normal aging, before the emergence of neuropathology.

0197



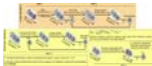
#### Measuring Biological Gradients along the Human Dorsal Striatum in vivo using Quantitative MRI

Elior Drori<sup>1</sup>, Shir Filo<sup>1</sup>, and Aviv Mezer<sup>1</sup>

<sup>1</sup>The Edmond and Lily Safra Center for Brain Sciences, The Hebrew University of Jerusalem, Jerusalem, Israel

To date there are no *in vivo* tools for quantifying spatial changes in the microstructure of subcortical gray-matter nuclei. We have developed a quantitative MRI tool, with which we measured variations along the human dorsal striatum, using quantitative T1. We found monotonic gradients along the main axes, consistent with known biological gradients of the striatum. In addition, we found effects of laterality, as well as aging effects. Our method can prove useful for detection and quantification of microstructural irregularities in the striatum in patients suffering from basal ganglia disorders, such as Parkinson's disease and ADHD.

0198



#### Development of a spatio-temporally consistent longitudinal structural template of the older adult brain

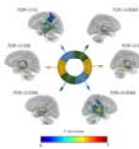
Abdur Raquib Ridwan<sup>1</sup>, Mohammad Rakeen Niaz<sup>1</sup>, Yingjuan Wu<sup>1</sup>, Xiaoxiao Qi<sup>1</sup>, David A. Bennett<sup>2</sup>, and Konstantinos Arfanakis<sup>1,2</sup>

<sup>1</sup>Biomedical Engineering, Illinois Institute of Technology, Chicago, IL, United States, <sup>2</sup>Rush Alzheimer's Disease center, Rush University Medical Center, Chicago, IL, United States

One of the major challenges in constructing a longitudinal structural template of the older adult brain is to ensure spatio-temporal consistency. In this work, a new method was introduced to construct a spatio-temporally consistent longitudinal structural template of the older adult brain based on high quality cross-sectional older adult data from a large cohort. The new template was compared to templates generated with previously published methods in terms of spatio-temporal consistency, image quality, and representativeness of age-related brain changes, and was shown to have superior performance.



0199



Diffusion measures and Connectometry in the Human Hippocampal-Subfields Using Super-Resolution HYDI.

Nahla M H Elsaid<sup>1,2</sup>, Pierrick Coupé<sup>3,4</sup>, Andrew J Saykin<sup>1,2</sup>, and Yu-Chien Wu<sup>1,2</sup>

<sup>1</sup>Department of Radiology and Imaging Sciences, Indiana University, Indianapolis, IN, United States, <sup>2</sup>Indiana Alzheimer Disease Center, Indiana University, Indianapolis, IN, United States, <sup>3</sup>LaBRI, UMR 5800, University of Bordeaux, Talence, France, <sup>4</sup>LaBRI, UMR 5800, PICTURA, F-33400, CNRS, Talence, France

The aging process is known to cause morphological and structural alterations in the human brain. Using a sub-millimeter super-resolution hybrid diffusion imaging (HYDI), we studied the effects of aging on the structural connectivity between the hippocampal subfields as well as between the hippocampus and the cerebral cortex.

0200



A multi-center study to investigate the relationship between iron content in deep gray matter nuclei and age

Yan Li<sup>1</sup>, Sean K. Sethi<sup>2,3</sup>, Chengyan Wang<sup>4</sup>, Weibo Chen<sup>5</sup>, Naying He<sup>1</sup>, Ewart Mark Haacke<sup>3</sup>, and Fuhua Yan<sup>1</sup>

<sup>1</sup>Department of Radiology, Ruijin Hospital, Shanghai Jiao Tong University School of Medicine, Shanghai, China, <sup>2</sup>The MRI Institute for Biomedical Research, Magnetic Resonance Innovations, Inc., Detroit, MI, United States, <sup>3</sup>Department of Radiology, Wayne State University, Detroit, MI, United States, <sup>4</sup>Human Phenome Institute, Fudan University, Shanghai, China, <sup>5</sup>Philips Healthcare, Shanghai, China

To investigate the correlation of iron content in deep gray matter nuclei as a function of age by reconstructed quantitative susceptibility mapping (QSM) using both whole-structural and regional perspectives from three different MRI sites and three different scanners to show that QSM is a robust technology across manufacturers and resolution.

## Oral

### Neurodegeneration 1 - Extrapyrimal Disease

Monday Parallel 2 Live Q&A

Monday 14:30 - 15:15 UTC

Moderators: Maria Eugenia Caligiuri

0201



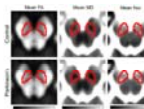
Introducing Substantia Nigra Iron Content and Neuromelanin Overlap to Distinguish Parkinson's Patients from Healthy Controls

Naying He<sup>1</sup>, Kiarash Ghassaban<sup>2,3</sup>, Pei Huang<sup>4</sup>, Zenghui Cheng<sup>1</sup>, Yan Li<sup>1</sup>, Mojtaba Jokar<sup>5</sup>, Sean K. Sethi<sup>2,5</sup>, Weibo Chen<sup>6</sup>, Shengdi Chen<sup>4</sup>, Fuhua Yan<sup>1</sup>, and Ewart Mark Haacke<sup>1,2,5</sup>

<sup>1</sup>Radiology, Ruijin Hospital, Shanghai Jiaotong Univ. School of Medicine, Shanghai, China, Shanghai, China, <sup>2</sup>Department of Radiology, Wayne State University, Detroit, MI, United States, <sup>3</sup>Department of Biomedical Engineering, Wayne State University, Detroit, MI, United States, <sup>4</sup>Department of Neurology, Ruijin Hospital, Shanghai Jiao Tong University School of Medicine, Shanghai, China, <sup>5</sup>Magnetic Resonance Innovations, Inc., Bingham Farms, Bingham Farms, MI, United States, <sup>6</sup>Philips Healthcare, Shanghai, China

A total of 40 Parkinson's disease (PD) patients and 40 age- and sex-matched healthy controls (HC) were scanned using a single 3D gradient echo magnetization transfer sequence to measure neuromelanin and iron content, and the overlap between them. These measures showed reliable results indicative of powerful diagnostic biomarkers to differentiate PD patients from HCs. An increase in iron content was seen in the substantia nigra for the PD patients while the neuromelanin volume decreased. The best predictor, however, was found to be the combination of neuromelanin volume and its overlap with iron-containing substantia nigra which yielded an AUC of 98%.

0202



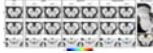
Reinterpreting Parkinson's disease-related diffusion signal changes in substantia nigra

Jason Langley<sup>1</sup>, Daniel E Huddleston<sup>2</sup>, Evan Oculam<sup>3</sup>, Stewart Factor<sup>2</sup>, and Xiaoping Hu<sup>1,3</sup>

<sup>1</sup>Center for Advanced Neuroimaging, University of California Riverside, Riverside, CA, United States, <sup>2</sup>Neurology, Emory University, Atlanta, GA, United States, <sup>3</sup>Bioengineering, University of California Riverside, Riverside, CA, United States

Parkinson's disease is a progressive, neurodegenerative disorder characterized by asymmetrical onset of motor symptoms such as bradykinesia, rigidity, and tremor. The principal pathology in Parkinson's disease is the loss of melanized dopamine neurons in the substantia nigra pars compacta (SNpc) with iron deposited alongside this neuronal loss. Loss of SNpc neurons should remove barriers for diffusion and increase diffusivity of water molecules in regions undergoing this loss. Studies examining Parkinsonian SNpc microstructural changes using a single tensor model have yielded conflicting results. Here, we investigate PD-related microstructural changes in multiple compartment and single tensor models.

0203



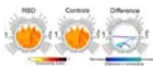
### Investigating Spatiotemporal Changes in the Substantia Nigra of Patients with Prodromal and Clinical Parkinson's Disease

Emma Biondetti<sup>1,2,3</sup>, Rahul Gaurav<sup>1,2,3</sup>, Lydia Yahia-Cherif<sup>1,3</sup>, Graziella Mangone<sup>4</sup>, Nadya Pyatigorskaya<sup>1,2,3,5</sup>, Romain Valabrègue<sup>1,3</sup>, Claire Ewenczyk<sup>2,3</sup>, Matthew Hutchison<sup>6</sup>, Jean-Christophe Corvol<sup>3,4,7</sup>, Marie Vidailhet<sup>2,3,7</sup>, and Stéphane Lehéricy<sup>1,2,3,5</sup>

<sup>1</sup>Brain and Spine Institute - ICM, Centre for NeuroImaging Research - CENIR, Paris, France, <sup>2</sup>Brain and Spine Institute - ICM, Team "Movement Investigations and Therapeutics", Paris, France, <sup>3</sup>Brain and Spine Institute - ICM, INSERM U 1127, CNRS UMR 7225, Sorbonne University, Paris, France, <sup>4</sup>National Institute of Health and Medical Research - INSERM, Clinical Investigation Centre, Pitié-Salpêtrière Hospital, Paris, France, <sup>5</sup>Department of Neuroradiology, Pitié-Salpêtrière Hospital, Public Assistance - Paris Hospitals (AP-HP), Paris, France, <sup>6</sup>Biogen Inc., Cambridge, MA, United States, <sup>7</sup>Department of Neurology, Pitié-Salpêtrière Hospital, Public Assistance - Paris Hospitals (AP-HP), Paris, France

Parkinson's disease (PD) and idiopathic rapid eye movement sleep behaviour disorder (iRBD, a prodromal condition of Parkinsonism) are characterised by the progressive loss of neuromelanin-containing neurons in the substantia nigra (SN). Based on longitudinal neuromelanin-sensitive magnetic resonance imaging (NM-MRI) of healthy controls, patients with iRBD and patients with PD, and voxel-wise analysis of NM-MRI on a study-specific anatomical brain template, we showed the temporal evolution of SN atrophy in disease. We also found significant correlations between temporal changes in the NM-MRI signal-to-noise ratio and clinical scores of disease severity, reflecting the functional organisation (motor, cognition and behaviour/mood) of the SN.

0204



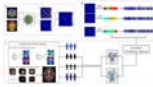
### Brainstem structural connectivity changes in prodromal Parkinson's disease by 7 Tesla HARDI

María Guadalupe García-Gomar<sup>1</sup>, Kavita Singh<sup>1</sup>, Matthew Stauder<sup>2</sup>, Laura D. Lewis<sup>1</sup>, Lawrence L. Wald<sup>1</sup>, Bruce R. Rosen<sup>1</sup>, Aleksandar Videnovic<sup>2</sup>, and Marta Bianciardi<sup>1</sup>

<sup>1</sup>Department of Radiology, Athinoula A. Martinos Center for Biomedical Imaging, Massachusetts General Hospital and Harvard Medical School, Boston, MA, United States, <sup>2</sup>Department of Neurology, Massachusetts General Hospital and Harvard Medical School, Boston, MA, United States

REM-sleep-behavior-disorder (RBD) is a sleep disorder characterized by the absence of muscular atonia during REM sleep. RBD patients have a high risk of developing Parkinson's disease (PD) within 10 years from RBD diagnosis. Thus, RBD allows the investigation of early/prodromal neurodegenerative-stages. Changes in brainstem-nuclei-connectivity are expected in RBD/prodromal-PD based on animal and *ex-vivo* human-studies. Yet, their investigation in living-humans is understudied. Through high-spatial-resolution 7 Tesla HARDI MRI and a recently-developed probabilistic-brainstem-nuclei-atlas, we built a brainstem-based structural-connectome in living RBD-patients and age-matched controls. Interestingly, in RBD-patients we detected structural-connectivity-changes within the brainstem in line with the pathophysiology of RBD in animal-models.

0205



### Clinical-related connectivity features define three biotypes of Parkinson's disease

Tao Guo<sup>1</sup>, Xiaojun Guan<sup>1</sup>, Cheng Zhou<sup>1</sup>, Ting Gao<sup>2</sup>, Jingjing Wu<sup>1</sup>, Peiyu Huang<sup>1</sup>, Xiaojun Xu<sup>1</sup>, and Minming Zhang<sup>1</sup>

<sup>1</sup>Department of Radiology, Second Affiliated Hospital of Zhejiang University School of Medicine, Hangzhou, China, <sup>2</sup>Department of Neurology, Second Affiliated Hospital of Zhejiang University School of Medicine, Hangzhou, China

We establish brain connectivity features that represented the disease signatures and identify Parkinson's disease (PD) subtypes by data-driven approaches. Canonical correlation analysis (CCA) was performed to define the clinical related connectivity features, which were then used in hierarchical cluster analysis to identify the distinct biotypes of PD. Multimodal MRI including gray matter functional connectivity and white matter microstructure were further used to explore the neuropsychological significance of these biotypes. CCA revealed two significant clinical-related patterns in PD. Hierarchical cluster analysis identified three neurophysiological biotypes: mild, progressive depression-dominant and progressive motor-dominant. These three biotypes characterized by different neural substrate.

0206



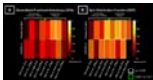
### Association of ApoE gene polymorphism and caudate functional connectivity in mild cognitive impairment of Parkinson's disease

Song'an Shang<sup>1</sup>, Weiqiang Dou<sup>2</sup>, Hongying Zhang<sup>3</sup>, Jing Ye<sup>3</sup>, and Jingtao Wu<sup>3</sup>

<sup>1</sup>Department of Radiology, Nanjing First Hospital, Nanjing Medical University, Nanjing, China, <sup>2</sup>GE Healthcare, MR Research China, Beijing, China, <sup>3</sup>Northern Jiangsu People's Hospital, Yangzhou, China

In this study, we aimed to investigate the association of Apolipoprotein E (ApoE) gene polymorphism and caudate functional connectivity in mild cognitive impairment of Parkinson's disease (PD-MCI), using resting-state functional magnetic resonance imaging (rs-fMRI) and genotyping. Our findings revealed that gene-brain-behavior associations involve alterations of caudate activity with posterior cortical, thereby provide potential imaging-based markers that contribute to the early diagnosis and monitoring of PD-MCI.

0207



### Dopaminergic premotor and motor pathways are dominant in the progression of motor disability in Parkinson's disease

Yao Chia Shih<sup>1</sup>, Septian Hartono<sup>2,3</sup>, Amanda Choo<sup>2</sup>, Celeste Chen<sup>2</sup>, Isabel Chew<sup>1</sup>, Zheyu Xu<sup>2,3</sup>, Louis Tan<sup>2,3</sup>, ChingYu Cheng<sup>3,4</sup>, Eng King Tan<sup>2,3</sup>, and Ling Ling Chan<sup>1,3</sup>

<sup>1</sup>Department of Diagnostic Radiology, Singapore General Hospital, Singapore, Singapore, <sup>2</sup>Department of Neurology, National Neuroscience Institute – SGH Campus, Singapore, Singapore, <sup>3</sup>Duke-NUS Medical School, Singapore, Singapore, <sup>4</sup>Department of Ophthalmology, Yong Loo Lin School of Medicine, National University of Singapore, Singapore, Singapore

White matter microstructural changes in relation to the neurotransmitter systems in Parkinson's disease (PD) progression remains unclear. We used diffusion spectrum imaging and local connectome fingerprint analysis to investigate microstructural integrity of the the premotor and motor pathways in associations with various neurotransmitter systems in the brainstem, and disease duration and severity of motor-related symptoms. We found greater microstructural changes in the dopaminergic pathways in association with motor progression than for the other neurochemical pathways. Patients with longer disease duration or more severe motor dysfunctions showed increased anisotropic water diffusion in these pathways, suggesting a compensatory effect of axonal sprouting.

0208



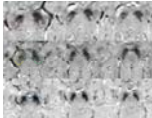
### QUANTITATIVE SUSCEPTIBILITY MAPPING AS A DIAGNOSTIC TOOL TO DISTINGUISH TREMOR DOMINANT PD FROM ESSENTIAL TREMOR.

Shumyla Jabeen<sup>1</sup>, Jitender Saini<sup>1</sup>, Jaladhar Neelavalli<sup>2</sup>, Narayankrishna Rolla<sup>2</sup>, Shweta Prasad<sup>3</sup>, and Ravi Yadav<sup>4</sup>

<sup>1</sup>Neuroimaging and Interventional Radiology, National Institute of Mental Health and Neurosciences, Bangalore, India, <sup>2</sup>Philips India, Bangalore, India, <sup>3</sup>Clinical neurosciences, National Institute of Mental Health and Neurosciences, Bangalore, India, <sup>4</sup>Neurology, National Institute of Mental Health and Neurosciences, bangalore, India

Tremor dominant PD and ET often pose a diagnostic difficulty in view of overlapping clinical features. We aimed at distinguishing the two using the novel technique of QSM to measure iron deposition in various gray matter nuclei including the substantia nigra pars compacta(SNPc). A statistically significant difference was seen in the QSM values of the SNPc, SNPc and caudate nucleus. ROC curve analysis showed a sensitivity and specificity of 90 and 87.5% respectively using a cut off value of 12 ppb for the SNPc. Thus, QSM is a potentially useful problem solving technique for distinguishing tremor dominant PD from ET.

0210



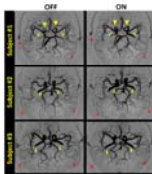
Total loss of "swallow tail sign": a potential substitute of PET for detecting dopaminergic degeneration in early-stage Parkinson's disease

Na Wang<sup>1</sup>, XueLing Liu<sup>2</sup>, and YuXin Li<sup>2</sup>

<sup>1</sup>Fudan university Huashan hospital, Shanghai, China, <sup>2</sup>Huashan Hospital, Fudan University,, Shanghai, China

Whether swallow tail sign (STS) could serve as a substitute or complement for nuclear medical imaging remains unclear. In this study, we compared STS features on MRI with striatal uptake on positron emission tomography (PET) at per nuclei level, construct an evaluation scale based on bilateral STS changes at the patient level, and estimate the diagnostic performance of the scale in 39 early-stage PD and 28 healthy controls. STS alterations corresponded well with striatal uptake on PET in early-stage PD. Total loss of STS is a reliable sign of nigrostriatal dopaminergic degeneration and might be a potential substitute for PET.

0210



Effects of Levodopa Therapy on Cerebral Arteries and Brain Tissue Perfusion in Parkinson's Disease Patients

Yuhui Xiong<sup>1,2</sup>, Lanxin Ji<sup>1</sup>, Le He<sup>1</sup>, Li Chen<sup>3</sup>, Xue Zhang<sup>1</sup>, Zhensen Chen<sup>3</sup>, Xuesong Li<sup>4</sup>, Huilin Zhao<sup>3</sup>, Manabu Shirakawa<sup>3</sup>, Chun Yuan<sup>3</sup>, Yu Ma<sup>5</sup>, and Hua Guo<sup>1</sup>

<sup>1</sup>Center for Biomedical Imaging Research, Department of Biomedical Engineering, School of Medicine, Tsinghua University, Beijing, China, <sup>2</sup>Neusoft Medical Systems Co., Ltd., Shanghai, China, <sup>3</sup>Vascular Imaging Laboratory, Department of Radiology, University of Washington, Seattle, WA, United States, <sup>4</sup>School of Computer Science and Technology, Beijing Institute of Technology, Beijing, China, <sup>5</sup>Tsinghua University Yuquan Hospital, Beijing, China

Parkinson's Disease (PD) has shown to be associated with cerebrovascular abnormalities, but its non-dopaminergic pathological mechanism is less studied. This study investigated the regulatory effect of levodopa, the most-commonly used therapy for PD, on cerebral arteries and blood flow. 57 PD patients and 17 age-matched healthy controls were scanned for artery morphologic and cerebral perfusion imaging at baseline, then the patients were re-scanned 50 minutes after taking levodopa. Results indicated that levodopa elevated blood perfusion level of PD brains to normal levels and dilated proximal arteries. Plus, blood perfusion showed related to motor syndrome scale post-levodopa.

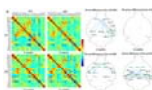
## Oral

### Neurodegeneration 1 - Dementia

Monday Parallel 2 Live Q&A

Monday 14:30 - 15:15 UTC

Moderators: In-Young Choi



Spatio-temporal alterations in functional connectivity, microstructure and cerebral glucose metabolism in a rat model of sporadic Alzheimer's

0211

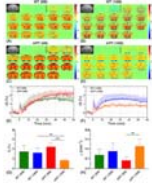


Yujian Diao<sup>1</sup>, Catarina Tristão Pereira<sup>2</sup>, Carole Poitry-Yamate<sup>1</sup>, Ting Yin<sup>1</sup>, Analina Raquel da Silva<sup>1</sup>, Rolf Gruetter<sup>1</sup>, and Ileana Ozana Jelescu<sup>1</sup>

<sup>1</sup>Ecole Polytechnique Fédérale de Lausanne, Lausanne, Switzerland, <sup>2</sup>Faculdade de Ciências da Universidade de Lisboa, Lisbon, Portugal

Impaired brain glucose consumption is a possible trigger of Alzheimer's disease (AD). Animal models can help characterize each contributor to the cascade independently. Here we report a comprehensive longitudinal study of functional connectivity, white matter microstructure and brain glucose metabolism using resting-state fMRI, diffusion MRI and FDG-PET in the intracerebroventricular-streptozotocin rat model of AD. Our study highlights the dynamics of how brain insulin resistance affects brain structure and function, and identifies potent MRI-derived biomarkers to track neurodegeneration in human AD and diabetic populations.

0212



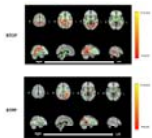
Dynamic glucose enhanced (DGE) MRI at 3T detects alterations in glucose uptake and clearance in young and old Alzheimer's mice

Jianpan Huang<sup>1</sup>, Xiongqi Han<sup>1</sup>, Celia M. Dong<sup>2</sup>, Gerald W. Y. Cheng<sup>3</sup>, Kai-Hei Tse<sup>3</sup>, Lin Chen<sup>4,5</sup>, Joseph H. C. Lai<sup>1</sup>, Ed X. Wu<sup>2</sup>, Peter C. M. van Zijl<sup>4,5</sup>, Jiadi Xu<sup>4,5</sup>, and Kannie W. Y. Chan<sup>1,4</sup>

<sup>1</sup>Department of Biomedical Engineering, City University of Hong Kong, Hong Kong, China, <sup>2</sup>Department of Electrical and Electronic Engineering, The University of Hong Kong, Hong Kong, China, <sup>3</sup>Department of Health Technology and Informatics, The Hong Kong Polytechnic University, Hong Kong, China, <sup>4</sup>Russell H. Morgan Department of Radiology and Radiological Science, The Johns Hopkins University School of Medicine, Baltimore, MD, United States, <sup>5</sup>F.M. Kirby Research Center for Functional Brain Imaging, Kennedy Krieger Research Institute, Baltimore, MD, United States

On-resonance variable delay multiple pulse (onVDMP) CEST MRI was applied to detect dynamic D-glucose enhanced signal in brain parenchyma and CSF of 6- and 16-month old APP/PS1 AD mice. A significantly slower D-glucose clearance from CSF was observed in young AD mice compared to age-matched wild type (WT) mice. Moreover, a reduced D-glucose uptake was observed both in parenchyma and CSF of old APP/PS1 mice. D-glucose kinetics detected by onVDMP can be used to assess the alterations in D-glucose uptake and clearance in AD and in the course of AD progression at 3T, a clinical relevant MRI field.

0213



Assessing White Matter Microstructural Changes Associated with Mild Cognitive Impairment using Laplacian-Regularized MAP MRI

Jason F. Moody<sup>1</sup>, Douglas C. Dean III<sup>1,2,3</sup>, Steven R. Keckskemeti<sup>3</sup>, Jennifer M. Oh<sup>4</sup>, Nagesh Adluru<sup>3</sup>, Sterling C. Johnson<sup>4,5</sup>, Barbara B. Bendlin<sup>4</sup>, and Andrew L. Alexander<sup>1,2,3,6</sup>

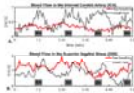
<sup>1</sup>Department of Medical Physics, University of Wisconsin-Madison, Madison, WI, United States, <sup>2</sup>Department of Pediatrics, University of Wisconsin-Madison, Madison, WI, United States, <sup>3</sup>Waisman Center, University of Wisconsin-Madison, Madison, WI, United States, <sup>4</sup>Wisconsin Alzheimer's Disease Research Center, University of Wisconsin-Madison, Madison, WI, United States, <sup>5</sup>Geriatric Research Education and Clinical Center, Middleton Memorial VA Hospital, University of Wisconsin-Madison, Madison, WI, United States, <sup>6</sup>Department of Psychiatry, University of Wisconsin-Madison, Madison, WI, United States

We implement Laplacian-regularized MAP MRI to investigate distinct white matter (WM) microstructural changes associated with mild cognitive impairment (MCI).

Comparisons of diffusion parameters (via TBSS) between healthy controls and MCI patients revealed significant group differences in a wide variety of WM pathways previously shown to be altered in MCI and Alzheimer's Dementia (AD). In particular, the MCI group exhibited WM clusters with lower return to origin probability (RTOP) and return to plane probability (RTPP) magnitudes, suggesting structurally affected axons in those tracts.

Our findings provide an early quantitative framework for identifying specific WM microstructural deficiencies characteristic of MCI and AD.

0214



#### Assessment of Intracranial Vascular Flow Oscillations in Alzheimer's Disease using Real Time 4D Flow MRI

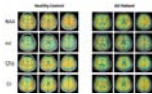
Leonardo A Rivera-Rivera<sup>1</sup>, Laura B Eisenmenger<sup>2</sup>, Sterling C Johnson<sup>3</sup>, and Kevin M Johnson<sup>1,2</sup>

<sup>1</sup>Department of Medical Physics, University of Wisconsin - Madison, Madison, WI, United States,

<sup>2</sup>Department of Radiology, University of Wisconsin - Madison, Madison, WI, United States, <sup>3</sup>Department of Medicine, University of Wisconsin - Madison, Madison, WI, United States

Microvascular oscillations have been speculated to be markers of autoregulation and to be driving forces of glymphatic clearance of interstitial fluid, A $\beta$ , and other soluble metabolites of the brain. To probe spontaneous low frequency oscillations (LFO) in the brain vasculature, measures of blood flow variance during several minutes might hold potential. In this study, we investigated induced LFOs in blood flow with 4D flow using 3D radial sampling and low-rank regularization for real time blood flow variance estimates. Preliminary results showed significant increased blood flow fluctuations in age-matched controls compared to AD subjects.

0215



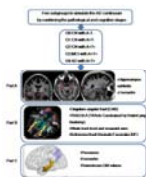
#### Fast 3D High-Resolution Metabolic Imaging in Alzheimer's Disease using SPICE

Jialin Hu<sup>1</sup>, Miao Zhang<sup>2</sup>, Rong Guo<sup>3,4</sup>, Yudu Li<sup>3,4</sup>, Wanqing Sun<sup>1</sup>, Danni Wang<sup>1</sup>, Hui Huang<sup>1</sup>, Yibo Zhao<sup>3,4</sup>, Ziyu Meng<sup>1,3</sup>, Biao Li<sup>2</sup>, Jun Liu<sup>5</sup>, Binyin Li<sup>5</sup>, Jie Luo<sup>1</sup>, Zhi-Pei Liang<sup>3,4</sup>, and Yao Li<sup>1</sup>

<sup>1</sup>Institute for Medical Imaging Technology, School of Biomedical Engineering, Shanghai Jiao Tong University, Shanghai, China, <sup>2</sup>Department of Nuclear Medicine, Ruijin Hospital, Shanghai Jiao Tong University School of Medicine, Shanghai, China, <sup>3</sup>Beckman Institute for Advanced Science and Technology, University of Illinois at Urbana-Champaign, Urbana, IL, United States, <sup>4</sup>Department of Electrical and Computer Engineering, University of Illinois at Urbana-Champaign, Urbana, IL, United States, <sup>5</sup>Department of Neurology and Institute of Neurology, Ruijin Hospital, Shanghai Jiao Tong University School of Medicine, Shanghai, China

As a progressive neurodegenerative disease, early diagnosis of Alzheimer's disease (AD) is important but remains difficult. MRSI is a useful tool for detecting neurometabolic alterations in AD, but most studies were limited by using single-slice or single-voxel techniques with low spatial resolution and long data acquisition time. In this study, we performed 3D MRSI of AD patients at a nominal spatial resolution of  $2.0 \times 3.0 \times 3.0$  mm<sup>3</sup> in a 7-min scan using a new technique called SPICE (SPectroscopic Imaging by exploiting spatioSpectral Correlation). Our experimental results showed noticeable neurometabolic changes in AD patients.

0216



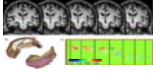
#### Progressive memory circuit impairments along with Alzheimer's disease neuropathology spread: evidence from in vivo neuroimaging

Shuyue Wang<sup>1</sup>, Kaicheng Li<sup>1</sup>, Xiao Luo<sup>1</sup>, Qingze Zeng<sup>1</sup>, Yeerfan Jiaerken<sup>1</sup>, Xiaopei Xu<sup>1</sup>, Yong Zhang<sup>2</sup>, Peiyu Huang<sup>1</sup>, and Minming Zhang<sup>1</sup>

<sup>1</sup>The 2nd Affiliated Hospital of Zhejiang University, School of Medicine, Hangzhou, China, <sup>2</sup>GE Healthcare, Shanghai, China

Along with Alzheimer's disease (AD) continuum, AD neuropathologies propagate trans-neuronally, causing the memory circuit disorganization. The 'misfolded tau protein propagation theory' indicates that tau pathology spread through synaptic connectivity and cause the structural impairments. Here, we hypothesized that HP is the first to suffer from AD neuropathology, then followed by the connected tract and downstream cortex. We defined the memory circuit as the hippocampus (HP), cingulum-angular bundles (CAB), and precuneus cortex, respectively representing the starting point, core connecting fibre and connected downstream cortex. Our results support the **tau propagation theory in the memory circuit in vivo**.

0217



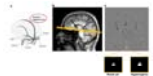
### Association of Hippocampus Fimbria Iron level measured by QSM with AD stages, Hippocampus Atrophy and Aging

Chun Ki Franklin Au<sup>1</sup>, Jill Abrigo<sup>1</sup>, Jack Lee<sup>2</sup>, Chunlei Liu<sup>3</sup>, Wing Chi Lisa Au<sup>4</sup>, Queenie Chan<sup>5</sup>, Qianyun Maxine Chen<sup>1</sup>, Chung Tong Vincent Mok<sup>4</sup>, and Weitian Chen<sup>1</sup>

<sup>1</sup>Department of Imaging and Interventional Radiology, The Chinese University of Hong Kong, Hong Kong, Hong Kong, <sup>2</sup>Centre For Clinical Research And Biostatistics, Centre for Clinical Research and Biostatistics, The Chinese University of Hong Kong, Hong Kong, Hong Kong, <sup>3</sup>Department of Electrical Engineering and Computer Sciences, University of California, Berkeley, USA, CA, United States, <sup>4</sup>Division of Neurology, The Chinese University of Hong Kong, Hong Kong, Hong Kong, <sup>5</sup>Philips, Hong Kong, Hong Kong

**Iron accumulation has been reported in specific brain regions of Alzheimer disease patients. In this study, we used Quantitative Susceptibility Mapping to show iron deposition in hippocampal fimbria and its strong correlation with hippocampus volume and AD stages. Our result might provide further insight of potential disconnection injury in AD pathophysiology.**

0218



### Quantitative assessment of cerebrovascular reactivity in older individuals: relationship to diagnosis, cognition and physical function

Sandeepa Sur<sup>1</sup>, Zixuan Lin<sup>1</sup>, Yang Li<sup>1</sup>, Sevil Yasar<sup>2</sup>, Paul Rosenberg<sup>3</sup>, Abhay Moghekar<sup>4</sup>, Shruti Agarwal<sup>1</sup>, Xirui Hou<sup>1</sup>, Rita Kalyani<sup>5</sup>, Kaisha Hazel<sup>1</sup>, George Pottanat<sup>1</sup>, Cuimei Xu<sup>1</sup>, Peter van Zijl<sup>6</sup>, Jay Pillai<sup>7</sup>, Peiying Liu<sup>1</sup>, Marilyn Albert<sup>4</sup>, and Hanzhang Lu<sup>1</sup>

<sup>1</sup>Department of Radiology, Johns Hopkins University, Baltimore, MD, United States, <sup>2</sup>Department of Gerontology, Johns Hopkins University, Baltimore, MD, United States, <sup>3</sup>Department of Psychiatry and Behavioral Sciences, Johns Hopkins University, Baltimore, MD, United States, <sup>4</sup>Department of Neurology, Johns Hopkins University, Baltimore, MD, United States, <sup>5</sup>Department of Medicine, Johns Hopkins University, Baltimore, MD, United States, <sup>6</sup>F.M. Kirby Research Center, Kennedy Krieger Institute, Baltimore, MD, United States, <sup>7</sup>Department of Neurosurgery, Johns Hopkins University, Baltimore, MD, United States

This study addresses the question, whether quantitative cerebrovascular reactivity (CVR) is a potential vascular biomarker in dementia with Alzheimer's and vascular pathologies. This was tested in a cross-sectional study, where CBF-CVR assessed via Phase-Contrast-MRI during a CO<sub>2</sub> breathing-challenge predicted cognitive and functional performance, disease-severity, and diabetes-risk, in 67 normal and mild-cognitive-impairment subjects. The performance and severity relationships remained robust after adjusting for Alzheimer's disease and competing vascular markers. These findings suggest that quantitative CBF-CVR has potential as a sensitive biomarker for early changes in cognitive and functional performance, and of disease severity in dementia, independent of Alzheimer's disease.

0219



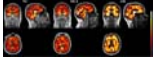
### The neurocognitive effects of VSOP training in mild cognitive impairment (CogTE study): A phase-II clinical trial

Feng Vankee Lin<sup>1</sup>

<sup>1</sup>Center for Advanced Imaging and Neurophysiology, University of Rochester, ROCHESTER, NY, United States

The current lack of effective pharmacological treatments for managing clinical symptoms in Alzheimer's dementia highlights the urgent need for developing non-pharmacological interventions in the field. Here we report a phase II randomized controlled trial that examined the immediate and mid-term effect of a cognitive process based training on multiple cognitive domains in mild cognitive impairment. We found robust intervention effect on processing speed/attention and working memory. These cognitive improvements were associated with both activation changes and network changes involving ACC, a hub for maintaining successful cognitive aging. These results provide new insights about non-pharmacological interventions in preventing dementia.

0220



### Evaluation of neuroinflammation in Alzheimer's disease on human subjects using third-generation TSPO ligand [18F]-GE180

Zhengshi Yang<sup>1</sup>, Karthik Sreenivasan<sup>1</sup>, Xiaowei Zhuang<sup>1</sup>, Aaron Ritter<sup>1</sup>, Jessica Caldwell<sup>1</sup>, Sarah J Banks<sup>2</sup>, Virendra Mishra<sup>1</sup>, Marwan Sabbagh<sup>1</sup>, Dietmar Cordes<sup>1,3</sup>, and Jeffrey Cummings<sup>1,4</sup>

<sup>1</sup>Cleveland Clinic Lou Ruvo Center for Brain Health, Las Vegas, NV, United States, <sup>2</sup>Department of Neuroscience, University of California, San Diego, CA, United States, <sup>3</sup>Department of Psychology and Neuroscience, University of Colorado, Boulder, CO, United States, <sup>4</sup>Department of Brain Health, School of Integrated Health Sciences, University of Nevada, Las Vegas, NV, United States

Inflammatory reactions contribute to disease progression and severity of Alzheimer's disease (AD). While multiple animal studies have suggested that increased neuroinflammation occurs in AD, few studies have investigated neuroinflammation in human subjects. This is the first study using the third-generation TSPO ligand [18F]-GE180 to evaluate the neuroinflammation in AD on human subjects. Our study suggests that neuroinflammation accumulates together with amyloid deposition and reaches a plateau when the regional amyloid SUVR reaches 1.1 threshold. Compared to amyloid pathology, neuroinflammation is more closely related to hyperconnectivity in MCI/AD subjects.

## Oral

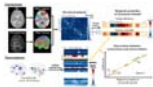
### Pediatric Neuro: Fetal to Adolescence - Pediatric Neuro: Fetal/Newborn/Developmental

Monday Parallel 3 Live Q&A

Monday 14:30 - 15:15 UTC

Moderators: Peiyong Liu & Xin Xu

0221



### Deciphering transcriptomic basis of the human brain structural connectome in the 3rd trimester

Chenyong Zhao<sup>1,2</sup>, Gabriel Santpere<sup>3</sup>, David Andrijevic<sup>3</sup>, Minhui Ouyang<sup>1</sup>, Nenad Sestan<sup>3</sup>, and Hao Huang<sup>1,4</sup>

<sup>1</sup>Department of Radiology, Children's Hospital of Philadelphia, Philadelphia, PA, United States, <sup>2</sup>Department of Bioengineering, School of Engineering and Applied Science, University of Pennsylvania, Philadelphia, PA, United States, <sup>3</sup>Department of Neuroscience and Kavli Institute for Neuroscience, Yale School of Medicine, New Haven, CT, United States, <sup>4</sup>Department of Radiology, Perelman School of Medicine, University of Pennsylvania, Philadelphia, PA, United States

Dramatic development of brain connectome takes place during the 3<sup>rd</sup> trimester, mediated by transcriptome. Transcriptome is complete set of gene-expressed mRNAs and is heterogeneous across brain regions and dynamic throughout development. The transcriptomic basis of structural connectome in this critical developmental stage is unknown. In this study, we identified transcription genes most significantly correlated to nodal efficiency and degree centrality of macroscale structural connectome based on diffusion MRI of 77 preterm brains and over 60,000 quantified transcriptomes. These identified transcription genes such as *MYRF* regulating oligodendrocyte differentiation and myelination may shed light into the transcriptomic basis of structural connectome development.



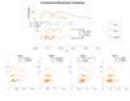
### THE NEONATAL PRETERM BRAIN: A CONNECTOME ANALYSIS

Joana S. de Almeida<sup>1</sup>, Djalel-Eddine Meskaldji<sup>1,2</sup>, Serafeim Loukas<sup>1,3</sup>, Lara Lordier<sup>1</sup>, Laura Gui<sup>4</sup>, François Lazeyras<sup>4</sup>, and Petra S. Hüppi<sup>1</sup>



<sup>1</sup>Department of Women-Children-Teenagers, Hôpitaux Universitaires de Genève, Genève, Switzerland, <sup>2</sup>Institute of Mathematics, Ecole Polytechnique Fédérale de Lausanne, Lausanne, Switzerland, <sup>3</sup>Institute of Bioengineering, Ecole Polytechnique Fédérale de Lausanne, Lausanne, Switzerland, <sup>4</sup>Department of Radiology and Medical Informatics, CIBM, University of Geneva, Genève, Switzerland

Prematurity disrupts brain maturation during a critical period of development, leading to structural brain alterations that might underlie the observed later neurodevelopmental impairments in preterm children. Using diffusion MRI based whole-brain constrained spherical deconvolution tractography, we constructed structural connectomes to study the impact of prematurity on neonatal brain network organization at term-equivalent age. We found that, globally, in comparison to full-term infants, structural networks of very-preterm infants at term showed an increased segregation and decreased capacity to integrate information across brain regions and, in particular, a diminished connectivity strength in subnetworks localized mainly in frontal, limbic and para-limbic regions.

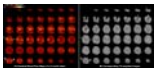


### Hierarchical complexity of the neonatal brain

Manuel Blesa Cabeza<sup>1</sup>, Paola Galdi<sup>1</sup>, Simon R Cox<sup>1</sup>, David Q. Stoye<sup>1</sup>, Gemma Sullivan<sup>1</sup>, Gillian J. Lamb<sup>1</sup>, Alan J Quigley<sup>2</sup>, Michael J. Thrippleton<sup>1</sup>, Javier Escudero Rodriguez<sup>1</sup>, Mark E Bastin<sup>1</sup>, Keith M Smith<sup>1</sup>, and James P Boardman<sup>1</sup>

<sup>1</sup>University of Edinburgh, Edinburgh, United Kingdom, <sup>2</sup>Royal Hospital for Sick Children, Edinburgh, United Kingdom

Preterm birth is associated with long term cognitive deficits and alterations to structural connectivity of developing brain networks. Diversity of connectivity patterns within hierarchically equivalent nodes (hierarchical complexity, HC), is a prominent feature of the adult human connectome. In this work, we show that HC of the structural connectome at birth shares similar properties to HC seen in the adult connectome. Infants born preterm have different HC to infants born at term. In addition, we show that high-level order may be necessary to create structural stability, and this high-level order is resilient to environmental challenges such as preterm birth.

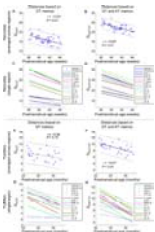


### High-resolution infant cerebral blood flow map measured with 3D multi-shot, stack-of-spirals pCASL

Minhui Ouyang<sup>1</sup>, John Detre<sup>2</sup>, Samantha Linh Lam<sup>1</sup>, J. Christopher Edgar<sup>1,2</sup>, and Hao Huang<sup>1,2</sup>

<sup>1</sup>Department of Radiology, The Children's Hospital of Philadelphia, Philadelphia, PA, United States, <sup>2</sup>Department of Radiology, Perelman School of Medicine, University of Pennsylvania, Philadelphia, PA, United States

During early infancy, dramatic structural and functional maturation of infant brains requires rapid increases of regional cerebral blood flow (rCBF). In this study, we optimized a 3D multi-shot, stack-of-spirals pCASL sequence to obtain high-resolution rCBF maps at isotropic 2.5mm for infants at different maturational stages. Distinctive rCBF distribution patterns at different infant stages of 0-6 months and 7-18 months were revealed. The age-dependent trend lines of rCBF at specific regions were charted. Infant rCBF increases heterogeneously across brain regions, with rCBF increasing faster in visual, prefrontal and parietal cortices than that in precentral and thalamus during this critical period.



### Multivariate Evaluation of White Matter Maturation on Neonates and Toddlers by Diffusion Kurtosis Imaging with Mahalanobis Distance

Xianjun Li<sup>1</sup>, Miaomiao Wang<sup>1</sup>, Fan Wu<sup>1</sup>, Qinli Sun<sup>1</sup>, Heng Liu<sup>1</sup>, Yuli Zhang<sup>1</sup>, Mengxuan Li<sup>1</sup>, Chao Jin<sup>1</sup>, Congcong Liu<sup>1</sup>, Xiaocheng Wei<sup>1</sup>, and Jian Yang<sup>1</sup>

<sup>1</sup>Department of Radiology, the First Affiliated Hospital of Xi'an Jiaotong University, Xi'an, China

Mahalanobis distance is a feasible multivariate approach. This work compared performances of Mahalanobis distances based on different combinations of metrics in assessing the white matter maturation on neonates and toddlers. Mahalanobis distance based on the combination of diffusion tensor and kurtosis tensor metrics demonstrated various advantages: stronger correlation with the postmenstrual age and higher developmental speeds could be revealed; distances from the developing to the adult brains and the changes from neonates to toddlers were enlarged. Results in the current work suggest that diffusion kurtosis imaging with the Mahalanobis distance would benefit the characterization of white matter maturation.

0226



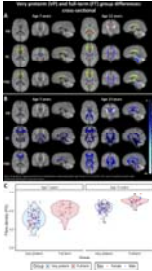
### Prematurity-related brain injuries disrupt thalamocortical reciprocal growth

Audrey Yin<sup>1</sup>, Mengting Liu<sup>1</sup>, Arthur W. Toga<sup>1</sup>, Duan Xu<sup>2</sup>, James Barkovich<sup>2</sup>, and Hosung Kim<sup>1</sup>

<sup>1</sup>USC Stevens Neuroimaging and Informatics Institute, Keck School of Medicine of USC, University of Southern California, Los Angeles, CA, United States, <sup>2</sup>Department of Radiology and Biomedical Imaging, UCSF School of Medicine, University of California, San Francisco, San Francisco, CA, United States

Prematurity-related injuries often result in aberrant brain maturation, specifically on peri-thalamic white matter. We investigated the effects of these injuries on the intra-thalamic tissue integrity and on thalamocortical connectivity. We found that injuries did not substantially affect thalamic volume or thalamic DTI parameters, but did have a substantial effect on the correlative growth between the thalamus and cortex. This implies that brain injuries disrupt the reciprocal development of the thalamus and cortex, which may indicate abnormal thalamocortical connectivity.

0227



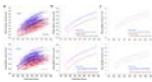
### Longitudinal development of white matter fibre density and morphology in children born very preterm

Claire E Kelly<sup>1,2</sup>, Deanne K Thompson<sup>1,2,3,4</sup>, Sila Genc<sup>2,5</sup>, Jian Chen<sup>2</sup>, Joseph YM Yang<sup>2,3,6,7</sup>, Chris Adamson<sup>2</sup>, Richard Beare<sup>2</sup>, Marc L Seal<sup>2,3</sup>, Jeanie LY Cheong<sup>1,8,9</sup>, Lex W Doyle<sup>1,3,8,9</sup>, and Peter J Anderson<sup>1,10</sup>

<sup>1</sup>Victorian Infant Brain Study (ViBeS), Murdoch Children's Research Institute, Melbourne, Australia, <sup>2</sup>Developmental Imaging, Murdoch Children's Research Institute, Melbourne, Australia, <sup>3</sup>Department of Paediatrics, The University of Melbourne, Melbourne, Australia, <sup>4</sup>Florey Institute of Neuroscience and Mental Health, Melbourne, Australia, <sup>5</sup>Cardiff University Brain Research Imaging Centre (CUBRIC), Cardiff University, Cardiff, United Kingdom, <sup>6</sup>Department of Neurosurgery, The Royal Children's Hospital, Melbourne, Australia, <sup>7</sup>Neuroscience Research, Murdoch Children's Research Institute, Melbourne, Australia, <sup>8</sup>Newborn Research, The Royal Women's Hospital, Melbourne, Australia, <sup>9</sup>Department of Obstetrics and Gynaecology, The University of Melbourne, Melbourne, Australia, <sup>10</sup>Turner Institute for Brain and Mental Health, Monash University, Melbourne, Australia

In this long-term follow-up of children following very preterm (VP) birth, we applied fixel-based analysis to study white matter development. At ages 7 and 13 years, VP children had reduced fibre density and cross-section throughout the white matter compared with full-term controls. Longitudinally, VP children had slower macrostructural development of commissural and motor pathways between ages 7 and 13 years. Younger gestational age, smaller birth weight and neonatal brain abnormalities were associated with lower fibre density and cross-section at both ages. Thus, VP birth and concomitant perinatal risk factors are associated with long-term delays and/or disruptions to white matter development.

0228



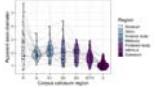
### Influences of Gender, Physical Growth, and Socioeconomic Characteristics on Early Brain Growth in Children from an LMIC Setting.

Sean Deoni<sup>1</sup>, Aarti Kumar<sup>2</sup>, Vishwajeet Kumar<sup>2</sup>, Madhuri Tiwari<sup>2</sup>, John Spencer<sup>3</sup>, and Muriel Bruchhage<sup>4</sup>

<sup>1</sup>MNCHD&T, Bill & Melinda Gates Foundation, Seattle, WA, United States, <sup>2</sup>CEL, Lucknow, India, <sup>3</sup>University of East Anglia, Norwich, United Kingdom, <sup>4</sup>Brown University, Providence, RI, United States

Early brain development is influenced by a myriad of environmental and psychosocial exposures that are often amplified in children in low and middle income countries (LMICs). However, few neuroimaging studies have been performed in these settings. Here we report on the first longitudinal neuroimaging study of young children in rural Uttar Pradesh (UP) India, showing the importance of early weight gain and socioeconomic factors on brain growth. We also find significant male-female differences, which may derive from the lesser societal importance of women, including lower education levels, increased malnutrition, and reduced healthcare seeking for girls.

0229



### Uncovering regional maturation of axon diameter across child and adolescent brain development

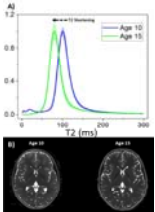
Sila Genc<sup>1</sup>, Erika P Raven<sup>1</sup>, Mark Drakesmith<sup>1</sup>, and Derek K Jones<sup>1,2</sup>

<sup>1</sup>Cardiff University Brain Research Imaging Centre (CUBRIC), Cardiff University, Cardiff, United Kingdom,

<sup>2</sup>Mary MacKillop Institute for Health Research, Australian Catholic University, Melbourne, Australia

The maturation of white matter across childhood and adolescence is predominantly driven by the thickening of myelin and increasing axon density. Previous post-mortem studies have suggested that axon count in the corpus callosum reaches adult levels in the early post-natal period, suggesting that the radial growth of axons may be driving the apparent increases in axon density. In this novel application of paediatric microstructural development, we estimate apparent axon diameter using ultra-strong gradient MRI (300 mT/m) for the first time. Our findings reveal age-related maturation of axon diameter in the genu and body of the corpus callosum.

0230



### Longitudinal Changes of the Extremely Preterm Brain from Age 10 to Age 15: Myelination and Hydration.

Ryan McNaughton<sup>1</sup>, Hernan Jara<sup>2</sup>, Xin Zhang<sup>1</sup>, Mina Botros<sup>2</sup>, Robert M Joseph<sup>2</sup>, Asim Z Mian<sup>2</sup>, Laurie Douglass<sup>2</sup>, Karl Kuban<sup>2</sup>, Rebecca C Fry<sup>3</sup>, and Michael O'Shea<sup>3</sup>

<sup>1</sup>Mechanical Engineering, Boston University, Boston, MA, United States, <sup>2</sup>Boston University Medical Center, Boston, MA, United States, <sup>3</sup>University of North Carolina at Chapel Hill School of Medicine, Chapel Hill, NC, United States

Purpose: To identify new qMRI markers for assessing changes in hydration and myelination during development of the extremely preterm (EP) brain. Methods: Quantitative MR algorithms create maps of the transverse relaxation time (T2) and normalized proton density (PD) for 7 EP born individuals using MR images obtained at age 10 and age 15 years. Results: White and grey matter of the EP brain demonstrate increases in proton density and significant decreases in tissue T2. Conclusion: Decreases in T2 potentially describes the evolution of a more myelin rich environment with age, motivating a new method to assess myelination during brain development.

## Oral

### Pediatric Neuro: Fetal to Adolescence - Pediatric Neuro: Epilepsy & Brain Injury

Monday Parallel 3 Live Q&A

Monday 14:30 - 15:15 UTC

Moderators: Matthew Barkovich & Ashley Harris

0231



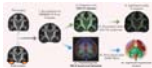
### Towards clinical implementation of multi-shell diffusion MRI: visual pathway investigation in paediatric epilepsy surgery

Luis Miguel Lacerda<sup>1</sup>, Jon Clayden<sup>1</sup>, Sian Handley<sup>2</sup>, Martin Tisdall<sup>3</sup>, Enrico Kaden<sup>4</sup>, Gavin Winston<sup>5</sup>, Alki Liasis<sup>2,6</sup>, Helen Cross<sup>7</sup>, and Chris Clark<sup>1</sup>

<sup>1</sup>Developmental Imaging and Biophysics Section, UCL Great Ormond Street Institute of Child Health, London, United Kingdom, <sup>2</sup>Clinical and Academic Department of Ophthalmology, Great Ormond Street Hospital for Children NHS Foundation Trust, London, United Kingdom, <sup>3</sup>Neurosurgery, Great Ormond Street Hospital for Children NHS Foundation Trust, London, United Kingdom, <sup>4</sup>Centre for Medical Image Computing, University College London, London, United Kingdom, <sup>5</sup>Department of Clinical and Experimental Epilepsy, UCL Institute of Neurology, London, United Kingdom, <sup>6</sup>University of Pittsburgh Medical Centre, Children's Hospital of Pittsburgh, Pittsburgh, PA, United States, <sup>7</sup>Clinical Neurosciences, UCL Great Ormond Street Institute of Child Health, London, United Kingdom

We used multi-shell diffusion imaging to investigate differences in the visual pathways of children undergoing epilepsy surgery and demonstrated its potential for clinical practice. In particular, we compared the traditional Diffusion Tensor Imaging model with the Spherical Mean Technique model and evaluated its potential to produce measures of tissue microstructure not confounded by orientation effects in both a healthy and patient population. Furthermore, we explored the effect of brain surgery and applied Constrained Spherical Deconvolution derived tractography to determine the frequency and influence of the extent and location of resection on the integrity of the visual system after the operation.

0232



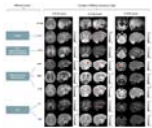
Emergence of distinct structural reorganization patterns in children as a result of temporal lobe epilepsy surgery – beyond voxel-based analysis

Luis Miguel Lacerda<sup>1</sup>, Pedro Luque Laguna<sup>2,3</sup>, Flavio Dell'acqua<sup>2,3</sup>, and Chris Clark<sup>1</sup>

<sup>1</sup>Developmental Imaging and Biophysics Section, Institute of Child Health, University College London, London, United Kingdom, <sup>2</sup>Forensic & Neurodevelopmental Sciences, King's College London, London, United Kingdom, <sup>3</sup>Sackler Institute for Translational Neurodevelopment, Institute of Psychiatry, Psychology and Neuroscience, King's College London, London, United Kingdom

We compared Tract-based Spatial Statistics (TBSS) with a recent method which relies on non-statistical parametric mapping in a tractography derived anatomical framework – tract-based cluster analysis (TBCA) - to explore the effect of surgery in Temporal Lobe Epilepsy. In particular, we investigated differences in fractional anisotropy (FA) as an effect of surgery, and if those changes depended on operated hemisphere. We found the same patterns of increased FA on the corona radiata and decreased FA in tracts traversing the temporal lobe with TBSS, whilst TBCA allowed for an increase in anatomical specificity when interpreting differences in this group.

0233

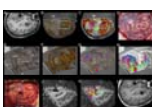


MRI profiling of focal cortical dysplasia using advanced diffusion models

Sara Lorio<sup>1</sup>, Sophie Adler<sup>2</sup>, Roxana Gunny<sup>3</sup>, Felice D'Arco<sup>3</sup>, Enrico Kaden<sup>2</sup>, Konrad Wagstyl<sup>2</sup>, Thomas Jacques<sup>2,3</sup>, Chris Clark<sup>2</sup>, Helen Cross<sup>2</sup>, Torsten Baldeweg<sup>2</sup>, and David W. Carmichael<sup>1</sup>

<sup>1</sup>King's College London, LONDON, United Kingdom, <sup>2</sup>UCL, London, United Kingdom, <sup>3</sup>Great Ormond Street Hospital, London, United Kingdom

Lesion detection and sub-typing for focal cortical dysplasia (FCD), a frequent cause of drug-resistant epilepsy, remain challenging on conventional MRI. New diffusion models such as the spherical mean techniques (SMT) and the neurite orientation dispersion and density imaging (NODDI) provide measurements that are potentially more specific to abnormal tissue microstructure. Quantitative analysis of lesion profiling demonstrated significant changes on NODDI and SMT maps proportional to neurites density, as well on microscopic mean, radial and axial diffusivities. Moreover, signal changes specific to FCD lesions sub-types were observed on those maps, suggesting they can provide features useful for automated lesion detection.

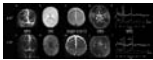


One-stage, language-dominant, opercular-insular epilepsy surgery with multimodal structural and functional neuroimaging evaluation

Joseph Yuan-Mou Yang<sup>1,2,3,4</sup>, Ramshekhar Menon<sup>5,6</sup>, Sarah Barton<sup>2,3,4,5</sup>, Simone Mandelstam<sup>7,8,9</sup>, Rachel Kerr<sup>10</sup>, Jacque Wrennall<sup>11,12</sup>, Catherine Bailey<sup>5</sup>, Jeremy Freeman<sup>2,5</sup>, Wirginia Maixner<sup>1,2</sup>, and A Simon Harvey<sup>2,3,5</sup>

<sup>1</sup>Neurosurgery, Royal Children's Hospital, Melbourne, Australia, <sup>2</sup>Neuroscience Research group, Murdoch Children's Research Institution, Melbourne, Australia, <sup>3</sup>Paediatrics, University of Melbourne, Melbourne, Australia, <sup>4</sup>Developmental Imaging group, Murdoch Children's Research Institution, Melbourne, Australia, <sup>5</sup>Neurology, Royal Children's Hospital, Melbourne, Australia, <sup>6</sup>Neurology, Sree Chitra Tirunal Institute for Medical Sciences and Technology, Thiruvananthapuram, India, <sup>7</sup>Medical Imaging, Royal Children's Hospital, Melbourne, Australia, <sup>8</sup>Medicine and Radiology, University of Melbourne, Melbourne, Australia, <sup>9</sup>The Florey Institute of Neuroscience and Mental Health, Melbourne, Australia, <sup>10</sup>Speech pathology, Royal Children's Hospital, Melbourne, Australia, <sup>11</sup>Clinical neuropsychology, Royal Children's Hospital, Melbourne, Australia, <sup>12</sup>Melbourne School of Psychological Sciences, University of Melbourne, Melbourne, Australia

Language dominant, insular-opercular epilepsies are challenging to manage due complex seizure presentations and proximity to language cortex and associated white matter tracts. Most centres elected for extensive invasive stereo-electroencephalogram recordings and ablative procedures. We demonstrated in our retrospective cohort of 11 patients that focal resections can be undertaken safely and effectively using neuroimaging of seizures, lesions, language fMRI and high order tractography reconstructions based on a multi-fibre white matter modelling technique, and careful microsurgical techniques. This avoids risks associated with invasive procedures. Surgery performed under direct vision is more precise, likely safer, allows tailoring with intraoperative electrocorticography, and provides histopathology.



Introduction of ultra-high field Magnetic Resonance Imaging in neonates: preparations and feasibility

Evita Wieggers<sup>1</sup>, Kim Annink<sup>2</sup>, Niek van der Aa<sup>2</sup>, Jeroen Dudink<sup>2</sup>, Thomas Alderliesten<sup>2</sup>, Floris Groenendaal<sup>2</sup>, Maarten Lequin<sup>1</sup>, Floor Jansen<sup>3</sup>, Koenraad Rhebergen<sup>4</sup>, Peter Luijten<sup>1</sup>, Jeroen Hendrikse<sup>1</sup>, Hans Hoogduin<sup>1</sup>, Erik Huijting<sup>1</sup>, Edwin Versteeg<sup>1</sup>, Fredy Visser<sup>1</sup>, Alexander Raaijmakers<sup>1</sup>, Dennis Klomp<sup>1</sup>, Manon Benders<sup>2</sup>, and Jannie Wijnen<sup>1</sup>

<sup>1</sup>Department of Radiology, University Medical Center Utrecht, Utrecht, Netherlands, <sup>2</sup>Department of Neonatology, University Medical Center Utrecht, Utrecht, Netherlands, <sup>3</sup>Department of Paediatric neurology, University Medical Center Utrecht, Utrecht, Netherlands, <sup>4</sup>Department of Otorhinolaryngology and Head & Neck Surgery, University Medical Center Utrecht, Utrecht, Netherlands

The aim of this study was to investigate the safety and feasibility of 7T MRI in neonates. RF safety simulations showed that the global and peak specific absorption rates in a baby model do not exceed the specific absorption rates in adult models at 7T. Furthermore an (acoustic) noise damping hood was developed to guarantee hearing protection. In 10 neonates, we show that it is feasible to obtain good quality images at 7T; safety parameters (heart rate, peripheral oxygen saturation, peripheral temperature and comfort scales) were monitored before, during and after the MR scans, no (MRI related) adverse events occurred.



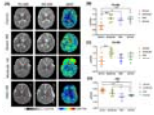
Deep convolution neural network-based DWI tractography connectome analysis to predict language improvement after pediatric epilepsy surgery

Jeong-Won Jeong<sup>1,2,3,4</sup>, Min-Hee Lee<sup>1,2</sup>, Nolan O'Hara<sup>2,4</sup>, Eishi Asano<sup>1,3,4</sup>, and Csaba Juhasz<sup>1,2,3,4</sup>

<sup>1</sup>Pediatrics, Wayne State University, Detroit, MI, United States, <sup>2</sup>Translational Imaging Lab, Children's Hospital of Michigan, Detroit, MI, United States, <sup>3</sup>Neurology, Wayne State University, Detroit, MI, United States, <sup>4</sup>Translational Neuroscience Program, Wayne State University, Detroit, MI, United States

Early surgery helps improve language function in pediatric epilepsy. We investigate if an advanced DWI approach combining deep convolution network-based tract classification with DWI connectome can help early surgery by providing preoperative imaging markers which indicate a high likelihood of postoperative language improvement. Our approach revealed two nodes in preoperative DWI data, including left middle temporal gyrus and left angular gyrus, of which preoperative local efficiency values are not significantly different in patients having postoperative improvement of receptive language, compared with age-matched healthy controls, which can be as effective imaging markers for prediction of the postoperative language improvement.

0237



Feasibility of oscillating and pulsed gradient diffusion MRI to assess neonatal hypoxia-ischemia on clinical system

Fusheng Gao<sup>1</sup>, Xiaoxia Shen<sup>1</sup>, Hongxi Zhang<sup>1</sup>, Yi Zhang<sup>2</sup>, Xiaolu Ma<sup>1</sup>, Jiangyang Zhang<sup>3</sup>, and Dan Wu<sup>2</sup>

<sup>1</sup>Children's Hospital, Zhejiang University School of Medicine, Hangzhou, China, <sup>2</sup>Key Laboratory for Biomedical Engineering of Ministry of Education, College of Biomedical Engineering & Instrument Science, Zhejiang University, Hangzhou, China, <sup>3</sup>Department of Radiology, New York University School of Medicine, New York, NY, United States

Despite the success of diffusion time ( $t_d$ ) dependent diffusion MRI in simulation and preclinical studies, clinical applications of the technique are challenged by difficulties in accessing short  $t_d$ , limited primarily by the clinical gradient system. This study demonstrated the feasibility of  $t_d$ -dependent dMRI using oscillating and pulsed gradients on a 3T clinical system to investigate neonatal hypoxic-ischemic encephalopathy (HIE). Results demonstrated that the  $t_d$ -dependency ( $\Delta MD$ ) increased in the deep gray matter of infants during the first year. In HIE patients,  $\Delta MD$  increased in the basal ganglia of the severe and moderate HIE, as well as in the penumbra of lesions.

0238



Growth Charting of Grey Matter and White Matter Functional Network among Normal Children and Adolescents

Xuan Bu<sup>1</sup>, Kaili Liang<sup>1</sup>, Yingxue Gao<sup>1</sup>, Lu Lu<sup>1</sup>, Hailong Li<sup>1</sup>, Lianqing Zhang<sup>1</sup>, Shi Tang<sup>1</sup>, Yanlin Wang<sup>1</sup>, Xinyu Hu<sup>1</sup>, Qiyong Gong<sup>1</sup>, Bharat Biswal<sup>2</sup>, and Xiaoqi Huang<sup>1</sup>

<sup>1</sup>Huaxi MR Research Center (HMRRC), Functional and molecular imaging Key Laboratory of Sichuan Province, Department of Radiology, Sichuan University, Chengdu, China, <sup>2</sup>Department of Biomedical Engineering, New Jersey Institute of Technology, Newark, NJ, United States

In current study, we used a network growth charting method to map the normative maturational trajectories of major functional network activity in both grey matter and white matter. A quadratic maturation trajectory of functional activity was observed in DMN, SMN and FPN for both grey matter and white matter. The coherent maturational trajectory between these grey matter and white matter network suggests the corresponding refinements of brain network function plays an important role in improvements in higher-order cognitive abilities during normative adolescent development.

0239



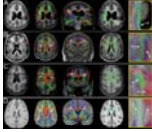
Disconnectome-Symptom Mapping in Traumatic Brain Injury: Application to Paediatric Populations

Adam J Shephard<sup>1</sup>, Jan Novak<sup>1</sup>, Cathy Catroppa<sup>2</sup>, Vicki Anderson<sup>2</sup>, and Amanda G Wood<sup>1,3</sup>

<sup>1</sup>School of Life & Health Sciences & Aston Neuroscience Institute, Aston University, Birmingham, United Kingdom, <sup>2</sup>Clinical Sciences, Murdoch Children's Research Institute, Melbourne, Australia, <sup>3</sup>School of Psychology, Deakin University, Geelong, Australia

Disconnectome-symptom mapping (DSM) was used to identify relationships between brain and behaviour, by assessing the effect of pathology-intersected white matter tracts on neuropsychological outcomes. This study used DSM to see how IQ, two years post-injury, related to disconnections in the brain, following paediatric traumatic brain injury. For this, two approaches were employed: the *BCBtoolkit*, designed for use in adults, and a child-analogue. This study found the *BCBtoolkit* to be less sensitive than the child-analogue, however, in both methods, disconnections in the superior longitudinal fasciculus and external capsule correlated with a reduced IQ when comparing disconnected patients to controls.

0240



#### White matter tracts organization in patients with polymicrogyria and lissencephaly

Filippo Arrigoni<sup>1</sup>, Denis Peruzzo<sup>1</sup>, Simone Mandelstam<sup>2,3,4,5</sup>, Gabriele Amorosino<sup>1</sup>, Daniela Redaelli<sup>1</sup>, Romina Romaniello<sup>6</sup>, Richard Leventer<sup>2,3,4</sup>, Renato Borgatti<sup>6</sup>, Marc Seal<sup>2,4</sup>, and Joseph Yuan-Mou Yang<sup>2,3,4</sup>

<sup>1</sup>Neuroimaging Lab, Scientific Institute, IRCCS E. Medea, Bosisio Parini, Italy, <sup>2</sup>Murdoch Children's Research Institute, Parkville, Australia, <sup>3</sup>Royal Children's Hospital, Parkville, Australia, <sup>4</sup>The University of Melbourne, Parkville, Australia, <sup>5</sup>The Florey Institute of Neuroscience and Mental Health, Parkville, Australia, <sup>6</sup>Scientific Institute, IRCCS E. Medea, Bosisio Parini, Italy

White matter (WM) tracts organization in 42 polymicrogyria (PMG) and 8 lissencephaly (LIS) patients were characterized using the tissue-specific Constrained Spherical Deconvolution modelling technique. Structural appearance of 9 major WM tracts were judged using fiber orientation distribution based direction-encoded color maps and probabilistic algorithm based tractography reconstructions. More abnormal-appearing WM tracts were identified in LIS compared to PMG. Degrees of superior longitudinal fasciculus and cingulum abnormalities were associated with PMG distribution and severity. Thickened superior fronto-occipital fasciculus was demonstrated in three patients. Patterns of WM tracts involvement were related to PMG and LIS distribution and subgroups.

## Oral

### Emerging Methods and Machine Learning in Musculoskeletal MRI - Machine Learning in Musculoskeletal

Monday Parallel 4 Live Q&A

Monday 14:30 - 15:15 UTC

Moderators: Akshay Chaudhari & Martijn Froeling

0241



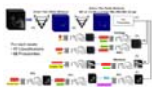
#### Deep Learning Predicts Total Knee Replacement from Magnetic Resonance Images

Aniket A. Tolpadi<sup>1,2</sup>, Jinhee J. Lee<sup>1</sup>, Valentina Padoia<sup>1</sup>, and Sharmila Majumdar<sup>1</sup>

<sup>1</sup>Department of Radiology and Biomedical Imaging, UCSF, San Francisco, CA, United States, <sup>2</sup>Department of Bioengineering, University of California, Berkeley, Berkeley, CA, United States

Total Knee Replacement (TKR) can relieve pain from osteoarthritis (OA), but patient dissatisfaction is not uncommon, making TKR delay advisable until absolutely necessary. Models could identify at-risk patients requiring nonsurgical treatment, prolonging good health and delaying TKR. We present a pipeline that uses DenseNet-121 to predict TKR onset from MRI images, integrates clinical information by ensembling logistic regression models, and sensitively and specifically predicts TKR, particularly at early-stage OA. Occlusion maps show many OA progression imaging biomarkers are implicated in TKR, and many tissues involved in knee flexion and extension preferentially affect TKR probability at early-stage and late-stage OA, respectively.

0242



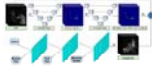
#### Deep Learning Assisted Full Knee 3D MRI-Based Lesion Severity Staging

Bruno Astuto Arouche Nunes<sup>1</sup>, Io Flament<sup>1</sup>, Nikan K. Namiri<sup>1</sup>, Rutwik Shah<sup>2,3</sup>, Matthew Bucknor<sup>1</sup>, Thomas Link<sup>2</sup>, Valentina Padoia<sup>2,3</sup>, and Sharmila Majumdar<sup>2</sup>

<sup>1</sup>Department of Radiology and Biomedical Imaging, UCSF, San Francisco, CA, United States, <sup>2</sup>Department of Radiology and Biomedical Imaging, UCSF, San Francisco, CA, United States, <sup>3</sup>Center for Digital Health Innovation, UCSF, San Francisco, CA, United States

The goal of this study is to capitalizing on recent developments in Deep Learning (DL) applied to medical imaging. Specifically, we aim to (i) identify cartilage, meniscus, bone marrow edema (BEM) and ACL ligament lesions and assess severity providing full knee lesion severity assessment, and (ii) provide a condensed clinical history of patients in an automated manner.

0243



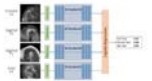
#### Semi-Quantitative Grading of the Anterior Cruciate Ligament using Deep Learning

Nikan K Namiri<sup>1</sup>, Io Flament<sup>1</sup>, Bruno Astuto<sup>1</sup>, Rutwik Shah<sup>1</sup>, Radhika Tibrewala<sup>1</sup>, Francesco Caliva<sup>1</sup>, Thomas M Link<sup>1</sup>, Valentina Pedoia<sup>1</sup>, and Sharmila Majumdar<sup>1</sup>

<sup>1</sup>Department of Radiology and Biomedical Imaging, University of California, San Francisco, San Francisco, CA, United States

In this study we present a fully-automated anterior cruciate ligament (ACL) detection and classification framework which provides multi-class severity staging of ACL tears using state-of-the-art deep learning architectures. We compared the performances of a 3D and a 2D convolutional neural network (CNN) in ACL lesion classification. A higher overall accuracy (84%) and linear-weighted kappa (.92) were observed with the 2D model; however, it underperformed compared to the 3D CNN in classifying partial tears. This is the first reported deep learning detection and classification pipeline for ACL severity staging, including reconstructed, fully torn, partially torn, and intact ligaments.

0244



#### Deep-learning Diagnosis of Supraspinatus Tendon Tears: Comparison of Multi-sequence Versus Single Sequence Input

Dana J. Lin, MD<sup>1</sup>, JinHyeong Park, PhD<sup>2</sup>, Michael Schwier, PhD<sup>2</sup>, Bernhard Geiger, PhD<sup>2</sup>, Esther Raithe, PhD<sup>3</sup>, and Michael P. Recht, MD<sup>1</sup>

<sup>1</sup>Department of Radiology, NYU School of Medicine, New York, NY, United States, <sup>2</sup>Siemens Healthineers, Princeton, NJ, United States, <sup>3</sup>Siemens Healthineers, Erlangen, Germany

Rotator cuff tears are a common cause of shoulder pain and typically diagnosed on shoulder MRI. Using 1,218 MR examinations performed at multiple field strengths and from multiple vendors, we developed a deep-learning (DL) model for the diagnosis of supraspinatus tendon tears on MRI using an ensemble of 3D ResNets combined via logistic regression to classify tears into no tear, partial tear, and full-thickness tear. We compared the effect of using multiple sequences as input versus a single sequence. Our results show that deep-learning diagnosis of supraspinatus tendon tears is feasible and that multi-sequence input improves model performance.

0245



#### Deep Shoulder CT Image Synthesis from MR via Context-aware 2.5D Generative Adversarial Networks

Yucheng Liu<sup>1</sup>, Yulin Liu<sup>2</sup>, Michael Z. Liu<sup>1</sup>, Pawas S. Shukla<sup>1</sup>, Richard Ha<sup>1</sup>, Tim Duong<sup>3</sup>, Sachin R. Jambawalikar<sup>1</sup>, and Tony T. Wong<sup>1</sup>

<sup>1</sup>Radiology, Columbia University Irving Medical Center, New York, NY, United States, <sup>2</sup>Information and Computer Engineering, Chung Yuan Christian University, Taoyuan City, Taiwan, <sup>3</sup>Radiology, Stony Brook Medicine, Stony Brook, NY, United States



We developed a context-aware 2.5D Generative Adversarial Network (GAN) to generate synthetic CT images from MRI. Adjacent 2D slices with in plane matrix of 512 x 512 and user defined slice context (from 3 to 41-slices) were provided as input. This allows the network to learn out-of-plane information for the slice of interest thereby alleviating the intensity discontinuity problem seen in 2D networks. In addition, this approach uses less GPU memory than a 3D GAN. Our results indicated that the network trained with larger number of adjacent slices outperform the fewer slice network.

0246



### Compressed Sensing with and without Deep Learning Reconstruction: Comparison of Capability for Improving Lumbar Spine MRI with Parallel Imaging

Yuki Obama<sup>1</sup>, Yoshiharu Ohno<sup>1</sup>, Kaori Yamamoto<sup>2</sup>, Akiyoshi Iwase<sup>3</sup>, Takahiro Ueda<sup>1</sup>, Kazuhiro Murayama<sup>4</sup>, and Hiroshi Toyama<sup>1</sup>

<sup>1</sup>Radiology, Fujita Health University School of Medicine, Toyoake, Japan, <sup>2</sup>Canon Medical Systems Corporation, Otawara, Japan, <sup>3</sup>Radiology, Department of Radiology, Fujita Health University Hospital, Toyoake, Japan, <sup>4</sup>Radiology, Joint Research Laboratory of Advanced Medical Imaging, Fujita Health University School of Medicine, Toyoake, Japan

There have been no major reports for assessing the utility of compressed sensing (CS) and deep learning reconstruction (DLR) as compared with routinely applied parallel imaging (PI) on lumbar spine MRI. We hypothesized that CS with DLR was able to improve image quality and shorten examination time on lumbar spine MRI, when compared with PI. The purpose of this study was to directly compare the capability for improving lumbar spine MRI among CS with and without DLR and PI in patients with different lumbar spinal diseases.

0247



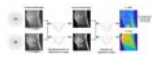
### Deep learning for the detection and differentiation of vertebral fracture

Yang Zhang<sup>1</sup>, Lee-Ren Yeh<sup>2</sup>, Jeon-Hor Chen<sup>1,2</sup>, Ning Lang<sup>3</sup>, Xiaoying Xing<sup>3</sup>, Yongye Chen<sup>3</sup>, Qizheng Wang<sup>3</sup>, Peter Chang<sup>1</sup>, Daniel Chow<sup>1</sup>, Huishu Yuan<sup>3</sup>, and Min-Ying Su<sup>1</sup>

<sup>1</sup>Department of Radiological Science, University of California, Irvine, CA, United States, <sup>2</sup>Department of Radiology, E-Da Hospital and I-Shou University, Kaohsiung, Taiwan, <sup>3</sup>Department of Radiology, Peking University Third Hospital, Beijing, China

This study investigated the value of deep learning for the detection and differential diagnosis of vertebral fracture. A model using ResNet50 was developed and tested in a separate dataset. The results were compared with the interpretation of an experienced radiologist. Our study noted that the analysis based on single vertebral body without inclusion of the soft tissue, the posterior elements, and the skipped lesions might be the reason why the radiologist's reading was better than deep learning approach. For the identification of malignant fracture using whole images from training set, the prediction accuracy was only moderate, with rooms for improvement.

0248



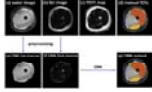
### Quantitative T1 Mapping from Incoherently Undersampled MR Images Using Self-Attention Convolutional Neural Networks

Yan Wu<sup>1</sup>, Yajun Ma<sup>2</sup>, Jiang Du<sup>2</sup>, and Lei Xing<sup>3</sup>

<sup>1</sup>Stanford University, Stanford, CA, United States, <sup>2</sup>Radiology, University of California San Diego, La Jolla, CA, United States, <sup>3</sup>Radiation Oncology, Stanford University, Stanford, CA, United States

The application of current quantitative MRI techniques is limited by the long scan time. In this study, we propose a deep learning strategy to derive quantitative T1 map and B1 map from two incoherently undersampled variable contrast images. Furthermore, radiofrequency field (B1) inhomogeneity is automatically corrected in the derived T1 map. The tasks are accomplished in two steps: joint reconstruction and parameter quantification, both employing self-attention convolutional neural networks. Significant reduction in data acquisition time has been successfully achieved, including an acceleration in variable contrast image acquisition caused by undersampling and a waiver of B1 map measurement.

0249



Deep learning-based thigh muscle segmentation for reproducible fat fraction quantification using fat-water decomposition MRI

Jie Ding<sup>1</sup>, Varut Vardhanabhuti<sup>1</sup>, Eric Lai<sup>2</sup>, Yuan Gao<sup>3</sup>, Sophelia Chan<sup>4</sup>, and Peng Cao<sup>1</sup>

<sup>1</sup>Department of Diagnostic Radiology, Li Ka Shing Faculty of Medicine, The University of Hong Kong, Hong Kong, Hong Kong, <sup>2</sup>Li Ka Shing Faculty of Medicine, The University of Hong Kong, Hong Kong, Hong Kong, <sup>3</sup>Division of Neurology, Department of Medicine, Queen Mary Hospital, The University of Hong Kong, Hong Kong, Hong Kong, <sup>4</sup>Department of Paediatrics and Adolescent Medicine, Li Ka Shing Faculty of Medicine, The University of Hong Kong, Hong Kong, Hong Kong

Time-efficient thigh muscle segmentation is a major challenge in moving from primarily qualitative assessment of thigh muscle MRI in clinical practice, to potentially more accurate and quantitative methods. In this work, we trained a convolutional neural network to automatically segment four clinically relevant muscle groups using fat-water MRI. Compared to cumbersome manual annotation which ordinarily takes at least 5-6 hours, this fully automated method provided sufficiently accurate segmentation within several seconds for each thigh volume. More importantly, it yielded more reproducible fat fraction estimations, which is extremely useful for quantifying fat infiltration in ageing and in diseases like neuromuscular disorders.

---

## Combined Educational & Scientific Session

### Emerging Methods and Machine Learning in Musculoskeletal MRI - Machine Learning in MSK

Organizers: Jung-Ah Choi, Riccardo Lattanzi, Kimberly Amrami, Jan Fritz, Miika Nieminen, Hiroshi Yoshioka

Monday Parallel 4 Live Q&A

Monday 14:30 - 15:15 UTC

Moderators: Richard Kijowski & Valentina Pedoia

Machine Learning for MSK Image Acquisition & Reconstruction

Fang Liu<sup>1</sup>

<sup>1</sup>Radiology, Harvard University, Boston, MA, United States

This talk will provide an overview of the latest deep learning techniques that have been applied to image reconstruction of musculoskeletal MRI. The topics focus on rapid imaging for both static MRI and quantitative MRI, such as T2 and T1rho mapping. The talk will conclude by highlighting potential challenges in deep learning-based reconstruction that warrant further investigation.

---

Machine Learning for MSK Image Processing & Interpretation

Cem M Deniz<sup>1</sup>

<sup>1</sup>Radiology, New York University Langone Health, New York, NY, United States

This educational lecture will provide an overview of the machine learning approaches applied in MR image processing and interpretation for musculoskeletal disorders.

---

Task-Based UltraFast MRI: Simultaneous Image Reconstruction and Tissue Segmentation

0250



Francesco Caliva<sup>1</sup>, Adam Noworolski<sup>2</sup>, Andrew Leynes<sup>1,3</sup>, Claudia Iriondo<sup>1,3</sup>, Sharmila Majumdar<sup>1</sup>, Peder Larson<sup>1</sup>, and Valentina Pedoia<sup>1</sup>

<sup>1</sup>Department of Radiology and Biomedical Imaging, University of California, San Francisco, San Francisco, CA, United States, <sup>2</sup>EECS, University of California, Berkeley, Berkeley, CA, United States, <sup>3</sup>Department of Bioengineering, University of California, Berkeley, Berkeley, CA, United States

We propose a novel task based deep learning framework for simultaneous MRI reconstruction and segmentation. On a dataset of retrospectively undersampled knee-DESS volumes we demonstrate that irrespective of ultra-high acceleration factors (i.e. 48×) a multitask 3D encoder-decoder is capable of reconstructing with high fidelity the knee MRI, accurately segment cartilaginous and meniscal tissues and reliably provide cartilage thickness. Our multitask solution outperforms two other methods: a compressed sensing reconstruction step, followed by a deep learning-based tissue segmentation. The other method comprises a cascade of two convolutional neural networks that sequentially perform image reconstruction and segmentation.

0251

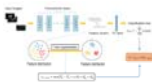


Computer Aided Detection AI Reduces Inter-Reader Variability in Grading Hip Abnormalities from MRI  
Radhika Tibrewala<sup>1</sup>, Eugene Ozhinsky<sup>1</sup>, Rutwik Shah<sup>1</sup>, Io Flament<sup>1</sup>, Kay Crossley<sup>2</sup>, Ramya Srinivasan<sup>1</sup>, Thomas M Link<sup>1</sup>, Valentina Pedoia<sup>1</sup>, and Sharmila Majumdar<sup>1</sup>

<sup>1</sup>Radiology and Biomedical Imaging, University of California San Francisco, San Francisco, CA, United States, <sup>2</sup>La Trobe Sport and Exercise Medicine Research Centre, Melbourne, Australia

MRI based hip degeneration grading is difficult, time-intensive and prone to inter-reader variability, aggravated by the lack of a standard hip grading scale. Recent research using deep learning based clinical classification tasks has shown efficiency in knee degenerative changes. In this study, we aim to develop a deep learning based hip degenerative changes classification model (for cartilage lesions, bone marrow edemas and cysts) and evaluate its performance. In addition to that, we develop an AI-assist tool based on model predictions to test on two radiologists to see if the inter-reader agreement increases by using the AI-assist.

0252

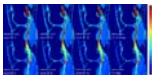


Automated Grading of Lumbar Disc Degeneration Using T-test Regularized Network  
Shui Liu<sup>1</sup>, Fei Gao<sup>2</sup>, Xiaodong Zhang<sup>1</sup>, Jue Zhang<sup>2,3</sup>, Xiaoying Wang<sup>1,3</sup>, and Jing Fang<sup>2,3</sup>

<sup>1</sup>Department of Radiology, Peking University First Hospital, Beijing, China, <sup>2</sup>College of Engineering, Peking University, Beijing, China, <sup>3</sup>Academy for Advanced Interdisciplinary Studies, Peking University, Beijing, China

To enrich the representation capability of the CNN model and achieve more accurate lumbar disc degeneration grading, inspired by student T-test in statistics, we propose a T-test regularization strategy focusing on pushing away different categories from each other in feature space.

0253



Deep Learning MR Relaxometry with Joint Spatial-Temporal Under-sampling  
Hongyu Li<sup>1</sup>, Mingrui Yang<sup>2</sup>, Jeehun Kim<sup>2</sup>, Ruiying Liu<sup>1</sup>, Chaoyi Zhang<sup>1</sup>, Peizhou Huang<sup>1</sup>, Sunil Kumar Gaire<sup>1</sup>, Dong Liang<sup>3</sup>, Xiaojuan Li<sup>2</sup>, and Leslie Ying<sup>1</sup>

<sup>1</sup>Department of Biomedical Engineering, Department of Electrical Engineering, The State University of New York at Buffalo, Buffalo, NY, United States, <sup>2</sup>Program of Advanced Musculoskeletal Imaging (PAMI), Cleveland Clinic, Cleveland, OH, United States, <sup>3</sup>Paul C. Lauterbur Research Center for Biomedical Imaging, Medical AI research center, SIAT, CAS, Shenzhen, China

This abstract presents a deep learning method to generate MR parameter maps from very few subsampled echo images. The method uses deep convolutional neural networks to learn the nonlinear relationship between the subsampled T1rho/T2-weighted images and the T1rho/T2 maps, bypassing the conventional exponential decay models. Experimental results show that the proposed method is able to generate T1rho/T2 maps from only 2 subsampled echo images with quantitative values comparable to those of the T1rho/T2 maps generated from fully-sampled 8 echo images using the conventional exponential decay curve fitting.

---

---

## Oral

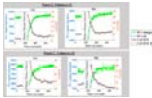
### Emerging Methods and Machine Learning in Musculoskeletal MRI - Musculoskeletal Emerging Methods

Monday Parallel 4 Live Q&A

Monday 14:30 - 15:15 UTC

Moderators: James MacKay

0254



Intermuscular Variability of Phosphocreatine Recovery Constants in Exercised Muscle Measured using 31PMRS and CrCEST at 7.0T

Dushyant Kumar<sup>1</sup>, Ravi Prakash Reddy Nanga<sup>1</sup>, Deepa Thakuri<sup>1</sup>, Neil Wilson<sup>2</sup>, Hari Hariharan<sup>1</sup>, and Ravinder Reddy<sup>1</sup>

<sup>1</sup>Radiology, University of Pennsylvania, Philadelphia, PA, United States, <sup>2</sup>Siemens Medical Solutions USA Inc, Malvern, PA, United States

Synopsis: As a noninvasive imaging biomarker, phosphorous magnetic resonance spectroscopy (31PMRS) has traditionally been used to measure the metabolic response of exercised skeletal muscle in humans and has contributed immensely to the vital understanding of muscle energetics. However, due to lack of spatial resolution in 31PMRS, it is difficult to resolve the intermuscular variabilities of creatine kinase kinetics. In this study we demonstrate that with proper placement of surface coil in a mild exercise study, the recovery constant for PCr determined from 31PMRS matches well with recovery constant measured from CrCEST using a volume coil for the same muscle group.

---

0255



Noise and Bias Reduction in Two-Point Dixon Peripheral Nerve Imaging and Muscle Denervation Assessment

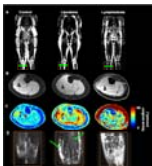
Ek T Tan<sup>1</sup>, Julia Sternberg<sup>1</sup>, Bin Lin<sup>1</sup>, Hollis G Potter<sup>1</sup>, and Darryl B Sneag<sup>1</sup>

<sup>1</sup>Radiology and Imaging, Hospital for Special Surgery, New York, NY, United States

High resolution, T2-weighted two-point Dixon is an effective technique for MR neurography (MRN) and can potentially also provide quantitative assessment of muscle 'edema' and fatty infiltration, which occur in acute and chronic muscle denervation, respectively. However, low SNR and residual off-resonance can introduce severe bias that impedes accurate interpretation. This study demonstrated that principal component analysis (PCA) denoising and off-resonance correction methods significantly improved proton density fat fraction (PDFF) measurements in 28 patient datasets and in signal simulations. Reduced bias allowed for further application of a proposed water-weighted processing enhances nerve conspicuity by suppressing perineural fat signal.

---

0256



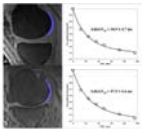
Lymphatic insufficiency observed by noninvasive MR lymphangiography and multi-nuclear 23Na-MRI in patients with lymphedema and lipedema

Rachelle Crescenzi<sup>1</sup>, Paula M.C. Donahue<sup>2,3</sup>, Kalen J Petersen<sup>1</sup>, Maria Garza<sup>1</sup>, Kelsey Guerreso<sup>1</sup>, Yu Luo<sup>1</sup>, Joshua A. Beckman<sup>4</sup>, and Manus J. Donahue<sup>1,5,6</sup>

<sup>1</sup>Radiology, Vanderbilt University Medical Center, Nashville, TN, United States, <sup>2</sup>Dayani Center for Health and Wellness, Vanderbilt University Medical Center, Nashville, TN, United States, <sup>3</sup>Physical Medicine and Rehabilitation, Vanderbilt University Medical Center, Nashville, TN, United States, <sup>4</sup>Cardiovascular Medicine, Vanderbilt University Medical Center, Nashville, TN, United States, <sup>5</sup>Neurology, Vanderbilt University Medical Center, Nashville, TN, United States, <sup>6</sup>Psychiatry, Vanderbilt University Medical Center, Nashville, TN, United States

The lymphatic system comprises a central component of the circulatory system, yet imaging approaches to visualize lymphatics remain underdeveloped. We utilized MR lymphangiography and sodium MRI to confirm lymphatic impairment in patients with lymphedema of known causes, and in patients with the adipose disorder lipedema of unknown etiology. We report distinct profiles on MR lymphangiography that correlate with tissue sodium and fat deposition. Results provide evidence of lymphatic involvement in lipedema that informs disease mechanisms related to swelling, and more broadly relates to lymphatic clearance dysfunction in a range of diseases where sodium and fat are implicated.

0257



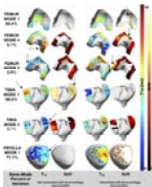
### Quantitative Assessment of Articular Cartilage Degeneration Using 3D Ultrashort Echo Time Cones Adiabatic T1 $\rho$ (3D UTE Cones AdiabT1 $\rho$ ) Imaging

Mei Wu<sup>1,2</sup>, Yanping Xue<sup>1</sup>, Yajun Ma<sup>1</sup>, Claire Tang<sup>1</sup>, Meghan Shen<sup>1</sup>, Saeed Jerban<sup>1</sup>, Eric Y Chang<sup>1,3</sup>, and Jiang Du<sup>1</sup>

<sup>1</sup>Department of Radiology, University of California, San Diego, San Diego, CA, United States, <sup>2</sup>Department of Radiology, Guangzhou First People's Hospital, School of Medicine, South China University of Technology, Guangzhou, China, <sup>3</sup>Radiology Service, VA San Diego Healthcare System, San Diego, CA, United States

The study protocol included three-dimensional Ultrashort Echo Time Cones actual flip angle imaging (3D UTE-Cones-AFI) for T1 measurement and UTE-Cones with adiabatic T1 $\rho$  (AdiabT1 $\rho$ ) preparation for AdiabT1 $\rho$  measurement. We applied the 3D UTE-Cones AdiabT1 $\rho$  sequence to healthy volunteers and patients with different degrees of OA for a systematic evaluation of its clinical performance. Results showed that the 3D UTE-Cones AdiabT1 $\rho$  sequence could be used for high resolution imaging and quantitative assessment of the knee cartilage, and that the AdiabT1 $\rho$  biomarker showed a significant positive relationship with WORMS.

0258



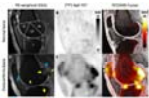
### Principal Component Analysis of Simultaneous PET/MRI Reveals Patterns of Cartilage-Bone Interactions in Osteoarthritis

Radhika Tibrewala<sup>1</sup>, Valentina Pedoia<sup>1</sup>, Matthew Bucknor<sup>1</sup>, and Sharmila Majumdar<sup>1</sup>

<sup>1</sup>Radiology and Biomedical Imaging, University of California San Francisco, San Francisco, CA, United States

Osteoarthritis (OA) is a joint disorder, consisting of cartilage degeneration and metabolic bone changes, which have previously been correlated by using [<sup>18</sup>F]-NaF PET/MRI in the knee. However, these correlations were derived using averaging methods in areas of [<sup>18</sup>F] uptake in the bone and surrounding cartilage T<sub>1 $\rho$</sub> /T<sub>2</sub> mean values, which could miss potential multifaceted mechanisms that are not spatially correlated in the joint. The goal of this study is to find complex patterns in OA by building a cartilage-bone interface and using principal component analysis to find cartilage-bone interactions and find associations with known manifestations of OA.

0259



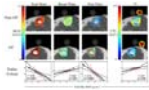
### Evaluating the Relationship Between Dynamic [18F]-Sodium Fluoride Uptake Parameters and MRI Knee Osteoarthritic Findings

Lauren Watkins<sup>1</sup>, James MacKay<sup>2,3</sup>, Bryan Haddock<sup>4</sup>, Valentina Mazzoli<sup>5</sup>, Scott Uhlrich<sup>6</sup>, Garry Gold<sup>5</sup>, and Feliks Kogan<sup>5</sup>

<sup>1</sup>Bioengineering, Stanford University, Stanford, CA, United States, <sup>2</sup>Radiology, University of East Anglia, Norwich, United Kingdom, <sup>3</sup>Radiology, University of Cambridge, Cambridge, United Kingdom, <sup>4</sup>Department of Clinical Physiology, Nuclear Medicine and PET, Copenhagen University Hospital, København, Denmark, <sup>5</sup>Radiology, Stanford University, Stanford, CA, United States, <sup>6</sup>Mechanical Engineering, Stanford University, Stanford, CA, United States

Abnormal bone physiology is a potential mechanism for the progression of knee osteoarthritis. Molecular information derived from PET imaging has shown promise in early detection of bone metabolic abnormalities. Here we investigated kinetic parameters of PET tracer ( $[^{18}\text{F}]\text{-NaF}$ ) uptake in subjects with knee osteoarthritis and evaluated the relationship between kinetic tracer uptake parameters and structural MRI findings. The kinetic parameters for  $[^{18}\text{F}]\text{-NaF}$  delivery and uptake to regions of bone containing osteophytes, bone marrow lesions, and adjacent to cartilage lesions identified on MRI were significantly different compared to normal-appearing bone, suggesting strong spatial relationships between structural damage and bone metabolic abnormalities.

0260



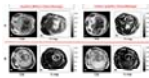
#### Quantitative Measurements of Bone Water and $^{31}\text{P}$ in Postmenopausal Women: A Preliminary Study

Brandon Clinton Jones<sup>1</sup>, Cheng-Chieh Cheng<sup>1</sup>, Xia Zhao<sup>1</sup>, Mona Al Mukaddam<sup>2</sup>, Peter J Snyder<sup>2</sup>, Chamith S Rajapakse<sup>1</sup>, Hee Kwon Song<sup>1</sup>, and Felix W Wehrli<sup>1</sup>

<sup>1</sup>Radiology, University of Pennsylvania, Philadelphia, PA, United States, <sup>2</sup>Medicine, University of Pennsylvania, Philadelphia, PA, United States

Seven osteoporotic treatment-naïve and 13 non-osteoporotic postmenopausal women have been examined in an ongoing MRI study to evaluate cortical bone properties.  $^1\text{H}$  dual-echo UTE and  $^1\text{H}$  IR-prepared rapid-UTE sequences were used for evaluation of pore and bound water concentrations in the tibial cortex, and a  $^{31}\text{P}$  PETRA-ZTE sequence for quantification of cortical bone mineralization. Elevated total water and pore water were found in the osteoporotic group ( $p=0.036$ ,  $p=0.032$ ), whereas  $^{31}\text{P}$  and bound water concentrations were not significantly different. Since pore water is a known surrogate of bone porosity, our preliminary results suggest it may be useful in evaluating bone health.

0261

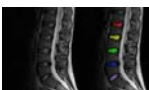


#### Can Tumor T1 Serve as Early Response Imaging Biomarker for Neoadjuvant Chemotherapy in Osteosarcoma? A Preliminary Study

Esha Baidya Kayal<sup>1</sup>, Nikhil Sharma<sup>1</sup>, Sameer Bakhshi<sup>2</sup>, Raju Sharma<sup>3</sup>, Devasenathipathy Kandasamy<sup>3</sup>, and Amit Mehndiratta<sup>1,4</sup>

<sup>1</sup>Centre for Biomedical Engineering, Indian Institute of Technology, Delhi, New Delhi, India, <sup>2</sup>Department of Medical Oncology, Dr. B.R. Ambedkar Institute-Rotary Cancer Hospital (IRCH), All India Institute of Medical Sciences, New Delhi, New Delhi, India, <sup>3</sup>Radio Diagnosis, All India Institute of Medical Sciences, New Delhi, New Delhi, India, <sup>4</sup>Department of Biomedical engineering, All India Institute of Medical Sciences, New Delhi, New Delhi, India

Histopathological examination is the current gold standard for evaluating tumor response to anti-cancer therapy; though it is possible only after surgery. Non-invasive imaging biomarkers of tumor response to therapy may be useful in optimizing existing treatments improving overall outcome. The spin-lattice relaxation time of water protons (T1) reflects therapeutic changes in tumor and is thus a generic marker of tumor response to therapy. Experimental results showed T1 relaxation time reduces upon successful chemotherapy and thus, a change in tumor T1 may be a non-invasive imaging marker of chemo-sensitivity and chemotherapy response.



#### Accelerated T2 Mapping of the Lumbar Intervertebral Discs: Robust Quantification in Clinically Feasible Acquisition Times

Marcus Raudner<sup>1</sup>, Markus Schreiner<sup>1,2</sup>, Tom Hilbert<sup>3,4,5</sup>, Tobias Kober<sup>3,5,6</sup>, Anna Szelenyi<sup>7</sup>, Vladimir Juras<sup>1</sup>, and Siegfried Trattnig<sup>1</sup>

<sup>1</sup>High Field MR Centre, Department of Biomedical Imaging and Image-guided Therapy, Medical University of Vienna, Vienna, Austria, <sup>2</sup>Department of Orthopedics and Trauma Surgery, Medical University of Vienna, Vienna, Austria, <sup>3</sup>Advanced Clinical Imaging Technology, Siemens Healthcare, Lausanne, Switzerland, <sup>4</sup>Department of Radiology, Lausanne University Hospital and University of Lausanne, Lausanne, Switzerland, <sup>5</sup>LTS5, Ecole Polytechnique Fédérale de Lausanne (EPFL), Lausanne, Switzerland, <sup>6</sup>Department of Radiology, University Hospital and University of Lausanne, Lausanne, Switzerland, <sup>7</sup>Department of Biomedical Imaging and Image-guided Therapy, Medical University of Vienna, Vienna, Austria

The physiological biochemical state of the intervertebral disc (IVD) allows for passive water-storing capabilities because of a high concentration of glycosaminoglycans (GAG) and an inherent structural integrity. T<sub>2</sub> mapping can quantitatively assess the IVD's water content and GAG concentration, but a typical 2D multi echo spin echo (MESE) sequence suffers from clinically prohibitive scan times. To resolve this, we compared the MESE sequence against GRAPPATINI, an accelerated sequence combining parallel imaging and a model-based reconstruction for T<sub>2</sub> quantification which uses undersampling to shorten the scan time from 13:18 to 2:27 minutes.

## Oral

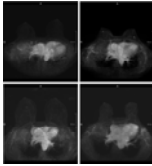
### Cancer Imaging: Machine Learning & Advanced Imaging - Cancer Imaging: Machine Learning

Monday Parallel 5 Live Q&A

Monday 14:30 - 15:15 UTC

Moderators: Bradford Moffat & Natarajan Raghunand

0263



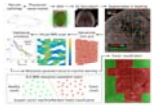
#### Triaging dense breast screening MR images using a dilated convolutional neural network

Angelo Zuffianò<sup>1</sup>, Bob de Vos<sup>1</sup>, Jorrit Glastra<sup>1</sup>, Pim Moeskops<sup>1</sup>, Valerio Fortunati<sup>1</sup>, Ivana Išgum<sup>2</sup>, Tim Leiner<sup>3</sup>, Carla van Gils<sup>3</sup>, and Wouter Veldhuis<sup>3</sup>

<sup>1</sup>Quantib, Utrecht, Netherlands, <sup>2</sup>Biomedical Engineering and Physics, Radiology and Nuclear Medicine, Amsterdam University Medical Center, Amsterdam, Netherlands, <sup>3</sup>Radiology, Utrecht University Medical Center, Utrecht, Netherlands

Dynamic contrast enhanced (DCE) MRI is the key series to analyze for the detection of breast cancer in women with extremely dense breasts. Given the increasing number of women receiving dense breast MRI screening we aimed to reduce radiologist workload without reducing the high sensitivity of MRI. We developed a convolutional neural network (CNN) based method able to defer 8.1% of the workload by identifying non-enhancing scans with a sensitivity of 96.3%.

0264



#### Proof-of-principle for endogenous signal classification towards voxel-wise tumor detection using statistical machine learning

Artur Hahn<sup>1,2</sup>, Julia Krüwel-Bode<sup>3</sup>, Yannis Seemann<sup>2</sup>, Sarah Schuegger<sup>2</sup>, Johann M. E. Jende<sup>1</sup>, Anja Hohmann<sup>4</sup>, Volker J. F. Sturm<sup>1</sup>, Ke Zhang<sup>5</sup>, Sabine Heiland<sup>1</sup>, Martin Bendszus<sup>1</sup>, Michael O. Breckwoldt<sup>1,6</sup>, Christian H. Ziener<sup>1,5</sup>, and Felix T. Kurz<sup>1,5</sup>

<sup>1</sup>Department of Neuroradiology, Heidelberg University Hospital, Heidelberg, Germany, <sup>2</sup>Department of Physics and Astronomy, University of Heidelberg, Heidelberg, Germany, <sup>3</sup>Molecular Mechanisms of Tumor Invasion (V077), German Cancer Research Center (DKFZ), Heidelberg, Germany, <sup>4</sup>Department of Neurology, Heidelberg University Hospital, Heidelberg, Germany, <sup>5</sup>Department of Radiology (E010), German Cancer Research Center (DKFZ), Heidelberg, Germany, <sup>6</sup>Clinical Cooperation Unit Neuroimmunology and Brain Tumor Immunology, German Cancer Research Center (DKFZ), Heidelberg, Germany

Based on the microvasculature of entire healthy and tumor-bearing mouse brains, imaged with high-resolution fluorescence microscopy, the transverse relaxation process within virtual MRI voxels was simulated. Extended parametrizations of the non-Lorentzian signal decay were used to train support vector machine and random forest classifiers to differentiate healthy brain and tumor voxel signals. A proof-of-principle is presented with U87 and GL261 glioblastoma at different SNR levels. This automated workflow enables the in-silico development of specialized MRI sequences to maximize classification accuracy with minimal NMR measurements for experimental analogies.

0265



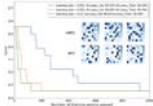
### Radiomic features of cervical tumors: identifying volume thresholds for transition to a poor prognosis phenotype

Benjamin W Wormald<sup>1,2</sup>, Thomas EJ Ind<sup>2,3</sup>, and Nandita M deSouza<sup>1,4</sup>

<sup>1</sup>Imaging, The Institute of Cancer Research, Sutton, Surrey, United Kingdom, <sup>2</sup>Gynaecological Oncology, The Royal Marsden NHS Foundation Trust, London, United Kingdom, <sup>3</sup>Surgery, St. Georges University Hospital, London, United Kingdom, <sup>4</sup>MRI Unit, The Royal Marsden NHS Foundation Trust, Sutton, Surrey, United Kingdom

Cervical cancer recurs post-trachelectomy often because of close surgical margins or lymph-node micrometastases. We show that 5 texture features distinguish good- from poor-prognosis tumors (low/high volume, without/with parametrial invasion, without/with lymph node metastases). For tumors suitable for trachelectomy ( $<4.19\text{cm}^3$ ), linear regression of feature value with volume (using 3 features with high discrimination of groups and 1 standard deviation from median from good prognosis group as threshold) indicated that radiomic features tended towards values representing poor prognosis at  $1.8\pm 0.2\text{cm}^3$  (T2-W images) and  $1.8\pm 0.06\text{cm}^3$  (ADC maps). Above  $1.8\text{cm}^3$  textural features of cervical cancer shift towards a phenotype likely to spread and metastasize.

0266



### Identification of Sarcomatoid De-Differentiation in Renal Cell Carcinoma by Machine Learning on Multiparametric MRI

Asim M. Mazin<sup>1</sup>, Samuel H. Hawkins<sup>1</sup>, Olya Stringfield<sup>2</sup>, Jasreman Dhillon<sup>3</sup>, Brandon J. Manley<sup>4</sup>, Daniel K. Jeong<sup>5</sup>, and Natarajan Raghunand<sup>1</sup>

<sup>1</sup>Department of Cancer Physiology, Moffitt Cancer Center, Tampa, FL, United States, <sup>2</sup>IRAT Shared Service, Moffitt Cancer Center, Tampa, FL, United States, <sup>3</sup>Department of Anatomic Pathology, Moffitt Cancer Center, Tampa, FL, United States, <sup>4</sup>Department of Genitourinary Oncology, Moffitt Cancer Center, Tampa, FL, United States, <sup>5</sup>Department of Diagnostic & Interventional Radiology, Moffitt Cancer Center, Tampa, FL, United States

We report a machine learning approach using Self-Organizing Maps (SOM) and Learning Vector Quantization (LVQ) to analyze multiparametric MRI for the purpose of differentiating between renal cell carcinoma tumor with (sRCC) and without (nsRCC) sarcomatoid de-differentiation, a transformation that is associated with poorer outcomes. The SOM+LVQ model was trained on mpMRI data from 9 nsRCC and 9 sRCC tumors, validated on a separate cohort of 3 nsRCC and 3 sRCC tumors, and tested on a held-out set of 5 nsRCC and 5 sRCC tumors. An overall classification accuracy of 70% was achieved on the test cohort.

0267



### Artificial Intelligence for Predicting Pathological Complete Response to Neoadjuvant Chemotherapy from MRI and Prognostic Clinical Features

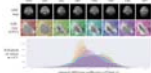
Hongyi Duanmu<sup>1</sup>, Pauline Huang<sup>1</sup>, Srinidhi Brahmavar<sup>1</sup>, Fusheng Wang<sup>1</sup>, and Tim Q Duong<sup>1</sup>

<sup>1</sup>Stony Brook University, Stony Brook, NY, United States



Pathological complete response (pCR) is a measurement of the effectiveness of neoadjuvant chemotherapy (NAC). While there are several studies about predicting the pCR, no one system can fully automate this prediction process. We proposed a 3D convolutional neural network (CNN) system, integrating information on breast MRI images and prognostic clinical features, to predict pCR pre-NAC. This system achieved inspiring results in the ISPY1 Clinical Trial dataset, with 77% accuracy. This approach shows the potential in breast cancer diagnose and assessment. Furthermore, the mechanism of integrating images and features information can be used and generalized to other tasks.

0268



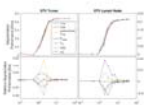
### The impact of radiomic feature reproducibility on a head and neck cancer radiotherapy response model: a comparison of two common analysis packages

James C Korte<sup>1,2</sup>, Carlos E Cardenas<sup>3</sup>, Tomas Kron<sup>1,4</sup>, Nicholas Hardcastle<sup>1,5</sup>, Jihong Wang<sup>3</sup>, Houda Bahig<sup>6</sup>, Baher Elgohari<sup>7</sup>, Laurence E Court<sup>3</sup>, Clifton D Fuller<sup>7</sup>, and Sweet Ping Ng<sup>7,8</sup>

<sup>1</sup>Department of Physical Science, Peter MacCallum Cancer Centre, Melbourne, Australia, <sup>2</sup>Department of Biomedical Engineering, The University of Melbourne, Melbourne, Australia, <sup>3</sup>Department of Radiation Physics, The University of Texas MD Anderson Cancer Center, Houston, TX, United States, <sup>4</sup>Sir Peter MacCallum Department of Oncology, The University of Melbourne, Melbourne, Australia, <sup>5</sup>Centre for Medical Radiation Physics, University of Wollongong, Wollongong, Australia, <sup>6</sup>Radiation Oncology Department, Centre Hospitalier de l'Université de Montréal, Montreal, QC, Canada, <sup>7</sup>Department of Radiation Oncology, University of Texas MD Anderson Cancer Center, Houston, TX, United States, <sup>8</sup>Department of Radiation Oncology, Peter MacCallum Cancer Centre, Melbourne, Australia

Radiomics is a promising technique for discovering image based biomarkers of therapy response in cancer. Reproducibility of radiomic features is a known issue that is being addressed by standardisation initiatives, but it remains a challenge to interpret previously published radiomic signatures. We investigate the reproducibility of radiomic features calculated with two common software packages and explore the impact of including non-reproducible diffusion features in a head and neck cancer (HNC) radiotherapy response model. Our results demonstrate that equivalent models can be generated from either software, but only when restricting the model to reproducible features identified with a correlation threshold method.

0269



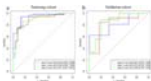
### Evaluating Noise Robustness of CNN-based Head&Neck Tumor Segmentations on Multiparametric MRI Data

Lars Bielak<sup>1,2</sup>, Nicole Wiedenmann<sup>2,3</sup>, Arnie Berlin<sup>4</sup>, Leonard Hägele<sup>1</sup>, Thomas Lottner<sup>1</sup>, Sebastian Gross<sup>5</sup>, Anca-Ligia Grosu<sup>2,3</sup>, and Michael Bock<sup>1,2</sup>

<sup>1</sup>Dept. of Radiology, Medical Physics, Medical Center - University of Freiburg, Faculty of Medicine, Freiburg, Germany, <sup>2</sup>German Cancer Consortium (DKTK), Partner Site Freiburg, Freiburg, Germany, <sup>3</sup>Dept. of Radiation Oncology, Medical Center - University of Freiburg, Faculty of Medicine, Freiburg, Germany, <sup>4</sup>The MathWorks, Inc., Novi, MI, United States, <sup>5</sup>The MathWorks, Inc., Ismaning, Germany

Multiparametric MRI imaging in combination with PET/CT is the basis for precise tumor segmentation in radiation therapy. We trained a segmentation CNN on the multiparametric MRI data of head and neck squamous cell carcinoma patients and investigated the network robustness against noise corruption in the input channels. Overall noise robustness and differences between seven different input contrasts were compared.

1243



### Radiomics analysis for Characterizing Ovarian Tumor Based on a DCE-MRI Pharmacokinetic Protocol

Xiao-li Song<sup>1</sup>, Jia-Liang Ren<sup>2</sup>, Kaiyu Wang<sup>3</sup>, and JinLiang Niu<sup>1</sup>

<sup>1</sup>Shanxi Medical University Second Affiliated Hospital, Taiyuan, China, <sup>2</sup>GE Healthcare, Beijing, China., Beijing, China, <sup>3</sup>GE Healthcare, MR Research China, Beijing, China, Beijing, China

DCE-MRI and its subsequently derived pharmacokinetic parameters have been adopted to explore tumor angiogenesis and vascular permeability changes inside tumors and improve the diagnostic accuracy of ovarian tumors. Radiomics can convert medical images to mineable high-dimensional quantitative imaging features based on automatic feature extraction algorithms. In this study, we present a radiomics model based on a DCE-MRI PK protocol and establish an effective and noninvasive 3-class classification prediction model for the discrimination among benign, borderline and malignant ovarian tumors.

---

---

**Oral**

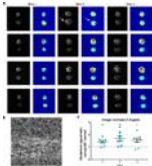
**Cancer Imaging: Machine Learning & Advanced Imaging - Cancer Imaging: Non-Proton & Exogenous Contrast**

Monday Parallel 5 Live Q&A

Monday 14:30 - 15:15 UTC

*Moderators:* Matthew Grech-Sollars & Esther Warnert

0270



**Deuterium MRI imaging of xenografted tumors following in vivo deuterated water labeling**

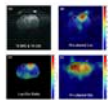
Julian C. Assman<sup>1</sup>, Jeffrey R. Brender<sup>2</sup>, Don E. Farthing<sup>1</sup>, Keita Saito<sup>2</sup>, Kathrynne A. Warrick<sup>1</sup>, Natella Maglakelidze<sup>1</sup>, Hellmut R. Merkle<sup>3</sup>, Murali C. Krishna<sup>2</sup>, Ronald E. Gress<sup>1</sup>, and Nataliya P. Buxbaum<sup>1</sup>

<sup>1</sup>Experimental Transplantation and Immunotherapy Branch, National Cancer Institute, National Institutes of Health, Bethesda, MD, MD, United States, <sup>2</sup>Radiation Biology Branch, Center for Cancer Research, National Cancer Institute, National Institutes of Health, Bethesda, MD, MD, United States, <sup>3</sup>Laboratory for Functional and Molecular Imaging, National Institute of Neurological Disorders and Stroke, National Institutes of Health, Bethesda, MD, MD, United States

Water is a substrate for many biochemical reactions. If D<sub>2</sub>O is ingested, it will be incorporated into proliferating cells. We hypothesized that rapidly proliferating cancer cells would become preferentially labeled with <sup>2</sup>H which would allow visualization by deuterium MRI following a short in vivo D<sub>2</sub>O labeling period. We initiated systemic D<sub>2</sub>O labeling in HT-29 and MiaPaCa-2 xenograft models and performed deuterium MRI following 7 and 14 days of in vivo tumor growth and labeling. We show that small tumors could be distinguished from normal tissue by the incorporation D<sub>2</sub>O into lipids with a greater sensitivity and selectivity than anatomical MRI.

---

0271



**Dynamic Deuterium MRS Imaging of Brain Tumor with Enhanced Sensitivity and Spatiotemporal Resolution**

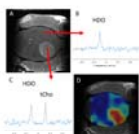
Xiao-Hong Zhu<sup>1</sup>, Tao Wang<sup>1</sup>, Yibo Zhao<sup>2,3</sup>, Yudu Li<sup>2,3</sup>, Rong Guo<sup>2,3</sup>, Yi Zhang<sup>1</sup>, Walter Low<sup>4</sup>, Zhi-Pei Liang<sup>2,3</sup>, and Wei Chen<sup>1</sup>

<sup>1</sup>CMRR, Department of Radiology, University of Minnesota, Minneapolis, MN, United States, <sup>2</sup>Beckman Institute for Advanced Science and Technology, University of Illinois at Urbana-Champaign, Urbana, IL, United States, <sup>3</sup>Departments of Electrical and Computer Engineering, University of Illinois at Urbana-Champaign, Urbana, IL, United States, <sup>4</sup>Department of Neurosurgery, University of Minnesota, Minneapolis, MN, United States

Noninvasive MR-based metabolic imaging of brain tumor may offer new tools for clinic diagnosis and monitoring of tumor growth or assessment of treatment efficacy. One potential candidate is the dynamic deuterium MRS (DMRS) imaging technique recently developed. To reach its full potential, we integrated advanced data processing with D-MRSI to enhance its sensitivity or spatiotemporal resolution. We demonstrated in this pilot study that quantitative “Warburg Effect” map and kinetic time courses of deuterated metabolites can be achieved with good spatiotemporal scales in rat brain tumor using Deep-SPICE based deuterium MRSI, which could potentially be applied to brain tumor patients.

---

0272

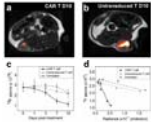


**Mapping of exogenous choline uptake in brain tumors in vivo using Deuterium Metabolic Imaging (DMI)**

Kevan L. Ip<sup>1</sup>, Monique A. Thomas<sup>1</sup>, Akshay Khunte<sup>1</sup>, Kevin L. Behar<sup>2</sup>, Robin A. de Graaf<sup>1</sup>, and Henk M. De Feyter<sup>1</sup>

A high level of intracellular choline is an established marker of malignancy in brain tumors. Here we investigate the uptake of exogenous choline *in vitro* using high resolution <sup>1</sup>H NMR into rodent glioblastoma cell lines. To map bloodborne uptake *in vivo*, we used the novel technique Deuterium Metabolic Imaging (DMI), combined with intravenous infusion of [<sup>2</sup>H<sub>3</sub>]-choline in two orthotopic rat (RG2) and mouse (GL261) models of glioblastoma. DMI-based metabolic maps revealed high uptake of choline in the tumors, in a stark image contrast with normal-appearing brain, illustrating the potential of [<sup>2</sup>H<sub>3</sub>]-choline chloride as metabolic imaging agent.

0273



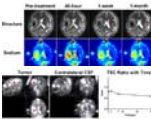
In vivo fluorine-19 MRI of intracellular oximetry response to chimeric antigen receptor T cell therapy against glioma

Fanny Chapelin<sup>1</sup>, Wenlian Zhu<sup>2</sup>, Benjamin Leach<sup>2</sup>, Hideho Okada<sup>3</sup>, and Eric Ahrens<sup>2</sup>

<sup>1</sup>Biomedical Engineering, University of Kentucky, Lexington, KY, United States, <sup>2</sup>Radiology, University of California San Diego, La Jolla, CA, United States, <sup>3</sup>Neurological Surgery, University of California San Francisco, San Francisco, CA, United States

We explore the temporal dynamics of tumor and T cell intracellular partial pressure of oxygen (pO<sub>2</sub>) in a murine flank glioma model receiving chimeric antigen receptor (CAR) T cell therapy. Tumor cells or T cells are intracellularly labeled with perfluorocarbon nanoemulsion prior to injection. <sup>19</sup>F MRI relaxation rate measurements are used to elucidate intracellular pO<sub>2</sub> *in vivo*. The tumor pO<sub>2</sub> peaks at 3 days post-infusion, commensurate with CAR T cell infiltration and tumor cell killing. Moreover, the absolute <sup>19</sup>F signal scales with tumor burden. Overall, <sup>19</sup>F pO<sub>2</sub> MRI measurements can assay cell-mediated apoptosis and provide insight into effector cell function.

0274



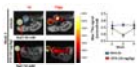
Quantitative Sodium MRI at 7T for the Early Efficacy Evaluation of Stereotactic Radiotherapy for Intracranial Tumors

Zihao Zhang<sup>1,2,3</sup>, Lichao Huang<sup>4</sup>, Xubin Chai<sup>1,2,3</sup>, Zhentao Zuo<sup>1,2,3</sup>, Zhe Wang<sup>1,2,3</sup>, Jing An<sup>5</sup>, Longsheng Pan<sup>4</sup>, and Yan Zhuo<sup>1,2,3</sup>

<sup>1</sup>State Key Laboratory of Brain and Cognitive Science, Institute of Biophysics, Chinese Academy of Sciences, Beijing, China, <sup>2</sup>University of Chinese Academy of Sciences, Beijing, China, <sup>3</sup>CAS Center for Excellence in Brain Science and Intelligence Technology, Beijing, China, <sup>4</sup>Department of Neurosurgery, PLA General Hospital, Beijing, China, <sup>5</sup>Siemens Shenzhen Magnetic Resonance Ltd., Shenzhen, China

Follow-up efficacy evaluation of stereotactic radiotherapy (SRT) helps to provide individualized treatment for intracranial tumors. However, biological changes at cytological level happen earlier than structural MRI can detect. Tissue sodium concentration (TSC) is sensitive to changes of tissue metabolic state and cell membrane integrity. In this study, we used sodium MRI at 7T to noninvasively quantify TSC and monitor the evolution of intracranial tumors after SRT. The results demonstrated that quantitative sodium MRI at 7T can reflect the efficacy of SRT, predict the volume change of tumor, and has the potential of finding the relapse of tumors in early stage.

0275



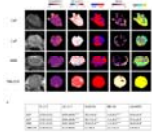
Utilising preclinical <sup>23</sup>Na MRI to probe the ionic microenvironment of breast cancer: developing novel diagnostics to probe treatment efficacy.

Andrew D James<sup>1,2</sup>, Theresa K Leslie<sup>1,2</sup>, Marie-Christine BD Labarthe<sup>3</sup>, Michaela Nelson<sup>1</sup>, Frank Riemer<sup>4</sup>, Gabrielle Baxter<sup>5</sup>, Joshua D Kaggie<sup>5</sup>, Fiona J Gilbert<sup>5</sup>, William Brackenbury<sup>1,2</sup>, and Aneurin J Kennerley<sup>2,3</sup>

<sup>1</sup>Biology, University of York, York, United Kingdom, <sup>2</sup>York Biomedical Research Institute, University of York, York, United Kingdom, <sup>3</sup>Chemistry, University of York, York, United Kingdom, <sup>4</sup>MMIV, Haukeland University Hospital, Bergen, Norway, <sup>5</sup>Department of Radiology, University of Cambridge, Cambridge, United Kingdom

Here we applied  $^{23}\text{Na}$  MRI, as part of a multiparametric imaging approach to measure ionic sodium concentration ( $[\text{Na}^+]$ ) levels in a longitudinal in-vivo mouse model of breast cancer. We investigated tumour  $[\text{Na}^+]$  in response to neoadjuvant chemotherapy and ion channel inhibitors as a novel therapeutic means of reducing metastasis. Results show that  $[\text{Na}^+]$  is decreased in tumour-bearing mice receiving standard chemotherapy. Data suggest that elevated tumour  $[\text{Na}^+]$  in breast cancer may represent a potential imaging biomarker for malignancy and response to chemotherapy.

0276



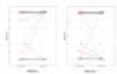
#### Imaging hypoxia in head and neck cancer xenografts with oxygen-enhanced MRI

Elise Lepicard<sup>1</sup>, Jessica Boulton<sup>1</sup>, Yann Jamin<sup>1</sup>, Konstantinos Zormpas-Petridis<sup>1</sup>, Adam Featherstone<sup>2</sup>, Carol Box<sup>1</sup>, Rafal Panek<sup>3</sup>, James O'Connor<sup>2</sup>, and Simon Robinson<sup>1</sup>

<sup>1</sup>Radiotherapy & Imaging, Institute of Cancer Research, Sutton, United Kingdom, <sup>2</sup>Centre for Imaging Sciences, University of Manchester, Manchester, United Kingdom, <sup>3</sup>Nottingham University Hospital, Nottingham, United Kingdom

Oxygen-enhanced (OE)-MRI was used to map and quantify hypoxia in head and neck squamous cell carcinoma xenografts, a tumour type in which hypoxia adversely affects patient prognosis. Application of a refined OE-MRI protocol revealed a markedly high proportion of voxels refractory to hyperoxia-induced changes in  $R_1$ , shown to be hypoxic in imaging-aligned tissue sections stained for the hypoxia marker pimonidazole.

0277



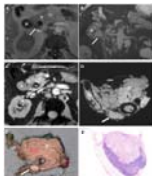
#### USPIO-enhanced MRI for pre-operative lymph node staging after neoadjuvant chemoradiotherapy in esophageal cancer

Didi de Gouw<sup>1</sup>, John Hermans<sup>2</sup>, Bastiaan Klarenbeek<sup>1</sup>, Marnix Maas<sup>2</sup>, Atsushi Nakamoto<sup>3</sup>, Tom Scheenen<sup>2</sup>, and Camiel Rosman<sup>1</sup>

<sup>1</sup>surgery, Radboudumc, Nijmegen, Netherlands, <sup>2</sup>radiology and nuclear medicine, Radboudumc, Nijmegen, Netherlands, <sup>3</sup>radiology, Osaka University Graduate School of Medicine, Osaka, Japan

Lymph node dissections during esophagectomy may be omitted or minimized in patients with esophageal cancer without or with limited lymph node metastases, thereby reducing associated morbidity. A promising technique to detect lymph node metastases is T2\*-weighted MRI after the injection of ultrasmall superparamagnetic iron oxide nanoparticles (USPIO, ferumoxtran-10). The aim of this study is to evaluate the feasibility of USPIO-enhanced MRI in the detection of locoregional lymph node metastases in patients with esophageal cancer whom underwent nCRT, and to study the effect of nCRT on the evaluation of USPIO-enhanced MRI.

0278



#### USPIO-enhanced MRI for pre-operative lymph node staging in patients with pancreatic and periampullary carcinoma: a feasibility study

Geke Litjens<sup>1</sup>, Atsushi Nakamoto<sup>2</sup>, Lodewijk Brosens<sup>3,4</sup>, Erwin van Geenen<sup>5</sup>, Marnix Maas<sup>1</sup>, Mathias Prokop<sup>1</sup>, Tom Scheenen<sup>1</sup>, Patrik Zámečník<sup>1</sup>, Kees van Laarhoven<sup>6</sup>, Jelle Barentsz<sup>1</sup>, and John Hermans<sup>1</sup>

<sup>1</sup>Radiology and Nuclear Medicine, Radboudumc, Nijmegen, Netherlands, <sup>2</sup>Diagnostic and Interventional Radiology, Osaka University Graduate School of Medicine, Suita, Japan, <sup>3</sup>Pathology, Radboudumc, Nijmegen, Netherlands, <sup>4</sup>Pathology, UMC Utrecht, Utrecht, Netherlands, <sup>5</sup>Gastroenterology and Hepatology, Radboudumc, Nijmegen, Netherlands, <sup>6</sup>Surgery, Radboudumc, Nijmegen, Netherlands

Detecting lymph node metastases is important but challenging in patients with pancreatic or periampullary carcinoma. USPIO-MRI is a promising tool to detect lymph node metastases. In 13 patients we detected on USPIO-MRI 86/307 suspect lymph nodes (28/78 regional and 58/229 distant). All patients with suspect regional lymph nodes had positive regional lymph nodes at histopathology. In evaluation of paraaortic lymph nodes discrimination between ganglions and lymph nodes showed to be important. Node-to-node analysis and follow-up of this study will give more accurate information on the value of USPIO-MRI for the detection of lymph node metastases in these patients.

---

## Oral - Power Pitch

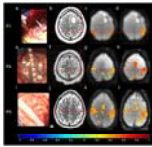
### Cancer Imaging: Machine Learning & Advanced Imaging - Advanced Cancer Imaging

Monday Parallel 5 Live Q&A

Monday 14:30 - 15:15 UTC

Moderators: Nima Gilani

0279



#### Presurgical Mapping in Brain Tumors with High-Speed Resting-State fMRI: Comparison with Task-fMRI and Intra-Operative Mapping

Stefan Posse<sup>1</sup>, Kishore Vakamudi<sup>1</sup>, Bruno Sa De La Rocque Guimaraes<sup>1</sup>, Rex Jung<sup>2</sup>, and Muhammad Omar Chohan<sup>2</sup>

<sup>1</sup>Neurology, University of New Mexico, Albuquerque, NM, United States, <sup>2</sup>Neurosurgery, University of New Mexico, Albuquerque, NM, United States

We investigated presurgical resting-state fMRI (rsfMRI) in 9 patients with brain tumors using high-speed multiband-EPI (TR:400ms) with real-time data quality monitoring for seed-based localization of sensorimotor and language networks. The Euclidean distance between intra-operative electrocortical-stimulation (ECS) and rsfMRI connectivity and task-activation in motor cortex, Broca's and Wernicke's areas was 5-13mm, except for discordant rsfMRI localization of Wernicke's area in one patient due to possible altered neurovascular coupling. A secondary objective was to accelerate encoding using echo-volumar-imaging. This study demonstrates the potential of high-speed rsfMRI for presurgical mapping and clinically-acceptable concordance with task-based fMRI and ECS localization.

0280



#### Patient Specific Planning of Thermal Magnetic Resonance: An EMF Simulation Study in Realistic Glioblastoma Multiforme Models

Eva Oberacker<sup>1</sup>, Cecilia Diesch<sup>1</sup>, Jacek Nadobny<sup>2</sup>, Andre Kuehne<sup>3</sup>, Thomas Wilhelm Eigentler<sup>1</sup>, Pirus Ghadjar<sup>2</sup>, Peter Wust<sup>2</sup>, and Thoralf Niendorf<sup>1,3,4</sup>

<sup>1</sup>Berlin Ultrahigh Field Facility (B.U.F.F.), Max Delbrück Center for Molecular Medicine in the Helmholtz Association, Berlin, Germany, <sup>2</sup>Clinic for Radiation Oncology, Charité Universitätsmedizin, Berlin, Germany, <sup>3</sup>MRI.TOOLS GmbH, Berlin, Germany, <sup>4</sup>Experimental and Clinical Research Center (ECRC), joint cooperation between the Charité Medical Faculty and the Max-Delbrück-Center for Molecular Medicine in the Helmholtz Association, Berlin, Germany

Ultrahigh-field MR employs higher radio frequencies (RF) than conventional MR and has unique potential to provide focal temperature manipulation and high resolution imaging in an integrated device (ThermalMR). The advantage of integrated therapy monitoring and guidance benefits thermal interventions in brain tumor treatments. To approach this goal this work examines the inter-patient variability in a heterogeneous group of glioma multiforme patients using EMF simulations. Our findings provide useful indicators as potential patient inclusion criteria for thermal treatment of brain tumors and form the technological basis for treatment planning and RF applicator developments *en route* to clinical applications of Thermal MR.

0281

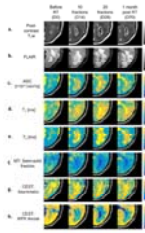


#### Characterization of CT-2A neurosphere-derived high-grade glioma in mice.

Uwe Himmelreich<sup>1</sup>, Matteo Riva<sup>2</sup>, Sarah Belderbos<sup>1</sup>, Roxanne Wouters<sup>2</sup>, Akila Weerasekera<sup>1</sup>, Thais Baert<sup>2</sup>, Willy Gsell<sup>1</sup>, and An Coosemans<sup>2</sup>

Several promising treatments against high-grade gliomas (HGGs) failed to provide significant benefit when translated from the preclinical setting to patients. Improving animal models is fundamental to overcome this translational gap. We have developed and comprehensively characterized in-vivo model based on the orthotopic implantation of CT-2A cells cultured in neurospheres (NS). Anatomical, metabolic (MRS) and perfusion MRI indicated that CT-2A NS-derived tumors showed a more HGG-like behavior, which was supported by survival data, increased glioma stem cell population and enhanced neoangiogenesis. Because of these specific features, the CT-2A NS-derived model represents a high-translational platform for the search of new HGG treatments.

0282



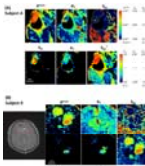
### Magnetization Transfer and Chemical Exchange Saturation Transfer in Glioblastoma at 1.5T: Comparison of Early and Late Tumor Progression

Rachel W Chan<sup>1</sup>, Sten Myrehaug<sup>2</sup>, Greg J Stanisiz<sup>1,3,4</sup>, James Stewart<sup>2</sup>, Mark Ruschin<sup>2</sup>, Arjun Sahgal<sup>2,3</sup>, and Angus Z Lau<sup>1,3</sup>

<sup>1</sup>Physical Sciences, Sunnybrook Research Institute, Toronto, ON, Canada, <sup>2</sup>Department of Radiation Oncology, Sunnybrook Health Sciences Centre, University of Toronto, Toronto, ON, Canada, <sup>3</sup>Medical Biophysics, University of Toronto, Toronto, ON, Canada, <sup>4</sup>Department of Neurosurgery and Pediatric Neurosurgery, Medical University, Lublin, Poland

This study aims to quantify the MT and CEST parameters in glioblastoma at 1.5T over four time points of chemoradiation. Previous approaches to quantify the MT/CEST signal in terms of response to treatment were at higher field strengths. Additionally, we analyzed different subregions within the clinical target volume and gross tumor volume, generated by thresholding based on the T<sub>1</sub>-weighted, FLAIR and DWI scans, for comparing the MT/CEST parameters between the early and late tumor progression. Results indicated that MT/CEST at 1.5T can be used for monitoring therapy and that the results depend on the specific tumor region analyzed.

0283



### A Comprehensive, Adaptive Approach for Shutter-Speed DCE-MRI Analyses of Heterogeneous Brain Tumor Data

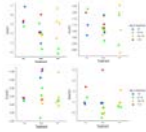
Ruiliang Bai<sup>1</sup>, Bao Wang<sup>2</sup>, Yinhang Jia<sup>1</sup>, Zhaoqing Li<sup>3</sup>, Yi-Cheng Hsu<sup>4</sup>, Charles S. Springer Jr.<sup>5</sup>, and Yingchao Liu<sup>6</sup>

<sup>1</sup>Interdisciplinary Institute of Neuroscience and Technology, School of Medicine, Zhejiang University, Hangzhou, China, <sup>2</sup>Department of Radiology, Shandong University Qilu Hospital, Jinan, China, <sup>3</sup>College of Biomedical Engineering and Instrument Science, Zhejiang University, Hangzhou, China, <sup>4</sup>MR Collaboration, Siemens Healthcare, Shanghai, China, <sup>5</sup>Advanced Imaging Research Center, Oregon Health & Science University, Portland, OR, United States, <sup>6</sup>Department of Neurosurgery, Provincial Hospital Affiliated to Shandong University, Jinan, China

The [Shutter-Speed-Model-Dynamic-Contrast-Enhanced] SSM-DCE-MRI pharmacokinetic analysis has a metabolic dimension. However, SSM must be applied thoughtfully, especially in Glioblastoma multiforme [GBM], because of strong tissue vascular heterogeneity across the brain field-of-view. Here, we present a method to select the appropriate SSM-DCE-MRI version to analyze such tissue, on a pixel-by-pixel basis. The supra-intensive parameters, vascular water efflux ( $k_{bo}$ ), cellular water efflux ( $k_{io}$ ), and vascular CA efflux ( $k_{pe}$ ) rate constants could be reliably determined. Pilot data on one recurrent and one pre-diagnosis GBM patient are presented to demonstrate method performance.

0284

Hippocampal MR Spectroscopy show chronic metabolic effects following cranial radiotherapy in childhood cancer survivors

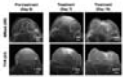


Maria Ljungberg<sup>1,2</sup>, Erik Fernström<sup>3</sup>, Oscar Jalnefjord<sup>1,2</sup>, Mikael Montelius<sup>1</sup>, Thomas Björk-Eriksson<sup>3</sup>, Marie Kalm<sup>4</sup>, and Marianne Jarfelt<sup>5</sup>

<sup>1</sup>Radiation Physics, Institute of Clinical Sciences, Sahlgrenska Academy, Gothenburg University, Göteborg, Sweden, <sup>2</sup>Medical Physics and Biomedical Engineering, Sahlgrenska University Hospital, Göteborg, Sweden, <sup>3</sup>Oncology, Institute of Clinical Sciences Sahlgrenska Academy Gothenburg University, Göteborg, Sweden, <sup>4</sup>Health and Rehabilitation, Institute of neuroscience and physiology, Sahlgrenska Academy Gothenburg University, Göteborg, Sweden, <sup>5</sup>Pediatrics, Institute of Clinical Sciences, Sahlgrenska Academy Gothenburg University, Göteborg, Sweden

Modern cranial radiotherapy (CRT) achieves high targeted doses of radiation to brain tumours, which has resulted in an increased population of long-term survivors of childhood cancer. Unfortunately, the CRT cause radiation damage to the healthy brain which results in cognitive deficits. In a group of adult childhood cancer survivors lower ratios of tNAA/tCho, Glu/tCho and Glu/tCr were obtained in the hippocampus for the patient group that received highest radiation doses to target volume as compared to the group that did not receive any CRT, indicating a still ongoing process of e.g inflammation, re-myelination and gliosis due to CRT

0285



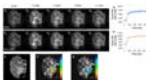
Longitudinal 3D intratumoral evaluation of an anti-angiogenic tumor treatment using a Gd-nano liposomal contrast agent and MR micro angiography

Nobuhiro Nitta<sup>1</sup>, Yoichi Takakusagi<sup>1</sup>, Daisuke Kokuryo<sup>2</sup>, Sayaka Shibata<sup>1</sup>, Akihiro Tomita<sup>3</sup>, Tatsuya Higashi<sup>1</sup>, Ichio Aoki<sup>1</sup>, and Masafumi Harada<sup>4</sup>

<sup>1</sup>Department of Molecular Imaging and Theranostics, National Institutes for Quantum and Radiological Science and Technology, Chiba, Japan, <sup>2</sup>Graduate School of System Informatics, Kobe University, Hyogo, Japan, <sup>3</sup>Department of Hematology, Fujita Health University School of Medicine, Aichi, Japan, <sup>4</sup>Graduate School of Medicine, Tokushima University, Tokushima, Japan

The enhanced permeability and retention (EPR) effect depends on nanoparticle properties and tumor/vessel conditions. We aimed to develop a tumor vasculature evaluation method and high-resolution nanoparticle-delivery imaging technique using magnetic resonance micro-imaging technology and a gadolinium (Gd)-dendron assembled liposomal contrast agent. We achieved 50- $\mu$ m isotropic MR angiography with clear visualization of tumor micro-vessel structure. The Gd-liposome-enhanced MR micro-imaging revealed differences in the vascular structures between two different types of grafted mice models. The MR micro-imaging methods facilitate the evaluation of intratumoral vascularization patterns, the quantitative assessment of vascular-properties that alter tumor malignancy, particle retentivity, and the effects of treatment.

0286



Radial sampling and KWIC-reconstruction reduce motion artifacts and improve spatial resolution for DCE-MRI of mouse pancreatic cancer

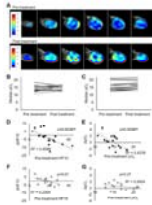
Jianbo Cao<sup>1</sup>, Stephen Pickup<sup>1</sup>, Hee Kwon Song<sup>1</sup>, and Rong Zhou<sup>1,2</sup>

<sup>1</sup>Department of Radiology, University of Pennsylvania, Philadelphia, PA, United States, <sup>2</sup>Abramson Cancer Center, University of Pennsylvania, Philadelphia, PA, United States

Genetically engineered mouse (GEM) model of pancreatic ductal adenocarcinoma (PDA) recapitulates a dense stroma exhibited in human disease and is thus relevant for testing stroma-directed drugs. However, the lesion location makes it highly susceptible to motion. We present a multi-slice 2D saturation-recovery technique using golden-angle radial k-space sampling combined with KWIC reconstruction for DCE-MRI of PDA. This method minimizes respiration motion artefacts in PDA tumors and increases the effective temporal resolution of the AIF.  $K^{trans}$  and  $k_{ep}$  maps derived from PK model fitting of DCE series exhibit adequate spatial resolution to reveal permeability and perfusion heterogeneity in the PDA tumor.

0287

Imaging assessment of pancreatic ductal adenocarcinoma xenograft treated with hypoxia activated prodrug Evofosfamide



Shun Kishimoto<sup>1</sup>, Nallathambiy Devasahayam<sup>1</sup>, Yu Saida<sup>1</sup>, Yasunori Otowa<sup>1</sup>, Kazutoshi Yamamoto<sup>1</sup>, Jeffrey R Brender<sup>1</sup>, and Murali C Krishna<sup>1</sup>

<sup>1</sup>NCI, Bethesda, MD, United States

TH-302 is designed to release cytotoxic bromo-isophosphoramidate (Br-IPM) moiety in hypoxic microenvironment. Therefore, this drug preferentially attacks the hypoxic region in cancer where other standard anti-cancer treatment such as chemotherapy and radiation therapy are ineffective. Here, we monitored the change in tumor hypoxia and perfusion in response to TH-302 treatment by EPR oximetry and DCE MRI using two pancreatic ductal adenocarcinoma xenograft models. The result showed improved oxygenation only in treatment sensitive MIA Paca-2 tumors without modulating tumor blood perfusion, suggesting that intratumor pO<sub>2</sub> is a useful biomarker to evaluate treatment response to TH-302.

0288



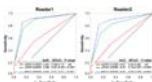
Extracellular pH Changes Induced by Immuno-Thermal Ablation in a Murine Colorectal Cancer Model

Daniel Coman<sup>1</sup>, Ryan J Slovak<sup>2,3</sup>, Fahmeed Hyder<sup>1,4,5</sup>, and Hyun S Kim<sup>1,2,5,6</sup>

<sup>1</sup>Radiology & Biomedical Imaging, Division of Bioimaging Sciences, Yale University School of Medicine, New Haven, CT, United States, <sup>2</sup>Radiology & Biomedical Imaging, Section of Interventional Radiology, Yale University School of Medicine, New Haven, CT, United States, <sup>3</sup>University of Connecticut School of Medicine, Farmington, CT, United States, <sup>4</sup>Department of Biomedical Engineering, Yale University School of Medicine, New Haven, CT, United States, <sup>5</sup>Yale Cancer Center, Yale University School of Medicine, New Haven, CT, United States, <sup>6</sup>Department of Internal Medicine, Section of Medical Oncology, Yale University School of Medicine, New Haven, CT, United States

Acidification of tumor microenvironment is associated with aggressive tumor growth and facilitate resistance to anti-cancer therapies. Extracellular pH (pH<sub>e</sub>) mapping with BIRDS is used to differentiate ablated and non-ablated tumors in the setting of systemic immunotherapy of murine colorectal cancer. Combination of Cryoablation with Dual Immune Checkpoint Blockade (DICB) resulted in a significant pH<sub>e</sub> increase compared to control tumors. This work demonstrates the feasibility of measuring pH<sub>e</sub> with BIRDS in a murine colorectal cancer model. pH<sub>e</sub> imaging could serve as a non-invasive imaging biomarker for tumor microenvironment assessment and monitoring of metabolic changes after immuno-thermal ablation therapy.

0289



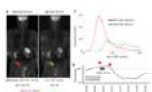
Utility of computed diffusion-weighted imaging for evaluating primary prostate cancer in whole-body MRI

Yuki Arita<sup>1,2</sup>, Yuma Waseda<sup>3</sup>, Soichiro Yoshida<sup>2,3</sup>, Taro Takahara<sup>2,4</sup>, Chikako Ishii<sup>2</sup>, Thomas C Kwee<sup>5</sup>, Ryota Ishii<sup>6</sup>, Shigeo Okuda<sup>1</sup>, Yasuhisa Fujii<sup>3</sup>, and Masahiro Jinzaki<sup>1</sup>

<sup>1</sup>Department of Radiology, Keio University School of Medicine, Tokyo, Japan, <sup>2</sup>Department of Radiology, Advanced Imaging Center Yaesu Clinic, Tokyo, Japan, <sup>3</sup>Department of Urology, Tokyo Medical and Dental University Graduate School, Tokyo, Japan, <sup>4</sup>Department of Biomedical engineering, Tokai University School of Engineering, Kanagawa, Japan, <sup>5</sup>Department of Radiology, Nuclear Medicine and Molecular Imaging, University Medical Center Groningen, Groningen, Netherlands, <sup>6</sup>Department of Biostatistics Unit, Clinical and Translational Research Center, Keio University Hospital, Tokyo, Japan

The purpose of this study is to determine the value of applying computed DWI to a whole-body MRI/DWI protocol to acquire computed high b-value (2000 s/mm<sup>2</sup>) diffusion-weighted images for local prostate cancer evaluation. Based on the results, computed diffusion-weighted images obtained from whole-body MRI provide a similar diagnostic performance compared to pelvic bi-parametric MRI for the detection of primary prostate cancer. Computed DWI is a straightforward postprocessing technique without the need for additional image acquisition time. It can be recommended for use in routine clinical practice in whole-body MRI protocols for concurrent evaluation of primary and metastatic prostate cancer.

0290



Progressive site-directed therapy for oligo-progressive castration-resistant prostate cancer

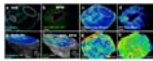


Soichiro Yoshida<sup>1</sup>, Taro Takahara<sup>2</sup>, Yuki Arita<sup>3,4</sup>, Chikako Ishii<sup>4</sup>, Kazuma Toda<sup>5</sup>, Kazuma Toda<sup>5</sup>, Tsuyoshi Sakamoto<sup>6</sup>, Toshiki Kijima<sup>1</sup>, Minato Yokoyama<sup>1</sup>, Junichiro Ishioka<sup>1</sup>, Yoh Matsuoka<sup>1</sup>, Kazutaka Saito<sup>1</sup>, Ryoichi Yoshimura<sup>5</sup>, and Yasuhisa Fujii<sup>1</sup>

<sup>1</sup>*Urology, Tokyo Medical and Dental University, Tokyo, Japan*, <sup>2</sup>*Biomedical Engineering, Tokai University School of Engineering, Kanagawa, Japan*, <sup>3</sup>*Radiology, Keio University School of Medicine, Tokyo, Japan*, <sup>4</sup>*Radiology, Advanced Imaging Center, Yaesu Clinic, Tokyo, Japan*, <sup>5</sup>*Radiation Therapeutics and Oncology, Tokyo Medical and Dental University, Tokyo, Japan*, <sup>6</sup>*PixSpace, Ltd., Fukuoka, Japan*

Locoregional therapy for oligometastatic prostate cancer has generated great interest. However, the benefit for castration-resistant prostate cancer (CRPC) has not been fully demonstrated. According to the current study, whole body-MRI incorporating DWI identified a substantial number of oligo-progressive CRPC patients (OP-CRPC) with a number of progressive lesions 3 or less. Progressive site-directed therapy (PSDT) to OP-CRPC provided a high treatment effect in terms of prostate-specific antigen (PSA) response, especially for patients with longer PSA-doubling time. Furthermore, this study identified the site-dependencies of the PSDT treatment effect; patients whose progressive site was localized in the pelvis were good candidates for PSDT.

0291



### A Multiscale, Multimodality Pipeline for “Image-based” Cancer Systems Biology

Akanksha Bhargava<sup>1</sup>, Manisha Aggarwal<sup>1</sup>, and Arvind Pathak<sup>1</sup>

<sup>1</sup>*Russell H. Morgan Department of Radiology and Radiological Science, Johns Hopkins University, Baltimore, MD, United States*

Preclinical imaging methods such as magnetic resonance microscopy ( $\mu$ MRI), micro-computed tomography ( $\mu$ CT) and optical techniques such as multiphoton microscopy (MPM) have been instrumental in advancing our understanding of the role of vasculature in cancer<sup>1</sup>. However, integrating vascular microenvironmental data across modalities and spatial scales for novel “image-based” cancer systems biology applications<sup>2</sup> remains a challenge. Therefore, we developed a multimodality imaging pipeline that achieves multiscale data integration, image co-registration and results in the generation of “cancer atlases” for systems and computational biology applications.

0292



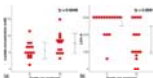
### Evaluating the sensitivity of ADC to childhood neuroblastoma pathology in vivo using Gaussian mixture modeling and computational pathology

Konstantinos Zormpas-Petridis<sup>1</sup>, Matthew D. Blackledge<sup>1</sup>, Louis Chesler<sup>2</sup>, Yinyin Yuan<sup>3</sup>, Simon P. Robinson<sup>1</sup>, and Yann Jamin<sup>1</sup>

<sup>1</sup>*Radiotherapy and Imaging, Institute of Cancer Research, London, Sutton, United Kingdom*, <sup>2</sup>*Clinical studies, Institute of Cancer Research, London, Sutton, United Kingdom*, <sup>3</sup>*Molecular pathology, Institute of Cancer Research, London, Sutton, United Kingdom*

We use Gaussian mixture modeling, computational pathology and MRI-histopathology registered datasets to evaluate *i)* the sensitivity of diffusion-weighted imaging to the rich histopathology of childhood neuroblastoma and *ii)* the sensitivity of the derived apparent diffusion coefficient, ADC, as a biomarker of response to a potent MYCN-targeted small molecule inhibitor in the Th-MYCN mouse, a faithful model of high-risk MYCN-driven disease.

0293



### Lactate concentration from double quantum filtered (DQF) MRS in human breast tumour is associated with tumour grading and patient prognosis

Sai Man Cheung<sup>1</sup>, Ehab Husain<sup>2</sup>, Yazan Masannat<sup>3</sup>, Klaus Wahle<sup>4</sup>, Steven Heys<sup>3</sup>, and Jiabao He<sup>1</sup>

<sup>1</sup>*Aberdeen Biomedical Imaging Centre, University of Aberdeen, Aberdeen, United Kingdom*, <sup>2</sup>*Pathology Department, Aberdeen Royal Infirmary, Aberdeen, United Kingdom*, <sup>3</sup>*Breast Unit, Aberdeen Royal Infirmary, Aberdeen, United Kingdom*, <sup>4</sup>*Institute of Pharmacy and Biological Sciences, University of Strathclyde, Glasgow, United Kingdom*

Upregulation of aerobic glycolysis and an elevated lactate accumulation have been linked to tumour aggressiveness. However, current evidence drawn from cell culture and small animal models remains controversial. Since lactate and lipid share the same spectral frequency, conventional MRS is inadequate in quantifying lactate under overwhelming lipid signal. Double quantum filtered (DQF) MRS allows excellent suppression of lipid signal from adipose breast tissues. We examined prognostic role of lactate concentration through a cross sectional study in grade II and III whole tumours freshly excised from patients with breast cancer using DQF MRS for the quantification of lactate concentration.

---

---

### Sunrise Session

#### Educational Q&A: Neuro Sunrise - Rodents vs. Humans: Multiple Sclerosis

Organizers: Cornelia Laule, John Port

Monday Parallel 2 Live Q&A

Monday 15:15 - 16:00 UTC

Moderators: Yan Bai

[Multiple Sclerosis: Lessons from Pre-Clinical Models](#)

Pascal Sati

---

[Multiple Sclerosis: Lessons from the Clinic](#)

Orhun Kantarci

---

---

### Sunrise Session

#### Educational Q&A: Neuro Sunrise - Rodents vs. Humans: Stroke

Organizers: Manabu Kinoshita, Nivedita Agarwal

Monday Parallel 2 Live Q&A

Monday 15:15 - 16:00 UTC

[Rodent Stroke Models for MRI and monitoring pathological processes](#)

Yuki Mori

---

[Non-Contrast-Enhanced MRI in Stroke](#)

Tetsuro Sekine

---

---

### Sunrise Session

#### Educational Q&A: Neuro Sunrise - Rodents vs. Humans: Traumatic Brain Injury

Organizers: Cornelia Laule, Pia Maly Sundgren

Monday Parallel 2 Live Q&A

Monday 15:15 - 16:00 UTC

Moderators: Hongxia Lei

[Traumatic Brain Injury: Lessons from Preclinical Models](#)

David Wright

---

[Traumatic Brain Injury: Lessons from Clinical Research](#)

Ivan Kirov

---

---

### Sunrise Session

#### Educational Q&A: Neuro Sunrise - Rodents vs. Humans: Neurodegeneration

Organizers: Nivedita Agarwal, Kader Oguz

Monday Parallel 2 Live Q&A

Monday 15:15 - 16:00 UTC

Preclinical Studies on Neurodegeneration  
Shu-Wei Sun

---

Advanced Neuroimaging in Neurodegenerative Diseases: Focus on Dementia  
Yan Bai

---

---

## Weekday Course

### Educational Q&A: Value - Value of MRI: A Global Perspective

Organizers: Vikas Gulani, Krishna Nayak, C. C. Tchoyoson Lim, Lawrence Wald

Monday Parallel 1 Live Q&A

Monday 15:15 - 16:00 UTC

Moderators: Sonal Krishan & Andrew Webb

#### Defining the Clinical Needs in Underserved Populations

Susan Sotardi<sup>1</sup>

<sup>1</sup>Children's Hospital Philadelphia, United States

---

#### Low-Cost Scanning: A Historical Overview

Raimo Sepponen<sup>1</sup>

<sup>1</sup>Aalto University, Espoo, Finland

A historical review of the experiences gained while introducing a 20 mT MRI unit for emergency and trauma clinics. The inherent high T1-contrast provided rather good sensitivity in the diagnosis of internal hemorrhages, some tumors, abscesses, and pneumonia. Due to the situation in the market, the argument of lower costs was not effective. However, the recent development of magnet materials and signal processing may give possibilities to develop niche concepts based on very low field MRI.

---

#### Affordable Magnet Configurations

Shaoying Huang<sup>1</sup>

<sup>1</sup>Singapore Univ. of Technology & Design, Singapore

---

#### Automatic Scanning: Can Computing Be Leveraged to Extend Scanning Capabilities?

Juan Santos<sup>1</sup>

<sup>1</sup>HeartVista, Inc., United States

Deep learning has dramatically improved the performance of computer vision and image analysis algorithms. Initial applications in MRI have focused on post-processing and, more recently, image reconstruction. We will explore how deep learning applied to automation in data acquisition and scan control can have a meaningful impact on image quality, consistency, ease of use, and translate to a significant reduction in total examination time.

---

#### Panel Discussion

Sonal Krishan<sup>1</sup>

<sup>1</sup>Medante Hospital, India

---

---

## Weekday Course

### Educational Q&A: Value - Junior Fellows Symposium: The Environmental Impact of MRI

Organizers: Timothy Bray, Stefanie Hectors, Nicole Seiberlich, Esther Warnert

Monday Parallel 1 Live Q&A

Monday 15:15 - 16:00 UTC

Moderators: Stefanie Hectors & Esther Warnert

#### Energy Consumption by MRI Scanners

Alastair Martin<sup>1</sup>

<sup>1</sup>University of California, San Francisco, United States

---

#### The Biological Fate of Gadolinium

Peter Caravan<sup>1</sup>

<sup>1</sup>Massachusetts General Hospital, United States

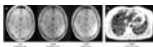
---

#### Getting Rid of Helium in MRI

Andrew Webb<sup>1</sup>

<sup>1</sup>Leiden University Medical Center, Netherlands

---



#### Engineering Solutions: Low-Field MRI

Rajiv Ramasawmy<sup>1</sup>

<sup>1</sup>National Heart, Lung & Blood Institute, National Institutes of Health, Bethesda, MD, United States

Systems with lower magnetic field strengths may reduce the environmental impact of MRI and could be combined with other engineering, efficiency and disposal solutions. Although these low field designs may not be suitable for all diagnostic imaging demands, all of these approaches towards lower field systems can pave the way towards both sustainable and accessible MRI.

---

#### Composite Recycled Permanent Magnet for MR Screening Device

Sunita Gudwani<sup>1</sup>

<sup>1</sup>Department of ENT, Escorts Heart Institute and Research Center, New Delhi, India

---

#### A Real-Time Updating Transport & Scheduling System Based on Machine Learning

Thomas Lindner<sup>1</sup>

<sup>1</sup>Neuroradiology, University Hospital Hamburg-Eppendorf, Hamburg, Germany

---

## Combined Educational & Scientific Session

### Educational Q&A: Value - Value of MRI

Organizers: Vikas Gulani, Krishna Nayak

Monday Parallel 1 Live Q&A

Monday 15:15 - 16:00 UTC

Moderators: Nicole Seiberlich & Kathryn Keenan

#### Introduction to Comparative Effectiveness Research

Nicholas K. Schiltz<sup>1</sup>

<sup>1</sup>Case Western Reserve University, Cleveland, OH, United States

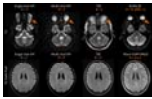
Comparative and cost-effectiveness approaches can be used to assess the value of MRI, but these studies have not traditionally been explored in the ISMRM community. This session will provide an introduction to comparative and cost-effectiveness research (CER), with particular focus on decision model approaches. Topics covered include: best practices for setting up a decision tree model, key measures and interpretation including incremental-cost effectiveness ratio, and the value of information. At the end of the session, audience members should know how to create an outline of a model for their own research questions to assess the value of MRI.

---

Case Study of Applying Comparative Effectiveness Research in MRI: Prostate MRI Before Biopsy  
Shivani Pahwa<sup>1</sup>

<sup>1</sup>Case Western Reserve University, United States

0294



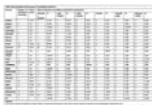
A comprehensive distortion-free 2-minute brain MR examination using BUDA and Wave-CAIPI

Wei-Ching Lo<sup>1</sup>, Kawin Setsompop<sup>2,3,4,5</sup>, Congyu Liao<sup>2</sup>, Susie Yi Huang<sup>2,3,4,5</sup>, John Conklin<sup>2,3,4</sup>, Stephen F. Cauley<sup>2,3,4</sup>, Wei Liu<sup>6</sup>, Bryan Clifford<sup>1</sup>, Steffen Bollmann<sup>1</sup>, Xiaozhi Cao<sup>2,7</sup>, Zijing Zhang<sup>2,8</sup>, Daniel Polak<sup>2,3,9,10</sup>, Daniel Nicolas Splitthoff<sup>9</sup>, Thorsten Feiweier<sup>9</sup>, Qiyuan Tian<sup>2,3,4</sup>, Jaejin Cho<sup>2</sup>, John E. Kirsch<sup>2,3,4</sup>, Shivraman Giri<sup>1</sup>, Otto Rapalino<sup>3,4</sup>, Pamela W. Schaefer<sup>3,4</sup>, Larry L. Wald<sup>2</sup>, and Berkin Bilgic<sup>2</sup>

<sup>1</sup>Siemens Medical Solutions, Boston, MA, United States, <sup>2</sup>Athinoula A. Martinos Center for Biomedical Imaging, Department of Radiology, Massachusetts General Hospital, Boston, MA, United States, <sup>3</sup>Department of Radiology, Massachusetts General Hospital, Boston, MA, United States, <sup>4</sup>Harvard Medical School, Boston, MA, United States, <sup>5</sup>Harvard-MIT Division of Health Sciences and Technology, Massachusetts Institute of Technology, Boston, MA, United States, <sup>6</sup>Siemens Shenzhen Magnetic Resonance Ltd., Shenzhen, China, <sup>7</sup>Center for Brain Imaging Science and Technology, Biomedical Engineering, Zhejiang University, Hangzhou, Zhejiang, China, <sup>8</sup>State Key Laboratory of Modern Optical Instrumentation, College of Optical Science and Engineering, Zhejiang University, Hangzhou, Zhejiang, China, <sup>9</sup>Siemens Healthcare GmbH, Erlangen, Germany, <sup>10</sup>Department of Physics and Astronomy, Heidelberg University, Heidelberg, Germany

We utilize Wave-CAIPI and BUDA techniques to develop a rapid 2-minute protocol that produces high in-plane resolution and distortion-free axial images for comprehensive evaluation of the brain. The protocol includes 3D T1-weighted Wave-CAIPI MPRAGE, 3D dark-fluid T2-weighted Wave-CAIPI SPACE-FLAIR, 2D T2\*-weighted gradient echo BUDA, 2D T2-weighted and diffusion-weighted spin-echo BUDA. The results of the optimized protocol demonstrate comparable image quality, tissue contrast, and spatial resolution to standard clinical scans while keeping the total scan time to less than 2 minutes. The advanced acquisition and reconstruction framework presented here offers a path toward increasing clinical acceptance of ultrafast brain examinations.

0295



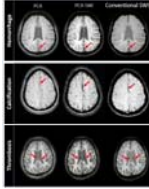
THE LONG ROAD FROM INVENTION TO IMPLEMENTATION: A PAN-EUROPEAN NEURORADIOLOGICAL SURVEY ON QUANTITATIVE MRI TECHNIQUES IN CLINICAL PRACTICE

Vera Catharina Keil<sup>1</sup>, Marion Smits<sup>2,3</sup>, Steffi Thust<sup>3,4</sup>, Jan Petr<sup>5</sup>, Laszlo Solymosi<sup>1</sup>, and Elia Manfrini<sup>1,6</sup>

<sup>1</sup>Neuroradiology, University Hospital Bonn, Bonn, Germany, <sup>2</sup>Department of Radiology and Nuclear Medicine (Ne-515), Erasmus MC, Rotterdam, Netherlands, <sup>3</sup>Lysholm Department of Neuroradiology, National Hospital for Neurology and Neurosurgery Queen Square, London, United Kingdom, <sup>4</sup>Department of Brain Rehabilitation and Repair, UCL Institute of Neurology Queen Square, London, United Kingdom, <sup>5</sup>Institute of Radiopharmaceutical Cancer Research, Helmholtz-Zentrum Dresden-Rossendorf, Dresden, Germany, <sup>6</sup>Universita Politecnica delle Marche. Facolta di Medicina e Chirurgia, Ancona, Italy

This pan-European online survey study revealed that clinically working Neuroradiologists appreciate the additional diagnostic accuracy rendered by quantitative MRI techniques. However, the clinical implementation of many techniques is hampered by a lack of knowledge on how to acquire, post-process and interpret results of multiple quantitative MRI techniques including ASL, CEST/APT, IVIM and others. With exception of DSC and DWI in tumor imaging and stroke, the number of indications is also still limited especially regarding head/neck Radiology and neurodegenerative diseases.

0296



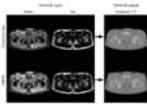
Free lunch may not exist, but free contrast does: Calculation of Susceptibility weighted Images from data acquired for Phase Contrast Angiography

Yogesh kannan Mariappan<sup>1</sup>, Jaladhar Neelavalli<sup>1</sup>, Nehul Makani<sup>1,2</sup>, Narayana Krishna Rolla<sup>1</sup>, Karthik Gopalakrishnan<sup>1</sup>, Nalini Pagadala<sup>1,2</sup>, and Jitendar Saini<sup>3</sup>

<sup>1</sup>Philips Healthcare, Bengaluru, India, <sup>2</sup>Indian Institute of Technology, Madras, Chennai, India, <sup>3</sup>National Institute for Mental Health and Neuroscience, Bengaluru, India

In Phase contrast Angiography (PCA), the flow is encoded as additional phase onto the background phase typically using a Fast field echo (FFE) based pulse sequence. This flow dependent phase is then extracted and is used in further downstream processing. The background phase is typically discarded. In this work, this background phase is processed to obtain Susceptibility weighted Imaging (SWI) contrast. Our preliminary results indicate that the additional SWI contrast (PCA-SWI) images can potentially provide clinically significant information like hemorrhage, calcification and thrombus etc. and are similar to the results obtained from conventional SWI images.

0297



Multiple-echo steady-state for MR-only prostate radiotherapy: Combined T1/T2-weighted imaging, water-fat separation, and synthetic CT

Frank Zijlstra<sup>1</sup>, Mateusz C Florkow<sup>1</sup>, and Peter R Seevinck<sup>1,2</sup>

<sup>1</sup>Image Sciences Institute, UMC Utrecht, Utrecht, Netherlands, <sup>2</sup>MRGuidance BV, Utrecht, Netherlands

We propose an efficient sequence for the acquisition of multiple contrasts for MR-only radiotherapy. By including T2-weighted echoes to a gradient echo sequence, this sequence provides T1- and T2-weighted imaging and water-fat separation in a single 4 minute acquisition. A previously trained deep neural network for synthetic CT generation was successfully applied to this new sequence, demonstrating that synthetic CT-based dose calculations can be performed. Furthermore, increased contrast between the anatomies of interest shows promise for (automatic) segmentation.

0298

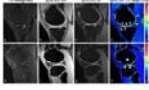


Acquisition Parameter Conditioned Generative Adversarial Network for Enhanced MR Image Synthesis

Jonas Denck<sup>1,2,3</sup>, George William Ferguson<sup>3</sup>, Jens Guehring<sup>3</sup>, Andreas Maier<sup>1</sup>, and Eva Rothgang<sup>2</sup>

<sup>1</sup>Pattern Recognition Lab, Department of Computer Science, Friedrich-Alexander-Universität Erlangen-Nürnberg, Erlangen, Germany, <sup>2</sup>Technical University of Applied Sciences Amberg-Weiden, Amberg, Germany, <sup>3</sup>Siemens Healthineers, Erlangen, Germany

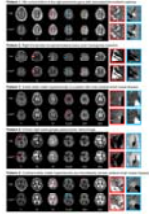
Current approaches for the synthesis of MR images are only trained on MR images with a specific set of acquisition parameter values, limiting the clinical value of these methods. We therefore trained a generative adversarial network (GAN) to generate synthetic MR knee images conditioned on various acquisition parameters (TR, TE, imaging orientation). This enables us to synthesize MR images with adjustable image contrast. This work can support radiologists and technologists during the parameterization of MR sequences, can serve as a valuable tool for radiology training, and can be used for customized data generation to support AI training.



Akshay S Chaudhari<sup>1</sup>, Murray Grissom<sup>2</sup>, Zhongnan Fang<sup>3</sup>, Bragi Sveinsson<sup>4</sup>, Jin Hyung Lee<sup>1</sup>, Garry E Gold<sup>1</sup>, Brian A Hargreaves<sup>1</sup>, and Kathryn J Stevens<sup>1</sup>

<sup>1</sup>Stanford University, Stanford, CA, United States, <sup>2</sup>Santa Clara Valley Medical Center, San Jose, CA, United States, <sup>3</sup>LVIS Corporation, Palo Alto, CA, United States, <sup>4</sup>Harvard Medical School, Boston, MA, United States

Knee MRI protocols usually require 20+ minutes of scan time, leading to great interest in expedited and high-value imaging examinations. Moreover, despite the popularity of quantitative imaging for osteoarthritis, it is not routinely implemented clinically. In this study, we use a 5-minute quantitative double-echo steady-state (qDESS) sequence that produces simultaneous morphological images and T2 relaxation time measurements. We prospectively enhance the slice-resolution of qDESS using deep learning. We show that qDESS provided high diagnostic accuracy compared to both diagnostic knee MRI and surgical findings. Additionally, automatic T2 maps increased reader diagnostic confidence and sensitivity to cartilage lesions.

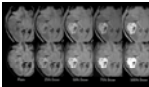


A comprehensive multi-shot EPI protocol for high-quality clinical brain imaging in 3 minutes

John Conklin<sup>1</sup>, Bryan Clifford<sup>2</sup>, Steffen Bollmann<sup>2</sup>, Wei-Ching Lo<sup>2</sup>, Berkin Bilgic<sup>3</sup>, Stephen Cauley<sup>3</sup>, Kawin Setsompop<sup>3</sup>, Thorsten Feiweier<sup>4</sup>, John Kirsch<sup>3</sup>, R. Gilberto Gonzalez<sup>3</sup>, Pamela Schaefer<sup>3</sup>, Otto Rapalino<sup>3</sup>, and Susie Huang<sup>3</sup>

<sup>1</sup>Radiology, Massachusetts General Hospital, Boston, MA, United States, <sup>2</sup>Siemens Medical Solutions, Boston, MA, United States, <sup>3</sup>Massachusetts General Hospital, Boston, MA, United States, <sup>4</sup>Siemens Healthcare GmbH, Erlangen, Germany

A comprehensive 3 minute whole-brain MRI exam based on multi-shot echoplanar imaging (ms-EPI) was optimized and evaluated in 5 patients with different clinical pathologies. This approach minimizes artifacts associated with single-shot echoplanar imaging, and provides image quality similar to that of a 10-minute clinical reference protocol based on turbo spin-echo imaging.



Possibility of the Reduction of Gd Dose using Spiral Spin-Echo Method for Contrast Enhanced Scans at 3.0T

Ravi Varma Dandu<sup>1</sup>, Rithika Varma Dandu<sup>2</sup>, Karthick Raj Rajendran<sup>3</sup>, Narayana Rolla<sup>4</sup>, and Indrajit Saha<sup>5</sup>

<sup>1</sup>Citi Neuro Centre, Hyderabad, India, <sup>2</sup>RV College of Engineering, Bengaluru, India, <sup>3</sup>Philips Healthcare, Eindhoven, Netherlands, <sup>4</sup>Philips Healthcare, Bangalore, India, <sup>5</sup>Philips Healthcare, Gurgaon, India

This study compares the performance of spin echo T1 with spiral k-space filling and three other techniques, for post contrast T1-weighted imaging of the brain. The lesion enhancement in each technique was evaluated after incremental fractional doses of gadolinium injection. The enhancement achieved on T1-FFE and T1-TSE techniques with full dose contrast could be achieved with 50% to 75% dose contrast in spiral imaging. Spiral imaging can thus be used to reduce the dose of injected contrast medium (by at least 25% and up to 50%) without compromising on the diagnostic quality of the post contrast study.



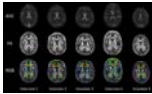
Determining the Value of Fit-for-Purpose MRI Exams of Multiple Sclerosis

Arijitt Borthakur<sup>1</sup>, Megan Frame<sup>1</sup>, Kristen Martin<sup>1</sup>, Melissa Mueller Gildea<sup>1</sup>, Charles E. Kahn, Jr<sup>1</sup>, and Mitchell D. Schnall<sup>1</sup>

<sup>1</sup>Radiology, Perelman School of Medicine at the University of Pennsylvania, Philadelphia, PA, United States

We compare the time savings and reduction in radiologists' workload after implementing ten new fit-for-purpose MRI protocols for imaging of multiple sclerosis patients at our academic medical center. A 2x2 framework was created to provide a method to monitor implementation of new imaging protocols in order to gauge success of adoption as well as determine areas for operational improvement.

0303



### Feasibility of Diffusion Tensor Imaging at 0.5T

Curtis N Wiens<sup>1</sup>, Chad T Harris<sup>1</sup>, Andrew T Curtis<sup>1</sup>, Philip J Beatty<sup>1</sup>, and Jeff A Stainsby<sup>1</sup>

<sup>1</sup>Research and Development, Synaptive Medical, Toronto, ON, Canada

This work examined the feasibility of diffusion tensor imaging (DTI) at 0.5T, a technique performed almost exclusively at field strengths of at least 1.5T. 2D diffusion-weighted axial spin-echo echo-planar imaging and 3D T1 weighted acquisitions were performed in the NIST isotropic diffusion phantom, a DTI phantom, and 5 healthy volunteers on a head-specific 0.5T MRI system. ADC measurements of the NIST phantom were in excellent agreement with previously recorded 3T measurements while DTI processing and tractography performed using Modus Plan was successful in all of the volunteers.

0304



### LI-RADS category 5 hepatocellular carcinoma: preoperative gadoxetic acid-enhanced MRI to predict early recurrence after curative resection

Hong Wei<sup>1</sup>, Hanyu Jiang<sup>1</sup>, and Bin Song<sup>1</sup>

<sup>1</sup>Department of Radiology, Sichuan University West China Hospital, Chengdu, China

This study aimed to investigate whether LI-RADS v2018 could indicate some prognostic information for high-risk patients with LR-5 hepatocellular carcinoma (HCC). We retrospectively evaluated 125 patients who underwent gadoxetic acid-enhanced MR examination within 1 month before surgical resection for HCC. The Cox proportional hazards model revealed that corona enhancement, peritumoral hypointensity on hepatobiliary phase, multifocality and serum alpha-fetoprotein were independent risk factors for early recurrence. The combined model derived from predictive biomarkers showed good performance, which could be used to effectively predict early recurrence after curative hepatectomy for LR-5 HCC.

## Oral

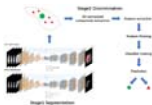
### Hepatobiliary & Pancreas - Liver: Methods & Applications

Monday Parallel 3 Live Q&A

Monday 15:15 - 16:00 UTC

Moderators: Shintaro Ichikawa

0305



### Automatic Liver Tumor Detection using Deep learning based segmentation and Radiomics guided Candidate Filtering

Rencheng Zheng<sup>1</sup>, Qidong Wang<sup>2</sup>, Ziyang Feng<sup>3</sup>, Chengyan Wang<sup>3</sup>, and He Wang<sup>1,3</sup>

<sup>1</sup>Institute of Science and Technology for Brain-Inspired Intelligence, Fudan University, Shanghai, China,

<sup>2</sup>Radiology department, The first affiliated hospital, College of medicine, Zhejiang University, Hangzhou, China,

<sup>3</sup>Human Phenome Institute, Fudan University, Shanghai, China

The objective of this study is to perform automatic multi DCE phases liver tumor detection using deep learning based segmentation and radiomics guided candidate filtering. The proposed model consists mainly of two stages, primary segmentation based on a U-net architecture neural network in stage1, and suspected tumor discrimination mechanism using multi DCE phases radiomics features including shape features, texture features, time dimension features and location information in stage 2. The proposed two-stage model exhibits superior performance in HCC tumor segmentation with a mean Dice score of 0.7928 in test set.

0306



### Improving the performance of non-enhanced MR for predicting the grade of hepatocellular carcinoma by transfer learning

Wu Zhou<sup>1</sup>, Wanwei Jian<sup>1</sup>, and Guangyi Wang<sup>2</sup>

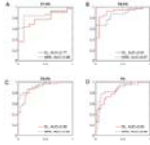
<sup>1</sup>School of Medical Information Engineering, Guangzhou University of Chinese Medicine, Guangzhou, China,

<sup>2</sup>Department of Radiology, Guangdong General Hospital, Guangzhou, China



Contrast agent has several limitations in clinical practice, and the diagnostic performance of non-enhanced MR for lesion characterization should be thoroughly exploited. Inspired by the work of cross-modal learning framework, we propose a deeply supervised cross-modal transfer learning method to remarkably improve the malignancy characterization of HCC in non-enhanced MR, in which the cross-modal relationship between the non-enhanced modal and contrast-enhanced modal is explicitly learned and subsequently transferred to another CNN model for improving the characterization performance of non-enhanced MR. The visualization method Grad-CAM is also applied to verify the effectiveness of the proposed cross-modal transfer learning model.

0307

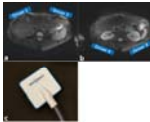


**Fully Automated Prediction of Liver Fibrosis using Deep Learning Analysis of Gadoxetic acid-enhanced MRI**  
Stefanie Hectors<sup>1,2,3</sup>, Paul Kennedy<sup>1,2</sup>, Kuang-Han Huang<sup>1,4</sup>, Hayit Greenspan<sup>5</sup>, Scott Friedman<sup>6</sup>, and Bachir Taouli<sup>1,2</sup>

<sup>1</sup>BioMedical Engineering and Imaging Institute, Icahn School of Medicine at Mount Sinai, New York, NY, United States, <sup>2</sup>Department of Diagnostic, Molecular and Interventional Radiology, Icahn School of Medicine at Mount Sinai, New York, NY, United States, <sup>3</sup>Department of Radiology, Weill Cornell Medicine, New York, NY, United States, <sup>4</sup>Prealize Health, Palo Alto, CA, United States, <sup>5</sup>Medical Imaging Processing Lab, Tel Aviv University, Tel Aviv, Israel, <sup>6</sup>Division of Liver Diseases, Icahn School of Medicine at Mount Sinai, New York, NY, United States

In this study we developed a fully automated deep learning algorithm based on gadoxetic acid-enhanced MRI for noninvasive prediction of liver fibrosis. We found good-to-excellent performance of the algorithm in an independent test set (AUC 0.77 – 0.91), which was equivalent to the diagnostic performance of MR elastography (AUC 0.86 – 0.92, p-values between methods >0.134). The developed algorithm may potentially allow for noninvasive liver fibrosis assessment, without the need for invasive biopsies.

0308



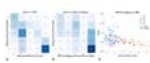
**Simultaneous stiffness measurement of the upper abdomen with multiple acoustic actuators MRE: feasibility and repeatability**

Jie Chen<sup>1,2</sup>, Jun Chen<sup>1</sup>, Jeremiah Heilman<sup>1</sup>, Kevin Glaser<sup>1</sup>, Richard Ehman<sup>1</sup>, and Meng Yin<sup>1</sup>

<sup>1</sup>Mayo Clinic, Rochester, MN, United States, <sup>2</sup>West China Hospital, Sichuan University, Chengdu, China

Simultaneous stiffness assessment of multiple organs in patients with systemic diseases may be beneficial. Here we used four passive MRE drivers to assess the feasibility and repeatability of simultaneous stiffness measurements of the liver, spleen and kidneys using 60-Hz vibrations. No significant bias was observed in the stiffness measurements of the liver and kidneys with 1 versus multiple drivers. Splenic stiffness was lower with four drivers. With four drivers, it is possible to obtain simultaneous stiffness measurements of the liver, spleen and kidneys with repeatability coefficients similar to those using a single driver while also overcoming attenuation in the liver.

0309



**Prospective Comparison of MR Elastography with MRI Cine-Tagging of Cardiac-Induced Motion for Noninvasive Staging of Liver Fibrosis**

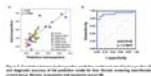
Thierry Lefebvre<sup>1,2,3</sup>, Léonie Petitclerc<sup>1,2,4</sup>, Giada Sebastiani<sup>5</sup>, Jeanne-Marie Giard<sup>2,6</sup>, Marie-Pierre Sylvestre<sup>2,7</sup>, Bich N. Nguyen<sup>8</sup>, Guillaume Gilbert<sup>1,9</sup>, Guy Cloutier<sup>1,10,11</sup>, and An Tang<sup>1,2,10</sup>



<sup>1</sup>Department of Radiology, Radio-Oncology and Nuclear Medicine, Université de Montréal, Montreal, QC, Canada, <sup>2</sup>Centre de recherche du Centre hospitalier de l'Université de Montréal (CRCHUM), Montréal, QC, Canada, <sup>3</sup>Medical Physics Unit, McGill University, Montréal, QC, Canada, <sup>4</sup>C.J. Gorter Center for High Field MRI, Department of Radiology, Leiden University Medical Center (LUMC), Leiden, Netherlands, <sup>5</sup>Department of Medicine, Division of Gastroenterology and Hepatology, McGill University Health Centre (MUHC), Montréal, QC, Canada, <sup>6</sup>Department of Medicine, Division of Hepatology and Liver Transplantation, Université de Montréal, Montréal, QC, Canada, <sup>7</sup>Department of Social and Preventive Medicine, École de santé publique de l'Université de Montréal (ESPUM), Montréal, QC, Canada, <sup>8</sup>Service of Pathology, Centre hospitalier de l'Université de Montréal (CHUM), Montréal, QC, Canada, <sup>9</sup>MR Clinical Science, Philips Healthcare Canada, Markham, ON, Canada, <sup>10</sup>Institute of Biomedical Engineering, Université de Montréal, Montréal, QC, Canada, <sup>11</sup>Laboratory of Biorheology and Medical Ultrasonics (LBUM), Centre de recherche du Centre hospitalier de l'Université de Montréal (CRCHUM), Montréal, QC, Canada

MR elastography for staging liver fibrosis assesses the right liver lobe and requires external hardware. MRI cine-tagging evaluates cardiac-induced strain and shows promise for assessing fibrosis in the left lobe without additional hardware. Shear modulus measured by MRE provided higher AUCs than that of strain measured on tagged images for distinguishing stages F0 vs.  $\geq$ F1 (0.87 vs. 0.81,  $P=0.083$ ) and  $\leq$ F3 vs. F4 (0.91 vs. 0.87,  $P=0.043$ ). Hence, MRE provided a diagnostic accuracy similar or higher than that of MRI cine-tagging for staging of liver fibrosis. Strain could be evaluated on screening abdominal MRI to assess the left liver.

0310



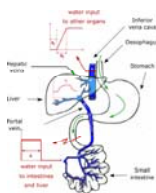
Noninvasive assessment of water content and collagen extent of liver tissue with multiparametric magnetic resonance elastography (MRE)

Jingbiao Chen<sup>1,2</sup>, Jin Wang<sup>3</sup>, Jiahui Li<sup>1</sup>, Jie Chen<sup>1</sup>, Xin Lu<sup>1</sup>, Hiroaki Yashiro<sup>4</sup>, Jenifer Siegelman<sup>4</sup>, Christopher T Winkelmann<sup>4</sup>, Richard L Ehman<sup>1</sup>, Vijay H Shah<sup>2</sup>, and Meng Yin<sup>1</sup>

<sup>1</sup>Radiology, Mayo Clinic, Rochester, MN, United States, <sup>2</sup>Gastroenterology and Hepatology, Mayo Clinic, Rochester, MN, United States, <sup>3</sup>the Third Affiliated Hospital of Sun Yat-Sen University, Guangzhou, China, <sup>4</sup>Research and Development, Takeda Pharmaceuticals International Co., Cambridge, MA, United States

Liver biopsy remains the gold standard for staging liver fibrosis. However, its invasive nature makes it unacceptable for long-term disease dynamic monitoring. In addition, current histopathological scoring systems for staging liver fibrosis are not quantitative. Also, the inflammatory response of increased interstitial fluid volume is precursory and occult with histological analysis. It is critical to address the overlooked fluid-associated inflammatory response and semi-quantitative fibrosis grading. Here, we use a novel technique, magnetic resonance elastography, combined with ALT, as a noninvasive quantitative method to quantify and monitor hepatic water and fibrosis content in a mouse model with varying disease progression/regression.

0311



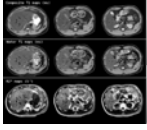
The thirsty liver: dynamic T1 mapping after fluid intake in healthy volunteers

Ferenc E. Mozes<sup>1</sup>, Emmanuel A. Selvaraj<sup>1</sup>, Michael Pavlides<sup>1,2</sup>, Matthew D. Robson<sup>1,3</sup>, and Elizabeth M. Tunnicliffe<sup>1</sup>

<sup>1</sup>OCMR, RDM Cardiovascular Medicine, University of Oxford, Oxford, United Kingdom, <sup>2</sup>Translational Gastroenterology Unit, University of Oxford, Oxford, United Kingdom, <sup>3</sup>Perspectum Diagnostics Ltd., Oxford, United Kingdom

Non-alcoholic fatty liver disease is on the rise and liver biopsies used to diagnose it need to be replaced by non-invasive methods such as T<sub>1</sub> mapping. Guidance for MRI scans allow for free water consumption before scans, increasing measurement variability. We therefore aimed to assess the effect of hydration on liver T<sub>1</sub> by acquiring serial shMOLLI T<sub>1</sub> maps after participants drank 1 litre of isotonic water. As water passed through the stomach and small intestines it first reached the portal circulation and later the systemic circulation, causing an increase in liver T<sub>1</sub> followed by an increase in spinal muscle T<sub>1</sub>.

0312



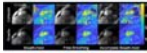
Rapid multi-slice fat and water separated T1 and composite R2\* mapping using a dual-echo radial inversion recovery SPGR pulse sequence

Zhitao Li<sup>1</sup>, John Pauly<sup>2</sup>, and Shreyas Vasanawala<sup>1</sup>

<sup>1</sup>Department of Radiology, Stanford University, Stanford, CA, United States, <sup>2</sup>Electrical Engineering, Stanford University, Stanford, CA, United States

A radial dual-echo IR-SPGR technique combined with a principal component based iterative reconstruction algorithm are demonstrated for fat and water separated rapid high-resolution abdominal multi-parameter mapping. This method can yield high-quality fat-signal-fraction map, B<sub>0</sub> field map, composite T<sub>1</sub> map, water component T<sub>1</sub> map as well as a R<sub>2</sub>\* map from a scan as fast as 3seconds/slice. The in-plane resolution of the resulting parameter maps is 1.25mm and the through-plane resolution is 5.00mm. With a selective inversion pulse, multiple slices can be acquired within a breath-hold.

0313



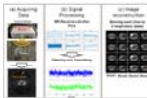
Ungated, Motion Robust, Simultaneous Cardiac and Liver T2\* Quantification via Rosette k-Space Sampling

Adam Michael Bush<sup>1</sup>, Christopher Michael Sandino<sup>2</sup>, Shreya Ramachandran<sup>3</sup>, Nicholas Dwork<sup>4</sup>, Frank Ong<sup>1</sup>, Marcus Alley<sup>1</sup>, and Shreyas Vasanawala<sup>1</sup>

<sup>1</sup>Radiology, Stanford University, Palo Alto, CA, United States, <sup>2</sup>Electrical Engineering, Stanford University, Palo Alto, CA, United States, <sup>3</sup>Electrical Engineering, University of California Berkeley, Berkeley, CA, United States, <sup>4</sup>Radiology, University of California San Francisco, San Francisco, CA, United States

In this work we introduce a novel method for T2\* determination using rosette k-space sampling and locally low-rank reconstruction. This approach produced comparable T2\* quantitation with higher spatial resolution, fewer motion artifacts and lessened variability without the use of gating. This approach offers a child-friendly, rapid, free-breathing, comprehensive assessment of liver and cardiac iron.

0314



Free-Breathing Radial Imaging using a Pilot-Tone RF Transmitter for Detection of Respiratory Motion

Eddy Solomon<sup>1</sup>, Thomas Vahle<sup>2</sup>, Jan Paska<sup>1</sup>, Kai Tobias Block<sup>1</sup>, Daniel K. Sodickson<sup>1</sup>, Fernando Boada<sup>1</sup>, and Hersh Chandarana<sup>1</sup>

<sup>1</sup>Radiology, New York University School of Medicine, New York, NY, United States, <sup>2</sup>Siemens Healthcare GmbH, Erlangen, Germany

The sensitivity of MRI sequences to motion impairs their reliability and diagnostic utility for examining the chest and abdomen. Established motion-compensation techniques are not accurate enough, come at the cost of patient comfort, and are limited by the MR imaging parameters. Here, we demonstrate a novel approach that detects respiratory signal from the amplitude modulation of a transmitted RF reference signal, termed 'pilot-tone' (PT). We show how the use of this simple RF transmitter, with its small dimensions, high sampling rate, and low interference with the MR acquisition, can produce motion corrected-images under free-breathing conditions.

## Oral

### Hepatobiliary & Pancreas - Diffuse Liver & Metabolism

Monday Parallel 3 Live Q&A

Monday 15:15 - 16:00 UTC

Moderators: Frederick Kelcz

0315



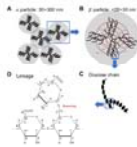
Assessment of obesity-induced metabolic disorders in adipose tissue by multi-parametric MR Elastography (MRE)

Jiahui Li<sup>1</sup>, Marzanna Obrzut<sup>1</sup>, Xin Lu<sup>1</sup>, Alina Allen<sup>2</sup>, Sudhakar K. Venkatesh<sup>1</sup>, Taofic Mounajjed<sup>3</sup>, Jun Chen<sup>1</sup>, Kevin J. Glaser<sup>1</sup>, Armando Manduca<sup>1</sup>, Vijay Shah<sup>2</sup>, Richard L. Ehman<sup>1</sup>, and Meng Yin<sup>1</sup>

<sup>1</sup>Radiology, Mayo Clinic, Rochester, MN, United States, <sup>2</sup>Gastroenterology, Mayo Clinic, Rochester, MN, United States, <sup>3</sup>Mayo Clinic, Rochester, MN, United States

We performed multiparametric 3D MR Elastography (MRE) in 37 obese patients who underwent bariatric surgeries. MRI/MRE, anthropometrics, and liver biopsy were obtained within three months of bariatric surgery and one year later. 12/37 (32%) patients have biopsy-proven non-alcoholic fatty liver disease (NAFLD) at the time of surgery. The MRE-assessed shear stiffness (SS) and loss modulus (LM) of subcutaneous adipose tissue decreased significantly after the surgery, as well as the liver tissue. MRE-assessed SS and LM have potential in distinguishing the obesity-induced metabolic disorder in the adipose tissues. The mechanical change may correlate with the therapeutic response in these obese patients.

0316



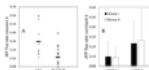
Mapping glycogen concentration in vivo based on the nuclear Overhauser enhancement (NOE) with water (glycoNOE)

Yang Zhou<sup>1,2</sup>, Peter C.M. van Zijl<sup>1,2</sup>, Xiang Xu<sup>1,2</sup>, Jiadi Xu<sup>1,2</sup>, Yuguo Li<sup>1,2</sup>, and Nirbhay N. Yadav<sup>1,2</sup>

<sup>1</sup>The Russell H. Morgan Department of Radiology, The Johns Hopkins University School of Medicine, Baltimore, MD, United States, <sup>2</sup>F.M. Kirby Research Center for Functional, Brain Imaging, Kennedy Krieger Institute, Baltimore, MD, United States

We recently reported a method for the enhanced detection of glycogen using the nuclear Overhauser enhancement (NOE) between glycogen and water (glycoNOE). Here we show that the glycoNOE signal is linearly dependent on glycogen concentration both in vitro and in mouse liver in vivo. The glycoNOE signal is affected by glycogen particle size, but not pH or temperature. glycoNOE MRI can non-invasively quantify liver glycogen levels in vivo and thus has the potential to assess disease where glycogen metabolism is altered.

0317



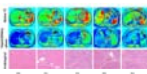
Mapping Metabolic Inflexibility in NAFLD: Comparison With Healthy Volunteers and Following L-Carnitine Intervention Using Advanced MRS.

Stephen Bawden<sup>1,2</sup>, Prarthana Thiagarajan<sup>1</sup>, Elizabeth Simpson<sup>1</sup>, Olivier Mouglin<sup>2</sup>, Paul Greenhaff<sup>3</sup>, Penny Gowland<sup>2</sup>, and Guruprasad P Aithal<sup>1</sup>

<sup>1</sup>NIHR Nottingham Biomedical Research Centre, University of Nottingham, Nottingham University Hospitals NHS Trust and the University of Nottingham, Nottingham, United Kingdom, <sup>2</sup>Sir Peter Mansfield Imaging Centre, University of Nottingham, Nottingham, United Kingdom, <sup>3</sup>School of Life Sciences, University of Nottingham, Nottingham, United Kingdom

Advanced MRI techniques such as <sup>1</sup>H MRS at 7T and saturation transfer <sup>31</sup>P MRS offer unique capabilities to map metabolic conditions and complement current physiological methodologies. The aim of this study was to build a metabolic profile for NAFLD v healthy volunteers by measuring physiological metabolic markers alongside <sup>1</sup>H MRS measurement of liver lipid, intra- (IMCL) and extra- (EMCL) myocellular lipid fraction, and dynamic <sup>31</sup>P MRS measurements of ATP flux rates, and to investigate the effect of a 24 week L-carnitine intervention. Interim analysis shows metabolic inflexibility in NAFLD patients compared with HV and a potential benefit of L-carnitine supplementation

0318



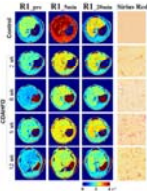
B1 inhomogeneity-corrected T1 mapping in quantitative evaluation of liver fibrosis using Gd-BOPTA enhanced MR imaging

Xinya Zhao<sup>1</sup>, Xianshun Yuan<sup>1</sup>, Xiang Feng<sup>2</sup>, Mengxiao Liu<sup>3</sup>, Xiangtao Lin<sup>1</sup>, and Ximing Wang<sup>1</sup>

<sup>1</sup>Department of Radiology, Shandong Provincial Hospital, Jinan, China, <sup>2</sup>MR Scientific Marketing, Siemens Healthcare, Beijing, China, <sup>3</sup>MR Scientific Marketing, Siemens Healthcare, Shanghai, China

The purpose of this study was to determine whether B1 inhomogeneity-corrected volumetric T1 mapping of Gd-BOPTA enhanced liver MR imaging are able to evaluate the degree of liver cirrhosis and to investigate their relationship with the histological grading. Our study found that B1 inhomogeneity-corrected T1 mapping using Gd-BOPTA enhanced MR imaging could be used in the quantitative evaluation of liver fibrosis.

0319



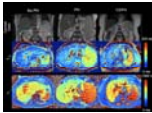
### Gd-EOB-DTPA-enhanced MRI in Nonalcoholic Steatohepatitis (NASH): Liver Fibrosis or Liver Function?

Iris Y. Zhou<sup>1</sup>, Chuantao Tu<sup>2</sup>, Veronica Clavijo Jordan<sup>1</sup>, Nicholas J. Rotile<sup>1</sup>, Mozhdeh Sojoodi<sup>3</sup>, Bryan C. Fuchs<sup>3</sup>, Kenneth K. Tanabe<sup>3</sup>, and Peter Caravan<sup>1</sup>

<sup>1</sup>Athinoula A. Martinos Center for Biomedical Imaging, Institute for Innovation in Imaging (i3), Department of Radiology, Massachusetts General Hospital and Harvard Medical School, Charlestown, MA, United States, <sup>2</sup>Department of Gastroenterology and Hepatology, Zhongshan Hospital, Fudan University, Shanghai, China, <sup>3</sup>Division of Surgical Oncology, Massachusetts General Hospital and Harvard Medical School, Boston, MA, United States

Nonalcoholic steatohepatitis (NASH) promotes fibrotic remodeling of the liver parenchyma, which may lead to cirrhosis, liver failure, or hepatocellular carcinoma. Gd-EOB-DTPA is a hepatobiliary T1 MRI contrast agent, receiving increasing attention as a tool for detecting and staging liver fibrosis. Here, using a choline-deficient high-fat diet (CDAHFD) for different durations we modeled NASH disease progression in rats and performed Gd-EOB-DTPA-enhanced MRI at different disease stages, correlating imaging histological measures of fibrosis as well as liver function tests. Gd-EOB-DTPA-enhanced MRI correlated well with liver function tests but not with liver fibrosis.

0320



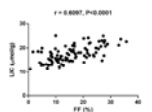
### Splenic T1p as a noninvasive biomarker for portal hypertension

Stefanie Hectors<sup>1,2,3</sup>, Octavia Bane<sup>1,2</sup>, Daniel Stocker<sup>1,2</sup>, Paul Kennedy<sup>1,2</sup>, Thomas Schiano<sup>4</sup>, Swan Thung<sup>5</sup>, Aaron Fischman<sup>2</sup>, and Bachir Taouli<sup>1,2</sup>

<sup>1</sup>BioMedical Engineering and Imaging Institute, Icahn School of Medicine at Mount Sinai, New York, NY, United States, <sup>2</sup>Department of Diagnostic, Molecular and Interventional Radiology, Icahn School of Medicine at Mount Sinai, New York, NY, United States, <sup>3</sup>Department of Radiology, Weill Cornell Medicine, New York, NY, United States, <sup>4</sup>Recanati/Miller Transplantation Institute, Icahn School of Medicine at Mount Sinai, New York, NY, United States, <sup>5</sup>Department of Pathology, Icahn School of Medicine at Mount Sinai, New York, NY, United States

In this study we explored the used of liver and spleen T1 and T1p parameters for noninvasive assessment of portal hypertension (PH) and compared the performance of the MRI relaxation parameters with that of radiological assessment. Spleen T1p showed a strong significant positive correlation with quantitative portal pressure measurements ( $r=0.613$ ,  $P=0.001$ ), while the other relaxation parameters did not. Spleen T1p also outperformed other relaxation parameters and radiological assessment for prediction of (clinically significant) PH (AUC 0.778 – 0.817). Our results indicate that spleen T1p may be a suitable noninvasive biomarker for prediction of PH.

0321



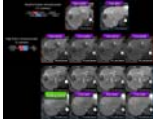
### Proton-density fat fraction-derived R2\* liver iron concentration – an exploratory study of Revita-2 phase II trial data

Manil D Chouhan<sup>1</sup>, Naomi Sakai<sup>1</sup>, Francisco Torrealdea<sup>2</sup>, Kelly White<sup>3</sup>, Juan Carlos Lopez Talavera<sup>3</sup>, Alan Bainbridge<sup>2</sup>, and Stuart A Taylor<sup>1</sup>

<sup>1</sup>UCL Centre for Medical Imaging, University College London, London, United Kingdom, <sup>2</sup>Department of Medical Physics, University College London Hospitals NHS Trust, London, United Kingdom, <sup>3</sup>Fractyl Laboratories Inc., Lexington, MA, United States

R2\* derived liver iron concentration (LIC) measurements from proton density fat fraction (PDFF) data obtained in patients with normal LIC levels may be useful. Here we present data from the Revita-2 trial demonstrating strong significant positive correlations between baseline liver fat fraction (FF) and LIC. Significant and stronger correlations between relative % change in liver FF and LIC in the treatment arms of the trial raise the possibility of treatment-related mechanistic effects on hepatic iron metabolism.

0322



#### Utility of Stack-of-stars Acquisition for Arterial Phase Imaging without Breath-holding on Dynamic MRI of the Liver

Shintaro Ichikawa<sup>1</sup>, Daiki Tamada<sup>1</sup>, Tetsuya Wakayama<sup>2</sup>, Sagar Mandava<sup>3</sup>, Ty A Cashen<sup>4</sup>, Hiroshi Onishi<sup>1</sup>, and Utaroh Motosugi<sup>1</sup>

<sup>1</sup>Department of Radiology, University of Yamanashi, Chuo, Japan, <sup>2</sup>MR Collaboration and Development, GE Healthcare, Hino, Japan, <sup>3</sup>MR Collaboration and Development, GE Healthcare, Tucson, AZ, United States, <sup>4</sup>MR Collaboration and Development, GE Healthcare, Madison, WI, United States

We compared arterial phase (AP) images using conventional (Cartesian) breath-hold liver acquisition with volume acceleration (LAVA) and stack-of-stars acquisition without breath-holding (LAVA-Star) on hepatic dynamic MRI. In Cartesian breath-hold LAVA group, 8.7% of patients showed inadequate scan timing of AP, while only 1 patient (4.0%) in LAVA-Star group (12 s/phase) showed inadequate scan timing. One advantage of LAVA-Star was that the adequate scan timing of AP can be obtained by using additional high frame rate reconstruction (3 s/phase) in the patient with inadequate scan timing in routine reconstruction. LAVA-Star was useful to obtain adequate scan timing in all patients.

0323



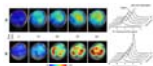
#### Quantitative MRI to assess portal hypertension in cirrhosis patients

Chris R Bradley<sup>1,2</sup>, Rob A Scott<sup>2</sup>, Eleanor F Cox<sup>1,2</sup>, Naaventhan Palaniyappan<sup>2</sup>, I Neil Guha<sup>2</sup>, Guruprasad P Aithal<sup>2</sup>, and Susan T Francis<sup>1,2</sup>

<sup>1</sup>Sir Peter Mansfield Imaging Centre, University of Nottingham, Nottingham, United Kingdom, <sup>2</sup>NIHR Nottingham Biomedical Research Centre, Nottingham University Hospitals NHS Trust and University of Nottingham, Nottingham, United Kingdom

Hepatic venous pressure gradient (HVPG) is the gold standard method for the assessment of portal pressure, but highly invasive. We scanned patients with portal hypertension at both 1.5T and 3T to assess MRI parameters related to portal pressure as defined by HVPG. Iron-corrected liver  $T_1$  highly correlated over the full range of HVPG (3T  $p < 0.0002$ , 1.5T  $p < 0.0001$ ), spleen  $T_1$  and superior mesenteric artery velocity correlated up to HVPG of 15 mmHg (spleen  $T_1$ : 3T  $p < 0.0003$ , 1.5T  $p < 0.0006$ ; SMA velocity:  $p < 0.00001$ ), after which at HVPG  $> 15$  mmHg no correlation was observed.

0324



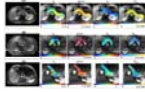
#### Visibility of deuterium-labeled liver glycogen in vivo.

Henk M. De Feyter<sup>1</sup>, Monique A. Thomas<sup>1</sup>, Kevin L. Behar<sup>2</sup>, and Robin A. de Graaf<sup>1</sup>

<sup>1</sup>Dept. of Radiology and Biomedical Imaging, Yale University, New Haven, CT, United States, <sup>2</sup>Dept. of Psychiatry, Yale University, New Haven, CT, United States

Deuterium metabolic imaging (DMI) is a novel technique for mapping metabolism in vivo, that combines  $^2\text{H}$  MRSI with administration of a  $^2\text{H}$ -labeled substrate. DMI combined with  $[6,6\text{-}^2\text{H}_2]$ -glucose has the potential to detect glycogen synthesis in the liver. However, the similar  $^2\text{H}$  chemical shifts of glucose and glycogen make unambiguous detection and separation difficult in vivo. Here we investigate the NMR-detectability of glycogen using high resolution  $^2\text{H}$  NMR of  $^2\text{H}$ -labeled glycogen isolated from mouse liver, and show that  $^2\text{H}$ -labeled glycogen is not detectable with DMI under in vivo conditions.

0325



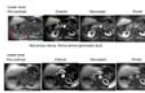
Six-Dimensional Quantitative DCE MR Multitasking in the Characterization of Pancreatic Ductal Adenocarcinoma Versus Chronic Pancreatitis

Nan Wang<sup>1,2</sup>, Srinivas Gaddam<sup>3</sup>, Lixia Wang<sup>1,4</sup>, Yibin Xie<sup>1</sup>, Zhaoyang Fan<sup>1</sup>, Simon Lo<sup>3</sup>, Stephen Pandol<sup>3</sup>, Anthony G Christodoulou<sup>1</sup>, and Debiao Li<sup>1</sup>

<sup>1</sup>Biomedical Imaging Research Institute, Cedars-Sinai Medical Center, Los Angeles, CA, United States, <sup>2</sup>Bioengineering, University of California, Los Angeles, Los Angeles, CA, United States, <sup>3</sup>Division of Digestive and Liver Diseases, Cedars-Sinai Medical Center, Los Angeles, CA, United States, <sup>4</sup>Chaoyang Hospital, Beijing, China

The differentiation of pancreatic ductal adenocarcinoma (PDAC) and chronic pancreatitis (CP) is crucial to the diagnosis and prognosis of PDAC. DCE MRI serves as a promising imaging tool, but still faces several technical challenges. In this work, we evaluated the characterization of PDAC versus CP using the proposed Multitasking DCE technique, which enables free-breathing acquisition, 3D whole-abdomen coverage, high temporal resolution at 500ms, and dynamic T1 mapping throughout all DCE phases. In vivo studies on 16 healthy volunteers, 14 PDAC patients, and 8 CP patients demonstrated the capability of Multitasking DCE in differentiating normal pancreas, PDAC, and CP.

0326



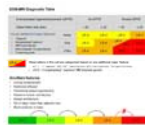
Free Breathing Dynamic Contrast Enhanced MR Imaging of the Hepatopancreatobiliary lesions with improved 3D Stack-of-Stars k-space trajectory

Takayuki Masui<sup>1</sup>, Motoyuki Katayama<sup>1</sup>, Yuji Iwadate<sup>2</sup>, Naoyuki Takei<sup>2</sup>, Mitsuharu Miyoshi<sup>2</sup>, Masako Sasaki<sup>1</sup>, Takahiro Yamada<sup>1</sup>, Ty Cashen<sup>3</sup>, Sagar Mandava<sup>4</sup>, and Kang Wang<sup>5</sup>

<sup>1</sup>Radiology, Seirei Hamamatsu General Hospital, Hamamatsu, Japan, <sup>2</sup>Global MR Applications and Workflow, GE Healthcare, Hino, Japan, <sup>3</sup>Global MR Applications and Workflow, GE Healthcare, Madison, WI, United States, <sup>4</sup>GE Healthcare, Tucson, AZ, United States, <sup>5</sup>GE Healthcare, Waukesha, WI, United States

The feasibility of dynamic Gd-contrast study for evaluation of hepatopancreatobiliary lesions under free breathing was demonstrated. Superb image quality with high temporal resolutions could be obtained using a stack-of-stars k-space trajectory with golden angle ordering a CG-SENSE algorithm that supports parallel imaging and soft-gating for accelerated motion robust imaging. Selective recognition of vasculatures and lesions in the liver and pancreas can be made with this technique, which may be equivalent to fast breath-hold dynamic contrast image in young and old aged population.

0327

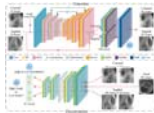


Modifying LI-RADS on gadoxetate disodium-enhanced MRI in a prospective cohort: toward improving simplicity and sensitivity

Hanyu Jiang<sup>1,2</sup>, Bin Song<sup>1</sup>, and Mustafa Shadi Rifaat Bashir<sup>2</sup>

<sup>1</sup>Department of Radiology, West China Hospital, Sichuan University, Chengdu, China, <sup>2</sup>Department of Radiology, Duke University Medical Center, Durham, NC, United States

We aimed to develop a modified Liver Imaging Reporting and Data System (mLI-RADS) with comparisons against original LI-RADS version 2018 (v2018) for diagnosing hepatocellular carcinoma (HCC) on gadoxetate disodium-enhanced magnetic resonance imaging (EOB-MRI). 1002 hepatic observations in 272 consecutive at-risk patients were prospectively included. Ancillary features were assessed based on inter-rater agreement, prevalence, diagnostic accuracy, and added value to the major features. Compared with the original LI-RADS v2018, mLI-RADS demonstrated superior simplicity, sensitivity and accuracy without substantial loss of specificity; hence should be the preferred diagnostic criteria for HCC in high-risk patients on EOB-MRI.



### Super-resolution Generative Adversarial Network for improving malignancy characterization of hepatocellular carcinoma

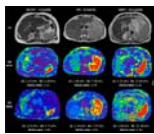
Wu Zhou<sup>1</sup>, Yunling Li<sup>1</sup>, Hui Huang<sup>1</sup>, Yaoqin Xie<sup>2</sup>, Lijuan Zhang<sup>2</sup>, and Guangyi Wang<sup>3</sup>

<sup>1</sup>School of Medical Information Engineering, Guangzhou University of Chinese Medicine, Guangzhou, China,

<sup>2</sup>Shenzhen Institutes of Advanced Technology, Chinese Academy of Sciences, Shenzhen, China,

<sup>3</sup>Department of Radiology, Guangdong General Hospital, Guangzhou, China

Deep feature derived from data-driven learning has consistently shown to outperform conventional texture features for lesion characterization. However, due to the slice thickness of medical imaging, through-plane has worse resolution than in-plane resolution. Therefore, the performance of deep feature extracted from the through plane slices may be worse, and their contributions to the final characterization may also be very limited. We propose an end-to-end super-resolution and self-attention framework based on generative adversarial network (GAN), in which the through-plane slices with low resolution are enhanced by learning the in-plane slices with high resolution to improve the performance of lesion characterization.



### Utility of magnetic resonance elastography and ultrasound shear wave elastography for assessment of portal hypertension

Paul Kennedy<sup>1,2</sup>, Octavia Bane<sup>1,2</sup>, Stefanie Hectors<sup>1,2,3</sup>, Daniel Stocker<sup>1,2</sup>, Bradley D Bolster Jr. <sup>4</sup>, Scott Friedman<sup>5</sup>, Thomas Schiano<sup>6</sup>, Isabel M Fiel<sup>7</sup>, Swan Thung<sup>7</sup>, Aaron Fischman<sup>2</sup>, and Bachir Taouli<sup>1,2</sup>

<sup>1</sup>BioMedical Engineering and Imaging Institute, Icahn School of Medicine at Mount Sinai, New York, NY, United States,

<sup>2</sup>Department of Diagnostic, Molecular and Interventional Radiology, Icahn School of Medicine at Mount Sinai, New York, NY, United States,

<sup>3</sup>Department of Radiology, Weill Cornell Medicine, New York, NY, United States,

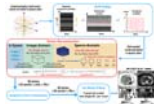
<sup>4</sup>Siemens Medical Solutions USA, Inc., Salt Lake City, UT, United States,

<sup>5</sup>Division of Liver Diseases, Icahn School of Medicine at Mount Sinai, New York, NY, United States,

<sup>6</sup>Department of Medicine, Icahn School of Medicine at Mount Sinai, New York, NY, United States,

<sup>7</sup>Department of Pathology, Icahn School of Medicine at Mount Sinai, New York, NY, United States

In this study we investigate the ability of MR elastography (MRE) and ultrasound shear wave elastography (SWE) to assess portal hypertension (PH) severity in patients with liver disease and hepatic venous pressure gradient (HVPG) measurement. 3D MRE spleen stiffness correlated with HVPG. 2D and 3D MRE of the spleen were significantly higher in patients with clinically significant PH (CSPH, HVPG>10mmHg) than those with no PH/PH (HVPG>5mmHg). 3D MRE spleen stiffness was significantly elevated in PH/CSPH patients compared to those with no PH and was an excellent predictor of CSPH. MRE spleen stiffness appears sensitive to hemodynamic changes associated with PH.



### Rapid Free-Breathing Volumetric Liver Fat and R2\* Quantification using Soft-Gating and Sparsity-Promoting Tensor Reconstruction

Shu-Fu Shih<sup>1,2</sup>, Tess Armstrong<sup>1</sup>, Sevgi Gokce Kafali<sup>1,2</sup>, Xiaodong Zhong<sup>3</sup>, Kara L. Calkins<sup>4</sup>, and Holden H. Wu<sup>1,2</sup>

<sup>1</sup>Radiological Sciences, University of California, Los Angeles, Los Angeles, CA, United States,

<sup>2</sup>Bioengineering, University of California, Los Angeles, Los Angeles, CA, United States,

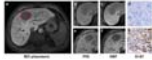
<sup>3</sup>Siemens Healthcare, Los Angeles, CA, United States,

<sup>4</sup>Pediatrics, University of California, Los Angeles, Los Angeles, CA, United States



MRI quantification of hepatic proton-density fat fraction (PDFF) and  $R_2^*$  enables non-invasive diagnosis and staging of non-alcoholic fatty liver disease (NAFLD) and liver iron overload, respectively. A recent 3D stack-of-radial technique enables free-breathing quantification, but requires scans of 2-4 minutes and motion may affect  $R_2^*$  accuracy. In this work, we propose an improved free-breathing stack-of-radial technique that combines soft-gating and a sparsity-promoting tensor reconstruction to compensate for motion effects and accelerate the scan to 31 seconds. Data from adult and pediatric NAFLD patients demonstrate good agreement of PDFF and  $R_2^*$  between the proposed method and the conventional breath-held Cartesian scan.

0331



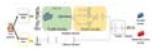
Preoperative prediction of HCC with highly aggressive characteristics using quantitative parameters derived from hepatobiliary phase

Zheng Ye<sup>1</sup>, Yi Wei<sup>1</sup>, Jie Chen<sup>1</sup>, and Bin Song<sup>1</sup>

<sup>1</sup>West China Hospital, Sichuan University, Chengdu, China

Hepatocellular carcinoma (HCC) with highly aggressive characteristics is usually actively proliferated and easily relapse, thereby requiring adjuvant therapies before surgery, like preoperative TACE, to improve the patients' prognosis. Ki-67 labeling index (LI) was reported to be highly correlated with aggressive propensity of HCC, and thus could affect the treatment response of the tumor and prognosis directly. Although most of HCC presented hypointensity on hepatobiliary phase (HBP), the absolute signal intensity and relative contrast enhancement ratio are not the same. In this study, we prospectively investigate the usefulness of HBP quantitative parameters for preoperative prediction of aggressiveness in HCC patients.

0332



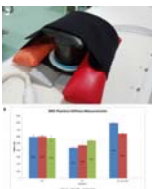
A Deep Transfer Learning Model for Liver Stiffness Classification using Clinical and T2-Weighted MRI Data

Hailong Li<sup>1,2</sup>, Lili He<sup>1,2,3</sup>, Jonathan Dudley<sup>2,4</sup>, Thomas Maloney<sup>2,4</sup>, Elanchezian Somasundaram<sup>4</sup>, Samuel L. Brady<sup>4,5</sup>, Nehal A. Parikh<sup>1,3</sup>, and Jonathan R. Dillman<sup>2,4,5</sup>

<sup>1</sup>The Perinatal Institute and Section of Neonatology, Perinatal and Pulmonary Biology, Cincinnati Children's Hospital Medical Center, Cincinnati, OH, United States, <sup>2</sup>Imaging Research Center, Cincinnati Children's Hospital Medical Center, Cincinnati, OH, United States, <sup>3</sup>Department of Pediatrics, University of Cincinnati College of Medicine, Cincinnati, OH, United States, <sup>4</sup>Department of Radiology, Cincinnati Children's Hospital Medical Center, Cincinnati, OH, United States, <sup>5</sup>Department of Radiology, University of Cincinnati College of Medicine, Cincinnati, OH, United States

Detection and monitoring of chronic liver diseases is typically assessed using a combination of clinical history, physical examination, laboratory testing, biopsy with histopathologic assessment, and imaging. The aim of this study is to develop a deep transfer learning model (DeepLiverNet) to categorically classify the severity of liver stiffening (no/mild vs. moderate/severe) using both anatomic T2-weighted MR images and clinical data. The DeepLiverNet model achieved accuracies of 88.0% and 80.0% on the risk stratification of liver stiffness in internal and external validation datasets, respectively. This demonstrates that a deep learning model may provide a means for stratifying liver stiffness without elastography.

0333



Multi-vendor Phantom and Intra-individual Comparison of Liver Stiffness Using Various MR Elastography Sequences at 1.5T & 3T

Justin Yu<sup>1</sup>, Anshuman Panda<sup>1</sup>, Kelly Tung-Smith<sup>1</sup>, Robert Nelson<sup>2</sup>, Akira Kawashima<sup>1</sup>, Ming Yang<sup>1</sup>, Chen Lin<sup>3</sup>, Aiden McGirr<sup>1</sup>, Sophia Fasani<sup>1</sup>, Kristina Flicek<sup>1</sup>, Sukhdeep Singh<sup>1</sup>, and Alvin Silva<sup>1</sup>

<sup>1</sup>Radiology, Mayo Clinic Arizona, Phoenix, AZ, United States, <sup>2</sup>National Institutes of Health, Phoenix, AZ, United States, <sup>3</sup>Mayo Clinic Florida, Jacksonville, FL, United States

The variability of stiffness data from GRE and SE EPI MRE sequences is tested on phantoms and in-vivo on 1.5T and 3T MRI scanners from two vendors. Large variability was observed in the phantom measurements for the GRE and EPI sequences on one of the vendor's scanner, ranging from 20-33% difference. Stiffness measurements were very similar (within 10%) between sequences on the other vendor's scanner. Similar results were found in several clinical subjects who had GRE and SE EPI sequences performed.

0334



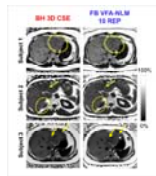
**Imaging-based Hepatic fibrosis staging of patients with hepatitis B: a radiomics analysis study on Gd-EOB-DTPA-enhanced MRI**

Rencheng Zheng<sup>1</sup>, Tian Qiu<sup>2</sup>, Nannan Shi<sup>2</sup>, Yuxin Shi<sup>2</sup>, Weibo Chen<sup>3</sup>, Chengyan Wang<sup>4</sup>, and He Wang<sup>4,5</sup>

<sup>1</sup>Fudan University, Shanghai, China, <sup>2</sup>Shanghai Public Health Clinical Center, Shanghai, China, <sup>3</sup>Philips Healthcare, Shanghai, China, <sup>4</sup>Human Phenome Institute, Fudan University, Shanghai, China, <sup>5</sup>Institute of Science and Technology for Brain-Inspired Intelligence, Fudan University, Shanghai, China

This study proposed an automatic hepatic fibrosis staging model based on transfer learning segmentation and radiomics analysis for hepatitis B patients. The automatic liver ROI extraction Time dimension features of multi DCE phases were included in feature set which played an important role in the classification. The proposed model exhibited a superior performance in significant fibrosis, advanced fibrosis and cirrhosis classification.

0335



**Motion-Robust, Free-Breathing, High-SNR Liver Fat Quantification Using a Variable Flip Angle Approach and Motion-Corrected Averaging**

Jitka Starekova<sup>1</sup>, Ruiyang Zhao<sup>1,2</sup>, Timothy J Colgan<sup>1</sup>, Kevin M Johnson<sup>1,2</sup>, Jennifer L Rehm<sup>3</sup>, Scott B Reeder<sup>1,2,4,5,6</sup>, and Diego Hernando<sup>1,2</sup>

<sup>1</sup>Department of Radiology, University of Wisconsin, Madison, Madison, WI, United States, <sup>2</sup>Department of Medical Physics, University of Wisconsin, Madison, Madison, WI, United States, <sup>3</sup>Department of Pediatrics, University of Wisconsin, Madison, Madison, WI, United States, <sup>4</sup>Department of Biomedical Engineering, University of Wisconsin, Madison, Madison, WI, United States, <sup>5</sup>Department of Medicine, University of Wisconsin, Madison, Madison, WI, United States, <sup>6</sup>Department of Emergency Medicine, University of Wisconsin, Madison, Madison, WI, United States

Chemical shift-encoded (CSE)-MRI enables accurate and precise quantification of proton density fat-fraction (PDFF) in the liver. Widely used 3D multi-echo spoiled gradient echo (SGRE) CSE-MRI requires reliable breath-holding to avoid motion-related artifacts. This is a major limitation for children, the elderly, and sick patients. Free-breathing 2D sequential CSE-MRI is motion-robust, however, suffers from low signal-to-noise-ratio (SNR). To overcome these limitations, we combined variable flip angle (VFA) 2D acquisitions and nonlocal means (NLM) motion-corrected averaging. In this prospective study, free-breathing multi-repetition VFA-NLM demonstrated high SNR and reduced artifacts compared to the conventional 3D-SGRE, while preserving accuracy of PDFF quantification.

0336

Parameter	Mean	SD	Min	Max
PDFF (%)	12.5	3.2	0.0	25.0
SNR	15.8	2.1	10.0	20.0
Artifact Score	1.2	0.3	0.0	2.0

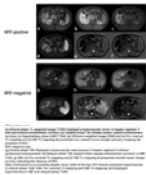
**A study of sensitivity of quantitative MRI measurements to the presence of iron in the liver**

Yurui Qian<sup>1</sup>, Jian Hou<sup>1</sup>, Yixiang Wang<sup>1</sup>, Vincent Wong<sup>2</sup>, Queenie Chan<sup>3</sup>, Weibo Chen<sup>4</sup>, Min Deng<sup>1</sup>, Franklin Au<sup>1</sup>, Anthony Chan<sup>5</sup>, Winnie Chu<sup>1</sup>, and Weitian Chen<sup>1</sup>

<sup>1</sup>Department of Imaging and Interventional Radiology, Chinese University of Hong Kong, Hong Kong, Hong Kong, <sup>2</sup>Department of Medicine & Therapeutics, Chinese University of Hong Kong, Hong Kong, Hong Kong, <sup>3</sup>Philips Healthcare, Hong Kong, Hong Kong, <sup>4</sup>Philips Healthcare, Shanghai, China, <sup>5</sup>Department of Anatomical and Cellular Pathology, Chinese University of Hong Kong, Hong Kong, Hong Kong

MRI is widely used as a non-invasive method to diagnose and monitor liver diseases. For certain quantitative MRI techniques, liver iron content may affect the measurement. In this work, we investigated the influence of liver iron content on several quantitative MRI methods, including macromolecular proton fraction, T1rho and intravoxel incoherent motion.

0337



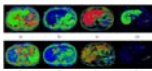
### Radiomic Analysis Based on Diverse Volumetric Interests Predicts Microvascular Invasion in Solitary Hepatocellular Carcinoma

Huanhuan Chong<sup>1</sup>, Li Yang<sup>1</sup>, Yangli Yu<sup>1</sup>, Dijia Wu<sup>2</sup>, Chun Yang<sup>1</sup>, and Mengsu Zeng<sup>1</sup>

<sup>1</sup>Department of Radiology, Shanghai Institute of Medical Imaging, Zhongshan Hospital of Fudan University, Shanghai, China, <sup>2</sup>Shanghai United Imaging Intelligence Co., Ltd, Shanghai, China

This study aims to construct a preoperative MVI prediction model in solitary HCC derived from gadoxetic acid-enhanced magnetic resonance imaging, and to further investigate its latent association with clinical indexes, imaging features and radiomics signatures based on diverse sequences and volumetric interests (VOIs) of tumor. The conclusion indicated that serum  $\alpha$ -fetoprotein, total bilirubin, higher value of tumor margin smoothness (prefer to non-smooth margin), non-intact capsule enhancement and peritumoral enhancement are independent and significant predictors for MVI, and the final nomogram incorporating clinical, imaging and the optimal radiomics model based on VOI\_entire\_5mm\_10mm\_liver achieves satisfactory prediction for MVI in solitary HCC.

0338



### Evaluation of liver function by using Hepatocyte fraction of Gd-EOB-DTPA-Enhanced MRI based on MELD score

Mao-Tong LIU<sup>1</sup>, Xue-Qin ZHANG<sup>1</sup>, Jian LU<sup>1</sup>, and Wei-Bo CHEN<sup>2</sup>

<sup>1</sup>Third Affiliated Hospital of Nantong University & Nantong Third People's Hospital, Nan Tong, China, <sup>2</sup>Philips Healthcare Shanghai, China, Shang Hai, China

The purpose of this study was to identify whether hepatocyte fraction that based on Gadoxetic Acid –enhanced MRI is useful for the assessment of liver function. Firstly, T1 mapping imaging was performed before and 20 minutes after Gd-EOB-DTPA administration, The following parameters are then obtained from the images: pre- and postcontrast T1 values of the liver (T1pre and T1post), increase in the T1 relaxation rate ( $\Delta R1$ ), rate of the decrease of the T1 relaxation time ( $\Delta T1$ ), hepatocyte fraction (HeF), and uptake coefficient (K). Our study showed that hepatocyte fraction can be used to evaluate the liver function of patients with hepatitis B cirrhosis, K value has high diagnostic efficiency.

## Oral

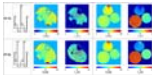
### Muscle, Cartilage, Knee stabilizers - Muscle

Monday Parallel 4 Live Q&A

Monday 15:15 - 16:00 UTC

Moderators: Chiara Girauda

0339



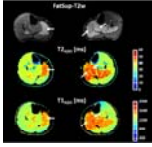
### T1, T2, and T1p Relaxation Mapping of the Lower Leg Muscle in Diabetic Neuropathy Patients with MR-Fingerprinting (MRF): Exercise Intervention

Azadeh Sharafi<sup>1</sup>, Smita Rao<sup>2</sup>, Martijn A. Cloos<sup>1</sup>, Ryan Brown<sup>1</sup>, and Ravinder R. Regatte<sup>1</sup>

<sup>1</sup>Radiology, NYU Langone Health, New York, NY, United States, <sup>2</sup>Physical Therapy, New York University, New York, NY, United States

Diabetic peripheral neuropathy (DPN) is characterized by metabolic and microvascular impairment (1) that damage peripheral nerves (2) and cause ischemic conditions and muscle degeneration in the lower extremities (3). Researchers have investigated the possibility of reversing DPN symptoms through exercise therapy (4). Such studies will benefit from quantitative biomarkers to evaluate therapeutic strategies targeting muscle function. In this work, we developed a magnetic resonance fingerprinting (MRF) technique that is insensitive to  $B_1$  imperfections for simultaneous  $T_1$ ,  $T_2$ , and  $T_{1\rho}$  relaxation mapping of skeletal muscle in DPN patients in response to exercise intervention at 3T.

0340



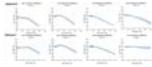
#### Water T1: a quantitative biomarker of disease activity in neuromuscular disorders

Benjamin Marty<sup>1,2</sup>, Harmen Reyngoudt<sup>1,2</sup>, Jean-Marc Boisserie<sup>1,2</sup>, Pierre-Yves Baudin<sup>3</sup>, and Pierre G. Carlier<sup>1,2</sup>

<sup>1</sup>NMR Laboratory, Neuromuscular Investigation Center, Institute of Myology, Paris, France, <sup>2</sup>NMR Laboratory, CEA/DRF/IBFJ/MIRCen, Paris, France, <sup>3</sup>Consultants for Research in Imaging and Spectroscopy, Tournai, Belgium

Recently, MR fingerprinting with water and fat separation was proposed to quantify water T1 ( $T_{1H_2O}$ ) in the muscles of patients with neuromuscular disorders. In this study, we investigated the sensitivity of  $T_{1H_2O}$  as a quantitative biomarker of disease activity, by comparing it with fat suppressed T2-weighted (FatSup-T2w) imaging and quantitative water T2 ( $T_{2H_2O}$ ) mapping, in a dataset of 61 subjects with different NMDs. We observed a significant increase of  $T_{1H_2O}$  values in muscles with FatSup-T2w signal hyperintensities. We also investigated different hypothesis explaining the moderate correlation ( $\rho = 0.54$ ) observed between  $T_{1H_2O}$  and  $T_{2H_2O}$  in the muscles of these patients.

0341



#### T2 mapping in healthy and diseased muscle using optimized extended phase graph algorithms in four clinical cohorts

Kevin Keene<sup>1,2</sup>, Jan-Willem Beenakker<sup>1,3</sup>, Melissa Hooijmans<sup>4</sup>, Karin Naarding<sup>2,5</sup>, Erik Niks<sup>2</sup>, Louise Otto<sup>6</sup>, Ludo van der Pol<sup>6</sup>, Martijn Tannemaat<sup>2</sup>, Hermien Kan<sup>1,5</sup>, and Martijn Froeling<sup>7</sup>

<sup>1</sup>Department of Radiology, C.J. Gorter center for high field MRI, Leiden University Medical Center, Leiden, Netherlands, <sup>2</sup>Department of Neurology, Leiden University Medical Center, Leiden, Netherlands, <sup>3</sup>Department of Ophthalmology, Leiden University Medical Center, Leiden, Netherlands, <sup>4</sup>Amsterdam University Medical Center, Amsterdam, Netherlands, <sup>5</sup>Duchenne Center Netherlands, Utrecht, Netherlands, <sup>6</sup>Department of Neurology, UMC Utrecht Brain Center, University Medical Center Utrecht, Utrecht, Netherlands, <sup>7</sup>Department of Radiology, University Medical Center Utrecht, Utrecht, Netherlands

Multi-echo spin-echo transverse relaxometry mapping using multi-component models is used to study disease activity in neuromuscular disease. A recent model using extended phase graphs (EPG) was introduced to obtain separate T2 values for water and fat, accounting for B1 and stimulated echoes. We improved this model and showed the importance of including flip angle slice profiles with a chemical shift displacement in the slice direction and correct calibration methods for the T2 of the fat component. We showed its performance in four clinical cohorts, and showed a gradual decline in  $T_{2water}$  with increasing fat fractions.

0342



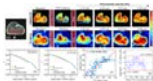
#### Multinuclear MRS at 7T uncovers exercise driven differences in skeletal muscle energy metabolism between young and seniors

Patrik Krumpolec<sup>1,2</sup>, Radka Klepochová<sup>1</sup>, Ivica Just Kukurová<sup>1</sup>, Marjeta Tušek Jelenc<sup>1</sup>, Jozef Ukropec<sup>2</sup>, Ivan Frollo<sup>3</sup>, Christopher Rodgers<sup>4,5</sup>, Barbara Ukropcová<sup>2,6</sup>, Siegfried Trattnig<sup>1,7</sup>, Martin Krššák<sup>1,7,8</sup>, and Ladislav Valkovič<sup>1,3,4</sup>

<sup>1</sup>High-field MR Center, Department of Biomedical Imaging and Image-guided Therapy, Medical University of Vienna, Vienna, Austria, <sup>2</sup>Institute of Experimental Endocrinology, Biomedical Research Center of Slovak Academy of Sciences, Bratislava, Slovakia, <sup>3</sup>Department of Imaging Methods, Institute of Measurements Science, Slovak Academy of Sciences, Bratislava, Slovakia, <sup>4</sup>Oxford Centre for Clinical Magnetic Resonance Research, BHF Centre of Research Excellence, University of Oxford, Oxford, United Kingdom, <sup>5</sup>Wolfson Brain Imaging Centre, Department of Clinical Neurosciences, University of Cambridge, Cambridge, United Kingdom, <sup>6</sup>Institute of Pathophysiology, Faculty of Medicine, Comenius University, Bratislava, Slovakia, <sup>7</sup>Christian Doppler Laboratory for Clinical Molecular MR Imaging, Vienna, Austria, <sup>8</sup>Division of Endocrinology and Metabolism, Department of Internal Medicine III, Medical University of Vienna, Vienna, Austria

The aim of this study was to investigate effect on the demand driven ATP production and carnosine content in the aging muscle. We utilized dynamic and saturation transfer <sup>31</sup>P- and <sup>1</sup>H-MRS. The dynamic experiment included acquisition of baseline data during two minutes of rest, six minutes of plantar flexion exercise (3.5 minutes long FAST measurement was performed), and six minutes of recovery. We report excessive Pi-to-ATP flux and increase of PME concentration during exercise as well as lower muscle carnosine concentration leading to lower pH after exercise in seniors, which could be linked to deprived metabolic flexibility in this population.

0343



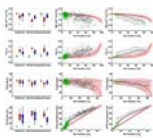
High-resolution phosphocreatine mapping using artificial neural network-based CEST MRI at 3T: A validation study

Lin Chen<sup>1,2</sup>, Michael Schär<sup>1,3</sup>, Kannie W.Y. Chan<sup>1,2,4</sup>, Jianpan Huang<sup>4</sup>, Zhiliang Wei<sup>1,2</sup>, Hanzhang Lu<sup>1,2</sup>, Qin Qin<sup>1,2</sup>, Robert G. Weiss<sup>1,3</sup>, Peter C.M. van Zijl<sup>1,2</sup>, and Jiadi Xu<sup>1,2</sup>

<sup>1</sup>Department of Radiology and Radiological Science, The Johns Hopkins University School of Medicine, Baltimore, MD, United States, <sup>2</sup>F.M. Kirby Research Center for Functional Brain Imaging, Kennedy Krieger Research Institute, Baltimore, MD, United States, <sup>3</sup>Division of Cardiology Department of Medicine, Johns Hopkins University School of Medicine, Baltimore, MD, United States, <sup>4</sup>Department of Biomedical Engineering, City University of Hong Kong, Hong Kong, China

Phosphocreatine (PCr) plays a vital role in neuron and myocyte energy homeostasis, and measurement of PCr provides a unique way to achieve insight into cellular energetics. Our previous study demonstrated that high-resolution PCr mapping of human skeletal muscle can be obtained on standard 3T clinical MRI scanner using artificial neural network-based chemical exchange saturation transfer (ANNCEST). Here, for further validation, we applied ANNCEST to measure PCr changes in exercised skeletal muscle and compared the measures with those from <sup>31</sup>P magnetic resonance spectroscopy. The feasibility of estimating spatially resolved PCr recovery rate constants using ANNCEST was also demonstrated.

0344

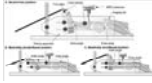


Quantitative MRI of skeletal muscle in a cross-sectional cohort of spinal muscular atrophy type 2 and type 3  
Louise A.M. Otto<sup>1</sup>, Ludo W.L. van der Pol<sup>1</sup>, Lara Schlauffke<sup>2</sup>, Camiel A. Wijngaarde<sup>1</sup>, Marloes Stam<sup>1</sup>, Renske I. Wadman<sup>1</sup>, Inge Cuppen<sup>3</sup>, Ruben P.A. van Eijk<sup>1,4</sup>, Fay-Lynn Asselman<sup>1</sup>, Bart Bartels<sup>5</sup>, Danny van der Woude<sup>5</sup>, Jeroen Hendrikse<sup>6</sup>, and Martijn Froeling<sup>6</sup>

<sup>1</sup>Neurology, UMC Utrecht Brain Center, University Medical Center, Utrecht, Utrecht, Netherlands, <sup>2</sup>Neurology, BG-University Hospital Bergmannsheil, Ruhr-University Bochum, Bochum, Germany, <sup>3</sup>Neurology and Child Neurology, UMC Utrecht Brain Center, University Medical Center, Utrecht, Utrecht, Netherlands, <sup>4</sup>Biostatistics & Research Support, Julius Center for Health Sciences and Primary Care, University Medical Center Utrecht, Utrecht, Netherlands, <sup>5</sup>Child Development and Exercise Center, UMC Utrecht Brain Center, University Medical Center, Utrecht, Utrecht, Netherlands, <sup>6</sup>Radiology, UMC Utrecht Brain Center, University Medical Center, Utrecht, Utrecht, Netherlands

qMRI of skeletal muscle has shown promising results in other neuromuscular diseases, but multi-parametric imaging has not been executed in Spinal Muscular Atrophy. We investigated a cohort of 31 patients and 20 controls with protocol consisting of DIXON, T2 mapping and DTI on a 3T MR scanner. All parameters differed significantly between patients and controls. DTI elucidates distinct properties of the muscle, suggesting atrophy by a lowered MD and increased FA. DTI shows correlation with muscle strength and motor function. This suggests the potential of diffusion tensor imaging of muscle in monitoring disease progression in SMA.

0345



### The effect of intramuscular fat on the large strain mechanical properties of skeletal muscle as measured by anisotropic MRE

Max Kaplan<sup>1,2</sup>, Alice Hatt<sup>1</sup>, Bezhad Babaei<sup>1,3</sup>, Lauriane Jugé<sup>1,2</sup>, and Lynne Bilston<sup>1,2</sup>

<sup>1</sup>Neuroscience Research Australia, Randwick, Australia, <sup>2</sup>University of New South Wales, Kensington, Australia, <sup>3</sup>University of Melbourne, Parkville, Australia

Intramuscular fat (IMF) increases with BMI and age, but it is unknown how it affects skeletal muscle viscoelastic properties, despite the key role skeletal muscle mechanical properties play in our capacity to move. We studied the effects of IMF on the anisotropic mechanical properties under large deformation of the calf muscles in healthy and obese participants, using an advanced approach incorporating diffusion tensor imaging data into magnetic resonance elastography reconstructions. Results show that intramuscular fat had no significant effect on muscle shear moduli, but stretching or shortening muscle altered the parallel and/or perpendicular stiffness and viscosity of some muscles.

0346



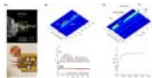
### Non Invasive Imaging of Human Motor Units

Matthew Birkbeck<sup>1,2,3</sup>, Linda Heskamp<sup>1</sup>, Ian Schofield<sup>1</sup>, Andrew Blamire<sup>1</sup>, and Roger Whittaker<sup>1</sup>

<sup>1</sup>Newcastle University, Newcastle upon Tyne, United Kingdom, <sup>2</sup>Newcastle Biomedical Research Centre, Newcastle upon Tyne, United Kingdom, <sup>3</sup>Regional Medical Physics, Newcastle upon Tyne, United Kingdom

Motor units are fundamental components in the process of contraction of skeletal muscle. Motor unit morphology changes in response to pathologies including motor neurone disease and sarcopenia. Currently the clinical method to investigate motor unit morphology and activity is invasive needle electromyography. Here we present a novel diffusion weighted imaging technique, motor unit MRI (MUMRI). MUMRI has been used to investigate the morphology of single human motor units, producing quantitative data on cross sectional area and dimensions of human motor units. This data agrees with current literature. MUMRI has detected statistically significant changes in the morphology of motor units.

0347



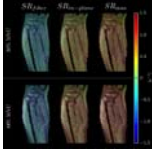
### Repeated Muscle Contraction increases Creatine Kinase Reaction Rate and Shortens Phosphocreatine Recovery in Mouse Skeletal Muscle

Kihwan Kim<sup>1</sup>, Yuning Gu<sup>1</sup>, Gahee Kim<sup>1</sup>, Mei Wong<sup>1</sup>, Bryan Clifford<sup>2,3</sup>, Sherry Huang<sup>1</sup>, Zhi-Pei Liang<sup>2,3</sup>, and Xin Yu<sup>1,4</sup>

<sup>1</sup>Department of Biomedical Engineering, Case Western Reserve University, Cleveland, OH, United States, <sup>2</sup>Electrical and Computer Engineering, University of Illinois at Urbana-Champaign, Urbana, IL, United States, <sup>3</sup>Beckman Institute for Advanced Science and Technology, University of Illinois at Urbana-Champaign, Urbana, IL, United States, <sup>4</sup>Case Center for Imaging Research, Case Western Reserve University, Cleveland, OH, United States

This study examined the effects of muscle contraction, induced by electrical stimulation, on creatine kinase (CK) reaction rate and the rate of phosphocreatine (PCr) recovery after its transient depletion in mouse skeletal muscle using phosphorous-31 (<sup>31</sup>P) magnetic resonance fingerprinting and dynamic <sup>31</sup>P magnetic resonance spectroscopy. Our results showed that electrical stimulation induced a significant increase in CK reaction rate by ~14%, as well as an increased in PCr recovery rate by 26%, suggesting a positive preconditioning effect induced by electrical stimulation.

0348



### Principal Axis and Fiber Aligned 3D Strain / Strain Rate Mapping with Compressed Sensing Velocity Encoded Phase Contrast MRI to study Aging Muscle

Vadim Malis<sup>1</sup>, Usha Sinha<sup>2</sup>, and Shantanu Sinha<sup>3</sup>

<sup>1</sup>Physics, UC San Diego, La Jolla, CA, United States, <sup>2</sup>Physics, San Diego State University, San Diego, CA, United States, <sup>3</sup>Radiology, UC San Diego, La Jolla, CA, United States

Strain and Strain rate tensors can be computed from velocity encoded phase contrast imaging. The study of the variation of deformation indices with force output (% Maximum Voluntary Contraction (MVC)) can provide information on the aging muscle. However, such studies have been limited by the long acquisition time precluding its use at high MVCs and in older subjects. We developed a compressed sensing VE-PC technique to enable acquisitions across a range of MVCs and applicable to older subjects as well. Significant differences in the deformation indices were seen between 11 young / 8 senior subjects as well between different %MVCs.

## Oral

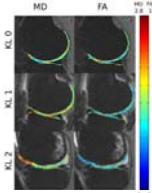
### Muscle, Cartilage, Knee stabilizers - Cartilage

Monday Parallel 4 Live Q&A

Monday 15:15 - 16:00 UTC

Moderators: Ashley Williams

0349



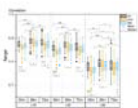
### DTI of articular cartilage as a biomarker for OA diagnosis, staging and progression in a population with early stages of the disease

Elisa Ramos Gavila<sup>1</sup>, Alejandra Duarte<sup>1</sup>, Jenny Bencardino<sup>2</sup>, Jonathan Samuel<sup>2</sup>, Svetlana Krasnokutsky<sup>2</sup>, and Jose Raya Garcia del Olmo<sup>2</sup>

<sup>1</sup>Radiology, NYU Langone Health Hospital, New York, NY, United States, <sup>2</sup>NYU Langone Health Hospital, New York, NY, United States

Early detection of knee osteoarthritis can be achieved by identifying early compositional changes of degenerative articular cartilage. The purpose of this case-control longitudinal study is to validate DTI as a biomarker for OA diagnosis, staging and progression in early stages of the disease. 60 patients with incipient OA (KL1) underwent 3 visits (baseline, 1.5 year and 3 years follow up). Clinical evaluation, Xray and MRI was performed. Positive correlation was demonstrated with morphological changes (KL and WOMBS score). In addition, DTI showed changes in the follow up at 1.5 years that were not apparent in clinical MRI.

0350



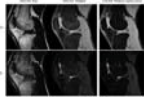
### Gray Level Co-occurrence Matrix Based 3D Texture Analysis of Knee Articular Cartilage using 3D DESS Images

Ari Väärälä<sup>1,2</sup>, Arttu Peuna<sup>3</sup>, Egor Panfilov<sup>1,2</sup>, Victor Casula<sup>1,2</sup>, Marianne Haapea<sup>2,4</sup>, Eveliina Lammentausta<sup>1,2,4</sup>, and Miika T Nieminen<sup>1,2,4</sup>

<sup>1</sup>Research Unit of Medical Imaging, Physics and Technology, University of Oulu, Oulu, Finland, <sup>2</sup>Medical Research Center, University of Oulu and Oulu University Hospital, Oulu, Finland, <sup>3</sup>Medical Imaging, Central Finland Health Care District, Jyväskylä, Finland, <sup>4</sup>Department of Diagnostic Radiology, Oulu University Hospital, Oulu, Finland

In the present study, a gray level co-occurrence matrix-based 3D texture analysis of knee 3D DESS images was used to investigate longitudinal changes in articular cartilage using data from the Osteoarthritis Initiative (baseline, 36-month and 72-month visits). At baseline, all subjects included in the study had Kellgren-Lawrence grade < 2. Three groups were defined, based on time of progression into radiographic osteoarthritis (Kellgren-Lawrence grades  $\geq 2$ ): control, slow progressor and fast progressor groups. 3D texture analysis of 3D DESS images was able to distinguish progressors from controls before radiographic signs of osteoarthritis and showed significant longitudinal changes across all groups.

0351



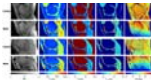
### Extending DESS to MESS: A 5 minute knee protocol for water-fat separation and T2 mapping

Frank Zijlstra<sup>1</sup> and Peter R Seevinck<sup>1</sup>

<sup>1</sup>Image Sciences Institute, UMC Utrecht, Utrecht, Netherlands

This study proposes a 5 minute knee protocol using an extension of the double-echo steady-state (DESS) sequence to include multiple readouts. This multiple-echo steady-state (MESS) sequence supports quantification of water, fat, and T2, in a single, efficient acquisition. These parameters may provide additional tissue-specific MRI biomarkers, for example in muscle and bone, on top of the T2 quantification of cartilage provided by the DESS sequence. In vivo results on 5 volunteers show robust water-fat separation and that T2 quantification using MESS corresponds well with quantification on water-selective DESS images.

0352



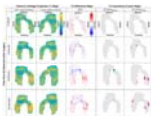
### Rapid Simultaneous T1, T2, and T1p Relaxation Mapping of the knee joint with MR-Fingerprinting (MRF)

Azadeh Sharafi<sup>1</sup>, Marcelo V. W. Zibetti<sup>1</sup>, Gregory Chang<sup>1</sup>, Martijn A. Cloos<sup>1</sup>, and Ravinder R. Regatte<sup>1</sup>

<sup>1</sup>Radiology, NYU Langone Health, New York, NY, United States

Osteoarthritis of the knee, the most common joint disease, is a degenerative heterogeneous musculoskeletal disease which is mainly recognized by the progressive loss of hyaline articular cartilage (1). Spin-lattice relaxation in the rotating frame ( $T_{1\rho}$ ) and spin-spin relaxation ( $T_2$ ) have been shown to be sensitive to the biochemical changes associated with osteoarthritis progression including: loss of proteoglycans, increased water content, and disruption of collagen and anisotropy (1, 2). In this study, we propose a novel MR fingerprinting sequence for in-vivo simultaneous T1, T2, and T1p relaxation mapping of knee joint at 3T.

0353



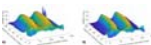
### Bilateral Femoral Cartilage T2 Asymmetry Analysis for the Detection of Early Osteoarthritic Degeneration

Marianne S Black<sup>1,2</sup>, Katherine A Young<sup>1</sup>, Akshay S Chaudhari<sup>1</sup>, Feliks Kogan<sup>1</sup>, Bragi Sveinsson<sup>3</sup>, Emily J McWalter<sup>4</sup>, Garry E Gold<sup>1,5</sup>, Marc E Levenston<sup>1,2</sup>, and Brian A Hargreaves<sup>1,5,6</sup>

<sup>1</sup>Radiology, Stanford University, Stanford, CA, United States, <sup>2</sup>Mechanical Engineering, Stanford University, Stanford, CA, United States, <sup>3</sup>Massachusetts General Hospital, Boston, MA, United States, <sup>4</sup>Mechanical Engineering, University of Saskatchewan, Saskatoon, SK, Canada, <sup>5</sup>Bioengineering, Stanford University, Stanford, CA, United States, <sup>6</sup>Electrical Engineering, Stanford University, Stanford, CA, United States

There is a pressing need for a single-time-point quantitative measure capable of predicting osteoarthritic change. Bilateral knee imaging with  $T_2$  cluster asymmetry analysis is a promising approach to achieve this goal. This study examines  $T_2$  cluster asymmetry in ACL-injured subjects and controls. ACL-injured subjects showed elevated  $T_2$  cluster asymmetry 9-months following reconstruction surgery relative to the controls in the superficial half of cartilage. This novel approach for analyzing  $T_2$  relaxation times in femoral cartilage shows promise in detecting changes that may be indicative of early osteoarthritis onset.

0354



### Collagen fiber anisotropy and orientation mapping of articular cartilage via T2 relaxation anisotropy

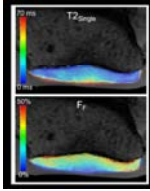
Henri Leskinen<sup>1</sup>, Nina E. Hänninen<sup>1,2</sup>, and Mikko J. Nissi<sup>1,2</sup>

<sup>1</sup>University of Eastern Finland, Kuopio, Finland, <sup>2</sup>University of Oulu, Oulu, Finland



Number of studies have investigated the orientation dependence of T2 relaxation in articular cartilage and, more importantly, connected the orientation dependence to the properties of the collagen fiber network in cartilage. The dependence arises from the non-averaging secular part of the dipolar coupling, which in turn has been attributed to the water-orienting properties of the collagenous network. Using high angular resolution sample rotation, this study aimed to measure the in-plane fiber angle, collagen anisotropy as well as the isotropic and anisotropic components of T2 relaxation in cartilage. Potential for extracting physically meaningful properties of cartilage from multi-orientation measurements was demonstrated.

0355



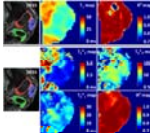
#### Correlation Between Single-Component and Bi-Component T2 Parameters and Proteoglycan Content and Mechanical Properties of Cartilage

Matthew Grondin<sup>1</sup>, Fang Liu<sup>2</sup>, Sami Faruqui<sup>2</sup>, Alexei Samsonov<sup>2</sup>, Wan-Ju Li<sup>3</sup>, Corinne Henak<sup>1</sup>, and Richard Kijowski<sup>2</sup>

<sup>1</sup>Mechanical Engineering, University of Wisconsin-Madison, Madison, WI, United States, <sup>2</sup>Radiology, University of Wisconsin-Madison, Madison, WI, United States, <sup>3</sup>Orthopedic Surgery, University of Wisconsin-Madison, Madison, WI, United States

Multi-component Driven Equilibrium Single Pulse Observation of T1 and T2 (mcDESPOT) was used to measure single-component T2 relaxation time ( $T_{2\text{Single}}$ ) and the fraction of the fast relaxing macromolecular bound water component ( $F_F$ ) of 24 human patellar cartilage samples at 3.0T. The cartilage samples underwent mechanical testing to measure linear modulus and energy dissipation and biochemical analysis to measure proteoglycan content. There were significant ( $p < 0.01$ ) and moderate positive correlations between  $F_F$  and proteoglycan content, linear modulus, and energy dissipation of cartilage. There were non-significant ( $p = 0.06-0.21$ ) and low negative correlations between  $T_{2\text{Single}}$  and proteoglycan content, linear modulus, and energy dissipation of cartilage.

0356



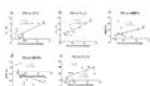
#### Ex Vivo Evaluation of Sodium Relaxation Times in Pediatric Articular-Epiphyseal Cartilage on a Whole-body 10.5T MR System – Initial Results

Stefan Zbyn<sup>1,2</sup>, Kai D. Ludwig<sup>1,2</sup>, Lauren Watkins<sup>3</sup>, Alexandra R. Armstrong<sup>4</sup>, Russell L. Lagore<sup>1,2</sup>, Amanda Nowacki<sup>1</sup>, Marc A. Tompkins<sup>5</sup>, Ferenc Toth<sup>4</sup>, Gregor Adriany<sup>1,2</sup>, Kevin G. Shea<sup>6</sup>, Garry Gold<sup>7</sup>, Armin M. Nagel<sup>8</sup>, Cathy S. Carlson<sup>4</sup>, Gregory J. Metzger<sup>1,2</sup>, and Jutta M. Ellermann<sup>1,2</sup>

<sup>1</sup>Center for Magnetic Resonance Research, University of Minnesota, Minneapolis, MN, United States, <sup>2</sup>Department of Radiology, University of Minnesota, Minneapolis, MN, United States, <sup>3</sup>Department of Bioengineering, Stanford University, Stanford, CA, United States, <sup>4</sup>Department of Veterinary Clinical Sciences, University of Minnesota, St. Paul, MN, United States, <sup>5</sup>Department of Orthopaedic Surgery, University of Minnesota, Minneapolis, MN, United States, <sup>6</sup>Department of Orthopaedic Surgery, Stanford Children's Hospital, Palo Alto, CA, United States, <sup>7</sup>Department of Radiology, Stanford University, Stanford, CA, United States, <sup>8</sup>Institute of Radiology, University Hospital Erlangen, Friedrich-Alexander-Universität Erlangen-Nürnberg, Erlangen, Germany

Sodium imaging is quantitative technique sensitive to changes in cartilage glycosaminoglycan content. Changes in cartilage matrix, due to maturation or degeneration, may influence sodium relaxation times which can lead to incorrect sodium concentration estimates when not addressed. This *ex vivo* study employs pediatric knee specimens to evaluate the relationship between sodium relaxation parameters and compositional changes in the developing cartilage matrix. Our preliminary evaluation suggests that cartilage maturation is accompanied by a decrease in sodium  $T_1$  and the short  $T_2^*$  component. Sodium concentrations in studies comparing healthy, diseased or immature cartilage should be corrected for possible changes in relaxation times.

0357



#### UTE-based biomarkers are selectively sensitive to enzymatic proteoglycan and collagen degradation in human articular cartilage

Lidi Wan<sup>1,2</sup>, Xin Cheng<sup>3</sup>, Adam C Searleman<sup>1</sup>, Yajun Ma<sup>1</sup>, Jonathan H Wong<sup>1,4</sup>, Mark E Murphy<sup>5</sup>, Jiang Du<sup>1</sup>, Guangyu Tang<sup>2</sup>, and Eric Y Chang<sup>1,4</sup>

<sup>1</sup>Department of Radiology, UC San Diego, San Diego, CA, United States, <sup>2</sup>Department of Radiology, Shanghai Tenth People's Hospital, Shanghai, China, <sup>3</sup>Division of Histology and Embryology, Jinan University, Guangzhou, China, <sup>4</sup>Radiology Service, VA San Diego Healthcare System, San Diego, CA, United States, <sup>5</sup>Orthopaedic Surgery Service, VA San Diego Healthcare System, San Diego, CA, United States

A panel of quantitative UTE techniques have been developed to assess articular cartilage. Osteoarthritis (OA) is a multifactorial disease characterized primarily by degeneration and loss of hyaline articular cartilage. This study investigated whether quantitative 3D UTE-Cones-based biomarkers are sensitive to proteoglycan (PG) loss and collagen degradation induced by enzyme in human cartilage, and also to determine the specificity of these biomarkers in quantitative cartilage imaging.

---

## Combined Educational & Scientific Session

### Muscle, Cartilage, Knee stabilizers - MRI of Knee Stabilizers

Organizers: Jan Fritz, Riccardo Lattanzi, Kimberly Amrami, Jung-Ah Choi, Miika Nieminen, Hiroshi Yoshioka

Monday Parallel 4 Live Q&A

Monday 15:15 - 16:00 UTC

Moderators: Bragi Sveinsson & Anup Singh

#### Structural MRI of the Knee Stabilizers

Darryl Sneag<sup>1</sup>

<sup>1</sup>Hospital for Special Surgery, United States

#### Functional & Quantitative MRI of the Knee Stabilizers

James Griffith<sup>1</sup>

<sup>1</sup>Chinese University of Hong Kong, Hong Kong, Hong Kong

0358



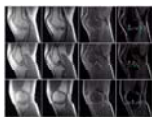
#### Feasibility of dynamic DTI exercise response and resistance dependence in quadriceps muscle

Eric E. Sigmund<sup>1</sup>, Steven H. Baete<sup>1</sup>, and Danielle Costanzo<sup>1</sup>

<sup>1</sup>Radiology, NYU Langone Health, New York, NY, United States

We describe measurement of resistance dependence diffusion metric exercise response in thigh muscle with a multiple echo diffusion tensor imaging (MEDITI) on a clinical 3 T scanner. With radial imaging, accelerated diffusion encoding, and compressed sensing reconstruction, spatial resolution of 3.4 mm and temporal resolution of 16 s was achieved. Using an MR-compatible ergometer with pneumatic resistance and force/displacement monitoring, post-exercise recovery of DTI metrics in the rectus femoris following quadriceps extension was monitored as a function of resistance. Significant dependences of response on resistance were observed.

0359



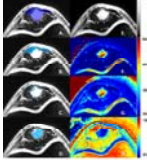
#### 3D UTE Cones Double Echo Steady State Imaging – a New Approach for High Resolution Morphological and Quantitative Evaluation of Short T2 Tissues

Hyungseok Jang<sup>1</sup>, Michael Carl<sup>2</sup>, Yajun Ma<sup>1</sup>, Mei Wu<sup>1</sup>, Zhao Wei<sup>1</sup>, Saeed Jerban<sup>1</sup>, Eric Chang<sup>1,3</sup>, and Jiang Du<sup>1</sup>

<sup>1</sup>University of California, San Diego, San Diego, CA, United States, <sup>2</sup>GE Healthcare, La Jolla, CA, United States, <sup>3</sup>VA San Diego Healthcare System, San Diego, CA, United States

Double echo steady state (DESS) imaging allows acquisition of two MR images with different contrasts from FID and echo images. In this study, we explored the feasibility and efficacy of 3D UTE Cones-based DESS (3D UTE-Cones-DESS) imaging of short T2 tissues in the knee joint. In ex vivo study of four cadaveric knees and in vivo study of three healthy volunteers, the UTE-Cones-DESS sequence provided high contrast imaging of the osteochondral junction (OCJ), the menisci, and other short T2 tissues, as well as T2 maps, under a total scan time of three minutes.

0360



### Sub-regional Quantification of Tissue-Specific Hydration State in Patellar Tendinopathy with 3D Ultrashort Echo Time MRI

Stephan Breda<sup>1</sup>, Dirk Poot<sup>1</sup>, Dorottya Papp<sup>1</sup>, Gabriel Krestin<sup>1</sup>, Robert-Jan de Vos<sup>2</sup>, and Edwin Oei<sup>1</sup>

<sup>1</sup>Radiology & Nuclear Medicine, Erasmus University Medical Center, Rotterdam, Netherlands, <sup>2</sup>Orthopedics & Sports Medicine, Erasmus University Medical Center, Rotterdam, Netherlands

Patellar tendinopathy (PT) is an overuse injury of the patellar tendon in athletes, often resulting from jumping activities such as playing basketball or volleyball. MR imaging with ultrashort echo times (3D-UTE MRI) is used to image the typical degenerative process of the proximal patellar tendon in PT. However, image analysis can be challenging within the heterogeneous patellar tendon affected by tendinopathy. Therefore, we propose a novel method for image analysis, in which voxels are sub-selected based on a parameter from bi-exponential fitting. This resulted in the identification of T2\* biomarkers, specific for distinct tissue-compartments within the patellar tendon.

0361



### Towards kinematic knee imaging with a liquid metal array

Andreas Port<sup>1</sup>, Roger Luechinger<sup>1</sup>, David Otto Brunner<sup>1</sup>, and Klaas Paul Pruessmann<sup>1</sup>

<sup>1</sup>Institute for Biomedical Engineering, ETH Zurich and University of Zurich, Zurich, Switzerland

Kinematic MR studies provide functional insights that corresponding static methods may not be able to provide. However, MR signal reception from body parts with large flexion ranges, such as the knee, can be challenging. Wearable RF coils that adapt well to a specific anatomy would offer good sensitivity and patient comfort at the same time. In the present work, we explore the practical utility of a wearable liquid metal coil. For this purpose a MR compatible knee bending setup is used. Static and kinematic imaging of a volunteer's knee confirm sensitivity and coverage over the whole range of flexion.

0362



### Compositional and Morphological Characterization of Knee Articular Cartilage in Collegiate Basketball Players using Multiparametric MRI

Kenneth T. Gao<sup>1</sup>, Valentina Pedoia<sup>1</sup>, Radhika Tibrewala<sup>1</sup>, Katherine A. Young<sup>2</sup>, Feliks Kogan<sup>2</sup>, Matthew F. Koff<sup>3</sup>, Garry E. Gold<sup>2</sup>, Hollis Potter<sup>3</sup>, and Sharmila Majumdar<sup>1</sup>

<sup>1</sup>Department of Radiology and Biomedical Imaging, University of California, San Francisco, San Francisco, CA, United States, <sup>2</sup>Department of Radiology, Stanford University, Stanford, CA, United States, <sup>3</sup>Department of Radiology and Imaging, Hospital for Special Surgery, New York, NY, United States

Magnetic resonance imaging (MRI) is commonly used to evaluate the morphology of athletes with high knee impact; however, the biochemical composition of their cartilage is not as well understood. In this study, we utilized voxel-based relaxometry (VBR), a fully automatic registration technique, to compare local distribution of knee articular cartilage T<sub>1ρ</sub> and T<sub>2</sub> relaxation times between high knee impact athletes (basketball players) and non-knee impact athletes (swimmers). Statistical analysis revealed laminar differences near the patella, with basketball players having prolonged values in the deep layer. These findings, amongst others, related well to morphological evaluation of the image set.

0363



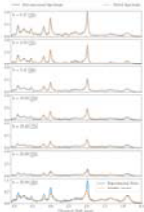
Calibration-free regional RF shims for localised MR spectroscopy

Adam Berrington<sup>1</sup>, Michal Povazan<sup>2</sup>, Christopher Mirfin<sup>1</sup>, Stephen Bawden<sup>1</sup>, Richard Bowtell<sup>1</sup>, and Penny Gowland<sup>1</sup>

<sup>1</sup>Sir Peter Mansfield Imaging Centre, School of Physics and Astronomy, University of Nottingham, Nottingham, United Kingdom, <sup>2</sup>Russel H. Morgan Department of Radiology and Radiological Science, Johns Hopkins University School Of Medicine, Baltimore, MD, United States

RF shimming can increase  $B_1^+$  availability, which is critical for robust localised MR spectroscopy at ultra-high field. Shim calibration is performed on a region-wise basis and is, therefore, time consuming. Additionally,  $B_1$  distributions become difficult to predict. Recent work has shown that 'universal' pulses can be generated offline – avoiding the need for calibration. Here, we determine static calibration-free RF shims, optimised over 5 heads, for 3 different brain regions.  $B_1^+$  availability using calibration-free shims was significantly higher than quadrature and comparable to tailored shimming. High quality spectra were also obtained from 3 regions with the calibration-free shims.

0364



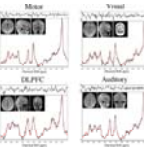
Diffusion-weighted MRS at short TE using a Connectom system: non-Gaussian metabolite diffusion and macromolecular signals in human brain

Kadir Şimşek<sup>1</sup>, André Döring<sup>1</sup>, André Pampel<sup>2</sup>, Harald E. Möller<sup>2</sup>, and Roland Kreis<sup>1</sup>

<sup>1</sup>Department of Radiology and Biomedical Research, University of Bern, Bern, Switzerland, <sup>2</sup>Max-Planck Institute For Human Cognitive and Brain Sciences, Leipzig, Germany

Diffusion-weighted MRS was successfully implemented on a 3T Connectom system reaching b-values of 25 ms/um<sup>2</sup> at a short TE of 30 ms and a moderate TM of 65 ms. Motion-compensation based on the water peak was found feasible up to the highest b-value and can be supplemented by scaling to the macromolecule peak intensity at 0.9 ppm. Non-Gaussian diffusion behavior was detected for multiple metabolites and was modeled with biexponential and kurtosis representations. In addition, a macromolecular spectrum could be determined by diffusion weighting and simultaneous modeling, which can now be used for quantification in clinical short TE MRS.

0365

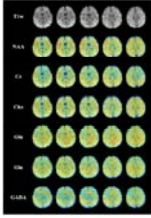


Intra-session and inter-subject variability of 3D-FID-MRSI using single-echo volumetric EPI navigators at 3T

Philipp Moser<sup>1</sup>, Korbinian Eckstein<sup>1</sup>, Lukas Hingerl<sup>1</sup>, Michael Weber<sup>1</sup>, Stanislav Motyka<sup>1</sup>, Bernhard Strasser<sup>1,2</sup>, Andre van der Kouwe<sup>3</sup>, Simon Robinson<sup>1</sup>, Siegfried Trattnig<sup>1,4</sup>, and Wolfgang Bogner<sup>1</sup>

<sup>1</sup>High Field MR Centre, Department of Biomedical Imaging and Image-guided Therapy, Medical University of Vienna, Vienna, Austria, <sup>2</sup>Athinoula A. Martinos Center for Biomedical Imaging, Department of Radiology, Harvard Medical School, Massachusetts General Hospital, Vienna, MA, United States, <sup>3</sup>Athinoula A. Martinos Center for Biomedical Imaging, Department of Radiology, Harvard Medical School, Massachusetts General Hospital, Boston, MA, United States, <sup>4</sup>Christian Doppler Laboratory for Clinical Molecular MR Imaging, Vienna, Austria

We demonstrate the combination of 3D free induction decay proton MR spectroscopic imaging and spatial encoding via concentric-ring trajectories at 3T. To improve the reliability as well as the temporal stability, single-echo, imaging-based volumetric navigators for real-time motion/shim-correction were additionally integrated. All intra-subject coefficients of variation and most of the inter-subject coefficients of variation obtained with motion/shim-correction were lower (i.e., better) than without and resulted in higher SNRs and lower CRLBs.

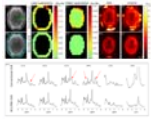


### Rapid High-Resolution Mapping of Brain Metabolites and Neurotransmitters Using Hybrid FID/SE-J-Resolved Spectroscopic Signals

Yibo Zhao<sup>1,2</sup>, Yudu Li<sup>1,2</sup>, Jiahui Xiong<sup>1,2</sup>, Rong Guo<sup>1,2</sup>, Yao Li<sup>3,4</sup>, and Zhi-Pei Liang<sup>1,2</sup>

<sup>1</sup>Department of Electrical and Computer Engineering, University of Illinois at Urbana-Champaign, Urbana, IL, United States, <sup>2</sup>Beckman Institute for Advanced Science and Technology, University of Illinois at Urbana-Champaign, Urbana, IL, United States, <sup>3</sup>School of Biomedical Engineering, Shanghai Jiao Tong University, Shanghai, China, <sup>4</sup>Med-X Research Institute, Shanghai Jiao Tong University, Shanghai, China

J-resolved MRSI is a powerful tool for separating overlapping resonances in conventional MRSI, which is especially useful for mapping neurotransmitters like  $\gamma$ -aminobutyric acid and glutamate. A major practical limitation of J-resolved MRSI lies in its long data acquisition time required to sample the high-dimensional data space using spin-echo-based sequences. In this work, we present a novel hybrid FID/SE data acquisition scheme to accelerate J-resolved MRSI. The proposed method has been validated using phantom and in vivo experimental data, producing high-quality 3D spatial maps of brain metabolites and neurotransmitters within clinically feasible time.

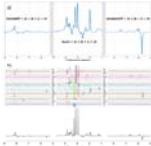


### Robust Outer Volume Suppression Utilizing Elliptical Pulsed Second Order Fields (ECLIPSE) for Human Brain Proton MRSI

Chathura Kumaragamage<sup>1</sup>, Henk M De Feyter<sup>1</sup>, Peter B Brown<sup>1</sup>, Scott McIntyre<sup>1</sup>, Terence W Nixon<sup>1</sup>, and Robin A de Graaf<sup>1</sup>

<sup>1</sup>Radiology and Biomedical Imaging, Yale University, New Haven, CT, United States

Extracranial lipid contaminants impede the reliable and accurate metabolite quantification with human brain MRSI. Elliptical localization with pulsed second order fields (ECLIPSE) was previously demonstrated for MRSI with inner volume selection (IVS), providing robust lipid suppression with improved elliptical brain coverage relative to a cubical ROI. In this work, alternative ECLIPSE-based OVS and IVS sequences were developed for human brain MRSI at 4T. Both ECLIPSE methods provide > 100-fold mean lipid suppression for short-TE MRSI. In addition, ECLIPSE-OVS consumes 30% of the power required by a traditional 8-slice OVS method, making ECLIPSE-OVS attractive for high field MRSI.



### HERCULES and ConCAT: Simultaneous modelling and fitting of 11 metabolites using LCMoDEL

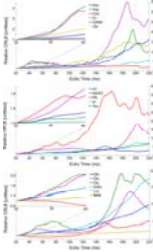
Diana Rotaru<sup>1</sup>, Georg Oeltzschner<sup>2,3</sup>, Richard Edden<sup>3,4</sup>, and David Lythgoe<sup>1</sup>

<sup>1</sup>Neuroimaging, King's College London, London, United Kingdom, <sup>2</sup>Russell H. Morgan Department of Radiology and Radiological Science, The Johns Hopkins University School of Medicine, Baltimore, MD, United States, <sup>3</sup>F. M. Kirby Research Center for Functional Brain Imaging, Kennedy Krieger Institute, Baltimore, MD, United States, <sup>4</sup>Radiology and Radiological Science, The Johns Hopkins University School of Medicine, Baltimore, MD, United States

Advanced spectral editing techniques have focused mainly on GABA and GSH discrimination and detection. HERCULES, unlike all predecessor sequences, delivers a reliable detection method for GABA and GSH, but also for ascorbate, aspartate, 2-hydroxyglutarate, lactate, NAA and NAAG. However, current analysis methods have not been optimized for HERCULES analysis. We investigated simultaneous LCMoDEL fitting of the concatenated sum and difference spectra calculated from HERCULES data. The concatenated (ConCAT) approach enables the use of all available spectral information. Compared to traditional single-spectrum analysis, ConCAT yielded improved results, with lower coefficients of variation obtained for concentration estimates and Cramér-Rao lower bounds.

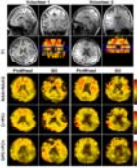
Optimization of echo time choice for seven common MRS pulse sequences through minimization of expected Cramér-Rao lower bounds.

Karl Landheer<sup>1</sup> and Christoph Juchem<sup>1,2</sup>



<sup>1</sup>Biomedical Engineering, Columbia University, New York, NY, United States, <sup>2</sup>Radiology, Columbia University, New York, NY, United States

It has recently been recommended to utilize the minimum echo time for non-editing magnetic resonance spectroscopic experiments. Despite this intuitive recommendation there is no comprehensive and systematic investigation into the choice of echo time across numerous sequences. Here the impact of echo time on the Cramér-Rao lower bounds for 17 different metabolites across the six most commonly used pulse sequences are investigated using simulated spectral shapes, as well as a MEGA-sLASER sequence for GABA quantification. Recommendations are provided for the choice of echo time which will minimize the expected Cramér-Rao lower bound for all metabolites and sequences in question.

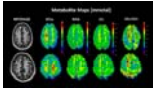


### Whole-brain MR Spectroscopic Imaging with stack of Spirals Out-In k-space Trajectory at 7T

Morteza Esmaeili<sup>1,2</sup>, Bernhard Strasser<sup>1</sup>, Wolfgang Bogner<sup>3</sup>, Philipp Moser<sup>3</sup>, Zhe Wang<sup>4</sup>, and Ovidiu C. Andronesi<sup>1</sup>

<sup>1</sup>Athinoula A. Martinos Center for Biomedical Imaging, Department of Radiology, Massachusetts General Hospital, Boston, MA, United States, <sup>2</sup>Department of Diagnostic Imaging, Akershus University Hospital, Lørenskog, Norway, <sup>3</sup>High-field MR Center, Department of Biomedical Imaging and Image-guided Therapy, Medical University of Vienna, Vienna, Austria, <sup>4</sup>Siemens Medical Solutions, Charlestown, MA, United States

Metabolic imaging using magnetic resonance spectroscopic imaging (MRSI) provides important biomarkers for brain neurochemistry. We developed a spiral-out-in (SOI) trajectory for human whole-brain MRSI at 7T to take advantage of increased sensitivity and spectral separation at ultra-high field. We hypothesized that spectral-spatial SOI sampling will provide higher signal-to-noise ratio(SNR) compared to spiral-out (SO) sampling by increasing the efficiency of data collection. We acquired data from phantom and six healthy volunteers. Metabolic maps, SNR, Cramér-Rao-Lower-Bounds (CRLB) were evaluated between SO and SOI acquisitions. By more efficient data points collection per repetition time, SOI provided a significant improvement in SNR and CRLB.

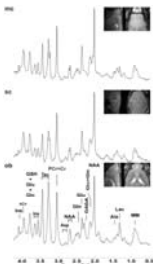


### Quantitative Metabolite Mapping of the Human Brain at 9.4 T

Andrew Martin Wright<sup>1,2</sup>, Saipavitra Murali Manohar<sup>1,3</sup>, and Anke Henning<sup>1,4</sup>

<sup>1</sup>MRZ, Max Planck Institute for Biological Cybernetics, Tuebingen, Germany, <sup>2</sup>International Max Planck Research School, University of Tuebingen, Tuebingen, Germany, <sup>3</sup>University of Tuebingen, Tuebingen, Germany, <sup>4</sup>Advanced Imaging Research Center, University of Texas Southwestern Medical Center, Dallas, TX, United States

Quantitative metabolite maps are reported from in vivo results at 9.4T. These maps are produced by quantifying with an internal water reference and utilize a novel T1 correction method applied to each voxel individually. Quantitative results allow cross-vendor and cross-site comparisons of results which may help to understand and characterize a variety neurological diseases.



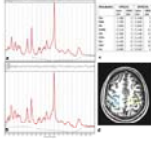
### Towards sub-microlitre MRS in the mouse brain in vivo at ultra-high field

Alireza Abaei<sup>1</sup>, Dinesh K Deelchand<sup>2</sup>, Francesco Roselli<sup>3</sup>, and Volker Rasche<sup>1</sup>

<sup>1</sup>Core Facility Small Animal Imaging, Ulm University, Medical Center, ulm, Germany, <sup>2</sup>Center for Magnetic Resonance Research, University of Minnesota, Minneapolis, MN, United States, <sup>3</sup>German Center for Neurodegenerative Diseases (DZNE), Ulm, Germany

Several pathological conditions affect only a small volume of the cortex (such as the motor cortex in amyotrophic lateral sclerosis) and its characterization in mouse models is made impossible by the interference of normal, nearby cortical tissue. A sub-microlitre preclinical MRS technique was successfully implemented to detect subtle changes of the neurometabolite concentrations in three cortical areas. Employing LASER together with using cryogenically cooled RF coils significantly reduces the acquisition time to enable sub-microlitre MRS acquisition. Our findings demonstrate that neurochemical profiles of individual cortical brain regions can be reliably collected in pre-clinically feasible scan times.

0373



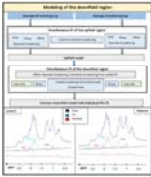
Adiabatic multiband inversion for simultaneous acquisition of  $^1\text{H}$  MR spectra from two voxels *in-vivo* at very short echo times

Layla Tabea Riemann<sup>1</sup>, Christoph Stefan Aigner<sup>1</sup>, Rüdiger Brühl<sup>1</sup>, Semiha Aydin<sup>1</sup>, Ralf Mекle<sup>2</sup>, Sebastian Schmitter<sup>1</sup>, Bernd Ittermann<sup>1</sup>, and Ariane Fillmer<sup>1</sup>

<sup>1</sup>Physikalisch-Technische Bundesanstalt (PTB), Braunschweig und Berlin, Germany, <sup>2</sup>Center for Stroke Research Berlin, Charité-Universitätsmedizin, Berlin, Germany

In this work, a novel  $^1\text{H}$  MR spectroscopy sequence is proposed that provides the advantages of single voxel spectroscopy, such as high spectral bandwidth, a narrower point spread function, shorter measurement time and larger signal-to-noise-ratio, as compared to spectroscopic imaging while exciting more than one voxel. A multi-band adiabatic RF pulse was implemented into a SPECIAL sequence to simultaneously acquire the signal of two disjunct voxels at short echo times. The overlapping signal was decomposed using the SENSE algorithm. The new sequence was validated using a two-compartment phantom and its feasibility for *in-vivo* application is demonstrated at 7 T.

0374



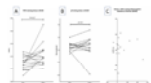
Quantification of phenylalanine with  $^1\text{H}$  MRS using optimized acquisition conditions and downfield background modeling

Maïke Hoefemann<sup>1</sup>, Raphaela Muri<sup>2</sup>, Stephanie Abgottspon<sup>2</sup>, Johannes Slotboom<sup>3</sup>, Regula Everts<sup>2,4</sup>, Roman Trepp<sup>2</sup>, and Roland Kreis<sup>1</sup>

<sup>1</sup>Departments of Radiology and Biomedical Research, University of Bern, Bern, Switzerland, <sup>2</sup>Department of Diabetes, Endocrinology, Clinical Nutrition and Metabolism, Bern University Hospital, University of Bern, Bern, Switzerland, <sup>3</sup>Support Center for Advanced Neuroimaging, University Institute of Diagnostic and Interventional Neuroradiology Inselspital, Bern, Switzerland, <sup>4</sup>Division of Neuropediatrics, Development & Rehabilitation, Pediatric University Hospital, University of Bern, Bern, Switzerland

For the quantification of the low-concentration metabolite phenylalanine (Phe) in patients with phenylketonuria using  $^1\text{H}$  magnetic resonance spectroscopy, optimal acquisition parameters and fitting procedures are crucial. Using a large voxel size and short TE helps to increase the signal-to-noise-ratio and allows restriction to a measurement time of 12min. Using the comparison of healthy controls vs. patients affords modeling of the unknown downfield region to develop a robust fitting model. Low CRLB of around 0.004mM proved the good precision of the quantification results, yielding cohort values of  $0.019\pm 0.01\text{mM}$  in controls and  $0.142\pm 0.02\text{mM}$  in patients.

0375



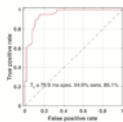
Myocardial Pi/PCr and pH during stress at 7T with STEAM  $^31\text{P}$  MRS in dilated cardiomyopathy; heart failure beyond the ejection fraction.

Andrew Apps<sup>1</sup>, Justin Lau<sup>1,2</sup>, Jane Ellis<sup>1</sup>, Mark Peterzan<sup>1</sup>, Moritz Hundertmark<sup>1</sup>, Damian Tyler<sup>3,4</sup>, Albrecht Ingo Schmid<sup>4,5</sup>, Stefan Neubauer<sup>6</sup>, Oliver Rider<sup>6</sup>, Ladislav Valkovic<sup>6,7</sup>, and Christopher T Rodgers<sup>8</sup>

<sup>1</sup>Cardiovascular Medicine, University of Oxford, Oxford, United Kingdom, <sup>2</sup>Physiology, Anatomy and Genetics, University of Oxford, Oxford, United Kingdom, <sup>3</sup>Physiology Anatomy and Genetics, University of Oxford, Oxford, United Kingdom, <sup>4</sup>Oxford Centre for Magnetic Resonance, University of Oxford, Oxford, United Kingdom, <sup>5</sup>Medical University of Vienna, Vienna, Austria, <sup>6</sup>Oxford Centre for Magnetic Resonance, University of Oxford, Oxford, United Kingdom, <sup>7</sup>Imaging Methods, Slovak Academy of Sciences, Bratislava, Slovakia, <sup>8</sup>Clinical Neurosciences, University of Cambridge, Cambridge, United Kingdom

The addition of Pi/PCr quantification adds value over PCr/ATP for the characterisation of myocardial energetics. In defining the chemical shift of the Pi resonance, pH can also be computed. Such measurements however are hampered in <sup>31</sup>P MRS due to the overlapping 2,3-DPG resonance. In harnessing the black blood contrast offered by STEAM, we successfully characterise Pi (and hence myocardial pH) in a cohort of patients with dilated cardiomyopathy. We go on to show that in these patients (but not controls) Pi/PCr rises significantly during dobutamine stress, a finding that would significantly impair the free energy of ATP hydrolysis during exertion.

0376



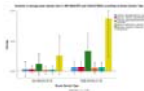
Fatty Acid Methylene T2 Can be Used to Separate Activatable Brown Adipose Tissue from Clavicular and Subcutaneous White Adipose Tissue in Humans

Ronald Ouwerkerk<sup>1</sup>, Jatin Raj Matta<sup>1</sup>, Ahmed Hamimi<sup>1</sup>, Aaron M Cypess<sup>2</sup>, Kong Y Chen<sup>3</sup>, and Ahmed Medhat Gharib<sup>1</sup>

<sup>1</sup>Biomedical and Metabolic Imaging Branch, NIDDK/NIH, Bethesda, MD, United States, <sup>2</sup>Translational Physiology Section, Diabetes, Endocrinology, and Obesity Branch, NIDDK/NIH, Bethesda, MD, United States, <sup>3</sup>Energy Metabolism Section, Diabetes, Endocrinology, and Obesity Branch, NIDDK/NIH, Bethesda, MD, United States

Localized <sup>1</sup>H-MRS was used to determine relaxation properties of fatty acid (FA) resonances in supraclavicular adipose tissue and distal white adipose tissue (WAT). Blinded to MRS results <sup>18</sup>F-FDG-PET was used to detect cold activated metabolism to identify active brown adipose tissue (BAT). Using the T2 of the FA methylene t a cutoff value of 76 ms this T2 can be used to distinguish BAT from distal or supraclavicular WAT with 85% sensitivity and 95% specificity

0377



In vivo 2D COSY reveals metabolic and lipid variations between low and high BI RADS density breasts in an average breast cancer risk cohort of 65 women

Natali Naude<sup>1,2,3</sup>, Gorane Santamaria<sup>1,2,3</sup>, Thomas Lloyd<sup>3</sup>, Ian Bennett<sup>3</sup>, Jeremy Khoo<sup>3</sup>, Peter Malycha<sup>1,3</sup>, and Carolyn Mountford<sup>1,2,3</sup>

<sup>1</sup>Translational Research Institute, Brisbane, Australia, <sup>2</sup>Queensland University of Technology, Brisbane, Australia, <sup>3</sup>Princess Alexandra Hospital, Brisbane, Australia

Breast density is a strong risk factor for breast cancer with a four to six fold increase for those in BI-RADS high density group versus low density group. The current study acquired MRI and MRS in 65 women at average lifetime risk of developing breast cancer, and found statistically significant differences in various MR-visible lipids and metabolites as well as cholesterol between low and high breast density groups. Results implicate that increased metabolic activity underlies increased mammographic breast density. 2D COSY offers a non-invasive window into breast tissue chemistry, without the use of gadolinium-based contrast media.

## Oral

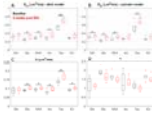
MRS: New Developments, Applications, & Fighting the Noise - MRS Applications

Monday Parallel 5 Live Q&A

Monday 15:15 - 16:00 UTC

Moderators: Nathalie Just & Gulim Oz



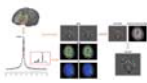


### Diffusion of brain metabolites highlights altered brain microstructure in chronic hepatic encephalopathy

Cristina Cudalbu<sup>1</sup>, Katarzyna Pierzchala<sup>1,2,3</sup>, Dunja Simicic<sup>1,2</sup>, Graham Knott<sup>4</sup>, Stephanie Clerc-Rosset<sup>4</sup>, Bernard Lanz<sup>2</sup>, and Ileana Jelescu<sup>1</sup>

<sup>1</sup>Centre d'Imagerie Biomedicale, École Polytechnique Fédérale de Lausanne, Lausanne, Switzerland, <sup>2</sup>Laboratory for functional and metabolic imaging, École Polytechnique Fédérale de Lausanne, Lausanne, Switzerland, <sup>3</sup>Service of Clinical Chemistry, University of Lausanne and University Hospital of Lausanne, Lausanne, Switzerland, <sup>4</sup>Biological Electron Microscopy Facility, École Polytechnique Fédérale de Lausanne, Lausanne, Switzerland

In chronic hepatic encephalopathy (HE), high ammonium delivery to the brain is causing the accumulation of glutamine (Gln) and gradual release of other osmolytes. We aimed to follow the longitudinal evolution of brain Gln and other metabolite properties in chronic-HE using diffusion-weighted spectroscopy (DW-MRS) and evaluate the potential changes in diffusion behavior which might provide information on Gln localization and potential microstructural alterations during chronic-HE. Increased diffusivity and reduced kurtosis in BDL rats, showcased by DW-MRS analysis, are fully consistent with a less complex microstructure and swollen soma as highlighted by fluorescence and electron microscopy leading to increased molecule mobility.

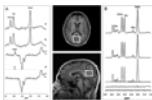


### Simultaneous High-Resolution 3D MRSI and Oxygen Extraction Fraction Mapping in Acute Stroke Using SPICE

Tianxiao Zhang<sup>1</sup>, Tianyao Wang<sup>2</sup>, Zengping Lin<sup>1</sup>, Rong Guo<sup>3,4</sup>, Yudu Li<sup>3,4</sup>, Yibo Zhao<sup>3,4</sup>, Ziyu Meng<sup>1,3</sup>, Jun Liu<sup>2</sup>, Danhong Wu<sup>5</sup>, Zheng Jin<sup>6</sup>, Xin Yu<sup>7</sup>, Zhi-Pei Liang<sup>3,4</sup>, and Yao Li<sup>1</sup>

<sup>1</sup>Institute for Medical Imaging Technology, School of Biomedical Engineering, Shanghai Jiao Tong University, Shanghai, China, <sup>2</sup>Radiology Department, The Fifth People's Hospital of Shanghai, Fudan University, Shanghai, China, <sup>3</sup>Beckman Institute for Advanced Science and Technology, University of Illinois at Urbana-Champaign, Urbana, IL, United States, <sup>4</sup>Department of Electrical and Computer Engineering, University of Illinois at Urbana-Champaign, Urbana, IL, United States, <sup>5</sup>Neurology Department, The Fifth People's Hospital of Shanghai, Fudan University, Shanghai, China, <sup>6</sup>Shanghai Minhang Hospital of Integrated Traditional Chinese and Western Medicine Hospital, Shanghai, China, <sup>7</sup>Department of Biomedical Engineering, Case Western Reserve University, Cleveland, OH, United States

Mapping the concurrent changes in oxygen extraction fraction (OEF) and neurometabolic markers could provide a powerful tool for evaluation of brain tissue viability after stroke. In this work, we investigated the feasibility of fast simultaneous 3D brain OEF and neurometabolic imaging noninvasively in acute ischemic stroke using SPICE. We achieved concurrent mapping of OEF (1.2×1.2×1.2 mm<sup>3</sup> nominal resolution) and MRSI (2.0×3.0×3.0 mm<sup>3</sup> nominal resolution) within a 7-minute scan. Our experimental results demonstrated the feasibility of mapping OEF and neurometabolic alterations in acute stroke.



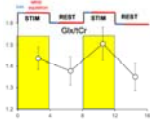
### Documentation of Anti-glutamatergic Effect of N-Acetylcysteine Treatment with 1H MRS Monitoring of Cortical Glutathione and Glutamate In Vivo

Dikoma C. Shungu<sup>1</sup>, Xiangling Mao<sup>1</sup>, Michelle Blate<sup>2</sup>, Diana Vu<sup>2</sup>, Guoxin Kang<sup>1</sup>, Halinder S. Mangat<sup>3</sup>, Claire Henchcliffe<sup>3</sup>, Benjamin Natelson<sup>2</sup>, and Nora Weiduschat<sup>1</sup>

<sup>1</sup>Radiology, Weill Cornell Medicine, New York, NY, United States, <sup>2</sup>Icahn School of Medicine at Mount Sinai, New York, NY, United States, <sup>3</sup>Neurology, Weill Cornell Medicine, New York, NY, United States

N-acetylcysteine (NAC), a glutathione (GSH) synthesis precursor, is thought to have anti-glutamatergic properties for which direct *in vivo* evidence is lacking. In this study, the postulated anti-glutamatergic properties of NAC were investigated by using <sup>1</sup>H MRS to monitor changes in brain levels of both GSH and glutamate (Glu) in response to 4 weeks of NAC supplementation in patients with chronic fatigue syndrome (CFS) and healthy volunteers (HV). Following NAC treatment, GSH levels increased significantly in CFS and numerically in HV, while Glu decreased significantly in both groups compared to baseline – a finding that supports NAC as an anti-glutamatergic agent.

0381



### Functional spectroscopic imaging (fMRSI) detects metabolite changes in the activated primary sensorimotor cortex at 7T

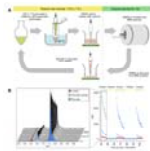
Petr Bednarik<sup>1</sup>, Lukas Hingerl<sup>1</sup>, Dario Goranovic<sup>1</sup>, Alena Svatkova<sup>1</sup>, Pedro de Lima Cardoso<sup>1</sup>, Siegfried Trattnig<sup>1</sup>, Rupert Lanzenberger<sup>2</sup>, and Wolfgang Bogner<sup>1</sup>

<sup>1</sup>Department of Medical Imaging and Image-guided Therapy, Medical University of Vienna, Vienna, Austria,

<sup>2</sup>Department of Psychiatry and Psychotherapy, Medical University of Vienna, Vienna, Austria

Functional single-voxel MRS (fMRS) was capable to sensitively detect metabolite responses to sensory stimulation, but suffered from large partial volume effects, that questioned the clinical utility of fMRS. Free-induction decay (FID)-MRSI promises to possess sufficient SNR to reach the sensitivity of SV-MRS and overcome its limitations by selective mapping the volume of interest with multiple voxels and thus, with higher spatial resolution, minimize the partial volume issue. Concentric-ring-trajectories (CRT)-based 3D FID-MRSI showed sufficient sensitivity and temporal stability to detect functional glutamate changes in the dominant sensorimotor region with expected most robust metabolite responses during finger tapping task.

0382



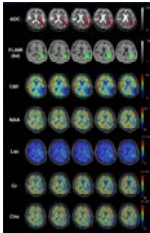
### Multi-sample measurement of pyruvate/lactate flux in melanoma cells using an HP micromagnetic resonance spectrometer and D2O solvation

Hannah J. Lees<sup>1</sup>, Micaela Millan<sup>1</sup>, Fayyaz Ahamed<sup>2</sup>, Roozbeh Eskandari<sup>1</sup>, Kristin L. Granlund<sup>1</sup>, Sangmoo Jeong<sup>1</sup>, and Kayvan R. Keshari<sup>1</sup>

<sup>1</sup>Memorial Sloan Kettering Cancer Center, NEW YORK, NY, United States, <sup>2</sup>University of California, Berkeley, Berkeley, CA, United States

The pyruvate-lactate flux,  $k_{PL}$ , shows promise as a biomarker of cancer presence and aggressiveness, and assessment of  $k_{PL}$  in patient-derived cells may be a useful tool to assess treatment response for advanced personalized medicine. Here we present a novel experimental protocol for the real-time measurement of pyruvate-lactate metabolic flux in multiple mass-limited cell suspension samples using a single dissolution, thereby increasing efficiency and providing greater control of the methodological variability associated with HP experiments. We then applied this protocol to the measurement of pyruvate-lactate flux in melanoma cells for the assessment of treatment response to BRAF inhibition.

0383



### Penumbra Identification in Acute Stroke Using Fast 3D 1H-MRSI

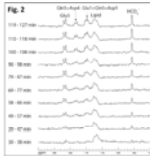
Yao Li<sup>1</sup>, Zengping Lin<sup>1</sup>, Tianyao Wang<sup>2</sup>, Tianxiao Zhang<sup>1</sup>, Rong Guo<sup>3,4</sup>, Yudu Li<sup>3,4</sup>, Yibo Zhao<sup>3,4</sup>, Ziyu Meng<sup>1,3</sup>, Jun Liu<sup>2</sup>, Xin Yu<sup>5</sup>, and Zhi-Pei Liang<sup>3,4</sup>

<sup>1</sup>Institute for Medical Imaging Technology, School of Biomedical Engineering, Shanghai Jiao Tong University, Shanghai, China, <sup>2</sup>Radiology Department, The Fifth People's Hospital of Shanghai, Fudan University, Shanghai, China, <sup>3</sup>Beckman Institute for Advanced Science and Technology, University of Illinois at Urbana-Champaign, Urbana, IL, United States, <sup>4</sup>Department of Electrical and Computer Engineering, University of Illinois at Urbana-Champaign, Urbana, IL, United States, <sup>5</sup>Department of Biomedical Engineering, Case Western Reserve University, Cleveland, OH, United States

Impaired metabolism was a key factor in the definition of ischemic penumbra. <sup>1</sup>H-MRSI has been recognized as a potentially powerful tool for metabolic imaging of stroke. In this proof of concept clinical study, we explored the potential of fast 3D high-resolution <sup>1</sup>H-MRSI to investigate brain neurometabolic changes at tissue-level in acute stroke. In a 6-min scan, we obtained N-acetylaspartate (NAA) and lactate (Lac) maps simultaneously. Our experimental results showed different NAA and Lac concentrations between hypoperfused tissue recruited to final infarct and that survived, indicating an improved delineation of penumbra by incorporating the tissue neuronal damage and acidosis information.

0384

Detection of Carbonic Anhydrase Activity in the Frontal Lobe of Human Brain

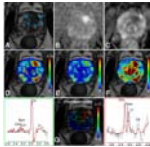


Shizhe Li<sup>1</sup>, Li An<sup>1</sup>, Christopher Johnson<sup>1</sup>, Maria Ferraris-Araneta<sup>1</sup>, Milalynn Victorino<sup>1</sup>, Jyoti Tomar<sup>1</sup>, and Jun Shen<sup>1</sup>

<sup>1</sup>National Institutes of Health, Bethesda, MD, United States

This study demonstrates the feasibility of detecting carbonic anhydrase activity in the frontal lobe of the human brain. Upon saturation of carbon dioxide, a very large magnetization transfer effect catalyzed by carbonic anhydrase was measured in the frontal lobe of healthy human subjects using <sup>13</sup>C MRS with oral administration of [U-<sup>13</sup>C<sub>6</sub>]glucose. The results showed that it is feasible to examine carbonic anhydrase activity using magnetization transfer <sup>13</sup>C MRS in the frontal cortex—where structural lesions, disturbed function, and morphology are strongly associated with many psychiatric symptoms.

0385



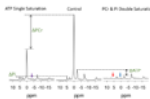
MRSI of the prostate revisited: The potential role of GOIA-sLASER in multiparametric MRI of central gland prostate cancer

Neda Gholizadeh<sup>1</sup>, Peter B Greer<sup>2,3</sup>, John Simpson<sup>2,3</sup>, Jonathan Goodwin<sup>2,3</sup>, Peter Lau<sup>4,5</sup>, Arend Heerschap<sup>6</sup>, and Saadallah Ramadan<sup>1,5</sup>

<sup>1</sup>Health Science, The University of Newcastle, Newcastle, Australia, <sup>2</sup>Radiation Oncology, Calvary Mater Newcastle, Newcastle, Australia, <sup>3</sup>Physics and mathematics, The University of Newcastle, Newcastle, Australia, <sup>4</sup>Radiology, Calvary Mater Newcastle, Newcastle, Australia, <sup>5</sup>Imaging Centre, Hunter Medical Research Institute (HMRI), Newcastle, Australia, <sup>6</sup>Radiology and Nuclear Medicine, Radboud University Medical Center, Nijmegen, Nijmegen, Netherlands

Due to histological heterogeneity of the central gland, accurate detection of central gland prostate cancer remains a challenge. A reliable and non-invasive imaging technique could increase the sensitivity and specificity for identification of central gland lesions missed by PI-RADS V2 or biopsies. This study evaluates the diagnostic performance of individual and combined parameters of an mp-MRI exam, employed for PI-RADS evaluations (T2WI, DWI, DCE) and advanced GOIA-sLASER MRSI using an external phased-array coil for central gland prostate cancer detection, localization and grading. The results demonstrate that MRSI using GOIA-sLASER considerably improves central gland prostate cancer detection and localization.

0386



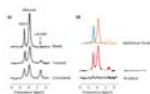
Phosphate Metabolite T1 Relaxation Times, ATP Hydrolysis Flux and Creatine Kinase Reaction Kinetics in the Human Skeletal Muscle.

Adil Bashir<sup>1</sup>, Jianyi Zhang<sup>2</sup>, and Thomas S Denney<sup>1</sup>

<sup>1</sup>Electrical and Computer Engineering, Auburn University, Auburn, AL, United States, <sup>2</sup>Biomedical Engineering, The University of Alabama at Birmingham, Birmingham, AL, United States

Long TR and low concentration makes the quantification of inorganic phosphate (Pi) difficult in <sup>31</sup>P magnetization saturation transfer experiments. An indirect method to measure Adenosine Triphosphate (ATP) turnover was demonstrated in animal studies, which does not require quantification of Pi. We demonstrate the application and validation of this technique in human studies. We measured the fluxes of ATP production and hydrolysis reactions using the indirect approach and validated the results against direct measurements. We also report the intrinsic T1 of Phosphocreatine, ATP and Pi in skeletal muscle at 7T. This will facilitate future studies of impaired bioenergetics in vivo.

0387



Deuterium (<sup>2</sup>H) magnetic resonance spectroscopy for monitoring chemotherapeutic response in vitro

Josephine L Tan<sup>1,2</sup>, Daniel Djayakarsana<sup>1,2</sup>, Rachel W Chan<sup>2</sup>, Colleen Bailey<sup>1,2</sup>, and Angus Z Lau<sup>1,2</sup>

<sup>1</sup>Medical Biophysics, University of Toronto, Toronto, ON, Canada, <sup>2</sup>Physical Sciences, Sunnybrook Research Institute, Toronto, ON, Canada

Deuterium ( $^2\text{H}$ ) magnetic resonance spectroscopy (MRS) is a novel metabolic imaging method that can measure aberrant glucose metabolism in cancer. In this abstract, we use  $^2\text{H}$  MRS to measure metabolic changes in acute myeloid leukemia (AML) cells after treatment with cisplatin. We show that this method is sensitive to differences in lactate levels, produced via glycolysis of deuterium-enriched glucose at 7T. These studies demonstrate the potential of  $^2\text{H}$  MRS to monitor chemotherapeutic response.

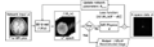
**Oral**  
**MRS: New Developments, Applications, & Fighting the Noise - MRS: Deep Learning & Denoising**

Monday Parallel 5 Live Q&A

Monday 15:15 - 16:00 UTC

Moderators: Wolfgang Bogner & Candace  
Fleischer

0388

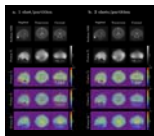


**High Resolution MR Spectroscopic Imaging Using Deep Image Prior Constrained Subspace Modeling**  
Kuang Gong<sup>1</sup>, Paul Kyu Han<sup>1</sup>, Thibault Marin<sup>1</sup>, Georges El Fakhri<sup>1</sup>, Quanzheng Li<sup>1</sup>, and Chao Ma<sup>1</sup>

<sup>1</sup>*Gordon Center for Medical Imaging, Department of Radiology, Massachusetts General Hospital, Harvard Medical School, Boston, MA, United States*

The subspace-based method, known as SPICE, is an emerging technique that achieves rapid high-resolution MRSI with good SNR. In SPICE, the spectrum at each voxel is represented as a low-dimensional subspace or manifold, where the basis functions or features are learned from training data. The spatial coefficients of the subspace model are estimated by fitting the model to the k-space data for image reconstruction. In this work, we propose to extend the SPICE framework by representing the spatial coefficients of the subspace model using deep image prior for improved image reconstruction.

0389



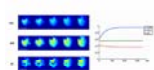
**Simultaneous 3D proton MRF and sodium MRI**

Zidan Yu<sup>1,2,3</sup>, Shota Hodono<sup>1,2,3</sup>, Bili Wang<sup>1</sup>, Olga Dergahyova<sup>1</sup>, Bei Zhang<sup>1,3</sup>, Ryan Brown<sup>1,3</sup>, Daniel K. Sodickson<sup>1,2,3</sup>, Guillaume Madelin<sup>1,2</sup>, and Martijn A. Cloos<sup>1,2,3</sup>

<sup>1</sup>*Center for Biomedical Imaging, Department of Radiology, New York University School of Medicine, New York, NY, United States*, <sup>2</sup>*Sackler Institute of Graduate Biomedical Sciences, NYU Langone Health, New York, NY, United States*, <sup>3</sup>*Center for Advanced Imaging Innovation and Research (CAI2R), NYU Langone Health, New York, NY, United States*

In this work, we present a 3D sequence that can simultaneously capture quantitative  $^1\text{H}$  density,  $T_1$ ,  $T_2$ ,  $B_1^+$  maps and a  $^{23}\text{Na}$  image of the whole head in a reasonable scan time (~10 min). The gradient momenta are strategically distributed to simultaneously acquire a full-radial trajectory for proton and a center-out radial trajectory for sodium in one single readout. A sodium SNR comparison, verification of the proton multi-parametric maps, and in-vivo results are shown.

0390



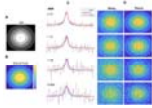
**High-Resolution Dynamic  $^{31}\text{P}$ -MRSI of Ischemia-Reperfusion in Rat Using Low-Rank Tensor Model with Deep Learning Priors**

Yudu Li<sup>1,2</sup>, Kihwan Kim<sup>3,4</sup>, Bryan Clifford<sup>1,2</sup>, Rong Guo<sup>1,2</sup>, Yuning Gu<sup>3,4</sup>, Zhi-Pei Liang<sup>1,2</sup>, and Xin Yu<sup>3,4,5,6</sup>

<sup>1</sup>*Department of Electrical and Computer Engineering, University of Illinois at Urbana-Champaign, Urbana, IL, United States*, <sup>2</sup>*Beckman Institute for Advanced Science and Technology, University of Illinois at Urbana-Champaign, Urbana, IL, United States*, <sup>3</sup>*Department of Biomedical Engineering, Case Western Reserve University, Cleveland, OH, United States*, <sup>4</sup>*Case Center for Imaging Research, Case Western Reserve University, Cleveland, OH, United States*, <sup>5</sup>*Department of Radiology, Case Western Reserve University, Cleveland, OH, United States*, <sup>6</sup>*Department of Physiology and Biophysics, Case Western Reserve University, Cleveland, OH, United States*

Dynamic  $^{31}\text{P}$ -MRS/MRSI is a promising tool for in vivo quantification of mitochondrial oxidative capacity. However, its practical utility is limited by the inherently low SNR of the  $^{31}\text{P}$  signal. This work is built upon our recent progress in accelerating dynamic  $^{31}\text{P}$ -MRSI using low-rank tensor models. We extended this method by learning the temporal priors with deep generative models and then incorporating them into the reconstruction via an information theoretical framework. This approach enabled high-resolution dynamic  $^{31}\text{P}$ -MRSI with  $1.5 \times 1.5 \times 2 \text{ mm}^3$  nominal spatial resolution and 5.1-sec temporal resolution in capturing the kinetics of metabolite changes in rat hindlimb during a stimulation-recovery protocol.

0391



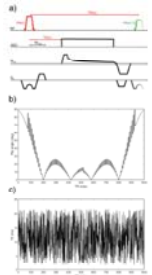
### A Deep Learning Method for Sensitivity Enhancement in Deuterium Metabolic Imaging (DMI)

Siyuan Dong<sup>1</sup>, Henk M. De Feyter<sup>2</sup>, Monique A. Thomas<sup>2</sup>, Robin A. de Graaf<sup>3</sup>, and James S. Duncan<sup>4</sup>

<sup>1</sup>Department of Electrical Engineering, Yale University, New Haven, CT, United States, <sup>2</sup>Department of Radiology and Biomedical Imaging, Yale University, School of Medicine, New Haven, CT, United States, <sup>3</sup>Department of Radiology and Biomedical Imaging, Department of Biomedical Engineering, Yale University, School of Medicine, New Haven, CT, United States, <sup>4</sup>Department of Radiology & Biomedical Imaging, Department of Electrical Engineering, Department of Statistics & Data Science, Yale University, New Haven, CT, United States

Deuterium Metabolic Imaging (DMI) is a novel approach providing 3D metabolic data from both animal models and human subjects. DMI relies on  $^2\text{H}$  MRSI in combination with administration of  $^2\text{H}$ -labeled substrates. Common to all MRI and MRSI methods, DMI's resolution is ultimately limited by the achievable SNR. This work proposes a data-driven method using a deep convolutional autoencoder to improve the SNR and increase the spatial resolution of DMI. The method was tested with simulated, phantom and in vivo experiments at various SNR levels to demonstrate its capability and precision for metabolic mapping using noisy DMI data.

0392



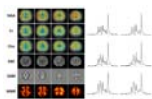
### Sodium Relaxometry using Magnetic Resonance Fingerprinting

Fabian J. Kratzer<sup>1,2</sup>, Sebastian Schmitter<sup>1,3</sup>, Armin M. Nagel<sup>1,4,5</sup>, Nicolas G. R. Behl<sup>6</sup>, Benjamin R. Knowles<sup>1</sup>, Peter Bachert<sup>1,2</sup>, Mark E. Ladd<sup>1,2,7</sup>, and Sebastian Flassbeck<sup>1</sup>

<sup>1</sup>Medical Physics in Radiology, German Cancer Research Center (DKFZ), Heidelberg, Germany, <sup>2</sup>Faculty of Physics and Astronomy, Ruprecht-Karls University Heidelberg, Heidelberg, Germany, <sup>3</sup>Physikalisch-Technische Bundesanstalt (PTB), Braunschweig and Berlin, Germany, <sup>4</sup>Institute of Radiology, University Hospital Erlangen, Friedrich-Alexander-Universität Erlangen-Nürnberg (FAU), Erlangen, Germany, <sup>5</sup>Institute of Medical Physics, Friedrich-Alexander-Universität (FAU), Erlangen, Germany, <sup>6</sup>Siemens Healthcare GmbH, Erlangen, Germany, <sup>7</sup>Faculty of Medicine, Ruprecht-Karls University Heidelberg, Heidelberg, Germany

Sodium relaxation times have been shown to be altered in several diseases. However, due to short relaxation times and low in-vivo signal, measurement times in sodium relaxometry on the order of 1h were reported for both, longitudinal and transversal relaxation constants. In this work, a novel sodium relaxometry method based on Magnetic Resonance Fingerprinting (MRF) principles is presented, which enables simultaneous quantification of  $T_1$ ,  $T_{2s}^*$ ,  $T_{2l}^*$ ,  $T_2^*$  and  $\Delta B_0$ , with automatic distinction between bi- and monoexponential transverse relaxation.

0393



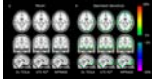
### Making SPICE Spicier with Sparse Sampling of (k, t)-Space and Learned Subspaces

Rong Guo<sup>1,2</sup>, Yudu Li<sup>1,2</sup>, Yibo Zhao<sup>1,2</sup>, Yao Li<sup>3,4</sup>, and Zhi-Pei Liang<sup>1,2</sup>

<sup>1</sup>Department of Electrical and Computer Engineering, University of Illinois at Urbana-Champaign, Urbana, IL, United States, <sup>2</sup>Beckman Institute for Advanced Science and Technology, University of Illinois at Urbana-Champaign, Urbana, IL, United States, <sup>3</sup>School of Biomedical Engineering, Shanghai Jiao Tong University, Shanghai, China, <sup>4</sup>Med-X Research Institute, Shanghai Jiao Tong University, Shanghai, China

SPICE has recently provided a unique capability for simultaneous acquisition of metabolite and water spectroscopic signals. While the water signals are often removed as nuisance components in traditional MRSI experiments, SPICE utilizes the water signals for QSM, MWF mapping, etc. In this work, we further extend SPICE data acquisition to achieve much larger k-space coverage and improve its processing scheme for simultaneous MRSI/QSM/SWI/MWF mapping. In vivo experiments demonstrated that this new scheme improved the accuracy of water/lipid removal, reduced the effects of field inhomogeneity, and achieved higher resolution for QSM, SWI and MWF using the unsuppressed water signals.

0394



Deep learning based T1-enhanced selection of linear attenuation coefficients for PET/MR attenuation correction: accuracy and repeatability

Chunwei Ying<sup>1</sup>, Yasheng Chen<sup>2</sup>, Michael M. Binkley<sup>2</sup>, Meher R. Juttukonda<sup>3,4</sup>, Shaney Flores<sup>1</sup>, Tammie L. S. Benzinger<sup>1,5</sup>, and Hongyu An<sup>1</sup>

<sup>1</sup>Mallinckrodt Institute of Radiology, Washington University School of Medicine, St. Louis, MO, United States,

<sup>2</sup>Department of Neurology, Washington University School of Medicine, St. Louis, MO, United States,

<sup>3</sup>Athinoula A. Martinos Center for Biomedical Imaging, Massachusetts General Hospital, Charlestown, MA,

United States, <sup>4</sup>Department of Radiology, Harvard Medical School, Boston, MA, United States, <sup>5</sup>Department

of Neurological Surgery, Washington University School of Medicine, St. Louis, MO, United States

We proposed a 3D patch based residual U-Net method to estimate pseudo CT images for PET/MR attenuation correction by including quantitative R1 maps as input. The proposed deep learning based T1-enhanced selection of linear attenuation coefficients (DL-TESLA) method outperformed the deep learning methods using UTE-R2\* or MPRAGE as inputs with a similar network structure. Moreover, we demonstrated that DL-TESLA had an excellent PET test-retest repeatability that was comparable to PET/CT, supporting its use for PET/MR AC in longitudinal studies of neurodegenerative diseases.

0395



MP-PCA denoising dramatically improves SNR in large-sized MRS data: an illustration in diffusion-weighted MRS

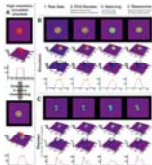
Ileana Ozana Jelescu<sup>1</sup>, Jelle Veraart<sup>2</sup>, and Cristina Cudalbu<sup>1</sup>

<sup>1</sup>Center for Biomedical Imaging, Ecole Polytechnique Fédérale de Lausanne, Lausanne, Switzerland, <sup>2</sup>Dept.

of Radiology, New York University School of Medicine, New York, NY, United States

MRS is an inherently low signal-to-noise technique resulting in substantial spectral averaging and large voxel volumes. The problem is further amplified for diffusion-weighted MRS. Here we test the performance of denoising using principal component analysis coupled with Marchenko-Pastur's random matrix theory in the context of DW-MRS. We report 50 – 100% increase in SNR, reduction in Cramer-Rao bounds and a potential eight-fold reduction in scan time. This technique is expected to also bring significant improvements in the context of fMRS, X-nuclei MRS and CSI.

0396



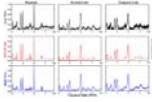
Processing of muscle phosphorus 7T CSI data using PCA denoising and deconvolution

Martijn Froeling<sup>1</sup>, Tijl A van der Velden<sup>1</sup>, Jeanine J Prompers<sup>1</sup>, and Dennis WJ Klomp<sup>1</sup>

<sup>1</sup>Department of Radiology, UMC Utrecht, Utrecht, Netherlands

Chemical shift imaging generally suffers from low SNR and low spatial resolution, especially for x-nuclei. State of the art image processing methods from the MRI domain, e.g. DTI pre-processing, can be applied to CSI data. In this study we show the feasibility of PCA denoising combined with deconvolution to enhance CSI SNR and spatial localization.

Spectral Wavelet-feature Analysis and Classification Assisted Denoising Approach for Enhancing Signal to Noise Ratios of MRS Data



Bing Ji<sup>1</sup>, Zahra Hosseini<sup>2</sup>, Liya Wang<sup>3</sup>, Lei Zhou<sup>4</sup>, Xinhua Tu<sup>5</sup>, and Hui Mao<sup>6</sup>

<sup>1</sup>Department of Radiology and Imaging Sciences, Emory University School of Medicine, Emory University, Atlanta, GA, Georgia, <sup>2</sup>MR R&D Collaborations, Siemens Healthineers, Atlanta, Georgia, <sup>3</sup>Department of Radiology, The People's Hospital of Longhua, Shenzhen, China, <sup>4</sup>Department of Radiology and Imaging Sciences, Emory University School of Medicine, Emory University, Atlanta, Georgia, <sup>5</sup>School of Communication and Information Engineering, Nanjing University of Posts and Telecommunication, Nanjing, China, <sup>6</sup>Department of Radiology and Imaging Sciences, Emory University School of Medicine, Emory University, Atlanta, GA, United States

Low signal-to-noise ratio (SNR) and long acquisition time limit the clinical applications of magnetic resonance spectroscopy (MRS). This work presents a data-driven machine-learning assisted Spectral Wavelet-feature Analysis and Classification Assisted Denoising (SWANCAD) approach to extract the specific spectral wavelets of signals and noises for reducing noise and improving SNR of MRS data. The effective denoise by SWANCAD enabled resolving prominent metabolic peaks but also identify the smaller concentration metabolites which are merged in the noises. Potential applications of the SWANCAD includes the possibility of improving the signal to noise ratio (SNR) of MRS data collected in sub-minute or sub-cm voxels.

## Corporate Symposium

### Gold Corporate Symposium: Siemens Healthineers

Plenary Hall (Grand Ballroom) Monday 19:30 - 20:30 UTC

Tuesday, 11 August 2020

## Corporate Symposium

### Bronze Corporate Evening Symposium: Hitachi, Ltd. Healthcare Business Unit

Room C3.3 Tuesday 1:00 - 3:00 UTC

## Plenary Session

### Plenary Session Tuesday - NIBIB New Horizons Lecture: MR Platforms for an Information Age

Tuesday Plenary Tuesday 12:00 - 13:30 UTC

## Plenary Session

### Plenary Session Tuesday - Translating to Translate: Fostering Collaborations Between Basic & Clinician Scientists

Organizers: Vikas Gulani, Tim Leiner, Christoph Juchem

Tuesday Plenary Tuesday 12:00 - 13:30 UTC

Moderators: Tim Leiner & Vikas Gulani

#### Value of Translation

Thomas Grist<sup>1</sup>

<sup>1</sup>University of Wisconsin - Madison, United States

#### Learning Each Other's Language

Laura Schreiber<sup>1</sup>

<sup>1</sup>Comprehensive Heart Failure Center, Germany

#### Aligning the Incentives

Garry Gold<sup>1</sup>

<sup>1</sup>Stanford University, United States

---

---

### Sunrise Session

#### Educational Q&A: fMRI/Diffusion/Perfusion Sunrise - Hemodynamic Modelling of fMRI Time Signals

Organizers: Susan Francis, Richard Buxton, Benedikt Poser

Tuesday Parallel 1 Live Q&A

Tuesday 13:45 - 14:30 UTC

Moderators: Richard Buxton

[Biophysical Modelling to Deconvolve Neurovascular Signals](#)

Jingyuan Chen

---

---

### Sunrise Session

#### Educational Q&A: fMRI/Diffusion/Perfusion Sunrise - Modelling ASL Perfusion Signals

Organizers: Benedikt Poser, Susan Francis, Richard Buxton, Xin Yu

Tuesday Parallel 1 Live Q&A

Tuesday 13:45 - 14:30 UTC

Moderators: Susan Francis

[Kinetic Modelling of ASL](#)

Patricia Figueiredo

---

---

[Hands-On Perfusion Modelling](#)

Michael Chappell

---

---

### Sunrise Session

#### Educational Q&A: fMRI/Diffusion/Perfusion Sunrise - Simulation of Diffusion

Organizers: Dmitry Novikov, Carl-Fredrik Westin

Tuesday Parallel 1 Live Q&A

Tuesday 13:45 - 14:30 UTC

[How to Set Up Monte Carlo Simulations of Diffusion](#)

Hong-Hsi Lee

---

---

[Using Simulations to Validate Models](#)

Marco Palombo

---

---

### Sunrise Session

#### Educational Q&A: fMRI/Diffusion/Perfusion Sunrise - Microstructure: Non-Diffusion

Organizers: Jongho Lee, Masaaki Hori

Tuesday Parallel 1 Live Q&A

Tuesday 13:45 - 14:30 UTC

[Myelin Water Imaging: Multiple Compartmental Model](#)

Irene Vavasour

---

---

[Magnetic Susceptibility Imaging: White Matter Fiber Model](#)

Daeun Kim

---

---



## Weekday Course

### Thoracic/Lung MRI - Lung MRI: Getting Started

Organizers: Mustafa Shadi Bashir, Vikas Gulani

Tuesday Parallel 3 Live Q&A

Tuesday 13:45 - 14:30 UTC

Moderators: Geoff Parker

#### Xenon Lung MRI

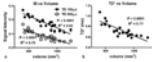
Talissa Altes<sup>1</sup>

<sup>1</sup>University of Missouri Health System, United States

#### Proton Lung MRI

Susan Hopkins<sup>1</sup>

<sup>1</sup>UCSD, San Diego, CA, United States



#### UTE & Other Techniques for Lung MRI

Masaya Takahashi<sup>1</sup>

<sup>1</sup>Guerbet Japan, Japan

Purpose: Pulmonary function tests (PFTs) are global measurements where contributions from regions of normal and varying degrees of alteration in function are combined. Non-uniform disruption of lung architecture is usually assessed by high-resolution computed tomography (CT), which incurs radiation exposure and yields only static anatomical data. Our purpose was to evaluate and define the applications of functional thoracic MRI to bridge anatomical and functional assessment of the lung in regional parenchymal diseases.

## Oral

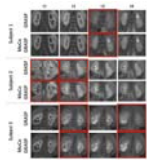
### Managing Motion and Artifacts - Keep Still: Managing Motion in the Body

Tuesday Parallel 4 Live Q&A

Tuesday 13:45 - 14:30 UTC

Moderators: Claudia Prieto & Daniel Staeb

0452

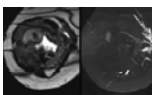


#### Bulk Motion Compensated Image Reconstruction for Renal Function Estimation with DCE-MRI

Jaume Coll-Font<sup>1,2</sup>, Onur Afacan<sup>1,2</sup>, Alto Stemmer<sup>3</sup>, Richard S. Lee<sup>2,4</sup>, Jeanne Chow<sup>1,2</sup>, Simon Warfield<sup>1,2</sup>, and Sila Kurugol<sup>1,2</sup>

<sup>1</sup>Radiology, Boston Children's Hospital, Boston, MA, United States, <sup>2</sup>Harvard Medical School, Boston, MA, United States, <sup>3</sup>Siemens Healthcare GmbH, Erlangen, Germany, <sup>4</sup>Urology, Boston Children's Hospital, Boston, MA, United States

Dynamic Radial VIBE (DRV) DCE-MRI can provide high spatio-temporal resolution in the dynamic series of volumes used to evaluate the kidney function. However, bulk motion during the scan corrupts the volumes and deteriorates the quality of the kidney function estimation. We introduce a bulk-motion robust image reconstruction technique to mitigate the effects of motion. Our algorithm detects corrupted k-space data, reconstructs the volumes without signal dropout and aligns them. We applied this approach on non-sedated babies undergoing feed-and-wrap DCE-MRI with DRV. Our results show that our method improves the image quality and the estimation of the kidney function parameters.



#### Motion corrected reconstruction of abdominal SWEEP data using local similarity graphs and deformable slice to volume registration

Laurence H Jackson<sup>1</sup>, Alena Uus<sup>1</sup>, Dafnis Batalle<sup>2,3</sup>, Jana M Hutter<sup>1</sup>, Thomas A Roberts<sup>1</sup>, Anthony N Price<sup>1</sup>, Alison Ho<sup>2,4</sup>, Laura McCabe<sup>2</sup>, Maria Deprez<sup>1</sup>, Lucy Chappell<sup>4</sup>, Mary Rutherford<sup>2</sup>, and Joseph V Hajnal<sup>1,2</sup>

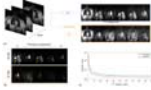
0453



<sup>1</sup>Biomedical Engineering, School of Biomedical Engineering & Imaging Sciences, Kings College London, London, United Kingdom, <sup>2</sup>Centre for the Developing Brain, School of Biomedical Engineering & Imaging Sciences, Kings College London, London, United Kingdom, <sup>3</sup>Department of Forensic and Neurodevelopmental Science, Institute of Psychiatry, Psychology & Neuroscience, Kings College London, London, United Kingdom, <sup>4</sup>Department of Women and Children's Health, School of Life Course Sciences, Kings College London, London, United Kingdom

In this work we introduce a novel pipeline for motion correction of SWEEP style acquisition data. The method utilizes local similarity graphs for efficient generation of static volumes by extracting the most coherent slices within a local neighborhood and interpolating over missing data. These static volumes are then used as registration targets for a patch-based deformable slice-to-volume registration. The pipeline produces highly coherent 3D volumes and is demonstrated in adult abdominal and fetal/placental imaging using 2D SWEEP bSSFP and SPGR acquisitions.

0454



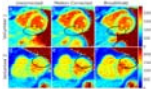
Motion Compensated Low-Rank (MoCoLoR) constrained reconstruction with application to motion resolved lung MRI

Xucheng Zhu<sup>1,2</sup>, Frank Ong<sup>3</sup>, Michael Lustig<sup>4</sup>, and Peder Larson<sup>1,2</sup>

<sup>1</sup>Radiology and Biomedical Imaging, University of California, San Francisco, San Francisco, CA, United States, <sup>2</sup>UC Berkeley-UCSF Graduate Program in Bioengineering, University of California, San Francisco and University of California, Berkeley, Berkeley, CA, United States, <sup>3</sup>Electrical Engineering, Stanford University, Stanford, CA, United States, <sup>4</sup>Electrical Engineering and Computer Sciences, University of California, Berkeley, Berkeley, CA, United States

Respiratory motion is one of the most challenging problems in thoracic and abdominal MRI. Motion resolved reconstruction is introduced to reduce the respiratory motion effects by grouping the data to different motion states, then using compressed sensing techniques to reconstruct different motion states images. Spatio-temporal low-rank constrained reconstruction is one of the widely used techniques. In this work, we proposed a new method incorporating motion compensation into the low-rank model, called MoCoLoR. The proposed method is applied to high resolution free breathing lung MRI, and the results show that MoCoLoR outperforms the standard low-rank constrained reconstruction.

0455



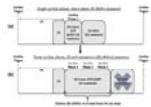
Pilot tone-based respiratory motion correction for 2D myocardial T1 mapping

Juliane Ludwig<sup>1</sup>, Kirsten Miriam Kerkering<sup>1</sup>, Peter Speier<sup>2</sup>, Frank Seifert<sup>1</sup>, Tobias Schaeffter<sup>1,3,4</sup>, and Christoph Kolbitsch<sup>1,3</sup>

<sup>1</sup>Physikalisch-Technische Bundesanstalt (PTB), Braunschweig and Berlin, Germany, <sup>2</sup>Siemens Healthcare, Erlangen, Germany, <sup>3</sup>Division of Imaging Sciences and Biomedical Engineering, King's College London, London, United Kingdom, <sup>4</sup>Biomedical Engineering and Einstein Center Digital Future, Technische Universität Berlin, Berlin, Germany

Respiratory heart motion during T<sub>1</sub> data acquisition can lead to strong motion artefacts, compromising the quality of reconstructed T<sub>1</sub> maps. Commonly, breathhold techniques are used to minimize respiratory motion but they suffer from low scan efficiency and require patient cooperation. Here, we propose a Pilot tone-based respiratory motion correction approach for free-breathing myocardial T<sub>1</sub> mapping. First, through-plane motion is corrected for by performing prospective slice tracking online during data acquisition. Second, in-plane motion is corrected for retrospectively by applying a phase shift to k-space data before image reconstruction. The feasibility of the proposed approach was demonstrated in four healthy volunteers.

0456



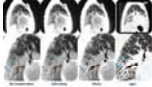
3D Self-Navigator Acquisition for Translational and Nonrigid Motion Correction in Multiphase Coronary MR Angiography

Kristin Quah<sup>1</sup>, Srivathsan P. Koundinyan<sup>1</sup>, Frank Ong<sup>1</sup>, Mario O. Malavé<sup>1</sup>, and Dwight Nishimura<sup>1</sup>

<sup>1</sup>Stanford University, Stanford, CA, United States

A whole-heart multiphase coronary angiography method has been developed that extracts a 3D navigator image every heartbeat from the 3D cones high-resolution imaging data. Such 3D self-navigators (sNAVs) enable direct beat-to-beat respiratory motion tracking of the heart for translational and nonrigid correction. 3D sNAVs are derived from the inner k-space region of phyllotaxis-ordered 3D cones interleaves collected over multiple cardiac phases. A multiscale low-rank method is used for reconstruction.

0457



### Motion Compensation in Pulmonary Ultra-short Echo Time MRI: Preliminary results in Idiopathic Pulmonary Fibrosis

Luis A Torres<sup>1</sup>, Xucheng Zhu<sup>2,3</sup>, Nathan Sandbo<sup>4</sup>, Mark L Shiebler<sup>4,5</sup>, Peder Larson<sup>2,3</sup>, and Sean B Fain<sup>1,5,6</sup>

<sup>1</sup>Dept. of Medical Physics, University of Wisconsin - Madison, Madison, WI, United States, <sup>2</sup>Dept. of Radiology and Biomedical Imaging, University of California - San Francisco, San Francisco, CA, United States, <sup>3</sup>UCSF/UC Berkeley Graduate Program in Bioengineering, University of California - San Francisco, San Francisco, CA, United States, <sup>4</sup>Dept. of Medicine, University of Wisconsin - Madison, Madison, WI, United States, <sup>5</sup>Dept. of Radiology, University of Wisconsin - Madison, Madison, WI, United States, <sup>6</sup>Dept. of Biomedical Engineering, University of Wisconsin - Madison, Madison, WI, United States

Acquiring pulmonary MRI images without motion corruption is a challenging task. In this work, we evaluate several conventional and advanced retrospective motion compensation techniques in subjects with idiopathic pulmonary fibrosis (IPF). We evaluate the effectiveness of each technique using concomitantly acquired CT scans, contrast to noise, and sharpness measures. We find that registration-based techniques show a significant improvement in CNR and sharpness. We also observe significantly improved image quality when referenced side-by-side with CT. We conclude that registration-based techniques could be used to better resolve subtle fibrotic textures in IPF.

0458



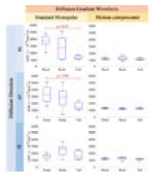
### Free-Breathing Abdominal Magnetic Resonance Fingerprinting Using a Pilot Tone Navigator

Sherry Huang<sup>1</sup>, Rasim Boyacioglu<sup>2</sup>, Reid Bolding<sup>3</sup>, Yong Chen<sup>2</sup>, and Mark A. Griswold<sup>2</sup>

<sup>1</sup>Biomedical Engineering, Case Western Reserve University, Cleveland, OH, United States, <sup>2</sup>Radiology, Case Western Reserve University, Cleveland, OH, United States, <sup>3</sup>Physics, Case Western Reserve University, Cleveland, OH, United States

This study presents a novel free-breathing technique which addresses some of the difficulties in quantitative  $T_1$  and  $T_2$  mapping of the abdomen. The technique integrates Magnetic Resonance Fingerprinting (MRF) and pilot tone (PT) navigator to retrospectively provide simultaneous quantification of multiple tissue properties in the abdomen in inhalation and expiration states of the respiratory motion. The proposed method can be implemented with both 2D and 3D MRF acquisitions.

0459



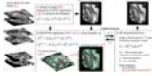
### Characterization and Correction of Cardiovascular Pulsation Artifacts in Diffusion-Weighted Imaging of the Pancreas

Ruiqi Geng<sup>1,2</sup>, Yuxin Zhang<sup>1,2</sup>, Jitka Starekova<sup>1</sup>, Lloyd Estkowski<sup>3</sup>, and Diego Hernando<sup>1,2</sup>

<sup>1</sup>Department of Radiology, University of Wisconsin-Madison, Madison, WI, United States, <sup>2</sup>Medical Physics, University of Wisconsin-Madison, Madison, WI, United States, <sup>3</sup>MR, GE Healthcare, Waukesha, WI, United States

Diffusion-weighted imaging (DWI) of the abdomen faces multiple challenges, particularly artifacts induced by respiratory, peristaltic, and cardiovascular-related motions. Effects of cardiovascular pulsation on pancreas DWI have not been previously characterized. This motion introduces artifactual signal voids and unreliable apparent diffusion coefficient (ADC) values across the pancreas in DWI, regardless of cardiac phases and diffusion directions. Importantly, these artifacts can be addressed by motion-compensated diffusion gradient waveforms. These findings may facilitate the development of reliable and reproducible DWI of the pancreas.

0460



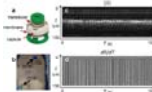
#### Non-rigid Motion Correction for Fetal Body MRI

Alena Uus<sup>1</sup>, Jacqueline Matthew<sup>1</sup>, Milou P. M. van Poppel<sup>1</sup>, Johannes Steinweg<sup>1</sup>, Laurence Jackson<sup>1</sup>, Mary Rutherford<sup>1</sup>, Joseph V. Hajnal<sup>1</sup>, and Maria Deprez<sup>1</sup>

<sup>1</sup>Biomedical Engineering Department, School of Biomedical Engineering and Imaging Sciences, King's College London, London, United Kingdom

Motion correction for fetal body MRI is particularly challenging due to non-rigid deformations of organs caused by bending and stretching. Rigid slice-to-volume registration (SVR) methods are efficient for 3D fetal brain reconstruction. However, for full body reconstruction, misregistration errors caused by deformable motion lead to degradation of features. We propose a novel deformable SVR (DSVR) method based on hierarchical deformable registration for reconstruction of 3D fetal trunk from multiple motion corrupted stacks. The method is quantitatively evaluated by comparison to the state-of-the-art methods on 20 iFIND fetal MRI datasets. Furthermore, DSVR reconstruction quality is assessed on 100 fetal MRI cases.

0461



#### Motion monitoring using MR-compatible ultrasound-based sensors

Bruno Madore<sup>1</sup>, Frank Preiswerk<sup>1</sup>, Jeremy Bredfeldt<sup>1</sup>, Shenyan Zong<sup>1</sup>, and Cheng-Chieh Cheng<sup>1</sup>

<sup>1</sup>Brigham and Women's Hospital, Harvard Medical School, Boston, MA, United States

The purpose of this work is to develop MR-compatible sensors that can attach to the patient's skin, to monitor breathing in a comprehensive manner. In contrast, alternatives such as MRI navigator echoes and optical tracking are typically rigidly fixed to walls or floors and as such cannot accompany a given patient through serial diagnostic and/or therapeutic procedures. We show here that these sensors capture breathing motion in much of its complexity, as validated against MRI and optical tracking data. These sensors could be used to help combine information from different modalities in a manner that takes internal motion into account.

## Oral

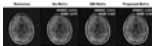
### Managing Motion and Artifacts - Mind Your Head: Managing Motion in the Brain

Tuesday Parallel 4 Live Q&A

Tuesday 13:45 - 14:30 UTC

Moderators: Berkin Bilgic

0462



#### Motion-compensated 3D radial MRI using self-encoded FID navigators

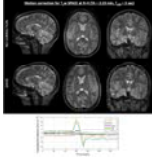
Tess E. Wallace<sup>1,2</sup>, Davide Piccini<sup>3,4,5</sup>, Tobias Kober<sup>3,4,5</sup>, Simon K. Warfield<sup>1,2</sup>, and Onur Afacan<sup>1,2</sup>

<sup>1</sup>Computational Radiology Laboratory, Boston Children's Hospital, Boston, MA, United States, <sup>2</sup>Department of Radiology, Harvard Medical School, Boston, MA, United States, <sup>3</sup>Advanced Clinical Imaging Technology, Siemens Healthcare, Lausanne, Switzerland, <sup>4</sup>Radiology, Lausanne University Hospital and University of Lausanne, Lausanne, Switzerland, <sup>5</sup>LTS5, École Polytechnique Fédérale de Lausanne (EPFL), Lausanne, Switzerland



We propose a novel motion compensation strategy for 3D radial MRI that directly estimates rigid-body motion parameters from the central k-space signal, which acts as a self-encoded FID navigator. By modelling trajectory deviations as low-spatial-order field variations, motion parameters can be recovered using a model that predicts the impact of motion and field changes on the FID signal. The proposed method enabled robust compensation for deliberate head motion in volunteers, with position estimates and image quality equivalent to that obtained with electromagnetic tracking. Our approach is suitable for robust neuroanatomical imaging in subjects that exhibit patterns of large, frequent motion.

0463



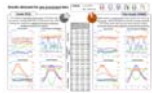
#### Scout Acquisition enables rapid Motion Estimation (SAME) for retrospective motion mitigation.

Daniel Polak<sup>1,2,3</sup>, Stephen Cauley<sup>2,4,5</sup>, Berkin Bilgic<sup>2,4,5</sup>, Daniel Nicolas Splitthoff<sup>3</sup>, Peter Bachert<sup>1</sup>, Lawrence L. Wald<sup>2,4,5</sup>, and Kawin Setsompop<sup>2,4,5</sup>

<sup>1</sup>Department of Physics and Astronomy, Heidelberg University, Heidelberg, Germany, <sup>2</sup>Department of Radiology, A. A. Martinos Center for Biomedical Imaging, Charlestown, MA, United States, <sup>3</sup>Siemens Healthcare GmbH, Erlangen, Germany, <sup>4</sup>Department of Radiology, Harvard Medical School, Boston, MA, United States, <sup>5</sup>Harvard-MIT Health Sciences and Technology, Massachusetts Institute of Technology, Cambridge, MA, United States

Navigation-free retrospective motion-correction typically requires estimating hundreds of coupled temporal motion parameters by solving a large non-linear inverse problem. This can be extremely demanding computationally, which has impeded implementation/adoption in clinical settings. We propose a technique that utilizes a *single* rapid scout scan ( $T_{\text{add}}=3\text{sec}$ ) to drastically reduce the computation cost of this motion-estimation and create a pathway for clinical acceptance. We optimized this scout along with the sequence acquisition reordering in a 3D Turbo-Spin-Echo acquisition. Our approach was evaluated in-vivo with up to R=6-fold acceleration and robust motion-mitigation was achieved using a scout with differing contrast to the imaging sequence.

0464



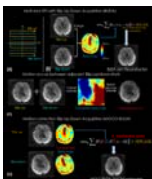
#### Measurement of head motion using a field camera in a 7T scanner

Laura Bortolotti<sup>1</sup>, Olivier Mougin<sup>1</sup>, and Richard Bowtell<sup>1</sup>

<sup>1</sup>Physics, Sir Peter Mansfield Imaging Centre, University of Nottingham, Nottingham, United Kingdom

In this work, a step towards a non-contact motion correction technique has been made. Measurements of extra-cranial field perturbations made using a 16-channel magnetic field camera have been used to predict head motion parameters with good accuracy. The prediction was performed using both linear (PLS) and non-linear (NARX) methods. The number of field probes used for the prediction was reduced by performing Principal Component Analysis. Magnetic field data was also pre-processed to reduce the unwanted effect of chest movement in respiration. NARX outperformed the PLS approach producing good predictions of head position changes for a wider range of movements.

0465



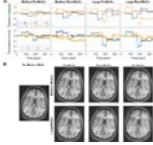
#### MOCO-BUDA: motion-corrected blip-up/down acquisition with joint reconstruction for motion-robust and distortion-free diffusion MRI of brain

Xiaozhi Cao<sup>1,2,3</sup>, Congyu Liao<sup>2,3</sup>, Zijong Zhang<sup>2,4</sup>, Mary Kate Manhard<sup>2,3</sup>, Hongjian He<sup>1</sup>, Jianhui Zhong<sup>1</sup>, Berkin Bilgic<sup>2,3,5</sup>, and Kawin Setsompop<sup>2,3,5</sup>

<sup>1</sup>Center for Brain Imaging Science and Technology, Department of Biomedical Engineering, Zhejiang University, Hangzhou, China, <sup>2</sup>Athinoula A. Martinos Center for Biomedical Imaging, Massachusetts General Hospital, Charlestown, MA, United States, <sup>3</sup>Department of Radiology, Harvard Medical School, Charlestown, MA, United States, <sup>4</sup>State Key Laboratory of Modern Optical Instrumentation, College of Optical Science and Engineering, Zhejiang University, Hangzhou, China, <sup>5</sup>Harvard-MIT Department of Health Sciences and Technology, Cambridge, MA, United States

We proposed a motion-correction method for joint reconstruction of blip-up/down EPI acquisition (BUDA-EPI) of brain diffusion MRI. Motion parameters were estimated and incorporated into the joint parallel imaging reconstruction of the blip-up/down multi-shot data, which included B0 field maps and Hankel structured low-rank constraint. The proposed motion-corrected reconstruction approach was demonstrated in vivo to provide motion-robust reconstruction of blip-up/down multi-shot EPI diffusion data.

0466



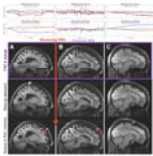
#### Comparison of Prospective and Retrospective Motion Correction for 3D Structural Brain MRI

Jakob Slipsager<sup>1,2,3,4</sup>, Stefan Glimberg<sup>4</sup>, Liselotte Højgaard<sup>2</sup>, Rasmus Paulsen<sup>1</sup>, Andre van der Kouwe<sup>3,5</sup>, Oline Olesen<sup>1,4</sup>, and Robert Frost<sup>3,5</sup>

<sup>1</sup>DTU Compute, Technical University of Denmark, Kgs. Lyngby, Denmark, <sup>2</sup>Department of Clinical Physiology, Nuclear Medicine & PET, Rigshospitalet, University of Copenhagen, Copenhagen, Denmark, <sup>3</sup>Athinoula A. Martinos Center for Biomedical Imaging, Massachusetts General Hospital, Charlestown, MA, United States, <sup>4</sup>TraCInnovations, Ballerup, Denmark, <sup>5</sup>Department of Radiology, Harvard Medical School, Boston, MA, United States

This work compares prospective and retrospective motion correction based on their capabilities to remove motion artifacts from 3D-encoded MPRAGE scans. Motion artifacts in clinical and research brain MRI are a major concern and the outcome of this problem includes repeated scans and the need for patient sedation or anesthesia, causing increased study time and cost. The prospective and retrospective correction approaches substantially improve the image quality of in-vivo scans for similar motion patterns. Prospective motion correction resulted in higher image quality than retrospective correction for larger discrete movements, and for periodic motion.

0467



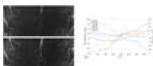
#### Scan-specific assessment of vNav motion artifact mitigation in the HCP Aging study using reverse motion correction

Robert Frost<sup>1,2</sup>, M. Dylan Tisdall<sup>3</sup>, Malte Hoffmann<sup>1,2</sup>, Bruce Fischl<sup>1,2,4</sup>, David H. Salat<sup>1,2</sup>, and André J. W. van der Kouwe<sup>1,2</sup>

<sup>1</sup>Athinoula A. Martinos Center for Biomedical Imaging, Massachusetts General Hospital, Charlestown, MA, United States, <sup>2</sup>Department of Radiology, Harvard Medical School, Boston, MA, United States, <sup>3</sup>Department of Radiology, Perelman School of Medicine, University of Pennsylvania, Philadelphia, PA, United States, <sup>4</sup>Computer Science and Artificial Intelligence Laboratory, Massachusetts Institute of Technology, Cambridge, MA, United States

In studies that acquire a single prospectively-corrected scan it is unclear whether motion correction was beneficial when inspecting residual artifacts and the motion profiles. Here we used reverse motion correction to estimate images that would have resulted without vNav prospective motion correction (PMC). Matched motion tests were used to assess whether the reverse correction step was an accurate representation of images acquired during similar motion but without PMC. Using reverse motion correction on a subset of scans from the Human Connectome Project Aging study suggests that vNav PMC and selective reacquisition substantially improved image quality when there was motion.

0468



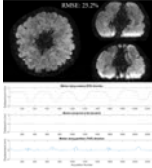
#### Preserved high resolution brain MRI by data-driven DISORDER motion correction

Lucilio Cordero-Grande<sup>1</sup>, Raphael Tomi-Tricot<sup>2</sup>, Giulio Ferrazzi<sup>3</sup>, Jan Sedlacik<sup>1</sup>, Shaihan Malik<sup>1</sup>, and Joseph V Hajnal<sup>1</sup>

<sup>1</sup>Centre for the Developing Brain and Biomedical Engineering Department, School of Biomedical Engineering and Imaging Sciences, King's College London, London, United Kingdom, <sup>2</sup>Centre for the Developing Brain and Biomedical Engineering Department, School of Biomedical Engineering and Imaging Sciences / MR Research Collaborations, King's College London / Siemens Healthcare Limited, London / Frimley, United Kingdom, <sup>3</sup>Biomedical Engineering Department, School of Biomedical Engineering and Imaging Sciences, King's College London, London, United Kingdom

Retrospective motion correction is applied for preserved image resolution on ultra-high field volumetric in-vivo brain MRI. Correction is based on the synergistic combination of appropriate view reorderings for increasing the sensitivity to motion and aligned reconstructions for deconvolving the effect of motion. Resolution loss introduced by motion is reverted without resorting to external motion tracking systems, navigators or training data. Contrast and sharpness improvements are shown on high resolution flow and susceptibility sensitive T1- and T2\*-weighted spoiled gradient echo sequences acquired on cooperative volunteers.

0469



Motion estimation and correction with joint optimization for wave-CAIPI acquisition

Zhe Wu<sup>1</sup> and Kâmil Uludağ<sup>1,2,3</sup>

<sup>1</sup>Techna Institute, University Health Network, Toronto, ON, Canada, <sup>2</sup>Koerner Scientist in MR Imaging, University Health Network, Toronto, ON, Canada, <sup>3</sup>Center for Neuroscience Imaging Research, Institute for Basic Science & Department of Biomedical Engineering, Sungkyunkwan University, Suwon, Korea, Republic of

Wave-CAIPI is a recently introduced parallel imaging method with high reduction factor and low g-factor penalty, thus is less prone to motion for the patients who cannot hold steady for long time. This study revealed that wave-CAIPI is still sensitive to during-scan motion, and proposed a joint optimization method to estimate motion and mitigate the introduced artifacts in wave-CAIPI images.

0470



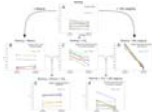
A method for controlling wireless hardware using the pulse sequence, applications in prospective motion correction.

Adam M. J. van Nierkerk<sup>1</sup>, Tim Sprenger<sup>2,3</sup>, Henric Rydén<sup>1,2</sup>, Enrico Avventi<sup>1,2</sup>, Ola Norbeck<sup>1,2</sup>, and Stefan Skare<sup>1,2</sup>

<sup>1</sup>Clinical Neuroscience, Karolinska Intitutet, Stockholm, Sweden, <sup>2</sup>Neuroradiology, Karolinska University Hospital, Stockholm, Sweden, <sup>3</sup>MR Applied Science Laboratory Europe, GE Healthcare, Stockholm, Sweden

We explore a real-time method of controlling a wireless device using the pulse sequence - with a series of short RF pulses. We show that it is possible to encode and detect eight unique identifiers with a high reliability in 52  $\mu$ s. Some identifiers are followed by short (< 1 ms) navigators that encode the pose of the device in the imaging volume. Other identifiers are followed by more RF pulses that encode information used for device configuration. These tools minimise the impact on the main pulse sequence and allow the device to tailor feedback precision to the pulse sequence requirements.

0471



Correcting motion registration errors caused by global intensity changes during CVR and CBF measurements.

Ryan Beckerleg<sup>1</sup>, Joseph Whittaker<sup>1</sup>, Daniel Gallichan<sup>2</sup>, and Kevin Murphy<sup>1</sup>

<sup>1</sup>CUBRIC, School of Physics and Astronomy, Cardiff University, Cardiff, United Kingdom, <sup>2</sup>CUBRIC, School of Engineering, Cardiff University, Cardiff, United Kingdom

Motion correction is an important preprocessing step in fMRI research<sup>1</sup>. Motion artefacts not only affect image quality but can lead to erroneous results which are normally corrected using a volume registration algorithm (VRA). Here we demonstrate that when global intensity changes are present in the data (e.g., caused by a CO<sub>2</sub> challenge during measurement of cerebrovascular reactivity (CVR) or by ASL tagging), the VRA misinterprets such intensity changes as motion. We compare the motion derived from the VRA with motion parameters derived from an external optical tracking system to determine the extent of the problem.

0398



### Metabolic characterization of human glioma subtypes using simultaneous pH- and oxygen-sensitive amine CEST-SAGE-EPI

Jingwen Yao<sup>1,2,3</sup>, Talia Oughourlian<sup>1,2,4</sup>, Timothy Cloughesy<sup>5,6</sup>, Phioanh L. Nghiemphu<sup>5,6</sup>, Albert Lai<sup>5,6</sup>, Linda M. Liau<sup>7</sup>, Richard G. Everson<sup>7</sup>, Whitney B. Pope<sup>2</sup>, Noriko Salamon<sup>2</sup>, David A. Nathanson<sup>8</sup>, and Benjamin M. Ellingson<sup>1,2,3,4,5</sup>

<sup>1</sup>Brain Tumor Imaging Laboratory (BTIL), Center of Computer Vision and Imaging Biomarker, David Geffen School of Medicine, UCLA, Los Angeles, CA, United States, <sup>2</sup>Department of Radiological Sciences, David Geffen School of Medicine, UCLA, Los Angeles, CA, United States, <sup>3</sup>Department of Bioengineering, Henry Samueli School of Engineering and Applied Science, UCLA, Los Angeles, CA, United States, <sup>4</sup>Neuroscience Interdepartmental Program, David Geffen School of Medicine, UCLA, Los Angeles, CA, United States, <sup>5</sup>UCLA Neuro-Oncology Program, David Geffen School of Medicine, UCLA, Los Angeles, CA, United States, <sup>6</sup>Department of Neurology, David Geffen School of Medicine, UCLA, Los Angeles, CA, United States, <sup>7</sup>Department of Neurosurgery, David Geffen School of Medicine, UCLA, Los Angeles, CA, United States, <sup>8</sup>Department of Molecular and Medical Pharmacology, David Geffen School of Medicine, UCLA, Los Angeles, CA, United States

We simultaneously quantified acidity and hypoxia of human gliomas with IDH, 1p/19q, and EGFR genotypes using CEST-SAGE-EPI. Results suggest IDH mutant gliomas are significantly less acidic and hypoxic than IDH wild-type tumors. Within IDH mutants, 1p/19q codeletion is associated with lower tumor acidity, while IDH wild-type, EGFR amplified tumors were more hypoxic. Both MRI-derived acidity and hypoxia were correlated with patient survival, suggesting metabolic characteristics may be prognostic. CEST-SAGE-EPI may be useful for exploring metabolic changes that result from particular genetic alterations or useful as a biomarker for accelerating drug development in human brain tumors.

0399



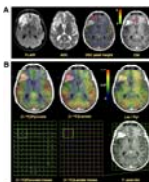
### Discrimination between lower-grade glioma and glioblastoma with amide proton transfer and diffusion kurtosis imaging at 3 Tesla

Zongwei Xu<sup>1</sup>, Chao Ke<sup>2</sup>, Xiaofei Lv<sup>3</sup>, Jie Liu<sup>1</sup>, Long Qian<sup>4</sup>, Shijie Xu<sup>2</sup>, Xin Liu<sup>1</sup>, Hairong Zheng<sup>1</sup>, and Yin Wu<sup>1</sup>

<sup>1</sup>Paul C. Lauterbur Research Center for Biomedical Imaging, Shenzhen Institutes of Advanced Technology, Chinese Academy of Sciences, Shenzhen, China, <sup>2</sup>Department of Neurosurgery, Sun Yat-Sen University Cancer Center, Guangzhou, China, <sup>3</sup>Department of Medical Imaging, Sun Yat-Sen University Cancer Center, Guangzhou, China, <sup>4</sup>GE Healthcare, Beijing, China

Preoperative assessment of histological tumor characteristics plays an essential role in evaluating prognosis and optimizing therapeutic strategies for glioma patients. This study aims to evaluate the feasibility of DKI and APT in differentiating lower-grade glioma (LGG) from glioblastoma at 3T. Twenty-four untreated patients were recruited and classified into LGG (grade II and III, N=10) and glioblastoma (grade VI, N=14). Results show comparable diagnostic performance of APTw and MK in differentiating the two groups with AUCs>0.85, superior to other DKI indices. Combining them further improves the discrimination accuracy, that may greatly facilitate prompt diagnosis and treatment decisions.

0400



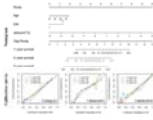
### Initial experience: detection of aberrant HP-13C metabolism in patients with glioblastoma prior to resection

Adam Autry<sup>1</sup>, Jeremy Gordon<sup>1</sup>, Marisa LaFontaine<sup>1</sup>, Hsin-Yu Chen<sup>1</sup>, Javier Villanueva-Meyer<sup>1</sup>, Susan Chang<sup>2</sup>, Duan Xu<sup>1</sup>, Peder EZ Larson<sup>1</sup>, Daniel B Vigneron<sup>1</sup>, Jennifer Clarke<sup>2</sup>, Janine Lupo<sup>1</sup>, and Yan Li<sup>1</sup>

<sup>1</sup>Department of Radiology and Biomedical Imaging, University of California San Francisco, San Francisco, CA, United States, <sup>2</sup>Department of Neurological Surgery, University of California San Francisco, San Francisco, CA, United States



0401



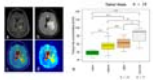
Radiomics profiling identifies the incremental value of MRI features to key molecular biomarkers for risk stratification of high-grade gliomas

Guoqiang Yang<sup>1</sup>, Shuaitong Zhang<sup>2</sup>, Xiaochun Wang<sup>1</sup>, Yan Tan<sup>1</sup>, Jingwei Wei<sup>2</sup>, Xiaoxu Chen<sup>3</sup>, Jie Tian<sup>2</sup>, and Hui Zhang<sup>1</sup>

<sup>1</sup>Department of Radiology, First Clinical Medical College, Shanxi Medical University, Taiyuan, Shanxi Province, China, <sup>2</sup>Key Laboratory of Molecular Imaging, Institute of Automation, Chinese Academy of Sciences, Beijing, China, <sup>3</sup>School of Economics and Management, Shanxi University, Taiyuan, Shanxi Province, China

To identify the incremental value of MRI features to the key molecular biomarkers for risk stratification of high-grade gliomas (HGGs). A comprehensive radiomics analysis integrated MRI features, clinical characteristics and genetic information was performed on 137 patients from TCGA/TCIA dataset and our institution. The combined model integrated radiomics signature with age and IDH genotype holds the best prognostic value. The radiomics signature has incremental prognostic value beyond the key molecular biomarkers, and could identify risk subgroups in various clinical and molecular subgroups. Our comprehensive radiomics analysis provided a potential tool to guide an individual diagnosis and treatment decisions for HGGs.

0402



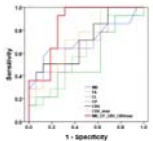
Sodium MRI at 7 Tesla as quantitative biomarker to assess tumor heterogeneity and histologic subtypes in glioma patients

Daniel Paech<sup>1</sup>, Sebastian Regnery<sup>2</sup>, Nicolas Behl<sup>3</sup>, Tanja Platt<sup>3</sup>, Nina Weinfurter<sup>1</sup>, Mark Edward Ladd<sup>3</sup>, Jürgen Debus<sup>2</sup>, Sebastian Adeberg<sup>2</sup>, and Heinz-Peter Schlemmer<sup>1</sup>

<sup>1</sup>Radiology, German Cancer Research Center, Heidelberg, Germany, <sup>2</sup>Radiooncology, University Hospital Heidelberg, Heidelberg, Germany, <sup>3</sup>Medical Physics in Radiology, German Cancer Research Center, Heidelberg, Germany

<sup>23</sup>Na MRI provides information on physiologic and pathophysiologically altered tissue sodium concentrations in vivo. In this prospective trial, we investigated the potential of <sup>23</sup>Na MRI at 7.0 Tesla to predict the tumor grade and genetic subtypes (such as isocitrate dehydrogenase (IDH) mutation and O6-methylguanine DNA methyltransferase (MGMT) promotor methylation) in a study cohort of 28 glioma patients. We show that that the quantitative <sup>23</sup>Na signal correlates with tissue-specific tumor subcompartments and that the contrast may allow non-invasive assessment of the tumor grade and IDH mutation.

0403



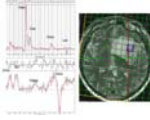
Differentiation of IDH Mutant from IDH wild-type High-grade Gliomas using Combined Analysis of Diffusion and Perfusion MRI

Santosh Kumar Yadav<sup>1</sup>, Sumei Wang<sup>2</sup>, Shadi Asadollahi<sup>2</sup>, MacLean Nasrallah<sup>3</sup>, Steven Brem<sup>4</sup>, Mohammad Haris<sup>1</sup>, Suyash Mohan<sup>2</sup>, and Sanjeev Chawla<sup>2</sup>

<sup>1</sup>Research, Sidra Medicine, Doha, Qatar, <sup>2</sup>Department of Radiology, Perelman School of Medicine at the University of Pennsylvania, Philadelphia, PA, United States, <sup>3</sup>Department of Pathology and Lab Medicine, Perelman School of Medicine at the University of Pennsylvania, Philadelphia, PA, United States, <sup>4</sup>Department of Neurosurgery, Perelman School of Medicine at the University of Pennsylvania, Philadelphia, PA, United States

Accurate identification of isocitrate dehydrogenase (IDH) mutant high-grade glioma is clinically important. We investigated the combined utility of diffusion (DTI) and perfusion (DSC-PWI) MR imaging in distinguishing IDH mutant from IDH wild-type high-grade gliomas. Treatment naïve patients (n=30) with IDH-mutant (n=14) and IDH-wild-type (n=16) high-grade gliomas were recruited. A classification model comprising of mean diffusivity, coefficient of planar anisotropy and maximum relative cerebral blood volume differentiated two genotypes of gliomas with an accuracy of 85%, a sensitivity of 87.2%, and a specificity of 81.5%. Combined analysis of DTI and DSC-PWI may be helpful in distinguishing IDH profiles of high-grade gliomas.

0404



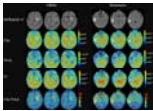
**Glioma 2HG threshold setting based on normal appearing white matter increases the diagnostic value of 3D MEGA-LASER for IDH mutation detection**

Marzena Wylezinska-Arridge<sup>1,2</sup>, Enrico De Vita<sup>2,3</sup>, Laura Mancini<sup>1,2</sup>, Ovidiu Andronesi<sup>4</sup>, Wolfgang Bogner<sup>5</sup>, Bernhard Strasser<sup>4</sup>, Tarek Yousry<sup>1,2</sup>, John Thornton<sup>1,2</sup>, and Sotirios Bisdas<sup>1,2</sup>

<sup>1</sup>Department of Neuroradiology, National Hospital for Neurology and Neurosurgery, London, United Kingdom, <sup>2</sup>Institute of Neurology, University College London, London, United Kingdom, <sup>3</sup>Department of Biomedical Engineering, School of Biomedical Engineering and Imaging Sciences, Kings College London, London, United Kingdom, <sup>4</sup>Athinoula A. Martinos Center for Biomedical Imaging, Massachusetts General Hospital, Harvard Medical School, Boston, MA, United States, <sup>5</sup>High Field MR Centre, Department of Biomedical Imaging and Image-guided Therapy, Medical University of Vienna, Vienna, Austria

It has been established that 2-hydroxyglutarate (2HG) MRS is important for non-invasive diagnosis of isocitrate dehydrogenase (IDH) status that holds prognostic value for the patient and is important for treatment planning. The purpose of this work was to investigate whether the threshold determination for identification of IDH mutation could be improved by using 'control' spectra from normal-appearing white matter, NAWM, in multi-voxel 3D MEGA-LASER acquisitions. The proposed approaches to threshold determination for 2HG detection in the tumour voxels provided increased sensitivity and specificity as compared with the cut-off thresholds based on CRLB% relative error.

0405



**Differentiation between Glioblastomas and Cerebral Metastases using High-Resolution 3D MRSI**

Pengcheng Yu<sup>1</sup>, Tianyao Wang<sup>2</sup>, Yujie Hu<sup>1</sup>, Yudu Li<sup>3,4</sup>, Rong Guo<sup>3,4</sup>, Yibo Zhao<sup>3,4</sup>, Ziyu Meng<sup>1,3</sup>, Hong Zhu<sup>5</sup>, Jun Liu<sup>6</sup>, Xin Yu<sup>7</sup>, Zhi-Pei Liang<sup>3,4</sup>, and Yao Li<sup>1</sup>

<sup>1</sup>Institute for Medical Imaging Technology, School of Biomedical Engineering, Shanghai Jiao Tong University, Shanghai, China, <sup>2</sup>Radiology Department, The Fifth People's Hospital of Shanghai, Fudan University, Shanghai, China, <sup>3</sup>Beckman Institute for Advanced Science and Technology, University of Illinois at Urbana-Champaign, Urbana, IL, United States, <sup>4</sup>Department of Electrical and Computer Engineering, University of Illinois at Urbana-Champaign, Urbana, IL, United States, <sup>5</sup>Department of Radiation Oncology, Minhang Branch of Cancer Hospital, Fudan University, Shanghai, China, <sup>6</sup>Radiology department, The Fifth People's Hospital of Shanghai, Fudan University, Shanghai, China, <sup>7</sup>Department of Biomedical Engineering, Case Western Reserve University, Cleveland, OH, United States

Differentiation between glioblastomas (GBMs) and cerebral metastases based on MR structural images is often challenging due to the poor specificity. MRSI is a useful tool for mapping the metabolic fingerprints of tumors. In this study, we investigate the use of a high-resolution MRSI technique known as SPICE for differentiation between GBMs and cerebral metastases in 28 patients. Our results show the metabolic biomarkers are different between GBMs and metastases as well as in the enhancing ring and the core of neoplasms. SPICE potentially provides a non-invasive metabolic measure to differentiate GBMs from cerebral metastases with high resolution.

0406



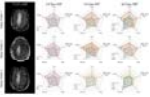
**The Effect of Tumor Grade within IDH Wild-Type and IDH Mutant Gliomas Assessed by Proton Magnetic Resonance Spectroscopy at 3T**

Esin Ozturk-Isik<sup>1,2</sup>, Banu Sacli Bilmmez<sup>1</sup>, Ayca Ersen Danyeli<sup>2,3</sup>, Cengiz Yakicier<sup>4</sup>, Alpay Ozcan<sup>2,5,6</sup>, M. Necmettin Pamir<sup>2,5,7</sup>, Koray Ozduman<sup>2,5,7</sup>, and Alp Dincer<sup>2,5,8</sup>

<sup>1</sup>Institute of Biomedical Engineering, Bogaziçi University, Istanbul, Turkey, <sup>2</sup>Brain Tumor Research Group, Acibadem Mehmet Ali Aydinlar University, Istanbul, Turkey, <sup>3</sup>Department of Pathology, Acibadem Mehmet Ali Aydinlar University, Istanbul, Turkey, <sup>4</sup>Department of Molecular Biology and Genetics, Acibadem Mehmet Ali Aydinlar University, Istanbul, Turkey, <sup>5</sup>Center for Neuroradiological Applications and Research, Acibadem Mehmet Ali Aydinlar University, Istanbul, Turkey, <sup>6</sup>Department of Medical Device Technologies, Acibadem Mehmet Ali Aydinlar University, Istanbul, Turkey, <sup>7</sup>Department of Neurosurgery, Acibadem Mehmet Ali Aydinlar University, Istanbul, Turkey, <sup>8</sup>Department of Radiology, Acibadem Mehmet Ali Aydinlar University, Istanbul, Turkey

Isocitrate dehydrogenase (*IDH*) mutation highly affects the overall survival of gliomas. In addition to the *IDH* mutation, the tumor histologic grade might play a role in patient prognosis. The aim of this study was to assess the metabolic variations between different tumor grades within *IDH* mutant (*IDH*-mut) and *IDH* wild-type (*IDH*-wt) gliomas using proton MR spectroscopy. Higher glycine in glioblastoma (GBM) within *IDH*-mut, and lower Cr and mIns in GBM within *IDH*-wt were the only statistically significant differences. Our study indicated similar metabolic profiles of different grades within *IDH* mutational subgroups, supporting *IDH* as a better predictor of clinical outcome.

0407



### Long-Term Monitoring of Brain Tumors Using MR Metabolic Phenotyping

Eduardo Coello<sup>1</sup>, Raymond Huang<sup>1</sup>, Molly F. Charney<sup>1</sup>, Wufan Zhao<sup>1</sup>, Huijun Liao<sup>1</sup>, Changho Choi<sup>2</sup>, and Alexander Lin<sup>1</sup>

<sup>1</sup>Radiology, Brigham and Women's Hospital, Boston, MA, United States, <sup>2</sup>Radiology, University of Texas Southwestern Medical Center, Dallas, TX, United States

This work introduces the concept of MR metabolic phenotyping (MRMP), a method that combines the high-resolution anatomical context of MRI and the highly specific metabolic information of MR spectroscopic imaging via unsupervised learning. The value of this technique was shown for the long-term follow up of *IDH*-mutated low-grade gliomas where high sensitivity to changes in the metabolic composition of the major tissue compartments was achieved.

## Oral

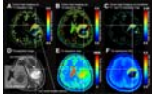
### Brain tumors - Brain Tumour: Quantitative MR Imaging

Tuesday Parallel 2 Live Q&A

Tuesday 13:45 - 14:30 UTC

Moderators: Kader Oguz & Koji Sakai

0408



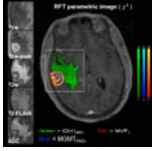
### Stereotactic tissue sampling and T1-, T2-relaxometry compared with ADC for tissue cell density quantification in gliomas imaging

Manabu Kinoshita<sup>1,2</sup>, Masato Uchikoshi<sup>3</sup>, Souichiro Tateishi<sup>2</sup>, Shohei Miyazaki<sup>2</sup>, Mio Sakai<sup>2</sup>, Tomohiko Ozaki<sup>2</sup>, Katsunori Asai<sup>2</sup>, Yuya Fujita<sup>2</sup>, Takahiro Matsushashi<sup>2</sup>, Yonehiro Kanemura<sup>4</sup>, Eku Shimosegawa<sup>1</sup>, Jun Hatazawa<sup>1</sup>, Shin-ichi Nakatsuka<sup>2</sup>, Haruhiko Kishima<sup>1</sup>, and Katsuyuki Nakanishi<sup>2</sup>

<sup>1</sup>Osaka University Graduate School of Medicine, Suita, Japan, <sup>2</sup>Osaka International Cancer Institute, Osaka, Japan, <sup>3</sup>Canon Medical Systems Corporation, Tochigi, Japan, <sup>4</sup>National Hospital Organization Osaka National Hospital, Osaka, Japan

The authors attempted to elucidate the correlation of tumor cell density within the brain in glioma patients and T1-, T2-relaxometry and ADC. First, an exploratory study compared T1-, T2-relaxometry, and ADC with 11C-methionine PET followed by a validation study using intraoperative stereo-tactically obtained tissues. A range of T1 values indicative of high cell density was identified, which finding was confirmed by stereotactic tissue sampling. For T2 values and ADC, however, no statistically significant correlation was confirmed regarding tumor cell density. The proposed technique was further able to create predictive tumor cell density map by T1 supplemented by T2 values.

0409



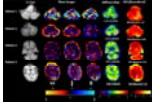
Statistical multiscale mapping of IDH1, MGMT, and microvasculature in human brain tumors from multiparametric MR and registered core biopsy

Jason Glenn Parker<sup>1</sup>, Emily E Diller<sup>2</sup>, Sha Cao<sup>3</sup>, Jeremy T Nelson<sup>4</sup>, Kristen Yeom<sup>5</sup>, Chang Ho<sup>1</sup>, and Robert Lober<sup>6</sup>

<sup>1</sup>Radiology & Imaging Sciences, Indiana University School of Medicine, Indianapolis, IN, United States, <sup>2</sup>School of Health Sciences, Purdue University, West Lafayette, IN, United States, <sup>3</sup>Biostatistics, Indiana University School of Medicine, Indianapolis, IN, United States, <sup>4</sup>Military Health Institute, University of Texas Health San Antonio, San Antonio, TX, United States, <sup>5</sup>Neuroradiology, Lucile Salter Packard Children's Hospital and Stanford University Medical Center, Palo Alto, CA, United States, <sup>6</sup>Neurosurgery, Dayton Children's Hospital, Dayton, OH, United States

We demonstrate statistical relationships between routine multiparametric imaging signatures and underlying cellular and molecular properties of brain tumors. We apply advanced statistical methods to correct for the family-wise error rate problem associated with whole-brain statistical parametric mapping, and show that the results have strong agreement with surgical biopsy. These results imply that cellular and molecular mapping of tumor heterogeneity from minimally-invasive images may be possible in the near future.

0410



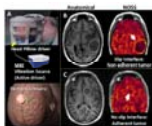
Preoperative assessment of stiffness and tumor-brain adhesion in schwannoma and meningioma patients and its comparison with surgical findings

Prateek Kalra<sup>1</sup>, Varun Varadarajan<sup>2</sup>, Michael S Harris<sup>3</sup>, Ashonti Harper<sup>3</sup>, Omar Mohamed<sup>3</sup>, Oliver Adunka<sup>2</sup>, Daniel M. Prevedello<sup>4</sup>, and Arunark Kolipaka<sup>1</sup>

<sup>1</sup>Radiology, Ohio State University Wexner Medical Center, Columbus, OH, United States, <sup>2</sup>Otolaryngology, Ohio State University Wexner Medical Center, Columbus, OH, United States, <sup>3</sup>Ohio State University Wexner Medical Center, Columbus, OH, United States, <sup>4</sup>Neurological Surgery, Ohio State University Wexner Medical Center, Columbus, OH, United States

Microsurgery in brain tumor patients aim to complete tumor resection without compromising neurological functionality. Inadequate preoperative knowledge of tumor may prolong surgical time and increase risk of postoperative complications which may depends upon tumor-brain adhesion and tumor stiffness. Previous studies have only looked into adhesion and stiffness separately using Magnetic Resonance Elastography (MRE). Previously, we proposed both adhesion and stiffness in vestibular schwannoma patients. Aim of this study is to also include meningioma cases in the analysis in order to broaden the tumor types and complexity. Preliminary results show good correlation between MRE-derived preoperative assessment of tumor and surgical findings.

0411



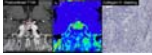
Quantification of meningioma-brain adhesion using MR-elastography based slip interface imaging

Ziying Yin<sup>1</sup>, Xin Lu<sup>1</sup>, Salomon Cohen Cohen<sup>2</sup>, Yi Sui<sup>1</sup>, Armando Manduca<sup>3</sup>, Jamie J Van Gompel<sup>2</sup>, Richard L. Ehman<sup>1</sup>, and John III Huston<sup>1</sup>

<sup>1</sup>Radiology, Mayo Clinic, Rochester, MN, United States, <sup>2</sup>Neurosurgery, Mayo Clinic, Rochester, MN, United States, <sup>3</sup>Physiology and Biomedical Engineering, Mayo Clinic, Rochester, MN, United States

Brain tumor adherence has been long recognized to impact surgical resection difficulty. Recently-developed slip interface imaging (SII) can preoperatively predict tumor-brain adhesion. In previous studies, subjectively-determined SII assessment of tumor adhesion has been shown to agree well with intraoperative findings. The purpose of this work was to develop an objective quantitative method for analyzing SII data for adherence, thereby minimizing inter- and intraobserver variability. We developed a radiomics-based metric (termed “adhesion degree”) based on SII to quantify the degree of tumor adhesion. In 46 meningiomas, the adhesion degree showed excellent accuracy in predicting completely adherent tumors (AUROC=0.96) from non-adherent tumors.

0412



Pharmacokinetic analysis of DCE-MRI in pituitary adenoma: evaluation of tumor consistency and comparison with histological collagen content

Kiyohisa Kamimura<sup>1</sup>, Masanori Nakajo<sup>1</sup>, Tomohide Yoneyama<sup>1</sup>, Manisha Bohara<sup>1</sup>, Yoshihiko Fukukura<sup>1</sup>, Shingo Fujio<sup>2</sup>, Takashi Iwanaga<sup>3</sup>, Hiroshi Imai<sup>4</sup>, Marcel Dominik Nickel<sup>5</sup>, and Takashi Yoshiura<sup>1</sup>

<sup>1</sup>Radiology, Kagoshima University Graduate School of Medical and Dental Sciences, Kagoshima, Japan,

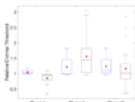
<sup>2</sup>Neurosurgery, Kagoshima University Graduate School of Medical and Dental Sciences, Kagoshima, Japan,

<sup>3</sup>Clinical Engineering Department Radiation Section, Kagoshima University Hospital, Kagoshima, Japan,

<sup>4</sup>Siemens Healthcare K.K., Tokyo, Japan, <sup>5</sup>Siemens Healthcare, Erlangen, Germany

Preoperative information of tumor consistency is important in patients with pituitary adenoma. Our aim was to evaluate the possible role of high-temporal and spatial resolution dynamic contrast enhanced MR imaging (DCE-MRI) and quantitative pharmacokinetic analysis in differentiation of a hard adenoma from soft adenoma. The hard adenoma showed significantly higher extravascular extracellular space per unit volume of tissue ( $v_e$ ) than soft adenoma and the  $v_e$  was significantly correlated to collagen IV content of pituitary adenomas. This quantitative pharmacokinetic parameter  $v_e$  may be useful for differentiation of the hard adenoma from soft adenoma.

0413



Evaluating the use of rCBV as a tumor grade classifier across NCI Quantitative Imaging Network sites: Part II of the DSC-MRI DRO Challenge

Laura C. Bell<sup>1</sup>, Natanael B. Semmineh<sup>1</sup>, Leland S. Hu<sup>2</sup>, Yuxiang Zhou<sup>2</sup>, Melissa Prah<sup>3</sup>, Kathleen M. Schmainda<sup>3</sup>, Jerrold L. Boxerman<sup>4</sup>, Hongyu An<sup>5</sup>, Cihat Eldeniz<sup>5</sup>, Richard Wahl<sup>5</sup>, Bradley Erickson<sup>6</sup>, Panagiotis Korfiatis<sup>6</sup>, Chengyue Wu<sup>7</sup>, Thomas Yankeelov<sup>7</sup>, Anna Sorace<sup>7</sup>, Neal Rutledge<sup>7</sup>, Thomas Chenevert<sup>8</sup>, Dariya Malyarenko<sup>8</sup>, Yichu Liu<sup>9</sup>, Andrew Brenner<sup>9</sup>, Yi-Fen Yen<sup>10</sup>, Jayashree Kalpathy-Cramer<sup>10</sup>, Andrew Beers<sup>10</sup>, Mark Muzi<sup>11</sup>, Ananth J. Madhuranthakam<sup>12</sup>, Marco Pinho<sup>12</sup>, Brian Johnson<sup>12</sup>, and C. Chad Quarles<sup>1</sup>

<sup>1</sup>Barrow Neurological Institute, Phoenix, AZ, United States, <sup>2</sup>Mayo Clinic, Scottsdale, AZ, United States,

<sup>3</sup>Medical College of Wisconsin 53226, Milwaukee, WI, United States, <sup>4</sup>Rhode Island Hospital and Alpert

Medical School of Brown University, Providence, RI, United States, <sup>5</sup>Washington University in St. Louis, St.

Louis, MO, United States, <sup>6</sup>Mayo Clinic, Rochester, MN, United States, <sup>7</sup>The University of Texas at Austin,

Austin, TX, United States, <sup>8</sup>University of Michigan, Ann Arbor, MI, United States, <sup>9</sup>University of Texas Health

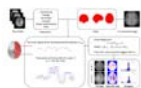
Science Center at San Antonio, San Antonio, TX, United States, <sup>10</sup>Massachusetts General Hospital, Boston,

MA, United States, <sup>11</sup>University of Washington, Seattle, WA, United States, <sup>12</sup>The University of Texas

Southwestern, Dallas, TX, United States

Using a dynamic susceptibility contrast (DSC) MRI DRO we previously characterized brain tumor relative cerebral blood volume (rCBV) reproducibility across 12 sites employing a range of imaging protocols and software platforms. Our goal in this study is to determine the impact of rCBV reproducibility for tumor grade classification. We found that varying software platforms produced a range of optimal thresholds, but the performance of these thresholds were similar. These results indicate that different software platforms are able to classify tumor grades, but the site-specific thresholds underscore the importance of standardizing acquisition and analysis protocols across sites and software benchmarking.

0414



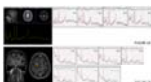
### Altered Systemic Fluctuations of Blood Flow in Brains with Glioma: An Investigation with Temporal-Shift Resting-State fMRI

Siqi Cai<sup>1</sup>, Zhifeng Shi<sup>2</sup>, Shihui Zhou<sup>1,3</sup>, Chunxiang Jiang<sup>1,3</sup>, and Lijuan Zhang<sup>1</sup>

<sup>1</sup>Shenzhen Institutes of Advanced Technology, Chinese Academy of Sciences, Shenzhen, China, <sup>2</sup>Huashan Hospital of Fudan University, Shanghai, China, <sup>3</sup>University of Chinese Academy of Science, Beijing, China

The systemic oscillation of the blood flow in cerebrum and cerebellum may vary with gliomas of different malignancy, resulting in neurovascular uncoupling and abnormal perfusion. In this study, we investigated the implication of glioma on the oscillation of cerebral blood flow based on time-shifted rs-fMRI. HGGs induces more widely alterations in the spontaneous fluctuations of cerebral and cerebellar blood flow at the global scale. Vascular oscillation changes derived from rs-fMRI may provide a novel insight for the assessment of the functional plasticity and its clinical relevance in the interpretation of the psychological and psychiatric symptoms in subjects with glioma.

0415



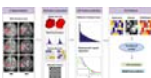
### Multimodal MRI to aid prediction of low-grade glioma growth characteristics

Franklyn Howe<sup>1</sup>, Timothy Jones<sup>2</sup>, Philip Rich<sup>2</sup>, Jordan Colman<sup>3</sup>, Guang Yang<sup>4</sup>, Felix Raschke<sup>5</sup>, Venus Liang<sup>1</sup>, Alex Denley<sup>1</sup>, and Thomas Barrick<sup>1</sup>

<sup>1</sup>Neurosciences Research Centre, St George's, University of London, London, United Kingdom, <sup>2</sup>St George's University Hospitals NHS Foundation Trust, London, United Kingdom, <sup>3</sup>Ashford and St Peter's Hospitals NHS Foundation Trust, Surrey, United Kingdom, <sup>4</sup>National Lund and Heart Institute, Imperial College, London, United Kingdom, <sup>5</sup>OncoRay—National Center for Radiation Research in Oncology, Dresden, Germany

<sup>1</sup>H MRS and DTI measures were assessed for their ability to predict the future growth and malignant transformation of low-grade gliomas. The tumour core NAA concentration and the mean diffusivity (MD) within the MRS voxel, combined with the FLAIR tumour volume, provided a good predictor of tumours with higher growth rates. A ROC analysis gave an AUC of 0.86 to predict tumours likely to undergo malignant progression, and AUC of 0.98 when including those undergoing early debulking. The combined NAA, MD and volumetric parameter provided a single time-point assessment of future growth characteristics.

0416



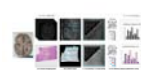
### Whole-tumor radiomics analysis of DKI and DTI may improve the prediction of genotypes for astrocytomas: a preliminary study

Yan Tan<sup>1,2</sup>, Wei Mu<sup>3</sup>, Xiaochun Wang<sup>1,2</sup>, Guoqiang Yang<sup>1,2</sup>, Robert James Gillies<sup>3</sup>, and Hui Zhang<sup>1,2</sup>

<sup>1</sup>Department of Radiology, First Hospital of Shanxi Medical University, Taiyuan, China, <sup>2</sup>College of Medical Imaging, Shanxi Medical University, Taiyuan, China, <sup>3</sup>Department of Cancer Physiology, H. Lee Moffitt Cancer Center and Research Institute, Tampa, FL, United States

Assessment of glioma genotypes by quantifying MR diffusion imaging heterogeneity of whole tumour may serve as a powerful tool to instruct therapeutic decision-making. This study evaluated the role and incremental value of whole-tumor radiomics analysis based on DKI and DTI images in determining the IDH and MGMTmet genotypes of astrocytomas. A radiomics models based on whole-tumor MK and MD maps showed good diagnostic efficiency in predicting IDH and MGMTmet genotypes. Furthermore, the combined model constructed by radiomics score, edema degree and age further improved the performance of predicting IDH, while the combined model did not benefit for MGMTmet prediction.

0417



### Information-based assessment of the radiomic-histomic relationship in brain cancer patients

Samuel Bobholz<sup>1</sup>, Allison Lowman<sup>2</sup>, Alexander Barrington<sup>3</sup>, Michael Brehler<sup>2</sup>, Sean McGarry<sup>1</sup>, Jennifer Connelly<sup>4</sup>, Elizabeth Cochran<sup>5</sup>, Anjishnu Banerjee<sup>6</sup>, and Peter LaViolette<sup>2,3</sup>

<sup>1</sup>Biophysics, Medical College of Wisconsin, Wauwatosa, WI, United States, <sup>2</sup>Radiology, Medical College of Wisconsin, Wauwatosa, WI, United States, <sup>3</sup>Biomedical Engineering, Medical College of Wisconsin, Wauwatosa, WI, United States, <sup>4</sup>Neurology, Medical College of Wisconsin, Wauwatosa, WI, United States, <sup>5</sup>Pathology, Medical College of Wisconsin, Wauwatosa, WI, United States, <sup>6</sup>Biostatistics, Medical College of Wisconsin, Wauwatosa, WI, United States

This study sought to provide a biological basis of radiomics-based analyses by assessing the relationship between MR features and analogous histomic features of the underlying tissue using coregistered histology samples taken at autopsy from brain cancer patients. Several radiomic features demonstrated substantial mutual information with their histomic analogs, with first order features showing the strongest associations. These histomic-preserving features were shown to be stable across potential confounds such as differences in scanner vendor and acquisition field strength. These findings suggest that MR radiomic features reflect information about the texture of the underlying tissue.

## Oral

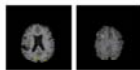
### Brain tumors - Emerging AI Applications in Neuro-Oncology

Tuesday Parallel 2 Live Q&A

Tuesday 13:45 - 14:30 UTC

Moderators: Christopher Filippi

0418



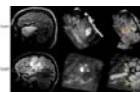
[An RNN and Autoencoder-based Deep Learning Approach for Detecting Brain Metastases in MRI](#)

Shuyang Zhang<sup>1</sup>, Min Zhang<sup>2</sup>, Xinhua Cao<sup>3</sup>, Geoffrey S Young<sup>2</sup>, and Xiaoyin Xu<sup>2</sup>

<sup>1</sup>University of Michigan-Ann Arbor, Ann Arbor, MI, United States, <sup>2</sup>Brigham and Women's Hospital and Harvard Medical School, Boston, MA, United States, <sup>3</sup>Boston Children's Hospital, Boston, MA, United States

Cancer metastases to the brain is a major cause of fatality in patients. Finding all the metastases is crucial to clinical treatment planning as today's radiation therapy can target up to 20 individual metastases, making it necessary for clinicians to detect and marking multiple metastases in practice. Detecting brain metastases, however, is very challenging because the objects are small and of low contrast. Computer-aided detection of metastases can be highly valuable to improve the accuracy and efficiency of a human reader. In this work, we developed a deep learning-based pipeline for finding metastases on brain MRI.

0419



[Fast multimodal image fusion with deep 3D convolutional networks for neurosurgical guidance – A preliminary study](#)

Jhimli Mitra<sup>1</sup>, Soumya Ghose<sup>1</sup>, David Mills<sup>1</sup>, Lowell Scott Smith<sup>1</sup>, Sarah Frisken<sup>2</sup>, Alexandra Golby<sup>2</sup>, Thomas K. Foo<sup>1</sup>, and Desmond Teck-Beng Yeo<sup>1</sup>

<sup>1</sup>General Electric Research, Niskayuna, NY, United States, <sup>2</sup>Brigham and Women's Hospital, Boston, MA, United States

Multimodality fusion in neurosurgical guidance aids neurosurgeons in making critical clinical decisions regarding safe maximal resection of tumors. It is challenging to have registration methods that automatically update pre-surgical MRI on intra-operative ultrasound, adjusting for the brain-shift for surgical guidance. A 3D deep learning-based convolutional network was developed for fast, multimodal alignment of pre-surgical MRI and intra-operative ultrasound volumes. The neural network is a combination of some well-known deep-learning architectures like FlowNet, Spatial Transformer Networks and UNet to achieve fast alignment of multimodal images. The CuRIOUS 2018 challenge training data was used to evaluate the accuracy of the developed method.

0420



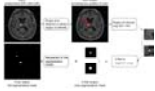
[A radiomic signature for predicting recurrence of FLAIR abnormality in glioblastomas using multi-modal MRI](#)

Tanay Chougule<sup>1</sup>, Rakesh Gupta<sup>2</sup>, Jitender Saini<sup>3</sup>, Shaleen Agarwal<sup>4</sup>, Rana Patir<sup>4</sup>, and Madhura Ingalthalikar<sup>1</sup>

<sup>1</sup>Symbiosis Center for Medical Image Analysis, Symbiosis International University, Pune, India, <sup>2</sup>Department of Radiology, Fortis Hospital, Gurgaon, India, <sup>3</sup>Department of Radiology, National Institute of Mental Health and Neurosciences, Bangalore, India, <sup>4</sup>Radiation Oncology and Neurosurgery, Fortis Hospital, Gurgaon, India

Standard post-operative radiation therapy in glioblastoma delivers radiation uniformly across the hyper-intense areas from pre-operative FLAIR images and does not account for the regions where the infiltration might relapse. This work creates a non-invasive prognostic signature of the extent of recurrent hyper-intense FLAIR using radiomics features extracted from multi-modal MRI. Results demonstrate that the area of recurrence can be accurately predicted earlier with some radiomic features as beacon of recurrence than others when tested temporally across multiple time-points.

0421



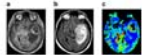
### Computer-aided detection and segmentation of brain metastases in MRI for stereotactic radiosurgery via a deep learning ensemble

Zijian Zhou<sup>1</sup>, Jeremiah W. Sanders<sup>1</sup>, Jason M. Johnson<sup>2</sup>, Tina M. Briere<sup>3</sup>, Mark D. Pagel<sup>4</sup>, Jing Li<sup>5</sup>, and Jingfei Ma<sup>1</sup>

<sup>1</sup>Imaging Physics, The University of Texas MD Anderson Cancer Center, Houston, TX, United States, <sup>2</sup>Diagnostic Radiology, The University of Texas MD Anderson Cancer Center, Houston, TX, United States, <sup>3</sup>Radiation Physics, The University of Texas MD Anderson Cancer Center, Houston, TX, United States, <sup>4</sup>Cancer Systems Imaging, The University of Texas MD Anderson Cancer Center, Houston, TX, United States, <sup>5</sup>Radiation Oncology, The University of Texas MD Anderson Cancer Center, Houston, TX, United States

Manual delineation of brain metastases for stereotactic radiosurgery (SRS) is time consuming and labor intensive. We successfully constructed a deep learning ensemble, including a single shot detector and U-Net, to detect and subsequently segment brain metastases in MRI for SRS treatment planning. Postcontrast 3D T1-weighted gradient echo MR images from 266 patients were randomly split by 212:54 for model training-validation and testing. For the testing group, an overall sensitivity of 80.4% (189/235 metastases) with 4 false positives per patient, and a median segmentation Dice of 77.9% (61.4% - 86.3%) for the detected metastases were achieved.

0422



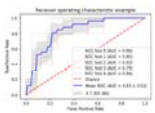
### Identifying Overall Survival in Glioblastoma Patients Using VASARI Features at 3T

Banu Sacli-Bilmez<sup>1</sup>, Zeynep Firat<sup>2</sup>, Melih Topcuoglu<sup>2</sup>, C. Kaan Yaltirik<sup>3</sup>, Uğur Türe<sup>3</sup>, and Esin Ozturk-Isik<sup>1</sup>

<sup>1</sup>Institute of Biomedical Engineering, Bogazici University, Istanbul, Turkey, <sup>2</sup>Department of Radiology, Yeditepe University, Istanbul, Turkey, <sup>3</sup>Department of Neurosurgery, Yeditepe University, Istanbul, Turkey

Glioblastoma (GBM) is the most common primary brain tumor in adults with 15 months median overall survival. The purpose of this study was to identify overall survival of GBM patients based on clinical and Visually AcceSable Rembrandt Images (VASARI) features using machine learning. According to our results, a support vector machine (SVM) model worked better for categorical data classification. With the help of adaptive synthetic (ADASYN) oversampling, a fine Gaussian SVM model identified short overall survival at 12 and 24 months thresholds with 99.78% and 88.80% accuracies, respectively.

0423



### Using anatomic and diffusion MRI with deep convolutional neural networks to distinguish treatment-induced injury from recurrent glioblastoma

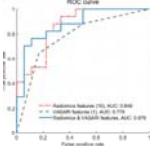
Julia Cluceru<sup>1,2</sup>, Paula Alcaide-Leon<sup>1</sup>, Valentina Pedoia<sup>1</sup>, Joanna Phillips<sup>3</sup>, Devika Nair<sup>1</sup>, Yannet Interian<sup>4</sup>, Susan Chang<sup>5</sup>, Javier E. Villanueva-Meyer<sup>1</sup>, Tracy Luks<sup>1</sup>, Annette Molinaro<sup>5</sup>, Mitchel Berger<sup>5</sup>, and Janine Lupo<sup>1,6</sup>



<sup>1</sup>Radiology and Biomedical Imaging, UCSF, San Francisco, CA, United States, <sup>2</sup>Bioengineering and Therapeutic Sciences, UCSF, San Francisco, CA, United States, <sup>3</sup>UCSF, Neurological Surgery, CA, United States, <sup>4</sup>Data Science, USF, San Francisco, CA, United States, <sup>5</sup>Neurological Surgery, UCSF, San Francisco, CA, United States, <sup>6</sup>Graduate Program in Bioengineering, UCSF/UC Berkeley, San Francisco and Berkeley, CA, United States

In this study, we leverage a promising new centrally restricted diffusion pattern<sup>1</sup> together with modern advances in deep learning to create a novel method for detecting treatment-related injury in the context of suspected recurrent glioblastoma. We report a 5-fold cross-validation average AUC ROC of 0.83 +/- 0.2 for the classification of lesions into two categories: those induced by treatment, and those that are true incidences of recurrent glioblastoma.

0424



IDH1 genotype prediction in lower-grade gliomas: a machine learning study with VASARI and ADC radiomics  
Shiteng Suo<sup>1</sup>, Mengqiu Cao<sup>1</sup>, Xiaoqing Wang<sup>1</sup>, Wei Yang<sup>2</sup>, Jianrong Xu<sup>1</sup>, and Yan Zhou<sup>1</sup>

<sup>1</sup>Renji Hospital, School of Medicine, Shanghai Jiao Tong University, Shanghai, China, <sup>2</sup>Guangdong Provincial Key Laboratory of Medical Image Processing, School of Biomedical Engineering, Southern Medical University, Guangzhou, China

Preoperative noninvasive prediction of IDH mutation status is crucial for prognosis and therapeutic decision making. In this study, we evaluated the qualitative and quantitative MRI features, namely, Visually Accessible Rembrandt Images (VASARI) features and apparent diffusion coefficient radiomics features in identifying IDH1 mutation status in lower-grade gliomas (WHO grade II-III). Results by machine learning methods showed that the combination achieved a better prediction performance. Our model may have the potential to serve as an alternative to the conventional workflow for the noninvasive identification of the molecular profiles.

0425



Automatic stratification of gliomas into WHO 2016 molecular subtypes using diffusion-weighted imaging and a pre-trained deep neural network

Julia Cluceru<sup>1,2</sup>, Yannet Interian<sup>3</sup>, Joanna Phillips<sup>4</sup>, Devika Nair<sup>1</sup>, Susan Chang<sup>4</sup>, Paula Alcaide-Leon<sup>1</sup>, Javier E. Villanueva-Meyer<sup>1</sup>, and Janine Lupo<sup>1,5</sup>

<sup>1</sup>Radiology and Biomedical Imaging, UCSF, San Francisco, CA, United States, <sup>2</sup>Bioengineering and Therapeutic Sciences, UCSF, San Francisco, CA, United States, <sup>3</sup>Data Science, USF, San Francisco, CA, United States, <sup>4</sup>UCSF, Neurological Surgery, CA, United States, <sup>5</sup>Graduate Program in Bioengineering, UCSF/UC Berkeley, San Francisco and Berkeley, CA, United States

In this abstract, we use diffusion and anatomical MR imaging together with a pre-trained RGB ImageNet to classify patients into major genetic entities defined by the WHO. We achieved 91% accuracy on our validation set with high per-class accuracy, precision, and recall; and 81% accuracy on a separate test dataset.

0426



MRI-based Radiomics as a Predictive Biomarker of Survival in High Grade Gliomas Treated with Chimeric Antigen Receptor T-Cell Therapy

Sohaib Naim<sup>1</sup>, Chi Wah Wong<sup>2</sup>, Eemon Tizpa<sup>1</sup>, Hannah Jade Young<sup>1</sup>, Kimberly Jane Bonjoc<sup>1</sup>, Seth Michael Hilliard<sup>1</sup>, Aleksandr Filippov<sup>1</sup>, Saman Tabassum Khan<sup>1</sup>, Christine Brown<sup>3</sup>, Behnam Badie<sup>4</sup>, and Ammar Ahmed Chaudhry<sup>1</sup>

<sup>1</sup>Diagnostic Radiology, City of Hope National Medical Center, Duarte, CA, United States, <sup>2</sup>Applied AI and Data Science, City of Hope National Medical Center, Duarte, CA, United States, <sup>3</sup>Hematology & Hematopoietic Cell Transplantation and Immuno-Oncology, City of Hope National Medical Center, Duarte, CA, United States, <sup>4</sup>Surgery, City of Hope National Medical Center, Duarte, CA, United States

High grade gliomas (HGG) is the most common malignant primary brain tumors in adults. In this study, 61 patients with recurrent HGGs underwent surgical resection and chimeric antigen receptor-T cell therapy. Volumetric segmentations of contrast-enhanced (CE) and non-enhanced tumors (NET) using T1-weighted CE MR images were used to identify shape- and texture-based features from these regions of interest. We evaluated radiomic characteristics of these HGGs to determine novel imaging biomarkers to predict treatment response. Exponentially-filtered textural radiomic features based on Neighboring Gray Tone Difference Matrix and Gray Level Co-occurrence Matrix derived from NET were the strongest predictors of overall survival.

---

## Oral

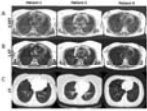
### Thoracic/Lung MRI - Thoracic MRI

Tuesday Parallel 3 Live Q&A

Tuesday 13:45 - 14:30 UTC

Moderators: Bastiaan Driehuys

0427



#### Structural and functional lung imaging using a high performance 0.55T MRI system

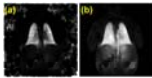
Ipshita Bhattacharya<sup>1</sup>, Rajiv Ramasawmy<sup>1</sup>, Joel Moss<sup>1</sup>, Marcus Y Chen<sup>1</sup>, Waqas Majeed<sup>2</sup>, Thomas Benkert<sup>3</sup>, Robert S Balaban<sup>1</sup>, and Adrienne Campbell-Washburn<sup>1</sup>

<sup>1</sup>National Institutes of Health, Bethesda, MD, United States, <sup>2</sup>Siemens Medical Solutions, Malvern, PA, United States, <sup>3</sup>Siemens Healthcare GmbH, Erlangen, Germany

Lung imaging using conventional MRI has several limitations for clinical use. A contemporary low-field MRI (0.55T) system offers several advantages for structural and functional imaging of lung owing to low magnetic susceptibility and increased oxygen relaxivity. In this abstract we present an improved structural imaging method and functional imaging method for patients with lymphangioleiomyomatosis (LAM) at low-field. Anatomical imaging offers improved delineation of cystic structures in the lung parenchyma. Oxygen-enhanced lung MRI is used to measure ventilation and regional texture in healthy volunteers and this patient group with abnormal pulmonary function.

---

0428

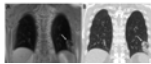


#### Feasibility of Structural and Phase-Resolved Functional Lung (PREFUL) MRI in Free-Breathing Neonates

Brandon Zanette<sup>1</sup>, Samal Munidasa<sup>1,2</sup>, Marcus J Couch<sup>1</sup>, Elaine Stirrat<sup>1</sup>, Eric Schrauben<sup>1</sup>, Robert Grimm<sup>3</sup>, Andreas Voskrebenezov<sup>4,5</sup>, Jens Vogel-Claussen<sup>4,5</sup>, Ravi Seethamraju<sup>6</sup>, Christopher K Macgowan<sup>1,2</sup>, Mary-Louise C Greer<sup>7,8</sup>, Emily Tam<sup>9,10</sup>, and Giles Santyr<sup>1,2</sup>

<sup>1</sup>Translational Medicine, The Hospital for Sick Children, Toronto, ON, Canada, <sup>2</sup>Medical Biophysics, University of Toronto, Toronto, ON, Canada, <sup>3</sup>MR Predevelopment, Siemens Healthcare, Erlangen, Germany, <sup>4</sup>Diagnostic and Interventional Radiology, Hannover Medical School, Hannover, Germany, <sup>5</sup>Biomedical Research in Endstage and Obstructive Lung Disease Hannover (BREATH), Member of the German Center for Lung Research (DZL), Hannover, Germany, <sup>6</sup>MR Collaborations North East, Siemens Healthineers, Boston, MA, United States, <sup>7</sup>Diagnostic Imaging, The Hospital for Sick Children, Toronto, ON, Canada, <sup>8</sup>Medical Imaging, University of Toronto, Toronto, ON, Canada, <sup>9</sup>Neurosciences and Mental Health, The Hospital for Sick Children, Toronto, ON, Canada, <sup>10</sup>Neurology, The Hospital for Sick Children, Toronto, ON, Canada

MRI of the neonatal pulmonary system can be a useful tool for the clinical evaluation of lung structure and function without ionizing radiation. Despite this, the inherent challenges associated with MRI of the lung make this difficult. This work demonstrates the feasibility of structural and functional imaging of the neonatal lung without exogenous contrast using a clinical whole-body 3T system with standard coils in neonates without any cardiorespiratory history. The imaging protocol includes T1-weighted, T2-weighted, and ultrashort echo time (UTE) imaging for structural imaging as well as novel free-breathing Phase-Resolved Function Lung (PREFUL) MRI for ventilation/perfusion imaging.

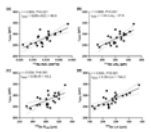


### Non-contrast-enhanced 3D-UTE MRI for pulmonary Imaging of Immunocompromised Patients during Hematopoietic Stem Cell Transplantation

Corona Metz<sup>1</sup>, David Böckle<sup>2</sup>, Julius Frederik Heidenreich<sup>1</sup>, Andreas Max Weng<sup>1</sup>, Thomas Benkert<sup>3</sup>, Götz Ulrich Grigoleit<sup>2</sup>, Herbert Köstler<sup>1</sup>, Thorsten Alexander Bley<sup>1</sup>, and Simon Veldhoen<sup>1</sup>

<sup>1</sup>Department of Diagnostic and Interventional Radiology, University Hospital Würzburg, Würzburg, Germany, <sup>2</sup>Department of Internal Medicine II, University Hospital Würzburg, Würzburg, Germany, <sup>3</sup>Application Development, Siemens Healthcare GmbH, Erlangen, Germany

Immunocompromised patients during HSCT procedure commonly need repeated MDCT examinations resulting in a high cumulative radiation dose. 3D-UTE MRI using a stack-of-spirals trajectory, enables contrast-free and radiation-free imaging of the lungs within a single breath-hold with increased signal yield due to echo times being well below parenchymal T2\*. 3D-UTE MRI allows diagnostics of inflammatory consolidations and pleural effusions with high sensitivity, specificity and consistency when compared to MDCT. Moreover, 3D-UTE sequences improve detection rates of ground glass opacities in pulmonary MRI.

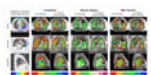


### Benchmarking acinar airway measurements from inhaled nanoparticles with hyperpolarized <sup>129</sup>Xe diffusion-weighted MRI

Ho-Fung Chan<sup>1</sup>, Madeleine Petersson Sjögren<sup>2</sup>, Paul J.C. Hughes<sup>1</sup>, Oliver I Rodgers<sup>1</sup>, Guilhem J Collier<sup>1</sup>, Graham Norquay<sup>1</sup>, Lars E Olsson<sup>3</sup>, Per Wollmer<sup>3</sup>, Jakob Löndahl<sup>2</sup>, and Jim M Wild<sup>1</sup>

<sup>1</sup>Academic Radiology, University of Sheffield, Sheffield, United Kingdom, <sup>2</sup>Division of Ergonomics and Aerosol Technology, Lund University, Lund, Sweden, <sup>3</sup>Department of Translational Medicine, Lund University, Malmö, Sweden

Airspace Dimension Assessment with inhaled nanoparticles (AiDA) and hyperpolarized <sup>129</sup>Xe diffusion-weighted (DW)-MRI was performed in twenty-three healthy volunteers to benchmark measurements from AiDA against those from <sup>129</sup>Xe DW-MRI. Significant correlations were observed between AiDA derived root mean square distal airspace radius, and <sup>129</sup>Xe apparent diffusion coefficient and diffusion model derived acinar airway dimensions. Furthermore, the AiDA recovery at zero-second breath-hold significantly correlated with <sup>129</sup>Xe alpha index from the stretched exponential model, a marker of acinar airspace heterogeneity. This benchmarking study demonstrates the potential of AiDA as an alternative method for the clinical evaluation of acinar airway microstructure changes.

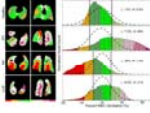


### Quantitative dose-dependent changes in regional lung function after radiation therapy detected using xenon-129 gas exchange MRI

Leith Rankine<sup>1,2</sup>, Ziyi Wang<sup>1</sup>, Elianna Bier<sup>1</sup>, Christopher Kelsey<sup>3</sup>, Shiva Das<sup>2</sup>, Lawrence Marks<sup>2</sup>, and Bastiaan Driehuys<sup>1</sup>

<sup>1</sup>Center for In Vivo Microscopy, Duke University, Durham, NC, United States, <sup>2</sup>Department of Radiation Oncology, University of North Carolina, Chapel Hill, NC, United States, <sup>3</sup>Department of Radiation Oncology, Duke University Medical Center, Durham, NC, United States

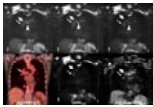
Radiation therapy (RT) is widely used to treat lung cancer, but damage to surrounding healthy tissues can lead to compromised lung function. In this study, patients undergoing RT were imaged pre- and post-treatment using hyperpolarized <sup>129</sup>Xe gas exchange MRI to assess for RT-induced changes in regional lung function. At 3-months post-treatment, a dose-response was evident in ventilation and gas exchange. Lung regions receiving  $\geq 20$ Gy exhibited significantly increased barrier uptake and decreased RBC transfer. This may help radiation oncologists further understand the dose-dependence of RT-induced lung injury, and design dose distributions with fewer treatment toxicities.



Peter James Niedbalski<sup>1</sup>, Elianna A Bier<sup>2,3</sup>, Ziyi Wang<sup>2,3</sup>, Matthew M Willmering<sup>1</sup>, Bastiaan Driehuys<sup>2,3,4</sup>, and Zackary I Cleveland<sup>1,5</sup>

<sup>1</sup>Center for Pulmonary Imaging Research, Cincinnati Children's Hospital Medical Center, Cincinnati, OH, United States, <sup>2</sup>Department of Biomedical Engineering, Duke University, Durham, NC, United States, <sup>3</sup>Center for In Vivo Microscopy, Duke University Medical Center, Durham, NC, United States, <sup>4</sup>Department of Radiology, Duke University Medical Center, Durham, NC, United States, <sup>5</sup>Department of Pediatrics, University of Cincinnati Medical Center, Cincinnati, OH, United States

Hyperpolarized <sup>129</sup>Xe MRI offers the ability to analyze pulmonary gas transfer by imaging <sup>129</sup>Xe dissolved in red blood cells (RBCs) separately from <sup>129</sup>Xe in other tissues. A notable feature of the dissolved <sup>129</sup>Xe signal is the presence of small cardiogenic oscillations in the <sup>129</sup>Xe RBC signal, which have been used to characterize global abnormalities in pulmonary microvascular hemodynamics. Here, we demonstrate that these cardiogenic oscillations can be mapped 3-dimensionally to image capillary bed hemodynamics. Our approach uses keyhole reconstruction of standard <sup>129</sup>Xe gas exchange MR acquisitions. Metrics obtained from these maps distinguished healthy from disease cohorts and predicted disease progression.

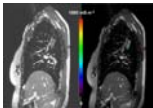


Computed Diffusion-Weighted Imaging in the Thorax: Determination of Appropriate b Value for Improving N-Stage Assessment in NSCLC Patients

Yoshiharu Ohno<sup>1,2</sup>, Masao Yui<sup>3</sup>, Daisuke Takenaka<sup>4</sup>, Yoshimori Kassai<sup>3</sup>, Kazuhiro Murayama<sup>1</sup>, and Takeshi Yoshikawa<sup>2</sup>

<sup>1</sup>Radiology, Fujita Health University School of Medicine, Toyoake, Japan, <sup>2</sup>Radiology, Kobe University Graduate School of Medicine, Kobe, Japan, <sup>3</sup>Canon Medical Systems Corporation, Otawara, Japan, <sup>4</sup>Diagnostic Radiology, Hyogo Cancer Center, Akashi, Japan

No major papers that determined the utility of cDWI for diagnosis of lymph node metastasis have been reported. We hypothesize that cDWI has a potential for improving diagnostic performance of N-stage in NSCLC patients as compared with aDWI and FDG-PET/CT, when set appropriate b value. The purpose of this study is to determine the utility of cDWI for differentiating metastatic from non-metastatic lymph nodes in NSCLC patients as compared with aDWI and FDG-PET/CT.

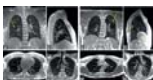


Noninvasive Assessment of Electrical Conductivity of Lung and Mediastinal Mass Lesions: Feasibility and Potential Clinical Value

Khin Khin Tha<sup>1,2</sup>, Ulrich Katscher<sup>3</sup>, Eiki Kikuchi<sup>4</sup>, Yasuka Kikuchi<sup>1</sup>, Yuki Yoshino<sup>1</sup>, Kinya Ishizaka<sup>5</sup>, Noriko Manabe<sup>1,2</sup>, Kohsuke Kudo<sup>1,2</sup>, and Hiroki Shirato<sup>2</sup>

<sup>1</sup>Department of Diagnostic and Interventional Radiology, Hokkaido University Hospital, Sapporo, Japan, <sup>2</sup>Global Station for Quantum Medical Science and Engineering, Hokkaido University, Sapporo, Japan, <sup>3</sup>Philips Research Laboratories, Hamburg, Germany, <sup>4</sup>First Department of Medicine, Hokkaido University Hospital, Sapporo, Japan, <sup>5</sup>Department of Radiological Technology, Hokkaido University Hospital, Sapporo, Japan

We evaluated the feasibility of  $\sigma$  measurable by EPT in evaluating lung and mediastinal mass lesions. EPT was performed in 21 patients with lung or mediastinal mass lesions. The lesion  $\sigma$  distribution, its relationship with histological findings, lesion size, location and the number of successful scans were evaluated. The malignant tumors had larger maximum  $\sigma$  and intralesional standard deviation and contrast. The larger the lesions, the greater were the intralesional contrast and entropy. The number of possible dynamic scans for reconstruction appeared to be larger in the upper lobe tumors, but the findings need to be confirmed with larger samples.

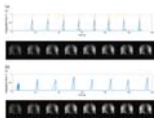


Thoracic imaging using balanced steady-state free precession with half-radial dual-echo readout (bSTAR)

Grzegorz Bauman<sup>1,2</sup> and Oliver Bier<sup>1,2</sup>

This work demonstrates the application of single-breathhold thoracic MRI with balanced steady-state free precession half-radial dual-echo readout technique (bSTAR) in human subjects. The proposed imaging technique combines a minimal-TR acquisition with a smoothly interleaved Archimedean spiral trajectory, which results in markedly improved signal intensity from low proton lung parenchyma tissue, improved visualization of the pulmonary vascular tree as well as a successful mitigation of eddy current and cardiac motion artifacts.

0436



### Volume-controlled <sup>19</sup>F MR imaging of fluorinated gas wash-in

Arnd Jonathan Obert<sup>1,2</sup>, Marcel Gutberlet<sup>1,2</sup>, Agilo Luitger Kern<sup>1,2</sup>, Frank Wacker<sup>1,2</sup>, and Jens Vogel-Claussen<sup>1,2</sup>

<sup>1</sup>Institute of Diagnostic and Interventional Radiology, Hannover Medical School, Hannover, Germany, <sup>2</sup>Biomedical Research in Endstage and Obstructive Lung Disease Hannover (BREATH), German Center for Lung Research (DZL), Hannover, Germany

Since Perfluoropropane is highly inert, and can be mixed with oxygen, patients can inhale up to 30 liters of gas during one examination without a significant physiological impact. This enables detailed measurements of gas wash-in dynamics using <sup>19</sup>F magnetic resonance imaging. In this work, an experimental setup for volume-controlled imaging of multiple breath-holds is realized using a pneumotachometer and pneumatic valves as well as MR triggering. In three healthy volunteers, the stability of the breathing volumes and the positions of the diaphragm, as well as the standard deviation of wash-in times, were analyzed comparing volume-controlled to non-controlled scans.

## Oral - Power Pitch

### Thoracic/Lung MRI - Pulmonary Power

Tuesday Parallel 3 Live Q&A

Tuesday 13:45 - 14:30 UTC

Moderators: Peter Thelwall

0437

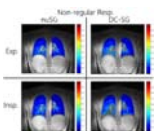


### Which is the Best Method for NSCLC Recurrence Evaluation among MRI, PET/MRI, PET/CT and Standard Examination in Large Prospective Cohort?

Yoshiharu Ohno<sup>1,2</sup>, Masao Yui<sup>3</sup>, Kota Aoyagi<sup>3</sup>, Yoshimori Kassaï<sup>3</sup>, Daisuke Takenaka<sup>4</sup>, Kazuhiro Murayama<sup>1</sup>, and Takeshi Yoshikawa<sup>2</sup>

<sup>1</sup>Radiology, Fujita Health University School of Medicine, Toyoake, Japan, <sup>2</sup>Radiology, Kobe University Graduate School of Medicine, Kobe, Japan, <sup>3</sup>Canon Medical Systems Corporation, Otawara, Japan, <sup>4</sup>Diagnostic Radiology, Hyogo Cancer Center, Akashi, Japan

Direct comparison of non-small cell lung cancer (NSCLC) recurrence evaluation among these four methods in large prospective cohort more than 400 patients had not been reported. We hypothesize that whole-body MRI as well as PET/MRI had better potential for postoperative NSCLC recurrence than PET/CT and standard radiological examination in large prospective cohort. The purpose of this study was thus to compare the diagnostic performance of whole-body MRI, PET/MRI, PET/CT and standard radiological examination for postoperative NSCLC recurrence assessment in large prospective cohort more than 400 patients.



### Lung Imaging and Proton Fraction Quantification for Highly Irregular Respiratory Patterns Using Nonuniform Self-Gating

Patrick Metzke<sup>1</sup>, Tobias Speidel<sup>2</sup>, Fabian Straubmüller<sup>1</sup>, and Volker Rasche<sup>1,2</sup>

<sup>1</sup>Department of Internal Medicine II, University Ulm Medical Center, Ulm, Germany, <sup>2</sup>Core Facility Small Animal Imaging (CF-SANI), Ulm University, Ulm, Germany

Most self-gating methods rely on information that is extracted either from *k*-space itself or from high temporal resolution sliding-window images. The obtained one-dimensional gating signal is analysed with respect to a dominant and characteristic frequency. These approaches are prone to fail in case of highly non-uniform motion.

The presented application of nonuniform Self-Gating based on a two-dimensional correlation matrix is capable of achieving high resolution proton fraction maps in human subjects with non-regular respiratory motion without the need of time consuming respiratory gating during acquisition.

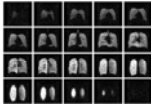


### 3D-SBCSI Xenon-129 lung MRI: Comparison of Healthy, CF, IPF, and COPD Subjects

Vicki Huang<sup>1</sup>, Steven Guan<sup>1</sup>, Nick Tustison<sup>1</sup>, Kun Qing<sup>1</sup>, Yun Shim<sup>2</sup>, John Mugler<sup>1</sup>, Talissa Altes<sup>3</sup>, Dana Albon<sup>2</sup>, Deborah Froh<sup>2</sup>, Borna Mehrad<sup>4</sup>, James Patrie<sup>5</sup>, Allan Ropp<sup>1</sup>, Lucy Gettle<sup>2</sup>, Mu He<sup>1</sup>, and Jaime Mata<sup>1</sup>

<sup>1</sup>Radiology & Medical Imaging, University of Virginia, Charlottesville, VA, United States, <sup>2</sup>Medicine, University of Virginia, Charlottesville, VA, United States, <sup>3</sup>Radiology, University of Missouri, Columbia, MO, United States, <sup>4</sup>University of Florida, Gainesville, FL, United States, <sup>5</sup>Public Health, University of Virginia, Charlottesville, VA, United States

The results of this study indicated that hyperpolarized Xe-129 MR 3D-SBCSI is sensitive to physiology of lung diseases and can therefore be used to differentiate lung disease and monitor disease progression on regional level and characterizing disease phenotypes and co-morbidities in the future.



### <sup>19</sup>F-MRI of inhaled perfluoropropane for assessment of pulmonary ventilation: a multi-centre reproducibility study in healthy volunteers

Mary Neal<sup>1,2</sup>, Benjamin Pippard<sup>1,2</sup>, Adam Maunder<sup>3</sup>, Rod Lawson<sup>4</sup>, Holly F. Fisher<sup>5</sup>, John N. S. Matthews<sup>5</sup>, Kieren Hollingsworth<sup>1,2</sup>, A. John Simpson<sup>2</sup>, Jim M. Wild<sup>3</sup>, and Pete Thelwall<sup>1,2</sup>

<sup>1</sup>Newcastle Magnetic Resonance Centre, Newcastle University, Newcastle upon Tyne, United Kingdom, <sup>2</sup>Translational and Clinical Research Institute, Newcastle University, Newcastle upon Tyne, United Kingdom, <sup>3</sup>POLARIS, Academic Radiology, University of Sheffield, Sheffield, United Kingdom, <sup>4</sup>Sheffield Teaching Hospitals NHS Foundation Trust, Sheffield, United Kingdom, <sup>5</sup>Institute of Health and Society, Newcastle University, Newcastle upon Tyne, United Kingdom

<sup>19</sup>F-MRI of inhaled perfluoropropane can be used to assess regional pulmonary ventilation. We conducted a prospective multi-centre reproducibility study in 40 healthy volunteers. Same-day static breath-hold <sup>19</sup>F-MR images with 1 cm isotropic resolution were acquired on four occasions for each volunteer following inhalation of a perfluoropropane/oxygen gas mixture. Percentage ventilated lung volume (%VV) was calculated for all volunteers, reflecting the inhalation protocol, imaging protocol, and image registration and segmentation process applied. Volunteer %VV was determined to within  $\pm 1.7\%$  (95% CI). Gas inhalations were well tolerated by all volunteers with no adverse events.



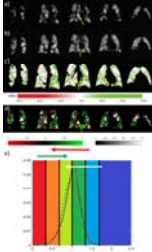
### Novel MRI-based Clusters of Asthma: Pulmonary Functional MRI and CT

Rachel L Eddy<sup>1,2</sup>, Christopher Liciskai<sup>3</sup>, David G McCormack<sup>3</sup>, and Grace Parraga<sup>1,2,3</sup>

<sup>1</sup>Robarts Research Institute, London, ON, Canada, <sup>2</sup>Department of Medical Biophysics, Western University, London, ON, Canada, <sup>3</sup>Division of Respiriology, Department of Medicine, Western University, London, ON, Canada

Pulmonary functional MRI measurements have never been evaluated for the generation of imaging-based asthma patient clusters, although computed tomography (CT)-based clusters have been determined. Here we investigated hyperpolarized inhaled gas MRI ventilation in combination with CT airway measurements in 60 patients with asthma and identified 6 pulmonary structure-function imaging-based clusters using MRI ventilation defect percent (VDP) and CT airway measurements. These clusters reflect proximal and distal airway abnormalities in asthma and may be used to stratify patients for treatment decisions.

0442



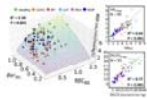
Binning method for treatment response mapping with hyperpolarized gas lung MRI: application in subjects with asthma

Guilhem Jean Collier<sup>1</sup>, Alberto Biancardi<sup>1</sup>, Paul J Hughes<sup>1</sup>, Laurie Smith<sup>1</sup>, Grace T Mussel<sup>1</sup>, Helen Marshall<sup>1</sup>, Ho F Chan<sup>1</sup>, Graham Norquay<sup>1</sup>, and Jim M Wild<sup>1</sup>

<sup>1</sup>Department of Infection, Immunity & Cardiovascular Disease, University of Sheffield, Sheffield, United Kingdom

This work applies a clustering method developed for image analysis of hyperpolarised gas lung ventilation MRI to a cohort of patients referred from a severe asthma clinic for investigation of breathlessness. Patients underwent spirometry tests and imaging at baseline and after inhalation of Salbutamol to assess reversibility. In a subset of patients, images pre and post bronchodilator were registered and a novel treatment response mapping method was applied. Results show significant correlations at baseline between imaging markers and FEV1% and between their percentage changes and the reversibility testing. The treatment response mapping method offers additional robust additional insights.

0443



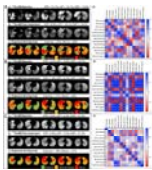
A Model for Interpreting Hyperpolarized <sup>129</sup>Xe Gas Exchange MRI

Ziyi Wang<sup>1</sup>, Leith Rankine<sup>1</sup>, Aparna Swaminathan<sup>1</sup>, Elianna A Bier<sup>1</sup>, Matthew P Thorpe<sup>2</sup>, Robert Tighe<sup>1</sup>, Yuh Chin Huang<sup>1</sup>, Sudarshan Rajagopal<sup>1</sup>, and Bastiaan Driehuys<sup>1</sup>

<sup>1</sup>Duke University, Durham, NC, United States, <sup>2</sup>Mayo Clinic, Rochester, MN, United States

Hyperpolarized <sup>129</sup>Xe gas exchange (GX) MR imaging of pulmonary ventilation, barrier uptake and red blood cell (RBC) transfer has shown sensitivity to a wide range of pathology. However, the physiological interpretation of regional RBC transfer defects is not yet fully established and its connection to conventional measures has yet to be studied in a broad range of pathology. Here we evaluate the extent to which <sup>129</sup>Xe RBC transfer reflects local perfusion, by testing its spatial correlation to <sup>99m</sup>Tc scintigraphy and propose a generalized model connecting <sup>129</sup>Xe gas exchange metrics to the membrane and capillary blood volume components of DL<sub>CO</sub>.

0444



Longitudinal lobar analysis to assess variable dynamic airflow changes in asthma with hyperpolarized helium-3 MRI

Mu He<sup>1</sup>, Lindsay A. L. Somerville<sup>1</sup>, Nicolas J. Tustison<sup>2</sup>, Jaime F. Mata<sup>2</sup>, Joanne M. Cassani<sup>3</sup>, Roselove Nunoo-Asare<sup>2</sup>, Alan M. Ropp<sup>2</sup>, Wilson G. Miller<sup>2</sup>, Yun M. Shim<sup>1</sup>, Talissa A. Altes<sup>3</sup>, John P. Mugler<sup>2</sup>, and Eduard E. de Lange<sup>2</sup>

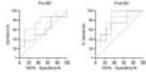
<sup>1</sup>Department of Pulmonary and Critical Care, University of Virginia, Charlottesville, VA, United States,

<sup>2</sup>Department of Radiology and Medical Imaging, University of Virginia, Charlottesville, VA, United States,

<sup>3</sup>Department of Radiology, University of Missouri, Columbia, MO, United States

With hyperpolarized  $^3\text{He}$  MRI regional differences in airflow can be assessed. We sought to evaluate the changes in regional ventilation following bronchodilator therapy in patients with asthma. Baseline and post-treatment  $^3\text{He}/^1\text{H}$  scans were co-registered, and normalized to enable serial comparison. Linear binning quantification was applied to the ventilation scan data to obtain quantitative metrics. Baseline and post-treatment scans were compared for regions of ventilation improvement or worsening. Lobar analysis was performed to identify ventilation abnormalities in each lobe. It was found that in asthmatics with bronchodilator response, ventilation improved globally, with most significant improvement in the upper and middle lobes.

0445



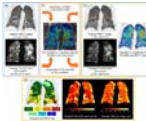
Supervised shallow learning of  $^{129}\text{Xe}$  MRI texture features to predict response to Anti-IL-5 biologic therapy in severe asthma

Marrissa McIntosh<sup>1</sup>, Rachel Eddy<sup>1</sup>, Danielle Knipping<sup>2</sup>, Tamas Lindenmaier<sup>2</sup>, David McCormack<sup>3</sup>, Christopher Liciskai<sup>3</sup>, Cory Yamashita<sup>3</sup>, and Grace Parraga<sup>4</sup>

<sup>1</sup>Department of Medical Biophysics, Robarts Research Institute, Western University, London, ON, Canada, <sup>2</sup>Robarts Research Institute, Western University, London, ON, Canada, <sup>3</sup>Division of Respiriology, Department of Medicine, Western University, London, ON, Canada, <sup>4</sup>Department of Medical Biophysics, Division of Respiriology, Department of Medicine, Robarts Research Institute, Western University, London, ON, Canada

$^{129}\text{Xe}$  MRI ventilation images consist of embedded texture features that help explain abnormal ventilation heterogeneity. We postulated that such texture features may help predict severe asthma patient response to anti-IL-5 therapies. Therefore, we employed supervised shallow learning techniques to identify specific  $^{129}\text{Xe}$  MRI features that help predict anti-IL-5 responders. Texture analysis yielded features that were superior to clinical measurements in identifying severe asthma patients that responded to anti-IL-5 therapy after 28 days. These promising results suggest that texture analysis may help predict asthmatics more likely to respond, before treatment is initiated.

0446



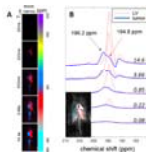
Voxel-wise comparison of co-registered quantitative CT and hyperpolarized gas diffusion-weighted MRI measurements in IPF

Ho-Fung Chan<sup>1</sup>, Alberto Biancardi<sup>1</sup>, Bilal A Tahir<sup>1</sup>, Nicholas D Weatherley<sup>1</sup>, Ronald A Karwoski<sup>2</sup>, Brian J Bartholmai<sup>2</sup>, Stephen M Bianchi<sup>3</sup>, and Jim M Wild<sup>1</sup>

<sup>1</sup>Academic Radiology, University of Sheffield, Sheffield, United Kingdom, <sup>2</sup>Biomedical Imaging Resource, Mayo Clinic, Rochester, MN, United States, <sup>3</sup>Academic Directorate of Respiratory Medicine, Sheffield Teaching Hospitals NHS Foundation Trust, Sheffield, United Kingdom

A framework for spatial co-registration of  $^3\text{He}$  diffusion-weighted (DW)-MRI and high resolution CT (HRCT) images was developed and implemented in a cohort of fifteen idiopathic pulmonary fibrosis participants. Voxel-wise comparison of  $^3\text{He}$  DW-MRI derived apparent diffusion coefficient (ADC) and mean alveolar dimension ( $L_{mD}$ ) with CALIPER image analysis software classifications revealed that the largest DW-MRI metrics are in voxels classified as honeycombing. Furthermore,  $L_{mD}$  values in voxels classified as normal by CALIPER were larger than those from age-matched healthy volunteers, suggesting DW-MRI may detect microstructural changes even in areas of the lung determined as macroscopically normal by HRCT.

0447



Hyperpolarized  $^{129}\text{Xe}$  Imaging of Oxygenated and Deoxygenated Blood in a Free-Breathing Mouse

Luis A Loza<sup>1</sup>, Stephen J Kadlecsek<sup>1</sup>, Mehrdad Pourfathi<sup>1</sup>, Kai Ruppert<sup>1</sup>, Tahmina S Achekzai<sup>1</sup>, Ian F Duncan<sup>1</sup>, and Rahim R Rizzi<sup>1</sup>

<sup>1</sup>Radiology, University of Pennsylvania, Philadelphia, PA, United States



<sup>129</sup>Xe's high solubility in tissue and blood, coupled with its dramatic change in chemical shift based on local chemical environment, enables quantitative measurements of blood oxygenation. In this work, we demonstrate a technique for distinguishing oxygenated vs. deoxygenated blood in the mouse circulatory system in vivo. Time-resolved dissolved-phase images and spectra were used to identify spectral signatures for <sup>129</sup>Xe dissolved in oxygenated and deoxygenated blood, which were then applied to a mouse model of lung cancer to temporally assess regional changes in pulmonary blood oxygenation. The results presented here demonstrate

0448



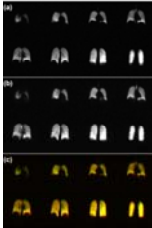
#### Dual Center and Dual Vendor feasibility of perfusion-weighted phase resolved functional lung (PREFUL) MRI in CF patients

Lea Behrendt<sup>1,2</sup>, Andreas Voskrebenezv<sup>1,2</sup>, Cristian Crisosto Gonzalez<sup>1,2</sup>, Marcel Gutberlet<sup>1,2</sup>, Helen Marshall<sup>3</sup>, Anna-Maria Dittrich<sup>4</sup>, Laurie Smith<sup>3</sup>, Paul Hughes<sup>3</sup>, Jim Wild<sup>3</sup>, and Jens Vogel-Claussen<sup>1,2</sup>

<sup>1</sup>Institute of Diagnostic and Interventional Radiology, Hannover Medical School, Hannover, Germany, <sup>2</sup>Biomedical Research in Endstage and Obstructive Lung Disease Hannover (BREATH), German Center for Lung Research (DZL), Hannover, Germany, <sup>3</sup>University of Sheffield, Sheffield, United Kingdom, <sup>4</sup>Paediatric Pneumology and Neonatology, Hannover Medical School, Hannover, Germany

Dynamic contrast enhanced (DCE) MRI is an established technique for measurement of lung perfusion, but requires the administration of contrast agents and a breath hold. Thus, methods for contrast agent free assessment of lung perfusion in free breathing, like phase resolved functional lung (PREFUL) MRI, are desirable. Therefore, in this dual center and dual vendor feasibility study, we validated PREFUL MRI against DCE MRI in patients with CF. Perfusion defect percentage (QDP) maps of both methods were calculated, showing an overlap of 61% for the whole lung. Further, a strong correlation between QDP<sub>PREFUL</sub> and QDP<sub>DCE</sub> was found ( $r=0.70$ ,  $p=0.005$ ).

0449



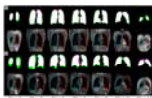
#### Comparison of 3D Stack-of-Spirals and 2D Gradient Echo for Ventilation Mapping using Hyperpolarized <sup>129</sup>Xe

Brandon Zanette<sup>1</sup>, Yonni Friedlander<sup>1,2</sup>, Samal Munidasa<sup>1,2</sup>, and Giles Santyr<sup>1,2</sup>

<sup>1</sup>Translational Medicine, The Hospital for Sick Children, Toronto, ON, Canada, <sup>2</sup>Medical Biophysics, University of Toronto, Toronto, ON, Canada

Hyperpolarized <sup>129</sup>Xe MRI is an emergent tool for the quantification of ventilation defects in the lungs. <sup>129</sup>Xe is typically imaged with 2D gradient recalled echo (2D-GRE) which may require lengthy breath-holds (up to 16s) to image the lung. This may be problematic in subjects who are not able to comply with these breath-hold constraints. Non-Cartesian spiral imaging samples k-space more efficiently, reducing the acquisition duration. In this work a 3D stack-of-spirals (3D-SoS) imaging sequence was developed and tested in healthy adults alongside conventional 2D-GRE for hyperpolarized <sup>129</sup>Xe ventilation mapping, showing equivalent ventilation defect percent quantification in a ~2 s scan.

0450



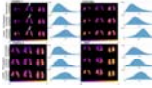
#### Fully-automated 1H MRI Thoracic Cavity Segmentation for Hyperpolarized Gas Imaging using a Convolutional Neural Network

Alexander M Matheson<sup>1</sup>, Rachel L Eddy<sup>1</sup>, Jonathan L MacNeil<sup>2</sup>, Marrison L McIntosh<sup>1</sup>, and Grace Parraga<sup>1,2</sup>

<sup>1</sup>Medical Biophysics, Robarts Research Institute, Western University, London, ON, Canada, <sup>2</sup>School of Biomedical Engineering, Robarts Research Institute, Western University, London, ON, Canada

Thoracic segmentations are crucial for accurate measurements of normalized lung ventilation, perfusion and gas exchange. Current semi-automated methods are time consuming, require experienced readers, and lack the standardization of fully-automated methods, such as convolutional neural networks. We retrospectively pooled data from 449 healthy and respiratory disease participants, resulting in a 55,000 slice augmented data set to train a dense v-net neural network. The network produced segmentations qualitatively matching semi-automated methods, with high Dice scores and an area under the receiver operating characteristic curve of 0.997. Implementation on the NiftyNet platform permits quick model dissemination for multi-site validation.

0451



### Bias Field Correction in Hyperpolarized $^{129}\text{Xe}$ Gas Ventilation MRI

Junlan Lu<sup>1</sup>, Ziyi Wang<sup>2</sup>, John C. Nouls<sup>3</sup>, Kush Gulati<sup>2</sup>, Elianna Bier<sup>2</sup>, David Mummy<sup>3</sup>, and Bastiaan Driehuys<sup>3</sup>

<sup>1</sup>Medical Physics Graduate Program, Duke University, Durham, NC, United States, <sup>2</sup>Biomedical Engineering, Duke University, Durham, NC, United States, <sup>3</sup>Radiology, Duke University, Durham, NC, United States

The presence of RF inhomogeneity in hyperpolarized  $^{129}\text{Xe}$  ventilation MRI affects quantitative analysis and interpretation. These inhomogeneities are commonly corrected using the N4ITK algorithm, which retrospectively calculates a smoothly varying bias field with non-uniform intensity normalization. However, this algorithm has not been rigorously validated for functional imaging. Here we show, using flip angle maps derived directly from 3D-radial acquisitions of ventilation, that N4ITK may over-correct bias field and remove inherent physiological gradients. We illustrate this comparison by a combination of simulation, phantom, and in vivo ventilation imaging.

## Combined Educational & Scientific Session

### Other Nuclei MRI and MRS to Study Metabolism - Biophysics & Metabolism Studied with Imaging & Spectroscopy of Non-Hyperpolarized X-Nuclei

Organizers: Ronald Ouwerkerk

Tuesday Parallel 5 Live Q&A

Tuesday 13:45 - 14:30 UTC

Moderators: Ravinder Reddy

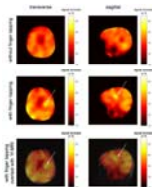
#### Imaging Biophysics & Metabolism with Other Nuclei ( $^{23}\text{Na}$ , $^{17}\text{O}$ , $^{39}\text{K}$ )

Jean-Philippe Ranjeva<sup>1</sup>

<sup>1</sup>CRMBM, France

In light of technical advancements supporting exploration of MR signals other than  $^1\text{H}$ , MRI of other nuclei having magnetic properties such as sodium ( $^{23}\text{Na}$ ), Oxygen ( $^{17}\text{O}$ ) or potassium ( $^{39}\text{K}$ ) is developing in parallel with the increase of the magnetic fields of clinical MR scanners. These modalities receive attention as markers of ionic homeostasis and cell viability ( $^{23}\text{Na}$ ,  $^{39}\text{K}$ ) or provide non-invasive way to determine cerebral metabolic rate of oxygen ( $\text{CMRO}_2$ ) consumption using  $^{17}\text{O}$  MRI. During this course, we will present the practical issues to conduct MRI of these particular nuclei, hypotheses and proxy to derive the biophysical parameters from these images

0472



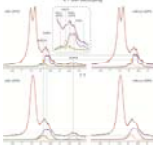
### Mapping neuronal activity associated with finger tapping using direct measurement of $^{17}\text{O}$ at 7 Tesla: proof-of-concept experiment

Tanja Platt<sup>1</sup>, Louise Ebersberger<sup>2,3</sup>, Vanessa L Franke<sup>1,4</sup>, Armin M Nagel<sup>1,5,6</sup>, Reiner Umathum<sup>1</sup>, Heinz-Peter Schlemmer<sup>2</sup>, Peter Bachert<sup>1,4</sup>, Mark E Ladd<sup>1,3,4</sup>, Andreas Korzowski<sup>1</sup>, Sebastian C Niesporek<sup>1</sup>, and Daniel Paech<sup>2</sup>

<sup>1</sup>Medical Physics in Radiology, German Cancer Research Center, Heidelberg, Germany, <sup>2</sup>Radiology, German Cancer Research Center, Heidelberg, Germany, <sup>3</sup>Faculty of Medicine, University of Heidelberg, Heidelberg, Germany, <sup>4</sup>Faculty of Physics and Astronomy, University of Heidelberg, Heidelberg, Germany, <sup>5</sup>Institute of Radiology, University Hospital Erlangen, Erlangen, Germany, <sup>6</sup>Institute of Medical Physics, Friedrich-Alexander-Universität Erlangen-Nürnberg (FAU), Erlangen, Germany

Dynamic  $^{17}\text{O}$ -MRI enables direct quantification of the cerebral metabolic rate of oxygen ( $\text{CMRO}_2$ ) consumption. We investigated hemispherical dependence of the method in three healthy volunteers as well as its potential for mapping neuronal activity associated with finger tapping in one healthy volunteer. Our findings were consistent with previous results, demonstrating higher  $\text{CMRO}_2$  values in gray compared to white matter. Evaluation of left/right hemispheric  $\text{CMRO}_2$  values without sensorimotor stimulation demonstrated hemispherical independence of the technique. The finger-tapping experiment demonstrated increased  $^{17}\text{O}$ -signal in the stimulated sensorimotor cortex and adjacent brain tissue, indicating that dynamic  $^{17}\text{O}$ -MRI may permit visualization of physiological neuronal activity.

0473



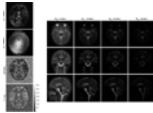
In vivo NAD<sup>+</sup>/NADH Measurements in the Human Brain using 31P MRS at 4 T and 7 T

Xi Chen<sup>1</sup>, Elliot Kuan<sup>2</sup>, Dost Ongur<sup>1</sup>, Wei Chen<sup>3</sup>, and Fei Du<sup>1</sup>

<sup>1</sup>McLean Hospital; Harvard Medical School, Belmont, MA, United States, <sup>2</sup>McLean Hospital, Belmont, MA, United States, <sup>3</sup>University of Minnesota, Minneapolis, MN, United States

Nicotinamide adenine dinucleotides play a crucial role in human health, but measuring the redox ratio (NAD<sup>+</sup>/NADH) in vivo is technically challenging and the confounding effects from UDPG remain unclear. In this study, for the first time we observed that the NAD<sup>+</sup>/NADH values decreased in 4T proton-decoupling spectra when the UDPG contribution was accounted for as well as confirming the opposite trend at 7T. Furthermore, we revealed different overlapping patterns at 4T and 7T which lead to this result. Finally, individual redox ratio measures with and without UDPG quantification are strongly correlated with one another at both 4T and 7T.

0474



Multiplexed Measurement of Multiple Nuclei (M3N) for integrated multi-nuclei imaging and parametric mapping in  $^{23}\text{Na}$  and  $^1\text{H}$  MRI

Yasmin Blunck<sup>1,2</sup>, Daniel Staeb<sup>3</sup>, Rebecca K Glarin<sup>2,4,5</sup>, Bradford A Moffat<sup>2,4</sup>, Kieran O'Brien<sup>6</sup>, and Leigh A Johnston<sup>1,2</sup>

<sup>1</sup>Department of Biomedical Engineering, University of Melbourne, Parkville, Australia, <sup>2</sup>Melbourne Brain Centre Imaging Unit, University of Melbourne, Parkville, Australia, <sup>3</sup>MR Research Collaborations, Siemens Healthcare Pty Ltd, Melbourne, Australia, <sup>4</sup>Department of Medicine & Radiology, University of Melbourne, Parkville, Australia, <sup>5</sup>Department of Radiology, Royal Melbourne Hospital, Parkville, Australia, <sup>6</sup>MR Research Collaborations, Siemens Healthcare Pty Ltd, Brisbane, Australia

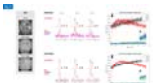
X-nuclei imaging like sodium MRI offers complementary information to  $^1\text{H}$ -based imaging. However, its clinical translation is hampered by the significant increase in scan time required for the acquisition of an additional nuclei. Addressing this challenge, this work introduces Multiplexed Measurement of Multiple Nuclei (M<sup>3</sup>N) sequences and proposes MERINA-MP2RAGE, a multi-nuclei sequence, that embeds sodium MRI in a  $^1\text{H}$ -MP2RAGE acquisition. The developed sequence was implemented on a 7T MRI and tested in phantom and human in vivo experiments. Merging  $^1\text{H}$ -MP2RAGE and  $^{23}\text{Na}$ -MERINA reduces the total scan time by 40% compared to sequential acquisitions while maintaining uncompromised image quality.

Metabolic Processes Studied with Non-Hyperpolarized Other Nuclei (Deuterium)

Henk M. De Feyter<sup>1</sup>

<sup>1</sup>Department of Radiology and Biomedical Imaging, Yale University School of Medicine, United States

0475



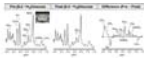
Dynamic assessment of early metabolic perturbations in glioma-bearing mice using denoised  $^2\text{H}$ -MRS

Rui V Simoes<sup>1</sup>, Javier Istúriz<sup>2</sup>, Jonas L Olesen<sup>3</sup>, Sune N Jespersen<sup>3</sup>, and Noam Shemesh<sup>1</sup>

<sup>1</sup>Champalimaud Research, Champalimaud Centre for the Unknown, Lisbon, Portugal, <sup>2</sup>Neos Biotec, Pamplona, Spain, <sup>3</sup>Center of Functionally Integrative Neuroscience (CFIN) and MINDLab, Department of Clinical Medicine, Aarhus University, Aarhus, Denmark

As our understanding of cancer metabolism advances, novel methods are needed to dynamically assess its heterogeneity in preclinical models, with high temporal resolution. Here we show the feasibility of dynamic <sup>2</sup>H-MRS in glioma-bearing mice to monitor glucose metabolism with <3s resolution. This was achieved with a new <sup>2</sup>H/<sup>1</sup>H RF coil design for the mouse brain and a novel application of Marchenko–Pastur denoising. We are now adapting this methodology to <sup>2</sup>H-MRSI, with high spatial resolution.

0476



Combining <sup>1</sup>H MRS with deuterium labeled glucose: A new strategy to assess dynamics of neural metabolism in vivo

Laurie J Rich<sup>1</sup>, Puneet Bagga<sup>1</sup>, Gabor Mizsei<sup>1</sup>, Mitchell D Schnell<sup>1</sup>, John A Detre<sup>2</sup>, Mohammad Haris<sup>3</sup>, and Ravinder Reddy<sup>1</sup>

<sup>1</sup>Radiology, University of Pennsylvania, Philadelphia, PA, United States, <sup>2</sup>Neurology, University of Pennsylvania, Philadelphia, PA, United States, <sup>3</sup>Research Branch, Qatar University, Doha, Qatar

Proton magnetic resonance spectroscopy (<sup>1</sup>H MRS) is a powerful technique capable of detecting a range of endogenous metabolites, but with currently existing approaches does not enable tracking of metabolic fluxes and pathways. We report a new strategy which utilizes <sup>1</sup>H MRS in conjunction with administration of deuterium (<sup>2</sup>H) labeled glucose to track downstream labeling of neural metabolites. Since <sup>2</sup>H is invisible on <sup>1</sup>H MRS, replacement of <sup>1</sup>H with <sup>2</sup>H leads to an overall reduction in <sup>1</sup>H MRS signal for the corresponding metabolites. Therefore, this approach makes it possible to monitor neural metabolism using conventional and widely available <sup>1</sup>H MRS methodologies.

## Oral

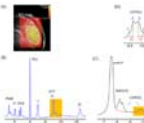
### Other Nuclei MRI and MRS to Study Metabolism - X-Nuclei MRS/MRI

Tuesday Parallel 5 Live Q&A

Tuesday 13:45 - 14:30 UTC

Moderators: Wafaa Zaaraoui & Xiao-Hong Zhu

0477



Detection of Multiple Nucleotide Sugars Including Uridine Diphosphate Hexoses and N-Acetyl Hexosamines in Human Brain by <sup>31</sup>P MRS at 7T

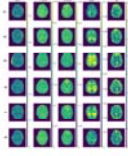
Jimin Ren<sup>1,2</sup>, Craig R Malloy<sup>1,2,3</sup>, and A Dean Sherry<sup>1,2,4</sup>

<sup>1</sup>Advanced Imaging Research Center, UT Southwestern Medical Center, Dallas, TX, United States, <sup>2</sup>Department of Radiology, UT Southwestern Medical Center, Dallas, TX, United States, <sup>3</sup>VA North Texas Health Care System, Dallas, TX, United States, <sup>4</sup>Department of Chemistry, University of Texas at Dallas, Richardson, TX, United States

A variety of nucleotide sugars (NS) are required for glycosylation of proteins and lipids to enhance and diversify cellular functions. The current 7T <sup>31</sup>P MRS study, for the first time, reports the detection of four different NS species in human brain in vivo. They are tentatively assigned to UDP-glucose, UDP-galactose, UDP-N-acetylglucosamine, and UDP-N-acetylgalactosamine, collectively denoted as UDP(G). These UDP (G) species are responsible for the observation of a “quartet-like” signal at -9.8 ppm, which cannot be explained by the presence of only a single UDP(G) species such as UDP-glucose (as expected to be a simple doublet).

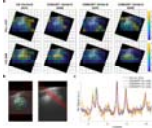
Phosphorus metabolic images of the human brain at 9.4 T using Chemical Shift Imaging: Investigation of differences in grey and white matter tissue

Loreen Ruhm<sup>1</sup>, Johanna Dorst<sup>1</sup>, Nikolai Avdievich<sup>1</sup>, and Anke Henning<sup>1,2</sup>



<sup>1</sup>Max Planck Institute for Biological Cybernetics, Tübingen, Germany, <sup>2</sup>UT Southwestern Medical Center, Dallas, TX, United States

<sup>31</sup>P Magnetic Resonance Spectroscopic Imaging (MRSI) is a non-invasive method that can reveal information about the energy and phospholipid metabolism. In this work, we investigate the differences in signal amplitudes of different <sup>31</sup>P metabolites between grey and white matter tissue in the human brain. We acquired highly resolved <sup>31</sup>P MRSI data at an ultrahigh field strength  $B_0$  of 9.4 T from the brain of six healthy volunteers. For the quantification of the <sup>31</sup>P MRSI data, different correction were applied to the signal amplitudes.

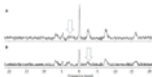


### <sup>31</sup>P-MRSI of the human heart in 2 ½ minutes at 7T using concentric rings (CONCEPT)

William T Clarke<sup>1</sup>, Lukas Hingerl<sup>2</sup>, Wolfgang Bogner<sup>2</sup>, Ladislav Valkovic<sup>3,4</sup>, and Christopher T Rodgers<sup>3,5</sup>

<sup>1</sup>Wellcome Centre for Integrative Neuroimaging, NDCN, University of Oxford, Oxford, United Kingdom, <sup>2</sup>High-field MR Centre, Department of Biomedical Imaging and Image-guided Therapy, Medical University of Vienna, Vienna, Austria, <sup>3</sup>Oxford Centre for Clinical Magnetic Resonance Research, Radcliffe Department of Medicine, University of Oxford, Oxford, United Kingdom, <sup>4</sup>Department of Imaging Methods, Institute of Measurement Science, Slovak Academy of Sciences, Bratislava, Slovakia, <sup>5</sup>Wolfson Brain Imaging Centre, Department of Clinical Neurosciences, University of Cambridge, Cambridge, United Kingdom

A density-weighted concentric ring trajectory MRSI sequence is implemented for cardiac <sup>31</sup>P-MRS at 7T. The sequence is characterised in phantoms and in five healthy participants. Quantitative comparisons are made against a previously implemented acquisition weighted CSI sequence with matched acquisition time and voxel size. The proposed sequence (CONCEPT) was found to robustly measure 3D localised PCr/ATP ratios of the human myocardium 2.59 times faster or with 1.73 times smaller nominal volume than standard acquisition weighted CSI.

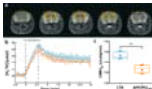


### Comparison of methods for measuring cerebral mitochondrial function with magnetisation transfer <sup>31</sup>P-MRS

Sam Keaveney<sup>1</sup>, Ross Maxwell<sup>1</sup>, Maelene Lohézić<sup>2</sup>, Rolf Schulte<sup>3</sup>, Ralph Noeske<sup>4</sup>, and Andrew Blamire<sup>1</sup>

<sup>1</sup>Newcastle Magnetic Resonance Centre, Newcastle University, Newcastle upon Tyne, United Kingdom, <sup>2</sup>GE Healthcare, Manchester, United Kingdom, <sup>3</sup>GE Healthcare, Munich, Germany, <sup>4</sup>GE Healthcare, Berlin, Germany

Mitochondrial function in the brain can be measured with magnetisation transfer <sup>31</sup>P-MRS. The conventional approach to magnetisation transfer incurs lengthy acquisition times, limiting the available spatial information. An accelerated approach, based on kinetic modelling, allows the technique to be extended to a multi-voxel implementation. Both approaches were applied in a group of healthy subjects to measure the rate of the creatine kinase reaction. There was good agreement between the reaction rates measured with the two methods in equivalently positioned voxels, validating the use of the accelerated approach to provide greater spatial resolution in future patient studies.



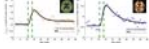
### Direct 17O-ZTE-MRI reveals decreased cerebral metabolic rate of oxygen consumption in a murine model of amyloidosis

Celine Baligand<sup>1,2</sup>, Jean-Baptiste Perot<sup>1,2</sup>, Didier Thenadey<sup>1,2</sup>, Julien Flament<sup>1,2</sup>, Marc Dhenain<sup>1,2</sup>, and Julien Valette<sup>1,2</sup>

<sup>1</sup>Molecular Imaging Research Center (MIRCent), Commissariat à l'Energie Atomique et aux Energies Alternatives (CEA), Fontenay-aux-Roses, France, <sup>2</sup>Neurodegenerative Diseases Laboratory (UMR 9199), Centre National de la Recherche Scientifique (CNRS), Université Paris-Sud, Université Paris-Saclay, Fontenay-aux-Roses, France

The cerebral metabolic rate of oxygen consumption (CMRO<sub>2</sub>) is an important metric of brain metabolism. It is of particular interest in preclinical studies of Alzheimer's disease, where amyloidosis has been associated with impaired mitochondrial function. CMRO<sub>2</sub> can be measured by direct <sup>17</sup>O-MRI of H<sub>2</sub><sup>17</sup>O signal changes during inhalation of <sup>17</sup>O-labeled oxygen gas. In this study, we used 3D zero echo time <sup>17</sup>O-(ZTE)-MRI at 11.7T to measure CMRO<sub>2</sub> in the APP/PS1<sub>dE9</sub> mouse model of amyloidosis and show that it is significantly lower than in control mice.

0482



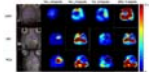
### Regional Analysis of CMRO<sub>2</sub> in Human Brain Using Dynamic <sup>17</sup>O-MRI

Hao Song<sup>1</sup>, Yanis Taege<sup>1</sup>, Johannes Fischer<sup>1</sup>, Ali Caglar Özen<sup>1,2</sup>, and Michael Bock<sup>1,2</sup>

<sup>1</sup>Dept. of Radiology, Medical Physics, Medical Center University of Freiburg, Faculty of Medicine, University of Freiburg, Freiburg, Germany, <sup>2</sup>German Consortium for Translational Cancer Research (DKTK) Partner Site Freiburg, German Cancer Research Center (DKFZ), Heidelberg, Germany

In this work, regional quantification of the cerebral metabolic rate of oxygen consumption (CMRO<sub>2</sub>) was performed using dynamic <sup>17</sup>O-MRI with inhalation of isotope-enriched <sup>17</sup>O<sub>2</sub>. First, global mean CMRO<sub>2</sub> values were determined in cortical grey matter and white matter. Then, local CMRO<sub>2</sub> was investigated in frontal, parietal and occipital areas, respectively. The results were in good agreement with previously reported PET values especially for the cortical grey matter. For regional analysis, the CMRO<sub>2</sub> values show good consistency across the white matter and in both frontal and parietal cortical grey matter.

0483



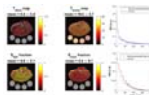
### Quantitative imaging of the transmembrane sodium gradient in brain tumors

Muhammad H. Khan<sup>1</sup>, John J. Walsh<sup>1</sup>, Sandeep K. Mishra<sup>2</sup>, Daniel Coman<sup>2</sup>, and Fahmeed Hyder<sup>1,2</sup>

<sup>1</sup>Biomedical Engineering, Yale University, New Haven, CT, United States, <sup>2</sup>Radiology & Biomedical Imaging, Yale University, New Haven, CT, United States

The transmembrane sodium gradient (difference between extracellular and intracellular concentrations) is necessary for the proper functioning of many bodily mechanisms, including action potential propagation and osmoregulation. While unbound sodium-23 (<sup>23</sup>Na) is fully detectable by NMR, it is not possible to discriminate between compartments because all <sup>23</sup>Na signals resonate at the same frequency. Our objective is to induce <sup>23</sup>Na chemical shift differences across cellular compartments with exogenous contrast agents that occupy the interstitial space. We applied this approach successfully *in vivo* to determine the variation of the transmembrane gradient in glioblastoma.

0484



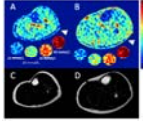
### Fast In Vivo <sup>23</sup>Na Imaging and T<sub>2</sub>\* Mapping Using Non-Localized 2D FID Magnetic Resonance Spectroscopic Imaging at 3 T

Ahmad Alhulail<sup>1,2</sup>, Pingyu Xia<sup>1</sup>, Xin Shen<sup>3</sup>, Miranda Nichols<sup>1</sup>, Srijyotsna Volety<sup>1</sup>, Nicholas Farley<sup>1</sup>, Armin M Nagel<sup>4</sup>, Ulrike Dydak<sup>1,5</sup>, and Uzay E Emir<sup>1,3</sup>

<sup>1</sup>School of Health Sciences, Purdue University, West Lafayette, IN, United States, <sup>2</sup>Department of Radiology and Medical Imaging, Prince Sattam bin Abdulaziz University, Al Kharj, Saudi Arabia, <sup>3</sup>Weldon School of Biomedical Engineering, Purdue University, West Lafayette, IN, United States, <sup>4</sup>Institute of Radiology, University Hospital Erlangen, Friedrich-Alexander-Universität Erlangen-Nürnberg (FAU), Erlangen, Germany, <sup>5</sup>Department of Radiology and Imaging Sciences, Indiana University School of Medicine, Indianapolis, IN, United States

Sodium signal decays quickly and bi-exponentially, which make  $T_2$  relaxation fitting and absolute quantification challenging. Estimating  $T_2$  with enough data points using multiple echoes requires an impractical acquisition time. Alternatively, we propose a fast sodium 2D-FID-MRSI sequence to collect the decaying signal with a high sampling frequency (625 Hz) starting at 0.55 ms within only 4 minutes at 3T. We demonstrate an absolute concentration map and separate maps of fast (mean:  $0.4 \pm 0.4$  ms) and slow (mean:  $19.6 \pm 5.7$  ms)  $T_2^*$  components from human calf muscles, showing that rapid data collection for  $T_2^*$  correction is feasible with this  $^{23}\text{Na}$ -MRSI method.

0485



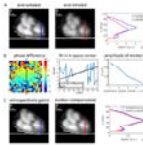
#### Multi-nuclear MRI identifies elevated skin sodium in adults with salt-sensitive blood pressure

Kalen J. Petersen<sup>1</sup>, Maria Garza<sup>1</sup>, Cassandra Reynolds<sup>2</sup>, Deepak Gupta<sup>2</sup>, Manus J. Donahue<sup>1,3,4</sup>, and Rachelle Crescenzi<sup>1</sup>

<sup>1</sup>Radiology, Vanderbilt University Medical Center, Nashville, TN, United States, <sup>2</sup>Cardiology, Vanderbilt University Medical Center, Nashville, TN, United States, <sup>3</sup>Neurology, Vanderbilt University Medical Center, Nashville, TN, United States, <sup>4</sup>Psychiatry, Vanderbilt University Medical Center, Nashville, TN, United States

Salt sensitive blood pressure (SSBP) is a cardiovascular disease risk factor, yet clinically-feasible biomarkers of SSBP have not been developed. We tested the hypothesis that peripheral tissue sodium content (TSC), measured with  $^{23}\text{Na}$ -MRI, is higher in persons with vs. without SSBP (n=39 total; age=29.4±7.4 years; sex=21/18 F/M). SSBP was confirmed by independent measurement of BP increase >5 mmHg after high-salt diet compared to low-salt diet. SSBP participants (n=13) had elevated leg skin TSC (p=0.04), and TSC was inversely correlated with leg fat-fraction (ρ=-0.57; p<0.001). Findings suggest that multi-nuclear  $^{23}\text{Na}/^1\text{H}$ -MRI could provide a radiological screening tool for SSBP.

0486



#### Respiratory motion compensation for human cardiac $^{23}\text{Na}$ MRI

Johanna Lott<sup>1,2</sup>, Armin M. Nagel<sup>1,3,4</sup>, Sebastian C. Niesporek<sup>1</sup>, Thoralf Niendorf<sup>5,6</sup>, Peter Bachert<sup>1,2</sup>, Mark E. Ladd<sup>1,2,7</sup>, and Tanja Platt<sup>1</sup>

<sup>1</sup>Medical Physics in Radiology, German Cancer Research Center (DKFZ), Heidelberg, Germany, <sup>2</sup>Faculty of Physics and Astronomy, University of Heidelberg, Heidelberg, Germany, <sup>3</sup>Institute of Radiology, University Hospital Erlangen, Erlangen, Germany, <sup>4</sup>Institute of Medical Physics, Friedrich-Alexander-Universität Erlangen-Nürnberg (FAU), Erlangen, Germany, <sup>5</sup>Berlin Ultrahigh Field Facility (B.U.F.F.), Max Delbrueck Center for Molecular Medicine in the Helmholtz Association, Berlin, Germany, <sup>6</sup>MRI. TOOLS GmbH, Berlin, Germany, <sup>7</sup>Faculty of Medicine, University of Heidelberg, Heidelberg, Germany

Sodium ( $^{23}\text{Na}$ ) ion distribution plays a fundamental role in biological processes, in particular in myocardial function.  $^{23}\text{Na}$  MRI provides noninvasive information about the total tissue sodium concentration. However, short relaxation times, low signal-to-noise ratio, breathing and heart motion render quantitative cardiac  $^{23}\text{Na}$  MRI challenging and result in long acquisition times. We present a method to compensate for respiratory motion in  $^{23}\text{Na}$  MRI by adding a linear phase in k-space with the goal to determine myocardial tissue sodium concentration. This enables a reduced measurement time for quantitative cardiac  $^{23}\text{Na}$  MRI compared to retrospective sorting into one respiratory state.

## Oral

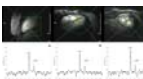
### Other Nuclei MRI and MRS to Study Metabolism - Simultaneous or Interleaved MRS & X-Nuclei

Tuesday Parallel 5 Live Q&A

Tuesday 13:45 - 14:30 UTC

Moderators: Joshua Kaggie

0487



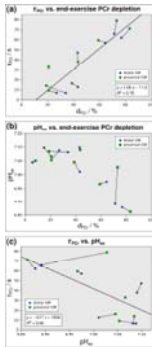
#### Cardiac $^{31}\text{P}$ MR Spectroscopy With Interleaved $^1\text{H}$ Image Navigation for Prospective Respiratory Motion Compensation – Initial Results

Stefan Wampfl<sup>1,2</sup>, Tito Körner<sup>1,2</sup>, Sigrun Roat<sup>1,2</sup>, Michael Wolzt<sup>3</sup>, Ewald Moser<sup>1,2</sup>, Siegfried Trattning<sup>2,4</sup>, Martin Meyerspeer<sup>1,2</sup>, and Albrecht Ingo Schmid<sup>1,2</sup>

<sup>1</sup>Center for Medical Physics and Biomedical Engineering, Medical University of Vienna, Vienna, Austria, <sup>2</sup>MR Center of Excellence, Medical University of Vienna, Vienna, Austria, <sup>3</sup>Department of Clinical Pharmacology, Medical University of Vienna, Vienna, Austria, <sup>4</sup>Department of Biomedical Imaging and Image-guided Therapy, Medical University of Vienna, Vienna, Austria

Cardiac phosphorus (<sup>31</sup>P) magnetic resonance spectroscopy (MRS) offers unique insights into the metabolism of the human heart. To further improve cardiac <sup>31</sup>P MRS acquisitions, the implementation of a proton (<sup>1</sup>H) magnetic resonance imaging (MRI) navigator into a <sup>31</sup>P MRS pulse sequence using multinuclear interleaving is demonstrated. In this feasibility study we further apply a method to robustly detect the heart on low-resolution navigator images. Combined with multinuclear interleaving this facilitates time-efficient position updates of the <sup>31</sup>P MRS voxel to prospectively correct for respiratory motion.

0488



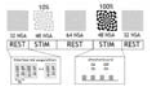
### Studying Human Plantar Flexor Muscles at Low-Intensity Exercise by Interleaving Perfusion <sup>1</sup>H MRI with Localised <sup>31</sup>P MRS

Fabian Niess<sup>1,2</sup>, Albrecht Ingo Schmid<sup>1,2</sup>, Siegfried Trattnig<sup>2,3</sup>, Ewald Moser<sup>1,2</sup>, and Martin Meyerspeer<sup>1,2</sup>

<sup>1</sup>Center for Medical Physics and Biomedical Engineering, Medical University of Vienna, Wien, Austria, <sup>2</sup>High-Field MR Centre, Medical University of Vienna, Wien, Austria, <sup>3</sup>Department of Biomedical Imaging and Image-guided Therapy, Medical University of Vienna, Wien, Austria

The purpose of this study is to show the effect of low-intensity exercise on localised <sup>31</sup>P MR spectra and <sup>1</sup>H images of human muscle. It was determined which PCr depletion is sufficient for quantifying the PCr recovery time constant ( $\tau_{PCr}$ ), while incurring minimal pH drop in a predominantly glycolytic muscle. PCr depletion during exercise was measured, PCr recovery was fitted and pH was quantified with dynamic localised <sup>31</sup>P MRS, while perfusion and BOLD <sup>1</sup>H images were simultaneously acquired in time-resolved measurements. Prolongation of  $\tau_{PCr}$  with acidification was confirmed, while very short  $\tau_{PCr}$  was found with neutral and slightly acidic pH.

0489

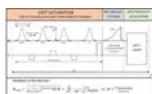


### A 7T interleaved fMRS and fMRI study on visual contrast dependency in the human brain.

Anouk Schrantee<sup>1</sup>, Chloe Najac<sup>2</sup>, Chris Jungerius<sup>2</sup>, Aart J Nederveen<sup>1</sup>, Vincent O Boer<sup>3</sup>, Wietske van der Zwaag<sup>4</sup>, Silvia Mangia<sup>5</sup>, and Itamar Ronen<sup>2</sup>

<sup>1</sup>Department of Radiology and Nuclear Medicine, Amsterdam University Medical Center, University of Amsterdam, Amsterdam, Netherlands, <sup>2</sup>C.J. Gorter Center for High Field MRI, Department of Radiology, Leiden University Medical Center, Leiden, Netherlands, <sup>3</sup>Danish Research Centre for Magnetic Resonance, Centre for Functional and Diagnostic Imaging and Research, Copenhagen University Hospital Hvidovre, Hvidovre, Denmark, <sup>4</sup>Spinoza Centre for Neuroimaging, Royal Netherlands Academy of Arts and Sciences, Amsterdam, Netherlands, <sup>5</sup>Center for Magnetic Resonance Research, Department of Radiology, University of Minnesota, Minneapolis, MN, United States

Functional magnetic resonance spectroscopy can non-invasively measure changes in local concentrations of neurometabolites and has been used to demonstrate changes in lactate and glutamate levels in response to visual stimulation. However, whether the neurometabolite response scales with the level of neuronal stimulation like the BOLD response, has not been extensively investigated. We here show that lactate, but not glutamate levels, change dependent on visual contrast levels (baseline, 10%, 100% contrast). Although we also demonstrate a significant contrast dependence in the BOLD response, we do not find a significant association between the lactate response and the BOLD response.



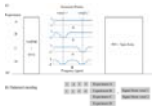
### Combining CEST and <sup>1</sup>H MR Spectroscopy for simultaneous determination of metabolite concentrations and effects of magnetization exchange

Maike Hoefemann<sup>1</sup>, André Döring<sup>1</sup>, and Roland Kreis<sup>1</sup>



A new sequence design was used to combine the CEST saturation method with traditional MRS. Using non-water suppressed metabolite-cycled spectroscopy offers the time-saving simultaneous recording of the traditional CEST z-spectrum and the metabolite spectrum under frequency selective saturation and allows the detection of exchange and magnetization transfer effects on metabolites and macromolecules. This technique might offer additional possibilities for quantifying the metabolite and macromolecular content or give further insight into the composition of the traditional CEST z-spectrum and is also relevant for judging the influence of water-suppression on absolute metabolite signals.

0491

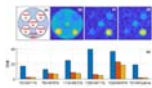


Simultaneous ultra-short TE-MRS in two voxels using a SPECIAL sequence with Hadamard encoding  
Masoumeh Dehghani<sup>1,2</sup>, Richard Edden<sup>3</sup>, and Jamie Near<sup>1,2</sup>

<sup>1</sup>McGill University, Montreal, QC, Canada, <sup>2</sup>Centre d'Imagerie Cérébrale, Montreal, QC, Canada, <sup>3</sup>Johns Hopkins University, Baltimore, MD, United States

The spin echo, full Intensity acquired localized (SPECIAL) sequence consists of a localized spin-echo, preceded by an alternating ISIS pre-inversion for voxel localization. In this study we modified the SPECIAL sequence to simultaneously localize the signal at two different positions. The technique relies on a four-step inversion scheme involving two different inversion positions, followed by a Hadamard encoding reconstruction. Comparing the in vivo performance of dual-SPECIAL sequence to the conventional SPECIAL sequence demonstrated that the dual-Special sequence provides simultaneous metabolite profile from two different regions, reducing the acquisition time by a factor of two, and without any penalty in SNR.

0492



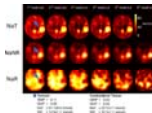
Simultaneous Acquisition of Spin-density-weighted and SNR-enhanced Fluid-attenuated <sup>23</sup>Na MRI Images (SELA)

Chengchuan Wu<sup>1</sup>, Yasmin Blunck<sup>1</sup>, and Leigh Johnston<sup>1</sup>

<sup>1</sup>Biomedical Engineering, The University of Melbourne, Parkville, Australia

This work presents SELA, a <sup>23</sup>Na MRI sequence that can simultaneously acquire spin-density-weighted (SDW) and SNR-enhanced fluid-attenuated (FLAIR) images in one scan. The sequence was examined by numerical simulation and phantom experiment in a 7T preclinical scanner. Preliminary results support the design purpose to improve <sup>23</sup>Na MRI efficiency and <sup>23</sup>Na-FLAIR image quality.

0493



Quantitative Multiple Quantum Filtered Sodium MRI and [<sup>18</sup>F]-FET-PET: Complementary Imaging Techniques for the Study of Cerebral Gliomas

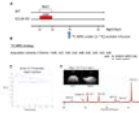
Wieland A Worthoff<sup>1</sup>, Aliaksandra Shymanskaya<sup>2</sup>, Karl-Josef Langen<sup>1,3,4</sup>, and N. Jon Shah<sup>1,2,4,5</sup>

<sup>1</sup>Institute of Neuroscience and Medicine - 4, Forschungszentrum Jülich GmbH, Jülich, Germany, <sup>2</sup>Institute of Neuroscience and Medicine - 11, Forschungszentrum Jülich GmbH, Jülich, Germany, <sup>3</sup>Department of Nuclear Medicine, RWTH Aachen University, Aachen, Germany, <sup>4</sup>Section JARA-Brain, Jülich-Aachen Research Alliance, Aachen, Germany, <sup>5</sup>Department of Neurology, RWTH Aachen University, Aachen, Germany

A cohort of patients with untreated cerebral gliomas underwent consecutive [<sup>18</sup>F]-FET-PET and sodium MRI exams. It is shown that quantitative results from multiple quantum filtered sodium MRI using the enhanced SISTINA sequence offer access to the metabolic properties of tumours beyond what is observed by [<sup>18</sup>F]-FET-PET alone, thus presenting the potential to serve as an additional marker in tumour diagnostics.

0494

Cerebral energy metabolism and neurotransmission in a schizophrenia mouse model: a combined <sup>1</sup>H-[<sup>13</sup>C] MRS and <sup>13</sup>C MRS study at 14.1T

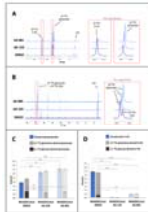


Bernard Lanz<sup>1</sup>, Radek Skupiński<sup>2,3,4</sup>, Kim Q Do<sup>2</sup>, and Lijing Xin<sup>3</sup>

<sup>1</sup>LIFMET, Ecole Polytechnique Fédérale de Lausanne, Lausanne, Switzerland, <sup>2</sup>Center for Psychiatric Neuroscience, Department of Psychiatry, Lausanne University Hospital (CHUV), Prilly, Switzerland, <sup>3</sup>Center for Biomedical Imaging (CIBM), Ecole Polytechnique Fédérale de Lausanne, Lausanne, Switzerland, <sup>4</sup>HES-SO, University of Applied Sciences of Western Switzerland, HEIA-FR, Institute of Chemical Technology, Fribourg, Switzerland

In this study, we applied interleaved localized <sup>1</sup>H-[<sup>13</sup>C]-MRS and direct <sup>13</sup>C MRS with polarization transfer to characterize brain energy metabolism in the early development of a GCLM-KO mouse model with infusion of [2-<sup>13</sup>C]acetate. This strategy enabled to measure simultaneously the [2-<sup>13</sup>C]acetate input function, glutamate and glutamine C4 and C3 enrichment and pool size changes. Two-compartment metabolic modelling was then applied to characterize mitochondrial metabolism and glutamate/glutamine cycling and compare it to a control group.

0495



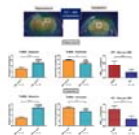
Metabolic reprogramming associated with IDH1-targeted treatments in low-grade glioma cell models: a <sup>1</sup>H and <sup>13</sup>C MRS study

Abigail R Molloy<sup>1</sup>, Chloé Najac<sup>1</sup>, Aliya Lakhani<sup>1</sup>, Elavarasan Subramani<sup>1</sup>, Georgios Batsios<sup>1</sup>, Anne Marie Gillespie<sup>1</sup>, Russell O Pieper<sup>2,3</sup>, Pavithra Viswanath<sup>1</sup>, and Sabrina M Ronen<sup>1,3</sup>

<sup>1</sup>Radiology and Biomedical Imaging, University of California, San Francisco, San Francisco, CA, United States, <sup>2</sup>Department of Neurological Surgery, University of California, San Francisco, San Francisco, CA, United States, <sup>3</sup>Brain Tumor Research Center, University of California, San Francisco, San Francisco, CA, United States

Mutant IDH1 (IDH1mut) drives glioma development, and targeted IDH1mut inhibitors show promising results in clinical trials. However, treatment is not associated with tumor shrinkage, and there is an urgent need for early imaging biomarkers of response. Our studies in IDH1mut-expressing glioma cells indicate that treatment with IDH1mut inhibitors leads to <sup>1</sup>H and <sup>13</sup>C-MRS-detectable metabolic changes. Specifically, we show a decrease in 2-HG and increase in glutamate, as well as an increase in metabolic flux from glutamine to glutamate. Furthermore, hyperpolarized [1-<sup>13</sup>C] α-ketoglutarate can probe these alterations in metabolism. This identifies potential non-invasive biomarkers of response to IDH1mut inhibition in glioma.

0496



Multimodal assessment of brain energy metabolism in a rat model of hepatic encephalopathy using <sup>1</sup>H-MRS and <sup>18</sup>F-FDG PET – a pilot study

Jessie Mosso<sup>1,2</sup>, Carole Poitry-Yamate<sup>1</sup>, Dunja Simicic<sup>1,2</sup>, Mario Lepore<sup>1</sup>, Cristina Cudalbu<sup>1</sup>, and Bernard Lanz<sup>2</sup>

<sup>1</sup>Center for biomedical imaging (CIBM), EPFL, Lausanne, Switzerland, <sup>2</sup>Laboratory for functional and metabolic imaging (LIFMET), EPFL, Lausanne, Switzerland

Hepatic encephalopathy (HE) is a severe complication of chronic liver disease which drastically affects patient lives. Its underlying mechanisms are still unknown and energy metabolism studies are of key interest. Here, we combined <sup>18</sup>F-FDG PET and <sup>1</sup>H-MRS and found a 2-fold decrease in brain glucose uptake in a rat model of HE compared to SHAM rats, associated with a previously reported increase in brain glutamine and decrease in osmolytes. Although the difference in glucose uptake measured by PET results from a combination of brain and systemic effects, this finding provides a new perspective on HE pathophysiology.

## Weekday Course

### MRS and Molecular Imaging, Development and Applications - Spectroscopy & Molecular Imaging of Cancer

Organizers: Catherine Hines, Kannie WY Chan, Hai-Ling Cheng, Ronald Ouwerkerk

Tuesday Parallel 5 Live Q&A

Tuesday 14:30 - 15:15 UTC

Moderators: Eva-Maria Ratai & Patrick Rolan

## MR in Cancer Theranostics

Zaver Bhujwala<sup>1</sup>

<sup>1</sup>Johns Hopkins University, School of Medicine, United States

---

## MRS to Probe Metabolites & In Vitro Assessment of Cancer

Ellen Ackerstaff<sup>1</sup>

<sup>1</sup>Memorial Sloan Kettering Cancer Center, United States

---

## Preclinical High Field Imaging of the Tumor Microenvironment

Vikram Kodibagkar<sup>1</sup>

<sup>1</sup>Arizona State University, United States

---

## Current & Future Clinical Oncology Applications

Eduard Chekmenev<sup>1</sup>

<sup>1</sup>Wayne State University, Detroit, MI, United States

---

## Oral

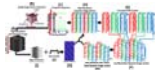
### Novel Pulse Sequences and Reconstruction Techniques - Novel Acquisitions & Reconstructions

Tuesday Parallel 4 Live Q&A

Tuesday 14:30 - 15:15 UTC

Moderators: Jonathan Tamir & Julia Velikina

0594



#### Complex-Valued Spatial-Temporal Super-Resolution Combined with Multi-Band Technique on T<sub>2</sub><sup>\*</sup>-Weighted Dynamic MRI

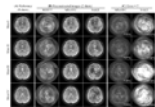
Duohua Sun<sup>1</sup>, Jean-Philippe Galons<sup>2</sup>, Chidi Ugonna<sup>1</sup>, Silu Han<sup>1</sup>, Mahesh Keerthivasan<sup>3</sup>, Marc Lindley<sup>4</sup>, and Nan-kuei Chen<sup>1</sup>

<sup>1</sup>Biomedical Engineering, The University of Arizona, Tucson, AZ, United States, <sup>2</sup>Medical Imaging, The University of Arizona, Tucson, AZ, United States, <sup>3</sup>Siemens healthineers, Tucson, AZ, United States, <sup>4</sup>GE Healthcare, Waukesha, WI, United States

We present an approach for improving spatial and temporal resolution of complex-valued T<sub>2</sub><sup>\*</sup>-weighted dynamic MRI. Compared with the conventional magnitude-valued super-resolution approaches, our technique utilizes phase information to better recover signal loss caused by susceptibility gradients and generate finer representations of temporal dynamic signal variation. Results from numerical and hybrid simulation show that promising improvements in image resolution, susceptibility artifact reduction and temporal signal variation representation can be achieved using our complex-valued super-resolution MRI scheme when compared to magnitude-valued super-resolution.

---

0595



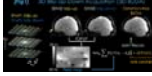
#### Calibrationless Multi-slice Spiral MRI Reconstruction via Low Rank Hankel Tensor Completion

Yilong Liu<sup>1,2</sup>, Zheyuan Yi<sup>1,2,3</sup>, Yujiao Zhao<sup>1,2</sup>, Hua Guo<sup>4</sup>, and Ed X. Wu<sup>1,2</sup>

<sup>1</sup>Laboratory of Biomedical Imaging and Signal Processing, The University of Hong Kong, Hong Kong, China, <sup>2</sup>Department of Electrical and Electronic Engineering, The University of Hong Kong, Hong Kong, China, <sup>3</sup>Department of Electrical and Electronic Engineering, Southern University of Science and Technology, Shenzhen, China, <sup>4</sup>Center for Biomedical Imaging Research, Department of Biomedical Engineering, Tsinghua University, Beijing, China

This study presents a calibrationless multi-slice spiral MRI reconstruction method based on low rank Hankel tensor completion (MS-HTC). In this study, the sampling pattern of adjacent slices complements each other by using the spiral trajectories of different rotation angles, and MS-HTC exploits the similarities of coil sensitivities, spatial support, and image content. The proposed method was evaluated with human brain spin-echo spiral MR data. The results show that MS-HTC can significantly reduce residual error compared to single-slice reconstruction with simultaneous autocalibrating and k-space estimation (SAKE).

0596



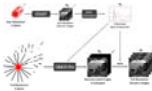
### 3D-BUDA Enables Rapid Distortion-Free QSM Acquisition

Berkin Bilgic<sup>1</sup>, Benedikt A Poser<sup>2</sup>, Christian Langkammer<sup>3</sup>, Kawin Setsompop<sup>1</sup>, and Congyu Liao<sup>1</sup>

<sup>1</sup>Martinos Center for Biomedical Imaging, Charlestown, MA, United States, <sup>2</sup>Maastricht University, Maastricht, Netherlands, <sup>3</sup>Department of Neurology, Medical University of Graz, Graz, Austria

We introduce 3D blip-up and -down acquisition (3D-BUDA) for 3D echo planar imaging (3D-EPI). We acquire two-shots of 3D-EPI with alternating phase-encoding to estimate  $B_0$  information. Incorporating this into the joint reconstruction of the shots eliminates distortion and enables signal averaging, permitting a 22-second, high-SNR acquisition at 1 mm<sup>3</sup> resolution. While shifted sampling between the shots provides complementary k-space coverage, using low-rank regularization eliminates shot-to-shot variations. SNR gain of 7T allows for additional partition acceleration, enabling a 9-second whole-brain scan at  $R_{\text{inplane}} \times R_z = 5 \times 2$ . These are combined with a self-supervised dipole inversion algorithm for Quantitative Susceptibility Mapping (QSM) which outperforms state-of-the-art reconstructions.

0597



### High Spatiotemporal Resolution Motion-Resolved MRI using XD-GRASP-Pro

Li Feng<sup>1</sup> and Fang Liu<sup>2,3</sup>

<sup>1</sup>Biomedical Engineering and Imaging Institute and Department of Radiology, Icahn School of Medicine at Mount Sinai, New York, NY, United States, <sup>2</sup>Gordon Center for Medical Imaging, Massachusetts General Hospital, Harvard Medical School, Boston, MA, United States, <sup>3</sup>Department of Radiology, University of Wisconsin Madison, Madison, WI, United States

This work presents a free-breathing motion-resolved golden-angle image reconstruction method called XD-GRASP-Pro, which extends the original XD-GRASP (eXtra-Dimensional Golden-angle RAdial Sparse Parallel MRI) method with imProved reconstruction performance through an additional self-estimated/calibrated low-rank subspace-constraint. The temporal basis used to construct the subspace is estimated from an intermediate reconstruction step on the low-resolution portion of radial k-space, which eliminates the need of using auxiliary data or a physical signal model that is not always available. XD-GRASP-Pro were tested for high spatiotemporal resolution motion-resolved liver MRI.

0598



### Real-time 3D respiratory motion estimation for MR-guided radiotherapy using low-rank MR-MOTUS

Niek R.F. Huttinga<sup>1,2</sup>, Tom Bruijnen<sup>1,2</sup>, Cornelis A.T. van den Berg<sup>1,2</sup>, and Alessandro Sbrizzi<sup>1,2</sup>

<sup>1</sup>Computational Imaging Group for MR diagnostics and Therapy, Center for Image Sciences, University Medical Center Utrecht, Utrecht, Netherlands, <sup>2</sup>Department of Radiology, Division of Imaging and Oncology, University Medical Center Utrecht, Utrecht, Netherlands

We propose low-rank MR-MOTUS, a framework for real-time reconstructions of 3D respiratory motion-fields for MR-guided radiotherapy. Low-rank MR-MOTUS factorizes space-time motion-fields into static spatial components and dynamic temporal components. This allows to 1) exploit spatial and temporal correlations in motion, and 2) split the reconstruction into a large-scale off-line training phase, and a small-scale on-line inference phase. Results show that in the on-line inference phase 3D respiratory motion can be estimated in 130ms, from data acquired in 24ms. This yields a total latency of 154ms, and low-rank MR-MOTUS thereby paves the way for real-time MR-guided radiotherapy on the MR-linac.

0599



Deep subspace learning: Enhancing speed and scalability of deep learning-based reconstruction of dynamic imaging data

Christopher M. Sandino<sup>1</sup>, Frank Ong<sup>1</sup>, and Shreyas S. Vasanawala<sup>2</sup>

<sup>1</sup>Department of Electrical Engineering, Stanford University, Stanford, CA, United States, <sup>2</sup>Department of Radiology, Stanford University, Stanford, CA, United States

Unrolled neural networks (UNNs) have surpassed state-of-the-art methods for dynamic MR image reconstruction from undersampled k-space measurements. However, 3D UNNs suffer from high computational complexity and memory demands, which limit applicability to large-scale reconstruction problems. Previously, subspace learning methods have leveraged low-rank tensor models to reduce their memory footprint by reconstructing simpler spatial and temporal basis functions. Here, a deep subspace learning reconstruction (DSLRL) framework is proposed to learn iterative procedures for estimating these basis functions. As proof of concept, we train DSLRL to reconstruct undersampled cardiac cine data with 5X faster reconstruction time than a standard 3D UNN.

0600



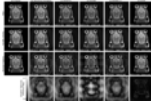
The total ellipse of the heart: Cardiac CINE imaging using frequency-modulated bSSFP and the elliptical signal model

Anne Slawig<sup>1</sup> and Herbert Köstler<sup>1</sup>

<sup>1</sup>Department of Diagnostic and Interventional Radiology, University Hospital Würzburg, Würzburg, Germany

Balanced steady state free precession sequences are well suited for cardiac imaging as they are fast, yield high signal and provide excellent contrast between blood and myocardium. To avoid the typical banding artifacts in such sequences, conventionally, multiple phase-cycled acquisitions are performed and combined to one image. Using a frequency-modulated bSSFP sequence the acquisition of many off-resonances can be performed in one single scan and a model-based reconstruction using the elliptical signal model performs well to reconstruct such measurements. Therefore, it allows the reconstruction of multiple off-resonance states for multiple heart phases from a single frequency-modulated bSSFP measurement.

0601



A Novel Image Reconstruction Algorithm for Radial MRI Data Acquired with a Rotating Radio-frequency Coil (RRFC)

Andrew Phair<sup>1</sup>, Michael Brideson<sup>1</sup>, Jin Jin<sup>2,3,4</sup>, Mingyan Li<sup>2</sup>, Stuart Crozier<sup>2</sup>, and Lawrence Forbes<sup>1</sup>

<sup>1</sup>School of Natural Sciences, University of Tasmania, Hobart, Australia, <sup>2</sup>School of Information Technology and Electrical Engineering, University of Queensland, Brisbane, Australia, <sup>3</sup>ARC Training Centre for Innovation in Biomedical Imaging Technology, University of Queensland, Brisbane, Australia, <sup>4</sup>Mark and Mary Stevens Neuroimaging and Informatics Institute, University of Southern California, Los Angeles, CA, United States

We present WARF, a novel reconstruction algorithm for radial MRI data acquired with a rotating radio-frequency coil (RRFC). The algorithm reconstructs each pixel as a weighted sum of all acquired data, with the weights determined by the k-space sampling pattern. The theory behind WARF leading to the derivation of appropriate weights is presented, and then WARF is applied to both simulated and experimental data sets. The results indicate WARF is achieving an improved robustness to RRFC angular velocity variability and k-space trajectory deviation compared with existing reconstruction methods.

0602



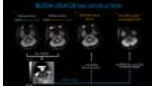
On the Influence of Prior Knowledge in Learning Non-Cartesian 2D CINE Image Reconstruction

Kerstin Hammernik<sup>1</sup>, Gastao Cruz<sup>2</sup>, Thomas Kuestner<sup>2</sup>, Claudia Prieto<sup>2</sup>, and Daniel Rueckert<sup>1</sup>

<sup>1</sup>Department of Computing, Imperial College London, London, United Kingdom, <sup>2</sup>School of Biomedical Engineering and Imaging Sciences, Kings College London, London, United Kingdom

In this work, we study the influence of prior knowledge in learning-based non-Cartesian 2D CINE MR image reconstruction. The proposed approach uses a novel minimal deep learning setup to embed the acquired non-Cartesian multi-coil data and conventional spatio-temporal (3D and 2D+t) Fields-of-Experts regularization in a proximal gradient variational network, achieving promising results for up to 12-fold retrospectively undersampled tiny golden-angle radial CINE imaging.

0603



### dSAGE enables distortion-free diffusion, spin and gradient echo imaging in 1 minute

Zijing Zhang<sup>1,2</sup>, Congyu Liao<sup>2</sup>, Jaejin Cho<sup>2</sup>, Mary Kate Manhard<sup>2</sup>, Wei-Ching Lo<sup>3</sup>, Jinmin Xu<sup>1,2</sup>, Kawin Setsompop<sup>2,4,5</sup>, Huafeng Liu<sup>1</sup>, and Berkin Bilgic<sup>2,4</sup>

<sup>1</sup>State Key Laboratory of Modern Optical Instrumentation, College of Optical Science and Engineering, Zhejiang University, Hangzhou, China, <sup>2</sup>Department of Radiology, A. A. Martinos Center for Biomedical Imaging, Massachusetts general hospital, Charlestown, MA, United States, <sup>3</sup>Siemens Medical Solutions, Boston, MA, United States, <sup>4</sup>Harvard Medical School, Boston, MA, United States, <sup>5</sup>Harvard-MIT Health Sciences and Technology, Massachusetts Institute of Technology, Cambridge, MA, United States

We propose dSAGE, a new EPI sequence for diffusion, Spin- and Gradient-echo imaging. We exploit unused sequence time during the  $b=0$  acquisition in a diffusion experiment to collect additional  $T2^*$ - and  $T2'$ -weighted contrasts with high in-plane resolution for free. We use a multi-shot acquisition with high in-plane acceleration to achieve  $1 \times 1$  mm<sup>2</sup> resolution, and alternate the phase-encoding polarities across the shots to eliminate geometric distortion using the navigator-free Blip Up-Down Acquisition (BUDA) technique(1). We demonstrate the ability of BUDA-dSAGE to provide whole-brain, distortion-free, high-SNR images with  $T2^*$ -,  $T2'$ -,  $T2$ -weighted contrasts and 3-direction dMRI and apparent diffusion coefficient (ADC) maps in 1-minute.

## Oral

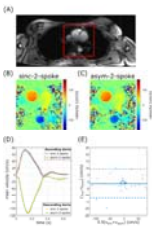
### Novel Pulse Sequences and Reconstruction Techniques - RF Pulses & Pulse Sequences

Tuesday Parallel 4 Live Q&A

Tuesday 14:30 - 15:15 UTC

Moderators: Emre Kopanoglu & Sydney Williams

0604



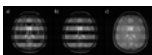
### Velocity encoded/compensated asymmetric multi-spoke RF pulses

Simon Schmidt<sup>1</sup>, Sebastian Flassbeck<sup>1</sup>, Mark E. Ladd<sup>1</sup>, and Sebastian Schmitter<sup>1,2</sup>

<sup>1</sup>Medical Physics in Radiology, German Cancer Research Center (DKFZ), Heidelberg, Germany, <sup>2</sup>Physikalisch-Technische Bundesanstalt (PTB), Braunschweig and Berlin, Germany

In this work, we investigate the feasibility of velocity encoded/compensated asymmetric multi-spoke RF pulses. Bloch simulations, phantom studies, and in-vivo measurements are conducted to characterize the pulse performance. Compared to conventional multi-spoke RF pulses, the results indicate that asymmetric multi-spoke RF pulses are suitable for both 2D and 3D acquisitions and can significantly reduce the repetition time without compromising on velocity quantification. The hereby gained acceleration can be additionally combined with techniques such as GRAPPA or compressed-sensing to further decrease the total acquisition time.

0605



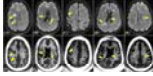
### Multiband Adiabatic Inversion Using Multiphoton Excitation

Victor Han<sup>1</sup> and Chunlei Liu<sup>1,2</sup>

<sup>1</sup>Electrical Engineering and Computer Sciences, University of California, Berkeley, Berkeley, CA, United States, <sup>2</sup>Helen Wills Neuroscience Institute, University of California, Berkeley, Berkeley, CA, United States

We present a technique for power-efficient multiband adiabatic inversion using the concept of multiphoton excitation. In this case, multiphoton excitation occurs with one photon from our traditional RF source and one or more photons from oscillating gradients. By a proper choice of oscillating gradients, we can meet multiphoton resonance conditions at multiple spatial locations, and thus achieve multiband multiphoton adiabatic inversions. Only a slightly scaled standard adiabatic pulse is needed on the traditional RF side. We demonstrate the technique with simulations, phantom and in vivo experiments on a 3T scanner.

0606



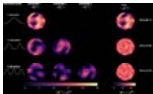
### Robust Morphological Myelin Imaging Using a Short TR Adiabatic Inversion Recovery Prepared Ultrashort Echo Time (STAIR-UTE) Sequence

Yajun Ma<sup>1</sup>, Hyungseok Jang<sup>1</sup>, Zhao Wei<sup>1</sup>, Zhenyu Cai<sup>1</sup>, Yanping Xue<sup>1</sup>, Eric Y Chang<sup>2</sup>, Jody Corey-Bloom<sup>1</sup>, and Jiang Du<sup>1</sup>

<sup>1</sup>UC San Diego, San Diego, CA, United States, <sup>2</sup>VA health system, San Diego, CA, United States

To image myelin in brain more robustly on clinical scanners, we propose a Short TR Adiabatic Inversion Recovery prepared UTE (STAIR-UTE) sequence for volumetric myelin imaging in vivo. With STAIR technique, long T2 tissues with a broad range of T1s can be sufficiently suppressed. High myelin contrast can be robustly obtained with a TR less than 250 ms. The resultant myelin imaging shows a clear loss of myelin signal in multiple sclerosis (MS) lesions.

0607



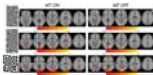
### Direct Saturation Control for Magnetization Transfer Imaging at 7T

David Leitão<sup>1</sup>, Raphael Tomi-Tricot<sup>2</sup>, Patrick Liebig<sup>3</sup>, Rene Gumbrecht<sup>3</sup>, Dieter Ritter<sup>3</sup>, Ana Baburamani<sup>4</sup>, Jan Sedlacik<sup>1,4</sup>, Joseph V. Hajnal<sup>1,4</sup>, and Shaihan J. Malik<sup>1,4</sup>

<sup>1</sup>Biomedical Engineering Department, School of Biomedical Engineering and Imaging Sciences, King's College London, London, United Kingdom, <sup>2</sup>MR Research Collaborations, Siemens Healthcare Limited, Frimley, United Kingdom, <sup>3</sup>Siemens Healthcare GmbH, Erlangen, Germany, <sup>4</sup>Centre for the Developing Brain, School of Biomedical Engineering and Imaging Sciences, King's College London, London, United Kingdom

Systems with Magnetization Transfer (MT) are particularly sensitive to  $B_1^+$  inhomogeneity, as the semisolid magnetization saturation is proportional to the square of  $B_1^+$ . This can be problematic at 7T imaging, where  $B_1^+$  inhomogeneity is more severe, compromising the MT contrast obtained. This work proposes applying a composite MT prep-pulse with varying RF complex weights for each sub-pulse. These weights are optimized to deliver in the end a homogenous  $\langle B_1^{+2} \rangle$ , such that the MT contrast obtained is spatially uniform. Simulation and phantom results showed great improvement in the  $\langle B_1^{+2} \rangle$  and MT ratio maps.

0608



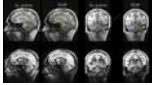
### Magnetization transfer enhanced functional contrast for short TE fMRI

Jenni Schulz<sup>1</sup>, Zahra Fazal<sup>1</sup>, Riccardo Metere<sup>1</sup>, José P Marques<sup>1</sup>, and David G Norris<sup>1,2</sup>

<sup>1</sup>Donders Institute for Brain, Cognition and Behaviour, Radboud University Nijmegen, Nijmegen, Netherlands, <sup>2</sup>Erwin L. Hahn Institute for Magnetic Resonance Imaging, University Duisburg-Essen, Essen, Germany

Magnetization-transfer can be used to suppress tissue signal but not blood. This sensitises the signal to CBV variations. By minimising TE we can maximise the sensitivity to CBV variation while minimising BOLD contrast. We implemented a short TE (7.5 ms) GE-EPI protocol with MT preparation, and performed a brain activation study on three healthy volunteers using a visual stimulus paradigm. Tissue suppression factors of typically 53% were achieved with MT-on. Both MT-on and -off conditions gave significant activation owing to residual BOLD contrast in MT-off. However, the group level contrast MT-on > MT-off gave standard activation maps with significant activation.

0609



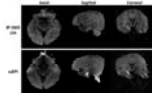
### Time-optimized universal non-selective pulses for 7T MRI with parallel transmission

Léo Van Damme<sup>1,2</sup>, Frank Mauconduit<sup>2</sup>, Thomas Chambrion<sup>1,3</sup>, Nicolas Boulant<sup>2</sup>, and Vincent Gras<sup>2</sup>

<sup>1</sup>Institut Elie Cartan, Université de Lorraine, Vandoeuvre-lès-Nancy, France, <sup>2</sup>Neurospin, CEA Saclay, Gif-sur-Yvette, France, <sup>3</sup>INRIA Nancy Grand Est, Vandœuvre, France

Parallel transmission is a promising technology in high field MRI to mitigate the RF field inhomogeneity problem. In that context, the so-called Universal  $k_T$ -point technique proves useful to achieve uniform spin excitation at no cost in terms of radio-frequency field calibration, although localized artefacts can occasionally appear due to the presence of very large resonance frequency offsets. By exploring more general RF pulse and magnetic field gradient waveforms than  $k_T$ -points, this work introduces time-minimized universal pulses presenting better broadband behavior. In-vivo acquisitions on 5 volunteers at 7T have been performed to demonstrate the improvements.

0610



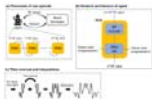
### In-plane simultaneous multi-segment imaging: example employing diffusion-weighted imaging using a 2D RF pulse

Kaibao Sun<sup>1</sup>, Zheng Zhong<sup>1,2</sup>, Zhongbiao Xu<sup>3</sup>, Guangyu Dan<sup>1,2</sup>, M. Muge Karaman<sup>1,2</sup>, and Xiaohong Joe Zhou<sup>1,2,4</sup>

<sup>1</sup>Center for MR Research, University of Illinois at Chicago, Chicago, IL, United States, <sup>2</sup>Department of Bioengineering, University of Illinois at Chicago, Chicago, IL, United States, <sup>3</sup>Department of Radiotherapy, Cancer Center, Guangdong Provincial People's Hospital & Guangdong Academy of Medical Science, Guangzhou, China, <sup>4</sup>Departments of Radiology and Neurosurgery, University of Illinois at Chicago, Chicago, IL, United States

Reduced field of view (rFOV) imaging offers several advantages, including high spatial resolution and reduced image distortion. We propose an in-plane simultaneous multi-segment (IP-SMS) imaging method to extend the benefits of rFOV to full FOV imaging. Unlike the conventional simultaneous multi-slice imaging, IP-SMS performs in-plane simultaneous multi-segment excitation by utilizing the periodic replicas of excitation profile of a 2D RF pulse, followed by parallel segment reconstruction using a set of "virtual" coil sensitivity profiles. We have demonstrated the IP-SMS imaging technique on phantoms and human brains where high-resolution diffusion images were obtained with minimal distortion.

0611



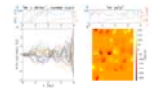
### DeepRF: Designing an RF pulse using a self-learning machine

Dongmyung Shin<sup>1</sup> and Jongho Lee<sup>1</sup>

<sup>1</sup>Department of Electrical and Computer Engineering, Seoul National University, Seoul, Korea, Republic of

Designing an RF pulse or developing a design rule requires a deep understanding of MR physics, and, therefore, is not easy. In this work, we demonstrate that an AI agent can self-learn the design strategy of an RF pulse and successfully generate a complex RF pulse (adiabatic RF) that satisfies given design criteria. The machine-designed pulse has a substantially different shape but shows performance comparable to the conventional adiabatic pulse.

0612



### INSTANT (INtegrated Shimming and Tip-Angle NormalizaTion): 3D flip-angle mitigation using joint optimization of RF and shim array currents

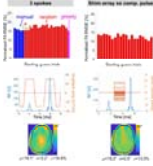
Mads Sloth Vinding<sup>1,2</sup>, Torben Ellegaard Lund<sup>1,2</sup>, Jason P Stockmann<sup>3,4</sup>, and Bastien Guérin<sup>3,4</sup>

<sup>1</sup>Department of Clinical Medicine, Aarhus University, Aarhus, Denmark, <sup>2</sup>Center of Functionally Integrative Neuroscience, Aarhus University Hospital, Aarhus, Denmark, <sup>3</sup>A. A. Martinos Center for Biomedical Imaging, Massachusetts General Hospital, Charlestown, MA, United States, <sup>4</sup>Harvard Medical School, Boston, MA, United States



We generalize a composite pulse approach used with an RF/multi-coil shim array, whereby we optimize the RF and shim array waveforms played simultaneously for 3D flip-angle homogenization at 7 Tesla in the human head. We show that this approach yields shorter pulses at a given excitation error than when optimizing the RF alone. In other words, the original intuition of the composite pulse approach of RF pulses surrounding DC shim current blips is extended to concurrent RF and shim current and the additional degrees-of-freedom played as continuous shim waveforms significantly improves the excitation quality (uniform 90° excitation).

0613



Improvements in flip-angle uniformization at 7 Tesla using an integrated RF/B0 shim array coil and composite pulses

Bastien Guerin<sup>1,2</sup>, Eugene Milshteyn<sup>1,2</sup>, Lawrence L Wald<sup>1,2</sup>, and Jason Stockmann<sup>1,2</sup>

<sup>1</sup>Martinos Center for Biomedical Imaging, Massachusetts General Hospital, Charlestown, MA, United States, <sup>2</sup>Harvard Medical School, Boston, MA, United States

We compare the RF/B0 shim array composite pulses of Rudrapatna [1] to kT-point and spoke pulses for flip-angle (FA) uniformization using a birdcage coil at 7T. Using 3 kT-points, it is possible to obtain highly uniform flip-angle distributions in the brain within 3ms, as long as the kT-points locations are optimized. The RF/B0 shim array pulses perform less well than this optimized 3-kT-points strategy for non-selective flip-angle mitigation, but better than optimized 3-spoke pulses for flip-angle mitigation in a slice. The DOFs provided by shim array coils could prove invaluable for integrated B0 shimming and flip-angle uniformization at 7T.

## Oral

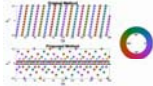
### Novel Pulse Sequences and Reconstruction Techniques - Data Sampling & Spatial Encoding Techniques

Tuesday Parallel 4 Live Q&A

Tuesday 14:30 - 15:15 UTC

Moderators: Gigi Galiana & Jason Stockmann

0614



Improved 3D real-time MRI with Stack-of-Spiral (SOSP) trajectory and variable density randomized encoding of speech production

Ziwei Zhao<sup>1</sup>, Yongwan Lim<sup>1</sup>, Dani Byrd<sup>2</sup>, Shrikanth Narayanan<sup>1</sup>, and Krishna Nayak<sup>1</sup>

<sup>1</sup>Ming Hsieh Department of Electrical and Computer Engineering, Viterbi School of Engineering, University of Southern California, Los Angeles, CA, United States, <sup>2</sup>Department of Linguistics, Dornsife College of Letters, Arts and Sciences, University of Southern California, Los Angeles, CA, United States

3D real-time (RT) MRI is a useful tool in speech production research, as it enables full visualization of the dynamics of vocal tract shaping during natural speech. Limited spatial and temporal resolution, and a tradeoff between them, is however common in highly accelerated MRI. In this work, we demonstrate improved spatio-temporal resolution by using variable density randomized stack-of-spiral sampling and a constrained reconstruction. We can capture rapid movement of articulators, specifically lips and tongue body movements at both normal and rapid speech rates, yielding a substantial improvement over prior approaches in measuring fine details of human speech production.

0615



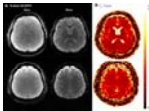
Sub-millisecond 2D MRI of the Vocal Fold Oscillation using Single Point Imaging with Rapid Encoding (SPIRE)

Johannes Fischer<sup>1</sup>, Ali Caglar Özen<sup>1,2</sup>, Matthias Echtenach<sup>3</sup>, Bernhard Richter<sup>4</sup>, and Michael Bock<sup>1</sup>

<sup>1</sup>Dept. of Radiology, Medical Physics, Medical Center University of Freiburg, Faculty of Medicine, University of Freiburg, Freiburg, Germany, <sup>2</sup>German Consortium for Translational Cancer Research Freiburg Site, German Cancer Research Center (DKFZ), Heidelberg, Germany, <sup>3</sup>Division of Phoniatrics and Pediatric Audiology, Department of Otorhinolaryngology, Head and Neck Surgery, Ludwig-Maximilians-University, Munich, Germany, <sup>4</sup>Institute of Musicians' Medicine, Medical Center University of Freiburg, Faculty of Medicine, University of Freiburg, Freiburg, Germany

We use single point imaging with rapid encoding (SPIRE) to image the vocal fold oscillations in the coronal plane. SPIRE is able to image fast, repetitive and two-dimensional motion, because the temporal resolution does not depend on TR but on the duration of the fast-switching phase encoding gradients, which is below one millisecond in this work. Data are gated using electroglottography and projection navigators are acquired during the sequence to detect shifts in larynx position which is corrected during reconstruction.

0616



### Spiral Crisscrossing Echo Planar Time-resolved Imaging (SCEPTI)

Gilad Liberman<sup>1</sup>, Fuyixue Wang<sup>1</sup>, Zijng Dong<sup>1</sup>, and Kawin Setsompop<sup>1</sup>

<sup>1</sup>A. A. Martinos Center for Biomedical Imaging, Department of Radiology, Massachusetts General Hospital, Charlestown, MA, United States

A new technique, termed Spiral Echo Planar Time-resolved Imaging (SKEPTIC), was developed to address both EPI's geometric distortion and blurring and augment the recently introduced Echo Planar Time-resolved Imaging (EPTI). In SKEPTIC, the (2+1)-D k-t space is traversed using several matching out-in spirals within a single shot, and can benefit from additional rotated and time-jittered shots. The out-in multi-spiral trajectory is incoherent with field inhomogeneity phase evolution in both axes. This results in the ability to deliver single-shot 1.9mm<sup>2</sup> in-plane resolution distortion-less, sharp multi-echo images with B<sub>0</sub> and T<sub>2</sub><sup>\*</sup> mapping, and inherent motion, phase and B<sub>0</sub>-variation estimates for multi-shot imaging.

0617



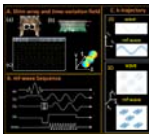
### Dual axis gradient insert for supersonic MRI

Edwin Versteeg<sup>1</sup>, Tjil Van der Velden<sup>1</sup>, Jeroen Hendrikse<sup>1</sup>, Dennis Klomp<sup>1</sup>, and Jeroen Siero<sup>1,2</sup>

<sup>1</sup>Radiology, University Medical Center Utrecht, Utrecht, Netherlands, <sup>2</sup>Spinoza Centre for Neuroimaging Amsterdam, Amsterdam, Netherlands

A silent gradient axis can be achieved by driving a gradient insert above 20 kHz. In this work, we investigate a prototype silent gradient insert that features two axes. Such a setup would enable both silent and fast imaging. The two axes were driven with an audio amplifier at 20 kHz and 22 kHz, and produced gradient amplitudes of 20.8 and 22 mT/m. We simulated the acceleration potential to be a factor of 9 and showed the feasibility of imaging with this setup on a phantom.

0618



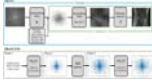
### Multi-frequency wave-encoding (mf-wave) on gradients and multi-coil shim-array hardware for highly accelerated acquisition

Jinmin Xu<sup>1,2</sup>, Jason Stockmann<sup>2</sup>, Berkin Bilgic<sup>2</sup>, Thomas Witzel<sup>2,3</sup>, Jaejin Cho<sup>2</sup>, Congyu Liao<sup>2</sup>, Zijng Zhang<sup>1,2</sup>, Huafeng Liu<sup>1</sup>, and Kawin Setsompop<sup>2,3,4</sup>

<sup>1</sup>State Key Laboratory of Modern Optical Instrumentation, College of Optical Science and Engineering, Zhejiang University, Hangzhou, China, <sup>2</sup>Department of Radiology, A.A. Martinos Center for Biomedical Imaging, Massachusetts General Hospital, Charlestown, MA, United States, <sup>3</sup>Harvard Medical School, Boston, MA, United States, <sup>4</sup>Massachusetts Institute of Technology, Harvard-MIT Health Sciences and Technology, Cambridge, MA, United States

Wave-CAIPI is a parallel imaging technique that can provide high accelerations with negligible g-factor and artifact penalties. However, gradient amplitude & slew rate limits impose a limitation on the amount of wave-encoding and hence the acceleration capability of this technique. In this study, we propose a multi-frequency wave-encoding method (mf-wave) that uses both the gradients and a combined RF and  $B_0$  shim array (32-channel) to perform wave-encoding simultaneously and synergistically at different wave frequencies during the acquisition. We demonstrate that mf-wave can enable ~20-fold acceleration with an acceptable g-factor noise penalty at 3T in vivo.

0619



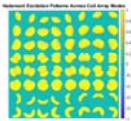
### PILOT: Physics-Informed Learned Optimal Trajectories for Accelerated MRI

Tomer Weiss<sup>1</sup>, Ortal Senouf<sup>2</sup>, Sanketh Vedula<sup>2</sup>, Oleg Michailovich<sup>3</sup>, Michael Zibulevsky<sup>2</sup>, and Alex Bronstein<sup>2</sup>

<sup>1</sup>CS, Technion, Haifa, Israel, <sup>2</sup>Technion, Haifa, Israel, <sup>3</sup>University of Waterloo, Waterloo, ON, Canada

We propose a novel approach to the learning of conjoint acquisition and reconstruction of MRI scans. The acquisition is encoded in the form of general k-space trajectories, which constrained to obey the hardware requirements (peak currents and maximum slew rates of magnetic gradients). We demonstrate the effectiveness of the proposed solution in both image reconstruction and image segmentation, reporting substantial improvements in terms of acceleration factors and the quality of these end tasks. To the best of our knowledge, our proposed algorithm is the first to do data- and task-driven learning over the space of all physically feasible k-space trajectories.

0620



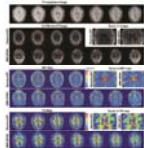
### MR Barcoding: Gradient-Free MRI Using B1-Selective Parallel Transmission

Christopher E. Vaughn<sup>1,2</sup>, Mark A. Griswold<sup>3</sup>, and William A. Grissom<sup>1,2</sup>

<sup>1</sup>Vanderbilt University Institute of Imaging Science, Nashville, TN, United States, <sup>2</sup>Department of Biomedical Engineering, Vanderbilt University, Nashville, TN, United States, <sup>3</sup>Radiology, Case Western Reserve University, Cleveland, OH, United States

Conventional MR imaging uses linear  $B_0$  gradients for spatial encoding, which have high cost and bulk, and lead to patient discomfort via noise and PNS. We introduce MR Barcoding as a silent, low-profile, and low-cost replacement for  $B_0$  gradients. The technique is based on non-linear RF magnitude gradients synthesized by an array of conventional transmit coils, combined with B1+-selective Hadamard encoding pulses. A proof-of-principle simulation shows that a 64x64 image could be reconstructed using an MRF model and a sub-30s scan duration. Experimental results at 47.5 mT validate the encoding capabilities of the B1+-selective Hadamard encoding pulses.

0621



### Rapid volumetric 3D MRI via simultaneous-multi-slab, multi-echo spatiotemporal encoding (SMS-ME SPEN)

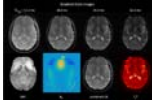
Lingceng Ma<sup>1,2</sup>, Martins Otikovs<sup>1</sup>, Samuel F Cousin<sup>3</sup>, Gilad Liberman<sup>4</sup>, Qingjia Bao<sup>1</sup>, and Lucio Frydman<sup>1</sup>

<sup>1</sup>Department of Chemical and Biological Physics, Weizmann Institute of Science, Rehovot, Israel, <sup>2</sup>College of Electronic science and technology, Xiamen University, Xiamen, China, <sup>3</sup>Centre de RMN à Très Haut Champs, Lyon, France, <sup>4</sup>Massachusetts General Hospital, Boston, MA, United States

SPatiotemporal ENcoding (SPEN) is a 2D single-shot MRI method with higher immunity to artifacts than EPI-based counterparts. The present study extends SPEN scans to 3D volumetric measurements, to achieve imaging over a 3<sup>rd</sup> dimension at higher resolution in minimal acquisition times. simultaneous multi-slab (SMS) and multi-echo (ME)  $k_z$ -encoding procedures are here combined to cope with the SAR complications that would ensue from simply repeating 2D acquisitions over multiple slices. A framework to appropriately reconstruct and process 3D SMS-ME SPEN data to ensure the image quality by taking motion artifacts derived from different dimensions into account is also proposed, and demonstrated.

0622

Simultaneous Multi-Slice Radial Echo Volumar Imaging for Fast Simultaneous Multi-Parametric Imaging



Christoph Alexander Rettenmeier<sup>1</sup>, Danilo Maziero<sup>2</sup>, Kai Tobias Block<sup>3</sup>, and V. Andrew Stenger<sup>1</sup>

<sup>1</sup>Medicine, University of Hawaii, Honolulu, HI, United States, <sup>2</sup>University of Hawaii, Honolulu, HI, United States, <sup>3</sup>New York University, New York, NY, United States

Echo Planar Imaging (EPI) is one of the most widely used fast acquisitions and has been shown to be useful for high-resolution Simultaneous Multi-Parametric (SMP) imaging. However, obtaining high spatial resolutions requires k-space segmentation which has a high sensitivity to motion. Radial sampling is promising because of its continuous k-space center update which can be used for self-navigation and its suitability for undersampling because of benign artifacts. We describe a new k-t sampling strategy based on a Radial Echo Volumar Imaging method for fast SMP imaging. Whole brain images including susceptibility, B0 and T2\* maps acquired at 3T are presented.

## Oral

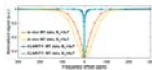
### CEST, MT, Zero-TE and Relaxometry - Chemical Exchange & Magnetisation Transfer: Mechanisms & Applications

Tuesday Parallel 1 Live Q&A

Tuesday 14:30 - 15:15 UTC

Moderators: Rosa Tamara Branca

0497



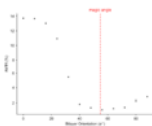
The CLARITY procedure of lipid removal from brain tissue sample reveals the lipid-origin of MT contrast in CEST imaging experiment

Anna Orzylowska<sup>1</sup>, Tymoteusz Słowik<sup>2</sup>, Agata Chudzik<sup>1</sup>, Anna Pankowska<sup>3</sup>, Wilfred W Lam<sup>4</sup>, and Greg J Stanisz<sup>1,4,5</sup>

<sup>1</sup>Department of Neurosurgery and Paediatric Neurosurgery, Medical University of Lublin, Lublin, Poland, <sup>2</sup>Center of Experimental Medicine, Medical University of Lublin, Lublin, Poland, <sup>3</sup>Department of Radiography, Medical University of Lublin, Lublin, Poland, <sup>4</sup>Physical Sciences, Sunnybrook Research Institute, Toronto, ON, Canada, <sup>5</sup>Department of Medical Biophysics, University of Toronto, Toronto, ON, Canada

The study compares the differences between Z-spectra derived from CEST imaging of rat brain in vivo and after post-mortem CLARITY lipids removal procedure. The lipids removal nulled-out MT macromolecular-originating signal measured with B<sub>1</sub> saturation amplitudes of 3 and 5 μT as compared to in vivo, and resulted in negligible MT contribution to CEST Z-spectra acquired with B<sub>1</sub>s of 0.5 and 0.75 μT, as opposite to living tissue, where the MT effect was significant. Our results showed that the macromolecular MT contribution into in vivo Z-spectra originates mostly from lipids, since the CLARITY technique removed the MT component from the spectrum.

0498



Orientation dependence of inhomogeneous magnetization transfer and dipolar order relaxation time in a phospholipid bilayer sample

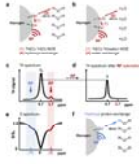
Sarah Rosemary Morris<sup>1,2,3</sup>, Rebecca Frederick<sup>1</sup>, Alex L MacKay<sup>1,2,4</sup>, Cornelia Laule<sup>1,2,3,5</sup>, and Carl A. Michal<sup>1</sup>

<sup>1</sup>Physics & Astronomy, University of British Columbia, Vancouver, BC, Canada, <sup>2</sup>Radiology, University of British Columbia, Vancouver, BC, Canada, <sup>3</sup>International Collaboration on Repair Discoveries, Vancouver, BC, Canada, <sup>4</sup>UBC MRI Research Centre, Vancouver, BC, Canada, <sup>5</sup>Pathology & Laboratory Medicine, University of British Columbia, Vancouver, BC, Canada

Inhomogeneous magnetization transfer ratio (ihMTR) is reported to have significant orientation dependence in the brain, likely due to the anisotropy of dipolar couplings between methylene protons on the oriented lipids in myelin bilayers. We measured the orientation dependence of linewidth, dipolar relaxation time (T<sub>1D</sub>) and ihMTR in an aligned phospholipid bilayer sample at 9.4T. ihMTR was maximized when the bilayers were parallel to B<sub>0</sub> and minimized near the magic angle (~54.7°) despite the fact that T<sub>1D</sub> is maximized there. This is in contrast to previous in vivo results which show maximal ihMTR for bilayers perpendicular to B<sub>0</sub>.

0499

Understanding the magnetization transfer pathway for water-based detection of the aliphatic protons in glycogen

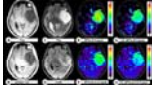


Yang Zhou<sup>1,2</sup>, Peter C.M. van Zijl<sup>1,2</sup>, Jiadi Xu<sup>1,2</sup>, and Nirbhay N. Yadav<sup>1,2</sup>

<sup>1</sup>The Russell H. Morgan Department of Radiology, The Johns Hopkins University School of Medicine, Baltimore, MD, United States, <sup>2</sup>F.M. Kirby Research Center for Functional, Brain Imaging, Kennedy Krieger Institute, Baltimore, MD, United States

Recently a new MRI method was developed for the sensitivity enhanced detection of glycogen based on magnetization transfer between glycogen aliphatic protons and water, yet the mechanism of this transfer pathway is still not well understood. Here, we show that the magnetization transfer occurs via the relayed-NOE (rNOE) CEST effect. A theoretical model is proposed to quantitatively describe the rNOE signal in these magnetization transfer MRI experiments. This study provides insight into the rNOE mechanism that commonly occurs in magnetization transfer MRI on systems such as proteins and carbohydrate polymers.

0500



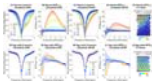
Fluid suppression in CEST imaging affects predominantly IDH-mutant 1p/19q retained gliomas with T2-FLAIR mismatch

Stefano Casagrande<sup>1</sup>, Laura Mancini<sup>2,3</sup>, Guillaume Gautier<sup>1</sup>, Philippe Peter<sup>1</sup>, Bruno Lopez<sup>1</sup>, Sebastian Brandner<sup>4,5</sup>, Enrico De Vita<sup>2,6</sup>, Xavier Golay<sup>2,3</sup>, and Sotirios Bisdas<sup>2,3</sup>

<sup>1</sup>Olea Medical, La Ciotat, France, <sup>2</sup>Lysholm Dept of Neuroradiology, University College of London Hospitals NHS Foundation Trust, London, United Kingdom, <sup>3</sup>Institute of Neurology UCL, London, United Kingdom, <sup>4</sup>National Hospital for Neurology & Neurosurgery, University College of London Hospitals NHS Foundation Trust, London, United Kingdom, <sup>5</sup>Department of Neurodegenerative Disease, Institute of Neurology UCL, London, United Kingdom, <sup>6</sup>Biomedical Engineering Department, School of Biomedical Engineering and Imaging Sciences, King's College London, London, United Kingdom

CEST is a novel MR technique helpful for predicting IDH and 1p/19q status in gliomas. The asymmetry-based methods however are sensitive to fluid signal and recent studies have shown that a significant proportion of IDH-mutant 1p/19q retained gliomas have T2-FLAIR mismatch, indicating the presence of a more fluid microenvironment. This work shows how fluid-suppressed CEST imaging metrics have an impact on amide and amine signals in glioma, with highest effect on IDH-mutant 1p/19q retained with T2-FLAIR mismatch. The combined use of asymmetry-based and fluid-suppressed CEST metrics could be a valuable tool for glioma staging more robust than asymmetry-based metrics alone.

0501

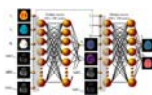


Influence of phosphate concentration on amine and amide chemical exchange saturation transfer (CEST) contrast

Jingwen Yao<sup>1,2,3</sup>, Chencai Wang<sup>1,2</sup>, and Benjamin M. Ellingson<sup>1,2,3</sup>

<sup>1</sup>Brain Tumor Imaging Laboratory (BTIL), Center of Computer Vision and Imaging Biomarker, David Geffen School of Medicine, UCLA, Los Angeles, CA, United States, <sup>2</sup>Department of Radiological Sciences, David Geffen School of Medicine, UCLA, Los Angeles, CA, United States, <sup>3</sup>Department of Bioengineering, Henry Samueli School of Engineering and Applied Science, UCLA, Los Angeles, CA, United States

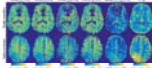
Effects of the catalytic in vivo chemical environment have often been neglected or underestimated in CEST-MRI studies. Phosphate is the predominant exchange catalyst in intracellular fluid and is essential for biosynthesis and bioenergetics. In this study, we evaluated the influence of phosphate on amine and amide CEST contrast using Bloch-McConnell simulations applied to physical phantom data. We demonstrate that amine proton exchange is greatly catalyzed by phosphate, under a physiological concentration range. We propose that catalytic agents should be considered as confounding factors in future CEST-MRI researches. This new dimension may also benefit the development of novel phosphate-sensitive imaging method.



Early Detection of Tumor Apoptotic Response to Oncolytic Virotherapy using Deep CEST MR Fingerprinting Or Perlman<sup>1</sup>, Hirotaka Ito<sup>2</sup>, Kai Herz<sup>3,4</sup>, Hiroshi Nakashima<sup>2</sup>, Moritz Zaiss<sup>3,5</sup>, E. Antonio Chiocca<sup>2</sup>, Christopher Nguyen<sup>1</sup>, Ouri Cohen<sup>6</sup>, Matthew S. Rosen<sup>1,7</sup>, and Christian T. Farrar<sup>1</sup>

<sup>1</sup>Athinoula A. Martinos Center for Biomedical Imaging, Massachusetts General Hospital and Harvard Medical School, Charlestown, MA, United States, <sup>2</sup>Brigham and Women's Hospital and Harvard Medical School, Boston, MA, United States, <sup>3</sup>Magnetic Resonance Center, Max Planck Institute for Biological Cybernetics, Tübingen, Germany, <sup>4</sup>IMPRS for Cognitive and Systems Neuroscience, University of Tübingen, Tübingen, Germany, <sup>5</sup>Department of Neuroradiology, University Clinic Erlangen, Erlangen, Germany, <sup>6</sup>Memorial Sloan Kettering Cancer Center, New York, NY, United States, <sup>7</sup>Department of Physics, Harvard University, Cambridge, MA, United States

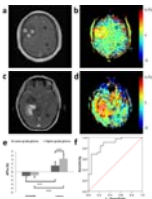
Oncolytic virotherapy (OV) is a promising treatment for high mortality cancers. To optimize the clinical outcome, non-invasive monitoring is essential. The goal of this work was to develop a deep-learning-based technique for quantitative and rapid molecular imaging of OV treatment response. Two CEST MR-fingerprinting protocols were sequentially implemented (105s each) and incorporated within a deep-reconstruction-network, trained to output the quantitative semi-solid and amide pool exchange parameters. The resulting molecular maps allowed early apoptosis detection in brain tumor OV mouse models. Clinical translation of CEST-MRF is demonstrated in a normal human subject and yielded parameters in good agreement with literature values.



CEST and qMT Properties of Brain Metastases from Radio-resistant and Radio-sensitive Primary Tumours  
Hatef Mehrabian<sup>1</sup>, Wilfred W Lam<sup>1</sup>, Hany Soliman<sup>1,2,3</sup>, Sten Myrehaug<sup>2,3</sup>, Arjun Sahgal<sup>1,2,3</sup>, and Greg J Stanisz<sup>1,4</sup>

<sup>1</sup>Physical Sciences, Sunnybrook Research Institute, Toronto, ON, Canada, <sup>2</sup>Radiation Oncology, Sunnybrook Health Sciences Centre, Toronto, ON, Canada, <sup>3</sup>Radiation Oncology, University of Toronto, Toronto, ON, Canada, <sup>4</sup>Medical Biophysics, University of Toronto, Toronto, ON, Canada

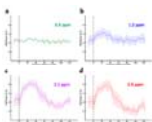
Previous animal studies have shown differences in CEST properties of radio-resistant and radio-sensitive renal cell carcinoma xenografts. The current study probed the differences in CEST and MT properties of brain metastases from radio-resistant and radio-sensitive primary tumours. We observed significantly lower amount of magnetization transfer,  $RM_{0B}/R_A$ , and direct water saturation effect,  $1/(R_A T_{2A})$  in brain metastases from radio-resistant tumours compared to those from radio-sensitive tumours. However, the CEST effects of the two cohorts were not different. Such information should be considered when investigating brain metastases and their response to treatment.



Prediction of prognostic characteristics in glioma patients using amide proton transfer imaging at 3 Tesla  
Jie Liu<sup>1</sup>, Xiaofei Lv<sup>2</sup>, Chao Ke<sup>3</sup>, Zongwei Xu<sup>1</sup>, Long Qian<sup>4</sup>, Shijie Xu<sup>3</sup>, Xin Liu<sup>1</sup>, Hairong Zheng<sup>1</sup>, and Yin Wu<sup>1</sup>

<sup>1</sup>Paul C. Lauterbur Research Center for Biomedical Imaging, Shenzhen Institutes of Advanced Technology, Chinese Academy of Sciences, Shenzhen, China, <sup>2</sup>Department of Medical Imaging, Sun Yat-Sen University Cancer Center, Guangzhou, China, <sup>3</sup>Department of Neurosurgery, Sun Yat-Sen University Cancer Center, Guangzhou, China, <sup>4</sup>GE Healthcare, Beijing, China

Early identification of glioma prognostic characteristics is of great clinical importance. This study aims to evaluate the feasibility of APT in the prediction of tumor grade, IDH mutation and MGMT promoter methylation status at 3 Tesla. A total of 50 patients were recruited. Results show that although APTw effect exhibits no substantial difference based on MGMT methylation status, it enables the discrimination of histopathological grade and IDH mutant status with AUCs higher than 0.88. The results suggest APTw is a valuable imaging biomarker for prediction of tumor prognostic parameters, that may benefit accurate diagnosis and prompt treatment decisions.



Unveiling the fate of glycolytic substrates using multi-spectral CEST: proof of concept with 2DG in the rat brain

Yohann Mathieu-Daudé<sup>1,2</sup>, Mélissa Vincent<sup>1,2</sup>, Julien Valette<sup>1,2</sup>, and Julien Flament<sup>1,2</sup>

0505



<sup>1</sup>Molecular Imaging Research Center (MIRGen), Commissariat à l'Energie Atomique et aux Energies Alternatives (CEA), Fontenay-aux-Roses, France, <sup>2</sup>UMR 9199, Neurodegenerative Diseases Laboratory, Centre National de la Recherche Scientifique (CNRS), Université Paris-Sud, Université Paris-Saclay, Fontenay-aux-Roses, France

2-Deoxy-D-glucose (2DG), an analogue of glucose similarly transported but with metabolism blocked after the first phosphorylation into 2DG-6-phosphate (2DG6P), has already been used to study glycolytic metabolism using gluCEST. However, origin of gluCEST signal is still an open question important to be addressed. In this study, we measured for the first time variations of CEST signal in the rat brain at different resonance frequencies following 2DG injection. The richness of CEST signal can help assessing the fate of glycolytic substrates and would constitute a first step toward quantitative measurement of glucose metabolism using CEST method.

0506



High-resolution pH imaging with ratiometric CEST and BIRDS using dual paramagnetic DOTA–tetraglycinate agents

Jelena Mihailovic<sup>1,2</sup>, Yuegao Huang<sup>1</sup>, John Walsh<sup>1</sup>, Daniel Coman<sup>1</sup>, Sara Samuel<sup>3</sup>, and Fahmeed Hyder<sup>1,3</sup>

<sup>1</sup>(1)Magnetic Resonance Research Center (MRRC), Yale University, New Haven, CT, United States, <sup>2</sup>(2) Department of Diagnostic Radiology, Yale University, New Haven, CT, United States, <sup>3</sup>Core Center for Quantitative Neuroscience with Magnetic Resonance (QNMR), Yale University, New Haven, CT, United States

Chemical Exchange Saturation Transfer (CEST) and Biosensor Imaging of Redundant Deviation in Shifts (BIRDS) biosensing methods differ respectively by detecting exchangeable and non-exchangeable protons on the agent. Given that CEST and BIRDS properties observed from the same paramagnetic agent are complimentary, we describe a novel approach for high-resolution pH imaging using dual agents of europium and thulium complexed with DOTA-tetraglycinate. In vitro results test the hypothesis that ratiometric paraCEST attributes are conserved when temperature from paraBIRDS is detected simultaneously, enabling absolute pH imaging. In vivo results in glioblastoma demonstrate feasibility of this dual paraCEST-paraBIRDS biosensing method for high-resolution pH imaging.

## Oral - Power Pitch

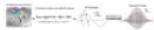
### CEST, MT, Zero-TE and Relaxometry - Contrast Mechanisms: Acquisition & Fitting Methods

Tuesday Parallel 1 Live Q&A

Tuesday 14:30 - 15:15 UTC

Moderators: Puneet Bagga & Ferdinand Schweser

0507

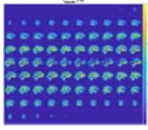


Tailored spectral-spatial saturation pulses for spatially uniform saturation in CEST imaging

Huiwen Luo<sup>1</sup>, Wissam AlGhuraibawi<sup>2</sup>, Kevin Godines<sup>2</sup>, Daniel Gochberg<sup>3</sup>, Moriel Vandsburger<sup>2</sup>, and William A Grissom<sup>1</sup>

<sup>1</sup>Biomedical Engineering, Vanderbilt University, Nashville, TN, United States, <sup>2</sup>Department of Bioengineering, University of California Berkeley, Berkeley, CA, United States, <sup>3</sup>Radiology and Radiological Sciences, Vanderbilt University, Nashville, TN, United States

A tailored spectral-spatial saturation pulse was developed to produce a flat flip angle profile across the heart and achieve more uniform CEST saturation despite B<sub>1</sub> inhomogeneity at 3 Tesla. The tailored saturation pulse train was simulated for a two-pool system to evaluate the z-spectrum at each spatial location in the heart, based on an in vivo 3 Tesla B<sub>1</sub> map. Whereas CEST saturation generated with a conventional Gaussian pulse yielded CEST contrast of 2.60±1.59% across the ventricle, the tailored pulse produced more uniform saturation across the heart which resulted in both greater and more uniform CEST contrast of 4.64±0.34%.

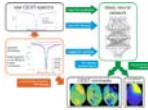


### Towards clinical CEST-MRF: whole brain snapshot CEST MR Fingerprinting at 3T using spin-lock saturation and a centric 3D-EPI readout

Kai Herz<sup>1</sup>, Sebastian Mueller<sup>1</sup>, Or Perlman<sup>2</sup>, Ruediger Stirnberg<sup>3</sup>, Tony Stoecker<sup>3,4</sup>, Klaus Scheffler<sup>1,5</sup>, Christian Farrar<sup>2</sup>, and Moritz Zaiss<sup>1,6</sup>

<sup>1</sup>Magnetic Resonance Center, Max Planck Institute for Biological Cybernetics, Tuebingen, Germany, <sup>2</sup>Athinoula A. Martinos Center for Biomedical Imaging, Department of Radiology, Massachusetts General Hospital and Harvard Medical School, Charlestown, MA, United States, <sup>3</sup>German Center for Neurodegenerative Diseases (DZNE), Bonn, Germany, <sup>4</sup>Department of Physics and Astronomy, University of Bonn, Bonn, Germany, <sup>5</sup>Department of Biomedical Magnetic Resonance, Eberhard Karls University Tuebingen, Tuebingen, Germany, <sup>6</sup>Department of Neuroradiology, University Hospital Erlangen, Erlangen, Germany

Quantitative CEST imaging is still not applied in clinical routine, as both quantification and whole brain coverage require usually long scan times. In this work, we present a CEST-MRF protocol using spin-lock saturation pulses and a fast 3D-EPI readout with whole brain coverage. This enables a fast generation of quantitative amide proton concentration maps of the entire brain at a clinical scanner.

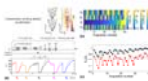


### DeepCEST 3T: Robust neural network prediction of 3T CEST MRI parameters including uncertainty quantification

Felix Glang<sup>1</sup>, Anagha Deshmane<sup>1</sup>, Sergey Prokudin<sup>2</sup>, Florian Martin<sup>1</sup>, Kai Herz<sup>1</sup>, Tobias Lindig<sup>3</sup>, Benjamin Bender<sup>3</sup>, Klaus Scheffler<sup>1,4</sup>, and Moritz Zaiss<sup>1,5</sup>

<sup>1</sup>Magnetic Resonance Center, Max Planck Institute for Biological Cybernetics, Tübingen, Germany, <sup>2</sup>Department of Perceiving Systems, Max Planck Institute for Intelligent Systems, Tübingen, Germany, <sup>3</sup>Department of Diagnostic and Interventional Neuroradiology, Eberhard Karls University Tübingen, Tübingen, Germany, <sup>4</sup>Department of Biomedical Magnetic Resonance, Eberhard Karls University Tübingen, Tübingen, Germany, <sup>5</sup>Department of Neuroradiology, University Clinic Erlangen, Erlangen, Germany

Analysis of CEST data often requires complex mathematical modeling before contrast generation, which can be error prone and time-consuming. Here, a probabilistic deep learning approach is introduced to shortcut conventional Lorentzian fitting analysis of 3T in-vivo CEST data by learning from previously evaluated data. It is demonstrated that the trained networks generalize to data of a healthy subject and a brain tumor patient, providing CEST contrasts in a fraction of the conventional evaluation time. Additionally, the probabilistic network architecture enables uncertainty quantification, indicating if predictions are trustworthy, which is assessed by perturbation analysis.



### Unsupervised Deep Learning-based Magnetization Transfer Contrast (MTC) MR Fingerprinting and CEST MRI

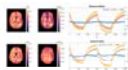
Beomgu Kang<sup>1</sup>, Byungjai Kim<sup>1,2</sup>, Michael Schar<sup>2</sup>, Hyunwook Park<sup>1</sup>, and Hye Young Heo<sup>2,3</sup>

<sup>1</sup>Department of Electrical Engineering, Korea Advanced Institute of Science and Technology, Daejeon, Korea, Republic of, <sup>2</sup>Russell H Morgan Department of Radiology and Radiological Science, Johns Hopkins University, Baltimore, MD, United States, <sup>3</sup>F.M. Kirby Research Center for Functional Brain Imaging, Kennedy Krieger Institute, Baltimore, MD, United States

Most currently used MTC/CEST imaging protocols depend on the acquisition of qualitative weighted images, limiting the detection sensitivity to quantitative parameters, their exchange rate and concentration. Here, we propose a fast, quantitative 3D MTC/CEST imaging framework based on a combined 1) time-interleaved parallel RF transmission, 2) compressed sensing, 3) MR fingerprinting, and 4) deep-learning techniques. Typically, supervised deep learning requires a massive amount of labeled images for training, which is limited particularly in MTC/CEST MRI field. However, the proposed unsupervised learning architecture requires only small amounts of unlabeled MTC/CEST data.



0511



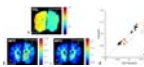
### Transient-State Inhomogeneous Magnetisation Transfer: Towards Magnetisation Transfer Fingerprinting

Daniel J. West<sup>1</sup>, Gastao Cruz<sup>1</sup>, Olivier Jaubert<sup>1</sup>, Rui P. A. G. Teixeira<sup>1,2</sup>, Torben Schneider<sup>3</sup>, Jacques-Donald Tournier<sup>1,2</sup>, Jo Hajnal<sup>1,2</sup>, Claudia Prieto<sup>1</sup>, and Shaihan J. Malik<sup>1,2</sup>

<sup>1</sup>School of Biomedical Engineering and Imaging Sciences, King's College London, London, United Kingdom, <sup>2</sup>Centre for The Developing Brain, King's College London, London, United Kingdom, <sup>3</sup>Philips Healthcare, Guildford, United Kingdom

Inhomogeneous magnetisation transfer (ihMT) is a contrast mechanism that has shown high specificity towards myelinated tissue. Contrast is typically generated using sequences comprising a preparation phase with several RF saturation pulses, followed by multiple readout periods for measurement. Here, we present a transient acquisition scheme that alternates between periods of multi-band and single-band RF pulses, to efficiently generate ihMT contrast during a single data acquisition. Since signal is transiently varying throughout, we use a dictionary-based low-rank inversion reconstruction method originally proposed for magnetic resonance fingerprinting. Simulation, phantom and human in-vivo experiments are included.

0512



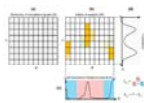
### Towards Absolute Quantification of Macromolecular Proton Content using Cross-Relaxation Imaging

Alexey Samsonov<sup>1</sup>, Aaron Field<sup>1</sup>, Vasily Yarnykh<sup>2</sup>, and Julia Velikina<sup>3</sup>

<sup>1</sup>Radiology, University of Wisconsin, Madison, WI, United States, <sup>2</sup>Radiology, University of Washington, Seattle, WA, United States, <sup>3</sup>Medical Physics, University of Wisconsin, Madison, WI, United States

Macromolecular proton fraction (MPF), the key two-pool MT model parameter, was established as a robust myelin-sensitive index, with clinical relevance in demyelinating diseases. However, as MPF assesses macromolecules relative to tissue water, its specificity to myelin is limited. i.e., MPF changes may occur independent of myelin, e.g., in the setting of inflammation and edema. Further, relating MPF to macromolecules may be ambiguous due to unequal concentrations of protons in macromolecular and water compartments. We demonstrate implications of these effects for MPF interpretation using phantom and ex-vivo experiments and propose a new macromolecular measure that explicitly accounts for tissue water effects.

0513

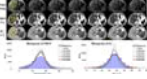


### Fat fraction mapping using bSSFP Signal Profile Asymmetries for Robust multi-Compartment Quantification (SPARCQ)

Giulia MC Rossi<sup>1,2</sup>, Tom Hilbert<sup>1,2,3</sup>, Adèle LC Mackowiak<sup>1,2</sup>, Katarzyna Pierzchała<sup>4,5</sup>, Tobias Kober<sup>1,2,3</sup>, and Jessica AM Bastiaansen<sup>1</sup>

<sup>1</sup>Department of Diagnostic and Interventional Radiology, Lausanne University Hospital and University of Lausanne, Lausanne, Switzerland, <sup>2</sup>Advanced Clinical Imaging Technology, Siemens Healthcare AG, Lausanne, Switzerland, <sup>3</sup>LTS5, Ecole Polytechnique Fédérale de Lausanne (EPFL), Lausanne, Switzerland, <sup>4</sup>Laboratory for Functional and Metabolic Imaging, Ecole Polytechnique Fédérale de Lausanne (EPFL), Lausanne, Switzerland, <sup>5</sup>Center for Biomedical Imaging (CIBM), Ecole Polytechnique Fédérale de Lausanne (EPFL), Lausanne, Switzerland

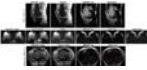
**A novel quantitative framework for detection of different tissue compartments based on bSSFP signal profile asymmetries (SPARCQ) is reported. SPARCQ uses a dictionary-based weight optimization algorithm to estimate voxel-wise off-resonance frequency and relaxation time ratio spectra from acquired bSSFP signal profiles. From the obtained spectra, quantitative parameters (i.e. fractions of the components of interest, thermal equilibrium magnetization) can be extracted. Validation and proof-of-concept are provided for voxel-wise water-fat separation and fat fraction mapping. Accuracy and repeatability of SPARCQ are demonstrated with phantom and in vivo experiments.**



Ante Zhu<sup>1,2</sup>, Yuxin Zhang<sup>2,3</sup>, Alan McMillan<sup>2</sup>, Fang Liu<sup>2</sup>, Timothy J Colgan<sup>2</sup>, Scott B. Reeder<sup>1,2,3,4,5</sup>, and Diego Hernando<sup>1,2,3,6</sup>

<sup>1</sup>Biomedical Engineering, University of Wisconsin-Madison, Madison, WI, United States, <sup>2</sup>Radiology, University of Wisconsin-Madison, Madison, WI, United States, <sup>3</sup>Medical Physics, University of Wisconsin-Madison, Madison, WI, United States, <sup>4</sup>Emergency Medicine, University of Wisconsin-Madison, Madison, WI, United States, <sup>5</sup>Medicine, University of Wisconsin-Madison, Madison, WI, United States, <sup>6</sup>Electrical and Computer Engineering, University of Wisconsin-Madison, Madison, WI, United States

Multi-echo chemical shift-encoded (CSE)-MRI techniques enable liver PDFFF and  $R_2^*$  quantification, which enable staging and treatment monitoring of liver fat and iron content, respectively. However, the common requirement of breath-holding in CSE-MRI acquisitions is challenging for many patients. Furthermore, the required specialized multi-echo acquisition and reconstruction are not available in all scanners. In this work, we assessed the accuracy of deep learning (DL)-based PDFFF and  $R_2^*$  quantification using reduced numbers of echoes. Preliminary results demonstrate the potential of this approach and suggest that at least four echoes are needed for quantifying PDFFF and  $R_2^*$  at 1.5T and 3.0T.

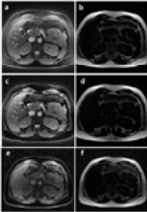


Simultaneous Multiple Resonance Frequency (SMURF) imaging: Fat-water imaging using multi-band principles

Beata Bachrata<sup>1,2,3</sup>, Bernhard Strasser<sup>1,2,4</sup>, Wolfgang Bogner<sup>1,2</sup>, Albrecht Ingo Schmid<sup>1,5</sup>, Siegfried Trattnig<sup>1,2,3</sup>, and Simon Daniel Robinson<sup>1,2,6,7</sup>

<sup>1</sup>High Field MR Centre, Medical University of Vienna, Vienna, Austria, <sup>2</sup>Department of Biomedical Imaging and Image-guided Therapy, Medical University of Vienna, Vienna, Austria, <sup>3</sup>Christian Doppler Laboratory for Clinical Molecular MR Imaging, Vienna, Austria, <sup>4</sup>Athinoula A. Martinos Center for Biomedical Imaging, Department of Radiology, Massachusetts General Hospital, Harvard Medical School, Boston, MA, United States, <sup>5</sup>Center for Medical Physics and Biomedical Engineering, Medical University of Vienna, Vienna, Austria, <sup>6</sup>Centre for Advanced Imaging, The University of Queensland, Brisbane, Australia, <sup>7</sup>Department of Neurology, Medical University of Graz, Graz, Austria

Imaging of body regions containing both water-based and fat-based structures is affected by artefacts arising from the chemical shift difference between water and fat. Recently, a single-echo water-fat separation technique was proposed which used multi-band principles to generate separate water and fat images as well as chemical shift-corrected, recombined water-fat images. We demonstrate the performance of gradient-echo and turbo spin-echo variants of this approach in the knee, breasts and abdomen. The separation of water and fat was similar to or better than with current state-of-the-art techniques and chemical shift effects were fully eliminated in recombined water-fat images.



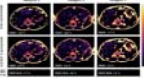
Fat suppression using a rosette trajectory for low field magnetic resonance imaging

Dominique Franson<sup>1</sup>, Yuchi Liu<sup>1,2</sup>, Rajiv Ramasawmy<sup>3</sup>, Adrienne Campbell-Washburn<sup>3</sup>, and Nicole Seiberlich<sup>1,2</sup>

<sup>1</sup>Case Western Reserve University, Cleveland, OH, United States, <sup>2</sup>University of Michigan, Ann Arbor, MI, United States, <sup>3</sup>National Heart, Lung, and Blood Institute, National Institutes of Health, Bethesda, MD, United States

Fat/water separation at low field strengths can be difficult due to the small difference between resonance frequencies. Rosette trajectories have previously been shown to be effective for spectral separation and fat suppression, and the approach is not dependent on a large frequency difference. Here, a rosette trajectory is used to significantly suppress fat signal in water images, and to produce separate fat images at 0.55T. B0 maps are calculated from two of the rosette echoes, and are used to improve the fat/water separation. Initial examples are shown in an oil/water phantom, and in the heart and abdomen.

0517



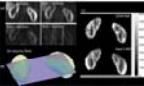
### Correcting gradient chain-induced fat quantification errors in multi-echo SoS acquisition using the gradient impulse response function

Christoph C. Zöllner<sup>1</sup>, Sophia Kronthaler<sup>1</sup>, Stefan A. Ruschke<sup>1</sup>, Holger Eggert<sup>2</sup>, Jürgen Rahmer<sup>2</sup>, Peter Börner<sup>2</sup>, Rickmer F. Braren<sup>1</sup>, Daniela Franz<sup>1</sup>, and Dimitrios C. Karampinos<sup>1</sup>

<sup>1</sup>Department of Diagnostic and Interventional Radiology, School of Medicine, Technical University of Munich, Munich, Germany, <sup>2</sup>Philips Research Laboratory, Hamburg, Germany

Multi-echo Stack-of-stars-type radial k-space trajectories employing golden-angle ordering have been becoming popular for abdominal fat quantification. Gradient chain imperfections including eddy currents and gradient delays are known to affect the image quality of radial imaging. Most methods for compensating radial k-space trajectory errors are based either on the acquisition of calibration lines with opposite polarity or on the processing of approximately anti-parallel spokes from the actual radial acquisition. This work shows that a trajectory correction based on a gradient system impulse response function improves fat quantification in gated golden-angle radial Dixon imaging.

0518



### Perfusion Quantification Validation on a Numerical Vascular Network of the Kidney: Traditional Kety's Method vs Quantitative Transport Mapping

Liangdong Zhou<sup>1</sup>, Qihao Zhang<sup>1,2</sup>, Pascal Spincemaille<sup>1</sup>, Thanh D Nguyen<sup>1</sup>, John Morgan<sup>1</sup>, Weiyang Dai<sup>1</sup>, Ajay Gupta<sup>1</sup>, Martin R Prince<sup>1</sup>, and Yi Wang<sup>1,2</sup>

<sup>1</sup>Weill Medical College of Cornell University, New York, NY, United States, <sup>2</sup>Cornell University, Ithaca, NY, United States

Perfusion quantification is important for the diagnosis of many diseases. Validation of perfusion quantification methods remains challenging due to the various assumptions and lack of the ground truth. We built a numerical phantom of microvascular network in the kidney. In the phantom, the ground truth blood velocity and flow were computed from Navier-Stokes equation. Tracer concentration was simulated based on the mass transport equation. Comparison between Kety's method and our recently proposed AIF-free QTM method was performed using the numerical phantom. It turns out that QTM method reduces the flow error by more than 3 folds compare with Kety's method.

0519



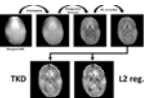
### A non-local filtering based approach for high quality quantitative susceptibility mapping reconstruction

Srikant Kamesh Iyer<sup>1</sup>, Brianna F Moon<sup>2</sup>, Nicholas J Josselyn<sup>1</sup>, Eileen Hwuang<sup>2</sup>, Jeffrey B Ware<sup>1</sup>, David Roalf<sup>3</sup>, Jae W Song<sup>1</sup>, S. Ali Nabavizadeh<sup>1</sup>, and Walter R Witschey<sup>1</sup>

<sup>1</sup>Radiology, Perelman School of Medicine, University of Pennsylvania, Philadelphia, PA, United States, <sup>2</sup>Bioengineering, Perelman School of Medicine, University of Pennsylvania, Philadelphia, PA, United States, <sup>3</sup>Psychiatry, University of Pennsylvania, Philadelphia, PA, United States

This abstract presents a novel non-local filtering based reconstruction approach for high quality quantitative susceptibility mapping (QSM). Popular QSM techniques that use fixed sparsity priors such as total variation or total generalized variation often suffer from blurring of fine features (e.g. edges). Since QSM images have non-local spatial redundancies in the form of self-similarity, we develop an approach that uses non-local grouping by 4D cube-matching and collaborative filtering in a plug-and-play (PnP) alternating direction method of multiplier (ADMM) framework. We show that the proposed non-local filtering based reconstruction approach achieves sharper edges and better preservation of fine features.

0520



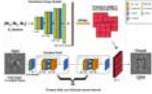
### Quantitative Susceptibility Mapping from 3D Magnetic Resonance Fingerprinting with Quadratic RF Phase Data

Rasim Boyacioglu<sup>1</sup> and Mark Griswold<sup>1</sup>

<sup>1</sup>Radiology, Case Western Reserve University, Cleveland, OH, United States

Magnetic Resonance Fingerprinting with Quadratic RF Phase (MRFqRF) can simultaneously map T1, T2, T2\* and off-resonance. It has been shown that local field inhomogeneities due to susceptibility is encoded in MRFqRF off-resonance maps. Here publicly available standard QSM processing tools were used to analyze two high resolution 3D MRFqRF datasets from 3T. Susceptibility contrast is revealed after phase unwrapping, background removal and B1 correction. QSM preprocessed data was further analyzed with two dipole kernel inversion algorithms. Susceptibility encoding in MRF framework is novel and brings immediate additional value to MRI exam.

0521



### OG-DNN: Orientation-Grasp Deep Neural Network for Quantitative Susceptibility Mapping

Kuo-Wei Lai<sup>1,2</sup>, Jeremias Sulam<sup>1</sup>, Manisha Aggarwal<sup>3</sup>, Peter van Zijl<sup>2,3</sup>, and Xu Li<sup>2,3</sup>

<sup>1</sup>Department of Biomedical Engineering, Johns Hopkins University, Baltimore, MD, United States, <sup>2</sup>F.M. Kirby Research Center for Functional Brain Imaging, Kennedy Krieger Institute, Baltimore, MD, United States, <sup>3</sup>Department of Radiology and Radiological Sciences, Johns Hopkins University, Baltimore, MD, United States

We designed a method called Orientation-Grasp Deep Neural Network (OG-DNN) for Quantitative Susceptibility Mapping (QSM). OG-DNN has dynamically adaptive convolutional filters that adjust themselves according to the input  $B_0$  orientation in the subject frame of reference. Our experimental results demonstrate that OG-DNN can reconstruct high-quality and consistent susceptibility maps from MR phase data acquired at different head orientations with respect to  $B_0$  within a consistent subject frame of reference. OG-DNN is expected to provide improved flexibility in practice and may potentially facilitate the development of deep learning-based Susceptibility Tensor Imaging (STI) reconstructions.

## Oral

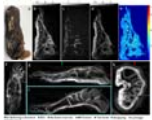
### CEST, MT, Zero-TE and Relaxometry - Relaxometry & Zero-TE

Tuesday Parallel 1 Live Q&A

Tuesday 14:30 - 15:15 UTC

Moderators: Hai-Ling Cheng & Martijn Cloos

0522



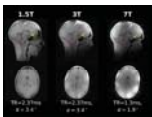
### Short-T2 MRI of Ancient Egyptian Mummified Human Tissue

Emily Louise Baadsvik<sup>1</sup>, Markus Weiger<sup>1</sup>, Romain Froidevaux<sup>1</sup>, Manuela Barbara Rösler<sup>1</sup>, David Otto Brunner<sup>1</sup>, Lena Öhrström<sup>2</sup>, Patrick Eppenberger<sup>2</sup>, Frank J. Rühli<sup>2</sup>, and Klaas Paul Pruessmann<sup>1</sup>

<sup>1</sup>Institute for Biomedical Engineering, ETH Zurich and University of Zurich, Zurich, Switzerland, <sup>2</sup>Institute of Evolutionary Medicine, University of Zurich, Zurich, Switzerland

Evolutionary medicine aims to study disease development over long timescales, and through the study of mummified human remains, tissue information dating back thousands of years becomes accessible. Due to their status as ancient relics, noninvasive techniques are preferable, and to date CT imaging is the most common modality. However, CT images lack soft-tissue contrast, making complementary MRI data desirable. Due to the extensively dehydrated nature and short T2 times of mummified tissues, acquiring such data is challenging. This research explored the use of the zero echo-time sequences and a high-performance gradient in mummy MRI, yielding yet unparalleled image quality.

0523



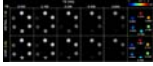
### ZTE Imaging Across Field Strengths; Opportunities for Low-Field Imaging

Emil Ljungberg<sup>1</sup>, Brian Burns<sup>2</sup>, Tobias Wood<sup>1</sup>, Ana Beatriz Solana<sup>3</sup>, Peder E.Z. Larson<sup>4</sup>, Gareth J. Barker<sup>1</sup>, and Florian Wiesinger<sup>1,3</sup>

<sup>1</sup>Neuroimaging, King's College London, London, United Kingdom, <sup>2</sup>ASL West, GE Healthcare, Menlo Park, CA, United States, <sup>3</sup>ASL Europe, GE Healthcare, Munich, Germany, <sup>4</sup>Univeristy of California, San Francisco, San Francisco, CA, United States

Zero Echo Time (ZTE) imaging enables ultra-fast, near silent data acquisition. In this work we demonstrate how contrast-to-noise, between white and gray matter in the brain, with a ZTE acquisition changes with field strength. At low field strength, maximum contrast is achievable with low RF power, which is promising for implementation on low field systems. We demonstrate through in vivo experiment that ZTE imaging can be performed at 1.5T/3T/7T, and how variable flip angle data at, for instance, 1.5T can be used for synthesising high quality  $T_1$ -weighted MR images.

0524



#### Efficient mapping of ultra-fast $T_2^*$ decay

Romain Froidevaux<sup>1</sup>, Markus Weiger<sup>1</sup>, Manuela Barbara Rösler<sup>1</sup>, David Otto Brunner<sup>1</sup>, Benjamin Emanuel Dietrich<sup>1</sup>, and Klaas Paul Pruessmann<sup>1</sup>

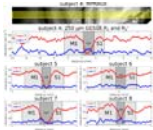
<sup>1</sup>Institute for Biomedical Engineering, ETH Zurich and University of Zurich, Zurich, Switzerland

With recent developments in gradient hardware even tissues with  $T_2$ s down to tens of microseconds have become accessible for MRI. Hence, mapping signal decay or imaging short- $T_2$  tissues selectively is of particular interest.

This can be performed using ultra-short echo time imaging with multiple TEs. However, for typical resolutions this approach is limited to  $T_2$ s down to hundreds of microseconds.

In this work, the PETRA and HYFI techniques are utilized to map the signal decay of samples with  $T_2$ s down to 54  $\mu$ s. Considerably larger scan efficiency is obtained for the HYFI approach.

0525



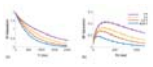
#### In vivo irreversible and reversible transverse relaxation rates in human cerebral cortex via line scans at 7T with 250 micron radial resolution

Mukund Balasubramanian<sup>1,2</sup>, Robert V. Mulkern<sup>1,2</sup>, and Jonathan R. Polimeni<sup>1,3,4</sup>

<sup>1</sup>Harvard Medical School, Boston, MA, United States, <sup>2</sup>Department of Radiology, Boston Children's Hospital, Boston, MA, United States, <sup>3</sup>Athinoula A. Martinos Center for Biomedical Imaging, Department of Radiology, Massachusetts General Hospital, Charlestown, MA, United States, <sup>4</sup>Harvard-MIT Division of Health Sciences and Technology, Massachusetts Institute of Technology, Cambridge, MA, United States

A novel "line-scan GESSE" pulse sequence was used to measure irreversible and reversible transverse relaxation rates— $R_2$  and  $R_2'$ , respectively—in the cerebral cortex of eight healthy human subjects, scanned at 7T with extremely high resolution (250  $\mu$ m) in the radial direction, i.e., perpendicular to the cortical surface. Within primary visual (V1), motor (M1) and somatosensory (S1) cortex, we observed patterns of  $R_2$  versus cortical depth that were quite consistent across subjects. These patterns are also consistent with the intracortical non-heme iron content in these areas, known from prior histology studies.

0526



#### Field-Dependence of White Matter $T_1$ Through Macromolecular Relaxation and Magnetization Transfer

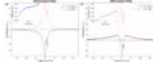
Yicun Wang<sup>1</sup>, Peter van Gelderen<sup>1</sup>, Jacco A. de Zwart<sup>1</sup>, and Jeff H. Duyn<sup>1</sup>

<sup>1</sup>AMRI, LFMI, NINDS, National Institutes of Health, Bethesda, MD, United States

Brain tissue  $T_1$  predominately reflects local macromolecular content and is magnetic field strength dependent. In this study, we quantified the field dependence of macromolecular proton  $T_1$  (or rate  $R_m$ ) in white matter by evaluating its effect exerted on the water signal through magnetization transfer. Inversion recovery and saturation recovery experiments were performed on a group of eight volunteers at 0.55, 1.5, 3 and 7 T, and were jointly analyzed using a two-pool exchange model.  $R_m$  was found to be close to inversely proportional to  $B_0$ , consistent with previous in vitro findings at very low fields.



0527

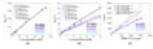


Luke A. Reynolds<sup>1</sup>, Alex L. MacKay<sup>1,2,3</sup>, and Carl A. Michal<sup>1</sup>

<sup>1</sup>Physics & Astronomy, University of British Columbia, Vancouver, BC, Canada, <sup>2</sup>Radiology, University of British Columbia, Vancouver, BC, Canada, <sup>3</sup>MRI Research Centre, University of British Columbia, Vancouver, BC, Canada

Adiabatic pulses are commonly used in clinical MRI due to their insensitivity to  $B_1$  inhomogeneity and uniform flip angle over a selected bandwidth. When applied to white matter, they are generally assumed to saturate the magnetization of the non-aqueous protons in myelin. We performed adiabatic inversion recovery experiments on bovine brain in vitro using a solid state NMR spectrometer to directly observe the effects of adiabatic inversions on the non-aqueous signal. Substantial non-aqueous magnetization remains after typical adiabatic pulses. The state of the non-aqueous magnetization seriously impacts measurement of  $T_1$ , yielding values dependent on the form of inversion pulse used.

0528



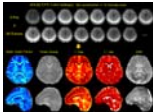
Short  $T_1$  Measurement Using an Inversion Recovery Prepared Three-Dimensional Ultrashort Echo Time Cones (3D IR-UTE-Cones) Method

Zhao Wei<sup>1,2,3</sup>, Yajun Ma<sup>1</sup>, Hyungseok Jang<sup>1</sup>, Wenhui Yang<sup>3</sup>, and Jiang Du<sup>1</sup>

<sup>1</sup>Department of Radiology, UC San Diego, San Diego, CA, United States, <sup>2</sup>University of Chinese Academy of Sciences, Beijing, China, <sup>3</sup>Institute of Electrical Engineering, Chinese Academy of Sciences, Beijing, China

In magnetic resonance imaging (MRI),  $T_1$  is an important biomarker for many diseases and plays a key role in affecting image contrast. We propose a novel  $T_1$  measurement method combining adiabatic inversion recovery with 3D ultrashort echo time cones pulse sequences (3D IR-UTE-Cones). This study aimed to verify the feasibility of using 3D IR-UTE-Cones to accurately calculate  $T_1$ s of short  $T_2^*$  tissues. The results indicated that this method could precisely measure a broad range of  $T_1$ s and that it performed better than commonly used clinical protocols in ultrashort  $T_1$  measurement.

0529



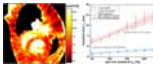
Variable Flip Angle 3D Echo Planar Time-Resolved Imaging (vFA 3D-EPTI) for Fast Multi-Compartment Quantitative Mapping

Zijing Dong<sup>1,2</sup>, Fuyixue Wang<sup>1,3</sup>, Kwok-Shing Chan<sup>4</sup>, Timothy G. Reese<sup>1</sup>, Berkin Bilgic<sup>1</sup>, José P. Marques<sup>4</sup>, and Kawin Setsompop<sup>1,3</sup>

<sup>1</sup>Athinoula A. Martinos Center for Biomedical Imaging, Massachusetts General Hospital, Charlestown, MA, United States, <sup>2</sup>Department of Electrical Engineering and Computer Science, MIT, Cambridge, MA, United States, <sup>3</sup>Harvard-MIT Health Sciences and Technology, MIT, Cambridge, MA, United States, <sup>4</sup>Donders Institute for Brain, Cognition and Behaviour, Radboud University, Nijmegen, Netherlands

Multi-compartment models have been developed to detect the microstructure properties of brain tissue using multi-modal MRI, but are limited by the long scan time of multi-contrast multi-parametric acquisition. In this work, a novel variable flip angle EPTI (vFA 3D-EPTI) technique is developed to quickly acquire rich multi-contrast information for multi-compartment analysis. The optimized 'temporal variant CAIPI' sampling was used, and an augmented subspace reconstruction with multi-compartment modelling is also developed to accurately reconstruct complex signal evolution. Through this approach, myelin water fraction, proton density, multi-compartment  $T_1$ ,  $T_2^*$  maps can be acquired simultaneously in 12 minutes at 1-mm isotropic resolution.

0530



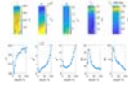
Synthetic  $T_1\rho$  dispersion imaging for improved myocardial tissue characterization using dispersion reconstruction

Maximilian Gram<sup>1,2</sup>, Daniel Gensler<sup>1,3</sup>, Patrick Winter<sup>1,2</sup>, Michael Seethaler<sup>2,3</sup>, Peter Jakob<sup>2</sup>, and Peter Nordbeck<sup>1,3</sup>

<sup>1</sup>Department of Internal Medicine I, University Hospital Würzburg, Würzburg, Germany, <sup>2</sup>Experimental Physics 5, University of Würzburg, Würzburg, Germany, <sup>3</sup>Comprehensive Heart Failure Center (CHFC), University Hospital Würzburg, Würzburg, Germany

$T_{1\rho}$  dispersion imaging is a very time-consuming process because full  $T_{1\rho}$ -mapping at different spin-lock amplitudes is required. Due to this issue, investigation of  $T_{1\rho}$  dispersion is hardly feasible in the limited measurement time of a small animal experiment. In this work, we present a novel approach for the rapid measurement of cardiac  $T_{1\rho}$  dispersion called dispersion reconstruction. With our new concept a  $T_{1\rho}$  dispersion image is generated by only acquiring a fraction of the required mapping data. Phantom and *in vivo* experiments confirm the applicability of our new method as part of a conventional protocol for small animal studies.

0531



### Correlation Time as a New MRI Contrast

Hassaan Elsayed<sup>1,2</sup>, Jouni Karjalainen<sup>1,2</sup>, Nina Hänninen<sup>1,3</sup>, Isabel Stavenuiter<sup>3</sup>, Stefan Zbyn<sup>1,4</sup>, Mikko Nissi<sup>1,3</sup>, Miika T. Nieminen<sup>1,2,5</sup>, and Matti Hanni<sup>1,2,5</sup>

<sup>1</sup>Research Unit of Medical Imaging, Physics and Technology, University of Oulu, Oulu, Finland, <sup>2</sup>Medical Research Center, University of Oulu and Oulu University Hospital, Oulu, Finland, <sup>3</sup>Department of Applied Physics, University of Eastern Finland, Kuopio, Finland, <sup>4</sup>Center for Magnetic Resonance Research, Department of Radiology, University of Minnesota, Minneapolis, MN, United States, <sup>5</sup>Department of Diagnostic Radiology, Oulu University Hospital, Oulu, Finland

In this study, we determined correlation time ( $\tau_c$ ), a parameter that we propose as MRI contrast indicative of the structure of articular cartilage.  $T_{1\rho}$  dispersion data were acquired from intact patellar bovine cartilage samples and  $\tau_c$  maps were obtained by fitting a Lorentzian model function to the  $T_{1\rho}$  dispersion. The association between  $\tau_c$  and the tissue properties was assessed by correlation analysis between  $\tau_c$  and histology. The results suggest that the proposed parameter  $\tau_c$  as well as other fitting parameters can reveal cartilage structure. More investigation is needed to establish correlation between  $\tau_c$  and histology.

## Oral - Power Pitch

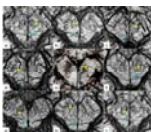
### Acquisition & Processing in Neuro - Novel Neuroimaging Techniques

Tuesday Parallel 2 Live Q&A

Tuesday 14:30 - 15:15 UTC

Moderators: Yuki Kanazawa & Qin Qin

0532

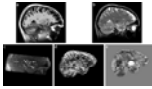


### Subvoxel Vascular Imaging of the Midbrain Using USPIO-Enhanced MRI

Sagar Buch<sup>1</sup>, Ying Wang<sup>2</sup>, Pavan K. Jella<sup>1</sup>, Min-Gyu Park<sup>3</sup>, Yongsheng Chen<sup>1,4</sup>, Jiani Hu<sup>1</sup>, Yulin Ge<sup>5</sup>, Kamran Shah<sup>1</sup>, and E. Mark Haacke<sup>1,2</sup>

<sup>1</sup>Department of Radiology, Wayne State University, Detroit, MI, United States, <sup>2</sup>Magnetic Resonance Innovations, Inc., Detroit, MI, United States, <sup>3</sup>Department of Neurology, Pusan National University School of Medicine, Yangsan, Korea, Republic of, <sup>4</sup>Department of Neurology, Wayne State University, Detroit, MI, United States, <sup>5</sup>Department of Radiology, New York University School of Medicine, New York, NY, United States

We demonstrate the utility of low dose Ferumoxytol in microvasculature imaging of the midbrain using susceptibility weighted imaging (SWI). Mapping the brain's vasculature has implications for understanding the etiology of many neurovascular and neurodegenerative diseases such as Parkinson's disease. By administering this strongly paramagnetic agent, SWI was able to visualize both arteries and veins; and its sensitivity to detect sub-voxel vessels increased tremendously. However, the use of Ferumoxytol exacerbates the signal loss of large vessels, confounding the ability to visualize nearby smaller vessels. Hence, we propose the use of multiple time point SWI to effectively see through the blooming artifacts.



### The human phantom: Comprehensive ultrahigh resolution whole brain in vivo single subject dataset

Falk Luesebrink<sup>1,2</sup>, Mattern Hendrik<sup>2</sup>, Renat Yakupov<sup>3</sup>, Steffen Oeltze-Jafra<sup>1,4</sup>, and Oliver Speck<sup>2,3,4,5</sup>

<sup>1</sup>Medicine & Digitalization, Otto-von-Guericke University, Magdeburg, Germany, <sup>2</sup>Biomedical Magnetic Resonance, Otto-von-Guericke University, Magdeburg, Germany, <sup>3</sup>German Center for Neurodegenerative Diseases, Magdeburg, Germany, <sup>4</sup>Center for Behavioral Brain Sciences, Magdeburg, Germany, <sup>5</sup>Leibniz Institute for Neurobiology, Magdeburg, Germany

Here, we present an extension to our previously published  $T_1$ -weighted dataset with an ultrahigh isotropic resolution of 250  $\mu\text{m}$ , consisting of multiple additional contrasts. Included are up to 150  $\mu\text{m}$  ToF, an updated 250  $\mu\text{m}$  MPRAGE, 330  $\mu\text{m}$  QSM, up to 450  $\mu\text{m}$   $T_2$ -weighted SPACE, 750  $\mu\text{m}$  MPM, 800  $\mu\text{m}$  DTI, one hour continuous rs-fMRI as well as more than 130 MPRAGE volumes collected over 10 years (with varying spatial resolution between 450  $\mu\text{m}$  and 1 mm). All data were acquired on the same 7 T scanner and of the same subject. Basic pre-processing of all data were conducted.

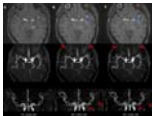


### Low $b$ -value DTI for Analyzing Pseudo-random Flow of CSF

Yoshitaka Bito<sup>1</sup>, Kuniaki Harada<sup>1</sup>, Hisaaki Ochi<sup>2</sup>, and Kohsuke Kudo<sup>3</sup>

<sup>1</sup>Healthcare Business Unit, Hitachi, Ltd., Tokyo, Japan, <sup>2</sup>Research and Development Group, Hitachi, Ltd., Tokyo, Japan, <sup>3</sup>Department of Diagnostic Imaging, Hokkaido University Graduate School of Medicine, Sapporo, Japan

Cerebrospinal fluid (CSF) plays an important role in the clearance system of the brain. Low  $b$ -value DTI is reported to be useful for observing the CSF flow; however, the precise flow property observed by low  $b$ -value DTI has not been fully investigated. We proposed a mathematical framework of low  $b$ -value DTI for analyzing a pseudo-random flow and applied this framework to investigation into CSF. Measured DTI shows high and anisotropic diffusivity, representing large variance of flow velocity, in some segments of CSF. It demonstrates that low  $b$ -value DTI can be used for analyzing pseudo-random flow of CSF.

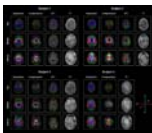


### 3D Flow Compensated Interleaved EPI with Partial Fourier Acquisition: A Feasibility Study for Fast Intracranial TOF-MRA

Wei Liu<sup>1</sup> and Kun Zhou<sup>1</sup>

<sup>1</sup>Siemens Shenzhen Magnetic Resonance Ltd., Shenzhen, China

As commonly used for intracranial vasculature, 3D TOF usually requires long acquisition time. In this study, we implemented a 3D-iEPI sequence with partial flow compensation, combined with partial Fourier acquisition to further reduce the flow artifacts. In specific, each interleave is sequentially acquired twice with alternating readout polarities to reduce the systematic inconsistencies between odd and even echoes. We explored the feasibility of such a sequence for fast intracranial TOF-MRA and demonstrated that the proposed sequence can reduce the acquisition time by approximately a factor of 2 with comparable vasculature depiction to 3D-GRE, which is promising for future applications.



### Strain Tensor Imaging (STI): Voxelwise assessment of cardiac-induced brain tissue strain at 7T MRI.

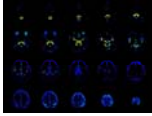
Jacob-Jan Sloots<sup>1</sup>, Alberto De Luca<sup>1</sup>, Geert Jan Biessels<sup>2</sup>, and Jaco Zwanenburg<sup>1</sup>

<sup>1</sup>Radiology, University Medical Center Utrecht, Utrecht, Netherlands, <sup>2</sup>Neurology, University Medical Center Utrecht, Utrecht, Netherlands



The heartbeat induces microvascular blood volume pulsations and subsequent tissue deformations in the brain. Although subtle (typically <1%), these deformations are highly relevant as they accelerate clearance of brain waste products. Moreover, they enable non-invasive assessment of mechanical tissue properties. We developed a sensitive MRI technique with full brain coverage for voxelwise quantification of the cardiac-induced brain tissue strain tensor with 3mm isotropic resolution, based on displacement encoding with stimulated echoes (DENSE). We visualize the strain tensor similar to diffusion tensor imaging. Strain tensor imaging opens a window on brain tissue mechanics and physiological blood volume dynamics in the brain.

0537



Multi b-value Diffusion weighted image Diphase Map (MbDDM) to evaluate cerebrospinal fluid dynamics.

Toshiaki Taoka<sup>1,2</sup>, Rintaro Ito<sup>1,2</sup>, Rei Nakamichi<sup>2</sup>, Toshiki Nakane<sup>2</sup>, Hisashi Kawai<sup>2</sup>, and Shinji Naganawa<sup>2</sup>

<sup>1</sup>Department of Innovative Biomedical Visualization, Nagoya University, Nagoya, Japan, <sup>2</sup>Department of Radiology, Nagoya University, Nagoya, Japan

To visualize the dynamics of cerebrospinal fluid (CSF) motion within the cranium, we evaluated the distribution of the motion-related signal dephasing by CSF on a Multi b-value Diffusion-weighted image Diphase Map (MbDDM). The MbDDM indicated that CSF motion was prominent in areas that included the ventral portion of the posterior fossa, the suprasellar cistern and the Sylvian fissure. Whereas, CSF motion was less in the lateral ventricles and the parietal subarachnoid space, casting doubt on the classical model of CSF dynamics.

0538



Transforming The Experience of Having MRI Using Virtual Reality

Kun Qian<sup>1</sup>, Tomoki Arichi<sup>1</sup>, Jonathan Eden<sup>2</sup>, Sofia Dall'Orso<sup>2</sup>, Rui Pedro A G Teixeira<sup>3</sup>, Kawal Rhode<sup>3</sup>, Mark Neil<sup>4</sup>, Etienne Burdet<sup>2</sup>, A David Edwards<sup>1</sup>, and Jo V Hajnal<sup>1</sup>

<sup>1</sup>Centre for the Developing Brain, School of Biomedical Engineering and Imaging Sciences, King's College London, London, United Kingdom, <sup>2</sup>Department of Bioengineering, Imperial College London, London, United Kingdom, <sup>3</sup>School of Biomedical Engineering and Imaging Sciences, King's College London, London, United Kingdom, <sup>4</sup>Department of Physics, Imperial College London, London, United Kingdom

Patients undergoing MRI often experience anxiety and sometimes distress prior to and during scanning. We have developed a non-intrusive MR compatible Virtual Reality (VR) system, providing a tailored immersive experience that the user can interact with and control using gaze tracking. Dedicated VR content has been created and tested on adults and children. A key feature is congruency between the VR world and physical sensations during MRI, including VR features corresponding to table motion and scanner noise/vibration. Results suggest the approach has huge clinical potential, and it could represent a platform for conducting a new generation of "natural" fMRI experiments.

0539



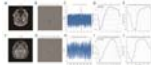
Three-Dimensional Simultaneous Quantitative T1-T2-T2\* Mapping of Whole Brain (SQUMA): Sequence Design and In-vivo Feasibility

Huiyu Qiao<sup>1</sup>, Shuo Chen<sup>1</sup>, Dandan Yang<sup>1</sup>, Hualu Han<sup>1</sup>, Zihan Ning<sup>1</sup>, and Xihai Zhao<sup>1</sup>

<sup>1</sup>Tsinghua University School of Medicine, Beijing, China

The feasibility of T1, T2 and T2\* in brain imaging and lesion quantification has been proved. However, studies about quantitative imaging seldom quantify T1, T2 and T2\* together. This study proposed a three-dimensional (3D) simultaneous quantitative T1-T2-T2\* mapping (SQUMA) for the whole brain. SQUMA sequence was composed of five dynamic scans using variable flip angles, variable T2 preparation duration and multi-echo acquisitions. **SQUMA sequence showed excellent agreement with reference imaging in measuring T1, T2 and T2\* values ( $R^2=0.98$ , 0.84 and 0.90, respectively) and good to excellent repeatability in in-vivo studies. It is feasible to use SQUMA in clinical applications.**

0540



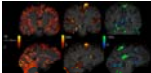
#### Real-Time EPI Phase Contrast Acquisition for Imaging of CSF Dynamics

Petrice Mostardi Cogswell<sup>1</sup>, Sandeep K Ganji<sup>2</sup>, Daniel D Borup<sup>1</sup>, Jeffrey L Gunter<sup>1</sup>, John Huston III<sup>1</sup>, and Clifford R Jack Jr<sup>1</sup>

<sup>1</sup>Radiology, Mayo Clinic, Rochester, MN, United States, <sup>2</sup>Philips Healthcare, Gainesville, FL, United States

CSF flow has been most commonly evaluated using a gated 2D phase contrast (PC) acquisition at the cerebral aqueduct or foramen magnum. However, real-time acquisitions that allow for evaluation of changes in flow with the cardiac and respiratory may provide additional insight into CSF dynamics disorders. In this study we apply a real-time EPI based PC acquisition for imaging of intracranial CSF flow at multiple intracranial locations. Quantitative analyses are validated by comparison with a standard phase contrast acquisition. Frequency spectra analysis demonstrates dominant variations in CSF flow with the cardiac and respiratory cycles.

0541



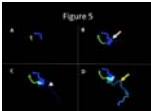
#### Short-term effects of transcranial direct current stimulation (tDCS) on cerebral blood flow measured with ASL MRI

Iris Asllani<sup>1,2</sup>, Francesco Di Lorenzo<sup>3</sup>, Katerina Gialopsou<sup>3</sup>, Joseph G Woods<sup>4,5</sup>, Marco Bozzali<sup>3</sup>, and Mara Cercignani<sup>3</sup>

<sup>1</sup>Neuroscience, University of Sussex, Brighton, United Kingdom, <sup>2</sup>Biomedical Engineering, Rochester Institute of Technology, Rochester, NY, United States, <sup>3</sup>University of Sussex, Brighton, United Kingdom, <sup>4</sup>Radiology, University of California San Diego, San Diego, CA, United States, <sup>5</sup>University of Oxford, Oxford, United Kingdom

Short-term effects of transcranial direct current stimulation (tDCS) on CBF were measured using arterial spin labeling (ASL) MRI. Results showed that anodal surface stimulation of the motor region was followed by an increase in gray matter CBF in that region. Conversely, CBF in the stimulated region following a cathodal stimulation decreased. There was no effect of sham stimulation on the CBF of the stimulated area. These findings may help forge a new path toward a better understanding of the neuro-physiological effects of tDCS in humans.

0542



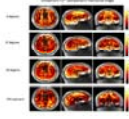
#### Venous Mapping of Vascular Malformations using Cranial 4D Flow MRI with Improved 'Virtual Injections'

Laura Eisenmenger<sup>1</sup>, Grant Steven Roberts<sup>2</sup>, Michael Loecher<sup>3</sup>, Leonardo Rivera-Rivera<sup>1</sup>, Patrick Turski<sup>1</sup>, Kevin M Johnson<sup>1,2</sup>, and Oliver Wieben<sup>1,2</sup>

<sup>1</sup>Radiology, University of Wisconsin - Madison, Madison, WI, United States, <sup>2</sup>Medical Physics, University of Wisconsin - Madison, Madison, WI, United States, <sup>3</sup>Radiology, Stanford University, Palo Alto, CA, United States

Endovascular intervention via a venous approach, or trans-venous embolization (TVE), has been increasing employed in the management of intracranial vascular lesions such as arteriovenous malformations (AVMs) and dural arteriovenous fistulas (DAVFs). Current pre-procedural planning is limited by overlapping, complex vascular anatomy and a lack of quantitative hemodynamic feature characterization. Using novel 4D flow MRI methods, high-resolution retrograde venous flow mapping with anatomical detail and dynamic flow fields can provide valuable information prior to TVE. We will present our institutional experience using this method in representative intracranial vascular lesions.

0543



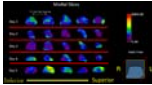
#### Quantification of T<sub>1</sub> and relative proton density in the brain ultrashort-T<sub>2</sub>\* component

Nikhil Deveshwar<sup>1</sup>, Emil Ljungberg<sup>2</sup>, Misung Han<sup>1</sup>, and Peder E. Z. Larson<sup>1</sup>

<sup>1</sup>Department of Radiology and Biomedical Imaging, University of California, San Francisco, San Francisco, CA, United States, <sup>2</sup>Department of Neuroimaging, King's College London, London, United Kingdom

This study presents a VFA approach for quantification of T<sub>1</sub> and relative proton density of the brain ultrashort-T<sub>2</sub>\* component. Measured T<sub>1</sub> values corresponding to the ultrashort-T<sub>2</sub>\* component were lower compared to T<sub>1</sub> values corresponding to long-T<sub>2</sub>\* components, and did not exhibit gray/white matter differences. Qualitatively, ultrashort-T<sub>2</sub>\* component fraction maps showed better gray/white matter contrast and clearer white matter structure delineation which we expect to be a more accurate representation of relative proton density. These results show that added VFA T<sub>1</sub> encoding in characterization of the brain ultrashort-T<sub>2</sub>\* component can more accurately differentiate white matter anatomy.

0544



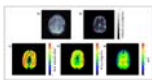
#### Feasibility for MR Elastography to Meet Unmet Need in Intracerebral Hemorrhage Surgical Planning

Robert Moskwa<sup>1</sup>, Dipul Chawla<sup>2</sup>, Corinne Henak<sup>2</sup>, Azam Ahmed<sup>3</sup>, and Walter Block<sup>1</sup>

<sup>1</sup>Medical Physics, University of Wisconsin-Madison, Madison, WI, United States, <sup>2</sup>Mechanical Engineering, University of Wisconsin-Madison, Madison, WI, United States, <sup>3</sup>Neurological Surgery, University of Wisconsin-Madison, Madison, WI, United States

It is hypothesized that the proper surgical approach for intracerebral hemorrhage (ICH) victims should depend on clot rigidity. Neurosurgical experience indicates that brain clot rigidity varies across patients and varies spatially and temporally within each patient. We hypothesize that the wide range of clot rigidity in ICH will allow MR elastography (MRE) techniques to depict the heterogeneity over a wide dynamic range of rigidity. Longitudinal MRE, ultrasound elastography, and mechanical compression testing were performed on large ex-vivo swine blood clots. MR elastography shows promise for characterizing the rigidity of intracerebral hemorrhage as indicated by these ex-vivo tests.

0545



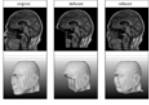
#### Measurement of Blood-Brain Barrier Permeability in Human Brain using Magnetization Transfer Effect at 7T.

Sultan Zaman Mahmud<sup>1,2</sup>, Thomas S. Denney<sup>1,2</sup>, Ronald J. Beyers<sup>2</sup>, and Adil Bashir<sup>1,2</sup>

<sup>1</sup>Department of Electrical and Computer Engineering, Auburn University, Auburn, AL, United States, <sup>2</sup>Auburn University MRI Research Center, Auburn, AL, United States

Blood-brain barrier (BBB) plays a very important role in regulating water and nutrients delivery between vascular circulation and central nervous system (CNS). Any disruption in the blood brain barrier may cause the alteration of normal functional activity of the nervous system. The techniques currently available to measure BBB permeability are prone to certain limitations and potential side effects. In this study we demonstrated a non-invasive technique of evaluating BBB permeability using the magnetization transfer (MT) effect on endogenous water labeled by arterial spin labeling (ASL) technique as a perfusion tracer.

0546



Till Huelnhagen<sup>1,2,3</sup>, Mário João Fartaria<sup>1,2,3</sup>, Ricardo Corredor-Jerez<sup>1,2,3</sup>, Mazen Fouad A. Wali Mahdi<sup>1</sup>, Gian Franco Piredda<sup>1,2,3</sup>, Bénédicte Maréchal<sup>1,2,3</sup>, Jonas Richiardi<sup>1,2</sup>, and Tobias Kober<sup>1,2,3</sup>

<sup>1</sup>Advanced Clinical Imaging Technology, Siemens Healthcare AG, Lausanne, Switzerland, Lausanne, Switzerland, <sup>2</sup>Department of Radiology, Lausanne University Hospital and University of Lausanne, Lausanne, Switzerland, <sup>3</sup>LTS5, École Polytechnique Fédérale de Lausanne (EPFL), Lausanne, Switzerland

A growing amount of imaging data is made publicly available. While this is desirable for science and its reproducibility, privacy concerns increase. As the shape of a face can be recovered based on MR images, an increased number of studies remove the face from the data to prevent biometric identification. This defacing can, however, pose a challenge to existing post-processing pipelines e.g. brain volume assessment. This work investigates the impact of regenerating facial structures in defaced images on morphometry in a large cohort using a deep neural network. The results show that refacing can prevent volumetric errors induced by defacing.

## Oral

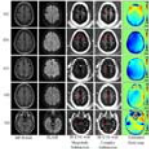
### Acquisition & Processing in Neuro - Neuroimaging Techniques: Acquisition & Processing 1

Tuesday Parallel 2 Live Q&A

Tuesday 14:30 - 15:15 UTC

Moderators: Jennifer McNab

0547



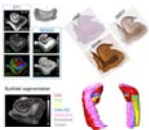
Improved Volumetric Myelin Imaging in Human Brain Utilizing Inversion Recovery Prepared Ultrashort Echo Time with Complex Echo Subtraction

Hyungseok Jang<sup>1</sup>, Zhao Wei<sup>1</sup>, Mei Wu<sup>1</sup>, Yajun Ma<sup>1</sup>, Eric Chang<sup>1,2</sup>, Jody Corey-Bloom<sup>1</sup>, and Jiang Du<sup>1</sup>

<sup>1</sup>University of California, San Diego, San Diego, CA, United States, <sup>2</sup>VA San Diego Healthcare System, San Diego, CA, United States

Myelin accelerates neural signaling in the central and peripheral nervous systems. Ultrashort echo time (UTE)-based imaging techniques have been proposed for direct capture of magnetic resonance (MR) signal from myelin lipid protons with extremely short T2\* (~0.3 ms). To suppress signal from long T2 water components and thereby improve myelin imaging, inversion recovery (IR)-based UTE techniques have been proposed. In this study, we explored the efficacy and feasibility of qualitative myelin imaging in vivo combining dual-echo IR-UTE with complex echo subtraction.

0548



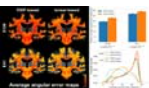
Post-mortem Diffusion MRI Analysis of Neuronal Pathways in the Human Hippocampus

Choong Heon Lee<sup>1</sup>, Jing Li<sup>2</sup>, Yulin Ge<sup>1</sup>, Timothy M Shepherd<sup>1</sup>, Youssef Zaim Wadghiri<sup>1</sup>, Jianguang Zhang<sup>1</sup>, and David W Nauen<sup>3</sup>

<sup>1</sup>Radiology, New York University School of Medicine, New York, NY, United States, <sup>2</sup>Peking Union Medical College Hospital, Beijing, China, <sup>3</sup>Pathology, Johns Hopkins University School of Medicine, Baltimore, MD, United States

High-resolution diffusion MRI data of post-mortem adult human hippocampus specimens were acquired and compared to histology to identify major axonal pathways in the hippocampus. The complex microstructural organization in the hippocampus made it difficult to resolve axonal pathways based on conventional diffusion tensor data. In comparison, neurite density map using the NODDI toolbox revealed the locations of the perforant path, mossy fibers, and Schaffer collaterals confirmed by histology. We were able to reconstruct the fimbria/alveus and perforant pathways using tractography, and the results resembled in vivo results from the HCP dataset. Other pathways in the hippocampus remained difficult to delineate.

0549

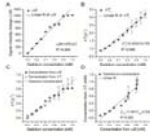


Spatial matching of fiber orientation distribution functions (fODFs) & brain structure using fODF-based vs. tensor-based registration

Xiaoxiao Qi<sup>1</sup>, Yingjuan Wu<sup>1</sup>, Abdur Raquib Ridwan<sup>1</sup>, Shengwei Zhang<sup>1</sup>, Mohammad Rakeen Niaz<sup>1</sup>, and Konstantinos Arfanakis<sup>1,2</sup>

Group-wise spatial normalization of fiber orientation distribution functions (fODF) is an important step in fixel-based analysis. This work compared the accuracy in matching fODFs using fODF-based and tensor-based registration. It demonstrated superior fODF matching with fODF-based registration, as expected, even in conditions that are optimal for tensor but not fODF reconstruction. Nevertheless, it was shown that tensor-based registration has the ability to spatially match fODF features rather well, though less accurately than fODF-based registration. Finally, this work demonstrated that fODF-based transformations resulted in worse matching of structural information than tensor-based transformations.

0550



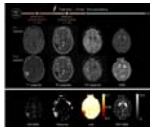
### A real-time quantitative method of Gd-DTPA concentration in neuroimaging using T1 3D MP-RAGE sequence at 3.0T

Yumeng Cheng<sup>1,2,3</sup>, Hongbin Han<sup>1,2,3</sup>, Yajuan Gao<sup>2,3</sup>, Rui Wang<sup>2,3</sup>, Yu Song<sup>3</sup>, Xianjie Cai<sup>1,2,3</sup>, and Zeqing Tang<sup>1,2,3</sup>

<sup>1</sup>Institute of Medical Technology(IMT), Peking University Health Science Center(PKUHSC), Beijing, China, <sup>2</sup>Department of Radiology, Peking University Third Hospital, Beijing, China, <sup>3</sup>Key Laboratory of Magnetic Resonance Imaging Equipment and Technique, Beijing, China

We proposed a simple quantitative method based on the linear relationship between MR signal enhancement and Gd-DTPA concentration (C) by using T1 3D MP-RAGE for the real-time in vivo measurement of Gd-DTPA concentration in neuroimaging at 3.0 T. A good linear relationship between  $\Delta SI$  and Gd-DTPA concentration existed over the concentration range of 0–1 mM ( $R^2=0.985$ ). Further, six human subjects with different brain tumors were enrolled for in vivo application of the novel method. All the results revealed that the quantitative method presented by our study is accurate, real-time and applicable.

0551



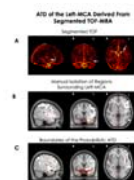
### Calculation of Concentration of Contrast Media, Relaxivity, Extracellular pH and Oxygen Extraction Fraction for Brain Tumor Characterization

Yuki Matsumoto<sup>1</sup>, Masafumi Harada<sup>1</sup>, Yuki Kanazawa<sup>1</sup>, Takashi Abe<sup>1</sup>, Maki Otomo<sup>1</sup>, Yo Taniguchi<sup>2</sup>, Masaharu Ono<sup>3</sup>, and Yoshitaka Bito<sup>3</sup>

<sup>1</sup>Tokushima University, Tokushima, Japan, <sup>2</sup>Research & Development Group, Hitachi, Ltd., Tokyo, Japan, <sup>3</sup>Healthcare Business Unit, Hitachi, Ltd., Tokyo, Japan

Concentration of contrast agent (CM), relaxivity ( $r_1$ ), extracellular pH (pHe), and oxygen extraction fraction (OEF), maps were calculated for detecting changes in tissue environment of brain diseases. As a result, the pHe value on glioblastoma or brain metastasis region was significantly lower than that on radiation necrosis (see Fig.3;  $P < 0.001$ ). The OEF value on glioblastoma region recorded significantly lower values than radiation necrosis and lung metastasis ( $P < 0.001$ ) while there was no significant difference amongst glioblastoma, breast metastasis, and lung metastasis ( $P > 0.05$ ).

0552



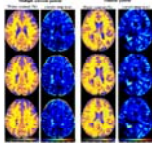
### Downloadable Probabilistic Map of the Territorial Distribution of the Left – Middle Cerebral Artery Derived from TOF-MRA

Samantha Cote<sup>1</sup>, Jean-Francois Lepage<sup>2</sup>, and Kevin Whittingstall<sup>3</sup>

<sup>1</sup>Médecine Nucléaire et Radiobiologie, Université de Sherbrooke, Sherbrooke, QC, Canada, <sup>2</sup>Pédiatrie, Université de Sherbrooke, Sherbrooke, QC, Canada, <sup>3</sup>Radiologie Diagnostique, Université de Sherbrooke, Sherbrooke, QC, Canada

Standardized artery territorial distributions (ATD) are derived from variable post-mortem ATD yet assume a homogenous distribution. We developed a downloadable probabilistic territorial distribution of the left-MCA derived from Time-of-Flight Magnetic-Resonance-Angiography that can be used with other MRI modalities. We examined the probability of the arterial territory in Broca's and Wernicke's area and found it to be almost 3 times higher in Broca area than Wernicke's area; however, both are traditionally believed to be supplied by the left-MCA. Combining the variability of arterial territories with functionally defined regions of interest can advance our knowledge of the consequences of cerebrovascular incidents.

0553



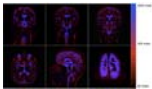
#### A novel MRI-based quantitative water content atlas of the human brain

N. Jon Shah<sup>1,2,3</sup>, Zaheer Abbas<sup>1</sup>, Dominik Ridder<sup>1</sup>, Markus Zimmermann<sup>1</sup>, and Ana-Maria Oros-Peusquens<sup>1</sup>

<sup>1</sup>Medical Imaging Physics, Institute of Neuroscience and Medicine 4, Jülich, Germany, <sup>2</sup>Institute of Neuroscience and Medicine 11, INM 11, JARA, Jülich, Germany, <sup>3</sup>Department of Neurology, Faculty of Medicine, Aachen, Germany

Measurement of quantitative, tissue-specific MR properties such as water content or relaxation times using quantitative-MRI at clinical field strength is a well-explored topic. However, none of the commonly used standard brain atlases, e.g., MNI or JHU, provide quantitative information. Utilising the framework of quantitative-MRI of the brain, this work reports on the development of the first quantitative in-vivo water content atlas based on twenty healthy volunteers datasets. Additionally, water content maps from patients with pathological changes in the brain were compared voxel-wise. These results suggest that quantitative-MRI in combination with water content atlas allows careful and quantitative interpretation of disease.

0554



#### CSF Protein Content Estimation By T2 Component Analysis

Koichi Oshio<sup>1</sup>, Masao Yui<sup>2</sup>, Seiko Shimizu<sup>2</sup>, and Shinya Yamada<sup>3,4</sup>

<sup>1</sup>Department of Diagnostic Radiology, Keio University School of Medicine, Tokyo, Japan, <sup>2</sup>Canon Medical Systems Corporation, Otawara-shi, Japan, <sup>3</sup>Kugayama Hospital, Tokyo, Japan, <sup>4</sup>Juntendo University, Tokyo, Japan

Although there is no lymphatic system in the CNS, there seems to be a mechanism to remove macro molecules from the brain. CSF and ISF are thought to be parts of this pathway, but the details are not known. In this study, MR signal of the extracellular water, including CSF, was decomposed into components with distinct T2's, to estimate content of macromolecules in each compartment. Assuming that protein content is relatively high along the clearance pathway, it might be possible to have some insight about this pathway from the obtained T2 map.

0555



#### Use Environments and Clinical Feasibility of Portable Point-of-Care Bedside Brain MRI

E. Brian Welch<sup>1</sup>, Samantha By<sup>1</sup>, Gang Chen<sup>1</sup>, Hadrien Dyvorne<sup>1</sup>, Cedric Hugon<sup>1</sup>, Christopher McNulty<sup>1</sup>, Anne Nelson<sup>1</sup>, Rafael O'Halloran<sup>1</sup>, Michael Poole<sup>1</sup>, Laura Sacolick<sup>1</sup>, Nicholas Zwart<sup>1</sup>, Sean C.L. Deoni<sup>2</sup>, Joel M. Stein<sup>3</sup>, Christopher Raio<sup>4</sup>, Kimon Bekelis<sup>5</sup>, Gerardo Chiricolo<sup>6</sup>, Kevin N. Sheth<sup>7</sup>, and Jonathan M. Rothberg<sup>1</sup>

<sup>1</sup>Hyperfine, Guilford, CT, United States, <sup>2</sup>Advanced Baby Imaging Lab, Brown University School of Engineering, Providence, RI, United States, <sup>3</sup>Department of Radiology, Hospital of the University of Pennsylvania, Philadelphia, PA, United States, <sup>4</sup>Emergency Department, Good Samaritan Hospital Medical Center, West Islip, NY, United States, <sup>5</sup>Department of Neurological Surgery, Good Samaritan Hospital Medical Center, West Islip, NY, United States, <sup>6</sup>Department of Emergency Medicine, New York Presbyterian Brooklyn Methodist Hospital, Brooklyn, NY, United States, <sup>7</sup>Department of Neurology, Yale University School of Medicine, New Haven, CT, United States

Using the world's first truly portable point-of-care (POC) MRI scanner, it is possible to acquire the fundamental neuro MR imaging contrasts in settings such as the neuro intensive care unit, emergency department, outpatient clinic, and pediatric clinic. Results are presented of neuro MRI exams of children and adults (some with known pathology) using T1W, T2W, FLAIR, and DWI from a low-field portable MRI scanner that transports directly to the patient's bedside.

## Oral

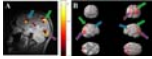
### Acquisition & Processing in Neuro - Neuroimaging Techniques: Acquisition & Processing 2

Tuesday Parallel 2 Live Q&A

Tuesday 14:30 - 15:15 UTC

Moderators: Yunhong Shu

0556



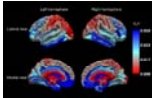
#### Hyperpolarized $^{129}\text{Xe}$ functional brain mapping

Yurii Shepelytskyi<sup>1,2</sup>, Francis T Hane<sup>2,3</sup>, Vira Grynko<sup>1,2</sup>, Tao Li<sup>3</sup>, Ayman Hassan<sup>4</sup>, and Mitchell S Albert<sup>2,3,5</sup>

<sup>1</sup>Chemistry and Materials Science Program, Lakehead University, Thunder Bay, ON, Canada, <sup>2</sup>Thunder Bay Regional Health Research Institute, Thunder Bay, ON, Canada, <sup>3</sup>Chemistry, Lakehead University, Thunder Bay, ON, Canada, <sup>4</sup>Thunder Bay Regional Health Science Centre, Thunder Bay, ON, Canada, <sup>5</sup>Northern Ontario School of Medicine, Thunder Bay, ON, Canada

Functional magnetic resonance imaging (fMRI) localizes active regions of the brain during brain stimuli. In this work, we demonstrate hyperpolarized (HP)  $^{129}\text{Xe}$  fMRI in two classical fMRI experiments: a flashing visual stimulus and a fist-clenching motor stimulus. Using a chemical shift saturation recovery (CSSR) pulse sequence, our processed images localize brain activity to regions of the brain correlated to those identified using conventional Blood Oxygenation Level Dependent fMRI. The sensitivity of Xe fMRI was nearly two orders of magnitude greater than that of BOLD fMRI. In addition,  $^{129}\text{Xe}$  fMRI allows presenting stimuli with significantly smaller repetition frequencies.

0557



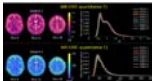
#### Water content for brain mapping at 7T: sub-mm resolution, sub-one percent precision

Ana-Maria Oros-Peusquens<sup>1</sup>, Ricardo Loução<sup>1</sup>, Monica Ferreira<sup>1</sup>, and N. Jon Shah<sup>1,2,3</sup>

<sup>1</sup>Research Centre Juelich, Juelich, Germany, <sup>2</sup>Section JARA-Brain, Jülich -Aachen Research Alliance (JARA), Aachen, Germany, <sup>3</sup>Department of Neurology, RWTH Aachen University, Aachen, Germany

We present a method for high resolution, high precision measurements of water content in vivo, validated by comparison of the values obtained in the same brains at 3T and 7T. Applications relevant to brain structure and function are illustrated. The cortical distribution of water content simultaneously reflects its complement, the macromolecular content of tissue. Furthermore, a 3D "long TR" single-scan mapping method with 3deg excitation angle is proposed at 7T and delivers results consistent with the 2D method. Structural scans reflecting quantitative properties of tissue can thus be obtained in a short (7min or less) measurement time.

0558



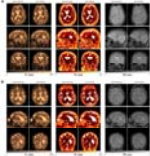
#### A five-minute multi-parametric high-resolution whole-brain MR-STAT exam: first results from a clinical trial

Stefano Mandija<sup>1,2</sup>, Federico D'Agata<sup>1,3</sup>, Hongyan Liu<sup>1,2</sup>, Oscar van der Heide<sup>1,2</sup>, Beyza Koktas<sup>2</sup>, Cornelis A.T. van den Berg<sup>1,2</sup>, Jeroen Hendrikse<sup>2</sup>, Anja van der Kolk<sup>2</sup>, and Alessandro Sbrizzi<sup>1,2</sup>

<sup>1</sup>Computational Imaging Group for MR diagnostic and therapy, Center for Image Sciences, University Medical Center Utrecht, Utrecht, Netherlands, <sup>2</sup>Department of Radiology, University Medical Center Utrecht, Utrecht, Netherlands, <sup>3</sup>Department of Neurosciences, University of Turin, Turin, Italy

MR-STAT is a recently developed technique which aims at reconstructing multi-parametric quantitative maps (T1, T2, PD, etc.) from a short cartesian acquisition. Previous research efforts have focused on the feasibility of the MR-STAT framework from a technical point of view. In this work, we present the implementation of a five-minute long high-resolution whole-brain MR-STAT protocol in a clinical trial and show the first results obtained from nine subjects. Synthetically generated contrast images as well as quantitative parametric maps show the robustness and the practical feasibility of the 5 minute long comprehensive MR-STAT protocol.

0559



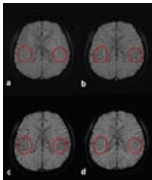
#### Accelerated 3D multiparametric MRI in glioma patients - Initial clinical experience

Carolin M Pirkel<sup>1,2</sup>, Laura Nuñez-Gonzalez<sup>3</sup>, Pedro A Gómez<sup>1</sup>, Sebastian Endt<sup>1,2</sup>, Rolf F Schulte<sup>2</sup>, Guido Buonincontri<sup>4,5</sup>, Marion Smits<sup>3</sup>, Bjoern H Menze<sup>1</sup>, Marion I Menzel<sup>2,6</sup>, and Juan A Hernandez-Tamames<sup>3</sup>

<sup>1</sup>Informatics, Technical University of Munich, Munich, Germany, <sup>2</sup>GE Healthcare, Munich, Germany, <sup>3</sup>Radiology & Nuclear Medicine, Erasmus MC, University Medical Center Rotterdam, Rotterdam, Netherlands, <sup>4</sup>Fondazione Imago7, Pisa, Italy, <sup>5</sup>IRCCS Fondazione Stella Maris, Pisa, Italy, <sup>6</sup>Physics, Technical University of Munich, Munich, Germany

In brain tumor diagnosis, fully quantitative, multiparametric MRI offers great opportunities as it allows for comprehensive tissue and hence tumor characterization which is essential for treatment planning and monitoring the treatment response. With its highly accelerated acquisition, advanced rapid MR mapping techniques facilitate multiparametric imaging in clinically acceptable scan times, providing quantitative, reproducible and accurate diagnostic information that is less affected by system and interpretation biases. In this work, we present initial clinical results and demonstrate the feasibility of a novel 3D multiparametric quantitative transient-state imaging (QTI) acquisition scheme in glioma patients.

0560



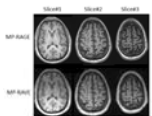
#### 3D Flow Compensated Interleaved EPI with a Centric Reordering Scheme for Fast High-Resolution Susceptibility-Weighted Imaging

Wei Liu<sup>1</sup> and Kun Zhou<sup>1</sup>

<sup>1</sup>Siemens Shenzhen Magnetic Resonance Ltd., Shenzhen, China

In this study, we implemented a novel centric reordering scheme in a partial flow compensated 3D-iEPI to further reduce the flow effect and assessed its feasibility for a fast high-resolution SWI application. By properly dividing one interleave into two EPI shots sequentially acquired with opposite phase encoding gradient polarities and overlapping one line in the interleave center, we demonstrated that the partial flow compensated 3D-iEPI with such centric reordering scheme can significantly reduce the arterial contamination and obtain comparable contrast and image quality to 3D-GRE, whilst enjoying an approximate 2-fold reduction in acquisition time.

0561



#### MP-RAVE: IR-Prepared T1-Weighted Radial Stack-of-Stars 3D GRE Imaging with Retrospective Motion Correction

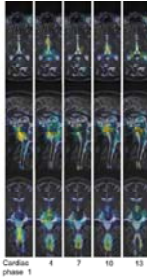
Eddy Solomon<sup>1</sup>, Houchun H. Hu<sup>2</sup>, Kai Tobias Block<sup>1</sup>, Daniel K. Sodickson<sup>1</sup>, and Hersh Chandarana<sup>1</sup>

<sup>1</sup>Radiology, New York University School of Medicine, New York, NY, United States, <sup>2</sup>Radiology, Nationwide Children's Hospital, Columbus, OH, United States



Inversion-recovery 3D T1 gradient echo sequences are commonly used in brain examinations for their excellent gray-/white-matter contrast. However, prominent motion artifacts can arise during lengthy Cartesian k-space sampling (typically 5-7 minutes) if the patient is not able to hold still, as is often the case for pediatric or elderly patients. Here, we present an alternative based on radial stack-of-stars imaging and show that comparable image contrast can be achieved, with lower sensitivity to head motion. Moreover, we demonstrate how the radial acquisition scheme can be utilized for additional retrospective motion correction to further improve robustness without increasing acquisition time.

0562



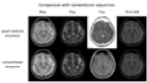
### 3D amplified MRI (aMRI) for visualizing pulsatile brain motion

Itamar Terem<sup>\*1</sup>, Leo Dang<sup>\*2</sup>, Allen Champagne<sup>3</sup>, Javid Abderezaei<sup>4</sup>, Zainab Almadan<sup>2</sup>, Anna-Maria Lydon<sup>5</sup>, Mehmet Kurt<sup>4,6</sup>, Miriam Scadeng<sup>2,7,8</sup>, and Samantha J Holdsworth<sup>2,8</sup>

<sup>1</sup>Department of Electrical Engineering & Department of Structural Biology, Stanford University, Stanford, CA, United States, <sup>2</sup>Department of Anatomy and Medical Imaging & Centre for Brain Research, University of Auckland, Auckland, New Zealand, <sup>3</sup>Centre for Neuroscience Studies, Queen's University, Kingston, ON, Canada, <sup>4</sup>Department of Mechanical Engineering, Stevens Institute of Technology, Hoboken, NJ, United States, <sup>5</sup>Centre for Advanced MRI, University of Auckland, Auckland, New Zealand, <sup>6</sup>Translational and Molecular Imaging Institute, Icahn School of Medicine at Mount Sinai, New York, NY, United States, <sup>7</sup>Department of Radiology, University of California, San Diego, CA, United States, <sup>8</sup>Mātai Medical Research Institute, Gisborne-Tairāwhiti, New Zealand

Amplified Magnetic Resonance Imaging (aMRI) has been introduced as a new brain motion detection and visualization method. Originally employed to amplify pulsatile brain motion in 2D, aMRI has shown to be promising for differentiating abnormal from normal pulsatile brain motion in obstructive brain disorders. Here, we further improve aMRI with the introduction of a combined 3D aMRI acquisition and post-processing tool, with subsequent image processing with optical flow and strain mapping. The 3D aMRI tool is then tested on both multi-slice and volumetric data and its ability to capture 3D brain motion is analyzed.

0563



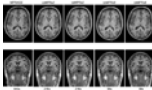
### Quad-contrast imaging with quantitative relaxation maps for clinical neuro-evaluation

Sooyeon Ji<sup>1</sup>, Se-Hong Oh<sup>2</sup>, and Jongho Lee<sup>1</sup>

<sup>1</sup>Electrical and Computer Engineering, Seoul National University, Seoul, Korea, Republic of, <sup>2</sup>Biomedical Engineering, Hankuk University of Foreign Studies, Yongin, Korea, Republic of

A 2D quad-contrast sequence is developed to generate four different contrast images commonly used in the clinical patient scan (PDw, T<sub>2</sub>w, T<sub>1</sub>w, and FLAIR) and two quantitative maps (T<sub>1</sub>- and T<sub>2</sub>- maps) in 4:14 of scan time. The proposed sequence provides comparable tissue contrasts to that of conventional sequences. In particular, native FLAIR contrast is acquired, which does not display hyperintense brain surface that arises from partial volume error during parameter mapping. Pseudo-contrast images with different TE and TI are also synthesized utilizing the quantitative maps, analogous to MAGIC.

0564



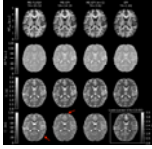
### Optimizing rapid compressed-sensing MPRAGE acquisitions for repeat sampling of brain morphometry within individuals

Ross W. Mair<sup>1,2</sup>, Lindsay C. Hanford<sup>1,3</sup>, Emilie Mussard<sup>4,5,6</sup>, Tom Hilbert<sup>4,5,6</sup>, Tobias Kober<sup>4,5,6</sup>, and Randy L. Buckner<sup>1,2,3</sup>

<sup>1</sup>Center for Brain Science, Harvard University, Cambridge, MA, United States, <sup>2</sup>Martinos Center for Biomedical Imaging, Massachusetts General Hospital, Charlestown, MA, United States, <sup>3</sup>Department of Psychology, Harvard University, Cambridge, MA, United States, <sup>4</sup>Advanced Clinical Imaging Technology, Siemens Healthcare, Lausanne, Switzerland, <sup>5</sup>Department of Radiology, Lausanne University Hospital and University of Lausanne, Lausanne, Switzerland, <sup>6</sup>LTS5, École Polytechnique Fédérale de Lausanne, Lausanne, Switzerland

Incoherent under-sampling and compressed-sensing reconstructions can reduce the scan time for a 1.0 mm MPRAGE down to as little as 60-90 seconds. Such time-savings permit the acquisition of multiple scans per session, allowing the variation of image metrics and brain morphometrics around their mean values to be quantified. We compared MPRAGE scans accelerated up to eight-fold with a fully-sampled MPRAGE; and using SNR, cortical thickness and gray matter volume, assessed the optimal regularization in the compressed-sensing reconstruction for each acceleration level to best match the values from the fully-sampled scan.

0565



### Fast Quantitative Multiparametric Mapping using 3D-EPI with Segmented CAIPIRINHA Sampling at 3T

Difei Wang<sup>1</sup>, Tony Stöcker<sup>1,2</sup>, and Rüdiger Stirnberg<sup>1</sup>

<sup>1</sup>German Center for Neurodegenerative Diseases (DZNE), Bonn, Germany, <sup>2</sup>Department of Physics and Astronomy, University of Bonn, Bonn, Germany

By comparison to a gold standard multiparametric mapping (MPM) protocol at 3T, this study shows that multi-echo 3D-EPI with highly segmented CAIPIRINHA sampling can yield whole-head  $T_1$ ,  $PD^*$ ,  $MT_{sat}$  and  $R_2^*$  maps of high quality at 1mm isotropic resolution in less than 3 minutes scan time. Even less than 1 minute of single-echo 3D-EPI is sufficient to yield accurate quantitative  $T_1$ ,  $PD^*$  and  $MT_{sat}$  maps. If necessary, SNR can be improved by including repeated EPI measurements. Optional motion- and distortion-correction across measurements may further improve results. Motion-robust MPM thus renders assessing quantitative parameter maps in clinical or population studies feasible.

## Oral

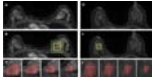
### Women's Imaging - Breast

Tuesday Parallel 3 Live Q&A

Tuesday 14:30 - 15:15 UTC

Moderators: Min Sun Bae & Linda Moy

0566



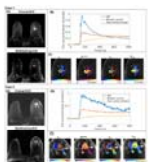
### Diagnosis of Benign and Malignant Breast Lesions on DCE-MRI by Using Radiomics and Deep Learning with Consideration of Peri-Tumor Tissue

Jiejie Zhou<sup>1</sup>, Yang Zhang<sup>2</sup>, Kai-Ting Chang<sup>3</sup>, Kyoung Eun Lee<sup>4</sup>, Ouchen Wang<sup>1</sup>, Jiance Li<sup>1</sup>, Yezhi Lin<sup>5</sup>, Zhifang Pan<sup>5</sup>, Peter Chang<sup>3</sup>, Daniel Chow<sup>3</sup>, Meihao Wang<sup>1</sup>, and Min-Ying Su<sup>3</sup>

<sup>1</sup>First Affiliate Hospital of Wenzhou Medical University, Wenzhou, China, <sup>2</sup>University of California, Irvine, CA, United States, <sup>3</sup>University of California, Irvine, Irvine, CA, United States, <sup>4</sup>Inje University Seoul Paik Hospital, Seoul, Korea, Republic of, <sup>5</sup>Wenzhou Medical University, Wenzhou, China

A total of 91 malignant/62 benign lesions were used for training, and 48 malignant/26 benign lesions for independent testing. Deep learning with ResNet50 were performed for differential diagnosis. To investigate the contribution of peri-tumor tissue, the tumor alone, smallest bounding box, and 1.2, 1.5, 2.0 times enlarged boxes were used as inputs. For per-lesion diagnosis, The accuracy was 91% for smallest bounding box, 84% for tumor alone and 1.2 times box, and further to 73% for 1.5 times box and 69% for 2.0 times box. In the independent testing dataset, the highest accuracy was 89% for the smallest bounding box.

0567



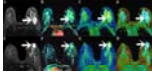
### Low-Dose, High-Temporal-Resolution Dynamic Contrast Enhanced MRI With Dynamic T1 Mapping Using Multitasking: An Initial Study on Breast Cancer

Nan Wang<sup>1,2</sup>, Yibin Xie<sup>1</sup>, Lixia Wang<sup>1,3</sup>, Sen Ma<sup>1,2</sup>, Stephen L. Shiao<sup>4</sup>, Anthony G. Christodoulou<sup>1</sup>, and Debiao Li<sup>1,2</sup>

<sup>1</sup>Biomedical Imaging Research Institute, Cedars-Sinai Medical Center, Los Angeles, CA, United States, <sup>2</sup>Department of Bioengineering, University of California, Los Angeles, Los Angeles, CA, United States, <sup>3</sup>Beijing Chaoyang Hospital, Beijing, China, <sup>4</sup>Radiation Oncology, Cedars-Sinai Medical Center, Los Angeles, CA, United States

DCE MRI is a well-accepted tool in the management of breast cancer, but continues to face technical challenges and concerns regarding gadolinium deposition. In this work, we proposed a novel Multitasking DCE technique, which enables adequate breast coverage, 0.9-mm isotropic spatial resolution, 1.5-s temporal resolution, dynamic T1 mapping throughout all DCE phases, and reduced dose of 0.02mmol/kg for the imaging of breast cancer. The in vivo studies demonstrated that the low-dose Multitasking DCE showed equivalent tumor delineation compared to standard DCE. The quantitative DCE parameters were repeatable in vivo and significantly different between normal breast and breast cancer.

0568



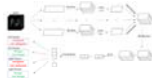
### The Utility of Amide Proton Transfer-weighted Imaging and Diffusion Kurtosis Imaging in the Diagnosis of Benign and Malignant Breast Lesions

Nan Meng<sup>1</sup>, Xuejia Wang<sup>2</sup>, Dongming Han<sup>2</sup>, Jing Sun<sup>3</sup>, Wenling Liu<sup>2</sup>, Kaiyu Wang<sup>4</sup>, and Meiyun Wang<sup>\*5</sup>

<sup>1</sup>Department of Radiology, Zhengzhou University People's Hospital & Henan Provincial People's Hospital, Academy of Medical Sciences, Zhengzhou University, Zhengzhou, China, <sup>2</sup>Department of MRI, the First Affiliated Hospital of Xinxiang Medical University, Weihui, China, <sup>3</sup>Department of Pediatrics, Zhengzhou Central Hospital, Zhengzhou University, Zhengzhou, China, <sup>4</sup>GE Healthcare, MR Research China, Beijing, China, <sup>5</sup>Department of Radiology, Zhengzhou University People's Hospital & Henan Provincial People's Hospital, Zhengzhou, China

Amide proton transfer-weighted imaging (APTWI) has unique advantages in displaying the metabolism of diseased proteins. Diffusion kurtosis imaging (DKI) can quantify the diffusion state water molecules in tissues with a non-gaussian model, thus correcting the deviation of the DWI model and improving the detection of lesions. Our results show that compared with APTWI, the DKI is more effective in the diagnosis of benign and malignant breast tumors.

0569



### Large-scale classification of breast MRI exams using deep convolutional networks

Shizhan Gong<sup>1</sup>, Matthew Muckley<sup>1</sup>, Nan Wu<sup>1</sup>, Taro Makino<sup>1</sup>, Gene Kim<sup>1</sup>, Laura Heacock<sup>1</sup>, Linda Moy<sup>1</sup>, Florian Knoll<sup>1</sup>, and Krzysztof Geras<sup>1</sup>

<sup>1</sup>New York University, New York, NY, United States

In this paper we trained an end-to-end classifier using a deep convolutional neural network on a large data set of 8632 3D MR exams. Our model can achieve an AUC of 0.8486 in identifying malignant cases on a test set reflecting the full spectrum of the patients who undergo the breast MRI examination. We studied the effect of the data set size and the effect of using different T1-weighted images in the series on the performance of our model. This work will serve as a guideline for optimizing future deep neural networks for breast MRI interpretation.

0570

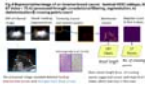
### Differentiating benign from malignant breast lesions: a feasibility study with synthetic MRI

Weibo Gao<sup>1</sup>, Quanxin Yang<sup>1</sup>, Xin Chen<sup>1</sup>, Xiaocheng Wei<sup>2</sup>, Qiujuan Zhang<sup>1</sup>, Honghong Sun<sup>1</sup>, Xiaohui Li<sup>1</sup>, Lin Wang<sup>1</sup>, Xiao na Zhang<sup>1</sup>, Baobin Guo<sup>1</sup>, Ali Shang<sup>1</sup>, and Xiao xia Lu<sup>1</sup>

<sup>1</sup>The second affiliated hospital of xi 'an jiaotong university, xi an, China, <sup>2</sup>MR Research, GE Healthcare, Beijing, China

In this study, we aim to investigate the feasibility of quantitative measurements obtained from magnetic resonance image compilation (MAGIC) MRI technology in the breast lesions and to further evaluate the application value of quantitative measurements in differentiating malignant from benign breast lesions. It was concluded that quantitative T2 relaxation time and PD value measured by MAGIC-MRI sequence can be applied in the breast lesions. The measured lower quantitative T2 and PD value is closely related to breast malignancy, which worth further study.

0571



### Quantitative Evaluation of Tumor-related Vessels on Ultrafast Dynamic Contrast-enhanced MRI: Image Biomarker of Breast Cancer Proliferation

Kango Kawase<sup>1</sup>, Masako Y Kataoka<sup>2</sup>, Tomohiro Takemura<sup>1</sup>, Takuto Fukutome<sup>1</sup>, Kojiro Yano<sup>3</sup>, Maya Honda<sup>2</sup>, Mami Iima<sup>2</sup>, Dominik Marcel Nickel<sup>4</sup>, Tatsuki Kataoka<sup>5</sup>, Masakazu Toi<sup>6</sup>, and Kaori Togashi<sup>2</sup>

<sup>1</sup>Faculty of Medicine, Kyoto University, Kyoto, Japan, <sup>2</sup>Department of Diagnostic Imaging and Nuclear Medicine, Kyoto University Graduate School of Medicine, Kyoto, Japan, <sup>3</sup>Osaka Institute of Technology, Osaka, Japan, <sup>4</sup>Siemens Healthcare GmbH, Erlangen, Germany, <sup>5</sup>Department of Diagnostic Pathology, Kyoto University Graduate School of Medicine, Kyoto, Japan, <sup>6</sup>Department of Breast Surgery, Kyoto University, Kyoto, Japan

For quantitative evaluation of tumor-related vessels, convolution filter processing was applied to ultrafast dynamic contrast-enhanced (UF-DCE) MRI of 51 lesions to obtain vessel length and crossing count as quantitative markers. The current analysis showed that these imaging markers were associated with a subtype of invasive breast cancer, the Ki-67 index, among invasive breast cancers. This opens a new approach to the evaluation of tumor-related vessels and tumor microenvironment.

0572



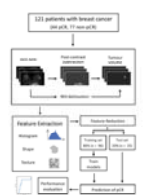
### Early Prediction of Breast Cancer Response to Neoadjuvant Chemotherapy Using Multi-Modal Diffusion MRI with Machine-Learning

Muge Karaman<sup>1,2</sup>, Shunan Che<sup>3</sup>, Rahul Mehta<sup>1,2</sup>, Guangyu Dan<sup>1,2</sup>, Zheng Zhong<sup>1,2</sup>, Han Ouyang<sup>3</sup>, X. Joe Zhou<sup>1,4</sup>, and Xinming Zhao<sup>3</sup>

<sup>1</sup>Center for Magnetic Resonance Research, University of Illinois at Chicago, Chicago, IL, United States, <sup>2</sup>Department of Bioengineering, University of Illinois at Chicago, Chicago, IL, United States, <sup>3</sup>Department of Radiology, Cancer Hospital, Chinese Academy of Medical Sciences, Beijing, China, <sup>4</sup>Departments of Radiology and Neurosurgery, University of Illinois at Chicago, Chicago, IL, United States

An early imaging assessment of breast cancer's response to neoadjuvant chemotherapy (NAC) is critical for timely planning of treatment strategies. In this study, we develop a machine-learning-based approach to investigate whether the combined features obtained from the intravoxel incoherent motion and continuous-time random-walk diffusion models provide an early prediction of pathologic response in patients receiving NAC. Our results have shown that a gradient boosting classifier trained with the early-treatment parametric changes within tumor can predict the response with an accuracy that is 96% of the accuracy achieved by using the post-treatment parametric changes.

0573



### Predicting response to neoadjuvant chemotherapy in breast cancer: machine learning-based analysis of radiomics features from baseline DCE-MRI

Gabrielle Baxter<sup>1</sup>, Andrew J Patterson<sup>2</sup>, Leonardo Rundo<sup>1</sup>, Ramona Woitek<sup>1</sup>, Reem Bedair<sup>2</sup>, Julia Carmona-Bozo<sup>1</sup>, Roido Manavaki<sup>1</sup>, Mary A McLean<sup>3</sup>, Scott A Reid<sup>4</sup>, Martin J Graves<sup>2</sup>, and Fiona J Gilbert<sup>1</sup>

<sup>1</sup>Department of Radiology, University of Cambridge, Cambridge, United Kingdom, <sup>2</sup>Department of Radiology, Addenbrooke's Hospital, Cambridge, United Kingdom, <sup>3</sup>Cancer Research UK, Cambridge, United Kingdom, <sup>4</sup>GE Healthcare, Amersham, United Kingdom

This study investigated the prediction of pathological complete response (pCR) to neoadjuvant chemotherapy in breast cancer using radiomics features derived from pre-treatment DCE-MRI. 121 women with biopsy-confirmed breast cancers (44 pCR and 77 non-pCR) were imaged before treatment. 384 radiomics features were extracted from 5 post-contrast images. A logistic regression model trained on 21 of these features was able to predict pCR with an AUC of 0.78. The highest AUC (0.85) was achieved by using 7 features from only the 3<sup>rd</sup> post-contrast time point. Clinical and pathological features should be included to improve the accuracy of prediction.

0574



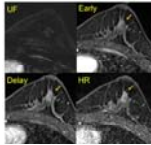
### The additive value of quantitative contralateral background parenchymal enhancement for the prediction of residual disease in the I-SPY 2 TRIAL

Wen Li<sup>1</sup>, Natsuko Onishi<sup>1</sup>, Vignesh Arasu<sup>1</sup>, David C. Newitt<sup>1</sup>, Alex Nguyen<sup>1</sup>, Jessica Gibbs<sup>1</sup>, Lisa J. Wilmes<sup>1</sup>, Ella F. Jones<sup>1</sup>, John Kornak<sup>1</sup>, Bonnie N. Joe<sup>1</sup>, The I-SPY 2 Investigator Network<sup>2</sup>, Laura J. Esserman<sup>1</sup>, and Nola M. Hylton<sup>1</sup>

<sup>1</sup>University of California, San Francisco, San Francisco, CA, United States, <sup>2</sup>Quantum Leap Healthcare Collaborative, San Francisco, CA, United States

This study tested the additive value of quantitative background parenchymal enhancement (BPE) assessed in the contralateral breast in the prediction of treatment response for patients with locally advanced breast cancer undergoing neoadjuvant chemotherapy (NAC). BPE predictors were added to the prediction models together with functional tumor volume predictors. Our results showed that combined model achieved better prediction for pathologic complete response in HER2-positive HR-negative cancer subtype after 3 weeks of NAC. The additive values of BPE were also observed at inter-regimen (12-week) for triple negatives, and at the pre-surgery for HR-positive subtypes.

0575



### Post-NAC evaluation using ultrafast breast dynamic contrast-enhanced MRI

Maya Honda<sup>1</sup>, Masako Kataoka<sup>1</sup>, Mami Iima<sup>1</sup>, Kanae Kawai Miyake<sup>1</sup>, Akane Ohashi<sup>1</sup>, Ayami Ohno Kishimoto<sup>1</sup>, Rie Ota<sup>1</sup>, Marcel Dominik Nickel<sup>2</sup>, Tatsuki Kataoka<sup>3</sup>, Masakazu Toi<sup>4</sup>, and Kaori Togashi<sup>1</sup>

<sup>1</sup>Department of Diagnostic Imaging and Nuclear Medicine, Graduate School of Medicine, Kyoto University, Kyoto, Japan, <sup>2</sup>MR Application Predevelopment, Siemens Healthcare GmbH, Erlangen, Germany, <sup>3</sup>Department of Diagnostic pathology, Graduate School of Medicine, Kyoto University, Kyoto, Japan, <sup>4</sup>Department of breast surgery, Graduate School of Medicine, Kyoto University, Kyoto, Japan

The study evaluated the accuracy to predict pathologic complete response (pCR) after neo-adjuvant chemotherapy (NAC) using ultrafast dynamic contrast-enhanced (UF-DCE) MRI. The sensitivity to predict pCR was higher on UF-DCE MRI compared with conventional dynamic contrast-enhanced (DCE) MRI. The difference in image and pathological sizes on UF-DCE MRI was smaller than on conventional DCE MRI. UF-DCE MRI potentially assesses post-NAC status in breast cancer patients accurately in a shorter acquisition time.

## Oral

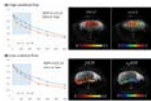
### Women's Imaging - Placenta

Tuesday Parallel 3 Live Q&A

Tuesday 14:30 - 15:15 UTC

Moderators: Simon Shah & KyungHyun Sung

0576



### Probing ballistic flow in the placenta using flow-compensated and non-compensated diffusion MRI

Ling Jiang<sup>1,2</sup>, Taotao Sun<sup>1,2</sup>, Yuhao Liao<sup>3</sup>, Yi Sun<sup>4</sup>, Yi Zhang<sup>3</sup>, Zhaoxia Qian<sup>1,2</sup>, and Dan Wu<sup>3</sup>

<sup>1</sup>Maternity and Child Health Hospital, School of Medicine, Shanghai Jiao Tong University, Shanghai, China, <sup>2</sup>Shanghai Key Laboratory of Embryo Original Diseases, Shanghai, China, <sup>3</sup>Key Laboratory for Biomedical Engineering of Ministry of Education, Department of Biomedical Engineering, College of Biomedical Engineering & Instrument Science, Zhejiang University, Hangzhou, China, <sup>4</sup>MR Collaboration, Siemens Healthcare Ltd., Shanghai, China

Intravoxel incoherent motion (IVIM) imaging is frequently used to evaluate microcirculatory flow. With the conventional diffusion MRI, IVIM effects include both pseudo-diffusive microcirculatory flow and bulk (or ballistic) blood flow. We propose a joint use of flow-compensated (FC) and non-FC diffusion gradient waveforms to specifically probe the fraction and velocity of ballistic flow in the placenta. The measured ballistic flow velocity showed a high correlation with umbilical flow based on Doppler ultrasound and a negative correlation with gestational age. These results demonstrated the potential of using FC/NC dMRI to noninvasively measure flow velocity inside the placenta.

0577



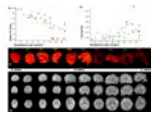
### Quantitative Perfusion Measurements of the Human Placenta with FAIR and pCASL Arterial Spin Labeling at 3T: Initial Feasibility

Quyên N. Do<sup>1</sup>, Christina Herrera<sup>2</sup>, Matthew A. Lewis<sup>1</sup>, Yin Xi<sup>1,3</sup>, Catherine Y. Spong<sup>2</sup>, Diane M. Twickler<sup>1,2</sup>, and Ananth J. Madhuranthakam<sup>1,4</sup>

<sup>1</sup>Radiology, UT Southwestern Medical Center, Dallas, TX, United States, <sup>2</sup>Obstetrics and Gynecology, UT Southwestern Medical Center, Dallas, TX, United States, <sup>3</sup>Population and Data Sciences, UT Southwestern Medical Center, Dallas, TX, United States, <sup>4</sup>Advanced Imaging Research Center, UT Southwestern Medical Center, Dallas, TX, United States

Quantitative measurement of placental perfusion is important for the assessment of placental function. We have developed and optimized a non-contrast perfusion MR imaging technique utilizing pseudo-continuous arterial spin labeling (pCASL) to quantitatively measure human placental perfusion at 3T. Placental perfusion was also assessed using flow-sensitive alternating inversion recovery (FAIR). The average placental blood flow ( $108 \pm 47$  mL/100g/min) was comparable to published literature values.

0578



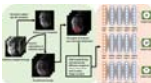
### CARDiac and Placental imaging (CARP) in pregnancy to assess etiology of preeclampsia and predict cardiovascular disease risk in later life

Jana Hutter<sup>1</sup>, Kathleen Colford<sup>1</sup>, Anthony Price<sup>1</sup>, Johannes Steinweg<sup>1</sup>, Lisa Story<sup>1</sup>, Kuberan Pushparajah<sup>1</sup>, Laura McCabe<sup>1</sup>, Alison Ho<sup>2</sup>, Adam J Lewandowski<sup>3</sup>, Joseph Hajnal<sup>1</sup>, Lucy Chappell<sup>2</sup>, Pablo Lamata<sup>1</sup>, and Mary Rutherford<sup>1</sup>

<sup>1</sup>Biomedical Engineering Department, School of Biomedical Engineering and Imaging Sciences, King's College London, London, United Kingdom, <sup>2</sup>Academic Women's Health, King's College London, London, United Kingdom, <sup>3</sup>Division of Cardiovascular Medicine, University of Oxford, Oxford, United Kingdom

Pre-eclampsia (PE) is one of the most common, yet serious, complications of pregnancy. Its manifestations during pregnancy -high blood pressure, proteinuria and placental lesions- are associated with both maternal and fetal morbidity and mortality. Maternal symptoms resolve after delivery but a lifelong elevated risk for cardiovascular disease (CVD) remains. The CARP study combines functional placental and fetal MRI with (maternal) cardiovascular MR during pregnancy at the time of maximal stress to the maternal heart, in an attempt to disentangle the complex cardiac and placental interactions in disease etiology and to predict maternal cardiovascular risk in later life.

0579

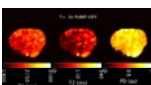


### Learning-based approach for accelerated IVIM imaging in the placenta

Fan Huang<sup>1</sup>, Shi-Ming Wang<sup>2</sup>, Guohui Yan<sup>3</sup>, Zhihao Wen<sup>4</sup>, Yuhao Liao<sup>1</sup>, Yi Zhang<sup>1</sup>, Yu Zou<sup>3</sup>, and Dan Wu<sup>1</sup>

<sup>1</sup>Key Laboratory for Biomedical Engineering of Ministry of Education, Department of Biomedical Engineering, College of Biomedical Engineering & Instrument Science, Zhejiang University, Hangzhou, China, <sup>2</sup>Department of Medical Imaging and Radiological Sciences, Chang Gung University, Taoyuan, Taiwan, <sup>3</sup>Department of Radiology, Women's Hospital, School of Medicine, Zhejiang University, Hangzhou, China, <sup>4</sup>Purple-river software corporation, Shenzhen, China

Q-space learning has shown its potential in accelerating Q-space sampling in diffusion MRI. This study proposed a new deep learning framework to accelerate intravoxel incoherent motion (IVIM) imaging and to estimate IVIM parameters from a small number of b values in the human placenta. The results demonstrated the feasibility of a reduced IVIM protocol using the proposed framework, which may help to accelerate the acquisition and reduce motion for placental IVIM.



### Placental MRI: Using a novel ex vivo placental perfusion chamber to validate in vivo magnetic resonance fingerprinting (MRF) relaxometry

Jeffrey N Stout<sup>1</sup>, Shahin Rouhani<sup>1,2</sup>, Congyu Liao<sup>3</sup>, Esra Abaci Turk<sup>1</sup>, Christopher G Ha<sup>1</sup>, Karen Rich<sup>4</sup>, Lawrence L. Wald<sup>3</sup>, William H. Barth, Jr<sup>5</sup>, Drucilla J. Roberts<sup>2</sup>, Elfar Adalsteinsson<sup>6</sup>, and P. Ellen Grant<sup>1</sup>

<sup>1</sup>Fetal-Neonatal Neuroimaging & Developmental Sciences Center, Boston Children's Hospital, Boston, MA, United States, <sup>2</sup>Department of Pathology, Massachusetts General Hospital, Boston, MA, United States, <sup>3</sup>A. Martinos Center for Biomedical Imaging, Massachusetts General Hospital, Boston, MA, United States, <sup>4</sup>Department of Radiology, Massachusetts General Hospital, Boston, MA, United States, <sup>5</sup>Maternal-Fetal Medicine, Obstetrics and Gynecology, Massachusetts General Hospital, Boston, MA, United States, <sup>6</sup>Institute for Medical Engineering and Science; Department of Electrical Engineering and Computer Science, Massachusetts Institute of Technology, Cambridge, MA, United States

The placenta is a challenging MRI target. Acquisition schemes developed for other organs, with implicit assumptions about motion, tissue composition and perfusion, should be vetted for applicability to the placenta. We have developed an ex vivo placental perfusion chamber with integrated MRI receive coil for high SNR and imaging acceleration to validate in vivo acquisitions in a controlled environment. Here we examine the effect of flowing spins on MRF relaxometry. We offer evidence that T1 is sensitive to overall fluid volume, while T2 is additionally sensitive spin inflow. Our placental perfusion system appears promising for validating in vivo quantitative MRI.

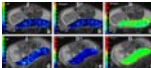


### Placental MRI: Effect of maternal position, breath hold and oxygen state on placental T<sub>2</sub>\* measurements

Esra Abaci Turk<sup>1</sup>, Jeffrey N. Stout<sup>1</sup>, Borjan Gagoski<sup>1</sup>, Mary Katherine Manhard<sup>2</sup>, Elfar Adalsteinsson<sup>3,4,5</sup>, Kawin Setsompop<sup>2</sup>, Polina Golland<sup>3,6</sup>, Drucilla J. Roberts<sup>7</sup>, William H. Barth Jr<sup>8</sup>, and P. Ellen Grant<sup>1</sup>

<sup>1</sup>Fetal-Neonatal Neuroimaging & Developmental Science Center, Boston Children's Hospital, Boston, MA, United States, <sup>2</sup>Athinoula A. Martinos Center for Biomedical Imaging, Massachusetts General Hospital, Charlestown, MA, United States, <sup>3</sup>Department of Electrical Engineering and Computer Science, Massachusetts Institute of Technology, Cambridge, MA, United States, <sup>4</sup>Harvard-MIT Health Sciences and Technology, Massachusetts Institute of Technology, Cambridge, MA, United States, <sup>5</sup>Institute for Medical Engineering and Science, Massachusetts Institute of Technology, Cambridge, MA, United States, <sup>6</sup>Computer Science and Artificial Intelligence Laboratory (CSAIL), Massachusetts Institute of Technology, Cambridge, MA, United States, <sup>7</sup>Pathology, Massachusetts General Hospital, Boston, MA, United States, <sup>8</sup>Maternal-Fetal Medicine, Massachusetts General Hospital, Boston, MA, United States

T<sub>2</sub>\* relaxometry has been proposed as a semi-quantitative measure for placental oxygen transport. However, to use T<sub>2</sub>\* as a diagnostic tool, it is necessary to define the normal range of results and factors that influence those results. In this study we investigated the effect of maternal position, breath-holds and oxygen state on placental T<sub>2</sub>\*. We observed lower T<sub>2</sub>\* with breath-hold protocol compared to no breath-hold protocol in left lateral position. Additionally, lower T<sub>2</sub>\* was measured in supine position during normoxic episode compared to left lateral position with no breath-hold protocol. Further studies are needed to understand these factors better.

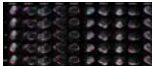


### Placental perfusion in Fetuses with congenital heart disease and normal pregnancy assessed with intravoxel incoherent motion imaging

Cong Sun<sup>1</sup>, Xin Chen<sup>1</sup>, Jinxia Zhu<sup>2</sup>, Robert Grimm<sup>3</sup>, and Guangbin Wang<sup>1</sup>

<sup>1</sup>Shandong Medical Imaging Research Institute, Shandong University, Jinan, China, <sup>2</sup>MR Collaboration, Healthcare Siemens Ltd., Beijing, China, Beijing, China, <sup>3</sup>Healthcare GmbH, Erlangen, Germany, Erlangen, Germany

To determine whether placental perfusion alterations are evident in utero in fetuses with congenital heart disease (CHD), we quantitatively investigated perfusion in 28 fetuses with CHD and 39 healthy gestational age-matched controls using intravoxel incoherent motion imaging (IVIM). We found that the f values were significantly higher in the CHD group compared with the normal pregnancy group (37.8% vs. 30.2%, p < 0.0001), and there was no significant difference in the D value and D\* value between the two groups. The increased placental perfusion in fetuses with CHD might represent an attempt to compensate for a perfusion deficit in fetal circulation.

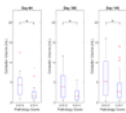


### Placenta Accreta Spectrum (PAS) Disorders Investigated with Multi-Compartment Placental MRI

Nada Mufti<sup>1,2</sup>, Patrick O'Brien<sup>3</sup>, George Attilakos<sup>3</sup>, Magdalena Sokolska<sup>4</sup>, Priya Narayanan<sup>3</sup>, Rosalind Aughwane<sup>1</sup>, Neil Sebire<sup>5</sup>, Imen Ben-Salha<sup>3</sup>, Nafisa Wilkinson<sup>3</sup>, Giles Kendall<sup>1,3</sup>, Jan Deprest<sup>1,3,6</sup>, David Atkinson<sup>7</sup>, Tom Vercauteren<sup>2,6</sup>, Sebastien Ourselin<sup>2</sup>, Anna L David<sup>1,3,6</sup>, and Andrew Melbourne<sup>2,8</sup>

<sup>1</sup>Institute for Women's Health, University College London (UCL), London, United Kingdom, <sup>2</sup>School of Biomedical Engineering and Imaging Sciences (BMEIS), Kings College London, London, United Kingdom, <sup>3</sup>University College London Hospital, London, United Kingdom, <sup>4</sup>Department of Medical Physics and Biomedical Engineering, University College London Hospital (UCLH), London, United Kingdom, <sup>5</sup>Great Ormond Street Hospital for Children, London, United Kingdom, <sup>6</sup>University Hospitals, KU Leuven, Leuven, Belgium, <sup>7</sup>Centre for Medical Imaging (CMI), University College London (UCL), London, United Kingdom, <sup>8</sup>Department of Medical Physics and Biomedical Engineering, University College London (UCL), London, United Kingdom

Uterine scarring from caesarean section (CS) can lead to subsequent abnormally adherent or invasive placenta. Failure to recognise Placenta Accreta Spectrum disorders prior to delivery can potentially cause catastrophic bleeding and death. Complex surgical interventions may be required to remove placental invasion of the uterine myometrium and nearby organs. Antenatal detection and correct PAS grading are important to plan delivery. Current ultrasound and MRI imaging are limited to subjective assessment of vascular invasion. We propose a multi-compartment model<sup>1</sup> that can quantify vascularity and proportion of abnormal placentation across the previous CS scar for objective diagnosis and to assist surgical planning.



### Quantitative Ferumoxytol Dynamic Contrast Enhanced (DCE) MRI Evaluation of the Placenta after Zika Virus Infection in the Rhesus Macaque

Daniel Seiter<sup>1</sup>, Kai D. Ludwig<sup>1</sup>, Sydney Nguyen<sup>2,3,4</sup>, Megan E Murphy<sup>2,3,4</sup>, Kathleen M Antony<sup>2,3,4</sup>, Ruiming Chen<sup>1</sup>, Terry K Morgan<sup>5</sup>, Ante Zhu<sup>6,7</sup>, Archana Dhyani<sup>8</sup>, Sean B Fain<sup>1,6,7</sup>, Kevin M Johnson<sup>1,7</sup>, Thaddeus G. Golos<sup>2,3,4</sup>, and Oliver Wieben<sup>1,7</sup>

<sup>1</sup>Medical Physics, University of Wisconsin-Madison, Madison, WI, United States, <sup>2</sup>Comparative Biosciences, University of Wisconsin-Madison, Madison, WI, United States, <sup>3</sup>Wisconsin National Primate Research Center, University of Wisconsin-Madison, Madison, WI, United States, <sup>4</sup>Obstetrics & Gynecology, University of Wisconsin-Madison, Madison, WI, United States, <sup>5</sup>Pathology, Oregon Health & Science University, Portland, OR, United States, <sup>6</sup>Biomedical Engineering, University of Wisconsin-Madison, Madison, WI, United States, <sup>7</sup>Radiology, University of Wisconsin-Madison, Madison, WI, United States, <sup>8</sup>Computer Science, University of Wisconsin-Madison, Madison, WI, United States

Proper placental development is crucial to fetal health. Here we report preliminary results characterizing the effects of Zika virus on the placenta of the rhesus macaque using dynamic contrast enhanced (DCE) MRI scans. DCE data were processed to identify individual cotyledons, their volume, and blood flow at three time points during gestation and were compared with pathological findings from term placenta dissection. Analysis shows a statistically significant decrease in cotyledon volume with pathology, measurable as early as 64 days gestation.



### High resolution diffusion and perfusion MRI of normal, preeclamptic and growth-restricted mice models reveal clear fetoplacental differences

Qingjia Bao<sup>1</sup>, Eddy Solomon<sup>1</sup>, Ron Hadas<sup>1</sup>, Stefan Markovic<sup>1</sup>, Odelia Chitrit<sup>1</sup>, Maxime Yon<sup>1</sup>, Michal Neeman<sup>1</sup>, and Lucio Frydman<sup>1</sup>

<sup>1</sup>Weizmann Institute of Science, Rehovot, Israel



DWI can evaluate pregnancy-related dysfunctions, yet EPI's sensitivity to motions and air/water/fat heterogeneities complicate these studies in preclinical settings. We have developed DWI methodologies based on SPatiotemporal ENcoding (SPEN) for overcoming these obstacles, delivering single-shot images at  $\approx 100\mu\text{m}$  in-plane resolutions. These methods were used to monitor fetoplacental differences between naïve and knockout mice strains mimicking preeclampsia and IUGR. High definition ADC/DTI maps could resolve the placental layers (maternal, fetal, trophoblastic), umbilical cords, and various brain compartments in the developing fetuses. Daily monitoring also showed differences in the development of placental and fetal (e.g. brain) structures among normal and disease models.

## Oral

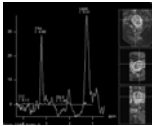
### Women's Imaging - Female Pelvis

Tuesday Parallel 3 Live Q&A

Tuesday 14:30 - 15:15 UTC

Moderators: Victoria Chernyak & Nandita deSouza

0586



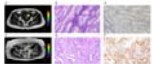
#### Total Choline Level on MRS Predicts Overall Survival for Endometrial Cancer and Correlates with Tissue Choline Metabolism

Gigin Lin<sup>1</sup>, Shang-Yueh Tsai<sup>2</sup>, Yu-Chun Lin<sup>1</sup>, Chiao-Yun Lin<sup>1</sup>, Ren-Chin Wu<sup>1</sup>, and Chyong-Huey Lai<sup>1</sup>

<sup>1</sup>Chang Gung Memorial Hospital, Linkou, Taiwan, <sup>2</sup>National Chengchi University, Taipei, Taiwan

Endometrial cancer is the most common gynecologic cancer in the developed countries but responses differently to the standard treatment. We aim to investigate and characterize the values of endometrial total choline levels on 1H MR spectroscopy in predicting overall survival, with tissue metabolomics and biochemistry corroboration. We found that increased total choline levels on MRS depicted high-risk cancer group for nodal metastasis, overall survival and disease-free survival for endometrial cancers, supported by increased tissue GPC levels and overexpression of EDI3.

0587



#### 3D TSE Amide Proton Transfer and IVIM Imaging for Type I Endometrial Carcinoma: Correlation with Ki-67 Proliferation Status

Yong-Lan He<sup>1</sup>, Yuan Li<sup>1</sup>, Cheng-Yu Lin<sup>1</sup>, Ya-Fei Qi<sup>1</sup>, Xiaoqi Wang<sup>2</sup>, Hai-Long Zhou<sup>1</sup>, Hua-Dan Xue<sup>1</sup>, and Zheng-Yu Jin<sup>1</sup>

<sup>1</sup>Peking Union Medical College Hospital, Beijing, China, <sup>2</sup>Philips Healthcare China, Beijing, China

This study demonstrates the first attempt of 3D TSE APTw MR imaging for endometrial carcinoma with excellent inter-observer measurement agreement. APT values on 22 type I endometrial carcinoma lesions were moderately positively correlated with Ki-67 labelling index ( $r = 0.583$ ,  $p=0.004$ ). APT values of Ki-67 low-proliferation group were significantly lower than high-proliferation group ( $p=0.016$ ) with AUC 0.768. However, no correlation was found between IVIM-derived parameters and Ki-67 labeling index (Dt,  $p=0.717$ ; D\*  $p=0.151$ ; f,  $p=0.153$ ).

0588

Parameter	Mean	SD	Min	Max
APTw	1.25	0.15	0.95	1.55
IVIM	0.85	0.10	0.75	0.95
Dt	0.15	0.02	0.12	0.18
D*	0.15	0.02	0.12	0.18
f	0.15	0.02	0.12	0.18

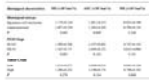
#### Accelerated T2 Mapping for Evaluating Cervical Cancer Features: A Preliminary Study

Shujian Li<sup>1</sup>, Jie Liu<sup>1</sup>, Jinxia Zhu<sup>2</sup>, Tobias Kober<sup>3</sup>, Tom Hilbert<sup>3</sup>, and Jingliang Cheng<sup>1</sup>

<sup>1</sup>Department of Magnetic Resonance, the First Affiliated Hospital of Zhengzhou University, Zhengzhou, China, <sup>2</sup>MR Collaboration, Siemens Healthcare Ltd, Beijing, China, <sup>3</sup>Advanced Clinical Imaging Technology, Siemens Healthcare AG, Lausanne, Switzerland

This study investigated the feasibility of an accelerated T2-mapping sequence to evaluate cervical cancer (CC) pathological type, grade, stage and lymphovascular space invasion (LVSI) status. The results showed that quantitative T2 values can effectively grade and predict the CC LVSI status, and the ADC values can stratify CC grading. The synthetic T2-weighted (T2W) images showed comparable staging accuracy to the morphological T2W images acquired by a conventional sequence. This suggests that this accelerated T2-mapping sequence may facilitate CC staging and grading. Quantitative T2 values may be superior to ADC values in predicting the LVSI status of CC.

0589



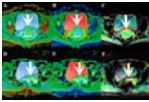
### Diffusion Kurtosis Imaging of Cervical Carcinoma: Correlation between Imaging Parameters and Histological Findings

Qi Zhang<sup>1</sup>, Xiaoduo Yu<sup>1</sup>, Jieying Zhang<sup>1</sup>, Han Ouyang<sup>1</sup>, Xinming Zhao<sup>1</sup>, and Lizhi Xie<sup>2</sup>

<sup>1</sup>Department of Radiology, National Cancer Center/Cancer Hospital, Chinese Academy of Medical Sciences and Peking Union Medical, Beijing, China, <sup>2</sup>GE healthcare, China, Beijing, China

Cervical cancer is the leading cause of death in gynecological malignancy around the world. The most important prognostic factors include stage at diagnosis, histological subtype, tumor differentiation and et al, which are critical to make the optimal treatment strategies. However, there are still huge challenges in accurate assessment tumor characteristics even by clinical examination and biopsy. DWI has showed promising results in assessment tumor characteristics in cervical cancer. Diffusion kurtosis imaging (DKI), an extension of DWI, is more sensitive to tissue heterogeneity and water exchange. This study demonstrated that DKI-derived parameters are helpful in assessment histological features of cervical cancer.

0590



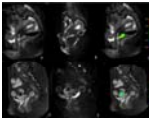
### Comparative Analysis of the Value of APTWI and DKI in Evaluating the Histological Features of Uterus Cervical Cancer

Nan Meng<sup>1</sup>, Xuejia Wang<sup>2</sup>, Dongming Han<sup>2</sup>, Xiaoyue Ma<sup>1</sup>, Yan Bai<sup>3</sup>, Kaiyu Wang<sup>4</sup>, and Meiyun Wang<sup>\*3</sup>

<sup>1</sup>Department of Radiology, Zhengzhou University People's Hospital & Henan Provincial People's Hospital, Academy of Medical Sciences, Zhengzhou University, Zhengzhou, China, <sup>2</sup>Department of MRI, the First Affiliated Hospital of Xinxiang Medical University, Weihui, China, <sup>3</sup>Department of Radiology, Zhengzhou University People's Hospital & Henan Provincial People's Hospital, Zhengzhou, China, <sup>4</sup>GE Healthcare, MR Research China, Beijing, China

Amide proton transfer-weighted imaging (APTWI) has unique advantages in displaying the metabolism of diseased proteins. Diffusion kurtosis imaging (DKI) can quantify the diffusion state water molecules in tissues with a non-gaussian model, thus correcting the deviation of the DWI model and improving the detection of lesions. Our results show that compared with APTWI, the DKI is more effective in evaluating the pathological and physiological characteristics of uterus cervical cancer (UCC).

0591



### Application of amide proton transfer in differential diagnosis of mass cervical carcinoma and typical uterine leiomyoma

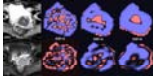
Xing Meng<sup>1</sup>, Ailian Liu<sup>1</sup>, Shifeng Tian<sup>1</sup>, Zhiwei Shen<sup>2</sup>, Yishi Wang<sup>2</sup>, Yaxin Niu<sup>1</sup>, and Wan Dong<sup>1</sup>

<sup>1</sup>Department of Radiology, the First Affiliated Hospital of Dalian Medical University, Dalian, China, <sup>2</sup>Philips Healthcare, Beijing, China

Amide proton transfer (APT) imaging technology has been applied in the diagnosis of central nervous system tumors to some extent. However, it is only used in the diagnosis of cervical carcinoma in uterine tumors, and there is no study on the differentiation of cervical carcinoma and related tumors with APT. We investigated the value of APT in the differential diagnosis of mass cervical carcinoma and typical uterine leiomyoma.

0592

### MRI Texture Analysis in the Characterization of Cervical Carcinoma



Mandi Wang<sup>1</sup>, Jose Angelo Perucho<sup>1</sup>, Queenie Chan<sup>2</sup>, and Elaine Lee<sup>1</sup>

<sup>1</sup>Department of Diagnostic Radiology, The University of Hong Kong, Hong Kong, Hong Kong, <sup>2</sup>Philips Healthcare, Hong Kong, China

MRI texture analysis was performed in 100 patients with cervical carcinoma. TexRAD software was used for texture extraction and analysis on ADC maps and T1c images. Texture features were compared between histological subtypes, tumour grades, FIGO stages and nodal status. Feature selection was achieved with AUC  $\geq$  0.70. ADC-derived MPP5 was significantly lower in SCC than ACA, Entropy6 derived from both ADC and T1c increased from FIGO I-II to FIGO III-IV, and ADC-derived Entropy3 was higher in positive nodal status than negative. No texture features could differentiate tumour grades with acceptable diagnostic efficiency.

0593



Prognosis of Focused Ultrasound Ablation Therapy Adenomyosis by Radiomics

Jing Zhang<sup>1</sup>, Zhicong Li<sup>2</sup>, Yang Song<sup>1</sup>, Han Wang<sup>2</sup>, Yefeng Yao<sup>1</sup>, and Guang Yang<sup>1</sup>

<sup>1</sup>Shanghai Key Laboratory of Magnetic Resonance, Department of Physics, East China Normal University, shanghai, China, <sup>2</sup>Department of Radiology, Shanghai General Hospital, Shanghai Jiao Tong University School of Medicine, shanghai, China

Patients with adenomyosis can be treated using Magnetic Resonance Imaging (MRI)-guided Focused Ultrasound Surgery (MRgFUS). However, not all patients have a good response to MRgFUS, some even require pain management such as with Non-Steroidal Anti-inflammatory Drugs (NSAIDs) following MRgFUS. To evaluate the prognosis of MRgFUS using only MRI images, we used radiomics features together with clinical features to build a machine learning model with our homemade open-source software, namely Feature Explorer (FAE), based on scikit-learn. We obtained a candidate model with AUC of 0.806 in test cohort.

## Oral - Power Pitch

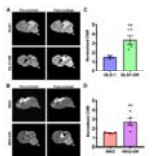
### MRS and Molecular Imaging, Development and Applications - Molecular Imaging Technical Developments & Novel Applications

Tuesday Parallel 5 Live Q&A

Tuesday 14:30 - 15:15 UTC

Moderators: René Botnar

0623



MRMI of Extradomain-B Fibronectin for Assessing Drug Resistance in Colon Cancer

Zheng-Rong Lu<sup>1</sup>, Amita Vaidya<sup>1</sup>, Nadia Ayat<sup>1</sup>, Helen Wang<sup>1</sup>, and Megan Buford<sup>1</sup>

<sup>1</sup>Biomedical Engineering, Case Western Reserve University, Cleveland, OH, United States

Non-invasive active surveillance and risk-stratification of drug-resistant colon cancer is imperative, in order to facilitate disease management and tailor therapeutic interventions. This research demonstrates that acquired drug resistance in colon cancer is associated with enhanced expression of extracellular matrix oncoprotein extradomain-B fibronectin (EDB-FN). MR molecular imaging of EDB-FN at a subclinical dose of macrocyclic ZD2-targeted contrast agent ZD2-N<sub>3</sub>-Gd(HP-DO3A) facilitates effective assessment of drug-resistant colon cancer in two independent models, highlighting the potential of EDB-FN as a diagnostic molecular marker for invasive colon cancer.

0624



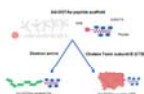
An MRI Method for Labeling and Imaging Decellularized Extracellular Matrix Scaffolds for Tissue Engineering

Daniel Andrzej Szulc<sup>1,2</sup>, Mohammadali Ahmadipour<sup>1,3</sup>, Fabio Gava Aoki<sup>3,4</sup>, Thomas K. Waddell<sup>1,3,5</sup>, Golnaz Karoubi<sup>5,6,7</sup>, and Hai-Ling Margaret Cheng<sup>1,2,7,8,9</sup>

<sup>1</sup>Institute of Biomaterials and Biomedical Engineering, University of Toronto, Toronto, ON, Canada, <sup>2</sup>Translational Biology & Engineering Program, Ted Rogers Centre for Heart Research, Toronto, ON, Canada, <sup>3</sup>Latner Thoracic Surgery Laboratories, Toronto General Hospital Research Institute, University Health Network, Toronto, ON, Canada, <sup>4</sup>Biomedical Engineering Laboratory, University of Sao Paulo, Sao Paulo, Brazil, <sup>5</sup>Department of Mechanical and Industrial Engineering, University of Toronto, Toronto, ON, Canada, <sup>6</sup>Latner Thoracic Surgery Laboratories, University of Toronto, Toronto, ON, Canada, <sup>7</sup>Ontario Institute for Regenerative Medicine, Toronto, ON, Canada, <sup>8</sup>Heart & Stroke/Richard Lewar Centre of Excellence for Cardiovascular Research, Toronto, ON, Canada, <sup>9</sup>Edward S. Rogers Sr. Department of Electrical & Computer Engineering, University of Toronto, Toronto, ON, Canada

Extracellular matrix (ECM) forms the underlying complex structure of bodily tissues, for this reason, ECM has been greatly explored as an ideal scaffold for tissue engineering. To better understand and optimize scaffold-based therapies we require sensitive and non-invasive imaging techniques. In this study, a novel and facile method for labelling and imaging decellularized ECM scaffolds is presented. A series of tissue-specific (bladder, lung, and tracheal smooth muscle and cartilage) dECM scaffolds are labelled with a small molecule manganese porphyrin, MnPNH<sub>2</sub>. The labelled scaffolds are biocompatible and exhibit significant and sustained signal in vitro and in vivo.

0625



### Multivalent Gadolinium-decorated Peptides for Versatile Bioconjugation of Molecular MRI Probes

Nikorn Pothayee<sup>1</sup>, Deepak Sail<sup>2</sup>, Stephen Dodd<sup>1</sup>, Rolf Swenson<sup>2</sup>, and Alan Koretsky<sup>1</sup>

<sup>1</sup>Laboratory of Functional and Molecular Imaging, National Institutes of Health, Bethesda, MD, United States,

<sup>2</sup>Imaging Probe Development Center, National Institutes of Health, Rockville, MD, United States

One of the most important goals of brain imaging is to define the anatomical connections within the brain. In addition to revealing normal circuitry, studies of neural connections and their transports can show rewiring and outgrowth during degeneration following brain injury and diseases. Ultrasensitive agents that can reveal neuroconnectivity and axonal transport dynamics in vivo will be very useful and allow for the interrogation of changes in brain connections and circuitry. In this work, we report two novel MR-visible neural tracers that can be used to visualize neuroconnectivity in vivo.

0626



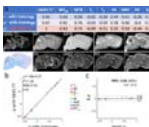
### Image-guided tumor resection of head and neck carcinoma (HNSCC) in rabbit models with targeting MRI-Raman nanoprobe

Pengpeng Sun<sup>1</sup>, Yunfei Zhang<sup>2</sup>, Kaicheng Li<sup>1</sup>, Cong Wang<sup>3</sup>, Feng Zeng<sup>3</sup>, Jinyu Zhu<sup>1</sup>, Yongming Dai<sup>2</sup>, Xiaofeng Tao<sup>1</sup>, and Yinwei Wu<sup>1</sup>

<sup>1</sup>Shanghai Ninth People's Hospital, Shanghai, China, <sup>2</sup>United Imaging Healthcare, Shanghai, China, <sup>3</sup>Fudan University, Shanghai, China

Accurately defining infiltrative tumor margin is extremely crucial for complete resection and avoiding mistaken removal of normal tissue. Currently, pre-operative MRI imaging is the most widely-used strategy for defining tumor margin. However, there are plenty of insurmountable disadvantages in terms of accuracy, low resolution, mismatch and so on. This research aims to develop one targeting MRI-Raman nanoprobe able to pre-operatively and intra-operatively evaluate infiltrative margin of head and neck carcinoma (HNSCC) and real-time guide tumor resection. The results showed that the nanoprobe greatly benefits the complete resection of HNSCC. As a result, the prognosis of tumor-bearing rabbits were considerably improved.

0627



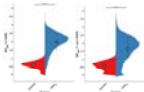
### Myelin-specific imaging using synchrotron X-ray scattering and comparison to MRI myelin-sensitive methods and histology

Marios Georgiadis<sup>1,2,3</sup>, Els Fieremans<sup>2</sup>, Aileen Schroeter<sup>3</sup>, Manuel Guizar-Sicairos<sup>4</sup>, Zirui Gao<sup>4</sup>, Aleezah Balolia<sup>5</sup>, Piotr Walczak<sup>6,7</sup>, Lin Yang<sup>8</sup>, Gergely David<sup>9</sup>, Jiangyang Zhang<sup>2</sup>, Dmitry S. Novikov<sup>10</sup>, Markus Rudin<sup>3,11</sup>, and Michael Zeineh<sup>1</sup>

<sup>1</sup>Radiology, Stanford University, Stanford, CA, United States, <sup>2</sup>NYU School of Medicine, New York, NY, United States, <sup>3</sup>Institute for Biomedical Engineering, ETH Zurich, Zurich, Switzerland, <sup>4</sup>Swiss Light Source, Paul Scherrer Institute, Villigen, Switzerland, <sup>5</sup>Psychology, University of Colorado Denver, Denver, CO, United States, <sup>6</sup>Radiology, Johns Hopkins Medicine, Baltimore, MD, United States, <sup>7</sup>Diagnostic Radiology & Nuclear Medicine, University of Maryland School of Medicine, Baltimore, MD, United States, <sup>8</sup>National Synchrotron Light Source II, Brookhaven National Laboratory, Upton, NY, United States, <sup>9</sup>Balgrist University Hospital, University of Zurich, Zurich, Switzerland, <sup>10</sup>Center for Biomedical Imaging, NYU School of Medicine, New York, NY, United States, <sup>11</sup>Institute of Pharmacology and Toxicology, University of Zurich, Zurich, Switzerland

Axonal myelination is an important indicator of brain development and is implicated in many neurologic diseases. However, MRI methods to probe myelin are sensitive but not specific. Small-angle X-ray scattering (SAXS) produces signal specific to myelin's nanostructural periodicity. Here we apply the recently developed SAXS tensor tomography (SAXS-TT) to non-invasively retrieve myelin levels in mouse brains, and compare them to myelin-sensitive MRI methods. We demonstrate SAXS-TT myelin specificity i) using myelin histology, ii) on a dysmyelination model and iii) by selectively probing central and peripheral nervous system myelin. We propose SAXS-TT as quantitative tomographic method for validating MRI myelin-sensitive sequences.

0628



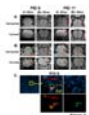
#### mGLUR5 and GABAA Receptor's Association with fMRI BOLD Signals in the Default Mode Network as Assessed via Simultaneously recorded PET/MR data

Ravichandran Rajkumar<sup>1,2,3</sup>, Claudia Régio Brambilla<sup>1,2,3</sup>, Christine Wyss<sup>1,4</sup>, Shukti Ramkiran<sup>1,2</sup>, Linda Orth<sup>1,2</sup>, Joshua Lewis Bierbrier<sup>1,5</sup>, Elena Rota Kops<sup>1</sup>, Jürgen Scheins<sup>1</sup>, Bernd Neumaier<sup>6</sup>, Johannes Ermer<sup>6</sup>, Hans Herzog<sup>1</sup>, Karl Joseph Langen<sup>1,3,7</sup>, Christoph Lerche<sup>1</sup>, N. Jon Shah<sup>1,3,8,9</sup>, and Irene Neuner<sup>1,2,3</sup>

<sup>1</sup>Institute of Neuroscience and Medicine 4 (INM-4), Forschungszentrum Jülich, Jülich, Germany, <sup>2</sup>Department of Psychiatry, Psychotherapy and Psychosomatics, RWTH Aachen University, Aachen, Germany, <sup>3</sup>JARA – BRAIN – Translational Medicine, Aachen, Germany, <sup>4</sup>Department of Psychiatry, Psychotherapy and Psychosomatics, University of Zurich, Zürich, Switzerland, <sup>5</sup>Department of Electrical and Computer Engineering, McMaster University, Hamilton, ON, Canada, <sup>6</sup>Institute of Neuroscience and Medicine 5 (INM-5), Forschungszentrum Jülich, Jülich, Germany, <sup>7</sup>Department of Nuclear Medicine, RWTH Aachen University, Aachen, Germany, <sup>8</sup>Institute of Neuroscience and Medicine 11 (INM-11), Forschungszentrum Jülich, Jülich, Germany, <sup>9</sup>Department of Neurology, RWTH Aachen University, Aachen, Germany

fMRI-BOLD signals reflect the synaptic activity and glucose energy metabolism in the brain. This study investigated the association between excitatory (mGLUR5), inhibitory (GABA<sub>A</sub>) neuroreceptors, and glucose metabolism using PET imaging with resting-state fMRI for the first time. The significantly higher mGLUR5 and GABA<sub>A</sub> neuroreceptor availability and glucose metabolism within the DMN and its correlations show a possible association between increased energy requirements and neuronal activity in the DMN. Further correlations with fMRI measurements show that higher energy demand is utilised for higher functional connectivity, and consecutively higher connectivity within the DMN is more strongly associated with inhibitory receptors.

0629



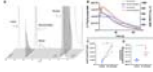
#### MRI Investigation of Adoptive T Cell Transfer and Microbleeds during Vesicular Stomatitis Virus Infection of the Brain

Li Liu<sup>1</sup>, Stephen Dodd<sup>1</sup>, Ryan Hunt<sup>1</sup>, Nikorn Pothayee<sup>1</sup>, Nadia Bouraoud<sup>1</sup>, Dragan Maric<sup>1</sup>, E Ashley Moseman<sup>1</sup>, Dorian B McGavern<sup>1</sup>, and Alan P Koretsky<sup>1</sup>

<sup>1</sup>National Institute of Neurological Disorders and Stroke, National Institutes of Health, Bethesda, MD, United States

A method to label non-phagocytic CD8 T cells with a micron-sized iron oxide particle (MPIO) has been developed which enables MRI single cell detection. Adoptive transfer of T cells showed therapeutic effects in mice causing less bleeding after intranasal virus infection. MPIO-labeled CD8 T cells entered the brain and the combination of labeled T cells and blood made sites of microbleeds easily detectable by MRI. The ability to track individual immune cells by MRI should open new possibilities for early detection of inflammation as well as to monitor the rapidly expanding field of immune cell therapies.

0630



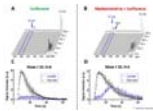
### Non-invasive Detection of M1 Activation in Macrophages using Hyperpolarized $^{13}\text{C}$ MRS of Pyruvate and DHA at 1.47 Tesla

Kai Qiao<sup>1,2</sup>, Lydia Le Page<sup>1,2</sup>, Celine Taglang<sup>1,2</sup>, and Myriam M Chaumeil<sup>1,2</sup>

<sup>1</sup>Physical Therapy and Rehabilitation Science, University of California, San Francisco, San Francisco, CA, United States, <sup>2</sup>Radiology and Biomedical Imaging, University of California, San Francisco, San Francisco, CA, United States

The immune system plays an essential role in various diseases, and macrophage activation patterns can vary greatly - impacting intervention. We propose that  $^{13}\text{C}$  Magnetic Resonance Spectroscopy (MRS) of hyperpolarized [ $1\text{-}^{13}\text{C}$ ] Pyruvate and [ $1\text{-}^{13}\text{C}$ ] Dehydroascorbic acid (DHA) can differentiate between non-activated and M1 classically activated macrophages at the clinically-relevant field strength of 1.47T. In M1-activated macrophages we report increased HP Lactate from Pyruvate, and increased HP Ascorbic Acid from DHA compared to Control cells. This study is a first in differentiating between activated and non-activated macrophages with HP probes at this field strength and could become a powerful translational tool.

0631



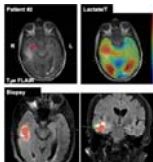
### Cerebral metabolism of hyperpolarized [ $2\text{H}_7$ , U- $^{13}\text{C}_6$ ]D-glucose in the healthy mouse under different anesthetic conditions

Emmanuelle Flatt<sup>1</sup>, Bernard Lanz<sup>1</sup>, Andrea Capozzi<sup>1</sup>, Magnus Karlsson<sup>2</sup>, Mathilde H.Lerche<sup>2</sup>, Rolf Grütter<sup>1,3</sup>, and Mor Mishkovsky<sup>1</sup>

<sup>1</sup>LIFMET, Ecole Polytechnique Fédérale de Lausanne, Lausanne, Switzerland, <sup>2</sup>Danmarks Tekniske Universitet, Lyngby, Denmark, <sup>3</sup>CIBM, Ecole Polytechnique Fédérale de Lausanne, Lausanne, Switzerland

Glucose is the primary fuel for the brain and its metabolism is linked with cerebral function. Isoflurane anesthesia is commonly employed in preclinical MRS but influences functional connectivity. The combination of isoflurane and medetomidine is regularly used in rodent fMRI and show similar functional connectivity as in awake animals. Here we compared the cerebral metabolism of hyperpolarized [ $2\text{H}_7$ , U- $^{13}\text{C}_6$ ]D-glucose under these two anesthetic conditions. When using the combination, the [ $1\text{-}^{13}\text{C}$ ]lactate signal and lactate-to-glucose ratio were more than doubled compared to isoflurane solely, showing that the change of anesthesia had a high impact on cerebral glucose uptake and glycolytic flux.

0632



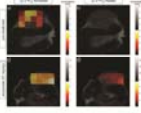
### Hyperpolarized $^{13}\text{C}$ Pyruvate Imaging of Glioblastoma Patients

Jun Chen<sup>1</sup>, Toral Patel<sup>2</sup>, Crystal E Harrison<sup>1</sup>, Galen D Reed<sup>3</sup>, Craig R Malloy<sup>1</sup>, Bruce Mickey<sup>2</sup>, and Jae Mo Park<sup>1,4,5</sup>

<sup>1</sup>Advanced Imaging Research Center, University of Texas Southwestern Medical Center, Dallas, TX, United States, <sup>2</sup>Neurosurgery, University of Texas Southwestern Medical Center, Dallas, TX, United States, <sup>3</sup>GE Healthcare, GE Healthcare, Dallas, TX, United States, <sup>4</sup>Radiology, University of Texas Southwestern Medical Center, Dallas, TX, United States, <sup>5</sup>Electrical Engineering, University of Texas Dallas, Richardson, TX, United States

Noninvasive tumor characterization is extremely beneficial for brain tumor patients for establishing surgical procedure and treatment plans. In this study, we imaged newly diagnosed glioblastoma patients using hyperpolarized [1-<sup>13</sup>C]pyruvate few days prior to surgical procedures and compared the imaging and biopsy results to evaluate the diagnostic values of hyperpolarized pyruvate imaging. Brain regions with increased <sup>13</sup>C-lactate production are confirmed as glioblastoma from stereotactic tissue-biopsy. This pilot study with treatment-naïve or newly diagnosed brain tumor patients suggest that preoperative metabolic imaging with hyperpolarized [1-<sup>13</sup>C]pyruvate may have strong diagnostic value with potential to be an alternative method for tissue biopsy.

0633



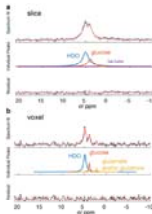
Assessing tumor cell death in vivo using <sup>2</sup>H-labeled fumarate and deuterium magnetic resonance spectroscopic imaging

Friederike Hesse<sup>1</sup>, Vencel Somai<sup>1,2</sup>, Flaviu Bulat<sup>1</sup>, Felix Kreis<sup>1</sup>, and Kevin Brindle<sup>1,3</sup>

<sup>1</sup>Cancer Research UK Cambridge Institute, Cambridge, United Kingdom, <sup>2</sup>Department of Radiology, University of Cambridge, Cambridge, United Kingdom, <sup>3</sup>Department of Biochemistry, University of Cambridge, Cambridge, United Kingdom

Monitoring tumor responses to treatment using metabolic imaging can give an early indication of outcome. We show here that Deuterium Metabolic Imaging (DMI) with <sup>2</sup>H-labelled fumarate can be used to detect early evidence of cell death following drug treatment in a pre-clinical murine lymphoma model. <sup>2</sup>H spectra were acquired from tumors with a time resolution of 5 min, following a bolus injection of <sup>2</sup>H-labelled fumarate. Within 48 h of etoposide treatment the rate of tumor malate production from the labelled fumarate increased significantly. Increased levels of labelled malate were also evident in spectroscopic images of the tumors.

0634



Deuterium MR spectroscopy to probe Krebs cycle metabolism of the in-vivo heart

Felix Kreis<sup>1</sup>, Grzegorz Kwiatkowski<sup>1</sup>, and Sebastian Kozerke<sup>1</sup>

<sup>1</sup>Institute for Biomedical Engineering, University and ETH Zurich, Zurich, Switzerland

We investigated whether deuterium MR spectroscopy using <sup>2</sup>H-labeled glucose can be used to assess Krebs cycle metabolism in the in-vivo heart. Localized <sup>2</sup>H spectra were acquired from a slice containing the whole heart and from a voxel containing only the left ventricle of the heart using a temporal resolution of ~12 min following a bolus injection of [6,6'-<sup>2</sup>H<sub>2</sub>]glucose. Single voxel spectra show the production of labelled Glutamate/Glutamine (Glx) ~36 min after the administration of the glucose. The Glx concentration reflects Krebs cycle activity which holds potential to probe various metabolic states of the heart.

## Oral

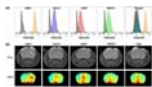
### MRS and Molecular Imaging, Development and Applications - Molecular Imaging: Non-Hyperpolarized

Tuesday Parallel 5 Live Q&A

Tuesday 14:30 - 15:15 UTC

Moderators: Jeff Bulte & Lingzhi Hu

0635



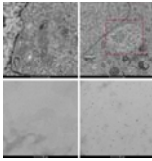
Label-free Tracking of Transplanted Mesenchymal Stem Cells Using manCEST MRI

Yue Yuan<sup>1</sup>, Congxiao Wang<sup>1</sup>, Jia Zhang<sup>1</sup>, and Jeff W.M. Bulte<sup>1</sup>

<sup>1</sup>The Russell H. Morgan Department of Radiology and Radiological Science, The Johns Hopkins University School of Medicine, Baltimore, Maryland, USA., Baltimore, MD, United States

Human mesenchymal stem cells (hMSCs) overexpress high-mannose-type (HM) N-glycans on their membrane surface. Taking advantage of the five exchangeable hydroxyl groups on mannose that provide CEST MRI contrast, we present a label-free method for tracking hMSCs in vivo. The mannose-sensitive CEST (manCEST) signal of hMSCs was clearly distinguishable from the surrounding host tissue and stood out against several other transplanted cell lines tested.

0636



### Bright-Ferritin: A novel MRI gene reporter complex for sensitive and longitudinal cell tracking

Daniel Andrzej Szulc<sup>1,2</sup>, Xavier Alexander Lee<sup>2,3</sup>, Hai-Ying Mary Cheng<sup>4,5</sup>, and Hai-Ling Margaret Cheng<sup>1,2,6</sup>

<sup>1</sup>Institute of Biomaterials and Biomedical Engineering, University of Toronto, Toronto, ON, Canada,

<sup>2</sup>Translational Biology & Engineering Program, Ted Rogers Centre for Heart Research, Toronto, ON,

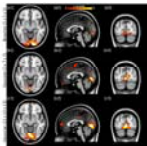
Canada, <sup>3</sup>Department of Physiology, University of Toronto, Toronto, ON, Canada, <sup>4</sup>Biology, University of

Toronto Mississauga, Toronto, ON, Canada, <sup>5</sup>Department of Cell & Systems Biology, University of Toronto,

Toronto, ON, Canada, <sup>6</sup>Edward S. Rogers Sr. Department of Electrical & Computer Engineering, University of Toronto, Toronto, ON, Canada

Tissue engineering with transplanted cells has the potential to repair and regenerate almost every tissue and organ of the body. One major obstacle of cell therapies is the inability to longitudinally assess injected cells. Non-invasive imaging with contrast-enhanced MRI is highly suited for this task but is limited with current methods. In this study, we report a novel method for producing bright endogenous cellular contrast through a genetic MRI reporter that results in the formation of in situ ferritin-manganese nanoparticles. The signal produced by these cells is significantly higher than traditional iron labelled ferritin-overexpressing cells and manganese-permeable cell lines.

0637



### MRI-assisted high temporal resolution dynamic FDG-PET imaging for assessing brain functions

Viswanath Pamulakanty Sudarshan<sup>1,2,3</sup>, Shengpeng Li<sup>4</sup>, Anthony Fernandez<sup>1</sup>, Phillip Ward<sup>4,5</sup>, Sharna Jamadar<sup>4,5</sup>, Gary Egan<sup>4,5</sup>, Suyash Awate<sup>3</sup>, and Zhaolin Chen<sup>4</sup>

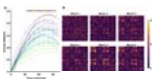
<sup>1</sup>Monash University, Clayton, Australia, <sup>2</sup>IITB Monash Research Academy, Mumbai, India, <sup>3</sup>Indian Institute of

Technology, Bombay, Mumbai, India, <sup>4</sup>Monash Biomedical Imaging, Clayton, Australia, <sup>5</sup>Turner Institute for

Brain and Mental Health, Clayton, Australia

Simultaneous positron emission tomography (PET) and magnetic resonance imaging (MRI) provide complementary structural and functional information. Recent developments in continuous infusion functional PET (fPET) have shown promising results to track dynamic changes in brain metabolism. Although fPET provides opportunities to investigate functional metabolism in the brain, the temporal resolution still remains a major challenge compared to functional MRI (fMRI). In this work, we use anatomical MRI information modeled as a Bowsher prior to improve the sensitivity of fPET at higher temporal resolution. We validate our MRI-assisted fPET analysis framework using both *in-silico* and *in-vivo* experiments.

0638



### Multimodal resting-state functional and metabolic connectivity with simultaneous MR-PET

Phillip G.D. Ward<sup>1,2,3</sup>, Xingwen Liang<sup>1</sup>, Gary F Egan<sup>1,2,3</sup>, and Sharna D Jamadar<sup>1,2,3</sup>

<sup>1</sup>Monash Biomedical Imaging, Monash University, Melbourne, Australia, <sup>2</sup>Turner Institute for Brain and

Mental Health, School of Psychological Sciences, Monash University, Melbourne, Australia, <sup>3</sup>Australian

Research Council Centre of Excellence for Integrative Brain Function, Melbourne, Australia

Metabolic connectivity measured using FDG-PET has been proposed as a biomarker for disease, however static FDG-PET cannot provide subject-level measures of connectivity. We applied constant infusion functional FDG-fPET to measure subject-level metabolic connectivity simultaneously with BOLD-fMRI connectivity. Group-average FDG-fPET and BOLD-fMRI connectivity profiles showed similarities and differences. FDG-fPET and BOLD-fMRI connectivity was most similar in superior cortex, and least similar in subcortical regions. Group-average FDG-fPET within-subject connectivity showed little similarity with static FDG-PET connectivity. Our new method opens up the opportunity for new metabolic neuroimaging biomarkers for disease, as well as approaches for multimodality MR-PET imaging.

Quantitative multiparametric PET-MRI of blood-brain barrier damage after stroke recanalization:



nanoparticles versus small contrast agent



0639

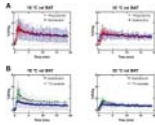


Justine Debatisse<sup>1,2</sup>, Omer Eker<sup>3,4</sup>, Oceane Wateau<sup>5</sup>, Tae-Hee Cho<sup>1,6</sup>, Marlene Wiart<sup>1</sup>, Nicolas Costes<sup>7</sup>, Ines Merida<sup>7</sup>, Christelle Leon<sup>1</sup>, Jean-Baptiste Langlois<sup>7</sup>, Thomas Troalen<sup>2</sup>, Christian Tourvielle<sup>7</sup>, Thibault Iecker<sup>7</sup>, Didier Le Bars<sup>7</sup>, Sophie Lancelot<sup>7</sup>, Norbert Nighoghossian<sup>1,6</sup>, Michel Ovize<sup>1,8</sup>, Hugues Contamin<sup>5</sup>, Francois Lux<sup>9</sup>, Olivier Tillement<sup>9</sup>, and Emmanuelle Canet Soulas<sup>1</sup>

<sup>1</sup>CarMeN lab, U1060 INSERM, University of Lyon, Lyon, France, <sup>2</sup>Siemens Healthcare SAS, Saint-Denis, France, <sup>3</sup>Interventional Neuroradiology, Hospices Civils de Lyon, Lyon, France, <sup>4</sup>CREATIS lab, UMR CNRS 5220, INSERM U1206, INSA, University of Lyon, Villeurbanne, France, <sup>5</sup>Cynbiose SAS, Marcy l'Etoile, France, <sup>6</sup>Neurology, Hospices Civils de Lyon, Lyon, France, <sup>7</sup>CERMEP, Lyon, France, <sup>8</sup>Cardiology, Hospices Civils de Lyon, Lyon, France, <sup>9</sup>ILM, CNRS UMR5306, University of Lyon, Villeurbanne, France

Quantification of blood-brain barrier (BBB) leakage is of main interest in the stroke field to identify patients susceptible to develop hemorrhage and to identify the therapeutic window for neuroprotective drugs administration. We used small (Gd-DOTA) and medium size (nanoparticles AGuIX) contrast agents (CA) to quantify BBB permeability 60-to-90 minutes post-recanalization in a model of stroke using dynamic contrast-enhanced (DCE) MRI. We confirmed 1) Early BBB leakage with both CA and 2) BBB opening to nanoparticles at post-recanalization provides opportunity for selective neuroprotection drug delivery.

0640



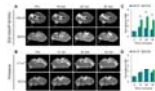
Estimation of brown adipose tissue perfusion by DCE-MRI improves measurement of oxidative metabolism by <sup>11</sup>C-acetate PET in a rat model

Gabriel Richard<sup>1</sup>, Christophe Noll<sup>1</sup>, Mélanie Archambault<sup>1</sup>, Luc Tremblay<sup>1</sup>, Serge Phoenix<sup>1</sup>, Samia Ait-Mohand<sup>1</sup>, Réjean Lebel<sup>1</sup>, Brigitte Guérin<sup>1</sup>, André C. Carpentier<sup>1</sup>, and Martin Lepage<sup>1</sup>

<sup>1</sup>Université de Sherbrooke, Sherbrooke, QC, Canada

Brown adipose tissue (BAT) oxidative metabolism can be measured by <sup>11</sup>C-acetate PET with a 3-tissue pharmacokinetic model. However, this model can have trouble distinguishing between increased oxidation and increased blood volume, both of which occur in active BAT. A sequential DCE-MRI and <sup>11</sup>C-acetate PET protocol was performed in male Wistar rats with and without BAT activation. DCE-MRI perfusion measures were comparable to those obtained previously with <sup>68</sup>Ga-DOTA PET. Incorporating the DCE-MRI blood volume information into the <sup>11</sup>C-acetate model revealed higher oxidation in activated BAT than indicated by the unconstrained model.

0641



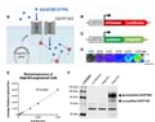
MR Molecular Imaging of EDB-Fibronectin for Precision Imaging of Oral Squamous Cell Carcinoma

Ryan Hall<sup>1</sup>, Nadia Ayat<sup>1</sup>, Peter Qiao<sup>1</sup>, Amita Vaidya<sup>1</sup>, and Zheng-Rong Lu<sup>1</sup>

<sup>1</sup>Department of Biomedical Engineering, Case Western Reserve University, Cleveland, OH, United States

Oral squamous cell carcinoma (OSCC) has maintained poor prognosis due to its aggressive nature and lack of targetable biomarkers for early and accurate detection. We have developed a targeted MRI contrast agent specific to extracellular matrix protein closely associated with tumor aggressiveness. Immunohistochemical analysis revealed strong EDB-FN expression in OSCC with minimal expression in normal tongue tissue. MR molecular imaging with our targeted contrast agent demonstrated the ability for differential contrast enhancement of aggressive OSCC tumors, underscoring the potential for using EDB-FN as a targetable biomarker for precision molecular imaging of OSCC.

0642



Whole-body profiling of early cancer metastasis using multimodality reporter gene imaging

Niviv N Nyström<sup>1,2</sup>, Timothy J Scholl<sup>2,3</sup>, and John Andrew Ronald<sup>1,2,4</sup>

<sup>1</sup>Medical Biophysics, University of Western Ontario, London, ON, Canada, <sup>2</sup>Medical Imaging Laboratories, Robarts Research Institute, London, ON, Canada, <sup>3</sup>Medical Biophysics, Robarts Research Institute, London, ON, Canada, <sup>4</sup>Lawson Health Research Institute, London, ON, Canada

Organic anion-transporting polypeptide 1b3 (Oatp1b3) is a protein derived from the human liver that is capable of taking up Gd-EOB-DTPA, a clinical contrast agent, into cells. We synthetically express the *Oatp1b3* gene on breast cancer cells and are able to track them throughout the bodies of preclinical animal models with high sensitivity and resolution as they metastasize. In the future, we hope to develop *Oatp1b3* as a tool to track the activation and location of gene and cellular therapies in patients on MRI.

---

---

## Sunrise Session

### Educational Q&A: Body Sunrise - Rectal Cancer

Organizers: Johannes Heverhagen, Utaroh Motosugi, Mustafa Shadi Bashir

Tuesday Parallel 3 Live Q&A

Tuesday 15:15 - 16:00 UTC

Treatment Challenges: What Does the Surgeon Need to Know?

Brian Allen

---

Diagnostic Challenges in Rectal Cancer: What Do We Need to Answer?

Kirsten Gormly

---

---

## Sunrise Session

### Educational Q&A: Body Sunrise - Benign Pelvic Diseases

Organizers: Reiko Woodhams, Daniel Margolis, Johannes Heverhagen, Mustafa Shadi Bashir

Tuesday Parallel 3 Live Q&A

Tuesday 15:15 - 16:00 UTC

Moderators:

: Aki Kido

: Victoria Chernyak

Benign Bowel Disease in the Pelvis

Verena Obmann

---

MR Imaging of Endometriosis: What Radiologists Should Know

Yuko IRAHA

---

---

## Sunrise Session

### Educational Q&A: Body Sunrise - DWI in the Body

Organizers: Utaroh Motosugi, Vikas Gulani, Mustafa Shadi Bashir

Tuesday Parallel 3 Live Q&A

Tuesday 15:15 - 16:00 UTC

Moderators: Chang-Hee Lee

DWI of the Breast

Mami Iima

---

Whole-Body DWI

Taro Takahara

---

---

## Sunrise Session

### Educational Q&A: Body Sunrise - The Heart of the Liver

Organizers: Dianna Bardo, Mustafa Shadi Bashir

Tuesday Parallel 3 Live Q&A

Tuesday 15:15 - 16:00 UTC

Moderators: Akira Yamada

## Liver Disease & the Single Ventricle Heart: The Ties That Bind

Mark Fogel

---

## Cardiogenic Liver Disease

Hina Arif Tiwari

---

---

### Weekday Course

#### Educational Q&A: P&E - Fundamentals of MRI Physics & Engineering I

Organizers: Nicole Seiberlich, Michael Lustig, Elizabeth Hecht

Tuesday Parallel 1 Live Q&A

Tuesday 15:15 - 16:00 UTC

#### Spin Gymnastics

Walter Kucharczyk<sup>1</sup>

<sup>1</sup>University Health Network, Canada

The physics of MRI will be reviewed with the goal of presenting an intuitive and graphically centered conceptual framework. The lecture is given in two components; the physics of NMR followed by the principles of MR imaging. Throughout the lecture, unique 3D animations are used to illustrate complex concepts in a graphically intuitive manner. The overall goal is to provide a working knowledge of the basic physics of MRI in a way that is both intuitive and true to the physics of MRI.

---

#### k-Space & Image Quality

Walter Witschey<sup>1</sup>

<sup>1</sup>University of Pennsylvania, United States

---

#### Basic MRI Hardware Components

Martijn Cloos<sup>1</sup>

<sup>1</sup>Centre for Advanced Imaging, The University of Queensland, Australia

This lecture will cover the basic hardware components found in an MRI system. Imagine it is 1972 and you just had a wonder full idea. Employing principles from NMR, you plan to “form images through local interactions”. As you arrive in the lab you immediately start discussions with the engineering team to build such a system. We will use these imagined discussions to better understand the functional role and design constrains of the basic components found in modern day MRI systems. Although some essential MR physics will be covered in passing, basic familiarity with the MRI process is assumed.

---

---

### Weekday Course

#### Educational Q&A: P&E - Fundamentals of MRI Physics & Engineering II

Organizers: Nicole Seiberlich, Michael Lustig, Elizabeth Hecht

Tuesday Parallel 1 Live Q&A

Tuesday 15:15 - 16:00 UTC

Moderators: Jesse Hamilton

#### Spin Echo Imaging

Sean Deoni<sup>1</sup>

<sup>1</sup>Brown University, United States

---

## Gradient Echo Imaging

Armin M. Nagel<sup>1</sup>

<sup>1</sup>*Institute of Radiology, University Hospital Erlangen, Friedrich-Alexander-University (FAU) Erlangen-Nürnberg, Germany*

Magnetic resonance imaging (MRI) techniques can usually be classified into spin-echo (SE) and gradient-echo (GRE) pulse sequences. In this presentation, the basic physical principles of GRE imaging, as well as different mechanisms to generate image contrast will be explained. Differences between SE and GRE MRI will be discussed. Additionally, the influence of different pulse sequence parameters (e.g. echo time, repetition time, flip angle; as well as spoiling techniques and preparation pulses) on the image contrast will be covered. Clinical applications of GRE imaging techniques will be shown exemplarily.

---

## Diffusion-Weighted Imaging

Maxime Descoteaux<sup>1</sup>

<sup>1</sup>*Computer Science, Université de Sherbrooke, Canada*

---

## Weekday Course

### Educational Q&A: P&E - Fundamentals of MRI Physics & Engineering III

Organizers: Nicole Seiberlich, Michael Lustig, Elizabeth Hecht

Tuesday Parallel 1 Live Q&A

Tuesday 15:15 - 16:00 UTC

#### MR Angiography

Oliver Wieben<sup>1</sup>

<sup>1</sup>*University of Wisconsin - Madison, United States*

---

#### Parallel Imaging

Felix Breuer<sup>1</sup>

<sup>1</sup>*Fraunhofer Institute for Integrated Circuits IIS, Würzburg, Germany*

---

#### Sparse Reconstruction Techniques

Anthony G Christodoulou<sup>1</sup>

<sup>1</sup>*Biomedical Imaging Research Institute, Cedars-Sinai Medical Center, Los Angeles, CA, United States*

MRI is a powerful but slow imaging modality, presenting challenges for scanner throughput, motion corruption, and observation of fast dynamic processes. Modern sparse reconstruction techniques break the classical speed limits of MRI, opening new opportunities and solving several long-standing problems. These approaches exploit the redundancy within images and across image sequences, representing images more efficiently than classical approaches to allow efficient acquisition. This talk will provide an overview of various sparse reconstruction techniques for static and dynamic imaging, with particular focus on compressed sensing and low-rank approaches.

---

## Weekday Course

### Educational Q&A: P&E - Fundamentals of MRI Physics & Engineering IV

Organizers: Nicole Seiberlich, Michael Lustig, Elizabeth Hecht

Tuesday Parallel 1 Live Q&A

Tuesday 15:15 - 16:00 UTC



## Contrast Agents

Scott Reeder<sup>1</sup>

<sup>1</sup>Radiology, University of Wisconsin, Madison, WI, United States

Contrast agents are an indispensable tool that can be used to improve the detection and characterization of a plethora of diseases, in a wide variety of clinical and research applications. GBCAs are the most widely used agents with tremendous experience over the last 30 years. Despite their outstanding safety records, safety concerns NSF and gadolinium deposition warrant attention in the literature as this subject evolves. Attention to optimization of pulse sequences to best exploit the use of contrast agents for disease detection should always be considered and can bear great fruit for maximizing the benefit of contrast with clinical MRI.

---

## Ultra-High Field Imaging

Kamil Ugurbil<sup>1</sup>

<sup>1</sup>University of Minnesota, United States

---

## Artifacts: Their Causes & Uses

Vikas Gulani<sup>1</sup>

<sup>1</sup>University of Michigan, United States

---

---

## Weekday Course

### CSF flow & Glymphatic Imaging - Emerging Methods for Imaging the Glymphatic System

Organizers: Thomas Okell, Krishna Nayak

Tuesday Parallel 2 Live Q&A

Tuesday 15:15 - 16:00 UTC

Moderators: Lydiane Hirschler

#### Contrast Agent-Based Methods for Visualizing Glymphatic System

Toshiaki Taoka<sup>1</sup>

<sup>1</sup>Nagoya University, Japan

The glymphatic system hypothesis is a concept associated with the dynamics of cerebrospinal fluid and interstitial fluid in the central nervous system. Tracer studies are one of the most efficient methods to visualize or evaluate mass transport systems in the living body. Tracer study using gadolinium based contrast agent is a method that provides tomographic images and evaluation of the whole brain which can be also applied to human subjects.

---

#### Non-Invasive Approaches

Yolanda Ohene<sup>1</sup>

<sup>1</sup>University College London, London, United Kingdom

Emerging non-invasive imaging approaches have been developed to investigate aspects of the glymphatic system. Many of these techniques have potential as clinical tools to better understand the human glymphatic system in health and disease. In this lecture, I will review these emerging non-invasive techniques and how they have been applied to probe the glymphatic system.

---

---

## Weekday Course

## CSF flow & Glymphatic Imaging - Imaging Perivascular Spaces in the Brain

Organizers: Nivedita Agarwal, Anja van der Kolk, C. C. Tchoyoson Lim

Tuesday Parallel 2 Live Q&A

Tuesday 15:15 - 16:00 UTC

Moderators: Lydiane Hirschler

### Zooming In on Perivascular Spaces: Brain

Nivedita Agarwal<sup>1</sup> and Roxana Octavia Carare<sup>2</sup>

<sup>1</sup>APSS Ospedale Santa Maria del Carmine, Italy, <sup>2</sup>University of Southampton, Southampton, United Kingdom

Perivascular spaces are fluid filled spaces around cerebral arterioles in the brain parenchyma. They play an important role in the exchange and drainage of interstitial fluid through mechanisms such as intramural periarterial drainage pathway and the glymphatic system. Such processes may fail and accelerate neurodegeneration in the brain. Neuroimaging methods are still lacking in advancing our knowledge of how exchange and drainage of solutes occurs through these spaces in the brain.

---

### Interstitial Fluid Dynamics: A Mathematical Approach

Lynne Bilston<sup>1</sup>

<sup>1</sup>Neuroscience Research Australia, Sydney, Australia

---

### Perivascular Spaces & Neurodegeneration

Matt Paradise<sup>1</sup>

<sup>1</sup>University of New South Wales, Sydney, Australia

---

## Oral

### System Imperfections, Artifacts, and More - Measuring & Correcting System Imperfections

Tuesday Parallel 3 Live Q&A

Tuesday 15:15 - 16:00 UTC

Moderators: Stephan Orzada & Rudolf Stollberger

0653



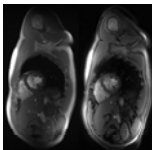
#### Optical Field Probes for MRI

Hans Stærkind<sup>1,2</sup>, Vincent Oltman Boer<sup>1</sup>, Kasper Jensen<sup>3</sup>, Eugene Simon Polzik<sup>2</sup>, and Esben Thade Petersen<sup>1,4</sup>

<sup>1</sup>Danish Research Centre for Magnetic Resonance, Centre for Functional and Diagnostic Imaging and Research, Copenhagen University Hospital Hvidovre, Hvidovre, Denmark, <sup>2</sup>Quantop, Niels Bohr Institute, University of Copenhagen, Copenhagen, Denmark, <sup>3</sup>School of Physics and Astronomy, University of Nottingham, Nottingham, United Kingdom, <sup>4</sup>Department of Health Technology, Technical University of Denmark, Kgs. Lyngby, Denmark

A novel optical field probe is described for the precision measurement of high magnetic fields. The advantages over traditional field probes are two-fold. First, there is no electromagnetic interference with the other parts of the MRI system such as the RF coil. Secondly, the setup allows for a continuous and long readout of the magnetic field during an MRI sequence, where traditional NMR probes typically operate in a pulsed mode.

0654



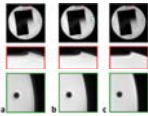
#### Spiral real-time cardiac MR imaging using a GSTF-based pre-emphasis

Philipp Eirich<sup>1,2</sup>, Tobias Wech<sup>1</sup>, Julius F. Heidenreich<sup>1</sup>, Manuel Stich<sup>1,3</sup>, Nils Petri<sup>4</sup>, Peter Nordbeck<sup>4</sup>, Thorsten A. Bley<sup>1</sup>, and Herbert Köstler<sup>1</sup>

<sup>1</sup>Department of Diagnostic and Interventional Radiology, University Hospital Würzburg, Würzburg, Germany, <sup>2</sup>Comprehensive Heart Failure Center Würzburg, Würzburg, Germany, <sup>3</sup>Siemens Healthcare, Erlangen, Germany, <sup>4</sup>Department of Internal Medicine I, University Hospital Würzburg, Würzburg, Germany

An automatic pre-emphasis based on the Gradient System Transfer Function (GSTF) was applied to real-time cardiac MR imaging at 3T to compensate for deviations of spiral k-space trajectories. This yielded cine series with coverage of the whole heart in free-breathing, less than 40 s total scan time and a temporal resolution of 50 ms. The developed framework was compared to a gated Cartesian acquisition in multiple breath-holds, in one healthy volunteer and one patient suffering from cardiac arrhythmia.

0655



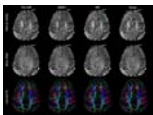
Trajectory calculation for spiral imaging based on concurrent reading of the gradient amplifiers' internal current sensors

Jürgen Rahmer<sup>1</sup>, Ingo Schmale<sup>1</sup>, Peter Mazurkewitz<sup>1</sup>, and Peter Börnert<sup>1</sup>

<sup>1</sup>Philips Research, Hamburg, Germany

Spiral sequences sample data during gradient variation and are therefore susceptible to dynamic field deviations caused by eddy currents, timing inaccuracies, or gradient amplifier non-linearities. Linear effects can be corrected using a gradient impulse response function for trajectory calculation. Non-linear effects require a measurement-based approach, e.g. measurement of the gradient fields during imaging using a field camera or an induction-based field measurement. To avoid the need for additional hardware, we propose a hybrid method that combines current measurements using the amplifier-internal current sensors with correction based on the current-to-gradient impulse response function. The approach improves trajectory accuracy in spiral imaging.

0656



Concurrent Field Monitoring in HCP dMRI at 7T: Correction for Eddy Current Induced Signal Blurring and Geometric Distortion.

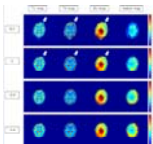
Ruoyun Emily Ma<sup>1</sup>, Mehmet Akçakaya<sup>1,2</sup>, Steen Moeller<sup>1</sup>, Connor Benson<sup>1</sup>, Edward Auerbach<sup>1</sup>, Kâmil Uğurbil<sup>1</sup>, and Pierre-François Van de Moortele<sup>1</sup>

<sup>1</sup>Center for Magnetic Resonance Research, University of Minnesota, Minneapolis, MN, United States,

<sup>2</sup>Electrical and Computer Engineering, University of Minnesota, Minneapolis, MN, United States

DW-EPI at high diffusion gradients suffers from eddy current induced signal blurring and geometric distortion. In this study, concurrent monitoring of field evolution with NMR probes was implemented for HCP diffusion MRI acquisition at 7T. After image reconstruction with field correction, eddy current induced geometric distortion was largely removed, yielding similar level of correction obtained by data driven approaches such as EDDY. Signal blurring was further reduced than with EDDY. Future efforts will be made to quantify the impact on cortical tractography of this improved DW-EPI reconstruction.

0657



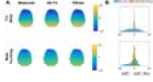
A simple method to estimate gradient delay for MRF

Koji Fujimoto<sup>1</sup>, Martijn A. Cloos<sup>2</sup>, and Tomohisa Okada<sup>1</sup>

<sup>1</sup>Human Brain Research Center, Graduate School of Medicine, Kyoto University, Kyoto, Japan, <sup>2</sup>Center for Advanced Imaging Innovation and Research (CAI2R) and Bernard and Irene Schwartz Center for Biomedical Imaging, Department of Radiology, New York University School of Medicine, New York, NY, United States

A self-contained method to estimate the gradient delay for radial based MRF sequences based on the residual error after dictionary matching was presented. Under IRB approval, MRF was performed in two healthy volunteers at 7T. Images were reconstructed with varying degrees of gradient offset in the readout direction. The correlation of the dictionary match (i.e. inner product of the compressed data with the matched dictionary entry) was recorded. The average signal intensity within the head ROI in the "match map" gave the best result, and hence could be an easy and reliable metric for gradient delay correction.

0658



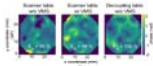
### Measurement and correction of spatiotemporal B<sub>0</sub> fluctuations using an FID-navigated EPI sequence

Tess E. Wallace<sup>1,2</sup>, Jonathan R. Polimeni<sup>2,3</sup>, Jason P. Stockmann<sup>2,3</sup>, W. Scott Hoge<sup>2,4</sup>, Tobias Kober<sup>5,6,7</sup>, Simon K. Warfield<sup>1,2</sup>, and Onur Afacan<sup>1,2</sup>

<sup>1</sup>Computational Radiology Laboratory, Boston Children's Hospital, Boston, MA, United States, <sup>2</sup>Department of Radiology, Harvard Medical School, Boston, MA, United States, <sup>3</sup>Athinoula A. Martinos Center for Biomedical Imaging, Massachusetts General Hospital, Boston, MA, United States, <sup>4</sup>Brigham and Women's Hospital, Boston, MA, United States, <sup>5</sup>Advanced Clinical Imaging Technology, Siemens Healthcare, Lausanne, Switzerland, <sup>6</sup>Radiology, Lausanne University Hospital and University of Lausanne, Lausanne, Switzerland, <sup>7</sup>LTS5, École Polytechnique Fédérale de Lausanne (EPFL), Lausanne, Switzerland

Spatiotemporal B<sub>0</sub> field fluctuations give rise to dynamic susceptibility-induced distortions in EPI time-series, which reduces signal stability, particularly at higher field strengths. In this work, we propose a novel method for rapid measurement of B<sub>0</sub> field changes from FIDnavs embedded in an EPI sequence. We demonstrate the ability of the proposed method to accurately characterize field changes up to second order in controlled phantom and volunteer experiments. Dynamic slice-wise distortion correction using FIDnav field estimates reduced normalized root-mean-square error and improved temporal SNR in volunteers performing deliberate arm motion.

0659



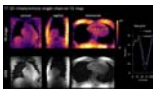
### Reduction of vibration-induced signal loss by matching mechanical vibrational states: application in high b-value diffusion weighted MRS

Dominik Weidlich<sup>1</sup>, Mark Zamskiy<sup>1</sup>, Marcus Maeder<sup>2</sup>, Stefan Ruschke<sup>1</sup>, Steffen Marburg<sup>2</sup>, and Dimitrios C. Karampinos<sup>1</sup>

<sup>1</sup>Department of Diagnostic and Interventional Radiology, Technical University of Munich, Munich, Germany, <sup>2</sup>Chair of Vibroacoustics of Vehicles and Machines, Technical University of Munich, Munich, Germany

Diffusion gradients are known to yield MR hardware vibrations, which may lead to signal loss in DW measurements especially at high b-values. The present work proposes to mitigate vibration-induced signal loss by introducing a vibration matching gradient (VMG). Laser interferometry was employed to measure the displacements induced by high b-value DW MR spectroscopy, focusing on the quantification of lipids ADC. The measured displacement patterns during the two diffusion gradients were more similar when using the VMG. The application of VMG showed an improvement in lipid ADC quantification in both a water-fat phantom and a volunteer's tibial bone marrow.

0660



### Respiration-Resolved 3D Multi-Channel B<sub>1</sub> mapping of the body at 7T

Sebastian Dietrich<sup>1</sup>, Christoph Stefan Aigner<sup>1</sup>, Juliane Ludwig<sup>1</sup>, Johannes Mayer<sup>1</sup>, Simon Schmidt<sup>2</sup>, Christoph Kolbitsch<sup>1,3</sup>, Tobias Schaeffter<sup>1,3</sup>, and Sebastian Schmitter<sup>1,2</sup>

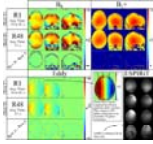
<sup>1</sup>Physikalisch-Technische Bundesanstalt (PTB), Braunschweig and Berlin, Germany, <sup>2</sup>Medical Physics in Radiology, German Cancer Research Center (DKFZ), Heidelberg, Germany, <sup>3</sup>Division of Imaging Sciences and Biomedical Engineering, King's College London, London, United Kingdom

A major challenge of ultra-high field MRI is the spatially inhomogeneous transmit radio frequency field that induces spatial contrast variations. In this work we present a novel technique to retrieve channel-wise, motion-resolved absolute 3D FA maps of the human body at 7T. Free breathing 3D scans of the thorax were performed and B<sub>1</sub> maps without motion artifacts are obtained for the two motion states inhale and exhale. It allows acquiring B<sub>1</sub> libraries that can be used for offline RF pulse calculation including motion-robust RF pulses.

PhysiCal: A rapid calibration scan for B<sub>0</sub>, B<sub>1+</sub>, coil sensitivity and Eddy current mapping.



0661

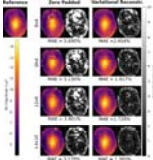


Siddharth Srinivasan Iyer<sup>1,2</sup>, Congyu Liao<sup>2</sup>, Qing Li<sup>3</sup>, Mary Katherine Manhard<sup>2</sup>, Avery Berman<sup>2</sup>, Berkin Bilgic<sup>2</sup>, and Kawin Setsompop<sup>2</sup>

<sup>1</sup>Electrical Engineering and Computer Science, Massachusetts Institute of Technology, Cambridge, MA, United States, <sup>2</sup>Athinoula A. Martinos Center for Biomedical Imaging, Charlestown, MA, United States, <sup>3</sup>MR Collaborations, Siemens Healthcare Ltd, Shanghai, China

Calibration scans that acquire coil sensitivity,  $B_0$  and  $B_{1+}$  inhomogeneities information play an important role in enabling modern acquisition and reconstruction techniques. This work proposes a unified, rapid calibration sequence termed Physics Calibration (*PhysiCal*) to obtain accurate  $B_0$ , Eddy,  $B_{1+}$  and coil sensitivity maps. *PhysiCal* utilizes a carefully designed mix of full and variable density sampling acquisitions across echoes with synergistic constrained and eigenvalue reconstruction for robust and accurate recovery of whole-brain  $B_0$ ,  $B_{1+}$ , Eddy and 32-channel coil sensitivity maps in just 11 seconds at 1 mm x 2 mm x 2mm resolution at 3T.

0662



Highly 3D accelerated Bloch Siebert  $B_{1+}$  Mapping at 7T

Andreas Lesch<sup>1</sup>, Christoph Aigner<sup>2</sup>, and Rudolf Stollberger<sup>1</sup>

<sup>1</sup>Institute of Medical Engineering, Graz University of Technology, Graz, Austria, <sup>2</sup>Physikalisch-Technische Bundesanstalt (PTB), Braunschweig and Berlin, Berlin-Charlottenburg, Germany

For many applications in MRI fast and accurate  $B_{1+}$ -mapping is an important prerequisite to correct for spatially varying RF-field variations. We recently proposed a reconstruction algorithm to reconstruct highly undersampled Bloch Siebert data, which was applied to 3T data. In this work we investigated the applicability of this algorithm to 7T data in terms of accuracy and possible acquisition time. We could successfully show that the proposed algorithm can be applied to 7T data with only slightly increased error compared to 3T. The minimum scan time at 7T is in the order of 45s-1min for a 3D volume.

## Oral

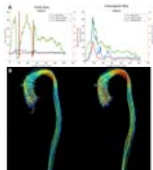
### System Imperfections, Artifacts, and More - Mitigating Sample-Induced Artifacts

Tuesday Parallel 3 Live Q&A

Tuesday 15:15 - 16:00 UTC

Moderators: Tolga Cukur & Megan Poorman

0663



Multiple phase unwrapping of 4D-flow MRI in cardiovascular valves and vessels

Joao Filipe Fernandes<sup>1</sup>, Alessandro Faraci<sup>1</sup>, Marzia Rigolli<sup>2</sup>, Umar Shehzad<sup>1</sup>, Saul Myerson<sup>2</sup>, David Nordsletten<sup>1,3</sup>, and Pablo Lamata<sup>1</sup>

<sup>1</sup>School of Biomedical Engineering & Imaging Sciences, King's College London, London, United Kingdom, <sup>2</sup>Division of Cardiovascular Medicine, Radcliffe Department of Medicine, University of Oxford, Oxford, United Kingdom, <sup>3</sup>Department of Surgery and Biomedical Engineering, University of Michigan, Ann Arbor, MI, United States

Accurate quantification of both high and low blood velocities is important for clinical decision-making in cardiovascular conditions like aortic valve stenosis. Multi-VENC acquisition is a potential solution. An alternative, without increasing acquisition time, is enabled here by correcting 4D-Flow MRI multi-aliasing along tubular structures. Our solution is based on continuity principles in successive cross-section planes, outperforming the state-of-the-art Laplacian-based solution which only performs single-wrap corrections. The accuracy of proposed method is verified in 4D-Flow MRI of 25 aortic stenosis patients with VENC of 1m/s, where double and triple unwrapping were needed to match velocity values measured by Doppler echocardiography.



Edge-preserving  $B_0$  inhomogeneity distortion correction for high-resolution multi-echo ex vivo MRI at 7T

0664

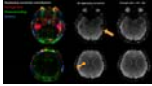


Divya Varadarajan<sup>1,2</sup>, Robert Frost<sup>1,2</sup>, Andre van der Kouwe<sup>1,2</sup>, Leah Morgan<sup>1</sup>, Bram Diamond<sup>1</sup>, Emma Boyd<sup>1</sup>, Morgan Fogarty<sup>1</sup>, Allison Stevens<sup>1</sup>, Bruce Fischl<sup>1,2</sup>, and Jonathan R Polimeni<sup>1,2,3</sup>

<sup>1</sup>Athinoula A. Martinos Center for Biomedical Imaging, Massachusetts General Hospital, Boston, MA, United States, <sup>2</sup>Harvard Medical School, Boston, MA, United States, <sup>3</sup>Harvard-MIT HST, Cambridge, MA, United States

High-resolution multi-echo MRI at ultra-high field for ex vivo imaging is time consuming, SNR starved and suffers from  $B_0$  inhomogeneity induced geometric distortions due to low-bandwidth in the readout direction. Fieldmap-based correction cannot correct singularities in regions of severe distortion, and reversed gradient (RG) approaches double the scan time. We propose to combine an alternating-polarity acquisition scheme for multi-echo MRI with a low-resolution fieldmap based novel distortion correction algorithm that can correct singularities in half the scan time of RG and enhance SNR while preserving edges. We show several ex vivo corrected results and demonstrate generalizability to in vivo MRI.

0665



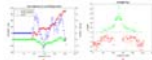
Accounting for  $B_0$  field-inhomogeneity-gradient induced dephasing in Cartesian and in time-resolved sequences.

Gilad Liberman<sup>1</sup> and Kawin Setsompop<sup>1</sup>

<sup>1</sup>Department of Radiology, Massachusetts General Hospital, Charlestown, MA, United States

The spatial derivative of the field inhomogeneity acts as a gradient, inducing growing intravoxel dephasing along the acquisition time, resulting in blurring, void regions ("signal loss") and artifacts. We tackle this issue through modelling and through Cartesian time-segmentation. We show that under typical settings, field inhomogeneity gradients cause significant artifact both through-plane and in-plane, and that these artifacts can be greatly mitigated with improved reconstruction at minimal computational cost. We formalize the description of the effects of these additional gradients in k-t space in temporal units, allowing for quick apprehension of the consequences to trajectory design and reconstruction approach.

0666



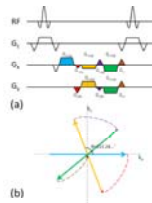
Alleviate motion artifacts in magnetic resonance imaging images using deep learning and compressed sensing

Long Cui<sup>1</sup>, Yang Song<sup>1</sup>, Yida Wang<sup>1</sup>, Haibin Xie<sup>1</sup>, Jianqi Li<sup>1</sup>, and Guang Yang<sup>1</sup>

<sup>1</sup>Shanghai Key Laboratory of Magnetic Resonance, Department of Physics, East China Normal University, Shanghai, China

We proposed a data-driven approach to alleviate motion artifacts in Magnetic Resonance (MR) images. Firstly, MR images were acquired using a pseudo-random k-space sampling sequence. Then a convolutional network was trained to denoise MR images containing motion artifacts, before the k-space of the denoised images were compared with the raw k-space to find out k-space lines influenced by the motion. Finally, compressed sensing (CS) was applied to those unaffected lines to reconstruct the final image. Simulated experiments proved that this approach can accurately detect k-space lines influenced by motion and reconstruct images better than those reconstructed directly by CS.

0667



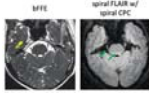
Echo-train radial SSFP with golden angle

Kaibao Sun<sup>1</sup>, Zheng Zhong<sup>1,2</sup>, and Xiaohong Joe Zhou<sup>1,2,3</sup>

<sup>1</sup>Center for MR Research, University of Illinois at Chicago, Chicago, IL, United States, <sup>2</sup>Department of Bioengineering, University of Illinois at Chicago, Chicago, IL, United States, <sup>3</sup>Departments of Radiology and Neurosurgery, University of Illinois at Chicago, Chicago, IL, United States

Golden-angle radial sampling based on bSSFP is widely used in time-resolved imaging. The temporal resolution of this technique can be improved by extending a single-echo acquisition to echo-train acquisition per TR. In this study, we demonstrate an echo-train golden-angle radial bSSFP (ETGAR-bSSFP) sequence by acquiring multiple spokes in k-space to improve the temporal resolution. In addition, we introduce an integrated phase correction method and a variation of ETGAR-bSSFP to manage the image artifacts. Results from phantom and human brain have showed high quality images can be acquired from the ETGAR-bSSFP sequences and be potentially used for dynamic imaging studies.

0668



### An improved spiral technique for imaging gamma knife subject with metal frame

Zhiqiang Li<sup>1</sup>, Sharmeen Maze<sup>1</sup>, Shiv Srivastava<sup>2</sup>, Stephen Sorensen<sup>2</sup>, and John P Karis<sup>1</sup>

<sup>1</sup>Neuroradiology, Barrow Neurological Institute, Phoenix, AZ, United States, <sup>2</sup>St Joseph's Hospital and Medical Center, Phoenix, AZ, United States

SSFP is widely used in gamma knife treatment planning in patients with trigeminal neuralgia. A metal frame worn by the patient often causes image artifacts. A spiral FLAIR technique is proposed with an improved approach for concomitant field induced phase error compensation, which is insensitive to the presence of the metal frame. Volunteer results demonstrate good delineation of the trigeminal nerve root entry zone, good adjacent CSF suppression, and good brain stem tissue contrast, therefore providing a potential alternative to SSFP for gamma knife treatment planning.

0669



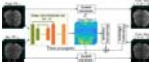
### Robust Coil Combination for bSSFP Elliptical Signal Model

Nicholas McKibben<sup>1,2</sup>, Grayson Tarbox<sup>3</sup>, Edward V. DiBella<sup>1,2</sup>, and Neal K. Bangerter<sup>4</sup>

<sup>1</sup>Biomedical Engineering, University of Utah, Salt Lake City, UT, United States, <sup>2</sup>Radiology and Imaging Sciences, University of Utah, Salt Lake City, UT, United States, <sup>3</sup>Electrical and Computer Engineering, Brigham Young University, Provo, UT, United States, <sup>4</sup>Bioengineering, Imperial College London, London, United Kingdom

Elliptical parametric models of the bSSFP signal equation are used to derive band-free images given multiple phase-cycled images. For large multicoil datasets, we desire coil combination before debanding to significantly reduce computational burden. Conventional coil combination methods fail as nonlinear mappings lead to distortions of the elliptical representation. We propose phase-substitutions that can be applied with any coil combination method including sum-of-squares and which allow coil combination before computationally expensive debanding operations.

0670



### An Unsupervised Deep Learning Method for Correcting the Susceptibility Artifacts in Reversed Phase-encoding EPIs

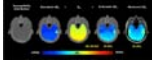
Soan Thi Minh Duong<sup>1</sup>, Sui Paul Ang<sup>1</sup>, and Mark Matthias Schira<sup>2</sup>

<sup>1</sup>School of Electrical, Computer and Telecommunications Engineering, University of Wollongong, Wollongong, Australia, <sup>2</sup>School of Psychology, University of Wollongong, Wollongong, Australia

We introduce a deep learning method, named S-Net, to correct the susceptibility artifacts in a pair of reversed phase-encoding (PE) echo-planar imaging images. The S-Net is trained in an unsupervised manner using a set of reversed-PE pairs. For a new reversed-PE pair, the corrected images are computed rapidly by evaluating the learned S-Net. Evaluation of three datasets demonstrates equally good correction performance as much lower computation time (1-3s) than state-of-the-art SAC methods such as AISAC (50-60s) or TOPUP (over 1000s). This fast performance provides a dramatic speedup for medical imaging processing pipelines and makes the real-time correction for MR-scanners feasible.

0671

B0 field estimation using Ultrashort echo time/Dixon imaging with a 4-class tissue segmentation



Jiazheng Zhou<sup>1,2</sup>, Ali Aghaeifer<sup>1</sup>, Gisela Hagberg<sup>1,3</sup>, and Klaus Scheffler<sup>1,3</sup>

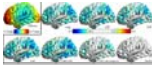
<sup>1</sup>High-Field Magnetic Resonance, Max Planck Institute of Biological Cybernetics, Tübingen, Germany,

<sup>2</sup>Graduate Training Centre of Neuroscience, IMPRS, University of Tübingen, Tübingen, Germany,

<sup>3</sup>Biomedical Magnetic Resonance, University Hospital Tübingen (UKT), Tübingen, Germany

We use a UTE sequence combining with Dixon method to obtain the subject specific susceptibility distribution, with 4-class tissue segmentation. The susceptibility model was then used to simulate motion-induced  $B_0$  change for two head positions. A good agreement between the simulated and measured field map has been observe. A forward field map predicting strategy was explored using the susceptibility model.

0672



Disentangling time series between gray matter and non-gray matter tissue using deep neural network improves resting state fMRI data quality

Zhengshi Yang<sup>1</sup>, Xiaowei Zhuang<sup>1</sup>, Karthik Sreenivasan<sup>1</sup>, Virendra Mishra<sup>1</sup>, and Dietmar Cordes<sup>1,2</sup>

<sup>1</sup>Cleveland Clinic Lou Ruvo Center for Brain Health, Las Vegas, NV, United States, <sup>2</sup>Department of

Psychology and Neuroscience, University of Colorado, Boulder, CO, United States

The fluctuation introduced by head motion, cardiac and respiratory fluctuations and other noise sources considerably confounds the interpretation of resting-state fMRI data. These noise fluctuations widely spread the whole brain regardless of the kinds of brain tissues, however, neural activity is more likely limited to gray matter tissue. Considering that the contribution of neural activity varies in different brain tissues, we hypothesized that disentangling gray matter and non-gray matter time series can clean fMRI data and improve the data quality. With such a hypothesis, we proposed a deep neural network method to denoise resting state fMRI data.

## Oral - Power Pitch

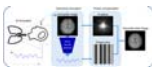
### System Imperfections, Artifacts, and More - Machine Learning: Artifact Correction, Quantification & Reconstruction

Tuesday Parallel 3 Live Q&A

Tuesday 15:15 - 16:00 UTC

Moderators: Teresa Correia & Joshua Trzasko

0673



DeepRespi: Retrospective correction for respiration-induced  $B_0$  fluctuation artifacts using deep learning

Hongjun An<sup>1</sup>, Hyeong-Geol Shin<sup>1</sup>, Woojin Jung<sup>1</sup>, and Jongho Lee<sup>1</sup>

<sup>1</sup>Department of Electrical and computer Engineering, Seoul National University, Seoul, Korea, Republic of

$B_0$  fluctuation from respiration can induce significant artifacts in MRI images. In this study, a new retrospective correction method that requires no modification in sequences (e.g. no navigator) is proposed. This method utilizes a convolution neural network (CNN), DeepRespi, to extract a respiration pattern from a corrupted image. The respiration pattern is applied back to the corrupted image for phase compensation. When tested, the CNN successfully extracted the respiration pattern (correlation coefficient =  $0.94 \pm 0.04$ ) and the corrected images showed on average  $68.9 \pm 13.2\%$  reduction in NRMSE when comparing the corrupted vs. corrected images.

0674



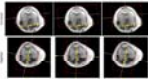
Convolutional Neural Network for Slice Encoding for Metal Artifact Correction (SEMACE) MRI

Sunghun Seo<sup>1</sup>, Won-Joon Do<sup>1</sup>, Huan Minh Luu<sup>1</sup>, Ki Hwan Kim<sup>1</sup>, Seung Hong Choi<sup>2</sup>, and Sung-Hong Park<sup>1</sup>

<sup>1</sup>Department of Bio and Brain Engineering, Korea Advanced Institute of Science and Technology, Daejeon, Korea, Republic of, <sup>2</sup>Department of Radiology, Seoul National University College of Medicine, Seoul, Korea, Republic of

We propose convolutional neural network (CNN) to accelerate Slice Encoding for Metal Artifact Correction (SEMAC). The concept was tested on metal-embedded agarose phantoms and patients with metallic neuro plates in the cerebral region. CNN was trained to output images with high SEMAC factor from input images with low SEMAC factor, achieving acceleration factors of 2 or 3. The metal artifacts in low SEMAC factor data were visually and quantitatively suppressed well in the output of CNN ( $p < 0.01$ ), which was comparable to that of the high SEMAC factor. The study shows the feasibility of reducing scan time of SEMAC through CNN.

0675



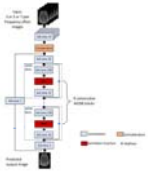
#### Consistency in human and machine-learning based scan-planes for clinical knee MRI planning

Chitresh Bhushan<sup>1</sup>, Dattesh D. Shanbhag<sup>2</sup>, Andre Maximo<sup>3</sup>, Uday Patil<sup>2</sup>, Radhika Madhavan<sup>1</sup>, Matthew Frick<sup>4</sup>, Kimberly K. Amrami<sup>4</sup>, Desmond Teck Beng yeo<sup>1</sup>, and Thomas Foo<sup>1</sup>

<sup>1</sup>GE Research, Niskayuna, NY, United States, <sup>2</sup>GE Healthcare, Bengaluru, India, <sup>3</sup>GE Healthcare, Rio de Janeiro, Brazil, <sup>4</sup>Mayo Clinic, Rochester, MN, United States

We evaluate the consistency and clinical applicability of our automated deep-learning based intelligent slice placement (ISP) approach for knee scan planning. We use 146 clinical knee exams that were retrospectively selected to have anatomically consistent scan planning along with manual-marking from in-house radiologist to access the variability across MR technicians. The results indicate that our automated ISP approach has better consistency than the variability seen across MR technicians for coronal and sagittal knee scan planning, indicating promising clinical applicability of our automated ISP approach.

0676



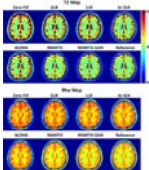
#### Accelerating the B0 Inhomogeneity Correction for GluCEST Imaging Using Deep Learning

Yiran Li<sup>1</sup>, Danfeng Xie<sup>1</sup>, Abigail Cember<sup>2</sup>, Ravi Prakash Reddy Nanga<sup>2</sup>, Hanlu Yang<sup>1</sup>, Dushyant Kumar<sup>2</sup>, Hari Hariharan<sup>2</sup>, Li Bai<sup>1</sup>, John A. Detre<sup>3</sup>, Ravinder Reddy<sup>2</sup>, and Ze Wang<sup>4</sup>

<sup>1</sup>Department of Electrical and Computer Engineering, Temple University, Philadelphia, PA, United States, <sup>2</sup>Department of Radiology, University of Pennsylvania Perelman School of Medicine, Philadelphia, PA, United States, <sup>3</sup>Department of Neurology, University of Pennsylvania Perelman School of Medicine, Philadelphia, PA, United States, <sup>4</sup>Department of Diagnostic Radiology and Nuclear Medicine, University of Maryland School of Medicine, Baltimore, MD, United States

Glutamate Chemical Exchange Saturation Transfer (GluCEST) MRI is a noninvasive technique for mapping parenchymal glutamate in the brain. GluCEST signal is sensitive to magnetic field (B0) inhomogeneity. Corrections for B0 inhomogeneity often require repeated data acquisitions at several saturation offset frequencies, which however dramatically prolongs the total acquisition time and can cause practical issues such as increased sensitive to patient motions. Another technique challenge in GluCEST MRI is the low signal-to-noise-ratio (SNR) as the signal is derived from the small z-spectrum difference. Both issues were addressed in this study with a novel deep learning-based algorithm armed with wide activation neurons.

0677



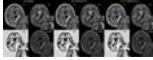
#### High-Performance Rapid Quantitative Imaging with Model-Based Deep Adversarial Learning

Fang Liu<sup>1,2</sup> and Li Feng<sup>3</sup>

<sup>1</sup>Gordon Center for Medical Imaging, Massachusetts General Hospital, Harvard Medical School, Boston, MA, United States, <sup>2</sup>Radiology, University of Wisconsin-Madison, Madison, WI, United States, <sup>3</sup>Biomedical Engineering and Imaging Institute and Radiology, Icahn School of Medicine at Mount Sinai, New York, NY, United States

The purpose of this work was to develop a novel deep learning-based reconstruction framework for rapid MR parameter mapping. Building upon our previously proposed Model-Augmented Neural network with Incoherent k-space Sampling (MANTIS) technique combining efficient end-to-end CNN mapping and k-space consistency to enforce joint data and model fidelity, this new method further extends to incorporate the latest adversarial training (MANTIS-GAN), so that more realistic parameter maps can be directly estimated from highly-accelerated k-space data. The performance of MANTIS-GAN was demonstrated for fast T2 mapping. Our study showed that MANTIS-GAN represents a promising approach for efficient and accurate MR parameter mapping.

0678



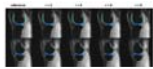
#### Joint Parallel Imaging reconstruction with Deep Learning for Multi-Contrast Synthetic MRI

Jae-Hun Lee<sup>1</sup>, Kanghyun Ryu<sup>1</sup>, Sung-Min Gho<sup>2</sup>, Ho-Sung Kim<sup>3</sup>, Mohammed A. Al-masni<sup>1</sup>, and Dong-Hyun Kim<sup>1</sup>

<sup>1</sup>Department of Electrical & Electronic Engineering, Yonsei Univ., Seoul, Korea, Republic of, <sup>2</sup>MR Collaboration and Development, GE Healthcare, Seoul, Korea, Republic of, <sup>3</sup>Department of Radiology, Asan medical center, Seoul, Korea, Republic of

Synthetic MRI or magnetic resonance imaging compilation (MAGiC) uses multiple-dynamic multiple-echo acquisition (MDME) and acquires 8 contrast images in a single scan. SENSE or GRAPPA method is conventionally used to reconstruct undersampled acquisition for respective contrast images. However, the method enables limited acceleration up to 2~3. In this study, combined reconstruction method (Joint Parallel Imaging with Deep Learning) is explored. The proposed method shows acceptable image quality with RMSE (4.6%) at the higher acceleration factor (up to 8) comparable to conventional GRAPPA with acceleration rate of 2~3.

0679



#### Joint 3D parameter mapping and motion correction using a kernel low rank method with offline training

Chaoyi Zhang<sup>1</sup>, JeeHun Kim<sup>2</sup>, Hongyu Li<sup>1</sup>, Peizhou Huang<sup>3</sup>, Ruiying Liu<sup>1</sup>, Dong Liang<sup>4</sup>, Xiaoliang Zhang<sup>3</sup>, Xiaojuan Li<sup>2</sup>, and Leslie Ying<sup>1,3</sup>

<sup>1</sup>Electrical Engineering, University at Buffalo, SUNY, Buffalo, NY, United States, <sup>2</sup>Biomedical Engineering, Program of Advanced Musculoskeletal Imaging (PAMI), Cleveland Clinic, OH, United States, <sup>3</sup>Biomedical Engineering, University at Buffalo, SUNY, Buffalo, NY, United States, <sup>4</sup>Paul C Lauterbur Research Center for Biomedical Imaging, Shenzhen institutes of Advanced Technology, Shenzhen, China

Magnetic resonance parameter mapping (e.g. T1, T2, T2\* and T1ρ) has shown potential in quantitative assessment while the clinical applications are limited by long acquisition time especially in 3D acquisition. In our previous work, we use single-exponential model to generate off-line single-exponential training data instead of low resolution training data, which reduced the reconstruction time. In clinical use, when motion is introduced in acquisition, single-exponential model is not satisfied and the reconstruction may fail. With this motivation, this abstract alternatively reconstruct the images and correct motion in 3D parameter mapping.

0680



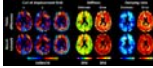
#### Construction of water-fat separation deep learning model combined with multi-echo nature of gradient-recalled echo sequence

Kewen Liu<sup>1</sup>, Xiaojun Li<sup>1</sup>, Qinjia Bao<sup>2</sup>, Chaoyang Liu<sup>3</sup>, Hongxia Xiong<sup>4</sup>, Zhao Li<sup>3</sup>, Yuan Ma<sup>1</sup>, Panpan Fang<sup>1</sup>, and Yalei Chen<sup>1</sup>

<sup>1</sup>School of Information Engineering, Wuhan University of Technology, Wuhan, China, <sup>2</sup>United Imaging of Scientific Instruments, Shanghai, China, <sup>3</sup>State Key Laboratory of Magnetic Resonance and Atomic and Molecular Physics, Wuhan Institute of Physics and Mathematics, Innovation Academy for Precision Measurement Science and Technology, Wuhan, China, <sup>4</sup>School of Civil Engineering & Architecture, Wuhan University of Technology, Wuhan, China

We proposed a novel deep learning network architecture (MEBC-RCAN) for water-fat separation based on multi-echo GRE sequence. The network architecture contains three main components: the first part is Multi-Echo Bidirectional Convolutional (MEBC) to explore the correlations of successive images in multi-echo GRE; the second part is Residual Channel Attention (RCA) network to mimic the iterative optimization in traditional water-fat separation method; and the third part is Multi-Layer Feature Fusion (MLFF) to combine separation information learned from every RCA network. The results show that the proposed network could effectively obtain the high-quality water and fat images from clinical multi-echo GRE data.

0681

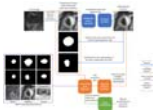


Artificial neural networks for numerical differentiation with application to magnetic resonance elastography  
Matthew C Murphy<sup>1</sup>, Joshua D Trzasko<sup>1</sup>, Jonathan M Scott<sup>1</sup>, Armando Manduca<sup>1</sup>, John Huston, III<sup>1</sup>, and Richard L Ehman<sup>1</sup>

<sup>1</sup>Mayo Clinic, Rochester, MN, United States

An artificial neural network (ANN) was trained to estimate the partial derivatives of a spatially varying field, and compared against a finite difference approach. For the application of elastography, training data were generated using a wave equation. After the training examples were corrupted by noise and missing data, the network was trained to estimate the analytical solution to the partial derivatives. In simulation, the ANN improved accuracy in noisy data but blurred sharp boundaries relative to a finite difference method. In vivo, using the ANN to compute the curl of the displacement field improved confidence in subsequent property estimates.

0682



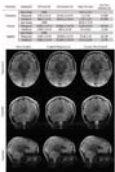
Visualizing and utilizing latent features of MR vessel wall images using weakly supervised deep learning analysis workflow

Li Chen<sup>1</sup>, Wenjin Liu<sup>1</sup>, Gador Canton<sup>1</sup>, Niranjana Balu<sup>1</sup>, Thomas Hatsukami<sup>1</sup>, John C. Waterton<sup>2</sup>, Jenq-Neng Hwang<sup>1</sup>, and Chun Yuan<sup>1</sup>

<sup>1</sup>University of Washington, Seattle, WA, United States, <sup>2</sup>Centre for Imaging Sciences, Manchester Academic Health Science Centre, The University of Manchester, Manchester, United Kingdom

Atherosclerotic plaque information can be extracted from MR vessel wall images through transforming the images into a high dimensional feature space. However, a huge amount of human supervision has traditionally been required to achieve a meaningful feature space representation. We demonstrated that by using a weakly supervised deep learning workflow including transfer learning, active learning, and metric learning, a meaningful feature space for vessel wall analysis can be generated, which can help us to visualize the high dimensional representations of normal and diseased vessel walls images, and lead to a plaque classification area under the curve of 0.93.

0683



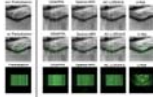
Investigating the robustness of convolutional neural network based B1+ prediction from localizer scans for SAR efficient 7T FLAIR imaging

Shahrokh Abbasi-Rad<sup>1</sup>, Kieran O'Brien<sup>1,2,3</sup>, Samuel Kelly<sup>1</sup>, Viktor Vegh<sup>1,3</sup>, Anders Rodell<sup>2</sup>, Yasvir Tesiram<sup>1</sup>, Jin Jin<sup>2,3,4,5</sup>, Markus Barth<sup>1,3,4</sup>, and Steffen Bollmann<sup>1,3</sup>

<sup>1</sup>Centre for Advanced Imaging, University of Queensland, Brisbane, Australia, <sup>2</sup>Siemens Healthcare Pty Ltd, Brisbane, Australia, <sup>3</sup>ARC Centre for Innovation in Biomedical Imaging Technology, University of Queensland, Brisbane, Australia, <sup>4</sup>School of Information Technology and Electrical Engineering, University of Queensland, Brisbane, Australia, <sup>5</sup>Mark and Mary Stevens Neuroimaging and Informatics Institute, University of Southern California, Los Angeles, CA, United States

In 7T MRI adiabatic pulses enable robust inversion of spins at the cost of increased SAR and longer scan times. A convolutional neural network was used to estimate the  $B_1^+$  profile from a localizer scan, Bloch equation simulations were used to calculate the required  $B_1^+$  for adiabaticity, and adiabatic pulse power was scaled accordingly reducing SAR by up to 38%. We investigated the robustness and efficiency of this approach and showed a substantial SAR reduction is possible without an additional B1 map acquisition. This resulted in an up to 27% faster T2-FLAIR acquisition with full brain coverage.

0684



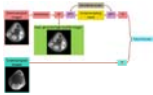
Local Perturbation Responses: A tool for understanding the characteristics of advanced nonlinear MR reconstruction algorithms

Chin-Cheng Chan<sup>1</sup> and Justin P. Haldar<sup>1</sup>

<sup>1</sup>Electrical and Computer Engineering, University of Southern California, Los Angeles, CA, United States

As MR image reconstruction algorithms become increasingly nonlinear, data-driven, and difficult to understand intuitively, it becomes more important that tools are available to assess the confidence that users should have about image reconstruction results. In this work, we suggest that a quantity known as the “local perturbation response” (LPR) provides useful information that can be used for this purpose. The LPR is analogous to a conventional point-spread function, but is well-suited to general image reconstruction methods that may have nonlinear and/or shift-varying characteristics. We illustrate the LPR in the context of several common image reconstruction techniques.

0685



Unsupervised Image Reconstruction using Deep Generative Adversarial Networks

Elizabeth Cole<sup>1</sup>, Frank Ong<sup>1</sup>, John Pauly<sup>1</sup>, and Shreyas Vasanaawala<sup>2</sup>

<sup>1</sup>Electrical Engineering, Stanford University, Stanford, CA, United States, <sup>2</sup>Radiology, Stanford University, Stanford, CA, United States

Many deep learning-based reconstruction methods require fully-sampled ground truth data for supervised training. However, instances exist where acquiring fully sampled data is either difficult or impossible, such as in dynamic contrast enhancement (DCE), 3D cardiac cine, 4D flow, etc. for training a reconstruction network. We present a deep learning framework for reconstructing MRI without using any fully sampled data. We test the method in two scenarios, and find the method produces higher quality images which reveal vessels and recover more anatomical structure. This method has potential in applications, such as DCE, cardiac cine, low contrast agent imaging, and real-time imaging.

0686



Highly Accelerated MPRAGE Imaging of the Brain Incorporating Deep Learning Priors with Subject-Specific Novel Features

Yue Guan<sup>1</sup>, Yudu Li<sup>2,3</sup>, Ziyu Meng<sup>3,4</sup>, Tianyao Wang<sup>5</sup>, Rong Guo<sup>2,3</sup>, Ruihao Liu<sup>4</sup>, Yao Li<sup>4</sup>, Yiping Du<sup>4</sup>, and Zhi-Pei Liang<sup>2,3</sup>

<sup>1</sup>Institute for Medical Imaging Technology, School of Biomedical Engineering, Shanghai Jiao Tong University, Shanghai, China, <sup>2</sup>Department of Electrical and Computer Engineering, University of Illinois at Urbana-Champaign, Urbana, IL, United States, <sup>3</sup>Beckman Institute for Advanced Science and Technology, University of Illinois at Urbana-Champaign, Urbana, IL, United States, <sup>4</sup>Shanghai Jiao Tong University, Shanghai, China, <sup>5</sup>Department of Radiology, The Fifth People's Hospital of Shanghai, Shanghai, China



MPRAGE imaging has been widely used in clinical applications and various attempts have been made for its acceleration. This paper presents a new method to accelerate MPRAGE imaging using sparse and random sampling of k-space and constrained reconstruction incorporating image priors and subject-specific novel features. In our current implementation, the MPRAGE image priors were obtained using deep learning on data from the Human Connectome Project, and novel localized features were recovered by solving a sparsity-constrained reconstruction. In vivo experimental results demonstrated that the proposed method can produce high-quality whole-brain MPRAGE images in 0.7x0.7x0.7 mm<sup>3</sup> nominal resolution from a 1.5-min scan.

---

---

## Oral

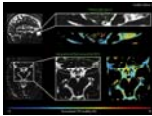
### CSF flow & Glymphatic Imaging - Glymphatic System & CSF Flow

Tuesday Parallel 2 Live Q&A

Tuesday 15:15 - 16:00 UTC

Moderators: Nivedita Agarwal & Olivier Baledent

0643



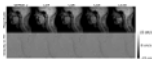
The driving force of glymphatics: influence of the cardiac cycle on CSF-mobility in perivascular spaces in humans

Lydiane Hirschler<sup>1</sup>, Bobby A Runderkamp<sup>2</sup>, Suzanne L Franklin<sup>1,3</sup>, Thijs van Harten<sup>1</sup>, Aart Nederveen<sup>2</sup>, Matthan WA Caan<sup>4</sup>, and Matthias JP van Osch<sup>1</sup>

<sup>1</sup>Leiden University Medical Center, Leiden, Netherlands, <sup>2</sup>Radiology and Nuclear Medicine, Amsterdam UMC, University of Amsterdam, Amsterdam, Netherlands, <sup>3</sup>University Medical Centre Utrecht, Utrecht, Netherlands, <sup>4</sup>Department of Biomedical Engineering & Physics, Amsterdam University Medical Center, Amsterdam, Netherlands

Recently, flow of cerebrospinal fluid (CSF) has been shown to play an important role in the waste clearance of the brain, ushering in the concepts of glymphatics and intramural periarterial drainage. Despite the importance of brain waste removal, the exact clearance mechanisms such as its driving force are still poorly understood and remain highly controversial. In this study, we image how the cardiac cycle influences the CSF-mobility in the human brain, in the perivascular spaces of the basal ganglia as well as in large CSF-filled spaces, i.e. ventricles and subarachnoid space around large arteries.

0644



Compressed sensing accelerated 4D flow magnetic resonance imaging of the cerebrospinal fluid.

Kristina Sonnabend<sup>1</sup>, Elena Jäger<sup>1</sup>, David Maintz<sup>1</sup>, Kilian Weiss<sup>1,2</sup>, and Alexander Bunck<sup>1</sup>

<sup>1</sup>University of Cologne, Faculty of Medicine and University Hospital Cologne, Institute for Diagnostic and Interventional Radiology, Cologne, Germany, <sup>2</sup>Philips GmbH, Hamburg, Germany

Cerebrospinal fluid (CSF) flow dynamics are relevant parameters in the diagnosis of neurological diseases and can be accessed by three-dimensional time-resolved phase-contrast MRI (4D flow MRI). However, these measurements are accompanied by long scan times making acquisition acceleration necessary to accomplish clinical feasibility. The aim of this study was to evaluate the feasibility of compressed sensing (CS) acceleration in 4D flow MRI of the CSF. CS factors 4 to 10 were compared against the conventional SENSE in 16 healthy subjects. Preliminary results show feasibility of CS factor 6 with comparable image and velocity data quality.

0645



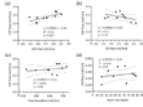
Cyclic Intracerebral Coherent Motion on Peripheral-Pulse-Gated Ultra-Low VENC MRI: Noninvasive Depiction of Glymphatic Flow?

Robert Y Shih<sup>1,2</sup>, J Kevin DeMarco<sup>1,2</sup>, J Kent Werner<sup>1,2</sup>, Justin E Costello<sup>1,2</sup>, Isabelle Heukensfeldt Jansen<sup>3</sup>, Luca Marinelli<sup>3</sup>, Thomas K Foo<sup>3</sup>, and Vincent B Ho<sup>1,2</sup>

<sup>1</sup>Uniformed Services University of the Health Sciences, Bethesda, MD, United States, <sup>2</sup>Walter Reed National Military Medical Center, Bethesda, MD, United States, <sup>3</sup>GE Global Research, Niskayuna, NY, United States

A combination of pressure gradients from arterial pulsatility, respiratory cycles, and resistance changes is thought to drive convective influx of CSF into paraarterial spaces for rapid exchange with ISF, followed by efflux into paravenous spaces toward arachnoid granulations, meningeal lymphatics, or cranial nerves. Visualization of this phenomenon was attempted with peripheral-pulse-gated phase contrast sequences at VENC = 5 mm/s (gradient echo) and 0.24 mm/s (spin echo) in four healthy adults using an ultra-high-performance MAGNUS gradient coil. Very slow intracerebral coherent motion was depicted, cerebropetal during systole, cerebrofugal during diastole, possibly reflecting bulk flow in paravascular spaces of the lymphatic system.

0646



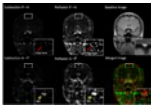
Blood flow in the internal carotid arteries is correlated with CSF outflow from the ventricular system

Karin Markenroth Bloch<sup>1</sup>, Tekla M. Kylkilahti<sup>2,3</sup>, Olle Haglund<sup>1</sup>, Linn C. Lingehall<sup>2,3</sup>, Nils Fregne<sup>2,3</sup>, Johannes Töger<sup>4</sup>, and Iben Lundgaard<sup>2,3</sup>

<sup>1</sup>National 7T facility, LBIC, Lund University, Lund, Sweden, <sup>2</sup>Department of Experimental Medical Science, Lund University, Lund, Sweden, <sup>3</sup>Wallenberg Centre for Molecular Medicine, Lund University, Lund, Sweden, <sup>4</sup>Department of Clinical Sciences, Lund University, Lund, Sweden

Little is known about which physiological parameters regulate CSF production. In this work, we tested the hypothesis that cerebral blood flow and heart rate play roles in CSF regulation. We used 7T MR to quantify CSF flow in the cerebral aqueduct and blood flow in the carotid arteries of healthy volunteers. We found that CSF outflow from the ventricular system correlated with blood flow in the internal carotid arteries, whereas there was no significant effect of heart rate on CSF outflow. This suggests that cerebral blood flow affects CSF flow and production.

0647



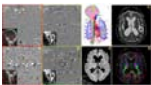
Human meningeal lymphatic vessels can be imaged by inversion recovery alternate ascending/descending directional navigation (ALADDIN)

Jun-Hee Kim<sup>1</sup> and Sung-Hong Park<sup>1</sup>

<sup>1</sup>Department of Bio and Brain engineering, Korea Advanced Institute of Science and Technology, Daejeon, Korea, Republic of

Recent studies showed meningeal lymphatic vessels significantly contribute to the clearance mechanisms of cerebrospinal fluid (CSF) and the immune system in central nervous system. In this study, we tried to image human dural meningeal lymphatic vessels (mLVs) using inversion recovery alternate ascending/descending directional navigation (IR-ALADDIN). The IR-ALADDIN imaging technique clearly showed not only structural dural mLVs, but also the flow direction of dural mLVs, and it can be applied for studying many lymphatic vessels in human neurological diseases.

0648



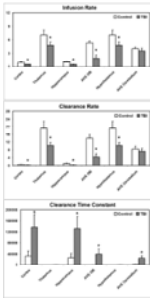
Impact of cerebrospinal and blood flow pulsilities on periventricular white matter in patients with hydrocephalus

Fadoua Saadani-Makki<sup>1,2,3</sup>, Malek Makki<sup>3</sup>, Serge Metanbou<sup>4</sup>, Cyrille Capel<sup>5</sup>, and Olivier Balédent<sup>1,2</sup>

<sup>1</sup>Department of Image Processing, University Hospital, Amiens, France, <sup>2</sup>CHIMERE EA 7516, Research Team for Head & Neck, University of Picardie Jules Verne, Amiens, France, <sup>3</sup>GIE Faire Face, CHU Amiens Picardie, Amiens, France, <sup>4</sup>Department of Radiology, University Hospital, Amiens, France, <sup>5</sup>Department of Neurosurgery, University Hospital, Amiens, France

The aim of this study was to assess the relationship between neuro-fluids dynamic and microstructure architecture of white matter fibers in hydrocephalus patients. Twenty-eight hydrocephalus patients underwent simultaneously diffusion tensor and phase contrast imaging. A statistical correlation between diffusion and flow parameters has shown a biological causal relationship between abnormal brain neuro-fluids dynamic and white matter alterations in hydrocephalus patients.

0649



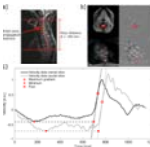
### MRI Detection of Impairment of Glymphatic Function in Rat after Mild Traumatic Brain Injury

Lian Li<sup>1</sup>, Michael Chopp<sup>1,2</sup>, Guangliang Ding<sup>1</sup>, Esmail Davoodi-Bojd<sup>1</sup>, Qingjiang Li<sup>1</sup>, Yanlu Zhang<sup>1</sup>, Ye Xiong<sup>1</sup>, and Quan Jiang<sup>1</sup>

<sup>1</sup>Henry Ford Hospital, Detroit, MI, United States, <sup>2</sup>Oakland University, Rochester, MI, United States

Using dynamic MRI glymphatic measurement and our advanced mathematic model, the alterations of glymphatic function in the brain with mild TBI were investigated. Our data show that mild TBI leads to both impaired influx and efflux of contrast agent along the glymphatic pathway. The reduced efficiency of glymphatic function affects the multiple regions across the brain, which may decrease the clearance of waste metabolites and facilitate protein aggregation, contributing to subsequent cognitive deficits. The global change in brain clearance function, rather than the appearance of focal lesions, appears to provide a reliable measure indicating the injury of the brain.

0650



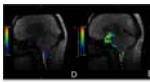
### Cerebrospinal fluid pulse wave velocity measurements using multiband CINE phase-contrast MRI

Kristina Sonnabend<sup>1</sup>, Gerrit Brinker<sup>2</sup>, David Maintz<sup>1</sup>, Alexander Bunck<sup>1</sup>, and Kilian Weiss<sup>1,3</sup>

<sup>1</sup>University of Cologne, Faculty of Medicine and University Hospital Cologne, Institute for Diagnostic and Interventional Radiology, Cologne, Germany, <sup>2</sup>University of Cologne, Faculty of Medicine and University Hospital Cologne, Department of General Neurosurgery, Center for Neurosurgery, Cologne, Germany, <sup>3</sup>Philips GmbH, Hamburg, Germany

Intraspinal compliance is related to neurological diseases and can be measured by pulse wave velocity (PWV). A multiband CINE phase-contrast MRI sequence was developed to measure the intraspinal PWV between two simultaneously acquired slices along spine. The method was evaluated in-vitro, in healthy-subjects and in a normal pressure hydrocephalus patient. In-vitro results show good reproducibility and dependency on transmural pressure in agreement with theory. A higher PWV compared to healthy subjects is observed in the patient. A decline in PWV after shunt surgery is detected, making it a promising tool for investigation and treatment follow-up of neurological diseases.

0651



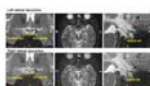
### Evaluation of Cerebrospinal Fluid Dynamics in endoscopic third ventriculostomy for treating obstructive hydrocephalus with 4D Flow MRI

Liu Jia<sup>1</sup>, Cheng Xiaoqing<sup>1</sup>, Lu Guang ming<sup>1</sup>, Dou Weiqiang<sup>2</sup>, and Shen Yong<sup>2</sup>

<sup>1</sup>Department of Medical Imaging, Jinling Hospital, Medical School of Nanjing University, Nanjing, China, <sup>2</sup>GE Healthcare, MR Research, Beijing, P.R. China, Nanjing, China

We aim to investigate the clinical value of 4D flow MRI in assessing cerebrospinal fluid (CSF) dynamics. The optimal velocity encoding factor (VENC) and high test-retest reproducibility was firstly obtained in CSF measurements for healthy volunteers. Ensured by these, 4D flow MRI has been further applied to evaluate the CSF dynamics for patients with obstructive hydrocephalus before and after endoscopic third ventriculostomy (ETV). Notable cerebrospinal fluid flow at the stoma has been found, indicating that a new cerebrospinal fluid circulation pathway was established. Our study thus demonstrated that 4D flow MRI is an effective tool to assess CSF dynamics quantitatively.

0652



### Analysis of Physiological Brain Shift and Optic Chiasm in the Closed Cranium due to Postural Position

Etsuko Kumamoto<sup>1</sup>, Shigeto Hayashi<sup>1,2</sup>, Ari Shinjima<sup>3</sup>, Koshi Yokota<sup>4</sup>, and Eiji Kohmura<sup>5</sup>

<sup>1</sup>Kobe University, Kobe, Japan, <sup>2</sup>Department of Neurosurgery, Hyogo Emergency Medical Center, Kobe, Japan, <sup>3</sup>Keio University, Tokyo, Japan, <sup>4</sup>Japan Aerospace Exploration Agency, Tsukuba, Japan, <sup>5</sup>school of medicine, Kobe University, Kobe, Japan

Methodological analysis related to physiological brain shift in the closed cranium is lacking. The spaceflight-associated neuro-ocular syndrome is attributed to the upward shift of the brain. We analyzed the relationship of brain shift and optic nerve shift by using MR volume data acquired in different body positions. The movement and rotation of each voxel, divided into  $20 \times 20 \times 20$  pixels<sup>3</sup>, were calculated using the block matching method. Experimental results show that the optic nerve transforms and deforms with the movement of the brain because of a change in body position.

---

## Combined Educational & Scientific Session

### Hyperpolarized MR - Hyperpolarized <sup>13</sup>C Metabolic Imaging for Clinical Research

Organizers: Yi-Fen Yen, Christoffer Laustsen, Malgorzata Marjanska

Tuesday Parallel 5 Live Q&A

Tuesday 15:15 - 16:00 UTC

Moderators: Jeremy Gordon & Jack Miller

#### From Mouse to Man: The Value & Future Outlook

Kayvan R. Keshari<sup>1</sup>

<sup>1</sup>Memorial Sloan-Kettering Cancer Center, New York, NY, United States

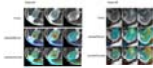
---

#### Hyperpolarized <sup>13</sup>C Imaging in 2030: A Clinician's View

Ferdia Gallagher<sup>1</sup>

<sup>1</sup>University of Cambridge, United Kingdom

0687



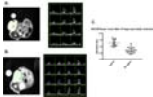
#### Initial Experience of Hyperpolarized <sup>13</sup>C Pyruvate MRI in Patients with Renal Tumors

Shuyu Tang<sup>1</sup>, Peder E.Z. Larson<sup>1</sup>, Maxwell Meng<sup>1</sup>, James Slater<sup>1</sup>, Jeremy Gordon<sup>1</sup>, Daniel B. Vigneron<sup>1</sup>, and Zhen J. Wang<sup>1</sup>

<sup>1</sup>University of California, San Francisco, San Francisco, CA, United States

We present our initial experience of applying HP <sup>13</sup>C pyruvate MRI in patients with renal tumors. Distinct tumor metabolic pattern and heterogeneity can be observed on HP <sup>13</sup>C pyruvate MRI. Our data from subjects with two injections also suggests that the metabolite measurements are reproducible. This initial experience paves the way for this metabolic imaging technique to be applied for differentiating between benign renal tumors, low grade RCCs and high grade RCCs.

0688



#### Hyperpolarized [1-<sup>13</sup>C] dehydroascorbic acid imaging of ascorbate-mediated oxidative stress in pancreatic cancer

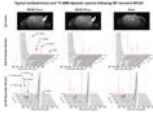
Nathaniel Kim<sup>1</sup>, Arsen Mamakhanyan<sup>1</sup>, Kristin Granlund<sup>1</sup>, Elisa de Stanchina<sup>2</sup>, Manish Shah<sup>3</sup>, Lewis Cantley<sup>3,4</sup>, and Kayvan A. Keshari<sup>1,3</sup>

<sup>1</sup>Department of Radiology, Memorial Sloan Kettering Cancer Center, New York, NY, United States,

<sup>2</sup>Antitumor Assessment Core Facility, Memorial Sloan Kettering Cancer Center, New York, NY, United States,

<sup>3</sup>Weill Cornell Medical College, New York, NY, United States, <sup>4</sup>Meyer Cancer Center, Weill Cornell Medical College, New York, NY, United States

We investigated hyperpolarized [1-<sup>13</sup>C] dehydroascorbic acid (HP DHA) as an imaging agent for probing oxidative stress in patient derived xenograft models (PDXs) of pancreatic cancer. By increasing the T<sub>1</sub> via D<sub>2</sub>O solvation and increasing the dose administered via awake mouse injection, conversion of DHA to ascorbate was readily observed in *BRAF* and *KRAS* mutant cancers. HP DHA was then used to characterize oxidative stress in these PDX models and their biochemical mechanism of response to ascorbate therapy. Changes in DHA/ascorbate metabolism were measured in these tumor models, demonstrating a proof of concept method for assessing ascorbate therapy in pancreatic cancer.

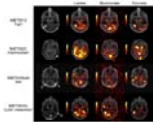


### Metabolism of the hyperpolarized neuroprotective agents [1-<sup>13</sup>C] lactate and [1-<sup>13</sup>C] pyruvate in a mouse model of transient ischemic stroke

Thanh Phong Lê<sup>1,2</sup>, Lara Buscemi<sup>3</sup>, Elise Vinckenbosch<sup>1</sup>, Mario Lepore<sup>4</sup>, Lorenz Hirt<sup>3</sup>, Jean-Noël Hyacinthe<sup>1,5</sup>, and Mor Mishkovsky<sup>2</sup>

<sup>1</sup>Geneva School of Health Sciences, HES-SO University of Applied Sciences and Arts Western Switzerland, Geneva, Switzerland, <sup>2</sup>Laboratory of Functional and Metabolic Imaging, École polytechnique fédérale de Lausanne (EPFL), Lausanne, Switzerland, <sup>3</sup>Department of Clinical Neurosciences, Lausanne University Hospital (CHUV), Lausanne, Switzerland, <sup>4</sup>Center for Biomedical Imaging - Animal Imaging and Technology (CIBM-AIT), École polytechnique fédérale de Lausanne (EPFL), Lausanne, Switzerland, <sup>5</sup>Image Guided Intervention Laboratory, University of Geneva (UNIGE), Geneva, Switzerland

Stroke is a major cause of death and disability. Neuroprotective strategies could ameliorate patient recovery. Pyruvate and lactate were found neuroprotectant in preclinical studies of stroke models. Hyperpolarized <sup>13</sup>C MRI provides a new way for real-time molecular imaging. In this work, we hyperpolarize those neuroprotective agents to study changes of their metabolism when administered at their therapeutic dose after ischemic stroke. We found that the metabolism of hyperpolarized lactate is significantly altered after transient cerebral ischemia, whereas moderate changes were depicted with hyperpolarized pyruvate. Those imply that hyperpolarized lactate would potentially be a better theranostic biosensor for stroke.

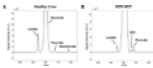


### Assessment of Intracranial Metastases in Patients using Hyperpolarized <sup>13</sup>C MRI

Casey Y Lee<sup>1,2</sup>, Hany Soliman<sup>3</sup>, Benjamin J Geraghty<sup>1,2</sup>, Nadia D Bragagnolo<sup>1,2</sup>, Albert P Chen<sup>4</sup>, William J Perks<sup>5</sup>, Arjun Sahgal<sup>3</sup>, Michael W Chan<sup>6</sup>, Sean Symons<sup>7</sup>, and Charles H Cunningham<sup>1,2</sup>

<sup>1</sup>Medical Biophysics, University of Toronto, Toronto, ON, Canada, <sup>2</sup>Physical Sciences, Sunnybrook Research Institute, Toronto, ON, Canada, <sup>3</sup>Radiation Oncology, Sunnybrook Health Sciences Centre, Toronto, ON, Canada, <sup>4</sup>GE Healthcare Technologies, Toronto, ON, Canada, <sup>5</sup>Pharmacy, Sunnybrook Health Sciences Centre, Toronto, ON, Canada, <sup>6</sup>Diagnostic Imaging, Trillium Health Partners, Mississauga, ON, Canada, <sup>7</sup>Radiology, Sunnybrook Health Sciences Centre, Toronto, ON, Canada

Hyperpolarized <sup>13</sup>C MRI was used to acquire images of [1-<sup>13</sup>C]lactate and <sup>13</sup>C-bicarbonate from the injected [1-<sup>13</sup>C]pyruvate in 8 patients with brain metastases. Lesions were manually contoured and the mean tumor <sup>13</sup>C-lactate signal was converted to a z-score by extending the approach previously described in Lee *et al.* (2019). As expected, the z-score ranks of the anatomical regions were less concordant in patients compared to controls. A range of lactate z-scores were observed in metastatic lesions, showing metabolic heterogeneity consistent with the known heterogeneity in metastatic features and clinical status. The lesions with the highest and 5<sup>th</sup> highest lactate z-scores progressed.



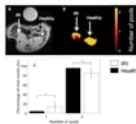
### Hyperpolarized [1-<sup>13</sup>C] Glycerate as Probe to Assess Glycolytic Activity in a Rat Model of Hepatocellular Carcinoma

Jun Chen<sup>1</sup>, Evan LaGue<sup>2</sup>, Junjie Li<sup>1</sup>, Edward Hackett<sup>1</sup>, Ian Corbin<sup>1</sup>, Kelvin Billingsley<sup>2</sup>, and Jae Mo Park<sup>3,4</sup>

<sup>1</sup>AIRC, UT Southwestern Medical Center at Dallas, Dallas, TX, United States, <sup>2</sup>Chemistry and Biochemistry, California State University Fullerton, Fullerton, CA, United States, <sup>3</sup>UT Southwestern Medical Center at Dallas, Dallas, TX, United States, <sup>4</sup>Electrical Engineering, University of Texas at Dallas, Richardson, TX, United States

Hyperpolarized [1-<sup>13</sup>C] glycerate was used to study the *in vivo* glycolytic activity in a rat model of hepatocellular carcinoma (HCC). Carbon-13 labeled glycolytic intermediate phosphoenolpyruvate (PEP) was detected in the tumor in addition to pyruvate and lactate peaks. The *in vivo* results were confirmed by high resolution <sup>13</sup>C NMR spectra of tissue extracts, after steady-state infusion of [2,3-<sup>13</sup>C<sub>2</sub>] glycerate. The results illustrate the potential of [1-<sup>13</sup>C] glycerate as a metabolic probe for assessing glycolytic flux.

0692



Hyperpolarized  $^{13}\text{C}$  Urea Laplacian relaxation processing reveals differences between healthy and ischemic renal  $T_2$  relaxation.

James Timothy Grist<sup>1</sup>, Christian Mariager<sup>2</sup>, and Christoffer Laustsen<sup>2</sup>

<sup>1</sup>University of Birmingham, Birmingham, United Kingdom, <sup>2</sup>Aarhus University, Aarhus, Denmark

Hyperpolarized  $^{13}\text{C}$  urea  $T_2$  relaxometry has been previously used to assess the diabetic and ischemic kidney. In this study we utilise a novel fitting method (Laplacian) to visualise the extent of damage, through a reduction in bi-exponential relaxation behaviour, in a rodent model of renal ischemia.

This opens up a number of potential pre-clinical and clinical uses of hyperpolarized  $^{13}\text{C}$  urea imaging providing a novel, and useful, readout of renal ischemia.

## Oral

### Hyperpolarized MR - New Frontiers in Hyperpolarization

Tuesday Parallel 5 Live Q&A

Tuesday 15:15 - 16:00 UTC

Moderators: Jessica Bastiaansen & Franz Schilling

0693



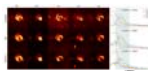
Transportable hyperpolarized glucose samples: towards remote dissolution DNP

Andrea Capozzi<sup>1,2</sup>, Jan Kilund<sup>1</sup>, Magnus Karlsson<sup>1</sup>, Mathilde Hauge Lerche<sup>1</sup>, and Jan Henrik Ardenkjaer-Larsen<sup>1</sup>

<sup>1</sup>Health Technology, Danish Technical University, Kongens Lyngby, Denmark, <sup>2</sup>IPHYS, EPFL, Lausanne, Switzerland

Our vision is to enable **delivery of hyperpolarized compounds to MR-facilities that currently have no access to hyperpolarization technology**. Today this is not the case and represents a main shortcoming of hyperpolarized-MR via dissolution Dynamic Nuclear Polarization (dDNP). The cause is the presence, in the dDNP sample, of **organic free radicals** necessary to generate the hyperpolarization. We herein present a paradigm shift in the technique built on the employment of **photo-induced thermally-labile free radicals**. We demonstrate quenching of the paramagnetic species while preserving most of the polarization in the case of **hyperpolarized glucose**.

0694



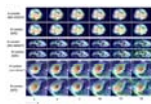
Accelerating cardiac hyperpolarized  $^{13}\text{C}$  imaging using variational networks for reconstruction

Andreas Dounas<sup>1</sup>, Valery Vishnevskiy<sup>1</sup>, Maximilian Fuetterer<sup>1</sup>, Julia Traechtler<sup>1</sup>, and Sebastian Kozerke<sup>1</sup>

<sup>1</sup>Institute for Biomedical Engineering, University and ETH Zurich, Zurich, Switzerland

A variational network (VN) was implemented and trained on synthetic data to reconstruct multi-echo hyperpolarized  $^{13}\text{C}$  data acquired in the in vivo heart. VN reconstruction performance was studied using 2D and 3D synthetic data under low SNR conditions and for acceleration factors of 3 and 9, respectively. Relative to standard gradient descent based reconstruction, the network offers improved reconstruction accuracy and reduced signal leakage between metabolites while preserving information on lactate-to-bicarbonate ratios.

0695



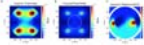
A Metabolite Specific 3D Stack-of-Spiral bSSFP Sequence for Improved Lactate Imaging in Hyperpolarized  $[1-^{13}\text{C}]$ Pyruvate Studies on a 3T Scanner

Shuyu Tang<sup>1</sup>, Robert Bok<sup>1</sup>, Hecong Qin<sup>1</sup>, Galen Reed<sup>2</sup>, Mark VanCrickinge<sup>1</sup>, Romelyn Delos Santos<sup>1</sup>, William Overall<sup>2</sup>, Juan Santos<sup>2</sup>, Jeremy Gordon<sup>1</sup>, Zhen J. Wang<sup>1</sup>, Daniel Vigneron<sup>1</sup>, and Peder E.Z. Larson<sup>1</sup>

<sup>1</sup>University of California, San Francisco, San Francisco, CA, United States, <sup>2</sup>HeartVista, Los Altos, CA, United States

This work describes a novel 3D bSSFP sequence that integrates a lactate specific excitation pulse and stack-of-spiral readouts for improved lactate dynamic imaging in hyperpolarized [1-<sup>13</sup>C]pyruvate studies on a clinical 3T scanner. Compared with metabolite specific GRE sequences, the MS-3DSSFP sequence showed an overall 2.5X SNR improvement for lactate imaging in rat kidneys, tumors of TRAMP mice and human kidneys.

0696



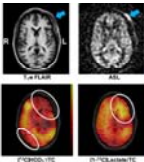
Providing a clinical pipeline for using the sodium-23 resonance to calibrate for in vivo hyperpolarized carbon-13 experiments.

James Timothy Grist<sup>1,2</sup>, Esben S Hansen<sup>3</sup>, Juan D Sanchez<sup>4</sup>, Mary A McLean<sup>5</sup>, Frank Riemer<sup>6</sup>, Rolf F Schulte<sup>7</sup>, Jan Henrik Ardenkjaer-Larsen<sup>4</sup>, Christoffer Laustsen<sup>3</sup>, and Ferdia A Gallagher<sup>6</sup>

<sup>1</sup>University of Cambridge, Cambridge, United Kingdom, <sup>2</sup>University of Birmingham, Birmingham, United Kingdom, <sup>3</sup>Aarhus University, Aarhus, Denmark, <sup>4</sup>Technical University of Denmark, Copenhagen, Denmark, <sup>5</sup>Cancer Research UK, Cambridge Institute, University of Cambridge, Cambridge, United Kingdom, <sup>6</sup>University of Cambridge, Cambridge, United Kingdom, <sup>7</sup>GE Healthcare, Munich, Germany

Hyperpolarized <sup>13</sup>C MRI is an emerging clinical technique to probe metabolism. Calibration of transmit gain and centre frequency is challenging, due to the low endogenous <sup>13</sup>C signal. Pre-scan is typically performed by adding an external phantom for reference, however this is challenged by the shim volume inside the subject and the RF coil excitation and reception profiles. We demonstrate the ability to use the sodium-23 resonance to accurately prescan prior to <sup>13</sup>C experiments, using single tuned <sup>13</sup>C coils in a 3T MRI system. This provides an important workflow improvement for the adoption of hyperpolarized <sup>13</sup>C imaging into clinical practise.

0697



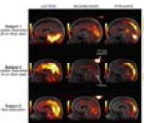
Imaging Acute Metabolic Changes in Mild Traumatic Brain Injury Patients using Hyperpolarized [1-<sup>13</sup>C] Pyruvate

Edward P Hackett<sup>1</sup>, Marco C Pinho<sup>2</sup>, Crystal E Harrison<sup>1</sup>, Galen D Reed<sup>3</sup>, Surendra Barshikar<sup>4</sup>, Christopher J Madden<sup>5</sup>, and Jae Mo Park<sup>1,2,6</sup>

<sup>1</sup>Advanced Imaging Research Center, University of Texas Southwestern Medical Center, Dallas, TX, United States, <sup>2</sup>Radiology, University of Texas Southwestern Medical Center, Dallas, TX, United States, <sup>3</sup>GE Healthcare, GE Healthcare, Dallas, TX, United States, <sup>4</sup>Physical Medicine and Rehabilitation, University of Texas Southwestern Medical Center, Dallas, TX, United States, <sup>5</sup>Neurosurgery, University of Texas Southwestern Medical Center, Dallas, TX, United States, <sup>6</sup>Electrical Engineering, University of Texas Dallas, Richardson, TX, United States

A major challenge of treating traumatic brain injury (TBI) patients is the simultaneously occurring complex secondary injury processes following the primary injury. The secondary events such as cerebral hyperglycolysis and mitochondrial failure develop over minutes to months after the primary injury. This case report details the first time hyperpolarized [1-<sup>13</sup>C]pyruvate imaging in TBI patients to examine regional metabolic changes in the brain post-traumatic injury. We observed an increased conservation of pyruvate to lactate at the injured sites as well as reduced bicarbonate production.

0698



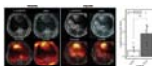
Is [1-<sup>13</sup>C]Lactate Converted to <sup>13</sup>C-Bicarbonate in the Human Brain?

Casey Y Lee<sup>1,2</sup>, Hany Soliman<sup>3</sup>, Nadia D Bragagnolo<sup>1,2</sup>, Albert P Chen<sup>4</sup>, William J Perks<sup>5</sup>, Chris Heyn<sup>6</sup>, Sandra E Black<sup>7</sup>, and Charles H Cunningham<sup>1,2</sup>

<sup>1</sup>Medical Biophysics, University of Toronto, Toronto, ON, Canada, <sup>2</sup>Physical Sciences, Sunnybrook Research Institute, Toronto, ON, Canada, <sup>3</sup>Radiation Oncology, Sunnybrook Health Sciences Centre, Toronto, ON, Canada, <sup>4</sup>GE Healthcare Technologies, Toronto, ON, Canada, <sup>5</sup>Pharmacy, Sunnybrook Health Sciences Centre, Toronto, ON, Canada, <sup>6</sup>Radiology, Sunnybrook Health Sciences Centre, Toronto, ON, Canada, <sup>7</sup>Department of Medicine (Neurology) and Hurvitz Brain Sciences Research Program, Sunnybrook Health Sciences Centre, Toronto, ON, Canada

Hyperpolarized [1-<sup>13</sup>C]lactate and <sup>13</sup>C-bicarbonate images were acquired with and without spectral-spatial lactate saturation in the brains of control participants. A previously published atlas-based analysis was used to convert [1-<sup>13</sup>C]lactate and <sup>13</sup>C-bicarbonate signals into z-scores to quantify the effect of [1-<sup>13</sup>C]lactate saturation. The analysis showed that lactate z-scores were changed in the saturation regions, as expected. The saturation of [1-<sup>13</sup>C]lactate signals did not significantly affect <sup>13</sup>C-bicarbonate signals.

0699



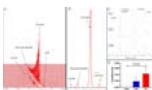
#### Metabolic Imaging of a Porcine Model of Acute Lung Injury Using Hyperpolarized [1-<sup>13</sup>C] Pyruvate MRI

Mehrdad Pourfathi<sup>1</sup>, Hooman Hamedani<sup>1,2</sup>, Yi Xin<sup>1,2</sup>, Michael Rosalino<sup>1</sup>, Stephen J Kadlecsek<sup>1</sup>, Ian Duncan<sup>1</sup>, Maurizio Cereda<sup>1,3</sup>, Sarmad Siddiqui<sup>1</sup>, Harrilla Profka<sup>1</sup>, Luis Loza<sup>1</sup>, Faraz Amzajerian<sup>1,2</sup>, Tahmina Achekzai<sup>1</sup>, Kai Ruppert<sup>1</sup>, Federico Sertic<sup>1,4</sup>, Ryan Baron<sup>1</sup>, Jon Snow<sup>1</sup>, Yiwen Qian<sup>1,2</sup>, Gabriel Unger<sup>1</sup>, Shampa Chatterjee<sup>5</sup>, and Rahim R. Rizzi<sup>1</sup>

<sup>1</sup>Radiology, University of Pennsylvania, Philadelphia, PA, United States, <sup>2</sup>Bioengineering, University of Pennsylvania, Philadelphia, PA, United States, <sup>3</sup>Anesthesiology and Critical Care, University of Pennsylvania, Philadelphia, PA, United States, <sup>4</sup>Surgery, University of Pennsylvania, Philadelphia, PA, United States, <sup>5</sup>Physiology, University of Pennsylvania, Philadelphia, PA, United States

Transpulmonary lactate gradient is strongly correlated with the severity of lung injury and inflammation in ARDS patients. Hyperpolarized [1-<sup>13</sup>C] pyruvate MRI allows us to quantitatively study altered pyruvate-to-lactate conversion in cancerous and inflamed tissues. We sought to demonstrate the translational potential of this technology for pulmonary metabolic imaging in humans. We performed [1-<sup>13</sup>C] pyruvate lung MRI in an experimental model of aspiration pneumonitis in pigs, demonstrating this technology's capacity to detect changes in pulmonary anaerobic metabolism after inflammatory injury in larger species.

0700



#### Investigation of Dormant and Metastatic Breast Cancer Metabolism via Hyperpolarized <sup>13</sup>C-MRS and Fluorescence Lifetime Imaging Microscopy

Paul Begovatz<sup>1</sup>, Sarah Erickson-Bhatt<sup>2,3,4</sup>, Benjamin Cox<sup>2</sup>, Suzanne Ponik<sup>4</sup>, Kevin Eliceiri<sup>1,2,3</sup>, and Sean Fain<sup>1,5,6</sup>

<sup>1</sup>Medical Physics, University of Wisconsin-Madison, Madison, WI, United States, <sup>2</sup>Morgridge Institute for Research, Madison, WI, United States, <sup>3</sup>Laboratory for Optical and Computational Instrumentation, University of Wisconsin-Madison, Madison, WI, United States, <sup>4</sup>Cell and Regenerative Biology, University of Wisconsin-Madison, Madison, WI, United States, <sup>5</sup>Radiology, University of Wisconsin-Madison, Madison, WI, United States, <sup>6</sup>Biomedical Engineering, University of Wisconsin-Madison, Madison, WI, United States

Hyperpolarized <sup>13</sup>C-Magnetic resonance spectroscopy (<sup>13</sup>C-MRS) and NADH fluorescence lifetime imaging (FLIM) have evolved as methods to detect metabolic shifts in aerobic glycolysis and oxidative phosphorylation which are associated with metastatic potential in cancer metabolism. This study set out to investigate the differences in cancer metabolism between murine non-metastatic, metastatic-dormant, and highly metastatic breast cancer cell lines. FLIM analysis revealed no differences in free and bound NADH between cell lines, indicative of uniform ATP production through oxidative phosphorylation; however, hyperpolarized <sup>13</sup>C-MRS measurements detected an increase in lactate production, or aerobic glycolysis, which was associated with greater breast cancer metastatic potential.

0701

In Vivo Spectroscopic Detection of Glutaminase Enzyme Activity with Hyperpolarized [5-<sup>13</sup>C,4-<sup>2</sup>H<sub>2</sub>,5-<sup>15</sup>N]-L-Glutamine



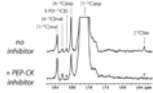


Roozbeh Eskandari<sup>1</sup>, Arsen Mamakhanyan<sup>1</sup>, Kristin L Granlund<sup>1</sup>, Kayvan R Keshari<sup>1</sup>, and Craig B Thompson<sup>2</sup>

<sup>1</sup>Radiology, Memorial Sloan Kettering Cancer Center, New York, NY, United States, <sup>2</sup>Cancer Biology & Genetics, Memorial Sloan Kettering Cancer Center, New York, NY, United States

Aberrations in glutaminase enzyme expression are associated with a variety of pathologies, and an in vivo probe to quantify flux through this pathway may provide a new layer of information. We developed a custom-synthesized compound, [5-<sup>13</sup>C,4-<sup>2</sup>H<sub>2</sub>,5-<sup>15</sup>N]-L-Glutamine, as a hyperpolarized MRI probe for glutaminase activity. Triple labeling of glutamine and D<sub>2</sub>O solvation reduces quadrupolar relaxation and extends both T<sub>1</sub> and T<sub>2</sub>, facilitating in vivo imaging. We were able to acquire <sup>13</sup>C spectroscopic data on a subcutaneous RCC xenograft murine model and detect in vivo conversion of hyperpolarized glutamine to glutamate, which permits further exploration of this imaging probe in the future.

0702



Detection of renal PEP-CK activity with hyperpolarized 13C-aspartate

Hikari A. I. Yoshihara<sup>1</sup> and Juerg Schwittr<sup>2,3</sup>

<sup>1</sup>Laboratory for Functional and Metabolic Imaging, Swiss Federal Institute of Technology (EPFL), Lausanne, Switzerland, <sup>2</sup>Division of Cardiology, Lausanne University Hospital (CHUV), Lausanne, Switzerland, <sup>3</sup>Cardiac MR Center, Lausanne University Hospital (CHUV) and University of Lausanne (UNIL), Lausanne, Switzerland

Renal gluconeogenesis contributes to glucose homeostasis and is elevated in diabetes. Aspartate is an efficient gluconeogenic substrate in the kidney, and its conversion to glucose proceeds via phosphoenolpyruvate carboxykinase (PEP-CK), which is a rate-limiting enzyme. Scanning the kidney of rats infused with hyperpolarized [1-<sup>13</sup>C]aspartate, the metabolites detected include [1-<sup>13</sup>C]malate and [4-<sup>13</sup>C]malate, 3-phospho[1-<sup>13</sup>C]glycerate, and a trace of bicarbonate. Using [1,4-<sup>13</sup>C<sub>2</sub>]aspartate resulted in higher bicarbonate signal, consistent with PEP-CK activity, and bicarbonate was undetectable after inhibiting PEP-CK. Compared to fed rats, the bicarbonate-to-malate ratio was 3-fold higher in fasted rats, indicating the potential of hyperpolarized aspartate to probe renal gluconeogenesis.

## Corporate Symposium

### Gold Corporate Symposium: GE Healthcare

Plenary Hall (Grand Ballroom)

Tuesday 19:15 - 20:15 UTC

## Wednesday, 12 August 2020

### Evening Event

#### ISMRM Business Meeting

Room C3.3

Wednesday 1:00 - 2:00 UTC

### Evening Event

#### EDI (Equity, Diversity & Inclusion) Forum: ISMRM for All

Plymouth Theatre

Wednesday 2:00 - 3:00 UTC

## Plenary Session

### Plenary Session Wednesday - Presidential Lecture: Windows into the Secret Lives of Cells

Wednesday Plenary

Wednesday 12:00 - 13:30 UTC

## Plenary Session

### Plenary Session Wednesday - Bringing MRI to Low-Resource Areas

Organizers: Christopher Filippi, Vikas Gulani, Cornelia Laule, Daniel Margolis, Ronald Ouwerkerk, Peng Hu

Wednesday Plenary

Wednesday 12:00 - 13:30 UTC

Moderators: Christopher Filippi & Vikas Gulani

[Accessible and Affordable MRI to make world healthier : An Indian Initiative](#)

Rajesh Harsh<sup>1</sup>

<sup>1</sup>SAMEER, India

---

[Extending Imaging Technology into Rural & Developing Sites: Where Does MRI Fit In?](#)

Adriana Velazquez Berumen<sup>1</sup>

<sup>1</sup>World Health Organization, Switzerland

---

[Life at the Bottom: Millitesla MRI in the 21st Century](#)

Matthew S Rosen<sup>1,2,3</sup>

<sup>1</sup>A.A. Martinos Center for Biomedical Imaging, Massachusetts General Hospital, Boston, MA, United States, <sup>2</sup>Department of Radiology, Harvard Medical School, Boston, MA, United States, <sup>3</sup>Department of Physics, Harvard University, Cambridge, MA, United States

---

---

## Sunrise Session

### Educational Q&A: CV Sunrise - CMR for Cardiac Function Beyond Ejection Fraction: Cardiac Physiology & Function: More Than Cardiac Ejection Fraction

Organizers: Dana Peters, Peng Hu

Wednesday Parallel 1 Live Q&A

Wednesday 13:45 - 14:30 UTC

Moderators: Michael Salerno

[Basics of Cardiac Physiology](#)

Marcus Carlsson

---

[Cardiac Function Assessment for the LV & Beyond](#)

Stuart Grieve

---

---

## Sunrise Session

### Educational Q&A: CV Sunrise - CMR for Cardiac Function Beyond Ejection Fraction: Myocardial Strain Imaging

Organizers: Dana Peters, Peng Hu

Wednesday Parallel 1 Live Q&A

Wednesday 13:45 - 14:30 UTC

[Methods for Myocardial Strain Imaging](#)

Frederick Epstein

---

[Methods for Myocardial Strain Imaging Beyond the LV](#)

Liang Zhong

---

---

## Sunrise Session

### Educational Q&A: CV Sunrise - CMR for Cardiac Function Beyond Ejection Fraction: Phase-Contrast for Evaluation of Cardiac Function

Organizers: Dana Peters, Peng Hu

Wednesday Parallel 1 Live Q&A

Wednesday 13:45 - 14:30 UTC

Overview of Methods for 2D & 4D Phase-Contrast

Oliver Wieben

---

Phase-Contrast MRI: Its Future Applications to Cardiac Function

Emilie Bollache

---

---

**Sunrise Session**

**Educational Q&A: CV Sunrise - CMR for Cardiac Function Beyond Ejection Fraction: Relationships Between Function & Myocardial Remodeling**

*Organizers:* Dana Peters, Peng Hu

Wednesday Parallel 1 Live Q&A

Wednesday 13:45 - 14:30 UTC

*Moderators:* Sebastien Roujol

[Imaging Myocardial Fibrosis](#)

Michael Jerosch-Herold

---

[Myocardial Tissue Remodeling: Fibrosis & Function](#)

Jeanette Schulz-Menger

---

---

**Sunrise Session**

**Educational Q&A: MRS Sunrise - Non-Gadolinium-Based Exogenous Contrast Agents**

*Organizers:* Hai-Ling Cheng, Kannie WY Chan

Wednesday Parallel 2 Live Q&A

Wednesday 13:45 - 14:30 UTC

[MRI With Non-Gadolinium Metals](#)

Ali Barandov

---

[Dynamic Glucose-Enhanced MRI](#)

Xiang Xu

---

---

**Sunrise Session**

**Educational Q&A: MRS Sunrise - Body MRS: Cancer**

*Organizers:* Wolfgang Bogner, Malgorzata Marjanska

Wednesday Parallel 2 Live Q&A

Wednesday 13:45 - 14:30 UTC

*Moderators:* Patrick Bolan & Savannah Partridge

[MRS of the Breast](#)

Paola Clauser

---

[MRS of the Prostate](#)

John Kurhanewicz

---

---

**Sunrise Session**

**Educational Q&A: MRS Sunrise - Body MRS: Non-Cancer**

*Organizers:* Wolfgang Bogner, Malgorzata Marjanska

Wednesday Parallel 2 Live Q&A

Wednesday 13:45 - 14:30 UTC

[MRS of Skeletal Muscle](#)

Alison Sleigh

---

MRS of the Heart

Ladislav Valkovic

---

---

## Sunrise Session

### Educational Q&A: MRS Sunrise - Deep Learning in MRS(I)

Organizers: Wolfgang Bogner, Malgorzata Marjanska

Wednesday Parallel 2 Live Q&A

Wednesday 13:45 - 14:30 UTC

Moderators: Roland Kreis

[How Can CNNs Improve the Quality of My Acquired MRS/MRSI Data?](#)

Zohaib Iqbal

---

[How Can Deep Learning Help Me Quantify & Understand MRS Data?](#)

Saumya Gurbani

---

---

## Weekday Course

### Prostate MRI - Prostate MRI: Easy as PI-RADS

Organizers: Daniel Margolis, Mustafa Shadi Bashir

Wednesday Parallel 3 Live Q&A

Wednesday 13:45 - 14:30 UTC

Moderators: Tom Scheenen

[PI-RADS: Prostate MRI from the Urologist's Point of View](#)

Phillip Stricker<sup>1</sup>

<sup>1</sup>(Private), Suite 1001, St Vincent's Clinic 438 Victoria Stree, Australia

---

[Not PI-RADS: Benign Mimics & Post-Treatment Imaging](#)

Varaha Satya Sairam Tammiseti<sup>1</sup>

<sup>1</sup>Diagnostic and Interventional Imaging, University of Texas Health Science Center at Houston, Houston, TX, United States

---

[Imaging of Prostate Cancer for Radiation Treatment Planning & Follow-Up](#)

Nandita deSouza<sup>1</sup>

<sup>1</sup>Institute for Cancer Research, London, United Kingdom

Localised prostate cancer is treated with prostatectomy, external beam radiotherapy with or without androgen deprivation therapy (ADT), brachytherapy and in selected cases, active surveillance. Because of its superior soft-tissue contrast, MRI plays an important role not only in staging disease, but in planning radiation-based treatment and in assessing recurrence following treatment.

---

[Quantitative & Functional Prostate MRI: The Future of PI-RADS](#)

KyungHyun Sung<sup>1</sup>

<sup>1</sup>UCLA, United States

---

---

## Weekday Course

### RF technologies - Future Receive Array Technology

Organizers: Greig Scott

Wednesday Parallel 5 Live Q&A

Wednesday 13:45 - 14:30 UTC

Moderators: Hiroyuki Fujita & Leigh Johnston

#### Future Rx Array Technology

Fraser Robb<sup>1</sup>

<sup>1</sup>GE Healthcare, United States

#### Wearable Receive Arrays

Andreas Port<sup>1</sup>

<sup>1</sup>Institute for Biomedical Engineering, ETH Zurich and University of Zurich, Zurich, Switzerland

This talk will give an overview of flexible and stretchable electrical conductor concepts, from which textile-embedded coil elements and fully wearable receive arrays are formed. It will also touch on the electronic interface particular to wearable coil arrays in terms of tuning, matching, signal digitization and transmission.



#### Options for Wireless MR Data Transmission

Roberta Frass-Kriegl<sup>1</sup> and Lena Nohava<sup>1,2</sup>

<sup>1</sup>Division MR Physics, Center for Medical Physics and Biomedical Engineering, Medical University of Vienna, Vienna, Austria, <sup>2</sup>BioMaps, Université Paris-Saclay, CEA, CNRS, Inserm, Orsay, France

Key requirements and possible strategies for a wireless radiofrequency (RF) signal chain comprising signal digitization, data compression and different wireless transmission technologies are presented. Current advances related to wireless receive coils are discussed, e.g. wireless control signals and clock synchronization to the MRI system. Furthermore, a perspective on wireless power delivery strategies for additional on-coil components is given, e.g. energy harvesting and wireless power transfer systems tested in the MR environment, complemented by considerations concerning the MR compatibility of components required for wireless RF coils.

#### Does Wireless MRI Have a Future?

Johan Overweg<sup>1</sup>

<sup>1</sup>Philips, Germany

This presentation discusses the impact wireless RF receive coils could have on diagnostic quality, safety, workflow, reliability and cost of an MR system. All of these factors will determine whether this technology will become a feature of future MRI systems.

## Oral

### Prostate MRI - Prostate

Wednesday Parallel 3 Live Q&A

Wednesday 13:45 - 14:30 UTC

Moderators: Andreas Loening

0703



Prostate MRI	Prostate MRI	Prostate MRI	Prostate MRI
Biopsy	61%	61%	76%
Biopsy	61%	61%	61%
Biopsy	61%	61%	61%
Biopsy	61%	61%	61%
Biopsy	61%	61%	61%
Biopsy	61%	61%	61%
Biopsy	61%	61%	61%
Biopsy	61%	61%	61%
Biopsy	61%	61%	61%
Biopsy	61%	61%	61%

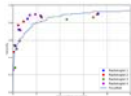
#### Prospective Validation of an Automated Hybrid Multidimensional MRI Based Tool to Identify Areas for Prostate Cancer Biopsy: Preliminary results

Aritrick Chatterjee<sup>1</sup>, Carla Harmath<sup>1</sup>, Roger Engelmann<sup>1</sup>, Ajit Devaraj<sup>2</sup>, Ambereen Yousuf<sup>1</sup>, Scott Eggener<sup>3</sup>, Glenn Gerber<sup>3</sup>, Gregory Karczmar<sup>1</sup>, and Aytekin Oto<sup>1</sup>

<sup>1</sup>Department of Radiology, University of Chicago, Chicago, IL, United States, <sup>2</sup>Philips Research North America, Chicago, IL, United States, <sup>3</sup>Department of Urology, University of Chicago, Chicago, IL, United States

This prospective clinical trial evaluates whether HM-MRI identifies PCa more reliably than random biopsy and/or targets detected based on PI-RADSv2. Patients underwent 3T mpMRI along with HM-MRI. Patients received 12-core TRUS-guided sextant random biopsy. Additional biopsy targets selected by radiologist ( $\geq$ PI-RADS 3) and suspected PCa based on HM-MRI tissue composition estimates were biopsied, using a UroNav MR-US fusion biopsy device. The diagnostic accuracy of HM-MRI for detecting clinically significant cancers was higher than that of mpMRI on per-tumor (0.74 vs 0.61) and sextant analysis (0.84 vs 0.75). HM-MRI had higher accuracy, sensitivity, specificity and PPV than mpMRI, with similar NPV.

0704



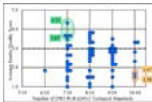
#### A Comparison between Radiologists versus Deep Learning for Prostate Cancer Detection in Multi-parameter MRI

Ruiming Cao<sup>1</sup>, Xinran Zhong<sup>2</sup>, Sohrab Afshari Mirak<sup>3</sup>, Ely Felker<sup>3</sup>, Voraparee Suvannarerg<sup>3,4</sup>, Teeravut Tubtawee<sup>3,5</sup>, Fabien Scalzo<sup>6</sup>, Steve Raman<sup>3</sup>, and Kyunghyun Sung<sup>3</sup>

<sup>1</sup>Bioengineering, UC Berkeley, Berkeley, CA, United States, <sup>2</sup>UT Southwestern, Dallas, TX, United States, <sup>3</sup>Radiology, UCLA, Los Angeles, CA, United States, <sup>4</sup>Radiology, Faculty of Medicine Siriraj Hospital, Mahidol University, Bangkok, Thailand, <sup>5</sup>Radiology, Faculty of Medicine, Prince of Songkla University, Songkhla, Thailand, <sup>6</sup>Computer Science, UCLA, Los Angeles, CA, United States

We evaluated our recently developed deep learning system, FocalNet, for prostate cancer detection in multi-parametric MRI (mpMRI). This study performed a head-to-head comparison between FocalNet and four genitourinary radiologists in an independent evaluation cohort consisting of 126 mpMRI scans untouched during the development. FocalNet demonstrated similar detection performance to radiologists under the high specificity condition or the high sensitivity condition, while radiologists outperformed FocalNet in moderate specificity and sensitivity.

0705



#### Does Compliance with PIRADSV2 Technical Requirements Guarantee Image Quality or Adequacy in Prostate mpMRI Reads?

Jonathan J. Sackett<sup>1</sup>, Joanna Shih<sup>1</sup>, Sarah Reese<sup>1</sup>, Jeffrey R. Brender<sup>1,2</sup>, Stephanie Harmon<sup>1</sup>, Tristan Barrett<sup>1</sup>, Mehmet Coskun<sup>1</sup>, Manuel Madariaga<sup>1</sup>, Jamie Marko<sup>1</sup>, Yan Mee Law<sup>1</sup>, Evrim Turkbey<sup>1</sup>, Sherif Mehralivand<sup>1</sup>, Thomas Sanford<sup>1</sup>, Nathan Lay<sup>1</sup>, Peter A. Pinto<sup>1</sup>, Bradford J. Wood<sup>2</sup>, Peter L. Choyke<sup>2</sup>, Murali C. Krishna<sup>2</sup>, and Baris I Turkbey<sup>2</sup>

<sup>1</sup>Molecular Imaging Program, National Cancer Institute, National Institutes of Health, Bethesda, MD, MD, United States, <sup>2</sup>National Cancer Institute, National Institutes of Health, Bethesda, MD, MD, United States

High quality MRIs are needed for prostate cancer screening and accurate targeting in MRI guided biopsies. Based on blind image quality assessment by image readers, compliance with the PIRADSV2 Minimum Technical Standards was determined to be neither necessary nor sufficient in ensuring quality in prostate T2 and DWI images.

0706



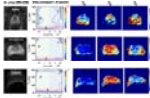
#### Radio-pathomic mapping models trained with annotations from multiple pathologists reliably distinguish high-grade prostate cancer

Sean D McGarry<sup>1</sup>, John D Bukowy<sup>2</sup>, Kenneth Iczkowski<sup>3</sup>, Allison K Lowman<sup>2</sup>, Michael Brehler<sup>2</sup>, Samuel Bobholz<sup>1</sup>, Alex Barrington<sup>2</sup>, Kenneth Jacobsohn<sup>4</sup>, Jackson Unteriner<sup>2</sup>, Petar Duvnjak<sup>2</sup>, Michael Griffin<sup>2</sup>, Mark Hohenwarter<sup>2</sup>, Tucker Keuter<sup>5</sup>, Wei Huang<sup>6</sup>, Tatjana Antic<sup>7</sup>, Gladell Paner<sup>7</sup>, Watchareepohn Palanghmonthip<sup>3,8</sup>, Anjishnu Banerjee<sup>5</sup>, and Peter S LaViolette<sup>2</sup>

<sup>1</sup>Biophysics, Medical College of Wisconsin, Milwaukee, WI, United States, <sup>2</sup>Radiology, Medical College of Wisconsin, Milwaukee, WI, United States, <sup>3</sup>Pathology, Medical College of Wisconsin, Milwaukee, WI, United States, <sup>4</sup>Urological Surgery, Medical College of Wisconsin, Milwaukee, WI, United States, <sup>5</sup>Biostatistics, Medical College of Wisconsin, Milwaukee, WI, United States, <sup>6</sup>Pathology, University of Wisconsin Madison, Madison, WI, United States, <sup>7</sup>Pathology, University of Chicago, Chicago, IL, United States, <sup>8</sup>Pathology, Chiang Mai University, Chiang Mai, Thailand

This study demonstrates that radio-pathomic maps of epithelium density derived from annotations performed by different pathologists distinguish high-grade prostate cancer from G3 and benign atrophy. In a test set of 5 patients epithelium density maps consistently demonstrate an AUC greater than 0.9 independent of which pathologist's annotations trained the model or which pathologist's annotations the model is applied to. The results in a larger test set largely mirror the results in the small test set. We also showed that radio-pathomic maps of epithelium density out-performed ADC maps independent of which observer was used to train the model.

0707

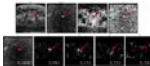


Towards In Vivo Prostate Microstructure Mapping Using Diffusion-Relaxation Correlation Spectrum Imaging  
Zhaohuan Zhang<sup>1,2</sup> and Holden Wu<sup>1,2</sup>

<sup>1</sup>Department of Radiological Sciences, University of California, Los Angeles, Los Angeles, CA, United States, <sup>2</sup>Department of Bioengineering, University of California, Los Angeles, Los Angeles, CA, United States

Recent work has demonstrated the ability of Diffusion-Relaxation Correlation Spectrum Imaging (DR-CSI) to quantify prostate microscopic tissue compartments (epithelium, stroma and lumen) in *ex vivo* prostate specimens at 3T using whole-mount digital histopathology as the reference. This study further developed DR-CSI for *in vivo* characterization of prostate microstructure using high resolution *ex vivo* DR-CSI as the reference. Consistent trends in DR-CSI signal component fraction variations in different prostate regions were found using *in vivo* DR-CSI across subjects, and agreed with trends on *ex vivo* DR-CSI.

0708



Improved characterization of prostate tumors through multi-compartmental analysis of restriction spectrum imaging data

Christopher C Conlin<sup>1</sup>, Christine H Feng<sup>2</sup>, Ana E Rodriguez-Soto<sup>1</sup>, Roshan A Karunamuni<sup>2</sup>, Joshua M Kuperman<sup>1</sup>, Dominic Holland<sup>1</sup>, Rebecca Rakow-Penner<sup>1</sup>, Tyler M Seibert<sup>2</sup>, Anders M Dale<sup>1,3</sup>, and Michael E Hahn<sup>1</sup>

<sup>1</sup>Department of Radiology, UC San Diego School of Medicine, La Jolla, CA, United States, <sup>2</sup>Department of Radiation Medicine and Applied Science, UC San Diego School of Medicine, La Jolla, CA, United States, <sup>3</sup>Department of Neurosciences, UC San Diego School of Medicine, La Jolla, CA, United States

Restriction spectrum imaging (RSI) is an advanced multi-shell diffusion technique that models the diffusion-weighted signal as a linear combination of exponential decays. While RSI shows promise for assessing prostate cancer, an optimal RSI model that effectively characterizes the diffusion properties of both normal and cancerous prostate tissue is essential to ensuring an accurate evaluation of prostate cancer lesions. In this study, we determined optimal ADC values for several RSI models of the prostate and assessed the number of tissue compartments required to best describe diffusion in both normal and cancerous prostate tissue.

0709



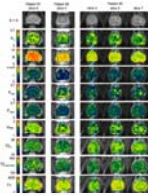
Comparing the Diagnostic Accuracy of Luminal Water Imaging versus PI-RADSv2.1 in Detection of Prostate Cancer

Shirin Sabouri<sup>1</sup>, Silvia Chang<sup>2,3,4</sup>, Emily Pang<sup>2</sup>, Rehab Mohammedid<sup>2</sup>, Edward Jones<sup>5</sup>, Larry Goldenberg<sup>3,4</sup>, Peter Black<sup>3,4</sup>, and Piotr Kozlowski<sup>1,2,3,4</sup>

<sup>1</sup>UBC MRI Research Centre, Vancouver, BC, Canada, <sup>2</sup>Department of Radiology, The University of British Columbia, Vancouver, BC, Canada, <sup>3</sup>Department of Urologic Sciences, The University of British Columbia, Vancouver, BC, Canada, <sup>4</sup>Vancouver Prostate Centre, Vancouver, BC, Canada, <sup>5</sup>Department of Pathology and Laboratory Medicine, The University of British Columbia, Vancouver, BC, Canada

Luminal water imaging (LWI) is an MRI technique that detects regions of decreased lumen volume in prostate. Recent studies on LWI have shown promising results regarding the accuracy of this technique in diagnosis of prostate cancer. However, to the best of our knowledge no study has yet compared the performance of LWI against the current clinical assessment. In this study, we perform a comparison between the diagnostic accuracy of LWI with the PI-RADSv2.1 assessment. Our results show that LWI performs similar to the PI-RADSv2.1 in the entire prostate and peripheral zone, and outperforms significantly in transition zone.

0710



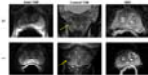
**Relaxed-VERDICT: decoupling relaxation and diffusion for comprehensive microstructure characterization of prostate cancer.**

Marco Palombo<sup>1</sup>, Saurabh Singh<sup>2</sup>, Hayley Whitaker<sup>2</sup>, Shonit Puwani<sup>2</sup>, Daniel C. Alexander<sup>1</sup>, and Eleftheria Panagiotaki<sup>1</sup>

<sup>1</sup>Centre for Medical Image Computing, Department of Computer Science, University College London, London, United Kingdom, <sup>2</sup>Centre for Medical Imaging, University College London, London, United Kingdom

This work presents a comprehensive VERDICT prostate model (relaxed-VERDICT) that includes compartment-specific relaxation effects providing prostate microstructural estimates unbiased by the relaxation properties of the tissue. We compare relaxed-VERDICT with the original VERDICT model and use it to provide estimates of T2 and T1 in benign and tumor prostate tissue. Our results suggest that original VERDICT's  $f_{ic}$  contrast is mostly driven by diffusion, supporting its use as imaging marker of apparent cellular volume fraction. Relaxed-VERDICT estimates of T1/T2 values are in very good agreement with literature. Finally, we propose a machine learning based processing pipeline that provides ultra-fast quantitative maps.

0711



**Prostate cancer multiparametric MRI comparison study of 3T versus 7T: lesion detection and study design considerations**

Ethan Leng<sup>1</sup>, Benjamin Spilseth<sup>2</sup>, Anil Chauhan<sup>2</sup>, Joseph Gill<sup>2</sup>, Ana Rosa<sup>2</sup>, Arcan Erturk<sup>1</sup>, Naoharu Kobayashi<sup>1</sup>, Xiaoxuan He<sup>1</sup>, Christopher Warlick<sup>3</sup>, and Gregory Metzger<sup>1</sup>

<sup>1</sup>Center for Magnetic Resonance Research, University of Minnesota, Minneapolis, MN, United States, <sup>2</sup>Radiology, University of Minnesota, Minneapolis, MN, United States, <sup>3</sup>Urology, University of Minnesota, Minneapolis, MN, United States

Recent works have demonstrated the feasibility of prostate multiparametric MRI (mpMRI) at 7T with improved resolution compared to mpMRI at 3T. However, the clinical relevance of finer anatomic details versus the drawbacks of increased imaging artifacts at 7T has yet to be investigated. In this work, we conducted a retrospective, multi-reader clinical evaluation of 19 paired mpMRI studies at 3T and 7T. The primary outcome of interest was accuracy of prostate cancer detection, with image quality and artifacts as secondary outcomes.

## Oral

### Diffusion Microstructure Modeling and Validation - Diffusion: Microstructure Modelling

Wednesday Parallel 4 Live Q&A

Wednesday 13:45 - 14:30 UTC

Moderators: Maryam Afzali & Marco Palombo

0712

The impact of axon orientation dispersion and 3D diameter variations on the transverse apparent diffusion coefficient



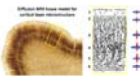


Mariam Andersson<sup>1,2</sup>, Jonathan Rafael-Patino<sup>3</sup>, Hans Martin Kjer<sup>1,2</sup>, Vedrana Andersen Dahl<sup>1</sup>, Alexandra Pacureanu<sup>4</sup>, Martin Bech<sup>5</sup>, Anders Bjorholm Dahl<sup>1</sup>, Jean-Philippe Thiran<sup>3,6</sup>, and Tim B. Dyrby<sup>1,2</sup>

<sup>1</sup>Department of Applied Mathematics and Computer Science, Technical University of Denmark, Kgs. Lyngby, Denmark, <sup>2</sup>Danish Research Centre for Magnetic Resonance, Hvidovre, Denmark, <sup>3</sup>Ecole Polytechnique Fédérale de Lausanne, Lausanne, Switzerland, <sup>4</sup>The European Synchrotron, Grenoble, France, <sup>5</sup>Department of Medical Radiation Physics, Clinical Science, Lund University, Lund, Sweden, <sup>6</sup>Radiology Department, Centre Hospitalier Universitaire Vaudois and University of Lausanne, Lausanne, Switzerland

We extract the orientation dispersion (OD) and 3D axon diameter variations of long axons ( $>100 \mu\text{m}$ ) from an ultra-high resolution, synchrotron X-ray nano-holotomography (XNH) scan of the monkey splenium. From this, we discover a relationship between mean axon diameter and along-axon diameter variations. Monte Carlo simulations are then performed on the intra-axonal spaces (IAS) of different substrates which inherit their morphological features from the segmented axons. These simulations show that the OD significantly affects the transverse apparent diffusion coefficient ( $\text{ADC}_{\perp}$ ) of the axon substrate at diffusion times up to 50 ms, while diameter variations do not.

0713



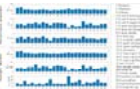
Modeling cortical architectonic features by analyzing diffusion MRI data in the cortical reference frame

Alexandru V Avram<sup>1,2</sup>, Kadharbatcha Saleem<sup>1,2</sup>, Frank Q Ye<sup>3</sup>, Cecil Yen<sup>4</sup>, Michal E Komlosh<sup>1,2</sup>, and Peter J Basser<sup>1</sup>

<sup>1</sup>NICHD, National Institutes of Health, Bethesda, MD, United States, <sup>2</sup>The Henry Jackson Foundation, Bethesda, MD, United States, <sup>3</sup>NIMH, National Institutes of Health, Bethesda, MD, United States, <sup>4</sup>NINDS, National Institutes of Health, Bethesda, MD, United States

We quantified the alignment between the DTI reference frame (DRF) and the cortical reference frame (CRF) throughout the entire cerebral cortex in a macaque brain, and found relatively good correspondence, especially in regions with high curvature such as the gyral walls and the cortical sulci. Based on this correspondence, we analyze cortical diffusion signals in the CRF and construct a simple model of cortical diffusion with distinct radial (columnar) and tangential (sheet-like) diffusion processes in cortical layers. The variation of model parameters with cortical depth reflects architectonic features described in a histologically defined digital macaque brain atlas.

0714



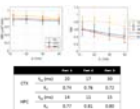
In vivo observation and interpretation of time-dependent diffusion in human brain gray matter

Hong-Hsi Lee<sup>1</sup>, Antonios Papaioannou<sup>1</sup>, Dmitry S Novikov<sup>1</sup>, and Els Fieremans<sup>1</sup>

<sup>1</sup>Center for Biomedical Imaging, Department of Radiology, NYU School of Medicine, New York, NY, United States

The purpose of this work is to identify the relevant microstructural features for the human brain gray matter. For that, we estimate the diffusivity and kurtosis time-dependence in 25 gray matter sub-regions of 10 healthy subjects, and compare the effects of the structural disorder and exchange (Karger model). The estimated power-law dynamical exponent  $\theta \approx 1/2$  is consistent with the structural disorder picture in a 1-dimensional micro-geometry of randomly positioned restrictions along neurites. In contrast, Karger model yields exchange time much shorter than values in previous studies, and below our shortest diffusion time.

0715



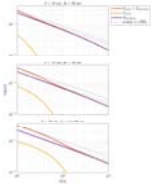
Water exchange time between gray matter compartments in vivo

Ileana Ozana Jelescu<sup>1</sup> and Dmitry S Novikov<sup>2</sup>

<sup>1</sup>Center for Biomedical Imaging, Ecole Polytechnique Fédérale de Lausanne, Lausanne, Switzerland, <sup>2</sup>Dept. of Radiology, New York University School of Medicine, New York, NY, United States

In the absence of a myelin sheath, exchange generally is non-negligible over the typical diffusion times of MRI experiments (10 – 100 ms) and should be accounted for in gray matter modeling. Here we use time-dependent kurtosis and the Kärger model (KM) of two slowly exchanging compartments to evaluate water exchange time between intra-neurite and extra-cellular compartments in rat GM *in vivo*. We report exchange times on the order of 10 – 30 ms. Future work will focus on exploring a broader range of diffusion times to test the asymptotic decay of kurtosis toward zero.

0716



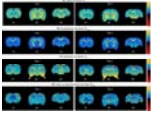
Stick power law scaling in neurons withstands realistic curvature and branching

Jonas Lynge Olesen<sup>1,2</sup> and Sune Nørhøj Jespersen<sup>1,2</sup>

<sup>1</sup>Center of Functionally Integrative Neuroscience (CFIN) and MINDLab, Department of Clinical Medicine, Aarhus University, Aarhus, Denmark, <sup>2</sup>Department of physics and Astronomy, Aarhus University, Aarhus, Denmark

A main idea contained in the standard model of diffusion is to model neurons with zero-width sticks. A resulting signature is the prediction that in the large  $b$  limit, the isotropically averaged signal scales as  $1/\sqrt{b}$  which has been verified in white matter but not gray matter. This has multiple proposed causes including dendrite curvature and branching. Here, we report on Monte Carlo simulations in 3D reconstructed neurons and find that branching and curvature do not break the power law scaling. On the other hand, the soma is found to limit the regime in which stick scaling is observed.

0717



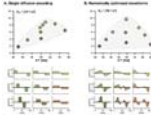
Correlation Tensor Imaging - resolving non-Gaussian diffusion sources of *in vivo* tissues

Rafael Neto Henriques<sup>1</sup>, Sune Nørhøj Jespersen<sup>2,3</sup>, and Noam Shemesh<sup>1</sup>

<sup>1</sup>Champalimaud Research, Champalimaud Centre for the Unknown, Lisbon, Portugal, <sup>2</sup>Center of Functionally Integrative Neuroscience (CFIN) and MINDLab, Clinical Institute, Aarhus University, Aarhus, Denmark, <sup>3</sup>Department of Physics and Astronomy, Aarhus University, Aarhus, Denmark

Resolving the different sources of diffusional kurtosis can increase DKI's specificity towards different microstructural features. Such sources can be resolved using the correlation tensor imaging (CTI) – a novel double diffusion encoding technique that does not rely on common assumptions of time-independent diffusion. Here, a minimal acquisition protocol for CTI is designed and used to characterize the diffusional kurtosis of living rat brains for the first time. We here develop an approach to acquire CTI data *in vivo* and show that it can robustly decouple inter-compartmental kurtosis sources (anisotropic and isotropic diffusivity variances) from intra-compartmental kurtosis sources.

0718



A unified framework for analysis of time-dependent diffusion: numerical validation of a restriction-exchange correlation experiment

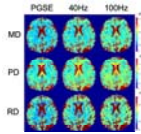
Markus Nilsson<sup>1</sup>, Carl-Fredrik Westin<sup>2</sup>, Jan Brabec<sup>1</sup>, Samo Lasic<sup>3</sup>, and Filip Szczepankiewicz<sup>1</sup>

<sup>1</sup>Clinical Sciences Lund, Lund University, Lund, Sweden, <sup>2</sup>Brigham and Women's hospital, Harvard Medical School, Boston, MA, United States, <sup>3</sup>Random Walk Imaging AB, Lund, Sweden

Probing time-dependence with diffusion MRI enables mapping of microstructure features such as cell sizes (restrictions) and membrane permeability (exchange). However, restrictions and exchange have opposite effects on the MR signal, and cannot be distinguished by just varying the diffusion time. We propose a unified framework for analysis of time-dependent diffusion that enables the design of efficient restriction-exchange correlation experiments. A signal representation was developed featuring parameters connected to restricted diffusion and exchange. This connection was validated by numerical simulations.

0719

Oscillating Gradient Diffusion-Encoding In Human Brain Shows Linear Frequency Correlation in High Amplitude and Slew Rate Head Gradient System

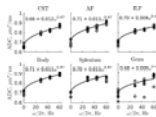


Ek T Tan<sup>1,2</sup>, Robert Y Shih<sup>3</sup>, Jhimli Mitra<sup>1</sup>, Yihe Hua<sup>1</sup>, Tim Sprenger<sup>4</sup>, Chitresh Bhushan<sup>1</sup>, Jennifer A McNab<sup>5</sup>, Matt A Bernstein<sup>6</sup>, and Thomas KF Foo<sup>1</sup>

<sup>1</sup>GE Research, Niskayuna, NY, United States, <sup>2</sup>Radiology and Imaging, Hospital for Special Surgery, New York, NY, United States, <sup>3</sup>Walter Reed National Military Medical Center, Bethesda, MD, United States, <sup>4</sup>GE Healthcare, Stockholm, Sweden, <sup>5</sup>Stanford University, Stanford, CA, United States, <sup>6</sup>Radiology, Mayo Clinic, Rochester, MN, United States

High gradient amplitude, high gradient slew rate, and high peripheral nerve stimulation thresholds are required for oscillating gradient spin-echo (OGSE) diffusion imaging on human MRI systems. With 200 mT/m amplitude and 500 T/m/s slew rate, the MAGNUS head gradient coil was used to evaluate OGSE imaging in six healthy subjects at frequencies up to 100 Hz and  $b=450$  s/mm<sup>2</sup>. Comparisons were made against standard pulsed gradient spin-echo (PGSE) diffusion in-vivo, which show up to 27% increased OGSE diffusivity, excellent linear correlation with frequency, and correlation length scales of 0.8 $\mu$ m in white matter. Diffusivity changes were negligible in an isotropic phantom.

0720



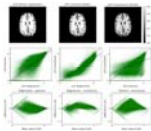
Evidence for Short Range Disorder in the in vivo Human Brain using OGSE Diffusion MRI

Aidin Arbabi<sup>1</sup>, Jason Kai<sup>1</sup>, Ali R Khan<sup>1</sup>, and Corey A Baron<sup>1</sup>

<sup>1</sup>Robarts Research Institute, University of Western Ontario, London, ON, Canada

Oscillating gradient spin-echo (OGSE) diffusion MRI enables probing of the frequency content of the apparent diffusion coefficient (ADC). A square root dependence of ADC on frequency has been demonstrated in both healthy and globally ischemic rodent brain tissue, which is consistent with short range structural disorder along neurites. In this work, OGSE data was acquired at multiple frequencies to explore the power law scaling of the ADC in the human brain in vivo, where evidence of a square root dependence of ADC on frequency was obtained for the first time in the in vivo human brain.

0721



Accuracy and precision of microscopy anisotropy estimation using q-space trajectory encoding - a model comparison study

Leevi Kerkelä<sup>1</sup>, Fabio Nery<sup>1</sup>, Feng-Lei Zhou<sup>2</sup>, Geoff J.M. Parker<sup>2,3,4</sup>, Filip Szczepankiewicz<sup>5,6,7</sup>, Matt G. Hall<sup>1,8</sup>, and Chris A. Clark<sup>1</sup>

<sup>1</sup>UCL Great Ormond Street Institute of Child Health, University College London, London, United Kingdom, <sup>2</sup>Centre for Medical Image Computing, University College London, London, United Kingdom, <sup>3</sup>Bioxydyn Limited, Manchester, United Kingdom, <sup>4</sup>CRUK and EPSRC Cancer Imaging Centre in Cambridge and Manchester, Manchester, United Kingdom, <sup>5</sup>Department of Radiology, Brigham and Women's Hospital, Boston, MA, United States, <sup>6</sup>Harvard Medical School, Boston, MA, United States, <sup>7</sup>Medical Radiation Physics, Clinical Sciences Lund, Lund University, Lund, Sweden, <sup>8</sup>National Physical Laboratory, Teddington, United Kingdom

Estimation of microscopic fractional anisotropy ( $\mu$ FA) using multidimensional diffusion MRI is a promising novel method for characterising clinically relevant microstructural properties of neural tissue. In this study, three commonly used methods for calculating  $\mu$ FA were compared by imaging a fibre phantom and healthy volunteers. Statistically significant differences were observed in accuracy and precision of the  $\mu$ FA estimates calculated using the covariance tensor model, the gamma distributed diffusivities model, and the direct regression approach. The differences between the methods have to be carefully considered when this promising new metric is applied in characterising microstructural properties of tissue or pathologies.

Oral

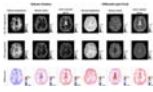
Diffusion Microstructure Modeling and Validation - Microstructure: Validation

Wednesday Parallel 4 Live Q&A

Wednesday 13:45 - 14:30 UTC

Moderators: Tim Dyrby

0722



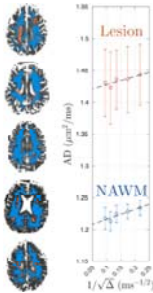
### High-Resolution Neural Soma Imaging with FLAIR: Eliminating CSF Contamination in Grey Matter

Noemi G Gyori<sup>1,2</sup>, Iulius Dragonu<sup>3</sup>, Christopher A Clark<sup>2</sup>, Daniel C Alexander<sup>1</sup>, and Enrico Kaden<sup>1</sup>

<sup>1</sup>Centre for Medical Image Computing, University College London, London, United Kingdom, <sup>2</sup>Great Ormond Street Institute of Child Health, University College London, London, United Kingdom, <sup>3</sup>Siemens Healthcare Ltd, Frimley, United Kingdom

In-vivo microstructure imaging in cortical grey matter is limited by low imaging resolution and signal contamination from CSF. In this work, we use FLAIR to eliminate free water signal in the brain, and thus enhance sensitivity to microscopic tissue architecture in the cortex. We present the advantage of CSF suppression in Neural Soma Imaging, a state-of-the-art diffusion technique that focuses on the salient features of grey matter. We show high-resolution maps (1.5 mm isotropic) of neural tissue microstructure and T1- and T2-relaxation times, and demonstrate that neural projection density estimates are significantly higher when the CSF signal is eliminated.

0723



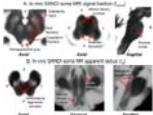
### Characterizing white matter lesions in multiple sclerosis with time-dependent diffusion MRI reveals the signature of axonal beading

Hong-Hsi Lee<sup>1</sup>, Dmitry S Novikov<sup>1</sup>, and Els Fieremans<sup>1</sup>

<sup>1</sup>Center for Biomedical Imaging, Department of Radiology, NYU School of Medicine, New York, NY, United States

We observe diffusivity time-dependence along white matter axons in normal-appearing white matter (NAWM) and lesions in 5 relapse remitting multiple sclerosis (MS) patients. The long-time diffusivity along axons is higher in MS lesion than that in NAWM due to persistent demyelination and axonal loss, consistent with previous studies. Further, the axial diffusivity time-dependence is weaker in MS lesions than in NAWM, probably caused by beading due to increased mitochondria in astrocytes/axons in MS lesions. We propose the axial diffusivity time-dependence as a potential specific biomarker for beading, to monitor the progression and treatment response of MS.

0724

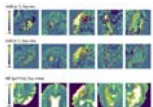


### Validation and application of soma and neurite density imaging (SANDI) for in-vivo human brainstem nuclei atlasing

Marta Bianciardi<sup>1</sup>, Maria G. García-Gomar<sup>1</sup>, Kavita Singh<sup>1</sup>, Michele Guerreri<sup>2</sup>, Alejandra Sierra<sup>3</sup>, Jussi Tohka<sup>3</sup>, Ali Abdollahzadeh<sup>3</sup>, Hui Zhang<sup>2</sup>, and Marco Palombo<sup>2</sup>

<sup>1</sup>Department of Radiology, A.A. Martinos Center for Biomedical Imaging, MGH and Harvard Medical School, Boston, MA, United States, <sup>2</sup>Centre for Medical Image Computing, Department of Computer Science, University College London, London, United Kingdom, <sup>3</sup>A.I. Virtanen Institute for Molecular Sciences, University of Eastern Finland, Kuopio, Finland

Despite the development of detailed *in-vivo* human cortical atlases, *in-vivo* brainstem nuclei atlasing is still at its early stages due to reduced gray-white matter MRI-contrast in the brainstem compared to the cortex. Recently, we generated an *in-vivo* probabilistic atlas of 16 human brainstem nuclei based on multi-contrast 7Tesla MRI. Nevertheless, to further expand the *in-vivo* brainstem nuclei atlas, there is an unmet need from additional MRI-contrast reflecting brainstem cytoarchitecture. We found that recently developed *in-vivo* Soma-And-Neurite-Density-Imaging (SANDI) provides original MRI-contrast directly related to *ex-vivo* brainstem nuclei cytoarchitecture, and can be used to expand the current *in-vivo* human brainstem nuclei atlas.



### Diffusion time dependence and tissue outcome in ischemic stroke

Björn Lampinen<sup>1</sup>, Jimmy Lätt<sup>2</sup>, Johan Wasselius<sup>3</sup>, Danielle van Westen<sup>4</sup>, and Markus Nilsson<sup>4</sup>

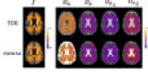
0725



<sup>1</sup>Medical Radiation Physics, Lund University, Lund, Sweden, <sup>2</sup>Center for Medical Imaging and Physiology, Skåne University Hospital, Lund, Sweden, <sup>3</sup>Clinical Sciences Lund, Neurology, Lund University, Lund, Sweden, <sup>4</sup>Clinical Sciences Lund, Diagnostic Radiology, Lund University, Lund, Sweden

Many patients with ischemic stroke that would benefit from 'late' recanalization go untreated, as current imaging-based predictions of outcome are insufficiently individualized. This study investigated whether diffusion MRI (dMRI), a standard tool in stroke diagnostics, provides additional information through effects of diffusion time dependence. Results showed elevated rates of water exchange within lesions of subacute stroke patients. The absence of such exchange appeared predictive of tissue viability in the chronic stage, even in regions normally considered irreversibly injured. Information on diffusion time dependence may thus improve penumbra definitions and help identifying subjects with favorable outcome of late recanalization.

0726



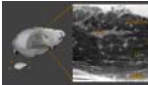
Testing white matter tissue modeling with multiple diffusion encoding MRI

Hunter G Moss<sup>1,2</sup>, Emilie T McKinnon<sup>1,2,3</sup>, and Jens H Jensen<sup>1,2</sup>

<sup>1</sup>Neuroscience, Medical University of South Carolina, Charleston, SC, United States, <sup>2</sup>Center for Biomedical Imaging, Medical University of South Carolina, Charleston, SC, United States, <sup>3</sup>Neurology, Medical University of South Carolina, Charleston, SC, United States

The validation of white matter (WM) tissue modeling for diffusion MRI is challenging, in part, because some of the predicted microstructural parameters (e.g., compartment-specific diffusivities) cannot be easily measured with independent methods such as histology. Most WM tissue models are designed to utilize single diffusion encoding (SDE) MRI data as provided by conventional diffusion MRI sequences. Since multiple diffusion encoding (MDE) MRI yields more information than SDE, it allows for tissue modeling that requires fewer assumptions. Hence, MDE can be applied to help validate the predictions for all SDE model parameters. Here we give an explicit example of this.

0727



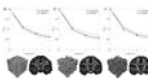
Streamline tractography for 3D mapping of axon bundle organization in one MRI voxel using ultra-high resolution synchrotron radiation imaging

Hans Martin Kjer<sup>1,2</sup>, Mariam Andersson<sup>1,2</sup>, Yi He<sup>2</sup>, Marie Louise Elkjaer<sup>3</sup>, Alexandra Pacureanu<sup>4,5</sup>, Zsolt Illes<sup>3</sup>, Bente Pakkenberg<sup>6</sup>, Anders Bjorholm Dahl<sup>1</sup>, Vedrana Andersen Dahl<sup>1</sup>, and Tim B. Dyrby<sup>1,2</sup>

<sup>1</sup>DTU Compute, Technical University of Denmark, Kgs. Lyngby, Denmark, <sup>2</sup>Danish Research Centre for Magnetic Resonance, Hvidovre, Denmark, <sup>3</sup>Department of Neurology, Odense University Hospital, Odense, Denmark, <sup>4</sup>X-ray Nanoprobe Group, ID16A, The European Synchrotron, Grenoble, France, <sup>5</sup>University College London, London, United Kingdom, <sup>6</sup>Research Laboratory for Stereology and Neuroscience, Bispebjerg University Hospital, Copenhagen NV, Denmark

We present an efficient image analysis pipeline that enables us to reveal white matter organization in high-resolution 3D non-MRI structural datasets, in cases where a strict image segmentation is not required nor possible. We apply the method to a synchrotron X-ray holographic tomography scan from a healthy mouse sample, and show the organization of axon bundles in a region covering parts of the corpus callosum and the cingulum. The method has a potential to improve our general understanding of white matter organization and our ability to generate realistic phantoms for validation of microstructure modelling from low-resolution diffusion MRI scans.

0728



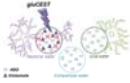
Improved contextual fibre growth for generating white matter numerical phantoms with realistic microstructure

Ross Callaghan<sup>1</sup>, Daniel C Alexander<sup>1</sup>, Marco Palombo<sup>1</sup>, and Hui Zhang<sup>1</sup>

<sup>1</sup>Department of Computer Science & Centre for Medical Image Computing, University College London, London, United Kingdom

We present an improved version of the ConFiG white matter numerical phantom generator to create realistic white matter microstructure. Building on ConFiG's novel fibre growth algorithm, the enhancement incorporates a dynamic growth network and global optimisation of fibre positions. Resulting phantoms represent a significant improvement over those from the original ConFiG algorithm, with realistic morphology and an increase in packing density of up to 30%. These improved phantoms result in much more realistic simulated diffusion MRI signals, reducing RMSE to real data by ten times. This improvement demonstrates the potential of ConFiG as a computational model of white matter microstructure.

0729



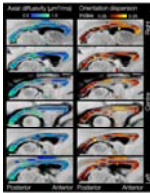
### Using glutamate-CEST to characterize water diffusion inside neurons: initial results

Mélissa Vincent<sup>1,2</sup>, Yohann Mathieu-Daudé<sup>1,2</sup>, Julien Flament<sup>1,2</sup>, and Julien Valette<sup>1,2</sup>

<sup>1</sup>Molecular Imaging Research Center (MIRGen), Commissariat à l'Energie Atomique et aux Energies Alternatives (CEA), Fontenay-aux-Roses, France, <sup>2</sup>UMR 9199, Neurodegenerative Diseases Laboratory, Centre National de la Recherche Scientifique (CNRS), Université Paris-Sud, Université Paris-Saclay, Fontenay-aux-Roses, France

It is still unclear how diffusion properties of water differ from one compartment to another (neurons, glial cells, extracellular space...). Here we propose the idea that Chemical Exchange Saturation Transfer of Glutamate (gluCEST) may be used to specifically reduce the contribution of intraneural water to the overall signal attenuation, thus providing enhanced sensitivity to non-neuronal compartments. Acquisitions performed in two rats yields water ADC slightly but significantly higher when gluCEST is performed, supporting the idea that water diffusion is slower inside neurons.

0730



### Estimating intra-axonal axial diffusivity with diffusion MRI in the presence of fibre orientation dispersion

Amy FD Howard<sup>1</sup>, Alexandre A Khrapitchev<sup>2</sup>, Jeroen Mollink<sup>1,3</sup>, Rogier B Mars<sup>1,4</sup>, Nicola Sibson<sup>2</sup>, Jerome Sallet<sup>5</sup>, Saad Jbabdi<sup>1</sup>, and Karla L Miller<sup>1</sup>

<sup>1</sup>FMRIB Centre, Wellcome Centre for Integrative Neuroimaging, Nuffield Department of Clinical Neurosciences, University of Oxford, Oxford, United Kingdom, <sup>2</sup>CR-UK/MRC Oxford Institute for Radiation Oncology, Department of Oncology, University of Oxford, Oxford, United Kingdom, <sup>3</sup>Department of Anatomy, Donders Institute for Brain, Cognition and Behaviour, Radboud University Medical Center, Nijmegen, Netherlands, <sup>4</sup>Donders Institute for Brain, Cognition and Behaviour, Radboud University Nijmegen, Nijmegen, Netherlands, <sup>5</sup>Wellcome Centre for Integrative Neuroimaging, Experimental Psychology, Medical Sciences Division, University of Oxford, Oxford, United Kingdom

Intra-axonal axial diffusivity could be interesting biomarker of disease, yet it is often assumed constant across the white matter. Furthermore, when intra-axonal diffusivity is estimated, few models account for fibre orientation dispersion which (when not explicitly modelled) will greatly affect the estimates of axial diffusion. Here we combine the stick model of intra-axonal diffusion with a simple model of fibre dispersion to simultaneously estimate intra-axonal axial diffusivity and fibre dispersion on a voxel-wise basis in high b-value data. Our results demonstrate considerable variability in the intra-axonal axial diffusivity across the white matter.

## Oral - Power Pitch

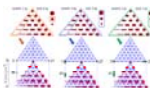
### Diffusion Microstructure Modeling and Validation - Diffusion & Microstructure: Modelling & Validation

Wednesday Parallel 4 Live Q&A

Wednesday 13:45 - 14:30 UTC

Moderators: Daan Christiaens

0731



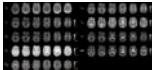
### Optimal experimental design in multidimensional diffusion MRI for parameter estimation of biophysical tissue models

Santiago Coelho<sup>1,2</sup>, Jose M Pozo<sup>1</sup>, Sune N Jespersen<sup>2,3,4</sup>, Alejandro F Frangi<sup>1</sup>, Dmitry S Novikov<sup>2</sup>, and Els Fieremans<sup>2</sup>

<sup>1</sup>Centre for Computational Imaging & Simulation Technologies in Biomedicine (CISTIB), School of Computing and School of Medicine, University of Leeds, Leeds, United Kingdom, <sup>2</sup>Radiology, School of Medicine, New York University, New York City, NY, United States, <sup>3</sup>Center of Functionally Integrative Neuroscience (CFIN) and MINDLab, Department of Clinical Medicine, Aarhus University, Aarhus, Denmark, <sup>4</sup>Department of Physics and Astronomy, Aarhus University, Aarhus, Denmark

It was recently shown that multidimensional diffusion MRI enables well-posed estimation of the Standard Model (SM) for diffusion in white matter. However, various multidimensional acquisitions can achieve this, and there are currently no criteria for efficient data acquisition for SM. We propose an optimal experiment design framework based on Cramér-Rao bounds to maximise accuracy and precision of SM parameter estimation. We explore the high-dimensional continuous acquisition space and identify the optimal combination of b-tensors that minimises estimation error. Simulations and *in vivo* experiments demonstrate that our optimised acquisition has a reduced estimation error on all SM microstructural parameters.

0732



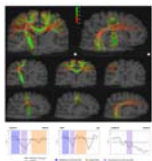
Towards unconstrained compartment modeling in white matter using diffusion-relaxation MRI with tensor-valued diffusion encoding

Björn Lampinen<sup>1</sup>, Filip Szczepankiewicz<sup>2,3</sup>, Johan Mårtensson<sup>4</sup>, Danielle van Westen<sup>2</sup>, Oskar Hansson<sup>5</sup>, Carl-Fredrik Westin<sup>3</sup>, and Markus Nilsson<sup>2</sup>

<sup>1</sup>Clinical Sciences Lund, Medical Radiation Physics, Lund University, Lund, Sweden, <sup>2</sup>Clinical Sciences Lund, Diagnostic Radiology, Lund University, Lund, Sweden, <sup>3</sup>Brigham and Women's Hospital, Harvard Medical School, Boston, MA, United States, <sup>4</sup>Clinical Sciences Lund, Department of Logopedics, Phoniatrics and Audiology, Lund University, Lund, Sweden, <sup>5</sup>Clinical Sciences Malmö, Clinical Memory Research Unit, Lund University, Lund, Sweden

Microstructure imaging aims to estimate specific quantities such as the axonal density through modeling of diffusion MRI (dMRI) data. However, the low information content of conventional dMRI necessitates assumptions limiting the estimates' accuracy. Here, we show how to replace model assumptions with independent information from tensor-valued diffusion encoding and diffusion-relaxation experiments. We present sampling protocols optimized using Cramér-Rao lower bounds allowing precise whole-brain estimation of compartment-specific fractions, diffusivities and  $T_2$  values in 15 minutes and show results from subjects of different ages. The approach greatly expands the set of parameters measurable with dMRI and provides parameter relations informing model constraints.

0733



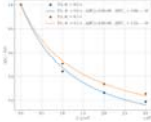
Resolving bundle-specific intra-axonal  $T_2$  within a voxel using a microstructure-informed approach

Muhamed Barakovic<sup>1,2,3</sup>, Chantal MW Tax<sup>1</sup>, Umesh S Rudrapatna<sup>1</sup>, Jonathan Rafael-Patino<sup>2</sup>, Cristina Granziera<sup>3</sup>, Jean-Philippe Thiran<sup>2,4</sup>, Alessandro Daducci<sup>5</sup>, Erick J Canales-Rodriguez<sup>2,4,6</sup>, and Derek K Jones<sup>1,7</sup>

<sup>1</sup>Cardiff University Brain Research Imaging Centre, Cardiff University, Cardiff, United Kingdom, <sup>2</sup>Signal Processing Laboratory 5 (LTS5), Ecole Polytechnique Fédérale de Lausanne, Lausanne, Switzerland, <sup>3</sup>Translational Imaging in Neurology (ThINK) Basel, Department of Biomedical Engineering, University Hospital Basel and University of Basel, Basel, Switzerland, <sup>4</sup>Radiology Department, Centre Hospitalier Universitaire Vaudois and University of Lausanne, Lausanne, Switzerland, <sup>5</sup>Department of Computer Science, University of Verona, Verona, Italy, <sup>6</sup>FIDMAG Germanes Hospitalaries Research Foundation, Barcelona, Spain, <sup>7</sup>Mary MacKillop Institute for Health Research, Faculty of Health Sciences, Australian Catholic University, Melbourne, Australia

At the typical spatial resolution of MRI, approximately 60-90% of voxels in the human brain contain multiple fibre populations. Quantifying microstructural properties of distinct fibre bundles within a voxel is challenging. While progress has been made for diffusion and  $T_1$ -relaxation properties, resolving intra-voxel  $T_2$  heterogeneity remains an open question. Here we proposed a novel framework, COMMIT- $T_2$ , that uses tractography-based spatial regularization. Unlike previously-proposed voxel-based methods, COMMIT- $T_2$  can recover bundle-specific  $T_2$  values within a voxel. Adding this new dimension to the microstructural characterisation of white matter pathways improves the power of tractometry to detect subtle differences in tissue properties.

0734



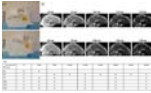
Orientation-dependent biases in powder averaging caused by inhomogeneous distributions of magnetic susceptibility in white matter

Sidsel Winther<sup>1,2</sup>, Henrik Lundell<sup>2</sup>, Mariam Andersson<sup>1,2</sup>, and Tim Dyrby<sup>1,2</sup>

<sup>1</sup>DTU Compute, Technical University of Denmark, Kgs. Lyngby, Denmark, <sup>2</sup>Danish Research Center for Magnetic Resonance, Functional and Diagnostic Imaging and Research, Copenhagen University Hospital Hvidovre, Hvidovre, Denmark

Numerical experiments show orientation dependency of the powder averaged diffusion signal (commonly assumed orientation-invariant) when susceptibility-induced inhomogeneity in white matter is taken into account. This implies an axon-orientation-dependent bias of the diffusion signal from white matter regions containing non-uniformly dispersed myelinated axons, which would lead to an over-estimation of the anisotropy. This implies a potential bias between the interpretation of the signal from eg. the internal capsule (oriented inferior-superior) and corpus callosum (oriented left-right).

0735



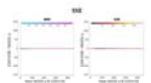
Incorporating T2-orientational dependence into diffusion-T2 correlation experiments using a tiltable coil

Chantal M.W. Tax<sup>1</sup>, Elena Kleban<sup>1</sup>, Muhamed Barakovic<sup>1,2,3</sup>, Maxime Chamberland<sup>1</sup>, and Derek K. Jones<sup>1</sup>

<sup>1</sup>CUBRIC, Cardiff University, Cardiff, United Kingdom, <sup>2</sup>Signal Processing Laboratory 5, Ecole Polytechnique Federale de Lausanne, Lausanne, Switzerland, <sup>3</sup>Translational Imaging in Neurology Basel, Department of Biomedical Engineering, University Hospital Basel, Basel, Switzerland

The anisotropy of white matter is reflected in various white matter contrasts. Transverse relaxation rates can be probed as a function of fibre-orientation with respect to the main magnetic field, while diffusion properties are probed as a function of fibre-orientation with respect to the gradient field. While the latter is easy to obtain in the same head position, the former involves reorientation of the subject's head inside the scanner. In this work we deployed a tiltable RF-coil to study R2 anisotropy of the brain white matter in diffusion-T2 correlation experiments.

0736



Tortuosity assumption not the cause of NODDI's incompatibility with tensor-valued diffusion encoding

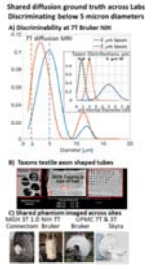
Michele Guerreri<sup>1</sup>, Filip Szczepankiewicz<sup>2,3</sup>, Björn Lampinen<sup>4</sup>, Marco Palombo<sup>1</sup>, Markus Nilsson<sup>2</sup>, and Hui Zhang<sup>1</sup>

<sup>1</sup>Computer Science & Centre for Medical Image Computing, University College London, London, United Kingdom, <sup>2</sup>Clinical Sciences Lund, Department of Radiology, Lund University, Lund, Sweden, <sup>3</sup>Radiology, Brigham and Women's Hospital, Harvard Medical School, Boston, MA, United States, <sup>4</sup>Clinical Sciences Lund, Department of Medical Radiation Physics, Lund University, Lund, Sweden



This work shows that the tortuosity assumption in NODDI can not be identified as the source of incompatibility when the model is extended to data acquired with tensor-valued diffusion encoding. NODDI, originally developed for multi-shell linear tensor encoded (LTE) data, was shown to be inadequate when extended to LTE and spherical tensor encoded (STE) data jointly. The adoption of tortuosity assumption by NODDI has been suggested as a plausible explanation. We conduct a systematic model-comparison study to show that this explanation is inaccurate. We identify a different assumption of the model, the equal-axial-diffusivity, as a source of incompatibility.

0737



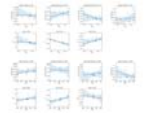
### Diffusion ground truth quantification of axon scale phantom: Limits of diffusion MRI on 7T, 3T and Connectome 1.0

Sudhir Pathak<sup>1</sup>, Walter Schneider<sup>1</sup>, Anthony Zuccolotto<sup>2</sup>, Susie Huang<sup>3</sup>, Qiuyun Fan<sup>4</sup>, Thomas Witzel<sup>5</sup>, Lawrence Wald<sup>4</sup>, Els Fieremans<sup>6</sup>, Michal E. Komlosh<sup>7</sup>, Dan Benjamini<sup>7</sup>, Alexandru V Avram<sup>7</sup>, and Peter J. Basser<sup>7</sup>

<sup>1</sup>University of Pittsburgh, Pittsburgh, PA, United States, <sup>2</sup>Psychology Software Tools, Inc, Pittsburgh, PA, United States, <sup>3</sup>Athinoula A. Martinos Center for Biomedical Imaging, Massachusetts General Hospital, Boston, MA, United States, <sup>4</sup>Department of Radiology, Massachusetts General Hospital, Boston, MA, United States, <sup>5</sup>Massachusetts General Hospital, Boston, MA, United States, <sup>6</sup>Department of Radiology, New York University, New York City, NY, United States, <sup>7</sup>National Institutes of Health, Bethesda, DC, United States

We have constructed a novel Taxon (textile water filled tubes) anisotropic diffusion phantom to provide “ground truth” verification of the current limits of diffusion imaging. This phantom is designed to contain 0.8 micron ID tubes with, a packing density of  $10^6$  per  $\text{mm}^2$ , matched to human axon histology, and allows parametric control of diameters, density, and angle dispersion. On a 7T small-bore scanner, we report the ability to distinguish fine Taxon diameter changes between 2-5 micron diameters and approximate 5 micron ID tubes on the 3T Connectome. This is approaching the anatomical scale of axons found in human brain.

0738



### Comparison of microstructural models of Sodium and Diffusion Basis Spectrum Images

Simona Schiavi<sup>1,2</sup>, Lazar Fleysher<sup>3</sup>, Peng Sun<sup>4</sup>, Nicole Graziano<sup>1</sup>, Arielle Falcone<sup>1</sup>, Yongxian Qian<sup>5</sup>, Fernando E. Boada<sup>5</sup>, Sheng-Kwei Song<sup>4,6,7</sup>, and Matilde Inglese<sup>1,2,3</sup>

<sup>1</sup>Department of Neurology, Icahn School of Medicine at Mount Sinai, New York, NY, United States, <sup>2</sup>DINOEMI, University of Genoa/IRCCS AOU San Martino-IST, Genoa, Italy, <sup>3</sup>Department of Radiology, Icahn School of Medicine at Mount Sinai, New York, NY, United States, <sup>4</sup>Biomedical MR Laboratory, Department of Radiology, Washington University School of Medicine, St. Louis, MO, United States, <sup>5</sup>Department of Radiology, NYU Langone Medical Center, New York, NY, United States, <sup>6</sup>Hope Center for Neurological Disorders, Washington University School of Medicine, St. Louis, MO, United States, <sup>7</sup>Biomedical Engineering, Washington University, St. Louis, MO, United States

Both diffusion weighted MRI and Sodium MRI are imaging techniques sensitive to tissue microstructure. The two methods provide complementary information and use tissue models to interpret observed signals to obtain tissue-specific parameters. We investigated the relationship between several tissue-parameters of the two models in the white matter and in the Corpus Callosum. Our results suggests that, the measured cell volume fraction of sodium agrees with diffusion basis spectrum images features. This opens to the possibility of using sodium MRI to investigate pathological tissues and recover complementary information to those we can retrieve with diffusion MRI.

0739



### Single-shot isotropic diffusion-weighted NMR spectroscopy in the human brain at 7T using tetrahedral encoding

Chloé Najac<sup>1</sup>, Henrik Lundell<sup>2</sup>, Hermien E. Kan<sup>1</sup>, Andrew G. Webb<sup>1</sup>, and Itamar Ronen<sup>1</sup>

<sup>1</sup>C.J. Gorter Center for High Field MRI, Department of Radiology, Leiden University Medical Center, Leiden, Netherlands, <sup>2</sup>Danish Research Centre for Magnetic Resonance, Copenhagen, Denmark

We propose a single-shot isotropic diffusion-weighted magnetic resonance spectroscopy (DW-MRS) sLASER-based sequence which enables single-shot measurement of metabolite apparent diffusion coefficient (ADC) at relatively short diffusion times and reasonable echo times in the human brain at 7T. Five brain metabolites and water ADC values were measured in two brain regions that differs significantly in white (WM) and grey matter (GM) content. Significantly higher  $ADC_{\text{metabolites}}$  and lower  $ADC_{\text{water}}$  were observed in WM compared to GM, illustrating microstructural tissue-specific differences.

0740



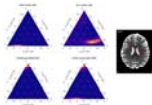
#### Whole-brain mapping of cortical architectonic features with high-resolution MAP-MRI

Alexandru V. Avram<sup>1,2</sup>, Kadharbatcha Saleem<sup>1,2</sup>, Frank Q Ye<sup>3</sup>, Cecil Yen<sup>4</sup>, Michal E Komlos<sup>1,2</sup>, and Peter J Basser<sup>1</sup>

<sup>1</sup>NICHD, National Institutes of Health, Bethesda, MD, United States, <sup>2</sup>The Henry Jackson Foundation, Bethesda, MD, United States, <sup>3</sup>NIMH, National Institutes of Health, Bethesda, MD, United States, <sup>4</sup>NINDS, National Institutes of Health, Bethesda, MD, United States

We apply high-resolution mean apparent propagator (MAP)-MRI to quantify cortical architectonic features in a fixed rhesus macaque brain. Cortical depth profiles of MAP-derived parameters, such as the propagator anisotropy (PA), correlate well with histological stains in corresponding brain regions, and may be used to automatically detect boundaries between cortical areas with distinct cyto- and myeloarchitectonic organization. Mapping cortical architectonic features non-invasively could provide a new radiological tool for diagnosis of developmental and neurodegenerative disorders and improve our understanding of how the human brain is organized and connected.

0741



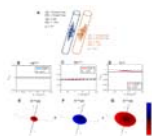
#### Towards Clinical Translation of Microscopic Diffusion Spectrum Imaging

Enrico Kaden<sup>1</sup>, Noemi G Gyori<sup>1,2</sup>, Iulius Dragonu<sup>3</sup>, Chris A Clark<sup>2</sup>, and Daniel C Alexander<sup>1</sup>

<sup>1</sup>Centre for Medical Image Computing, University College London, London, United Kingdom, <sup>2</sup>Great Ormond Street Institute of Child Health, University College London, London, United Kingdom, <sup>3</sup>Siemens Healthcare Ltd, Frimley, United Kingdom

Conventional wisdom suggests that it is necessary to average the diffusion signal over the gradient directions to map microstructural features in the presence of orientational heterogeneity. Contrary to this belief, we show that powder-averaging the signal is redundant and leverage this insight to perform, within the same scan time, diffusion experiments with many rather than few  $b$ -values and with many rather than few gradient waveforms for  $b$ -tensor encoding and beyond, facilitating the translation of advanced techniques such as microscopic diffusion spectrum imaging to clinical practice.

0742



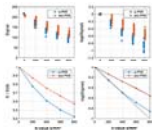
#### Measuring the full diffusional intra- and inter-compartmental kurtosis tensors using double diffusion encoding

Rafael Neto Henriques<sup>1</sup>, Jonas Lyng Olesen<sup>2,3</sup>, Sune Nørhøj Jespersen<sup>2,3</sup>, and Noam Shemesh<sup>1</sup>

<sup>1</sup>Champalimaud Research, Champalimaud Centre for the Unknown, Lisbon, Portugal, <sup>2</sup>Center of Functionally Integrative Neuroscience (CFIN) and MINDLab, Clinical Institute, Aarhus University, Aarhus, Denmark, <sup>3</sup>Department of Physics and Astronomy, Aarhus University, Aarhus, Denmark

Diffusional kurtosis imaging (DKI) quantifies the non-Gaussian degree of diffusion using the kurtosis tensor. However, kurtosis can depend on conflicting sources of non-Gaussian diffusion such as Gaussian diffusion variance (inter-compartmental kurtosis) or the presence of restricted and hindered effects inside compartments (intra-compartmental kurtosis). Here, we develop and apply a novel double diffusion encoding method that is capable of providing the full directional dependence of both inter- and intra-compartmental kurtosis which can be summarized into two distinct kurtosis tensors and thereby improving kurtosis specificity and potentially providing information for diffusion model validation.

0743



Perivascular space fluid contribute to diffusion signal attenuation at low b-value, revisiting extra-cellular space diffusion

Farshid Sepehrband<sup>1</sup>

<sup>1</sup>Stevens Neuroimaging and Informatics Institute, Keck School of Medicine, USC, Los Angeles, CA, United States

Figure 3. Top row: high resolution T2 SPACE image at 7T and manual segmentation results of PVS, highlighting the large presence of PVS across the brain. Second row: a schematic representation of a given conservatively drawn PVS is shown (high resolution images suggested that the PVS has a higher thickness compared to what is shown here). The PVS is presented aside electron microscopy images of white matter axons (as a rough reference).

0744



Impeded diffusion fraction model for multi-exponential DWI: demonstration in kurtosis phantom and prostate cancer

Dariya Malyarenko<sup>1</sup>, Scott D Swanson<sup>1</sup>, and Thomas L Chenevert<sup>1</sup>

<sup>1</sup>University of Michigan, Ann Arbor, MI, United States

Majority of current clinical MRI protocols continue to use DWI qualitatively, as an indicator of impeded diffusion evident from sustained signal at high  $b$ -values. Quantitative microenvironment description relying on multi-exponential diffusion models is precluded by required prolonged multi- $b$  acquisition and high resolution/SNR not routinely achievable in clinical setting. This study presents a model based on multi-compartment formalism to quantify impeded diffusion fraction (IDF, of water coordinated by macromolecules) from conventional clinical DWI acquisition. The physical origin for IDF is verified using two-compartment diffusion kurtosis phantom, and application example is demonstrated for prostate cancer.

## Oral - Power Pitch

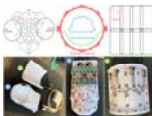
### RF technologies - RF Components & Coils

Wednesday Parallel 5 Live Q&A

Wednesday 13:45 - 14:30 UTC

Moderators: Boris Keil & Xiaotong Zhang

0745



An 8-CH Dipole Transceiver Array with 24-CH Loop Receiver Array for Non-Human Primate Head Imaging at 10.5T

Russell Luke Lagore<sup>1</sup>, Steen Moeller<sup>1</sup>, Lance DelaBarre<sup>1</sup>, Andrea Grant<sup>1</sup>, Jerahmie Radder<sup>1</sup>, Kamil Ugurbil<sup>1</sup>, Essa Yacoub<sup>1</sup>, Noam Harel<sup>1</sup>, and Gregor Adriany<sup>1</sup>

<sup>1</sup>Center for Magnetic Resonance Research, University of Minnesota, Minneapolis, MN, United States

In this work we developed an 8-CH dipole transceiver with 24-channel loop receive array (for a total of 32 receive channels) for head imaging of anesthetized non-human primates at 10.5T. We demonstrate the benefits of receiving with both the dipole array and loop arrays to recapture SNR in deep brain structures and allow for accelerated acquisitions with near lossless parallel imaging performance up to  $R=3$  in either AP or LR. Presented are diffusion and anatomical MR images acquired with this coil.

0746



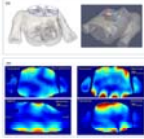
Effect of Coaxial Feed Cables on the Performance of Loop & Dipole Arrays at Ultra High Frequencies

Myung Kyun Woo<sup>1</sup>, Lance DelaBarre<sup>1</sup>, Russell Lagore<sup>1</sup>, Andrea Grant<sup>1</sup>, Steve Jungst<sup>1</sup>, Yigitcan Eryaman<sup>1</sup>, Kamil Ugurbil<sup>1</sup>, and Gregor Adriany<sup>1</sup>

<sup>1</sup>Center for Magnetic Resonance Research, Minneapolis, MN, United States

We designed and built three elliptically arranged 8- and 16-channel transceiver dipole and loop arrays for the human head applications and evaluated the influence of coaxial feed cables on the overall array performance. The influence of coaxial feed cables was evaluated in simulation and compared against actual built arrays in terms of B1+ and SAR efficiency. For all three arrays we consistently observed ~30 % performance reduction compared to the “ideal” coil with no coaxial cables.

0747



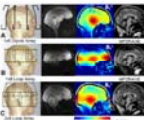
Customized B1+-Shaping using Multi-Channel Transceiver Array Prototype for 7T Cardiac MRI with Central Elements Symmetry

Maxim Terekhov<sup>1</sup>, Ibrahim A. Elabyad<sup>1</sup>, Frank Resmer<sup>2</sup>, Titus Lanz<sup>2</sup>, Theresa Reiter<sup>1,3</sup>, David Lohr<sup>1</sup>, Wiebke Schlöttelburg<sup>1,4</sup>, and Laura M. Schreiber<sup>1</sup>

<sup>1</sup>Chair of Cellular and Molecular Imaging, Comprehensive Heart Failure Center (CHFC), University Hospital Würzburg, Wuerzburg, Germany, <sup>2</sup>RAPID Biomedical, Rimpfing, Germany, <sup>3</sup>Department of Internal Medicine I, University Hospital Würzburg, Wuerzburg, Germany, <sup>4</sup>Institute of Diagnostic and Interventional Radiology, University Hospital Würzburg, Wuerzburg, Germany

Multiple element transmits and receive (mTx) phased arrays allow for improvement of the image quality in ultra-high-field ( $B_0 \geq 7T$ ) cardiac MRI (cMRI). The optimization performed for both transmit and receive requires novel approaches regarding mTx element geometry and positioning making a B1-shimming of such arrays a complicated problem. We have demonstrated the initial experience of the case-specific B1-shimming of the mTx-array design for cMRI at 7T. The design with a central symmetry of elements and tailored cost function used for driving phases optimization allows for high flexibility in shaping of predefined target B1+ profiles.

0748



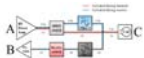
Asymmetric Dipole Head Array for Ultra-High-Field Magnetic Resonance Imaging Turns “Dielectric Resonance” from an Enemy to a Friend.

Nikolai Avdievich<sup>1</sup>, Georgiy Solomakha<sup>2</sup>, Loreen Ruhm<sup>1</sup>, Jonas Bause<sup>1,3</sup>, Anke Henning<sup>1,4</sup>, and Klaus Scheffler<sup>1,5</sup>

<sup>1</sup>Max Planck Institute for Biological Cybernetics, Tuebingen, Germany, <sup>2</sup>Nanophotonics and Metamaterials, ITMO University, St.Petersburg, Russian Federation, <sup>3</sup>Graduate School of Neural and Behavioral Sciences, Tuebingen, Germany, <sup>4</sup>Advanced Imaging Research Center, University of Texas Southwestern Medical Center, Dallas, TX, United States, <sup>5</sup>Department for Biomedical Magnetic Resonance, University of Tübingen, Tuebingen, Germany

We developed a novel 9.4T (400MHz) human head transceiver array consisted of 8 optimized bent folded dipole antennas. Due to an asymmetrical shape of dipoles (bending) and the RF shield, the array simultaneously excites two modes including a circular polarized mode of the array itself, and the TE mode of the human head. Mode mixing can be easily controlled by changing the folded length. As a result, the new array provides superior whole-brain coverage compared to various 8-element loop and dipole arrays or even to a more complicated 16-element loop array. In addition, the maximum local SAR is substantially reduced.

0749



Design of frequency division duplex RF system for frequency encoding using Bloch-Siegert shift

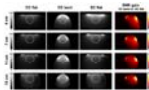
Yonghyun Ha<sup>1</sup>, Kartiga Selvaganesan<sup>1</sup>, Charles Rogers III<sup>1</sup>, Baosong Wu<sup>1</sup>, Sajad Hosseinnzhadian<sup>1</sup>, Gigi Galiana<sup>1</sup>, and R. Todd Constable<sup>1</sup>

<sup>1</sup>Department of Radiology and Biomedical Imaging, Yale School of Medicine, New Haven, CT, United States

In this work, we designed a frequency division duplex RF system for frequency encoding using Bloch-Siegert shift at very low field, with a modification of dual-band pass filters. Although the off-resonance frequency (870 kHz) is very close to the Larmor frequency (1 MHz), the applied off-resonance signal can be filtered out by a modified dual-band pass filter on the receive path. This system allows us to apply a 870 kHz transmit pulse while receiving 1 MHz signal from the RF coil.

---

0750



### Flexible receive-only coaxial coils with multiple turns and gaps for 3 T MRI

Lena Nohava<sup>1,2</sup>, Raphaela Czerny<sup>2</sup>, Michael Obermann<sup>1,2</sup>, Jacques Felbinger<sup>3</sup>, Roberta Frass-Kriegl<sup>2</sup>, Jean-Christophe Ginefri<sup>1</sup>, and Elmar Laistler<sup>2</sup>

<sup>1</sup>IR4M (Imagerie par Résonance Magnétique et Multi-Modalités), UMR8081, Université Paris-Sud/CNRS, Université Paris-Saclay, Orsay, France, <sup>2</sup>Division MR Physics, Center for Medical Physics and Biomedical Engineering, Medical University of Vienna, Vienna, Austria, <sup>3</sup>Université de Lorraine, Inserm, IADI, Nancy, France

A bench and 3 T MRI study of flexible multi-turn multi-gap coaxial coils and standard copper wire coils with 4, 7, 10 and 15 cm loop diameter is presented. The coaxial coils are made of four different cable types and can be employed for different biomedical applications where form-fitting the coil to the subject anatomy is advantageous. We evaluate the receive-only coaxial coils' active detuning performance, their robustness upon bending and demonstrate a significant SNR gain when using bent coaxial coils instead of flat standard coils.

---

0751



### Practical eight-channel pTx system for 7 T MRI with optically controlled and monitored on-coil current-source RF amplifiers

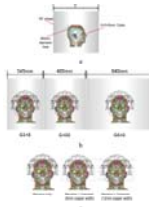
Natalia Gudino<sup>1</sup>, Jacco A de Zwart<sup>1</sup>, and Jeff H Duyn<sup>1</sup>

<sup>1</sup>LFMI, NINDS, National Institutes of Health, Bethesda, MD, United States

We present an eight channel pTx-Rx system built with optically controlled and monitored on-coil Tx amplifiers and optical pTx control optimized for 7 T imaging. We show preliminary results of the technology implemented for human head imaging.

---

0752



### Shielding Effects on Signal-to-Noise Ratio at Ultra-High Field MRI

Bei Zhang<sup>1,2</sup>, Gregor Adriany<sup>3</sup>, Andrea Grant<sup>3</sup>, Russell Lagore<sup>3</sup>, Brian Rutt<sup>4</sup>, Kamil Ugurbil<sup>3</sup>, and Riccardo Lattanzi<sup>1,5</sup>

<sup>1</sup>Center for Advanced Imaging Innovation and Research, New York University School of Medicine, New York, NY, United States, <sup>2</sup>Advanced Imaging Research Center, University of Texas Southwestern Medical Center, Dallas, TX, United States, <sup>3</sup>Center for Magnetic Resonance Research, University of Minnesota, Minneapolis, MN, United States, <sup>4</sup>Stanford University, Stanford, CA, United States, <sup>5</sup>The Sackler Institute of Graduate Biomedical Sciences, New York University School of Medicine, New York, NY, United States

We evaluated the effect of a radio frequency shield on the signal-to-noise ratio (SNR) of a loop coil at various field strengths in simulation. At 7T, SNR constantly improves as the shield diameter increases. At higher field strengths, SNR is maximized when using an optimal shield diameter, which is inversely proportional to the frequency. We also show that central SNR for a 32-channel receive array could drop by a factor of two when using a non-optimal shield diameter at 10.5T. Inserting a transmit array between the receiver and an optimally-sized shield could considerably deteriorate SNR.

---

0753



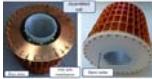
### A 22-channel high impedance glove array for dynamic hand and wrist imaging at 3T

Bei Zhang<sup>1,2</sup>, Justin Ho<sup>1</sup>, Shota Hodono<sup>1,3</sup>, Bili Wang<sup>1</sup>, Ryan Brown<sup>1,3</sup>, Riccardo Lattanzi<sup>1,3</sup>, Markus Vester<sup>4</sup>, Robert Rehner<sup>4</sup>, and Martijn Cloos<sup>1,3</sup>

<sup>1</sup>Center for Advanced Imaging Innovation and Research, New York University School of Medicine, New York, NY, United States, <sup>2</sup>Advanced Imaging Research Center, University of Texas Southwestern Medical Center, Dallas, TX, United States, <sup>3</sup>The Sackler Institute of Graduate Biomedical Sciences, New York University School of Medicine, New York, NY, United States, <sup>4</sup>Siemens Healthcare, Erlangen, Germany

We constructed a 22-channel high impedance glove array for dynamic hand and wrist imaging. The glove array has a robust, flexible, comfortable, safe, and cleanable construction. Siemens Tim4G technology was used to connect coils to the scanner through a single bundled cable to streamline the workflow and permit hand postures that are uninhibited by bulky components. Compared to a rigid commercial 16-channel Hand/Wrist coil, our 22-channel glove array showed higher SNR on fingers and wrist and comparable SNR on the palm and top of the hand. Further analysis revealed low coupling between the coils that resulted in good acceleration performance.

0754

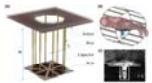


**Experimental Characterization of Artificial Magnetic Shield for Improvement of Small-Animal Birdcage at 7 T**  
Ksenia Lezhennikova<sup>1</sup>, Redha Abdeddaim<sup>2</sup>, Anna Hurshkainen<sup>1</sup>, Alexandre Vignaud<sup>3</sup>, Marc Dubois<sup>2,4</sup>, Konstantin Simovski<sup>5</sup>, Alexander Raaijmakers<sup>6</sup>, Irina Melchakova<sup>1</sup>, Stefan Enoch<sup>2</sup>, Pavel Belov<sup>1</sup>, and Stanislav Glybovski<sup>1</sup>

<sup>1</sup>Faculty of Physics and Engineering, ITMO University, St.Petersburg, Russian Federation, <sup>2</sup>CNRS, Centrale Marseille, Institut Fresnel, Aix Marseille Univ, Marseille, France, <sup>3</sup>CEA-Saclay, DRF/I2BM/Neurospin/UNIR, Université Paris-Saclay, Gif-sur-Yvette Cedex, Paris, France, <sup>4</sup>CNRS, CRMBM, Aix Marseille Univ, Marseille, France, <sup>5</sup>Department of Electronics and Nanoengineering, AALTO University, AALTO, Finland, <sup>6</sup>Biomedical Engineering, Eindhoven University of Technology, Eindhoven, Netherlands

We proposed a practical realization of an artificial shield for a small-animal birdcage coil for 7T MRI based on a cylindrical miniaturized corrugated structure, which demonstrates the property of a constructive interference inside the coil. The presence of a conventional metallic shield around the birdcage significantly limits the coil efficiency because of the destructive interference between the magnetic field of the shield and the primary field of the coil in the subject. We numerically and experimentally demonstrated that the proposed structure placed around the birdcage could increase the efficiency for relatively small samples due to its in-phase reflection.

0755



**A novel RF-resonator for penile imaging**

Evgeniy Alekseevich Koreshin<sup>1</sup>, Mikhail Zubkov<sup>1</sup>, Alexander Yurievich Efimtcev<sup>2</sup>, Alexandr Mikhailovich Gulko<sup>3</sup>, and Irina Valerievna Melchakova<sup>1</sup>

<sup>1</sup>Faculty of Physics and Engineering, ITMO University, Saint-Petersburg, Russian Federation, <sup>2</sup>Department of Radiology, Federal Almazov North-West Medical Research Center, Saint-Petersburg, Russian Federation, <sup>3</sup>1st urology department, City Center of Endourology and New Technologies, Saint-Petersburg, Russian Federation

We present a new design of a radiofrequency resonator for urological applications. The resonator functions by inductively coupling to the body coil of a 1.5 T MR-scanner. This configuration of the Tx-Rx path allows increasing the transmission efficiency and signal to noise ratio (SNR) while reducing the specific absorption rate (SAR). Phantom and *in-vivo* imaging shows that the resonator provides around 100-fold SAR reduction and 10-fold transmission efficiency increase. Phantom imaging shows doubled SNR compared to the commercial flexible 4-element Rx coil. *In-vivo* imaging shows only a 50% increase in SNR, improved patient positioning and reduced the artifacts rate.

0756



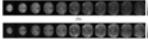
**High impedance coils versus conventional loop coils for transmit purposes: a comparison using an eight channel head coil array for 7 Tesla**

Carel Costijn van Leeuwen<sup>1</sup>, Masoud Mazraeh Mollaei Sharifian<sup>2</sup>, Luca van Dijk<sup>1</sup>, Konstantin Simovski<sup>2</sup>, and Alexander J. E. Raaijmakers<sup>1,3</sup>

<sup>1</sup>Department of radiology, University Medical Center Utrecht, Utrecht, Netherlands, <sup>2</sup>Aalto University, Espoo, Finland, <sup>3</sup>Biomedical Engineering, Eindhoven University of Technology, Eindhoven, Netherlands

This study compares high impedance coils to conventional loop coils for transmit purposes at 7 Tesla. A new design for high impedance coils is presented. Two eight-channel head arrays of equal dimensions were created; one using high impedance coils, one with conventional loops. B1 field maps are produced to compare transmit efficiency. Scattering parameters are measured in various loading conditions to compare inter-element coupling. The high impedance coils perform worse in terms of transmit efficiency, and better in terms of coupling.

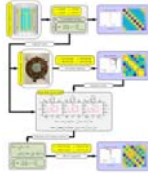
---

0757  Optimization of a close-fitting volume RF coil using linear programming for brain imaging at 6.5 mT  
Sheng Shen<sup>1,2</sup>, Zheng Xu<sup>1</sup>, Neha Koonjoo<sup>2,3,4</sup>, and Matthew S. Rosen<sup>2,3,4</sup>

<sup>1</sup>State Key Laboratory of Power Transmission Equipment and System Security and New Technology, Chongqing University, Chongqing, China, <sup>2</sup>MGH/A.A. Martinos Center for Biomedical Imaging, Cambridge, MA, United States, <sup>3</sup>Department of Physics, Harvard University, Cambridge, MA, United States, <sup>4</sup>Harvard Medical School, Boston, MA, United States

The use of a close-fitting roughly head-shaped volume coil for MRI has the merit of improving the SNR from the brain. However, the surface of the RF coil follows that of the head, making it difficult to determine the optimal coil winding pattern. Here, we proposed a method which combines finite element method simulation and linear programming to optimize the coil pattern of a close-fitted RF coil with the objective of maximizing its SNR and RF-magnetic-field homogeneity for operation at ultra-low field (6.5 mT, 276 kHz). We then tested the optimized coil by imaging a water-filled phantom using a 3D-bSFFP.


---

0758  Design of an 8-channel transmit array coil using the equivalent circuit model of the manufactured structure  
Ehsan Kazemivalipour<sup>1,2</sup>, Alireza Sadeghi-Tarakameh<sup>1,2</sup>, Ugur Yilmaz<sup>2</sup>, and Ergin Atalar<sup>1,2</sup>

<sup>1</sup>Electrical and Electronics Engineering Department, Bilkent University, Ankara, Turkey, <sup>2</sup>National Magnetic Resonance Research Center (UMRAM), Bilkent University, Ankara, Turkey

We propose a practical approach to designing transmit array (TxArray) precisely by integrating the equivalent circuit model of the manufactured structure and its EM simulation results to reduce the measurements and simulations differences caused by the imperfection in manufacturing. We investigate the performance of a shielded 8-channel degenerate birdcage head TxArray at 123.2MHz together with simulation and experiment to validate the proposed method. All self/mutual-inductances and self/mutual-resistances of the manufactured TxArray have been computed to determine the optimum capacitor values by minimization of the total return power from the coil.

---

0759  BPSK/ASK Wireless Link Assessment for MRI  
Greig Cameron Scott<sup>1</sup>, Shreyas Vasanawala<sup>2</sup>, Fraser Robb<sup>3</sup>, and John Pauly<sup>2</sup>

<sup>1</sup>Electrical Engineering, Stanford University, Stanford, CA, United States, <sup>2</sup>Stanford University, Stanford, CA, United States, <sup>3</sup>GE Healthcare, Aurora, OH, United States

We assess the use of binary phase shift keyed and amplitude shift keyed modulation to develop a very short range wireless link. Here the signal integrity for transmission of 200 Mbps at 3.2 GHz carrier frequencies were demonstrated in a mock MRI bore environment. This approach provides a viable path for wireless MRI receive coil data transfer.

---

## Oral

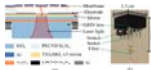
### RF technologies - Novel RF Approaches

Wednesday Parallel 5 Live Q&A

Wednesday 13:45 - 14:30 UTC

Moderators: Lucia Navarro de Lara & Manuela Rösler

0760



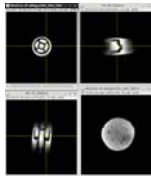
### Magnetic resonance imaging with direct optical detection

Anders Simonsen<sup>1</sup>, Juan D. Sánchez-Heredia<sup>2</sup>, Sampo Saarinen<sup>1</sup>, Jan H. Ardenkjær-Larsen<sup>2</sup>, Albert Schliesser<sup>1</sup>, and Eugene S. Polzik<sup>1</sup>

<sup>1</sup>Niels Bohr Institute, University of Copenhagen, Copenhagen, Denmark, <sup>2</sup>Department of Health Technology, Technical University of Denmark, Kgs. Lyngby, Denmark

A new approach to MRI detection is reported, where an optomechanical transducer directly converts and amplifies the MR signal to amplitude modulation of laser light. The transducer, which is simultaneously a capacitor and an optical cavity, is connected directly in parallel to the receive coil. The mechanical Q-factor of the transducer is 1500, providing a 3 dB bandwidth of 1 kHz. We show here for the first time that this technology can be used to directly acquire a <sup>13</sup>C MRI at 3T (32.13 MHz), and reconstruct it using the standard pipeline of a commercial MR scanner.

0761



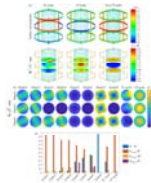
### A Non-Magnetic Staggered Commutation Based Circulator to Achieve Time-Efficient Simultaneous Transmit and Receive (STAR) MRI

Hazal Yuksel<sup>1</sup>, Lance DelaBarre<sup>2</sup>, Djaudat Idiyatullin<sup>3</sup>, Julie Kabil<sup>4</sup>, Gregor Adriany<sup>3</sup>, Sung-Min Sohn<sup>5</sup>, Harish Krishnaswamy<sup>1</sup>, John Thomas Vaughan<sup>4</sup>, and Michael Garwood<sup>3</sup>

<sup>1</sup>Electrical Engineering, Columbia University, New York, NY, United States, <sup>2</sup>Center for Magnetic Resonance Research, University of Minnesota, Minneapolis, MN, United States, <sup>3</sup>University of Minnesota, Minneapolis, MN, United States, <sup>4</sup>Columbia University, New York, NY, United States, <sup>5</sup>Arizona State University, Tempe, AZ, United States

Traditional MRI relies on the temporal separation of the receiver (RX) and transmitter (TX) to solve the problem of self-interference. Often, the TX signal is billions of times larger than the RX signal, and T/R switches are used so the TX does not saturate or destroy the RX. This leads to an inefficient method of acquiring imaging data for especially fast decaying signals. We propose a magnetic-free, PCB based circulator to remove the T/R switch and achieve simultaneous transmit and receive MRI. We present images of a phantom acquired with a continuous SWIFT sequence to validate the concept.

0762



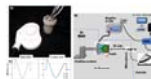
### Design of transmit array coils for MRI by minimizing the modal reflection coefficients

Ehsan Kazemivalipour<sup>1,2</sup>, Alireza Sadeghi-Tarakameh<sup>1,2</sup>, and Ergin Atalar<sup>1,2</sup>

<sup>1</sup>Electrical and Electronics Engineering Department, Bilkent University, Ankara, Turkey, <sup>2</sup>National Magnetic Resonance Research Center (UMRAM), Bilkent University, Ankara, Turkey

We propose a general analysis based on minimization of modal reflection coefficients, providing a simple tool for quantifying the performance of transmit array (TxArray) coils in terms of power efficiency. We investigate the performance of various dual-row birdcage TxArrays, with an additional degree of freedom to correct B<sub>1+</sub>-field inhomogeneities by adding RF shimming ability in the longitudinal-direction, together with simulations and experiments. The chosen structure of the TxArray allows the coil to act like degenerate birdcage coils. We demonstrate when TxArrays are properly designed, in some critical excitation modes such as circularly-polarized (CP) mode, the total reflection becomes negligibly small.

0763



### Assessment of MR compatibility for multichannel stimulation using three-axis TMS coil elements

Lucia Navarro de Lara<sup>1,2</sup>, Mohammad Daneshzand<sup>1,2</sup>, Anthony Mascarenas<sup>3</sup>, Douglas Paulson<sup>3</sup>, Sergey Makarov<sup>1,4</sup>, Jason Stockmann<sup>1,2</sup>, Larry Wald<sup>1,2,5</sup>, and Aapo Nummenmaa<sup>1,2</sup>



<sup>1</sup>Radiology, A.A Martinos Center for Biomedical Imaging/MGH, Charlestown, MA, United States, <sup>2</sup>Harvard Medical School, Boston, MA, United States, <sup>3</sup>Tristan Technologies, San Diego, CA, United States, <sup>4</sup>Department of Electrical and Computer Engineering, A.A Martinos Center for Biomedical Imaging/MGH, Worcester, MA, United States, <sup>5</sup>HST/MIT, Cambridge, MA, United States

We investigate the feasibility of using small-diameter three-axis TMS coil as a basis for constructing a simultaneous stimulation and imaging array. We present an MR-compatible 3-axis TMS coil prototype comprising of three orthogonal coil X/Y/Z units. We assess the influence of the TMS coil element on the MRI images and measure the sound pressure levels with systematically varying the current amplitudes and coil orientation with respect to the magnetic field. Supported by simulations, we conclude that construction of a large-scale multichannel; system using such a 3-axis TMS elements as a basis appears feasible but the acoustic properties should be improved

0764



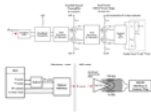
#### A 64-Channel 7T array coil for accelerated brain MRI

Azma Mareyam<sup>1</sup>, John E. Kirsch<sup>1,2</sup>, Yulin Chang<sup>3</sup>, Gunjan Madan<sup>3</sup>, and Lawrence L. Wald<sup>1,2</sup>

<sup>1</sup>Athinoula A. Martinos Center for Biomedical Imaging, Massachusetts General Hospital, Charlestown, MA, United States, <sup>2</sup>Harvard Medical School, Boston, MA, United States, <sup>3</sup>Siemens Medical Solutions USA, Boston, MA, United States

We construct and test a prototype 64-channel brain array coil for 7T and compare it to a 32-channel coil of similar design. Coil characteristics like signal to noise ratio, noise correlation matrix, and noise amplification (G-factor) for parallel imaging are described as well as and a comparison of the B1+ maps to assess birdcage coil efficiency and homogeneity. The coil was designed on a split-half former with a sliding top half to facilitate patient entry and utilizes a sliding birdcage coil for transmit

0765



#### Dual-Tuned Optically Controlled On-Coil Switch-Mode Amplifier

Natalia Gudino<sup>1</sup>, Stephen J Dodd<sup>1</sup>, Steve Li<sup>2</sup>, and Jeff H Duyn<sup>1</sup>

<sup>1</sup>LFMI, NINDS, National Institutes of Health, Bethesda, MD, United States, <sup>2</sup>MIB, NIMH, National Institutes of Health, Bethesda, MD, United States

Optically controlled on-coil amplifiers have been presented for the practical implementation of pTx system at ultra-high field MRI. We present a new prototype that can transmit power to excite <sup>1</sup>H and X-nuclei. We show bench and MRI data with a dual-tuned on-coil amplifier implementation for <sup>1</sup>H and <sup>31</sup>P excitation at 7T. We expect this technology can allow a simpler and more versatile implementation of a multinuclear multichannel hardware compared to the traditional multinuclear setup based on 50 Ω broadband voltage mode amplification.

0766



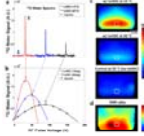
#### First prototype of a Stream-Function-based Multi-Coil Array dedicated to human brain shimming at Ultra-High-Field

Bruno Pinho Meneses<sup>1,2</sup>, Jason Stockmann<sup>3,4</sup>, and Alexis Amadon<sup>1</sup>

<sup>1</sup>Neurospin/CEA-Saclay, Gif-sur-Yvette, France, <sup>2</sup>Université Paris-Saclay, Saclay, France, <sup>3</sup>Athinoula A. Martinos Center for Biomedical Imaging, Charlestown, MA, United States, <sup>4</sup>Harvard Medical School, Boston, MA, United States

Using Singular Value Decomposition of optimal Stream Functions computed from a database of 100 B<sub>0</sub> fieldmaps, a 13-channel cylindrical optimized Multi-Coil Array for shimming of the human brain is built and tested in an experimental setup for field measurement at 7T. Such measurements are compared to expected performances, serving as proof of concept for this novel design methodology. Performance is compared to what would be achieved by matrix multi-coil array designs patterned on a cylinder.

0767



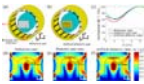
### Permittivity-Tunable Ceramic Technology for Largely Improving B<sub>1</sub> fields and SNR for Broad MR Imaging Applications

Byeong-Yeul Lee<sup>1</sup>, Xiao-Hong Zhu<sup>1</sup>, Hannes M. Wiesner<sup>1</sup>, Maryam Sarkarat<sup>2</sup>, Sebastian Rupprecht<sup>3</sup>, Michael T Lanagan<sup>2</sup>, Qing X Yang<sup>3</sup>, and Wei Chen<sup>1</sup>

<sup>1</sup>CMRR, Radiology, University of Minnesota, Minneapolis, MN, United States, <sup>2</sup>Department of Engineering Science and Mechanics, Pennsylvania State University, University Park, PA, United States, <sup>3</sup>Center for NMR Research, Neurosurgery, Pennsylvania State College of Medicine, Hershey, PA, United States

We present an innovative technique of tunable ultrahigh dielectric constant (tuHDC) ceramics incorporating RF coil(s) for MR imaging applications. The ceramic has a very high permittivity tunability of 2000-15000 by varying the ceramic temperature between few to 40 °C to achieve optimal performance at the nuclide Larmor frequency of interest, resulting in larger B<sub>1</sub> field and SNR improvements for <sup>1</sup>H MRI at 1.5T clinic scanner and <sup>17</sup>O MRSI at 10.5T human scanner. We found a large denoising effect in <sup>17</sup>O MRSI, which further boosts the SNR gain. The technology should benefit for biomedical research and clinical diagnosis.

0768



### Design and demonstration of an artificial dielectric for 7 T MRI

Vsevolod Vorobyev<sup>1</sup>, Alena Shchelokova<sup>1</sup>, Irena Zivkovic<sup>2</sup>, Alexey Slobozhanyuk<sup>1</sup>, Juan Domingo Baena<sup>3</sup>, Juan Pablo del Risco<sup>4</sup>, Redha Abdeddaim<sup>5</sup>, Andrew Webb<sup>2,6</sup>, and Stanislav Glybovski<sup>1</sup>

<sup>1</sup>Department of Nanophotonics and Metamaterials, ITMO University, Saint Petersburg, Russian Federation, <sup>2</sup>Department of Radiology, C.J.Gorter Center for High Field MRI, Leiden University Medical Center, Leiden, Netherlands, <sup>3</sup>Department of Physics, Universidad Nacional de Colombia, Bogota, Colombia, <sup>4</sup>School of Exact Sciences and Engineering, Universidad Sergio Arboleda, Bogota, Colombia, <sup>5</sup>Aix Marseille University, CNRS, Centrale Marseille, Institut Fresnel, Marseille, France, <sup>6</sup>Stevens Research Center, Carle Foundation Hospital, Urbana, IL, United States

We present a new approach replacing high-permittivity water-based dielectric pads with a non-resonant low-cost artificial dielectric to improve MR image quality by modifying the interferences present in the radiofrequency field at 7T MRI. The artificial dielectric comprises a stack of metal patches printed on dielectric substrates. Numerical studies and imaging of a head-phantom with the proposed structure showed the same increase in the transmit radiofrequency field distribution at the area of interest as for conventional dielectric pads. The advantages of the new structure include ease of manufacture and long-term stability.

## Oral

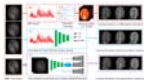
### Advances in Quantitative MRI - Advances in MR Fingerprinting

Wednesday Parallel 5 Live Q&A

Wednesday 14:30 - 15:15 UTC

Moderators: Guido Buonincontri & Debra McGivney

0867



### High Fidelity Direct-Contrast Synthesis from Magnetic Resonance Fingerprinting in Diagnostic Imaging

Ke Wang<sup>1</sup>, Mariya Doneva<sup>2</sup>, Thomas Amthor<sup>2</sup>, Vera C. Keil<sup>3</sup>, Ekin Karasan<sup>1</sup>, Fei Tan<sup>4</sup>, Jonathan I. Tamir<sup>1,5</sup>, Stella X. Yu<sup>1,6</sup>, and Michael Lustig<sup>1</sup>

<sup>1</sup>Electrical Engineering and Computer Sciences, University of California, Berkeley, Berkeley, CA, United States, <sup>2</sup>Philips Research, Hamburg, Germany, <sup>3</sup>Universitätsklinikum Bonn, Bonn, Germany, <sup>4</sup>Bioengineering, UC Berkeley-UCSF, San Francisco, CA, United States, <sup>5</sup>Electrical and Computer Engineering, The University of Texas at Austin, Austin, TX, United States, <sup>6</sup>International Computer Science Institute, University of California, Berkeley, Berkeley, CA, United States

MR Fingerprinting is an emerging attractive candidate for multi-contrast imaging since it quickly generates reliable tissue parameter maps. However, contrast-weighted images generated from parameter maps often exhibit artifacts due to model and acquisition imperfections. Instead of direct modeling, we propose a supervised method to learn the mapping from MRF data directly to synthesized contrast-weighted images, *i.e.*, direct contrast synthesis (DCS). *In-vivo* experiments on both volunteers and patients show substantial improvements of our proposed method over previous DCS method and methods that derive synthetic images from parameter maps.

0868



#### Feasibility of MR fingerprinting using a high-performance 0.55T MRI system

Adrienne E. Campbell-Washburn<sup>1</sup>, Yun Jiang<sup>2</sup>, Gregor Kördörfer<sup>3,4</sup>, Mathias Nittka<sup>3</sup>, and Mark A. Griswold<sup>2</sup>

<sup>1</sup>National Heart, Lung, and Blood Institute, National Institutes of Health, Bethesda, MD, United States, <sup>2</sup>Department of Radiology, Case Western Reserve University, Cleveland, OH, United States, <sup>3</sup>Siemens Healthcare GmbH, Erlangen, Germany, <sup>4</sup>Friedrich-Alexander-Universität Erlangen-Nürnberg, Erlangen, Germany

We assess the feasibility of T1 and T2 mapping with MR fingerprinting implemented on a high-performance 0.55T system that combines contemporary hardware and imaging methods with a lower magnetic field strength. Quantitative values correlated closely to spin-echo measurements in the NIST phantom. Brain MRF was evaluated in 12 healthy volunteers and liver MRF was evaluated in one volunteer as a proof-of-concept. At 0.55T, T1 was 539ms (white matter) and 660ms (gray matter), and T2 was 64ms (white matter) and 76ms (gray matter). The combination of MRI fingerprinting and low-field MRI systems provides an opportunity for rapid, low-cost, quantitative imaging.

0869



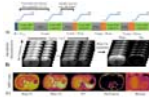
#### An attempt to understand why we measure longer relaxation times in quantitative muscle MRI using MRF than using conventional methods

Kirsten Koolstra<sup>1</sup>, Andrew Webb<sup>1</sup>, and Peter Börner<sup>1,2</sup>

<sup>1</sup>Leiden University Medical Center, Leiden, Netherlands, <sup>2</sup>Philips Research Hamburg, Hamburg, Germany

Fast relaxation time quantification is important in dynamic muscle studies and can be achieved using Magnetic Resonance Fingerprinting (MRF). The  $T_2$  values in muscle measured with MRF are consistently higher than those measured with the conventionally used multi-echo turbo-spin-echo (MSE) method, while  $T_1$  values are closer to reference measurements. We hypothesize that this increase can in part be attributed to an increased sensitivity of MRF to flow compared to MSE. In this work we test the sensitivity of MRF to flow in muscle by saturating a slab at different distances above the imaging slice for variable suppression of inflowing spins.

0870



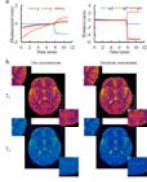
#### Liver Dixon MR Fingerprinting: T1, T2, T2\* and fat fraction tissue characterization

Olivier Jaubert<sup>1</sup>, Cristobal Arrieta<sup>2,3</sup>, Gastao Cruz<sup>1</sup>, Aurelien Bustin<sup>1</sup>, Torben Schneider<sup>4</sup>, Georgios Georgiopoulos<sup>1</sup>, Pier-Giorgio Masci<sup>1</sup>, Carlos Sing-Long<sup>3,5,6</sup>, Rene Michael Botnar<sup>1</sup>, and Claudia Prieto<sup>1</sup>

<sup>1</sup>Biomedical Engineering Department, School of Biomedical Engineering and Imaging Sciences, King's College London, London, United Kingdom, <sup>2</sup>Biomedical Imaging Center, Pontificia Universidad Católica de Chile, Santiago, Chile, <sup>3</sup>Millennium Nucleus for Cardiovascular Magnetic Resonance, Santiago, Chile, <sup>4</sup>Philips Healthcare, London, United Kingdom, <sup>5</sup>Instituto de Ingeniería Matemática y Computacional, Pontificia Universidad Católica de Chile, Santiago, Chile, <sup>6</sup>Millennium Nucleus Center for the Discovery of Structures in Complex Data, Chile, Santiago, Chile

Quantitative  $T_1$ ,  $T_2$ ,  $T_2^*$  and fat fraction (FF) maps are promising imaging biomarkers for the assessment of liver disease. Magnetic Resonance Fingerprinting has been recently proposed for fast  $T_1$ ,  $T_2$  and  $M_0$  mapping of the liver, however in the presence of high iron or fat concentrations corrections using separately acquired  $T_2^*$  and FF maps are needed. Here we propose a novel approach which enables simultaneous liver  $T_1$ ,  $T_2$ ,  $T_2^*$  and FF maps from a single  $\sim 15$ s breath-hold scan. The proposed approach was evaluated on phantoms, 8 healthy subjects and 2 patients in comparison to conventional mapping techniques.

0871



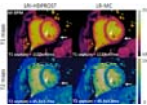
### Improving motion robustness of 3D MR Fingerprinting using fat navigator

Yong Chen<sup>1</sup>, Xiaopeng Zong<sup>2</sup>, Dan Ma<sup>1</sup>, Weili Lin<sup>2</sup>, and Mark Griswold<sup>1</sup>

<sup>1</sup>Radiology, Case Western Reserve University, Cleveland, OH, United States, <sup>2</sup>Radiology, University of North Carolina at Chapel Hill, Chapel Hill, NC, United States

In this study, we developed a 3D MRF method in combination with fat navigator to improve its motion sensitivity for neuroimaging. A rapid fat navigator sampling was achieved at 3T by using the stack-of-spirals acquisition and non-Cartesian spiral GRAPPA. The improvement in motion robustness was achieved without increasing the scan time for quantitative tissue mapping. Our preliminary results demonstrate that 1) the added fat navigator sampling does not influence the accuracy of  $T_1$  and  $T_2$  quantification, and 2) the motion robustness for quantitative tissue mapping using MRF was largely improved with the proposed method.

0872



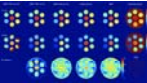
### Generalised Low-Rank Non-rigid Motion Corrected reconstruction for 2D Cardiac MRF

Gastao Cruz<sup>1</sup>, Haikun Qi<sup>1</sup>, Olivier Jaubert<sup>1</sup>, Aurelien Bustin<sup>1</sup>, Thomas Kuestner<sup>1</sup>, Torben Schneider<sup>2</sup>, René M. Botnar<sup>1</sup>, and Claudia Prieto<sup>1</sup>

<sup>1</sup>Biomedical Engineering Department, School of Biomedical Engineering and Imaging Sciences, King's College London, London, United Kingdom, <sup>2</sup>Philips Healthcare, Guildford, United Kingdom

Cardiac Magnetic Resonance Fingerprinting (cMRF) has been proposed for simultaneous myocardial  $T_1$  and  $T_2$  mapping. This approach uses ECG-triggering to synchronize data acquisition to a small mid-diastolic window, reducing cardiac motion artefacts but also limiting the amount of acquired data per heartbeat. This low scan efficiency can limit the spatial resolution achievable in a breath-held scan. Here we introduce a novel approach for contrast-resolved motion-corrected reconstruction, that combines the generalized matrix description formalism for non-rigid motion correction with low-rank compression of temporally varying contrast. This approach enables longer acquisition windows and higher scan efficiency in cMRF, correcting for cardiac motion.

0873

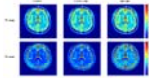


### Evaluation of transmit sensitivity ( $B_1^+$ ) encoding in MR fingerprinting at 7T

Ding Xia<sup>1,2</sup>, Zidan Yu<sup>1,2,3</sup>, Riccardo Lattanzi<sup>1,2,3</sup>, and Martijn A Cloos<sup>1,2</sup>

<sup>1</sup>Center for Advanced Imaging Innovation and Research, Department of Radiology, New York University School of Medicine, New York, NY, United States, <sup>2</sup>Center for Biomedical Imaging, Department of Radiology, New York University School of Medicine, New York, NY, United States, <sup>3</sup>Sackler Institute of Graduate Biomedical Sciences, New York University School of Medicine, New York, NY, United States

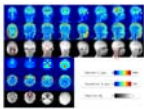
We evaluated the ability of three reported MR fingerprinting methods to mitigate the effect of  $B_1^+$  inhomogeneity at 7T. Results from each method were compared with gold standard results. All methods provided relatively accurate  $T_1$  quantification. We show that  $T_2$  cannot be accurately quantified at 7T without accounting for  $B_1^+$  in the MR fingerprinting dictionary. The Inversion-Recovery-FISP-FLASH (IRFF) method provided the most accurate  $T_2$  values. We conclude that the use of both FISP and FLASH segments best encodes  $B_1^+$  into the fingerprint.



Lixian Zou<sup>1,2</sup>, Huihui Ye<sup>3</sup>, Shi Su<sup>1</sup>, Haifeng Wang<sup>1</sup>, Dong Liang<sup>1,4</sup>, Xin Liu<sup>1</sup>, and Hairong Zheng<sup>1</sup>

<sup>1</sup>Shenzhen Institutes of Advanced Technology, Chinese Academy of Sciences, Shenzhen, China, <sup>2</sup>Shenzhen College of Advanced Technology, University of Chinese Academy of Sciences, Shenzhen, China, <sup>3</sup>State Key Laboratory of Modern Optical Instrumentation, College of Optical Science and Engineering, Zhejiang University, Zhejiang, China, <sup>4</sup>Research Center for Medical AI, Shenzhen Institutes of Advanced Technology, Chinese Academy of Sciences, Shenzhen, China

MRF is a time-efficient technique to simultaneously measure of multiple parameters through pattern recognition. The completeness of dictionary to describe the signal evolution process in NMR system is very important to acquire the accurate  $T_1$  and  $T_2$  values. A new dictionary, generated by using fractional Bloch equations and  $B_1$  correction, is proposed to improve the MRF-FISP accuracy. In this work, we compared the accuracy of relaxation values with three dictionary models through phantom and in-vivo experiments. Results illustrated that dictionary generated through fractional Bloch equation with  $B_1$  correction is the best to approach  $T_1$  and  $T_2$  standards.

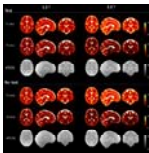


3D UTE-MRF for multiple parametric maps with sub-millimeter isotropic resolution using multi-dimensional golden-angle radial trajectory

Qing Li<sup>1,2</sup>, Xiaozhi Cao<sup>1</sup>, Huihui Ye<sup>1,3</sup>, Zihan Zhou<sup>1</sup>, Hongjian He<sup>1</sup>, and Jianhui Zhong<sup>1</sup>

<sup>1</sup>Center for Brain Imaging Science and Technology, Key Laboratory for Biomedical Engineering of Ministry of Education, College of Biomedical Engineering and Instrumental Science, Zhejiang University, Hangzhou, China, <sup>2</sup>Siemens Healthcare Ltd., Shanghai, China, <sup>3</sup>State Key Laboratory of Modern Optical Instrumentation, College of Optical Science and Engineering, Zhejiang University, Hangzhou, China

In this study, we used a 3D ultrashort-echo-time MR Fingerprinting (UTE-MRF) method to generate distortion-free quantitative  $T_1$ ,  $T_2$ , and proton density maps with an isotropic resolution of  $0.8 \times 0.8 \times 0.8 \text{ mm}^3$ .



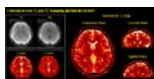
Three-dimensional MRF obtains highly repeatable and reproducible multi-parametric estimations in the healthy human brain at 1.5T and 3T

Guido Buonincontri<sup>1,2</sup>, Jan W Kurzwaski<sup>2,3</sup>, Joshua Kaggie<sup>4</sup>, Tomasz Matys<sup>4</sup>, Ferdia Gallagher<sup>4</sup>, Matteo Cencini<sup>2,5</sup>, Graziella Donatelli<sup>2,6</sup>, Paolo Cecchi<sup>6</sup>, Mirco Cosottini<sup>2,6,7</sup>, Nicola Martini<sup>8</sup>, Francesca Frijia<sup>9</sup>, Domenico Montanaro<sup>9</sup>, Pedro A Gómez<sup>2,10</sup>, Rolf F Schulte<sup>11</sup>, Alessandra Retico<sup>3</sup>, and Michela Tosetti<sup>1,2</sup>

<sup>1</sup>IRCCS Stella Maris, Pisa, Italy, <sup>2</sup>Imago7 Foundation, Pisa, Italy, <sup>3</sup>Istituto Nazionale di Fisica Nucleare, Pisa, Italy, <sup>4</sup>Department of Radiology, University of Cambridge, Cambridge, United Kingdom, <sup>5</sup>University of Pisa, Department of Physics, Pisa, Italy, <sup>6</sup>U.O. Neuroradiologia, Azienda Ospedaliera Universitaria Pisana (AOUP), Pisa, Italy, <sup>7</sup>University of Pisa, Department of Translational Research and New Technologies in Medicine and Surgery, Pisa, Italy, <sup>8</sup>Fondazione Toscana Gabriele Monasterio, Pisa, Italy, <sup>9</sup>U.O.C. Risonanza Magnetica Specialistica e Neuroradiologia, Fondazione CNR/Regione Toscana G. Monasterio, Pisa, Italy, <sup>10</sup>Technical University of Munich, Munich, Germany, <sup>11</sup>GE Healthcare, Munich, Germany

Three-dimensional magnetic resonance fingerprinting with spiral projection k-space trajectory offers fully-quantitative estimations at a high spatial resolution. To assess the repeatability and reproducibility of the estimations, we acquired test/re-test data in the human brain at 1.5T and 3.0T in a travelling head study involving a total of 12 subjects and 8 different MR scanners. Our approach estimated voxel-wise performance in the CNS: variability was assessed using coefficients-of-variation, bias using a GLM analysis. Solid matter repeatability CVs were under 2% for  $nPD/T_1$ , and 5% for  $T_2$ , while reproducibility biases were under 10% in solid matter compartments for  $T_1/T_2$ .

0877



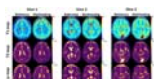
### Fast Simultaneous T1, T2 and T2\* Mapping at High Spatial Resolution using 3D Echo-planar Time-resolved Imaging (3D-EPTI)

Fuyixue Wang<sup>1,2</sup>, Zijing Dong<sup>1,3</sup>, Timothy G. Reese<sup>1</sup>, Lawrence L. Wald<sup>1,2</sup>, and Kawin Setsompop<sup>1,2</sup>

<sup>1</sup>A. A. Martinos Center for Biomedical Imaging, Massachusetts General Hospital, Charlestown, MA, United States, <sup>2</sup>Harvard-MIT Health Sciences and Technology, MIT, Cambridge, MA, United States, <sup>3</sup>Department of Electrical Engineering and Computer Science, MIT, Cambridge, MA, United States

An efficient quantitative mapping sequence based on 3D Echo-Planar Time-resolved Imaging (3D-EPTI) is proposed. The acquisition contains inversion recovery gradient echo readouts followed by GRASE-like readouts to provide sensitivity to  $T_1$ ,  $T_2$  and  $T_2^*$ . Fast k-TI-TE coverage is achieved by fusing highly-accelerated spatiotemporal CAIPI sampling with golden-angle radial-blade Cartesian under-sampling, where the reconstruction is performed using the subspace model. We demonstrate the high-efficiency of the proposed technique by obtaining multi-contrast images and quantitative maps at 1-mm isotropic resolution whole-brain in 3 minutes.

0878



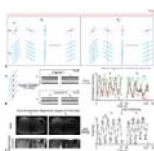
### Motion-Resolved, 3D Whole-Brain Simultaneous T1, T2, and T1p Mapping using Multitasking with Application to Multiple Sclerosis: A Pilot Study

Sen Ma<sup>1,2</sup>, Anthony G. Christodoulou<sup>2</sup>, Nan Wang<sup>1,2</sup>, Marwa Kaisey<sup>3</sup>, Nancy L. Sicotte<sup>3</sup>, and Debiao Li<sup>1,2</sup>

<sup>1</sup>Department of Bioengineering, University of California, Los Angeles, Los Angeles, CA, United States, <sup>2</sup>Biomedical Imaging Research Institute, Cedars-Sinai Medical Center, Los Angeles, CA, United States, <sup>3</sup>Department of Neurology, Cedars-Sinai Medical Center, Los Angeles, CA, United States

Quantitative multi-parametric relaxometry MRI (e.g.,  $T_1$ ,  $T_2$ , and  $T_{1\rho}$  mapping) can demonstrate longitudinal brain changes and enhance lesion contrasts against normal appearing matters in multiple sclerosis. Conventional methods that quantify these relaxation parameters are time-consuming and subject to motion, thus challenging for clinical practice. We present a novel approach that simultaneously quantifies  $T_1$ ,  $T_2$ , and  $T_{1\rho}$  with whole brain coverage in 9min, using the recently developed Multitasking framework that models the multidimensional image as a low-rank tensor. This technique is validated on healthy volunteers. We also demonstrate the feasibility of lesion characterization on relapsing remitting multiple sclerosis patients.

0879



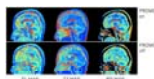
### Free-Breathing Simultaneous Quantification of Liver T1, Fat and $R_2^*$ with Variable Flip Angle Golden-Angle-Ordered 3D Stack-of-Radial MRI

Le Zhang<sup>1</sup>, Shu-Fu Shih<sup>1,2</sup>, Tess Armstrong<sup>1,3</sup>, and Holden H. Wu<sup>1,2,3</sup>

<sup>1</sup>Radiological Sciences, University of California, Los Angeles, Los Angeles, CA, United States, <sup>2</sup>Bioengineering, University of California, Los Angeles, Los Angeles, CA, United States, <sup>3</sup>Physics and Biology in Medicine, University of California, Los Angeles, Los Angeles, CA, United States

Quantification of  $T_1$ , proton-density fat fraction (PDFF), and  $R_2^*$  in the liver can provide information about a range of diseases. Existing Cartesian acquisition schemes generally require breath-holding, which limits spatial coverage and may be difficult for sick, elderly or pediatric patients. In this study, we propose a variable-flip-angle (VFA) golden-angle-ordered (GA) 3D stack-of-radial sequence that can provide multiparametric mapping with volumetric liver coverage in three minutes during free-breathing and with intrinsic motion compensation capability. Pilot studies in healthy subjects demonstrate agreement with reference breath-held scans and good measurement repeatability.

0880



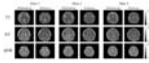
### Prospective motion corrected 3D multi-parametric imaging

Naoyuki Takei<sup>1</sup>, David Shin<sup>2</sup>, Dan Rettmann<sup>3</sup>, Shohei Fujita<sup>4,5</sup>, Issei Fukunaga<sup>4</sup>, Akifumi Hagiwara<sup>4</sup>, Ken-Pin Hwang<sup>6</sup>, Marcel Warntjes<sup>7</sup>, Shigeki Aoki<sup>4</sup>, Suchandrima Banerjee<sup>2</sup>, and Hiroyuki Kabasawa<sup>1</sup>

<sup>1</sup>GE Healthcare, Tokyo, Japan, <sup>2</sup>GE Healthcare, Menlo Park, CA, United States, <sup>3</sup>GE Healthcare, Rochester, MN, United States, <sup>4</sup>Juntendo University School of Medicine, Tokyo, Japan, <sup>5</sup>The University of Tokyo Graduate School of Medicine, Tokyo, Japan, <sup>6</sup>The University of Texas M.D. Anderson Cancer Center, Houston, TX, United States, <sup>7</sup>SyntheticMR, Linköping, Sweden

To aim for reliable parametric mapping to motion artifact, prospective motion correction was integrated to a multi-parametric technique, 3D QALAS. 2D Spiral navigators were inserted into wait times in the QALAS without impacting scan time for motion tracking and correction. The effectiveness of prospective motion correction was demonstrated. The proposed technique is expected to yield prospectively motion corrected 3D brain volumetric images of multiple contrasts and quantitative mappings.

0881



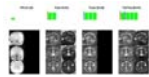
### Simultaneous quantitative mapping of T1, R2\* and susceptibility with magnetic resonance multitasking

Tianle Cao<sup>1,2</sup>, Nan Wang<sup>1,2</sup>, Sen Ma<sup>1,2</sup>, Yibin Xie<sup>1</sup>, Sara Gharabaghi<sup>3</sup>, E. Mark Haacke<sup>3,4,5</sup>, Anthony G. Christodoulou<sup>1</sup>, and Debiao Li<sup>1</sup>

<sup>1</sup>Biomedical Imaging Research Institute, Cedars Sinai Medical Center, Los Angeles, CA, United States, <sup>2</sup>Bioengineering Department, University of California, Los Angeles, Los Angeles, CA, United States, <sup>3</sup>Magnetic Resonance Innovations, Inc, Bingham Farms, MI, United States, <sup>4</sup>Wayne State University School of Medicine, Detroit, MI, United States, <sup>5</sup>The MRI Institute for Biomedical Research, Bingham Farms, MI, United States

A new approach for simultaneous quantitative mapping of T1, R2\* and susceptibility was presented in this work. This technique employed IR pulses followed by N=152 segments of multi-echo FLASH readout. We were able to reconstruct the images for each echo time and inversion time under the multitasking framework for further analysis. Results of both visual comparison and statistical analysis showed that our proposed method agreed well with the reference but were more time efficient and robust to interscan motion.

0882



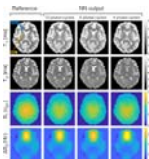
### PSST ... Parameter mapping Swift and SilenT

Florian Wiesinger<sup>1,2</sup>, Emil Ljungberg<sup>2</sup>, Mathias Engström<sup>3</sup>, Sandeep Kaushik<sup>1</sup>, Tobias Wood<sup>2</sup>, Steven Williams<sup>2</sup>, Gareth Barker<sup>2</sup>, and Ana Beatriz Solana<sup>1</sup>

<sup>1</sup>GE Healthcare, Munich, Germany, <sup>2</sup>King's College London, London, United Kingdom, <sup>3</sup>GE Healthcare, Stockholm, Sweden

Here we describe a new framework for 3D, high-resolution Parameter mapping in a Swift and SilenT manner, termed PSST. The method combines T1 and T2 contrast preparation with segmented, silent, zero TE (ZTE) image encoding and an analytical signal model. Four canonical schemes are presented and demonstrated in phantom and in-vivo brain experiments.

0883



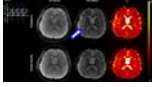
### Deep-Learning Driven Acceleration of Multi-Parametric Quantitative Phase-Cycled bSSFP Imaging

Rahel Heule<sup>1</sup>, Jonas Bause<sup>1</sup>, Orso Pusterla<sup>2,3,4</sup>, and Klaus Scheffler<sup>1,5</sup>

<sup>1</sup>High Field Magnetic Resonance, Max Planck Institute for Biological Cybernetics, Tübingen, Germany, <sup>2</sup>Institute for Biomedical Engineering, University and ETH Zurich, Zurich, Switzerland, <sup>3</sup>Division of Radiological Physics, Department of Radiology, University Hospital Basel, Basel, Switzerland, <sup>4</sup>Department of Biomedical Engineering, University of Basel, Basel, Switzerland, <sup>5</sup>Department of Biomedical Magnetic Resonance, University of Tübingen, Tübingen, Germany

Prominent asymmetries in the bSSFP frequency profile in tissues with distinct fiber pathways are known to be a confounding factor in the quantification of relaxation times from a series of phase-cycled scans. It has been demonstrated that the resulting bias can be eliminated by training artificial neural networks using gold standard relaxation times as target. Here, the ability of neural networks to not only provide gold standard brain tissue  $T_1$  and  $T_2$  values as well as field map estimates ( $B_1$ ,  $\Delta B_0$ ) but also to highly accelerate the acquisition by reducing the number of phase-cycles is explored.

0884



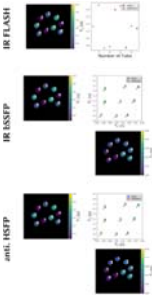
Flexible model-based reconstruction through generalized cycled parameter splitting approach.

Gilad Liberman<sup>1</sup>, Fuyixue Wang<sup>1</sup>, Zijong Dong<sup>1</sup>, and Kawin Setsompop<sup>1</sup>

<sup>1</sup>Department of Radiology, Massachusetts General Hospital, Charlestown, MA, United States

Model-based reconstruction approaches benefit from tight representation of the signal and from optimization on meaningful quantitative parameter maps, while requiring advanced algorithms and increased computational resources. We propose a generalized iterative thresholding algorithm with parameter splitting for model-based reconstruction, along with an efficient implementation. The approach is flexible and generalizable to problems in various MRI domains. We demonstrate it on the common image with phase evolution and signal decay model tackled with multi-echo GRE and Echo-Planar Time-resolved Imaging (EPTI), resulting in better image quality in comparison with GRAPPA and subspace constrained reconstruction, and increased z-scores in a low-SNR functional experiment.

0885



Generic Quantitative MRI using Model-Based Reconstruction with the Bloch Equations

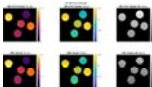
Nick Scholand<sup>1,2</sup>, Xiaoqing Wang<sup>1,2</sup>, Sebastian Rosenzweig<sup>1,2</sup>, H. Christian M. Holme<sup>1,2</sup>, and Martin Uecker<sup>1,2</sup>

<sup>1</sup>Department of Interventional and Diagnostic Radiology, University Medical Center, Göttingen, Germany,

<sup>2</sup>German Centre for Cardiovascular Research, Göttingen, Germany

Conventional quantitative MRI estimates parameters by fitting a known analytical signal model to pixels of images with different contrasts. By combining image reconstruction and the signal model into one non-linear inverse problem, model-based reconstruction methods can estimate the parameters directly from k-space. Avoiding the acquisition and reconstruction of intermediate images they require much less data. Furthermore, they can be directly combined with parallel imaging and compressed sensing, but still rely on analytical models and carefully designed MRI sequences. Here, we generalize this framework to work with arbitrary sequences using a Runge-Kutta based simulation of spin dynamics.

0886



Extension of MR-STAT to non-Cartesian and gradient-spoiled sequences

Oscar van der Heide<sup>1,2</sup>, Alessandro Sbrizzi<sup>1,2</sup>, Tom Bruijnen<sup>1,3</sup>, and Cornelis van den Berg<sup>1,2</sup>

<sup>1</sup>Computational Imaging Group for MR Diagnostics and Therapy, Center for Image Sciences, University Medical Center Utrecht, Utrecht, Netherlands, <sup>2</sup>Department of Radiology, Division of Imaging and Oncology, University Medical Center Utrecht, Utrecht, Netherlands, <sup>3</sup>Department of Radiotherapy, Division of Imaging & Oncology, University Medical Center Utrecht, Utrecht, Netherlands

MR-STAT is a framework for obtaining multi-parametric quantitative MR maps using data from single short scans. A single large-scale optimization problem is solved in which spatial localisation of signal and estimation of tissue parameters are performed simultaneously. In previous work, MR-STAT was presented using gradient-balanced sequences with linear, Cartesian readouts. To demonstrate the generic nature of the MR-STAT framework and to explore potentially more efficient acquisition schemes, we extend MR-STAT to non-Cartesian gradient trajectories as well as gradient-spoiled sequences. We compare our results from golden angle radial, gradient-spoiled acquisitions to low-rank ADMM MRF reconstructions on the same data sets.



---

---

Oral

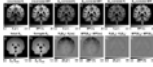
Advances in Quantitative MRI - Quantitative Relaxation Parameter Mapping: Better, Faster, Stronger

Wednesday Parallel 5 Live Q&A

Wednesday 14:30 - 15:15 UTC

Moderators: Christian Guenther & Leigh Johnston

0887



Correction of B<sub>1</sub> non-uniformity errors in fast macromolecular proton fraction and R<sub>1</sub> mapping without B<sub>1</sub> maps

Vasily L. Yarnykh<sup>1</sup>

<sup>1</sup>Radiology, University of Washington, Seattle, WA, United States

Correction of B<sub>1</sub> field non-uniformity is critical for quantitative MRI methods including fast macromolecular proton fraction (MPF) and variable flip angle T<sub>1</sub> mapping. However, B<sub>1</sub> mapping sequences increase the examination time and are not commonly available in clinics. A new algorithm is presented to enable simultaneous B<sub>1</sub> correction in R<sub>1</sub>=1/T<sub>1</sub> and MPF mapping without acquisition of B<sub>1</sub> maps. The principle of the algorithm is based on different mathematical dependences of B<sub>1</sub>-related errors in R<sub>1</sub> and MPF allowing extraction of a surrogate B<sub>1</sub> map from uncorrected R<sub>1</sub> and MPF maps. The method demonstrated excellent agreement with actual B<sub>1</sub> mapping at 3T.

0888



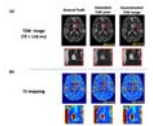
A fast T2 mapping protocol for prostate clinical applications using compressed sensing with low-rank and sparsity constraints

Jochen Keupp<sup>1</sup>, Doneva Mariya<sup>1</sup>, Jakob Meineke<sup>1</sup>, and Peter Forthmann<sup>1</sup>

<sup>1</sup>Philips Research, Hamburg, Germany

T2w-MRI plays an important role in prostate cancer providing information on the location/grade in diagnosis or surveillance. T2-mapping may provide objective characterization but is hampered by long acquisition time, which has been addressed by dedicated acceleration techniques (e.g. kt-T2 mapping). We investigate further acceleration of T2-mapping by prospective variable sub-sampling in the echo time domain, comparing regular or irregular patterns in combination with compressed sensing using low rank and sparsity constraints, towards a routine clinical T2 mapping protocol with increased volume coverage. Prostate and phantom T2-maps with 24 slices (1×1×3mm<sup>3</sup> voxel) were acquired in 5½ minutes with promising map quality.

0889



Accelerated T2 Mapping by Integrating Two-Stage Learning with Sparse Modeling

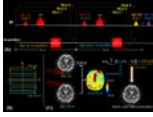
Ziyu Meng<sup>1,2</sup>, Yudu Li<sup>2,3</sup>, Rong Guo<sup>2,3</sup>, Yibo Zhao<sup>2,3</sup>, Tianyao Wang<sup>4</sup>, Fanyang Yu<sup>2,5</sup>, Brad Sutton<sup>2,5</sup>, Yao Li<sup>1</sup>, and Zhi-Pei Liang<sup>2,3</sup>

<sup>1</sup>Institute for Medical Imaging Technology, School of Biomedical Engineering, Shanghai Jiao Tong University, Shanghai, China, <sup>2</sup>Beckman Institute of Advanced Science and Technology, University of Illinois at Urbana-Champaign, Urbana, IL, United States, <sup>3</sup>Department of Electrical and Computer Engineering, University of Illinois at Urbana-Champaign, Urbana, IL, United States, <sup>4</sup>Department of Radiology, The Fifth People's Hospital of Shanghai, Fudan University, Shanghai, China, <sup>5</sup>Department of Bioengineering, University of Illinois at Urbana-Champaign, Urbana, IL, United States

We propose a new method to learn the multi-TE image priors for accelerated T2 mapping. The proposed method has the following key features: a) fully leveraging the Human Connectome Project (HCP) database to learn T2-weighted image priors for a single TE, b) transferring the learned single-TE T2-weighted image priors to multi-TE via deep histogram mapping, c) reducing the learning complexity using a tissue-based training strategy, and d) recovering subject-dependent novel features using sparse modeling. The proposed method has been validated using experimental data, producing very encouraging results.

---

0890



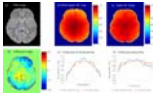
### T2-BUDA-gSlider: fast T2 mapping with blip-up/down acquisition, generalized SLIce Dithered Enhanced Resolution and subspace reconstruction

Xiaozhi Cao<sup>1,2,3</sup>, Congyu Liao<sup>2,3</sup>, Zijing Zhang<sup>2,4</sup>, Siddharth Srinivasan Iyer<sup>2,5</sup>, Hongjian He<sup>1</sup>, Kawin Setsompop<sup>2,3,6</sup>, Jianhui Zhong<sup>1</sup>, and Berkin Bilgic<sup>2,3,6</sup>

<sup>1</sup>Center for Brain Imaging Science and Technology, Department of Biomedical Engineering, Zhejiang University, Hangzhou, China, <sup>2</sup>Athinoula A. Martinos Center for Biomedical Imaging, Massachusetts General Hospital, charlestown, MA, United States, <sup>3</sup>Department of Radiology, Harvard Medical School, charlestown, MA, United States, <sup>4</sup>State Key Laboratory of Modern Optical Instrumentation, College of Optical Science and Engineering, Zhejiang University, Hangzhou, China, <sup>5</sup>Department of Electrical Engineering and Computer Science, Massachusetts Institute of Technology, Cambridge, MA, United States, <sup>6</sup>Harvard-MIT Department of Health Sciences and Technology, Cambridge, MA, United States

We propose to combine the gSlider acquisition and blip-up/down acquisition (BUDA) to achieve high-resolution and distortion-free  $T_2$  mapping. Firstly, we incorporate Hankel structured low-rank constraint into BUDA reconstruction to recover distortion-free images from blip-up/down shots without navigation. To utilize the similarity among RF-encodings and TEs, we introduce a model-based shuffling-gSlider joint reconstruction to recover high-resolution thin-slice images by gradually eliminating the weak coefficient components during the iterative reconstruction. Finally, the reconstructed images are used to obtain quantitative  $T_2$  maps. The proposed method enables distortion-free high-quality whole-brain  $T_2$  mapping with 1 mm isotropic resolution within ~1 minute.

0891



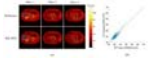
### Bloch Modelling Enables Robust T2 Mapping using Retrospective Proton Density and T2-weighted Images from Different Vendors and Sites

Gitanjali Chhetri<sup>1</sup>, Kelly C McPhee<sup>1</sup>, and Alan H Wilman<sup>1</sup>

<sup>1</sup>Biomedical Engineering, University of Alberta, Edmonton, AB, Canada

Differences in pulse sequences between vendors can result in variation in  $T_2$  mapping, if not accounted for. We show that Bloch simulation based Indirect and Stimulated Echo Compensation minimizes these differences in  $T_2$  maps across different scanners. In contrast, standard exponential fitting results in highly variable  $T_2$  values across MR systems even if echo and repetition times are identical. By overcoming errors in  $T_2$  quantification through sequence modelling,  $T_2$  mapping can be applied in studies across multiple sites and vendors.

0892



### Joint Calibrationless Multi-slice Multi-echo Parallel Imaging Reconstruction for Abdominal $T_2^*$ Mapping

Xiaochuan Wu<sup>1,2</sup>, Zheyuan Yi<sup>1,2,3</sup>, Yilong Liu<sup>1,2</sup>, Fei Chen<sup>3</sup>, Yanqiu Feng<sup>4</sup>, and Ed X. Wu<sup>1,2</sup>

<sup>1</sup>Laboratory of Biomedical Imaging and Signal Processing, The University of Hong Kong, Hong Kong, China,

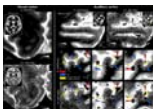
<sup>2</sup>Department of Electrical and Electronic Engineering, The University of Hong Kong, Hong Kong, China,

<sup>3</sup>Department of Electrical and Electronic Engineering, Southern University of Science and Technology, Shenzhen, China,

<sup>4</sup>School of Biomedical Engineering, Southern Medical University, Guangzhou, China

$T_2^*$  mapping in abdominal imaging is challenging due to respiration motions that can result in severe artifacts and affect the accuracy of  $T_2^*$  quantification. Traditional simultaneous autocalibrating and k-space estimation (SAKE) provides a calibrationless parallel imaging approach to reduce the image acquisition time. However, SAKE does not utilize the highly sharable image contents and coil sensitivities among multi-slice multi-echo data. In this study, we proposed a joint calibrationless reconstruction of multi-slice multi-echo images from undersampled MR data for abdominal imaging. Results demonstrated that the resulting  $T_2^*$  maps were in excellent agreement with those from the fully sampled data.

0893

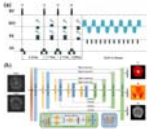


### 7T in-vivo human $T_2^*$ mapping at 350 $\mu$ m isotropic resolution using ME-GRE with flow artifact mitigation reveals cortical layers & vessels

Omer Faruk Gulban<sup>1</sup>, Benedikt Poser<sup>1</sup>, Martin Havlicek<sup>1</sup>, Federico De Martino<sup>1</sup>, and Dimo Ivanov<sup>1</sup>

Spatial misencoding of the vascular signal due to flow is an imaging artifact that presents a significant challenge for in vivo MRI at high resolutions ( $\leq 0.5\text{mm}$ ). Here we propose a method for mitigating this artifact in multi-echo gradient recalled echo (ME-GRE) images at **350 $\mu\text{m}$  isotropic resolution** by applying  $90^\circ$  rotations to their phase-encoding direction. After applying our method, we demonstrate clearly visible stria of Gennari, intracortical veins, and pial vessels while mitigating the flow artifact. In addition, we report  $T_2^*$  estimates of several human brain tissues (artery, vein, gray/white matter, CSF) in-vivo which are valuable for future hemodynamic signal modeling.

0894



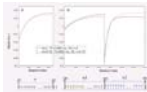
#### Deep Learning-based Single-shot $T_2^*$ Mapping Using Multiple Overlapping-Echo Detachment Acquisition

Qinqin Yang<sup>1</sup>, Jian Wu<sup>1</sup>, Wei Wang<sup>1</sup>, Jiyang Dong<sup>1</sup>, Shuhui Cai<sup>1</sup>, and Congbo Cai<sup>1</sup>

<sup>1</sup>Department of Electronics Science, Xiamen University, Xiamen, Fujian, China

Quantitative MRI is of great value to both clinical diagnosis and scientific research. In this study, a novel  $T_2^*$  mapping method, gradient-echo multiple overlapping-echo detachment acquisition (GRE-MOLED) sequence with deep learning-based reconstruction algorithm was proposed. The method is capable of acquiring reliable  $T_2^*$ ,  $M_0$  and  $B_0$  maps simultaneously in a single shot and is robust to  $B_0$ -inhomogeneities. As a rapid  $T_2^*$  quantitative tool, GRE-MOLED reduces the scan time of  $T_2^*$  mapping to less than 75 ms per slice and has great potential in clinical real-time applications.

0895



#### Dual Flip-angle IR-FLASH for B1+ Insensitive T1 Mapping: Application to T1 CMR Multitasking.

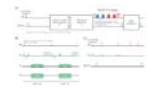
Fardad Michael Serry<sup>1</sup>, Sen Ma<sup>1,2</sup>, Debiao Li<sup>1,2</sup>, and Anthony G Christodoulou<sup>1</sup>

<sup>1</sup>Biomedical Imaging Research Institute, Cedars-Sinai Medical Center, Los Angeles, CA, United States,

<sup>2</sup>Department of Bioengineering, University of California, Los Angeles, Los Angeles, CA, United States

T1 mapping is important for many diseases, from cancer [1] to cardiovascular disease [2], and more. Many fast T1 mapping protocols rely on an IR-FLASH sequence, especially in the heart. However, the accuracy and repeatability of T1 mapping with IR-FLASH are compromised by B1+ inhomogeneity. Here we present a simple dual-flip-angle (DFA) modification of the IR-FLASH pulse sequence to provide B1+-robust T1 mapping that obviates the need for a separate B1+ scan. We show the improved agreement of DFA-IR-FLASH to IR-TSE in a phantom study as well as its feasibility for in vivo cardiac T1 mapping with MR Multitasking.

0896



#### Simultaneous measurements of blood flow and blood water T2: a general-purpose sequence for T2-based measurement of whole-organ O<sub>2</sub> consumption

Cheng-Chieh Cheng<sup>1</sup>, Pei-Hsin Wu<sup>1</sup>, Michael C. Langham<sup>1</sup>, and Felix W. Wehrli<sup>1</sup>

<sup>1</sup>University of Pennsylvania, Philadelphia, PA, United States

A  $T_2$ -based oximetry method for quantifying whole-organ metabolic rate of oxygen ( $\text{MRO}_2$ ): A velocity-encoded acquisition module with golden-angle radial sampling was inserted into a background-suppressed  $T_2$ -prepared sequence specifically for blood water  $T_2$  quantification. Parallel imaging and compressed-sensing techniques were applied to the reconstruction of the sparsely-sampled velocity-encoded  $k$ -space data to generate velocity maps. Whole-organ oxygen metabolic rate was estimated by converting  $T_2$  to blood oxygenation level via a calibration curve. A pilot study in the superior sagittal sinus showed the method's ability to estimate whole-brain  $\text{CMRO}_2$  ( $136 \pm 23 \mu\text{mol}/\text{minute}/100\text{g}$ , mean  $\pm$  S.D.) in a single pass.

## Combined Educational & Scientific Session

### Machine Learning and Tissue Characterisation in CMR - Machine Learning in Cardiovascular Imaging

Organizers: Jennifer Steeden, Jennifer Keegan

Wednesday Parallel 1 Live Q&A

Wednesday 14:30 - 15:15 UTC

Moderators: Eric Gibbons & Pedro Ferreira

#### Applications of Machine Learning in Clinical Cardiovascular MRI

Albert Hsiao<sup>1</sup>

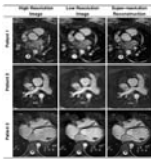
<sup>1</sup>University of California, San Diego, United States

#### Machine Learning & Future Clinical Practice in Cardiovascular MRI

Claudia Prieto<sup>1</sup>

<sup>1</sup>King's College London, United Kingdom

0769



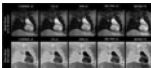
#### Rapid Whole-Heart CMR with Single Volume Super-Resolution

Jennifer Steeden<sup>1</sup>, Michael Quail<sup>2</sup>, Alexander Gotschy<sup>2,3</sup>, Andreas Hauptmann<sup>1,4</sup>, Rodney Jones<sup>1</sup>, and Vivek Muthurangu<sup>1</sup>

<sup>1</sup>University College London, London, United Kingdom, <sup>2</sup>Great Ormond Street Hospital, London, United Kingdom, <sup>3</sup>University and ETH Zurich, Institute for Biomedical Engineering, Zurich, Switzerland, <sup>4</sup>University of Oulu, Oulu, Finland

Three-dimensional (3D), whole heart, balanced steady state free precession (WH-bSSFP) sequences provides excellent delineation of both intra-cardiac and vascular anatomy. However, they are usually cardiac triggered and respiratory navigated, resulting in long acquisition times (10-15minutes). Here, we propose a machine-learning single-volume super-resolution reconstruction (SRR), to recover high-resolution features from rapidly acquired low-resolution WH-bSSFP data. We show that it is possible to train a network using synthetically down-sampled WH-bSSFP data. We tested the network on synthetic test data and 40 prospective data sets, showing ~3x speed-up in acquisition time, with excellent agreement with reference standard high resolution WH-bSSFP images.

0770



#### A Multi-Scale Variational Neural Network for accelerating bright- and black-blood 3D whole-heart MRI in patients with congenital heart disease

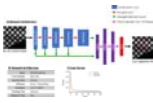
Niccolo Fuin<sup>1</sup>, Giovanna Nordio<sup>1</sup>, Thomas Kuestner<sup>1</sup>, Radhouene Nejj<sup>2</sup>, Karl Kunze<sup>2</sup>, Yaso Emmanuel<sup>3</sup>, Alessandra Frigiola<sup>1,3</sup>, Rene Botnar<sup>1,4</sup>, and Claudia Prieto<sup>1,4</sup>

<sup>1</sup>Biomedical Engineering Department, School of Biomedical Engineering and Imaging Sciences, King's College London, London, United Kingdom, <sup>2</sup>MR Research Collaborations, Siemens Healthcare Limited, Frimley, United Kingdom, <sup>3</sup>Guy's and St Thomas' Hospital, NHS Foundation Trust, London, United Kingdom, <sup>4</sup>Pontificia Universidad Católica de Chile, Santiago, Chile

Bright- and black-blood MRI sequences provide complementary diagnostic information in patients with congenital heart disease (CHD). A free-breathing 3D whole-heart sequence (MTC-BOOST) has been recently proposed for contrast-free simultaneous bright- and black-blood MRI, demonstrating high-quality depiction of arterial and venous structures. However, high-resolution fully-sampled MTC-BOOST acquisitions require long scan times of ~12min. Here we propose a joint Multi-Scale Variational Neural Network (MS-VNN) which enables the acquisition of high-quality bright- and black blood MTC-BOOST images in ~2-4 minutes, and their joint reconstruction in ~20s. The technique is compared with Compressed-Sensing reconstruction for 5x acceleration, in CHD patients.

Cardiac Tag Tracking with Deep Learning Trained with Comprehensive Synthetic Data Generation

0771

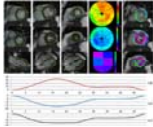


Michael Loecher<sup>1</sup>, Luigi E Perotti<sup>2</sup>, and Daniel B Ennis<sup>1,3,4,5</sup>

<sup>1</sup>Radiology, Stanford, Palo Alto, CA, United States, <sup>2</sup>Mechanical Engineering, University of Central Florida, Orlando, FL, United States, <sup>3</sup>Radiology, Veterans Administration Health Care System, Palo Alto, CA, United States, <sup>4</sup>Cardiovascular Institute, Stanford, Palo Alto, CA, United States, <sup>5</sup>Center for Artificial Intelligence in Medicine & Imaging, Stanford, Palo Alto, CA, United States

A convolutional neural network based tag tracking method for cardiac grid-tagged data was developed and validated. An extensive synthetic data simulator was created to generate large amounts of training data from natural images with analytically known ground-truth motion. The method was validated using both a digital cardiac deforming phantom and tested using in vivo data. Very good agreement was seen in tag locations (<1.0mm) and calculated strain measures (<0.02 midwall Ecc)

0772



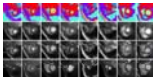
Deep Learning-based Strain Quantification from CINE Cardiac MRI

Teodora Chitiboi<sup>1</sup>, Bogdan Georgescu<sup>1</sup>, Jens Wetzel<sup>2</sup>, Indraneel Borgohain<sup>1</sup>, Christian Geppert<sup>2</sup>, Stefan K Piechnik<sup>3</sup>, Stefan Neubauer<sup>3</sup>, Steffen Petersen<sup>4</sup>, and Puneet Sharma<sup>1</sup>

<sup>1</sup>Siemens Healthineers, Princeton, NJ, United States, <sup>2</sup>Magnetic Resonance, Siemens Healthcare, Erlangen, Germany, <sup>3</sup>Division of Cardiovascular Medicine, Radcliffe Department of Medicine, University of Oxford, Oxford, United Kingdom, <sup>4</sup>NIHR Biomedical Research Centre at Barts, Queen Mary University of London, London, United Kingdom

Deep learning enables fully automatic strain analysis from CINE MRI on large subject cohorts. Deep learning neural nets were trained to segment the heart chambers from CINE MRI using manually annotated ground truth. After validation on more than 1700 different patient datasets, the models were used to generate segmentations as the first step of a fully automatic strain analysis pipeline for 460 subjects. We found significant differences associated with gender (strain magnitude smaller for males), height (lower strain magnitude for patients taller than 170 cm) and age (lower circumferential and longitudinal strain for subjects older than 60 years).

0773



Leveraging Anatomical Similarity for Unsupervised Model Learning and Synthetic MR Data Generation

Thomas Joyce<sup>1</sup> and Sebastian Kozerke<sup>1</sup>

<sup>1</sup>Institute for Biomedical Engineering, University and ETH Zurich, Zurich, Switzerland

We present a method for the controllable synthesis of 3D (volumetric) MRI data. The model is comprised of three components which are learnt simultaneously from unlabelled data through self-supervision: i) a multi-tissue anatomical model, ii) a probability distribution over deformations of this anatomical model, and, iii) a probability distribution over 'renderings' of the anatomical model (where a rendering defines the relationship between anatomy and resulting pixel intensities). After training, synthetic data can be generated by sampling the deformation and rendering distributions.

## Oral

### Machine Learning and Tissue Characterisation in CMR - Cardiovascular Machine Learning: Image Processing & Beyond

Wednesday Parallel 1 Live Q&A

Wednesday 14:30 - 15:15 UTC

Moderators: Mehdi Hedjazi Moghari & Shanshan Wang

0774



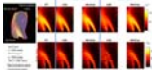
In-vivo application of a trained neural network using a fusion of computational fluid dynamic and 4D flow MRI data

David R Rutkowski<sup>1,2</sup>, Alejandro Roldán-Alzate<sup>1,2,3</sup>, and Kevin M Johnson<sup>1,4</sup>

<sup>1</sup>Radiology, University of Wisconsin, Madison, WI, United States, <sup>2</sup>Mechanical Engineering, University of Wisconsin, Madison, WI, United States, <sup>3</sup>Biomedical Engineering, University of Wisconsin, Madison, WI, United States, <sup>4</sup>Medical Physics, University of Wisconsin, Madison, WI, United States

Augmentation of 4D flow MRI data with computational fluid dynamics (CFD) -informed training networks may provide a method to produce highly accurate physiological flow fields. In this preliminary work, the potential utility of such a method was demonstrated by using high resolution patient-specific CFD data to train a neural network, and then using the trained network to enhance MRI-derived velocity fields.

0775



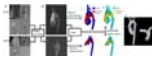
### Improved In Vivo Estimation of the Reynolds Stress Tensor from 4D and 5D Flow MRI Using Cholesky Decomposition-Based Neural Networks

Valery Vishnevskiy<sup>1,2</sup>, Hannes Dillinger<sup>1,2</sup>, Jonas Walheim<sup>1,2</sup>, Lin Zhang<sup>1</sup>, and Sebastian Kozerke<sup>1,2</sup>

<sup>1</sup>ETH Zurich, Zurich, Switzerland, <sup>2</sup>University of Zurich, Zurich, Switzerland

A novel approach using Cholesky decomposition-based neural networks for the estimation of Reynolds stress tensors in 4D Flow MRI is presented. Evaluation is carried out for simulated MRI signals using particle tracking velocimetry data and tested on in-vivo data obtained in a healthy volunteer and a patient with bioprosthetic aortic valve. The proposed method allows to account for non-Gaussian acquisition noise and guarantees positive-definiteness of the estimated tensors, which yields 68% improvement in turbulent shear stress estimation compared to standard least squares estimation.

0776



### Fully Automated Multivendor and Multisite Artificial Intelligence-based 3D Segmentation of the Proximal Arteries from 4D flow MRI

Haben Berhane<sup>1</sup>, Michael Scott<sup>2</sup>, Takashi Fujiwara<sup>3</sup>, Lorna Browne<sup>3</sup>, Joshua Robinson<sup>1</sup>, Cynthia Rigsby<sup>1</sup>, Michael Markl<sup>2</sup>, and Alex Barker<sup>3</sup>

<sup>1</sup>Lurie Children's Hospital of Chicago, Chicago, IL, United States, <sup>2</sup>Northwestern University, Chicago, IL, United States, <sup>3</sup>University of Colorado, Anschutz Medical Campus, Aurora, CO, United States

We trained and validated a multi-label convolutional neural network for the segmentation of the aorta and pulmonary arteries from 4D flow MRI for rapid flow analysis across multiple vendors and centers. Using 67 whole-heart 4D flow MRI scans, including 29 with cardiac pathologies, across two institutions and vendors, we trained and tested our CNN using 10-fold cross validation. For flow analysis, We calculated net flow, peak velocity, and Qp-Qs. Across all flow metrics, we found that automated segmentations showed moderate to strong agreement with the manual segmentations, while taking a fraction of the time.

0777



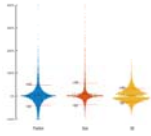
### Automatic quantification of ultra-high resolution quantitative first-pass perfusion imaging using deep-learning based segmentation and MOCO

Matthew Van Houten<sup>1</sup>, Xue Feng<sup>1</sup>, Yang Yang<sup>2</sup>, Austin Robinson<sup>3</sup>, Craig Meyer<sup>1</sup>, and Michael Salerno<sup>1,3</sup>

<sup>1</sup>Department of Biomedical Engineering, University of Virginia, Charlottesville, VA, United States, <sup>2</sup>Biomedical Engineering and Imaging Institute and Department of Radiology, Icahn School of Medicine at Mount Sinai, New York, NY, United States, <sup>3</sup>Department of Medicine, University of Virginia, Charlottesville, VA, United States

While quantitative first-pass quantitative perfusion imaging is an excellent non-invasive tool for the evaluation of coronary artery disease, current processing shortcomings have kept it from widespread clinical use. In this study, we developed a pipeline which robustly and automatically segments, registers, and quantifies flow with our ultra-high resolution quantitative perfusion sequence.

0778



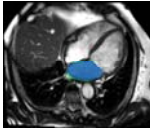
n-Standard deviations from remote is unreliable for scar quantification – evaluation using multicenter multivendor clinical trial data

Einar Heiberg<sup>1,2</sup>, Henrik Engblom<sup>1</sup>, Marcus Carlsson<sup>1</sup>, David Erlinge<sup>3</sup>, Dan Atar<sup>4</sup>, Anthony H Aletras<sup>1,5</sup>, and Hakan Arheden<sup>1</sup>

<sup>1</sup>Department of Clinical Sciences Lund, Clinical Physiology, Skåne University Hospital, Lund University, Lund, Sweden, <sup>2</sup>Lund University, Wallenberg Center for Molecular Medicine, Lund, Sweden, <sup>3</sup>Lund University, Department of Clinical Sciences Lund, Cardiology, Skåne University Hospital, Lund, Sweden, Lund, Sweden, <sup>4</sup>Department of Cardiology, Oslo University Hospital Ullevål, and Institute of Clinical Sciences, University of Oslo, Oslo, Norway, <sup>5</sup>School of Medicine, Aristotele University of Thessaloniki, Laboratory of Computing, Medical Informatics and Biomedical – Imaging Technologies, Thessaloniki, Greece

The purpose of this study is to systematically evaluate sources to variability in the n-SD from remote method for infarct quantification. Remote ROI position, size, and number of standard deviations all to a large extent affected infarct size. The main driver of infarct variability in the n-SD method are the differences in myocardial SD level, that varies between subjects, site and vendors. Based on the source of variability in infarct size we conclude the n-SD method lack accuracy for infarct quantification, especially in multi-center, multi-vendor setting.

0779



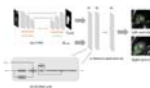
AI-supported Segmentation of the Whole Left Atrium in Cine MRI Identifies a New Geometrical Predictor of Outcome in Atrial Fibrillation

Maurice Pradella<sup>1</sup>, Sven Knecht<sup>2</sup>, Manuela Moor<sup>1</sup>, Shan Yang<sup>1</sup>, Constantinos Anastasopoulos<sup>1</sup>, Gian Voellmin<sup>2</sup>, Philip Haaf<sup>2</sup>, Stefan Osswald<sup>2</sup>, Michael Kuehne<sup>2</sup>, Christian Sticherling<sup>2</sup>, Bram Stieltjes<sup>1</sup>, and Jens Bremerich<sup>1</sup>

<sup>1</sup>Department for Radiology, University Hospital Basel, Basel, Switzerland, <sup>2</sup>Department for Cardiology, University Hospital Basel, Basel, Switzerland

Deep learning based, automatic segmentation of the whole left atrium in cine MRI makes detailed geometrical analysis possible by fitting of an ellipsoid into the contours of the left atrium. Therefore, we could identify the ellipsoidal volume at the time-point before atrial contraction as an independent predictor of recurrence of atrial fibrillation after catheter ablation in a multivariable analysis.

0780



A level-set reformulated as deep recurrent network for left/right ventricle segmentation on cardiac cine MRI

Fan Huang<sup>1</sup>, Vince Varut Vardhanabhuti<sup>1</sup>, Pek-Lan Khong<sup>1</sup>, Ming-Yen NG<sup>1</sup>, and Peng Cao<sup>1</sup>

<sup>1</sup>Department of Diagnostic Radiology, The University of Hong Kong, Hong Kong, Hong Kong

We proposed a segmentation method, which is based on a level-set reformulated via a deep recurrent network (RLSNet). This network takes the advantage of U-Net in terms of medical pattern recognition and level-set algorithm in terms of keeping the enclosed and smooth shape of the segmentation contour. We evaluate the network by the segmentation of the left and right ventricles of the heart on cardiac cine Magnetic Resonance Images, which gives greater performance than using U-Net only.

0781



Stop copying contours from Cine to LGE: multimodal learning with disentangled representations needs zero annotations

Agisilaos Chatsias<sup>1</sup>, Haochuan Jiang<sup>1</sup>, Giorgos Papanastasiou<sup>2,3</sup>, Chengjia Wang<sup>2,3</sup>, Colin Stirrat<sup>2,3</sup>, Scott Semple<sup>2,3</sup>, David Newby<sup>2,3</sup>, Rohan Dharmakumar<sup>4</sup>, and Sotirios A Tsaftaris<sup>1,5</sup>

<sup>1</sup>School of Engineering, University of Edinburgh, Institute of Digital Communications, Edinburgh, United Kingdom, <sup>2</sup>Edinburgh Imaging Facility QMRI, Edinburgh, United Kingdom, <sup>3</sup>Centre for Cardiovascular Science, Edinburgh, United Kingdom, <sup>4</sup>Cedars Sinai Medical Center, Los Angeles, CA, United States, <sup>5</sup>The Alan Turing Institute, London, United Kingdom

We propose a novel deep learning method, Multi-modal Spatial Disentanglement Network (MMSDNet), to segment anatomy in medical images. MMSDNet takes advantage of complementary information provided by multiple sequences of the same patient. Even when trained without annotations, it can segment anatomy (e.g., myocardium) in Late Gadolinium Enhancement (LGE) images, which is essential for assessing myocardial infarction. This is achieved by transferring knowledge from the simultaneously acquired cine-MR data where annotations are easier to be obtained. MMSDNet outperforms classical methods including non-linear registration, and simple copying of contours, as well as the state-of-the-art U-Net model.

0782



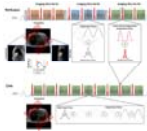
**A Joint Multi-Scale Variational Neural Network for Accelerating Free-breathing Whole-Heart qBOOST-T2 mapping**

Niccolo Fuin<sup>1</sup>, Giorgia Milotta<sup>1</sup>, Thomas Kuestner<sup>1</sup>, Aurelien Bustin<sup>1</sup>, Gastao Cruz<sup>1</sup>, Rene Botnar<sup>1,2</sup>, and Claudia Prieto<sup>1,2</sup>

*<sup>1</sup>Biomedical Engineering Department, School of Biomedical Engineering and Imaging Sciences, King's College London, London, United Kingdom, <sup>2</sup>Pontificia Universidad Católica de Chile, Santiago, Chile*

T2 mapping is a promising technique for the characterization of myocardial inflammation and oedema. We recently proposed a quantitative 3D whole-heart sequence (qBOOST-T2) which provides co-registered 3D high-resolution bright-blood and T2 map volumes from a single free-breathing scan. However, high-resolution qBOOST-T2 requires long scan times of ~10 min. Here we propose a joint Multi-Scale Variational Neural Network (jMS-VNN) to enable the acquisition of 3D high-resolution bright-blood and accurate T2 map volumes in ~3 mins, and their reconstruction in ~30s. The proposed jMS-VNN jointly reconstructs data from multiple contrasts and efficiently apply dictionary-based signal matching for fast T2 map generation.

0783



**Improved SMS Reconstruction using ReadOut-Concatenated K-space SPIRiT (ROCK-SPIRiT)**

Omer Burak Demirel<sup>1,2</sup>, Sebastian Weingärtner<sup>1,2,3</sup>, Steen Moeller<sup>2</sup>, and Mehmet Akçakaya<sup>1,2</sup>

*<sup>1</sup>Electrical and Computer Engineering, University of Minnesota, Minneapolis, MN, United States, <sup>2</sup>Center for Magnetic Resonance Research, University of Minnesota, Minneapolis, MN, United States, <sup>3</sup>Department of Imaging Physics, Delft University of Technology, Delft, Netherlands*

Simultaneous Multi-slice (SMS) imaging has great potential for high acceleration rates with minimal loss in SNR. However, due to the unfavorable coil geometry only moderate acceleration rates have been achieved in cardiac applications. Outer volume suppression (OVS) has been proposed to overcome this limitation by suppressing unwanted signal from extra-cardiac tissues such as chest and back. Despite OVS, existing reconstruction techniques may suffer from residual leakage artifacts or noise amplification. In this work, we sought to extend SPIRiT to a readout-concatenated space to improve image quality in highly accelerated perfusion and cine imaging while mitigating leakage and noise amplification.

## Oral

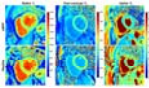
### Machine Learning and Tissue Characterisation in CMR - CMR Tissue Characterisation

Wednesday Parallel 1 Live Q&A

Wednesday 14:30 - 15:15 UTC

Moderators: Walter Witschey

0784



**Cardiac MR fingerprinting with a short acquisition window in healthy volunteers and 62 consecutive patients referred for clinical CMR**

Simone Rumac<sup>1</sup>, Anna Giulia Pavon<sup>2</sup>, Jesse Hamilton<sup>3</sup>, David Rodrigues<sup>1</sup>, Nicole Seiberlich<sup>3</sup>, Juerg Schwitler<sup>2</sup>, and Ruud B. van Heeswijk<sup>1</sup>

*<sup>1</sup>Department of Radiology, Lausanne University Hospital (CHUV), Lausanne, Switzerland, <sup>2</sup>Cardiology Service, Lausanne University Hospital (CHUV), Lausanne, Switzerland, <sup>3</sup>Department of Radiology, University of Michigan, Ann Arbor, MI, United States*



Cardiac magnetic resonance fingerprinting (cMRF) can be used to simultaneously acquire myocardial  $T_1$  and  $T_2$  maps in a single breath-hold. However, the common 250 ms acquisition window of cMRF might leave it vulnerable to motion artefacts. The goal of this study was therefore to compare the performance of cMRF with a short acquisition window (150ms) and low-rank reconstruction to that of routine cardiac parametric mapping techniques. In 7 healthy volunteers, and 62 cardiac patients, cMRF resulted in similar native relaxation times, but slightly different post-contrast  $T_1$  and ECV values compared to routine techniques.

0785



16-fold accelerated, single-shot late gadolinium enhancement CMR using GRASP for multi-TI reconstruction  
Daming Shen<sup>1,2</sup>, Kyungpyo Hong<sup>3</sup>, Bradley D Allen<sup>2</sup>, Daniel C Lee<sup>4</sup>, and Daniel Kim<sup>1,2</sup>

<sup>1</sup>Biomedical Engineering, Northwestern University, Evanston, IL, United States, <sup>2</sup>Radiology, Northwestern University Feinberg School of Medicine, Chicago, IL, United States, <sup>3</sup>Biomedical Engineering and Imaging Institute, Icahn School of Medicine at Mount Sinai, New York, NY, United States, <sup>4</sup>Division of Cardiology, Internal Medicine, Northwestern University Feinberg School of Medicine, Chicago, IL, United States

Late gadolinium enhanced (LGE) CMR is the gold standard test for assessment of myocardial scarring. There is unmet need for high resolution, free-breathing LGE CMR for patients with arrhythmia and/or dyspnea. The purpose of this study was to develop and clinically evaluate a high resolution, free-breathing LGE CMR sequence combined with radial k-space sampling and compressed sensing (CS), which enables image contrast optimization without a TI scout.

0786

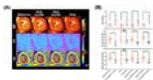


3D sub-millimeter personalized estimation of cardiomyocyte orientation using dimensionality reduction  
Johanna Stimm<sup>1</sup>, Stefano Buoso<sup>1</sup>, Martin Genet<sup>2,3,4</sup>, Sebastian Kozerke<sup>1</sup>, and Christian T Stoeckl<sup>1</sup>

<sup>1</sup>Institute for Biomedical Engineering, University and ETH Zurich, Zurich, Switzerland, <sup>2</sup>Laboratoire de Mécanique des Solides, École Polytechnique, Paris, France, <sup>3</sup>C.N.R.S./Université Paris-Saclay, Palaiseau, France, <sup>4</sup>M3DISIM team, Inria / Université Paris-Saclay, Palaiseau, France

We propose a parametric low-rank representation of major characteristics of cardiomyocyte orientation in a shape-adapted coordinate system from 3D high-resolution ex-vivo cDTI data by exploiting structural similarity across hearts. We compare two dimensionality reduction methods, namely Proper Orthogonal Decomposition and Proper Generalized Decomposition. These low-order descriptions can be fit to sparse, noisy or low-resolution target data. Transferring high-resolution microstructural information with this parametric representation shows potential for in-vivo denoising and 3D extrapolation.

0787



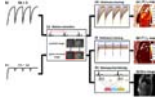
Accelerated In Vivo Cardiac Diffusion Tensor MRI with Residual Deep Learning based Denoising in Lean and Obese Subjects

Kellie Phipps<sup>1</sup>, Robert Eder<sup>1</sup>, Sam Allen Michelhaugh<sup>2</sup>, Aferdita Spahillari<sup>2</sup>, Maaïke van den Boomen<sup>1,3,4</sup>, Joan Kim<sup>1</sup>, Shestruma Parajuli<sup>1</sup>, Timothy G Reese<sup>3,5</sup>, Choukri Mekkaoui<sup>3,5</sup>, David Sosnovik<sup>1,3,6</sup>, Denise Gee<sup>7,8</sup>, Ravi Shah<sup>1,6</sup>, and Christopher Nguyen<sup>1,3,6</sup>

<sup>1</sup>Cardiovascular Research Center, Massachusetts General Hospital, Charlestown, MA, United States, <sup>2</sup>Cardiology Division, Massachusetts General Hospital, Charlestown, MA, United States, <sup>3</sup>Martinos Center for Biomedical Imaging, Massachusetts General Hospital, Charlestown, MA, United States, <sup>4</sup>Department of Radiology, University Medical Center Groningen, Groningen, Netherlands, <sup>5</sup>Department of Radiology, Harvard Medical School, Boston, MA, United States, <sup>6</sup>Department of Medicine, Harvard Medical School, Boston, MA, United States, <sup>7</sup>Weight Center, Massachusetts General Hospital, Boston, MA, United States, <sup>8</sup>Department of Surgery, Harvard Medical School, Boston, MA, United States

In vivo cardiac DT-MRI allows for imaging of the underlying myocardial fiber orientations but is hindered by clinically infeasible scan times. We developed and tested a residual deep learning denoising algorithm, DnCNN-54, on cardiac DT-MRI scans with fewer averages (4, 2, and 1) than the conventional 8-average 30 minute scan. We demonstrated a 2-fold acceleration can be achieved after DnCNN-54 is applied to 4 average dataset compared with the reference 8-average scan that preserves signal to noise ratio and cardiac DT-MRI parameter quantification. This 2-fold acceleration via DnCNN-54 denoising also maintained cardiac DT-MRI mean differences between obese and lean subjects.

0788



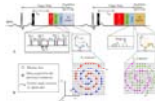
Free-breathing continuous cine and T1 mapping acquisition using a motion-corrected dual flip angle inversion-recovery spiral technique at 3 T

Ruixi Zhou<sup>1</sup>, Daniel S. Weller<sup>2</sup>, Yang Yang<sup>3</sup>, Junyu Wang<sup>1</sup>, John P. Mugler<sup>4</sup>, and Michael Salerno<sup>5</sup>

<sup>1</sup>Biomedical Engineering, University of Virginia, Charlottesville, VA, United States, <sup>2</sup>Electrical and Computer Engineering, University of Virginia, Charlottesville, VA, United States, <sup>3</sup>Biomedical Engineering and Imaging Institute and Department of Radiology, Icahn School of Medicine at Mount Sinai, New York, NY, United States, <sup>4</sup>Radiology, Biomedical Engineering, University of Virginia, Charlottesville, VA, United States, <sup>5</sup>Cardiology, Radiology, Biomedical Engineering, University of Virginia, Charlottesville, VA, United States

We propose a technique to obtain cine images and accurate B1-corrected T1 maps in a single free-breathing continuous Look-Locker inversion-recovery acquisition modified to use two excitation flip angles. Data are acquired using a single spiral interleaf, rotated by the golden-angle in time, with an inversion RF pulse applied every four seconds. Cine images are reconstructed from the steady state portion of the signal, while T1 mapping fits the model using maps with two flip angles. This strategy provides cine images and T1 maps, as well as a flip angle scale factor map, in a single free-breathing continuous acquisition.

0789



Respiratory Motion-compensated High-resolution 3D Whole-heart T1p Mapping

Haikun Qi<sup>1</sup>, Aurelien Bustin<sup>1</sup>, Thomas Kuestner<sup>1</sup>, Reza Hajhosseiny<sup>1</sup>, Gastao Cruz<sup>1</sup>, Karl Kunze<sup>1,2</sup>, Radhouene Neji<sup>1,2</sup>, René Botnar<sup>1</sup>, and Claudia Prieto<sup>1</sup>

<sup>1</sup>School of Biomedical Engineering and Imaging Sciences, King's College London, London, United Kingdom, <sup>2</sup>MR Research Collaborations, Siemens Healthcare Limited, Frimley, United Kingdom

Cardiac T1p mapping has shown promising results for detecting ischemic cardiomyopathy without the need of exogenous contrast agents. Current 2D myocardial T1p mapping requires multiple breath-holds and provides limited coverage of the heart. In this study, we proposed a free-breathing 3D T1p mapping technique featuring whole heart coverage, near-isotropic spatial resolution ( $1.7 \times 1.7 \times 2 \text{mm}^3$ ) and 100% respiratory acquisition efficiency. With the proposed technique, five T1p weightings were acquired in a clinically feasible scan time (~6 min), based on which 3D T1p maps were estimated. The accuracy and feasibility of the 3D technique was investigated in phantoms, healthy subjects and patient.

0790



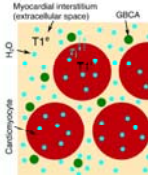
Reproducibility, Repeatability and Preliminary Clinical Results of Free-Breathing Isotropic 3D Whole-Heart T2 Mapping

Aurelien Bustin<sup>1</sup>, Alina Hua<sup>1</sup>, Giorgia Milotta<sup>1</sup>, Olivier Jaubert<sup>1</sup>, Reza Hajhosseiny<sup>1</sup>, Tefvik Ismail<sup>1</sup>, René Botnar<sup>1</sup>, and Claudia Prieto<sup>1</sup>

<sup>1</sup>Biomedical Engineering Department, School of Biomedical Engineering and Imaging Sciences, King's College London, London, United Kingdom

Myocardial T2 mapping has emerged as a promising tool for edema characterization and detection of myocardial inflammation. T2 mapping is conventionally performed under breath-hold by acquiring multiple T2-prepared images using 2D bSSFP. However, 2D imaging and breath-holding impedes high spatial resolution, limits whole-heart coverage and can be challenging in some patients. We developed a free-breathing 3D whole-heart T2 mapping framework that achieves high isotropic resolution in a clinically feasible scan time in healthy subjects. Here we sought to quantify the reproducibility and repeatability of this technique and assess its performance to detect myocardial inflammation in a clinical setting.

0791



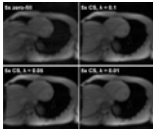
Quantifying the underestimation of myocardial extra cellular volume fraction measurements due to transcytolemmal water exchange

Andrew D Scott<sup>1,2</sup>, Peter D Gatehouse<sup>1,2</sup>, and David N Firmin<sup>1,2</sup>

<sup>1</sup>CMR Unit, The Royal Brompton Hospital, London, United Kingdom, <sup>2</sup>National Heart and Lung Institute, Imperial College London, London, United Kingdom

MR based measures of myocardial extra cellular volume fraction (ECV) obtained from pre and post-contrast T1 mapping are frequently used in research studies. However, typically ECV calculations rely on rapid exchange of water molecules between the intra and extracellular space. We assess the validity of the shutter speed approximation of the full two-compartment model and use this model to assess the effect of limited water exchange rate between the cardiomyocytes and interstitial fluid. For typical conditions used in measuring ECV, we demonstrate an underestimation of ECV on a similar magnitude to the changes attributed to disease in some studies.

0792



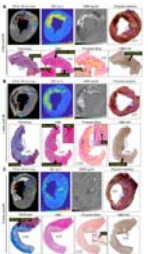
Effects of Accelerated Acquisition of Myocardial Creatine CEST MRI in the Healthy Human Heart at 3T

Kevin Godines<sup>1</sup>, Wissam AlGhuraibawi<sup>1</sup>, Bonnie Lam<sup>1</sup>, and Moriel Vandsburger<sup>1</sup>

<sup>1</sup>Bioengineering, University of California Berkeley, Berkeley, CA, United States

CEST-MRI is emerging as a powerful modality for molecular imaging of cardiac metabolites and fibrosis. In order to derive all contrasts (amide proton transfer: APT, creatine, and magnetization transfer: MT) a substantial number of differently CEST-weighted images must be acquired. Application of compressed sensing for cardiac CEST enables a 5x acceleration of acquisition with preserved accuracy.

0793



Magnetic susceptibility, R2\* and iron evolve during reperfusion injury wound healing

Brianna F. Moon<sup>1</sup>, Srikant Kamesh Iyer<sup>2</sup>, Eileen Hwuang<sup>1</sup>, Nicholas J. Josselyn<sup>2</sup>, James J. Pilla<sup>2</sup>, Joseph H. Gorman III<sup>3</sup>, Robert C. Gorman<sup>3</sup>, Cory Tschabrunn<sup>4</sup>, Samuel J. Keeney<sup>3</sup>, Estibaliz Castellero<sup>5</sup>, Giovanni Ferrari<sup>5</sup>, Steffen Jockusch<sup>6</sup>, Haochang Shou<sup>7</sup>, Elizabeth M. Higbee-Dempsey<sup>8</sup>, Andrew Tsourkas<sup>1</sup>, Victor A. Ferrari<sup>4</sup>, Yuchi Han<sup>4</sup>, Harold I. Litt<sup>2</sup>, and Walter R. Witschey<sup>2</sup>

<sup>1</sup>Bioengineering, University of Pennsylvania, Philadelphia, PA, United States, <sup>2</sup>Radiology, Perelman School of Medicine, University of Pennsylvania, Philadelphia, PA, United States, <sup>3</sup>Surgery, Perelman School of Medicine, University of Pennsylvania, Philadelphia, PA, United States, <sup>4</sup>Medicine, Perelman School of Medicine, University of Pennsylvania, Philadelphia, PA, United States, <sup>5</sup>Surgery, Columbia University Irving Medical Center, New York City, NY, United States, <sup>6</sup>Chemistry, Columbia University, New York City, NY, United States, <sup>7</sup>Biostatistics, Epidemiology and Informatics, Perelman School of Medicine, University of Pennsylvania, Philadelphia, PA, United States, <sup>8</sup>Biochemistry and Molecular Biophysics Graduate Group, Perelman School of medicine, University of Pennsylvania, Philadelphia, PA, United States

There are multiple forms of iron including protein bound and labile iron found in reperfusion injury of acute myocardial infarction (MI). This study investigated iron accumulation, molecular form of iron, and cellular response to reperfusion injury with respect to the duration of wound-healing, in a large animal model. We demonstrate with magnetic susceptibility and R2\* imaging biomarkers, there is a significant increase in infarct iron content in acute reperfusion injury that dissipates by 8-week post-MI and validate these findings with histology, iron concentration, and mRNA expression.

---

WITHDRAWN

---

## Combined Educational & Scientific Session

### Psychoradiology - Psychoradiology & AI

Organizers: Meiyun Wang, John Port

Wednesday Parallel 2 Live Q&A

Wednesday 14:30 - 15:15 UTC

Moderators: John Port & Liesbeth Reneman

#### Frontiers in Psychoradiology

Qiyong Gong<sup>1</sup>

<sup>1</sup>Huaxi MR Research Center (HMRRC), Department of Radiology, West China Hospital of Sichuan University, Chengdu, Sichuan Province, China

With the AI technical development, psychoradiology is primed to assist clinician for improving the clinical care of the psychiatric patients.

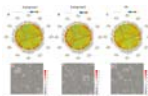
---

#### Machine Learning: Methods and Applications to Brain Disorders

Conor Liston<sup>1</sup>

<sup>1</sup>Department of Psychiatry, Weill Cornell Medical College, New York, NY, United States

0794



#### Clustering analysis differentiates clinical subtypes of major depressive disorder that identify symptom-specific brain connectivity

Shi Tang<sup>1</sup>, Yanlin Wang<sup>1</sup>, Yongbo Hu<sup>1</sup>, Lu Lu<sup>1</sup>, Lianqing Zhang<sup>1</sup>, Xuan Bu<sup>1</sup>, Hailong Li<sup>1</sup>, Yingxue Gao<sup>1</sup>, Lingxiao Cao<sup>1</sup>, Xinyue Hu<sup>1</sup>, Jing Liu<sup>1</sup>, Xinyu Hu<sup>1</sup>, Weihong Kuang<sup>2</sup>, Qiyong Gong<sup>1</sup>, and Xiaoqi Huang<sup>1</sup>

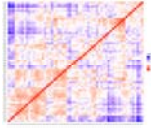
<sup>1</sup>Huaxi MR Research Center (HMRRC), Functional and molecular imaging Key Laboratory of Sichuan Province, Department of Radiology, West China Hospital, Sichuan University, Chengdu 610041, China, Chengdu, China, <sup>2</sup>Department of psychiatry, West China Hospital, Sichuan University, Chengdu 610041, China, Chengdu, China

Functional connectivity/network analyses using fMRI data have been applied to characterize diagnostic biomarkers in MDD. However, the association between brain connection and dimensional symptoms of this heterogeneous syndrome still remains unclear. In this work, we focused on first-episode and unmedicated MDD patients, firstly using unsupervised clustering analysis differentiated them into two subgroups on the basis of clinical features. Also, we compared the brain connectivity among subgroups plus healthy people. Then we used multivariate methods identified which clinical symptoms are significantly influenced by which brain connectivity. Our results may provide neurobiological mechanisms of MDD symptoms and serve as effective diagnostic biomarkers.

---

0795

#### Relapse Risk Revealed by Degree Centrality and Cluster Analysis in Heroin Addicts Undergoing Methadone Maintenance Treatment



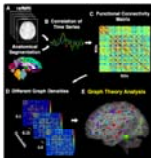
Yarong Wang<sup>1</sup> and Lei Wang<sup>2</sup>

<sup>1</sup>Department of Radiology, The First Affiliated Hospital of Xi'an Jiaotong University, Xi'an, China,

<sup>2</sup>Department of nuclear medicine, Tangdu Hospital of Air Force Medical University of PLA, Xi'an, China

The objective of this study is to identify the heroin dependents undertaking stable methadone maintenance treatment (MMT patients) at high risk for opioid relapse prospectively. First, a self-defined addiction-related brain network was constructed with 10 hubs of several circuits associated with addiction and their degree centrality. Next, sixty male MMT patients was classified into different subgroups through grouping their addiction-related network into distinct neuronal activity patterns by K-means clustering algorithm. By comparing relapse rate between subgroups with distinct network pattern, the one at high risk for relapse was identified. This finding implicated a novel strategy for improving MMT therapeutic effect.

0796



Aberrant Functional Brain Network Topology for Classification between Major Depressive Disorder and Healthy Controls

Yael Jacob<sup>1</sup>, Laurel S Morris<sup>1</sup>, Kuang-Han Huang<sup>1</sup>, Molly Schneider<sup>1</sup>, Gaurav Verma<sup>1</sup>, James W Murrrough<sup>1</sup>, and Priti Balchandani<sup>1</sup>

<sup>1</sup>Icahn School of Medicine at Mount Sinai, New York, NY, United States

Currently, diagnosis for major depressive disorder (MDD) is largely reliant on self-reported symptoms. The ability to identify MDD without self-report is greatly needed. Implementing a graph-theoretical analysis on resting state fMRI (rsfMRI), we tested whether whole-brain network topology can be used as predictors of MDD using a machine learning algorithm. We found that MDD patients exhibit aberrant network centrality measures within the right hippocampus, supramarginal and parsopercularis. Using these as predictors in a machine learning algorithm we were able to classify MDD and controls with total accuracy of 81%, demonstrating the applicability of rsfMRI for diagnostics of MDD.

0797

Model	Accuracy	Macro F1	Micro F1
Siamese Network	0.4606	0.4147	0.4147
MLP	0.4500	0.4000	0.4000
Random Forest	0.4400	0.3900	0.3900
SVM	0.4300	0.3800	0.3800
Decision Tree	0.4200	0.3700	0.3700
Logistic Regression	0.4100	0.3600	0.3600
Naive Bayes	0.4000	0.3500	0.3500
K-Nearest Neighbors	0.3900	0.3400	0.3400
Support Vector Machine	0.3800	0.3300	0.3300
Artificial Neural Network	0.3700	0.3200	0.3200

Multi-class identification for major depression, bipolar disorder and schizophrenia based on Siamese Network

Chao Li<sup>1,2,3</sup>, Yue Cui<sup>1,2,3</sup>, Yongfeng Yang<sup>4</sup>, Jing Sui<sup>1,2,3</sup>, Luxian Lv<sup>4</sup>, and Tianzi Jiang<sup>1,2,3</sup>

<sup>1</sup>Brainnetome Center, Institute of Automation, Chinese Academy of Sciences, Beijing, China, <sup>2</sup>National Laboratory of Pattern Recognition, Institute of Automation, Chinese Academy of Sciences, Beijing, China, <sup>3</sup>University of Chinese Academy of Sciences, Beijing, China, <sup>4</sup>Department of Psychiatry, Henan Mental Hospital, The Second Affiliated Hospital of Xinxiang Medical University, Xinxiang, China

Siamese Network is an artificial neural network that has been used in small sample sets multi-class classification studies. This study identified major depressive disorder (MDD), bipolar disorder (BD), and schizophrenia (SZ) based on combined gray matter, white matter and cerebrospinal fluid using Siamese Network. The participants included four groups: MDD (n = 102), BD (n = 44), SZ (n = 114), and healthy controls (n = 103). We found Siamese Network achieved improved performance than the multilayer perception network with different numbers of features. We achieved a classification accuracy of 46.06% and Macro F1 of 41.47% for this multi-class identification.

## Oral

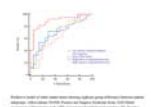
### Psychoradiology - Update on Schizophrenia

Wednesday Parallel 2 Live Q&A

Wednesday 14:30 - 15:15 UTC

Moderators: John Port

0798



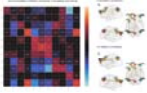
Pretreatment white matter integrity predicts one-year clinical outcome in first episode schizophrenia

Jiaxin Zeng<sup>1</sup>, Wenjing Zhang<sup>1</sup>, Gui Fu<sup>2</sup>, Lu Liu<sup>3</sup>, Biqu Tang<sup>1</sup>, Na Hu<sup>1</sup>, Yuan Xiao<sup>1</sup>, Qiyong Gong<sup>1</sup>, and Su Lui<sup>1</sup>

<sup>1</sup>West China Hospital of Sichuan University, Chengdu, China, <sup>2</sup>Sun Yat-sen University Cancer Center, Guangzhou, China, <sup>3</sup>The First People's Hospital of Ziyang, Ziyang, China

The unrevealing neuropathology underlying different clinical outcome has blocked effective treatment of schizophrenia. In this study, by prospectively recruited patients at baseline and followed them up for one-year, we have revealed the promising role of disrupted white matter integrity in discriminating good outcome from poor outcome schizophrenia. Further, the baseline white matter integrity in left anterior thalamus radiation is positively correlative with reduction of clinical ratings after one-year in all the patients. These findings indicated the underlying substrates in patients with different clinical outcomes and can serve as the potential imaging characteristic in differentiating these patients before initiating of antipsychotics.

0799



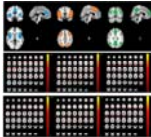
Triple Network Hypothesis-related disrupted connections are associated with positive and negative symptoms in first-episode schizophrenia

Yibin Xi<sup>1</sup>, Fan Guo<sup>1</sup>, Longbiao Cui<sup>1</sup>, Xiaocheng Wei<sup>2</sup>, Baojuan Li<sup>1</sup>, and Hong Yin<sup>1</sup>

<sup>1</sup>The Fourth Military Medical University, Xi'an, China, Xi'an, China, <sup>2</sup>MR Research China, GE Healthcare, Beijing, China

Schizophrenia is one complex mental disorder. However the dysregulated cross-network interactions among the SN, CEN and DMN and how they contributed to different symptoms is still not clear. By analyzing network interactions among the SN, CEN and DMN in patients and controls using DCM, as well as the relationship between network dynamics and clinical symptoms, our study provides strong evidence for the dysregulation among SN, CEN and DMN in a triple-network perspective in first-episode schizophrenia. We further proved that the connection between DMN and CEN could be clinically-relevant neurobiological signature of schizophrenia symptoms.

0800



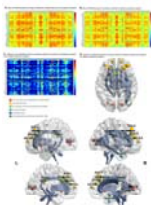
A Triple Network Connectivity Study in patients with first episode schizophrenia

Hui Zhang<sup>1,2</sup>, Pui Wai Chiu<sup>1,3</sup>, Simon S.Y. Lui<sup>4,5</sup>, Karen S.Y. Hung<sup>4</sup>, Raymond C.K. Chan<sup>5,6,7</sup>, Queenie Chan<sup>8</sup>, P.C. Sham<sup>3,7</sup>, Eric F.C. Cheung<sup>4</sup>, and Henry Ka Fung Mak<sup>1,2,3</sup>

<sup>1</sup>Department of Diagnostic Radiology, The University of Hong Kong, Hong Kong, Hong Kong, <sup>2</sup>Alzheimer's Disease Research Network, Hong Kong, Hong Kong, <sup>3</sup>State Key Laboratory of Brain and Cognitive Sciences, Hong Kong, Hong Kong, <sup>4</sup>Castle Peak Hospital, Hong Kong, Hong Kong, <sup>5</sup>Neuropsychology and Applied Cognitive Neuroscience Laboratory, CAS Key Laboratory of Mental Health, Institute of Psychology, Chinese Academy of Sciences, Beijing, China, <sup>6</sup>Department of Psychology, University of Chinese Academy of Sciences, Beijing, China, <sup>7</sup>Department of Psychiatry, The University of Hong Kong, Hong Kong, Hong Kong, <sup>8</sup>Philips Healthcare, Hong Kong, Hong Kong

To investigate the major psychopathology of first-episode schizophrenia (SCZ), the triple network model consisting of central executive network (CEN), salience network (SN) and default mode network (DMN) was employed. Group-level independent component analysis and group comparison between schizophrenia patients and healthy subjects within networks were applied. In the results, the SCZ group presented significant hyperconnectivity in bilateral insula within SN and hypoconnectivity in occipital lobe and medial prefrontal cortex within DMN. In addition to that, connectivity in bilateral insula within SN showed significant correlation with PANSS scores.

0801



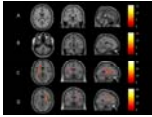
Altered functional synchrony between grey and white matter as a novel indicator of brain system dysconnectivity in schizophrenia

Naici Liu<sup>1</sup>, Wenjing Zhang<sup>1</sup>, Chengmin Yang<sup>1</sup>, Jiaxin Zeng<sup>1</sup>, Rebekka Lencer<sup>2</sup>, and Su Lui<sup>1</sup>

<sup>1</sup>Sichuan University, Chengdu, China, <sup>2</sup>University of Münster, Münster, Germany

Previous studies of white matter (WM) had been limited to structural assessment. In this study, by utilizing resting-state fMRI, the BOLD signals in WM and its functional correlations with BOLD signals in grey matter (GM) were assessed between antipsychotic-naive schizophrenia patients and healthy comparisons. The functional correlation coefficient defined as GM-WM functional synchrony were found widespread altered in patients, especially in WM connecting hemispheres, fronto-temporal, cortico-subcortical regions, and in prefrontal, cingulate, visual, temporal cortex. Additionally, age and illness-duration related alternations in functional synchrony shared the same trend. These findings described schizophrenia as a progressive disorder which was characterized by dysconnectivity.

0802



Altered resting-state functional activity characterizes white matter function in schizophrenia patients with long-term illness courses

Chengmin Yang<sup>1</sup>, Wenjing Zhang<sup>1</sup>, Naici Liu<sup>1</sup>, Li Yao<sup>1</sup>, Jiabin Zeng<sup>1</sup>, and Su Lui<sup>1</sup>

<sup>1</sup>Sichuan University, Chengdu, China

Increasing evidence has suggested white matter (WM) as well raised functional activity in brain and its functional information could be detected by resting-state functional MRI (rs-fMRI). Our study provided new insight into WM functional alterations over the long-term course of schizophrenia with and without the potential effects of antipsychotic medication. Functional changes in the splenium of the corpus callosum (SCC) were found in both treated and untreated patients, which may represent core WM functional changes in schizophrenia.

0803

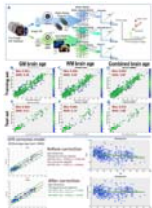
Volumetric Alterations in Treated and Never Treated Long-Term ill Schizophrenia Patients

Chandan Shah<sup>1</sup>, Youjin Zhao<sup>1</sup>, Na Hu<sup>1</sup>, Yuan Xiao<sup>1</sup>, Wenjing Zhang<sup>1</sup>, Jiabin Zeng<sup>1</sup>, and Lui Su<sup>1</sup>

<sup>1</sup>Radiology, Sichuan University, Chengdu, China

This project aims at determining specific thalamic nuclei changes in schizophrenia patients with long term illness without the confounding effects of antipsychotics as well as to determine the individual thalamic changes after long term antipsychotics.

0804



Multiple Brain Age Metrics Reveal Premature Brain Aging Network and Association with Clinical Factors in Schizophrenia

Chang-Le Chen<sup>1</sup>, Li-Ying Yang<sup>1</sup>, Yu-Hung Tung<sup>2</sup>, Yung-Chin Hsu<sup>3</sup>, Chih-Min Liu<sup>4</sup>, Tzung-Jeng Hwang<sup>4</sup>, Hai-Gwo Hwu<sup>4</sup>, and Wen-Yih Isaac Tseng<sup>1,5</sup>

<sup>1</sup>Institute of Medical Device and Imaging, College of Medicine, National Taiwan University, Taipei, Taiwan,

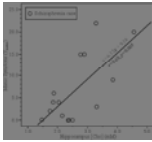
<sup>2</sup>Department of Medicine, College of Medicine, National Taiwan University, Taipei, Taiwan, <sup>3</sup>AcroViz Technology Inc., Taipei, Taiwan, <sup>4</sup>Department of Psychiatry, National Taiwan University Hospital, Taipei, Taiwan, <sup>5</sup>Molecular Imaging Center, National Taiwan University, Taipei, Taiwan

It is unclear how brain regions contribute to the premature aging in schizophrenia and whether different brain age metrics would reveal distinct clinical relevance. Therefore, we developed multiple bias-free brain age metrics based on volumetric and microstructural information to quantify the brain aging of patients with schizophrenia. The results showed that the cortical areas and fiber tracts located in the prefrontal, temporal, and limbic regions manifested dominantly to the premature brain aging compared to the other areas. Also, white matter brain age showed the significant correlation with age of onset, medication dose, and negative symptom, manifesting better clinical sensitivity.

0805

Hippocampal Metabolic MR Spectroscopic Imaging Associations with Psychotic and Manic Symptoms in Patients with Schizophrenia

Eyal Lotan<sup>1</sup>, Dolores Malaspina<sup>2</sup>, Henry Rusinek<sup>1</sup>, and Oded Gonen<sup>1</sup>



<sup>1</sup>NYU Langone Medical Center, New York, NY, United States, <sup>2</sup>Icahn School of Medicine at Mount Sinai, New York, NY, United States

Previous proton MR spectroscopic imaging of the hippocampus distinguished schizophrenia cases from controls by elevated creatine [Cr] and more variable N-acetylaspartate [NAA] and choline [Cho] concentrations. Here we examine these metabolite's concentrations in 15 cases against their research diagnostic interviews and symptom ratings. Despite modest cohort size we find: (a) elevated [Cho] predicts psychotic; and (b) manic symptoms severity; and (c) lower [NAA] trended with negative symptoms. These findings suggest that microgliosis and demyelination, reflected by reduced [NAA] and elevated [Cho], may be related to active psychotic and manic symptoms, potentially benefiting precision medicine in selection and monitoring schizophrenia treatment.

0806

Year	Country	Region	City	Population
2018	Chile	Santiago	Santiago	6,000,000
2019	Chile	Santiago	Santiago	6,000,000
2020	Chile	Santiago	Santiago	6,000,000

Longitudinal study of quantitative susceptibility mapping in patients with the first episode of psychosis

Marisleydis García<sup>1,2,3</sup>, Néstor Muñoz<sup>1,2,3</sup>, Carlos Milovic<sup>1,2,3</sup>, Luz María Alliende<sup>4</sup>, Bárbara Iruretagoyena<sup>4</sup>, Alfonso Gonzalez<sup>5</sup>, Julio Acosta Carbonero<sup>6</sup>, Cristián Montalba<sup>2,3</sup>, Nicolás Crossley<sup>2,4</sup>, Sergio Uribe<sup>2,3</sup>, and Cristián Tejos<sup>1,2,3</sup>

<sup>1</sup>Departament Electrical Engineering, Pontificia Universidad Catolica de Chile, Santiago de Chile, Chile, <sup>2</sup>Biomedical Imaging Center, Pontificia Universidad Catolica de Chile, Santiago de Chile, Chile, <sup>3</sup>Millennium Nucleus for Cardiovascular Magnetic Resonance, Pontificia Universidad Catolica de Chile, Santiago de Chile, Chile, <sup>4</sup>Neurology Department, School of Medicine, Pontificia Universidad Catolica de Chile, Santiago de Chile, Chile, <sup>5</sup>Instituto Psiquiátrico Horwitz, Santiago de Chile, Chile, <sup>6</sup>Tenoke Ltd., Cambridge, United Kingdom

Psychosis has been related with dopamine alterations in deep brain nuclei. Neuromelanin is a by-product of the synthesis of dopamine and it is synthesized via iron-dependent oxidation. Thus, susceptibility might give a window to study the progression of dopamine levels at deep brain nuclei of psychotic patients. We studied a cohort of patients with First Episode of Psychosis (FEP) using QSM at two time points and compared them with healthy controls. We found susceptibility changes in seven subcortical areas at FEP onset. We also found susceptibility changes at the left globus pallidus interna after three months of pharmacological treatment.

Oral

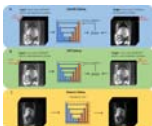
Machine Learning, Imaging Optimization, and Cancer - Machine Learning in Body MRI

Wednesday Parallel 3 Live Q&A

Wednesday 14:30 - 15:15 UTC

Moderators: Eva Gombos & Frank Zoellner

0807



Phase2Phase: Reconstruction of free-breathing MRI into multiple respiratory phases using deep learning without a ground truth

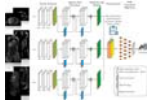
Cihat Eldeniz<sup>1</sup>, Weijie Gan<sup>1</sup>, Sihao Chen<sup>1</sup>, Jiaming Liu<sup>1</sup>, Ulugbek S. Kamilov<sup>1</sup>, and Hongyu An<sup>1</sup>

<sup>1</sup>Washington University in St. Louis, Saint Louis, MO, United States

Radial MRI can be used for reconstructing multiple respiratory phases with retrospective binning. However, short acquisitions suffer from significant streaking artifacts. Compressed sensing (CS)-based methods are commonly used; nevertheless, CS is computational intensive and the image quality depends on the regularization parameters. We hereby propose a deep learning method that does not need an artifact-free target during training. The method can reconstruct high-quality volumes with ten respiratory phases, even for acquisitions close to 1 minute in length. The method outperforms CS for the same acquisition duration and can yield slightly better results than Unet3D trained using a surrogate ground truth.



0808

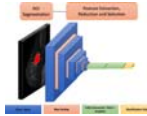


Thomas Küstner<sup>1,2,3</sup>, Tobias Hepp<sup>2</sup>, Karim Armanious<sup>2,3</sup>, Konstantin Nikolaou<sup>4</sup>, Sergios Gatidis<sup>2,4</sup>, and Bin Yang<sup>3</sup>

<sup>1</sup>Biomedical Engineering Department, School of Biomedical Engineering and Imaging Sciences, King's College London, London, United Kingdom, <sup>2</sup>Medical Image and Data Analysis (MIDAS), University Hospital Tübingen, Tübingen, Germany, <sup>3</sup>Institute of Signal Processing and System Theory, University of Stuttgart, Stuttgart, Germany, <sup>4</sup>Department of Radiology, University Hospital Tübingen, Tübingen, Germany

Age is one of the most important clinical parameters describing patients in a medical context. The chronological age (CA) does however not necessarily reflect the true underlying biological age (BA) which can depend on multiple factors such as lifestyle, social environment, medical history, genetics and ethnicity. It is therefore desirable to measure BA quantitatively and objectively. In this proof-of-principle study, we examine if CA can be estimated from whole-body MRI. We propose a novel deep learning architecture to perform an accurate CA estimation.

0809



Transfer Learning-Based Preoperative Prediction of Lymph Node Metastasis

Renee Cattell<sup>1</sup>, Jie Ding<sup>1</sup>, Shenglan Chen<sup>1</sup>, and Chuan Huang<sup>1,2,3</sup>

<sup>1</sup>Biomedical Engineering, Stony Brook University, Stony Brook, NY, United States, <sup>2</sup>Radiology, Stony Brook University, Stony Brook, NY, United States, <sup>3</sup>Psychiatry, Stony Brook University, Stony Brook, NY, United States

A tool to preoperatively predict sentinel lymph node status in patients with breast cancer could minimize the need for invasive surgical examination. Radiomics has been shown to have predictive power in many classification tasks. Fully automated deep learning methods would integrate more easily into clinical workflow because they do not require manual feature extraction. However, convolutional neural networks are computationally demanding and require large datasets to train. Transfer learning can be applied to allow for shortened training time and applicable to relatively small datasets.

0810



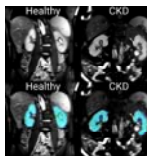
Deep Learning for Determination of Myometrial Invasion Depth and Automatic Lesion Identification Based on Endometrial Cancer MR Imaging

Yida Wang<sup>1</sup>, Yinqiao Yi<sup>1</sup>, Minhua Shen<sup>2</sup>, He Zhang<sup>2</sup>, Xu Yan<sup>3</sup>, and Guang Yang<sup>1</sup>

<sup>1</sup>Shanghai Key Laboratory of Magnetic Resonance, East China Normal University, Shanghai, China, <sup>2</sup>Department of Radiology, Obstetrics and Gynecology Hospital, Fudan University, Shanghai, China, <sup>3</sup>MR Scientific Marketing, Siemens Healthcare, Shanghai, China

We proposed an deep learning approach to locate lesion and evaluate the myometrial invasion (MI) depth automatically on magnetic resonance (MR) images. Firstly, we trained a detection model based on YOLOv3 to locate lesion area on endometrial cancer MR (ECM) images. Then, the detected lesion regions on both sagittal and coronal images were simultaneously fed into a classification model based on Resnet to identify MI depth. Precision-recall curve, receiver operating characteristic curve and confusion matrix were used to evaluate the performance of the proposed method. The proposed model achieved good and time-efficient performance.

0811



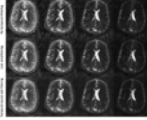
Automated Renal Segmentation in Healthy and Chronic Kidney Disease Subjects Using A Convolutional Neural Network

Alexander J Daniel<sup>1</sup>, Charlotte E Buchanan<sup>1</sup>, Thomas Allcock<sup>1</sup>, Daniel Scerri<sup>1</sup>, Eleanor F Cox<sup>1</sup>, Benjamin L Prestwich<sup>1</sup>, and Susan T Francis<sup>1</sup>

<sup>1</sup>Sir Peter Mansfield Imaging Centre, University of Nottingham, Nottingham, United Kingdom

Manual segmentation of the kidneys in renal MRI is a time consuming process in many processing pipelines. Existing automated methods using classical imaging processing are specific to a single pathology. Here we implement a convolutional neural network for rapid and automatic segmentation of the kidneys from both a healthy control and Chronic Kidney Disease cohort. When validated on unseen data, the network achieved a mean Dice score of  $0.93 \pm 0.02$  with mean error in total kidney volume of  $2.0 \pm 16.5$  ml which, in the majority of subjects, was better than human precision from manual segmentation.

0812



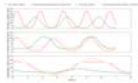
#### Unsupervised radial streak artifact reduction in time resolved MRI

Sagar Mandava<sup>1</sup>, Ty Cashen<sup>2</sup>, Daniel V Litwiller<sup>3</sup>, Tetsuya Wakayama<sup>4</sup>, and Ersin Bayram<sup>5</sup>

<sup>1</sup>Global MR Applications & Workflow, GE Healthcare, Tucson, AZ, United States, <sup>2</sup>Global MR Applications & Workflow, GE Healthcare, Madison, WI, United States, <sup>3</sup>Global MR Applications & Workflow, GE Healthcare, New York, NY, United States, <sup>4</sup>Global MR Applications & Workflow, GE Healthcare, Hino, Japan, <sup>5</sup>Global MR Applications & Workflow, GE Healthcare, Houston, TX, United States

Radial magnetic resonance imaging is attractive due to its inherently high motion robustness and its ability to support accelerated imaging but is plagued by streaking artifact. The problem is exacerbated in time resolved imaging, like DCE-MRI, which deal with higher levels of undersampling due to the need to jointly deliver high spatial and temporal resolution. While reconstructive methods typically based on sparse or low rank methods exist to minimize streak artifact, their use is currently limited due to their high computational complexity. As an alternative, we describe a temporal neural network to suppress streak artifact from a time-series of images.

0813



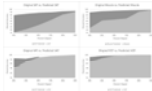
#### Diaphragm motion prediction with a LSTM network using MRI k-space data

Carola Fischer<sup>1,2</sup>, Florian Friedrich<sup>1,2</sup>, Peter Bachert<sup>1,2</sup>, Mark E. Ladd<sup>1</sup>, and Benjamin R. Knowles<sup>1</sup>

<sup>1</sup>Medical Physics in Radiology, German Cancer Research Center (DKFZ), Heidelberg, Germany, <sup>2</sup>Department of Physics and Astronomy, Heidelberg University, Heidelberg, Germany

Hybrid MRI linear accelerators (MR-linac) enable real-time tracking of tumor motion during treatment. Due to system latencies that delay treatment adjustments, one has to predict as well as track motion. This abstract presents a feasibility study to predict diaphragm motion using MRI k-space data using a long short-term memory (LSTM) recurrent neural network, by comparing simulation, phantom and an *in vivo* study. First experiments show that prediction accuracies of approximately 1.7mm are possible at 400ms latencies for the diaphragm with guided breathing.

0814



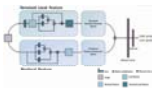
#### Automating Image-Based Body Composition Analysis with Missing Data

Clint R Frandsen<sup>1,2</sup>, Alexander D Weston<sup>1,2</sup>, Kenneth R Philbrick<sup>1,2</sup>, Gian Marco Conte<sup>1,2</sup>, Bradley J Erickson<sup>1,2</sup>, and Timothy Kline<sup>1,2</sup>

<sup>1</sup>Radiology Informatics Lab, Mayo Clinic, Rochester, MN, United States, <sup>2</sup>Physiology & Biomedical Engineering, Mayo Clinic College of Medicine & Science, Rochester, MN, Rochester, MN, United States

We have developed and evaluated an automated algorithm that learns to synthesize representative segmentations of the missing anatomy in partial abdominal MR images using a deep learning-based approach. These synthesized segmentations are optimal for studies focusing on the analyzes of body composition.

0815



#### Local feature denoising and global feature extraction for malignancy characterization of hepatocellular carcinoma

Wu Zhou<sup>1</sup>, Hui Huang<sup>1</sup>, Guangyi Wang<sup>2</sup>, and Honglai Zhang<sup>1</sup>

Convolutional neural network (CNN) has been regarded to be powerful for lesion characterization in clinical practice. However, local deep feature derived from CNN has two main shortcomings for characterization. First, the convolutional operations typically process within a local neighborhood while ignoring the global dependency. Furthermore, it is unstable to small perturbations in images (e.g., noise or artifacts). Therefore, we propose a denoised local fusion and nonlocal deep feature fusion method to alleviate the above two problems. The proposed method is a general module, which can be integrated into any CNN-based architecture for improving performance of lesion characterization in clinical routine.

---

## Oral - Power Pitch

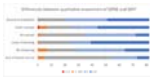
### Machine Learning, Imaging Optimization, and Cancer - Image Optimization & Innovation

Wednesday Parallel 3 Live Q&A

Wednesday 14:30 - 15:15 UTC

Moderators: Rebecca Rachow-Pener

0816



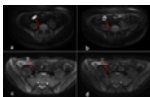
Cine SSFSE for reduced susceptibility artifact and increased diagnostic accuracy in MR enterography

Peter Wei<sup>1</sup>, Anugayathri Jawahar<sup>1</sup>, Daniel V. Litwiller<sup>2</sup>, and Andreas M. Loening<sup>1</sup>

<sup>1</sup>Department of Radiology, Stanford University, Stanford, CA, United States, <sup>2</sup>Global MR applications and Workflow, GE Healthcare, New York, NY, United States

A steady-state free precession (SSFP) sequence is used in many MR enterography (MRE) protocols for acquiring cine images to assess bowel motility, inflammation, and strictures. However, SSFP suffers from susceptibility and banding artifacts that become more significant at high field strengths. In this IRB approved retrospective study, we compared a cine SSFP sequence to a cine T2-weighted single-shot fast spin echo (SSFSE) sequence in 41 patients. We found SSFSE demonstrated significantly superior subjective assessments of image quality, improved diagnostic performance compared to cine SSFP, and successfully mitigated SSFP artifacts that can otherwise limit the exam.

0817



The Application of High-resolution Multi-shot DWI with MUSE reconstruction in the Diagnosis of Active Inflammation in Crohn's Disease

Guangtao Chen<sup>1</sup>, Hing-Chiu Chang<sup>1</sup>, and Keith Wan-Hang Chiu<sup>1</sup>

<sup>1</sup>The Department of Diagnostic Radiology, The University of Hong Kong, Hong Kong, China

Diffusion-weighted imaging (DWI) has been shown to be useful in evaluation of active bowel inflammation. Single-shot diffusion-weighted echo-planar imaging (ssDW-EPI) was commonly used in previous studies. However, ssDW-EPI suffers from geometric distortion and low spatial resolution. Moreover, the data acquisition of ssDW-EPI in bowel region become more difficult due to off-resonance effect. A recently developed multiplexed sensitivity-encoding (MUSE) framework can produce multi-shot DW-EPI (msDW-EPI) data with improved spatial resolution and reduced distortions. In this study, we demonstrated that the higher resolution and better overall image quality of msDW-EPI using MUSE framework potentially increased the accuracy in diagnosing active bowel inflammation.

0818

Robustness of Texture Features on 3 Tesla Liver MRI.

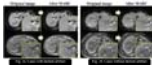
Vinay Prabhu<sup>1</sup>, Nicolas Gillingham<sup>1</sup>, Mary T. Bruno<sup>1</sup>, James Babb<sup>1</sup>, Henry Rusinek<sup>1</sup>, and Hersh Chandarana<sup>1</sup>

<sup>1</sup>Radiology, NYU Langone Health, New York, NY, United States

We studied the robustness of liver MRI texture features by scanning five healthy volunteers at 3T, first using standard institutional acquisition parameters, and then introducing slight variation in acquisition parameters. Our results demonstrate that a number of texture features were not robust to acquisition parameter changes.

---

0819



### Erasing artifacts from arterial phase MRI: Motion Artifact Reduction using a Convolutional network (MARC)

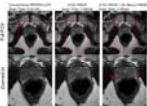
Shinya Kojima<sup>1,2</sup>, Daiki Tamada<sup>2</sup>, Tetsuya Wakayama<sup>3</sup>, Shintaro Ichikawa<sup>2</sup>, Hiroyuki Morisaka<sup>4</sup>, Shigeru Suzuki<sup>1</sup>, and Utaroh Motosugi<sup>2</sup>

<sup>1</sup>Department of Radiology, Tokyo Women's Medical University Medical Center East, Arakawa, Japan, <sup>2</sup>Department of Radiology, University of Yamanashi, Yamanashi, Japan, <sup>3</sup>MR Collaboration and Development, GE Healthcare, Hino, Japan, <sup>4</sup>Department of Radiology, Saitama Medical University International Medical Center, Saitama, Japan

Motion artifact by irregular respiration disturbs accurate diagnosis in dynamic contrast-enhanced MRI of the liver. We developed a motion artifact reduction algorithm using a convolutional network (MARC). The training was performed using U-net with the arterial phase images with and without simulated artifacts. For verifying the ability of MARC algorithm, contrast-to-noise ratio measurement and visual assessment were performed in 120 cases. The image quality of arterial phase images with motion artifacts were significantly improved after applying MARC algorithm, while no particular difference was observed in the images without motion artifacts. MARC provides motion artifacts reduction without variation of image contrast.

---

0820



### High Resolution T2W imaging using Deep Learning Reconstruction and Reduced Field-of-View PROPELLER

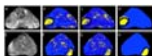
Xinzeng Wang<sup>1</sup>, Daniel Litwiller<sup>2</sup>, Marc Lebel<sup>3</sup>, Ali Ersoz<sup>4</sup>, Lloyd Estkowski<sup>4</sup>, Jason Stafford<sup>5</sup>, and Ersin Bayram<sup>6</sup>

<sup>1</sup>GE Healthcare, Houston, TX, United States, <sup>2</sup>Global MR Applications & Workflow, GE Healthcare, New York, NY, United States, <sup>3</sup>Global MR Applications & Workflow, GE Healthcare, Calgary, AB, Canada, <sup>4</sup>Global MR Applications & Workflow, GE Healthcare, Waukesha, WI, United States, <sup>5</sup>Department of Imaging Physics, MD Anderson Cancer Center, Houston, TX, United States, <sup>6</sup>Global MR Applications & Workflow, GE Healthcare, Houston, TX, United States

T2W FSE-PROPELLER is robust to susceptibility artifacts and bulk motion, but requires longer acquisition times compared to conventional FSE methods. Recently, a reduced Field-Of-View PROPELLER sequence using rotating outer volume suppression method has been proposed and optimized to reduce the scan time for small FOV and high-resolution T2W imaging. However, image SNR is comparatively lower compared to the conventional PROPELLER with phase oversampling. In this work, a deep learning based PROPELLER reconstruction method was used to improve the SNR and image quality of the reduced Field-Of-View PROPELLER.

---

0821



### End-to-end Deep Learning Strategy To Segment Prostate Cancer From Multi-parametric MR Images

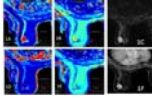
David Hoar<sup>1</sup>, Peter Lee<sup>2</sup>, Alessandro Guida<sup>3</sup>, Steven Patterson<sup>3</sup>, Chris Bowen<sup>3,4</sup>, Jennifer Merrimen<sup>5</sup>, Cheng Wang<sup>5</sup>, Ricardo Rendon<sup>6</sup>, Steven Beyea<sup>3,4</sup>, and Sharon Elizabeth Clarke<sup>3,4</sup>

<sup>1</sup>Department of Electrical and Computer Engineering, Dalhousie University, Halifax, NS, Canada, <sup>2</sup>Faculty of Computer Science, Dalhousie University, Halifax, NS, Canada, <sup>3</sup>Biomedical Translational Imaging Centre, Nova Scotia Health Authority and IWK Health Centre, Halifax, NS, Canada, <sup>4</sup>Diagnostic Radiology, Dalhousie University, Halifax, NS, Canada, <sup>5</sup>Pathology, Dalhousie University, Halifax, NS, Canada, <sup>6</sup>Urology, Dalhousie University, Halifax, NS, Canada

The purpose of this study was to develop a convolutional neural network (CNN) for dense prediction of prostate cancer using mp-MRI datasets. Baseline CNN outperformed logistic regression and random forest models. Transfer learning and unsupervised pre-training did not significantly improve CNN performance; however, test-time augmentation resulted in significantly higher F1 scores over both baseline CNN and CNN plus either of transfer learning or unsupervised pre-training. The best performing model was CNN with transfer learning and test-time augmentation (F1 score of 0.59, AUPRC of 0.61 and AUROC of 0.93).

---

0822



### T1 and T2 relaxation time in synthetic MRI for differentiating benign and malignant breast lesions

Shi yun SUN<sup>1</sup>, Zhuo lin Li<sup>1</sup>, Ying ying Ding<sup>1</sup>, Yi fan Liu<sup>1</sup>, Dong xue ZHANG<sup>1</sup>, Li sha NIE<sup>2</sup>, Ke XUE<sup>1</sup>, and Dian Ke DU<sup>1</sup>

<sup>1</sup>Radiology, Yunnan Cancer Hospital, The Third Affiliated Hospital of Kunming Medical University, Kunming, China, <sup>2</sup>GE Healthcare, MR Research China, Beijing, China, China

It is reported that dynamic contrast imaging and T2 relaxation time can be used to differentiate benign and malignant breast lesions. However, few researches have investigated T1 and T2 relaxation time changes before and after contrast injection. But it's important for the diagnosis of breast diseases. Thus, the study aims to utilize the T1 and T2 mapping in synthetic MR to differentiate benign and malignant lesions. Our results demonstrated that T1 and T2 mapping could constitute a new adjunct in the MRI diagnosis of breast diseases.

0823



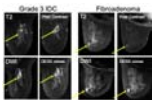
### Water and Fat Separation with a Dixon Conditional Generative Adversarial Network (DixonCGAN)

Jong Bum Son<sup>1</sup>, Ken-Pin Hwang<sup>1</sup>, Marion E. Scoggins<sup>2</sup>, Basak E. Dogan<sup>3</sup>, Gaiane M. Rauch<sup>2</sup>, Mark D. Pagel<sup>4</sup>, and Jingfei Ma<sup>1</sup>

<sup>1</sup>Imaging Physics Department, The University of Texas MD Anderson Cancer Center, Houston, TX, United States, <sup>2</sup>Diagnostic Radiology Department, The University of Texas MD Anderson Cancer Center, Houston, TX, United States, <sup>3</sup>Department of Diagnostic Radiology, The University of Texas Southwestern Medical Center, Dallas, TX, United States, <sup>4</sup>Cancer Systems Imaging Department, The University of Texas MD Anderson Cancer Center, Houston, TX, United States

A Dixon conditional generative adversarial network (DixonCGAN) was developed for Dixon water and fat separation. For the robust water image reconstruction, DixonCGAN performs water and fat separation with three processing steps: (1) phase-correction with DixonCGAN, (2) error-correction for DixonCGAN processing, and (3) the final water and fat separation. A conditional generative adversarial network (CGAN) originally designed to change photo styles could be successfully modified to perform phase-correction with improved global and local image details. Moreover, localized deep-learning processing errors could be effectively recovered with the proposed deep-learning error-correction processes.

0824



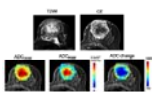
### Double Echo Steady State (DESS) Cones for Non-Contrast-Enhanced Breast MRI

Catherine Judith Moran<sup>1</sup>, Christopher M Sandino<sup>2</sup>, Joseph Cheng<sup>1</sup>, Marcus T Alley<sup>1</sup>, Bruce Daniel<sup>1</sup>, and Brian A. Hargreaves<sup>1</sup>

<sup>1</sup>Radiology, Stanford University, Stanford, CA, United States, <sup>2</sup>Electrical Engineering, Stanford University, Stanford, CA, United States

Breast MRI without a contrast injection has the potential to increase accessibility and compliance to the method in women who are recommended to undergo annual MRI to screen for breast cancer. Steady-state diffusion weighted methods provide robust image quality in comparison to conventional diffusion weighted methods which can suffer from variable image quality due to distortion, blurring and low-resolution. Double Echo Steady State (DESS) acquisition with a cones k-space trajectory is investigated for non-contrast enhanced breast MRI in 30 women undergoing clinically indicated breast MRIs.

0825



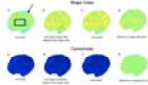
### Clinical Diffusion Time Dependency of Breast Tumors and Associations with Prognostic Factors

Mami Iima<sup>1,2</sup>, Masako Kataoka<sup>1</sup>, Maya Honda<sup>1</sup>, Ayami Ohno Kishimoto<sup>1</sup>, Rie Ota<sup>1</sup>, Akane Ohashi<sup>1</sup>, Yuta Urushibata<sup>3</sup>, Thorsten Feiweier<sup>4</sup>, Masakazu Toji<sup>5</sup>, and Kaori Togashi<sup>1</sup>

<sup>1</sup>Diagnostic Imaging and Nuclear Medicine, Kyoto University Graduate School of Medicine, Kyoto, Japan, <sup>2</sup>Clinical Innovative Medicine, Institute for Advancement of Clinical and Translational Science, Kyoto University Hospital, Kyoto, Japan, <sup>3</sup>Siemens Healthcare K.K., Tokyo, Japan, <sup>4</sup>Siemens Healthcare GMBH, Erlangen, Germany, <sup>5</sup>Breast Surgery, Kyoto University Graduate School of Medicine, Kyoto, Japan

We investigated the variation of ADC values obtained at diffusion times that are clinically available for differentiation of human breast tumors. The ADC values in both malignant and benign breast tumors decreased with increased diffusion time, and a larger change in ADC values was found in malignant tumors. The significant association found between ADC change and Ki-67 expression might indicate the potential of diffusion time-dependent ADC values as a tool to differentiate these prognostic biomarkers and assess tumor heterogeneity without the need for contrast agents.

0826



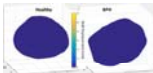
**Cortical Surface Spectral Matching of the Fetal Brain Pre and Post Fetal Surgery for Open Spina Bifida**

Nada Mufti<sup>1,2,3</sup>, Michael Aertsen<sup>4</sup>, Michael Ebner<sup>2,3</sup>, Lucas Fidon<sup>2</sup>, Tom Vercauteren<sup>2,5</sup>, Luc De Catte<sup>5</sup>, Philippe Demaerel<sup>4</sup>, Jan Deprest<sup>1,5</sup>, Sebastien Ourselin<sup>2</sup>, Anna L David<sup>1,6</sup>, and Andrew Melbourne<sup>2,3</sup>

<sup>1</sup>Institute for Women's Health and Department of Medical Physics and Biomedical Engineering, University College London (UCL), London, United Kingdom, <sup>2</sup>School of Biomedical Engineering and Imaging Sciences (BMEIS), King's College London, London, United Kingdom, <sup>3</sup>Department of Medical Physics and Biomedical Engineering, University College London (UCL), London, United Kingdom, <sup>4</sup>Department of Radiology, University Hospitals Katholieke Universiteit (KU) Leuven, Leuven, Belgium, <sup>5</sup>Department of Obstetrics and Gynaecology, University Hospitals Katholieke Universiteit (KU) Leuven, Leuven, Belgium, <sup>6</sup>University Hospitals KU Leuven, Leuven, Belgium

Comprehensive evaluation of the fetal central nervous system (CNS) is required to select the most suitable candidates, to counsel parents about fetal spina bifida surgery, and to monitor post-op response. In children and adolescents with spina bifida, MRI assessment of gyrification correlates with motor and cognitive function. Our aim is to determine if MRI can quantify fetal brain gyrification and folding before and after fetal spina bifida surgery. If successful, mapping the gyrification changes to different lobes in the brain may prove useful in the prediction of motor and cognitive function after fetal surgery.

0827



**Comprehensive Analysis of Bladder Wall Perfusion and Deformation in BPH patients using MRI**

Ryan J Pewowaruk<sup>1</sup>, David R Rutkowski<sup>2</sup>, Cody J Johnson<sup>2</sup>, Colin K Kim<sup>2</sup>, Shane A Wells<sup>2</sup>, Wade A Bushman<sup>3</sup>, Diego Hernando<sup>2,4</sup>, and Alejandro Roldán-Alzate<sup>1,2,5</sup>

<sup>1</sup>Biomedical Engineering, University of Wisconsin, Madison, WI, United States, <sup>2</sup>Radiology, University of Wisconsin, Madison, WI, United States, <sup>3</sup>Urology, University of Wisconsin, Madison, WI, United States, <sup>4</sup>Medical Physics, University of Wisconsin, Madison, WI, United States, <sup>5</sup>Mechanical Engineering, University of Wisconsin, Madison, WI, United States

Male urogenital disease is a common problem, and non-invasive methods for diagnosis and disease progression tracking are limited. This study was aimed at developing an MRI-based method to characterize urogenital tissue morphology, bladder-prostate interaction, and blood flow perfusion. These methods were tested in three patients with BPH and three healthy volunteers. Strong correlation between void fraction and prostate volume was found. Future work will be aimed at applying these methods to larger cohorts so that clinical utility may be further understood.

0828



**3D O2-Enhanced MR Imaging vs. Thin-Section CT: Capability for Pulmonary Functional Loss Assessment and Clinical Stage Classification in Smokers**

Yoshiharu Ohno<sup>1,2</sup>, Masao Yui<sup>3</sup>, Daisuke Takenaka<sup>4</sup>, Yoshimori Kassai<sup>3</sup>, Kazuhiro Murayama<sup>1</sup>, and Takeshi Yoshikawa<sup>2</sup>

<sup>1</sup>Radiology, Fujita Health University School of Medicine, Toyoake, Japan, <sup>2</sup>Radiology, Kobe University Graduate School of Medicine, Kobe, Japan, <sup>3</sup>Canon Medical Systems Corporation, Otawara, Japan, <sup>4</sup>Diagnostic Radiology, Hyogo Cancer Center, Akashi, Japan

No one directly compare this new technique with quantitatively assessed CT for pulmonary functional loss evaluation and The Global Initiative for Chronic Obstructive Lung Disease (GOLD) classification in smokers. We hypothesized that regional  $\Delta T1$  change from 3D O<sub>2</sub>-enhanced MRI has a potential for pulmonary functional loss assessment and clinical stage classification as well as quantitatively assessed thin-section CT in smokers. The purpose of this study was to prospectively and directly compare the quantitative capability for pulmonary functional loss assessment and clinical stage classification between 3D O<sub>2</sub>-enhanced MRI and thin-section CT in smokers.

---

---

## Oral - Power Pitch

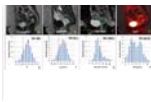
### Machine Learning, Imaging Optimization, and Cancer - Body Trunk Cancer

Wednesday Parallel 3 Live Q&A

Wednesday 14:30 - 15:15 UTC

Moderators: Oliver Gurney-Champion & Tom Scheenen

0829



#### Early Prediction of Treatment Response and Mortality in Advanced Cervical Cancer: Temporal Changes of Functional MRI and <sup>18</sup>FDG PET/CT Radiomics

Murat Alp Oztek<sup>1,2</sup>, Stephen R Bowen<sup>2</sup>, Savannah C Partridge<sup>1</sup>, Daniel S Hippe<sup>1</sup>, William T. Yuh<sup>1</sup>, Aaron S Nelson<sup>3</sup>, Simon S Lo<sup>2</sup>, Elaine Y Lee<sup>4</sup>, Eric Leung<sup>5</sup>, John C Grecula<sup>6</sup>, Matthew Harkenrider<sup>7</sup>, Michael V Knopp<sup>6</sup>, Wei Wu<sup>1</sup>, and Nina A Mayr<sup>2</sup>

<sup>1</sup>Radiology, University of Washington, Seattle, WA, United States, <sup>2</sup>Radiation Oncology, University of Washington, Seattle, WA, United States, <sup>3</sup>MIM Software, Beachwood, OH, United States, <sup>4</sup>Radiology, The University of Hong Kong, Hong Kong, Hong Kong, <sup>5</sup>Sunnybrook Health Sciences Centre, University of Toronto, Toronto, ON, Canada, <sup>6</sup>Ohio State University, Columbus, OH, United States, <sup>7</sup>Loyola University, Chicago, IL, United States

DCE, ADC and <sup>18</sup>FDG PET/CT radiomics parameters, obtained simultaneously before, early during and midway during ongoing radiation/chemotherapy correlate with tumor response and particularly mortality, and can serve as early predictors of treatment outcome in advanced cervical cancer. Longitudinal development of functional heterogeneity may be a sensitive measure reflecting responsiveness of individual tumors to a specific cytotoxic treatment regimen. Particularly the persistence of skewness of the dynamic contrast enhancement within the tumor volume predicted cancer mortality. Functional radiomics assessment may help address the unmet need for a patient- and treatment-specific early indicator of tumor responsiveness and survival.

---

0830



#### Delta Radiomic Features from serial bi-parametric MRI are associated with biopsy upgrading of prostate cancer patients on Active Surveillance

Rakesh Shiradkar<sup>1</sup>, Ruyuan Zuo<sup>1</sup>, Amr Mahran<sup>2</sup>, Lin Li<sup>1</sup>, Britt Conroy<sup>2,3</sup>, Lee Ponsky<sup>2,3</sup>, Sree Harsha Tirumani<sup>2,3</sup>, and Anant Madabhushi<sup>1</sup>

<sup>1</sup>Case Western Reserve University, Cleveland, OH, United States, <sup>2</sup>UH Cleveland Medical Center, Cleveland, OH, United States, <sup>3</sup>Case Western Reserve University School of Medicine, Cleveland, OH, United States

Serial MRI allows for non-invasive monitoring of prostate cancer patients on Active Surveillance (AS). However, repeat biopsies continue to be defacto standard for AS monitoring due to limitations of MRI. In this study, we sought to compute delta changes in radiomic features on serial bi-parametric MRI and evaluate their associations with biopsy upgrading. We observed that delta radiomic features that quantify underlying spatial, gradient based heterogeneity were associated with biopsy upgrading. On univariable and multivariable analysis with routine clinical variables, we observed that none of the clinical variables were significant while delta radiomic classifier predictions were significant and independently predictive.

0831



#### T2\*-weighted MRI as a non-contrast enhanced method for assessment of focal laser ablation zone extent in prostate cancer thermotherapy

Chongpeng Sun<sup>1,2</sup>, Shiyang Wang<sup>1,3</sup>, Aritrick Chatterjee<sup>1</sup>, Milica Medved<sup>1</sup>, Scott Eggner<sup>4</sup>, Gregory S Karczmar<sup>1</sup>, and Aytakin Oto<sup>1</sup>

<sup>1</sup>Radiology, University of Chicago, Chicago, IL, United States, <sup>2</sup>Radiology, The First Affiliated Hospital of Guangzhou Medical University, Guangzhou, China, <sup>3</sup>Medical Physics, University of Missouri, Columbia, MO, United States, <sup>4</sup>Urology, University of Chicago, Chicago, IL, United States

This study evaluated the utility of T2\*-weighted (T2\*W) MRI for intra-operative identification of ablation zone extent during focal laser ablation (FLA) of prostate cancer. Ablation zone ROI sizes and contrast-to-background ratio (CBR) were calculated on T2\*W and apparent diffusion coefficient (ADC) maps and compared to those in the reference standard subtracted contrast-enhanced T1-weighted (sceT1W) images. CBRs on T2\*W (TE=32,63 ms) did not differ significantly from those in sceT1W, and ROI sizes in T2\*W (TE=63 ms) and sceT1W were well-correlated and differed by only 15%. Therefore, T2\*W MRI with long TE visualizes post-procedure ablation zone comparably to contrast-enhanced T1W MRI.

0832



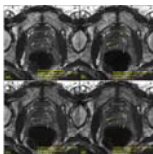
#### Added Value of DCE in Machine Learning-based Tumor Probability Maps for Predicting Clinically Significant Cancer Foci in Pre-biopsy MR images

Gabriel Addio Nketiah<sup>1</sup>, Léo Pallas<sup>2</sup>, Adrian L Breto<sup>3</sup>, Radka Stoyanova<sup>3</sup>, Mattijs Elschot<sup>1</sup>, and Tone F. Bathen<sup>1,4</sup>

<sup>1</sup>Circulation and Medical Imaging, Norwegian University of Science and Technology, Trondheim, Norway, <sup>2</sup>Department of Digital Science, CPE Lyon, Lyon, Norway, <sup>3</sup>Sylvester Comprehensive Cancer Center, University of Miami, Miami, FL, United States, <sup>4</sup>Clinic of Radiology and Nuclear Medicine, St. Olavs University Hospital, Trondheim, Norway

The utility of multiparametric (mp) versus biparametric (bp) MRI protocol in prostate cancer diagnosis has been compared in several large studies, but mainly using manual qualitative evaluation. In this study we employed machine learning models to investigate the added value of DCE (i.e. mpMRI) in predicting significant cancer foci in pre-biopsy MR images. Whereas both protocols had comparable results in the whole prostate and transition zone analyses, we found mpMRI model to be more useful in the peripheral zone, where significant differences ( $p < 0.05$ ) were found for all performance measures i.e. area under the curve, accuracy, sensitivity and specificity.

0833



#### Parallel imaging compressed sensing in fully balanced SSFP for prostate brachytherapy MRI without an endorectal coil: a prospective study

Jeremiah W Sanders<sup>1</sup>, Steven J Frank<sup>2</sup>, Aradhana M Venkatesan<sup>3</sup>, Tharakeswara K Bathala<sup>3</sup>, Chad Tang<sup>2</sup>, Rajat J Kudchadker<sup>4</sup>, Teresa L Bruno<sup>2</sup>, Mark D Pagel<sup>5</sup>, and Jingfei Ma<sup>1</sup>

<sup>1</sup>Imaging Physics, University of Texas MD Anderson Cancer Center, Houston, TX, United States, <sup>2</sup>Radiation Oncology, University of Texas MD Anderson Cancer Center, Houston, TX, United States, <sup>3</sup>Diagnostic Radiology, University of Texas MD Anderson Cancer Center, Houston, TX, United States, <sup>4</sup>Radiation Physics, University of Texas MD Anderson Cancer Center, Houston, TX, United States, <sup>5</sup>Cancer Systems Imaging, University of Texas MD Anderson Cancer Center, Houston, TX, United States





Parallel imaging and compressed sensing (PICS) techniques have demonstrated the ability to accelerate MRI acquisitions in a number of clinical MRI protocols. For postimplant prostate brachytherapy MRI, an endorectal coil (ERC) is currently used to achieve images of sufficient signal-to-noise ratio (SNR) for postimplant quality assessment. Previously we retrospectively demonstrated the feasibility of using PICS to accelerate postimplant prostate brachytherapy MRI. In this work, we prospectively demonstrate that combining PICS with fully balanced steady-state free precession MRI enables high resolution and high SNR images of the prostate without an ERC.

0834



Parameter	AA	CA
ADC	1.12 ± 0.12	1.05 ± 0.10
T2	102 ± 10	98 ± 10
DCE-MRI	1.12 ± 0.12	1.05 ± 0.10

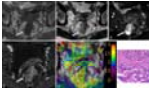
### Quantitative multi-parametric MRI of the prostate reveals differences between ethnicities

Aritrick Chatterjee<sup>1</sup>, Xiaobing Fan<sup>1</sup>, Ambereen Yousuf<sup>1</sup>, Tatjana Antic<sup>2</sup>, Gregory Karczmar<sup>1</sup>, and Aytekin Oto<sup>1</sup>

<sup>1</sup>Department of Radiology, University of Chicago, Chicago, IL, United States, <sup>2</sup>Department of Pathology, University of Chicago, Chicago, IL, United States

This study investigates whether quantitative MRI of the prostate reveals differences between ethnicities that can affect diagnosis. This study shows that the different ethnicities, specifically AAs and CAs have different quantitative MRI values that affects the utility of MRI in the diagnosis of PCa. Different thresholds are needed for PCa diagnosis for different ethnicities. Despite more high grade lesions in AA, the ADC and T2 for lesions in AA were nominally higher than in CA. DCE-MRI significantly improves differentiation of PCa from benign tissue in AA, due to significantly higher cancer signal enhancement rate in AA compared to CA.

0835



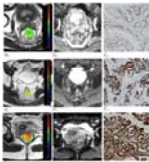
### Amide Proton Transfer Imaging of Rectal Cancer: Baseline values and Feasibility for Predicting Tumor Pathological Features

Lan Zhang<sup>1</sup>, Xin Li<sup>1</sup>, Ping Han<sup>1</sup>, and Fan Yang<sup>1</sup>

<sup>1</sup>Radiology, Union Hospital, Tongji Medical College, Huazhong University of Science and Technology, Wuhan, China

We speculate that APT value may be a useful biomarker for assessing rectal pathological characteristics, which could have a potential impact on the clinical therapeutic strategies for patients. We have established a baseline for the APT values in rectal cancer, which was shown significantly correlated with pathologic features (eg. tumor grade and Ki-67 index).

0836



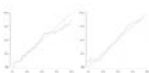
### 3D Amide proton transfer weighted imaging in predicting Ki-67 proliferation state of rectal adenocarcinoma

Ling Li<sup>1</sup>, Yingjie Mei<sup>2</sup>, Zhaoxian Yan<sup>3</sup>, Jieping Feng<sup>3</sup>, Bo Liu<sup>3</sup>, and Xian Liu<sup>3</sup>

<sup>1</sup>Guangzhou University of Chinese Medicine; The second Affiliated hospital of Guangzhou University of Chinese Medicine; Guangzhou, China, <sup>2</sup>Clinical Science, Philips Healthcare; Shanghai, China, <sup>3</sup>Radiology, The second Affiliated hospital of Guangzhou University of Chinese Medicine, Guangzhou, China

The Accurate preoperative staging and grading are significant on the treatment of protocol selection rectal adenocarcinoma. As a new molecular MR imaging technique, APT imaging could provide information that correlates with tumor cell proliferation. In this study, the capability of APT in differentiating WHO grades and pathologic stages of rectal adenocarcinoma was investigated and compared with DWI. The results show that APT value have a significantly positive correlation with the stage and grade of the rectal adenocarcinoma, and the prognosis factor Ki67.

0837



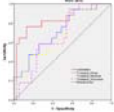
### CT and MRI based multi-modal and multi-parametric radiomics pre-operative prediction of perineural invasion in patients with rectal cancer

Xiangchun Liu<sup>1</sup>, Yu Fu<sup>1</sup>, Yan Guo<sup>2</sup>, Kan He<sup>1</sup>, Qi Yang<sup>1</sup>, and Huimao Zhang<sup>1</sup>

<sup>1</sup>The First Hospital of Jilin University, Changchun, China, <sup>2</sup>GE Healthcare, Beijing, China

Perineural invasion (PNI), defined by tumor invasion of nervous structures and nerve sheaths, which is thought an independent predictor of outcome in rectal cancer. However, for a radiologist, neither MRI nor CT can reliably evaluate PNI. Radiomics is an emerging and effective method for quantitative analysis and prediction using big data of medical imaging. Therefore, this study aims to develop and validate a radiomics prediction model based on MRI and CT for the preoperative prediction of PNI in rectal cancer. The results indicated that excellent diagnostic performance can be yielded with such multi-modal radiomics.

0838



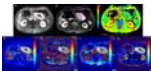
Synthetic magnetic resonance imaging-derived histogram metrics for prediction of lymph node metastasis in rectal cancer

Li Zhao<sup>1</sup>, Hongmei Zhang<sup>1</sup>, Lizhi Xie<sup>2</sup>, and Xinming Zhao<sup>1</sup>

<sup>1</sup>Diagnostic Radiology, Cancer Hospital, Chinese Academy of Medical Sciences and Peking Union Medical College, Beijing, China, <sup>2</sup>MR Research, GE Healthcare, Beijing, China

The aim of this study was to evaluate the feasibility of quantitative synthetic magnetic resonance imaging (SyMRI)-derived histogram of the primary tumor for predicting the regional lymph node (LN) metastasis in patients with rectal cancer (RC). Our study indicated that histogram parameters of primary tumor on T1 mapping and T2 mapping were associated with regional LN status in RC. Moreover, the combination of the quantitative SyMRI parameters, pathological extramural venous invasion (EMVI), and maximum tumor diameter may significantly improve the predictive performance of LN metastasis.

0839



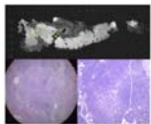
Value of quantitative DCE and DW-MRI in predicting extramural venous invasion in locally advanced gastric cancer and the prognostic significance

Yongjian Zhu<sup>1</sup>, Ying Li<sup>1</sup>, Jun Jiang<sup>1</sup>, Yutao Zhou<sup>1</sup>, Liming Jiang<sup>1</sup>, Liyan Xue<sup>2</sup>, and Lizhi Xie<sup>3</sup>

<sup>1</sup>Department of Imaging Diagnosis, National Cancer Center/National Clinical Research Center for Cancer/Cancer Hospital, Chinese Academy of Medical Sciences and Peking Union Medical College, Beijing, China, <sup>2</sup>Department of Pathology, National Cancer Center/National Clinical Research Center for Cancer/Cancer Hospital, Chinese Academy of Medical Sciences and Peking Union Medical College, Beijing, China, <sup>3</sup>GE healthcare, China, Beijing, China

Extramural vascular invasion (EMVI) has been found as an independent risk factor for recurrence and distant metastasis in patients with gastric cancer. Dynamic contrast-enhanced magnetic resonance imaging (DCE-MRI) and diffusion weighted imaging (DWI) has been applied in diagnosis of different cancers. In this study, we research into the value of DCE-MRI parameters and ADC in predicting EMVI and the prognostic significance. It was found that  $K^{trans}$ ,  $V_e$  and ADC are independent predictors of pathological EMVI in LAGC, and MRI-predicted EMVI (mrEMVI) confirmed to be a poor prognosis predictor in terms of 2-year recurrence-free survival (RFS).

0840



Ex Vivo MRI for Direct Radiologic-Histologic Correlation in the Pancreas: Protocol Development with Cadaver Specimens

Alexandra W. Acher<sup>1</sup>, TJ Colgan<sup>1</sup>, Yuxin Zhang<sup>1</sup>, Krisztian Kovacs<sup>2</sup>, Jitka Starekova<sup>1</sup>, Victoria Rendell<sup>3</sup>, Daniel E. Abbott<sup>3</sup>, Erin Brooks<sup>2</sup>, Rashmi Agni<sup>2</sup>, Emily Winslow<sup>4</sup>, and Scott B. Reeder<sup>5</sup>

<sup>1</sup>Department of Radiology, University of Wisconsin, Madison, WI, United States, <sup>2</sup>Department of Pathology, University of Wisconsin, Madison, WI, United States, <sup>3</sup>Department of Surgery, University of Wisconsin, Madison, WI, United States, <sup>4</sup>Department of Surgery, Georgetown University, Washington DC, MD, United States, <sup>5</sup>Department of Radiology and Department of Medical Physics, University of Wisconsin, Madison, WI, United States

The purpose of this study was to develop a protocol for use of a previously validated radiologic-histologic correlation device to evaluate the pancreas with ex vivo MRI. Precise radiologic-histologic correlation of pancreatic anatomy was achieved in cadaveric pancreas specimens. The final protocol will be applied to co-localize pancreas cancer margins radiologically and histologically, as well as nodal burden in pancreaticoduodenectomy specimens.

0841



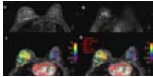
**Pulmonary MR Imaging with Ultra-Short TE: Capability of Nodule Detection and Lung RADS Classification for Lung Cancer Screening**

Yoshiharu Ohno<sup>1,2</sup>, Masao Yui<sup>3</sup>, Daisuke Takenaka<sup>4</sup>, Yoshimori Kassai<sup>3</sup>, Kazuhiro Murayama<sup>1</sup>, and Takeshi Yoshikawa<sup>2</sup>

<sup>1</sup>Radiology, Fujita Health University School of Medicine, Toyoake, Japan, <sup>2</sup>Radiology, Kobe University Graduate School of Medicine, Kobe, Japan, <sup>3</sup>Canon Medical Systems Corporation, Otawara, Japan, <sup>4</sup>Diagnostic Radiology, Hyogo Cancer Center, Akashi, Japan

No report has been found to compare the capability of pulmonary MR imaging with UTE for nodule detection and Lung-RADS classification as compared with low-dose CT (LDCT) and standard-dose CT (SDCT). We hypothesized that pulmonary MR imaging with UTE has a similar potential to detect pulmonary nodules and evaluate Lung-RADS classification as well as LDCT and SDCT. The purpose of this study was to compare the capability of pulmonary MR imaging with UTE for lung nodule detection and evaluation of Lung-RADS classification with LDCT and SDCT.

0842



**A Pilot Evaluation of Amide Proton Transfer-Weighted (APT<sub>w</sub>) MR Imaging in Characteristics and Diagnosis of Premenopausal Breast Tumors**

Nan Zhang<sup>1</sup>, Qingwei Song<sup>1</sup>, Lina Zhang<sup>1</sup>, Ailian Liu<sup>1</sup>, Haonan Zhang<sup>1</sup>, Yu Song<sup>1</sup>, Liangjie Lin<sup>2</sup>, Jiazheng Wang<sup>2</sup>, and Zhiwei Shen<sup>2</sup>

<sup>1</sup>The First Affiliated Hospital of Dalian Medical University, Dalian, China, <sup>2</sup>Philips Healthcare, Beijing, China

Amide proton transfer (APT) imaging is based on the chemical exchange between free bulk water protons and the amide protons (-NH) of endogenous mobile proteins and peptides in tissue. Previous studies have shown that APT-weighted (APT<sub>w</sub>) MRI could noninvasively identify and differentiate tumors in brain, head and neck etc. This study aims to explore the feasibility of APT<sub>w</sub>-MRI in characteristics and discrimination of premenopausal malignant and benign breast tumors. The results show that the APT<sub>w</sub> MR imaging efficiency of diagnosis of premenopausal breast tumors were 0.904.

**Combined Educational & Scientific Session**

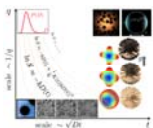
**Diffusion Modeling, Tractography and Applications - Microstructure: What Scales Are You Probing?**

Organizers: Carl-Fredrik Westin

Wednesday Parallel 4 Live Q&A

Wednesday 14:30 - 15:15 UTC

Moderators: Carl-Fredrik Westin & Dmitry Novikov



**Probing Microstructure Lengths Scales with Diffusion: Theory**

Valerij Kiselev<sup>1</sup>

<sup>1</sup>Medical Physics, Dpt. of Radiology, University Medical Center Freiburg, Freiburg, Germany

Regimes of diffusion weighting are discussed starting with the simplest measurement with narrow gradient pulses. Such measurements can be classified on a plane of diffusion time and the wave vector induced by the diffusion-sensitizing gradients. Beyond this simple picture are gradients with a finite duration, which radically change the signal behavior for the closed compartment. Versatile diffusion weighting scheme, the successors of the double diffusion encoding, are discussed under the overarching idea of geometry matching between the gradient encoding and the targeted cell population.

---

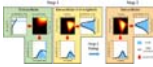
### Probing Microstructure Lengths Scales with Diffusion: Application

Joseph Ackerman<sup>1</sup>

<sup>1</sup>Washington University, United States

This didactic lecture will highlight illustrative measurements with physically-realizable model systems that provide simplifying parsimonious dMRI test platforms and deliver parameters useful for the modeling of microstructurally-complex real tissues. These dMRI test platforms will include: (i) perfused, cultured (in vitro), microbead-adherent HeLa cells; (ii) perfused, cultured (in vitro), microbead-adherent neurons and glia (aka, "brains-on-beads"); (iii) *Xenopus laevis* oocyte (aka, frog egg); and (iv) intracellular N-acetylaspartate (NAA) in rat brain in vivo.

0843



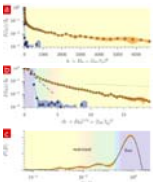
### Non-invasive mapping of non-parametric cell size distributions using MRI-cytometry

Junzhong Xu<sup>1</sup>, Xiaoyu Jiang<sup>1</sup>, Sean P Devan<sup>2</sup>, Lori R Arlinghaus<sup>1</sup>, Eliot T McKinley<sup>1</sup>, Jingping Xie<sup>1</sup>, Zhongliang Zu<sup>1</sup>, Qing Wang<sup>3</sup>, A Bapsi Chakravarthy<sup>1</sup>, Yong Wang<sup>3</sup>, and John C Gore<sup>1</sup>

<sup>1</sup>Vanderbilt University Medical Center, Nashville, TN, United States, <sup>2</sup>Vanderbilt University, Nashville, TN, United States, <sup>3</sup>Washington University, St. Louis, MO, United States

Non-invasive mapping of cell size distribution provides a unique means to probe biological tissues. We introduce a diffusion MRI based framework that does not require prior assumptions on distribution functions to provide tissue microstructural properties including non-cell-volume-weighted cell size distributions. We validated this approach, which we call MRI-cytometry, comprehensively using computer simulations in silico, cultured cells in vitro, and animal xenografts in vivo. We then demonstrate the implementation of MRI-cytometry in imaging breast cancer patients using clinical 3T MRI, indicating its potential clinical application such as more specific assessments of tumor status and therapeutic responses.

0844



### Unprecedented diffusion weighting and exchange resolution of cellular and sub-cellular structures in live and fixed neural tissue

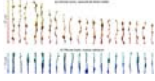
Nathan Hu Williamson<sup>1</sup>, Rea Ravin<sup>1</sup>, Dan Benjamini<sup>1</sup>, Hellmut Merkle<sup>2</sup>, Melanie Falgairolle<sup>2</sup>, Michael J O'Donovan<sup>2</sup>, Dvir Blivis<sup>2</sup>, Dave Ide<sup>2</sup>, Teddy Cai<sup>1</sup>, Nima Ghorashi<sup>3</sup>, Ruiliang Bai<sup>1,4</sup>, and Peter Basser<sup>1</sup>

<sup>1</sup>Eunice Kennedy Shriver National Institutes of Child Health and Human Development, National Institutes of Health, Bethesda, MD, United States, <sup>2</sup>National Institute of Neurological Disorders and Stroke, National Institutes of Health, Bethesda, MD, United States, <sup>3</sup>National Heart, Lung, and Blood Institute, National Institutes of Health, Bethesda, MD, United States, <sup>4</sup>College of Biomedical Engineering and Instrument Science, Zhejiang University, Hangzhou, China

Diffusion and exchange methods are developed using the large static gradient produced by a single-sided permanent magnet and provide resolution to water within sub-micron membrane structures. Using tissue delipidation methods, we show that water diffusion is restricted solely by lipid membranes. Most of the diffusion signal can be assigned to water in tissue which is far from membranes. The remaining 25% can be assigned to water restricted within membrane structures at the cellular, organelle, and vesicle levels. Diffusion exchange spectroscopy measures water exchanging between membrane structures and free environments at 100 s<sup>-1</sup>.

---

0845



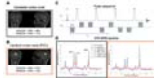
Random walk simulations of diffusion in human brain white matter from 3d EM validate diffusion time-dependence transverse and parallel to axons

Hong-Hsi Lee<sup>1</sup>, Qiyuan Tian<sup>2</sup>, Chanon Ngamsombat<sup>2</sup>, Daniel R Berger<sup>3</sup>, Jeff W Lichtman<sup>3</sup>, Susie Y Huang<sup>2</sup>, Dmitry S Novikov<sup>1</sup>, and Els Fieremans<sup>1</sup>

<sup>1</sup>Center for Biomedical Imaging, Department of Radiology, NYU School of Medicine, New York, NY, United States, <sup>2</sup>Athinoula A. Martinos Center for Biomedical Imaging, Massachusetts General Hospital, Charlestown, MA, United States, <sup>3</sup>Department of Molecular and Cellular Biology, Harvard University, Cambridge, MA, United States

We perform for the first time Monte Carlo simulations inside realistic human intra-axonal space segmented from electron microscopy. We observe non-Gaussian time-dependent diffusion in both radial and axial directions, and validate analytical models of these phenomena. We also compare the results in human axons with similar simulations in mouse axons, and discuss how the differences in axonal parameters (mean radius, radius variation, undulations) explain the differences in the simulation results between the human and mouse.

0846



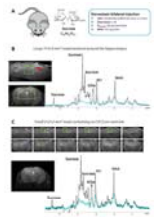
Characterizing the fine microstructure of cerebellar and cerebral cortex non-invasively with metabolite diffusion-weighted MRS

Marco Palombo<sup>1</sup>, Cecile Gallea<sup>2,3</sup>, Guglielmo Genovese<sup>3,4</sup>, Stephane Lehericy<sup>2,3</sup>, and Francesca Branzoli<sup>3,4</sup>

<sup>1</sup>Centre for Medical Image Computing, Department of Computer Science, University College London, London, United Kingdom, <sup>2</sup>Team "Movement Investigations and Therapeutics", Brain and Spine Institute - ICM, Paris, France, <sup>3</sup>INSERM U 1127, CNRS UMR 7225, Sorbonne University, Paris, France, <sup>4</sup>Brain and Spine Institute - ICM, Centre for Neuroimaging Research - CENIR, Paris, France

Diffusion-weighted magnetic resonance spectroscopy (DW-MRS) performed at ultra-high b-values enables the quantification of fine cell microstructural features such as dendritic spine density. Here, we measured in vivo the diffusion of total N-acetyl-aspartate (tNAA) and choline compounds (tCho) in the human cerebellar and cerebral cortex at 3 T, up to a b-value of 24 ms/μm<sup>2</sup>. We used biophysical modelling and numerical simulations to interpret the metabolite signal attenuation with the b-value. The diffusion of tNAA, a mostly neuronal metabolite, is compatible with a larger presence of spines and highly restricting granular cell soma in cerebellar compared to cerebral cortex.

0847



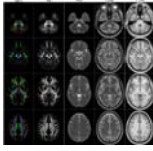
Characterizing extracellular diffusion properties using diffusion-weighted MRS of sucrose injected in the mouse brain

Mélissa Vincent<sup>1,2</sup>, Mylène Gaudin<sup>1,2</sup>, Covadonga Lucas-Torres<sup>3</sup>, Océane Guillemaud<sup>1,2</sup>, Carole Escartin<sup>1,2</sup>, Alan Wong<sup>3</sup>, and Julien Valette<sup>1,2</sup>

<sup>1</sup>Molecular Imaging Research Centre (MIRcen), Commissariat à l'Energie Atomique et aux Energies Alternatives (CEA), Fontenay-aux-Roses, France, <sup>2</sup>UMR 9199, Neurodegenerative Diseases Laboratory, Centre National de la Recherche Scientifique (CNRS), Université Paris-Sud, Université Paris-Saclay, Fontenay-aux-Roses, France, <sup>3</sup>NIMBE/Laboratoire de Structure et Dynamique par Résonance Magnétique (LSDRM), Commissariat à l'Energie Atomique et aux Energies Alternatives (CEA), Gif-sur-Yvette, France

Diffusion in the extracellular space is assessed by state-of-the-art diffusion-weighted MRS techniques following intracerebral injection of sucrose, which predominantly remains in the extracellular space. Sucrose diffusion appears to be not strictly Gaussian and different from intracellular metabolites diffusion. Signal attenuation is stronger and deviates from mono-exponential attenuation at very high b-values, suggesting the presence of some highly restricted pool. The ADC is higher and decreases when augmenting t<sub>0</sub>, indicating that the tortuosity regime is not reached yet. Lastly, unlike intracellular metabolites, sucrose diffusion does not exhibit microstructural anisotropy in double-diffusion-encoding experiments.

0848



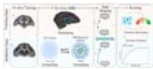
Diffusion MRI Atlases from the Human Connectome Project Data

M. Okan Irfanoglu<sup>1</sup>, Amritha Nayak<sup>1,2</sup>, and Carlo Pierpaoli<sup>1</sup>

<sup>1</sup>QMI, NIBIB/NIH, Bethesda, MD, United States, <sup>2</sup>The Henry Jackson Foundation for the Advancement of Military Medicine, Rockville, MD, United States

In this work, we have created diffusion MRI (dMRI) atlases from the young adult Human Connectome Project (HCP) data. In order to achieve increased anatomical detail and to enable subsequent morphological analysis, we have reprocessed the entire HCP1200 dataset. The DTI atlases, derived scalar maps and JHU atlas inspired white matter ROIs have been made publicly available. The reprocessed DWIs will be made available for HARDI analysis in the near future.

0849



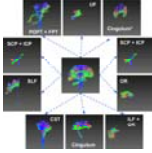
The IronTract challenge: Validation and optimal tractography methods for the HCP diffusion acquisition scheme

Chiara Maffei<sup>1</sup>, Gabriel Girard<sup>2,3</sup>, Kurt G. Schilling<sup>4</sup>, Nagesh Adluru<sup>5</sup>, Dogu Baran Aydogan<sup>6</sup>, Andac Hamamci<sup>7</sup>, Fang-Cheng Yeh<sup>8</sup>, Matteo Mancini<sup>9,10</sup>, Ye Wu<sup>11</sup>, Alessia Sarica<sup>12</sup>, Achille Teillac<sup>13,14,15</sup>, Steven H. Baete<sup>16,17</sup>, Davood Karimi<sup>18</sup>, Ying-Chia Lin<sup>16,17</sup>, Fernando Boada<sup>16,17</sup>, Nathalie Richard<sup>13</sup>, Bassam Hiba<sup>13</sup>, Aldo Quattrone<sup>12</sup>, Yoonmi Hong<sup>11</sup>, Dinggang Shen<sup>11</sup>, Pew-Thian Yap<sup>11</sup>, Tommy Boshkovski<sup>10</sup>, Jennifer S. W. Campbell<sup>19</sup>, Nikola Stikov<sup>10</sup>, G. Bruce Pike<sup>20</sup>, Barbara B. Bendlin<sup>5</sup>, Andrew L. Alexander<sup>5</sup>, Vivek Prabhakaran<sup>5</sup>, Adam Anderson<sup>21</sup>, Bennett A. Landman<sup>4,21</sup>, Erick J.Z. Canales-Rodríguez<sup>3,22,23</sup>, Muhamed Barakovic<sup>3,24</sup>, Jonathan Rafael-Patino<sup>3</sup>, Thomas Yu<sup>3</sup>, Gaëtan Rensonnet<sup>3,25</sup>, Simona Schiavi<sup>3,26</sup>, Alessandro Daducci<sup>26</sup>, Marco Pizzolato<sup>3</sup>, Elda Fischi-Gomez<sup>3,24</sup>, Jean-Philippe Thiran<sup>2,3</sup>, George Dai<sup>27</sup>, Giorgia Grisot<sup>28</sup>, Nikola Lazovski<sup>29</sup>, Albert Puente<sup>29</sup>, Matt Rowe<sup>29</sup>, Irina Sanchez<sup>29</sup>, Vesna Prchkovska<sup>29</sup>, Robert Jones<sup>1</sup>, Julia Lehman<sup>30</sup>, Suzanne Haber<sup>30</sup>, and Anastasia Yendiki<sup>1</sup>

<sup>1</sup>Athinoula A. Martinos Center for Biomedical Imaging, Massachusetts General Hospital and Harvard Medical School, Charlestown, MA, United States, <sup>2</sup>Radiology Department, Centre Hospitalier Universitaire Vaudois and University of Lausanne, Lausanne, Switzerland, <sup>3</sup>Signal Processing Lab (LTS5), École Polytechnique Fédérale de Lausanne, Lausanne, Switzerland, <sup>4</sup>Institute of Imaging Science, Vanderbilt University, Nashville, TN, United States, <sup>5</sup>University of Wisconsin, Madison, WI, United States, <sup>6</sup>Department of Neuroscience and Biomedical Engineering, Aalto University, Helsinki, Finland, <sup>7</sup>Department of Biomedical Engineering, Faculty of Engineering, Yeditepe University, Istanbul, Turkey, <sup>8</sup>Department of Neurological Surgery, University of Pittsburgh, Pittsburgh, PA, United States, <sup>9</sup>Department of Neuroscience, Brighton and Sussex Medical School, University of Sussex, Brighton, United Kingdom, <sup>10</sup>NeuroPoly Lab, Polytechnique Montreal, Montreal, QC, Canada, <sup>11</sup>Department of Radiology and BRIC, University of North Carolina, Chapel Hill, NC, United States, <sup>12</sup>Neuroscience Research Center, University Magna Graecia of Catanzaro, Catanzaro, Italy, <sup>13</sup>CNRS/ISC, Bron, France, <sup>14</sup>Université de Bordeaux, Bordeaux, France, <sup>15</sup>CNRS/INCLIA, Bordeaux, France, <sup>16</sup>Center for Advanced Imaging Innovation and Research (CAI2 R), NYU School of Medicine, New York, NY, United States, <sup>17</sup>Center for Biomedical Imaging, Dept. of Radiology, NYU School of Medicine, New York, NY, United States, <sup>18</sup>Boston Children's Hospital, Boston, MA, United States, <sup>19</sup>Montreal Neurological Institute, McGill University, Montreal, QC, Canada, <sup>20</sup>Hotchkiss Brain Institute and Department of Radiology, University of Calgary, Calgary, AB, Canada, <sup>21</sup>Department of Electrical Engineering, Vanderbilt University, Nashville, TN, United States, <sup>22</sup>FIDMAG Germanes Hospitalàries, Sant Boi de Llobregat, Barcelona, Spain, <sup>23</sup>Mental Health Research Networking Center (CIBERSAM), Madrid, Spain, <sup>24</sup>Translational Imaging in Neurology (ThINK), Department of Medicine and Biomedical Engineering, University Hospital and University of Basel, Basel, Switzerland, <sup>25</sup>ICTEAM Institute, Université Catholique de Louvain, Louvain-la-Neuve, Belgium, <sup>26</sup>Computer Science Department, University of Verona, Verona, Italy, <sup>27</sup>Wellesley College, Wellesley, Wellesley, MA, United States, <sup>28</sup>DeepHealth, Inc., Cambridge, MA, United States, <sup>29</sup>QMENTA, Inc., Barcelona, Spain, <sup>30</sup>Department of Pharmacology and Physiology, University of Rochester School of Medicine, Rochester, NY, United States

We present results from IronTract, the first challenge to evaluate tractography on the two-shell diffusion scheme of the Human Connectome Project (HCP). Accuracy was evaluated by comparison to tracer injections in the same macaque brains as the diffusion data. Training and validation datasets involved different injection sites. We observed that optimizing data analysis with respect to one injection site does not guarantee optimality for another; encouragingly, two teams could achieve consistently high performance in both datasets. We also found that, when analysis methods are optimized, the HCP scheme may achieve similar accuracy as a more demanding diffusion spectrum imaging acquisition.

0850



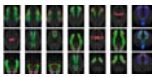
### Auto-encoded Latent Representations of White Matter Streamlines

Shenjun Zhong<sup>1</sup>, Zhaolin Chen<sup>1</sup>, and Gary Egan<sup>1,2</sup>

<sup>1</sup>Monash Biomedical Imaging, Monash University, Australia, Melbourne, Australia, <sup>2</sup>School of Psychological Sciences, Monash University, Australia, Melbourne, Australia

Clustering white matter streamlines is still a challenging task. The existing methods based on spatial coordinates rely on manually engineered features, and/or labeled dataset. This work introduced a novel method that solves the problem of streamline clustering without needing labeled data. This is achieved by training a deep LSTM-based autoencoder to learn and embed any lengths of streamlines into a fixed-length vector, i.e. latent representation, then perform clustering in an unsupervised learning manner.

0851



### Tract Dictionary Learning for Fast and Robust Recognition of Fiber Bundles

Ye Wu<sup>1</sup>, Yoonmi Hong<sup>1</sup>, Weili Lin<sup>1</sup>, Pew-Thian Yap<sup>1</sup>, and the UNC/UMN Baby Connectome Project Consortium<sup>1</sup>

<sup>1</sup>Department of Radiology and BRIC, University of North Carolina, Chapel Hill, Chapel Hill, NC, United States

Fiber bundle parcellation is key to bundle-specific analysis of white matter pathways. In this abstract, we propose an efficient framework for parcellation of white matter tractograms using discriminative dictionary learning. The key to our framework is to learn a compact dictionary for each fiber bundle so that the streamlines within the bundle can be succinctly represented. Experiments on a bundle-labeled HCP dataset and an infant dataset highlight the ability of our framework in grouping streamlines into anatomically plausible bundles.

0852



### TractLearn: a geodesic learning framework for quantitative dissection of brain bundles

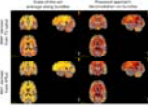
Arnaud Attyé<sup>1,2</sup>, Felix Renard<sup>3</sup>, Monica Baciu<sup>2</sup>, Elise Roger<sup>2</sup>, Laurent Lamalle<sup>4</sup>, Patrick Dehail<sup>5</sup>, H el ene Cassoudeulle<sup>5</sup>, and Fernando Calamante<sup>6,7</sup>

<sup>1</sup>School of Biomedical Engineering, University of Sydney, Sydney, Australia, <sup>2</sup>CNRS LPNC UMR 5105, University of Grenoble Alpes, Grenoble, France, <sup>3</sup>Laboratoire d'informatique de Grenoble, Grenoble, France, <sup>4</sup>University of Grenoble Alpes, Grenoble, France, <sup>5</sup>Bordeaux University Hospital, Bordeaux, France, <sup>6</sup>Sydney Imaging Lab, University of Sydney, Sydney, Australia, <sup>7</sup>School of Aerospace, Mechanical and Mechatronic Engineering, Sydney, Australia

Here we present a unified framework for brain fascicles quantitative analyses by geodesic learning (TractLearn) — as a data-driven unsupervised learning task. TractLearn allows a mapping between the image high-dimensional domain and the reduced latent space of brain fascicles. Besides providing a framework to test the reliability of various brain metrics with a global overview, it allows to identify subtle quantitative alteration in disease model with small subset of patients and/or data sparsity. With this regard, TractLearn is a ready-to-use algorithm for precision medicine.

Myelin weighted tractography: a new way to investigate bundles myelination in-vivo?

0853

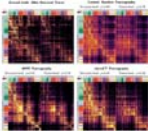


Simona Schiavi<sup>1,2</sup>, Po-Jui Lu<sup>3,4</sup>, Matthias Weigel<sup>3,4,5</sup>, Derek K. Jones<sup>6,7,8</sup>, Ludwig Kappos<sup>3,4</sup>, Cristina Granziera<sup>3,4</sup>, and Alessandro Daducci<sup>1</sup>

<sup>1</sup>Department of Computer Science, University of Verona, Verona, Italy, <sup>2</sup>DINOEMI, University of Genoa, Genoa, Italy, <sup>3</sup>Departments of Medicine, Clinical Research and Biomedical Engineering, University Hospital Basel and University of Basel, Basel, Switzerland, <sup>4</sup>Translational Imaging in Neurology (ThINk) Basel, Department of Medicine and Biomedical Engineering, University Hospital Basel and University of Basel, Basel, Switzerland, <sup>5</sup>Radiological Physics, Department of Radiology, University Hospital Basel and University of Basel, Basel, Switzerland, <sup>6</sup>Cardiff University Brain Research Imaging Centre, Cardiff University, Cardiff, United Kingdom, <sup>7</sup>Neuroscience and Mental Health Research Institute, Cardiff University, Cardiff, United Kingdom, <sup>8</sup>Mary MacKillop Institute for Health Research, Australian Catholic University, Melbourne, Australia

Tractometry is a widely used tool to investigate microstructural properties that reflect differences in white matter tracts. It consists in averaging tissue features (obtained from any voxel-wise map) along streamlines recovered with diffusion tractography. To overcome the bias introduced by the average, we propose a new method to deconvolve on each individual tract the actual value measured by the microstructural map. For the first time we were able to assess the bundle-specific myelin content by combining tractography with two myelin-sensitive sequences and we obtained good agreement with previously reported values on the cortex.

0854



Synchrotron microCT tractography connectomics: comparison with diffusion MRI and neural tracer injections  
Scott Trinkle<sup>1</sup>, Sean Foxley<sup>1</sup>, Narayanan Kasthuri<sup>2</sup>, and Patrick La Rivière<sup>1</sup>

<sup>1</sup>Department of Radiology, The University of Chicago, Chicago, IL, United States, <sup>2</sup>Department of Neurobiology, The University of Chicago, Chicago, IL, United States

In this study, we generated tractography-derived, mesoscale mouse “connectomes” from diffusion MRI and synchrotron microCT data on the same mouse brain and evaluated their accuracy using anterograde tracer data from the Allen Mouse Brain Connectivity Atlas. We are developing whole-brain synchrotron microCT, which provides micron-level isotropic resolution across whole mouse brains with no physical sectioning. Even when binning the microCT orientation information to the MRI resolution, microCT tractography outperformed MRI. However, both datasets performed similarly to a tractography connectome constructed entirely with random orientation data, highlighting the importance of understanding geometric biases in tractography connectome construction.

0855



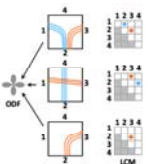
Anatomically informed multi-level fiber tractography for improved sensitivity of white matter bundle reconstruction in diffusion MRI

Andrey Zhylyka<sup>1</sup>, Alexander Leemans<sup>2</sup>, Josien Pluim<sup>1</sup>, and Alberto De Luca<sup>2</sup>

<sup>1</sup>Biomedical Engineering, Eindhoven University of Technology, Eindhoven, Netherlands, <sup>2</sup>Image Sciences Institute, University Medical Center Utrecht, Utrecht, Netherlands

Neurosurgery planning is an important application of fiber tractography which requires the results to be consistent and accurate. Deterministic tractography methods are generally characterized by high specificity and limited sensitivity, whereas the opposite typically holds for probabilistic methods. Here, we propose a multi-level fiber tractography strategy that takes fiber branching into account and incorporates an anatomical prior to provide a balance between true and false positive reconstructions. We evaluated our approach on the MASSIVE dataset and compared its performance to the existing state of art.

0856



Towards taking the guesswork (and the errors) out of diffusion tractography

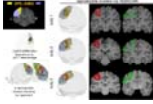
Anastasia Yendiki<sup>1</sup>, Robert Jones<sup>2</sup>, Adrian Dalca<sup>1,3</sup>, Hui Wang<sup>1</sup>, and Bruce Fischl<sup>1</sup>

<sup>1</sup>Radiology, Harvard Medical School & Massachusetts General Hospital, Charlestown, MA, United States, <sup>2</sup>Radiology, Massachusetts General Hospital, Charlestown, MA, United States, <sup>3</sup>Massachusetts Institute of Technology, Cambridge, MA, United States



Orientation distributions estimated from diffusion MRI have multiple peaks per voxel. Tractography algorithms must choose among them arbitrarily, leading to errors. We propose a novel approach to making this choice in a manner informed by the data. We use post mortem optical and MRI data to train a convolutional neural network that can recognize voxel-wise connection patterns directly from diffusion data, circumventing the conventional paradigm of an orientation distribution. We introduce TRACARIS (TRACT Architectures Recovered from Imaging Signals), a tractography algorithm that uses these network-predicted, local connection patterns. We present preliminary validation results from a post mortem human brain sample.

0857



Short-range Tractography with high Throughput And Reproducibility (STTAR) characterized by FDT tracing and HDBSCAN clustering

Chenyang Zhao<sup>1,2</sup>, Minhui Ouyang<sup>1</sup>, Qinlin Yu<sup>1</sup>, and Hao Huang<sup>1,3</sup>

<sup>1</sup>Department of Radiology, Children's Hospital of Philadelphia, Philadelphia, PA, United States, <sup>2</sup>Department of Bioengineering, School of Engineering and Applied Science, University of Pennsylvania, Philadelphia, PA, United States, <sup>3</sup>Department of Radiology, Perelman School of Medicine, University of Pennsylvania, Philadelphia, PA, United States

Short-range association fibers (SAFs), linking adjacent cortical regions, are dominant in structural connectome and associated with autism and schizophrenia. However, SAFs are not well characterized due to challenges in high-throughput tracing of SAF with diffusion MRI and challenges of identifying and labeling reproducible SAFs. The vast amount of SAFs also make it difficult to delineate them. To meet these challenges, we established a protocol "STTAR" including high-throughput streamline tracing with a regularized FDT probabilistic tractography and semi-automatic identification of reproducible SAFs with novel HDBSCAN clustering. Newly identified reproducible SAFs and those consistently reported in the literature are also demonstrated.

## Oral

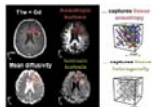
### Diffusion Modeling, Tractography and Applications - Diffusion: Applications

Wednesday Parallel 4 Live Q&A

Wednesday 14:30 - 15:15 UTC

Moderators: Stella Xing

0858



B-tensor encoding in gliomas: improved tumor grading by the isotropic kurtosis

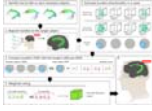
Jan Brabec<sup>1</sup>, Filip Szczepankiewicz<sup>2,3,4</sup>, Patrik Brynolfsson<sup>5</sup>, Lampinen Björn<sup>1</sup>, Faris Durmo<sup>4</sup>, Anna Rydelius<sup>6</sup>, Linda Knutsson<sup>1,7</sup>, Pia Sundgren<sup>4,8</sup>, and Markus Nilsson<sup>4</sup>

<sup>1</sup>Clinical Sciences Lund, Medical Radiation Physics, Lund University, Lund, Sweden, <sup>2</sup>Department of Radiology, Brigham and Women's Hospital, Boston, MA, United States, <sup>3</sup>Harvard Medical School, Boston, MA, United States, <sup>4</sup>Clinical Sciences Lund, Diagnostic Radiology, Lund University, Lund, Sweden, <sup>5</sup>Dept. of Translational Medicine, Division of Medical Radiation Physics, Lund University, Lund, Sweden, <sup>6</sup>Clinical Sciences Lund, Neurology, Lund University, Lund, Sweden, <sup>7</sup>Russell H. Morgan Department of Radiology and Radiological Science, Johns Hopkins University School of Medicine, Baltimore, MD, United States, <sup>8</sup>Lund University Bioimaging Center, Lund University, Lund, Sweden

B-tensor encoding enables mapping of the isotropic and anisotropic components of the diffusional kurtosis, which are sensitive to cell eccentricity and variance in cell density, respectively. We measured the kurtosis components in patients with glioma tumors and explored their ability to improve tumor classification. Results showed that the addition of isotropic kurtosis improves the ability to distinguish low- and high-grade gliomas compared with using post-Gd T1w enhancements alone. Also, non-enhancing glioblastomas and oligodendrogliomas could be distinguished based on the within-tumor standard deviation of the isotropic kurtosis.

0859

Lesion-Robust White-Matter Bundle Identification through Diffusion Driven Label Fusion

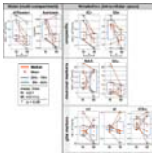


Guillermo Gallardo<sup>1</sup>, Gaston Zanitti<sup>2</sup>, Samuel Deslauriers-Gauthier<sup>3</sup>, Matthew Higger<sup>4</sup>, Sylvain Bouix<sup>4</sup>, Alfred Anwander<sup>5</sup>, and Demian Wassermann<sup>2</sup>

<sup>1</sup>Neuropsychology, Max Planck Institute for Human Cognitive and Brain Sciences, Leipzig, Germany, <sup>2</sup>Parietal, Inria Saclay - Ile de France, Paris, France, <sup>3</sup>Athena EPI, Universite Cote d'Azur, Inria, Sophia Antipolis, France, <sup>4</sup>Psychiatry Neuroimaging Laboratory, Brigham and Womens Hospital, Harvard Medical School, Boston, MA, United States, <sup>5</sup>Max Planck Institute for Human Cognitive and Brain Sciences, Leipzig, Germany

White-matter pathologies disrupt the white-matter organization, that manifests as deficits in brain function. When treating such pathologies, it is of great importance to infer which pathways are affected. However, the white-matter lesions hamper the use of tractography to track fiber bundles. In this work, leveraging diffusion imaging, we propose a novel diffusion-driven technique to improve the localization of brain pathways. Aggregating information from few healthy subjects, our technique is able to localize both the affected pathways and the lesion interrupting when tracking is not possible.

0860

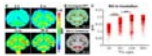


Investigation of potential effects of sleep on diffusion characteristics of metabolites and water: initial results  
André Döring<sup>1</sup>, Christian Rummel<sup>2</sup>, Sandra C. Röthlisberger<sup>3</sup>, Simone Duss<sup>3</sup>, Corinne Roth<sup>3</sup>, Claudio Bassetti<sup>3,4</sup>, and Roland Kreis<sup>1</sup>

<sup>1</sup>Depts. Radiology and Biomedical Research, University of Bern, Bern, Switzerland, <sup>2</sup>Support Center for Advanced Neuroimaging, University Institute for Diagnostic and Interventional Neuroradiology, Bern, Switzerland, <sup>3</sup>Sleep-Wake-Epilepsy-Center, University Hospital Bern, Bern, Switzerland, <sup>4</sup>Dept. of Neurology, University Hospital Inselspital Bern, Bern, Switzerland

Diffusion-weighted MR spectroscopy (DW-MRS) and imaging (DW-MRI) was applied to investigate potential effects of sleep on apparent diffusion coefficients (ADCs) of water and metabolites in human gray matter in 7 healthy subjects. Monitoring the transition from wake to sleep for a period of 4 hours did not reveal any significant alterations, while comparison of night measurements after slight sleep deprivation to morning examinations after a full night's sleep indicated that ADCs for some metabolites are lower in the morning than before sleep – though these results need corroboration in a larger cohort.

0861



Multidimensional Diffusion MRI Assists Myelin-sensitive Bound Pool Fraction in Differentiating Microstructural Maturity of Primate Brains

Yi He<sup>1</sup>, Henrik Lundell<sup>1</sup>, Ines Mexia Rodrigues<sup>1</sup>, Matthew D. Budde<sup>2</sup>, Mark D. Does<sup>3</sup>, Maurice Ptito<sup>4,5</sup>, and Tim Bjørn Dyrby<sup>1</sup>

<sup>1</sup>Danish Research Centre for Magnetic Resonance, Centre for Functional and Diagnostic Imaging and Research, Copenhagen University Hospital Hvidovre, Hvidovre, Denmark, <sup>2</sup>Neurosurgery, Medical College of Wisconsin, Milwaukee, WI, United States, <sup>3</sup>Department of Biomedical Engineering, Vanderbilt University, Nashville, TN, United States, <sup>4</sup>School of Optometry, Université de Montréal, Montreal, QC, Canada, <sup>5</sup>Department of Nuclear Medicine, University of Southern Denmark, Odense, Denmark

Myelin-sensitive bound pool fraction (BPF) enables the tracking process of myelination in primate brains. The 3D BPF maps demonstrated rapid development of myelination from a 2-day-old brain to a 12-month-old brain and a slower increase from 12 months to 30 months. Even though the process of myelination is slow, multidimensional diffusion MRI indices are indeed helpful in significantly differentiating the microstructural maturity of primate brains. Our findings suggest that both indices, isotropic kurtosis ( $MK_i$ , associated with cell density variance) and microscopic anisotropy ( $MK_A$ , correlated with cell eccentricity) are significant imaging markers for microstructural differentiation in the development of primate brains.



Grading bladder urothelial carcinoma using a non-Gaussian fractional order calculus diffusion model

0862

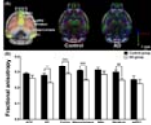


Cui Feng<sup>1,2</sup>, Yanchun Wang<sup>1</sup>, Guangyu Dan<sup>2,3</sup>, Zheng Zhong<sup>2,3</sup>, M. Muge Karaman<sup>2,3</sup>, Daoyu Hu<sup>1</sup>, and Xiaohong Joe Zhou<sup>2,3,4,5</sup>

<sup>1</sup>Radiology, Tongji Hospital, Tongji Medical College, Huazhong University of Science and Technology, Wuhan, China, <sup>2</sup>Center for MR Research, University of Illinois at Chicago, Chicago, IL, United States, <sup>3</sup>Department of Bioengineering, University of Illinois at Chicago, Chicago, IL, United States, <sup>4</sup>Department of Radiology, University of Illinois at Chicago, Chicago, IL, United States, <sup>5</sup>Department of Neurosurgery, University of Illinois at Chicago, Chicago, IL, United States

Diffusion-weighted imaging based on apparent diffusion coefficient (ADC) has been used for bladder urothelial carcinoma grading. However, a considerable overlap between the low- and high-grade bladder urothelial carcinoma has hindered its clinical acceptance. We employed high b-value diffusion imaging with a non-Gaussian fractional-order calculus (FROC) diffusion model for grading bladder urothelial carcinoma. Significant differences were observed in the FROC parameters  $D$ ,  $\beta$  and  $\mu$ , between the low- and high-grade urothelial carcinoma. The combination of the FROC parameters provided substantially better performance than ADC. These findings indicate a promising role of FROC parameters for characterizing bladder urothelial carcinoma and beyond.

0863



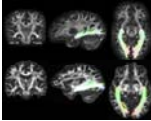
### Altered Brain and Gut in Alzheimer's Disease Model Using Diffusion MRI and Intestinal Bacteria Gene Analysis

Yao-Wen Liang<sup>1</sup>, Ching-Wen Chang<sup>1</sup>, Ssu-Ju Li<sup>1</sup>, Ting-Chun Lin<sup>1</sup>, Hsin-Tzu Lu<sup>1</sup>, You-Yin Chen<sup>1</sup>, and Yu-Chun Lo<sup>2</sup>

<sup>1</sup>National Yang-Ming University, Taipei, Taiwan, <sup>2</sup>Taipei Medical University, Taipei, Taiwan

Microbiota-gut-brain axis, a bidirectional communication, was proposed as an important role in Alzheimer's disease (AD). However, the correlation between gut microbiota and brain microstructure in AD remained unclear. Triple-transgenic mouse models of AD were used to investigate brain-behavior-gut-microbiome interaction. Diffusion MRI, behavior tasks, and intestinal bacteria gene analysis were applied in this study. The findings implied that the altered brain microstructure and atypical distribution of gut microbiota were associated with the cognitive dysfunction in AD.

0864



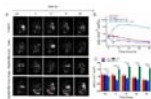
### Fully-Automated Delineation of the Optic Radiation

Lee Bremner Reid<sup>1</sup>, Eloy Martínez-Heras<sup>2</sup>, Magí Andorrà Inglés<sup>2</sup>, Elisabeth Solana<sup>2</sup>, Sara Llufríu<sup>2</sup>, José V Manjón<sup>3</sup>, and Jurgen Frapp<sup>1</sup>

<sup>1</sup>The Australian e-Health Research Centre, CSIRO, Brisbane, Australia, <sup>2</sup>Center of Neuroimmunology, Laboratory of Advanced Imaging in Neuroimmunological Diseases, Hospital Clinic Barcelona, Institut d'Investigacions Biomediques August Pi i Sunyer and Universitat de Barcelona, Barcelona, Spain, <sup>3</sup>ITACA, Universitat Politècnica de València, Valencia, Spain

The optic radiation (OR), is often severed during temporal lobe resection, resulting in permanent quadrantanopia. To date all published tractography methods that delineate the OR require manual input (e.g. region-of-interest placement and adjustment), or appear to underestimate Meyer's Loop, limiting their widespread clinical adoption. Here, we present and validate the CONSULT pipeline for OR delineation. This pipeline accepts unprocessed DICOM images as input and produces realistic subject-specific segmentations of the OR, including Meyer's Loop, without need for any human input. Its validation in 183 datasets demonstrated plausible delineations that are in line with previous dissection studies.

0865



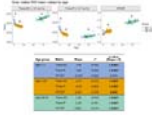
### Exploring multi-functions of MRI in PDT: imaging-guided tumor therapy, follow-up monitoring and early evaluation of therapeutic efficacy

Xiudong Shi<sup>1</sup>, Weitao Yang<sup>2</sup>, Qiong Ma<sup>1</sup>, and Yuxin Shi<sup>1</sup>

<sup>1</sup>Shanghai public health clinical center, Fudan University, Shanghai, China, <sup>2</sup>The Institute for Biomedical Engineering & Nano Science, Tongji University, Shanghai, China

Estimating the gross tumor volume by measuring the physical diameters of the tumor with calipers is a common method for evaluating the efficacy of photodynamic therapy (PDT). In this study, the optimal time for determining the efficacy of PDT treatment based on morphological and functional magnetic resonance (MR) imaging techniques is determined.

0866



Contribution of parenchymal water and CSF-like water to changes in brain water diffusivity in post-natal development and aging

Laura D. Reyes<sup>1</sup>, Amritha Nayak<sup>1,2</sup>, Alzheimer's Disease Neuroimaging Initiative <sup>\*3</sup>, and Carlo Pierpaoli<sup>1</sup>

<sup>1</sup>NIBIB, National Institutes of Health, Bethesda, MD, United States, <sup>2</sup>Henry M. Jackson Foundation, Bethesda, MD, United States, <sup>3</sup>Alzheimer's Disease Neuroimaging Initiative, Los Angeles, CA, United States

In this study, we used a biexponential dual compartment diffusion tensor imaging (DTI) model to characterize different pools of parenchymal water to investigate CSF-like free water and parenchymal diffusivity in childhood, early adulthood, and elderly adulthood, and examine how they change across the lifespan. We identified age-related changes in the contribution of parenchymal and CSF-like free water to age-related changes in overall diffusivity that can be linked to changes in tissue microstructure.

---

### Sunrise Session

#### Educational Q&A: Preclinical - Cutting-Edge Primers on Preclinical Imaging: Neuroscience

Organizers: Catherine Hines, Damian Tyler, Neil Harris, Arvind Pathak

Wednesday Parallel 1 Live Q&A

Wednesday 15:15 - 16:00 UTC

Primer on Transgenic Mouse Models for Neuropathologies

Piotr Walczak

Structural & Functional Neuroimaging in Rodents

Jianyang Zhang

---

### Sunrise Session

#### Educational Q&A: Preclinical - Cutting-Edge Primers on Preclinical Imaging: The 3 I's: Inflammation, Infection & Immuno-Oncology

Organizers: Catherine Hines, Damian Tyler, Neil Harris, Arvind Pathak

Wednesday Parallel 1 Live Q&A

Wednesday 15:15 - 16:00 UTC

Moderators: Susann Boretius

Primer on Animal Models of Infection and Immuno-Oncology

Cai Li

Advanced MRI technologies for detecting infection and inflammation

Guanshu Liu

---

### Sunrise Session

#### Educational Q&A: Preclinical - Cutting-Edge Primers on Preclinical Imaging: Cancer

Organizers: Catherine Hines, Damian Tyler, Neil Harris, Arvind Pathak

Wednesday Parallel 1 Live Q&A

Wednesday 15:15 - 16:00 UTC

Moderators: Ellen Ackerstaff & MASAKO KATAOKA

Primer on Mouse Models for Cancer: Transgenic, Humanized, In Vitro Assessment

Natalie Serkova

---

Imaging the Tumor Microenvironment

Geoff Parker

---

---

## Sunrise Session

### Educational Q&A: Preclinical - Cutting-Edge Primers on Preclinical Imaging: Cardiac

Organizers: Catherine Hines, Damian Tyler, Neil Harris, Arvind Pathak

Wednesday Parallel 1 Live Q&A

Wednesday 15:15 - 16:00 UTC

Primer on Small & Large Animal Cardiac Models

Dara Kraitchman

---

Beyond Cardiac Function: Microstructure & Metabolism

Jürgen Schneider

---

---

## Weekday Course

### Machine Learning for Image Reconstruction - Hands-On Deep Learning

Organizers: Florian Knoll, Michael Lustig, Demian Wassermann

Wednesday Parallel 5 Live Q&A

Wednesday 15:15 - 16:00 UTC

Moderators: Michael Lustig & Florian Knoll

Hands-On Deep Learning (Supporting Presenter)

Hemant Kumar Aggarwal<sup>1</sup>

<sup>1</sup>University of Iowa, United States

---

Hands-On Deep Learning

Peter Chang<sup>1</sup>

<sup>1</sup>University of California, Irvine, United States

---

Hands-On Deep Learning (Supporting Presenter)

Chen Qin<sup>1</sup>

<sup>1</sup>Imperial College London, United Kingdom

---

Hands-On Deep Learning (Supporting Presenter)

Matthew Muckley<sup>1</sup>

<sup>1</sup>New York University School of Medicine, United States

---

---

## Oral - Power Pitch

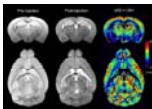
### Educational Q&A: Preclinical - Preclinical Imaging Advances

Wednesday Parallel 1 Live Q&A

Wednesday 15:15 - 16:00 UTC

Moderators: Simon Robinson

0897



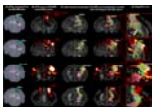
Toward high spatial resolution functional MRI: In vivo 50-micron cerebral blood volume mapping of the mouse brain

Akira Sumiyoshi<sup>1</sup>, Keigo Hikishima<sup>2</sup>, and Ichio Aoki<sup>1</sup>

<sup>1</sup>National Institutes for Quantum and Radiological Science and Technology (QST), Chiba, Japan, <sup>2</sup>Okinawa Institute of Science and Technology Graduate University (OIST), Okinawa, Japan

We report here in vivo 50-micron cerebral blood volume (CBV) mapping of the mouse brain using intraperitoneal injection protocol of gadolinium-based contrast agent. Based on k-means clustering we identified different vascular clusters that separately range from macro- to micro-vasculature. The CBV map demonstrated layer-dependent macro- and micro-vascular densities in the cortex where different cortical regions exhibited different vascular patterns. The CBV map also identified different vascular densities and patterns in the hippocampus. These results suggest that CBV map would be a useful and alternative tool that assesses brain function and metabolism at extremely high spatial resolution.

0898



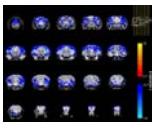
A quantitative approach to validate the mouse thalamo-cortical structural network reconstructed using diffusion MRI tractography

Tanzil Mahmud Arefin<sup>1</sup>, Choong Heon Lee<sup>1</sup>, Zifei Liang<sup>1</sup>, and Jiangyang Zhang<sup>1</sup>

<sup>1</sup>Radiology, NYU School of Medicine, New York, NY, United States

In this work, we used our previously reported high-resolution dMRI-based mouse brain atlas<sup>8</sup> to trace node-to-node thalamo-cortical structural connectivity in the mouse brain. Taking advantage of the rich viral tracer data from the Allen Mouse Brain Connectivity Atlas (AMBCA)<sup>4</sup>, the tractography results were examined using the tracer data as ground truth. Our findings pinpoint the potentiality of mapping reliable structural connectivity in gray matter structures using tractography and at the same time, highlight the necessity of further investigation on determining the imaging and tractography parameters for accurate estimation of such connectivity.

0899



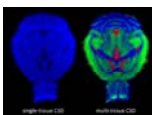
Brain structure in the homozygous FUSDelta14 mouse recapitulates amyotrophic lateral sclerosis phenotypes

Aurea B. Martins Bach<sup>1</sup>, Lily Qiu<sup>1</sup>, Jacob Ellegood<sup>2</sup>, Nick Wang<sup>2</sup>, Brian J. Nieman<sup>2</sup>, John G. Sled<sup>2</sup>, Remya R. Nair<sup>3</sup>, Elizabeth M. C. Fisher<sup>3,4</sup>, Thomas J. Cunningham<sup>3</sup>, Jason Lerch<sup>1</sup>, and Karla L. Miller<sup>1</sup>

<sup>1</sup>Wellcome Centre for Integrative Neuroimaging, FMRIB, Nuffield Department of Clinical Neurosciences, University of Oxford, Oxford, United Kingdom, <sup>2</sup>Mouse Imaging Centre, The Hospital for Sick Children, Toronto, ON, Canada, <sup>3</sup>Mammalian Genetics Unit, MRC Harwell Institute, Oxfordshire, United Kingdom, <sup>4</sup>Department of Neuromuscular Diseases, Institute of Neurology, University College London, London, United Kingdom

This study assesses changes in brain anatomy with MRI in the homozygous humanized FUSDelta14 mouse model of amyotrophic lateral sclerosis (ALS). Post-mortem brain T2w-images were acquired at 7T, with 40µm isotropic resolution. After registration, the deformation fields were compared between mutant and wild-type mice. Homozygous FUSDelta14 mice exhibited atrophy in multiple grey and white matter structures. These results are in agreement with observations such as cortical thinning and alterations in white matter microstructure in ALS patients. Homozygous humanized FUSDelta14 mice show an early brain phenotype and are therefore a promising model for the study of ALS pathogenic mechanisms.

0900



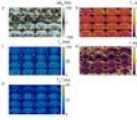
Multi-tissue constrained spherical deconvolution in a murine brain

Steven Jillings<sup>1</sup>, Jan Morez<sup>2</sup>, Nicholas Vidas-Guscic<sup>3</sup>, Johan Van Audekerke<sup>3</sup>, Floris Wuyts<sup>1</sup>, Marleen Verhoye<sup>3</sup>, Jan Sijbers<sup>2</sup>, and Ben Jeurissen<sup>2</sup>

<sup>1</sup>Lab for Equilibrium Investigations and Aerospace, Dept. of Physics, University of Antwerp, Antwerp, Belgium, <sup>2</sup>imec-Vision Lab, Dept. of Physics, University of Antwerp, Antwerp, Belgium, <sup>3</sup>Bio Imaging Lab, Dept. of Biomedical Sciences, University of Antwerp, Antwerp, Belgium

Multi-tissue constrained spherical deconvolution (MT-CSD) leverages the unique b-value dependency of each brain tissue type to estimate the full white matter (WM) fiber orientation density function (fODF) as well as the apparent densities of gray matter (GM) and cerebrospinal fluid (CSF), directly from multi-shell diffusion MRI (dMRI) data. Currently, its adoption is focussed almost entirely on imaging of the human brain. In this work, we demonstrate that the sequence, the pipeline and the advantages that are now well established for human brains, can be transferred to murine brains, bringing the technique into the preclinical realm.

0901



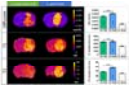
3D Magnetic Resonance Fingerprinting with Quadratic Phase in Mouse Brain on Preclinical 7T System

Charlie Wang<sup>1</sup>, Yuning Gu<sup>2</sup>, Rasim Boyacioglu<sup>2</sup>, Charlie Androjna<sup>3</sup>, Mark Alan Griswold<sup>2</sup>, and Xin Yu<sup>2</sup>

<sup>1</sup>Metrohealth Hospital, Cleveland, OH, United States, <sup>2</sup>Case Western Reserve University, Cleveland, OH, United States, <sup>3</sup>Cleveland Clinic, Cleveland, OH, United States

Magnetic Resonance Fingerprinting with Quadratic Phase (qRF-MRF) was previously validated in 2D clinical imaging for simultaneous off-resonance, T1, T2, and T2\* mapping. Translation of qRF-MRF to high-field preclinical systems for small animal imaging is challenging due to the higher field inhomogeneity and the higher spatial resolution required. Here, a 3D qRF-MRF method was explored to address these challenges. High-resolution simultaneous mapping of off-resonance, T1, T2, and T2\* on *in vivo* mouse brain at 7T was demonstrated. Computational limitations for large dictionary parameter space and reconstruction times were addressed using randomized SVD time compression and quadratic fitting methods.

0902



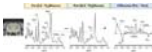
*In vivo* MRI can assess differences in cell density and size of different *Cryptococcus* species in brain lesions.

Liesbeth Vanherp<sup>1</sup>, Kristof Govaerts<sup>1</sup>, Amy Hillen<sup>2</sup>, Jennifer Poelmans<sup>3</sup>, Katrien Lagrou<sup>4</sup>, Greetje Vande Velde<sup>1</sup>, and Uwe Himmelreich<sup>1</sup>

<sup>1</sup>Biomedical MRI, University of Leuven, Leuven, Belgium, <sup>2</sup>Department of Cell and Molecular Biology, Karolinska Institutet, Stockholm, Sweden, <sup>3</sup>Janssen Pharmaceutical Companies of Johnson & Johnson, Beerse, Belgium, <sup>4</sup>Laboratory of Clinical Bacteriology and Mycology, University of Leuven, Leuven, Belgium

Multi-parametric MRI was correlated with *in vivo* Fibred Confocal Fluorescence Microscopy and histology in two preclinical models of cryptococcosis. Increased ADCs and T2 relaxation times were linked to differences in capsule size and associated fungal density in brain lesions caused by the two pathogenic fungi *Cryptococcus neoformans* and *C. gattii*. This provides not only a non-invasive means to assess one of the most important virulence factors of Cryptococci in preclinical research but may also affect patient management by providing a method for differential diagnosis.

0903



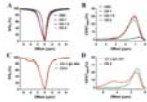
Investigating cerebral energetics and neurotransmission using *in vivo* <sup>1</sup>H MRS and [6,6'-<sup>2</sup>H<sub>2</sub>]glucose in a preclinical model

Puneet Bagga<sup>1</sup>, Laurie J Rich<sup>1</sup>, Neil E Wilson<sup>1</sup>, Mark Elliott<sup>1</sup>, Mitch D Schnell<sup>1</sup>, Mohammad Haris<sup>2,3</sup>, John A Detre<sup>4</sup>, and Ravinder Reddy<sup>1</sup>

<sup>1</sup>Department of Radiology, University of Pennsylvania, Philadelphia, PA, United States, <sup>2</sup>Sidra Medicine, Doha, Qatar, <sup>3</sup>LARC, Qatar University, Doha, Qatar, <sup>4</sup>Department of Neurology, University of Pennsylvania, Philadelphia, PA, United States

Energy metabolism and neurotransmission are two crucial processes affecting almost all aspects of cerebral function and  $^1\text{H}$  MRS allows the non-invasive detection and quantification of neurochemicals. In this study, we performed  $^1\text{H}$  MRS in conjunction with the administration of  $[6,6'\text{-}^2\text{H}_2]\text{glucose}$  to measure turnover kinetics of glutamate, glutamine and GABA in rat brain. As  $^2\text{H}$  is invisible on  $^1\text{H}$  MRS, the turnover of metabolites leads to a corresponding drop in their  $^1\text{H}$  MR signal visualized by subtraction of the Post- $[6,6'\text{-}^2\text{H}_2]\text{glucose}$  administration from the Pre-administration  $^1\text{H}$  MR spectra. The fractional enrichment data can be fitted to evaluate the rates of cerebral energetics.

0904



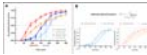
#### CEST imaging of self-healing hydrogels for drug delivery to the brain

Xiongqi Han<sup>1</sup>, Jianpan Huang<sup>1</sup>, and Kannie Wai Yan Chan<sup>1,2</sup>

<sup>1</sup>Department of Biomedical Engineering, City University of Hong Kong, Hong Kong, Hong Kong, <sup>2</sup>Russell H. Morgan Department of Radiology and Radiological Science, Johns Hopkins Medicine, Baltimore, MD, United States

Self-healing hydrogels can adapt to the dynamic and mechanically demanding environment in the brain when compare to conventional brittle hydrogels. Herein, we developed a series of self-healing chitosan-dextran based hydrogels (CDgels) which were mechanically soft and its composition could be detected via CEST-MRI. Once crosslinked, CEST-MRI contrast at 1.2 ppm decreased when the crosslinking density increased. Interestingly, this phenomenon was observed when we further incorporated barbituric acid (BA) into CDgels to form part of the Schiff-base interaction. The resultant BA-loaded CDgels showed both CEST contrast at 3T, demonstrating a robust approach for imaging-guided hydrogel-based therapy in brain.

0905



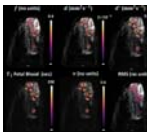
#### Oxygen carrier therapy slows infarct growth in large vessel occlusion dog model based on perfusion- and diffusion-weighted MRI analysis

Mohammed Salman Shazeeb<sup>1,2</sup>, Robert King<sup>1,2</sup>, Josephine Kolstad<sup>1</sup>, Christopher Raskett<sup>1</sup>, Natacha Le Moan<sup>3</sup>, Jonathan A. Winger<sup>3</sup>, Lauren Kelly<sup>3</sup>, Ana Krtolica<sup>3</sup>, Nils Henninger<sup>1</sup>, and Matthew Gounis<sup>1</sup>

<sup>1</sup>University of Massachusetts Medical School, Worcester, MA, United States, <sup>2</sup>Worcester Polytechnic Institute, Worcester, MA, United States, <sup>3</sup>Omniox Inc., San Carlos, CA, United States

The dog large vessel occlusion (LVO) model mimics the clinical trend observed in patients where the brain infarct follows either a slow or fast progression. The dog LVO model can be used in the design of new therapeutics to improve clinical outcome in patients. This study examined the effect of an oxygen carrier in its ability to slow infarct growth in the dog LVO model. In fast evolvers, the oxygen carrier therapy prolonged infarct progression and reduced the final normalized infarct volume. Delaying infarct progression can potentially extend the time-window for thrombectomy enabling more patients to receive this critical treatment.

0906



#### A Bayesian Approach for Diffusion-Weighted Imaging to study placenta development and function in pregnancy in a large animal model

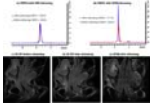
Dimitra Flouri<sup>1,2</sup>, Jack RT Darby<sup>3</sup>, Stacey L Holman<sup>3</sup>, Sunthara R Perumal<sup>4</sup>, Anna L David<sup>5,6</sup>, Janna L Morrison<sup>3</sup>, and Andrew Melbourne<sup>1,2</sup>

<sup>1</sup>School of Biomedical Engineering & Imaging Sciences, King's College London, London, United Kingdom, <sup>2</sup>Department of Medical Physics & Biomedical Engineering, University College London, London, United Kingdom, <sup>3</sup>Early Origins of Adult Health Research Group, University of South Australia, Adelaide, Australia, <sup>4</sup>Preclinical Imaging and Research Laboratories, South Australian Health and Medical Research Institute, Adelaide, Australia, <sup>5</sup>Institute for Women's Health, University College London, London, United Kingdom, <sup>6</sup>NIHR University College London Hospitals Biomedical Research Center, London, United Kingdom



Abnormalities of placental development and function result in fetal growth restriction. There is growing interest in understanding placenta structure and function throughout pregnancy to gain better understanding of placenta dysfunction. Advances in technology enables derivation of quantitative indices that reflect tissue microcapillary perfusion and tissue diffusivity from MRI. Despite recent progress, in-vivo diffusion-weighted MRI remains challenging due to long scan times, respiratory motion and low signal-to-noise ratio. Sheep provide a relevant large-scale model for invasive validation studies for MRI measurements. We aimed to improve parameter mapping using Bayesian inference. Bayesian analysis yields improved parameter maps relative to conventional least-squares fitting.

0907



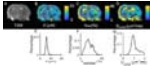
A robust shimming method for in vivo abdominal mice studies based on ultrafast pulse sequences

Qingjia Bao<sup>1</sup>, Ricardo Martinho<sup>1</sup>, and Lucio Frydman<sup>1</sup>

<sup>1</sup>Weizmann Institute of Science, Rehovot, Israel

A challenge in functional, diffusivity and spectroscopic MRI studies of mouse body regions is B0 inhomogeneity, especially at ultrahigh fields. To map and correct these B0s, phase difference images are usually acquired using gradient echo sequences. These, however, are hard to obtain with good quality in abdominal studies due to motion artifacts. In this study we report a fully automated 3D map-based shimming method based on an ultrafast sequence that can overcome these artifacts, delivering optimal B0 homogeneity over the targeted ROIs. This technique is exemplified with mice studies at 15.2T, where its usefulness and reproducibility is demonstrated.

0908



In vivo Quantification of Restriction Sizes in Gray Matter of Rat Brain Using Temporal Diffusion Spectroscopy

xiaoyu jiang<sup>1</sup>, junzhong xu<sup>1</sup>, sean p. devan<sup>1</sup>, and john c. gore<sup>1</sup>

<sup>1</sup>Vanderbilt University Institute of Imaging Science, nashville, TN, United States

The diffusion time ( $t_{diff}$ ) dependence of diffusion MRI signals provides a means to characterize tissue microstructure at cellular levels. Several studies have reported the diffusion time dependence of diffusion signals from rodent brains in health and disease, as well as human brains. Here, we apply IMPULSED (Imaging Microstructural Parameters Using Limited Spectrally Edited Diffusion), a temporal diffusion spectroscopy-based method that we have described previously, to map the mean restriction size for water diffusion in gray matter of the rat brain *in vivo* by fitting the  $t_{diff}$  dependence of diffusion signals to a simple biophysical model.

## Oral

### Machine Learning for Image Reconstruction - Machine Learning for Image Reconstruction

Wednesday Parallel 5 Live Q&A

Wednesday 15:15 - 16:00 UTC

Moderators: Fang Liu

0987



$\Sigma$ -net: Ensembled Iterative Deep Neural Networks for Accelerated Parallel MR Image Reconstruction

Kerstin Hammernik<sup>1</sup>, Jo Schlemper<sup>1,2</sup>, Chen Qin<sup>1</sup>, Jinming Duan<sup>3</sup>, Gavin Seegoolam<sup>1</sup>, Cheng Ouyang<sup>1</sup>, Ronald M Summers<sup>4</sup>, and Daniel Rueckert<sup>1</sup>

<sup>1</sup>Department of Computing, Imperial College London, London, United Kingdom, <sup>2</sup>Hyperfine Research Inc., Guilford, CT, United States, <sup>3</sup>School of Computer Science, University of Birmingham, Birmingham, United Kingdom, <sup>4</sup>NIH Clinical Center, Bethesda, MD, United States

We propose an ensembled  $\Sigma$ -net for fast parallel MR image reconstruction, including parallel coil networks, which perform implicit coil weighting, and sensitivity networks, involving explicit sensitivity maps. The networks in  $\Sigma$ -net are trained with various ways of data consistency, i.e., gradient descent, proximal mapping, and variable splitting, and with a semi-supervised finetuning scheme to adapt to the k-space data at test time. We achieved robust and high SSIM scores by ensembling all models to a  $\Sigma$ -net. At the date of submission,  $\Sigma$ -net is the leading entry of the public fastMRI multicoil leaderboard.

0988



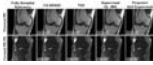
### Deep Model-based MR Parameter Mapping Network (DOPAMINE) for Fast MR Reconstruction

Yohan Jun<sup>1</sup>, Hyungseob Shin<sup>1</sup>, Taejoon Eo<sup>1</sup>, Taeseong Kim<sup>1</sup>, and Dosik Hwang<sup>1</sup>

<sup>1</sup>Electrical and Electronic Engineering, Yonsei University, Seoul, Republic of Korea

In this study, a deep model-based MR parameter mapping network termed as “DOPAMINE” was developed to reconstruct MR parameter maps from undersampled multi-channel k-space data. It consists of two models: 1) MR parameter mapping model which estimates initial parameter maps from undersampled k-space data with a deep convolutional neural network (CNN-based mapping), 2) parameter map reconstruction model which removes aliasing artifacts with a deep CNN (CNN-based reconstruction) and interleaved data consistency layer by embedded MR model-based optimization procedure.

0989



### Physics-Based Self-Supervised Deep Learning for Accelerated MRI Without Fully Sampled Reference Data

Burhaneddin Yaman<sup>1,2</sup>, Seyed Amir Hossein Hosseini<sup>1,2</sup>, Steen Moeller<sup>2</sup>, Jutta Ellermann<sup>2</sup>, Kamil Ugurbil<sup>2</sup>, and Mehmet Akcakaya<sup>1,2</sup>

<sup>1</sup>Electrical and Computer Engineering, University of Minnesota, Minneapolis, MN, United States, <sup>2</sup>Center for Magnetic Resonance Research, University of Minnesota, Minneapolis, MN, United States

Recently, deep learning (DL) has emerged as a means for improving accelerated MRI reconstruction. However, most current DL-MRI approaches depend on the availability of ground truth data, which is generally infeasible or impractical to acquire due to various constraints such as organ motion. In this work, we tackle this issue by proposing a physics-based self-supervised DL approach, where we split acquired measurements into two sets. The first one is used for data consistency while training the network, while the second is used to define the loss. The proposed technique enables training of high-quality DL-MRI reconstruction without fully-sampled data.

0990



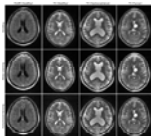
### Synchronizing dimension reduction and parameter inference in 3D multiparametric MRI: A hybrid dual-pathway neural network approach

Carolin M Pirk<sup>1,2</sup>, Izabela Horvath<sup>1,2</sup>, Sebastian Endt<sup>1,2</sup>, Guido Buonincontri<sup>3,4</sup>, Marion I Menze<sup>2,5</sup>, Pedro A Gómez<sup>1</sup>, and Bjoern H Menze<sup>1</sup>

<sup>1</sup>Informatics, Technical University of Munich, Munich, Germany, <sup>2</sup>GE Healthcare, Munich, Germany, <sup>3</sup>Fondazione Imago7, Pisa, Italy, <sup>4</sup>IRCCS Fondazione Stella Maris, Pisa, Italy, <sup>5</sup>Physics, Technical University of Munich, Munich, Germany

Complementing the fast acquisition of coupled multiparametric MR signals, multiple studies have dealt with improving and accelerating parameter quantification using machine learning techniques. Here we synchronize dimension reduction and parameter inference and propose a hybrid neural network with a signal-encoding layer followed by a dual-pathway structure, for parameter prediction and recovery of the artifact-free signal evolution. We demonstrate our model with a 3D multiparametric MRI framework and show that it is capable of reliably inferring T1, T2 and PD estimates, while its trained latent-space projection facilitates efficient data compression already in k-space and thereby significantly accelerates image reconstruction.

0991



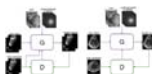
### Deep Learning MRI Reconstruction in Application to Point-of-Care MRI

Jo Schlemper<sup>1</sup>, Seyed Sadegh Mohseni Salehi<sup>1</sup>, Carole Lazarus<sup>1</sup>, Hadrien Dyvorne<sup>1</sup>, Rafael O'Halloran<sup>1</sup>, Nicholas de Zwart<sup>1</sup>, Laura Sacolick<sup>1</sup>, Samantha By<sup>1</sup>, Joel M. Stein<sup>2</sup>, Daniel Rueckert<sup>3</sup>, Michal Sofka<sup>1</sup>, and Prantik Kundu<sup>1,4</sup>

<sup>1</sup>Hyperfine Research Inc., Guilford, CT, United States, <sup>2</sup>Hospitals of the University of Pennsylvania, Philadelphia, PA, United States, <sup>3</sup>Computing, Imperial College London, London, United Kingdom, <sup>4</sup>Icahn School of Medicine at Mount Sinai, New York City, NY, United States

The goal of low-field (64 mT) portable point-of-care (POC) MRI is to produce low cost, clinically acceptable MR images in reasonable scan times. However, non-ideal MRI behaviors make the image quality susceptible to artifacts from system imperfections and undersampling. In this work, a deep learning approach is proposed for fast reconstruction from hardware and sampling-associated imaging artifacts. The proposed approach outperforms the reference deep learning approaches for retrospectively undersampled data with simulated system imperfections. Furthermore, we demonstrate that it yields better image quality and faster reconstruction than compressed sensing approach for unseen, prospectively undersampled low-field POC MR images.

0992



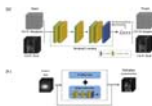
### Wasserstein GANs for MR Imaging: from Paired to Unpaired Training

Ke Lei<sup>1</sup>, Morteza Mardani<sup>1,2</sup>, Shreyas S. Vasawala<sup>2</sup>, and John M. Pauly<sup>1</sup>

<sup>1</sup>Electrical Engineering, Stanford University, Stanford, CA, United States, <sup>2</sup>Radiology, Stanford University, Stanford, CA, United States

Lack of ground-truth MR images impedes the common supervised training of deep networks for image reconstruction. This work leverages WGANs for unpaired training of reconstruction networks. The reconstruction network is an unrolled neural network with a cascade of residual blocks and data consistency modules. The discriminator network is a multilayer CNN that acts like a critic, scoring the generated and label images. Our experiments demonstrate that unpaired WGAN training with minimal supervision is a viable option when there exists insufficient or no fully-sampled training label images that match the input images. Adding WGANs to paired training is also shown effective.

0993



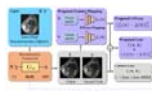
### RED-N2N: Image reconstruction for MRI using deep CNN priors trained without ground truth

Jiaming Liu<sup>1</sup>, Cihat Eldeniz<sup>1</sup>, Yu Sun<sup>1</sup>, Weijie Gan<sup>1</sup>, Sihao Chen<sup>1</sup>, Hongyu An<sup>1</sup>, and Ulugbek S. Kamilov<sup>1</sup>

<sup>1</sup>Washington University in St. Louis, St. Louis, MO, United States

We propose a new MR image reconstruction method that systematically enforces data consistency while also exploiting deep-learning imaging priors. The prior is specified through a convolutional neural network (CNN) trained to remove undersampling artifacts from MR images without any artifact-free ground truth. The results on reconstructing free-breathing MRI data into ten respiratory phases show that the method can form high-quality 4D images from severely undersampled measurements corresponding to acquisitions of about 1 minute in length. The results also highlight the improved performance of the method compared to several popular alternatives, including compressive sensing and UNet3D.

0994



### High-Fidelity Reconstruction with Instance-wise Discriminative Feature Matching Loss

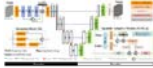
Ke Wang<sup>1</sup>, Jonathan I. Tamir<sup>1,2</sup>, Stella X. Yu<sup>1,3</sup>, and Michael Lustig<sup>1</sup>

<sup>1</sup>Electrical Engineering and Computer Sciences, University of California, Berkeley, Berkeley, CA, United States, <sup>2</sup>Electrical and Computer Engineering, The University of Texas at Austin, Austin, TX, United States, <sup>3</sup>International Computer Science Institute, University of California, Berkeley, Berkeley, CA, United States



Machine-learning based reconstructions have shown great potential to reduce scan time while maintaining high image quality. However, commonly used per-pixel losses for the training don't capture perceptual differences between the reconstructed and the ground truth images, leading to blurring or reduced texture. Thus, we incorporate a novel feature representation-based loss function with the existing reconstruction pipelines (e.g. MoDL), which we called Unsupervised Feature Loss (UFLoss). In-vivo results on both 2D and 3D reconstructions show that the addition of the UFLoss can encourage more realistic reconstructed images with much more detail compared to conventional methods (MoDL and Compressed Sensing).

0995

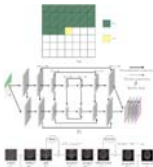


A spatially adaptive cross-modality based three-dimensional reconstruction network for susceptibility imaging  
Lijun Bao<sup>1</sup> and Hongyuan Zhang<sup>1</sup>

<sup>1</sup>Xiamen University, Xiamen, China

In this work, we propose a spatially adaptive cross-modality based three-dimensional reconstruction network to determine the susceptibility distribution from the magnetic field measurement. To compensate the information lost in previous encoder layers, a set of spatially adaptive modules in different resolutions are embedded into multiscale decoders, which extract features from magnitude images and field maps adaptively. Thus, the magnitude regularization is incorporated into the network architecture while the training stability is improved. It is potential to solve inverse problems of three-dimensional data, especially for cross-modality related reconstructions.

0996



MRI Reconstruction Using Deep Bayesian Inference  
Guanxiong Luo<sup>1</sup> and Peng Cao<sup>1</sup>

<sup>1</sup>The University of Hong Kong, Hong Kong, China

A deep neural network provides a practical approach to extract features from existing image database. For MRI reconstruction, we presented a novel method to take advantage of such feature extraction by Bayesian inference. The innovation of this work includes 1) the definition of image prior based on an autoregressive network, and 2) the method uniquely permits the flexibility and generality and caters for changing various MRI acquisition settings, such as the number of radio-frequency coils, and matrix size or spatial resolution.

## Oral

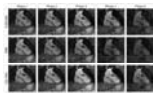
### Machine Learning for Image Reconstruction - Machine Learning Reconstruction of Dynamic Acquisitions

Wednesday Parallel 5 Live Q&A

Wednesday 15:15 - 16:00 UTC

Moderators: Li Feng & Shanshan Wang

0997



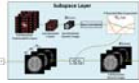
A Model-Based Variational Neural Network for Accelerated and Respiratory Motion-resolved 4D Cartesian Cardiac MRI

Niccolo Fuin<sup>1</sup>, Thomas Kuestner<sup>1</sup>, Gastao Cruz<sup>1</sup>, Aurelien Bustin<sup>1</sup>, René Botnar<sup>1,2</sup>, and Claudia Prieto<sup>1,2</sup>

<sup>1</sup>Biomedical Engineering Department, School of Biomedical Engineering and Imaging Sciences, King's College London, London, United Kingdom, <sup>2</sup>Pontificia Universidad Católica de Chile, Santiago, Chile

Long scan times and susceptibility to respiratory motion are major challenges in free-breathing 3D cardiac MRI. Respiratory-resolved 4D approaches deal with motion by assigning data to different respiratory bins and exploiting motion redundancies during reconstruction. However, for accelerated acquisitions this leads to highly undersampled respiratory bins, affecting image quality. Here we propose a novel unrolled VNN that reconstructs undersampled 4D cardiac MRI by exploiting motion redundancies and by using conjugate gradient to enforce data-consistency within every stage of the VNN, providing generalization of the network to the unpredictable sampling of each bin due to subject-specific respiratory motion.

0998



### k-t SANTIS: Subspace Augmented Neural neTwork with Incoherent Sampling for dynamic image reconstruction

Fang Liu<sup>1,2</sup> and Li Feng<sup>3</sup>

<sup>1</sup>Gordon Center for Medical Imaging, Massachusetts General Hospital, Harvard Medical School, Boston, MA, United States, <sup>2</sup>Radiology, University of Wisconsin-Madison, Madison, WI, United States, <sup>3</sup>Biomedical Engineering and Imaging Institute and Radiology, Icahn School of Medicine at Mount Sinai, New York, NY, United States

A novel deep learning-based dynamic image reconstruction technique called k-t SANTIS (Subspace Augmented Neural neTwork with Incoherent Sampling) is presented in this study. Different from prior deep learning-based reconstruction approaches that rely primarily on data-driven learning, k-t SANTIS incorporates a low-rank subspace model into the deep-learning reconstruction architecture, which is implemented by adding a subspace layer to enforce an explicit subspace constraint during network training. k-t SANTIS represents a new deep image reconstruction framework with hybrid data-driven and physics-informing learning, taking additional prior knowledge available in the dataset into consideration during the training process to achieve better reconstruction performance.

0999



### Dynamic Real-time MRI with Deep Convolutional Recurrent Neural Networks and Non-Cartesian Fidelity

Yufei Zhang<sup>1</sup>, Zhijun Wang<sup>1</sup>, Quan Chen<sup>1</sup>, Shuo Li<sup>1</sup>, Zekang Ding<sup>1</sup>, Chenfei Shen<sup>1</sup>, Xudong Chen<sup>1</sup>, Kang Yan<sup>1</sup>, Cong Zhang<sup>2</sup>, Xiaodong Zhou<sup>2</sup>, Yiping P. Du<sup>1</sup>, and Huajun She<sup>1</sup>

<sup>1</sup>Institute for Medical Imaging Technology, School of Biomedical Engineering, Shanghai Jiao Tong University, Shanghai, China, <sup>2</sup>United Imaging Healthcare, Shanghai, China

A convolutional recurrent neural networks (CRNN) with Non-Cartesian fidelity for 2D real-time imaging was proposed. 3D stack-of-star GRE radial sequence with self-navigator was used to acquire the data. Multiple respiratory phases were extracted from the navigator and the sliding window method was used to get the training data. The Fidelity constraints the reconstruction image to be consistent to the undersampled non-Cartesian k-space data. Convolution and recurrence improve the quality of the reconstructed images by using temporal dimension information. The reconstruction speed is around 10 frames/second, which fulfills the requirement of real-time imaging.

1000

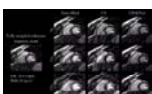


### An Unsupervised Deep Learning Method for Parallel MR Cardiac Imaging via Time Interleaved Sampling

Ziwen Ke<sup>1,2</sup>, Yanjie Zhu<sup>3</sup>, Jing Cheng<sup>2,3</sup>, Leslie Ying<sup>4</sup>, Xin Liu<sup>3</sup>, Hairong Zheng<sup>3</sup>, and Dong Liang<sup>1,3</sup>

<sup>1</sup>Research Center for Medical AI, Shenzhen Institutes of Advanced Technology, Chinese Academy of Sciences, Shenzhen, China, <sup>2</sup>Shenzhen College of Advanced Technology, University of Chinese Academy of Sciences, Shenzhen, China, <sup>3</sup>Paul C. Lauterbur Research Center for Biomedical Imaging, Shenzhen Institutes of Advanced Technology, Chinese Academy of Sciences, Shenzhen, China, <sup>4</sup>Department of Biomedical Engineering and Department of Electrical Engineering, The State University of New York, Buffalo, NY, United States

Deep learning has achieved good success in cardiac MRI. However, these methods are all based on big data, and only deal with single-channel imaging. In this paper, we propose an unsupervised deep learning method for parallel MR cardiac imaging via time interleaved sampling. Specifically, a set of full-encoded reference data were built by merging the data from adjacent time frames, and used to train a network for reconstructing each coil image separately. Finally, coil images were combined via another CNN. The validation on in vivo data show that our method can achieve improved reconstruction compared with other competing methods.

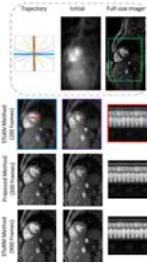


### CINENet: Deep learning-based 3D Cardiac CINE Reconstruction with multi-coil complex 4D Spatio-Temporal Convolutions

Thomas Küstner<sup>1</sup>, Niccolo Fuin<sup>1</sup>, Kerstin Hammernik<sup>2</sup>, Aurelien Bustin<sup>1</sup>, Radhouene Nejj<sup>1,3</sup>, Daniel Rueckert<sup>2</sup>, René M Botnar<sup>1</sup>, and Claudia Prieto<sup>1</sup>

<sup>1</sup>Biomedical Engineering Department, School of Biomedical Engineering and Imaging Sciences, King's College London, London, United Kingdom, <sup>2</sup>Department of Computing, Imperial College London, London, United Kingdom, <sup>3</sup>MR Research Collaborations, Siemens Healthcare Limited, Frimley, United Kingdom

CINE MRI is the gold-standard for the assessment of cardiac function. Compressed Sensing (CS) reconstruction has enabled 3D CINE acquisition with left ventricular (LV) coverage in a single breath-hold. However, maximal achievable acceleration is limited by the performance of the selected reconstruction method. Deep learning has shown to provide good-quality reconstructions of highly accelerated 2D CINE imaging. In this work, we propose a novel 4D (3D+time) reconstruction network for prospectively undersampled 3D Cartesian cardiac CINE that utilizes complex-valued spatial-temporal convolutions. The proposed network outperforms CS in visual quality and shows good agreement for LV function to gold-standard 2D CINE.



### DYNAMIC MRI USING DEEP MANIFOLD SELF-LEARNING

Abdul Haseeb Ahmed<sup>1</sup>, Hemant Aggarwal<sup>1</sup>, Prashant Nagpal<sup>1</sup>, and Mathews Jacob<sup>1</sup>

<sup>1</sup>University of Iowa, Iowa City, IA, United States

We propose a deep self-learning algorithm to learn the manifold structure of free-breathing and ungated cardiac data and to recover the cardiac CINE MRI from highly undersampled measurements. Our method learns the manifold structure in the dynamic data from navigators using autoencoder network. The trained autoencoder is then used as aprior in the image reconstruction framework. We have tested the proposed method on free-breathing and ungated cardiac CINE data, which is acquired using a navigated golden-angle gradient-echo radial sequence. Results show the ability of our method to better capture the manifold structure, thus providing us reduced spatial and temporal blurring as compared to the SToRM reconstruction.

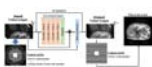


### Deep Learning for Robust Accelerated Dynamic MRI Reconstruction for Active Acquisition Pipelines

Gavin Seegoolam<sup>1</sup>, Anthony Price<sup>2</sup>, Joseph V Hajnal<sup>2,3</sup>, and Daniel Rueckert<sup>1</sup>

<sup>1</sup>BioMedIA, Department of Computing, Imperial College London, London, United Kingdom, <sup>2</sup>Biomedical Engineering Department, School of Biomedical Engineering and Imaging Sciences, Kings College London, London, United Kingdom, <sup>3</sup>Centre for the Developing Brain, School of Biomedical Engineering and Imaging Sciences, Kings College London, London, United Kingdom

With the advent of active acquisition-reconstruction pipelines, this study shows that by exploiting motion, robust intermediate reconstructions can be used to exploit the entire k-space budget and stabilise deep learning methods for accelerated dynamic MRI. The generated intermediate reconstructions are known as data-consistent motion-augmented cines (DC-MAC). A motion-exploiting convolutional neural network (ME-CNN), which incorporates the DC-MAC, is evaluated against a similar model to that used in a recent active acquisition-reconstruction study, the data-consistent convolutional neural network (DC-CNN). We find that the ME-CNN outperforms DC-CNN but also the DC-MAC offers better reconstructions at low acceleration rates.



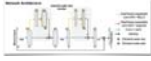
### FITs-CNN: A Very Deep Cascaded Convolutional Neural Networks Using Folded Image Training Strategy for Abdominal MRI Reconstruction

Satoshi Funayama<sup>1</sup>, Tetsuya Wakayama<sup>2</sup>, Hiroshi Onishi<sup>1</sup>, and Utaroh Motosugi<sup>1</sup>

<sup>1</sup>Department of Radiology, University of Yamanashi, Yamanashi, Japan, <sup>2</sup>GE Healthcare Japan, Tokyo, Japan

For faster abdominal MR imaging, deep learning-based reconstruction is expected to be a powerful reconstruction method. One of the challenges in deep learning-based reconstruction is its memory consumption when it is combined with parallel imaging. To handle the problem, we propose a very deep cascaded convolutional neural networks (CNNs) using folded image training strategy (FITs). We also present that the network can be trained with FITs and shows good quality of reconstructed images.

1005



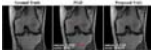
### Attention-Gated Convolutional Neural Networks for Off-Resonance Correction of Spiral Real-Time Magnetic Resonance Imaging

Yongwan Lim<sup>1</sup>, Shrikanth S Narayanan<sup>1</sup>, and Krishna S Nayak<sup>1</sup>

<sup>1</sup>University of Southern California, Los Angeles, CA, United States

Spiral acquisitions are preferred in real-time MRI because of their efficiency, which has made it possible to capture vocal tract dynamics during natural speech. A fundamental limitation of spirals is blurring and signal loss due to off-resonance, which degrades image quality at air-tissue boundaries. Here, we present a new CNN-based off-resonance correction method that incorporates an attention-gate mechanism. This leverages spatial and channel relationships of filtered outputs and improves the expressiveness of the networks. We demonstrate improved performance with the attention-gate, on 1.5T spiral speech RT-MRI, compared to existing off-resonance correction methods.

1006



### Unrolled Physics-Based Deep Learning MRI Reconstruction with Dense Connections using Nesterov Acceleration

Seyed Amir Hossein Hosseini<sup>1,2</sup>, Burhaneddin Yaman<sup>1,2</sup>, Steen Moeller<sup>2</sup>, Kamil Ugurbil<sup>2</sup>, Mingyi Hong<sup>1</sup>, and Mehmet Akcakaya<sup>1,2</sup>

<sup>1</sup>Electrical and Computer Engineering, University of Minnesota, Minneapolis, MN, United States, <sup>2</sup>Center for Magnetic Resonance Research, University of Minnesota, Minneapolis, MN, United States

Numerous studies have recently employed deep learning (DL) for accelerated MRI reconstruction. Physics-based DL-MRI techniques unroll an iterative optimization procedure into a recurrent neural network, by alternating between linear data consistency and neural network-based regularization units. Data consistency unit typically implements a gradient step. We hypothesize that further gains can be achieved by allowing dense connections within unrolled network, facilitating information flow. Thus, we propose to unroll a Nesterov-accelerated gradient descent that considers the history of previous iterations. Results indicate that this method considerably improves reconstruction over unrolled gradient descent schemes without skip connections.

## Oral

### Neurodegeneration 2 - Neurodegeneration

Wednesday Parallel 2 Live Q&A

Wednesday 15:15 - 16:00 UTC

Moderators: Yuhei Takado

0909



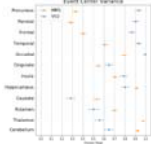
### Neurodegenerative and functional signatures of the cerebellar cortex in m.3243A>G patients

Roy AM Haast<sup>1</sup>, Dimo Ivanov<sup>2</sup>, Ali R Khan<sup>1,3</sup>, Irenaeus FM de Co<sup>4</sup>, Elia Formisano<sup>2,5</sup>, and Kamil Uludag<sup>6,7</sup>

<sup>1</sup>Robarts Research Institute, Western University, London, ON, Canada, <sup>2</sup>Department of Cognitive Neuroscience, Maastricht University, Maastricht, Netherlands, <sup>3</sup>Department of Medical Biophysics, Schulich School of Medicine and Dentistry, Western University, London, ON, Canada, <sup>4</sup>Department of Genetics and Cell Biology, Maastricht University, Maastricht, Netherlands, <sup>5</sup>Maastricht Center for Systems Biology, Maastricht University, Maastricht, Netherlands, <sup>6</sup>Institute for Basic Science, Center for Neuroscience Imaging Research, Department of Biomedical Engineering, Sungkyunkwan University, Suwon, Republic of Korea, <sup>7</sup>University Health Network, Toronto, ON, Canada

The m.3243A>G mutation is the most commonly observed mitochondrial mutation in humans. It causes a wide range of phenotypes, ranging from normal healthy aging to a severely affected quality of life through neuroradiological changes and cognitive impairment. Here, we studied the cerebellar changes in these patients and showed significant local reductions in gray matter tissue volume and functional connectivity using 7T MRI. Interestingly, its white matter remains relatively intact. Taken together, the current results contributes to the still limited understanding of brain pathologies in m.3243A>G patients.

0910



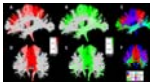
### Modelling the temporal cascade of abnormalities in diffusion magnetic resonance imaging in sporadic Creutzfeldt-Jakob disease

Riccardo Pascuzzo<sup>1</sup>, Vikram Venkatraghavan<sup>2</sup>, Marco Moscatelli<sup>1</sup>, Marina Grisoli<sup>1</sup>, Esther E. Bron<sup>2</sup>, Stefan Klein<sup>2</sup>, Janis Blevins<sup>3</sup>, Gianmarco Castelli<sup>1</sup>, Lawrence B. Schonberger<sup>4</sup>, Pierluigi Gambetti<sup>5</sup>, Brian S. Appleby<sup>3</sup>, and Alberto Bizzi<sup>1</sup>

<sup>1</sup>Neuroradiology Unit, Fondazione IRCCS Istituto Neurologico Carlo Besta, Milan, Italy, <sup>2</sup>Biomedical Imaging Group Rotterdam, Departments of Medical Informatics & Radiology, Erasmus MC, University Medical Center Rotterdam, Rotterdam, Netherlands, <sup>3</sup>National Prion Disease Pathology Surveillance Center, Case Western Reserve University, School of Medicine, Cleveland, OH, United States, <sup>4</sup>National Center for Emerging and Zoonotic Infectious Diseases, Centers for Disease Control and Prevention, Atlanta, GA, United States, <sup>5</sup>Department of Pathology, Case Western Reserve University, School of Medicine, Cleveland, OH, United States

The subtypes of sporadic Creutzfeldt-Jakob disease (sCJD), determined only at autopsy, may have different abnormality patterns in diffusion-weighted magnetic resonance imaging (DW-MRI) according to few reports. For the first time, we provide temporal cascades of the DW-MRI abnormalities in seven distinct sCJD subtypes using a data-driven technique named “discriminative event-based model”. Based on these cascades, we propose a novel procedure to identify the subtype of a patient. We found that sCJD subtypes have either initial cortical (MM/MV1, MM/MV2C, VV1 subtypes) or subcortical involvement (MV2K and VV2) with specific orderings of DW-MRI abnormalities, allowing a correct subtype prediction in most cases.

0911



### Why white matter matters – Interplay of white matter hyperintensities, white matter tracts, and processing speed – The Maastricht Study

Laura W.M. Vergoossen<sup>1,2</sup>, Jacobus F.A. Jansen<sup>1,2,3</sup>, Thomas T. van Sloten<sup>4,5</sup>, Miranda T. Schram<sup>2,4,5</sup>, Walter H. Backes<sup>1,2</sup>, and on behalf of The Maastricht Study<sup>4</sup>

<sup>1</sup>Radiology and Nuclear Medicine, Maastricht University Medical Center, Maastricht, Netherlands, <sup>2</sup>Mental Health and Neuroscience, Maastricht University, Maastricht, Netherlands, <sup>3</sup>Electrical Engineering, Eindhoven University of Technology, Eindhoven, Netherlands, <sup>4</sup>Internal Medicine, Maastricht University Medical Center, Maastricht, Netherlands, <sup>5</sup>School for Cardiovascular Disease, Maastricht University, Maastricht, Netherlands

White matter hyperintensities interfere with the course of white matter tracts, and disrupt connections between gray matter regions. This process might potentially underlie cognitive decline. In the large population-based Maastricht Study (n=5083), we found an association of lower processing speed scores with larger white matter hyperintensities and smaller total tract volumes in important processing speed related white matter tracts. These findings provide more insight into how white matter hyperintensities seem to influence the cognition-sensitive organization of white matter tracts.

0912



### Neurochemical alterations in the visual cortex of glaucoma patients

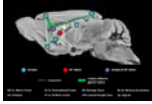
Ji Won Bang<sup>1</sup>, Anna M Chen<sup>1,2</sup>, Carlos Parra<sup>1</sup>, Gadi Wollstein<sup>1</sup>, Joel S Schuman<sup>1</sup>, and Kevin Chan<sup>1,3</sup>

<sup>1</sup>Department of Ophthalmology, New York University, New York, NY, United States, <sup>2</sup>Sackler Institute of Graduate Biomedical Sciences, New York University, New York, NY, United States, <sup>3</sup>Department of Radiology, New York University, New York, NY, United States



Glaucoma is considered to involve neurochemical alterations in the visual system. While the role of excitotoxicity in glaucoma remains controversial, we showed that the balance between glutamate, a main excitatory signal, and gamma-aminobutyric acid (GABA), a main inhibitory signal, is involved in glaucoma pathogenesis. We demonstrated that the visual cortex of glaucoma patients changes to an excitatory-dominant state and that this change is driven by reduced GABA. Additionally, we showed that visual field loss is associated with reduced N-acetyl-aspartate, a marker for neuronal integrity. Taken together, these findings suggest that neurochemical alterations may serve as informative markers for glaucoma.

0913



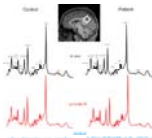
Vulnerable brain network in a mouse model of Huntington's disease revealed by gluCEST, magnetization transfer and anatomic imaging.

Jean-Baptiste Perot<sup>1,2</sup>, Clement M. Garin<sup>1,2</sup>, Salma Bougacha<sup>1,2,3,4</sup>, Alexandra Durr<sup>5,6</sup>, Marc Dhenain<sup>1,2</sup>, Sandrine Humbert<sup>7</sup>, Emmanuel Brouillet<sup>1,2</sup>, and Julien Flament<sup>1,2</sup>

<sup>1</sup>Molecular Imaging Research Center (MIRcen), Commissariat à l'Energie Atomique et aux Energies Alternatives (CEA), Fontenay-aux-Roses, France, <sup>2</sup>UMR 9199, Neurodegenerative Diseases Laboratory, Centre National de la Recherche Scientifique (CNRS), Université Paris-Sud, Université Paris-Saclay, Fontenay-aux-Roses, France, <sup>3</sup>Inserm UMR-S U1237, Normandie University, UNICAEN, GIP Cyceron, Caen, France, <sup>4</sup>Inserm U1077 Neuropsychologie et Imagerie de la mémoire Humaine, Normandie University, UNICAEN, EPHE, CHU de Caen, Caen, France, <sup>5</sup>Inserm UMR-S U1127, Institut du Cerveau et de la Moelle épinière (ICM), Sorbonne Université, Paris, France, <sup>6</sup>Département de génétique, Groupe Hospitalier Pitié-Salpêtrière, APHP, Paris, France, <sup>7</sup>Inserm U1216, Grenoble Institut des Neurosciences (GIN), Univ. Grenoble Alpes, Grenoble, France

Huntington's disease (HD) is an inherited neurodegenerative disease characterized by cognitive, motor and psychiatric symptoms. Despite tremendous efforts made during past years, there is a need for more predictive and functional biomarkers of disease pathogenesis and progression. In the present study, we developed a longitudinal and multimodal imaging protocol to elucidate HD pathogenesis in a mouse model of HD and to evaluate the potential of different biomarkers. Our approach combining volume, gluCEST and magnetization transfer imaging and automated brain segmentation revealed a brain network particularly vulnerable in this model.

0914



Metabolic and microstructural MPSII brain alteration revealed by multiparametric MR imaging and spectroscopy – a combined 3T and 7T study

Alena Svatkova<sup>1</sup>, Lenka Minarikova<sup>2</sup>, Petr Bednarik<sup>2</sup>, Verena Rosenmayr<sup>3</sup>, Gilbert Hangel<sup>2</sup>, Bernhard Strasser<sup>4</sup>, Lukas Hingerl<sup>2</sup>, Thomas Stulnig<sup>3</sup>, and Stephan Gruber<sup>2</sup>

<sup>1</sup>Department of Medicine III, Medical University of Vienna, Vienna, Austria, <sup>2</sup>High Field MR Centre, Department of Biomedical Imaging and Image-guided Therapy, Medical University of Vienna, Vienna, Austria, <sup>3</sup>Clinical Division for Endocrinology and Metabolism, Department of Medicine III, Medical University of Vienna, Vienna, Austria, <sup>4</sup>Athinoula A. Martinos Center for Biomedical Imaging, Boston, MA, United States

While glycosaminoglycan deposition in Mucopolysaccharidosis type II, a rare X-linked lysosomal storage disorder, unquestionably alters the brain, metabolic and microstructural MR markers have not been yet established. Thus, we utilized 3T diffusion MRI and fine-tuned semi-LASER MR spectroscopy as well as in-house developed 7T 3D-FID-MRS imaging to examine differences between seven MPSII and eight age-matched healthy males. Analyses revealed profound deficit in the supratentorial white matter consistent with de/dysmyelination on both diffusion and spectroscopy as well as decrease of neuronal population or hypometabolism measured as glutamate deficit in the posterior cingulate cortex, which is a critical hub of neurocognitive networks.

0915



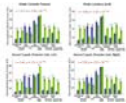
Neurocognitive and psychiatric features among primary Sjögren's syndrome patients: from clinical outcomes to brain MRI

Radjiv Goulabchand<sup>1,2,3</sup>, Veronica Ravano<sup>4,5,6</sup>, Mário João Fartaria<sup>4,5,6</sup>, Ricardo Corredor-Jerez<sup>4,5,6</sup>, Elodie Castille<sup>1,3</sup>, Sophie Navucet<sup>7</sup>, Alexandre Maria<sup>1,2,8</sup>, Alain Le Quellec<sup>1,2</sup>, Emmanuelle Le Bars<sup>9,10,11</sup>, Audrey Gabelle<sup>2,7,12</sup>, Philippe Guilpain<sup>1,3,8</sup>, Nicolas Menjot de Champfleu<sup>9,10</sup>, and Bénédicte Maréchal<sup>4,5,6</sup>

<sup>1</sup>Département de médecine interne et maladies multi-organiques, Hôpital Saint Eloi, CHRU Montpellier, Montpellier, France, <sup>2</sup>Médecine interne, CHU de Nîmes, Nîmes, France, <sup>3</sup>Faculté de médecine, Université de Montpellier, Montpellier, France, <sup>4</sup>Advanced Clinical Imaging Technology, Siemens Healthcare AG, Lausanne, Switzerland, <sup>5</sup>Department of Radiology, Lausanne University Hospital and University of Lausanne, Lausanne, Switzerland, <sup>6</sup>LTS 5, École Polytechnique Fédérale de Lausanne (EPFL), Lausanne, Switzerland, <sup>7</sup>Centre Mémoire de Ressources et de Recherche, Hôpital Gui De Chauliac, CHRU Montpellier, Montpellier, France, <sup>8</sup>IRMB, INSERM, CHU Montpellier, Montpellier, France, <sup>9</sup>Département d'imagerie médicale, Hôpital Gui de Chauliac, CHRU Montpellier, Montpellier, France, <sup>10</sup>Institut d'Imagerie Fonctionnelle Humaine (I2FH), Hôpital Gui de Chauliac, Centre Hospitalier Régional Universitaire de Montpellier, Montpellier, France, <sup>11</sup>Laboratoire Charles Coulomb, CNRS UMR 5221, Université de Montpellier, Montpellier, France, <sup>12</sup>Laboratoire de Biochimie-Protéomique Clinique - IRMB - CCBHM - Inserm U1183, CHU Montpellier, Hôpital St-Eloi - Université Montpellier, Montpellier, France

To date, neuropsychiatric profiles in Sjögren's syndrome patients are not explained by the immunological profile or clinical symptoms. Consequently, there is a lack of biomarkers potentially characterizing such profiles for this rare autoimmune disease. Our goal was to investigate the potential of MRI-based features to objectively explain fatigue, depression and cognitive complaints in twenty-nine patients with primary Sjögren's syndrome. Specifically, we explored features from automated brain morphometry and brain lesion segmentation as potential imaging biomarkers. Z-score differences in certain brain structures (thalamus, corpus callosum, ventricles, and insula) were found, suggesting an association between MRI-based biomarkers and patient's neuropsychiatric profiles.

0916



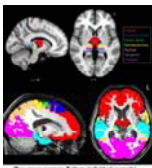
Gait - related white matter tracts damage in idiopathic normal pressure hydrocephalus

shuai xu<sup>1</sup>, ye yao<sup>2</sup>, jing ding<sup>3</sup>, and he wang<sup>\*4,5</sup>

<sup>1</sup>Fudan University, Shanghai, China, <sup>2</sup>School of Public Health, Fudan University, Shanghai, China, <sup>3</sup>Department of Neurology, Zhongshan Hospital, Fudan University, Shanghai, China, <sup>4</sup>Institute of Science and Technology for Brain-Inspired Intelligence, Fudan University, Shanghai, China, <sup>5</sup>Human Phenome Institute, Fudan University, shanghai, China

Grouping based on white matter hyperactivities (WMH) of each white matter tract, 15 idiopathic normal pressure hydrocephalus (iNPH) patients' 10 gait index were compared by double sample t test. The results showed some white matter tracts with strongest gait index relationships located in motor and sensory pathways including middle cerebellar peduncle (MCP), left medial lemniscus, left posterior limb of internal capsule and right posterior limb of internal capsule.

0917



Subcortical abnormality reveal disease specific changes in amyotrophic lateral sclerosis

Sicong Tu<sup>1,2</sup>, Matthew Kiernan<sup>1</sup>, and Martin Turner<sup>2</sup>

<sup>1</sup>Brain and Mind Centre, The University of Sydney, Sydney, Australia, <sup>2</sup>Nuffield Department of Clinical Neuroscience, University of Oxford, Oxford, United Kingdom

Amyotrophic lateral sclerosis (ALS) is a rapidly progressive neurodegenerative condition affecting the motor system, but increasingly recognised as a multi-system disease. We present two studies that highlight disease specific patterns of abnormality in the thalamus and corpus callosum that suggest regional variation in neural relay structures may be promising markers of disease progression in ALS.



A correlation analysis between DTI/DKI derived metrics and metabolite levels in the brain of HIV+ individuals

Teddy Salan<sup>1</sup>, Sameer Vyas<sup>2</sup>, Paramjeet Singh<sup>2</sup>, Mahendra Kumar<sup>3</sup>, Sulaiman Sheriff<sup>1</sup>, and Varan Govind<sup>1</sup>



<sup>1</sup>Radiology, University of Miami, Miami, FL, United States, <sup>2</sup>Postgraduate Institute for Medical Education & Research, Chandigarh, India, <sup>3</sup>Psychiatry and Behavioral Sciences, University of Miami, Miami, FL, United States

Several studies have focused on diffusion tensor imaging (DTI) as marker for structural damage in the brain due to infection from human immunodeficiency virus (HIV). However, few have associated the findings from diffusion kurtosis imaging (DKI) and magnetic resonance spectroscopic imaging (MRSI) measures. In this work, we correlate measures of DTI and DKI with MRSI in order to evaluate associations between structural alterations and changes in metabolite concentrations within the brain of HIV individuals.

## Oral

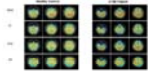
### Neurodegeneration 2 - Imaging & Spectroscopy of Traumatic Brain Injury

Wednesday Parallel 2 Live Q&A

Wednesday 15:15 - 16:00 UTC

Moderators: Rebecca Feldman

0919



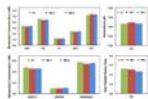
#### Altered neurometabolic changes in acute mild traumatic brain injury patients: a SPICE study

Tianyao Wang<sup>1</sup>, Jialin Hu<sup>2</sup>, Danni Wang<sup>2</sup>, Yujie Hu<sup>2</sup>, Jiahua Sun<sup>3</sup>, Jun Liu<sup>1</sup>, Yudu Li<sup>4,5</sup>, Rong Guo<sup>4,5</sup>, Yibo Zhao<sup>4,5</sup>, Ziyu Meng<sup>2,4</sup>, Zhipei Liang<sup>4,5</sup>, and Yao li<sup>2,6</sup>

<sup>1</sup>Radiology department, The Fifth People's Hospital of Shanghai, Shanghai, China, <sup>2</sup>Institute for Medical Imaging Technology, School of Biomedical Engineering, Shanghai Jiao Tong University, Shanghai, China, <sup>3</sup>Neurosurgery department, The Fifth People's Hospital of Shanghai, Shanghai, China, <sup>4</sup>Beckman Institute for Advanced Science and Technology, University of Illinois at Urbana-Champaign, Urbana, IL, United States, <sup>5</sup>Department of Electrical and Computer Engineering, University of Illinois at Urbana-Champaign, Urbana, IL, United States, <sup>6</sup>Med-X Research Institute, Shanghai Jiao Tong University, Shanghai, China

Mild traumatic brain injury (mTBI) is the most prevalent form of brain injury but the underlying physiological mechanisms are still not fully understood. MRSI has long been recognized as a potentially powerful tool for detection of neurometabolic alterations induced by TBI but most existing studies are limited by low resolution. In this study, we used a 3D high-resolution MRSI technique, known as SPICE, to study neurometabolic alterations in acute mTBI patients. Our experimental results showed various metabolic changes in different areas of patients, which lay a foundation for further investigation to gain new insights into the pathophysiology underlying acute mTBI.

0920



#### Quantitative <sup>31</sup>P MRS Assessment of Neurometabolic Derangement in Pediatric Concussion

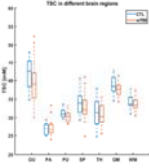
Xiao-Hong Zhu<sup>1</sup>, Byeong-Yeul Lee<sup>1</sup>, Katherine Ingram<sup>2</sup>, Wei Chen<sup>1</sup>, Robert Doss<sup>2,3</sup>, and Joseph Petronio<sup>2</sup>

<sup>1</sup>CMRR, Department of Radiology, University of Minnesota, Minneapolis, MN, United States, <sup>2</sup>Children's Minnesota Neuroscience Institute, St. Paul, MN, United States, <sup>3</sup>Department of Neurology, University of Minnesota, Minneapolis, MN, United States

Abnormal changes in brain metabolism and its role in pediatric concussion have not been well studied. We employed <sup>31</sup>P MRS technique at 7T to assess the neurometabolic alteration in children with concussion. Phosphorous metabolites concentrations and other key physiological parameters were measured in patient and control cohorts. Metabolic differences between healthy and concussed brains were detected at two time points after the injury. We also found that mild head trauma reduced the age-dependences of high-energy phosphates and NAD contents in the developing brain, and it took much longer than clinically defined "recovery time" to fully restore such relationship.

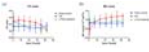
#### Quantitative <sup>23</sup>Na MRI of mild traumatic brain injury: Initial findings

Teresa Gerhalter<sup>1</sup>, Rosemary Peralta<sup>1</sup>, Mickael Tordjman<sup>1</sup>, Julia Zabludovsky<sup>1</sup>, Seena Dehkharghani<sup>1</sup>, Alejandro Zarate<sup>2</sup>, Soo-Min Shin<sup>3</sup>, Ilya Aylyarov<sup>3</sup>, Tamara Bushnick<sup>2</sup>, Jonathan M. Silver<sup>4</sup>, Stephen P. Wall<sup>3</sup>, Brian S. Im<sup>2</sup>, Ryan Brown<sup>1</sup>, Guillaume Madelin<sup>1</sup>, and Ivan I. Kirov<sup>1</sup>



<sup>1</sup>Center for Biomedical Imaging, Department of Radiology, New York University School of Medicine, New York, NY, United States, <sup>2</sup>Department of Rehabilitation Medicine, New York University School of Medicine, New York, NY, United States, <sup>3</sup>Ronald O. Perelman Department of Emergency Medicine, New York University School of Medicine, New York, NY, United States, <sup>4</sup>Department of Psychiatry, New York University School of Medicine, New York, NY, United States

In this quantitative sodium MRI study, 24 mild traumatic brain injury (mTBI) and 9 controls were scanned at 3 T. Total sodium content (TSC) was calculated in five different subcortical regions, as well as in global grey and white matter. TSC in mTBI did not differ statistically from controls for the examined regions. Patients with findings on conventional <sup>1</sup>H imaging (e.g. lesions, microhemorrhages) did not differ from patients without such findings in their TSC. More patients and controls are being recruited to strengthen the statistical power of these comparisons.

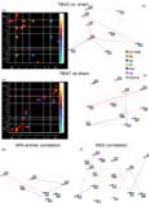


The usefulness of diffusion tensor imaging in evaluating the neuroprotective effect of LITUS to moderate traumatic brain injury with rat model

Zheng Tao<sup>1</sup>, Du Juan<sup>1</sup>, Yuan Yi<sup>2</sup>, Wu Shuo<sup>1</sup>, Wang Zhanqiu<sup>1</sup>, Liu Defeng<sup>1</sup>, Shi Qinglei<sup>3</sup>, Wang Xiaohan<sup>1</sup>, and Liu Lanxiang<sup>1</sup>

<sup>1</sup>MRI, Qinhuangdao Municipal No. 1 Hospital, Qinhuangdao, China, <sup>2</sup>Institute of Electrical Engineering, Yanshan University, Qinhuangdao, China, <sup>3</sup>Siemens Healthcare, MR Scientific Marketing, Beijing, China

In this study, we verified the feasibility of FA and MD values in evaluating the neuro therapeutic effect of LITUS with rat model. The neuro therapeutic effect of LITUS was attributed to promoting blood flow and the protein expression of BDNF.

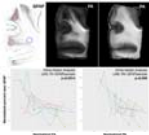


Repercussions of a single concussion in the mouse brain: insights from functional and structural Magnetic Resonance Imaging.

Xuan Vinh To<sup>1</sup> and Fatima A. Nasrallah<sup>1,2</sup>

<sup>1</sup>The Queensland Brain Institute, The University of Queensland, Australia, Queensland, Australia, <sup>2</sup>The Centre for Advanced Imaging, The University of Queensland, Australia, St Lucia, Australia

Resting-state functional connectivity in mouse model of concussion detected a process of functional adaptation at day 2 post-injury in compensation for white matter injuries: increased connectivity among the Default Mode and Hippocampal Networks and decreased or negative connectivity to the Midbrain. These adaptations maintained cognition and spatial learning but negatively affected the motor and balance functions. The functional adaptations were short-term: at day 7, increased cellularity were detected by Diffusion MRI in grey matter regions involved with day 2 functional adaptations.



Correspondence of diffusion tensor and propagator metrics with quantitative histologic outcomes in chronic traumatic encephalopathy

Mihika Gangolli<sup>1</sup>, Elizabeth Hutchinson<sup>2</sup>, Ann McKee<sup>3</sup>, Joong Hee Kim<sup>1</sup>, Sinisa Pajevic<sup>1</sup>, and Peter Basser<sup>1</sup>

<sup>1</sup>National Institutes of Health, Bethesda, MD, United States, <sup>2</sup>BME, University of Arizona, Tucson, AZ, United States, <sup>3</sup>Boston University, Boston, MA, United States

Diffusion tensor and propagator metrics are compared directly in post-mortem cortex specimens from humans with chronic traumatic encephalopathy. Significant correlation was found between fractional anisotropy and non-Gaussianity with pTau staining in the sulcal depths. Additionally, GFAP staining of astrocytosis in the white matter was significantly correlated with Trace, FA, return-to-origin probability and propagator anisotropy. Cluster-based methods were also applied to explore the multivariate diffusion signature associated with CTE pathology. These findings suggest that diffusion metrics may be sensitive to CTE-related pathology.

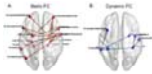
0925

Ultra-early versus early magnetic resonance imaging for mild traumatic brain injury: a CENTER-TBI Study  
Sophie Richter<sup>1</sup>, Stefan Winzeck<sup>1</sup>, Evgenios Kornaropoulos<sup>1</sup>, Marta Correia<sup>2</sup>, Jan Verheyden<sup>3</sup>, Thijs Vande Vyvere<sup>3</sup>, Guy Williams<sup>4</sup>, David Menon<sup>1</sup>, and Virginia Newcombe<sup>1</sup>

<sup>1</sup>University Division of Anaesthesia, University of Cambridge, Cambridge, United Kingdom, <sup>2</sup>MRC Cognition and Brain Sciences Unit, University of Cambridge, Cambridge, United Kingdom, <sup>3</sup>Icometrix, Leuven, Belgium, <sup>4</sup>Wolfson Brain Imaging Center, University of Cambridge, Cambridge, United Kingdom

Traumatic brain injury (TBI) is a major public health problem and is a leading cause of neurodisability. This study demonstrates the dynamic changes that occurs after mTBI as defined using conventional and advanced MRI including diffusion tensor imaging.

0926



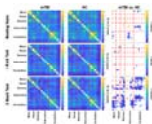
Abnormal static and dynamic functional connectivity in active professional fighters with repetitive head trauma: A resting-state fMRI study

Xiaowei Zhuang<sup>1</sup>, Virendra Mishra<sup>1</sup>, Zhengshi Yang<sup>1</sup>, Karthik Sreenivasan<sup>1</sup>, Sarah J Banks<sup>2</sup>, Lauren Bennett<sup>3</sup>, Bernick Charles<sup>1</sup>, and Dietmar Cordes<sup>1,4</sup>

<sup>1</sup>Lou Ruvo Center for Brain Health, Cleveland Clinic, Las Vegas, NV, United States, <sup>2</sup>Department of Neuroscience, University of California, San Diego, La Jolla, CA, United States, <sup>3</sup>Neuroscience Institute, Hoag Hospital, Irvine, CA, United States, <sup>4</sup>University of Colorado, Boulder, Boulder, CO, United States

Both static and dynamic functional connectivity differences between cognitively impaired and non-impaired active professional fighters were first explored. Significant decreased static functional connections and trend-level increased dynamic functional connections among regions involved in memory and executive functions were found in cognitively impaired fighters, which adds brain functional reorganizations to previously observed structural damages in brain deficits related to repetitive head trauma. We further demonstrated that both static and dynamic functional connectivity were sensitive to cognitive declines in this fighter's cohort, as both static and dynamic functional features can reliably predict cognitive impairment status in fighters.

0927



Association of Brain Functional Connectivity with Dizziness is Modulated by Executive Functions in Mild Traumatic Brain Injury

Jyun-Ru Chen<sup>1</sup>, Li-Chun Hsieh<sup>2,3,4</sup>, Cheng-Yu Chen<sup>2,3,4</sup>, and Chia-Feng Lu<sup>1</sup>

<sup>1</sup>Department of Biomedical Imaging and Radiological Sciences, National Yang Ming University, Taipei, Taiwan, <sup>2</sup>Department of Medical Imaging, Taipei Medical University Hospital, Taipei, Taiwan, <sup>3</sup>Department of Radiology, School of Medicine, College of Medicine, Taipei Medical University, Taipei, Taiwan, <sup>4</sup>Translational Imaging Research Center, Taipei Medical University Hospital, Taipei, Taiwan

Dizziness is one of the frequent post-concussion symptoms, however neuroimaging evidence that supports symptom occurrence was less explored. This study started with the investigation of modulation effects from executive functions on functional connectivity (FC) between brain regions related to dizziness and balance followed by the correlation analysis to identify the imaging biomarker for elucidating the dizziness symptoms after mTBI.

## Oral - Power Pitch

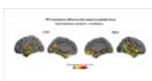
### Neurodegeneration 2 - Epilepsy

Wednesday Parallel 2 Live Q&A

Wednesday 15:15 - 16:00 UTC

Moderators: Thijs Dhollander & Claire Kelly

0928



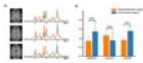
Extratemporal cortical morphological changes and hypometabolism revealed in radiological MRI-negative temporal lobe epilepsy

Julia Pia Simon<sup>1</sup>, Ben A. Duffy<sup>1</sup>, Yan Li<sup>2</sup>, Arthur W. Toga<sup>1</sup>, Wolfgang G. Muhlhofer<sup>3</sup>, Robert C. Knowlton<sup>2</sup>, and Hosung Kim<sup>1</sup>

<sup>1</sup>University of Southern California, Los Angeles, CA, United States, <sup>2</sup>Neurology and UCSF Weill Institute for Neurosciences, San Francisco, CA, United States, <sup>3</sup>University of Alabama at Birmingham Epilepsy Center, Birmingham, AL, United States

Radiological MRI-negative temporal lobe epilepsy (TLE) is a common, but challenging subtype for surgical treatment. Compared to MRI-positive cases, these patients often require invasive EEG for localization that may also involve extratemporal regions. Furthermore, these cases entail a lower likelihood of seizure-free surgical outcome. To better understand this important group, we studied cortical surface features of MRI and FDG-PET to relate occult extratemporal damage to epilepsy localization and surgical outcome prediction. Bilateral cortical morphological changes were found. FDG-PET hypometabolism was lateralized in the hemisphere ipsilateral to seizure focus. Extratemporal and bilateral hypometabolism tended to be associated with poor surgical outcome.

0929



### Simultaneous <sup>18</sup>F-FDG-PET and <sup>1</sup>H-MRSI Metabolic Imaging in Epilepsy Patients: A Feasibility Study

Hui Huang<sup>1</sup>, Miao Zhang<sup>2</sup>, Rong Guo<sup>3,4</sup>, Yudu Li<sup>3,4</sup>, Yibo Zhao<sup>3,4</sup>, Jialin Hu<sup>1</sup>, Hongping Meng<sup>2</sup>, Xinyun Huang<sup>2</sup>, Xiaozhu Lin<sup>2</sup>, Wei Liu<sup>5</sup>, Biao Li<sup>2</sup>, Bomin Sun<sup>5</sup>, Yao Li<sup>1</sup>, Zhi-Pei Liang<sup>3,4</sup>, and Jie Luo<sup>1</sup>

<sup>1</sup>Institute of Medical Imaging Technology, School of Biomedical Engineering, Shanghai Jiao Tong University, Shanghai, China, <sup>2</sup>Department of Nuclear Medicine, Ruijin Hospital, Shanghai Jiao Tong University School of Medicine, Shanghai, China, <sup>3</sup>Department of Electrical and Computer Engineering, University of Illinois at Urbana Champaign, Urbana, IL, United States, <sup>4</sup>Beckman Institute for Advanced Sciences and Technology, University of Illinois at Urbana Champaign, Urbana, IL, United States, <sup>5</sup>Department of Functional Neurosurgery, Ruijin Hospital, Shanghai Jiao Tong University School of Medicine, Shanghai, China

PET and MRSI could provide metabolic information of the epileptogenic zone, which could add value to presurgical planning of epilepsy patients. This study investigated the feasibility of simultaneous high-resolution MRSI and <sup>18</sup>F-FDG-PET for whole brain imaging in epilepsy patients, and studied the correlation between metabolic changes found in MRSI and hypometabolism found in FDG-PET. Our experimental results showed a decrease in NAA and an increase in Cho, concomitant with low FDG uptake.

0930



### Deep Learning Reconstruction Method for Improved Visualization of Hippocampal Anatomical Structures

Patrick Quarterman<sup>1</sup>, Angela Lignelli<sup>2</sup>, Marc Lebel<sup>3</sup>, and Sachin Jambawalikar<sup>4</sup>

<sup>1</sup>GE Healthcare, New York, NY, United States, <sup>2</sup>Radiology, Columbia University, New York, NY, United States, <sup>3</sup>GE Healthcare, Calgary, AB, Canada, <sup>4</sup>Columbia University, New York, NY, United States

The purpose of this study was to determine if deep learning reconstruction (DLRecon) method to reduce image noise could lead to improvement in in-vivo anatomical detail of the hippocampus structures without substantial increase in scan/exam time on a clinical 3T system. Evaluation of this new reconstruction technique was performed on a group of 5 volunteers with results indicating that higher resolution scans compared to current seizure protocol was free of imaging noise and led to higher confidence in identifying hippocampal key anatomical structures and temporal lobes.

0931

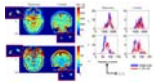
### White matter microstructure characterisation in left and right temporal lobe epilepsy (TLE) using TBSS

Nicolò Rolandi<sup>1</sup>, Fulvia Palesi<sup>1</sup>, Francesco Padelli<sup>2</sup>, Isabella Giachetti<sup>2</sup>, Domenico Aquino<sup>2</sup>, Giuseppe Didato<sup>3</sup>, Elio Maccagnano<sup>3</sup>, Paul Summers<sup>4</sup>, Giancarlo Germani<sup>4</sup>, Claudia AM Gandini Wheeler-Kingshott<sup>1,5,6</sup>, and Paolo Vitali<sup>4</sup>

<sup>1</sup>Department of Brain and Behavioral Science, University of Pavia, Pavia, Italy, <sup>2</sup>Fondazione I.R.C.C.S. Istituto Neurologico Carlo Besta, Milan, Italy, <sup>3</sup>Neuroradiology, Fondazione I.R.C.C.S. Istituto Neurologico Carlo Besta, Milan, Italy, <sup>4</sup>Neuroradiology Unit, Brain MRI 3T Research Center, IRCCS Mondino Foundation, Pavia, Italy, <sup>5</sup>Department of Neuroinflammation, UCL Queen Square Institute of Neurology, Faculty of Brain Sciences, University College London, NMR Research Unit, Queen Square MS Centre, London, United Kingdom, <sup>6</sup>Brain MRI 3T Research Center, IRCCS Mondino Foundation, Pavia, Italy

Tract-based spatial statistics investigations of temporal lobe epilepsy (TLE) have been using standard diffusion metrics, without distinguishing patients according to the lateralization of their epileptogenic zone. The aim of this study is to further our knowledge by identifying specific patterns of alteration in left and right TLE patients using diffusion kurtosis imaging and NODDI parameter maps. Our findings demonstrate the presence of specific patterns of white matter alterations, with the left TLE more widely affecting both cerebral and cerebellar regions. These results support the need to consider patients separately, according to the side of their pathology.

0932



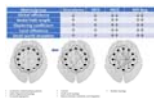
Visualization enhancement and quantitative analysis of relaxation time in medial temporal lobe epilepsy based on 3D high-resolution MRF

Xiaozhi Cao<sup>1,2,3</sup>, Kang Wang<sup>4</sup>, Congyu Liao<sup>2,3</sup>, Dengchang Wu<sup>4</sup>, Qing Li<sup>1</sup>, Ziyang Chen<sup>1</sup>, Jun Li<sup>1</sup>, Huihui Ye<sup>1</sup>, Hongjian He<sup>1</sup>, and Jianhui Zhong<sup>1</sup>

<sup>1</sup>Center for Brain Imaging Science and Technology, Department of Biomedical Engineering, Zhejiang University, Hangzhou, China, <sup>2</sup>Athinoula A. Martinos Center for Biomedical Imaging, Massachusetts General Hospital, Charlestown, MA, United States, <sup>3</sup>Department of Radiology, Harvard Medical School, Charlestown, MA, United States, <sup>4</sup>Department of Neurology, the First Affiliated Hospital, School of Medicine, Zhejiang University, Hangzhou, China

We propose to use a 3D MRF technique with multi-axis spiral projection acquisition to achieve 3D high-resolution whole-brain quantitative imaging for patients with MTLE. Isotropic 1-mm resolution relaxivity maps were achieved within 5 minutes. By incorporating Freesurfer's automatic subcortical segmentation, a whole-brain subcortical segmentation was obtained, enabling feasible and subjective quantitative analysis for each substructure. Additionally, volume information of the substructure was obtained during the process.

0933



CORTICAL THICKNESS COVARIANCE STRUCTURAL NETWORKS IN "FOCAL" EPILEPSY

Karthik Kulanthaivelu<sup>1</sup>, Kiran Raj V<sup>1</sup>, Raghavendra Kenchaiah<sup>2</sup>, Jitender Saini<sup>1</sup>, Rose Dawn Bharath<sup>1</sup>, and Sanjib Sinha<sup>2</sup>

<sup>1</sup>Department of Neuroimaging and Interventional Radiology, National Institute of Mental Health and Neurosciences, Bengaluru, India, <sup>2</sup>Department of Neurology, National Institute of Mental Health and Neurosciences, Bengaluru, India

"Focal" epilepsy is a network aberration. Network characteristics in focal epilepsy due to calcified Neurocysticercal granuloma have not been elucidated. Forty-two patients of focal epilepsy with MRI evidence of either calcified granuloma, malformation of cortical development, mesial temporal sclerosis, or no imaging abnormality were included. Group-level Cortical thickness covariance networks were generated and compared. Focal epilepsy patients (including those with calcific granuloma) had significantly reduced network global efficiency and higher nodal characteristic path length/ Clustering coefficient/ Nodal local efficiency ( $p < 0.05$ ). Networks in focal epilepsy ("including those due to calcific granuloma") have higher segregation and lesser integration.

0934

Radiomics Features of Hippocampal Regions in Conventional and Diffusion Tensor Imagings can Differentiate Temporal Lobe Epilepsy Patients

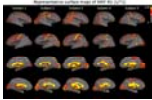
Yae Won Park<sup>1</sup>, Dongmin Choi<sup>2</sup>, Kyunghwa Han<sup>1</sup>, Sung Soo Ahn<sup>1</sup>, Hwiyoung Kim<sup>1</sup>, and Hyang Woon Lee<sup>3</sup>



<sup>1</sup>Yonsei University College of Medicine, Seoul, Republic of Korea, <sup>2</sup>Department of Computer Science, Yonsei University, Seoul, Republic of Korea, <sup>3</sup>Department of Neurology, Ewha Womans University College of Medicine, Seoul, Republic of Korea

A total of 92 subjects(66 TLE [35 right and 31 left] and 26 healthy controls) were allocated to training(n=66) and test(n=26) sets. Radiomics features (n=558) from the bilateral hippocampi were extracted from T1WI and DTI. Machine learning models were trained. Identical processes were performed to differentiate right TLE from HC and left TLE from HC. The radiomics model in test set showed better performance than hippocampal volume for identifying TLE (AUC 0.82 vs. AUC 0.62, P=0.08). Radiomics models of both subgroups showed better performance than those of hippocampal volume(AUC 0.76 vs. AUC 0.54 [P=0.12] and AUC 0.95 vs 0.68 [P=0.04]).

0935



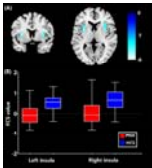
### Using High-resolution 3D MR Fingerprinting for Characterization of Focal Cortical Dysplasia

Joon Yul Choi<sup>1</sup>, Rasim Boyacioglu<sup>2</sup>, Stephen Jones<sup>3</sup>, Ken Sakaie<sup>3</sup>, Ingmar Blümcke<sup>1,4</sup>, Imad Najm<sup>1</sup>, Mark Griswold<sup>2</sup>, Dan Ma<sup>5</sup>, and Zhong Irene Wang<sup>1</sup>

<sup>1</sup>Epilepsy Center / Neurological Institute, Cleveland Clinic, Cleveland, OH, United States, <sup>2</sup>Radiology, Case Western Reserve University, Cleveland, OH, United States, <sup>3</sup>Imaging Institute, Cleveland Clinic, Cleveland, OH, United States, <sup>4</sup>Neuropathology, University of Erlangen, Erlangen, Germany, <sup>5</sup>Biomedical Engineering, Case Western Reserve University, Cleveland, OH, United States

We investigate in this study quantitative T1 and T2 values as potential biomarkers of tissue properties in epilepsy patients with focal cortical dysplasia (FCD) using a novel high-resolution 3D magnetic resonance fingerprinting (MRF) technique. We first investigated the quantitative T1 and T2 values in various Brodmann areas to verify the sensitivity of MRF in probing tissue properties of the human cortex. We then investigated the MRF T1 and T2 values in different subtypes of FCD lesions, which were higher than their corresponding cortical regions in the controls.

0936



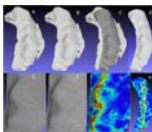
### Resting-state functional connectivity alterations in periventricular nodular heterotopia related epilepsy

Xinyu Hu<sup>1</sup>, Wenyu Liu<sup>2</sup>, Dong Zhou<sup>2</sup>, Qiyong Gong<sup>1</sup>, and Xiaoqi Huang<sup>1</sup>

<sup>1</sup>Huaxi MR Research Center (HMRRC), West China Hospital of Sichuan University, Chengdu, China, <sup>2</sup>Department of Neurology, West China Hospital of Sichuan University, Chengdu, China

We performed the first resting-state fMRI study integrating both whole-brain functional connectivity (FC) and seed-based FC analyses to explore the network-level neural function alterations in patients with periventricular nodular heterotopia (PNH). Our findings (i) identified lower functional connectivity strength (FCS, an index of whole-brain connectivity) in bilateral insula, higher FC in the precuneus and lower FC in the anterior cingulate cortex/medial prefrontal cortex and cerebellum networks in PNH patients and (ii) demonstrated that the significant insular hypoactivation represented the cortical hub of the whole-brain networks in PNH, which might be of clinical significance in predicting disability progression of PNH.

0937



### Quantifying Hippocampal Dentation in Epilepsy: a comparison of absolute mean curvature versus visual inspection and their memory correlates.

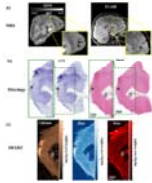
Lawrence Ver Hoef<sup>1,2</sup>, Mike Zhang<sup>3</sup>, and Anandh Kilpattu Ramaniharan<sup>3</sup>

<sup>1</sup>Neurology, University of Alabama at Birmingham, Birmingham, AL, United States, <sup>2</sup>Birmingham VA Medical Center, Birmingham, AL, United States, <sup>3</sup>University of Alabama at Birmingham, Birmingham, AL, United States



Hippocampal dentation (HD) is a morphologic feature of the human hippocampus that has been recently described and has been shown to correlate with aspects of verbal and visual memory. It varies dramatically across healthy individuals and can be affected by diseases such as epilepsy. We demonstrate a method to extract ultra-high-resolution surface contours from common MPRAGE images. We also propose a method based on absolute mean curvature to quantify HD and compare that to visual inspection in a cohort of temporal lobe epilepsy patients. Finally, we examine correlations between HD and measures of verbal and visual memory across methods.

0938



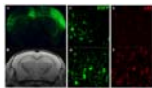
#### Quantitative susceptibility mapping reveals abnormal zinc, calcium and iron levels in focal cortical dysplasia lesions

Sara Lorio<sup>1</sup>, Po-Wah So<sup>1</sup>, Jan Sedlacik<sup>1</sup>, Derek Li<sup>2</sup>, Emma Dixon<sup>3</sup>, Sophie Adler<sup>3</sup>, Harold G. Parkers<sup>1</sup>, Helen J. Cross<sup>3</sup>, Torsten Baldeweg<sup>3</sup>, Thomas Jacques<sup>3</sup>, Karin Shmueli<sup>3</sup>, and David Carmichael<sup>1,3</sup>

<sup>1</sup>King's College London, London, United Kingdom, <sup>2</sup>UCL, London, United Kingdom, <sup>3</sup>UCL, LONDON, United Kingdom

We estimated quantitative susceptibility maps (QSM) in 19 children with histologically confirmed focal cortical dysplasia (FCD), a frequent cause of drug-resistant epilepsy. QSM allowed measurement of cortical and sub-cortical layered structure and its alteration in FCD lesions. Moreover, QSM was sensitive to abnormal deposits of calcium, zinc, and iron, which were validated using X-ray fluorescence in brain tissue specimens available following surgical treatment. QSM could provide a non-invasive biomarker of cortical tissue changes in epilepsy and could be used to determine alterations in mineral deposits in different brain disorders.

0939



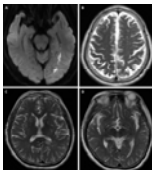
#### Assessing Focal Cortical Dysplasia Using Advanced Diffusion Imaging Sequences

Boyu Zhang<sup>1</sup>, Shaoping Zhong<sup>2</sup>, Yuwen Zhang<sup>1</sup>, Qianfeng Wang<sup>1</sup>, Jing Ding<sup>2</sup>, and He Wang<sup>1,3</sup>

<sup>1</sup>Institute of Science and Technology for Brain-Inspired Intelligence, Fudan University, Shanghai, China, <sup>2</sup>Department of Neurology, Zhongshan Hospital, Fudan University, Shanghai, China, <sup>3</sup>Human Phenome Institute, Fudan University, Shanghai, China

Focal cortical dysplasia (FCD) are neurodevelopmental disorders characterized by localized cortical malformation that is highly associated with the drug-resistant epilepsy. In this study, we examined the advanced diffusion MR imaging-neurite orientation dispersion and density imaging (NODDI) in the FCD mice model. The orientation dispersion index (ODI) that represents the dispersion of neurite is significantly higher in the FCD group compared with the control group which are compatible with the pathological observation. Meanwhile, no significant differences are observed in conventional DTI measurements FA and MD indicating that NODDI is more sensitive in detecting FCD lesion.

0940



#### Significance of Perivascular Spaces in Acute Ischemic Stroke and its Predictions of Epileptogenesis

Nian Yu<sup>1,2,3</sup>, Benjamin Sinclair<sup>4,5</sup>, Lina Maria Garcia Posada<sup>6</sup>, Ben Chen<sup>4</sup>, Qing Di<sup>1</sup>, Xingjian Lin<sup>1</sup>, Qingling Huang<sup>7</sup>, Scott Kolbe<sup>4</sup>, Patrick Kwan<sup>2,4,5,8</sup>, and Meng Law<sup>4,6</sup>

<sup>1</sup>Department of Neurology, The Nanjing Brain Hospital Affiliated to Nanjing Medical University, Nanjing, China, <sup>2</sup>Department of Neurology, Royal Melbourne Hospital, Melbourne, Australia, <sup>3</sup>Department of Radiology, The Nanjing Brain Hospital Affiliated to Nanjing Medical University, Melbourne, China, <sup>4</sup>Department of Neuroscience, Monash University, Melbourne, Australia, <sup>5</sup>Department of Neurology, Alfred Hospital, Melbourne, Australia, <sup>6</sup>Department of Radiology, Alfred Hospital, Melbourne, Australia, <sup>7</sup>Department of Radiology, The Nanjing Brain Hospital Affiliated to Nanjing Medical University, Nanjing, China, <sup>8</sup>Department of Medicine, University of Melbourne, Melbourne, Australia

Around 10% of patients with stroke go on to develop epilepsy, however, imaging biomarkers for post-stroke epilepsy (PSE) are lacking. Perivascular spaces (PVS) are small interstitial fluid filled spaces lining the blood vessels which have a role in waste clearance in the brain. They have been found to be abnormal in epilepsy, and here we investigate whether they could serve as an early predictor of PSE. We found that the overall number and scores of enlarged PVSs were not associated with PSE, but the inter-hemispheric asymmetry was an independently associated biomarker.

## Oral

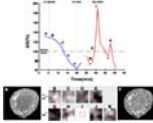
### MRI of the Kidneys - Kidney

Wednesday Parallel 3 Live Q&A

Wednesday 15:15 - 16:00 UTC

Moderators: Pim Pullens

0941



#### Single Nephron Glomerular Filtration and Macromolecular Dynamics in Perfused Kidneys using MRI

Edwin J. Baldelomar<sup>1</sup>, Scott C. Beeman<sup>2</sup>, Jennifer R. Charlton<sup>3</sup>, and Kevin M. Bennett<sup>4</sup>

<sup>1</sup>Radiology, Washington University in St. Louis, St. Louis, MO, United States, <sup>2</sup>Biomedical Engineering, Arizona State University, Tempe, AZ, United States, <sup>3</sup>Pediatrics, University of Virginia, Charlottesville, VA, United States, <sup>4</sup>Radiology, Washington University in St. Louis, Saint Louis, MO, United States

In this work, we use contrast agents cationic ferritin and gadolinium-DTPA (Gd-DTPA) to visualize dynamics of macromolecules and freely filtering particles in individual nephrons throughout entire perfused rat kidneys. Further, we also look at dynamics in kidneys that received a vasoconstriction agent, angiotension II (AngII). Voxel time courses were fitted with a bi-exponential model for each experiment (Experiment I, CF infusion and Experiment II, Gd-DTPA bolus). From fitting we assess CF uptake rates and measure single nephron glomerular filtration rate (snGFR). CF uptake rates and values of snGFR were mapped spatially and observed to be heterogeneously distributed throughout the kidney.

0942



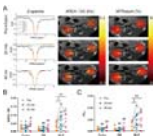
#### MRI Assessment of Renal Tubular Volume Fraction with an IVIM-NNLS Approach Under Increased Tubular Pressure

Joao Santos Periquito<sup>1</sup>, Kathleen Cantow<sup>2</sup>, Thomas Gladysz<sup>3</sup>, Bert Flemming<sup>2</sup>, Dirk Grosenick<sup>3</sup>, Erdmann Seeliger<sup>2</sup>, Thoralf Niendorf<sup>1</sup>, and Andreas Pohlmann<sup>1</sup>

<sup>1</sup>Max Delbrueck Center for Molecular Medicine, Berlin, Germany, <sup>2</sup>Institute for Vegetative Physiology, Charité – Universitaetsmedizin Berlin, Berlin, Germany, <sup>3</sup>Physikalisch-Technische Bundesanstalt (PTB), Berlin, Germany

The measurement of tubular volume fraction changes in the kidney may be valuable as a confounder of  $T_2^*$ -derived tissue oxygenation and as a potential biomarker. Diffusion weighted imaging provides information about *in-vivo* water mobility which can be linked to three sources: tissue water diffusion, blood perfusion within intrarenal microvasculature, and tubular fluid. In this work we explore the feasibility of assessing tubular volume fraction changes using the non-negative least squares (NNLS) approach under different physiological conditions.

0943



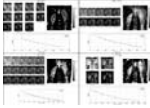
#### Delayed urea differential enhancement CEST (dudeCEST)-MRI with T1 correction for monitoring renal urea handling

Soo Hyun Shin<sup>1</sup>, Brandon Zhang<sup>1</sup>, K. L. Barry Fung<sup>1</sup>, Michael F. Wendland<sup>2</sup>, and Moriel H. Vandsburger<sup>1</sup>

<sup>1</sup>Department of Bioengineering, University of California, Berkeley, Berkeley, CA, United States, <sup>2</sup>Berkeley Preclinical Imaging Core (BPIC), University of California, Berkeley, Berkeley, CA, United States

Urea recycling is a major component of renal tubular function and may provide an in vivo surrogate for tubular dysfunction in renal diseases. We demonstrate an approach of delayed urea differential enhancement CEST (dudeCEST)-MRI, which detects enhanced urea CEST contrast specific to the inner medulla and papilla of the mouse kidney at 20 minutes after urea injection. To enhance quantification while accounting for different  $T_1$  values within the kidney, apparent exchange-dependent relaxation (AREX) correction was applied. The combination of dudeCEST with AREX analysis will be a useful platform for assessment of renal urea recycling as a surrogate for tubular dysfunction.

0944



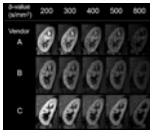
#### A Comparison of T<sub>2</sub> Mapping Methods in the Kidneys

Alexander J Daniel<sup>1</sup>, Eleanor F Cox<sup>1</sup>, Charlotte E Buchanan<sup>1</sup>, and Susan T Francis<sup>1</sup>

<sup>1</sup>Sir Peter Mansfield Imaging Centre, University of Nottingham, Nottingham, United Kingdom

Renal  $T_2$  mapping is still in its infancy with little consensus on methodology between studies, this leads to a variation in  $T_2$  measurements between studies. Here four  $T_2$  mapping methods (Spin Echo-Echo Planar Imaging (SE-EPI), Multi-Echo Turbo Spin Echo (ME-TSE), Gradient Spin Echo (GraSE), and Carr-Purcell-Meiboom-Gill  $T_2$  preparation ( $T_2$  prep)) are compared on both a calibrated phantom and in-vivo kidneys. The GraSE technique was found to produce the most accurate maps relative to the phantom and form the clearest maps of the kidneys in-vivo, showing clear differences between cortical and medullary tissues.

0945



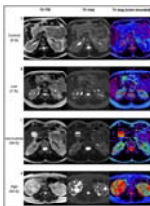
#### Travelling kidneys: Multicentre multivendor variability of renal diffusion-weighted imaging – preliminary results

Fabio Nery<sup>1</sup>, Charlotte Buchanan<sup>2</sup>, Andrew Priest<sup>3</sup>, João Sousa<sup>4</sup>, Michael Nation<sup>5</sup>, Iosif Mendichovszky<sup>3</sup>, Steven Sourbron<sup>6</sup>, Susan Francis<sup>2</sup>, and David Thomas<sup>7,8,9</sup>

<sup>1</sup>UCL Great Ormond Street Institute of Child Health, London, United Kingdom, <sup>2</sup>Sir Peter Mansfield Imaging Centre, University of Nottingham, University Park, Nottingham, United Kingdom, <sup>3</sup>Department of Radiology, Addenbrooke's Hospital, Cambridge University Hospitals NHS Foundation Trust, Cambridge, United Kingdom, <sup>4</sup>Imaging Biomarkers Group, Department of Biomedical Imaging Sciences, University of Leeds, Leeds, United Kingdom, <sup>5</sup>Kidney Research UK, Peterborough, United Kingdom, <sup>6</sup>Department of Infection, Immunity and Cardiovascular Disease, University of Sheffield, Sheffield, United Kingdom, <sup>7</sup>Neuroradiological Academic Unit, UCL Queen Square Institute of Neurology, University College London, London, United Kingdom, <sup>8</sup>Dementia Research Centre, UCL Queen Square Institute of Neurology, University College London, London, United Kingdom, <sup>9</sup>Wellcome Centre for Human Neuroimaging, UCL Queen Square Institute of Neurology, University College London, London, United Kingdom

Multicentre validation studies are required to enable clinical translation of renal MRI biomarkers. Here, we report on the feasibility of standardising renal diffusion weighting imaging protocols and on the variability of renal apparent diffusion coefficient across a range of vendors. Results suggest feasibility of implementing near-identical renal diffusion weighted imaging acquisition protocols with product sequences and the potential of the apparent diffusion coefficient as a robust metric to characterise renal microstructure in multi-centre studies.

0946



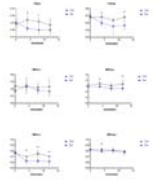
#### Novel magnetic resonance kidney biomarker Parenchyma-T2 for assessment of Autosomal dominant polycystic kidney disease

Florian Siedek<sup>1</sup>, Franziska Grundmann<sup>2</sup>, Kilian Weiss<sup>1</sup>, Daniel Pinto dos Santos<sup>1</sup>, Sita Arjune<sup>2</sup>, Stefan Haneder<sup>1</sup>, Thorsten Persigehl<sup>1</sup>, Roman-Ulrich Mueller<sup>2</sup>, and Bettina Baessler<sup>1</sup>

<sup>1</sup>Radiology, University of Cologne, Cologne, Germany, <sup>2</sup>Department II of Internal Medicine, University of Cologne, Cologne, Germany

Novel biomarkers for a more sensitive and quick assessment of ADPKD patients especially in those cases where kidney function is still preserved and can be maintained is urgently needed. We analyzed in 139 patients and 10 healthy controls if magnetic resonance T2 mapping of the kidneys allows a sufficient differentiation of cyst fraction as a surrogate marker for disease severity. The new biomarker parenchyma-T2 showed the strongest correlation to renal cyst fraction and was faster to determine than the established biomarker htTKV. Consequently, parenchyma-T2 has the potential to serve as a novel predictive biomarker especially in early stages of disease.

0947



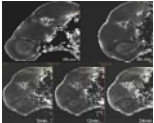
**Diffusional Kurtosis Imaging of kidney in STZ-induced Diabetic Rats.**

Youzhen Feng<sup>1</sup>, Zhongyuan Cheng<sup>1</sup>, Xiaoqiao Chen<sup>2</sup>, Xiaoqing Xiong<sup>1</sup>, Qiting Lin<sup>1</sup>, Dingkun SiTu<sup>1</sup>, Long Qian<sup>3</sup>, Huomei Chen<sup>1</sup>, and Xiangran Cai<sup>1</sup>

<sup>1</sup>Medical Imaging Center, First Affiliated Hospital, Jinan University, Guangzhou, Guangdong, China, Guangzhou, China, <sup>2</sup>Medical Imaging Center, The Eighth Hospital of Sun Yat-sen University, Shenzhen, China., Shenzhen, China, <sup>3</sup>MR Research, GE Healthcare., Beijing, China

Diffusional kurtosis imaging (DKI) is an advanced diffusion model and could identify the heterogeneity of cellularity and microstructural complexity. To test whether the DKI could detect the functional changes of kidney in early Diabetic kidney disease (DKD), the STZ-induced diabetic rats were applied in current study. Further, the biochemical and pathological evidences would also be provided to compare with the DKI biomarker.

0948



**Evaluation of hypoxia with T2' mapping in renal ischemia reperfusion injury**

Jing gang Zhang<sup>1</sup>, Wei Xing<sup>1</sup>, Jie Chen<sup>1</sup>, and Weiqiang Dou<sup>2</sup>

<sup>1</sup>Radiology, Third Affiliated Hospital of Soochow University, Changzhou, China, <sup>2</sup>MR Research China, GE Healthcare, Shanghai, China

The purpose was to explore if T2' mapping can assess renal oxygen in the ischemia-reperfusion injury (IRI). IRI models were established according to different ischemia time, followed by injection of furosemide 24 hours after IRI and consecutive MRI scans. Quantitative scores of oxygen were acquired with the hypoxic probe. We found that R2' values of the inner and outer medulla were statistically significant. R2' value of the outer medulla was highly correlated with oxygen scores. T2' mapping could serve as a quantitative biomarker to assess the renal oxygen and monitor the treatment in patients with IRI.

**Combined Educational & Scientific Session**

**MRI of the Kidneys - Renal MRI: Past, Present & Future**

Organizers: Christoffer Laustsen, Daniel Margolis, Mustafa Shadi Bashir

Wednesday Parallel 3 Live Q&A

Wednesday 15:15 - 16:00 UTC

Moderators: Steven Sourbron & Octavia Bane



**State-of-the-Art Focal Kidney MR Biomarkers**

Brian Allen<sup>1</sup>

<sup>1</sup>Duke University, United States

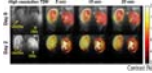
Many solid renal neoplasms have characteristic features on imaging. Imaging biomarkers can be used to non-invasively identify histology of the most common subtypes of renal cell carcinoma and can be used to assess response to therapy. No one biomarker can accurately differentiate all renal masses, as some renal masses have features in common, necessitating attention to all images, phases, or sequences.

## Emerging Focal Kidney Biomarkers

Cornelius von Morze<sup>1</sup>

<sup>1</sup>Department of Radiology, Washington University, St Louis, MO, United States

0949



### Iopamidol CEST MR Urography for Urinary Tract Obstructions

KowsalyaDevi Pavuluri<sup>1</sup>, Shaowei Bo<sup>1</sup>, Farazad Sedaghat<sup>1</sup>, Max Kates<sup>2</sup>, and Michael T McMahon<sup>1,3</sup>

<sup>1</sup>The Russell H. Morgan Department of Radiology and Radiological Science, The Johns Hopkins University School of Medicine, Baltimore, MD, United States, <sup>2</sup>Department of Urology, The Johns Hopkins University School of Medicine, Baltimore, MD, United States, <sup>3</sup>F.M. Kirby Research Center for Functional Brain Imaging, Kennedy Krieger Institute, Baltimore, MD, United States

Urinary tract obstructions (UTOs) are impairments in urine flow which can lead to pain, infection and irreversible kidney damage if left undiagnosed or untreated. Chemical exchange saturation transfer (CEST) is a novel MRI contrast mechanism that is particularly sensitive to environmental changes including changes in pH values. In this study we developed a protocol by administering the FDA approved iopamidol to obtain dynamic pH and perfusion MRI contrast maps of the kidneys and compared these with iopamidol administered multi-phase CT in a unilateral urinary obstruction mouse model.

0950



### T2 and diffusion tensor imaging of kidney disease in an epicutaneous TLR7 enhanced lupus mouse model

Luke Xie<sup>1</sup>, Vineela D. Gandham<sup>1</sup>, Kai H. Barck<sup>1</sup>, Eric Suto<sup>1</sup>, Wyne P. Lee<sup>1</sup>, Oded Foreman<sup>1</sup>, Richard A. D. Carano<sup>1</sup>, Alex J. De Crespigny<sup>1</sup>, and Robby M. Weimer<sup>1</sup>

<sup>1</sup>Genentech, South San Francisco, CA, United States

System lupus erythematosus (SLE) is an autoimmune disease that can lead to lupus nephritis and glomerulonephritis. Studies have evaluated kidneys from SLE patients using diffusion-weighted imaging. However, specific MRI metrics most related to the underlying disease has not been identified. In this study, we evaluate a lupus model with MRI and determine the physical properties that contribute to the MRI signal. This is achieved through structural analysis of glomeruli with whole kidney 3D micro-CT and pathological evaluation of glomeruli, tubules, interstitium, and arterioles. Finally, a comprehensive correlation analysis is performed to determine top MRI metrics most sensitive to the disease.

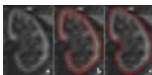
## Emerging Functional Kidney MR Biomarkers

Steffen Ringgaard<sup>1</sup>

<sup>1</sup>MR Research Centre, Aarhus University, Aarhus, Denmark

Non-invasive assessment of kidney function and microstructure is important for diagnosis and treatment monitoring of patients with kidney diseases. Besides its ability to make high-resolution diagnostic images, MR also has the potential for evaluating a number of functional parameters. In this lecture we will discuss the most promising of these MR biomarkers for assessing kidney function and microstructure, and we will briefly touch up on some arising methodologies. This includes ASL, phase contrast, BOLD imaging, diffusion imaging, relaxation mapping and some non-proton methods.

0951



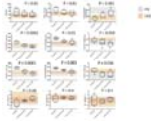
### Pulsed Arterial Spin Labeling and Pseudo-Continuous Arterial Spin Labeling MRI for Diagnosis of Renal Insufficiency

Zhiyong Lin<sup>1</sup>, Rui Wang<sup>1</sup>, Jing Liu<sup>1</sup>, Jinxia Zhu<sup>2</sup>, Chengwen Liu<sup>2</sup>, Bernd Kühn<sup>3</sup>, and Xiaoying Wang<sup>1</sup>

<sup>1</sup>Department of Radiology, Peking University First Hospital, Beijing, China, <sup>2</sup>MR Collaboration, Siemens Healthcare, Ltd., Beijing, China, <sup>3</sup>Siemens Healthcare GmbH, Erlangen, Germany

Patients with renal artery stenosis (RAS) exhibit changes in renal artery hemodynamics. This study investigated the clinical value of pulsed arterial spin labeling (PASL) and pseudo-continuous arterial spin labeling (pCASL) in diagnosing and grading renal insufficiency in patients with RAS. PASL performed better for measuring renal blood flow (RBF) in the renal cortex to provide differential diagnosis of renal function, while the RBF values obtained with pCASL were more closely correlated with the glomerular filtration rate (GFR). These findings indicate that PASL and pCASL MRI have utility for diagnosing and grading renal insufficiency in patients with RAS.

0952



### Assessment of Acute Kidney Injury and associated longitudinal changes with recovery using multiparametric renal MRI

Charlotte Elizabeth Buchanan<sup>1</sup>, Huda Mahmoud<sup>2</sup>, Eleanor F Cox<sup>1</sup>, Rebecca Noble<sup>2</sup>, Benjamin L Prestwich<sup>1</sup>, Isma Kazmi<sup>2</sup>, Maarten W Taal<sup>2</sup>, Nicholas Selby<sup>2</sup>, and Susan T Francis<sup>1</sup>

<sup>1</sup>Sir Peter Mansfield Imaging Centre, University of Nottingham, Nottingham, United Kingdom, <sup>2</sup>Centre for Kidney Research and Innovation, University of Nottingham, Derby, United Kingdom

Acute kidney injury (AKI) is defined clinically using serum creatinine. We use multiparametric renal MRI to assess longitudinal changes in AKI. Nine participants were assessed at time of AKI, 7 were re-scanned at 3-months and 1-year. At peak AKI, total kidney volume (TKV) and cortex and medulla T<sub>1</sub> were elevated, and cortex perfusion reduced compared to HVs. After 3-months, TKV reduced compared to peak AKI, cortex and medulla T<sub>1</sub> remained slightly elevated compared to HVs. Perfusion remained reduced compared to HVs after 1-year. MRI showed incomplete recovery at 3 months, despite normalisation of biochemistry, providing potential to identify maladaptive repair.

## Oral

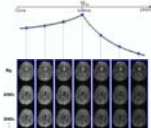
### Diffusion Acquisition and Reconstruction - Diffusion: Acquisition

Wednesday Parallel 4 Live Q&A

Wednesday 15:15 - 16:00 UTC

Moderators: Jennifer McNab

0953



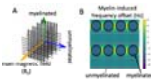
### Diffusion-PEPTIDE: rapid distortion-free diffusion-relaxometry imaging

Merlin J Fair<sup>1,2</sup>, Congyu Liao<sup>1,2</sup>, Daeun Kim<sup>3</sup>, Divya Varadarajan<sup>1,2</sup>, Justin P Haldar<sup>3,4</sup>, and Kawin Setsompop<sup>1,2,5</sup>

<sup>1</sup>A. A. Martinos Center for Biomedical Imaging, Massachusetts General Hospital, Charlestown, MA, United States, <sup>2</sup>Department of Radiology, Harvard Medical School, Boston, MA, United States, <sup>3</sup>Department of Electrical and Computer Engineering, University of Southern California, Los Angeles, CA, United States, <sup>4</sup>Department of Biomedical Engineering, University of Southern California, Los Angeles, CA, United States, <sup>5</sup>Harvard-MIT Health Sciences and Technology, MIT, Cambridge, MA, United States

Diffusion-PEPTIDE incorporates the recently developed rapid multi-shot relaxometry technique Propeller EPTI with Dynamic Encoding (PEPTIDE) into a diffusion acquisition scheme. PEPTIDE enables fast acquisition of distortion- and blurring-free images, time-resolved for different timepoints with varying T<sub>2</sub> & T<sub>2</sub><sup>\*</sup> weighting, with self-navigation for correction of shot-to-shot phase-variation and motion. Diffusion-PEPTIDE is demonstrated here to enable distortion-free in vivo diffusion-relaxometry with large parameter space in an sensible acquisition time.

0954



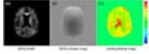
### Diffusion-weighted phase imaging: towards a tract-specific myelin measure

Michiel Cottaar<sup>1</sup>, Benjamin C. Tendler<sup>1</sup>, Wenchuan Wu<sup>1</sup>, Karla L. Miller<sup>1</sup>, and Saad Jbabdi<sup>1</sup>

<sup>1</sup>WIN@FMRIB, University of Oxford, Oxford, United Kingdom

We propose a novel sequence that adds a second asymmetric spin echo after a standard Stejskal-Tanner sequence. This allows the estimation of the off-resonance frequency of the diffusion-weighted signal due to the myelin magnetic susceptibility. Varying the orientation of the diffusion-weighting gradient dephases different fibre populations. In simulations we show that for a sufficiently high b-value ( $> \sim 3 \text{ ms}/\mu\text{m}^2$ ), the intra-axonal water will dominate leading to a simple relation between the myelin-induced frequency shift and the log  $g$ -ratio. This allows the difference in log  $g$ -ratio between crossing fibres to be measured and hence estimate the myelination of individual crossing tracts.

0955



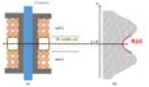
Simultaneous acquisition of diffusion weighted images and conductivity maps using a balanced double echo steady state (DESS) sequence

Jochen Keupp<sup>1</sup>, Bernhard Gleich<sup>1</sup>, and Ulrich Katscher<sup>1</sup>

<sup>1</sup>Philips Research, Hamburg, Germany

A combined acquisition of distortion-free diffusion-weighted images and tissue conductivity maps is explored using a fully balanced double echo steady state (DESS) sequence. Banding artifacts are avoided using sufficiently high gradient moments of the diffusion gradient, such that the banding is contained within single voxels. The stability of the B1 transceive phase measurement by the balanced DESS sequence allows the derivation of quantitative tissue conductivity based second derivative using standard EPT (electrical properties tomography) methods. Feasibility of simultaneous DWI and EPT is shown on a 3T MRI system in phantom and volunteer experiments (head).

0956



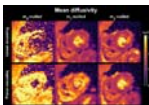
Diffusion phase-imaging using non-linear gradients in anisotropic synthetic fiber phantoms

Pamela Wochner<sup>1</sup>, Torben Schneider<sup>2</sup>, Jason Stockmann<sup>3</sup>, Jack Lee<sup>1</sup>, and Ralph Sinkus<sup>1,4</sup>

<sup>1</sup>School of Biomedical Engineering & Imaging Sciences, King's College London, London, United Kingdom, <sup>2</sup>Philips Healthcare, Guildford, United Kingdom, <sup>3</sup>Department of Radiology, Massachusetts General Hospital, Athinoula A. Martinos Center for Biomedical Imaging, Charlestown, MA, United States, <sup>4</sup>Inserm U1148, LVTS, University Paris Diderot, Paris, France

Diffusion MRI classically uses linear gradients to encode information about micro-structure in the loss of signal magnitude. When replaced by gradients varying quadratically in space, anisotropic diffusion results in a net phase shift, while the signal magnitude is largely preserved. This allows the extraction of information from signal phase inaccessible to other diffusion MRI methods. The phase evolution of anisotropic fiber phantoms were studied in simulations and diffusion experiments. Simulations confirm increasing phase change with increasing anisotropy and mixing time between diffusion gradients. First MR experiments with different mixing times show a phase shift in good agreement with theoretical estimate.

0957



Motion-compensated gradient waveform design for tensor-valued diffusion encoding by constrained numerical optimization

Filip Szczepankiewicz<sup>1,2,3</sup>, Irvin Teh<sup>4</sup>, Erica Dall'Armellina<sup>4</sup>, Sven Plein<sup>4</sup>, Jurgen E. Schneider<sup>4</sup>, and Carl-Fredrik Westin<sup>2,3</sup>

<sup>1</sup>Clinical Sciences Lund, Lund University, Lund, Sweden, <sup>2</sup>Radiology, Brigham and Women's Hospital, Boston, MA, United States, <sup>3</sup>Harvard Medical School, Boston, MA, United States, <sup>4</sup>Leeds Institute of Cardiovascular and Metabolic Medicine, University of Leeds, Leeds, United Kingdom

Motion compensation is vital for cardiac diffusion MRI. In this paper we propose an optimized gradient waveform design that allows tensor-valued diffusion encoding with motion compensation. We demonstrate that it works for in vivo cardiac imaging and we show that it is more efficient than previous designs.

0958

A TSE BLADE based distortion-free diffusion-weighted imaging method with Dixon water-fat separation

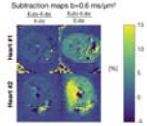


Kun Zhou<sup>1</sup>, Wei Liu<sup>1</sup>, and Yulin V Chang<sup>2</sup>

<sup>1</sup>Siemens Shenzhen Magnetic Resonance Ltd., Shenzhen, China, <sup>2</sup>Siemens Medical Solutions USA, Boston, MA, United States

Diffusion weighted imaging with EPI can suffer from image distortions due to sensitivity to B0 inhomogeneity and chemical shift related artifacts induced by incomplete fat suppression. In this study, we propose a TSE BLADE sequence with Dixon water-fat separation for DWI. With this technique, distortion-free DWI with robust fat suppression was shown to be feasible, even in body regions with strong B0 inhomogeneity.

0959



### Stay on the beat: tuning in on time-dependent diffusion in the heart

Henrik Lundell<sup>1</sup>, Samo Lasič<sup>1,2</sup>, Filip Szczepankiewicz<sup>3,4,5</sup>, Markus Nilsson<sup>3</sup>, Daniel Topgaard<sup>6</sup>, Jürgen E. Schneider<sup>7</sup>, and Irvin Teh<sup>7</sup>

<sup>1</sup>Danish Research Centre for Magnetic Resonance, Centre for Functional and Diagnostic Imaging and Research, Copenhagen University Hospital Hvidovre, Hvidovre, Denmark, <sup>2</sup>Random Walk Imaging AB, Lund, Denmark, <sup>3</sup>Clinical Sciences, Lund University, Lund, Sweden, <sup>4</sup>Harvard Medical School, Boston, MA, United States, <sup>5</sup>Brigham and Women's Hospital, Boston, MA, United States, <sup>6</sup>Physical Chemistry, Lund University, Lund, Sweden, <sup>7</sup>Leeds Institute of Cardiovascular and Metabolic Medicine, University of Leeds, Leeds, United Kingdom

Diffusion encoding with general gradient waveforms provides flexibility and experimental efficiency for multidimensional diffusion encoding (MDE). Here we investigate b-tensor shape and spectral content as two independent measurement dimensions for imaging myocardial microstructure. By tuning spectral content, we demonstrate that time-dependent diffusion can be controlled for across b-tensor shapes and that tuning in itself provide a strong image contrast in a clinically feasible setting. For encoding high frequencies alone, our isotropic encoding provides higher experimental efficiency.

0960



### Acquiring and predicting MUlti-dimensional Diffusion (MUDI) data: an open challenge

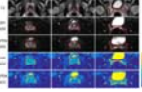
Marco Pizzolato<sup>1</sup>, Marco Palombo<sup>2</sup>, Elisenda Bonet-Carne<sup>2,3</sup>, Francesco Grussu<sup>2,4</sup>, Andrada Ianus<sup>5</sup>, Fabian Bogusz<sup>6</sup>, Tomasz Pieciak<sup>6,7</sup>, Lipeng Ning<sup>8</sup>, Stefano B. Blumberg<sup>2</sup>, Thomy Mertzanidou<sup>2</sup>, Daniel C. Alexander<sup>2</sup>, Maryam Afzali<sup>9</sup>, Santiago Aja-Fernández<sup>7,9</sup>, Derek K. Jones<sup>9,10</sup>, Carl-Fredrik Westin<sup>8</sup>, Yogesh Rathi<sup>8</sup>, Steven H. Baete<sup>11,12</sup>, Lucilio Cordero-Grande<sup>13</sup>, Thilo Ladner<sup>14</sup>, Paddy J. Slator<sup>2</sup>, Daan Christiaens<sup>13,15</sup>, Jean-Philippe Thiran<sup>1,16</sup>, Anthony N. Price<sup>13</sup>, Farshid Sepehrband<sup>17</sup>, Fan Zhang<sup>8</sup>, and Jana Hutter<sup>13</sup>

<sup>1</sup>Signal Processing Lab (LTS5), École Polytechnique Fédérale de Lausanne, Lausanne, Switzerland, <sup>2</sup>Department of Computer Science, Centre for Medical Image Computing, University College London, London, United Kingdom, <sup>3</sup>BCNatal Fetal Medicine Research Center, Barcelona, Spain, <sup>4</sup>Queen Square MS Centre, UCL Queen Square Institute of Neurology, Faculty of Brain Sciences, University College London, London, United Kingdom, <sup>5</sup>Champalimaud Research, Champalimaud Centre for the Unknown, Lisbon, Portugal, <sup>6</sup>AGH University of Science and Technology, Kraków, Poland, <sup>7</sup>Laboratorio de Procesado de Imagen (LPI), Universidad de Valladolid, Valladolid, Spain, <sup>8</sup>Brigham and Women's Hospital, Harvard Medical School, Boston, MA, United States, <sup>9</sup>Cardiff University Brain Research Imaging Center (CUBRIC), School of Psychology, University of Cardiff, Cardiff, United Kingdom, <sup>10</sup>Mary MacKillop Institute for Health Research, Faculty of Health Sciences, Australian Catholic University, Melbourne, Australia, <sup>11</sup>Center for Biomedical Imaging, Dept. of Radiology, New York University School of Medicine, New York, NY, United States, <sup>12</sup>Center for Advanced Imaging Imaging, Innovation and Research, New York University School of Medicine, New York, NY, United States, <sup>13</sup>Centre for Medical Engineering, Centre for the Developing Brain, King's College London, London, United Kingdom, <sup>14</sup>Department of Chemistry and Applied Biosciences, ETH Zurich, Zurich, Switzerland, <sup>15</sup>Department of Electrical Engineering (ESAT-PSI), KU Leuven, Leuven, Belgium, <sup>16</sup>Radiology Department, Centre Hospitalier Universitaire Vaudois and University of Lausanne, Lausanne, Switzerland, <sup>17</sup>Laboratory of Neuro Imaging (LONI), USC Stevens Neuroimaging and Informatics Institute, University of Southern California, Los Angeles, CA, United States



The variety of possible combinations of acquisition parameters is key to the versatility of MRI as a diagnostic modality. However, the full exploration of the parameter space defined by b-values, gradient directions, inversion and echo times comes at the expense of the acquisition time. We present the results of an open challenge where different methods were proposed to predict the content of a densely sampled acquisition, which explores such parameter space, from only a subset of parameter combinations. These indicate the possibility of leveraging the redundancy in the data to shorten the acquisition time while minimizing information loss.

0961



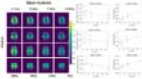
Overcoming geometric distortions in human prostate diffusion weighted imaging by spatio-temporal encoded (SPEN) MRI

Martins Otikovs<sup>1</sup>, Lingceng Ma<sup>1</sup>, and Lucio Frydman<sup>1</sup>

<sup>1</sup>Weizmann Institute of Science, Rehovot, Israel

Spatiotemporal encoding (SPEN) is an alternative ultrafast imaging technique which allows one to manipulate the bandwidth along the phase-encoding (PE) direction as well as to achieve  $T_2^*$  refocusing throughout the FID acquisition, thereby overcoming distortions observed along EPI's PE dimension. The study compares multislice 2D SPEN and a 3D SPEN sequence variants against EPI derivatives, evaluating their ability to deliver prostate diffusion-weighted imaging (DWI) data and apparent diffusion coefficient (ADC) maps on healthy human volunteers. Essentially distortion-free diffusion weighted images and ADC maps of prostate with good SNR were achieved by the 2D SPEN variant.

0962



Measuring Time-Dependent Diffusion Kurtosis Using the MAGNUS High-Performance Head Gradient

Grant Kaijuin Yang<sup>1,2</sup>, Ek Tsoon Tan<sup>3</sup>, Eric Fiveland<sup>4</sup>, Thomas Foo<sup>4</sup>, and Jennifer McNab<sup>2</sup>

<sup>1</sup>Electrical Engineering, Stanford University, Stanford, CA, United States, <sup>2</sup>Radiology, Stanford University, Stanford, CA, United States, <sup>3</sup>Hospital for Special Surgery in Manhattan, New York, NY, United States, <sup>4</sup>GE Global Research, Niskayuna, NY, United States

In this work, we measure time-dependent effects on diffusion kurtosis estimates in the in vivo human brain over an extended range of b-values(458-2000s/mm<sup>2</sup>) and frequencies(0-96Hz) using a high-performance head gradient coil on a whole-body 3T MRI.

## Oral - Power Pitch

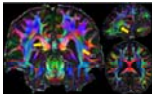
### Diffusion Acquisition and Reconstruction - Diffusion: Acquisition, Reconstruction & Processing

Wednesday Parallel 4 Live Q&A

Wednesday 15:15 - 16:00 UTC

Moderators: Daan Christiaens & Muge Karaman

0963



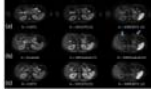
Acquisition of a reference Connectom diffusion MRI dataset: In vivo whole-brain diffusion MRI at 760  $\mu$ m isotropic averaged over 18 hours

Fuyixue Wang<sup>1,2</sup>, Zijong Dong<sup>1,3</sup>, Qiyuan Tian<sup>1</sup>, Congyu Liao<sup>1</sup>, Qiuyun Fan<sup>1</sup>, W. Scott Hoge<sup>4</sup>, Chanon Ngamsombat<sup>1</sup>, Boris Keil<sup>5</sup>, Jonathan R. Polimeni<sup>1,2</sup>, Lawrence L. Wald<sup>1,2</sup>, Susie Y. Huang<sup>1,2</sup>, and Kawin Setsompop<sup>1,2</sup>

<sup>1</sup>A. A. Martinos Center for Biomedical Imaging, Massachusetts General Hospital, Charlestown, MA, United States, <sup>2</sup>Harvard-MIT Health Sciences and Technology, MIT, Cambridge, MA, United States, <sup>3</sup>Department of Electrical Engineering and Computer Science, MIT, Cambridge, MA, United States, <sup>4</sup>Department of Radiology, Brigham and Women's Hospital, Boston, MA, United States, <sup>5</sup>Department of Life Science Engineering, Institute of Medical Physics and Radiation Protection, Giessen, Germany

We present a whole brain in vivo diffusion MRI dataset acquired at 760um isotropic resolution and sampled at 1260 q-space points across 9 two-hour sessions. The creation of this benchmark in vivo diffusion MRI dataset is possible through use of the Connectom scanner, custom-built 64-channel phased-array coil, gSlider acquisition, dual-polarity GRAPPA reconstruction, reverse phase encoding for distortion mitigation, and personalized motion-robust stabilizer. The data will enhance our understanding of gray and white matter structure with fine detail revealed at sub-mm resolution and serve as a reference dataset for new modeling and processing algorithms.

0964



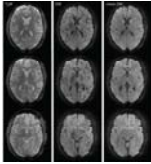
### Towards Single-shot Diffusion-weighted Spiral Abdominal Imaging on a Clinical Scanner

Peter Börner<sup>1,2</sup>, Holger Eggers<sup>1</sup>, Kay Nehrke<sup>1</sup>, Peter Mazurkewitz<sup>1</sup>, Jürgen Rahmer<sup>1</sup>, Johan van den Brink<sup>3</sup>, and Silke Hey<sup>3</sup>

<sup>1</sup>Philips Research Hamburg, Hamburg, Germany, <sup>2</sup>Radiology, LUMC, Leiden, Netherlands, <sup>3</sup>Philips Healthcare Best, Best, Netherlands

Single-shot diffusion-weighted imaging is predominantly performed with echo planar imaging today. Spiral imaging allows shorter echo times and thus promises higher SNR, but is more sensitive to various system imperfections. Previous work showed the feasibility of single-shot diffusion-weighted spiral imaging in the brain. This work explores the applicability to abdominal imaging. It shows that good image quality is achievable in volunteers, using the system demand trajectory for reconstruction, parallel imaging for acceleration, and static main field inhomogeneity mapping for corresponding deblurring.

0965



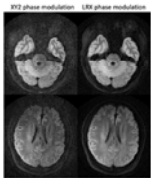
### Diffusion Imaging with Very High Resolution and Very Short Echo Time

Bertram Jakob Wilm<sup>1</sup>, Manuela Roesler<sup>1</sup>, Franciszek Hennel<sup>1</sup>, Markus Weiger<sup>1</sup>, and Klaas Paul Pruessmann<sup>1</sup>

<sup>1</sup>ETH and University of Zürich, Zürich, Switzerland

To achieve high-resolution diffusion imaging with short echo times, single-shot spiral DWI using a recently developed gradient insert (strength=200 mT/m, slew=600 T/m/s) was implemented. The high gradient strength in combination with the spiral readout allowed for an echo time as short as 19 ms at a b-factor of 1000 s/mm<sup>2</sup>. The high slew rate enabled shortening of the spiral readout duration which reduces sensitivity against static off-resonance and T<sub>2</sub>\* blurring artifacts, and allowed imaging with an in-plane image resolution of only 0.69 mm. First in-vivo results are presented.

0966



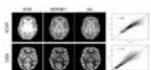
### An enhanced turboPROP+ technique for diffusion weighted imaging

Zhiqiang Li<sup>1</sup>, Melvyn B Ooi<sup>1,2</sup>, and John P Karis<sup>1</sup>

<sup>1</sup>Neuroradiology, Barrow Neurological Institute, Phoenix, AZ, United States, <sup>2</sup>Philips Healthcare, Gainesville, FL, United States

Diffusion weighted MRI is a useful technique for the diagnosis of neurological disorders. DW EPI is time efficient but suffer from geometric distortions. DW PROPELLER and its variants, including turboPROP and turboPROP+, have been proposed to generate distortion free images. This project improves the turboPROP+ technique by incorporating LRX RF phase modulation approach to improve SNR and signal stability, and by revising the phase correction algorithm to minimize residual artifacts. Volunteer results demonstrate reduced artifacts compared to the original phase correction algorithm, and increased SNR/image quality compared to original XY2 phase modulation.

0967



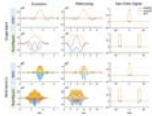
### Denosing of DWI signal using deep learning

Hu Cheng<sup>1</sup>, Jian Wang<sup>1,2</sup>, Shreyas Sanjeev Fadnavis<sup>3</sup>, Eleftherios Garyfallidis<sup>3</sup>, and Sharlene Newman<sup>1</sup>

<sup>1</sup>Psychological and Brain Sciences, Indiana University, Bloomington, IN, United States, <sup>2</sup>School of Information Science and Engineering, Shandong Normal University, Jinan, China, <sup>3</sup>Indiana University, Bloomington, IN, United States

We developed a simple deep learning method for DWI data denoising and tested it on correcting sum of square (SoS) noise. By acquiring two sets of diffusion images reconstructed with SoS and SENSE1 coil combination schemes on one subject as training data, the learned model can effectively denoise any SoS data acquired with the same DWI protocol. The denoised data produces similar results in diffusion tensor analysis and NODDI analysis as the SENSE1 data. This method also shed light on denoising techniques for diffusion imaging if a low-noise DWI dataset is available.

0968



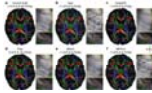
### SNR-Enhanced High-Resolution Diffusion Imaging Using 3D Simultaneous Multi-Slab (SMSlab) with Root-flipped RF Pulse Design

Simin Liu<sup>1</sup>, Erpeng Dai<sup>1,2</sup>, and Hua Guo<sup>1</sup>

<sup>1</sup>Center for Biomedical Imaging Research, Department of Biomedical Engineering, School of Medicine, Tsinghua University, Beijing, China, <sup>2</sup>Department of Radiology, Stanford University, Stanford, CA, United States

3D simultaneous multi-slab (SMSlab) is a technique to increase SNR efficiency in high-resolution diffusion imaging. However, it still suffers from the intrinsic low SNR of diffusion MRI, especially when using multi-band RF pulses, which increases the pulse duration and thus lengthens the echo time. In this study, root-flipped RF pulses were used in SMSlab to acquire 1 mm isotropic 3D diffusion images. With a multi-band factor of 2, the root-flipped pulses brought about 12 ms reduction of TE (from 91 to 79 ms), and 16% SNR gain, compared to traditional SINC pulses.

0969



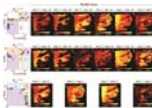
### DeepDTI: Six-direction diffusion tensor MRI using deep learning

Qiyuan Tian<sup>1,2</sup>, Berkin Bilgic<sup>1,2</sup>, Qiuyun Fan<sup>1,2</sup>, Congyu Liao<sup>1,2</sup>, Chanon Ngamsombat<sup>1</sup>, Yuxin Hu<sup>3</sup>, Thomas Witzel<sup>1</sup>, Kawin Setsompop<sup>1,2</sup>, Jonathan R. Polimeni<sup>1,2</sup>, and Susie Y. Huang<sup>1,2</sup>

<sup>1</sup>Martinos Center for Biomedical Imaging, Massachusetts General Hospital, Charlestown, MA, United States, <sup>2</sup>Department of Radiology, Harvard Medical School, Boston, MA, United States, <sup>3</sup>Department of Electrical Engineering, Stanford University, Stanford, CA, United States

Diffusion tensor imaging (DTI) is widely used clinically but typically requires acquiring diffusion-weighted images (DWIs) along many diffusion-encoding directions for robust model fitting, resulting in lengthy acquisitions. Here, we propose a joint denoising and q-space angular super-resolution method called "DeepDTI" achieved using data-driven supervised deep learning that minimizes the data requirement for DTI to the theoretical minimum of one b=0 image and six DWIs. Metrics derived from DeepDTI's results are equivalent to those obtained from three b=0 and 19 to 26 DWI volumes for different scalar and orientational DTI metrics, and superior to those derived from state-of-the-art denoising methods.

0970



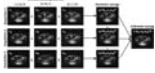
### Multidimensional correlation MRI of the brain

Kristofor Pas<sup>1,2</sup>, Michal Komlosh<sup>2,3</sup>, Daniel Perl<sup>4</sup>, Peter Basser<sup>2</sup>, and Dan Benjamini<sup>2,3</sup>

<sup>1</sup>University of Texas at Arlington, Arlington, TX, United States, <sup>2</sup>National Institutes of Health, Bethesda, MD, United States, <sup>3</sup>Uniformed Service University of the Health Sciences, Bethesda, MD, United States, <sup>4</sup>Uniformed Services University of the Health Sciences, Bethesda, MD, United States

Multidimensional correlation MRI is an emerging imaging modality that is capable of disentangling highly heterogeneous systems, according to chemical and physical interactions of water within them. Using this approach, the conventional three dimensional MR scalar images are replaced with spatially resolved multidimensional spectra. The ensuing abundance in microstructural and chemical information is a blessing that incorporates a real challenge: how does one distill and refine it into images? Here we introduce a method that robustly identifies the multidimensional spectral components in the image domain, defines the spectral regions of interest, and uses them to reconstruct images of sub-voxel components.

0971



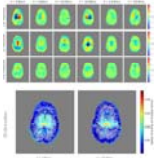
### Accelerating clinical diffusion-weighted MRI using deep learning: Potential utility in metastatic prostate cancer and malignant mesothelioma

Konstantinos Zormpas-Petridis<sup>1</sup>, Nina Tunariu<sup>1</sup>, Andra Curcean<sup>1</sup>, Christina Messiou<sup>1</sup>, David Collins<sup>1</sup>, Yann Jamin<sup>1</sup>, Dow-Mu Koh<sup>1</sup>, and Matthew D. Blackledge<sup>1</sup>

<sup>1</sup>Radiotherapy and Imaging, Institute of Cancer Research, London, Sutton, United Kingdom

Diffusion-weighted MR-imaging (DWI) is an attractive non-invasive tool for staging and response evaluation of myeloma and metastatic bone disease. However, scans can last up to 30 minutes in whole body studies, which can hinder the adoption of DWI in clinical practice, especially in patients who are unwell. Here, we use a deep learning approach to establish that sub-sampled, but rapidly acquired images, could be used to reconstruct 'clinical-grade' DWI images, potentially reducing acquisition times (from ~30 to ~5 minutes). Such time savings could reduce scanning costs and spare patient time/discomfort.

0972



### Simultaneous Imaging of Diffusion and Coherent Motion in Slow-Flow Compartments in the Brain

Isabelle Heukensfeldt Jansen<sup>1</sup>, Luca Marinelli<sup>1</sup>, Ek Tsoon Tan<sup>2</sup>, Robert Y Shih<sup>3,4</sup>, J Kevin DeMarco<sup>3,4</sup>, J Kent Werner<sup>3,4</sup>, Vincent B Ho<sup>3,4</sup>, and Thomas Foo<sup>1</sup>

<sup>1</sup>GE Global Research Center, Niskayuna, NY, United States, <sup>2</sup>Hospital for Special Surgery, New York, NY, United States, <sup>3</sup>Uniformed Services University of the Health Sciences, Bethesda, MD, United States, <sup>4</sup>Walter Reed National Military Medical Center, Bethesda, MD, United States

We demonstrate a method for simultaneous imaging of diffusion and slow motion in vivo. We use both the magnitude and phase information from image data to reconstruct coherent and incoherent motion (flow and diffusion). We modified a PGSE diffusion imaging sequence so that b-value and encoded velocity can be set independently. We imaged healthy volunteers with a 2-shell sequence with  $b_{\max}=2000 \text{ sec/mm}^2$  and  $v_{\text{enc}}=0.24 \text{ mm/s}$  at multiple phases during the cardiac cycle using peripheral gating. Results show a distinct periodic motion around the ventricles with RMS speed 0.065 mm/s, moving laterally during systole and medially during diastole

0973



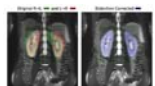
### Mitigating Gyral Bias via Active Cortex Tractography

Ye Wu<sup>1</sup>, Yoonmi Hong<sup>1</sup>, and Pew-Thian Yap<sup>1</sup>

<sup>1</sup>Department of Radiology and BRIC, University of North Carolina, Chapel Hill, Chapel Hill, NC, United States

We propose a tractography method, called active cortex tractography (ACT), to overcome gyral bias by enabling fiber streamlines to curve naturally into the cortex. We show that the cortex can play an active role in cortical tractography by affording anatomical knowledge to overcome orientation ambiguities as the streamlines enter the superficial white matter in gyral blades and approach the cortex.

0974



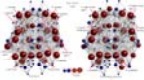
### Simultaneous distortion and motion correction in abdominal DW-MRI using dual echo EPI and slice-to-volume registration

Jaume Coll-Font<sup>1,2</sup>, Onur Afacan<sup>1,2</sup>, Scott Hoge<sup>2,3</sup>, Bahram Marami<sup>4</sup>, Ali Gholipour<sup>1,2</sup>, Jeanne Chow<sup>1,2</sup>, Simon Warfield<sup>1,2</sup>, and Sila Kurugol<sup>1,2</sup>

<sup>1</sup>Radiology, Boston Children's Hospital, Boston, MA, United States, <sup>2</sup>Harvard Medical School, Boston, MA, United States, <sup>3</sup>Radiology, Brigham and Women's Hospital, Boston, MA, United States, <sup>4</sup>Icahn School of Medicine at Mount Sinai, New York, NY, United States

Diffusion-weighted MRI (DW-MRI) has been increasingly used in abdominal applications. However, unavoidable respiratory motion, as well as B0 field inhomogeneities reduce the accuracy of the quantitative parameters and hinders clinical applicability. In this work, we present a dual echo EPI DW-MRI and slice-to-volume registration method to jointly correct for geometric distortion and motion of the kidneys. The results show that our method effectively reduced geometric distortions, improved alignment of the DW-MR volumes and increased the precision of the estimated quantitative parameters.

0975



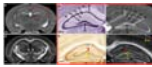
Analysis of hub-regions from the structural connectomes of preterm-born and control adolescents

Hassna Irzan<sup>1,2</sup>, Michael Hütel<sup>2</sup>, Sebastien Ourselin<sup>2</sup>, Neil Marlow<sup>3</sup>, and Andrew Melbourne<sup>1,2</sup>

<sup>1</sup>Medical Physics and Biomedical Engineering, University College London, London, United Kingdom, <sup>2</sup>Biomedical Engineering and Imaging Sciences, King's College London, London, United Kingdom, <sup>3</sup>Institute for Women's Health, London, United Kingdom

Preterm birth has been linked to white matter abnormalities in infants, however the functional implications of these abnormalities are poorly understood. Thus, the long-term effect of such alterations needs further investigation. By combining graph theory and statistical analysis methods, we identify and investigate the hub structure of the preterm brain. The results suggest that while the hub structure is preserved, the connectivity strength and capacity of information flow is reduced and that is linked to reduced brain volume as well as preterm birth.

0976



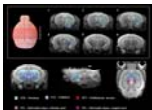
Structural Analysis of Whole Mouse Brain by Magnetic Resonance Histology

Nian Wang<sup>1</sup>, Leonard E. White<sup>2</sup>, Gary Cofer<sup>1</sup>, Yi Qi<sup>1</sup>, and G. Allan Johnson<sup>1</sup>

<sup>1</sup>Department of Radiology, Duke University, Durham, NC, United States, <sup>2</sup>Department of Neurology, Duke University, Durham, NC, United States

Diffusion MRI (dMRI) encompasses a broad range of scales, physical mechanisms and models and applications from clinical to the basic sciences. The recent development of compressed sensing allowed us to extend the spatial and contrast resolution to define more subtle brain architecture beyond the meso scale, solidly in the microscopic domain. We report here dMRI at spatial resolution down to 25  $\mu\text{m}$  i.e. voxels that are more 500,000 times smaller than that of the routine clinical scans.

0977



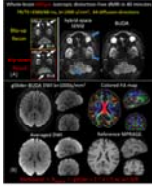
Semi-automated tractography analysis using an Allen mouse brain atlas : comparing DTI acquisition between NEX and SNR

SangJIn Im<sup>1</sup> and Hyeon-Man Baek<sup>2</sup>

<sup>1</sup>Gachon Advanced Institute for Health Sciences & Technology, Gachon university, Incheon, Korea, Republic of, <sup>2</sup>Gachon university, Incheon, Korea, Republic of

Although tractography research was focused primarily on the human brain, tractography was integrated into animal models to benefit from various preclinical experiments. Accurate segmentation is required for proper connectome of animal models. The Allen mouse brain atlas can provide accurate coordinates and segmentation information to the mouse brain, but it is difficult to use because it is not MRI data. In this study, we use the ABA to accurately segment the mouse brain and examine tractography. In addition, various NEX are used to determine the changes in tractography caused by an increase in the SNR of the DTI.

0978



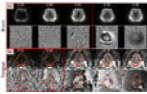
**Distortion-free, submillimeter-isotropic-resolution diffusion MRI with gSlider BUDA-EPI and multi-coil dynamic B0 shimming**

Congyu Liao<sup>1</sup>, Berkin Bilgic<sup>1</sup>, Qiyuan Tian<sup>1</sup>, Jason Stockmann<sup>1</sup>, Qiuyun Fan<sup>1</sup>, Siddharth Srinivasan Iyer<sup>1,2</sup>, Fuyixue Wang<sup>1,3</sup>, Chanon Ngamsombat<sup>1,4</sup>, Xiaozhi Cao<sup>1</sup>, Mary Kate Manhard<sup>1</sup>, Susie Y. Huang<sup>1</sup>, Lawrence L. Wald<sup>1</sup>, and Kawin Setsompop<sup>1</sup>

*<sup>1</sup>Athinoula A. Martinos Center for Biomedical Imaging, Massachusetts General Hospital, Harvard Medical School, Boston, MA, United States, <sup>2</sup>Department of Electrical Engineering and Computer Science, Massachusetts Institute of Technology, Cambridge, MA, United States, <sup>3</sup>Harvard-MIT Health Sciences and Technology, Massachusetts Institute of Technology, Cambridge, MA, United States, <sup>4</sup>Department of Radiology, Faculty of Medicine, Siriraj Hospital, Mahidol University, Thailand*

Diffusion magnetic resonance imaging (dMRI) is a highly sensitive imaging modality, but is limited in spatial resolution and signal-to-noise ratio (SNR). In this work, we combine an SNR-efficient acquisition and model-based reconstruction strategies with newly-available hardware instrumentation to achieve distortion-free in-vivo dMRI at 600-860  $\mu\text{m}$  isotropic voxel size with high fidelity and sensitivity on a clinical 3T scanner. At this resolution, it is possible to accurately probe the microstructure of different cortical layers in the human brain.

0979



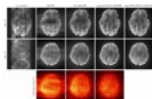
**Prospective Motion Detection and Re-acquisition in Diffusion MRI using Phase image-based Method (PITA-MDD)**

Xiao Liang<sup>1</sup>, Pan Su<sup>2</sup>, Sunil G. Patil<sup>2</sup>, Nahla M.H. Elsaid<sup>3</sup>, Steve Roys<sup>1</sup>, Maureen L. Stone<sup>4</sup>, Rao P. Gullapalli<sup>1</sup>, Jerry L. Prince<sup>5,6</sup>, and Jiachen Zhuo<sup>1</sup>

*<sup>1</sup>Department of Diagnostic Radiology and Nuclear Medicine, University of Maryland School of Medicine, Baltimore, MD, United States, <sup>2</sup>Siemens Medical Solutions USA Inc, Malvern, PA, United States, <sup>3</sup>Department of Radiology and Imaging Sciences, Indiana University School of Medicine, Indianapolis, IN, United States, <sup>4</sup>Department of Neural and Pain Sciences and Department of Orthodontics, University of Maryland School of Dentistry, Baltimore, MD, United States, <sup>5</sup>Department of Electrical and Computer Engineering, Johns Hopkins University, Baltimore, MD, United States, <sup>6</sup>Department of Computer Science, Johns Hopkins University, Baltimore, MD, United States*

We have applied phase image-based motion detection (PITA-MDD) in real-time prospective motion detection and re-acquisition. During image reconstruction, PITA-MDD motion detection is performed on each slice. A diffusion-weighted volume will be re-acquired if number of motion slices exceeds the pre-set threshold. dMRI data were acquired on a volunteer using a prospective PITA-MDD sequence for the brain and the tongue. The detected motion corrupted data were consistent with subject's motion. Denser tongue muscle fibers were visible after replacing motion volumes with re-acquired volumes. Prospective PITA-MDD motion detection and re-acquisition has improved dMRI acquisition, especially in challenging areas, such as the tongue.

0980



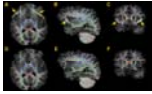
**Phase-matched Self-calibrated K-space Phase Correction Method for Multi-shot Diffusion Imaging**

Zhe Zhang<sup>1</sup>, Xiaodong Ma<sup>2</sup>, Lanxin Ji<sup>1</sup>, Jing Jing<sup>1</sup>, Wanlin Zhu<sup>1</sup>, Zhangxuan Hu<sup>3</sup>, Yishi Wang<sup>4</sup>, Hua Guo<sup>3</sup>, and Yongjun Wang<sup>1,5</sup>

*<sup>1</sup>China National Clinical Research Center for Neurological Diseases, Beijing Tiantan Hospital, Capital Medical University, Beijing, China, <sup>2</sup>Center for Magnetic Resonance Research, University of Minnesota, Minneapolis, MN, United States, <sup>3</sup>Center for Biomedical Imaging Research, Department of Biomedical Engineering, School of Medicine, Tsinghua University, Beijing, China, <sup>4</sup>Philips Healthcare, Beijing, China, <sup>5</sup>Department of Neurology, Beijing Tiantan Hospital, Capital Medical University, Beijing, China*

Multi-shot acquisition enables high-resolution diffusion imaging, but the artifacts caused by shot-to-shot phase variation must be corrected. Self-calibrated multi-shot DWI methods utilize parallel imaging reconstruction to solve the phase of each shot. Previously reported self-calibrated GRAPPA with a compact kernel (SC-ckGRAPPA) method is compromised by the high reduction factor when recovering the navigator information. In this work, PM-SC-ckGRAPPA was introduced with the phase-matched reconstruction, and evaluated via in-vivo experiment. Results show that PM-SC-ckGRAPPA provides improved reconstruction compared with conventional approaches, and PM-SC-ckGRAPPA can be a potential tool for high-resolution diffusion imaging.

0981



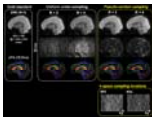
### Fat-shift suppression in diffusion MRI using rotating phase encoding and localised outlier weighting

Daan Christiaens<sup>1,2</sup>, Lucilio Cordero-Grande<sup>1,3</sup>, Jana Hutter<sup>3,4</sup>, Anthony N Price<sup>3,4</sup>, Jonathan O'Muircheartaigh<sup>1</sup>, Katy Vecchiato<sup>1</sup>, Joseph V Hajnal<sup>1,3</sup>, and J-Donald Tournier<sup>1,3</sup>

<sup>1</sup>Centre for the Developing Brain, School of Biomedical Engineering and Imaging Sciences, King's College London, London, United Kingdom, <sup>2</sup>Department of Electrical Engineering (ESAT/PSI), KU Leuven, Leuven, Belgium, <sup>3</sup>Biomedical Engineering Department, School of Biomedical Engineering and Imaging Sciences, King's College London, London, United Kingdom, <sup>4</sup>Centre for the Developing Brain, King's College London, London, United Kingdom

Diffusion MRI is prone to fat-shift artefacts, especially in accelerated diffusion MRI with higher b-values. Building on the property that the fat signal localisation depends on the phase encoding direction, we propose to suppress fat-shift artefacts in post-processing using localised outlier rejection across 4 different phase encoding directions. To this end, we extend a retrospective diffusion MRI motion correction framework with local outlier weights, defined as a voxel-wise measure of the MR reconstruction residuals. Comparative results in a pediatric brain imaging cohort show that the proposed method reduces fat-shift artefacts in the parenchyma without affecting the reconstruction in uncorrupted regions.

0982



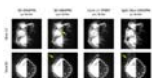
### High-Resolution 3D Multi-shot Diffusion-Weighted Imaging with Pseudo-Random Sampling and Compressed Sensing

Hing-Chiu Chang<sup>1</sup> and Xiaoxi Liu<sup>1,2</sup>

<sup>1</sup>Department of Diagnostic Radiology, The University of Hong Kong, Hong Kong, Hong Kong, <sup>2</sup>Department of Radiology and Biomedical Imaging, University of California San Francisco, San Francisco, CA, United States

3D multi-shot diffusion-weighted imaging (msDWI) with multi-slab acquisition can achieve high-resolution diffusion-tensor imaging (DTI), but additional correction is required to eliminate slab boundary artifact associated with multi-slab acquisition. A proposed 3D-MUSER technique can improve the feasible slab thickness by enabling 3D phase correction with a 3D single-shot navigator, thereby making single-slab 3D DTI feasible. However, the relatively long scantime can limit the applications of 3D DTI in neuroscience research, despite high spatial resolution attainable. In this study, we proposed a potential strategy to develop a 3D DTI technique capable of high scan acceleration.

0983



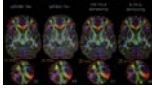
### Coil-joint-split N/2 Ghost Correction and Joint L1-SPIRiT for SMS-EPI Reconstruction: Demonstration Using 7T HCP-style Diffusion Acquisition

Ziyi Pan<sup>1</sup>, Hua Guo<sup>1</sup>, Erpeng Dai<sup>2</sup>, Edward J. Auerbach<sup>3</sup>, Kamil Ugurbil<sup>3</sup>, and Xiaoping Wu<sup>3</sup>

<sup>1</sup>Center for Biomedical Imaging Research, Department of Biomedical Engineering, School of Medicine, Tsinghua University, Beijing, China, <sup>2</sup>Department of Radiology, Stanford University, Stanford, CA, United States, <sup>3</sup>Center for Magnetic Resonance Research, Radiology, Medical School of the University of Minnesota, Minneapolis, MN, United States

Simultaneous Multislice (SMS) has become a major acceleration technique in Human Connectome Project (HCP) to acquire high-resolution diffusion and functional MRI. Conventional reconstruction for SMS-EPI includes using traditional Nyquist ghost correction and slice GRAPPA that usually requires single-band (SB) reference scans. In this work, we introduce a novel reference-less Nyquist ghost correction approach and a new joint L1-spirit reconstruction algorithm without the need of SB reference scans. We evaluated the performance of the proposed method by acquiring 7T HCP-style diffusion and show that the proposed method can effectively suppress the strong residual aliasing/ghosting as observed for when using conventional reconstruction.

0984



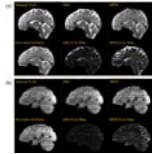
#### Structure preserving noise removal in Hilbert space from ultra-high resolution diffusion MRI data

Gabriel Ramos-Llordén<sup>1</sup>, Gonzalo Vegas-Sanchez-Ferrero<sup>1</sup>, Congyu Liao<sup>2</sup>, Carl-Fredrik Westin<sup>1</sup>, Kawin Setsompop<sup>2</sup>, and Yogesh Rathi<sup>1</sup>

<sup>1</sup>Brigham and Women's Hospital, Harvard Medical School, Boston, MA, United States, <sup>2</sup>Massachusetts General Hospital, Harvard Medical School, Charlestown, MA, United States

In-vivo submillimeter resolution diffusion MRI suffers from limited signal-to-noise ratio (SNR) due to the small voxel size. Denoising techniques can improve the SNR and facilitate further dMRI analysis. Among them, perhaps PCA-based (e.g. Marchenko-Pastur PCA) have shown the best performance. In this work, we introduce kernel PCA, a powerful nonlinear generalization of linear PCA to Hilbert spaces that is shown to suppress a substantial amount of noise (which MP-PCA is incapable of) and still reliably preserve dMRI signal. We showcase K-PCA noise removal with 660 micrometer gSlider data, where we compared it qualitatively and quantitatively with MP-PCA.

0985



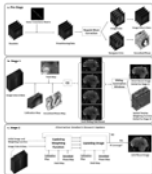
#### Rapid Boundary Artifacts Correction for Simultaneous Multi-slab (SMSlab) Acquisition Using Convolutional Network

Jieying Zhang<sup>1</sup>, Simin Liu<sup>1</sup>, Yuhsuan Wu<sup>1</sup>, and Hua Guo<sup>1</sup>

<sup>1</sup>Center for Biomedical Imaging Research, Department of Biomedical Engineering, School of Medicine, Tsinghua University, Beijing, China

Simultaneous multi-slab (SMSlab) technique is a 3D acquisition method that can achieve optimal signal-to-noise ratio (SNR) efficiency for high-resolution diffusion-weighted imaging (DWI) or functional MRI (fMRI). However, boundary artifacts may restrain its application. Nonlinear inversion for slab profile encoding (NPEN) has been proposed for its correction, which needs long computation time. In this study, we propose to use a convolutional network for boundary artifacts correction. It can solve the problem in a short time and improve the signal-to-noise ratio (SNR), which is of great meaning for high-resolution whole-brain DWI and fMRI.

0986



#### Sliding-Slab Profile Encoding (SLIPEN) for Eliminating Slab Boundary Artifact in Three-Dimensional Multi-slab Diffusion-Tensor Imaging

Xiaoxi Liu<sup>1,2</sup>, Di Cui<sup>1</sup>, Xucheng Zhu<sup>2</sup>, Edward S. Hui<sup>1,3</sup>, Queenie Chan<sup>4</sup>, Peder E.Z. Larson<sup>2</sup>, and Hing-Chiu Chang<sup>1</sup>

<sup>1</sup>Department of Diagnostic Radiology, The University of Hong Kong, Hong Kong, China, <sup>2</sup>Department of Radiology and Biomedical Imaging, University of California San Francisco, San Francisco, CA, United States, <sup>3</sup>The State Key Laboratory of Brain and Cognitive Sciences, Hong Kong, China, <sup>4</sup>Philips Healthcare, Hong Kong, China



3D multi-slab diffusion-tensor imaging (DTI) can enable high-resolution DTI at submillimeter voxel size. However, the slab boundary artifact and distortion along slab direction can deteriorate the data quality of 3D DTI, thereby limiting its applications. In this work, we proposed a sliding-slab profile encoding (SLIPEN) method to acquire the 3D multi-slab DTI data with sliding-slab technique, and to reconstruct the data free from slab boundary artifact. In addition, off-resonance correction can be incorporated into SLIPEN for producing high-quality artifact-free 3D DTI data.

---

---

## Corporate Symposium

### Gold Corporate Symposium: Philips Healthcare

Plenary Hall (Grand Ballroom)

Wednesday 19:15 - 20:15 UTC

---

---

Thursday, 13 August 2020

## Evening Event

### Closing Session

Thursday 2:00 - 5:00 UTC

---

---

## Plenary Session

### Plenary Session Thursday - MRI in Patients with Implantable Electronic Devices

Organizers: Vikas Gulani, Peng Hu, Tim Leiner, Yunhong Shu, Claude Sirlin

Thursday Plenary

Thursday 12:00 - 14:05 UTC

Moderators: Vikas Gulani & Peng Hu

#### MRI & Cardiovascular Implantable Electronic Devices (CIEDs): Best Practices

Pamela Woodard<sup>1</sup>

<sup>1</sup>Washington Univ. School of Medicine, United States

---

#### The Risks of MRI & Cardiovascular Implantable Electronic Devices: Separating Truth from Fiction

Robert Russo

---

#### MRI & Other Implantable Electronic Devices: Best Practices

Kagayaki Kuroda<sup>1</sup>

<sup>1</sup>School of Info Sci & Tech, Tokai University, Japan

---

---

## Plenary Session

### Plenary Session Thursday - Mansfield Lecture: Imaging the First 1000 Days of Life: Challenges & Opportunities

Thursday Plenary

Thursday 12:00 - 14:05 UTC

---

---

## Weekday Course

### Novel imaging techniques for CMR - Approaches to Pediatric Cardiovascular Imaging

Organizers: Jennifer Steeden, Peng Hu, Jennifer Keegan

Thursday Parallel 3 Live Q&A

Thursday 14:20 - 15:05 UTC

Moderators: J. Paul Finn

### Increasing Speed of Acquisition for Pediatric Imaging

Adrienne Campbell-Washburn<sup>1</sup>

<sup>1</sup>National Heart, Lung, and Blood Institute, National Institutes of Health, Bethesda, MD, United States

This presentation will provide an overview of fast imaging methods used for pediatric cardiovascular MR. Specifically, it will focus on: New developments in data undersampling paired with advanced image reconstruction, non-Cartesian acquisitions, rapid free-breathing methods, multi-parametric imaging approaches, and applications of machine learning for rapid imaging.

---

### Overcoming Problems With Motion for Pediatric Imaging

Mehdi Hedjazi Moghari<sup>1</sup>

<sup>1</sup>Harvard Medical School, United States

Pediatric cardiovascular magnetic resonance (CMR) imaging is challenging due to bulk, respiratory, and cardiac motion. This lecture will cover key concepts in motion correction, including sedation, electrocardiogram (ECG) gating, cardiac self-gating, respiratory navigators, respiratory self-gating, and the state-of-the-art comprehensive free-breathing 3-dimensional (3D) CMR imaging.

---

### State-of-the-Art Pediatric Cardiovascular MRI & Research Techniques

Vivek Muthurangu<sup>1</sup>

<sup>1</sup>University College London, United Kingdom

---

### Pediatric Cardiovascular MR: The Clinical Need, The Fun & The Challenges

Mark Fogel<sup>1</sup>

<sup>1</sup>Children's Hospital of Philadelphia, Philadelphia, PA, United States

---

## Oral - Power Pitch

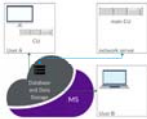
### Quantification, ML, and Tools - MRI Toolbox

Thursday Parallel 1 Live Q&A

Thursday 14:20 - 15:05 UTC

Moderators: Daniel Gallichan & Jon Nielsen

1037



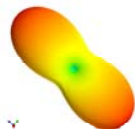
### CAMRI – Cloud-Accessible MRI Emulator

Eros Montin<sup>1,2</sup>, Giuseppe Carluccio<sup>1,2</sup>, Christopher Michael Collins<sup>1,2</sup>, and Riccardo Lattanzj<sup>1,2,3</sup>

<sup>1</sup>Department of Radiology, Bernard and Irene Schwartz Center for Biomedical Imaging, New York University School of Medicine, New York, NY, United States, <sup>2</sup>Department of Radiology, Center for Advanced Imaging Innovation and Research (CAI2R), New York University School of Medicine, New York, NY, United States, <sup>3</sup>Sackler Institute of Graduate Biomedical Sciences, New York University School of Medicine, New York, NY, United States

CAMRI is a web-based application designed to emulate MRI experiments. It provides a numerical simulator of the Bloch equations, and enables to import electromagnetic field distributions as well as voxelized objects. A user-friendly graphic user interface guides users through the selection of predefined object geometries, with corresponding B<sub>0</sub>, B<sub>1</sub> and gradient fields distributions. Users can then customize sequence parameters and simulate the full MRI experiment from k-space acquisition to image reconstruction. Results can be seamlessly visualized and compared across different settings. The application will be distributed via the Cloud MR portal, which allows running simulations on the cloud.

---

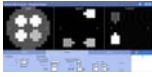


### Sycomore: an MRI simulation toolkit

Julien Lamy<sup>1</sup> and Paulo Loureiro de Sousa<sup>1</sup>

<sup>1</sup>*ICube, University of Strasbourg-CNRS, Strasbourg, France*

Sycomore is an open-source MRI simulation toolkit which provides a user-friendly and consistent interface in Python for five different simulation models (Bloch simulation, three variants of EPG and the Configuration Model). Its C++ computing core, additionally helped by OpenMP, offers efficient computation of those five simulation models on desktop computers. The interactive run-time achievable for classical MRI experiments make it a valuable tool for rapid development of sequence prototypes and for teaching.

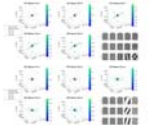


### Virtual Scanner: MRI Experiments in a Browser

Gehua Tong<sup>1,2</sup>, Sairam Geethanath<sup>2</sup>, Keerthi Sravan Ravi<sup>1,2</sup>, Marina Manso Jimeno<sup>1,2</sup>, Enlin Qian<sup>1,2</sup>, and John Thomas Vaughan, Jr.<sup>2</sup>

<sup>1</sup>*Department of Biomedical Engineering, Columbia University, New York, NY, United States*, <sup>2</sup>*Columbia Magnetic Resonance Research Center, Columbia University, New York, NY, United States*

Open-source standards for MR pulse sequences and data have been recently developed, but there is no unified platform for combining them with implemented simulation, reconstruction, and analysis tools to the best of our knowledge. We designed Virtual Scanner in order to provide a platform that allows rapid prototyping of new MR software and hardware. It also serves as a training tool for MR technicians and physicists. Two modes are provided: Standard Mode mimics MR scanner interfaces to assist training, while Advanced Mode allows customized simulation of each step in the signal chain.



### 3D Spatially-Resolved Phase Graph

Xiang Gao<sup>1</sup>, V.G. Kiselev<sup>1</sup>, Thomas Lange<sup>1</sup>, Jürgen Hennig<sup>1</sup>, and Maxim Zaitsev<sup>1</sup>

<sup>1</sup>*Medical Center University of Freiburg, Faculty of Medicine, University of Freiburg, Freiburg im Breisgau, Germany*

A new open source recursive magnetization evolution calculation algorithm is proposed for simulating arbitrary pulse sequences efficiently and intuitively. It lifts the sequence symmetry requirements of the Extended Phase Graph and avoids intensive computations associated with direct Bloch equation simulations. The method further allows for tracking the evolution of the MR signal and corresponding k-vectors in presence of time-variant gradients with arbitrary orientations in 3D domain.

To illustrate the developed technique, two simple examples are presented: spoiler design for the PRESS-based magnetic spectroscopic imaging (MRSI) and fast off-resonance calculation for dictionary building in Magnetic Resonance Fingerprinting (MRF).



### A dynamic digital phantom with realistic vasculature and perfusion based on MR histology

Chengyue Wu<sup>1</sup>, David A. Hormuth<sup>2</sup>, Federico Pineda<sup>3</sup>, Gregory S. Karczmar<sup>3</sup>, Robert D. Moser<sup>2,4</sup>, and Thomas E. Yankeelov<sup>1,2,5,6</sup>

<sup>1</sup>*Department of Biomedical Engineering, University of Texas at Austin, Austin, TX, United States*, <sup>2</sup>*Oden Institute for Computational Engineering and Sciences, University of Texas at Austin, Austin, TX, United States*, <sup>3</sup>*Department of Radiology, University of Chicago, Chicago, IL, United States*, <sup>4</sup>*Department of Mechanical Engineering, University of Texas at Austin, Austin, TX, United States*, <sup>5</sup>*Department of Diagnostic Medicine, University of Texas at Austin, Austin, TX, United States*, <sup>6</sup>*Department of Oncology, University of Texas at Austin, Austin, TX, United States*

Digital phantoms are valuable tools for developing or optimizing new imaging techniques, devices, and analyses. In this contribution, we seek to develop a dynamic digital phantom which contains a detailed representation of vascular structure, tissue properties, and perfusion based on high-resolution MRI data of a rat kidney (courtesy of the Duke Center for In Vivo Microscopy). This dynamic digital phantom can be used to simulate perfusion and diffusion MRI techniques, and systematically evaluate new magnetic resonance imaging acquisition reconstruction/image processing techniques.

1042



#### Numerical simulation of 4D Flow MRI

Thomas Puiseux<sup>1,2</sup>, Anou Sewonu<sup>1,3</sup>, Ramiro Moreno<sup>1,3,4</sup>, Simon Mendez<sup>2</sup>, and Franck Nicoud<sup>2</sup>

<sup>1</sup>SPIN UP, Toulouse, France, <sup>2</sup>IMAG, Univ. Montpellier, CNRS, Montpellier, France, <sup>3</sup>I2MC, INSERM U1048, Toulouse, France, <sup>4</sup>ALARA Expertise, Strasbourg, France

The present study proposes a novel approach to efficiently simulate 4D Flow MRI acquisitions in realistic complex flow conditions. Navier-Stokes and Bloch equations are simultaneously solved with Eulerian-Lagrangian coupling. A semi-analytic solution for the Bloch equation as well as a periodic particle re-injection strategy are implemented to reduce the computational cost. The Bloch solver and the velocity reconstruction pipeline were first validated in a steady flow configuration. The coupled 4D Flow MRI simulation procedure was validated in a complex pulsatile flow phantom cardiovascular-typical experiment. Besides, we compared simulated MR velocity data with experimental 4D Flow MRI measurements.

1043



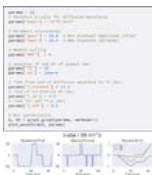
#### Event-Based Traversing of Hierarchical Sequences Allows Real-Time Execution and Arbitrary Looping in a Scanner-Independent MRI Framework

Daniel Christopher Hoinkiss<sup>1</sup>, Cristoffer Cordes<sup>1</sup>, Simon Konstandin<sup>1</sup>, and Matthias Günther<sup>1,2</sup>

<sup>1</sup>MR Physics, Fraunhofer MEVIS, Bremen, Germany, <sup>2</sup>MR-Imaging & Spectroscopy, Faculty 01 (Physics/Electrical Engineering), University of Bremen, Bremen, Germany

MR sequence development is either based on complex, platform-specific solutions or restricted by fixed sequence structures together with a strict hierarchical implementation of loops. This abstract introduces event-based traversing of  $\gamma^{\text{STAR}}$  sequences together with a buffered real-time execution at the scanner. The concept provides easy implementation of arbitrary, interleaved loop structures as well as memory efficient, real-time capable sequence execution in a vendor-agnostic environment. It is demonstrated for interleaved loop structures in a pCASL 3D GRASE sequence for brain perfusion imaging.

1044



#### Gradient Optimization (GrOpt) Toolbox: A Software Package for Fast Gradient Waveform Design

Michael Loecher<sup>1,2</sup>, Matthew Middione<sup>1,2</sup>, and Daniel B Ennis<sup>1,2,3,4</sup>

<sup>1</sup>Radiology, Stanford, Palo Alto, CA, United States, <sup>2</sup>Radiology, Veterans Administration Health Care System, Palo Alto, CA, United States, <sup>3</sup>Cardiovascular Institute, Stanford, Palo Alto, CA, United States, <sup>4</sup>Center for Artificial Intelligence in Medicine & Imaging, Stanford, Palo Alto, CA, United States

Objective: To introduce and demonstrate a software library for time-optimal gradient waveform optimization for a wide range of applications. The software allows for direct just-in-time gradient waveform design on scanner hardware for multiple vendors. The software is tested over a range of constraints and acquisition types for which compute times are on the order of (1-100ms). The sequences are also implemented on two different vendor scanners, demonstrating the interoperability of the method.



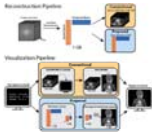
#### SigPy.RF: Comprehensive Open-Source RF Pulse Design Tools for Reproducible Research

Jonathan B Martin<sup>1</sup>, Frank Ong<sup>2</sup>, Jun Ma<sup>1</sup>, Jonathan I Tamir<sup>3,4</sup>, Michael Lustig<sup>3</sup>, and William A Grissom<sup>1</sup>



<sup>1</sup>Biomedical Engineering, Vanderbilt University, Nashville, TN, United States, <sup>2</sup>Electrical Engineering, Stanford University, Stanford, CA, United States, <sup>3</sup>Electrical Engineering and Computer Sciences, University of California, Berkeley, Berkeley, CA, United States, <sup>4</sup>Electrical and Computer Engineering, UT Austin, Austin, TX, United States

We present SigPy.RF, an extensive set of open-source, Python-based tools for MRI RF pulse design. This toolbox extends the SigPy Python software package and leverages SigPy's existing capabilities for GPU computation, iterative optimization, and powerful abstractions for linear operators, proximal operators, and applications. Tools are available for all steps of the excitation design process including trajectory/gradient design, pulse design, and simulation. Our implemented functions for pulse design include advanced SLR, multiband, adiabatic, optimal control, B<sub>1</sub>-selective and small-tip pTx designers. SigPy.RF pulse designs were validated in simulations and a pTx experiment.

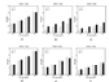


A Reconstruction Compatible, Fast and Memory Efficient Visualization Framework for Large-scale Volumetric Dynamic MRI

Cedric Yue Sik Kin<sup>1</sup>, Frank Ong<sup>2</sup>, Jonathan I Tamir<sup>3,4</sup>, Michael Lustig<sup>3</sup>, John M Pauly<sup>2</sup>, and Shreyas S Vasanaawala<sup>1</sup>

<sup>1</sup>Radiology, Stanford University, Stanford, CA, United States, <sup>2</sup>Electrical Engineering, Stanford University, Stanford, CA, United States, <sup>3</sup>Electrical and Computer Sciences, UC Berkeley, Berkeley, CA, United States, <sup>4</sup>Electrical and Computer Engineering, The University of Texas at Austin, Austin, TX, United States

We addressed the speed and memory shortcomings of conventional visualization consoles when processing high-dimensional MRI datasets by proposing a novel approach that leverages compressed representations of such datasets. We considered low rank reconstructions and operated on them directly for visualization, unlike traditional viewers which load entire uncompressed image datasets. We built a web viewer that utilizes this approach to demonstrate real time reformatting and slicing. We were able to achieve more than 15x reduction in both memory usage and loading times.



Specific Absorption Rate prediction for open source pulse sequence programming

Sairam Geethanath<sup>1</sup>, Jon-Fredrik Nielsen<sup>2</sup>, Douglas C Noll<sup>2</sup>, and John Thomas Vaughan Jr.<sup>1</sup>

<sup>1</sup>Columbia MR Research Center, Columbia University, New York, NY, United States, <sup>2</sup>University of Michigan, Ann Arbor, MI, United States

Flexibility in designing custom pulse sequences has a direct impact on the development of diverse MR techniques and strategies. However, it is important to be cognizant of the MR safety risks that are associated with such custom sequences. We develop and evaluate an open source software package to predict global Specific Absorption Rate for Pulseseq and TOPPE based sequences. We compare the resulting predictions with scanner reported SAR values for different flip angles and three sample weights, on two major MR vendor platforms. The predictions correlate highly with the scanner reported values: R<sub>2</sub> = 0.87 (vendor 1); 0.99 (vendor 2).



MRI Raw Data Compression for long-term storage in large-scale population imaging

Philipp Ehses<sup>1</sup>, Marten Veldmann<sup>1</sup>, Yiming Dong<sup>1</sup>, and Tony Stöcker<sup>1</sup>

<sup>1</sup>German Center for Neurodegenerative Diseases (DZNE), Bonn, Germany

In the overwhelming majority of MRI studies, only the reconstructed images are stored and the raw data that was used during the reconstruction process is lost. However, routine raw data storage would potentially allow imaging studies that are conducted now to benefit from future improved image reconstruction techniques. Unfortunately, the raw data storage requirements are often prohibitive, especially in large-scale population studies. We developed a flexible software tool that achieves high lossy compression of MRI raw data and is able to decompress the data back to the vendor-specific format to allow for retrospective reconstruction using the vendor's reconstruction pipeline.

1049



### Chemical sHift bAsed pRospective k-Space anyMizAtion (CHARISMA)

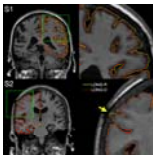
Hendrik Mattern<sup>1</sup>, Martin Knoll<sup>1</sup>, Falk Lüsebrink<sup>1,2</sup>, and Oliver Speck<sup>1,3,4,5</sup>

*<sup>1</sup>Biomedical Magnetic Resonance, Otto-von-Guericke University, Magdeburg, Germany, <sup>2</sup>Medicine and Digitalization, Otto-von-Guericke University, Magdeburg, Germany, <sup>3</sup>German Center for Neurodegenerative Disease, Magdeburg, Germany, <sup>4</sup>Center for Behavioral Brain Sciences, Magdeburg, Germany, <sup>5</sup>Leibniz Institute for Neurobiology, Magdeburg, Germany*

One key element of open science is to make all data publicly available. In case of neuroscience, reconstructed images can be defaced to prevent data privacy violations, but no strategy to anonymize raw data has been presented to our best knowledge.

Here, chemical shift based prospective k-Space anonymization is presented. The subject wears an oil-filled mask which is superimposed onto the subject's skin due to chemical shift. This low-cost solution (<15€) is easy to build and applicable for sequences with sufficient chemical shift in the A-P direction.

1050



### Longitudinal FreeSurfer with non-linear subject-specific template improves sensitivity to cortical thinning

Malte Hoffmann<sup>1,2</sup>, David Salat<sup>1,2</sup>, Martin Reuter<sup>\*1,2,3</sup>, and Bruce Fischl<sup>\*1,2,4</sup>

*<sup>1</sup>Athinoula A. Martinos Center for Biomedical Imaging, Charlestown, MA, United States, <sup>2</sup>Department of Radiology, Harvard Medical School, Boston, MA, United States, <sup>3</sup>German Center for Neurodegenerative Diseases, Bonn, Germany, <sup>4</sup>Computer Science and Artificial Intelligence Laboratory, Massachusetts Institute of Technology, Cambridge, MA, United States*

Longitudinal FreeSurfer creates a within-subject template by rigidly registering and median-filtering longitudinal timepoints (TP). Information common to all TPs is extracted from the template for unbiased TP initialization, resulting in substantial improvements over cross-sectional processing. However, this approach is not optimal in the presence of severe atrophy or other large-scale anatomical change, which causes voxels to be filtered across tissue classes. We address this problem by introducing an enhanced longitudinal stream that deforms each TP using non-linear registration to construct the template. We demonstrate considerable increases in sensitivity to cortical thinning, without affecting test-retest reliability.

1051



### Developing a Novel and Robust Preprocessing Pipeline for Intensity-Based High-Resolution Magnetic Resonance Angiogram

Wei Zhu<sup>1</sup>, Yi Zhang<sup>1</sup>, Xiao-Hong Zhu<sup>1</sup>, and Wei Chen<sup>1</sup>

*<sup>1</sup>Center for Magnetic Resonance Research, Department of Radiology, University of Minnesota, Minneapolis, MN, United States*

In-vivo high-resolution imaging of cerebral blood vessels is critical for brain functional research and clinical diagnosis. Despite well-developed magnetic resonance angiogram (MRA) techniques, a simple, robust preprocessing procedure has yet to be established. Thus, we propose a preprocessing pipeline that includes zero-fill interpolation, intensity non-uniformity correction, image denoising, vessel enhancement and segmentation. Specifically, we found that the most effective and robust denoising method is anisotropic total variation (ATV). By adopting and optimizing an improved 3D Hessian based tubular and spherical enhancement filter and a region-based level-set image segmentation method, we can automate the preprocessing of intensity-based MRAs with high fidelity.

## Oral - Power Pitch

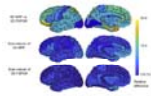
### Quantification, ML, and Tools - Quantitative MRI: Reproducibility, Robustness & New Directions

Thursday Parallel 1 Live Q&A

Thursday 14:20 - 15:05 UTC

Moderators: Gastao Cruz

1007



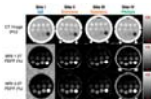
#### Reproducibility and Repeatability of Three-dimensional Magnetic Resonance Fingerprinting-based Human Brain Morphometry

Shohei Fujita<sup>1,2</sup>, Guido Buonincontri<sup>3,4</sup>, Matteo Cencini<sup>3,5</sup>, Naoyuki Takeji<sup>6</sup>, Rolf F. Schulte<sup>7</sup>, Issei Fukunaga<sup>1</sup>, Akifumi Hagiwara<sup>1</sup>, Wataru Uchida<sup>1,8</sup>, Masaaki Hori<sup>9</sup>, Ryusuke Irie<sup>1,2</sup>, Koji Kamagata<sup>1</sup>, Osamu Abe<sup>2</sup>, and Shigeki Aoki<sup>1</sup>

<sup>1</sup>Department of Radiology, Juntendo University, Tokyo, Japan, <sup>2</sup>Department of Radiology, The University of Tokyo, Tokyo, Japan, <sup>3</sup>Imago7 Foundation, Pisa, Italy, <sup>4</sup>IRCCS Stella Maris, Pisa, Italy, <sup>5</sup>Department of Physics, University of Pisa, Pisa, Italy, <sup>6</sup>MR Applications and Workflow, GE Healthcare, Tokyo, Japan, <sup>7</sup>GE Healthcare, Munich, Germany, <sup>8</sup>Department of Radiological Sciences, Tokyo Metropolitan University, Tokyo, Japan, <sup>9</sup>Department of Radiology, Toho University Omori Medical Center, Tokyo, Japan

Magnetic Resonance fingerprinting (MRF) provides simultaneous acquisition of T1 and T2 values with high reliability. However, the reproducibility and repeatability of human brain morphometry based on MRF still requires investigation. Here, we examined the feasibility of three-dimensional (3-D) MRF to evaluate the brain cortical thickness and volumetric analysis in healthy volunteers. Scan-rescan tests of both 3-D MRF and conventional 3D T1-weighted imaging were performed. For each sequence, the regional cortical thickness and volume of the subcortical structures were measured using automatic brain segmentation software. High agreement between conventional scans and scan-rescan repeatability in healthy human brains were observed.

1008



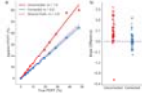
#### Multi-Site, Multi-Vendor Validation of the Accuracy and Reproducibility of Fat Quantification using a Novel MRI and CT Compatible Fat Phantom

Ruiyang Zhao<sup>1,2</sup>, Diego Hernando<sup>1,2</sup>, David T Harris<sup>1</sup>, Louis Hinshaw<sup>3</sup>, Ke Li<sup>1,2</sup>, Jessica Miller<sup>4</sup>, Perry J Pickhardt<sup>1</sup>, Ihab R Kamel<sup>5</sup>, Mahadevappa Mahesh<sup>5</sup>, Mounes Aliyari Ghasabeh<sup>5</sup>, Mustafa R Bashir<sup>6,7,8</sup>, Jean Shaffer<sup>6,7</sup>, Carolyn Lowry<sup>6</sup>, Daniele Marin<sup>6</sup>, Takeshi Yokoo<sup>9</sup>, Lakshmi Ananthakrishnan<sup>9</sup>, Xinhui Duan<sup>9</sup>, and Scott B Reeder<sup>1,2,3,10,11</sup>

<sup>1</sup>Radiology, University of Wisconsin-Madison, Madison, WI, United States, <sup>2</sup>Medical Physics, University of Wisconsin-Madison, Madison, WI, United States, <sup>3</sup>Biomedical Engineering, University of Wisconsin-Madison, Madison, WI, United States, <sup>4</sup>Human Oncology, University of Wisconsin-Madison, Madison, WI, United States, <sup>5</sup>Radiology, Johns Hopkins University, Baltimore, MD, United States, <sup>6</sup>Radiology, Duke University, Durham, NC, United States, <sup>7</sup>Center for Advanced Magnetic Resonance Development, Duke University, Durham, NC, United States, <sup>8</sup>Medicine, Duke University, Durham, NC, United States, <sup>9</sup>Radiology, University of Texas Southwestern, Dallas, TX, United States, <sup>10</sup>Medicine, University of Wisconsin-Madison, Madison, WI, United States, <sup>11</sup>Emergency Medicine, University of Wisconsin-Madison, Madison, WI, United States

Accurate quantification of liver fat content is needed for early detection, staging, and treatment monitoring of non-alcoholic fatty liver disease. Chemical shift encoded MRI techniques enable accurate fat quantification through proton density fat fraction maps. CT is capable of quantifying fat based on the decrease in attenuation with increasing liver fat concentration. Current MR quantitative fat phantoms do not accurately mimic CT-based attenuation in the presence of liver fat. Therefore, the purpose of this work was to develop and validate the performance of a novel multimodality phantom that mimics the signals of liver fat in both MRI and CT.

1009



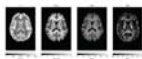
### Multi-Center Phantom Validation of a Novel Method for Temperature Correction in PDFF Estimation using Magnitude Chemical Shift-Encoded MRI

Ruvini Navaratna<sup>1,2</sup>, Timothy J Colgan<sup>1</sup>, Ruiyang Zhao<sup>1,2</sup>, Houchun Harry Hu<sup>3</sup>, Mark Bydder<sup>4</sup>, Takeshi Yokoo<sup>5</sup>, Mustafa R Bashir<sup>6,7,8</sup>, Michael S Middleton<sup>9</sup>, Suraj D Serai<sup>10</sup>, Daria Malyarenko<sup>11</sup>, Thomas Chenevert<sup>11</sup>, Mark Smith<sup>3</sup>, Walter Henderson<sup>9</sup>, Gavin Hamilton<sup>9</sup>, Yunhong Shu<sup>12</sup>, Claude B Sirlin<sup>9</sup>, Jean A Tkach<sup>13</sup>, Andrew T Trout<sup>13</sup>, Jean H Brittain<sup>14</sup>, Diego Hernando<sup>1,2</sup>, and Scott B Reeder<sup>1,2,15,16,17</sup>

<sup>1</sup>Radiology, University of Wisconsin-Madison, Madison, WI, United States, <sup>2</sup>Medical Physics, University of Wisconsin-Madison, Madison, WI, United States, <sup>3</sup>Radiology, Nationwide Children's Hospital, Columbus, OH, United States, <sup>4</sup>Radiological Sciences, University of California - Los Angeles, Los Angeles, CA, United States, <sup>5</sup>Radiology, University of Texas Southwestern Medical Center, Dallas, TX, United States, <sup>6</sup>Radiology, Duke University Medical Center, Durham, NC, United States, <sup>7</sup>Division of Gastroenterology, Duke University Medical Center, Durham, NC, United States, <sup>8</sup>Center for Advanced Magnetic Resonance Development, Duke University Medical Center, Durham, NC, United States, <sup>9</sup>Radiology, University of California - San Diego, San Diego, CA, United States, <sup>10</sup>Radiology, Children's Hospital of Philadelphia, Philadelphia, PA, United States, <sup>11</sup>Radiology, University of Michigan, Ann Arbor, MI, United States, <sup>12</sup>Radiology, Mayo Clinic, Rochester, MN, United States, <sup>13</sup>Radiology, Cincinnati Children's Hospital Medical Center, Cincinnati, OH, United States, <sup>14</sup>Calimetrix, LLC, Madison, WI, United States, <sup>15</sup>Biomedical Engineering, University of Wisconsin-Madison, Madison, WI, United States, <sup>16</sup>Medicine, University of Wisconsin-Madison, Madison, WI, United States, <sup>17</sup>Emergency Medicine, University of Wisconsin-Madison, Madison, WI, United States

Chemical shift-encoded MRI (CSE-MRI) is well-established to quantify proton density fat-fraction (PDFF) as a quantitative biomarker of hepatic steatosis.<sup>1</sup> However, temperature is known to affect the accuracy and precision of PDFF quantification.<sup>2</sup> In this study, we aim to characterize the effects of temperature on PDFF quantification using computer simulations, temperature-controlled phantom experiments, and a multi-center phantom study. Further, we present a novel method to minimize temperature-related fat quantification bias for magnitude-based CSE-MRI methods.

1010



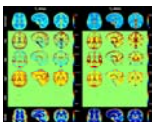
### Myelin-sensitive Quantitative Maps: Two's Company, Three's a Crowd?

Matteo Mancini<sup>1,2,3</sup>, Eva Alonso-Ortiz<sup>2</sup>, Mara Cercignani<sup>1</sup>, Julien Cohen-Adad<sup>2</sup>, and Nikola Stikov<sup>2</sup>

<sup>1</sup>Department of Neuroscience, Brighton and Sussex Medical School, University of Sussex, Brighton, United Kingdom, <sup>2</sup>NeuroPoly Lab, Polytechnique Montreal, Montreal, QC, Canada, <sup>3</sup>CUBRIC, Cardiff University, Cardiff, United Kingdom

Are myelin-sensitive maps interchangeable? We performed a scan-rescan study in 5 subjects using T1 mapping, magnetization transfer and myelin water fraction. We found overall that all metrics have high scan-rescan repeatability and that they are highly correlated with each other. However, isolating the main factor behind this shared variance is not straightforward because of the different interplays between the measures. In the end, what will matter is to what extent these relationships are preserved in the presence of pathology.

1011



### Large-scale quantitative atlases over the whole adult age range

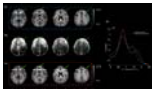
Gian Franco Piredda<sup>1,2,3</sup>, Peipeng Liang<sup>4</sup>, Tom Hilbert<sup>1,2,3</sup>, Hongjian He<sup>5</sup>, Jean-Philippe Thiran<sup>2,3</sup>, Yi Sun<sup>6</sup>, Jianhui Zhong<sup>5,7</sup>, Kuncheng Li<sup>8,9</sup>, and Tobias Kober<sup>1,2,3</sup>



<sup>1</sup>Advanced Clinical Imaging Technology, Siemens Healthcare AG, Lausanne, Switzerland, <sup>2</sup>Department of Radiology, Lausanne University Hospital and University of Lausanne, Lausanne, Switzerland, <sup>3</sup>LTS5, École Polytechnique Fédérale de Lausanne (EPFL), Lausanne, Switzerland, <sup>4</sup>School of Psychology, Capital Normal University, Beijing Key Laboratory of Learning and Cognition, Beijing, China, <sup>5</sup>Center for Brain Imaging Science and Technology, Key Laboratory for Biomedical Engineering of Ministry of Education, College of Biomedical Engineering and Instrumental Science, Zhejiang University, Hangzhou, Zhejiang, China, <sup>6</sup>MR Collaboration, Siemens Healthcare Ltd., Shanghai, China, <sup>7</sup>Department of Imaging Sciences, University of Rochester, Rochester, NY, United States, <sup>8</sup>Department of Radiology, Xuanwu Hospital, Capital Medical University, Beijing, China, <sup>9</sup>Beijing Key Laboratory of Magnetic Resonance Imaging and Brain Informatics, Beijing, China

It was recently shown that brain atlases of normative relaxation times enable automated detection of tissue alterations on a single-subject basis. In this work, normative quantitative  $T_1$  and  $T_2$  atlases were obtained from a large-scale adult cohort of healthy volunteers (#997) covering a comprehensive age range (19-72y) in a multi-centric study including eleven sites. Atlases were derived by linearly modelling the inter-subject variability of  $T_1/T_2$  while accounting for effects such as gender and age differences. Travelling subjects were scanned in nine centers with the same protocol, the comparison of the acquired maps showed good reproducibility of the employed relaxometry sequences.

1012



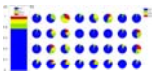
### Intra-volume motion correction via Bayesian imputation in multi-parametric mapping (MPM) quantitative imaging

Mikael Brudfors<sup>1</sup>, Yaël Balbastre<sup>1</sup>, John Ashburner<sup>1</sup>, Siawoosh Mohammadi<sup>2,3</sup>, and Martina F Callaghan<sup>1</sup>

<sup>1</sup>Wellcome Centre for Human Neuroimaging, University College London, London, United Kingdom, <sup>2</sup>Department of Systems Neuroscience, University Medical Center Hamburg-Eppendorf, Hamburg, Germany, <sup>3</sup>Department of Neurophysics, Max Planck Institute for Human Cognitive and Brain Sciences, Leipzig, Germany

Intra-scan motion is a common source of artefacts in magnetic resonance imaging (MRI), which cannot be easily corrected. However, in quantitative MRI (qMRI), several volumes with varying parameters are acquired, and some sort of data redundancy exists. In this abstract, we propose a general framework where corrupted voxels are treated as missing entries and imputed using a Bayesian model of differently weighted MRI volumes. We demonstrate its efficacy in the context of various multi-parameter mapping (MPM) qMRI protocols, in which one volume is corrupted by motion. We show that the model can efficiently recover the corrupted data without introducing bias.

1013

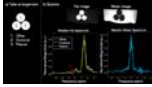


### Data-driven Motion Detection for MR Fingerprinting

Gregor Kördörfer<sup>1</sup>, Pedro Lima Cardoso<sup>2</sup>, Peter Bär<sup>2</sup>, Simone Kitzer<sup>2</sup>, Wolfgang Bogner<sup>2,3</sup>, Siegfried Trattnig<sup>2,3</sup>, and Mathias Nittka<sup>1</sup>

<sup>1</sup>Siemens Healthcare GmbH, Erlangen, Germany, <sup>2</sup>High Field MR Centre, Department of Biomedical Imaging and Image-guided Therapy, Medical University of Vienna, Vienna, Austria, <sup>3</sup>Christian Doppler Laboratory for Clinical Molecular MR Imaging, MOLIMA, Vienna, Austria

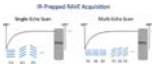
In contrast to qualitative MRI, motion artifacts can be more subtle in quantitative MRI methods such as Magnetic Resonance Fingerprinting (MRF). Errors caused by motion are not easily detectable by visual inspection of resulting maps. Hence, there is clear need for supporting the reliability of results with regard to motion-induced errors. We present a method to detect if significant through-plane motion occurred during an MRF scan, without external motion tracking devices or acquiring additional data. The method is based on classifying the spatiotemporal residuals either by eye or a neural network. The performance was successfully evaluated in a patient study.



Suma Anand<sup>1</sup>, Adam Michael Bush<sup>2</sup>, Christopher Michael Sandino<sup>3</sup>, Shreyas Vasanawala<sup>2</sup>, and Michael Lustig<sup>1</sup>

<sup>1</sup>Electrical Engineering and Computer Sciences, University of California, Berkeley, Berkeley, CA, United States, <sup>2</sup>Radiology, Stanford University, Palo Alto, CA, United States, <sup>3</sup>Electrical Engineering, Stanford University, Palo Alto, CA, United States

Obesity is a major cause of preventable morbidity and mortality in the US. A growing body of work suggests that triglyceride composition and its spatial distribution play a central role in this epidemic, necessitating the need for better non-invasive fat imaging. We propose a motion-robust acquisition scheme that combines the spatial resolution of MRI and the spectral resolution of MR spectroscopy using 2D multi-echo rosette k-space sampling. We validate the method with an oil phantom and demonstrate its motion robustness with a free-breathing in vivo acquisition.

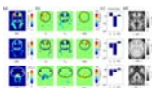


Stack-of-Stars Inversion-Recovery MRI for Free-Breathing T1 Mapping and IR-Prepared Fat/Water Separation

Li Feng<sup>1</sup>, Kai Tobias Block<sup>2</sup>, Thomas Benkert<sup>3</sup>, Ye Tian<sup>4</sup>, Chenyu Liu<sup>1</sup>, Fang Liu<sup>5,6</sup>, Zahi Fayad<sup>1</sup>, and Yang Yang<sup>1</sup>

<sup>1</sup>Biomedical Engineering and Imaging Institute and Department of Radiology, Icahn School of Medicine at Mount Sinai, New York, NY, United States, <sup>2</sup>Center for Advanced Imaging Innovation and Research (CAI2R), Department of Radiology, New York University School of Medicine, New York, NY, United States, <sup>3</sup>MR Applications Development, Siemens Healthcare GmbH, Erlangen, Germany, <sup>4</sup>Department of Radiology and Imaging Sciences, University of Utah, Salt Lake City, UT, United States, <sup>5</sup>Gordon Center for Medical Imaging, Massachusetts General Hospital, Harvard Medical School, Boston, MA, United States, <sup>6</sup>Department of Radiology, University of Wisconsin Madison, Madison, WI, United States

This work presents a framework for inversion-recovery (IR)-prepared stack-of-stars imaging and its applications for rapid free-breathing 3D liver MRI. Building upon a previously developed stack-of-stars 3D GRE sequence (RAVE: RAdial Volumetric Encoding), a non-selective 180° IR pulse has been implemented that is periodically played-out to achieve IR preparation (IR-Prepped RAVE). The new sequence allows (1) single-echo acquisition in combination with GRASP-Pro (imProved Golden-angle RAdial Sparse Parallel) reconstruction for free-breathing volumetric T1 mapping of the liver, and (2) multi-echo acquisition in combination with dynamic model-based reconstruction for IR-prepped and contrast-resolved fat/water separation.



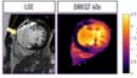
Identification and Correction of Errors in Quantitative Multi-Parameter Mapping (MPM)

Tobias Streubel<sup>1,2</sup>, Leonie Klock<sup>3</sup>, Martina Callaghan<sup>4</sup>, Simone Kühn<sup>3,5</sup>, Antoine Lutti<sup>6</sup>, Karsten Tabelow<sup>7</sup>, Nikolaus Weiskopf<sup>2</sup>, Gabriel Ziegler<sup>8,9</sup>, and Siawoosh Mohammadi<sup>1,2</sup>

<sup>1</sup>Institute for Systems Neuroscience, University Medical Center Hamburg-Eppendorf, Hamburg, Germany, <sup>2</sup>Department of Neurophysics, Max Planck Institute for Human Cognitive and Brain Sciences, Leipzig, Germany, <sup>3</sup>Department of Psychiatry and Psychotherapy, University Medical Center Hamburg-Eppendorf, Hamburg, Germany, <sup>4</sup>Wellcome Trust Centre for Neuroimaging, UCL Institute of Neurology, UCL, London, United Kingdom, <sup>5</sup>Center for Lifespan Psychology, Max Planck Institute for Human Development, Berlin, Germany, <sup>6</sup>Laboratory for Research in Neuroimaging, Department of Clinical Neuroscience, Lausanne, Switzerland, <sup>7</sup>Stochastic Algorithms and Nonparametric Statistics, Weierstrass Institute for Applied Analysis and Stochastics, Berlin, Germany, <sup>8</sup>Institute of Cognitive Neurology and Dementia Research, Otto-von-Guericke-University, Magdeburg, Germany, <sup>9</sup>German Center for Neurodegenerative Diseases, Magdeburg, Germany

We introduced novel error maps for proton density, longitudinal relaxation and magnetization transfer saturation rates that are more sensitive to artifacts than previously used error measures. We showed that they can be used to identify and down weigh local errors in the quantitative parameter maps for an experiment consisting of two successive multi-parameter mapping (MPM) measurements in a group of 10 healthy subjects.

1017



### Model-based quantitative mapping for highly accelerated first-pass perfusion cardiac MRI

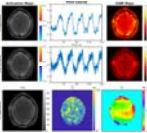
Teresa Correia<sup>1</sup>, Torben Schneider<sup>2</sup>, and Amedeo Chiribiri<sup>1</sup>

<sup>1</sup>*School of Biomedical Engineering and Imaging Sciences, King's College London, London, United Kingdom,*

<sup>2</sup>*Philips Healthcare, Guildford, United Kingdom*

First-pass perfusion cardiac MR (FP-CMR) is becoming essential for evaluating myocardial ischemia. However, FP-CMR requires ECG-gating and breath-holding, leading to a trade-off between spatial resolution and coverage. Moreover, perfusion abnormalities are often identified visually by highly trained operators. Recently, quantitative FP-CMR and compressed sensing (CS) have been proposed to reduce operator-dependency and moderately accelerate acquisitions, respectively. Here, a model-based reconstruction is proposed to directly estimate quantitative myocardial perfusion maps from highly undersampled acquisitions. Thus, allowing for higher spatial resolution and coverage than indirect methods, where dynamic images are reconstructed using CS and quantitative maps are obtained subsequently using tracer-kinetic modeling.

1018



### OSSI Manifold Model for High-Resolution fMRI Joint Reconstruction and Quantification

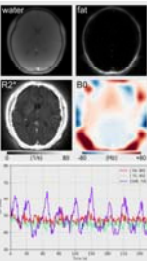
Shouchang Guo<sup>1</sup>, Douglas C. Noll<sup>2</sup>, and Jeffrey A. Fessler<sup>1</sup>

<sup>1</sup>*Electrical Engineering and Computer Science, University of Michigan, Ann Arbor, MI, United States,*

<sup>2</sup>*Biomedical Engineering, University of Michigan, Ann Arbor, MI, United States*

Oscillating Steady-State Imaging (OSSI) is a new fMRI acquisition method that can provide high SNR signals, but does so at the expense of imaging time. We previously used a physics-based regularizer for high-quality, undersampled reconstruction by modeling the oscillating signal with physics parameters. However, the reconstructions were not quantitative, as the key parameter  $\Delta R_2^*$  for BOLD effects was not studied. In this work, to quantify MRI parameters of physiological importance, we jointly reconstruct the images and the parameters. The proposed manifold model reconstructs high-resolution images from 12-fold undersampled data, while also providing quantitative  $\Delta R_2^*$  estimates for fMRI.

1019



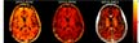
### Dynamic Water, Fat, $R_2^*$ and $B_0$ Field Inhomogeneity Quantification Using Multi-Echo Multi-Spoke Radial FLASH

Zhengguo Tan<sup>1,2</sup>, Peter Dechent<sup>3</sup>, Xiaoqing Wang<sup>1,2</sup>, Nick Scholand<sup>1,2</sup>, Dirk Voit<sup>4</sup>, Jens Frahm<sup>2,4</sup>, and Martin Uecker<sup>1,2</sup>

<sup>1</sup>*Diagnostic and Interventional Radiology, University Medical Center Göttingen, Göttingen, Germany,*

<sup>2</sup>*German Center for Cardiovascular Research (DZHK), Göttingen, Germany,* <sup>3</sup>*Cognitive Neurology, University Medical Center Göttingen, Göttingen, Germany,* <sup>4</sup>*Biomedizinische NMR, Max-Planck-Institute for Biophysical Chemistry, Göttingen, Germany*

To achieve dynamic and simultaneous access to  $R_2^*$  relaxation rates,  $B_0$  field inhomogeneities and water/fat separation, we developed a model-based reconstruction technique on BART for continuous acquisitions based on undersampled multi-echo multi-spoke radial FLASH. Beside spatial smoothness constraints on coil sensitivity and  $B_0$  field maps, L1 wavelet regularization is applied to the water, fat and  $R_2^*$  maps. Preliminary results of brain fMRI data demonstrate significant  $T_2^*$  change from 37 to 67 ms in the occipital visual cortex. In addition,  $R_2^*$  mapping of free-breathing liver with only 15 RF shots per frame (194 ms temporal resolution) reveals increased  $R_2^*$  during inspiration.

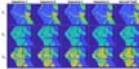


### Myelin Water Imaging Using STFR with Exchange

Steven T. Whitaker<sup>1</sup>, Gopal Nataraj<sup>2</sup>, Jon-Fredrik Nielsen<sup>3</sup>, and Jeffrey A. Fessler<sup>1</sup>

<sup>1</sup>Electrical Engineering and Computer Science, University of Michigan, Ann Arbor, MI, United States, <sup>2</sup>Medical Physics, Memorial Sloan Kettering Cancer Center, New York, NY, United States, <sup>3</sup>Biomedical Engineering, University of Michigan, Ann Arbor, MI, United States

Myelin water fraction (MWF) estimates are desirable for tracking the progression of demyelinating diseases such as multiple sclerosis. To address the long scan times of conventional MWF imaging methods, faster steady-state scans have been studied recently. One such steady-state scan is small-tip fast recovery (STFR). This work compares STFR-based MWF estimates using a two-compartment tissue model without exchange to those obtained using a three-compartment tissue model with exchange. Using a three-compartment model with exchange results in MWF estimates that are closer to traditional multi-echo spin echo (MESE) estimates.



### Quantification of T<sub>1ρ</sub> using magnetic resonance fingerprinting

Brendan Lee Eck<sup>1,2</sup>, Jeehun Kim<sup>2</sup>, Mingrui Yang<sup>2</sup>, and Xiaojuan Li<sup>2</sup>

<sup>1</sup>Cardiovascular and Metabolic Sciences, Cleveland Clinic, Cleveland, OH, United States, <sup>2</sup>Biomedical Engineering, Cleveland Clinic, Cleveland, OH, United States

Quantitative T<sub>1ρ</sub> imaging has been studied for evaluating changes in tissue composition, in particular for detecting early cartilage degeneration in osteoarthritis. Magnetic resonance fingerprinting (MRF) provides a framework for rapid, robust acquisition of quantitative tissue property maps. Simulation experiments using spin-lock prepared MRF with different pulse schedules were conducted to demonstrate the feasibility of quantification of T<sub>1ρ</sub> in addition to T<sub>1</sub> and T<sub>2</sub>. All tested sequences were sensitive to T<sub>1ρ</sub> and produced tissue property maps with major structures of interest. Differing accuracy and precision between sequences suggests opportunities for optimizing MRF for simultaneous T<sub>1</sub>, T<sub>2</sub>, and T<sub>1ρ</sub> quantification.

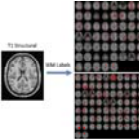
## Oral - Power Pitch

### Quantification, ML, and Tools - Machine Learning Potpourri: White Matter, Pharmacokinetics, Brain Age & Other Applications

Thursday Parallel 1 Live Q&A

Thursday 14:20 - 15:05 UTC

Moderators: Akshay Chaudhari & Jo Schlemper

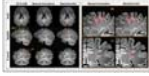


### Learning white matter fingerprints from structural information

Colin Hansen<sup>1</sup>, Qi Yang<sup>1</sup>, Francois Rheault<sup>2</sup>, Bramsh Qamar<sup>3</sup>, Owen Williams<sup>4</sup>, Susan Resnick<sup>4</sup>, Eleftherios Garyfallidis<sup>3</sup>, Adam W Anderson<sup>5,6</sup>, Maxime Descoteaux<sup>2</sup>, Bennett A Landman<sup>5,6,7,8</sup>, and Kurt G Schilling<sup>5</sup>

<sup>1</sup>Computer Science, Vanderbilt University, Nashville, TN, United States, <sup>2</sup>Sherbrooke Connectivity Imaging Laboratory (SCIL), Universite de Sherbrooke, Sherbrooke, QC, Canada, <sup>3</sup>Intelligent Systems Engineering, Indiana University Bloomington, Bloomington, IN, United States, <sup>4</sup>Laboratory of Behavioral Neuroscience, National Institute on Aging, Baltimore, MD, United States, <sup>5</sup>Vanderbilt University Institute of Imaging Science, Nashville, TN, United States, <sup>6</sup>Biomedical Engineering, Vanderbilt University, Nashville, TN, United States, <sup>7</sup>Radiology and Radiological Sciences, Vanderbilt University Medical Center, Nashville, TN, United States, <sup>8</sup>Electrical Engineering, Vanderbilt University, Nashville, TN, United States

Here, we present a tool and reconstruction method to label white matter pathways directly on structural images without the need for diffusion MRI or tractography. A 3D U-net was trained utilizing 1109 scan sessions where fiber pathways were segmented using two different segmentation schemes. Results on testing datasets show anatomically viable segmentations and moderate-to-high volume overlaps with gold-standard pathways, on par with scan-rescan reproducibility of tractography on the same datasets. We envision the use of this tool for visualizing the expected course of white matter pathways when diffusion data are not available.

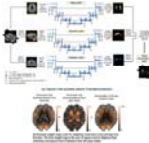


### StackGen-Net: A Stacked Generalization of 3D Orthogonal Convolutional Neural Networks for Improved Detection of White Matter Hyperintensities

Lavanya Umapathy<sup>1</sup>, Gloria J Guzman Perez-Carrillo<sup>2</sup>, Mahesh Bharath Keerthivasan<sup>2,3</sup>, Maria I Altbach<sup>2</sup>, Blair Winegar<sup>2</sup>, Craig Weinkauf<sup>4</sup>, and Ali Bilgin<sup>1,2,5</sup>

<sup>1</sup>Department of Electrical and Computer Engineering, University of Arizona, Tucson, AZ, United States, <sup>2</sup>Department of Medical Imaging, University of Arizona, Tucson, AZ, United States, <sup>3</sup>Siemens Healthcare USA, Tucson, AZ, United States, <sup>4</sup>Department of Surgery, University of Arizona, Tucson, AZ, United States, <sup>5</sup>Department of Biomedical Engineering, University of Arizona, Tucson, AZ, United States

Detection and quantification of White Matter Hyperintensities (WMH) on T2-FLAIR images can provide valuable information to assess neurological disease progression. We propose a fully automated stacked generalization ensemble of three orthogonal 3D Convolutional Neural Networks (CNNs), StackGen-Net, to detect WMH on 3D FLAIR images. Each orthogonal CNN predicts WMH on axial, sagittal, and coronal orientations. The posteriors are then combined using a Meta CNN. StackGen-Net outperforms individual CNNs in the ensemble, their ensemble combination, as well as some state-of-the-art deep learning-based models. StackGen-Net can reliably detect and quantify WMH in clinically feasible times, with performance comparable to human inter-observer variability.



### Detection of white matter hyperintensities using Triplanar U-Net ensemble network

Vaanathi Sundaresan<sup>1</sup>, Mark Jenkinson<sup>1</sup>, Giovanna Zamboni<sup>2</sup>, and Ludovica Griffanti<sup>1</sup>

<sup>1</sup>FMRIB, Wellcome Centre for Integrative Neuroimaging (WIN), Nuffield Department of Clinical Neurosciences, University of Oxford, Oxford, United Kingdom, <sup>2</sup>Centre for prevention of Stroke and Dementia, Nuffield Department of Clinical Neurosciences, University of Oxford, Oxford, United Kingdom

We propose a triplanar U-Net ensemble network (TrUE-Net) model for detecting white matter hyperintensities (WMHs) on structural brain MR images. The network uses a combination of loss functions based on the anatomical distribution of WMHs. The model takes T1-weighted and FLAIR images as input channels. The U-Nets in three planes (axial, coronal, sagittal) provides three 2D probability maps, which are combined by averaging across planes to obtain the final probability map. When evaluated on three different cohorts from the MICCAI WMH segmentation challenge dataset, TrUE-Net provided better average performance (Dice=0.78, voxel-wise TPR=0.75), when compared to FSL-BIANCA (Dice=0.69, voxel-wise TPR=0.74).

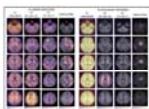


### Organ-based estimation of the chronological age based on 3D MRI scans

Sherif Abdulatif<sup>1</sup>, Karim Armanious<sup>1,2</sup>, Anish Rao Bhaktharaguttu<sup>1</sup>, Thomas Küstner<sup>2</sup>, Bin Yang<sup>1</sup>, and Sergios Gatidis<sup>2</sup>

<sup>1</sup>University of Stuttgart, Stuttgart, Germany, <sup>2</sup>University Hospital Tübingen, Tübingen, Germany

Age is an essential clinical parameter. It is often utilized as a risk factor for various disorders with the potential of influencing therapeutic decisions. However, a discrepancy exists between the chronological age (CA) and the biological age (BA) of an individual due to many factors such as medical history, genetics and lifestyle. In this preliminary work, we propose a novel deep-learning architecture for organ-specific CA estimation from 3D MR volumes for the brain and knee. We hypothesize that the introduced organ-specific approach would enable future analysis of the BA as different organs are expected to exhibit different aging characteristics.



### Assessing the effect of registration and model quality using attention gates for brain-age prediction with convolutional neural networks.

Nicola K Dinsdale<sup>1</sup>, Emma Bluemke<sup>2</sup>, Mark Jenkinson<sup>1</sup>, and Ana IL Namburete<sup>2</sup>

Nonlinear registration forms a part of standard MRI neuroimaging pipelines but leads to suppression of morphological information. Using attention gates within a convolutional neural network, we explore the effect of the nonlinear registration on age prediction, comparing to linear registration. We show that the network is driven by interpolation effects near the ventricles when trained with nonlinear data, whereas when trained with linear data it considers the whole brain volume. The network may, therefore, be missing cortical changes, limiting the utility of the networks in detecting the early stages of neurological disease.

1027



### Deep Learning-based Fetal-Uterine Motion Modeling from Volumetric EPI Time Series

Muheng Li<sup>1</sup>, Yi Xiao<sup>1</sup>, Tingyin Liu<sup>2</sup>, Junshen Xu<sup>3</sup>, Esra Turk<sup>4</sup>, Borjan Gagoski<sup>4,5</sup>, Karen Ying<sup>1</sup>, Polina Golland<sup>2,3</sup>, P. Ellen Grant<sup>4,5</sup>, and Elfar Adalsteinsson<sup>3,6</sup>

<sup>1</sup>Department of Engineering Physics, Tsinghua University, Beijing, China, <sup>2</sup>Computer Science and Artificial Intelligence Laboratory (CSAIL), Massachusetts Institute of Technology, Cambridge, MA, United States, <sup>3</sup>Department of Electrical Engineering and Computer Science, Massachusetts Institute of Technology, Cambridge, MA, United States, <sup>4</sup>Fetal-Neonatal Neuroimaging and Developmental Science Center, Boston Children's Hospital, Boston, MA, United States, <sup>5</sup>Harvard Medical School, Boston, MA, United States, <sup>6</sup>Institute for Medical Engineering and Science, Massachusetts Institute of Technology, Cambridge, MA, United States

We propose a three-dimensional convolutional neural network applied to echo planar EPI time series of pregnant women for the automatic segmentation of the uterus (placenta excluded) and fetal body. The segmentation results are utilized to create a dynamic model for the fetus for retrospective analyses. The 3D dynamic fetal-uterine motion model will provide quantitative information of fetal motion characteristics for diagnostic purposes and may guide future fetal imaging strategies where adaptive, online slice prescription is used to mitigate motion artifacts.

1028



### Multi-path Deformable Convolutional Neural Network with Label Distribution Learning for Fetal Brain Age Prediction

Lufan Liao<sup>1</sup>, Xin Zhang<sup>2</sup>, Fenqiang Zhao<sup>1</sup>, Jingjiao Lou<sup>1</sup>, Li Wang<sup>1</sup>, Xiangmin Xu<sup>2</sup>, He Zhang<sup>3</sup>, and Gang Li<sup>1</sup>

<sup>1</sup>Department of Radiology and BRIC, The University of North Carolina at Chapel Hill, Chapel Hill, CA, United States, <sup>2</sup>School of Electronic and Information Engineering, South China University of Technology, GUANGZHOU, China, <sup>3</sup>Department of Radiology, Obstetrics and Gynecology Hospital, Fudan University, ShangHai, China

In this study, an end-to-end framework, combining deformable convolution and label distribution learning, is developed for fetal brain age prediction based on MRI. Furthermore, a multi-path architecture is proposed to deal with multi-view MRI scenarios. Experiments on the collected dataset demonstrate that the proposed model achieves promising performance.

1029



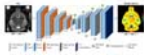
### Exploration of Feature Space in Semantic Segmentation Convolutional Neural Networks

Logan A Thorneloe<sup>1</sup>, Arjun D Desai<sup>2,3</sup>, Garry E Gold<sup>3,4,5</sup>, Brian A Hargreaves<sup>2,3,4</sup>, Neal K Bangerter<sup>6</sup>, and Akshay S Chaudhari<sup>3</sup>

<sup>1</sup>Electrical Engineering, Brigham Young University, Provo, UT, United States, <sup>2</sup>Electrical Engineering, Stanford University, Stanford, CA, United States, <sup>3</sup>Radiology, Stanford University, Stanford, CA, United States, <sup>4</sup>Bioengineering, Stanford University, Stanford, CA, United States, <sup>5</sup>Orthopedic Surgery, Stanford University, Stanford, CA, United States, <sup>6</sup>Bioengineering, Imperial College London, London, United Kingdom

Recent advances in deep learning and convolutional neural networks (CNNs) have shown promise for automatic segmentation in MR images. However, because of the stochastic nature of the training process, it is difficult to interpret what information networks learn to represent. In this study, we explore how differences in learned weights between networks can be used to express semantic relationships between different tissues. For cartilage and meniscus segmentation in the knee, we show that network generalizability for segmenting tissues can be measured by distances between networks. We also use these findings to motivate robust training policies for fine-tuning with limited data.

1030



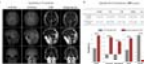
### SUBSTITUTING GADOLINIUM IN BRAIN MRI USING DEEPCONTRAST: A PROOF-OF-CONCEPT STUDY IN MICE

Haoran Sun<sup>1</sup>, Xueqing Liu<sup>1</sup>, Xinyang Feng<sup>1</sup>, Chen Liu<sup>2</sup>, Nanyan Zhu<sup>3</sup>, Sabrina Josefina Gjerswold-Selleck<sup>1</sup>, Hong-Jian Wei<sup>4,5</sup>, Pavan Shankar Upadhyayula<sup>5,6</sup>, Angeliki Mela<sup>5,6</sup>, Cheng-Chia Wu<sup>4,5</sup>, Peter Canoll<sup>5,6</sup>, Andrew F. Laine<sup>1</sup>, John Thomas Vaughan<sup>1</sup>, Scott A. Small<sup>7,8,9</sup>, and Jia Guo<sup>7,10</sup>

<sup>1</sup>Department of Biomedical Engineering, Columbia University, New York, NY, United States, <sup>2</sup>Department of Electrical Engineering, Columbia University, New York, NY, United States, <sup>3</sup>Department of Biological Science, Columbia University, New York, NY, United States, <sup>4</sup>Department of Radiation Oncology, Columbia University, New York, NY, United States, <sup>5</sup>Columbia University Irving Medical Center, Columbia University, New York, NY, United States, <sup>6</sup>Department of Pathology and Cell Biology, Columbia University, New York, NY, United States, <sup>7</sup>Department of Psychiatry, Columbia University, New York, NY, United States, <sup>8</sup>Departments of Neurology, Columbia University, New York, NY, United States, <sup>9</sup>Departments of Radiology, Columbia University, New York, NY, United States, <sup>10</sup>Mortimer B. Zickerman Mind Brain Behavior Institute, Columbia University, New York, NY, United States

Cerebral blood volume (CBV) is a hemodynamic correlate of oxygen metabolism and reflects brain activity and function. High-resolution CBV maps can be generated using the steady-state gadolinium-enhanced MRI technique. Recent studies suggest that the exogenous gadolinium based contrast agent (GBCA) can accumulate in the brain after frequent use. Here, we develop and optimize a deep learning algorithm, DeepContrast, which performs equally well as exogenous GBCA in mapping CBV of the normal brain tissue and enhancing glioblastoma. Together, these studies validate our hypothesis that a deep learning approach can potentially replace the need for GBCAs in brain MRI.

1031



### Substituting Gadolinium In Human Brain MRI Using DeepContrast

Chen Liu<sup>1,2</sup>, Nanyan Zhu<sup>1,3</sup>, Xinyang Feng<sup>4,5</sup>, Frank A Provenzano<sup>6</sup>, John T Vaughan<sup>4,7,8</sup>, Scott A Small<sup>6,7,9</sup>, and Jia Guo<sup>8,9</sup>

<sup>1</sup>These authors contribute equally to this work and are joint first authors, New York, NY, United States, <sup>2</sup>Electrical Engineering, Columbia University, New York, NY, United States, <sup>3</sup>Biological Science, Columbia University, New York, NY, United States, <sup>4</sup>Biomedical Engineering, Columbia University, New York, NY, United States, <sup>5</sup>Facebook, San Francisco, NY, United States, <sup>6</sup>Neurology, Columbia University, New York, NY, United States, <sup>7</sup>Radiology, Columbia University, New York, NY, United States, <sup>8</sup>Mortimer B. Zuckerman Mind Brain Behavior Institute, Columbia University, New York, NY, United States, <sup>9</sup>Psychiatry, Columbia University, New York, NY, United States

MRI estimation of cerebral blood volume (CBV) is useful in mapping potential brain function. To obtain high-resolution CBV maps, it typically requires intravenous (IV) injections of Gadolinium-based contrast agents (GBCAs), the use of which has come under new scrutiny. Here, we design and implement a deep learning algorithm, DeepContrast, to estimate GBCA contrast directly from T1-weighted (T1W) structural MRI. The predicted contrast performs equally well as the GBCA-enhanced CBV map even in mapping subtle age-related functional changes in the human brain. Therefore, our study demonstrates the feasibility of substituting GBCA in human brain MRI using DeepContrast.





<sup>1</sup>Queen Square MS Centre, Queen Square Institute of Neurology, Faculty of Brain Sciences, University College London, London, United Kingdom, <sup>2</sup>Centre for Medical Image Computing, Department of Computer Science, University College London, London, United Kingdom, <sup>3</sup>Champalimaud Research, Champalimaud Centre for the Unknown, Lisbon, Portugal, <sup>4</sup>Centre for Medical Imaging, University College London, London, United Kingdom, <sup>5</sup>Department of Brain and Behavioural Sciences, University of Pavia, Pavia, Italy, <sup>6</sup>Brain MRI 3T Center, IRCCS Mondino Foundation, Pavia, Italy

This work introduces the “Select and retrieve via direct up-sampling” network (SARDU-Net), a new method for model-free, data-driven quantitative MRI (qMRI) experiment design. SARDU-Net identifies informative measurements within lengthy acquisitions and reconstructs fully-sampled signals from a sub-protocol, without prior information on the MRI contrast. It combines two deep networks: a selector, which selects a signal sub-sample, and a predictor, which retrieves input signals. SARDU-Net can be run with standard computational resources and can increase the clinical appeal of qMRI. Here we demonstrate its potential on qMRI of prostate and spinal cord, two areas where fast acquisitions are key.

1036



### End-to-End Full Automated Pipeline using a Convolutional Neural Network for Lung Segmentation in Phase-Resolved Functional Lung (PREFUL) MRI

Cristian Crisosto<sup>1,2</sup>, Andreas Voskrebenez<sup>1,2</sup>, Marcel Gutberlet<sup>1,3</sup>, Filip Klimeš<sup>1,2</sup>, Frank Wacker<sup>1,2</sup>, Till Kaireit<sup>1,2</sup>, Gesa Poeler<sup>1,2</sup>, Lea Behrendt<sup>1,2</sup>, Christopher Korz<sup>1</sup>, and Jens Vogel-Claussen<sup>1,2</sup>

<sup>1</sup>Institute of Diagnostic and Interventional Radiology, Hanover Medical School, Hannover, Germany, <sup>2</sup>Biomedical Research in Endstage and Obstructive Lung Disease Hannover (BREATH), German Center for Lung Research (DZL), Hannover, Germany, <sup>3</sup>Biomedical Research in Endstage and 3 Obstructive Lung Disease Hannover (BREATH), German Center for Lung Research (DZL), Hannover, Germany

Translation and establishment of complex pulmonary magnetic resonance (MR) imaging techniques in the clinics requires a reliable, fully automated and fast calculation. In this work we present a semantic convolutional neural network (CNN) model for lung parenchyma and vessel segmentation in combination with parallelized computation on a high-performance computer to design an end-to-end pipeline for phase-resolved functional lung (PREFUL) MRI. The CNN was trained (n=1118) and validated (n=1064) with manually segmented images by a trained radiologist. Automatic segmentation of lung parenchyma was achieved for all tested images.

## Oral

### Neurovascular imaging - MRI in Diagnosis & Treatment of Cerebrovascular Diseases

Thursday Parallel 2 Live Q&A

Thursday 14:20 - 15:05 UTC

Moderators: Cristina Granziera

1052




### Comparison of Automated Cerebral Infarct Segmentation Techniques using DWI and FLAIR MRI

Ryan A. Rava<sup>1,2</sup>, Muhammad Waqas<sup>2,3</sup>, Kenneth V. Snyder<sup>2,3</sup>, Elad I. Levy<sup>2,3</sup>, Adnan H. Siddiqui<sup>2,3</sup>, Jason M. Davies<sup>2,3</sup>, Xiaoliang Zhang<sup>1</sup>, and Ciprian N. Ionita<sup>1,2,3</sup>


<sup>1</sup>Biomedical Engineering, University at Buffalo, Buffalo, NY, United States, <sup>2</sup>Canon Stroke and Vascular Research Center, University at Buffalo, Buffalo, NY, United States, <sup>3</sup>Neurosurgery, University at Buffalo, Buffalo, NY, United States

FLAIR MRI has the potential to provide more accurate ground truth infarct labels compared with DWI for the purpose of software validation and determination of ischemic stroke patient eligibility for thrombectomy. Currently, accurate segmentation of infarct has hindered the use of FLAIR infarct labels due to skull and erroneous image intensity values being similar to those of infarct lesions. In this study, an automated segmentation technique was developed for segmentation of infarct tissue from FLAIR MRI and performance metrics comparing this method to manually segmented infarct (FLAIR Sorenson-Dice=0.8168, DWI Sorenson-Dice=0.7922) indicate this technique is non-inferior to the current standard (DWI).

1053  FLAIR-based estimation of the stroke onset time: a magnetic field dependent study  
Tao Jin<sup>1</sup>

<sup>1</sup>Department of Radiology, University of Pittsburgh, Pittsburgh, PA, United States


Stroke onset time is a prerequisite for thrombolytic treatment but is unknown in ~25% of acute ischemic stroke patients. A fluid-attenuated inversion recovery (FLAIR)-based MRI index (e.g., DWI-FLAIR mismatch) has been suggested as a surrogate to determine whether the stroke duration is within the treatment window. In this work, we showed that the time when a positive FLAIR contrast appears between ischemic and normal tissue increases with  $B_0$ , and is dependent on the imaging parameters. Therefore, FLAIR-based studies of stroke onset should be designed or interpreted with care.

1054  Stable fractional anisotropy and mean diffusivity after treatment in patients with asymptomatic high grade internal carotid artery stenosis

Lena Schmitzer<sup>1</sup>, Stephan Kaczmarz<sup>1,2</sup>, Nico Sollmann<sup>1</sup>, Claus Zimmer<sup>1</sup>, Christine Preibisch<sup>1,3</sup>, and Jens Götter<sup>1,2,4</sup>

<sup>1</sup>School of Medicine, Department of Neuroradiology, Technical University of Munich, Munich, Germany, <sup>2</sup>MRRC, Yale University, New Haven, CT, United States, <sup>3</sup>School of Medicine, Clinic of Neurology, Technical University of Munich, Munich, Germany, <sup>4</sup>School of Medicine, Department of Radiology, Technical University of Munich, Munich, Germany

Internal carotid artery stenosis (ICAS) is a well-known risk factor for stroke. However, treatment efficacy evaluations are currently limited by widely unknown ICAS-effects on brain microstructure. Two promising parameters to study pathophysiological changes in white matter (WM) are fractional anisotropy (FA) and mean diffusivity (MD), derived from established diffusion-tensor imaging. We evaluated FA- and MD-maps in 15 ICAS-patients before and after revascularization. Our results demonstrated globally unimpaired FA and MD before treatment, even in watershed areas, which are especially vulnerable to hemodynamic impairments. Postinterventional structural results were stable. Thus, absence of ischemic events and successful treatment are indicated.

1055  Determining stroke onset time using T2 relaxation times: A comparison of reference and reference independent methods in ischemic stroke patients

Bryony L. McGarry<sup>1</sup>, Robin A. Damion<sup>1</sup>, Terence J. Norton<sup>1</sup>, Michael J. Knight<sup>1</sup>, Philip L. Clatworthy<sup>2</sup>, George W.J. Harston<sup>3</sup>, Keith W. Muir<sup>4</sup>, and Risto A. Kauppinen<sup>5</sup>

<sup>1</sup>School of Psychological Science, University of Bristol, Bristol, United Kingdom, <sup>2</sup>Stroke Neurology, North Bristol NHS Trust, Bristol, United Kingdom, <sup>3</sup>Acute Stroke Programme, Radcliffe Department of Medicine, University of Oxford, Oxford, United Kingdom, <sup>4</sup>Institute of Neuroscience and Psychology, University of Glasgow, Glasgow, United Kingdom, <sup>5</sup>Faculty of Engineering, University of Bristol, Bristol, United Kingdom

Unknown onset time is a common contradiction for anti-thrombolytic treatment of ischemic stroke.  $T_2$  relaxation times within the lesion estimate onset time, but accuracy may be affected by dependence on the non-ischemic hemisphere as reference for pre-ischemic values. In hyperacute ischemic stroke patients, we tested a reference-independent approach shown to be an accurate timer in a preclinical stroke model. This involved modelling the  $T_2$  distribution within ADC defined lesions to design linear regression models for onset time estimation. The reference-independent approach was accurate in grey matter and for lesions containing grey and white matter, the reference-dependent approach was more accurate.



Parameters	ASL-CBF	SWI-QSM	DWI	ASL-CBF
Mean	0.0000	0.0000	0.0000	0.0000
Std	0.0000	0.0000	0.0000	0.0000
Min	0.0000	0.0000	0.0000	0.0000
Max	0.0000	0.0000	0.0000	0.0000
Q1	0.0000	0.0000	0.0000	0.0000
Q3	0.0000	0.0000	0.0000	0.0000
Skewness	0.0000	0.0000	0.0000	0.0000
Kurtosis	0.0000	0.0000	0.0000	0.0000
Entropy	0.0000	0.0000	0.0000	0.0000
Information	0.0000	0.0000	0.0000	0.0000

A Comparative Analysis of CEST-APT, SWI-QSM, DWI and ASL-CBF in Ischemic Stroke Patients

Guomin Li<sup>1</sup>, Hui Liu<sup>2</sup>, Qi Liu<sup>2</sup>, Yongquan Ye<sup>2</sup>, Yichen Hu<sup>2</sup>, Haodong Qin<sup>3</sup>, Jun Xie<sup>3</sup>, Jianhao Yan<sup>4</sup>, Yang Xin<sup>3</sup>, and Guihua Jiang<sup>4</sup>

<sup>1</sup>Medical Imaging, Guangdong Second Provincial General Hospital, Guangzhou, China, <sup>2</sup>UIH America, Inc., Houston, TX, United States, <sup>3</sup>United Imaging Healthcare, Shanghai, China, <sup>4</sup>Guangdong Second Provincial General Hospital, Guangzhou, China

In this study, APT, SWI-QSM, ASL-CBF, and DWI imaging are compared and evaluated in stroke patients, with a focus on different values in identifying diseased area and helping to provide better prognosis.

1057



### Amide Proton Transfer Magnetic Resonance Imaging detecting early Wallerian degeneration of the pyramidal tract after ischemic stroke

Junxin Wang<sup>1</sup>, Yanwei Miao<sup>1</sup>, Jiazheng Wang<sup>2</sup>, Zhiwei Shen<sup>2</sup>, Bingbing Gao<sup>1</sup>, Yu Bing<sup>1</sup>, Yunan Cui<sup>1</sup>, Ailian Liu<sup>1</sup>, and Qingwei Song<sup>1</sup>

<sup>1</sup>Department of Radiology, the First Affiliated Hospital of Dalian Medical University, Dalian, China, <sup>2</sup>Phillips healthcare, China, China

The study aimed to evaluate the significance of amide proton transfer weighted (APT<sub>w</sub>) imaging in the early diagnosis of pyramidal tract Wallerian degeneration (WD) following cerebral infarction. This study included 25 patients with acute cerebral infarction and 12 healthy adult controls. Our data suggested that the value of APT<sub>w</sub> was significantly increased on ipsilateral compared to contralateral and the control group in the posterior limb of internal capsule. It proves the feasibility of APT<sub>w</sub> in early detection of WD.

1058



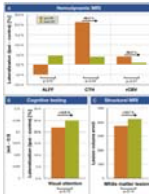
### Correlation between APT<sub>w</sub> changes and regional cerebral oxygen metabolism in ischemic tissue of patients with subacute ischemic stroke

Yuhan Jiang<sup>1</sup>, Yanwei Miao<sup>1</sup>, Peipei Chang<sup>1</sup>, Zhongping Zhang<sup>2</sup>, Yiwei Che<sup>1</sup>, Ailian Liu<sup>1</sup>, Qingwei Song<sup>1</sup>, and Jiazheng Wang<sup>2</sup>

<sup>1</sup>the First Affiliated Hospital of Dalian Medical University, Dalian, China, Dalian, China, <sup>2</sup>Philips Healthcare, Beijing, China, Beijing, China

The relationship between APT<sub>w</sub> and regional cerebral oxygen metabolism levels in the ischemic area is unclear. This study attempts to investigate the mechanism of ischemic tissue pH changes and its influencing factors by measuring the APT<sub>w</sub> value of ischemic tissue, combined with ASL and SWI. We found that the phase differences of the veins in the infarct ( $\Delta\phi_{\text{lesion}}$ ) is positively correlated with APT<sub>w</sub>max and APT<sub>w</sub>max-min in the ischemic penumbra at PLD1.5.

1059



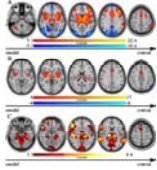
### Treatment efficacy of asymptomatic carotid artery stenosis patients evaluated by clinically applicable hemodynamic MRI and cognitive testing

Stephan Kaczmarz<sup>1,2</sup>, Jens Göttler<sup>1,2,3</sup>, Jan Petr<sup>4</sup>, Nico Sollmann<sup>1</sup>, Lena Schmitzer<sup>1</sup>, Andreas Hock<sup>5</sup>, Mikkel Bo Hansen<sup>6</sup>, Kim Mouridsen<sup>6</sup>, Claus Zimmer<sup>1</sup>, Fahmeed Hyder<sup>2</sup>, and Christine Preibisch<sup>1,7</sup>

<sup>1</sup>School of Medicine, Department of Neuroradiology, Technical University of Munich, Munich, Germany, <sup>2</sup>MRRC, Yale University, New Haven, CT, United States, <sup>3</sup>School of Medicine, Department of Radiology, Technical University of Munich, Munich, Germany, <sup>4</sup>Institute of Radiopharmaceutical Cancer Research, Helmholtz-Zentrum Dresden-Rossendorf, Dresden, Germany, <sup>5</sup>Philips Healthcare, Hamburg, Germany, <sup>6</sup>Institute of Clinical Medicine, Aarhus University, Aarhus, Denmark, <sup>7</sup>School of Medicine, Clinic of Neurology, Technical University of Munich, Munich, Germany

Hemodynamic MRI is highly promising to improve treatment decisions in asymptomatic internal carotid artery stenosis (ICAS). However, treatment efficacy evaluations require clinically applicable techniques, such as dynamic susceptibility contrast (DSC) and resting-state BOLD-based evaluations of amplitude of low-frequency fluctuations (ALFF). We present data from 16 asymptomatic ICAS patients before and after treatment and 17 age-matched healthy controls measuring cerebral blood volume (CBV) and capillary transit-time heterogeneity (CTH) by DSC and ALFF with additional cognitive testing. We hypothesized recovery of hemodynamic impairments after revascularization. Our results confirmed this hypothesis for all parameters. Interestingly, at the same time cognitive function remained impaired.

1060



### Network mapping of central post-stroke pain and analgesic neuromodulation

Gavin J B Elias<sup>1</sup>, Philippe De Vloo<sup>2</sup>, Jürgen Germann<sup>1</sup>, Alexandre Boutet<sup>1</sup>, Robert M Gramer<sup>1</sup>, Suresh E Joel<sup>3</sup>, Bart Morlion<sup>2</sup>, Bart Nuttin<sup>2</sup>, and Andres M Lozano<sup>1</sup>

<sup>1</sup>University Health Network, Toronto, ON, Canada, <sup>2</sup>University Hospitals Leuven, Leuven, Belgium, <sup>3</sup>GE Global Research, Bangalore, India

Despite the prevalence of central post-stroke pain (CPSP), pain-causing brain lesions remain incompletely understood. In 17 CPSP patients receiving invasive neuromodulation, we utilized voxelwise odds-ratio mapping and normative resting state fMRI to identify high-risk pain hotspots and describe functional networks associated with CPSP lesions and analgesic stimulation. Highest-risk CPSP hotspots were located in somatosensory thalamus/white matter and connected to a network comprising anterior cingulate cortex, insula, thalamus, and inferior parietal lobule. Posterior insula and thalamus were also coupled to therapeutic deep brain stimulation volumes. These findings elucidate CPSP's topography and connectivity while informing the network-level mechanism of analgesic neuromodulation.

## Oral

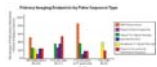
### Neurovascular imaging - Beyond the Lumen: Vessel Wall Imaging in Cerebrovascular Diseases

Thursday Parallel 2 Live Q&A

Thursday 14:20 - 15:05 UTC

Moderators: Jae Song & Lena Vaclavu

1061



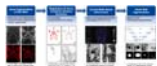
### Imaging Endpoints by Pulse Sequence Type for Intracranial Atherosclerosis using Vessel Wall MR Imaging

Jae W Song<sup>1</sup>, Athanasios Pavlou<sup>1</sup>, Jiayu Xiao<sup>2</sup>, Steven R Messe<sup>3</sup>, Scott E Kasner<sup>3</sup>, Zhaoyang Fan<sup>2</sup>, and Laurie A Loevner<sup>1</sup>

<sup>1</sup>Radiology, University of Pennsylvania, Philadelphia, PA, United States, <sup>2</sup>Radiology, Cedars Sinai Medical Center, Los Angeles, CA, United States, <sup>3</sup>Neurology, University of Pennsylvania, Philadelphia, PA, United States

Intracranial atherosclerosis is a common cause of ischemic stroke. Variability in protocol/pulse sequence design of intracranial vessel wall MR imaging (VWI) has led to different imaging endpoints to detect and characterize atherosclerosis. We systematically reviewed the literature to identify VWI investigations studying atherosclerosis to identify commonly reported imaging endpoints. The most common imaging endpoints using T1-weighting included wall enhancement, thickening, plaque quadrant in cross-section, and stenosis; on T2-weighting, intraplaque T2 signal intensity and wall thickening were common endpoints. Establishing diagnostically accurate imaging endpoints to validate as atherosclerosis biomarkers are critical to understand where efforts for technique optimization should be directed.

1062



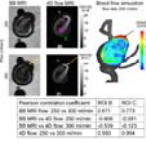
### Automated Morphology Analysis of Intracranial and Extracranial Vessel Wall Using Convolutional Neural Network

Liwen Wan<sup>1</sup>, Na Zhang<sup>1</sup>, Lei Zhang<sup>1</sup>, Shi Su<sup>1</sup>, Cheng Wang<sup>1</sup>, Baochang Zhang<sup>1</sup>, Hao Peng<sup>1</sup>, Haoxiang Li<sup>1</sup>, Dong Liang<sup>1</sup>, Xin Liu<sup>1</sup>, and Hairong Zheng<sup>1</sup>

<sup>1</sup>Shenzhen Institutes of Advanced Technology, Chinese Academy of Sciences, Shenzhen, China

Intracranial and extracranial atherosclerotic disease are major causes of ischemic stroke. Manual analyses of intracranial and extracranial artery vessel wall are time consuming and experience dependent. The purpose of this study was to develop an automated method to analyze 3D intra- and extracranial arterial vessel wall images, including vessel centerline tracking, vessel straightened reformation, vessel wall segmentation based on CNN, and morphological quantification. In conclusion, the proposed method facilitates the large-scale quantitative analysis of vessel wall, and is promising in promoting the clinical applications of MR vessel wall imaging.

1063



### Investigation of black blood MRI signal enhancement in a patient-specific aneurysm model.

Mariya Stanislavovna Pravdivtseva<sup>1</sup>, Carson Hoffman<sup>2</sup>, Leonardo A. Rivera-Rivera<sup>2</sup>, Rafael Medero<sup>2</sup>, Lindsay Bodart<sup>2</sup>, Alejandro Roldan-Alzate<sup>2</sup>, Michael A. Speidel<sup>2</sup>, Charles M. Strother<sup>2</sup>, Kevin M. Johnson<sup>2</sup>, Oliver Wieben<sup>2</sup>, Olav Jansen<sup>3</sup>, Naomi Larsen<sup>3</sup>, Philipp Berg<sup>4</sup>, Eva Peschke<sup>1</sup>, and Jan-Bernd Hövener<sup>1</sup>

<sup>1</sup>Neuroradiology and Radiology, Section Biomedical Imaging, Molecular Imaging North Competence Center (MOIN CC), Department of Radiology and Neuroradiology, University Medical Center Schleswig-Holstein (UKSH), Kiel University, Kiel, Germany, <sup>2</sup>Department of Medical Physics, University of Wisconsin School of Medicine and Public Health, Madison, Wisconsin, USA, Madison, WI, United States, <sup>3</sup>Neuroradiology and Radiology, Department of Radiology and Neuroradiology, University Medical Center Schleswig-Holstein (UKSH), Kiel, Germany, <sup>4</sup>Research Campus STIMULATE, University of Magdeburg, Magdeburg, Germany, Magdeburg, Germany

Intracranial aneurysm is a life-threatening disease. Vessel wall enhancement may be used as a marker to identify an aneurysm with a high risk of rupture. Accumulation of contrast agent in the vessel wall and slow or turbulent flow can contribute to the formation of vessel wall enhancement. In the current study enhanced signal on black blood MRI was observed in printed model of an intracranial aneurysm with and without Gd administration. The found signal was associated with the slow flow in the aneurysm. Additionally, the impact of spatial resolution, flow rate, MSDE preparation and contrast concentration was considered.

1064



### Atherosclerotic Plaques on Perforating Arteries Can be Detected by Vessel Wall Imaging at 7T in Patients with Single Subcortical Infarction

Qingle Kong<sup>1,2,3</sup>, Haiqiang Qin<sup>4</sup>, Ning Wei<sup>5</sup>, Jing An<sup>6</sup>, Yan Zhuo<sup>1,2,3</sup>, and Zihao Zhang<sup>1,2,3</sup>

<sup>1</sup>State Key Laboratory of Brain and Cognitive Science, Beijing MR Center for Brain Research, Institute of Biophysics, Chinese Academy of Sciences, Beijing, China, <sup>2</sup>University of Chinese Academy of Sciences, Beijing, China, <sup>3</sup>CAS Center for Excellence in Brain Science and Intelligence Technology, Beijing, China, <sup>4</sup>Department of neurology, Beijing Tiantan Hospital, Capital Medical University, Beijing, China, <sup>5</sup>China National Clinical Research Center for Neurological Diseases, Beijing Tiantan Hospital, Capital Medical University, Beijing, China, <sup>6</sup>Siemens Shenzhen Magnetic Resonance Ltd., Shenzhen, China

Branch atheromatous disease (BAD) refers to small, deep brain infarcts that are predominantly caused by the occlusion of perforating arteries, which may lead to single subcortical infarction (SSI). However, there is no in-vivo radiological evidence of plaques in the perforating arteries due to their small caliber. In this study, we used high-resolution black-blood imaging at 7T to display the vessel wall of the anterior choroidal artery (AChA), and analyzed atherosclerotic plaques of AChA in patients with isolated infarcts on the posterior limb of internal capsule. The delineation of AChA plaques provides direct imaging evidence for the etiological diagnosis of BAD.

1065



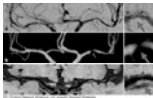
### Serial MR Vessel Wall Imaging Reveals Medical Treatment Response of Symptomatic Intracranial Atherosclerotic Plaque

Jiayu Xiao<sup>1</sup>, Shlee Song<sup>1</sup>, Konrad Schlick<sup>1</sup>, Shuang Xia<sup>2</sup>, Tao Jiang<sup>3</sup>, Tong Han<sup>4</sup>, Robert Jackson<sup>1</sup>, Oana Dumitrascu<sup>1</sup>, Marcel Maya<sup>1</sup>, Patrick Lyden<sup>1</sup>, Debiao Li<sup>1,5</sup>, Qi Yang<sup>6</sup>, and Zhaoyang Fan<sup>1,5</sup>

<sup>1</sup>Cedars-Sinai Medical Center, Los Angeles, CA, United States, <sup>2</sup>Tianjin First Central Hospital, Tianjin, China, <sup>3</sup>Beijing Chaoyang Hospital, Beijing, China, <sup>4</sup>Tianjin Huanhu Hospital, Tianjin, China, <sup>5</sup>University of California, Los Angeles, Los Angeles, CA, United States, <sup>6</sup>Beijing Xuanwu Hospital, Beijing, China

Ischemic stroke is a leading cause of disability and death, also has a high recurrence rate. Serial magnetic resonance vessel wall imaging (MR-VWI) was used to quantify the morphological changes of intracranial atherosclerotic plaque during the medical treatment of ischemic stroke patients. Changes of quantitative plaque features were compared between patients with different clinical outcomes. Our study showed an increasing trend in most progression patients. Maximum wall thickness, pre-contrast plaque-wall contrast ratio and post-contrast plaque enhancement ratio showed significant decreases in the non-progression group. Quantitative assessment of atherosclerotic lesion-specific responses to medical therapy is clinically feasible with serial MR-VWI.

1066



**Accuracy of 3D High-Resolution Vessel Wall Imaging in Evaluating Internal Carotid and Intracranial Arterial Stenotic Lesions**

Yan Gong<sup>1</sup>, Chen Cao<sup>2</sup>, Yu Guo<sup>3</sup>, Song Liu<sup>2</sup>, Zhu Jinxia<sup>4</sup>, Shuang Xia<sup>3</sup>, Xiudi Lu<sup>3</sup>, Ying Zou<sup>3</sup>, and Wen Shen<sup>3</sup>

<sup>1</sup>Tianjin Medical University NanKai Hospital, Tianjin, China, <sup>2</sup>Department of Radiology, Tianjin Huanhu Hospital, Tianjin, China, <sup>3</sup>Department of Radiology, Tianjin First Central Hospital, Tianjin, China, <sup>4</sup>siemens-healthineers, Tianjin, China

This study compared high-resolution vessel wall imaging (HR-VWI) and time-of-flight magnetic resonance angiography (TOF-MRA) for evaluation of stenosis using digital subtraction angiography (DSA) as the criterion standard. Compared with TOF-MRA, HR-VWI produced results that more closely agreed with DSA, showed better reproducibility and accuracy with smaller variance, and provided additional information on vessel wall pathology. HR-VWI may therefore be useful as an adjunct to DSA to diagnose stenosis and evaluate changes in intracranial vessel walls.

1067



Parameter	Asymptomatic	Symptomatic
Age	61.2 ± 10.5	61.8 ± 11.2
Gender	32 (64.0%)	31 (62.0%)
Diabetes	12 (24.0%)	15 (30.0%)
Hypertension	28 (56.0%)	30 (60.0%)
Hyperlipidemia	25 (50.0%)	28 (56.0%)
Smoking	18 (36.0%)	20 (40.0%)
Alcohol	15 (30.0%)	18 (36.0%)
ICAD	15 (30.0%)	30 (60.0%)
LDL	180.5 ± 45.2	195.3 ± 52.1
HDL	105.2 ± 35.1	98.7 ± 32.5
TC	215.3 ± 55.4	225.6 ± 60.2
Triglyceride	155.4 ± 45.3	165.7 ± 50.1
FBG	5.2 ± 0.8	5.5 ± 0.9
CRP	1.2 ± 0.5	1.5 ± 0.6
hs-CRP	1.8 ± 0.7	2.1 ± 0.8
hs-CRP/CRP	1.5 ± 0.4	1.6 ± 0.5

**Association of conventional vascular risk factors with asymptomatic and symptomatic intracranial atherosclerosis**

Yongjun Han<sup>1,2</sup>, Runhua Zhang<sup>3</sup>, DanDan Yang<sup>1,2</sup>, Hualu Han<sup>2</sup>, Huiyu Qiao<sup>2</sup>, Dongye Li<sup>4</sup>, Shuo Chen<sup>2</sup>, Gaifen Liu<sup>3</sup>, and Xihai Zhao<sup>2</sup>

<sup>1</sup>Center for Brain Disorders Research, Capital Medical University and Beijing Institute of Brain Disorders, Beijing, China, <sup>2</sup>Center for Biomedical Imaging Research, Department of Biomedical Engineering, Tsinghua University School of Medicine, Beijing, China, <sup>3</sup>Department of Neurology, Beijing Tiantan Hospital, Capital Medical University; China National Clinical Research Center for Neurological Diseases, Beijing, China, <sup>4</sup>Department of radiology, Sun Yat-sen Memorial hospital, Sun Yat-sen University, Beijing, China

This study investigated the association of vascular risk factors with asymptomatic and symptomatic ICAD using MR vascular wall imaging. Compared with controls, there was a positive association between hypertension and asymptomatic ICAD; and a positive association of hypertension, LDL, and diabetes and an inverse association of HDL with symptomatic ICAD (all p<0.05). Compared to asymptomatic ICAD, there was an inverse association between hyperlipidemia and symptomatic ICAD (p<0.001). We found that hypertension was a risk factor of asymptomatic ICAD and hypertension, diabetes and higher LDL were risk factors for symptomatic ICAD, whereas HDL was inversely associated with symptomatic ICAD.

**Oral - Power Pitch**

**Neurovascular imaging - Highlights in Cerebral Lumenography & Vascular Reactivity**

Thursday Parallel 2 Live Q&A

Thursday 14:20 - 15:05 UTC

Moderators: Henk Mutsaerts



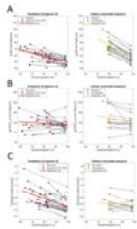
### Cerebrovascular reactivity mapping using resting-state fMRI: comparison with CO<sub>2</sub>-inhalation method in 170 controls and 50 Moyamoya patients

Gongkai Liu<sup>1</sup>, Hanzhang Lu<sup>1</sup>, Yang Li<sup>1</sup>, Binu Thomas<sup>2</sup>, Marco Pinho<sup>2</sup>, Judy Huang<sup>1</sup>, Babu G. Welch<sup>2</sup>, Denise C. Park<sup>3</sup>, and Peiyong Liu<sup>1</sup>

<sup>1</sup>Department of Radiology, Johns Hopkins University School of medicine, Baltimore, MD, United States,

<sup>2</sup>University of Texas Southwestern Medical Center, Dallas, TX, United States, <sup>3</sup>The University of Texas at Dallas, Dallas, TX, United States

Cerebral vascular reserve, which indicates the potential of the tissue to receive more blood flow when needed, is desired to evaluate the ischemic risk of brain tissue. However, it is cumbersome to measure vascular reserve using the current methods with Diamox or hypercapnia challenges. Therefore there is a growing interest in using resting-state MRI data to measure cerebrovascular reactivity (CVR). Here, using CO<sub>2</sub>-inhalation MRI as a gold standard and capitalizing on a large cohort of healthy controls (N=170) and Moyamoya patients (N=50), we sought to identify the optimal strategies for resting-state CVR mapping and establish benchmarks for this new technique.

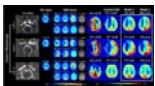


### Effects from inhalation of hypoxic air and carbon monoxide exposure on human cerebral perfusion, oxygen consumption and lactate production

Mark Bitsch Vestergaard<sup>1</sup>, Hashmat Ghanizada<sup>2</sup>, Ulrich Lindberg<sup>1</sup>, Nanna Arngim<sup>2</sup>, Olaf Paulson<sup>3</sup>, Messoud Ashina<sup>2</sup>, and Henrik Bo Wiberg Larsson<sup>1</sup>

<sup>1</sup>Functional Imaging Unit, Department of Clinical Physiology, Nuclear Medicine and PET, Copenhagen University Hospital Rigshospitalet, Glostrup, Denmark, <sup>2</sup>Danish Headache Center, Department of Neurology, Copenhagen University Hospital Rigshospitalet, Glostrup, Denmark, <sup>3</sup>Neurobiology Research Unit, Department of Neurology, Copenhagen University Hospital Rigshospitalet, Copenhagen, Denmark

In present study we demonstrate that in healthy humans the cerebral lactate concentration increases during inhalation of hypoxic air but not after exposure to carbon monoxide. This suggests a regulatory mechanism of cerebral glycolytic activity possibly mediated by sensing of arterial oxygen pressure and that the lactate production is not solely a result of hindered oxidative metabolism, at least during non-threatening hypoxic exposure. Phase-contrast mapping and susceptibility-based oximetry were used to acquire global cerebral blood flow and oxygen consumption and MR-spectroscopy was used to measure the lactate concentration in the occipital lobe in a total of 51 healthy humans.

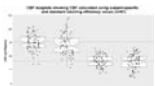


### Using Deep Learning to Predict PET Cerebrovascular Reserve in Moyamoya Disease from Baseline MRI

David Yen-Ting Chen<sup>1,2</sup>, Yosuke Ishii<sup>1,3</sup>, Moss Yize Zhao<sup>1</sup>, Audrey Peiwen Fan<sup>1</sup>, and Greg Zaharchuk<sup>1</sup>

<sup>1</sup>Radiology, Stanford University, Palo Alto, CA, United States, <sup>2</sup>Medical Imaging, Shuang Ho Hospital, Taipei Medical University, New Taipei City, Taiwan, <sup>3</sup>Neurosurgery, Tokyo Medical and Dental University, Tokyo, Japan

Cerebrovascular reserve (CVR) is an important hemodynamic parameter for moyamoya disease. Acetazolamide (ACZ) test is often used to measure CVR clinically. However, ACZ is contraindicated in patients with sulfa allergies, severe kidney and liver disease and potentially has severe adverse side effect. Thus, there is a need to assess CVR without pharmacological vasodilation. We utilized a simultaneous [15O]-water PET/MRI dataset to train a convolutional neural network (CNN) to predict CVR. The CNN combined multi-contrast information from baseline perfusion and structural images to predict whole-brain PET-level CVR, with high image quality, quantification accuracy, and diagnostic accuracy for identifying impaired CVR.

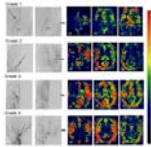


### Effect of subject-specific labelling efficiency for arterial spin labelling on cerebral blood flow in mild stroke patients

Michael S Stringer<sup>1,2</sup>, Nithya N Nair<sup>3</sup>, Una Clancy<sup>1,2</sup>, Alasadir Morgan<sup>1,2</sup>, Zahra Shirzadi<sup>4,5</sup>, Yulu Shi<sup>1,2,6</sup>, Francesca Chappell<sup>1,2</sup>, Antoine Vallatos<sup>1,2</sup>, Maria Valdes Hernandez<sup>1,2</sup>, Dany Jaime Garcia<sup>1,2</sup>, Gordon W Blair<sup>1,2</sup>, Rosalind Brown<sup>1,2</sup>, Bradley J MacIntosh<sup>4,5</sup>, Ian Marshall<sup>1,2</sup>, Fergus Doubal<sup>1,2</sup>, Michael J Thrippleton<sup>1,2</sup>, and Joanna M Wardlaw<sup>1,2</sup>

<sup>1</sup>Centre for Clinical Brain Sciences, University of Edinburgh, Edinburgh, United Kingdom, <sup>2</sup>UK DRI at the University of Edinburgh, Edinburgh, United Kingdom, <sup>3</sup>Centre for Discovery Brain Sciences, University of Edinburgh, Edinburgh, United Kingdom, <sup>4</sup>Department of Biomedical Physics, University of Toronto, Toronto, ON, Canada, <sup>5</sup>Hurvitz Brain Sciences, Sunnybrook Research Institute, University of Toronto, Toronto, ON, Canada, <sup>6</sup>Beijing Tiantan Hospital, Capital Medical University, Beijing, China

Accurate cerebral blood flow (CBF) quantification using arterial spin labelling (ASL) depends on physiological and MR parameters. Labelling efficiency is particularly relevant given it may vary between vascular disease patients. We determined subject-specific labelling efficiency values using phase-contrast MRI scans in a mild stroke cohort. Bland-Altman plots suggested a bias in CBF, with nominal labelling efficiency values underestimating at low and overestimating at high CBF. Using subject-specific, but not nominal, labelling efficiency showed plausible associations between white matter CBF and smoking status, pulse pressure, and age. Subject-specific labelling efficiencies appear to mitigate variance and improve CBF quantification in clinical ASL.

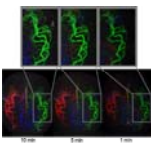


### Noninvasive Assessment of Cerebral Collaterals with 3D Multi-inversion Time Arterial Spin Labeling in Ischemic Stroke: Comparison with DSA

Hui Wang<sup>1</sup>, Chuili Kong<sup>2</sup>, Quanzhi Feng<sup>1</sup>, Yi Liu<sup>1</sup>, Yutian Li<sup>1</sup>, Jinli Li<sup>1</sup>, Josef Pfeuffer<sup>3</sup>, Xianchang Zhang<sup>4</sup>, and Tong Han<sup>1</sup>

<sup>1</sup>Radiology, Tianjin Huanhu Hospital, Tianjin, China, <sup>2</sup>Radiology, Liaocheng People's Hospital, Liaocheng, China, <sup>3</sup>Siemens Healthcare, Erlangen, Germany, <sup>4</sup>MR Collaboration, Siemens Healthcare Ltd, Beijing, China

This study proposed a new method that can directly visualize and assess the collateral status by post-processing multiphase perfusion-weighted images (PWI) generated by multi-inversion time arterial spin labeling (mTI-ASL), and evaluate its performance by comparison with digital subtraction angiography (DSA) in patients with ischemic stroke. Comparison of the results of 28 patients showed that the collateral status assessed by the 3D mTI-ASL grading system was greatly consistent (kappa coefficient  $k = 0.854$ ) with DSA. This technique is promising for the noninvasive assessment of the collateral status in stroke patients.

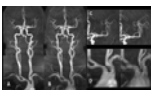


### High resolution 4D vessel selective angiography in under 5 minutes using a constrained reconstruction

Sophie Schauman<sup>1</sup>, Thomas W Okell<sup>1</sup>, and Mark Chiew<sup>1</sup>

<sup>1</sup>Wellcome Centre for Integrative Neuroimaging, NDCN, University of Oxford, Oxford, United Kingdom

Arterial spin labeling methods can be used to produce vessel selective angiograms. However, to do this in 3D or 4D is extremely time consuming as many encodings of high spatial (and temporal) resolution images are needed. We propose an optimized acquisition and reconstruction method to create high quality angiograms in five minutes or less. For the acquisition protocol we explore different sampling patterns across encoded images, and for the reconstruction method different ways of constraining the signal temporally.



### Comparison of Spiral and Cartesian k space filling strategies for Time of Flight MR angiography for cervicocerebral arteries – Pilot Study

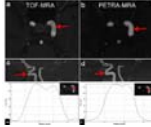
Ravi Varma Dandu<sup>1</sup>, Karthick Raj Rajendran<sup>2</sup>, Rithika Varma Dandu<sup>3</sup>, Sivakanth Nalubolu<sup>4</sup>, Kiran Barla<sup>1</sup>, Narayana Rolla<sup>5</sup>, and Indrajit Saha<sup>6</sup>



<sup>1</sup>Citi Neuro Centre, Hyderabad, India, <sup>2</sup>Philips Healthcare, Eindhoven, Netherlands, <sup>3</sup>RV College of Engineering, Bengaluru, India, <sup>4</sup>Narayana Health City, Bangalore, India, <sup>5</sup>Philips Healthcare, Bangalore, India, <sup>6</sup>Philips Healthcare, Gurgaon, India

This study compares the performance of Time of Flight MR angiography (ToF-MRA) with spiral k-space filling and ToF-MRA with cartesian filling, for evaluation of the cervicocerebral circulation in 16 healthy volunteers. The imaging protocols were adjusted to give similar coverage and scan times for both techniques. Spiral ToF-MRA showed better visualization of almost all arteries of the cervicocerebral circulation – especially in the small distal intracranial arteries. Artefactual signal drops in segments with slow flow were also fewer with spiral ToF-MRA. Spiral ToF-MRA can potentially evaluate the cervicocerebral arterial system with higher spatial resolution than Cartesian ToF-MRA.

1075



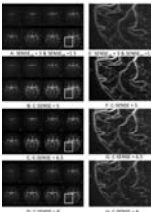
Clinical Evaluation of PETRA-MR Angiography in comparison with 3D-TOF-MRA for improved flow dephasing at 3 Tesla

Qing Fu<sup>1</sup>, Xiao-yong Zhang<sup>2</sup>, and Ding-xi Liu<sup>1</sup>

<sup>1</sup>Department of Radiology, Union Hospital, Tongji Medical College, Huazhong University of Science and Technology, Wuhan, China, <sup>2</sup>MR Collaborations, Siemens Healthcare Ltd., Shenzhen, China

This study aimed to demonstrate the image quality and diagnostic performance of subtraction-based pointwise encoding time reduction with radial acquisition (PETRA-MRA) for improved flow dephasing in the intracranial internal carotid artery (ICA) when compared with conventional 3D-TOF-MRA. Our findings showed that image quality and signal homogeneity within the ICA in PETRA-MRA were significantly better than those obtained with TOF-MRA. In conclusion, PETRA-MRA proved to be superior for depicting less flow dephasing artifacts and better image quality in comparison with 3D-TOF-MRA.

1076



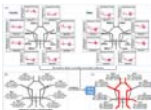
Compressed SENSE combined with Keyhole and View-Sharing accelerate Non-contrast enhanced 4D Intracranial MRA based on pCASL

Jilei Zhang<sup>1</sup>, Weibo Chen<sup>1</sup>, Jianqing Sun<sup>1</sup>, Queenie Chan<sup>1</sup>, Maoxue Wang<sup>2</sup>, and Bing Zhang<sup>2</sup>

<sup>1</sup>Clinical Science, Philips Healthcare, Shanghai, China, <sup>2</sup>Drum Tower Hospital, Medical School of Nanjing University, Nanjing, China

The non-contrast enhanced 4D MRA is time-consuming because of the needs to acquire high resolution data at multi-timepoints, which limited its clinical application. In current study, 4D-PACK combined with C-SENSE=6.5 can reduce 23% acquisition time (4 min 42s) for non-contrast enhanced 4D-MRA compared with 4D-PACK with SENSE acceleration, and the excellent acceleration advantage of C-SENSE can improve the clinical application for 4D MRA. The proposed acquisition scheme of 4DMRA with C-SENSE acceleration can be potentially used for evaluating arteriovenous malformation (AVM), arteriovenous fistulas (AVF), moyamoya disease, and stroke patients.

1077



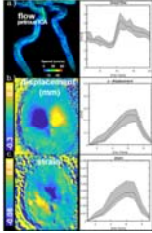
Heat Maps of Abnormal Intracranial Hemodynamics in Intracranial Atherosclerotic Disease using 4D Flow MRI

Yue Ma<sup>1,2</sup>, Maria Aristova<sup>1</sup>, Sameer Ansari<sup>1,3,4</sup>, Ann Ragin<sup>1</sup>, Michael Markl<sup>1</sup>, and Susanne Schnell<sup>5</sup>

<sup>1</sup>Radiology, Northwestern University, Chicago, IL, United States, <sup>2</sup>Radiology, Shengjing Hospital of China Medical University, Shenyang, China, <sup>3</sup>Neurology, Northwestern University, Chicago, IL, United States, <sup>4</sup>Neurosurgery, Northwestern University, Chicago, IL, United States, <sup>5</sup>Radiology, University of Greifswald, Chicago, IL, United States

Symptomatic intracranial atherosclerotic disease (ICAD) patients who present with stenosis and hemodynamic abnormalities are at higher risk of recurrent stroke. We propose a methodology that creates patient-specific 'heat maps' of abnormal hemodynamic parameters, based on intracranial dual-venic 4D flow MRI. The heat maps were created by detecting and highlighting outlier measurements from 95% confidence interval of normative parameter estimates in healthy controls. Elevated peak velocity (PV) was found in 75% of patients and 58.3% of them with abnormal PV in the uninvolved hemisphere. This novel approach to characterize intracranial hemodynamic impact may allow making patient-specific risk stratification and treatment strategies.

1078



#### Association of Brain Biomechanics and Vascular Dynamics using 4D Flow, MRE and DENSE MRI

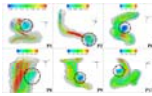
Leonardo A Rivera-Rivera<sup>1</sup>, Grant S Roberts<sup>1</sup>, Laura B Eisenmenger<sup>2</sup>, Oliver Wieben<sup>1,2</sup>, Sterling C Johnson<sup>3</sup>, and Kevin M Johnson<sup>1,2</sup>

<sup>1</sup>Department of Medical Physics, University of Wisconsin - Madison, Madison, WI, United States,

<sup>2</sup>Department of Radiology, University of Wisconsin - Madison, Madison, WI, United States, <sup>3</sup>Department of Medicine, University of Wisconsin - Madison, Madison, WI, United States

The coupling of brain biomechanics and hemodynamics is complex as it includes arterial pressure pulsations, venous and CSF flow, and tissue compliance. Experimental evidence has demonstrated alterations of each the multiple compartments in disease; however, the relationships and coupling between brain biomechanics (e.g. strain and stiffness) and vascular flow dynamics is not well characterized. This study investigates the relationships between brain blood flow, stiffness, and strain using a multi-scale brain imaging platform that includes 4D flow, MRE, and DENSE MRI. Results suggest strong correlations between blood flow, strain, and stiffness and age-related changes in these parameters.

1079



#### Three Dimensional Vortex Identification and Characterization in Small Intracranial Aneurysms based on Sub-millimetric 4D Flow MRI at 7 Tesla

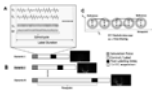
Ang Zhou<sup>1</sup>, Sean Moen<sup>2</sup>, Bharathi Jagadeesan<sup>2,3,4</sup>, and Pierre-Francois Van de Moortele<sup>1</sup>

<sup>1</sup>Center for Magnetic Resonance Research, University of Minnesota, Minneapolis, MN, United States,

<sup>2</sup>Department of Neurosurgery, University of Minnesota, Minneapolis, MN, United States, <sup>3</sup>Department of Radiology, University of Minnesota, Minneapolis, MN, United States, <sup>4</sup>Department of Neurology, University of Minnesota, Minneapolis, MN, United States

Asymptomatic small intracranial aneurysms affect about 1 in 50 people and are often considered at a low risk of rupture. There are no effective hemodynamic parameters accurately predicting the evolution of small aneurysms. Three dimensional vortex motion is observed in aneurysms which reflects the hemodynamic environment and potentially impact the development of small aneurysms. We propose an approach to describe the three dimensional main vortex motion as a whole inside small aneurysms based on 4D Flow MRI at 7 Tesla. This approach defines the high vortex motion region and gives the direction of the main vortex motion and its center.

1080



#### Vessel-selective 4D-MRA Using Superselective pCASL Combined with CENTRA-Keyhole (4D-S-PACK) for Intracranial Dural Arteriovenous Fistulas

Osamu Togao<sup>1</sup>, Akio Hiwatashi<sup>2</sup>, Makoto Obara<sup>3</sup>, Michael Helle<sup>4</sup>, Kazufumi Kikuchi<sup>1</sup>, Daichi Momosaka<sup>1</sup>, Yoshitomo Kikuchi<sup>1</sup>, Tatsuhiro Wada<sup>5</sup>, Hiroo Murazaki<sup>5</sup>, and Marc Van Cauteren<sup>3</sup>

<sup>1</sup>Department of Clinical Radiology, Graduate School of Medical Sciences, Kyushu University, Fukuoka,

Japan, <sup>2</sup>Department of Molecular Imaging & Diagnosis, Graduate School of Medical Sciences, Kyushu

University, Fukuoka, Japan, <sup>3</sup>Philips Japan, Tokyo, Japan, <sup>4</sup>Philips Research, Hamburg, Germany, <sup>5</sup>Division

of Radiology, Department of Medical Technology, Kyushu University Hospital, Fukuoka, Japan

In this study, we demonstrated the ability of 4D-S-PACK (4D-MRA based on superselective pCASL with CENTRA-keyhole and view-sharing) to visualize intracranial DAVFs. 4D-S-PACK enables a time-resolved and vessel-selective angiography within 5 minutes without a use of contrast agents. It was shown that good vessel selectivity for the internal and external carotid arteries was achieved with 4D-S-PACK. 4D-S-PACK enabled accurate identification of feeding arteries. Although the superselective labelling in 4D-S-PACK caused a slight reduction in CNR, compared to full labelling in 4D-PACK, this was acceptable since visualization was well preserved. 4D-PACK can be a non-invasive clinical tool for assessing intracranial DAVFs.

---

## Combined Educational & Scientific Session

### Novel imaging techniques for CMR - Multi-Contrast & High Dimensionality Cardiovascular MRI

Organizers: Jennifer Steeden, Bernd Wintersperger

Thursday Parallel 3 Live Q&A

Thursday 14:20 - 15:05 UTC

Moderators: Anthony Christodoulou & Eddy Solomon

#### Fingerprinting: Concept & State-of-the Art Techniques

Yong Chen<sup>1</sup>

<sup>1</sup>Radiology, Case Western Reserve University, Cleveland, OH, United States

Magnetic Resonance Fingerprinting is a novel imaging method for rapid quantitative imaging. This presentation will first cover the basic concepts of Magnetic Resonance Fingerprinting and then introduce its extension for cardiac imaging. We will further discuss recent advances in cardiac Magnetic Resonance Fingerprinting and the future directions in clinical applications.

---

#### High-Dimensionality Imaging: What More Does It Give Us?

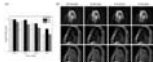
Ricardo Otazo<sup>1</sup>

<sup>1</sup>Memorial Sloan Kettering Cancer Center, United States

A recent paradigm shift in MRI has seen the capture of multiple dynamic dimensions in a single acquisition. At first glance, adding new dimensions would appear to make MRI more challenging, but recent developments in compressed sensing and low-rank tensor imaging have shown that this multidimensional image structure can be exploited to improve over conventional imaging performance and enable access to new physiological information of clinical interest. This talk will present the most significant developments in this paradigm shift along with relevant clinical applications.

---

1081



#### MR Multitasking based Multi-dimensional Assessment of Cardiovascular System (MT-MACS) Technique: Feasibility on the Thoracic Aorta

Zehao Hu<sup>1,2</sup>, Anthony G. Christodoulou<sup>1</sup>, Nan Wang<sup>1,2</sup>, Shlee S. Song<sup>3</sup>, Marcel M. Maya<sup>4</sup>, Mariko L. Ishimori<sup>5</sup>, Lindsay J. Forbess<sup>5</sup>, Jiayu Xiao<sup>1</sup>, Xiaoming Bi<sup>6</sup>, Fei Han<sup>6</sup>, Debiao Li<sup>1,2,7</sup>, and Zhaoyang Fan<sup>1,2,7</sup>

<sup>1</sup>Biomedical Imaging Research Institute, Cedars-Sinai Medical Center, Los Angeles, CA, United States,

<sup>2</sup>Bioengineering Department, University of California, Los Angeles, Los Angeles, CA, United States,

<sup>3</sup>Department of Neurology, Cedars-Sinai Medical Center, Los Angeles, CA, United States, <sup>4</sup>Department of

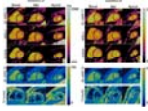
Imaging, Cedars-Sinai Medical Center, Los Angeles, CA, United States, <sup>5</sup>Department of Rheumatology,

Cedars-Sinai Medical Center, Los Angeles, CA, United States, <sup>6</sup>Siemens Healthineers, Los Angeles, CA,

United States, <sup>7</sup>Department of Medicine, University of California, Los Angeles, Los Angeles, CA, United States

Thoracic aortic diseases are one of the most common causes of cardiovascular morbidity and mortality, where imaging plays a central role in diagnosis. As a noninvasive technique, MR imaging has the potential to provide a comprehensive evaluation of the thoracic aorta from various aspects. However, clinical adoption of this modality is hindered by several limitations, i.e. long scan time and cumbersome setup for accommodating motion during data acquisition. In this work, we present an MR MultiTasking based 3D Multi-dimensional Assessment of Cardiovascular System (MT-MACS) technique that allows for ECG- and navigator-free thoracic aortic imaging within 6 minutes.

1082



### 3D Free-breathing Cardiac Magnetic Resonance Fingerprinting

Gastao Cruz<sup>1</sup>, Olivier Jaubert<sup>1</sup>, Haikun Qi<sup>1</sup>, Aurelien Bustin<sup>1</sup>, Giorgia Milotta<sup>1</sup>, Torben Schneider<sup>2</sup>, Peter Koken<sup>3</sup>, Mariya Doneva<sup>3</sup>, René M. Botnar<sup>1</sup>, and Claudia Prieto<sup>1</sup>

<sup>1</sup>Biomedical Engineering Department, School of Biomedical Engineering and Imaging Sciences, King's College London, London, United Kingdom, <sup>2</sup>Philips Healthcare, Guildford, United Kingdom, <sup>3</sup>Philips Research Hamburg, Hamburg, Germany

2D cardiac Magnetic Resonance Fingerprinting (cMRF) has been proposed for simultaneous and co-registered T1/T2 mapping using ECG-triggering and breath-holding. However, 2D cMRF provides limited coverage of the heart and is sensitive to residual through-plane respiratory motion. Here we propose respiratory motion-compensated 3D cMRF to enable whole-heart myocardial T1/T2 mapping in a single free-breathing scan. Respiratory bellows driven localized autofocus is proposed for beat-to-beat translational motion correction and patch-based low rank MRF reconstruction is employed to minimise residual aliasing. 3D cMRF enabled whole-heart T1/T2 mapping in ~7min scan time with comparable map quality to conventional 2D MOLLI, SASHA and T2-GraSE.

1083



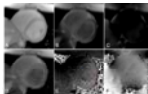
### Quantification of carotid plaque composition with Multi-contrast Atherosclerosis Characterization (MATCH) versus multisequence carotid MRI

Mohamed Kassem<sup>1,2</sup>, Ellen Boswijk<sup>2</sup>, Jochem Van der Pol<sup>2</sup>, Rik PM Moonen<sup>2</sup>, Jan Bucarius<sup>2</sup>, Zhaoyang Fan<sup>3</sup>, and M Eline Kooj<sup>1,2</sup>

<sup>1</sup>Radiology and Nuclear medicine, CARIM School for Cardiovascular Diseases, Maastricht, Netherlands, <sup>2</sup>Radiology and Nuclear medicine, Maastricht university Medical Centre, Maastricht, Netherlands, <sup>3</sup>Cedars-Sinai Medical Center, Biomedical Imaging Research Institute, Los Angeles, CA, United States

Multisequence MRI protocol usually includes an MP-RAGE sequence for the identification of plaque compositions. Multisequence MRI has some limitations including long scan time and image mis-registration errors. Multi-contrast Atherosclerosis Characterization (MATCH) was developed to overcome the above limitations. Eighteen patients with  $\geq 2$  mm carotid plaques underwent 3.0T carotid MRI including conventional multisequence and MATCH. For the artery-based component detection, excellent agreement was obtained for LRNC, substantial for IPH and slight agreement for calcifications. No significant difference between MATCH and conventional MRI was shown in measurement of volume of LRNC/IPH, IPH, calcifications, percentage wall volume and normalized wall index.

1084



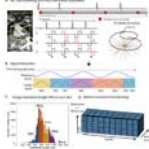
### B1 Inhomogeneity at 3T causes spatially non-reproducible and inaccurate cardiac creatine CEST-contrast in healthy controls

Wissam AlGhuraibawi<sup>1</sup>, Kevin Godines<sup>1</sup>, Mark Velasquez<sup>1</sup>, Sinyeob Ahn<sup>2</sup>, Wolfgang Rehwald<sup>3</sup>, and Moriel Vandsburger<sup>1</sup>

<sup>1</sup>Bioengineering, University of California Berkeley, Berkeley, CA, United States, <sup>2</sup>Siemens Healthineers, Concord, CA, United States, <sup>3</sup>Siemens Healthineers, Durham, NC, United States

CEST-MRI is an emerging molecular imaging method for non-invasive assessment of cardiomyocyte metabolites. In cardiac CEST-MRI, spatial  $B_1$  inhomogeneity across the myocardium significantly reduces the accuracy of measured CEST contrasts. Deviation from the prescribed  $B_1$  leads to altered creatine CEST contrast due to both reduced labeling efficiency and heightened magnetization transfer and direct water direct saturation across the heart. The final impact is measurement of falsely and substantially reduced creatine CEST contrast in the healthy heart.

1085



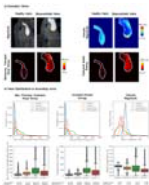
### Decoding the Effects of Rhythm on Hemodynamics in Patients with Atrial Fibrillation Using a 5D Flow Framework

Liliana Ma<sup>1,2</sup>, Jerome Yerly<sup>3</sup>, Lorenzo Di Sopra<sup>3</sup>, Davide Piccini<sup>3,4</sup>, Rod Passman<sup>5</sup>, Philip Greenland<sup>5</sup>, Daniel Kim<sup>1,2</sup>, Matthias Stuber<sup>3</sup>, and Michael Mark<sup>1,2</sup>

<sup>1</sup>Department of Radiology, Northwestern University, Feinberg School of Medicine, Chicago, IL, United States, <sup>2</sup>Department of Biomedical Engineering, Northwestern University, Evanston, IL, United States, <sup>3</sup>Department of Radiology, Lausanne University Hospital (CHUV) and University of Lausanne (UNIL), Lausanne, Switzerland, <sup>4</sup>Siemens Healthcare, Lausanne, Switzerland, <sup>5</sup>Department of Medicine and Preventive Medicine, Northwestern University, Feinberg School of Medicine, Chicago, IL, United States

Atrial fibrillation (AF) is the most common cardiac arrhythmia and is associated with increased risk of ischemic stroke. Arrhythmic heartbeats in AF may alter atrial flow characteristics and the influence of differences in heart rates on LA 3D hemodynamics has not yet been systematically investigated. Recently, a fully self-gated free-running 5D flow (4D flow+respiration) framework was introduced and validated. The purpose of this study was to expand the 5D flow framework to explore the influence of heart rates on thrombogenic hemodynamic parameters in AF patients.

1086



### 5D Flow Tensor MRI with Multipoint Encoding for Efficient Mapping of Reynolds Stresses in the In-vivo Aorta

Jonas Walheim<sup>1</sup>, Hannes Dillinger<sup>1</sup>, Alexander Gotschy<sup>1,2,3</sup>, and Sebastian Kozerke<sup>1</sup>

<sup>1</sup>Institute for Biomedical Engineering, University and ETH Zurich, Zurich, Switzerland, Zurich, Switzerland, <sup>2</sup>Great Ormond Street Hospital, London, United Kingdom, <sup>3</sup>Department of Cardiology, University Hospital Zurich, Zurich, Switzerland

In-vivo 5D Flow Tensor MRI with multipoint encoding for accurate assessment of Reynolds stresses in the aorta is presented. Based on distributions of turbulence intensity in healthy and pathological flows, a 6-directional multipoint encoding with 3 different encoding strengths is proposed. Using a 5D Flow compressed sensing acquisition in-vivo data are collected in 10 minutes irrespective of breathing motion. Data obtained in aortic valve patients and healthy controls demonstrate the feasibility of the method to quantify turbulence in healthy and pathological flow.

## Oral - Power Pitch

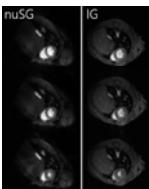
### Novel imaging techniques for CMR - Cardiovascular Power Pitch: Technical

Thursday Parallel 3 Live Q&A

Thursday 14:20 - 15:05 UTC

Moderators: Yang Yang

1087



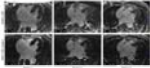
### Retrospective Compensation of Cardiac and Respiratory Motion in Mice using nonuniform Self-Gating

Tobias Speidel<sup>1</sup>, Patrick Metzke<sup>2</sup>, Fabian Straubmueller<sup>2</sup>, Hao Li<sup>1</sup>, and Volker Rasche<sup>2</sup>

<sup>1</sup>Core-Facility Small Animal Imaging, Ulm University, Ulm, Germany, <sup>2</sup>Experimental Cardiovascular MRI, Ulm University Medical Center, Ulm, Germany

The application of self-gating techniques to small animal imaging poses challenging problems, particularly dominated by the high respiratory frequencies. Established self-gating methods are based on information that is extracted either from the k-space itself or from low-resolution images, leading to one-dimensional gating signals. These approaches are prone to fail in the case of arrhythmic respiratory and/or cardiac motion. The concept of nonuniform self-gating is capable of retrospectively considering respiratory and cardiac motion despite significant changes in cardiac or respiratory frequencies by using a two-dimensional gating matrix for deriving the required gating information.

1088



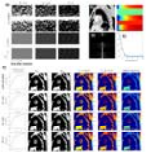
### Highly efficient respiratory motion-compensated 3D water/fat late gadolinium enhanced atrial wall imaging

Camila Munoz<sup>1</sup>, Iain Sim<sup>2</sup>, Aurelien Bustin<sup>1</sup>, Radhouene Neji<sup>1,3</sup>, Karl P Kunze<sup>3</sup>, Michaela Schmidt<sup>4</sup>, Mark O'Neill<sup>2</sup>, Steven E Williams<sup>2</sup>, Rene M Botnar<sup>1</sup>, and Claudia Prieto<sup>1</sup>

<sup>1</sup>Biomedical Engineering Department, School of Biomedical Engineering and Imaging Sciences, King's College London, London, United Kingdom, <sup>2</sup>Cardiovascular Imaging Department, School of Biomedical Engineering and Imaging Sciences, King's College London, London, United Kingdom, <sup>3</sup>MR Research Collaborations, Siemens Healthcare Limited, Frimley, United Kingdom, <sup>4</sup>Cardiovascular MR Predevelopment, Siemens Healthcare GmbH, Erlangen, Germany

3D late gadolinium enhanced (LGE) imaging is a promising technique for the non-invasive assessment of atrial fibrosis. In order to minimize respiratory motion, current 3D LGE atrial imaging relies on diaphragmatic navigator gating, leading to time-consuming scans with unpredictable duration. Here we introduce a highly efficient respiratory motion-compensated 3D water/fat IR-prepared LGE atrial imaging protocol with predictable scan time. Preliminary results demonstrate that the proposed approach enables depiction of atrial scar comparable to conventional 3D atrial LGE imaging, but with a significantly shorter scan time of <5 minutes. The proposed approach holds promise for high-resolution atrial wall imaging.

1089



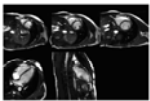
### Accelerating Myocardial Arterial Spin Labeling in Small Animals by Exploiting Spatiotemporal Correlations

Grzegorz Kwiatkowski<sup>1</sup>, Frank Kober<sup>2</sup>, and Sebastian Kozerke<sup>1</sup>

<sup>1</sup>Institute for Biomedical Engineering, ETH Zurich, Zurich, Switzerland, <sup>2</sup>Aix Marseille Univ, CNRS, CRMBM, Marseille, France

The feasibility of accelerating arterial spin labelling (ASL) by exploiting spatiotemporal correlations for assessing myocardial perfusion in small animals is demonstrated. Based on numerical simulations and retrospectively undersampled in-vivo data, three-fold acceleration yields errors below  $16 \pm 10\%$  in myocardial blood flow quantification and hence the method is considered promising to shorten the long scan times of myocardial ASL in small animals.

1090



### Real-Time free breathing cardiac CINE MRI with 84 channel high density receive array at 3 Tesla: Initial experience

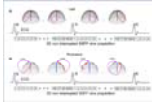
Mark Gosselink<sup>1</sup>, Hugo Klarenberg<sup>2</sup>, Hildo J. Lamb<sup>3</sup>, Gustav J. Strijkers<sup>2</sup>, Dennis W.J. Klomp<sup>1</sup>, Tim Leiner<sup>1</sup>, and Martijn Froeling<sup>1</sup>

<sup>1</sup>University Medical Center Utrecht, Utrecht, Netherlands, <sup>2</sup>Amsterdam University Medical Center, Amsterdam, Netherlands, <sup>3</sup>Leiden University Medical Center, Leiden, Netherlands

Cardiac triggered CINE imaging is used clinically for the assessment of cardiac function. The purpose of this study is to investigate the feasibility of real time free breathing CINE MRI using a high density receive array on a 3T clinical system with online compressed SENSE image reconstruction. We demonstrate feasibility of real-time 2D CINE imaging using a high-density coil array.

1091

Leaf: A Novel 3D Radial Trajectory for Free-breathing 3D Cine Cardiac Magnetic Resonance Imaging

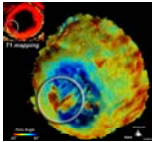


Lukas Braunstorfer<sup>1</sup>, Mehdi H. Moghari<sup>2</sup>, and Andrew H. Powell<sup>3</sup>

<sup>1</sup>Cardiology, Harvard Medical School, Cambridge, MA, United States, <sup>2</sup>Cardiology, Harvard Medical School, Boston, MA, United States, <sup>3</sup>Cardiology, Harvard Medical School, Boston, MA, United States

Free-breathing 3D cine steady-state free precession (SSFP) sequence with radial phyllotaxis trajectory is recently performed for making cardiac magnetic resonance imaging (MRI) exams easy and more comfortable for patients. Phyllotaxis trajectory is susceptible to the eddy current artifact due to a large gradient change during the 3D cine SSFP acquisition for measuring the centerline of k-space. We, therefore, developed and validated a novel leaf trajectory that minimizes the gradient change, and eddy current.

1092



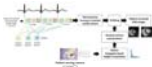
Cardiac Diffusion Tensor MRI Using M2-gSlider with a Real-Time Slice Tracking Respiratory Navigator

Christopher Nguyen<sup>1,2,3</sup>, Timothy G Reese<sup>3,4</sup>, Congyu Liao<sup>3,4</sup>, William J Kostis<sup>5</sup>, Marcel P Jackowski<sup>6</sup>, Kavin Setsompop<sup>3,4</sup>, and Choukri Mekkaoui<sup>3,4</sup>

<sup>1</sup>Cardiovascular Research Center, Massachusetts General Hospital, Charlestown, MA, United States, <sup>2</sup>Department of Medicine, Harvard Medical School, Boston, MA, United States, <sup>3</sup>Martinos Center for Biomedical Imaging, Massachusetts General Hospital, Charlestown, MA, United States, <sup>4</sup>Department of Radiology, Harvard Medical School, Boston, MA, United States, <sup>5</sup>Cardiovascular Institute, Rutgers Robert Wood Johnson Medical School, New Brunswick, NJ, United States, <sup>6</sup>Department of Computer Science, University of São Paulo, São Paulo, Brazil

Free-breathing isotropic cardiac diffusion tensor MRI (DT-MRI) of the left ventricle can be performed using second moment (M2) motion compensated spin echo encoding and generalized slice dithered enhanced resolution (gSlider). This technique provides substantial improvements in spatial resolution and consequently in the accuracy of diffusion-based indices. However, M2-gSlider's RF slice encoding is susceptible to through-slice motion, limiting the maximal improvement in slice resolution. Here, we evaluate the addition of a slice tracking respiratory navigator (NAV) to prospectively adjust slice position in real-time. M2-gSlider-NAV was validated in healthy volunteers and tested in a patient with a history of myocardial infarction.

1093



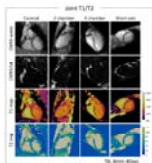
Rapid free breathing multi-slice radial CINE MRI using a patient sensing camera

Guruprasad Krishnamoorthy<sup>1,2</sup>, Joao Silva Tourais<sup>1,2</sup>, Jouke Smink<sup>1</sup>, Marc Kouwenhoven<sup>1</sup>, and Marcel Breeuwer<sup>1,2</sup>

<sup>1</sup>Philips Healthcare, Best, Netherlands, <sup>2</sup>Eindhoven University of Technology, Eindhoven, Netherlands

The benefits of the current cardiac CINE MRI are often limited by the requirement of patient co-operation for multiple breath-holds. To overcome this limitation, we present a new, free-breathing respiratory motion-compensated 2D multi-slice radial CINE method for left ventricular functional assessment. Our method utilizes the respiratory signal obtained from a patient sensing camera for performing motion weighted density compensation in radial gridding to minimize respiratory motion artifacts in the reconstructed image. The left-ventricular functional assessments from volunteers obtained using the proposed method are in good agreement with the results obtained using the standard Cartesian breath-hold method.

1094



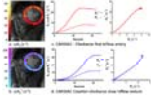
3D Whole-heart High-resolution Motion Compensated Joint T1/T2 Mapping

Giorgia Milotta<sup>1</sup>, Aurelien Bustin<sup>1</sup>, Olivier Jaubert<sup>1</sup>, Radhouene Neji<sup>1</sup>, Claudia Prieto<sup>1</sup>, and Rene Botnar<sup>1</sup>

<sup>1</sup>Biomedical Engineering Department, School of Biomedical Engineering and Imaging Sciences, King's College London, London, United Kingdom

Tissue characterization including identification and quantification of fibrosis and oedema plays an important role in many myocardial diseases. Conventionally 2D  $T_1$  and  $T_2$  maps are acquired sequentially under several breath-holds. However these approaches achieve limited spatial resolution and coverage. Furthermore, partial volume effects at water-fat interfaces may affect  $T_1$  and  $T_2$  quantification. In this work, we propose a free-breathing high-resolution whole-heart joint  $T_1$  and  $T_2$  mapping sequence with Dixon encoding which provides co-registered 3D  $T_1$  and  $T_2$  maps and complementary 3D anatomical water coronary magnetic resonance angiography (CMRA) and fat images in a single scan of ~9min.

1095



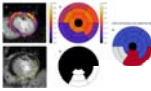
### Vessel architectural imaging in the human heart using heartbeat-to-heartbeat GESE-EPI

Maaïke van den Boomen<sup>1,2</sup>, Mary Kate Manhard<sup>1,3</sup>, Kyrre E. Emblem<sup>4</sup>, David E. Sosnovik<sup>1,5,6</sup>, Niek H.J. Prakken<sup>2</sup>, Christopher Nguyen<sup>1,5,6</sup>, Kawin Setsompop<sup>1,3,7</sup>, and Ronald J.H. Borra<sup>2,8</sup>

<sup>1</sup>A.A. Martinos Center for Biomedical Imaging, Massachusetts General Hospital, Boston, MA, United States, <sup>2</sup>Department of Radiology, University Medical Center Groningen, Groningen, Netherlands, <sup>3</sup>Department of Radiology, Harvard Medical School, Boston, MA, United States, <sup>4</sup>Department of Diagnostic Physics, Oslo University Hospital, Oslo, Norway, <sup>5</sup>Cardiovascular Research Center, Massachusetts General Hospital, Boston, MA, United States, <sup>6</sup>Department of Medicine, Harvard Medical School, Boston, MA, United States, <sup>7</sup>Division of Health Sciences and Technology, Harvard-MIT, Cambridge, MA, United States, <sup>8</sup>Department of Nuclear Medicine and Molecular Imaging, University Medical Center Groningen, Groningen, Netherlands

Vessel architectural imaging (VAI) is explored in the heart by using a heartbeat-to-heartbeat GESE-EPI sequence upon injection of Gd-DTPA. Cardiac VAI can provide the vascular type, caliber, density and blood volume fraction indices in the myocardium, in line with previous work performed in the brain. Further histological validation of these indices is needed, but our initial results demonstrates the feasibility of this technique to advance cardiovascular research into cardiac microvascular dysfunction.

1096



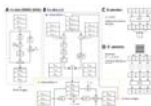
### Fully automated assessment of myocardial ischemic burden – a joint perfusion and viability mapping approach

Cian Michael Scannell<sup>1</sup>, Adriana Villa<sup>1</sup>, Stefano Figliozzi<sup>1</sup>, Jack Lee<sup>1</sup>, Mikto Veta<sup>2</sup>, Marcel Breeuwer<sup>2,3</sup>, and Amedeo Chiribiri<sup>1</sup>

<sup>1</sup>King's College London, London, United Kingdom, <sup>2</sup>Eindhoven University of Technology, Eindhoven, Netherlands, <sup>3</sup>Philips Healthcare, Best, Netherlands

Quantitative myocardial perfusion MRI has the potential to guide the management of patients with coronary artery disease. It has been shown to have high prognostic value and has the benefit of being automated and user-independent. However, a known limitation of the technique is that it cannot distinguish between perfusion defects that are due to a previous infarction and inducible ischemia. In this work we combine quantitative myocardial perfusion with a further automated pipeline for scar quantification from LGE images. It is shown that this combined assessment can identify areas of inducible ischemia in which the tissue is viable.

1097



### Multiband first-pass myocardial perfusion MRI using a slice-low-rank plus sparse model

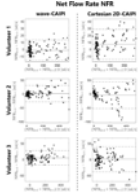
Changyu Sun<sup>1</sup>, Austin Robinson<sup>2</sup>, Christopher Schumann<sup>2</sup>, Daniel Weller<sup>1,3</sup>, Michael Salerno<sup>1,2,4</sup>, and Frederick Epstein<sup>1,4</sup>

<sup>1</sup>Biomedical Engineering, University of Virginia, Charlottesville, VA, United States, <sup>2</sup>Medicine, University of Virginia, Charlottesville, VA, United States, <sup>3</sup>Electrical and Computer Engineering, University of Virginia, Charlottesville, VA, United States, <sup>4</sup>Radiology, University of Virginia, Charlottesville, VA, United States



Multiband (MB) excitation and in-plane acceleration of first-pass perfusion imaging has the potential to provide a high aggregate acceleration rate. Our recent slice-SPIRiT work formulated MB reconstruction as a constrained optimization problem that jointly uses in-plane and through-plane coil information and MB data consistency. Here we extend these methods to develop k-t slice-SPARSE-SENSE and k-t slice-L+S reconstruction models. First-pass perfusion data with MB=3 and rate-2 k-t Poisson-disk undersampling were acquired in 6 patients. The slice-L+S reconstruction showed sharper borders and greater contrast than slice-SPARSE-SENSE and had better image quality scores as assessed by two cardiologists.

1098



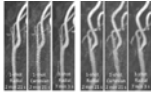
#### Accelerated 4D Flow MRI with wave-CAIPI

Julian A. J. Richter<sup>1,2</sup>, Tobias Wech<sup>1</sup>, Andreas M. Weng<sup>1</sup>, Manuel Stich<sup>1,3</sup>, Ning Jin<sup>4</sup>, Thorsten A. Bley<sup>1</sup>, and Herbert Köstler<sup>1</sup>

<sup>1</sup>Department of Diagnostic and Interventional Radiology, University Hospital Würzburg, Würzburg, Germany, <sup>2</sup>Comprehensive Heart Failure Center Würzburg, Würzburg, Germany, <sup>3</sup>Siemens Healthcare, Erlangen, Germany, <sup>4</sup>Siemens Medical Solutions USA, Inc., Chicago, IL, United States

The wave-CAIPI technique was applied to aortic 4D flow MRI. Three healthy volunteers were examined and flow parameters as well as hemodynamic flow patterns were derived from the measured data. The acquisitions were retrospectively accelerated and compared to conventional Cartesian 2D-CAIPI sampling. Using wave-CAIPI sampling, the deviations between flow parameters of the 6-fold accelerated scans and the references (2-fold accelerated) could be reduced by up to 47% compared to Cartesian sampling. As a consequence, the acquisition time of aortic 4D flow acquisitions could be decreased to 3.5 minutes with higher precision, concerning the calculated flow parameters and hemodynamic flow patterns.

1099



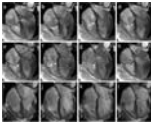
#### Feasibility of Rapid Quiescent-Interval Slice-Selective MRA of the Carotid Arteries Using Radial Sampling and Deep Learning Reconstruction

Ioannis Koktzoglou<sup>1,2</sup>, Rong Huang<sup>1</sup>, Pascale J Aouad<sup>1,3</sup>, Emily A Aherne<sup>1,3</sup>, Archie L Ong<sup>2,4</sup>, and Robert R Edelman<sup>1,3</sup>

<sup>1</sup>Radiology, NorthShore University HealthSystem, Evanston, IL, United States, <sup>2</sup>The University of Chicago Pritzker School of Medicine, Chicago, IL, United States, <sup>3</sup>Radiology, Northwestern University Feinberg School of Medicine, Chicago, IL, United States, <sup>4</sup>Neurology, NorthShore University HealthSystem, Evanston, IL, United States

Ungated quiescent-interval slice-selective (QISS)-based magnetic resonance angiography (MRA) of the extracranial carotid arteries normally carries scan times of approximately 7 minutes. This work evaluated the feasibility of 3-fold accelerated single-shot QISS MRA in under three minutes using radial k-space sampling and a patch-based deep learning image reconstructive strategy.

1100



#### On the Feasibility of Noncontrast Valvular Cine MRI with High Spatial Resolution and High Frame Rate Using Deep-learning-powered Acceleration

Peng Lai<sup>1</sup>, Christopher M Sandino<sup>2</sup>, Shreyas S Vasanawala<sup>3</sup>, Anne Menini<sup>1</sup>, Haonan Wang<sup>4</sup>, Anja C.S Brau<sup>1</sup>, and Martin A Janich<sup>5</sup>

<sup>1</sup>GE Healthcare, Menlo Park, CA, United States, <sup>2</sup>Electrical Engineering, Stanford University, Palo Alto, CA, United States, <sup>3</sup>Radiology, Stanford University, Palo Alto, CA, United States, <sup>4</sup>GE Healthcare, Waukesha, WI, United States, <sup>5</sup>GE Healthcare, Munich, Germany

Valvular imaging is challenging to conventional cine MRI due to its requirement of very high spatial and temporal resolution. This work preliminarily investigated valvular cine MRI with highly accelerated data acquisition powered by deep learning reconstruction. Our results demonstrated the feasibility to resolve valve anatomy and motion with nearly 1mm spatial resolution and 10ms frame rate, while flow-induced dephasing generates shading in blood pool and can complicate valve visualization.

---

---

## Combined Educational & Scientific Session

### fMRI Physiology - From Microvasculature Dynamics to Functional Signals

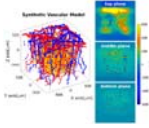
Organizers: Richard Buxton, Susan Francis, Benedikt Poser

Thursday Parallel 4 Live Q&A

Thursday 14:20 - 15:05 UTC

Moderators: Xin Yu & Luca Vizioli

1311



Investigation of the dynamic fingerprint of the BOLD fMRI signal based on a novel statistical 3D cortical vascular network of the human brain

Mario G. Báez-Yáñez<sup>1</sup>, Jeroen Siero<sup>1,2</sup>, and Natalia Petridou<sup>1</sup>

<sup>1</sup>Department of Radiology, Center for Image Sciences, UMC Utrecht, Utrecht, Netherlands, <sup>2</sup>Spinoza Centre for Neuroimaging Amsterdam, Royal Netherlands Academy of Arts and Sciences, Amsterdam, Netherlands

In order to quantify the hemodynamic contributions to the BOLD fMRI signal in humans, it is necessary to adopt a computational model that resembles the cortical vasculature and mimics hemodynamic changes triggered by neurovascular coupling. Moreover, simulation of the local magnetic disturbance induced by the geometry, hemodynamic changes, and the biophysical properties of the tissues can provide accurate insights on the physiological fingerprint of the BOLD fMRI signal. In this work, based on a realistic 3D computational approach of the human cortical vasculature, we simulate the biophysical effects produced by hemodynamic changes to compute a dynamic BOLD fMRI signal response.

---

Contrast Mechanisms & Field Strength Dependence

Klaus Scheffler<sup>1</sup>

<sup>1</sup>Max Planck Institute for Bio. Cybernetics, Germany



Vascular Network & Signal Origins

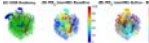
James Mester<sup>1</sup>, Paolo Bazzigaluppi<sup>1</sup>, Matthew Rozak<sup>1</sup>, and Bojana Stefanovic<sup>2</sup>

<sup>1</sup>Sunnybrook Research Institute, Toronto, ON, Canada, <sup>2</sup>Sunnybrook Research Institute, Canada

This lecture will review recent work characterizing neurovascular coupling on the microscopic level and underscore the significance of studying network-level behaviour.

---

1101



The role of rapid capillary resistance decreases in the BOLD response assessed through simulations in a realistic vascular network

Joerg Peter Pfannmoeller<sup>1</sup>, Louis Gagnon<sup>2</sup>, Avery Berman<sup>1</sup>, and Jonathan Polimeni<sup>1</sup>

<sup>1</sup>Imaging, Athinoula A. Martinos Center for Biomedical Imaging, Massachusetts General Hospital, Boston, MA, United States, <sup>2</sup>Physics, Engineering Physics and Optics, Laval University, Quebec, QC, Canada

The brain's physiology may fundamentally limit the achievable spatial and temporal specificity of gradient-echo fMRI. Even if the physiology does not pose such a limitation a better understanding would allow for data analysis techniques that improve the spatial specificity. Microscopy allows for highly detailed investigations of local physiological mechanism and provides a growing knowledge from which fMRI may benefit profoundly. A current challenge is the transition from focal mechanisms to their consequence on the mesoscopic scale of BOLD examinations. In this abstract we present our recent work on this transition using simulations of the BOLD effect.

---

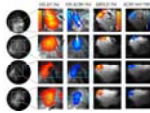


On the relation between positive and negative functional changes of cerebral blood flow and T2\* in the human visual cortex.

Ratnamanjuri Devi<sup>1</sup>, Toralf Mildner<sup>1</sup>, Torsten Schlumm<sup>1</sup>, Jöran Lepsien<sup>1</sup>, and Harald E. Möller<sup>1</sup>

<sup>1</sup>Max Planck Institute for Human Cognitive and Brain Sciences, Leipzig, Germany

Measurement of functional CBF is challenging due to inherently low SNR and signal amplitudes, especially in regions of negative BOLD response. Here, multi-echo center-out EPI is introduced which allows for simultaneous measurement of functional changes in CBF and T2\* with improved sensitivity. Using a visual stimulus inducing positive and negative BOLD responses, a linear relationship between absolute changes in CBF and T2\* along both positive and negative directions was found with similar coupling ratios. Negative absolute functional CBF changes were found to be almost independent of the baseline CBF, in agreement with previous work on the positive BOLD response.

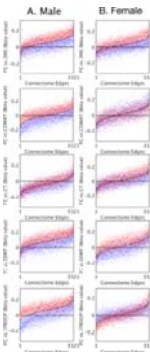


Cross species validation of the layer-fMRI VASO contrast mechanism: data comparison against pre-clinical 2D-OIS and CBV-MRI gold standards.

Aneurin J Kennerley<sup>1</sup>, Benedikt A Poser<sup>2</sup>, Frida H Torkelsen<sup>1</sup>, Rainer Goebel<sup>2</sup>, Amanda Kaas<sup>2</sup>, and Laurentius Huber<sup>2</sup>

<sup>1</sup>Chemistry, University of York, York, United Kingdom, <sup>2</sup>Maastricht Brain Imaging Centre, Maastricht University, Maastricht, Netherlands

With recent advances in ultra-high-field MRI hardware and sequence mechanisms, it has become possible to capture CBV-weighted fMRI signal across cortical layers. However, the exact contrast mechanisms of layer-dependent VASO has not been fully validated with gold-standard pre-clinical methods.



Individual differences in haemoglobin concentration influence BOLD fMRI functional connectivity and its correlations with behaviour

Phillip G D Ward<sup>1,2,3</sup>, Edwina R Orchard<sup>1,2,3</sup>, Stuart Oldham<sup>3</sup>, Aurina Arnatkevičiūtė<sup>3</sup>, Francesco Sforzini<sup>1</sup>, Alex Fornito<sup>3</sup>, Gary F Egan<sup>1,2,3</sup>, and Sharna D Jamadar<sup>1,2,3</sup>

<sup>1</sup>Monash Biomedical Imaging, Monash University, Melbourne, Australia, <sup>2</sup>Australian Research Council Centre of Excellence for Integrative Brain Function, Melbourne, Australia, <sup>3</sup>Turner Institute for Brain and Mental Health, Monash University, Melbourne, Australia

The BOLD signal detects changes in relative concentrations of oxy/deoxy-haemoglobin. Thus, individual blood haemoglobin levels may influence the BOLD signal-to-noise ratio in a manner independent of neural activity. In this study, we emulate group-differences in haemoglobin by performing a median split on 524 healthy elderly individuals based on individual measurements of haemoglobin. When compared, the two haemoglobin subgroups showed no differences in cognitive measures, however, significant differences in linear relationships between cognitive performance and functional connectivity were observed in four cognitive tests. Our findings confirm that haemoglobin levels are an important confounding variable in BOLD-fMRI-based studies in the elderly.

## Oral - Power Pitch

### fMRI Physiology - Probing Physiology with fMRI

Thursday Parallel 4 Live Q&A

Thursday 14:20 - 15:05 UTC

Moderators: Paula Croal

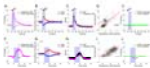


Geometrically accurate imaging of the pial arterial vasculature of the human brain in vivo with high-resolution time-of-flight angiography at 7T

Saskia Bollmann<sup>1,2</sup>, Michael I. Bernier<sup>1,2</sup>, Simon Daniel Robinson<sup>3,4,5</sup>, and Jonathan R. Polimeni<sup>1,2,6</sup>

<sup>1</sup>Athinoula A. Martinos Center for Biomedical Imaging, Massachusetts General Hospital, Charlestown, MA, United States, <sup>2</sup>Department of Radiology, Harvard Medical School, Charlestown, MA, United States, <sup>3</sup>Centre for Advanced Imaging, The University of Queensland, Brisbane, Australia, <sup>4</sup>High Field MR Centre, Department of Biomedical Imaging and Image-guided Therapy, Medical University of Vienna, Vienna, Austria, <sup>5</sup>Department of Neurology, Medical University of Graz, Graz, Austria, <sup>6</sup>Division of Health Sciences and Technology, Massachusetts Institute of Technology, Cambridge, MA, United States

Non-invasive imaging of the pial arterial vasculature using the inflow-based contrast provided by moving blood water spins requires sufficiently small voxel sizes (160  $\mu\text{m}$ ) to maintain high contrast in small pial arteries (200  $\mu\text{m}$  diameter). Additional acquisition of quantitative susceptibility values allows the differentiation of veins and arteries, turning magnetic resonance angiography into true *arteriography*. Importantly, flow compensation in all phase encoding directions is necessary to assure geometric accuracy, even for small vessels.

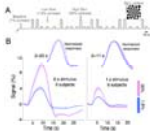


### Correcting hemodynamic crosstalk effects in fluorescent fiber-photometry signals for quantitative neurovascular coupling studies

Weiting Zhang<sup>1,2,3</sup>, Tzu-Hao Chao<sup>1,2,3</sup>, Yue Yang<sup>1,4</sup>, Tzu-Wen Wang<sup>1,2,3</sup>, Esteban Oyarzabal<sup>1,2,3</sup>, SungHo Lee<sup>1,2,3</sup>, Brittany Katz<sup>1,2,3</sup>, Guohong Cui<sup>5</sup>, and Yan-Yu Ian Shih<sup>1,2,3</sup>

<sup>1</sup>Center for Animal MRI, The University of North Carolina at Chapel Hill, Chapel Hill, NC, United States, <sup>2</sup>Biomedical Research Imaging Center, The University of North Carolina at Chapel Hill, Chapel Hill, NC, United States, <sup>3</sup>Department of Neurology, The University of North Carolina at Chapel Hill, Chapel Hill, NC, United States, <sup>4</sup>Department of Statistics, The University of North Carolina at Chapel Hill, Chapel Hill, NC, United States, <sup>5</sup>Neurobiology Branch, NIEHS/NIH, RTP, NC, United States

The number of fiber-photometry studies incorporating fMRI are rapidly increasing, as these compatible modalities have the ability to reveal neuronal ground-truths. We recently noticed that photometry recording suffers from hemodynamic contamination, leading to false negative results. In this study, we 1) demonstrate how changes in cerebrohemodynamics can yield false negative GCaMP data, 2) propose a method to derive HbO and HbR from spectrally resolved fiber-photometry, 3) validate the derive hemodynamic parameters against concurrently measured CBV and BOLD using photometry and fMRI, 4) implement the proposed correction in vivo, and 5) apply corrected photometric results to rapidly derive hemodynamic response functions.

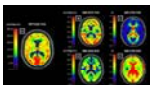


### Probing the neuronal and vascular origins of task contrast-dependent hemodynamic response functions

Jingyuan E Chen<sup>1,2</sup>, Nina E Fultz<sup>1</sup>, Gary Glover<sup>3</sup>, Bruce R Rosen<sup>1,2</sup>, Jonathan R Polimeni<sup>1,2</sup>, and Laura D Lewis<sup>4</sup>

<sup>1</sup>Athinoula A. Martinos Center for Biomedical Imaging, Massachusetts General Hospital, Boston, MA, United States, <sup>2</sup>Radiology, Harvard Medical School, Boston, MA, United States, <sup>3</sup>Radiology, Stanford University, Stanford, CA, United States, <sup>4</sup>Biomedical Engineering, Boston University, Boston, MA, United States

In this study, we employed concurrent EEG/fMRI to investigate the neuronal and vascular mechanisms driving task-contrast modulation of HRF shapes. Our results demonstrated that HRFs vary as a function of task contrast levels. Briefly, HRFs elicited by high-contrast stimuli exhibited delayed time-to-peaks and stronger post-stimulus undershoots that likely arose from neuronal origins, and wider full-width-at-half-maximums that were possibly driven by vascular changes.



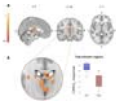
### Effective oxygen diffusivity mapping with multiparametric quantitative BOLD and pCASL: Comparison between healthy young and elderly subjects

Jan Kufer<sup>1</sup>, Jens Goettler<sup>1,2,3</sup>, Samira Epp<sup>1</sup>, Mikkel Bo Hansen<sup>4</sup>, Claus Zimmer<sup>1</sup>, Kim Mouridsen<sup>4</sup>, Fahmeed Hyder<sup>2</sup>, Christine Preibisch<sup>1,5</sup>, and Stephan Kaczmarz<sup>1,2</sup>

<sup>1</sup>School of Medicine, Department of Neuroradiology, Technical University of Munich, Munich, Germany, <sup>2</sup>MRRC, Yale University, New Haven, CT, United States, <sup>3</sup>School of Medicine, Department of Radiology, Technical University of Munich, Munich, Germany, <sup>4</sup>Institute of Clinical Medicine, Aarhus University, Aarhus, Denmark, <sup>5</sup>School of Medicine, Clinic of Neurology, Technical University of Munich, Munich, Germany

The effective oxygen diffusivity (EOD) of the capillary bed has gained increasing interest as a promising biomarker providing additional information on microvascular integrity. To overcome limitations in the applicability of existing and relatively complex EOD mapping techniques, we proposed a novel more easily applicable MR-based approach. We measured EOD in 16 young and 30 elderly healthy subjects. Our measurements of EOD by MRI in young subjects yielded comparably good results in comparison with PET-data as a reference. Furthermore, we found EOD reductions in elderly healthy subjects with concomitant capillary transit-time heterogeneity (CTH) increases, indicating disturbed capillary oxygen extraction ability.

1109

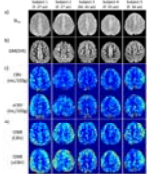


**Voxel-wise CMRO<sub>2</sub> mapping reveals focally-reduced task-related oxygen consumption in multiple sclerosis**  
Eleonora Patitucci<sup>1</sup>, Rachael C Stickland<sup>2</sup>, Hannah L Chandler<sup>1</sup>, Michael Germuska<sup>1</sup>, Catherine Foster<sup>1</sup>, Sharmila Khot<sup>1</sup>, Neeraj Saxena<sup>1</sup>, Valentina Tomassini<sup>1,3</sup>, and Richard G Wise<sup>1,3</sup>

<sup>1</sup>CUBRIC - Cardiff University Brain Research Imaging Centre -Psychology, Cardiff University, Cardiff, United Kingdom, <sup>2</sup>Department of Physical Therapy and Human Movement Sciences, Northwestern University, Chicago, IL, United States, <sup>3</sup>Institute for Advanced Biomedical Technologies (ITAB), Department of Neurosciences, Imaging and Clinical Sciences, University of Chieti-Pescara "G. d'Annunzio", Chieti, Italy

Calibrated fMRI can map the rate of cerebral oxygen consumption of the human brain, offering an important indicator of energy dysfunction in neurodegenerative and neuroinflammatory diseases. Previous studies investigated oxygen metabolism at rest or in response to tasks within BOLD signal defined region of interests (ROIs). Here, we investigate on a voxel-by-voxel basis the oxygen metabolic activity in patients with multiple sclerosis during the execution of a task. We show the feasibility of mapping task-induced CMRO<sub>2</sub> changes, demonstrating reduced oxygen consumption in the basal ganglia in MS patients that was not otherwise evident from BOLD or CBF signals.

1110



**Venular Cerebral Blood Volume (vCBV) Mapping Using Fourier-Transform Based Velocity-Selective Pulse Trains**

Wenbo Li<sup>1,2</sup>, Peter van Zijl<sup>1,2</sup>, and Qin Qin<sup>1,2</sup>

<sup>1</sup>Department of Radiology, Johns Hopkins University School of Medicine, Baltimore, MD, United States, <sup>2</sup>F.M. Kirby Research Center for Functional Brain Imaging, Kennedy Krieger Institute, Baltimore, MD, United States

A new method is proposed to quantify the venular cerebral blood volume (vCBV) by using Fourier-transform based velocity-selective inversion (FT-VSI) to null the arterial blood signal while using Fourier-transform based velocity-selective saturation (FT-VSS) to suppress the tissue signal. Compared to previous schemes, the proposed method potentially has higher SNR and is more robust to tissue signal fluctuations attributed to system instabilities and physiological motion. The contamination of cerebrospinal fluid (CSF) signal is also corrected for by taking an extra image at a second echo with long TE. Using this method, vCBV of five volunteers were measured at 3T.

1111



**Increased negative BOLD responses along the rat visual pathway with short inter-stimulus intervals**  
Rita Gil<sup>1</sup>, Francisca F. Fernandes<sup>1</sup>, and Noam Shemesh<sup>1</sup>

<sup>1</sup>Champalimaud Neuroscience Programme, Champalimaud Centre for the Unknown, Lisbon, Portugal

We investigated BOLD responses along the rat visual pathway via inter-stimulus-intervals (ISI) and stimulus pulse width (PW) modulation. PWs did not impact negative BOLD responses (NBRs) while shortening ISI resulted in very large increases in NBRs. Visual cortex (VC) NBRs at short ISIs were accompanied by decreased positive BOLD responses (PBRs) in lateral geniculate nucleus of the thalamus (LGN) and superior colliculus (SC). At the shortest ISI (30ms) NBRs were observed in SC. Along with reported reduced visual evoked potentials amplitude at short ISIs, our findings suggest decreased net excitability as a source for negative BOLD responses in this scenario.

1112

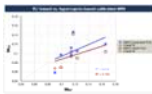


Short breathing tasks at the start of a resting state scan: feasible measures of cerebrovascular reactivity  
Rachael Stickland<sup>1</sup>, Apoorva Ayyagari<sup>1</sup>, Kristina Zvolanek<sup>1</sup>, and Molly Bright<sup>1</sup>

<sup>1</sup>Northwestern University, Chicago, IL, United States

Cerebrovascular reactivity (CVR), the blood flow response to a vasodilatory stimulus, is changed in many pathologies. CVR can be estimated without gas challenges by performing breathing tasks or by analyzing natural CO<sub>2</sub> fluctuations at rest. We added two short breathing tasks (hypercapnic: breath hold, hypocapnic: cued deep breathing) to the start of two resting state fMRI scans. When using all the data, or just the breathing segments, adequate CVR maps could be estimated; this was not the case when just using the resting portions. This paradigm can provide an estimate of CVR, and help improve analysis of resting state data.

1113



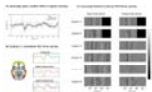
Comparison of calibrated fMRI with calibration factor M determined by hypercapnia vs. gas-free R<sub>2</sub>'

Stephan Kaczmarz<sup>1,2</sup>, Jan Kufer<sup>1</sup>, Lena Schmitzer<sup>1</sup>, Jens Göttler<sup>1,2,3</sup>, Mario Eduardo Archila Melendez<sup>1</sup>, Andreas Hock<sup>4</sup>, Christian Sorg<sup>1</sup>, Claus Zimmer<sup>1</sup>, Fahmeed Hyder<sup>2</sup>, and Christine Preibisch<sup>1,5</sup>

<sup>1</sup>School of Medicine, Department of Neuroradiology, Technical University of Munich, Munich, Germany, <sup>2</sup>MRRC, Yale University, New Haven, CT, United States, <sup>3</sup>School of Medicine, Department of Radiology, Technical University of Munich, Munich, Germany, <sup>4</sup>Philips Healthcare, Hamburg, Germany, <sup>5</sup>School of Medicine, Clinic of Neurology, Technical University of Munich, Munich, Germany

Calibrated-fMRI is highly promising to quantify human brain function via mapping changes of cerebral metabolic rate of oxygen. While the R<sub>2</sub>'-based approach is easily applicable, systematic differences to the well-established hypercapnia-calibration have been reported. We present data from an ongoing study in seven healthy young subjects correlating calibration factors M from R<sub>2</sub>' vs. hypercapnia. We hypothesized better correlation after methodological improvements in R<sub>2</sub>'-mapping and pseudo-continuous arterial spin labeling (pCASL). Our results confirmed this hypothesis, with good correlations between both fMRI-calibrations. However, we found potentially confounding hypercapnia effects on pCASL. Thus, our results suggest benefits of gas-free R<sub>2</sub>'-calibration for future applications.

1114



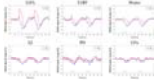
Probing dynamic cerebral autoregulation with BOLD fMRI using a thigh cuff challenge

Joseph R Whittaker<sup>1</sup>, Jessica Steventon<sup>1</sup>, Marcello Venzi<sup>1</sup>, and Kevin Murphy<sup>1</sup>

<sup>1</sup>CUBRIC, School of Physics and Astronomy, Cardiff University, Cardiff, United Kingdom

The Thigh Cuff Challenge (TCC) technique is a promising method for assessing dynamic cerebral autoregulation with fMRI. A TCC fMRI experiment was performed in order to better understand the BOLD fMRI signal changes associated with autoregulation. We demonstrate that TCC event-locked cortical fMRI signal changes are widespread across cortical grey matter, with varying response shape both within and between subjects. The TCC BOLD response is on average ~0.3%, which we estimate on a voxel-wise basis using a novel informed basis set, which provides a proof-of-concept demonstrating the potential of TCC and fMRI to probe cerebrovascular function.

1115



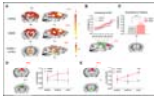
### Effect of inhibitory neural activities to BOLD fMRI

Hyun Seok Moon<sup>1,2</sup>, Haiyan Jiang<sup>1</sup>, Won Beom Jung<sup>1,2</sup>, JungMi Lee<sup>1</sup>, Gunsoo Kim<sup>1</sup>, and Seong-Gi Kim<sup>1,2</sup>

<sup>1</sup>Center for Neuroscience Imaging Research (CNIR), Institute for Basic Science (IBS), Suwon, Korea, Republic of, <sup>2</sup>Department of Biomedical Engineering, Sungkyunkwan University, Suwon, Korea, Republic of

BOLD fMRI combined with optogenetics allows for brain-wide neural network studies. Most studies have focused on activity of excitatory neurons, which is presumably to contribute BOLD fMRI dominantly. However, fMRI response evoked by inhibitory neural activities is unknown. Here, we investigated 15.2T BOLD response of optogenetically stimulated GABAergic neural activation, and verified the results with electrophysiology.

1116



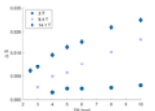
### Paradoxical fMRI overconnectivity upon neural silencing of fronto-cortical activity

Carola Canella<sup>1,2</sup>, Federico Rocchi<sup>1,2</sup>, Shahryar Noei<sup>3</sup>, Daniel Gutierrez-Barragan<sup>1</sup>, Ludovico Coletta<sup>1</sup>, Elizabeth de Guzman<sup>1</sup>, Alberto Galbusera<sup>1</sup>, Massimo Pasqualetti<sup>4</sup>, Giuliano Iurilli<sup>5</sup>, Stefano Panzeri<sup>3</sup>, and Alessandro Gozzi<sup>1</sup>

<sup>1</sup>Functional Neuroimaging Laboratory, Istituto Italiano di Tecnologia, Rovereto, Italy, <sup>2</sup>Center for Mind and Brain Sciences, University of Trento, Rovereto, Italy, <sup>3</sup>Neuronal Computational Laboratory, Istituto Italiano di Tecnologia, Rovereto, Italy, <sup>4</sup>Biology Department, University of Pisa, Pisa, Italy, <sup>5</sup>Systems Neurobiology Laboratory, Istituto Italiano di Tecnologia, Rovereto, Italy

Neuroimaging measurements of functional connectivity are commonly interpreted as an index of reciprocal interareal communication. However, direct testing of this hypothesis has been lacking. Using chemogenetics, electrophysiology and resting-state fMRI in the mouse, we show that acute and chronic silencing of the prefrontal cortex result in paradoxical rsfMRI overconnectivity of the mouse default mode network (DMN) and increased delta activity, an effect relayed to wider cortical territories by polymodal thalamic areas. Our results challenge prevailing interpretations of functional connectivity and implicate a critical contribution of sub-cortical rhythm generators to the establishment of large-scale functional coupling.

1117



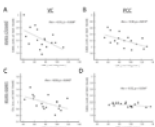
### Towards intravascular BOLD signal characterization in balanced SSFP experiments of human blood at high to ultra-high fields

Marlon Pérez-Rodas<sup>1,2</sup>, Hildegard Schulz<sup>1</sup>, Rolf Pohmann<sup>1</sup>, Klaus Scheffler<sup>1,3</sup>, and Rahel Heule<sup>1</sup>

<sup>1</sup>High-Field MR Center, Max Planck Institute for Biological Cybernetics, Tübingen, Germany, <sup>2</sup>Graduate Training Centre of Neuroscience, IMPRS for Cognitive and Systems Neuroscience, University of Tübingen, Tübingen, Germany, <sup>3</sup>Department of Biomedical Magnetic Resonance, University of Tübingen, Tübingen, Germany

To fully understand the neurovascular fingerprint observed in BOLD experiments, extravascular and intravascular contributions have to be identified separately. Balanced steady-state free precession (bSSFP) imaging has demonstrated the ability for distortion-free fMRI with high microvascular sensitivity. However, the underlying intravascular contribution to BOLD bSSFP is not yet entirely known as literature  $R_2$  relaxation rates do not reflect the apparent diffusion-related  $R_2$  decrease in blood with shorter bSSFP refocusing intervals (TRs). This work thus focuses on characterizing the oxygen sensitivity of bSSFP in blood samples at high to ultra-high fields by means of passband signal differences and intrinsic  $R_2$  estimation.

1118



### Metabolic basis of human brain network nodes in resting-states of eyes-closed and eyes-open

Yury Koush<sup>1</sup>, Robin A. de Graaf<sup>1</sup>, Peter Herman<sup>1</sup>, Douglas L. Rothman<sup>1</sup>, and Fahmeed Hyder<sup>1</sup>

<sup>1</sup>Yale University, New Haven, CT, United States

Resting-state fMRI studies are conducted with eyes-closed (EC) or eyes-open (EO) conditions. Given differences in spontaneous activity between EO and EC conditions, metabolic foundations of fMRI-derived networks, specifically activated (e.g., sensory network) and deactivated (e.g., default mode network, DMN) nodes, are poorly understood. We assessed aerobic glycolysis and excitatory-inhibitory balance in healthy volunteers' visual cortex (VC, a non-DMN node) and posterior cingulate cortex (PCC, a DMN node) using J-edited fMRS and calibrated fMRI. Functional changes between EO and EC conditions are regionally non-specific to aerobic glycolysis and flow-metabolism coupling, but neurovascular coupling in VC depends on EO and EC conditions.

---

## Oral

### Engineering and Safety of MRI - MRI Safety

Thursday Parallel 5 Live Q&A

Thursday 14:20 - 15:05 UTC

Moderators: Emine Saritas

1119

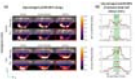
#### A 10-year Review of MRI-Related FDA Adverse Event Reports

Jana G Delfino<sup>1</sup>, Daniel M Krainak<sup>1</sup>, Stephanie A Flesher<sup>1</sup>, and Donald L Miller<sup>1</sup>

<sup>1</sup>US Food and Drug Administration, Silver Spring, MD, United States

We provide a breakdown of the adverse event reports received by FDA during a 10-year period (2008-2017). Reports were manually categorized into eight mutually-exclusive event types. Thermal events were further sub-categorized by probable root cause. Objects that became projectiles were sub-categorized. Adverse events related to MR systems consistent with the known hazards of the MR environment continue to be reported to FDA. Thermal events were the most commonly reported serious injury (59% of analyzed reports). Mechanical events (11%), projectile events (9%), image quality issues (6%), and acoustic events (6%) were also observed.

1120



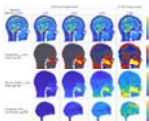
#### Impact of respiration on B1+ field and SAR distribution at 7 T using a novel EM simulation setup

Natalie Schön<sup>1</sup>, Johannes Petzold<sup>1</sup>, Frank Seifert<sup>1</sup>, Christoph Stefan Aigner<sup>1</sup>, Gregory J. Metzger<sup>2</sup>, Bernd Ittermann<sup>1</sup>, and Sebastian Schmitter<sup>1,2</sup>

<sup>1</sup>Physikalisch-Technische Bundesanstalt (PTB), Braunschweig and Berlin, Germany, <sup>2</sup>Center for Magnetic Resonance Research, University of Minnesota, Minneapolis, MN, United States

At 7T body imaging spatial variations of the transmit magnetic (B1+) and electric (E) fields are observed. Additionally, recent in-vivo studies showed that B1+ patterns vary throughout the respiratory cycle. We present a novel electromagnetic (EM) simulation setup that allows investigating respiration-induced changes of the E- and B1+ fields. Using such simulations, we aim to verify the aforementioned in-vivo results that demonstrated respiration-induced changes of B1+ and corresponding flip angle distributions in the heart. Furthermore, the hitherto neglected, corresponding SAR variations are investigated and we find an up to 100 % change in local SAR throughout the respiratory cycle.

1121



#### Parallel transmit local SAR vs. mesh resolution in EMF simulations of highly detailed anatomical models – a rigorous analysis

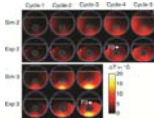
Andre Kuehne<sup>1</sup>, Eva Oberacker<sup>2</sup>, Helmar Waiczies<sup>1</sup>, Mostafa Berangi<sup>1</sup>, Jacek Nadobny<sup>3</sup>, Pirus Ghadjar<sup>3</sup>, Peter Wust<sup>3</sup>, and Thoralf Niendorf<sup>1,2,4</sup>



<sup>1</sup>MRI.TOOLS GmbH, Berlin, Germany, <sup>2</sup>Max Delbrück Center for Molecular Medicine in the Helmholtz Association, Berlin, Germany, <sup>3</sup>Clinic for Radiation Oncology, Charité Universitätsmedizin, Berlin, Germany, Berlin, Germany, <sup>4</sup>Experimental and Clinical Research Center (ECRC), joint cooperation between the Charité Medical Faculty and the Max Delbrück Center for Molecular Medicine in the Helmholtz Association, Berlin, Germany

Electromagnetic simulations are an important tool for RF coil and thermal RF applicator development. For rapid design evaluation, fast low mesh resolution simulations would be of benefit, which can however potentially introduce errors in regions of intricate tissue distributions. We rigorously analyze local power deposition errors introduced by using low-resolution meshes in simulations of a highly detailed head model at 297 MHz. Our results indicate, that even at 5mm the introduced error is acceptable. However, artificial current paths are formed in the oronasal cavity, leading to not critical albeit locally elevated power deposition, thus deserving additional attention.

1122

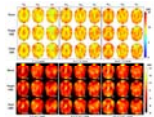


Validation of RF induced temperature increase in phantom and in living human tissue: a comparison study  
Shubham Gupta<sup>1</sup>, Keiji Tanaka<sup>1</sup>, and R. Allen Waggoner<sup>1</sup>

<sup>1</sup>Laboratory for Cognitive Brain Mapping, RIKEN Center for Brain Science, Wakoshi, Saitama, Japan

In this study, we compared the temperature increase in a phantom and three human legs that were calculated by the simulations, measured by the MR-thermometry, and the optical thermocouples (phantom only), with good agreement between the modalities. IEC guidelines require simulations of SAR along with validation in phantoms to ensure safety. While it is likely impossible to simulate every possible pulse shape and phase combination in a pTx system with a large number of transmit channels, the results we present here suggest that simulations plus MR-thermometry could provide the verification currently lacking in pTx studies.

1123



Convex Optimized Excitation Control to Reduce RF Heating for DBS Patients at UHF MRI  
Youngdae Cho<sup>1</sup> and Hyoungsuk Yoo<sup>1</sup>

<sup>1</sup>Biomedical Engineering, Hanyang University, Seoul, Republic of Korea

Patients having deep brain stimulation (DBS) can suffer from radio-frequency (RF) heating around the electrode during the MRI scan. Most of previous solutions were conducted based on the birdcage coil; the methods are inappropriate for ultra-high field (UHF) MRI system over 7 T using multi-channel RF coil. Our study introduced an optimized excitation control method by changing input weights of coil elements through convex optimization. Results demonstrated that proposed method effectively reduces RF heating around the electrode as well as acquires MR images of major brain regions with high resolution simultaneously.

1124



Surgical modification of extracranial trajectories of DBS leads can significantly reduce image artifact and RF heating during MRI at 3T

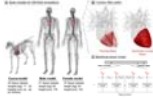
Bhumi Bhusal<sup>1</sup>, Joshua Rosenow<sup>2</sup>, Mark Nolt<sup>2</sup>, Roberto Lopez-Rosado<sup>1</sup>, Julie Pilitsis<sup>3</sup>, and Laleh Golestanirad<sup>1</sup>

<sup>1</sup>Northwestern University, Chicago, IL, United States, <sup>2</sup>Northwestern Medicine, Chicago, IL, United States,

<sup>3</sup>Albany Medical Center, Albany, NY, United States

Patients with deep brain stimulation (DBS) implants can significantly benefit from MRI, however the interaction between MRI electric fields and DBS leads induces RF currents in the leads that can cause tissue heating and image artifacts. Here we show that modifying the extracranial trajectory of a DBS lead implanted into a cadaver brain significantly reduces both heating in the tissue and the image artifact around electrode contacts during MRI at 3T. Electromagnetic simulations confirm that trajectory modification can reduce induced currents in the lead, which in turn reduces the SAR amplification and distortion of B1 fields around the electrodes.

1125



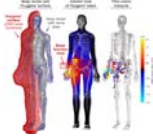
### Simulation of electromagnetic cardiac stimulation: Validation in dogs and application to human threshold limits for MRI gradient coils

Valerie Klein<sup>1,2</sup>, Mathias Davids<sup>1,2,3</sup>, Lothar R. Schad<sup>1</sup>, Lawrence L. Wald<sup>2,3,4</sup>, and Bastien Guérin<sup>2,3</sup>

<sup>1</sup>Computer Assisted Clinical Medicine, Medical Faculty Mannheim, Heidelberg University, Mannheim, Germany, <sup>2</sup>A. A. Martinos Center for Biomedical Imaging, Department of Radiology, Massachusetts General Hospital, Charlestown, MA, United States, <sup>3</sup>Harvard Medical School, Boston, MA, United States, <sup>4</sup>Harvard-MIT Division of Health Sciences and Technology, Cambridge, MA, United States

Lack of detailed data requires a conservative approach in the IEC 60601-2-33 safety limits to prevent cardiac stimulation (CS) by MRI gradient switching. Analogous to our previous peripheral nerve stimulation modeling, we use coupled electromagnetic and electrophysiological simulations to investigate magnetically induced CS in human and canine body models. Our CS simulation pipeline reproduces CS thresholds measured in previous dog experiments. The predicted human CS thresholds are significantly higher than the regulatory safety limits. With further validation, CS simulations could eventually play an important role in determining appropriate MRI safety limits.

1126



### Assembly of a PNS predicting "P-matrix" on a Huygens' surface for rapid PNS assessment of 2D or 3D gradient coil windings

Mathias Davids<sup>1,2,3</sup>, Bastien Guerin<sup>1,2</sup>, and Lawrence L Wald<sup>1,2,4</sup>

<sup>1</sup>A.A. Martinos Center for Biomedical Imaging, Massachusetts General Hospital, Dept. of Radiology, Charlestown, MA, United States, <sup>2</sup>Harvard Medical School, Boston, MA, United States, <sup>3</sup>Computer Assisted Clinical Medicine, Medical Faculty Mannheim, Heidelberg University, Mannheim, Germany, <sup>4</sup>Harvard-MIT Health Sciences and Technology, Cambridge, MA, United States

Peripheral Nerve Stimulation (PNS) modeling has a potential role for designing and operating therapeutic and diagnostic devices (such as MRI), but is computationally demanding due to the required simulations of EM fields and neural responses. We describe compression of the PNS modeling framework into a single versatile PNS matrix (*P*-matrix) defined on a Huygens' surface just outside the subject's body to allow fast detailed PNS analysis on arbitrary coil windings/formers. This *P*-matrix can be translated to any coil former within seconds, allowing for rapid PNS assessment or optimization of gradient coil windings with explicit PNS constraints.

1127



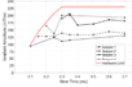
### Simple Anatomical Measures Correlate with Individual PNS Thresholds for kHz-range Homogeneous Magnetic Fields

Omer Burak Demirel<sup>1,2,3,4</sup>, Toygan Kilic<sup>1,2</sup>, Tolga Çukur<sup>1,2,5</sup>, and Emine Ulku Saritas<sup>1,2,5</sup>

<sup>1</sup>Electrical and Electronics Engineering, Bilkent University, Ankara, Turkey, <sup>2</sup>National Magnetic Resonance Research Center (UMRAM), Bilkent University, Ankara, Turkey, <sup>3</sup>Center for Magnetic Resonance Research, University of Minnesota, Minneapolis, MN, United States, <sup>4</sup>Electrical and Computer Engineering, University of Minnesota, Minneapolis, MN, United States, <sup>5</sup>Neuroscience Graduate Program, Bilkent University, Ankara, Turkey

This work shows for the first time that fat percentage strongly correlates with peripheral nerve stimulation (PNS) thresholds for kHz-range homogeneous magnetic fields. The correlations get even stronger after taking into account the effects of body part size that is exposed to the magnetic field. These types of magnetic fields are used as excitation field in Magnetic Particle Imaging (MPI). Hence, these results can potentially lead to subject specific threshold prediction, allowing high performance scans within subject specific safety limits.

1128



### Magneto-phosphenes in head-only gradient coils

Colin M McCurdy<sup>1</sup>, Amgad M Louka<sup>1</sup>, William B Handler<sup>1</sup>, and Blaine A Chronik<sup>1</sup>

<sup>1</sup>The xMR Labs, Department of Physics and Astronomy, Western University, London, ON, Canada

Magneto-phosphenes are caused by induced potentials in the retina, that result in visual stimulation, appearing as flashing lights. In the MR environment, magneto-phosphenes have been encountered with higher gradient strengths and longer slew times than are typically encountered in MRI. However, in a prototype head-only gradient coil we were able to repeatedly induce magneto-phosphenes in four subjects. We then tested the effects of slew times, external light, and eye direction on the subject's perception of magneto-phosphenes, finding that slew times had little effect but dimming lights and changing eye direction raised thresholds in most cases.

## Oral

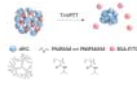
### Engineering and Safety of MRI - MR Engineering & Safety

Thursday Parallel 5 Live Q&A

Thursday 14:20 - 15:05 UTC

Moderators: Thomas Denney & Gigi Galiana

1129



### Temperature Triggered Release of a Protein from Thermoresponsive Nanogels Using Thermal Magnetic Resonance

Yiyi Ji<sup>1</sup>, Lukas Winter<sup>2</sup>, Lucila Navarro<sup>3,4</sup>, Min-Chi Ku<sup>1</sup>, João Periquito<sup>1</sup>, Michal Pham<sup>1</sup>, Werner Hoffmann<sup>2</sup>, Loryn E. Theune<sup>3</sup>, Marcelo Calderón<sup>3,5,6</sup>, and Thoralf Niendorf<sup>1,7</sup>

<sup>1</sup>Berlin Ultrahigh Field Facility (B.U.F.F.), Max Delbrück Center for Molecular Medicine in the Helmholtz Association (MDC), Berlin, Germany, <sup>2</sup>Physikalisch-Technische Bundesanstalt (PTB), Berlin, Germany, <sup>3</sup>Institute of Chemistry and Biochemistry, Freie Universität Berlin, Berlin, Germany, <sup>4</sup>Instituto de Desarrollo Tecnológico para la Industria Química (INTEC), Universidad Nacional del Litoral (UNL) - Consejo Nacional de Investigaciones Científicas y Técnicas (CONICET), Santa Fe, Argentina, <sup>5</sup>POLYMAT and Applied Chemistry Department, Faculty of Chemistry, University of the Basque Country UPV/EHU, Donostia-San Sebastián, Spain, <sup>6</sup>IKERBASQUE, Basque Foundation for Science, Bilbao, Spain, <sup>7</sup>Experimental and Clinical Research Center (ECRC), a joint cooperation between the Charité Medical Faculty and the Max Delbrück Center for Molecular Medicine, Berlin, Germany

Thermal Magnetic Resonance (ThermalMR) adds a thermal dimension to an MR device by exploiting the constructive interference of radiofrequency (RF) waves for temperature intervention. Here, the capacity of ThermalMR is demonstrated in a model system involving the release of a protein from thermoresponsive nanogels. Upon RF heating the nanogels ( $T=43^{\circ}\text{C}$ ), 29.3% of the protein were released after 6h which is in accordance with the release profile obtained for the reference data derived from a water bath setup. ThermalMR provides an ideal testbed for the study of temperature induced release of drugs, MR probes and other agents from thermoresponsive carriers.

1130



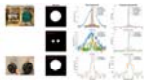
### Magnetic Resonance Fingerprinting with Quadratic RF Phase for Continuous Temperature Monitoring in Aqueous Tissues

Rasim Boyacioglu<sup>1</sup>, Megan Poorman<sup>2,3</sup>, Kathryn Keenan<sup>2</sup>, and Mark Griswold<sup>1</sup>

<sup>1</sup>Radiology, Case Western Reserve University, Cleveland, OH, United States, <sup>2</sup>Physical Measurement Laboratory, National Institute of Standards and Technology, Boulder, CO, United States, <sup>3</sup>Department of Physics, University of Colorado Boulder, Boulder, CO, United States

Conventional temperature monitoring is based on measurement of off-resonance via gradient-echo phase scans for non-adipose tissue. MRF with quadratic RF phase (MRFqRF) simultaneously quantifies off-resonance, T1, T2, and T2\*. For a proof of principle thermometry experiment with MRFqRF, an ex-vivo aqueous sample was heated with laser ablation, temperature was tracked, and multiple continuous MRFqRF scans were obtained with different temporal resolutions. Scanner frequency drifts were removed automatically with Independent Component Analysis. Residual changes in off-resonance predict the temperature change. However, MRFqRF temporal resolution (~10s) needs to be increased further for clinical relevance.

1131



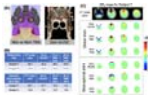
### Bloch-Optimized Dithered-Ultrasound-Pulse RF for Low-Field Inhomogeneous Permanent Magnet MR Imagers

Irene Kuang<sup>1</sup>, Nick Arango<sup>1</sup>, Jason Stockmann<sup>2,3</sup>, Elfar Adalsteinsson<sup>1,4</sup>, and Jacob White<sup>1</sup>

<sup>1</sup>Electrical Engineering and Computer Science, Massachusetts Institute of Technology, Cambridge, MA, United States, <sup>2</sup>A. A. Martinos Center for Biomedical Imaging, Massachusetts General Hospital, Charlestown, MA, United States, <sup>3</sup>Harvard Medical School, Boston, MA, United States, <sup>4</sup>Institute for Medical Engineering and Science, Massachusetts Institute of Technology, Cambridge, MA, United States

Declining costs of permanent magnets and embedded systems electronics has driven systems engineering of point-of-care diagnostics to the forefront of MR research. We present a low-cost RF signal chain (<\$100) for low-field imaging using a Teensy 4.0 microcontroller and STHV800 ultrasound pulser IC. Bloch-optimization simulation of programmable, dithered-pulses enables broadband excitation of the notably inhomogeneous permanent magnets employed in portable, hand-held MR systems.

1132



### Feasibility of using a 3-axis multi-channel TMS coil array for B0 shimming of the brain at 3T

Jason P. Stockmann<sup>1,2</sup>, Lucia Navarro de Lara<sup>1</sup>, Larry Wald<sup>1,2</sup>, and Aapo Nummenmaa<sup>1,2</sup>

<sup>1</sup>A. A. Martinos Center, Massachusetts General Hospital, Charlestown, MA, United States, <sup>2</sup>Harvard Medical School, Boston, MA, United States

We explore the local field control capability of a 48ch TMS coil array to perform B0 shimming in the brain. The array uses sixteen 3-axis TMS coils built using three independent orthogonal windings that provide added flexibility to orient the resultant magnetic dipole and thus facilitate tailoring the B0 shim field. We propose adapting the TMS coils to carry DC shim currents during EPI fMRI time series acquisitions to reduce artifact levels and improve the utility of TMS-fMRI for studying brain circuits.

1133



### In-bore voltage inversion with very low EMI by a switched capacitor converter

Christoph Michael Schildknecht<sup>1</sup>, David Otto Brunner<sup>1</sup>, and Klaas Paul Pruessmann<sup>1</sup>

<sup>1</sup>ETH Zurich and University of Zurich, Zurich, Switzerland

Complex in-bore electronics (e.g. motion trackers, digitizer etc.) frequently requires various voltage rails. This poses especially a challenge when bi-polar voltages are required because in-bore voltage inversion is typically not possible due to the EMI of such converter. The here presented switched capacitor voltage inverter allows in-bore operation without disturbing the MRI scanner due to the very low EMI. Lab and 3T MRI measurement were performed to verify the EMC compatibility and characterize the device.

1134

Single channel non-linear breast gradient coil for diffusion encoding

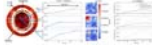


Sebastian Littin<sup>1</sup>, Feng Jia<sup>1</sup>, Philipp Amrein<sup>1</sup>, Huijun Yu<sup>1</sup>, Arthur Magill<sup>2</sup>, Tristan Kuder<sup>2</sup>, Mark E. Ladd<sup>2</sup>, Frederik Laun<sup>3</sup>, Sebastian Bickelhaupt<sup>4</sup>, and Maxim Zaitsev<sup>1</sup>

<sup>1</sup>Department of Radiology, Medical Physics, University of Freiburg, University Medical Center, Freiburg, Germany, <sup>2</sup>Medical Physics in Radiology, German Cancer Research Center, Heidelberg, Germany, <sup>3</sup>Department of Radiology, MR Physics, University Medical Center Erlangen, Erlangen, Germany, <sup>4</sup>Junior Group Medical Imaging and Radiology – Cancer Prevention, German Cancer Research Center (DKFZ), Heidelberg, Germany

The aim of this project is to design and implement a non-linear single channel breast gradient coil for diffusion encoding. Initial field maps of the prototype implementation are shown. The prototype should allow to generate gradient strengths between 1 and 3.6 [T/m].

1135



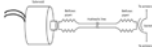
Measurement-based safety assessment, prediction and mitigation of RF induced implant heating with parallel transmission: temperature matrix

Berk Silemek<sup>1</sup>, Lukas Winter<sup>1</sup>, Frank Seifert<sup>1</sup>, Harald Pfeiffer<sup>1</sup>, and Bernd Ittermann<sup>1</sup>

<sup>1</sup>Physikalisch-Technische Bundesanstalt (PTB), Braunschweig and Berlin, Germany

A Measurement-based Temperature-Matrix approach is presented that enables a fast, patient and exam specific estimation and mitigation of RF hazards of implants. Various locations in phantom are tested using an 8-channel (300MHz) implant safety testbed. Heating reduction Based on T-Matrix Measurements resulted >3 times heating reduction vs. circularly-polarized mode and >19 times vs. worst-case mode. 2-channel MRI (3T) feasibility experiments using high temperature resolution showed good correlation with transmitted power. In addition, T-matrix-based temperature increase predictions successfully demonstrated. As summary, an easy to implement, cheap, sensor-based method, the T-matrix, to investigate, characterize and mitigate RF heating of implants is introduced.

1136



A Hydraulically Operated Wireless RF Switch to Control Antenna Tuning in MR-Mediated Radiofrequency Ablation

Jerome L. Ackerman<sup>1,2</sup>, Erez Nevo<sup>3</sup>, and Abraham Roth<sup>3</sup>

<sup>1</sup>Martinos Center for Biomedical Imaging, Department of Radiology, Massachusetts General Hospital, Charlestown, MA, United States, <sup>2</sup>Department of Radiology, Harvard Medical School, Boston, MA, United States, <sup>3</sup>Robin Medical, Inc., Baltimore, MD, United States

In magnetic resonance mediated radiofrequency ablation (MR-RFA) the RF energy for the ablation is captured by a wire antenna placed in the scanner bore, and channeled to the ablation needle. There are no external wired connections. The effective length of the antenna is adjusted physically or electrically to be resonant with the scanner RF to maximize energy capture. To suppress heating when desired, the antenna must be detuned. An electronic switch to do so reduces antenna efficiency, but a simple wireless hydraulically activated mechanical switch maintains full antenna efficiency and achieves high on-off ratio.

1137



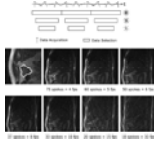
Conductive Elastomer for Wearable RF Coils

Andreas Port<sup>1</sup>, Roger Luechinger<sup>1</sup>, David Otto Brunner<sup>1</sup>, and Klaas Paul Pruessmann<sup>1</sup>

<sup>1</sup>Institute for Biomedical Engineering, ETH Zurich and University of Zurich, Zurich, Switzerland

Several stretchable conductor concepts have been proposed that rely on a continuous metal phase, rigid or liquid, as conductive path. Conductive elastomers, fundamentally different, form the conductive path through contact between particles such as carbon nano tubes, silver nanowires or silver microparticles. In the present work, we explore the feasibility and performance of MR detection with conductive elastomer coils. Evaluation is performed in terms of Q, SNR and in-vivo imaging. The results indicate that MR receive coils made from conductive elastomer provide good stretchability, adequate electrical performance and promise workflow enhancements as such a coil could even be washed.

1138



Comparison of tumor autosegmentation techniques from an undersampled dynamic radial bSSFP acquisition on a low-field MR-linac

Florian Friedrich<sup>1,2</sup>, C. Katharina Spindeldreier<sup>3</sup>, Juliane Hörner-Rieber<sup>3</sup>, Sebastian Klüter<sup>3</sup>, Peter Bachert<sup>1,2</sup>, Mark E. Ladd<sup>1</sup>, and Benjamin R. Knowles<sup>1</sup>

<sup>1</sup>Medical Physics in Radiology, German Cancer Research Center (DKFZ), Heidelberg, Germany,

<sup>2</sup>Department of Physics and Astronomy, Heidelberg University, Heidelberg, Germany, <sup>3</sup>Department of Radiation Oncology,, University Hospital of Heidelberg, Heidelberg, Germany

MR-linac hybrid systems can dynamically image a tumor during radiotherapy to aid in a more precise delivery of the radiation dose. Motion tracking of the target is required and is currently performed by a deformable image registration on Cartesian bSSFP images. This study compares three different tracking methods (convolutional neuronal network, multi-template matching, and deformable image registration) to track a lung tumor in Cartesian images, where the performance of the three methods did not differ significantly. The convolutional neuronal network provided minimal decrease in tracking accuracy in a healthy volunteer when undersampled radial images were used to accelerate image acquisition.

## Weekday Course

### Hot Topics & Cancer - Musculoskeletal Cancer Imaging

Organizers: Hiroshi Yoshioka, Riccardo Lattanzi, Jan Fritz, Jung-Ah Choi, Kimberly Amrami, Miika Nieminen

Thursday Parallel 1 Live Q&A

Thursday 15:05 - 15:50 UTC

Moderators: Andreas Weng

Advanced MRI Techniques for Imaging Musculoskeletal Tumors

Hakan Ilaslan<sup>1</sup>

<sup>1</sup>Cleveland Clinic, Cleveland, OH, United States

Clinical MRI of Musculoskeletal Tumors

Shivani Ahlawat<sup>1</sup>

<sup>1</sup>Musculoskeletal Imaging Division The Russell H. Morgan Department of Radiology & Radiological Science, Johns Hopkins University School of Medicine, Baltimore, MD, United States

Benign and malignant musculoskeletal soft tissue and bone tumors are frequently encountered in a routine clinical radiology practice. Accurate characterization of these tumors is challenging but necessary to inform patient management decisions such as the need for histologic sampling versus observation. A systematic use of clinical, radiographic and MRI-based quantitative and qualitative data can characterize a subset of MSK soft tissue and bone tumors as determinate lesions. If an MSK soft tissue or bone tumor cannot be characterized as benign, the tumor should be reported as indeterminate and the patient should undergo biopsy and/or orthopedic oncology consultation to exclude malignancy.

PET/MRI Applications in Musculoskeletal Cancer Imaging

Garry Gold<sup>1</sup> and Ali B. Syed<sup>2</sup>

## Post-Treatment Imaging of Response & Surveillance

Amanda Isaac<sup>1</sup>

<sup>1</sup>King's College London, London, United Kingdom

---

---

## Weekday Course

### Novel clinical applications of CMR - MRI in Cardio-Oncology

Organizers: Aleksandra Radjenovic, Tim Leiner

Thursday Parallel 3 Live Q&A

Thursday 15:05 - 15:50 UTC

Moderators: Michael Salerno & Yuchi Liu



#### Introduction to Cardio-Oncology

Mark Nolan<sup>1</sup>

<sup>1</sup>Australia

Cardio-Oncology is a new and rapidly expanding clinical field that challenges traditional treatment paradigms in helping a vulnerable population. Cardiovascular complications of novel chemotherapeutics are increasingly recognized and can affect nearly any dimension of cardiac function. Therefore there is a need for versatile cardiac imaging techniques which can guide physicians be looking beyond traditional imaging biomarkers, such as LVEF. Cardiovascular MRI is well-positioned to meet these challenges. This session will introduce the current landscape of cardio-oncology and how cardiovascular MRI may help.

---

#### Emerging Clinical Practice of Cardio-Oncology

Lauren A. Baldassarre<sup>1</sup>

<sup>1</sup>Internal Medicine (Cardiology), Yale University, NEW HAVEN, CT, United States

---

#### Current Role of MRI in Cardio-Oncology

Bernd Wintersperger<sup>1</sup>

<sup>1</sup>University of Toronto

Related to the continuously improved patient long term survival and improved personalized cancer therapy regimens, adverse cardiovascular effects of cancer therapy have become highly important considerations. Given its accuracy and precision as well its ability to assess details of the myocardial tissue characterization makes cardiac MRI a prime modality in assessment of potential cancer therapy related cardiac dysfunction (CTRCD) as well as tissue changes.

---

#### What Can MRI Bring to the Field of Cardio-Oncology in the Future?

Yoo Jin Hong<sup>1</sup>

<sup>1</sup>Yonsei University Health System, Republic of Korea

Current guidelines consider LVEF assessment using echocardiography as the standard diagnostic technique for detecting chemotherapy-induced cardiotoxicity. However, magnetic resonance imaging (MRI) may play an important role in the cardiac evaluation of cancer patients.

---

---

1139



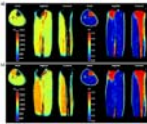
Multimodal qMRI Framework for Knee Imaging Biomarker Fusion and Osteoarthritis Prediction

Alejandro Morales Martinez<sup>1,2</sup>, Francesco Caliva<sup>1</sup>, Claudia Iriondo<sup>1,2</sup>, Sarthak Kamat<sup>1</sup>, Sharmila Majumdar<sup>1</sup>, and Valentina Pedoia<sup>1,2,3</sup>

<sup>1</sup>Department of Radiology and Biomedical Imaging, University of California, San Francisco, San Francisco, CA, United States, <sup>2</sup>Graduate Program in Bioengineering, University of California, Berkeley, Berkeley, CA, United States, <sup>3</sup>Center for Digital Health Innovation (CDHI), University of California San Francisco, San Francisco, CA, United States

Bone and cartilage segmentation models were trained and validated with a segmented dataset of 40 and 176 3D DESS MRI volumes respectively. The trained models were used to run inference on 20,989 3D DESS MRI volumes from the Osteoarthritis Initiative dataset. Biomarkers such as femoral bone shape, cartilage thickness and cartilage T2 average values were extracted from the segmentations. Point clouds representing each biomarker were transformed into spherical coordinates and merged using different fusion strategies. The spherical maps were used to train an OA diagnosis model with a test specificity, sensitivity and AUC was 84.1%, 78.7%, and 89.7% respectively.

1140



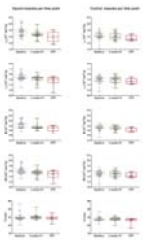
3D MR fingerprinting with water and fat separation

Benjamin Marty<sup>1,2</sup>

<sup>1</sup>NMR Laboratory, Neuromuscular Investigation Center, Institute of Myology, Paris, France, <sup>2</sup>NMR Laboratory, CEA/DRF/IBFJ/MIRcen, Paris, France

In this study, a fast 3D MR fingerprinting sequence with water and fat separation (3D MRF T1-FF) was developed for simultaneous measurement of FF and water T1 in the skeletal muscles of patients with fat infiltrations. The precision and accuracy of the sequence was evaluated on a multi-vial phantom and in vivo proofs of concept were obtained in the legs of a healthy volunteer before and after plantar dorsi-flexions and at rest in a patient suffering from inclusion body myositis.

1141



Diffusion Tensor Imaging detects recovery after acute muscle injury

Melissa Tamara Hooijmans<sup>1</sup>, Jithsa R. Monte<sup>2</sup>, Martijn Froeling<sup>3</sup>, Jos Oudeman<sup>4</sup>, Johannes L. Tol<sup>5</sup>, Mario Maas<sup>2</sup>, Gustav J. Strijkers<sup>1</sup>, and Aart J. Nederveen<sup>2</sup>

<sup>1</sup>Department of Biomedical Engineering & Physics, Amsterdam University Medical Centers, University of Amsterdam, Amsterdam, Netherlands, <sup>2</sup>Department of Radiology & Nuclear Medicine, Amsterdam University Medical Centers, University of Amsterdam, Amsterdam, Netherlands, <sup>3</sup>Department of Radiology, University Medical Center Utrecht, Utrecht, Netherlands, <sup>4</sup>Department of Orthopaedic Surgery, University Medical Center Utrecht, Utrecht, Netherlands, <sup>5</sup>Department of Orthopaedic Surgery, Amsterdam University Medical Centers, University of Amsterdam, Amsterdam, Netherlands

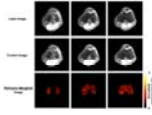
41 athletes with an acute hamstring injury underwent MRI examination of their injured leg and the uninjured contralateral leg at three different time points: (1) within one week after the index injury (baseline), (2) two weeks after baseline, and at (3) Return to Play (RTP). Baseline DTI values (MD, RD and the three eigenvalues) were elevated compared to control hamstring muscles and decreased during the RTP phase. qT2 values were elevated after the index injury and did not change over time. DTI is promising for monitoring recovery of hamstring injuries.

1142

Knee Epiphyseal Bone Marrow Perfusion Imaging Using FAIR RESOLVE

Xiufeng Li<sup>1</sup>, Casey P. Johnson<sup>1</sup>, and Jutta Ellermann<sup>1</sup>

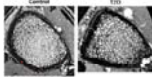




<sup>1</sup>Center for Magnetic Resonance Research, University of Minnesota, Minneapolis, MN, United States

Perfusion imaging can provide critical information to assess vasculature status and tissue viability of knee bone marrow. Arterial spin labeling, as a non-invasive and non-contrast-enhanced perfusion imaging approach, is well-suited for routine assessment of bone marrow perfusion, longitudinal monitoring of disease progression and repeated evaluation of therapy response. Recently, knee epiphyseal bone marrow ASL imaging has been demonstrated at 3T with promising results by using FAIR ss-FSE method. However, the ss-FSE image readout only supports single-slice acquisitions. To overcome this limitation, we implemented and evaluated FAIR RESOLVE for multi-slice knee epiphyseal bone marrow perfusion imaging.

1143



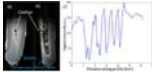
Multi-modality in vivo imaging of cortical bone vasculature: Comparison of diabetes patients to healthy controls

Po-hung Wu<sup>1</sup>, Misung Han<sup>1</sup>, Roland Krug<sup>1</sup>, Jing Liu<sup>1</sup>, Gabby B. Joseph<sup>1</sup>, Thomas Link<sup>1</sup>, and Galatea Kazakia<sup>1</sup>

<sup>1</sup>Department of Radiology and Biomedical Imaging, University of California - San Francisco, San Francisco, CA, United States

Type 2 diabetes is known to increase fracture risk, possibly through the development of pathological cortical bone porosity. However, the mechanisms of pathological pore growth are not understood. We hypothesize that T2D patients will display altered vascularization within cortical pores due to microvascular disease. In this study, 15 T2D patients and 22 controls were imaged by HR-pQCT and DCE-MRI to analyze vessel and perfusion metrics (eg. vessel density, transition time). The study results suggest that T2D patients have altered vessel distribution and perfusion characteristics, and that microvascular disease may be a factor in diabetic bone disease.

1144



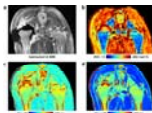
Visibility of artificial dental side root canals using MRI

Agazi Samuel Tesfai<sup>1</sup>, Andreas Vollmer<sup>2</sup>, Moritz Braig<sup>1</sup>, Johannes Fischer<sup>1</sup>, Ute Ludwig<sup>1</sup>, and Michael Bock<sup>1</sup>

<sup>1</sup>Dept. of Radiology, Medical Physics, Medical Center - University of Freiburg, Freiburg, Germany, <sup>2</sup>Dept. of Oral and Craniomaxillofacial Surgery, Center for Dental Medicine, Medical Center - University of Freiburg, Freiburg, Germany

Detection of root canals is vital for dental diagnosis, however it is difficult to locate these anatomies within sub-millimeter dimension. To determine the ability of MRI to display such structures, a bovine tooth with different sized artificial cavities was prepared. It was evaluated with a preclinical 7T system and a clinical 3T MR system against cone beam CT. 7T measurements with UTE offer precise distinction of cavities up to 200µm. 3T UTE allows only differentiation of 1000µm cavities due to blurring. Tooth immersed in contrast agent solution allows localization up to 200µm cavity with spin echo sequence and negative contrast.

1145



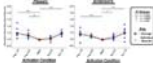
Quantitative T2, T1p, and Diffusion Mapping of Early-Stage Ischemic Osteonecrosis of the Femoral Head: An In Vivo Piglet Model Study at 3T MRI

Casey P. Johnson<sup>1,2</sup>, Ferenc Toth<sup>1</sup>, Alexandra R. Armstrong<sup>1</sup>, Harry K. W. Kim<sup>3,4</sup>, and Jutta M. Ellermann<sup>2,5</sup>

<sup>1</sup>Veterinary Clinical Sciences Department, University of Minnesota, Saint Paul, MN, United States, <sup>2</sup>Center for Magnetic Resonance Research, University of Minnesota, Minneapolis, MN, United States, <sup>3</sup>Texas Scottish Rite Hospital for Children, Dallas, TX, United States, <sup>4</sup>Department of Orthopaedic Surgery, UT Southwestern Medical Center, Dallas, TX, United States, <sup>5</sup>Department of Radiology, University of Minnesota, Minneapolis, MN, United States

This study tested whether T2 and T1 $\rho$  relaxation times are sensitive in detecting early-stage osteonecrosis of the femoral head in piglet model under *in vivo* conditions and at clinical 3T MRI. This study builds on recent *ex vivo* 9.4T studies assessing T2 and T1 $\rho$  in the piglet model. We also evaluated apparent diffusion coefficient for comparison. We found that T2, T1 $\rho$ , and ADC were all significantly increased in the ischemic vs. contralateral control femoral heads in n=6 piglets one week after onset of ischemia. These methods may be clinically useful to detect and characterize early-stage osteonecrosis to inform treatment decisions.

1146



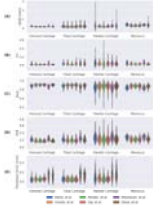
### Estimating contraction of individual muscles during isometric wrist torque using multi-muscle MR elastography (MM-MRE)

Daniel Smith<sup>1</sup>, Andrea Zonnino<sup>1</sup>, Fabrizio Sergi<sup>1</sup>, and Curtis Johnson<sup>1</sup>

<sup>1</sup>University of Delaware, Newark, DE, United States

In this study, we propose to use a technique called MM-MRE to identify states of contraction of individual forearm muscles based on the measurement of muscle shear wave speed. Using a custom protocol and passive driver device, we scanned four subjects through 45 MRE scans each in three wrist positions during five torque application states. We found significant correlations between increased wave speed and higher applied torques, in both agonist and antagonist motions. The results indicate that MM-MRE is an effective measurement tool for analyzing the contractile state of individual forearm muscle during isometric contractions of the wrist joint.

1147



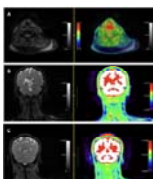
### A Report on the International Workshop on Osteoarthritis Imaging Segmentation Challenge: A Multi-Institute Evaluation on a Standard Dataset

Arjun D. Desai<sup>1,2</sup>, Francesco Caliva<sup>3</sup>, Claudia Iriondo<sup>3</sup>, Naji Khosravan<sup>4</sup>, Aliasghar Mortazi<sup>4</sup>, Sachin Jambawalikar<sup>5</sup>, Drew Torigian<sup>6</sup>, Jutta Ellerman<sup>7</sup>, Mehmet Akçakaya<sup>8</sup>, Ulas Bagci<sup>4</sup>, Radhika Tibrewala<sup>3</sup>, Io Flament<sup>3</sup>, Matt O'Brien<sup>3</sup>, Sharmila Majumdar<sup>3</sup>, Mathias Perslev<sup>9</sup>, Akshay Pai<sup>9</sup>, Christian Igel<sup>9</sup>, Erik B. Dam<sup>9</sup>, Sibaji Gaj<sup>10</sup>, Mingrui Yang<sup>10</sup>, Kunio Nakamura<sup>10</sup>, Xiaojuan Li<sup>10</sup>, Cem M. Deniz<sup>11</sup>, Vladimir Juras<sup>12</sup>, Ravinder Regatte<sup>11</sup>, Garry E. Gold<sup>2</sup>, Brian A. Hargreaves<sup>2</sup>, Valentina Pedoia<sup>3</sup>, and Akshay S. Chaudhari<sup>2</sup>

<sup>1</sup>Electrical Engineering, Stanford University, Stanford, CA, United States, <sup>2</sup>Radiology, Stanford University, Stanford, CA, United States, <sup>3</sup>Radiology, University of California San Francisco, San Francisco, CA, United States, <sup>4</sup>University of Central Florida, Orlando, FL, United States, <sup>5</sup>Radiology, Columbia University Medical Center, New York, NY, United States, <sup>6</sup>Radiology, University of Pennsylvania, Philadelphia, PA, United States, <sup>7</sup>Radiology, University of Minnesota, Minneapolis, MN, United States, <sup>8</sup>Electrical and Computer Engineering, University of Minnesota, Minneapolis, MN, United States, <sup>9</sup>Computer Science, University of Copenhagen, Copenhagen, Sweden, <sup>10</sup>Biomedical Engineering, Cleveland Clinic, Cleveland, OH, United States, <sup>11</sup>Radiology, New York University Langone Health, New York, NY, United States, <sup>12</sup>Biomedical Imaging and Image-Guided Therapy, Medical University of Vienna, Vienna, Austria

Cartilage thickness can be predictive of joint health. However, manual cartilage segmentation is tedious and prone to inter-reader variations. Automated segmentation using deep-learning is promising; yet, heterogeneity in network design and lack of dataset standardization has made it challenging to evaluate the efficacy of different methods. To address this issue, we organized a standardized, multi-institutional challenge for knee cartilage and meniscus segmentation. Results show that CNNs achieve similar performance independent of network architecture and training design and, given the high segmentation accuracy achieved by all models, only a weak correlation between segmentation accuracy metrics and cartilage thickness was observed.

1148



### Abnormal [18F]FDG PET/MRI Findings in Paraspinal Structures of Patients with Suspected Cerebrospinal Fluid Leak

Peter Cipriano<sup>1</sup>, Daehyun Yoon<sup>1</sup>, Ryan Penticuff<sup>1</sup>, Yingding Xu<sup>2</sup>, Ian Carroll<sup>3</sup>, and Sandip Biswal<sup>1</sup>

<sup>1</sup>Stanford University, Stanford, CA, United States, <sup>2</sup>Stanford University, Palo Alto, CA, United States,

<sup>3</sup>Stanford University, Redwood City, CA, United States

Six patients with suspected cerebrospinal fluid leak but in whom no site of leakage had been identified and six controls underwent simultaneous, whole-body [18F]FDG PET/MRI imaging. Increased [18F]FDG uptake was found in paraspinal structures in all six patients and was significantly greater than in the corresponding areas of controls. Temporary but significant relief in symptoms resulted from blood patches placed at locations coinciding with PET/MRI abnormalities.

1149



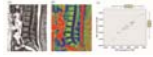
#### Classification of Spinal Metastases Coming from Different Primary Cancer Origin by Using Quantitative Radiomics Analysis with Multi-Class SVM

Yongye Chen<sup>1</sup>, Yang Zhang<sup>2</sup>, Enlong Zhang<sup>1</sup>, Xiaoying Xing<sup>1</sup>, Qizheng Wang<sup>1</sup>, Huishu Yuan<sup>1</sup>, Min-Ying Su<sup>2</sup>, and Ning Lang<sup>1</sup>

<sup>1</sup>Department of Radiology, Peking University Third Hospital, Beijing, China, <sup>2</sup>Department of Radiological Sciences, University of California, Irvine, CA, United States

For patients suspected to have spinal metastasis, a confirmed pathological diagnosis is needed to proceed with appropriate treatment. This study applied quantitative radiomics to differentiate 5 groups of patients with metastatic cancers in the spine, including 28 lung, 11 breast, 7 kidney, 11 prostate and 18 thyroid. The analysis was done on post-contrast images. A total of 107 features, including 32 first order and 75 texture, were extracted for each case by using PyRadiomics. The group differentiation was done by using multi-class support vector machine (SVM). The overall accuracy was 80%, with the highest accuracy of 27/28=96% for lung mets.

1150



#### Evaluation of the risk of osteoporosis by using IDEAL-IQ in diabetic patients

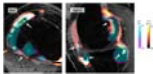
Yu Song<sup>1</sup>, Qingwei Song<sup>1</sup>, Aibo Wang<sup>2</sup>, Ailian Liu<sup>1</sup>, Yanwei Miao<sup>1</sup>, Nan Zhang<sup>1</sup>, Haonan Zhang<sup>1</sup>, and Lizhi Xie<sup>3</sup>

<sup>1</sup>Department of Radiology, the First Affiliated Hospital of Dalian Medical University, Dalian, China,

<sup>2</sup>Department of Radiology, Peking University Third Hospital, Beijing, China, <sup>3</sup>GE Healthcare, MR Research, Beijing, China

Diabetes is a metabolic disease that leads to a high risk of fracture related to osteoporosis. Noninvasive and reliable assessment of osteoporosis is essential for clinical practice. The aim of this study was to explore the agreement of the Proton Density Fat Fraction (PDFF) values of lumbar vertebra measured by Magnetic Resonance Imaging (MRI) IDEAL-IQ sequences at different field strengths and to investigate the value of IDEAL-IQ in the assessment of osteoporosis risk in diabetic.

1151



#### Imaging of Bone-Synovium Interactions Using Dynamic Contrast Enhanced MRI and 18F-Sodium Fluoride PET

James MacKay<sup>1,2</sup>, Lauren Watkins<sup>3</sup>, Garry Gold<sup>3</sup>, and Feliks Kogan<sup>4</sup>

<sup>1</sup>Radiology, University of East Anglia, Norwich, United Kingdom, <sup>2</sup>Radiology, University of Cambridge, Cambridge, United Kingdom, <sup>3</sup>Radiology, Stanford University, Stanford, CA, United States, <sup>4</sup>Stanford University, Stanford, CA, United States

Synovial inflammation is hypothesised to play a role in the development and progression of osteophytes in osteoarthritis (OA).

Here we use hybrid 3T PET-MRI to perform simultaneous bilateral knee MR imaging of 11 participants (22 knees) with knee OA. We use  $^{18}\text{F}$ -NaF PET to quantify osteophyte metabolic activity and dynamic contrast enhanced MR imaging to quantify synovitis.

We demonstrate that synovitis adjacent to osteophytes is more intense (as quantified by the DCE parameter  $K^{\text{trans}}$ ) than the whole-joint average, and that there is a significant association between increased osteophyte metabolic activity (as quantified by PET  $\text{SUV}_{\text{max}}$ ) and intensity of adjacent synovitis.

---

## Oral - Power Pitch

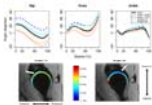
### Hot Topics & Cancer - Musculoskeletal 2

Thursday Parallel 1 Live Q&A

Thursday 15:05 - 15:50 UTC

Moderators: Jutta Ellermann & Hiroshi Yoshioka

1152



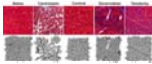
#### Linking multi-joint biomechanics with cartilage composition from qMRI

Koren Roach<sup>1</sup>, Valentina Padoia<sup>1</sup>, Jinhee J Lee<sup>1</sup>, Tijana Popovic<sup>1</sup>, Sharmila Majumdar<sup>1</sup>, and Richard B Souza<sup>1</sup>

<sup>1</sup>UCSF, San Francisco, CA, United States

Hip osteoarthritis is likely caused by changes in gait biomechanics and cartilage biochemistry and composition. In this study, we employed multivariate functional principal component analysis to identify gait waveform characteristics that were related to  $T_{1\rho}$  and  $T_2$  relaxation times in the femoral and acetabular cartilage. Our results indicated that transverse and sagittal plane waveform characteristics are significantly related to  $T_{1\rho}$  and  $T_2$  relaxation times in the femoral and acetabular cartilage and may be key planes of motion on which to focus preventative therapies for hip osteoarthritis.

1153



#### Using the random permeable barrier model to predict fiber size in histology informed simulated skeletal muscle models

David B Berry<sup>1</sup>, Erin K Englund<sup>2</sup>, Vitaly Galinsky<sup>3</sup>, Lawrence R Frank<sup>3</sup>, and Samuel R Ward<sup>2,3,4</sup>

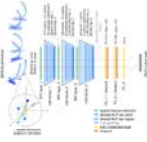
<sup>1</sup>Nanoengineering, University of California, San Diego, La Jolla, CA, United States, <sup>2</sup>Orthopaedic Surgery, University of California, San Diego, La Jolla, CA, United States, <sup>3</sup>Radiology, University of California, San Diego, La Jolla, CA, United States, <sup>4</sup>Bioengineering, University of California, San Diego, La Jolla, CA, United States

There is growing interest in using the Random Permeable Barrier Model (RPBM) to measure muscle microstructure. The goal of this study was to evaluate the accuracy of RPBM in predicting muscle fiber size in histology informed models of healthy and injured skeletal muscle from simulated DTI data. RPBM was found to systematically underestimate fiber size, but accurately predicted surface area to volume ratio (S/V) of the simulated muscle fibers. While the clinical interpretation of S/V ratio is unclear, this indicates that accurate measurement of S/V may serve as a proxy to changes in muscle fiber size and therefore function.

---

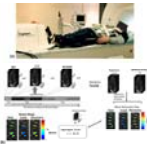
To the point: deep learning on dense T2 point clouds for improved feature extraction

Claudia Iriondo<sup>1</sup>, Alaleh Razmjoo<sup>2</sup>, Francesco Caliva<sup>2</sup>, Sharmila Majumdar<sup>2</sup>, and Valentina Padoia<sup>2</sup>



<sup>1</sup>Radiology and Biomedical Imaging, University of California, San Francisco, San Francisco, CA, United States, <sup>2</sup>University of California, San Francisco, San Francisco, CA, United States

To-the-point (TTP) is a novel approach for analyzing compositional MR imaging data. By representing tibial and femoral cartilage T2 values as a dense point cloud, our approach can leverage the data's inherent sparsity while maintaining local geometric properties, leading to improved feature extraction and faster image processing times. Experiments on the whole OAI T2 dataset show strong performance in an OA diagnosis task 82.44% sens, 82.59% spec, with extracted features even identifying patients who would become diagnosed with OA 1 to 2 years in the future.

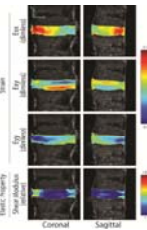


### 3D Internal dynamic strains in the intervertebral disc (IVD) of the lumbar spine with GRASP-MRI under mechanical loading

Rajiv G Menon<sup>1</sup>, Marcelo V. W. Zibetti<sup>1</sup>, and Ravinder R Regatte<sup>1</sup>

<sup>1</sup>Center for Biomedical Imaging, Department of Radiology, New York University Langone Health, New York, NY, United States

The goal of this study was to develop a non-invasive MRI technique to measure 3D dynamic internal strains in the intervertebral discs (IVDs) of lumbar spine during loading and recovery phases. For this purpose, a combination of static mechanical loading of the IVD using MR-compatible ergometer and continuous MRI-acquisition with a 3D-GRASP acquisition was used. Data was acquired on five healthy volunteers, and dynamic strains under loading and recovery conditions were calculated in 5-IVD segments from L1/L2 to L5/S1. By measuring temporal evolution of strain during rest, loading and recovery phases, dynamic strain information in the IVD may be investigated.

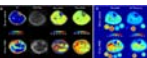


### Intervertebral Disc Elastography: Physiological Strain, Stiffness, and Relaxometry in Axial Compression and Bending

Deva D. Chan<sup>1,2</sup>, Paull C. Gossett<sup>2</sup>, Robert L. Wilson<sup>3</sup>, Woong Kim<sup>2</sup>, Yue Mei<sup>4,5,6</sup>, Kent Butz<sup>2</sup>, Nancy Emery<sup>7</sup>, Eric A. Nauman<sup>2</sup>, Stéphane Avril<sup>6</sup>, and Corey P. Neu<sup>2,3</sup>

<sup>1</sup>Biomedical Engineering, Rensselaer Polytechnic Institute, Troy, NY, United States, <sup>2</sup>Biomedical Engineering, Purdue University, West Lafayette, IN, United States, <sup>3</sup>Mechanical Engineering, University of Colorado Boulder, Boulder, CO, United States, <sup>4</sup>Engineering Mechanics, Dalian University of Technology, Dalian, China, <sup>5</sup>International Research Center for Computational Mechanics, Dalian University of Technology, Dalian, China, <sup>6</sup>Center for Biomedical and Healthcare Engineering, MINES Saint-Étienne, Saint-Étienne, France, <sup>7</sup>Ecology and Evolutionary Biology, University of Colorado Boulder, Boulder, CO, United States

IVD degeneration is the most recognized cause of low back pain, characterized by the decline of tissue structure and mechanics. MRI relaxometry is one quantitative measure of IVD degeneration, yet MRI metrics of mechanics have not been fully explored. We quantified patterns of IVD strain and mechanics during physiological compression and bending. Strains patterns depended on the loading mode, and shear modulus in the nucleus pulposus was typically an order of magnitude lower than the annulus fibrosis, except in bending, where the apparent stiffness depended on the loading direction. Strain and material properties provide new possible biomarkers for IVD degeneration.



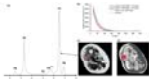
### Quantitative <sup>1</sup>H and <sup>23</sup>Na NMR imaging in the skeletal muscles of patients with fascioscapulohumeral muscular dystrophy

Benjamin Marty<sup>1,2</sup>, Teresa Gerhalter<sup>1,2,3</sup>, Lena V. Gast<sup>3</sup>, Katharina Porzelt<sup>4</sup>, Matthias Türk<sup>4</sup>, Matthias Hammon<sup>3</sup>, Michael Uder<sup>3</sup>, Rolf Schröder<sup>5</sup>, Pierre G. Carlier<sup>1,2</sup>, and Armin M. Nage<sup>3,6,7</sup>

<sup>1</sup>NMR Laboratory, Neuromuscular Investigation Center, Institute of Myology, Paris, France, <sup>2</sup>NMR Laboratory, CEA/DRF/IBFJ/MIRCen, Paris, France, <sup>3</sup>Institute of Radiology, University Hospital, FAU, Erlangen, Germany, <sup>4</sup>Institute of Neurology, FAU, Erlangen, Germany, <sup>5</sup>Department of Neuropathology, University Hospital Erlangen, FAU, Erlangen, Germany, <sup>6</sup>Division of Medical Physics in Radiology, DKFZ, Heidelberg, Germany, <sup>7</sup>Institute of Medical Physics, FAU, Erlangen, Germany

Facioscapulohumeral muscular dystrophy (FSHD) is a neuromuscular disorder characterized by structural changes affecting skeletal muscle tissues, resulting in muscle wasting and dysfunction. Here, we determined the value of quantitative <sup>1</sup>H and <sup>23</sup>Na muscle MRI approaches for providing variables related to disease severity (fat fraction) and disease activity (water T<sub>2</sub>, water T<sub>1</sub>, total sodium content and inversion-recovery <sup>23</sup>Na) in patients with FSHD. We found that MRI variables related to water mobility and ion homeostasis were increased at an early stage of the degeneration process in several muscles of FSHD patients and represent potential candidates for assessing treatment response in clinical trials.

1158



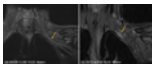
About the origin of decreased <sup>1</sup>H NMRS-based water T<sub>2</sub> in highly fatty infiltrated skeletal muscles of subjects with neuromuscular disorders

Harmen Reynhoudt<sup>1,2</sup>, Ericky Caldas de Almeida Araujo<sup>1,2</sup>, Pierre-Yves Baudin<sup>3</sup>, Benjamin Marty<sup>1,2</sup>, and Pierre G. Carlier<sup>1,2</sup>

<sup>1</sup>NMR Laboratory, Neuromuscular Investigation Center, Institute of Myology, Paris, France, <sup>2</sup>NMR Laboratory, CEA/DRF/IBFJ/MIRCen, Paris, France, <sup>3</sup>Consultants for Research in Imaging and Spectroscopy, Tournai, Belgium

<sup>1</sup>H NMRS-based water T<sub>2</sub> (T<sub>2w</sub>) has shown to be decreasing when muscle fat fraction levels are elevated (>60%). Here, two myopathy patient groups with similar fat fraction levels (>60%) emerged, being a group with T<sub>2w</sub>>30 ms and a group with T<sub>2w</sub><30 ms, which seemed to be correlated to the respective water resonance linewidths. Interpretation of these reduced T<sub>2w</sub> values at high fat fractions needs to be handled cautiously. The larger linewidths observed in the spectra characterized by shorter T<sub>2w</sub> may be due to the local B<sub>0</sub> gradients induced by susceptibility differences between muscle and fat.

1159



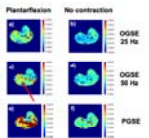
Radiologic evaluation of MSDE-CUBE-FLEX for imaging brachial plexus

Daehyun Yoon<sup>1</sup>, Neha Antil<sup>1</sup>, Sandip Biswal<sup>1</sup>, and Amelie Lutz<sup>1</sup>

<sup>1</sup>Radiology, Stanford university, Stanford, CA, United States

The conventional MRI examination of brachial plexus using 2D fast spin-echo sequences suffers from 1) long scan time due to a large field of view, 2) insufficient fat suppression due to strong off-resonance, 3) confusion between nerves and blood vessels. We recently presented a novel MSDE-CUBE-FLEX sequence addressing these issues by combining 1) outer volume suppression, 2) fast triple-echo Dixon technique, 3) magnitude-preparation to suppress blood signal. In this work, we compared the MSDE-CUBE-FLEX and 2D FSE sequences for imaging brachial plexus, which shows clear improvements in brachial plexus visualization with the MSDE-CUBE-FLEX sequence.

1160



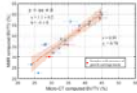
Imaging of skeletal muscle contraction using Oscillating Gradient Spin Echo (OGSE)

Valentina Mazzoli<sup>1</sup>, Kevin Moulin<sup>1</sup>, Feliks Kogan<sup>1</sup>, Brian Hargreaves<sup>1</sup>, and Garry E. Gold<sup>1</sup>

<sup>1</sup>Department of Radiology, Stanford University, Stanford, CA, United States

The apparent diffusion coefficient measured using DTI in skeletal muscles depends on the time allowed for diffusing water molecules to probe the local environment and on the size of muscle cells. Here we explore the use of Oscillating Gradient Spin Echo diffusion to obtain information on skeletal muscle microstructure over smaller distances than conventionally probed using PGSE. Our results show the ability to image skeletal muscle during active contraction (foot dorsiflexion and plantarflexion) using OGSE, and diffusion values are dependent on the oscillation frequency and on the contraction status of the muscle

1161



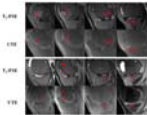
A new Trabecular BV/TV Estimation Method using Single-Sided NMR Devices through the Separation between Intra- and Inter-trabecular  $^1\text{H}$  Signals

Marco Barbieri<sup>1</sup>, Paola Fantazzini<sup>1</sup>, Anna Festa<sup>2</sup>, Fabio Baruffaldi<sup>2</sup>, Claudia Testa<sup>1</sup>, and Leonardo Brizi<sup>1</sup>

<sup>1</sup>Physics and Astronomy, University of Bologna, Bologna, Italy, <sup>2</sup>IRCCS Istituto Ortopedico Rizzoli, Bologna, Italy

Methods to improve the early detection of diseases associated with an increased bone fragility are objects of investigation. Single-sided NMR is an appealing approach for medical applications. In this work we propose a new methodology to assess the bone volume fraction (BV/TV) of trabecular bone (TB), without the need of using a reference sample, exploiting the separation between intra- and inter-trabecular  $^1\text{H}$  signals from quasi-continuous  $T_2$  distributions. BV/TV of TB samples estimated using NMR were found in strong agreement with micro-CT estimations. This is promising for the application of single-sided NMR scanners to in-vivo assessing of bone micro-structure.

1162



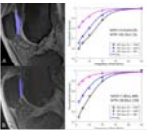
Osteochondral Junction (OCJ) Imaging Using a Fast T1-weighted 3D Ultrashort Echo Time Cones Sequence at 3T

Zhenyu Cai<sup>1,2</sup>, Zhao Wei<sup>2</sup>, Mingxin Chen<sup>2</sup>, Saeed Jerban<sup>2</sup>, Hyungseok Jang<sup>2</sup>, Eric Chang<sup>2,3</sup>, Jiang Du<sup>2</sup>, and Yajun Ma<sup>2</sup>

<sup>1</sup>Radiology, Fuwai Hospital Chinese Academy of Medical Sciences, Shenzhen, shenzhen, China, <sup>2</sup>Radiology, University of California San Diego, San Diego, CA, United States, <sup>3</sup>VA San Diego Healthcare System, San Diego, CA, United States

The osteochondral junction (OCJ) is the region where calcified cartilage meets subchondral bone (SCB), and is likely to be highly related to osteoarthritis (OA). However, it is difficult to image OCJ tissues due to their relatively short transverse relaxation times, which cause little or no signal to appear with conventional imaging sequences. In this study, we developed a 3D T1-weighted fast ultrashort echo time cones sequence with fat saturation (FS-UTE-Cones) to generate a high OCJ contrast image of the human knee on a clinical 3T MRI scanner.

1163



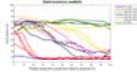
Quantitative 3D ultrashort echo time Cones magnetization transfer (3D UTE-Cones-MT) magnetic resonance imaging of knee cartilage degeneration

Yanping Xue<sup>1,2</sup>, Yajun Ma<sup>1</sup>, Zhao Wei<sup>1</sup>, Francis Tang<sup>1</sup>, Mei Wu<sup>1</sup>, Saeed Jerban<sup>1</sup>, Eric Y Chang<sup>1,3</sup>, and Jiang Du<sup>1</sup>

<sup>1</sup>University of California, San Diego, San Diego, CA, United States, <sup>2</sup>Radiology, Beijing Chao-Yang Hospital, Beijing, China, <sup>3</sup>VA San Diego Healthcare System, San Diego, CA, United States

Quantitative MRI biomarkers, such as  $T_2$ ,  $T_2^*$ , and  $T_1\rho$  have been used to detect cartilage degeneration. However, these biomarkers are sensitive to the magic angle effect. Magnetization transfer (MT) modeling provides magic angle insensitive parameters such as macromolecular proton fraction (MMF). This study focuses on the clinical evaluation of cartilage degeneration using 3D ultrashort echo time cones MT (3D UTE-Cones-MT) modeling in osteoarthritis (OA) patients. Both MMF and MT ratio (MTR) show significant negative correlations with WOMBS grading of knee cartilage. This study highlights the potential of 3D UTE-Cones-MT techniques for detection of early cartilage degeneration in OA.

1164



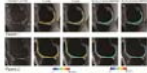
Muscular fat infiltration in FSHD starts with a “fat burst” near the distal tendon and advances towards the proximal tendon

Linda Heskamp<sup>1</sup>, Augustin C. Ogier<sup>2,3</sup>, David Bendahan<sup>3</sup>, and Arend Heerschap<sup>1</sup>

<sup>1</sup>Radiology and Nuclear Medicine, Radboud university medical center, Nijmegen, Netherlands, <sup>2</sup>Aix Marseille Univ, Université de Toulon, CNRS, LIS, Marseille, France, <sup>3</sup>Aix Marseille Univ, CNRS, CRMBM, Marseille, France

In patients with facioscapulohumeral muscular dystrophy (FSHD) it is known what the genetic origin of the disease is, but unknown how it is initiated and propagates along muscles. In a cross-sectional and longitudinal study we analyzed fat infiltration in lower leg muscles, tendon-to-tendon, with a 3D Dixon method. This revealed that fat infiltration starts with a distal “fat burst” in the first years of its initiation after which fat replacement further proceeds in a slower pace towards the proximal tendons. This indicates that the disease is triggered by an event typical for the distal parts of lower extremity muscles.

1165



Efficient Measurement of Composite Metric  $R_2-R_{1\rho}$  in Knee Cartilage

Misung Han<sup>1</sup>, Radhika Tibrewala<sup>1</sup>, Emma Bahroos<sup>1</sup>, Valentina Padoia<sup>1,2</sup>, and Sharmila Majumdar<sup>1,2</sup>

<sup>1</sup>Radiology and Biomedical Imaging, University of California, San Francisco, San Francisco, CA, United States, <sup>2</sup>Center for Digital Health Innovation, University of California, San Francisco, San Francisco, CA, United States

Cartilage degeneration, characterized by collagen structure disruption, proteoglycan depletion, and increased water content, has been shown to alter  $T_2$  and  $T_{1\rho}$  relaxation times. A composite metric,  $R_2-R_{1\rho}$ , which further reflects an anisotropic component of  $R_2$ , has recently demonstrated high sensitivity to cartilage degeneration; however, quantification of  $R_2$  and  $R_{1\rho}$  respectively requires long scan times. In this work, we validated the potential of assessing  $R_2-R_{1\rho}$  using one pair of signals with  $T_{1\rho}$  preparation and  $T_2$  preparation from a combined  $T_{1\rho}/T_2$  quantification sequence for in vivo knee MRI at 3T.

## Combined Educational & Scientific Session

### Spinal Cord, Head and Neck - Spinal Cord: Cool MR Tools & How to Use Them

Organizers: Cornelia Laule, John Port

Thursday Parallel 2 Live Q&A

Thursday 15:05 - 15:50 UTC

Moderators: Seth Smith & Cornelia Laule

A Soup of MR Sequences for the Spinal Cord

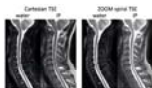
Virginie Callot<sup>1</sup>

<sup>1</sup>CRMBM-CEMEREM, CNRS / Aix-Marseille University, France

This presentation is intended to give a non-exhaustive overview of what can be done in the spinal cord using quantitative MRI. « Classical » sequences that can be robustly used will be described. For each of these sequence families, more advanced techniques will be briefly underlined. Sequences providing functional, metabolic and vascular information will also be discussed. We will finish with a brief overview of recent advances in SC MRI at 7T.

From this « soup » of sequences, attendees should be able to extract the best ingredients and recipes for their own investigation.

1166



A ZOOM spiral TSE technique for spinal imaging

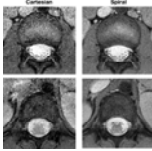
Zhiqiang Li<sup>1</sup>, Ryan K Robison<sup>2</sup>, Melvyn B Ooi<sup>1,3</sup>, and John P Karis<sup>1</sup>



<sup>1</sup>Neuroradiology, Barrow Neurological Institute, Phoenix, AZ, United States, <sup>2</sup>Radiology, Phoenix Children's Hospital, Phoenix, AZ, United States, <sup>3</sup>Philips Healthcare, Gainesville, FL, United States

Spine is a challenging area for MRI due to both anatomical features and motion. Spiral TSE has been proposed for spinal MRI. Aliasing in spiral spinal MRI is mitigated by combining oversampling with saturation band, with the latter not always achieving consistent and good signal suppression. In this work, the ZOOM technique has been incorporated into spiral TSE. Phantom and in vivo results demonstrate better signal suppression with ZOOM spiral TSE compared to spiral TSE acquired with a saturation band.

1167



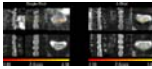
### Axial T2\*-Weighted Spiral MRI of the Spine at 1.5T

Ryan Robison<sup>1</sup>, Amber Pokorney<sup>1</sup>, Michael Kuwabara<sup>1</sup>, and Patricia Cornejo<sup>1</sup>

<sup>1</sup>Phoenix Children's Hospital, Phoenix, AZ, United States

This study evaluates spiral as an alternative to Cartesian in axial T2\*-weighted gradient echo imaging of the spine. SNR and CNR measurements were performed on spine data from a healthy volunteer. Expert reviewer ratings were also performed on data from 5 patients. Both the SNR/CNR measurements and reviewer ratings indicate that spiral can yield superior image quality without significant artifacts for a given scan time.

1168



### Spatial Specificity of BOLD Signal in the Spinal Cord at 7T Using a Noxious Thermal Stimulus

Alan C Seifert<sup>1,2,3</sup> and S Johanna Vannesjo<sup>4,5</sup>

<sup>1</sup>Biomedical Engineering and Imaging Institute, Icahn School of Medicine at Mount Sinai, New York, NY, United States, <sup>2</sup>Department of Radiology, Icahn School of Medicine at Mount Sinai, New York, NY, United States, <sup>3</sup>Graduate School of Biomedical Sciences, Icahn School of Medicine at Mount Sinai, New York, NY, United States, <sup>4</sup>Spinal Cord Injury Center, University Hospital Balgrist, University of Zurich, Zurich, Switzerland, <sup>5</sup>Wellcome Centre for Integrative Neuroimaging, FMRIB, University of Oxford, Oxford, United Kingdom

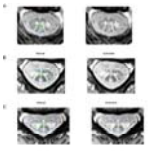
BOLD signal in gradient-echo images is a combination of macrovascular and microvascular contributions, where the macrovascular component, arising from larger veins draining the activated tissue, is less specific to the site of activation. In this work, we image activation produced in the cervical spinal cord by a noxious thermal stimulus at 7T. We consistently observed activation in the dorsal white matter medial to the dorsal horn, rather than in the gray matter itself. However, due to the relatively straightforward venous architecture of the spinal cord, this observed displaced activation does remain closely related to the true site of neuronal activation.

### Spicing Up Your Soup: Analysis Techniques for the Spinal Cord

Benjamin De Leener<sup>1</sup>

<sup>1</sup>École Polytechnique de Montréal, Canada

1169



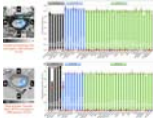
### Automatic Quantification Pipeline for Spinal Cord Grey and White Matter in Multiple Sclerosis

Charidimos Tsagkas<sup>1,2,3</sup>, Antal Horvath<sup>4</sup>, Alexandra Todea<sup>5</sup>, Jannis Mueller<sup>1,2</sup>, Anna Altermatt<sup>2,3</sup>, Marina Leimbacher<sup>6</sup>, Simon Pezold<sup>4</sup>, Matthias Weigel<sup>2,4,7</sup>, Tanja Haas<sup>7</sup>, Michael Amann<sup>1,3,4</sup>, Ludwig Kappos<sup>1,2</sup>, Till Sprenger<sup>1,8</sup>, Philippe Cattin<sup>4</sup>, Cristina Granziera<sup>1,2,4</sup>, and Katrin Parmar<sup>1,2</sup>

<sup>1</sup>Neurologic Clinic and Policlinic, Departments of Medicine, Biomedical Engineering and Clinical Research, University Hospital Basel, University of Basel, Basel, Switzerland, <sup>2</sup>Translational Imaging in Neurology (ThINK) Basel, Department of Medicine and Biomedical Engineering, University Hospital Basel, University of Basel, Basel, Switzerland, <sup>3</sup>Medical Image Analysis Center (MIAC AG), Basel, Switzerland, <sup>4</sup>Department of Biomedical Engineering, University of Basel, Allschwil, Switzerland, <sup>5</sup>Division of Diagnostic and Interventional Neuroradiology, Department of Radiology and Nuclear Medicine, University Hospital Basel, University of Basel, Basel, Switzerland, <sup>6</sup>Medical Faculty, University of Basel, Basel, Switzerland, <sup>7</sup>Division of Radiological Physics, Department of Radiology, University Hospital Basel, University of Basel, Basel, Switzerland, <sup>8</sup>Department of Neurology, DKD Helios Klinik Wiesbaden, Wiesbaden, Germany

Currently, there is no gold-standard for spinal cord (SC) grey and white matter (GM/WM) quantification in multiple sclerosis (MS). In this work, the cervical SC of 24 MS patients and 24 healthy controls (HC) was scanned on a 3T MRI-system using averaged magnetization inversion recovery acquisitions. Manual segmentations were provided to train a “Multi-Dimensional Gated Recurrent Unit” neural network for subsequent automatic SC GM/WM/lesion segmentation. Accuracy of automatic segmentations was high and decreased in the order WM→GM→lesions and HC→MS. MS patients had reduced SC GM and WM compared to HC. Finally, SC GM, WM and lesions correlated with physical disability.

1170



### Quantitative MRI of the spinal cord: reproducibility and normative values across 40 sites

Eva Alonso-Ortiz<sup>1</sup>, Charley Gros<sup>1</sup>, Alexandru Foias<sup>1</sup>, Mihael Abramovic<sup>2</sup>, Christoph Arneitz<sup>2</sup>, Nicole Atcheson<sup>3</sup>, Laura Barlow<sup>4</sup>, Robert Barry<sup>5,6,7</sup>, Markus Barth<sup>3</sup>, Marco Battiston<sup>8</sup>, Christian Buchel<sup>9</sup>, Matthew Budde<sup>10</sup>, Virginie Callot<sup>11,12</sup>, Benjamin De Leener<sup>13,14,15</sup>, Maxime Descoteaux<sup>16,17</sup>, Paulo Loureiro de Sousa<sup>18</sup>, Dostal Marek<sup>19</sup>, Julien Doyon<sup>15</sup>, Adam Dvorak<sup>20</sup>, Falk Eippert<sup>21</sup>, Karla Epperson<sup>22</sup>, Jürgen Finsterbusch<sup>9</sup>, Issei Fukunaga<sup>23</sup>, Claudia Wheeler-Kingshott<sup>8,24,25</sup>, Giancarlo Germani<sup>26</sup>, Guillaume Gilbert<sup>27</sup>, Francesco Grussu<sup>28,29</sup>, Akifumi Hagiwara<sup>23</sup>, Pierre-Gilles Henry<sup>30</sup>, Tomas Horak<sup>31</sup>, Masaaki Hori<sup>23</sup>, James Joers<sup>30</sup>, K Kamiya<sup>32</sup>, Haleh Karbasforoushan<sup>33</sup>, Ali Khatibi<sup>34,35</sup>, Joo-Won Kim<sup>36</sup>, Nawal Kinany<sup>37</sup>, Hagen Kitzler<sup>38</sup>, S Kolind<sup>39</sup>, Joe Yazhuo Kong<sup>40,41,42</sup>, Petr Kudlička<sup>31</sup>, Paul Kuntke<sup>43</sup>, Nyoman Kurniawan<sup>3</sup>, Slawomir Kusmia<sup>44</sup>, Rene Labounek<sup>45,46</sup>, Maria Marcella Laganà<sup>47</sup>, Corree Laule<sup>48</sup>, Christine Law<sup>49</sup>, Christophe Lenglet<sup>30</sup>, Tobias Leutritz<sup>21</sup>, Yaou Liu<sup>50,51</sup>, Sara Llufriu<sup>52</sup>, Sean Mackey<sup>53</sup>, Eloy Martinez<sup>52</sup>, Igor Nestrasil<sup>30,45</sup>, Nico Papinutto<sup>54</sup>, Daniel Papp<sup>55</sup>, Deborah Pareto<sup>56</sup>, Todd Parrish<sup>57</sup>, Anna Pichiecchio<sup>26,58</sup>, Alex Rovira Cañellas<sup>56</sup>, Marc Ruitenber<sup>59</sup>, Rebecca Samson<sup>28</sup>, Giorgio Savini<sup>26</sup>, Maryam Seif<sup>60</sup>, Alan Seifert<sup>36</sup>, Alex Smith<sup>55</sup>, Z A Smith<sup>57</sup>, Elisabeth Solana<sup>62</sup>, Y Suzuki<sup>61</sup>, G Tackley<sup>44</sup>, Alexandra Tinnermann<sup>9</sup>, Jan Valosek<sup>46</sup>, Marios Yiannakas<sup>28</sup>, Kenneth Weber<sup>62</sup>, Nikolaus Weiskopf<sup>21</sup>, Richard Wise<sup>44</sup>, P O Wyss<sup>2</sup>, Junqian Xu<sup>36</sup>, and Julien Cohen-Adad<sup>1,63</sup>

<sup>1</sup>NeuroPoly Lab, Institute of Biomedical Engineering, Polytechnique Montreal, Montreal, QC, Canada, <sup>2</sup>Department of Radiology, Swiss Paraplegic Centre, Nottwil, Switzerland, <sup>3</sup>Centre for Advanced Imaging, The University of Queensland, Brisbane, Australia, <sup>4</sup>Department of Radiology, University of British Columbia, Vancouver, BC, Canada, <sup>5</sup>Athinoula A. Martinos Center for Biomedical Imaging, Department of Radiology, Massachusetts General Hospital, Charlestown, MD, United States, <sup>6</sup>Department of Radiology, Harvard Medical School, Boston, MA, United States, <sup>7</sup>Harvard–Massachusetts Institute of Technology Health Sciences & Technology, Cambridge, MA, United States, <sup>8</sup>Queen Square MS Centre, Queen Square Institute of Neurology, Faculty of Brain Sciences, University College London, London, United Kingdom, <sup>9</sup>Institute of Systems Neuroscience, University Medical Center Hamburg-Eppendorf, Hamburg, Germany, <sup>10</sup>Department of Neurosurgery, Medical College of Wisconsin, Milwaukee, WI, United States, <sup>11</sup>CNRS, CRMBM, Aix-Marseille University, Marseille, France, <sup>12</sup>APHM, Hopital Universitaire Timone, CEMEREM, Marseille, France, <sup>13</sup>Department of Computer and Software Engineering, Polytechnique Montreal, Montreal, QC, Canada, <sup>14</sup>CHU Sainte-Justine Research Centre, Montreal, QC, Canada, <sup>15</sup>Montreal Neurological Institute, McGill University, Montreal, QC, Canada, <sup>16</sup>CIMS, Centre de Recherche CHUS, Sherbrooke, QC, Canada, <sup>17</sup>Sherbrooke Connectivity Imaging Lab (SCIL), Computer Science Department, Université de Sherbrooke, Sherbrooke, QC, Canada, <sup>18</sup>CNRS, ICube, FMTS, Université de Strasbourg, Strasbourg, France, <sup>19</sup>University Hospital Brno, Brno, Czech Republic, <sup>20</sup>Department of Physics and Astronomy, University of British Columbia, Vancouver, BC, Canada, <sup>21</sup>Max Planck Institute for Human Cognitive and Brain Sciences, Leipzig, Germany, <sup>22</sup>Richard M. Lucas Center, Stanford University School of Medicine, Stanford, CA, United States, <sup>23</sup>Department of Radiology, Juntendo University School of Medicine, Tokyo, Japan, <sup>24</sup>Department of Brain and Behavioural Sciences, University of Pavia, Pavia, Italy, <sup>25</sup>Brain MRI 3T Research Centre, IRCCS Mondino Foundation, Pavia, Italy, <sup>26</sup>Neuroradiology Unit, IRCCS Mondino Foundation, Pavia, Italy, <sup>27</sup>MR Clinical Science, Philips Healthcare, Markham, ON, Canada, <sup>28</sup>Queen Square MS Centre, Queen Square Institute of Neurology, Faculty of Brain Sciences, Faculty of Brain Sciences, University College London, London, United Kingdom, <sup>29</sup>Centre for Medical Image Computing, Department of Computer Science, University College London, London, United Kingdom, <sup>30</sup>Center for Magnetic Resonance Research, Department of Radiology, University of Minnesota, Minneapolis, MN, United States, <sup>31</sup>CEITEC - Central European Institute of Technology, Brno, Czech Republic, <sup>32</sup>University of Tokyo, Tokyo, Japan, <sup>33</sup>Interdepartmental Neuroscience Program, Northwestern University School of Medicine, Chicago, IL, United States, <sup>34</sup>Department of Neurology and Neurosurgery, McGill University, Montreal, QC, Canada, <sup>35</sup>Centre of Precision Rehabilitation for Spinal Pain (CPR Spine), School of Sport, Exercise and Rehabilitation Sciences, College of Life and Environmental Sciences, University of Birmingham, Birmingham, United Kingdom, <sup>36</sup>Translational and Molecular Imaging Institute, Department of Radiology, Icahn School of Medicine at Mount Sinai, New York, NY, United States, <sup>37</sup>Center for Neuroprosthetics, Institute of Bioengineering, Ecole Polytechnique Fédérale de Lausanne, Lausanne, Switzerland, <sup>38</sup>Department of Neuroradiology, Technische Universität Dresden, Dresden, Germany, <sup>39</sup>Departments of Medicine (Neurology), Physics & Astronomy, Radiology, University of British Columbia, Vancouver, BC, Canada, <sup>40</sup>CAS Key Laboratory of Behavioral Science, Institute of Psychology, Chinese Academy of Sciences, Beijing, China, <sup>41</sup>Department of Psychology, University of Chinese Academy of Sciences, Beijing, China, <sup>42</sup>Wellcome Centre for Integrative Neuroimaging, University of Oxford, Oxford, United Kingdom, <sup>43</sup>University Hospital Carl Gustav Carus, Dresden, Germany, <sup>44</sup>CUBRIC, Cardiff University, Wales, United Kingdom, <sup>45</sup>Division of Clinical Behavioral Neuroscience, Department of Pediatrics, University of Minnesota, Minneapolis, MN, United States, <sup>46</sup>Departments of Neurology and Biomedical Engineering, University Hospital Olomouc, Olomouc, Czech Republic, <sup>47</sup>IRCCS Fondazione Don Carlo Gnocchi, Milan, Italy, <sup>48</sup>Departments of Pathology & Laboratory Medicine, Physics & Astronomy, Radiology; International Collaboration on Repair Discoveries (ICORD), University of British Columbia, Vancouver, BC, Canada, <sup>49</sup>Department of Anesthesiology, Perioperative and Pain Medicine, Stanford University School of Medicine, Palo Alto, CA, United States, <sup>50</sup>Department of Radiology, Beijing Tiantan Hospital, Capital Medical University, Beijing, China, <sup>51</sup>Tiantan Image Research Center, China National Clinical Research Center for Neurological Diseases, Beijing, China, <sup>52</sup>Center of Neuroimmunology, Laboratory of Advanced Imaging in Neuroimmunological Diseases, Hospital Clinic Barcelona, Institut d'Investigacions Biomediques August Pi i Sunyer (IDIBAPS) and Universitat de Barcelona, Barcelona, Spain, <sup>53</sup>Stanford University School of Medicine, Stanford, CA, United States, <sup>54</sup>Department of Neurology, University of California San Francisco, San Francisco, CA, United States, <sup>55</sup>Wellcome Centre For Integrative Neuroimaging, FMRIB, NDCN, University of Oxford, Oxford, United Kingdom, <sup>56</sup>Neuroradiology Section, Vall Hebron University Hospital, Barcelona, Spain, <sup>57</sup>Feinberg School of Medicine, Northwestern University

School of Medicine, Chicago, IL, United States, <sup>58</sup>Department of Brain and Behavioural Neuroscience, University of Pavia, Pavia, Italy, <sup>59</sup>School of Biomedical Sciences, Faculty of Medicine, The University of Queensland, Brisbane, Australia, <sup>60</sup>Spinal Cord Injury Center Balgrist, University of Zurich, Zurich, Switzerland, <sup>61</sup>Department of Radiology, University of Tokyo, Tokyo, Japan, <sup>62</sup>Systems Neuroscience and Pain Laboratory, Stanford University, Stanford, CA, United States, <sup>63</sup>Functional Neuroimaging Unit, CRIUGM, University of Montreal, Montreal, QC, Canada

Normative quantitative MRI values are useful for establishing diagnosis in individuals with a suspected disease. Building on the recent creation of an open-access multi-center database (n=248 subjects) of spinal cord MRI, we processed those data to extract quantitative metrics that are commonly used (cross-sectional area, diffusion and magnetization transfer metrics). Inter-vendor (Siemens, Philips, GE), inter- and intra-site coefficients of variation (COV) were calculated. Overall results suggest that the spinal cord generic acquisition protocol is reproducible across sites and vendors (COVs within 2-8%). The data and processing pipeline are publicly available at <https://spine-generic.readthedocs.io/>.

## Oral - Power Pitch

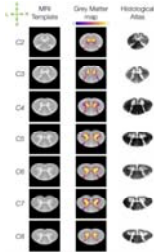
### Spinal Cord, Head and Neck - Spinal Cord: Anatomy, Acquisition & Assessment of Abnormalities

Thursday Parallel 2 Live Q&A

Thursday 15:05 - 15:50 UTC

Moderators: Kristin O'Grady

1171



#### Ex vivo MRI template of the human cervical cord at 80µm isotropic resolution

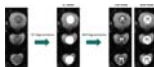
Charley Gros<sup>1</sup>, Abdullah Asiri<sup>2,3</sup>, Benjamin De Leener<sup>4</sup>, Charles Watson<sup>5</sup>, Gary Cowin<sup>6</sup>, Marc Ruitenberg<sup>7</sup>, Nyoman Kurniawan<sup>2</sup>, and Julien Cohen-Adad<sup>1,8</sup>

<sup>1</sup>NeuroPoly Lab, Institute of Biomedical Engineering, Polytechnique Montreal, Montreal, QC, Canada,

<sup>2</sup>Centre for Advanced Imaging, The University of Queensland, Brisbane, Australia, <sup>3</sup>Radiology department, College of applied medical sciences, Najran University, Najran, Saudi Arabia, <sup>4</sup>Department of Computer and Software Engineering, Polytechnique Montreal, Montreal, QC, Canada, <sup>5</sup>Faculty of Health Sciences, Curtin University of Technology, Perth, Australia, <sup>6</sup>National Imaging Facility, Centre for Advanced Imaging, The University of Queensland, Brisbane, Australia, <sup>7</sup>School of Biomedical Sciences, The University of Queensland, Brisbane, Australia, <sup>8</sup>Functional Neuroimaging Unit, CRIUGM, Université de Montréal, Montreal, QC, Canada

Spinal cord MRI templates allow reproducible and large scale atlas-based studies. However, current templates may have suboptimal resolutions (~0.5mm isotropic) to analyse high resolution data acquired at ultra-high field (e.g. 7T scanners). We generated a 3D human cervical cord template at 80µm isotropic resolution, from 13 ex vivo specimens, with a reference based on spinal levels. Further, the template was registered to the existing in vivo PAM50 template. Results showed consistency with histological studies in terms of grey matter morphology, and template generation achieved high accuracy (mean distance error: 0.10±0.01mm). The template and related scripts will be made publicly available.

1172



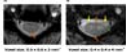
#### Spinal Cord Segmentation and T2\*-relaxation times of GM and WM within the Spinal Cord at 9.4T

Ole Geldschläger<sup>1</sup>, Dario Bosch<sup>1</sup>, Nikolai Avdievitch<sup>1</sup>, Klaus Scheffler<sup>1,2</sup>, and Anke Henning<sup>1,3</sup>

<sup>1</sup>High-field Magnetic Resonance, Max-Planck-Institut für biolog. Cybernetics, Tübingen, Germany, <sup>2</sup>Institute for Biomedical Magnetic Resonance, University Hospital Tübingen, Tübingen, Germany, <sup>3</sup>Advanced Imaging Research Center, University of Texas Southwestern Medical Center, Dallas, TX, United States

This study presents the first investigations with algorithmic spinal cord-segmentation, as well as gray matter/white matter-segmentation within the spinal cord, at the ultrahigh field strength of 9.4T. On multi-echo gradient-echo acquisitions from three subjects, the tested algorithms perform the segmentations correctly. Based on these multi-echo data, pixel-wise T2\*-relaxation time maps were calculated. By means of the segmentations, averaged T2\*-times of 24.88ms ± 6.68ms for gray matter and 19.37ms ± 8.66ms for white matter, were calculated.

1173



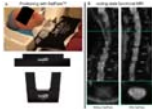
### A multi-element transceiver array for cervical spinal cord imaging at 7T

Ece Ercan<sup>1</sup>, Thomas Ruytenberg<sup>1</sup>, Kristin P. O'Grady<sup>2,3</sup>, Seth A. Smith<sup>2,3,4</sup>, Andrew Webb<sup>1</sup>, and Irena Zivkovic<sup>1</sup>

<sup>1</sup>C.J. Gorter Center for High Field MRI, Department of Radiology, Leiden University Medical Center, Leiden, Netherlands, <sup>2</sup>Vanderbilt University Institute of Imaging Science, Nashville, TN, United States, <sup>3</sup>Department of Radiology and Radiological Sciences, Vanderbilt University Medical Center, Nashville, TN, United States, <sup>4</sup>Department of Biomedical Engineering, Vanderbilt University, Nashville, TN, United States

Spinal cord imaging at 7T MRI is challenging and limited by the need for dedicated RF coils. In this study, we present a flexible coil design for cervical spinal cord imaging at 7T.  $B_1^+$  inhomogeneities were addressed by using multichannel array and phased-based RF shimming. Dorsal and ventral nerve roots, denticulate ligaments, and blood vessels were visible on axial  $T_2^*$ -weighted images. Cross-sectional area measurements from C3-C4 cervical levels were consistent with literature values.

1174



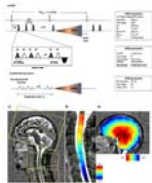
### Effect of non-protonated perfluorocarbon liquid-filled SatPads on spinal cord MR imaging

Benjamin De Leener<sup>1,2</sup>, Linda Soltrand Dahlberg<sup>2</sup>, Ali Khatibi<sup>2,3</sup>, Julien Cohen-Adad<sup>4,5</sup>, and Julien Doyon<sup>2</sup>

<sup>1</sup>Department of computer engineering and software engineering, Polytechnique Montreal, Montreal, QC, Canada, <sup>2</sup>Montreal Neurological Institute, McGill University, Montreal, QC, Canada, <sup>3</sup>Center of Precision Rehabilitation for Spinal Pain (CPR Spine), University of Birmingham, Birmingham, United Kingdom, <sup>4</sup>NeuroPoly Lab, Institute of Biomedical Engineering, Polytechnique Montreal, Montreal, QC, Canada, <sup>5</sup>Functional Neuroimaging Unit, CRIUGM, Université de Montréal, Montreal, QC, Canada

Acquiring high-quality functional MRI data of the spinal cord is challenging due to large susceptibility artifacts and high physiological noise, causing signal dropout and distortions, particularly in the cervical region. This study demonstrated the beneficial effect of using non-protonated perfluorocarbon liquid-filled SatPads™ during fMRI acquisition. Indeed, results show an increase of 31.51% for the global signal and 36.59% for the temporal signal-to-noise ratio for resting-state fMRI data acquired in the cervical spinal cord.

1175



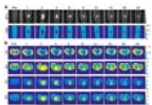
### Towards minimal T1 and B1 contributions in cervical spinal cord inhomogeneous magnetization transfer imaging

Arash Forodighasemabadi<sup>1,2,3,4</sup>, Thomas Troalen<sup>5</sup>, Lucas Soustelle<sup>1,2</sup>, Guillaume Duhamel<sup>1,2</sup>, Olivier Girard<sup>1,2</sup>, and Virginie Callot<sup>1,2,4</sup>

<sup>1</sup>Aix-Marseille Univ, CNRS, CRMBM, Marseille, France, <sup>2</sup>APHM, Hopital Universitaire Timone, CEMEREM, Marseille, France, <sup>3</sup>Aix-Marseille Univ, IFSTTAR, LBA, Marseille, France, <sup>4</sup>Lab-Spine International Research Laboratory, Marseille-Montréal, France, <sup>5</sup>Siemens Healthcare SAS, Saint-Denis, France

Inhomogeneous Magnetization Transfer (ihMT) is a promising MRI technique, sensitive to myelinated tissue that can be used to study demyelinating pathologies such as MS. But the conventional MT and ihMT ratio metrics could be sensitive to T1 and B1 variations, especially in the context of spinal cord imaging. In order to minimize these effects, this study focuses on 3D ihMT-RAGE sequence with high FA reference acquisition and ihMTR inverse metric computation. The quantifications within GM and WM along the cervical spinal cord demonstrate that this technique is promising for investigating SC pathologies.

1176



### Regional and longitudinal changes of multiple MRI parameters correlate with behavioral impairment and recovery after spinal cord injury

Feng Wang<sup>1,2</sup>, Tung-Lin Wu<sup>1</sup>, Pai-Feng Yang<sup>1,2</sup>, Nellie E. Byun<sup>1</sup>, Li Min Chen<sup>1,2</sup>, and John C. Gore<sup>1,2,3</sup>

<sup>1</sup>Vanderbilt University Institute of Imaging Science, Vanderbilt University Medical Center, Nashville, TN, United States, <sup>2</sup>Radiology and Radiological Sciences, Vanderbilt University Medical Center, Nashville, TN, United States, <sup>3</sup>Biomedical Engineering, Vanderbilt University, Nashville, TN, United States

Quantitative magnetization transfer (qMT) and diffusion tensor imaging (DTI) may detect and track compositional and structural changes in spinal cords before and after injury and during repair. This study aims to systematically evaluate the abilities of the qMT-derived pool size ratio (PSR) and DTI-derived diffusion parameters to assess injury-associated regional changes in spinal cords of monkeys, and to correlate them to specific sensorimotor behaviors. An overall goal is to evaluate the relationships between longitudinal changes in different regional MRI measures and sensorimotor behavioral impairment and recovery following spinal cord injury over a long period of time (months).

1177



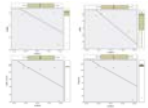
### Preoperative evaluation of multimodal spinal MRI in patients with acute traumatic spinal cord injury

Yuan Liu<sup>1</sup>, Fengzhao Zhu<sup>2</sup>, Xiangchuang Kong<sup>1</sup>, Jiazheng Wang<sup>3</sup>, Xiaodong Guo<sup>2</sup>, and Yang Lian<sup>1</sup>

<sup>1</sup>Radiology, Union Hospital, Wuhan, China, <sup>2</sup>orthopedics, Union Hospital, Wuhan, China, <sup>3</sup>Philips Healthcare, Beijing, China

Baseline MRI was recommended in acute spinal cord injury for clinical decision making and outcome prediction. The study presented a new quantitative method for evaluating the spinal cord severity to grade the retained fiber tracks by zoom DTI in pre-operation. For patients with ASIA A, no ASIA grade got promoted in FTClass A1 with completely fibers interruption and 3 out of 6 patients converted to C within 6-month follow-up in FTclass A2 with partially retention. The retained spinal cord fibers were critical for postoperative functional recovery. Multimodal MRI, especially accurate DTI provide potential quantitative predictive indicators for prognosis.

1178



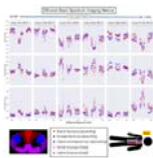
### Sodium concentration alterations in spinal cord injury and associations to motor and sensory function

Bhavana Shantilal Solanky<sup>1</sup>, Ferran Prados<sup>1</sup>, Carmen Tur<sup>1</sup>, Selma Al-Ahmad<sup>2</sup>, Xixi Yang<sup>1</sup>, Baris Kanber<sup>3</sup>, David Choi<sup>2</sup>, Jalesh N Panicker<sup>4</sup>, and Claudia A M Gandini Wheeler-Kingshott<sup>1</sup>

<sup>1</sup>NMR Research Unit, Queen Square MS Centre, Department of Neuroinflammation, NMR Research Unit, Queen Square MS Centre, Department of Neuroinflammation, UCL Queen Square Institute of Neurology, Faculty of Brain Sciences, UCL, London, United Kingdom, <sup>2</sup>National Hospital For Neurology and Neurosurgery, Queen Square, London, United Kingdom, <sup>3</sup>Translational Imaging Group, Centre for Medical Image Computing, Department of Medical Physics and Biomedical Engineering, University College London, London, United Kingdom, <sup>4</sup>Department of Uro-neurology, National Hospital for Neurology and Neurosurgery, London, United Kingdom

Sodium retention as a consequence of spinal cord injury is thought to impair the regenerative ability of neurons but also reduce damage. Studies have shown that sodium-blockers can lead to improved outcomes in some SCI patients. Here alterations in spinal cord total sodium concentrations in spinal cord injury patients and healthy controls were investigated using sodium MRS. The association of sodium concentration to cross sectional area and ASIA score was also explored.

1179



### Inhomogeneous Magnetization Transfer and DBSI detect downstream white matter damage in post-mortem human cervical spinal cord injury

Sarah Rosemary Morris<sup>1,2,3</sup>, Andrew Yung<sup>1,3,4</sup>, Valentin Prevost<sup>1,3,4</sup>, Shana I George<sup>5</sup>, Piotr Kozlowski<sup>1,2,3,4</sup>, Andrew Bauman<sup>1,3,4</sup>, Farah Samadi<sup>1,6</sup>, Caron Fournier<sup>1,6</sup>, Lisa Parker<sup>7</sup>, Kevin Dong<sup>1</sup>, Femke Streijger<sup>1</sup>, G.R. Wayne Moore<sup>1,6,7,8</sup>, Brian Kwon<sup>1,9,10</sup>, and Cornelia Laule<sup>1,2,3,6</sup>

<sup>1</sup>International Collaboration on Repair Discoveries, Vancouver, BC, Canada, <sup>2</sup>Physics & Astronomy, University of British Columbia, Vancouver, BC, Canada, <sup>3</sup>Radiology, University of British Columbia, Vancouver, BC, Canada, <sup>4</sup>UBC MRI Research Centre, Vancouver, BC, Canada, <sup>5</sup>Carson Graham Secondary School, Vancouver, BC, Canada, <sup>6</sup>Pathology & Laboratory Medicine, University of British Columbia, Vancouver, BC, Canada, <sup>7</sup>Vancouver General Hospital, Vancouver, BC, Canada, <sup>8</sup>Medicine, University of British Columbia, Vancouver, BC, Canada, <sup>9</sup>Vancouver Spine Surgery Institute, Vancouver, BC, Canada, <sup>10</sup>Orthopaedics, University of British Columbia, Vancouver, BC, Canada

Spinal cord injuries are heterogeneous, with complex microstructure which changes over time. We used 7T Diffusion Tensor Imaging (DTI), Diffusion Basis Spectrum Imaging (DBSI) and inhomogeneous Magnetization Transfer (ihMT) to investigate microstructural damage in post-mortem human spinal cord injury tissue. We measured sharp decreases in DTI fractional anisotropy and DBSI fiber fraction at the injury epicentre of the three cords with the most severe injuries. We found evidence for downstream demyelination (ihMT) and axonal loss (DTI FA, DBSI fiber fraction) in the two cords with the longest injury-death interval suggesting a time-frame for the detection of Wallerian degeneration by MRI.

1180



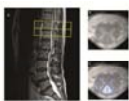
Is recovery from whiplash influenced by macromolecular changes in spinal cord white matter?

Mark Andrew Hoggarth<sup>1,2</sup>, James Elliott<sup>2,3</sup>, Mary Kwasny<sup>4</sup>, Marie Wasielewski<sup>2</sup>, Kenneth Weber<sup>5</sup>, and Todd Parrish<sup>1,6</sup>

<sup>1</sup>Biomedical Engineering, Northwestern University, Chicago, IL, United States, <sup>2</sup>Physical Therapy and Human Movement Sciences, Northwestern University, Chicago, IL, United States, <sup>3</sup>Northern Sydney Local Health District & Faculty of Health Sciences, The University of Sydney, Sydney, Australia, <sup>4</sup>Preventive Medicine, Northwestern University, Chicago, IL, United States, <sup>5</sup>Anesthesiology, Perioperative and Pain Medicine, Stanford University School of Medicine, Palo Alto, CA, United States, <sup>6</sup>Radiology, Northwestern University, Chicago, IL, United States

Whiplash injuries are the most common outcome from non-fatal motor vehicle collisions, affecting nearly four million people in the United States each year. The purpose of this cross-sectional study was to investigate the macromolecular environment of cervical spinal cord white matter in participants with persistent whiplash. This investigation of 76 individuals demonstrated changes in cervical white matter integrity following whiplash injuries using magnetization transfer imaging. Significant differences in the magnetization transfer ratio homogeneity of large cervical white matter tracts were observed in females with poor clinical outcome, indicating a spinal cord insult may contribute to chronic pain after whiplash injury.

1181



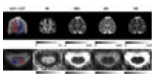
Structural MRI investigation caudal to degenerative cervical myelopathy: a clinical MRI application

Kevin Vallotton<sup>1</sup>, Maryam Seif<sup>1</sup>, Markus Hupp<sup>1</sup>, Armin Curt<sup>1</sup>, and Patrick Freund<sup>1,2,3</sup>

<sup>1</sup>Spinal Cord Injury Center, University Hospital Balgrist, University of Zurich, Zurich, Switzerland, <sup>2</sup>Department of Neurophysics, Max Planck Institute for Human Cognitive and Brain Sciences, Leipzig, Germany, <sup>3</sup>Wellcome Trust Centre for Neuroimaging, UCL Institute of Neurology, London, United Kingdom

Degenerative cervical myelopathy (DCM) is the most common form of non-traumatic spinal cord injury (SCI) and induces neurodegeneration in the cervical cord at and above the primary stenosis level. However, whether similar neurodegeneration occurs at the lumbar level remains unclear. We therefore applied high resolution T2\*-weighted MRI in the lumbar cord in both DCM patients and healthy controls to investigate potential injury-induced structural changes. Significant atrophy was found in mild DCM patients and its magnitude was associated with sensory impairment.

1182



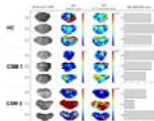
Spinal cord and brain DTI alterations in cervical spondylotic myelopathy (CSM)

Rebecca Sara Samson<sup>1</sup>, Jonathan Stutters<sup>1</sup>, Muhammad Ali Akbar<sup>2</sup>, Armin Curt<sup>3</sup>, Julien Cohen-Adad<sup>4,5</sup>, Michael Fehlings<sup>2,6</sup>, Patrick Freund<sup>3,7,8</sup>, Blair Innerarity<sup>1</sup>, Maryam Seif<sup>3</sup>, Carmen Tur<sup>1</sup>, and Claudia A. M. Gandini Wheeler-Kingshott<sup>1,9,10</sup>

<sup>1</sup>NMR Research Unit, Queen Square MS Centre, Department of Neuroinflammation, University College London, London, United Kingdom, <sup>2</sup>Institute of Medical Science, University of Toronto, Toronto, ON, Canada, <sup>3</sup>Spinal Cord Injury Center Balgrist, University of Zurich, Zurich, Switzerland, <sup>4</sup>NeuroPoly Lab, Institute of Biomedical Engineering, Polytechnique Montreal, Montreal, QC, Canada, <sup>5</sup>Functional Neuroimaging Unit, CRIUGM, Université de Montréal, Montreal, QC, Canada, <sup>6</sup>Kremsil Research Institute, University Health Network, Toronto, ON, Canada, <sup>7</sup>Department of Neurophysics, Wellcome Trust Centre for Neuroimaging, University College London, London, United Kingdom, <sup>8</sup>Max Planck Institute for Human Cognitive and Brain Sciences, Leipzig, Germany, <sup>9</sup>Department of Brain and Behavioural Sciences, University of Pavia, Pavia, Italy, <sup>10</sup>Brain MRI 3T Center, IRCCS Mondino Foundation, Pavia, Italy

We explored diffusion tensor imaging (DTI) metrics along the corticospinal tract (CST) from the cervical cord to the motor cortex, measured using separate brain and cervical cord DTI protocols in healthy subjects and cervical spondylotic myelopathy (CSM) patients at two sites. Instead of looking at either brain or cord separately, here, we combine brain and cord measurements and examine how the CST is affected in CSM, in addition to exploring correlations with clinical measures. Statistically significant changes were observed between CSM and HC when comparing cord and brain CST data, demonstrating the sensitivity of CST metrics to cord pathology.

1183



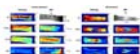
Dynamic Susceptibility Contrast imaging at 7T for spinal cord perfusion mapping in Cervical Spondylotic Myelopathy patients

Simon Lévy<sup>1,2,3,4</sup>, Pierre-Hugues Roche<sup>4,5</sup>, and Virginie Callot<sup>1,2,4</sup>

<sup>1</sup>Aix-Marseille Univ, CNRS, CRMBM, Marseille, France, <sup>2</sup>APHM, Hopital Universitaire Timone, CEMEREM, Marseille, France, <sup>3</sup>Aix-Marseille Univ, IFSTTAR, LBA, Marseille, France, <sup>4</sup>iLab-Spine International Research Laboratory, Marseille-Montreal, QC, France, <sup>5</sup>Neurosurgery Department, APHM, Hopital Nord, Marseille, France

The performance of Dynamic Susceptibility Contrast imaging at 7T for spinal cord perfusion mapping within clinical constraints was investigated. A cardiac-gated spin-echo EPI sequence with 0.7x0.7mm<sup>2</sup> in-plane resolution was used in one healthy volunteer and two Cervical Spondylotic Myelopathy patients. Relative blood volume and flow maps successfully revealed the higher perfusion of gray matter versus white matter for the volunteer and one patient. Results were limited for the patient with greater functional impairment and disadvantageous acquisition conditions. Although human spinal cord perfusion has never been mapped as precisely, several issues remain to address (image distortions, Specific-Absorption-Rate limitations, Arterial Input Function).

1184



New potential MRI markers of glial scarring and tissue damage in multiple sclerosis spinal cord pathology using diffusion MRI

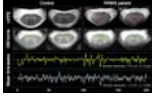
Marco Palombo<sup>1</sup>, Francesco Grussu<sup>1,2</sup>, Torben Schneider<sup>1,2,3</sup>, Gabriele C. DeLuca<sup>4</sup>, Daniel C. Alexander<sup>1</sup>, Claudia A. M. Gandini Wheeler-Kingshott<sup>2,5,6</sup>, and Hui Zhang<sup>1</sup>

<sup>1</sup>Centre for Medical Image Computing, Department of Computer Science, University College London, London, United Kingdom, <sup>2</sup>NMR Research Unit, Queen Square MS Centre, Queen Square Institute of Neurology, Faculty of Brain Sciences, University College London, London, United Kingdom, <sup>3</sup>Philips UK, Guildford, Surrey, United Kingdom, <sup>4</sup>Nuffield Department of Clinical Neurosciences, University of Oxford, Oxford, United Kingdom, <sup>5</sup>Department of Brain and Behavioural Sciences, University of Pavia, Pavia, Italy, <sup>6</sup>Brain MRI 3T Center, IRCCS Mondino Foundation, Pavia, Italy



Multiple sclerosis (MS) is characterized by demyelination, extra-cellular matrix disruption, inflammation and astrocytic scarring of WM lesions. This study investigates the use of a recently introduced MRI technique called SANDI (Soma And Neurite Density Imaging) to provide histologically meaningful estimates of cell body (namely soma) density in MS spinal cord pathology. Our results on ex-vivo human spinal cord specimens show significant positive correlation between SANDI metrics ( $f_{neurite}$  and  $f_{soma}$ ) and histological markers of myelination (plp) and astrocytes reactivity (gfap), respectively. The study suggests SANDI metrics as complementary imaging markers of demyelination ( $f_{neurite}$ ), astrocytic scarring ( $f_{soma}$ ) and extra-cellular matrix disruption ( $f_{extra}$ ).

1185



### Cervical cord resting-state fMRI shows preserved functional connectivity in low disability relapsing-remitting multiple sclerosis

Anna Combes<sup>1,2</sup>, Baxter P. Rogers<sup>1,2</sup>, Mereze Visagie<sup>2</sup>, Kristin P. O'Grady<sup>1,2</sup>, Richard D. Lawless<sup>2,3</sup>, Sanjana Satish<sup>2</sup>, Atlee Witt<sup>2</sup>, Shekinah Malone<sup>4</sup>, Colin D. McKnight<sup>2</sup>, Francesca R. Bagnato<sup>5</sup>, John C. Gore<sup>1,2,3</sup>, and Seth A. Smith<sup>1,2,3</sup>

<sup>1</sup>Radiology & Radiological Sciences, Vanderbilt University Medical Center, Nashville, TN, United States, <sup>2</sup>Vanderbilt University Institute of Imaging Science, Nashville, TN, United States, <sup>3</sup>Department of Biomedical Engineering, Vanderbilt University, Nashville, TN, United States, <sup>4</sup>School of Medicine, Meharry Medical College, Nashville, TN, United States, <sup>5</sup>Clinical Neurology, Vanderbilt University Medical Center, Nashville, TN, United States

Functional connectivity (FC) in the cervical spinal cord can be assessed with 3T resting-state fMRI. FC strength in the ventral and dorsal networks was measured in a group of relapsing-remitting multiple sclerosis (MS) patients with low disability, high cervical lesion load, and mildly impaired sensorimotor function and was found similar to matched healthy controls. There was no impact of the presence of cord lesions, suggesting FC is preserved even in the presence of structural damage. Future work will explore the longitudinal trajectories of cord FC in support of intact or impaired sensorimotor function in MS.

## Oral

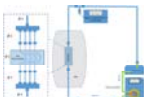
### Spinal Cord, Head and Neck - Head & Neck

Thursday Parallel 2 Live Q&A

Thursday 15:05 - 15:50 UTC

Moderators: Kirk Welker

1186



### 2D ungated PC-MRI for the exploration of small vessels in head and neck vascularisation

Agnès Paasche<sup>1</sup>, Jérémie Bettoni<sup>1</sup>, Stéphanie Dakpé<sup>1</sup>, and Olivier Balédent<sup>1</sup>

<sup>1</sup>CHU AMIENS-PICARDIE, AMIENS, France

2D ungated PC-MRI could be accurate enough to assess cervicofacial vascularization where vessels are often less than 4 mm in diameter but they are sensitive to the pulsatile flow and their accuracy and precision should be evaluate. We have designed a phantom model to determine the better MRI parameters for pulsatile flow in pipes of one millimeter of diameter. 108 sequences have been tested and 2 were selected as accurate and precise even in case of high pulsatility. The duration of the acquisition was 15 second. 2D ungated sequences should be suitable for daily clinical practice in small vessels evaluation.

1187



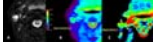
### Multi-parametric diffusion tensor imaging for early detection of dysthyroid optic neuropathy during thyroid-associated ophthalmopathy

Ping Liu<sup>1</sup>, Gui-hua Jiang<sup>1</sup>, and Jing Zhang<sup>2</sup>

<sup>1</sup>Radiology, Guangdong Second Provincial General Hospital, Guangzhou, China, <sup>2</sup>Radiology, The Affiliated Tongji Hospital, Tongji Medical College, Huazhong University of Science & Technology, Wuhan, China

Dysthyroid optic neuropathy (DON) is the most serious complication of Thyroid-Associated Ophthalmopathy (TAO). Untimely and ineffective treatment of could lead to permanent blindness. Early detection is the principle factor for timely intervention. Diffusion tensor imaging(DTI) is a noninvasive tool to reveal microstructural or non-overt damage and quantify pathological processes of nerve fiber bundle. We applied the multi-parametric of optic nerve to identify the DON from TAO. The result reveals that DTI can be considered a useful and noninvasive tool to differentiate DON from TAO with higher accuracy.

1188



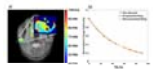
#### Evaluation of APT imaging in parotid glands and strategy in clinical usage

Yu Chen<sup>1</sup>, Tong Su<sup>1</sup>, Zhuhua Zhang<sup>1</sup>, Zhentan Xu<sup>1</sup>, Xiaoqi Wang<sup>2</sup>, Huadan Xue<sup>1</sup>, and Zhengyu Jin<sup>1</sup>

<sup>1</sup>Peking Union Medical College Hospital, Beijing, China, <sup>2</sup>Philips HealthCare, Beijing, China, Beijing, China

This study was to prospectively evaluate APT imaging for the parotid glands and lesions. 32 patients, confirmed cancer in parotid glands, underwent 3D TSE APTw imaging. Scores for integrity and for hyperintensity artifacts of both tumor lesions and normal parotid glands were evaluated. Tumor lesions had better integrity score than normal parotid glands. Scores for hyperintensity artifacts in APTw images showed no significant difference between tumor lesions and normal parotid glands. Most APTw images of parotid glands lesions were scored with good integrity and had acceptable image quality, while challenges still exist in some cases.

1189



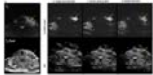
#### Bi-exponential T<sub>1p</sub> relaxation calculation of parotid glands in vivo at 3T

Huimin Zhang<sup>1</sup>, Qiyong Ai<sup>1</sup>, Queenie Chan<sup>2</sup>, Ann D. King<sup>1</sup>, and Weitian Chen<sup>1</sup>

<sup>1</sup>Department of Imaging and Interventional Radiology, The Chinese University of Hong Kong, Hong Kong, Hong Kong, <sup>2</sup>Philips Healthcare, Hong Kong, Hong Kong

T<sub>1p</sub> relaxation, known as the spin-lattice relaxation time in the rotating frame, is sensitive to molecular interactions including dipolar interactions, chemical exchange, and diffusion. T<sub>1p</sub> is often measured by mono-exponential relaxation models. Bi-exponential T<sub>1p</sub> relaxation have been previously observed in muscle, cartilage, menisci and brain. We report our observation of bi-exponential T<sub>1p</sub> relaxation in parotid glands.

1190



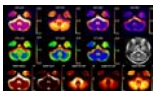
#### DW-EPI distortion reduction using Multi-shot EPI (MUSE) and Reverse Polarity Gradient (RPG) in Head & Neck Region

Maggie M Fung<sup>1</sup>, Amaresha Konar Shridhar<sup>2</sup>, Arnaud Guidon<sup>3</sup>, Amita Shukla-Dave<sup>2,4</sup>, and Vaios Hatzoglou<sup>4</sup>

<sup>1</sup>MR Apps & Workflow, GE Healthcare, New York City, NY, United States, <sup>2</sup>Department of Medical Physics, Memorial Sloan Kettering Cancer Center, New York City, NY, United States, <sup>3</sup>MR Apps & Workflow, GE Healthcare, Boston, MA, United States, <sup>4</sup>Department of Radiology, Memorial Sloan Kettering Cancer Center, New York City, NY, United States

The purpose of this study is to investigate the distortion correction performance and ADC value consistency of the single shot EPI (SSEPI), multi-shot EPI (MUSE) and reverse polarity gradient (RPG) method in phantom, and head & neck cancer patients. We observed improved distortion correction performance in MUSE, and best distortion correction in MUSE plus RPG method. Improved anatomical details, reduced artifacts and improved perceived clinical utility were also observed in MUSE (with and without RPG) as compare to SSEPI. ADC values remained consistent between these techniques.

1191



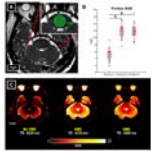
#### Detection of radiation brain injury in patients with nasopharyngeal carcinoma: A comparative study of DTI, DKI and MAP-MRI

Weike Zeng<sup>1</sup>, Mengzhu Wang<sup>2</sup>, Yaxuan Pi<sup>3</sup>, Yi Li<sup>3</sup>, Xu Yan<sup>4</sup>, Guang Yang<sup>5</sup>, and Jun Shen<sup>6</sup>

<sup>1</sup>Department of Radiology, SUN YAT-SEN Memorial Hospital, SUN YAT-SEN University, Guangzhou, China, <sup>2</sup>MR Scientific Marketing, Siemens Healthcare, Guangzhou, China, <sup>3</sup>department of NEUROLOGY, Sun Yat-sen Memorial Hospital, Sun Yat-sen University, Guangzhou, China, <sup>4</sup>MR Scientific Marketing, Siemens Healthineers, Shanghai, China, <sup>5</sup>Shanghai Key Laboratory of Magnetic Resonance, East China Normal University, Shanghai, China, <sup>6</sup>Sun Yat-sen Memorial Hospital, Sun Yat-sen University, Guangzhou, China

Mean apparent propagator (MAP)-MRI, which builds a powerful analytical framework based on the random motion distribution of real water molecules, can more accurately and comprehensively characterize microstructure features of brain tissues than conventional diffusion imaging. This study investigated the application of MAP-MRI in the early diagnosis of radiation-induced brain injury in patients with nasopharyngeal carcinoma, compared with diffusion tensor imaging (DTI) and diffusion kurtosis imaging (DKI).

1192



Trigeminal nerve tractography with accelerated simultaneous multislice readout-segmented echo planar diffusion tensor imaging

Yao Chia Shih<sup>1</sup>, Yeow Hoay Koh<sup>2</sup>, Soo Lee Lim<sup>1</sup>, Yen San Kiew<sup>1</sup>, Ee Wei Lim<sup>2</sup>, See Mui Ng<sup>1</sup>, Leon Qi Rong Ooi<sup>2</sup>, Wen Qi Tan<sup>1,3</sup>, Helmut Rumpel<sup>1</sup>, Eng King Tan<sup>2,3</sup>, and Ling Ling Chan<sup>1,3</sup>

<sup>1</sup>Department of Diagnostic Radiology, Singapore General Hospital, Singapore, Singapore, <sup>2</sup>Department of Neurology, National Neuroscience Institute – Outram Campus, Singapore, Singapore, <sup>3</sup>Duke-NUS Medical School, Singapore, Singapore

The impact of simultaneous multi-slice imaging (SMS) with short repetition time (TR) accelerated acquisition on diffusion tensor imaging (DTI) combined with readout-segmented echo planar imaging (RESOLVE) on the intra-cranial nerves is unexplored. Compared to non-SMS RESOLVE-DTI, two SMS RESOLVE-DTI protocols showed higher pontine signal-to-noise ratio (SNR). Consistent measures of different DTI metrics of cisternal trigeminal nerves across the three RESOLVE-DTI protocols and significant positive correlations of mean DTI metrics in pairwise comparison across these suggest that SMS RESOLVE-DTI allows fast and reliable evaluation of the microstructural integrity of the cisternal trigeminal nerve, with possible utility in trigeminal neuralgia.

1193



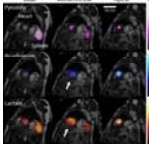
Predicting tumor aggressiveness in papillary thyroid cancers using multiparametric quantitative imaging metrics

Ramesh Paudyal<sup>1</sup>, Jung Hun Oh<sup>1</sup>, Vaios Hatzoglou<sup>2</sup>, Andre L. Moreira<sup>3</sup>, Ashok shaha<sup>4</sup>, R. Michael Tuttle<sup>5</sup>, and Amita Shukla-Dave<sup>1,2</sup>

<sup>1</sup>Medical Physics, Memorial Sloan Kettering Cancer Center, New York, NY, United States, <sup>2</sup>Radiology, Memorial Sloan Kettering Cancer Center, New York, NY, United States, <sup>3</sup>Pathology, NYU Langone Medical Center, New York, NY, United States, <sup>4</sup>Surgery, Memorial Sloan Kettering Cancer Center, New York, NY, United States, <sup>5</sup>Medicine, Memorial Sloan Kettering Cancer Center, New, NY, United States

Accurate risk stratification and predicting tumor aggressiveness is critically important for the management of papillary thyroid cancer. The results from the present study predict tumor aggressiveness in papillary thyroid cancer using noninvasive multi-parametric MRI (i.e. non-Gaussian intravoxel incoherent motion (NG-IVIM) diffusion weighted (DW) and dynamic contrast-enhanced (DCE)-MRI). The surrogate biomarkers of tumor vascularity ( $K^{\text{trans}}$ ) and tumor cellularity (D) were negatively correlated. The kurtosis coefficient (K) reflecting tissue microstructure showed a moderate and significant correlation with the contrast agent leakage space ( $v_e$ ). DWI and DCE-MRI derived metrics can predict tumor aggressiveness in PTC.

1194



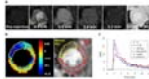
### Human 13C Hybrid-Shot Spiral (HYSS) Imaging of Pathological Cardiac Metabolism Following Myocardial Infarction

Justin YC Lau<sup>1,2</sup>, Andrew Apps<sup>1</sup>, Jack JJJ Miller<sup>1,2,3</sup>, Andrew Tyler<sup>2</sup>, Liam AJ Young<sup>1</sup>, Andrew JM Lewis<sup>1</sup>, Gareth Barnes<sup>4</sup>, Claire Trumper<sup>1</sup>, Stefan Neubauer<sup>1</sup>, Oliver J Rider<sup>1</sup>, and Damian J Tyler<sup>1,2</sup>

<sup>1</sup>Oxford Centre for Clinical Magnetic Resonance Research, Division of Cardiovascular Medicine, Radcliffe Department of Medicine, University of Oxford, Oxford, United Kingdom, <sup>2</sup>Department of Physiology, Anatomy & Genetics, University of Oxford, Oxford, United Kingdom, <sup>3</sup>Department of Physics, University of Oxford, Oxford, United Kingdom, <sup>4</sup>Royal Brompton & Harefield NHS Foundation Trust, Harefield, United Kingdom

This study reports the clinical translation of a hybrid-shot spiral sequence (HYSS) for imaging the diseased heart and spleen. Two subjects with myocardial infarction from coronary artery disease were imaged following administration of hyperpolarized [1-<sup>13</sup>C]pyruvate. High lactate and bicarbonate signal were seen in the region adjacent to the infarcted zone, with no signal within the infarct. A large splenic lactate signal was observed in a subject with an active systemic inflammatory response post myocardial infarction.

1195



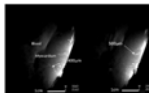
### Tracer kinetic modeling of nitroxide-enhanced MRI to quantify oxidative stress in mouse models of heart disease

Soham Shah<sup>1</sup>, Yu Wang<sup>1</sup>, Christopher Waters<sup>1</sup>, Lanlin Chen<sup>1</sup>, Brent French<sup>1</sup>, and Frederick Epstein<sup>1</sup>

<sup>1</sup>University of Virginia, Charlottesville, VA, United States

Oxidative stress plays a significant role in the pathogenesis of heart disease. Nitroxide free radicals have been used as redox-sensitive MRI contrast agents where oxidative stress is correlated to the nitroxide-enhanced signal decay rate. We developed a two-compartment exchange and reduction model (2CXRM) to quantify both myocardial nitroxide exchange and reduction and hypothesized that dynamic nitroxide-enhanced MRI can comprehensively assess nitroxide kinetics in mouse models of angiotensin II infusion (ANGII) and myocardial infarction (MI). The 2CXRM detected elevated reduction rates in ANGI and post-MI mice indicative of oxidative stress and reduced nitroxide delivery, consistent with microvascular damage, in post-MI mice.

1196

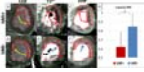


### Initial technical developments of local RF coil for sub-millimeter cardiovascular MRI.

Marylène Delcey<sup>1,2,3,4</sup>, Isabelle Saniour<sup>5</sup>, Pierre Bour<sup>1,2,4</sup>, Fanny Vaillant<sup>1,2,4</sup>, Emma Abell<sup>1,2,4</sup>, Wadie Benhassen<sup>3</sup>, Marie Poirier-Quinot<sup>5</sup>, and Bruno Quesson<sup>1,2,4</sup>

<sup>1</sup>IHU Liryc, Electrophysiology and Heart Modeling Institute, Fondation Bordeaux Université, Pessac, France, <sup>2</sup>Univ. Bordeaux, Centre de recherche Cardio-Thoracique de Bordeaux, U1045, Bordeaux, France, <sup>3</sup>Siemens Healthcare SAS, Saint-Denis, France, <sup>4</sup>INSERM, Centre de recherche Cardio-Thoracique de Bordeaux, U1045, Bordeaux, France, <sup>5</sup>IR4M, UMR8081, Université Paris-Sud/CNRS, Université Paris-Saclay, Orsay, France

In the context of cardiovascular diseases, precise determination of the extent and locations of the arrhythmogenic substrate could significantly improve diagnosis and treatment for both atrial and ventricular electrical diseases. However, the current spatial resolution and signal-to-noise ratio (SNR) in clinical scanners remain insufficient to provide relevant information of small structures like atrial wall or sub-millimeter fatty infiltration in ventricle. To address this limitation in SNR, two receiver coils were implemented at 1.5T for high resolution cardiac imaging, with different active decoupling techniques (safety aspects). Images at 200  $\mu$ m in-plane spatial resolution were successfully obtained on a beating heart.

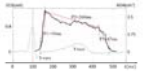


### Chronic Myocardial Infarcts with Iron Deposits Exhibit Lower Rest Perfusion and Elevated Nitric Oxide Synthase Activity

Eric Johnson<sup>1,2</sup>, Anand Nair<sup>2</sup>, Ivan Cokic<sup>1,2</sup>, Hsin-Yung Yang<sup>2</sup>, Andreas Kumar<sup>3</sup>, and Rohan Dharmakumar<sup>1,2</sup>

<sup>1</sup>UCLA, Los Angeles, CA, United States, <sup>2</sup>Cedars Sinai, Los Angeles, CA, United States, <sup>3</sup>Northern Ontario School of Medicine, Thunder Bay, ON, Canada

Hemorrhagic myocardial infarction (hMI) patients are predisposed to adverse outcomes in the chronic stage of MI, yet physiological underpinnings contributing to this observation are not well understood. We hypothesized that hMI areas containing iron deposits would negatively impact endothelial function and tested our hypothesis by evaluating perfusion defects in patients and dogs with a history of hMI; with histological staining for iron, endothelial cells and nitric oxide synthase (NOS) in excised myocardial sections of dogs with chronic MI. Hemorrhagic subjects had significantly reduced perfusion and markedly elevated NOS activity.

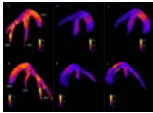


### Capture the Opening and Closing of Human Aortic Valve Using MRI with Sub-Millisecond Temporal Resolution

Zheng Zhong<sup>1,2</sup>, Kaibao Sun<sup>2</sup>, Guangyu Dan<sup>1,2</sup>, Muge Karaman<sup>1,2</sup>, and Xiaohong Joe Zhou<sup>1,2,3,4</sup>

<sup>1</sup>Bioengineering, University of Illinois at Chicago, Chicago, IL, United States, <sup>2</sup>CMRR, University of Illinois at Chicago, Chicago, IL, United States, <sup>3</sup>Radiology, University of Illinois at Chicago, Chicago, IL, United States, <sup>4</sup>Neurosurgery, University of Illinois at Chicago, Chicago, IL, United States

Stenosis and regurgitation are two common valvular diseases currently diagnosed using echocardiography. Cardiac MR has potential to diagnose these two diseases, however, faces the challenge of inadequate temporal resolution for capturing the rapid opening or closing of aortic valve. Using a variation of a recently proposed technique, coined Sub-millisecond Periodic Event Encoded Dynamic Imaging or SPEEDI (formerly called SMILE), we demonstrated that this process can be visualized using MRI with sub-millisecond temporal resolution. This new capability has improved the accuracy and reliability in studying the dynamics of aortic valve, opening new opportunities to detect stenosis and regurgitation using MRI.



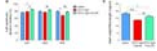
### Evaluation of potential hemodynamic biomarkers in experimental PAH using center-out stack-of-stars 4D phase contrast velocity mapping

Ali Nahardani<sup>1,2</sup>, Simon Leistikow<sup>2,3</sup>, Katja Grün<sup>4</sup>, Martin Krämer<sup>1</sup>, Karl Heinz Herrmann<sup>1</sup>, Andrea Schrepper<sup>5</sup>, Reinhard Bauer<sup>6</sup>, Christian Jung<sup>7</sup>, Alexander Berndt<sup>8</sup>, P. Christian Schulze<sup>4</sup>, Lars Linsen<sup>3</sup>, Jürgen R. Reichenbach<sup>1</sup>, Marcus Franz<sup>4</sup>, and Verena Hoerr<sup>1,2,9</sup>

<sup>1</sup>Institute of Diagnostic and Interventional Radiology, Medical Physics Group, University Hospital Jena, Jena, Germany, <sup>2</sup>Institute of Medical Microbiology, University Hospital Jena, Jena, Germany, <sup>3</sup>Institute of Computer Science, Department of Mathematics and Computer Science, Westfälische Wilhelms-Universität Münster, Muenster, Germany, <sup>4</sup>Department of Internal Medicine I, Division of Cardiology, Angiology, Pneumology, and Intensive Medical Care, University Hospital Jena, Jena, Germany, <sup>5</sup>Department of Cardiothoracic Surgery, University Hospital Jena, Jena, Germany, <sup>6</sup>Institute of Molecular Cell Biology, Center of Molecular Biomedicine, University Hospital Jena, Jena, Germany, <sup>7</sup>Department of Internal Medicine, Division of Cardiology, University Hospital Düsseldorf, Düsseldorf, Germany, <sup>8</sup>Institute of Legal Medicine, Section of Pathology, University Hospital Jena, Jena, Germany, <sup>9</sup>Department of Clinical Radiology, University Hospital Muenster, Muenster, Germany

Potential hemodynamic biomarkers of pulmonary arterial hypertension (PAH) and consecutive right ventricular remodeling were investigated by 4D flow center-out stack-of-stars velocity mapping in a rat model of monocrotaline induced PAH in comparison to healthy controls and a treatment group taking Macitentan. The averaged-mean values of blood flow velocities of pulmonary tract were substantially decreased in the diseased animal group compared to the control and under-treatment group. Diseased animals further showed a pronounced pressure gradient drop between the pulmonary artery bronchial branches and pulmonary veins. The effect of vascular resistance was additionally noted in the velocity-time curve of the pulmonary arteries.

1200



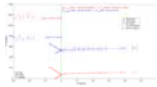
#### AICAR prevents heart failure in a rat model of doxorubicin-induced cardiotoxicity

Kerstin N Timm<sup>1</sup>, Vicky Ball<sup>1</sup>, Benjamin Thackray<sup>1</sup>, Michael P Murphy<sup>2</sup>, Lisa C Heather<sup>1</sup>, and Damian J Tyler<sup>1</sup>

<sup>1</sup>Department of Physiology, Anatomy and Genetics, University of Oxford, Oxford, United Kingdom, <sup>2</sup>MRC Mitochondrial Biology Unit, University of Cambridge, Cambridge, United Kingdom

Doxorubicin (DOX) is a commonly used chemotherapeutic agent for the treatment of many cancers. However, DOX has serious cardiotoxic side effects culminating in congestive heart failure. We have previously shown in a clinically-relevant rat model of DOX-induced heart failure (DOX-HF), that this is due to loss and dysfunction of mitochondria. We show here that 5-aminoimidazole-4-carboxamide ribonucleotide (AICAR), an activator of AMPK, can prevent heart failure in DOX-treated rats. This cardioprotective effect appears to be, at least in part, achieved through improved fatty acid oxidation in cardiac mitochondria which can be indirectly assessed with hyperpolarized [2-<sup>13</sup>C]pyruvate MRS.

1201



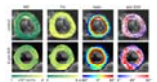
#### Estimating Blood Volume with Ferumoxytol at 0.55 T

Daniel A. Herzka<sup>1</sup>, Rajiv A. Ramasawmy<sup>1</sup>, Toby Rogers<sup>1</sup>, Kendall O'Brien<sup>1</sup>, Delaney McGuirt<sup>1</sup>, Adrienne Campbell-Washburn<sup>1</sup>, and Robert J. Lederman<sup>1</sup>

<sup>1</sup>National Heart Lung and Blood Institute, National Institutes of Health, Bethesda, MD, United States

Off-label use of ferumoxytol as an intravascular contrast agent for cardiovascular imaging is increasing. Measurements of circulating blood volume using dilution techniques has been previously demonstrated with ferumoxytol at 1.5 T. The relaxivity of ferumoxytol at low field (0.55 T) is increased, making it an attractive approach potentially requiring reduced dosages. Here we successfully demonstrate the feasibility of measurement of total circulating blood volume at lower field strength in swine.

1202



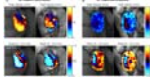
#### Microstructural cardiac remodelling in aortic stenosis and its reversibility following valve replacement – a CMR diffusion tensor imaging study

Alexander Gotschy<sup>1,2,3</sup>, Constantin von Deuster<sup>1</sup>, Lucas Weber<sup>4</sup>, Mareike Gast<sup>5</sup>, Martin O. Schmiady<sup>6</sup>, Robbert J. H. van Gorkum<sup>1</sup>, Jochen von Spiczak<sup>1,4</sup>, Robert Manka<sup>2,4</sup>, Sebastian Kozerke<sup>1</sup>, and Christian T. Stoeck<sup>1</sup>

<sup>1</sup>Institute for Biomedical Engineering, University and ETH Zurich, Zurich, Switzerland, <sup>2</sup>Department of Cardiology, University Hospital Zurich, Zurich, Switzerland, <sup>3</sup>Great Ormond Street Hospital, London, United Kingdom, <sup>4</sup>Institute of Diagnostic and Interventional Radiology, University Hospital Zurich, Zurich, Switzerland, <sup>5</sup>Division of Cardiology, Pulmonology and Vascular Medicine, University Hospital Duesseldorf, Duesseldorf, Germany, <sup>6</sup>Department of Cardiac Surgery, University Hospital Zurich, Zurich, Switzerland

CMR diffusion tensor imaging (CMR DTI) allows for the assessment of cardiac microstructure in diseased hearts. We investigated changes of myocardial diffusion properties and myocyte orientation in patients with aortic stenosis (AS) before and after valve replacement (AVR) using DTI and T1-mapping. Mean diffusivity (MD), fractional anisotropy (FA), E2A sheet angle and the transmural helix angle (HA)-slope were altered in AS patients, while native T1 was not significantly different. After AVR, the HA-slope was the only parameter with reversible changes, whereas MD, FA and E2A remained abnormal. This study indicates that AS-induced alterations of myocardial microstructure partly persist following AVR.

1203



**Cardiac Rhythm Impacts Left Atrial Hemodynamics Measured with 4D Flow and Real Time PC MRI in Controls and Patients with Atrial Fibrillation**

Amanda L DiCarlo<sup>1</sup>, Hassan Haji-Valizadeh<sup>2</sup>, Suvai Gunasekaran<sup>1</sup>, Patrick McCarthy<sup>3</sup>, Rod Passman<sup>4</sup>, Philip Greenland<sup>4</sup>, Daniel C Lee<sup>1</sup>, Daniel Kim<sup>1</sup>, and Michael Markl<sup>1,5</sup>

<sup>1</sup>Radiology, Northwestern University, Chicago, IL, United States, <sup>2</sup>Department of Medicine (Cardiovascular Division), Beth Israel Deaconess Medical Center & Harvard Medical School, Boston, MA, United States, <sup>3</sup>Cardiac Surgery, Northwestern University, Chicago, IL, United States, <sup>4</sup>Preventive Medicine, Northwestern University, Chicago, IL, United States, <sup>5</sup>Biomedical Engineering, Northwestern University, Chicago, IL, United States

Stroke prevention is a major therapeutic goal in atrial fibrillation (AF) management. Flow quantification using MRI can provide information about left atrium hemodynamics implicated in stroke risk. This study evaluates the impact of cardiac arrhythmia on velocity and stasis, reflective of slow flow, measurements using both 4D-flow and real time phase contrast techniques in a cohort of healthy controls and AF patients in sinus rhythm and arrhythmia. Both real time phase contrast and 4D-flow showed a similar increase in left atrium stasis between controls and patients and between patients with low and high heart rate variability, but real time phase contrast was more sensitive to differences.

**Oral - Power Pitch**

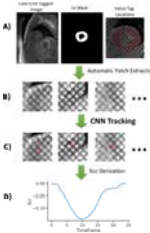
**Novel clinical applications of CMR - Cardiovascular Power Pitch: Applications**

Thursday Parallel 3 Live Q&A

Thursday 15:05 - 15:50 UTC

Moderators: Daniel Herzka

1204



**Measuring Cardiac Strain in Duchenne Muscular Dystrophy with a Convolutional Neural Net Tag Tracking Method**

Michael Loecher<sup>1,2</sup>, Luigi E Perotti<sup>3</sup>, Patrick Magrath<sup>4</sup>, and Daniel B Ennis<sup>1,2,5,6</sup>

<sup>1</sup>Radiology, Stanford, Palo Alto, CA, United States, <sup>2</sup>Radiology, Veterans Administration Health Care System, Palo Alto, CA, United States, <sup>3</sup>Mechanical Engineering, University of Central Florida, Orlando, FL, United States, <sup>4</sup>Radiology, University of California Los Angeles, Los Angeles, CA, United States, <sup>5</sup>Cardiovascular Institute, Stanford, Palo Alto, CA, United States, <sup>6</sup>Center for Artificial Intelligence in Medicine & Imaging, Stanford, Palo Alto, CA, United States

The objective of this work was to demonstrate the feasibility of using a convolutional neural net (CNN) based tag tracking algorithm for deriving strain measurements in grid tagged cardiac MR images. The method was tested in 23 subjects. When compared to commercial software the CNN-based method produces similar measurements for peak Ecc and shows lower strain in boys with DMD compared to healthy subjects [CNN =  $-0.15 \pm 0.03$  vs  $-0.21 \pm 0.03$ ] and [Conventional =  $-0.16 \pm 0.03$  vs  $-0.21 \pm 0.02$ ] ( $p < .001$ ). Peak Ecc was not significantly different within cohorts when compared between methods [DMD cohort:  $p=0.32$ , Healthy cohort:  $p=0.99$ ]

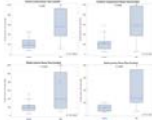


**Clinical Value of an Almost Automated Fast Free-breathing Cardiac Magnetic Resonance Workflow**

Keyan Wang<sup>1</sup>, Michaela Schmidt<sup>2</sup>, Jing An<sup>3</sup>, and Xiaoming Bi<sup>4</sup>

<sup>1</sup>1st affiliated hospital of Zhengzhou University, Zhengzhou, China, <sup>2</sup>Siemens Healthcare GmbH, Erlangen, Germany, <sup>3</sup>Siemens Shenzhen Magnetic Resonance Ltd, Shenzhen, China, <sup>4</sup>Siemens Healthineers, Los Angeles, CA, United States

The application of cardiac magnetic resonance (CMR) is limited in patients with arrhythmia or poor breath holding ability. In this study, clinical value of a rapid free-breathing workflow was assessed by employing real-time compressed-sensing for cardiac function and motion-corrected LGE embedded in a workflow engine for cardiac assessment. Results indicated that the proposed free-breathing fast workflow allowed in a short acquisition time to assess the morphological features of the heart and left ventricular function, especially in patients with severe heart failure.

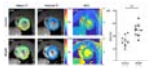


CrCEST energetics of calf muscle groups at 3T distinguish patients with peripheral arterial disease from age-matched normals

Helen Sporkin<sup>1</sup>, Christopher Schumann<sup>2</sup>, Roshin Mathew<sup>2</sup>, Christopher Kramer<sup>2,3</sup>, and Craig Meyer<sup>1,3</sup>

<sup>1</sup>Biomedical Engineering, University of Virginia, Charlottesville, VA, United States, <sup>2</sup>Cardiology, University of Virginia, Charlottesville, VA, United States, <sup>3</sup>Radiology and Medical Imaging, University of Virginia, Charlottesville, VA, United States

In Peripheral Arterial Disease, arterial occlusions in the lower limbs lead to tissue ischemia, which can lead to claudication pain or the need for amputation. Creatine CEST (CrCEST) imaging can indirectly image creatine as it exchanges protons with free water during metabolism after exercise. Ischemia in the skeletal reduces available oxygen, slowing metabolism. CrCEST data of three major calf muscle groups were fit to a monoexponential function in order to compare energetics between PAD patients and age-matched normal subjects. We have so far imaged 22 age-matched subjects and 19 PAD patients, and found a significant increase in the decay constant.

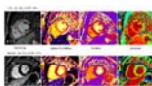


ECG-free, free-breathing myocardial T1/ECV mapping at high heart rates using MR Multitasking: A feasibility study in a HFpEF rat model

Pei Han<sup>1,2</sup>, Rui Zhang<sup>3,4</sup>, Anthony Christodoulou<sup>2</sup>, Shawn Wagner<sup>2</sup>, Yibin Xie<sup>2</sup>, Eugenio Cingolani<sup>3</sup>, Eduardo Marban<sup>3</sup>, and Debiao Li<sup>1,2,5</sup>

<sup>1</sup>Department of Bioengineering, UCLA, Los Angeles, CA, United States, <sup>2</sup>Biomedical Imaging Research Institute, Cedars-Sinai Medical Center, Los Angeles, CA, United States, <sup>3</sup>Smidt Heart Institute, Cedars-Sinai Medical Center, Los Angeles, CA, United States, <sup>4</sup>Department of Cardiology, Xin-Hua Hospital Affiliated to Shanghai Jiao Tong University School of Medicine, Shanghai, China, <sup>5</sup>Department of Medicine, UCLA, Los Angeles, CA, United States

CMR T1 and ECV quantification can be used to characterize focal or diffuse myocardial fibrosis. However, it is technically challenging to acquire high-quality maps in small animals for preclinical research because of high heart rates and high respiration rates. In this study, we developed an ECG-free, free-breathing MR Multitasking T1 mapping method on a 9.4T small animal MRI system. The feasibility of characterizing diffuse myocardial fibrosis was tested in a HFpEF rat model. Elevated ECV found in the HFpEF group is consistent with previous human studies and shows strong correlation with the histological data.



Tissue characterization by mapping and strain cardiac magnetic resonance imaging to evaluate myocardial inflammation in fulminant myocarditis

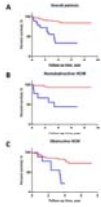
Hui Zhu<sup>1</sup>, Haojie Li<sup>1</sup>, Zhaoxia Yang<sup>1</sup>, and Liming Xia<sup>1</sup>

<sup>1</sup>Radiology, Tongji Hospital, Tongji Medical College, Huazhong University of Science and Technology, Wuhan, China



Fulminant myocarditis show significant different LGE patterns, increased edema and decreased strain measurements compared with non-fulminant acute myocarditis and global peak circumferential and radial strain were closely correlated with quantitative parameters of myocardial edema.

1209



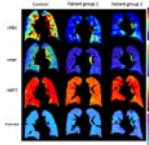
Global longitudinal diastolic strain rate predict adverse outcomes in hypertrophic cardiomyopathy assessed with CMR tissue tracking

Chunchao Xia<sup>1</sup>, Xiaoyue Zhou<sup>2</sup>, and Zhenlin Li<sup>1</sup>

<sup>1</sup>West China Hospital, Chengdu, China, <sup>2</sup>MR Collaboration, Siemens Healthineers Ltd., Shanghai, China

During hypertrophic cardiomyopathy (HCM), left ventricular (LV) diastolic dysfunction is regarded as one of the primary mechanisms responsible for the main adverse cardiovascular events (MACEs). Early evaluation of LV diastolic function is of great importance to risk stratification and management optimization in HCM patient populations. Our study indicated that the cardiac magnetic resonance tissue tracking (CMR-TT)–derived longitudinal global diastolic strain rate (PDSR) is a novel and easy-to-perform index for evaluating LV diastolic dysfunction and predicting adverse outcomes in HCM patient populations, which would also be beneficial for risk stratification.

1210



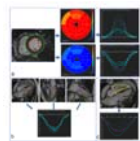
Assessing lung perfusion in pulmonary hypertension

Paul J.C. Hughes<sup>1</sup>, Andrew J. Swift<sup>1,2</sup>, Frederick J. Wilson<sup>3</sup>, Marcella Cogliano<sup>1</sup>, Faisal AA Alandejani<sup>1</sup>, Anthony Cahn<sup>3</sup>, Lindsay Kendall<sup>3</sup>, David G. Kiely<sup>2,4,5</sup>, and Jim M. Wild<sup>1,2</sup>

<sup>1</sup>POLARIS, Department of Infection, Immunity and Cardiovascular Disease, The University of Sheffield, Sheffield, United Kingdom, <sup>2</sup>Insigneo Institute for in silico Medicine, The University of Sheffield, Sheffield, United Kingdom, <sup>3</sup>GlaxoSmithKline R&D Ltd, Stevenage, United Kingdom, <sup>4</sup>Sheffield Pulmonary Vascular Disease, Sheffield Teaching Hospitals NHS Trust, Sheffield, United Kingdom, <sup>5</sup>Department of Infection, Immunity and Cardiovascular Disease, The University of Sheffield, Sheffield, United Kingdom

Pulmonary arterial hypertension (PAH) is a condition that impacts on lung perfusion and right ventricular function. This work aimed to assess i) the diagnostic utility of relative pulmonary perfusion parameters to distinguish patients with PAH from healthy controls and ii) changes in lung perfusion in 2 patient groups with PAH: newly diagnosed patients initiating and patients escalating treatment and clinically stable patients who had no escalation of treatment.

1211



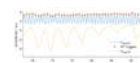
The relationship between CMR–derived myocardial strain and late gadolinium enhancement in asymptomatic heart transplant patients

Xuehua Shen<sup>1</sup>, Yating Yuan<sup>1</sup>, Ming Yang<sup>1</sup>, Xiaoyue Zhou<sup>2</sup>, Jing Wang<sup>1</sup>, Wei Sun<sup>3</sup>, Mingxing Xie<sup>3</sup>, Li Zhang<sup>3</sup>, and Bo Liang<sup>1</sup>

<sup>1</sup>Department of Radiology, Union Hospital, Tongji Medical College, Huazhong University of Science and Technology, Wuhan, Hubei, China, <sup>2</sup>MR Collaboration, Siemens Healthineers Ltd., Shanghai, China, Shanghai, China, <sup>3</sup>Department of Ultrasound, Union Hospital, Tongji Medical College, Huazhong University of Science and Technology, Wuhan, Hubei, China

No study has explored the relationship between CMR-derived myocardial strain and the extent of LGE in asymptomatic HT patients. The purpose of this study was to evaluate this relationship using DRA and FT strain analysis. In this study, there were strong correlation and good reproducibility between DRA and FT strain modalities. HT patients with LGE had reduced LVGLS and preserved LVGCS. CMR-derived LVGLS was significantly and independently correlated with LGE.

1212



Retrospective Analysis of Pilot Tone Derived Cardiac and Respiratory Motion Information in a Patient Cohort

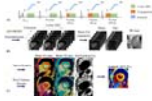
Mario Bacher<sup>1,2</sup>, Lorenzo Di Sopra<sup>1</sup>, Peter Speier<sup>2</sup>, Davide Piccini<sup>3</sup>, Anna-Giulia Pavon<sup>1</sup>, Christopher Roy<sup>1</sup>, Juerg Schwitter<sup>1</sup>, Jérôme Yerly<sup>1</sup>, and Matthias Stuber<sup>1</sup>

<sup>1</sup>Department of Radiology, Lausanne University Hospital and University of Lausanne, Lausanne, Switzerland,

<sup>2</sup>Siemens Healthineers, Erlangen, Germany, <sup>3</sup>Siemens Healthineers, Lausanne, Switzerland

The Pilot Tone is a novel motion sensing method capable of simultaneous, sequence independent measurement of respiratory and cardiac motion. Here, we show that Pilot Tone motion data can be used as an alternative to self-gating in a free-breathing, cardiac- and respiration resolved CMRI sequence. We demonstrate in a patient cohort that Pilot Tone motion information correlates well with ECG ground-truth and self-gating respiratory signals.

1213



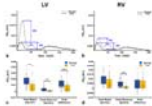
Reproducibility, Repeatability and Preliminary Clinical Results of Dixon Cardiac MRF: T<sub>1</sub>, T<sub>2</sub>, ECV and fat fraction tissue characterization

Olivier Jaubert<sup>1</sup>, Gastao Cruz<sup>1</sup>, Aurelien Bustin<sup>1</sup>, Torben Schneider<sup>2</sup>, Georgios Georgiopoulos<sup>1</sup>, Mariya Doneva<sup>3</sup>, Pier-Giorgio Masci<sup>1</sup>, Rene Michael Botnar<sup>1</sup>, and Claudia Prieto<sup>1</sup>

<sup>1</sup>Biomedical Engineering Department, School of Biomedical Engineering and Imaging Sciences, King's College London, London, United Kingdom, <sup>2</sup>Philips Healthcare, London, United Kingdom, <sup>3</sup>Philips Research Hamburg, Hamburg, Germany

Dixon cardiac Magnetic Resonance Fingerprinting (DcMRF) has been recently proposed to enable simultaneous water T<sub>1</sub>, water T<sub>2</sub> and fat fraction (FF) quantification in a single breath-hold scan. Here we investigate the reproducibility, repeatability and clinical feasibility of DcMRF in comparison to reference MOLLI, T2GRASE and 6 echo proton density FF measurements. Reproducibility and repeatability were investigated in healthy subjects, whereas native T<sub>1</sub>, T<sub>2</sub> and FF, and post contrast T<sub>1</sub> and synthetic ECV measurements were performed in patients with suspected cardiovascular disease.

1214



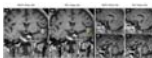
Evaluate Myocardial Circumferential Kinetic Energy for Patients with Repaired Tetralogy of Fallot

Shi-Ying Ke<sup>1</sup>, Meng-Chu Chang<sup>1</sup>, Ming-Ting Wu<sup>2</sup>, Ken-Pen Weng<sup>3,4</sup>, and Hsu-Hsia Peng<sup>1</sup>

<sup>1</sup>Department of Biomedical Engineering and Environmental Sciences, National TsingHua University, Hsinchu, Taiwan, <sup>2</sup>Department of Radiology, Kaohsiung Veterans General Hospital, Kaohsiung, Taiwan, <sup>3</sup>Department of Pediatrics, Kaohsiung Veterans General Hospital, Kaohsiung, Taiwan, <sup>4</sup>Department of Pediatrics, National Yang-Ming University, Taipei, Taiwan

This study aims to evaluate biventricular myocardial circumferential kinetic energy (KE<sub>θ</sub>) for assessment of regional myocardial function in repaired tetralogy of Fallot (rTOF) patients with preserved global cardiac function. The tissue phase mapping (TPM) was acquired in the basal, mid, and apical slices in the left and right ventricles. We found the altered KE values and abnormal distribution of three-directional %KE in rTOF patients. In conclusion, the altered myocardial KE<sub>θ</sub> may provide useful information for assessment of regional myocardial function in rTOF patients with preserved global cardiac function.

1215



Motion-Compensated 3D TSE for More Robust Intracranial MR Vessel Wall Imaging

Zhehao Hu<sup>1,2</sup>, Fei Han<sup>3</sup>, Andre J.W. Van der Kouwe<sup>4,5</sup>, Xiaoming Bi<sup>3</sup>, Bin Sun<sup>6</sup>, Jiayu Xiao<sup>1</sup>, Junzhou Chen<sup>1,2</sup>, Shlee S. Song<sup>7</sup>, Marcel M. Maya<sup>8</sup>, Debiao Li<sup>1,2,9</sup>, and Zhaoyang Fan<sup>1,2,9</sup>

<sup>1</sup>Biomedical Imaging Research Institute, Cedars-Sinai Medical Center, Los Angeles, CA, United States, <sup>2</sup>Bioengineering Department, University of California, Los Angeles, Los Angeles, CA, United States, <sup>3</sup>Siemens Healthineers, Los Angeles, CA, United States, <sup>4</sup>A. A. Martinos Center for Biomedical Imaging, Massachusetts General Hospital, Charlestown, MA, United States, <sup>5</sup>Department of Radiology, Harvard Medical School, Boston, MA, United States, <sup>6</sup>Department of Radiology, Fujian Medical University Union Hospital, Fuzhou, China, <sup>7</sup>Department of Neurology, Cedars-Sinai Medical Center, Los Angeles, CA, United States, <sup>8</sup>Department of Imaging, Cedars-Sinai Medical Center, Los Angeles, CA, United States, <sup>9</sup>Department of Medicine, University of California, Los Angeles, Los Angeles, CA, United States

While underexplored to date, motion susceptibility may critically undermine clinical translation of 3D intracranial MR vessel wall imaging (VWI). Motion artifacts observed in intracranial VWI are either caused by head bulk motion or internally localized movement. By combining volumetric navigators (vNav) and self-gating (SG) strategies, we propose a novel motion compensation approach that can simultaneously address these two motion issues. Our preliminary studies demonstrated the potential of using this technique to improve robustness of 3D intracranial MR VWI.

## Oral

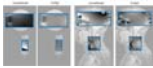
### High resolution fMRI - fMRI Acquisition & Analysis

Thursday Parallel 4 Live Q&A

Thursday 15:05 - 15:50 UTC

Moderators: Wietske van der Zwaag

1216



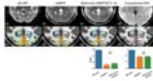
#### A Shim Algorithm to Improve the Field Homogeneity and Image Quality in Cortico-Spinal fMRI

Björn Fricke<sup>1</sup> and Jürgen Finsterbusch<sup>1</sup>

<sup>1</sup>Department of Systems Neuroscience, University Medical Center Hamburg-Eppendorf, Hamburg, Germany

Cortico-spinal functional MRI covering a brain and a cervical spinal cord volume in the same acquisition, e.g. to investigate the interaction of brain and spinal cord areas, requires a dynamic shim update of the frequency and linear shim terms to obtain a reasonable EPI image quality in both volumes. Unfortunately, the optimum values for static higher-order and volume-specific dynamic linear shim terms cannot be determined with the standard shim algorithms provided by manufacturers. Here, a shim algorithm has been implemented that overcomes this problem and provides a better field homogeneity in the brain and spinal cord volumes.

1217



#### Implementing multi-echo balanced SSFP with a sequential phase-encoding order at 7T

Huilou Liang<sup>1,2</sup>, Ziyi Pan<sup>3</sup>, Chencan Qian<sup>1,2</sup>, Kaibao Sun<sup>1</sup>, Fanhua Guo<sup>1,2</sup>, Dehe Weng<sup>4</sup>, Jing An<sup>4</sup>, Yan Zhuo<sup>1,2,5</sup>, Hua Guo<sup>3</sup>, Danny J.J. Wang<sup>6</sup>, and Rong Xue<sup>1,2,7</sup>

<sup>1</sup>State Key Laboratory of Brain and Cognitive Science, Beijing MRI Center for Brain Research, Institute of Biophysics, Chinese Academy of Sciences, Beijing, China, <sup>2</sup>University of Chinese Academy of Sciences, Beijing, China, <sup>3</sup>Center for Biomedical Imaging Research, Department of Biomedical Engineering, School of Medicine, Tsinghua University, Beijing, China, <sup>4</sup>Siemens Shenzhen Magnetic Resonance Ltd, Shenzhen, China, <sup>5</sup>CAS Center for Excellence in Brain Science and Intelligence Technology, Chinese Academy of Sciences, Beijing, China, <sup>6</sup>Laboratory of fMRI Technology (LOFT), Stevens Neuroimaging and Informatics Institute, University of Southern California, Los Angeles, CA, United States, <sup>7</sup>Beijing Institute for Brain Disorders, Beijing, China

In the past decade, passband bSSFP has emerged as an alternative method to the widely-used GE-EPI in fMRI studies at high-fields. Multiline bSSFP with an interleaved phase-encoding order was further proposed to accelerate bSSFP fMRI. However, it intrinsically suffers from high spatial frequency ghosts which blur the image. In this study, we developed a multi-echo bSSFP sequence using a sequential phase-encoding order, combined with the GRAPPA technique for ghost elimination. *In vivo* experiments demonstrated that this sequence could shorten the imaging time and provide high-quality structural and functional MR images of the human brain at 7T with sub-millimeter resolution.

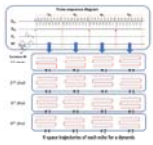


### Feasibility of high spatial and temporal resolution multi-echo multi-band whole brain resting-state functional MRI on a compact 3T system

Daehun Kang<sup>1</sup>, Hang Joon Jo<sup>1,2</sup>, Myung-Ho In<sup>1</sup>, Erin Gray<sup>1</sup>, Ek T Tan<sup>3,4</sup>, Thomas K Foo<sup>4</sup>, Uten Yarach<sup>1</sup>, Nolan K Meyer<sup>1</sup>, Joshua D Trzasko<sup>1</sup>, John Huston<sup>1</sup>, Matt A Bernstein<sup>1</sup>, and Yunhong Shu<sup>1</sup>

<sup>1</sup>Mayo Clinic, Rochester, MN, United States, <sup>2</sup>Hanyang University, Seoul, Republic of Korea, <sup>3</sup>Hospital of Special Surgery, New York, NY, United States, <sup>4</sup>GE Global Research, Niskayuna, NY, United States

Multi-echo fMRI has been shown to provide better denoising and result in improved functional analysis compared to single-echo acquisition, but it reduces the temporal resolution and inhibits high-resolution imaging. Multi-band imaging and in-plane acceleration can compensate for the reduced resolution. The high performance gradient on a compact 3T scanner can further reduce the echo-spacing and accelerate the acquisition. Here we demonstrate that high spatial-resolution ME-MB fMRI is achievable with high temporal resolution on the compact 3T. The effectiveness of ME acquisition is evaluated with different artifact reduction strategies in whole brain resting-state fMRI and compared with the standard SE acquisition.

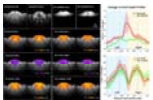


### Multi-Echo Multi-Segment EPI Based fMRI Using Sliding-Window Acquisition and Multiplexed Sensitivity Encoding (MUSE)

Shihui Chen<sup>1</sup>, Mei-Lan Chu<sup>2</sup>, Queenie Chan<sup>3</sup>, Nan-Kuei Chen<sup>4,5</sup>, Chun-Jung Juan<sup>6</sup>, Liyuan Liang<sup>1</sup>, and Hing-Chiu Chang<sup>1</sup>

<sup>1</sup>The University of Hong Kong, Hong Kong, Hong Kong, <sup>2</sup>Graduate Institute of Biomedical Electronics and Bioinformatics, National Taiwan University, Taipei, Taiwan, Taipei, Taiwan, <sup>3</sup>Philips Healthcare, Hong Kong, China, Hong Kong, Hong Kong, <sup>4</sup>Department of Biomedical Engineering, University of Arizona, Tucson, AZ, United States, Tucson, AZ, United States, <sup>5</sup>Brain Imaging and Analysis Center, Duke University Medical Center, Durham, NC, United States, Durham, NC, United States, <sup>6</sup>Department of Medical Imaging, China Medical University Hsinchu Hospital, Taiwan, Taipei, Taiwan

Multi-echo fMRI (ME-fMRI) has been shown to be useful in differentiating BOLD and non-BOLD signals, therefore improving the sensitivity of fMRI. Parallel imaging with high acceleration factor (e.g.,  $R \geq 3$ ) is indispensable to achieve reasonable TE interval and desired spatial resolution for ME-fMRI acquisition. However, the reconstructed multi-echo images with high acceleration factor may suffer from underside noise amplification due to SENSE reconstruction. In this work, we further modify multi-echo multi-segment EPI (MEMS-EPI) technique with sliding window acquisition to acquire multi-echo fMRI with high acceleration factor, and then reconstruct highly accelerated multi-echo fMRI images with MUSE algorithm.



### Ultrahigh-resolution Laminar fMRI Mapping of Cat Visual Cortex at 9.4T: Comparison of 2D GE-EPI and 3D iv-GRASE Sequences

Wei Zhu<sup>1</sup>, Djaudat Idiyatullin<sup>1</sup>, Shinho Cho<sup>1</sup>, Yi Zhang<sup>1</sup>, Kâmil Uğurbil<sup>1</sup>, Xiao-Hong Zhu<sup>1</sup>, and Wei Chen<sup>1</sup>

<sup>1</sup>Center for Magnetic Resonance Research, Department of Radiology, University of Minnesota, Minneapolis, MN, United States

Blood oxygenation-level dependent (BOLD) fMRI studies at the level mesoscopic organizations, such as cortical columns and layers, is challenged by the low signal-to-noise ratio (SNR) and the specificity of different fMRI sequences even at ultrahigh magnetic fields. In this work, we show that when mapping layer-specific activities in the cat visual cortex, ultrahigh-resolution 3D GRASE sequence with inner volume selection achieved similar specificity as at 9.4 Tesla CBV-fMRI using 2D GE-EPI sequence, while attains a higher BOLD sensitivity. Our results indicate that 3D iv-GRASE BOLD is promising for laminar and columnar mapping of brain functions.



### iZTE-fMRI

Martin John MacKinnon<sup>1</sup>, Sheng Song<sup>1</sup>, Li-Ming Hsu<sup>1</sup>, Sung-Ho Lee<sup>1</sup>, G. Allan Johnson<sup>2</sup>, and Yen-Yu Ian Shih<sup>1</sup>

<sup>1</sup>University of North Carolina at Chapel Hill, Chapel Hill, NC, United States, <sup>2</sup>Duke University, Durham, NC, United States

In this study we demonstrate how a zero-echo-time (ZTE) technique can overcome several limitations of traditional fMRI experiments. We demonstrate that ZTE fMRI can detect functional activations with positive iron oxide contrast, termed iZTE-fMRI, at an approximate three-fold magnitude increase in tCNR when compared to GRE-techniques in-vivo - with the further potential demonstrated from phantom studies to increase tCNR more significantly under optimal contrast agent dose. We also show that iZTE fMRI experiments can produce functional images with markedly less susceptibility artifacts and acoustic noise than standard GRE techniques.

1222

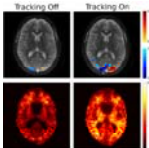


Novel resampling approach for 200-ms temporal resolution MB-SWIFT fMRI – application to DBS in rats  
Ekaterina Zhurakovskaya<sup>1</sup>, Lauri Lehto<sup>1</sup>, Jaakko Paasonen<sup>1</sup>, Lin Wu<sup>2</sup>, Sheng Sang<sup>2</sup>, Jun Ma<sup>2</sup>, Hanne Laakso<sup>1</sup>, Tiina Pirttimäki<sup>1</sup>, Olli Gröhn<sup>1</sup>, Silvia Mangia<sup>2</sup>, and Shalom Michaeli<sup>2</sup>

<sup>1</sup>University of Eastern Finland, Kuopio, Finland, <sup>2</sup>Center for Magnetic Resonance Research, University of Minnesota, Minneapolis, MN, United States

Deep brain stimulation (DBS) is widely used to treat several disorders. Given its minimal sensitivity to electrode-induced artifacts, fMRI with Multi-Band Sweep Imaging with Fourier Transformation (MB-SWIFT) is a powerful tool for identifying the DBS mechanism of action at a network level. However, MB-SWIFT generally suffers from low time resolution, thus limiting the characterization of temporal features. Here, we introduce a novel resampling approach applicable to radial k-space sampling such as used in MB-SWIFT, allowing to track repeating events with 200-ms time resolution. A proof of concept was demonstrated during DBS of the medial septal nucleus in rats.

1223



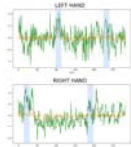
Real-Time Respiration Compensation in Oscillating Steady State fMRI

Amos A Cao<sup>1</sup> and Douglas Noll<sup>2</sup>

<sup>1</sup>University of Michigan, Ann Arbor, MI, United States, <sup>2</sup>Biomedical Engineering, University of Michigan, Ann Arbor, MI, United States

Oscillating Steady-State Imaging (OSSI) is a new steady-state sequence for high-SNR fMRI. Respiration-induced B<sub>0</sub> changes cause undesirable changes to the OSSI steady-state, resulting in signal artifacts. To address this problem, we present a prospective correction method which utilizes a self-navigating spiral trajectory to measure and correct for B<sub>0</sub> changes in real-time. In an initial fMRI proof-of-concept, our real-time correction method increased the number of activated voxels by 454% and increased mean tSNR by 81%. Real-time prospective correction has the potential to outperform retrospective correction methods by directly reducing perturbations to steady-state magnetization during acquisition.

1224



A Paradigm Free Regularization Approach to Recover Brain Activations: Validation on Task fMRI

Isa Costantini<sup>1</sup>, Samuel Deslauriers-Gauthier<sup>1</sup>, and Rachid Deriche<sup>1</sup>

<sup>1</sup>Athena Project-Team, Inria Sophia Antipolis - Méditerranée, Université Côte d'Azur, Biot, France

In this work we propose and validate a Paradigm-Free fMRI (PFFMRI) algorithm that acts directly on the 4-D fMRI image and recover the underlying brain activations without knowledge on the experimental paradigm. PFFMRI is based on the idea that large image variations should be preserved as they occur during brain activation, but small variations should be smoothed to remove noise. Starting from this, we were able to regularize the fMRI image with an anisotropic regularization, thus recovering the location of the brain activations in space and their timing and duration without knowledge of the experimental paradigm.

---

Oral

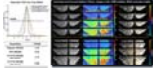
High resolution fMRI - Submillimeter 7-Tesla fMRI in Humans

Thursday Parallel 4 Live Q&A

Thursday 15:05 - 15:50 UTC

Moderators: Peter Bandettini & Jeroen Siero

1225



Highly Accelerated Sub-Millimeter Resolution 3D GRASE with Controlled T2 Blurring in T2-Weighted FMRI at 7T: Feasibility Study

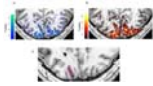
Suhung Park<sup>1</sup>, Salvatore Torrisi<sup>2</sup>, Jennifer Townsend<sup>2</sup>, Alexander Beckett<sup>2</sup>, and David Feinberg<sup>1,2</sup>

<sup>1</sup>University of California, Berkeley, Berkeley, CA, United States, <sup>2</sup>Advanced MRI Technologies, Sebastopol, CA, United States

3D GRASE is used for cortical layer and columnar fMRI in the absence of signal confounds from draining veins. Its use has been limited by limited slice coverage with blurring. We developed highly accelerated 3D GRASE with controlled T2 blurring by combining compressed sensing with variable flip angles. Compared with current GRASE acquisitions, the proposed method demonstrates that 1) through-plane random encoding with VFA increases the slice coverage with a sharper point spread function, 2) reduced TE from in-plane random encoding provides a high SNR efficiency, and 3) the resulting image sharpness and SNR efficiency lead to increased BOLD activation.

---

1226



Modelling the Laminar VASO Signal Change in Human V1 at 7T

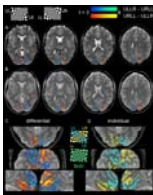
Atena Akbari<sup>1</sup>, Saskia Bollmann<sup>1</sup>, Tonima S Ali<sup>1</sup>, and Markus Barth<sup>1,2,3</sup>

<sup>1</sup>Centre for Advanced Imaging, The University of Queensland, Brisbane, Australia, <sup>2</sup>ARC Training Centre for Innovation in Biomedical Imaging Technology, The University of Queensland, Brisbane, Australia, <sup>3</sup>School of Information Technology and Electrical Engineering, The University of Queensland, Brisbane, Australia

In this study, we used the “cortical vascular model” for human V1 at 7T to simulate the laminar VASO-Space-Occupancy (VASO) signal change. For comparison, we conducted VASO experiments on a group of healthy subjects to measure laminar signal change in V1. Results show a very good agreement between the model prediction and the experimental results once the volume changes of the different vascular compartments (arterioles, capillaries, venules) are taken into account.

---

1227



Sub-Millimeter Spiral fMRI Combining Magnitude and Phase BOLD Contrast

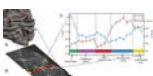
Lars Kasper<sup>1</sup>, Maria Engel<sup>1</sup>, Jakob Heinzle<sup>2</sup>, Matthias Mueller-Schrader<sup>2</sup>, Jonas Reber<sup>1</sup>, Thomas Schmid<sup>1</sup>, Christoph Barmet<sup>1</sup>, Bertram Jakob Wilm<sup>1</sup>, Klaas Enno Stephan<sup>2,3,4</sup>, and Klaas Paul Pruessmann<sup>1</sup>

<sup>1</sup>Institute for Biomedical Engineering, ETH Zurich and University of Zurich, Zurich, Switzerland, <sup>2</sup>Translational Neuromodeling Unit, Institute for Biomedical Engineering, University of Zurich and ETH Zurich, Zurich, Switzerland, <sup>3</sup>Wellcome Trust Centre for Neuroimaging, University College London, London, United Kingdom, <sup>4</sup>Max Planck Institute for Metabolism Research, Cologne, Germany

We investigate the spatial specificity of sub-millimeter (0.8mm) single-shot spiral fMRI, and its feasibility for functional phase contrast. Scrutinizing activation patterns of a visual paradigm in 6 subjects, we find that significant contrast changes occur between adjacent voxels, contributing to the evidence of spatial specificity of spiral acquisition as well as gradient echo BOLD contrast, and its possible applications in laminar or columnar fMRI. Furthermore, the vessel-localized nature of the phase activation suggests its suitability for masking macrovascular confound effects.

---

1228

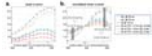


High-resolution line-scanning reveals distinct visual response properties across human cortical layers.

Andrew T. Morgan<sup>1</sup>, Nils Nothnagel<sup>1</sup>, Jozien Goense<sup>1</sup>, and Lars Muckli<sup>1</sup>

Motivated by recent functional line-scanning recordings in rodents, we developed a procedure to record human cortical layers at high spatial (200  $\mu\text{m}$ ) and temporal resolution (100 ms). Our technique addresses challenges associated with human line-scanning, such as planning around cortical folding and restrictive SAR limitations. Our results show that line-scanning of human cortical layers corroborates electrophysiological measurements of tuning properties in primary visual cortex. These results demonstrate that line-scanning is a promising technique for investigating local functional circuits in human cortex.

1229



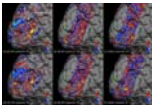
Cortical-depth dependence of pure T<sub>2</sub>-weighted BOLD fMRI with minimal T<sub>2</sub>' contamination using Echo-Planar Time-resolved Imaging (EPTI)

Fuyixue Wang<sup>1,2</sup>, Zijong Dong<sup>1,3</sup>, Qiyuan Tian<sup>1</sup>, Jingyuan Chen<sup>1</sup>, Anna Izabella Blazejewska<sup>1</sup>, Timothy G. Reese<sup>1</sup>, Jonathan R. Polimeni<sup>1,2</sup>, and Kawin Setsompop<sup>1,2</sup>

<sup>1</sup>A. A. Martinos Center for Biomedical Imaging, Massachusetts General Hospital, Charlestown, MA, United States, <sup>2</sup>Harvard-MIT Health Sciences and Technology, MIT, Cambridge, MA, United States, <sup>3</sup>Department of Electrical Engineering and Computer Science, MIT, Cambridge, MA, United States

BOLD fMRI based on T<sub>2</sub> contrast has the promise to provide exclusively microvascular specificity, which would optimize the ability of fMRI signals to accurately reflect and localize neuronal activity. However, it is challenging in practice to achieve pure T<sub>2</sub> weighting. Here we employ a new highly-efficient acquisition and reconstruction framework based on EPI, Echo-Planar Time-resolved Imaging (EPTI), and extend it to generate blurring- and distortion-free data with purely T<sub>2</sub> weighting. We evaluate the technique through a cortical-depth analysis of activation in human visual cortex and demonstrate that it achieves the desired microvascular specificity.

1230



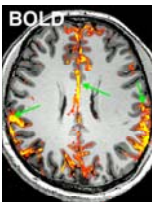
Mapping ocular dominance columns in humans using GE-EPI, SE-EPI and SS-SI-VASO at 7 T

Daniel Haenelt<sup>1,2</sup>, Nikolaus Weiskopf<sup>1</sup>, Lenka Vaculciakova<sup>1,2</sup>, Roland Mueller<sup>1</sup>, Shahin Nasr<sup>3,4</sup>, Jonathan Polimeni<sup>3,4</sup>, Roger Tootell<sup>3,4</sup>, Laurentius Huber<sup>5</sup>, Martin Sereno<sup>6</sup>, and Robert Trampel<sup>1</sup>

<sup>1</sup>Max Planck Institute for Human Cognitive and Brain Sciences, Leipzig, Germany, <sup>2</sup>International Max Planck Research School on Neuroscience of Communication: Function, Structure, and Plasticity, Leipzig, Germany, <sup>3</sup>Athinoula A. Martinos Center for Biomedical Imaging, Boston, MA, United States, <sup>4</sup>Department of Radiology, Harvard Medical School, Boston, MA, United States, <sup>5</sup>Department of Cognitive Neuroscience, Maastricht Brain Imaging Center, Maastricht, Netherlands, <sup>6</sup>Department of Psychology, San Diego State University, San Diego, CA, United States

Functional MRI studies classically rely on the use of GE-EPI sequences. However, the GE-based signal is inherently sensitive to large veins, which impairs its use in high-resolution fMRI application. Other BOLD- and CBV-based approaches like SE-EPI and SS-SI-VASO, respectively, promise a higher specificity at the expense of sensitivity. In the present work, we tested if ocular dominance columns (ODCs) can be detected using GE-EPI, SE-EPI and SS-SI-VASO at 7 T. ODCs could be reliably mapped using all three acquisition methods. Furthermore, we could show for the first time ODCs in humans by exploiting the functional CBV response using SS-SI-VASO.

1231



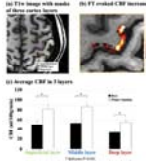
Mapping directional functional connectivity across brain-wide networks with layer-specific CBV-fMRI

Laurentius Huber<sup>1</sup>, Emily Finn<sup>2</sup>, Sean Marrett<sup>2</sup>, Sriranga Kashyap<sup>1</sup>, Arman Khojandi<sup>2</sup>, Rainer Goebel<sup>1</sup>, Peter Bandettini<sup>2</sup>, and Benedikt Poser<sup>1</sup>

<sup>1</sup>MBIC, Uni Maastricht, Faculty of Psychology and Neuroscience, Maastricht, Netherlands, <sup>2</sup>SFIM, NIMH, Bethesda, MD, United States

With recent advances in ultra-high-field MRI hardware and sequence mechanisms, it has become possible to measure CBV-weighted fMRI signal across cortical layers. While initial proof-of-principle layer-fMRI studies in primary brain areas with conventional fMRI task designs are promising, layer-fMRI has not yet realized its full potential to map layer-dependent functional connectivity across large-scale brain networks. In this study, we investigate the applicability of CBV-weighted layer-fMRI to assess functional connectivity during resting-state and naturalistic tasks. We can map common resting-state networks and characterize their internal layer-dependent signatures with respect to directionality and cortical hierarchy.

1232



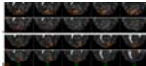
### In-vivo laminar CBF fMRI using high-resolution pseudo-continuous arterial spin labeling at 7T

Xingfeng Shao<sup>1</sup>, Kay Jann<sup>1,2</sup>, Kai Wang<sup>1</sup>, Fanhua Guo<sup>3</sup>, Peng Zhang<sup>3</sup>, and Danny JJ Wang<sup>1,2</sup>

<sup>1</sup>Mark & Mary Stevens Neuroimaging and Informatics Institute, Keck School of Medicine, University of Southern California, Los Angeles, CA, United States, <sup>2</sup>Department of Neurology, University of Southern California, Los Angeles, CA, United States, <sup>3</sup>State Key Laboratory of Brain and Cognitive Science, Beijing MRI Center for Brain Research, Institute of Biophysics, Chinese Academy of Sciences, Beijing, China

In-vivo laminar CBF fMRI was performed by high resolution ( $0.5 \times 0.5 \times 1.5 \text{ mm}^3$ ) inner-volume GRASE with optimized pCASL labeling at 7T. Activation of finger-tapping task (5 blocks, TA=10 min) was reliably detected in all 4 subjects. Both rest/FT CBF peaks in the middle layers, which corresponds to highest capillary density in cortex layer IV. FT evoked CBF increase shows one peak in middle layer, and a second shoulder in deep layer. The capability to provide quantitative CBF measurements at both baseline and task activation with high specificity to neuronal activities is a unique strength of ASL fMRI compared to other fMRI techniques.

1233



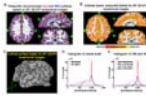
### On the feasibility of using single-shot perfusion labeling (SSPL) at 7 Tesla for laminar fMRI

Jacco A de Zwart<sup>1</sup>, Peter van Gelderen<sup>1</sup>, and Jeff H Duyn<sup>1</sup>

<sup>1</sup>Advanced MRI section, LFMI, NINDS, National Institutes of Health, Bethesda, MD, United States

Blood oxygen-level dependent (BOLD) functional MRI (fMRI) based on gradient-echo EPI is the most commonly used fMRI method due to its high sensitivity and robustness. However, large vein contribution negatively affects spatial localization of BOLD activation, of crucial importance for laminar and other high-resolution fMRI applications. Perfusion and blood volume-based methods have been shown to increase spatial accuracy of activation maps. Here we demonstrate feasibility of single-shot perfusion labeling (SSPL) fMRI at up to  $1 \text{ mm}^3$  resolution, a reference-less perfusion fMRI method twice as efficient as FAIR in which background signal is suppressed, improving temporal stability.

1234



### A magnetization transfer weighted anatomical reference allows laminar fMRI analysis in native functional image space

Yuhui Chai<sup>1</sup>, Linqing Li<sup>2</sup>, Yicun Wang<sup>3</sup>, Larentius Huber<sup>4</sup>, Benedikt Poser<sup>4</sup>, Jeff Duyn<sup>3</sup>, and Peter Bandettini<sup>1,2</sup>

<sup>1</sup>Section on Functional Imaging Methods, Laboratory of Brain and Cognition, NIMH, NIH, Bethesda, MD, United States, <sup>2</sup>Functional MRI Core, NIMH, NIH, Bethesda, MD, United States, <sup>3</sup>Advanced MRI Section, Laboratory of Functional and Molecular Imaging, NINDS, NIH, Bethesda, MD, United States, <sup>4</sup>Maastricht Brain Imaging Center, Faculty of Psychology and Neuroscience, University of Maastricht, Maastricht, Netherlands

In most previous laminar fMRI studies, cortical layers are defined based on an anatomical image that is collected by a different acquisition technique and exhibits different geometric distortion compared to the functional images. We introduce to generate a magnetization transfer (MT) weighted anatomical reference, using identical acquisition design as fMRI measurement. Cortical surface and depth can be reconstructed directly from this MT-weighted anatomical EPI image and all laminar analysis can be performed in the native fMRI image space without the need for distortion correction and registration.



---

## Oral - Power Pitch

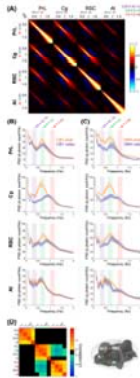
### High resolution fMRI - fMRI Applications

Thursday Parallel 4 Live Q&A

Thursday 15:05 - 15:50 UTC

Moderators: Giovanna Diletta Ielacqua & Scott Peltier

1235



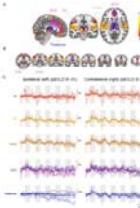
Simultaneous fMRI and multi-channel, spectrally resolved fiber-photometry reveals the neural basis of default mode network modulation in rats

Tzu-Hao Harry Chao<sup>1</sup>, Li-Ming Hsu<sup>1</sup>, Martin MacKinnon<sup>1</sup>, and Yen-Yu Shih<sup>1</sup>

<sup>1</sup>University of North Carolina at Chapel Hill, Chapel Hill, NC, United States

This study establishes a novel MR-compatible multi-channel fiber-photometry platform and demonstrates 1) photometry-CBV measured in PrL and Cg co-fluctuate with global DMN signal derived from CBV-fMRI, 2) significantly enhanced 0.6-0.8 Hz GCaMP power in PrL, Cg, and RSC, but not AI, between two DMN states, 3) significantly enhanced 0.25-0.45 Hz GCaMP power in PrL, Cg and RSC precedes DMN activation peak by 3-5 s, but not AI, and 4) significantly enhanced 0.6-0.8 Hz GCaMP power in AI precedes DMN deactivation valley by 11 s.

1236



Deciphering the Pain-Matrix with Ultrahigh functional MRI: En Route to Objective Biomarkers for Pain

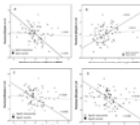
Gijs Jurjen Heij<sup>1</sup>, Thoralf Niendorf<sup>1,2</sup>, and Henning Matthias Reimann<sup>1</sup>

<sup>1</sup>Berlin Ultrahigh Field Facility (B.U.F.F.), Max-Delbrück-Center for Molecular Medicine, Berlin, Germany,

<sup>2</sup>Experimental and Clinical Research Center, a joint cooperation between the Charité Medical Faculty and the Max Delbrück Center for Molecular Medicine in the Helmholtz Association, Berlin, Germany

Despite millions of people suffering from chronic pain, clinicians still rely on self-reports for the assessment of pain. In attempts to identify objective biomarkers, fMRI studies have revealed an assembly of regions that consistently activates in response to noxious stimuli, but also to non-noxious equally salient stimuli. Since most studies have been performed at 3T or lower, higher field strengths might be able to differentiate pain from saliency. As a first step, we aimed to identify the pain-matrix at ultrahigh fields using an ON/OFF heat stimulation paradigm and show here that the regions associated with the pain-matrix could be identified.

1237

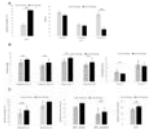


Disrupted Small-World Networks and Differences in Metabolite Concentration in Healthy Adults with Low and High Genetic Risk

Hui Zhang<sup>1,2</sup>, Pui Wai Chiu<sup>1,3</sup>, Isaac Ip<sup>4</sup>, Tianyin Liu<sup>5</sup>, Gloria Hoi Yan Wong<sup>5</sup>, You-Qiang Song<sup>6</sup>, Savio Wai Ho Wong<sup>4</sup>, Queenie Chan<sup>7</sup>, Karl Herrup<sup>8</sup>, and Henry Ka Fung Mak<sup>1,2,3</sup>

<sup>1</sup>Department of Diagnostic Radiology, The University of Hong Kong, Hong Kong, Hong Kong, <sup>2</sup>Alzheimer's Disease Research Network, Hong Kong, Hong Kong, <sup>3</sup>State Key Laboratory of Brain and Cognitive Sciences, Hong Kong, Hong Kong, <sup>4</sup>Department of Educational Psychology, the Chinese University of Hong Kong, Hong Kong, Hong Kong, <sup>5</sup>Department of Social Work and Administration, The University of Hong Kong, Hong Kong, Hong Kong, <sup>6</sup>Department of Biochemistry, The University of Hong Kong, Hong Kong, Hong Kong, <sup>7</sup>Philips Healthcare, Hong Kong, Hong Kong, <sup>8</sup>Alzheimer Disease Research Centre, University of Pittsburgh, Pittsburgh, PA, United States

To identify the relationship between the topological properties and glutamate in genetic-related subgroups (ApoE4 carriers and non-ApoE4 carriers), combined resting state fMRI (rs-fMRI) and MRS were applied in this study. Graph theory metrics of subgroups were calculated and compared. In the results, ApoE4 carriers had worse network segregation and integration. However, there was significant correlation between [Glx]<sub>abs</sub> in left hippocampus and topological metrics in high-risk group. We postulated that glutamatergic synaptic transmission modulates rs-fMRI activities in ApoE4 carriers.

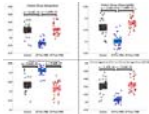


### Combined Working Memory and Attention Training Improves Cognition via Task-Specific and Transfer Effects

Daisuke Sawamura<sup>1,2</sup>, Ryusuke Suzuki<sup>3</sup>, Keita Ogawa<sup>4</sup>, Shinya Sakai<sup>2</sup>, Xinnan Li<sup>1</sup>, Hiroyuki Hamaguchi<sup>1</sup>, and Khin Khin Tha<sup>5,6</sup>

<sup>1</sup>Department of Biomarker Imaging Science, Graduate School of Biomedical Science and Engineering, Hokkaido University, Sapporo, Japan, <sup>2</sup>Department of Functioning and Disability, Faculty of Health Sciences, Hokkaido University, Sapporo, Japan, <sup>3</sup>Departments of Medical Physics, Hokkaido University Hospital, Sapporo, Japan, <sup>4</sup>Department of Rehabilitation, Hokkaido University Hospital, Sapporo, Japan, <sup>5</sup>Department of Diagnostic and Interventional Radiology, Hokkaido University, Sapporo, Japan, <sup>6</sup>Global Station for Quantum Medical Science and Engineering, Hokkaido University, Sapporo, Japan

Little is known about how neurocognition is modulated upon combined computerized cognitive training (CCT). We developed a combined CCT program designed to improve several cognitive functions simultaneously, and evaluated its effect on neurocognitive performance and functional connectivity (FC) of the brain. The results suggest that the CCT improves not only the targeted functions but also the other aspects of neurocognition via augmentation of transfer effect. The LPFC and fronto-parieto-occipital networks are thought to play role.



### Repetitive TMS increases whole brain metastability and dynamic integrity in Essential Tremor

SUJAS BHARDWAJ<sup>1</sup>, RAJANIKANT PANDA<sup>2</sup>, SHWETA PRASAD<sup>1</sup>, SUNIL KUMAR KHOKHAR<sup>3</sup>, SNEHA RAY<sup>3</sup>, ROSE DAWN BHARATH<sup>3</sup>, and PRAMOD KUMAR PAL<sup>1</sup>

<sup>1</sup>NEUROLOGY, NIMHANS, Bengaluru, India, <sup>2</sup>Coma Science Group, Université de Liège, Liège, Belgium, <sup>3</sup>NI & IR, NIMHANS, Bengaluru, India

We assessed the effect of repetitive transcranial magnetic stimulation (rTMS) on whole brain dynamics using fMRI. MRI was acquired before and after a single session of rTMS in 30 patients of Essential Tremor and 20 age matched healthy controls. Whole brain dynamic synchronization - "metastability", and propagation of integration - "intrinsic ignition", were studied in order to assess brain network topological fluctuations following rTMS. Single subject and group wise whole brain metastability, integration and ignition driven integration was found improve with a single session of rTMS.

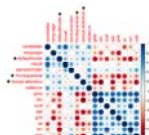


### Diminished default mode network connectivity in older individuals is associated with aberrant brain metabolism

Xirui Hou<sup>1</sup>, Zixuan Lin<sup>1</sup>, Peiyong Liu<sup>1</sup>, Corinne Pettigrew<sup>2</sup>, Anja Soldan<sup>2</sup>, Marilyn Albert<sup>2</sup>, and Hanzhang Lu<sup>1</sup>

<sup>1</sup>The Russell H. Morgan Department of Radiology, Johns Hopkins University School of Medicine, Baltimore, MD, United States, <sup>2</sup>Department of Neurology, Johns Hopkins University School of Medicine, Baltimore, MD, United States

Cerebral metabolic rate of oxygen (CMRO<sub>2</sub>), the rate at which O<sub>2</sub> is consumed in the brain, is thought to be a direct index of energy hemostasis and brain health. Recent studies have suggested that CMRO<sub>2</sub> is elevated but functional connectivity is declined with age. In this work, we demonstrated the diminished default network was associated with aberrant CMRO<sub>2</sub> in older healthy subjects. Network analysis indicated that the increasing amount of CMRO<sub>2</sub> was used to compensate for the inefficiency of degraded networks.



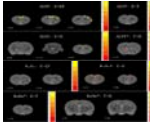
### Functional connectivity is associated with radiotherapy-induced vascular injury and cognitive impairment in young brain tumor survivors

Melanie Morrison<sup>1</sup>, Angela Jakary<sup>1</sup>, Erin Felton<sup>2</sup>, Schuyler Stoller<sup>2</sup>, Sabine Mueller<sup>2</sup>, and Janine Lupo<sup>1</sup>

<sup>1</sup>Radiology & Biomedical Imaging, University of California San Francisco, San Francisco, CA, United States, <sup>2</sup>Department of Pediatrics, University of California San Francisco, San Francisco, CA, United States

While radiation therapy plays an essential role in the management of brain tumor patients, exposure to radiation has been known to lead to declines in neurocognitive performance and vascular injury. As there remains a need for a reliable marker and predictor of patient outcome, this study explores the usefulness of functional connectivity measurements derived from 7T rsfMRI. We found that temporal properties, specifically low-frequency signals of some large-scale brain networks, are associated with more severe cognitive impairment and vascular injury, highlighting the potential benefit of using rsfMRI for treatment planning and prediction of patient outcome after RT.

1242



Effects of EGR3 transfection on behavior and resting-state fMRI in rats and evaluation of risperidone treatment in schizophrenia model

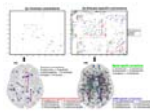
Xiaowei Han<sup>1,2</sup>, Guolin Ma<sup>1</sup>, and Lizhi Xie<sup>3</sup>

<sup>1</sup>Department of Radiology, China-Japan Friendship Hospital, Beijing, China, <sup>2</sup>Graduate School of Peking Union Medical College, Beijing, China, <sup>3</sup>GE Healthcare, MR Research China, Beijing, China

Schizophrenia is a neurodevelopmental psychiatric disorder with unclear etiology and no effective treatment. In this study, we established a new schizophrenia model in rats using early growth response (EGR3) gene transfection which was injected into the hippocampus and dentate gyrus of rats. The model was examined by evaluating the behavioral impact and cerebral alterations of schizophrenia model rats using behavioral phenotyping and resting-state functional magnetic resonance imaging (rs-fMRI). In addition, the efficacy of risperidone therapy was also evaluated in treated group rats. Briefly, we found several regional alterations in the cerebrum, which were consequently partially reversed by risperidone.

WITHDRAWN

1244



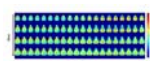
Estimation of stable whole-brain effective-connectivity characterization of mental disorders

Lipeng Ning<sup>1,2</sup> and Yogesh Rathi<sup>1,2</sup>

<sup>1</sup>Brigham and Women's Hospital, Boston, MA, United States, <sup>2</sup>Harvard Medical School, Boston, MA, United States

We propose an algorithm to estimate whole-brain effective connectivity measures by integrating structural connectivity matrix between brain regions and resting-state functional MRI data. Our algorithm first uses the Lyapunov inequality from control theory to ensure that the estimated whole-brain dynamic system is stable and physically meaningful. Then, the effective connectivity measure is characterized by a novel conditional causality measure. We applied the proposed algorithm to a public dataset which consisted of healthy controls (n=94), patients with schizophrenia (n=45), bipolar (n=44) and ADHD (n=37). Our results show that the proposed approach provides reliable estimation brain-network features of these brain disorders.

1245



Altered patterns of neural activity and functional connectivity revealed by dynamic rsfMRI in the Q175 mouse model of Huntington's disease

Tamara Vasilkovska<sup>1</sup>, Bram Callewaert<sup>1</sup>, Somaie Salajeghe<sup>1</sup>, Dorian Pustina<sup>2</sup>, Longbin Liu<sup>2</sup>, Mette Skinbjerg<sup>2</sup>, Celia Dominguez<sup>2</sup>, Ignacio Munoz-Sanjuan<sup>2</sup>, Annemie Van der Linden<sup>1</sup>, and Marleen Verhoye<sup>1</sup>

<sup>1</sup>Department of Biomedical Sciences, University of Antwerp, Antwerp, Belgium, <sup>2</sup>CHDI Foundation, Princeton, NJ, United States

Static FC changes in neurodegeneration can indicate underlining neural mechanism pathology present in pre-manifest disease stage. In addition to the spatial FC component, quasi-periodic patterns (QPPs) implement spatiotemporal information of neural activity, allowing integrated assessment of possible initial changes in large-scale brain dynamics. We measured Low Frequency (LF) BOLD changes using rsfMRI in Q175 HD mouse model at 3 and 12 months of age. Results indicate decreased FC between specific regions in heterozygous compared to wild-type mice at 12 months. Both at 3 and 12 months, additional QPPs are present in the heterozygous group, deviating from the wild type group.

1246



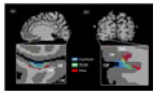
### Laminar fMRI using layer-specific optogenetic stimulations

Russell W Chan<sup>1</sup>, Mazen Asaad<sup>2</sup>, Bradley J Edelman<sup>1</sup>, Hyun Joo Lee<sup>1</sup>, Hillel Adesnik<sup>3</sup>, David Feinberg<sup>3</sup>, and Jin Hyung Lee<sup>1,4,5,6</sup>

<sup>1</sup>Neurology and Neurological Sciences, Stanford University, Stanford, CA, United States, <sup>2</sup>Molecular and Cellular Physiology, Stanford University, Stanford, CA, United States, <sup>3</sup>Helen Wills Neuroscience Institute, University of California, Berkeley, CA, United States, <sup>4</sup>Bioengineering, Stanford University, Stanford, CA, United States, <sup>5</sup>Neurosurgery, Stanford University, Stanford, CA, United States, <sup>6</sup>Electrical Engineering, Stanford University, Stanford, CA, United States

We attempted to establish the mesoscale layer-specific fMRI representation of neuronal activity using layer-specific Cre-driver mouse lines, optogenetic stimulations, fMRI and electrophysiological recordings. Although laminar fMRI responses were distinct during L2/3, L4, L5 and L6 stimulations, all fMRI responses increased along the cortical depth. This phenomenon was, however, not observed in LFP and spike recordings. This discrepancy between fMRI, LFP and spiking may be due to the draining veins transporting deoxyhemoglobin from the deeper layers to the superficial layers. Future studies may take into account of neurovasculature to elucidate the exact mechanisms of mesoscale layer-specific neurovascular coupling.

1247



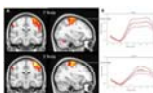
### Layer-dependent repetition suppression in the human visual cortex

Uk-Su Choi<sup>1,2</sup>, Seiji Ogawa<sup>3</sup>, and Ikuhiro Kida<sup>1,2</sup>

<sup>1</sup>Center for Information and Neural Networks, NICT, Suita, Japan, <sup>2</sup>Graduate School of Frontier Biosciences, Osaka University, Suita, Japan, <sup>3</sup>Kansei Fukushi Research Institute, Tohoku Fukushi University, Sendai, Japan

To examine the layer-dependent fMRI responses of face processing in human visual cortex, we acquired submillimeter functional and anatomical data at 7T. Here, we measured fMRI responses to left single and paired faces with various interstimulus intervals; furthermore, we calculated the repetition suppression (RS) ratio from three cortical layers in the right primary visual cortex (V1) and occipital face area (OFA). The fMRI response and RS ratio of superficial and middle layers of the right V1 were similar to those of all right OFA layers. Hence, the layers in different hierarchical visual areas were modulated in the same manner.

1248



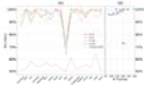
### Comparing stimulus and resting state fMRI at 3T and 7T reveal a superiority of 7T in detecting changes in subcortical networks

Silke Kreitz<sup>1,2</sup>, Angelika Mennecke<sup>1</sup>, Laura Cristina Konerth<sup>2</sup>, Armin Nagel<sup>3</sup>, Frederic Laun<sup>3</sup>, Michael Uder<sup>3</sup>, Arnd Doerfler<sup>1</sup>, and Andreas Hess<sup>2</sup>

<sup>1</sup>Department of Neuroradiology, University Hospital Erlangen, Friedrich-Alexander-University Erlangen-Nürnberg, Erlangen, Germany, <sup>2</sup>Institute of Experimental and Clinical Pharmacology and Toxicology, Friedrich-Alexander University Erlangen-Nürnberg, Erlangen, Germany, <sup>3</sup>Department of Radiology, University Hospital of the Friedrich-Alexander University Erlangen-Nürnberg, Erlangen, Germany

7T MRI is hoped to improve diagnostics, therapy and research of neurological diseases. Here, we characterize the influence of field strength on fMRI approaches including task based and RS-fMRI. Quality metrics revealed a basic separation of 3T and 7T fMRI data, mainly by tSNR, MDI, CNR and EFC. 7T fMRI showed higher BOLD response amplitudes, more functional connections and higher connectivity strength especially in inferior brain regions. Though higher variability between subjects at 7T likely requires enhanced statistical power in group comparisons, intra individual fMRI measurements might detect subtle connectivity changes at 7T useful for diagnosis and therapy.

1249



### Classifying Autism Spectrum Disorder Patients from Normal Subjects using a Connectivity-based Graph Convolutional Network

Lebo Wang<sup>1</sup>, Kaiming Li<sup>2</sup>, and Xiaoping Hu<sup>1,2</sup>

<sup>1</sup>Department of Electrical and Computer Engineering, University of California, Riverside, Riverside, CA, United States, <sup>2</sup>Department of Bioengineering, University of California, Riverside, Riverside, CA, United States

Traditional deep learning architectures have met with limited performance improvement on fMRI data analysis. Our connectivity-based graph convolutional network modeled fMRI data as graphs and performed convolutions within connectivity-based neighborhood. We demonstrate that our approach is substantially more robust in classifying Autism Spectrum Disorder (ASD) patients from normal subjects compared with those in published work. Extracting spatial features and averaging across frames are beneficial in reducing variance and improving classification accuracy.

## Oral

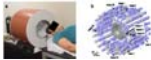
### Novel Hardware - New Directions in MR Systems

Thursday Parallel 5 Live Q&A

Thursday 15:05 - 15:50 UTC

Moderators: Andrew Webb

1250



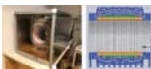
### A Point-of-Care MRI Scanner for Human Brain Imaging

Clarissa Zimmerman Cooley<sup>1,2</sup>, Patrick C McDaniel<sup>1,3</sup>, Jason P Stockmann<sup>1,2</sup>, Sai Abitha Srinivas<sup>1</sup>, and Lawrence L Wald<sup>1,2,4</sup>

<sup>1</sup>Athinoula A Martinos Center for Biomedical Imaging, Dept. of Radiology, Massachusetts General Hospital, Charlestown, MA, United States, <sup>2</sup>Harvard Medical School, Boston, MA, United States, <sup>3</sup>Dept. of Electrical Engineering, Massachusetts Institute of Technology, Cambridge, MA, United States, <sup>4</sup>Harvard-MIT Division of Health Sciences and Technology, Cambridge, MA, United States

Access to MRI scanners is limited by cost, size, and siting requirements. Specialized low-cost, compact, portable systems could greatly increase accessibility worldwide and enable point-of-care MRI. We present a portable MRI scanner for human brain imaging based on a compact 122kg Halbach cylinder with a built-in readout field. Designing for a built-in encoding field reduces the size of the magnet, the overall system power-consumption, cooling requirements, and acoustic noise. The generalized reconstruction method accounts for non-linearities in the gradient fields. T1 and T2-weighted in vivo images are presented with a resolution of 2x2x7mm.

1251



### Three-dimensional in-vivo human Imaging on a 50 mT low-cost portable Halbach Array

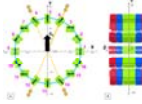
Thomas O'Reilly<sup>1</sup>, Wouter Teeuwisse<sup>1</sup>, Bart de Vos<sup>2</sup>, and Andrew Webb<sup>1</sup>

<sup>1</sup>C.J. Gorter Center for High Field MRI, Leiden University Medical Center, Leiden, Netherlands, <sup>2</sup>Circuits and Systems, Delft University of Technology, Delft, Netherlands



We show the first 3D in-vivo images acquired from our custom-built 50 mT low-cost Halbach based portable MRI scanner. 3D Images of a knee were acquired with a ~2 mm isotropic resolution using a 3D turbo spin echo sequence in less than 12 minutes. Gradient non-linearity induced image distortions are minimal within the central ~10 cm of the magnet bore length, but require correction beyond this point. These results represent the latest step towards our goal of creating a fully portable MRI scanner targeting pediatric neuroimaging in the developing world for less than 30 000 euros.

1252



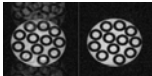
### Design of a Permanent Magnet for MRI of the Ankle on the International Space Station

Aaron R. Purchase<sup>1</sup>, Gordon E. Sarty<sup>2</sup>, Logi Vidarrson<sup>3</sup>, Keith Wachowicz<sup>1</sup>, Piotr Liszkowski<sup>4,5</sup>, Hongwei Sun<sup>1</sup>, Jonathan C. Sharp<sup>1</sup>, and Boguslaw Tomanek<sup>1,6</sup>

<sup>1</sup>Department of Oncology, University of Alberta, Edmonton, AB, Canada, <sup>2</sup>Department of Psychology and Division of Biomedical Engineering, University of Saskatchewan, Saskatoon, SK, Canada, <sup>3</sup>LT Imaging, Toronto, ON, Canada, <sup>4</sup>AGH University of Science and Technology, Krakow, Poland, <sup>5</sup>MRI-Tech Sp. z o.o, Krakow, Poland, <sup>6</sup>Institute of Nuclear Physics, Polish Academy of Sciences, Krakow, Poland

MRI is desired for monitoring bone and muscle deterioration in astronauts during long-term spaceflights and on the International Space Station (ISS). However, the magnet is generally too heavy to be transported to the ISS. Therefore, we designed a light (~10kg) magnet that allows transmit array spatial encoding (TRASE) MRI of the ankle on the ISS. The magnet is based on a sparse Halbach geometry with magnetic block-pairs. The positions of the block-pairs were optimized using a genetic algorithm. We intend to manufacture the magnet and test the entire MRI system on a Falcon 20 jet.

1253



### First Experiences with a Three-Bore Conduction-Cooled Cryogen-Free Extremity Scanner

Jerome L. Ackerman<sup>1,2</sup>, Shahin Pourrahimi<sup>3</sup>, Marcus Donaldson<sup>1,2</sup>, Nadder Pourrahimi<sup>3</sup>, Julien Rivoire<sup>4</sup>, Julien Muller<sup>4</sup>, Hizami Murad<sup>4</sup>, Ouri Cohen<sup>5</sup>, and Isabela Choi<sup>1</sup>

<sup>1</sup>Martinos Center, Dept of Radiology, Massachusetts General Hospital, Charlestown, MA, United States, <sup>2</sup>Department of Radiology, Harvard Medical School, Boston, MA, United States, <sup>3</sup>Superconducting Systems, Inc., Billerica, MA, United States, <sup>4</sup>RS2D, Mundolsheim, France, <sup>5</sup>Memorial Sloan Kettering Cancer Center, New York, NY, United States

We developed an MRI scanner designed for limb scanning based on a novel conduction-cooled three-bore cryogen-free 1.5T magnet. The two outer bores accommodate the unscanned leg for enhanced patient comfort. We describe the issues relevant to this unique magnet and scanner, including our solution to the field instability problem common in conduction-cooled MRI magnets. By recording the field variation as a function of the phase of the cold head cycle, a compensating waveform may be played out via the numerically-controlled oscillator of the scanner to reduce the periodic field excursion from 25 Hz to about 1-2 Hz.

WITHDRAWN

1255



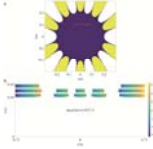
### Single sided magnet system for relaxometry and diffusion measurement

Dion Thomas<sup>1</sup>, Petrik Galvosas<sup>1</sup>, Paul D Teal<sup>2</sup>, Freya G Harrison<sup>3,4</sup>, Max Berry<sup>3,5</sup>, Yu-Chieh Tzeng<sup>3</sup>, and Sergei Obruchkov<sup>6</sup>

<sup>1</sup>School of Chemical and Physical Sciences, Victoria University of Wellington, Wellington, New Zealand, <sup>2</sup>School of Engineering and Computer Science, Victoria University of Wellington, Wellington, New Zealand, <sup>3</sup>Centre for Translational Physiology, University of Otago, Wellington, New Zealand, <sup>4</sup>Department of Surgery and Anaesthesia, University of Otago, Wellington, New Zealand, <sup>5</sup>Department of Paediatrics and Child Health, University of Otago, Wellington, New Zealand, <sup>6</sup>Robinson Research Institute, Victoria University of Wellington, Wellington, New Zealand

We have developed a new permanent magnet based single sided magnetic resonance system, which is suitable for relaxometry and diffusion measurement. Our design generates an external region of homogeneous  $B_0$  field, a sweet spot, from which signal can be detected. The magnet has been optimised to have a larger penetration depth and higher B field strength than currently existing systems. We have found the system provides good homogeneity and field strength, making it useful for relaxometry. Additionally, we demonstrate it can be used for diffusion-T2 measurements, which will allow further biomedical applications.

1256



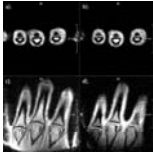
### A short-bore helium-off 7 T whole-body MRI superconducting magnet design

Yaohui Wang<sup>1</sup>, Qiuliang Wang<sup>1</sup>, Jianhua Liu<sup>1</sup>, Junsheng Cheng<sup>1</sup>, Zhongbiao Xu<sup>2</sup>, Zhifeng Chen<sup>3</sup>, and Feng Liu<sup>4</sup>

<sup>1</sup>Institute of Electrical Engineering, Chinese Academy of Sciences, Beijing, China, <sup>2</sup>Department of Radiotherapy Cancer Center, Guangdong Provincial People's Hospital & Guangdong Academy of Medical Science, Guangzhou, China, <sup>3</sup>School of Biomedical Engineering, Southern Medical University, Guangzhou, China, <sup>4</sup>School of Information Technology and Electrical Engineering, The University of Queensland, Brisbane, Australia

7T whole-body MRI system has received comprehensive praises from the worldwide users, but some patients feel claustrophobic when doing the scanning at the long tunnel. This work proposed a ultra-short design scheme for the 7 T MRI magnet, which is nearly a half of the presented commercial system. In addition, the magnet operates at helium-off environment, which saves the precious coolant liquid helium and is also convenient to maintain.

1257



### In vivo Two-photon Magnetic Resonance Imaging of Human Hand at 1T

Jianshu Chi<sup>1</sup>, Victor Han<sup>1</sup>, and Chunlei Liu<sup>1,2</sup>

<sup>1</sup>Electrical Engineering and Computer Sciences, University of California, Berkeley, Berkeley, CA, United States, <sup>2</sup>Helen Wills Neuroscience Institute, University of California, Berkeley, Berkeley, CA, United States

We demonstrate the first in vivo imaging experiment with a multiphoton excitation technique at 1T. To produce multiphoton excitation, we built a secondary RF coil that produces an RF field, parallel to the  $B_0$  field. Designed for kHz frequencies, this coil consists with two layers of traces in a spiral configuration on a printed circuit board (PCB). Adding this low-frequency coil to an Aspect 1T Wrist Scanner, we acquired gradient echo images with two-photon excitation of a human hand in vivo.

1258



### Improving Homogeneity in Delta Relaxation Enhanced Magnetic Resonance Using Boundary Element Method

Matthew A. McCready<sup>1</sup>, William B. Handler<sup>1</sup>, and Blaine A. Chronik<sup>1</sup>

<sup>1</sup>Physics and Astronomy, Western University, London, ON, Canada

Delta relaxation enhanced magnetic resonance (dreMR) is a field-shifting quantitative molecular imaging method using activatable MR probes. The dreMR method may be used to produce images with signal proportional to concentration of contrast agent and eliminate signal due to unbound agent. In this work we outline a novel design method for dreMR coils, using an inner layer of windings determined by the boundary element method (BEM). This new design method produces a strong, highly homogeneous field shift which, when coupled with a 0.5T MRI system and activatable MR probes, can reliably image on a larger volume than previous designs.

1259



### Wearable MRS system for blood glucose measurement: Proof of concept

Yongxian Qian<sup>1</sup>, Bei Zhang<sup>1</sup>, Shannon Haas<sup>1</sup>, and Aaron R. Chidake<sup>2</sup>

<sup>1</sup>Radiology, New York University, New York, NY, United States, <sup>2</sup>Endocrinology, New York University, New York, NY, United States

This study presents preliminary results supporting a new concept to build a wearable magnetic resonance spectroscopy (MRS) system for noninvasive blood glucose measurement in humans. Computer simulations, hardware buildups and subject studies demonstrated the promising of such a system.

## Oral

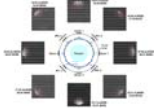
### Novel Hardware - Hardware Components

Thursday Parallel 5 Live Q&A

Thursday 15:05 - 15:50 UTC

Moderators: Aurelien Destruel & Ed Wu

1260



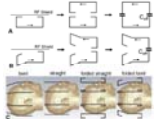
A novel interchangeable, double-tuned, twin head coil array design for <sup>1</sup>H/<sup>23</sup>Na MR imaging and <sup>1</sup>H/<sup>31</sup>P MR spectroscopy at 7 T

Chang-Hoon Choi<sup>1</sup>, Airat Galiamov<sup>1</sup>, Suk-Min Hong<sup>1</sup>, Jörg Felder<sup>1</sup>, Wieland A. Worthoff<sup>1</sup>, and N. Jon Shah<sup>1,2,3,4</sup>

<sup>1</sup>INM-4, Forschungszentrum Juelich, Juelich, Germany, <sup>2</sup>INM-11, Forschungszentrum Juelich, Juelich, Germany, <sup>3</sup>JARA-BRAIN-Translational Medicine, Aachen, Germany, <sup>4</sup>Department of Neurology, RWTH Aachen University, Aachen, Germany

X-nuclei MR offers unique access to important metabolic information in tissues. Multi-tuned coils are required for the X-nuclei measurements, but designing a well-performing coil is challenging. In this study, we present our novel design and performance evaluation of an interchangeable, twin, double-tuned, head coil array for <sup>1</sup>H/<sup>23</sup>Na MR imaging and <sup>1</sup>H/<sup>31</sup>P MR spectroscopy at 7 T. The outer proton array was built using an alternately positioned 4-channel dipole antenna and a 4-channel microstrip transmission line array to improve decoupling. The inner 8-channel X-nuclei loop arrays, orthogonal to the <sup>1</sup>H, were designed identically to enable conventionally switching between <sup>23</sup>Na and <sup>31</sup>P.

1261



Decoupling of Folded Dipole Antenna Elements of a Human Head Array at 9.4T.

Nikolai Avdievich<sup>1</sup>, Georgiy Solomakha<sup>2</sup>, Loreen Ruhm<sup>1</sup>, Anke Henning<sup>1,3</sup>, and Klaus Scheffler<sup>1,4</sup>

<sup>1</sup>Max Planck Institute for Biological Cybernetics, Tuebingen, Germany, <sup>2</sup>Nanophotonics and Metamaterials, ITMO University, St. Petersburg, Russian Federation, <sup>3</sup>Advanced Imaging Research Center, University of Texas Southwestern Medical Center, Dallas, TX, United States, <sup>4</sup>Department for Biomedical Magnetic Resonance, University of Tübingen, Tuebingen, Germany

Dipole antennas have been successfully utilized at ultra-high fields (UHF, >7 T) as elements of human body arrays. Usage of dipoles for UHF human head arrays is still under development. In this case, dipoles must be made much shorter, and placed at a relatively large distance to the head. As a result, dipoles are not well loaded and are often purely decoupled. In this work, we developed a novel method of decoupling of adjacent dipole antennas, and used this technique while constructing a novel 9.4 T human head TxRx dipole array coil. The array demonstrates good decoupling and full-brain coverage.

1262



Dual-Stream iPRES-W Head Coil Array for MR Imaging, Wireless Respiratory Tracking, and Wireless Localized B<sub>0</sub> Shimming

Jonathan Cuthbertson<sup>1,2</sup>, Trong-Kha Truong<sup>1,2</sup>, Vani Yadav<sup>1,2</sup>, Fraser Robb<sup>3</sup>, Allen Song<sup>1,2</sup>, and Dean Darnell<sup>1,2</sup>

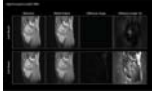
<sup>1</sup>Brain Imaging and Analysis Center, Duke University, Durham, NC, United States, <sup>2</sup>Medical Physics Graduate Program, Duke University, Durham, NC, United States, <sup>3</sup>GE Healthcare Inc., Aurora, OH, United States





The integrated RF/wireless coil design enables MRI imaging and wireless data transfer with the same coil thereby reducing the number of wired connections in the scanner. Here, we implement this design onto a 48-channel head coil array to enable two independent wireless data streams for two separate applications, specifically, wireless 1) control of the DC currents used for  $B_0$  shimming and 2) respiratory tracking with a respiratory belt. In vivo experiments in the brain showed that this coil array significantly reduced  $B_0$  inhomogeneities (-41%) and EPI distortions while simultaneously streaming respiratory data from the subject without data loss.

1263



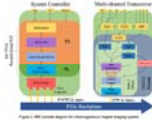
### Harmonic Balance Modeling of MRI Preamp Impairments

Chris Vassos<sup>1</sup>, Fraser Robb<sup>2</sup>, Shreyas Vasanawala<sup>3</sup>, John Pauly<sup>1</sup>, and Greig Scott<sup>1</sup>

<sup>1</sup>Electrical Engineering, Stanford University, Stanford, CA, United States, <sup>2</sup>GE Healthcare, Aurora, OH, United States, <sup>3</sup>Radiology, Stanford University, Stanford, CA, United States

A Silicon Germanium alternative to standard HEMT pre-amplifiers is proposed. This is intended to ameliorate the high power consumption associated with current implementations for the wireless use case in which power is a limiting factor. The proposed pre-amp is evaluated for linearity and gain through a behavioral model that is extracted from SPICE simulation to process k-space data. It is found that the non-linearities introduced by the SiGe device begin to have an impact on image quality in high dynamic range cases. This encourages further investigation into SiGe devices as low-power preamplifiers.

1264



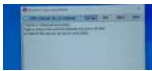
### An Open-Source Multichannel MRI Console

Guang Yang<sup>1</sup>, Sergei Obruchkov<sup>2</sup>, and Robin Dykstra<sup>1</sup>

<sup>1</sup>School of Engineering and Computer Science, Victoria University of Wellington, Wellington, New Zealand, <sup>2</sup>Robinson Research Institute, Victoria University of Wellington, Wellington, New Zealand

This abstract describes the development of a complete multi-channel MRI console that can be the basis for many MR projects. To support the growing open-source hardware MR community we are making a collection of PXIe modules and IP available to anyone to use and develop applications on. A System Controller Board, a 2-channel Tx and 4-channel Rx transceiver board, an FMC General Purpose Module, PXIe data transfer engine IP, Linux API and device drivers can be accessed online <https://github.com/mr-kit/>.

1265



### Misappropriation of the Scanner Synchronization Trigger for Serial Communication with any UART Device

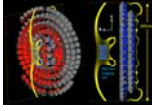
Andrew Dupuis<sup>1</sup>, Dominique Franson<sup>1</sup>, Nicole Seiberlich<sup>2</sup>, and Mark A Griswold<sup>1,3</sup>

<sup>1</sup>Biomedical Engineering, Case Western Reserve University, Cleveland, OH, United States, <sup>2</sup>Radiology, University of Michigan, Ann Arbor, MI, United States, <sup>3</sup>Department of Radiology, School of Medicine, Case Western Reserve University, Cleveland, OH, United States

Clinical MRI scanners are not designed to allow for easy communication with 3rd party devices, whether for development or clinical purposes. However, most modern scanners provide a synchronization trigger interface that is sequence (and therefore research-user) controllable. We investigated using the synchronization trigger as a serial data output for arbitrary data, and successfully implemented a 192 kilobaud simplex serial interface that can be implemented within any sequence to enable arbitrary data transfer to and control of any external UART device. This opens significant opportunities for 3rd party hardware and software research without manufacturer consent or firmware changes.

1266

Single-sided magnet design for an MR guided lumbar puncture (LP) device



Clarissa Zimmerman Cooley<sup>1,2</sup>, Patrick C McDaniel<sup>1,3</sup>, Jason P Stockmann<sup>1,2</sup>, Farrah J Mateen<sup>2,4</sup>, and Lawrence L Wald<sup>1,2,5</sup>

<sup>1</sup>Athinoula A Martinos Center for Biomedical Imaging, Dept. of Radiology, Massachusetts General Hospital, Charlestown, MA, United States, <sup>2</sup>Harvard Medical School, Boston, MA, United States, <sup>3</sup>Dept. of Electrical Engineering, Massachusetts Institute of Technology, Cambridge, MA, United States, <sup>4</sup>Dept. of Neurology, Massachusetts General Hospital, Boston, MA, United States, <sup>5</sup>Harvard-MIT Division of Health Sciences and Technology, Cambridge, MA, United States

Lumbar Punctures (LP) are generally guided by palpation only without visualization of the internal anatomy, leading to repeat attempts and/or avoidance in difficult cases. Image guidance with US and X-ray is possible, but US has poor depth and CSF contrast and radiation from X-ray complicates Point of Care (POC) use. We present a magnet design for a POC MR guided LP device that will couple to a mechanical track for needle insertion. The single-sided magnet is an NdFeB array and achieves a 40mT field and ~50mT/m built-in gradient in the ROI. Simulations of the magnet and imaging procedure are presented.

1267



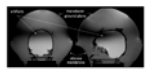
A deflatable positionally-localized Virtual Biopsy "Gun": Construct and initial testing

Ehud J Schmidt<sup>1,2</sup>, Yue Chen<sup>3</sup>, Anthony Gunderman<sup>3</sup>, Junichi Tokuda<sup>4</sup>, Hassan Elahi<sup>5</sup>, Ravi T Seethamraju<sup>6</sup>, Henry R Halperin<sup>5</sup>, and Akila N Viswanathan<sup>2</sup>

<sup>1</sup>Medicine (Cardiology), The Johns Hopkins University, Baltimore, MD, United States, <sup>2</sup>Radiation Oncology, Johns Hopkins University, Baltimore, MD, United States, <sup>3</sup>Mechanical Engineering, University of Arkansas, Fayetteville, AR, United States, <sup>4</sup>Radiology, Brigham and Womens Hospital, Boston, MA, United States, <sup>5</sup>Medicine (Cardiology), Johns Hopkins University, Baltimore, MD, United States, <sup>6</sup>MRI, Siemens Healthineers, Boston, MA, United States

Evaluating tissue properties prior-to or during therapy, such as locating cancerous and necrotic cells, or characterizing response to radiation or ablation, is conventionally performed by tissue excision, followed by pathologic examination. An alternative is diagnosing tissue *in-situ* without removing it, as performed using Optical-Coherence-Tomography or Intra-Vascular-UltraSound. We aim to perform tissue definition in soft-tissues not accessed through body-orifices or blood-vessels by combining; (1) Steerable tissue-puncture, (2) MR-Tracking-motion-localization, and (3) imaging along the punctured-holes' walls. Utilization requires rapid high-CNR multiple-contrast MRI. A deflatable virtual-biopsy "gun" for diagnosing cervical-cancer radiation-therapy response was developed. It imaged ~15mm surrounding punctured-holes created for brachytherapy seed-delivery.

1268

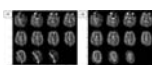


Improving Image Quality in Transcranial Magnetic Resonance Guided focused Ultrasound Using a Conductive Screen

J. Rock Hadley<sup>1</sup>, Henrik Odeen<sup>2</sup>, Robb Merrill<sup>2</sup>, Sam Adams<sup>2</sup>, Viola Rieke<sup>2</sup>, Allison Payne<sup>2</sup>, and Dennis Parker<sup>2</sup>

<sup>1</sup>Radiology and Imaging Sciences, University of Utah, Salt Lake City, UT, United States, <sup>2</sup>University of Utah, Salt Lake City, UT, United States

This work uses an RF screen, placed over the top of a human skull phantom, to reduce image banding artifacts that are common in transcranial transducer MRI. The goals of the study are to improve imaging homogeneity over the region of the brain by changing RF field patterns that cause the artifacts, and to find a solution that doesn't attenuate or distort the ultrasound properties of the transducer. Hydrophone and focused ultrasound heating studies are performed to measure ultrasound screen transparency and MRI studies are performed to evaluate the effects the screen has on homogeneity and artifact reduction.



Retrospective Electromagnetic interference mitigation in a portable low field MRI system

Sai Abitha Srinivas<sup>1</sup>, Clarissa Z Cooley<sup>1,2</sup>, Jason P Stockmann<sup>1,2</sup>, Patrick C McDaniel<sup>1,3</sup>, and Lawrence L Wald<sup>1,2,4</sup>



<sup>1</sup>Athinoula A Martinos Center for Biomedical Imaging, Charlestown, MA, United States, <sup>2</sup>Harvard Medical School, Boston, MA, United States, <sup>3</sup>Dept. of Electrical Engineering, Massachusetts Institute of Technology, Cambridge, MA, United States, <sup>4</sup>Harvard-MIT Division of Health Sciences and Technology, Cambridge, MA, United States

The performance of a low field Point of Care (POC) MRI system operating outside an RF shielded room is adversely affected by the presence of electromagnetic interference signals, which produce image artifacts, sometimes complicated enough to be confused with image noise. We demonstrate a post-processing interference suppression technique using an external reference coil and dynamically updated transfer function to detect the interference and remove it from the imaging data.

## Oral - Power Pitch

### Novel Hardware - Engineering in MR & Beyond

Thursday Parallel 5 Live Q&A

Thursday 15:05 - 15:50 UTC

Moderators: Stephan Orzada

1270



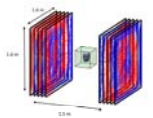
#### Implementation of Low-cost FPGA-based Magnetic Particle Imaging System

Congcong Liu<sup>1,2</sup>, Caiyun Shi<sup>1</sup>, Jianguo Cui<sup>2</sup>, Xin Liu<sup>1</sup>, Hairong Zheng<sup>1</sup>, Dong Liang<sup>1</sup>, and Haifeng Wang<sup>1</sup>

<sup>1</sup>Shenzhen Institutes of Advanced Technology, Chinese Academy of Sciences, Shenzhen, China, <sup>2</sup>Chongqing University of Technology, Chongqing, China

Conventional Magnetic Particle Imaging (MPI) systems are expensive and bulky, and most of them use CPU and MPU as controllers. Field Programmable Gate Arrays (FPGAs) have recently become widely utilized as controllers in many systems for flexibility and speed. In this paper, we proposed an implementation scheme of a low-cost, small-volume MPI system based on FPGA architecture. The experimental results showed that the complete operation of the MPI system signal link could be realized by the low-cost FPGA-based control system ( $\leq \$200$ ), and the distribution of the superparamagnetic iron oxide nanoparticles (SPION) could be imaged by the signal of the particle.

1271



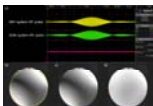
#### A wearable 50-channel magnetoencephalography (MEG) system

Ryan Hill<sup>1</sup>, Elena Boto<sup>1</sup>, Niall Holmes<sup>1</sup>, Gillian Roberts<sup>1</sup>, Jim Leggett<sup>1</sup>, Zelekha Seedat<sup>1</sup>, Molly Rea<sup>1</sup>, Tim Tierney<sup>2</sup>, Stephanie Mellor<sup>2</sup>, Vishal Shah<sup>3</sup>, James Osborne<sup>3</sup>, Gareth Barnes<sup>4</sup>, Richard Bowtell<sup>1</sup>, and Matthew Brookes<sup>1</sup>

<sup>1</sup>Sir Peter Mansfield Imaging Centre, University of Nottingham, Nottingham, United Kingdom, <sup>2</sup>Wellcome Centre for Human Neuroimaging, UCL, London, United Kingdom, <sup>3</sup>QuSpin Inc., Louisville, CO, United States, <sup>4</sup>Wellcome Trust Centre for Neuroimaging, UCL, London, United Kingdom

We have developed a wearable magnetoencephalography (MEG) system comprising 50, miniaturised optical pumped magnetometers (OPMs) fixed on an EEG-type cap. Large, bi-planar field and field-gradient coils sited inside a magnetically shielded room reduce the field around the head to  $< 1$  nT. This allows the subject to move their head during experiments without confounding the OPM signals. We report results from a simple finger abduction paradigm and a motor learning experiment in which a subject learns to play the ukulele. The results demonstrate the potential of OPM-MEG to overcome some limitations of neuroimaging investigations using fixed, cumbersome scanners.

1272



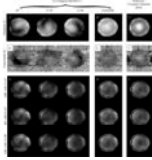
#### Triggered software defined radio for parallel transmission MRI research

Fred Tam<sup>1</sup>, Benson Yang<sup>1</sup>, and Simon J Graham<sup>1,2</sup>

<sup>1</sup>Physical Sciences, Sunnybrook Research Institute, Toronto, ON, Canada, <sup>2</sup>Department of Medical Biophysics, University of Toronto, Toronto, ON, Canada

Building a flexible setup for parallel transmission (PTx) MRI research is still challenging. A commercial software defined radio device was tested for suitability in a revised setup. Software was developed to make the device generate radiofrequency (RF) bursts in response to triggers. Preliminary bench tests showed quick and reliable triggering, consistent amplitude and phase across channels, and successful runtime adjustment. An initial PTx MRI demonstration showed capability for RF shimming in echo planar imaging of a phantom. Further troubleshooting is planned to reduce observed phase jitter, but the setup is already capable of a range of PTx research applications.

1273



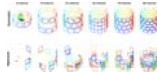
#### Time-multiplexed Excitation and Acquisition (TEA) with Rotating RF Coil Array (RRFCA)

Jin Jin<sup>1,2,3</sup>, Zhentao Zuo<sup>4,5</sup>, Mingyan Li<sup>2</sup>, Ewald Weber<sup>2</sup>, Aurelien Destruel<sup>2</sup>, Feng Liu<sup>2</sup>, Rong Xue<sup>4,5</sup>, and Stuart Crozier<sup>2</sup>

<sup>1</sup>Siemens Healthcare Pty Ltd, Brisbane, Australia, <sup>2</sup>The University of Queensland, St Lucia, Australia, <sup>3</sup>University of Southern California, Los Angeles, CA, United States, <sup>4</sup>Institute of Biophysics, Chinese Academy of Sciences, Beijing, China, <sup>5</sup>Sino-Danish College, University of Chinese Academy of Sciences, Beijing, China

RF shimming, by means of adjusting the relative amplitudes and phases of the independent transmit channels of a parallel transmit system, is widely used in ultra-high-field imaging to improve transmit homogeneity but has limited capabilities especially for large fields of view. This work designed and tested an 8-channel rotating transceiver array to provide more degrees-of-freedom for both transmission and reception. During transmission, the array achieved a uniform effective transmit magnetic field in a time-multiplexed fashion; during reception, the array provided more unique sensitivity profiles, facilitating higher image SNR. Parallel-imaging-like reconstruction was developed, assisted by a robust self-calibrated sensitivity estimation technique.

1274



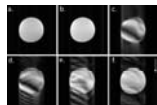
#### An optimized multi-coil shim setup matching inhomogeneity distribution in the human brain; positive and negative aspects

Ali Aghaeifar<sup>1</sup>, Jiazheng Zhou<sup>1</sup>, Feng Jia<sup>2</sup>, Maxim Zaitsev<sup>2</sup>, and Klaus Scheffler<sup>1</sup>

<sup>1</sup>Max Planck Institute for Biological Cybernetics, Tuebingen, Germany, <sup>2</sup>Dept. of Radiology, Medical Physics, Medical Center University of Freiburg, Faculty of Medicine, University of Freiburg, Freiburg, Germany

Multi-coil shim setup is a popular choice for  $B_0$  shimming. In contrast to conventional regular arrangement of the shim coils, one can effectively position the shim coil to match inhomogeneity distribution in the human brain. In this work, a comparison between regular and optimized arrangement of the local coils in a multi-coil shim setup is performed and the pros and cons of each design are evaluated.

1275



#### Imaging artefacts during simultaneous in-beam MR imaging and proton pencil beam irradiation

Sebastian Gantz<sup>1,2</sup>, Volker Hietschold<sup>3</sup>, Sergej Schneider<sup>1,2,4</sup>, and Aswin Louis Hoffmann<sup>1,2,5</sup>

<sup>1</sup>Institute of Radiooncology-OncoRay, Helmholtz-Zentrum Dresden - Rossendorf, Dresden, Germany, <sup>2</sup>OncoRay – National Center for Radiation Research in Oncology, Faculty of Medicine and University Hospital Carl Gustav Carus, Technische Universität Dresden, Helmholtz-Zentrum Dresden-Rossendorf, Dresden, Germany, <sup>3</sup>Department of Radiology, Faculty of Medicine and University Hospital Carl Gustav Carus, Technische Universität Dresden, Dresden, Germany, <sup>4</sup>Technische Universität Dresden, Carl Gustav Carus Faculty of Medicine, Dresden, Germany, <sup>5</sup>Department of Radiotherapy and Radiation Oncology, Faculty of Medicine and University Hospital Carl Gustav Carus, Technische Universität Dresden, Dresden, Germany

The targeting precision of proton therapy is expected to benefit from real-time MRI guidance. We developed a setup of a first prototype *in-beam* MRI scanner with a proton pencil beam scanning nozzle. Dipole magnets in the nozzle used for beam steering produce time-dependent magnetic fringe fields that may interfere with the MR image acquisition. In this study, we show that vertical beam steering shows no degradation of the MR image quality, whereas horizontal beam steering introduces severe ghosting artefacts in phase encoding direction. The origin of these artefacts is unraveled and strategies to eliminate or correct these artefacts are proposed.

1276



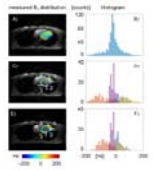
#### Low-profile AC/DC coils without RF Chokes

Jixin Xia<sup>1,2</sup>, Charlotte R. Sappo<sup>1,3</sup>, William A. Grissom<sup>1,3,4</sup>, and Xinqiang Yan<sup>3,4</sup>

<sup>1</sup>Department of Biomedical Engineering, Vanderbilt University, Nashville, TN, United States, <sup>2</sup>Department of Electrical Engineering, Vanderbilt University, Nashville, TN, United States, <sup>3</sup>Vanderbilt University Institute of Imaging Science, Nashville, TN, United States, <sup>4</sup>Department of Radiology, Vanderbilt University Medical Center, Nashville, TN, United States

Large RF chokes increase the inductance/resistance of the DC loop and thus lead to unwanted power dissipation and bulk. We theoretically analyzed the added coil loss induced by bridge inductors in AC/DC coils and found that large bridge chokes can be replaced by low-profile inductors with much smaller values, if the capacitance is adjusted to compensate the resonance frequency shift. This will reduce the footprint of AC/DC coils as well as the inductance/resistance and thus power dissipation, with a cost of slightly higher coil loss.

1277



#### Considerations for Cardiac Phase-Specific B<sub>0</sub> Shimming at 7 T

Michael Hock<sup>1</sup>, Maxim Terekhov<sup>1</sup>, Markus Johannes Ankenbrand<sup>1</sup>, David Lohr<sup>1</sup>, Theresa Reiter<sup>1,2</sup>, Christoph Juchem<sup>3</sup>, and Laura Maria Schreiber<sup>1</sup>

<sup>1</sup>Chair of Cellular and Molecular Imaging, Comprehensive Heart Failure Center (CHFC), University Hospital Wuerzburg, Wuerzburg, Germany, <sup>2</sup>Department of Internal Medicine I, University Hospital Wuerzburg, Wuerzburg, Germany, <sup>3</sup>Departments of Biomedical Engineering and Radiology, Columbia University, New York City, NY, United States

Spatio-temporal inhomogeneities of the static magnetic (B<sub>0</sub>) field are a major limiting factor in cardiac magnetic resonance applications at 7T. A previously developed shim strategy was demonstrated to correct spatial myocardial B<sub>0</sub>-field inhomogeneities in a preliminary *in vivo* implementation. To correct localized spots of B<sub>0</sub>-inhomogeneities, third-order terms were found to be beneficial. Cardiac phase-specific shimming was evaluated in simulations based on the *in vivo* field map data, and optimal shim settings were shown to differ between cardiac phases. Future work will address the application of a shim averaged over all cardiac phases to each individual phase.

1278



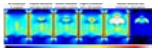
#### A compact vertical 1.5T human head scanner with shoulders outside the bore and window for studying motor coordination

Michael Garwood<sup>1</sup>, Michael Mullen<sup>1</sup>, Naoharu Kobayashi<sup>1</sup>, Lance delaBarre<sup>1</sup>, Steven Suddarth<sup>1</sup>, Djaudat Idiyatullin<sup>1</sup>, John Strupp<sup>1</sup>, Gregor Adriany<sup>1</sup>, Jarvis Haupt<sup>1</sup>, Alex Gutierrez<sup>1</sup>, Taylor Froelich<sup>1</sup>, Russell Lagore<sup>1</sup>, Benjamin Parkinson<sup>2</sup>, Konstantinos Bouloukakis<sup>2</sup>, Mark Hunter<sup>2</sup>, Mathieu Szmigiel<sup>2</sup>, Mailin Lemke<sup>2</sup>, Edgar Rodriguez-Ramirez<sup>2</sup>, Robin de Graaf<sup>3</sup>, Chathura Kumaragamage<sup>3</sup>, Scott McIntyre<sup>3</sup>, Terry Nixon<sup>3</sup>, Christoph Juchem<sup>4</sup>, Sebastian Theilenberg<sup>4</sup>, Yun Shang<sup>4</sup>, Jalal Ghazouani<sup>4</sup>, Alberto Tannús<sup>5</sup>, Mateus José Martins<sup>5</sup>, Edson Vidoto<sup>5</sup>, Fernando Paiva<sup>5</sup>, Daniel Pizetta<sup>5</sup>, Maurício Falvo<sup>5</sup>, Diego Turibio<sup>5</sup>, Christian Bones<sup>5</sup>, Eduardo Falvo<sup>5</sup>, John Thomas Vaughan<sup>4</sup>, Julie Kabil<sup>4</sup>, Hazal Yüksel<sup>4</sup>, Harish Krishnaswamy<sup>4</sup>, Sung-Min Sohn<sup>6</sup>, and Ramon Gilberto Gonzalez<sup>7</sup>

<sup>1</sup>Center for Magnetic Resonance Research, University of Minnesota, Minneapolis, MN, United States, <sup>2</sup>Victoria University of Wellington, Wellington, New Zealand, <sup>3</sup>Yale University, New Haven, CT, United States, <sup>4</sup>Columbia University, New York, NY, United States, <sup>5</sup>Centro de Imagens e Espectroscopia por Ressonância Magnética, Universidade de São Paulo in São Carlos, São Carlos, Brazil, <sup>6</sup>Arizona State University, Tempe, AZ, United States, <sup>7</sup>MGH/Harvard, Boston, MA, United States

A multi-disciplinary team of researchers in a multi-institutional consortium have designed and are building an easily relocatable head-only 1.5T MRI scanner weighing only ~500 kg. The goal is to develop a radically new type of MRI scanner that will enhance brain research, and ultimately, enable the diagnosis of neurological diseases in underserved populations throughout the world where MRI scanners are currently unavailable. To image with this system, pulse sequences have been developed and implemented to generate images using a highly inhomogeneous  $B_0$ .

1279



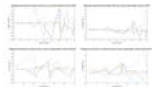
Improvement of SNR in MRgFUS with Strategic Design of Bath Medium and Transducer Ground Plane

Christopher M. Collins<sup>1,2</sup>, Ryan Brown<sup>1</sup>, and Daniel K. Sodickson<sup>1</sup>

<sup>1</sup>New York University School of Medicine, New York, NY, United States, <sup>2</sup>Center of Advanced Imaging, Innovation, and Research (CAI2R), New York, NY, United States

By adjusting the electrical permittivity of the material in the bath and adding slots to the conductive ground for the ultrasound array in MR-guided focused ultrasound it is possible to go from a situation where the ultrasound array and associated fluid bath detrimentally affect the RF fields for MRI and prohibit effective imaging in the Region of Interest, to where they actually enhance it, thereby improving image quality.

1280



Motion detection using reflected signals from an eight channel parallel transmit head coil at 7T

Hans Hoogduin<sup>1</sup>, Mark Gosselink<sup>1</sup>, Giel Mens<sup>1</sup>, Wim Prins<sup>2</sup>, Tijl van der Velden<sup>1</sup>, and Dennis Klomp<sup>1</sup>

<sup>1</sup>UMCU, Utrecht, Netherlands, <sup>2</sup>Philips, Best, Netherlands

Directional couplers are used to measure reflected waves from an eight channel PTx coil to detect head motion at 7T. The method doesn't require any changes to pulse sequences and has no time penalty. A general linear model is used to predict head motion from the signals measured at the couplers.

1281



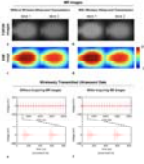
Multi-Channel RF Power and Phase Supervision Systems Technology for Thermal Magnetic Resonance: Development, Evaluation and Application

Haopeng Han<sup>1</sup>, Thomas Wilhelm Eigentler<sup>1</sup>, Eckhard Grass<sup>2,3</sup>, and Thoralf Niendorf<sup>1,4,5</sup>

<sup>1</sup>Berlin Ultrahigh Field Facility (B.U.F.F.), Max Delbrück Center for Molecular Medicine in the Helmholtz Association, Berlin, Germany, <sup>2</sup>IHP – Leibniz-Institut für innovative Mikroelektronik, Frankfurt (Oder), Germany, <sup>3</sup>Institute of Computer Science, Humboldt-Universität zu Berlin, Berlin, Germany, <sup>4</sup>Experimental and Clinical Research Center (ECRC), a joint cooperation between the Charité Medical Faculty and the Max Delbrück Center for Molecular Medicine, Berlin, Germany, <sup>5</sup>MRI.TOOLS GmbH, Berlin, Germany

Thermal Magnetic Resonance makes use of the physics of radio frequency waves applied at ultrahigh field-MRI. To achieve precise energy focal point formation, accurate thermal dose control and safety management, the transmitted RF signal amplitude and phase need to be supervised and regulated in real-time. In this work, a multi-channel power and phase supervision module was developed, evaluated and applied as an integral part of the Thermal MR hardware system. Preliminary experiments were conducted to demonstrate that the proposed module is suitable and essential for RF heating using a hybrid Thermal MR approach.

1282



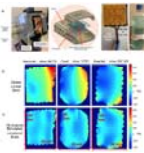
### Integrated RF/Wireless Coil and Ultrasound-Based Sensors to Enable Wireless Physiological Motion Monitoring in MRI

Devin Willey<sup>1,2</sup>, Julia Bresticker<sup>1,2</sup>, Trong-Kha Truong<sup>1,2</sup>, Allen Song<sup>1,2</sup>, Bruno Madore<sup>3</sup>, and Dean Darnell<sup>1,2</sup>

<sup>1</sup>Brain Imaging and Analysis Center, Duke University, Durham, NC, United States, <sup>2</sup>Medical Physics Graduate Program, Duke University, Durham, NC, United States, <sup>3</sup>Department of Radiology, Brigham and Women's Hospital, Harvard Medical School, Boston, MA, United States

An integrated RF/wireless coil, used to wirelessly transmit data and acquire MR images, and small ultrasound-based sensors, used to monitor physiological motion and correct MRI artifacts, were combined to enable wireless transmission of 1-MHz ultrasound data acquired from the sensors. Experiments were performed to validate that the coil could wirelessly transmit ultrasound data 1) while taking MR images and 2) from inside and outside the bore to a computer. This integrated system improves the mobility of the OCM sensors, thereby enabling them to accompany patients throughout the hospital, and demonstrates the coil's ability to transmit high-fidelity analog data while imaging.

1283



### B0 Shim Array Integrated into a Solenoid TRX Coil for Localized B0 in Permanent Magnet Scanners

Rafael Limgenco Calleja<sup>1</sup>, Celine Jeyda Veys<sup>1</sup>, and Michael Lustig<sup>1</sup>

<sup>1</sup>Electrical Engineering and Computer Sciences, University of California, Berkeley, Berkeley, CA, United States

Low-to-mid field systems have nearly been abandoned for high-field, high-performance systems. However, recent improvements in MR hardware, algorithms and computation are stimulating a resurgence in interest of upgrading lower-end magnets to achieve high-performance at significantly lower cost, improved accessibility, portability and siting. Here, we look at upgrading a wrist/animal 1T permanent-magnet system. We integrate a simple  $B_0$  array into a solenoid TRX coil for reducing  $B_0$  through localized targeted shimming. We demonstrate potential for improved field homogeneity with simulations, and demonstrate homogeneity improvements using a 6-channel prototype array with negligible effects on the transmit field and received SNR.

## Sunrise Session

### Emerging Clinical Applications in Musculoskeletal MRI Q&A - Emerging Clinical Applications in Musculoskeletal MR Imaging: Whole-Body Musculoskeletal Imaging

Organizers: Riccardo Lattanzi, Kimberly Amrami, Jung-Ah Choi, Jan Fritz, Miika Nieminen, Hiroshi Yoshioka

Thursday Parallel 1 Live Q&A

Thursday 15:50 - 16:35 UTC

Moderators: Erin Englund

Whole-Body MRI for Musculoskeletal Radiologists: Technical

Laura Fayad

Whole-Body MRI for Musculoskeletal Radiologists: Clinical Applications & Considerations

Stephen Broski

## Sunrise Session

### Emerging Clinical Applications in Musculoskeletal MRI Q&A - Emerging Clinical Applications in Musculoskeletal MR Imaging: Neuromuscular Imaging

Organizers: Riccardo Lattanzi, Kimberly Amrami, Jung-Ah Choi, Jan Fritz, Miika Nieminen, Hiroshi Yoshioka

Thursday Parallel 1 Live Q&A

Thursday 15:50 - 16:35 UTC

MRI for Neuromuscular Imaging: Technical

Martijn Froeling

MRI for Neuromuscular Imaging: Clinical  
Harmen Reyngoudt

---

---

### Sunrise Session

#### Emerging Clinical Applications in Musculoskeletal MRI Q&A - Emerging Clinical Applications in Musculoskeletal MR Imaging: Osteoarthritis

Organizers: Riccardo Lattanzi, Kimberly Amrami, Jung-Ah Choi, Jan Fritz, Miika Nieminen, Hiroshi Yoshioka

Thursday Parallel 1 Live Q&A

Thursday 15:50 - 16:35 UTC

Moderators: Manushka Vaidya

MRI of Osteoarthritis: Technical  
Valentina Pedoia

---

MRI of Osteoarthritis: Clinical  
Shadpour Demehri

---

---

### Sunrise Session

#### Emerging Clinical Applications in Musculoskeletal MRI Q&A - Emerging Clinical Applications in Musculoskeletal MR Imaging: Imaging of Tendinopathy

Organizers: Riccardo Lattanzi, Kimberly Amrami, Jung-Ah Choi, Jan Fritz, Miika Nieminen, Hiroshi Yoshioka

Thursday Parallel 1 Live Q&A

Thursday 15:50 - 16:35 UTC

Quantitative Ultrashort Echo Time MR Imaging of Tendon  
Yajun Ma

---

MR Imaging of Tendinopathy: Clinical  
Edwin Oei

---

---

### Sunrise Session

#### Hands-on Physics and Engineering Sunrise Q&A - EM Simulations in MRI

Thursday Parallel 5 Live Q&A

Thursday 15:50 - 16:35 UTC

EM Simulations for MRI Safety  
Kyoko Fujimoto

---

Hands-On Modeling  
Özlem Ipek

---

---

### Sunrise Session

#### Hands-on Physics and Engineering Sunrise Q&A - Hands-On: Making Custom Electronics

Organizers: Greig Scott, Yunhong Shu

Thursday Parallel 5 Live Q&A

Thursday 15:50 - 16:35 UTC

Moderators: Irena Zivkovic

Do-It-Yourself Electronics for MRI  
Natalia Gudino

---

The Design & Implementation of Digital Receivers for MRI  
Robin Dykstra

---

---



---

## Sunrise Session

### Hands-on Physics and Engineering Sunrise Q&A - Hands-On: Pulse Sequence & RF Pulse Design

Organizers: Kawin Setsompop, Mariya Doneva

Thursday Parallel 5 Live Q&A

Thursday 15:50 - 16:35 UTC

[Open-Source Pulse Sequence Programming](#)

Tony Stoecker

---

[Open-Source RF Pulse Design & Demo](#)

Jonathan Martin

---

---

## Sunrise Session

### Hands-on Physics and Engineering Sunrise Q&A - Hands-On: Image Reconstruction

Organizers: Mariya Doneva

Thursday Parallel 5 Live Q&A

Thursday 15:50 - 16:35 UTC

[Step-by-Step Iterative SENSE Reconstruction](#)

Zhaolin Chen

---

[Step-by-Step Reconstruction Using Learned Dictionaries](#)

Jon Tamir

---

---

## Weekday Course

### Brain-Gut Axis and AI in Neuroimaging - The Brain-Gut Axis: Imaging the Superorganism

Organizers: C. C. Tchoyoson Lim, Nivedita Agarwal

Thursday Parallel 2 Live Q&A

Thursday 15:50 - 16:35 UTC

Moderators: C. C. Tchoyoson Lim & Zhongming Liu

[Neuroimaging the Gut-Brain Axis: Influence of the Gut Microbiome on Brain Microstructure](#)

John-Paul J. Yu<sup>1</sup>

<sup>1</sup>University of Wisconsin-Madison, Madison, WI, United States

With well-established associations between gut microbiome populations, brain structure and function, and neurological disease and neuropsychiatric illness, the concomitant changes in neural tissue microstructure occurring parallel to these changes in the composition of the gut microbiome remain poorly characterized. We present new evidence for the neural microstructural correlates underpinning these mechanistic changes, the association between specific gut microbiome populations and brain microstructure, and the role of the human gut microbiome in the microstructural complexity of the developing brain.

---

[Neuroimaging of the Brain-Gut Axis](#)

Ling Ling Chan<sup>1</sup>

<sup>1</sup>Singapore General Hospital, Singapore, Singapore

---

---

## Oral

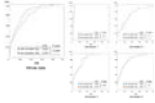
### Brain-Gut Axis and AI in Neuroimaging - AI Applications in Neuroimaging: High Novelty & Impact

Thursday Parallel 2 Live Q&A

Thursday 15:50 - 16:35 UTC

Moderators: Yunyan Zhang

1284



The neural network model that can consider the inhomogeneity of the judgements between different annotators: implementation for MRA diagnosis

Yasuhiko Tachibana<sup>1</sup>, Masataka Nishimori<sup>2</sup>, Masaaki Chiku<sup>3</sup>, Naoyuki Kitamura<sup>2</sup>, Kensuke Umehara<sup>4</sup>, Junko Ota<sup>4</sup>, Takayuki Obata<sup>1</sup>, and Tatsuya Higashi<sup>5</sup>

<sup>1</sup>Applied MRI Research, Department of Molecular Imaging and Theranostics, National Institute of Radiological Sciences, QST, Chiba, Japan, <sup>2</sup>MNES corporation, Tokyo, Japan, <sup>3</sup>Medical Check Studio Ginza Clinic, Tokyo, Japan, <sup>4</sup>Medical Informatics Section, QST Hospital, QST, Chiba, Japan, <sup>5</sup>Department of Molecular Imaging and Theranostics, National Institute of Radiological Sciences, QST, Chiba, Japan

The neural network model was designed to judge the existence of aneurysms from brain MR angiography images. On the hypothesis that each radiologist (annotator) has a unique bias for decision, the network was designed so that it accepts input of who the annotator was as an additional information to compute the output. The hypothesis might be reasonable, and the model design might be useful because the accuracy of the trained model (area under the curve (AUC) in receiver operating characteristic (ROC) analysis) elevated significantly ( $P < .0001$ , DeLong test) by adding the information of who the annotator was.

1285



Predicting brain function from anatomy with geometric deep learning using high-resolution MRI data

Fernanda Lenita Ribeiro<sup>1,2</sup>, Steffen Bollmann<sup>3</sup>, and Alexander M Puckett<sup>1,2</sup>

<sup>1</sup>School of Psychology, University of Queensland, Brisbane, Australia, <sup>2</sup>Queensland Brain Institute, University of Queensland, Brisbane, Australia, <sup>3</sup>Centre for Advanced Imaging, University of Queensland, Brisbane, Australia

Whether it be in a man-made machine or a biological system, form and function are often directly related. In the latter, however, this particular relationship is often unclear due to the intricate and involved nature of biology. Here we developed a geometric deep learning model capable of exploiting the actual structure of the cortex to learn the complex relationship between brain function and anatomy from structural and functional MRI data. Our model was not only able to predict the functional organization of human visual cortex from anatomical properties alone, but it was also able to predict nuanced variations across individuals.

1286



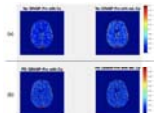
Toward a site and scanner-generic deep learning model for reduced gadolinium dose in contrast-enhanced brain MRI

Srivathsa Pasumarthi Venkata<sup>1</sup>, Jonathan Tamir<sup>1</sup>, Enhao Gong<sup>1</sup>, Greg Zaharchuk<sup>1</sup>, and Tao Zhang<sup>1</sup>

<sup>1</sup>Subtle Medical Inc., Menlo Park, CA, United States

Gadolinium-based contrast agents (GBCAs) create unique image contrast to facilitate identification of various clinical findings. However, recent discovery of gadolinium deposition after contrast-enhanced MRI raises new safety concerns of GBCAs. Deep learning (DL) has recently been used to predict the contrast-enhanced images using only a fraction of the standard dose. However, challenges remain in generalizing the DL methods across different protocols/vendors/institutions. In this work, we propose comprehensive technical solutions to improve DL model robustness and obtain high quality low-dose contrast-enhanced MRI across multiple scanners and institutions.

1287



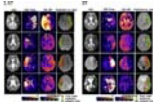
Estimating the capillary input function using deep learning approach for Dynamic Contrast-Enhanced MRI assessment of blood brain barrier

Jonghyun Bae<sup>1,2</sup>, Li Feng<sup>3</sup>, Krzysztof Geras<sup>4</sup>, Florian Knoll<sup>4</sup>, Yulin Ge<sup>4,5</sup>, and Sungheon Gene Kim<sup>4,5</sup>

<sup>1</sup>Sackler Institute of Graduate Biomedical Science, NYU School of Medicine, New York, NY, United States, <sup>2</sup>Radiology, Center for Advanced Imaging Innovation and Research, New York, NY, United States, <sup>3</sup>Icahn School of Medicine at Mount Sinai, New York, NY, United States, <sup>4</sup>Center for Advanced Imaging Innovation and Research, New York, NY, United States, <sup>5</sup>Center for Biomedical Imaging, NYU, New York, NY, United States

This study proposes a deep learning approach of estimating the capillary level of input function for kinetic model analysis on dynamic contrast enhanced (DCE)-MRI data. Our deep-learning network was trained with the numerically synthesized data generated with a wide range of contrast kinetic dynamics with different arterial input function (AIF). We hypothesize that the voxel level capillary input functions would be more accurate input functions for pharmacokinetic analysis. This hypothesis was tested with the DCE-MRI data of healthy subjects.

1288



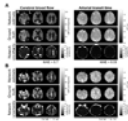
### Deep Learning Detection of Penumbra Tissue on Arterial Spin Labeling in Stroke

Kai Wang<sup>1</sup>, Qinyang Shou<sup>1</sup>, Samantha Ma<sup>1</sup>, David Liebeskin<sup>2</sup>, Xin Qiao<sup>2</sup>, Jeffrey Saver<sup>2</sup>, Noriko Salamon<sup>2</sup>, Songlin Yu<sup>3</sup>, Hosung Kim<sup>1</sup>, Yannan Yu<sup>4</sup>, Yuan Xie<sup>4</sup>, Greg Zaharchuk<sup>4</sup>, Fabien Scalzo<sup>2</sup>, and Danny Wang<sup>1</sup>

<sup>1</sup>University of Southern California, Los Angeles, CA, United States, <sup>2</sup>University of California, Los Angeles, Westwood, CA, United States, <sup>3</sup>Beijing Tiantan Hospital, Capital Medical University, Beijing, China, <sup>4</sup>Stanford University, Stanford, CA, United States

A deep learning (DL)-based algorithm was developed to automatically identify the hypoperfusion lesion and penumbra in ASL images of arterial ischemic stroke (AIS) patients. A total of 167 3D pCASL datasets from 137 AIS patients on Siemens MR were used for training, using concurrently acquired DSC MRI as the label. The DL model achieved a voxel-wise area under the curve (AUC) of 0.958, and 92% accuracy for retrospective determination for subject-level endovascular treatment eligibility. The DL-model was cross validated on 12 GE pCASL data with 92% accuracy without fine-tuning of parameters.

1289



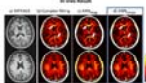
### A deep learning approach for hemodynamic parameter estimation from multi-delay arterial spin-labelled MRI

Nicholas J. Luciw<sup>1,2</sup>, Zahra Shirzadi<sup>2</sup>, Sandra E. Black<sup>2</sup>, Maged Goubran<sup>2</sup>, and Bradley J. MacIntosh<sup>1,2</sup>

<sup>1</sup>Department of Medical Biophysics, University of Toronto, Toronto, ON, Canada, <sup>2</sup>Sunnybrook Research Institute, Toronto, ON, Canada

Arterial spin-labelled (ASL) MRI is used to quantify cerebral blood flow and arterial transit time. Currently, these parameters are not calculated at the scanner given the time-consuming processing required. Fast, automated parameter estimation is therefore desirable to radiology clinics. Here, we trained a convolutional neural network to estimate cerebral blood flow and arterial transit time from multiple post-label delay ASL. The network produces estimates comparable to other approaches and was designed to evaluate model uncertainty. This fast, automated method is suitable for scan-time generation of accurate hemodynamic maps, important in the assessment of neurological disorders and neurodegeneration.

1290



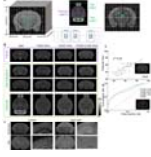
### Fiber orientation robust myelin water fraction mapping using complex-valued neural network in multi-echo gradient echo

Soozy Jung<sup>1</sup>, Kanghyun Ryu<sup>1</sup>, Jae Eun Song<sup>1</sup>, Mina Park<sup>2</sup>, and Dong-Hyun Kim<sup>1</sup>

<sup>1</sup>Department of Electrical and Electronic Engineering, Yonsei University, Seoul, Korea, Republic of, <sup>2</sup>Department of Radiology, Gangnam Severance Hospital, Seoul, Korea, Republic of

Recently, magnitude-based artificial neural network (ANN) method was implemented to estimate myelin water fraction (MWF) mapping using multi-echo gradient-echo (mGRE) data. However, MWF mapping in mGRE data requires phase information with the demand of considering frequency shifts in white matter. Here, we developed a complex-valued ANN for MWF mapping which could learn the phase information of the mGRE signal. According to simulation and in vivo analysis, complex-valued ANN is more robust to fiber orientation and noise than magnitude-based ANN and conventional fitting method.

1291



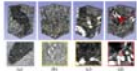
### Connecting Histology and MRI using Deep Learning

Zifei Liang<sup>1</sup>, Choong Heon Lee<sup>1</sup>, Tanzil M. Arefin<sup>1</sup>, Piotr Walczak<sup>2</sup>, Song-Hai Shi<sup>3</sup>, Florian Knoll<sup>1</sup>, Yulin Ge<sup>1</sup>, Leslie Ying<sup>4</sup>, and Jiangyang Zhang<sup>1</sup>

<sup>1</sup>Radiology, NYU Langone Health, New York, NY, United States, <sup>2</sup>Diagnostic Radiology & Nuclear Medicine, University of Maryland School of Medicine, Baltimore, MD, United States, <sup>3</sup>Center for Molecular Imaging & Nanotechnology, Memorial Sloan Kettering Cancer Center, New York, NY, United States, <sup>4</sup>Electrical Engineering, University at Buffalo, Buffalo, NY, United States

We developed a deep learning network that can generate new tissue contrasts from MRI data to match the contrasts of several histological methods. The network was trained using the carefully curated histological data from the Allen Institute mouse brain atlas and co-registered MRI data. In our tests, the new contrasts, which resembled Nissl, neurofilament, and myelin-basic-protein stained histology, demonstrated higher sensitivity and specificity than commonly used diffusion MRI markers to characterize neuronal, axonal, and myelin structures in the mouse brain. The contrasts were further validated using two mouse models with abnormal neuronal structures and dysmyelination.

1292



### The substantial influence of negative sampling and prevalence when presenting classification results: case study with TOF-MRA

Tommaso Di Noto<sup>1</sup>, Guillaume Marie<sup>1</sup>, Sebastien Tourbier<sup>1</sup>, Guillaume Saliou<sup>1</sup>, Meritxell Bach Cuadra<sup>1,2,3</sup>, Patric Hagmann<sup>1</sup>, and Jonas Richiardi<sup>1,4</sup>

<sup>1</sup>Faculty of Biology and Medicine, Department of Radiology, Lausanne University Hospital (CHUV) and University of Lausanne (UNIL), Lausanne, Switzerland, <sup>2</sup>Medical Image Analysis Laboratory (MIAL), Centre d'Imagerie BioMédicale (CIBM), Lausanne, Switzerland, <sup>3</sup>Signal Processing Laboratory (LTS 5), Ecole Polytechnique Fédérale de Lausanne (EPFL), Lausanne, Switzerland, <sup>4</sup>Advanced Clinical Imaging Technology, Siemens Healthcare, Lausanne, Switzerland

One recurrent problem for applying deep learning models in medical imaging is the reduced availability of labelled training data. A common approach is therefore to focus on image patches rather than whole volumes, thus increasing the number of samples. However, for many diseases anomalous patches (positive samples) are outnumbered by negative patches showing no anomaly. Here, we explore different strategies for negative sampling in the context of brain aneurysm detection. We show that classification performances can vary drastically with respect to negative sampling, and that real-world disease or anomaly prevalence can further degrade performance estimates.

1293



### Gaussian Process Progression Modelling of structural MRI changes in Huntington's disease

Peter A. Wijeratne<sup>1,2</sup>, Sara Garbarino<sup>3</sup>, Eileanoir B. Johnson<sup>2</sup>, Sarah Gregory<sup>2</sup>, Rachael I. Scahill<sup>2</sup>, Sarah J. Tabrizi<sup>2</sup>, Marco Lorenzi<sup>3</sup>, and Daniel C. Alexander<sup>1</sup>

<sup>1</sup>Department of Computer Science, University College London, London, United Kingdom, <sup>2</sup>Department of Neurodegenerative Disease, University College London, London, United Kingdom, <sup>3</sup>Université Côte d'Azur, Valbonne, France

Longitudinal measurements of brain atrophy using structural T1-weighted MRI (sMRI) can provide powerful biomarkers for clinical trials in neurodegenerative diseases. Here we use the latest advances in disease progression modelling, specifically the Gaussian Process Progression Model (GPPM), to untangle the effects of inter-subject variability, measurement noise and individual disease stage on longitudinal sMRI measurements in Huntington's disease (HD). We use GPPM to estimate, for the first time, the relative timescale of sub-cortical atrophy in HD, and identify when sMRI provides additional information to genetics. We conclude that GPPM could increase power over standard imaging biomarkers for clinical trials in HD.

---

## Oral - Power Pitch

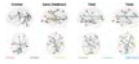
### Brain-Gut Axis and AI in Neuroimaging - Emerging Applications of AI in Neuroimaging

Thursday Parallel 2 Live Q&A

Thursday 15:50 - 16:35 UTC

Moderators: C. C. Tchoyoson Lim

1294



#### Hybrid structure-function connectome predicts individual cognitive abilities

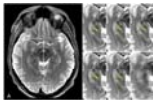
Elvisha Dhamala<sup>1,2</sup>, Keith W Jamison<sup>1</sup>, Sarah M Dennis<sup>3</sup>, Raihaan Patel<sup>4,5</sup>, M Mallar Chakravarty<sup>4,5,6</sup>, and Amy Kuceyeski<sup>1,2</sup>

<sup>1</sup>Radiology, Weill Cornell Medicine, New York, NY, United States, <sup>2</sup>Neuroscience, Weill Cornell Medicine, New York, NY, United States, <sup>3</sup>Sarah Lawrence College, Bronxville, NY, United States, <sup>4</sup>Biological and Biomedical Engineering, McGill University, Montreal, QC, Canada, <sup>5</sup>Cerebral Imaging Centre, Douglas Mental Health University Institute, Montreal, QC, Canada, <sup>6</sup>Psychiatry, McGill University, Montreal, QC, Canada

Structural connectivity (SC) and functional connectivity (FC) can be independently used to predict cognition and show distinct patterns of variance in relation to cognition. No work identified has yet investigated whether SC and FC can be combined to better predict cognitive abilities. In this work, we aimed to predict cognitive measures in 785 healthy adults using a hybrid structure-function connectome and quantify the most important connections. We show that: 1) hybrid connectomes explain 15% of the variance in individual cognitive measures, and 2) long-range cortico-cortical functional connections and short-range cortico-subcortical and subcortico-subcortical structural connections are most important for the prediction.

---

1295



#### Contrast-weighted SSIM loss function for deep learning-based undersampled MRI reconstruction

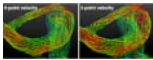
Sangtae Ahn<sup>1</sup>, Anne Menini<sup>2</sup>, Graeme McKinnon<sup>3</sup>, Erin M. Gray<sup>4</sup>, Joshua D. Trzasko<sup>4</sup>, John Huston<sup>4</sup>, Matt A. Bernstein<sup>4</sup>, Justin E. Costello<sup>5</sup>, Thomas K. F. Foo<sup>1</sup>, and Christopher J. Hardy<sup>1</sup>

<sup>1</sup>GE Research, Niskayuna, NY, United States, <sup>2</sup>GE Healthcare, Menlo Park, CA, United States, <sup>3</sup>GE Healthcare, Waukesha, WI, United States, <sup>4</sup>Department of Radiology, Mayo Clinic College of Medicine, Rochester, MN, United States, <sup>5</sup>Walter Reed National Military Medical Center, Bethesda, MD, United States

Deep learning-based undersampled MRI reconstructions can result in visible blurring, with loss of fine detail. We investigate here various structural similarity (SSIM) based loss functions for training a compressed-sensing unrolled iterative reconstruction, and their impact on reconstructed images. The conventional unweighted SSIM has been used both as a loss function, and, more generally, for assessing perceived image quality in various applications. Here we demonstrate that using an appropriately weighted SSIM for the loss function yields better reconstruction of small anatomical features compared to L1 and conventional SSIM loss functions, without introducing image artifacts.

---

1296



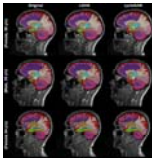
#### Accelerated 4D-flow MRI using Machine Learning (ML) Enabled Three Point Flow Encoding

Dahan Kim<sup>1,2</sup>, Laura Eisenmenger<sup>3</sup>, and Kevin M. Johnson<sup>3,4</sup>

<sup>1</sup>Department of Medical Physics, University of Wisconsin, Madison, WI, United States, <sup>2</sup>Department of Physics, University of Wisconsin, Madison, WI, United States, <sup>3</sup>Department of Radiology, University of Wisconsin, Madison, WI, United States, <sup>4</sup>Department of Medical Physics, University of Wisconsin, Middleton, WI, United States

4D-flow MRI suffers from long scan time due to a minimum of four velocity encodings necessary to solve for three velocity components and the reference background phase. We examine the feasibility of using machine learning (ML) to determine the background phase and hence three velocity components from only three flow encodings. The results show that ML is capable of estimating three-directional velocities from three flow encodings with high accuracy (1.5%-3.8% velocity underestimation) and high precision ( $R^2=0.975$ ). These findings indicate that 4D-flow MRI can be accelerated without requiring a dedicated reference scan, with a scan time reduction of 25%.

1297



A practical application of generative models for MR image synthesis: from post- to pre-contrast imaging

Gian Franco Piredda<sup>1,2,3</sup>, Virginie Piskin<sup>1</sup>, Vincent Dunet<sup>2</sup>, Gibran Manasseh<sup>2</sup>, Mário J Fartaria<sup>1,2,3</sup>, Till Huelnhagen<sup>1,2,3</sup>, Jean-Philippe Thiran<sup>2,3</sup>, Tobias Kober<sup>1,2,3</sup>, and Ricardo Corredor-Jerez<sup>1,2,3</sup>

<sup>1</sup>Advanced Clinical Imaging Technology, Siemens Healthcare AG, Lausanne, Switzerland, <sup>2</sup>Department of Radiology, Lausanne University Hospital and University of Lausanne, Lausanne, Switzerland, <sup>3</sup>LTS5, École Polytechnique Fédérale de Lausanne (EPFL), Lausanne, Switzerland

Multiple sclerosis studies following the widely accepted MAGNIMS protocol guidelines might lack non-contrast-enhanced  $T_1$ -weighted acquisitions as they are only considered optional. Most existing automated tools to perform morphological brain analyses are, however, tuned to non-contrast  $T_1$ -weighted images. This work investigates the use of deep learning architectures for the generation of pre-Gadolinium from post-Gadolinium image volumes. Two generative models were tested for this purpose. Both were found to yield similar contrast information as the original non-contrast  $T_1$ -weighted images. Quantitative comparison using an automated brain segmentation on original and synthesized non-contrast  $T_1$ -weighted images showed good correlation ( $r=0.99$ ) and low bias ( $<0.7$  ml).

1298



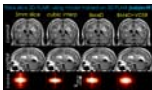
Quantification of Non-Water-Suppressed Proton Spectroscopy using Deep Neural Networks

Marcia Sahaya Louis<sup>1</sup>, Eduardo Coello<sup>2</sup>, Huijun Liao<sup>2</sup>, Ajay Joshi<sup>3</sup>, and Alexander Lin<sup>2</sup>

<sup>1</sup>ECE, Boston University, Boston, MA, United States, <sup>2</sup>Radiology, Brigham and Women's hospital, Boston, MA, United States, <sup>3</sup>Boston University, Boston, MA, United States

Water is present in the brain tissue at a concentration that is at least four orders of magnitude higher than metabolites of interest. As a result, it is necessary to suppress the water resonance so that the brain metabolites of interest can be better visualized and quantified. This work presents a neural network model for extracting the metabolites spectrum from non-water-suppressed proton magnetic resonance spectra. The autoencoder model learns a vector field for mapping the water signal to a lower-dimensional manifold and accurately reconstructs the metabolite spectra as compared to water-suppressed spectra from the same subject.

1299



From 2D thick slices to 3D isotropic volumetric brain MRI - a deep learning approach

Berkin Bilgic<sup>1,2</sup>, Long Wang<sup>1</sup>, Enhao Gong<sup>1</sup>, Greg Zaharchuk<sup>1,3</sup>, and Tao Zhang<sup>1</sup>

<sup>1</sup>Subtle Medical Inc, Menlo Park, CA, United States, <sup>2</sup>Martinos Center for Biomedical Imaging, MGH/Harvard, Charlestown, MA, United States, <sup>3</sup>Stanford University, Stanford, CA, United States

The long scan time of 3D isotropic MRI (often 5 minutes or longer) has limited the wide clinical adoption despite the apparent advantages. For many clinical sites, shorter 2D sequences are used routinely in brain MRI exams instead. The latest development of deep learning (DL) has demonstrated the feasibility of significant resolution improvement from low resolution acquisitions. In this work, we propose a deep learning method to synthesize 3D isotropic FLAIR images from 2D FLAIR acquisition with 5mm slice thickness. To demonstrate the generalizability, the proposed method is validated on both simulated and real 2D FLAIR datasets.

1300



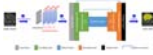
### Deep Learning Multi-class Segmentation Algorithm is more Resilient to the Variations of MR Image Acquisition Parameters

Yi-Tien Li<sup>1,2</sup>, Yi-Wen Chen<sup>1</sup>, David Yen-Ting Chen<sup>1,3</sup>, and Chi-Jen Chen<sup>1,4</sup>

*<sup>1</sup>Department of Radiology, Taipei Medical University - Shuang Ho Hospital, New Taipei, Taiwan, <sup>2</sup>Institute of Biomedical Engineering, National Taiwan University, Taipei, Taiwan, <sup>3</sup>Department of Radiology, Stanford University, Palo Alto, CA, United States, <sup>4</sup>School of Medicine, College of Medicine, Taipei Medical University, Taipei, Taiwan*

A huge amount of T2-FLAIR images with appearance of white matter hyperintensities (WMH) were used. 1368 cases from one hospital were selected as the training set. Another 100 cases from the same hospital and 200 cases from the other 2 different hospitals were treated as the independent test set. Based on multi-class U-SegNet approach, it can achieve the highest F1 score (same hospital: 90.01%; different hospital: 86.52%) in the test set compared with other approaches. The result suggested that the multi-class segmentation approach is more resilient to the variations of MR image parameters than the single label segmentation approach.

1301



### Accurate Brain Extraction Using 3D U-Net with Encoded Spatial Information

Hualei Shen<sup>1</sup>, Chenyu Wang<sup>1,2</sup>, Kain Kyle<sup>2</sup>, Chun-Chien Shieh<sup>2,3</sup>, Lynette Masters<sup>4</sup>, Fernando Calamante<sup>1,5</sup>, Dacheng Tao<sup>6</sup>, and Michael Barnett<sup>1,2</sup>

*<sup>1</sup>Brain and Mind Centre, the University of Sydney, Sydney, Australia, <sup>2</sup>Sydney Neuroimaging Analysis Centre, Sydney, Australia, <sup>3</sup>Sydney Medical School, the University of Sydney, Sydney, Australia, <sup>4</sup>I-MED Radiology Network, Sydney, Australia, <sup>5</sup>Sydney Imaging and School of Biomedical Engineering, the University of Sydney, Sydney, Australia, <sup>6</sup>School of Computer Science, the University of Sydney, Sydney, Australia*

Brain extraction from 3D MRI datasets using existing 3D U-Net convolutional neural networks suffers from limited accuracy. Our proposed method overcame this challenge by combining a 3D U-Net with voxel-wise spatial information. The model was trained with 1,615 T1 volumes and tested on another 601 T1 volumes, both with expertly segmented labels. Results indicated that our method significantly improved the accuracy of brain extraction over a conventional 3D U-Net. The trained model extracts the brain from a T1 volume in ~2 minutes and has been deployed for routine image analyses at the Sydney Neuroimaging Analysis Centre.

1302



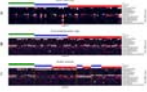
### 3D DUAL RECURSIVE REFINER NETWORK FOR ROBUST SEGMENTATION: APPLICATION TO BRAIN EXTRACTION

Maxime Bertrait<sup>1</sup>, Pascal Ceccaldi<sup>1</sup>, Boris Mailhé<sup>1</sup>, Youngjin Yoo<sup>1</sup>, and Mariappan S. Nadar<sup>1</sup>

*<sup>1</sup>Digital Technology and Innovation, Siemens Healthineers, Princeton, NJ, United States*

In Magnetic Resonance Imaging, acquisition protocol may varies from one clinical task to another affecting the resulting reconstructed scan in terms of field of view and resolution. In research, 3D acquired MRI scans are widely available providing high quality isotropic medical images but is far from what can exist in clinical environment such as 2D multi-slices with thick slices acquisition that can provide anisotropic medical images. We then present a framework, through a brain extraction task, called Dual Recursive Refiner able to work with both acquisitions. The presented framework outperforms baseline architectures for segmentation on both isotropic and anisotropic data.

1303



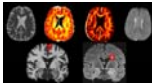
Characterisation of white matter lesion patterns in Systemic Lupus Erythematosus by an unsupervised machine learning approach.

Theodor Rumetshofer<sup>1</sup>, Tor Olof Strandberg<sup>2</sup>, Peter Mannfolk<sup>3</sup>, Andreas Jönsen<sup>4</sup>, Markus Nilsson<sup>1</sup>, Johan Mårtensson<sup>1</sup>, and Pia Maly Sundgren<sup>1,5</sup>

<sup>1</sup>Department of Clinical Sciences Lund/Diagnostic Radiology, Lund University, Lund, Sweden, <sup>2</sup>Clinical Memory Research Unit, Department of Clinical Sciences, Malmö, Lund University, Lund, Sweden, <sup>3</sup>Clinical Imaging and Physiology, Skåne University Hospital, Lund, Sweden, <sup>4</sup>Department of Rheumatology, Skåne University Hospital, Lund, Sweden, <sup>5</sup>Department of Clinical Sciences/Centre for Imaging and Function, Skåne University Hospital, Lund, Sweden

Evaluating white matter hyperintensities (WMHs) in neuropsychiatric systemic lupus erythematosus (NPSLE) is a challenging task. Multimodal MRI images in combination with unsupervised machine characterization can provide a powerful tool to investigate the spatial WHM distribution of relevant phenotypes. Automatically segmented WMH maps were spatially allocated to a white matter tract atlas. Cluster analysis was applied on this tract-wise lesion-load map to obtain subtypes with a distinct WMH damage profile. This approach on microstructural changes could help to identify specific progression pattern which may improve the accuracy of NPSLE classification.

1304



Attention-based convolutional network quantifying the importance of quantitative MR metrics in the multiple sclerosis lesion classification

Po-Jui Lu<sup>1,2,3</sup>, Reza Rahmanzadeh<sup>1,2</sup>, Riccardo Galbusera<sup>1,2</sup>, Matthias Weigel<sup>1,2,4</sup>, Youngjin Yoo<sup>3</sup>, Pascal Ceccaldi<sup>3</sup>, Yi Wang<sup>5</sup>, Jens Kuhle<sup>2</sup>, Ludwig Kappos<sup>1,2</sup>, Philippe Cattin<sup>6</sup>, Benjamin Odry<sup>7</sup>, Eli Gibson<sup>3</sup>, and Cristina Granziera<sup>1,2</sup>

<sup>1</sup>Translational Imaging in Neurology (ThINK) Basel, Department of Medicine and Biomedical Engineering, University Hospital Basel and University of Basel, Basel, Switzerland, <sup>2</sup>Neurologic Clinic and Policlinic, Departments of Medicine, Clinical Research and Biomedical Engineering, University Hospital Basel and University of Basel, Basel, Switzerland, <sup>3</sup>Digital Technology and Innovation, Siemens Healthineers, Princeton, NJ, United States, <sup>4</sup>Radiological Physics, Department of Radiology, University Hospital Basel, Basel, Switzerland, <sup>5</sup>Department of Radiology, Weill Cornell Medical College, New York, NY, United States, <sup>6</sup>Center for medical Image Analysis & Navigation, Department of Biomedical Engineering, University of Basel, Basel, Switzerland, <sup>7</sup>Covera Health, New York, NY, United States

White matter lesions in multiple sclerosis patients exhibit distinct characteristics depending on their locations in the brain. Multiple quantitative MR sequences sensitive to white matter micro-environment are necessary for the assessment of those lesions; but how to judge which sequences contain the most relevant information remains a challenge. In this abstract, we are proposing a convolutional neural network with a gated attention mechanism to quantify the importance of MR metrics in classifying juxtacortical and periventricular lesions. The results show the statistically significant order of quantitative importance of metrics, one step closer to combining more relevant metrics for better interpretation.

1305



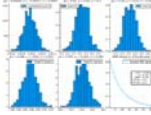
Deep Learning Segmentation of Lenticulostriate Arteries on 3D Black Blood MRI

Samantha J Ma<sup>1</sup>, Mona Sharifi Sarabi<sup>1</sup>, Kai Wang<sup>1</sup>, Soroush Heidari Pahlavian<sup>1</sup>, Wenli Tan<sup>1</sup>, Madison Lodge<sup>1</sup>, Lirong Yan<sup>1</sup>, Yonggang Shi<sup>1</sup>, and Danny JJ Wang<sup>1</sup>



Cerebral small vessels are largely inaccessible to existing clinical *in vivo* imaging technologies. As such, early cerebral microvascular morphological changes in small vessel disease (SVD) are difficult to evaluate. A deep learning (DL)-based algorithm was developed to automatically segment lenticulostriate arteries (LSAs) in 3D black blood images acquired at 3T. Using manual segmentations as supervision, 3D segmentation of LSAs is demonstrated to be feasible with relatively high performance and can serve as a useful tool for quantitative morphometric analysis in patients with cerebral SVD.

1306



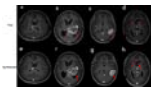
### Bayesian learning for fast parameter inference of multi-exponential white matter signals

Jonathan Doucette<sup>1,2</sup>, Christian Kames<sup>1,2</sup>, and Alexander Rauscher<sup>1,3,4</sup>

<sup>1</sup>UBC MRI Research Centre, Vancouver, BC, Canada, <sup>2</sup>Department of Physics & Astronomy, University of British Columbia, Vancouver, BC, Canada, <sup>3</sup>Department of Pediatrics, Faculty of Medicine, University of British Columbia, Vancouver, BC, Canada, <sup>4</sup>Division of Neurology, Faculty of Medicine, University of British Columbia, Vancouver, BC, Canada

In this work we use Bayesian learning methods to investigate data-driven approaches to parameter inference of multi-exponential white matter signals. Multi spin-echo (MSE) signals are simulated by solving the Bloch-Torrey on 2D geometries containing myelinated axons, and a conditional variational autoencoder (CVAE) model is used to learn to map simulated signals to posterior parameter distributions. This approach allows for the mapping of MSE signals directly to physical parameter vectors without expensive post-processing. We demonstrate the effectiveness of this model through the simultaneous inference of the myelin water fraction, flip angle, intra-/extracellular water  $T_2$ , myelin water  $T_2$ , and myelin g-ratio.

1307



### Clinical performance of reduced gadolinium dose for contrast-enhanced brain MRI using deep learning

Huanyu Luo<sup>1</sup>, Jing Xue<sup>1</sup>, Yunyun Duan<sup>1</sup>, Cheng Xu<sup>1</sup>, Jonathan Tamir<sup>2</sup>, Srivathsa Pasumarthi Venkata<sup>2</sup>, and Yaou Liu<sup>1</sup>

<sup>1</sup>Radiology, Beijing Tiantan Hospital, Beijing, China, <sup>2</sup>Subtle Medical Inc, Menlo Park, CA, United States

The reported gadolinium deposition phenomenon has caused extensive concern in the radiology community. This study focuses on validating the clinical performance of a proposed deep learning architecture which can significantly reduce the dosage of gadolinium-based contrast agents (GBCA) in brain MRI. The results suggest that the synthesized contrast images using deep learning with reduced GBCA dose can maintain its diagnostic quality under certain clinical circumstances.

1308



### Deep learning Assisted Radiological report (DART)

Keerthi Sravan Ravi<sup>1,2</sup>, Sairam Geethanath<sup>2</sup>, Girish Srinivasan<sup>3</sup>, Rahul Sharma<sup>4</sup>, Sachin R Jambawalikar<sup>4</sup>, Angela Lignelli-Dipple<sup>4</sup>, and John Thomas Vaughan Jr.<sup>2</sup>

<sup>1</sup>Biomedical Engineering, Columbia University, New York, NY, United States, <sup>2</sup>Columbia Magnetic Resonance Research Center, Columbia University, New York, NY, United States, <sup>3</sup>MediYantri Inc., Palatine, IL, United States, <sup>4</sup>Columbia University Irving Medical Center, New York, NY, United States

A 2015 survey indicates that burnout of radiologists was seventh highest among all physicians. In this work, two neural networks are designed and trained to generate text-based first read radiology reports. Existing tools are leveraged to perform registration and then brain tumour segmentation. Feature vectors are constructed utilising the information extracted from the segmentation masks. These feature vectors are fed to the neural networks to train against a radiologist's reports on fifty subjects. The neural networks along with image statistics are able to characterise tumour type, mass effect and edema and report tumour volumetry; compiled as a first-read radiology report.

---

## Oral

### Cardiovascular Techniques - Myocardial Perfusion & Function

Thursday Parallel 3 Live Q&A

Thursday 15:50 - 16:35 UTC

Moderators: Edward DiBella & Pedro Ferreira

1309  Multi-slice arterial spin labelled myocardial perfusion imaging with single shot EPI

Ahsan Javed<sup>1</sup> and Krishna S Nayak<sup>1</sup>

<sup>1</sup>Electrical and Computer Engineering, University of Southern California, Los Angeles, CA, United States

Arterial spin labelled cardiac magnetic resonance (ASL-CMR) imaging is a non-contrast myocardial perfusion (MP) imaging technique which can detect clinically relevant changes in MP under vasodilatory stress. Existing ASL-CMR techniques have limited spatial coverage because they cannot acquire multiple slices during the limited duration of pharmacologically induced peak stress (~3-4 min). In this work, we demonstrate the feasibility of a using carefully designed single shot echo planar imaging sequence for multi slice ASL-CMR at 3T.

1310  Interaction of Aortic Flow and Myocardial Motion in Patients with Repaired Tetralogy of Fallot

Xiao-Qing Zhang<sup>1</sup>, Meng-Chu Chang<sup>1</sup>, Ming-Ting Wu<sup>2</sup>, Ken-Pen Weng<sup>3,4</sup>, and Hsu-Hsia Peng<sup>1</sup>

<sup>1</sup>Department of Biomedical Engineering and Environmental Sciences, National Tsing Hua University, Hsinchu, Taiwan, <sup>2</sup>Department of Radiology, Kaohsiung Veterans General Hospital, Kaohsiung, Taiwan, <sup>3</sup>Department of Pediatrics, Kaohsiung Veterans General Hospital, Kaohsiung, Taiwan, <sup>4</sup>Department of Pediatrics, National Yang-Ming University, Taipei, Taiwan

We aimed to investigate the abnormal aortic flow and its adverse interaction with regional myocardial motion in repaired tetralogy of Fallot (rTOF) patients. The rTOF patients were divided into rTOF1 and rTOF2 groups according to their indexed right ventricular end-systolic volume (RVESVi). The rTOF2 group demonstrated increased aortic retrograde fraction and there was a correlation exhibited between retrograde fraction and systolic myocardial motion. In conclusion, the assessments of abnormal aortic flow and altered myocardial motion were helpful in elucidating the possibly adverse interaction between the characteristics of the aorta and myocardium in rTOF patients with different degrees of RV dilatation.

WITHDRAWN

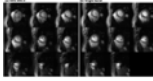
1312  Fully Self-gated Free-breathing 3D Cartesian Cardiac CINE with Isotropic Whole-heart Coverage in Less Than 2 Minutes

Thomas Küstner<sup>1</sup>, Aurelien Bustin<sup>1</sup>, Olivier Jaubert<sup>1</sup>, Radhouene Neji<sup>1,2</sup>, Claudia Prieto<sup>1</sup>, and René M Botnar<sup>1</sup>

<sup>1</sup>Biomedical Engineering Department, School of Biomedical Engineering and Imaging Sciences, King's College London, London, United Kingdom, <sup>2</sup>MR Research Collaborations, Siemens Healthcare Limited, Frimley, United Kingdom

Free-breathing continuous acquisitions, so called free-running, enable 3D whole-heart coverage for motion-resolved functional cardiac MRI. In prior work approaches based on 3D radial imaging were proposed with scan times of ~10-15min which also require computationally demanding reconstructions. In this work, we propose a 3D Cartesian free-running water-selective sequence that provides isotropic 3D whole-heart CINE imaging in <2min. Data is acquired with a variable-density spiral-like 3D Cartesian out-inward sampling and sequence-adaptive tiny-golden and golden angle increment. Respiratory motion-corrected and cardiac motion-resolved CINE images are obtained from a multi-bin-PROST reconstruction which exploits spatial-temporal redundancies. High agreement to conventional 2D CINE was observed.



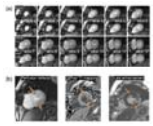


### High resolution spiral simultaneous multi-slice first-pass perfusion imaging with whole-heart coverage at 1.5 T and 3 T

Junyu Wang<sup>1</sup>, Yang Yang<sup>2,3</sup>, Ruixi Zhou<sup>1</sup>, Changyu Sun<sup>1</sup>, Mathews Jacob<sup>4</sup>, Daniel S. Weller<sup>5</sup>, Frederick H. Epstein<sup>1,6</sup>, and Michael Salerno<sup>1,3,6</sup>

<sup>1</sup>Biomedical Engineering, University of Virginia, Charlottesville, VA, United States, <sup>2</sup>Biomedical Engineering and Imaging Institute and Department of Radiology, Icahn School of Medicine at Mount Sinai, New York, NY, United States, <sup>3</sup>Medicine, University of Virginia, Charlottesville, VA, United States, <sup>4</sup>Electrical and Computer Engineering, University of Iowa, Iowa City, IA, United States, <sup>5</sup>Electrical and Computer Engineering, University of Virginia, Charlottesville, VA, United States, <sup>6</sup>Radiology, University of Virginia, Charlottesville, VA, United States

First-pass contrast-enhanced myocardial perfusion imaging is a useful noninvasive tool to evaluate patients with known or suspected coronary artery disease, but current techniques are still limited in spatial-temporal resolution and ventricular coverage. We designed a spiral pulse sequence with simultaneous multi-slice (SMS) acquisition and utilized the SMS-L1-SPIRiT reconstruction technique to achieve ultra-high resolution (1.5 mm at 1.5 T and 1.25 mm at 3 T) perfusion imaging with whole-heart coverage. The proposed spiral SMS perfusion acquisition strategy was tested on healthy volunteers and clinical patients. High image quality was demonstrated with an SMS factor of 3 at both 1.5T and 3T.

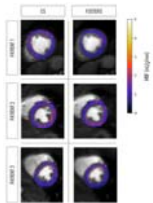


### Whole-heart, ungated, free-breathing myocardial perfusion MRI by using CRIMP

Ye Tian<sup>1</sup>, Jason Mendes<sup>1</sup>, Brent Wilson<sup>2</sup>, Alexander Ross<sup>2</sup>, Edward DiBella<sup>1</sup>, and Ganesh Adluru<sup>1</sup>

<sup>1</sup>Radiology, University of Utah, Salt Lake City, UT, United States, <sup>2</sup>Cardiology, University of Utah, Salt Lake City, UT, United States

We propose Continuous Radial Interleaved simultaneous Multi-slice acquisitions at spoiled steady-state (CRIMP) for whole-heart, ungated, free-breathing myocardial perfusion assessment. The simultaneous multi-slice (SMS) sequence captures multiple cardiac phases in all image slices simultaneously and keeps the inner slices at steady-state. We use a patch-based motion-compensated locally low-rank method to reconstruct the images. Quantitative perfusion analysis was also performed with an arterial input function estimated from a separate low-dose injection.

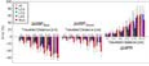


### High-Resolution Free-Breathing Quantitative Myocardial Perfusion MRI Using Multi-Echo Dixon

Joao Tourais<sup>1,2</sup>, Torben Schneider<sup>3</sup>, Cian Scannell<sup>4</sup>, Russell Franks<sup>4</sup>, Javier Sanchez-Gonzalez<sup>5</sup>, Mariya Doneva<sup>6</sup>, Christophe Schuelke<sup>6</sup>, Jakob Meineke<sup>6</sup>, Jochen Keupp<sup>6</sup>, Jouke Smink<sup>1</sup>, Marcel Breeuwer<sup>1,2</sup>, Amedeo Chiribiri<sup>4</sup>, Markus Henningson<sup>7</sup>, and Teresa Correia<sup>4</sup>

<sup>1</sup>MR R&D – Clinical Science, Philips Healthcare, Best, Netherlands, <sup>2</sup>Department of Biomedical Engineering, Eindhoven University of Technology, Eindhoven, Netherlands, <sup>3</sup>Philips Healthcare, Guildford, Surrey, United Kingdom, <sup>4</sup>School of Biomedical Engineering and Imaging Sciences, King's College London, London, United Kingdom, <sup>5</sup>Philips Healthcare Iberia, Madrid, Spain, <sup>6</sup>Philips Research Europe, Hamburg, Germany, <sup>7</sup>Department of Medical and Health Sciences, Linköping University, Linköping, Sweden

First-pass perfusion cardiac MR (FP-CMR) allows the detection of myocardial ischemia. Also, quantitative methods enable a reliable and operator-independent assessment of myocardial perfusion. However, conventional FP-CMR has limited spatial resolution and should be performed under breath-hold. Therefore, diagnostic accuracy is compromised by respiratory induced motion artifacts and false-positive defects due to dark-rim artifacts. We propose, a k-t accelerated dual-saturation FP-CMR multi-echo Dixon sequence to increase the spatial resolution, estimate respiratory motion from fat images and measure T2\*-related signal loss from the multi-echo images. Thus, perfusion quantification is improved by minimizing dark-rim artifacts, correcting for respiratory motion and T2\*.

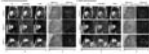


### Analysis of Location-dependent Errors of Myocardial Blood Flow (MBF) Estimates using Computational Fluid Dynamics (CFD)-Simulations

Tim A. Jedamzik<sup>1</sup>, Johannes Martens<sup>1</sup>, Sabine Panzer<sup>1</sup>, Maria Siebes<sup>2</sup>, Jeroen P. H. M. van den Wijngaard<sup>2,3</sup>, and Laura M. Schreiber<sup>1</sup>

<sup>1</sup>Chair of Cellular and Molecular Imaging, Comprehensive Heart Failure Center (CHFC), University Hospital Würzburg, Würzburg, Germany, <sup>2</sup>Dept. of Biomedical Engineering & Physics - Translational Physiology, Amsterdam UMC, University of Amsterdam, Amsterdam Cardiovascular Sciences, Amsterdam, Netherlands, <sup>3</sup>Dept. of Clinical Chemistry and Hematology, Diakenessenhuis, Utrecht, Netherlands

To analyze systematic errors and regional variability of the myocardial blood flow ( $\Delta$ MBF) and myocardial perfusion reserve ( $\Delta$ MPR) estimates in dynamic contrast-enhanced perfusion MRI, computational fluid dynamic (CFD)-simulations were performed in a realistic 3D coronary vasculature model of an *ex-vivo* porcine heart. Simulations were performed down to the pre-arteriolar level for the myocardial segments. The simulations show a strong spatial variance in the resulting  $\Delta$ MBF and  $\Delta$ MPR values of up to 60%. The errors are increasing with distance from the model inlet as well as with lower flow velocities. Errors are more pronounced in the right coronary artery.

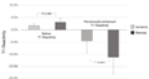


### Rapid Dealiasing of Undersampled, Radial First-Pass Cardiac Perfusion MR Images using 3D Residual U-Net

Lexiaozi Fan<sup>1,2</sup>, Daming Shen<sup>1,2</sup>, Hassan Haji-Valizadeh<sup>3</sup>, Nivedita K Naresh<sup>4</sup>, James C. Carr<sup>1</sup>, Benjamin H. Freed<sup>5</sup>, Daniel C. Lee<sup>5</sup>, and Daniel Kim<sup>1,2</sup>

<sup>1</sup>Department of Radiology, Northwestern University Feinberg School of Medicine, Chicago, IL, United States, <sup>2</sup>Department of Biomedical Engineering, Northwestern University, Evanston, IL, United States, <sup>3</sup>Department of Medicine (Cardiovascular Division), Beth Israel Deaconess Medical Center & Harvard Medical School, Boston, MA, United States, <sup>4</sup>Department of Radiology, University of Colorado Denver, Denver, CO, United States, <sup>5</sup>Division of Cardiology, Internal Medicine, Northwestern University Feinberg School of Medicine, Chicago, IL, United States

Compressed sensing (CS) is capable of accelerating cardiac perfusion MRI for achieving high spatial resolution (1.6 mm x 1.6 mm x 8 mm) and extensive spatial coverage (6+ slices per heartbeat), but the lengthy image reconstruction time (~8 min per slice with 64 frames using GPU) hinders its clinical translation. In this study, we sought to, for the first time, rapidly reconstruct accelerated cardiac perfusion data using a 3D residual U-net for clinical translation.



### Ferumoxytol contrast increases the normalized relative difference in T1 reactivity between remote and ischemic myocardium

Caroline M. Colbert<sup>1,2</sup>, Anna Le<sup>3</sup>, Jiaxin Shao<sup>1</sup>, Jesse Currier<sup>3</sup>, Peng Hu<sup>1</sup>, and Kim-Lien Nguyen<sup>1,2,3</sup>

<sup>1</sup>Department of Radiological Sciences, David Geffen School of Medicine at UCLA, Los Angeles, CA, United States, <sup>2</sup>Physics and Biology in Medicine Graduate Program, David Geffen School of Medicine at UCLA, Los Angeles, CA, United States, <sup>3</sup>Division of Cardiology, David Geffen School of Medicine at UCLA, Los Angeles, CA, United States

T1 reactivity can be used as a marker for myocardial perfusion reserve in the setting of ischemia or hypoperfusion. We hypothesize that ferumoxytol, as a pure intravascular agent with high  $r_1$  relaxivity, sensitizes T1 reactivity for assessment of myocardial perfusion. We selectively induced acute myocardial hypoperfusion in twelve healthy male Yorkshire swine. We then performed native and ferumoxytol-enhanced adenosine stress testing with the MOLLI sequence at 3.0T. Ferumoxytol increased absolute T1 reactivity in remote regions by 4.62-fold. The normalized difference in T1 was 4.5-fold greater in FE images compared to native T1.

1319



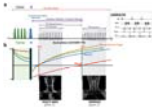
**Ultrashort TE Time-Spatial Labeling Inversion Pulse MRA for Simulated Visceral Arterial Diseases Indicated for Endovascular Interventions.**

Ryuichi Mori<sup>1</sup>, Hideki Ota<sup>2</sup>, Simon TUPIN<sup>3</sup>, Tomoyoshi Kimura<sup>1</sup>, Hironobu Sasaki<sup>1</sup>, Tatsuo Nagasaka<sup>1</sup>, Takashi Nishina<sup>4</sup>, Sho Tanaka<sup>4</sup>, Yoshiaki Morita<sup>2</sup>, Yoshimori kassai<sup>4</sup>, and Kei Takase<sup>2</sup>

<sup>1</sup>Department of Radiology, Tohoku University Hospital, Sendai, Japan, <sup>2</sup>Diagnostic Radiology, Tohoku University Hospital, Sendai, Japan, <sup>3</sup>Institute of Fluid Science, Tohoku University, Sendai, Japan, <sup>4</sup>Canon Medical Systems corp., Tochigi, Japan

Visceral arterial diseases should be evaluated before and after endovascular interventions. We compared ultrashort TE (UTE) and steady-state free precession (SSFP) time-SLIP MRAs regarding their signal decay in pulsatile flow phantoms reflecting stenosis, aneurysm, and metallic stents. In all phantom models, UTE time-SLIP MRA provided superior visualization of target lumens to SSFP time-SLIP MRA. UTE time-SLIP MRA demonstrated minimal signal decay except for in-stent lumen of a stainless-steel stent. Our results indicated robustness of UTE time-SLIP MRA for intra-voxel spin dephasing caused by accelerated flow at the stenosis, turbulent flow in the aneurysm and susceptibility effects from metallic devices.

1320



**REACT-MD: simultaneous non-contrast-enhanced subclavian MRA and fat suppressed direct thrombus imaging (MPRAGE) with a large field-of-view**

Masami Yoneyama<sup>1</sup>, Shuo Zhang<sup>2</sup>, Yasuhiro Goto<sup>3</sup>, Michinobu Nagao<sup>4</sup>, Kayoko Abe<sup>4</sup>, Osamu Togao<sup>5</sup>, Isao Shiina<sup>3</sup>, Kazuo Kodaira<sup>3</sup>, Yutaka Hamatani<sup>3</sup>, and Marc Van Cauteren<sup>6</sup>

<sup>1</sup>Philips Japan, Tokyo, Japan, <sup>2</sup>Philips Healthcare, Hamburg, Germany, <sup>3</sup>Department of Radiological Services, Tokyo Women's Medical University, Tokyo, Japan, <sup>4</sup>Department of Diagnostic Imaging and Nuclear Medicine, Tokyo Women's Medical University, Tokyo, Japan, <sup>5</sup>Department of Clinical Radiology, Graduate School of Medical Sciences, Kyushu University, Fukuoka, Japan, <sup>6</sup>Philips Healthcare, Best, Netherlands

Direct visualization of the plaques and vessel wall lesions in addition to luminal changes is of clinical importance for management of patients with atherosclerotic disease. In this work, the recently proposed REACT (Relaxation-Enhanced Angiography without Contrast and Triggering) technique was further developed and particularly optimized with Multiple Delays (REACT-MD) to simultaneously provide non-contrast-enhanced MR angiogram and MPRAGE (magnetization prepared rapid gradient echo) type images with uniform background tissue suppression over a large field of view. Initial results in patients showed great promise in detection of luminal changes and plaques for assessment of systemic atherosclerosis in one single scan.

1321



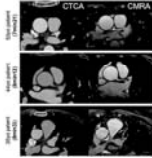
**Motion Compensated Coronary MRA using Focused Navigation (fNAV)**

Christopher W. Roy<sup>1</sup>, John Heerfordt<sup>1,2</sup>, Davide Piccini<sup>1,2</sup>, Juerg Schwitter<sup>3</sup>, and Matthias Stuber<sup>1,4</sup>

<sup>1</sup>Radiology, Lausanne University Hospital (CHUV) and University of Lausanne (UNIL), Lausanne, Switzerland, <sup>2</sup>Advanced Clinical Imaging Technology (ACIT), Siemens Healthcare AG, Lausanne, Switzerland, <sup>3</sup>Division of Cardiology and CMR-Center, Lausanne University Hospital (CHUV), Lausanne, Switzerland, <sup>4</sup>Center for Biomedical Imaging (CIBM), Lausanne, Switzerland

Robust visualization of the coronary vessels is challenging due to cardiac and respiratory motion. Several strategies exist that resolve respiratory motion (XD-GRASP) or compensate for it using N-dimensional image-based navigators to correct for N dimensions of motion. We present a novel self-navigation method wherein the minimization of an image metric is used to estimate 3D non-rigid respiratory motion from a 1D navigator signal (focused navigation: fNAV). We validate fNAV for free-breathing cardiac triggered whole-heart CMRA in a realistic numerical phantom, demonstrate its use in cohorts of healthy volunteers and patients, and quantitatively compare fNAV reconstructions to XD-GRASP.

1322



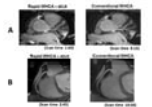
### Impact of sub-millimeter isotropic resolution on the visualization of coronary arteries in patients undergoing accelerated whole-heart CMRA

Aurelien Bustin<sup>1</sup>, Reza Hajhosseiny<sup>1</sup>, Imran Rashid<sup>1</sup>, Gastao Cruz<sup>1</sup>, Ronak Rajani<sup>1</sup>, Tefvik Ismail<sup>1</sup>, René Botnar<sup>1</sup>, and Claudia Prieto<sup>1</sup>

<sup>1</sup>Biomedical Engineering Department, School of Biomedical Engineering and Imaging Sciences, King's College London, London, United Kingdom

The recent integration of undersampled acquisitions with image-navigators and non-rigid motion-correction have enabled free-breathing 3D whole-heart coronary MR angiography (CMRA) with sub-millimeter isotropic resolution in clinically feasible scan times in healthy subjects. The high acceleration factor and spatial resolution however must be balanced with the need for a robust and high-quality image reconstruction. We sought to assess whether this highly accelerated sub-millimeter isotropic resolution contrast-free CMRA framework could reliably improve the visualization of coronary arteries in comparison to lower resolution (and lower acceleration factor) CMRA in patients with suspected coronary artery disease who underwent CT coronary angiography.

1323



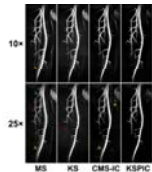
### Rapid Whole Heart Coronary MRA with 100% respiratory gating efficiency: Fast 3D Wheel data sampling with denoising deep learning reconstruction

Yoshiaki Morita<sup>1</sup>, Hideki Ota<sup>1</sup>, Atsuro Masuda<sup>1</sup>, Takashi Nishina<sup>2</sup>, Sho Tanaka<sup>2</sup>, Yuichi Yamashita<sup>2</sup>, Yoshimori Kassai<sup>2</sup>, and Kei Takase<sup>1</sup>

<sup>1</sup>Department of Radiology, Tohoku University Hospital, Sendai, Miyagi, Japan, <sup>2</sup>Canon Medical Systems Corporation, Otawara, Tochigi, Japan

Our proposed Whole Heart Coronary MR Angiography with 100% respiratory gating efficiency using Fast 3D Wheel data acquisition implementing denoising deep learning reconstruction allowed the rapid data acquisition consistently within 3 minutes in spite of irregular breath pattern while maintaining the image quality and contrast ratio of conventional scan. This technique will improve the ease-of-use of coronary artery imaging for practical use.

1324



### Highly Accelerated Subtractive NCE-MRA using Advanced k-space Subtraction and Magnitude Subtraction Reconstruction Methods

Hao Li<sup>1</sup>, Martin John Graves<sup>2</sup>, Nadeem Shaida<sup>2</sup>, Akash Prashar<sup>2</sup>, David John Lomas<sup>1</sup>, and Andrew Nicholas Priest<sup>2</sup>

<sup>1</sup>Department of Radiology, University of Cambridge, Cambridge, United Kingdom, <sup>2</sup>Department of Radiology, Addenbrooke's Hospital, Cambridge, United Kingdom

We implemented two advanced reconstruction methods for highly accelerated subtractive NCE-MRA, which can exploit the sparsity of subtracted angiograms. One method is based on  $k$ -space subtraction of complex raw data with phase and intensity correction (KSPIC). Another method is to reconstruct bright- and dark-blood data with an additional magnitude subtraction term in the cost function to exploit the sparsity. The performance of the two methods was evaluated in both retrospective and prospective accelerated datasets using quantitative metrics and qualitative scoring. Compared with conventional methods, they both showed improved image reconstruction quality, while KSPIC had the best performance.

1325



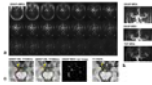
#### Highly accelerated vessel wall imaging using CAIPIRINHA accelerated SPACE and IFR-CS

Sen Jia<sup>1,2</sup>, Zhilang Qiu<sup>1,2</sup>, Lei Zhang<sup>2</sup>, Xin Liu<sup>2</sup>, Hairong Zheng<sup>2</sup>, and Dong Liang<sup>2</sup>

<sup>1</sup>University of Chinese Academy of Sciences, Shenzhen, China, <sup>2</sup>Shenzhen Institutes of Advanced Technology, Chinese Academy of Sciences, Shenzhen, China

Joint intracranial and carotid 3D vessel wall imaging (VWI) with an isotropic spatial resolution between 0.5-0.6 mm is promising in diagnosing arterial wall diseases but leads to clinically impractical scan time. CAIPIRINHA 3x3 undersampling with elliptical scanning is used to expedite the VWI by 11-fold without less sampling the high-frequency region of  $k$ -space. Iterative L1-ESPIRiT algorithm is employed for reconstruction with GRAPPA result as the initialization. The scheme of Iterative Feature Refinement is embedded into L1-ESPIRiT iteration to avoid potential over-smoothing issue. Finally, the 3D 11x VWI scan at an isotropic resolution of 0.6 mm takes only 3.5 minutes.

1326



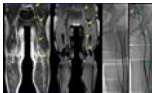
#### iSNAP sequence for simultaneous measurement of whole brain dynamic MRA, MRA, intracranial vessel wall and T1W structural brain MRI

Zhensen Chen<sup>1</sup>, Zechen Zhou<sup>2</sup>, Niranjan Balu<sup>1</sup>, Haikun Qi<sup>3</sup>, Baocheng Chu<sup>1</sup>, Thomas S Hatsukami<sup>4</sup>, and Chun Yuan<sup>1</sup>

<sup>1</sup>Vascular Imaging Lab and BioMolecular Imaging Center, Radiology, University of Washington, Seattle, WA, United States, <sup>2</sup>Philips Research North America, Cambridge, MA, United States, <sup>3</sup>Biomedical Engineering, King's College London, London, United Kingdom, <sup>4</sup>Surgery, University of Washington, Seattle, WA, United States

In this study, a whole brain sequence named iSNAP, with 0.8 mm isotropic voxel size and 6 min 30 sec acquisition time, was developed to simultaneously obtain four different image contrasts (dynamic MRA [dMRA] for blood flow monitoring, MRA for luminal stenosis measurement, black blood image for vessel wall [VW] measurement and T1W for brain structural imaging). Preliminary testing results on a healthy volunteer and two patients with cerebrovascular diseases demonstrated the feasibility and potential of the sequence.

1327



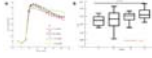
#### Outcome of Catheter-direct Thrombolysis for Deep Vein Thrombosis using T1-weighted Magnetic Resonance Black-blood Thrombus Imaging

Chen Huang<sup>1</sup>, Guoxi Xie<sup>2</sup>, Xueping He<sup>1</sup>, Yufeng Ye<sup>1</sup>, Wei Deng<sup>1</sup>, Jianke Liang<sup>1</sup>, Zhuonan He<sup>1</sup>, Xin Liu<sup>3</sup>, Debiao Li<sup>4</sup>, Zhaoyang Fan<sup>4</sup>, and Hanwei Chen<sup>1</sup>

<sup>1</sup>Guangzhou panyu central hospital, Guangzhou, China, <sup>2</sup>Guangzhou medical university, Guangzhou, China, <sup>3</sup>Shenzhen Institutes of Advanced Technology, Shenzhen, China, <sup>4</sup>Cedars-Sinai Medical Center, Los Angeles, CA, United States

The present study aims to evaluate the outcome of thrombolysis for acute DVT using the thrombus signal characteristics generated by a T1-weighted MR black-blood thrombus imaging (BTI) technique. The patients were divided into iso- or hyper-intense thrombus groups according to the BTI images and the additional CDT were performed. The thrombolysis ratio of patients with iso-intense signals was significantly higher than hyper-intense ones. However, the patients with iso-intense thrombus had a lower incidence rate of PTS at 6 and 12 months. So, the thrombus signal characteristics on BTI images maybe used to predict the outcome of DVT treated with the lytic therapy.

1328



Self-gated dynamic contrast enhanced magnetic resonance imaging of the aortic root in atherosclerotic mice: a natural progression study

Claudia Calcagno<sup>1</sup>, John David<sup>2</sup>, Abdallah Motaal<sup>2</sup>, Thijs Beldman<sup>2</sup>, Alexandra Corbin<sup>1</sup>, Arnav Kak<sup>1</sup>, Sarayu Ramachandran<sup>1</sup>, Alison Pruzan<sup>1</sup>, Raphael Soler<sup>1</sup>, Christopher Faries<sup>1</sup>, Zahi A. Fayad<sup>1</sup>, Willem Mulder<sup>1</sup>, and Gustav Strijkers<sup>2</sup>

<sup>1</sup>Icahn School of Medicine at Mount Sinai, New York, NY, United States, <sup>2</sup>University of Amsterdam, Amsterdam, Netherlands

Enhanced endothelial permeability is an important hallmark of atherosclerotic plaques at high-risk for causing severe cardiovascular events. Here we present the application of a novel, self-gated DCE-MRI acquisition combined with compressed sensing reconstruction to quantify endothelial permeability in the mouse aortic root. In a longitudinal natural disease progression study in ApoE<sup>-/-</sup> mice, we find that plaque contrast agent washout computed from this acquisition changes significantly over time, with washout being slower in older mice.

## Oral

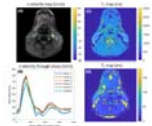
### Cardiovascular Techniques - Velocity & Flow

Thursday Parallel 3 Live Q&A

Thursday 15:50 - 16:35 UTC

Moderators: Liang Zhong

1329



Time-resolved 3D Flow-MRF for relaxation and velocity quantification in the carotid arteries

Lisa Leroi<sup>1</sup>, Sebastian Flassbeck<sup>2,3</sup>, and Sebastian Schmitter<sup>1,2</sup>

<sup>1</sup>Physikalisch-Technische Bundesanstalt Berlin (PTB), Braunschweig and Berlin, Germany, <sup>2</sup>Medical Physics in Radiology, German Cancer Research Center (DKFZ), Heidelberg, Germany, <sup>3</sup>Faculty of Physics and Astronomy, Heidelberg University, Heidelberg, Germany

The simultaneous quantification of blood velocity and tissue relaxation times could be a valuable tool for clinicians, especially in the carotid arteries, where atheroma plaques could occur. This can be achieved using the recently presented Flow-MRF technique that relies on the acquisition of randomly distributed gradients  $m_1$  momentum using a FISP MRF-sequence, with varying flip angle and fixed TR. In this work, Flow-MRF is extended to a time-resolved 3D acquisition and successfully applied in-vivo to the carotid bifurcation at 3T.  $T_1$ ,  $T_2$  and 3D time-resolved flow maps are recovered in a 3D slab.

1330



Retrospective camera-based respiratory binning for 4D flow MRI – A comparison with liver navigator and self-gating

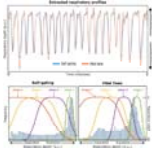
Lukas M. Gottwald<sup>1</sup>, Joao Tourais<sup>2,3</sup>, Eva S. Peper<sup>1</sup>, Jouke Smink<sup>2</sup>, Bram F. Coolen<sup>4</sup>, Gustav J. Strijkers<sup>4</sup>, Pim van Ooij<sup>1</sup>, and Aart J. Nederveen<sup>1</sup>

<sup>1</sup>Radiology and Nuclear Medicine, Amsterdam UMC, Amsterdam, Netherlands, <sup>2</sup>MR R&D – Clinical Science, Philips Healthcare, Best, Netherlands, <sup>3</sup>Department of Biomedical Engineering, University of Technology, Eindhoven, Netherlands, <sup>4</sup>Biomedical Engineering and Physics, Amsterdam UMC, Amsterdam, Netherlands



This study aimed to compare the performance of the novel camera-based respiratory navigation sensor (VitalEye) in retrospective respiratory binned Cartesian 4D flow MRI to conventional liver navigator and self-gating. Analyzed were the cross-correlation of the respiratory signals, peak flow rate error compared to 2D flow and the image quality in terms of edge sharpness of the liver/diaphragm border and signal-to-noise ratio. The novel camera-based respiratory navigation sensor VitalEye performed as good as conventional liver navigator and self-gating. Respiratory signal, flow rate error, and image quality showed no significant difference, but VitalEye has the advantage of a 10-times higher sampling frequency.

1331



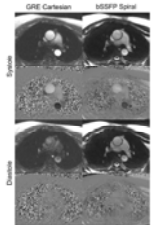
Extracting the respiratory signal from Pilot Tone for highly accelerated, respiratory-resolved whole-heart 4D flow imaging

Aaron Pruitt<sup>1</sup>, Peter Speier<sup>2</sup>, Chong Chen<sup>1</sup>, Yingmin Liu<sup>3</sup>, Ning Jin<sup>4</sup>, Orlando Simonetti<sup>5</sup>, and Rizwan Ahmad<sup>1</sup>

<sup>1</sup>Biomedical Engineering, The Ohio State University, Columbus, OH, United States, <sup>2</sup>Siemens Healthcare GmbH, Erlangen, Germany, <sup>3</sup>Dorothy M. Davis Heart and Lung Research Institute, The Ohio State University, Columbus, OH, United States, <sup>4</sup>Siemens Medical Solutions USA, Inc., Columbus, OH, United States, <sup>5</sup>Cardiovascular Medicine and Radiology, The Ohio State University, Columbus, OH, United States

Pilot Tone has recently been proposed as a novel approach towards physiological signal monitoring. Unlike self-gating, often relied upon by free-running, respiratory-resolved imaging sequences, Pilot Tone is generalizable to a multitude of imaging techniques without requiring additional pulse sequence modification or specialized k-space sampling. In this work, we combine Pilot Tone with our previously described highly accelerated and fully self-gated whole-heart 4D flow framework to reconstruct respiratory-resolved 4D flow images in three healthy subjects. We compare Pilot Tone and self-gating derived respiratory binning and demonstrate good agreement in aortic and pulmonary artery flow quantification between the two methods.

1332



Spiral bSSFP Phase-contrast Flow at 0.55T

Rajiv Ramasawmy<sup>1</sup>, Daniel Herzka<sup>1</sup>, Robert Lederman<sup>1</sup>, and Adrienne Campbell-Washburn<sup>1</sup>

<sup>1</sup>National Heart, Lung & Blood Institute, National Institutes of Health, Bethesda, MD, United States

A balanced SSFP (bSSFP) phase-contrast using a spiral readout was implemented for quantitative flow measurements at 0.55T. bSSFP flow is challenging at 1.5T and 3T due to off-resonance. However, at 0.55T, this sequence exploits the improved field inhomogeneity for a long readout (TR = 7.2ms) bSSFP spiral acquisition. This sequence provided improved signal-to-noise ratio (SNR) normalized by voxel, especially during diastole (Cartesian gradient echo SNR/voxel = 3.6, spiral bSSFP SNR/voxel = 9.4), to produce quality flow measurements at 0.55T.

1333

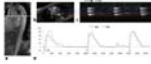
Longitudinal study of 4D flow MRI derived aortic hemodynamics in bicuspid aortic valve patients with repaired coarctation.

Gilles Soulat<sup>1</sup>, Michael Scott<sup>1</sup>, Ashitha Pathrose<sup>1</sup>, Kelly Jarvis<sup>1</sup>, Haben Berhane<sup>2</sup>, Bradley Allen<sup>1</sup>, Ryan Avery<sup>1</sup>, Cynthia Rigsby<sup>2</sup>, and Michael Markl<sup>3</sup>

<sup>1</sup>Department of Radiology, Feinberg School of Medicine, Northwestern University, Chicago, IL, United States, <sup>2</sup>Department of Medical Imaging, Ann & Robert H. Lurie Children's Hospital of Chicago, Chicago, IL, United States, <sup>3</sup>Department of Radiology, Feinberg School of Medicine, and Department of Biomedical Engineering, McCormick School of Engineering; Northwestern University, Chicago, IL, United States

Bicuspid aortic valve (BAV) patients with history of aortic coarctation are considered higher risk for aortic complications. We evaluated 4D flow aortic metrics in 15 BAV adults with coarctation repair (mean age 35y) retrospectively reviewed at baseline and follow-up (3.98y [2.10 to 4.96y]). Areas of higher wall shear stress were mainly located in the arch, and 4D flow metrics remained stable at follow-up. Aortic growth was slow, with a significant increase in the anterior arch (0.25mm/y) and diaphragmatic aorta (0.27mm/y). At baseline, peak velocity at the coarctation repair site was inversely correlated to mid arch and diaphragmatic aortic growth.

1334



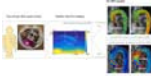
#### Evaluation of Vascular Reactivity of Maternal Cardiovascular Adaptations During Pregnancy with Quantitative MRI

Michael C Langham<sup>1</sup>, Felix W Wehrli<sup>1</sup>, Alessandra S Caporale<sup>1</sup>, and Nadav Schwartz<sup>2</sup>

<sup>1</sup>Radiology, University of Pennsylvania, Philadelphia, PA, United States, <sup>2</sup>Maternal Fetal Medicine, University of Pennsylvania, Philadelphia, PA, United States

Significant maternal cardiovascular adaptations take place during pregnancy. One such alteration is a decrease in peripheral vascular resistance to accommodate an increase in cardiac output. In this pilot study, we aimed to evaluate changes in vascular reactivity during normal pregnancy by quantifying MRI surrogate markers of endothelial function. A novel quantitative MRI protocol was performed on 14 healthy pregnant women to evaluate peripheral micro- and macrovascular reactivity and central arterial stiffness. Preliminary results indicate attenuated peripheral vascular reactivity consistent with previous studies of brachial artery reactivity using ultrasound in pregnant women.

1335



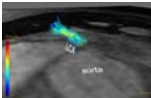
#### Screening Efficacy of Wearable Seismocardiography to Recommend MRI for Stratification of Aortic Valve Diseases

Ethan M I Johnson<sup>1</sup>, J. Alex Heller<sup>2</sup>, Flori Garcia Vicente<sup>2</sup>, Mozziyar Etemadi<sup>1,2</sup>, Alex Barker<sup>3</sup>, and Michael Markl<sup>1,4</sup>

<sup>1</sup>Biomedical Engineering, Northwestern University, Evanston, IL, United States, <sup>2</sup>Anesthesiology, Northwestern University, Chicago, IL, United States, <sup>3</sup>Radiology and Biomedical Engineering, University of Colorado, Anschutz Medical Campus, Aurora, CO, United States, <sup>4</sup>Radiology, Northwestern, Chicago, IL, United States

Aortic valve diseases (AVD) require regular monitoring of aortic size and blood speeds. MRI can quantify morphology and flow parameters, such as velocity and wall shear stress, with high accuracy and reproducibility, especially as compared to echocardiography. However, the value proposition may be low for performing repeated MRI if there has been no change in disease state. A quick, inexpensive and easy to use test that identifies potential need for MR imaging could significantly raise the cost-effectiveness of using MRI for monitoring AVD. Here we show high potential screening efficacy of using seismocardiography to select AVD patients needing MRI examination.

1336



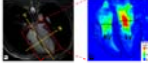
#### Towards Coronary Flow Reserve Assessment with 4D Flow MRI

Carmen PS Blanken<sup>1</sup>, Eva S Peper<sup>1</sup>, Lukas M Gottwald<sup>1</sup>, Bram F Coolen<sup>2</sup>, Gustav J Strijkers<sup>2</sup>, R Nils Planken<sup>1</sup>, Aart J Nederveen<sup>1</sup>, and Pim van Ooij<sup>1</sup>

<sup>1</sup>Radiology and Nuclear Medicine, Amsterdam UMC, Amsterdam, Netherlands, <sup>2</sup>Biomedical Engineering, Amsterdam UMC, Amsterdam, Netherlands

Coronary flow reserve (CFR) is a clinical test that interrogates the function of the entire coronary vasculature, indicating the presence of coronary stenoses, microvascular disease or both in patients with ischemic heart disease. We used 15 times accelerated 4D flow MRI with compressed sensing reconstruction at an isotropic spatial resolution of 1.0 mm to measure diastolic flow in the left coronary artery of six healthy subjects. Mean diastolic flow was  $1.15 \pm 0.18$  ml/s with a mean scan-rescan difference of 0.06 ml/s. 4D flow MRI-based diastolic flow quantification in the LCA is feasible and could enable non-invasive CFR measurement.

1337



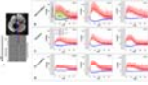
#### Myocardial and Intraventricular Kinetic Energy in Patients with Repaired Tetralogy of Fallot

Shi-Ying Ke<sup>1</sup>, Meng-Chu Chang<sup>1</sup>, Ming-Ting Wu<sup>2</sup>, Ken-Pen Weng<sup>3,4</sup>, and Hsu-Hsia Peng<sup>1</sup>

<sup>1</sup>Department of Biomedical Engineering and Environmental Sciences, National TsingHua University, Hsinchu, Taiwan, <sup>2</sup>Department of Radiology, Kaohsiung Veterans General Hospital, Kaohsiung, Taiwan, <sup>3</sup>Department of Pediatrics, Kaohsiung Veterans General Hospital, Kaohsiung, Taiwan, <sup>4</sup>Department of Pediatrics, National Yang-Ming University, Taipei, Taiwan

We aimed to investigate the interaction between myocardial kinetic energy ( $KE_{myo}$ ) and intraventricular KE ( $KE_{ven}$ ) in left- and right-ventricle (LV, RV) for repaired tetralogy of Fallot (rTOF) patients. The rTOF group displayed higher systolic RV  $KE_{ven}$ , earlier LV myocardial diastolic time-to-peak ( $TTP_{myo}$ ), earlier RV  $TTP_{myo}$  in both systole and diastole, earlier LV  $TTP_{ven}$  in both systole and diastole, and earlier RV  $TTP_{ven}$  in systole. In conclusion, from an insight of energy conversion, rTOF patients demonstrated undermined interaction between LV  $KE_{myo}$  and  $KE_{ven}$  in an early stage. The dilated RV potentially have impacts on the RV  $KE_{ven}$  in rTOF patients.

1338



#### Quantitative MRI and serum biomarkers detect acute and chronic vascular effects of e-cigarette use

Alessandra Caporale<sup>1</sup>, Shampa Chatterjee<sup>2</sup>, Michael C Langham<sup>1</sup>, Wensheng Guo<sup>3</sup>, Frank Leone<sup>4</sup>, Andrew Strasser<sup>5</sup>, and Felix W Wehrli<sup>1</sup>

<sup>1</sup>Radiology, Laboratory for Structural, Physiologic and Functional Imaging, Perelman School of Medicine, University of Pennsylvania, Philadelphia, PA, United States, <sup>2</sup>Physiology, Institute for Environmental Medicine, Perelman School of Medicine, Philadelphia, PA, United States, <sup>3</sup>Biostatistics and Epidemiology, Perelman School of Medicine, Philadelphia, PA, United States, <sup>4</sup>University of Pennsylvania Medical Center, Pulmonary, Allergy & Critical Care Division, Philadelphia, PA, United States, <sup>5</sup>Psychiatry, Center for Interdisciplinary Research on Nicotine Addiction, Philadelphia, PA, United States

The vascular effects of e-cigarette use were investigated in young adults (19-35 years). Blood draws and 3T-MRI data were collected from seven e-cigarette users, seven smokers, thirty nonsmokers, the latter replicating the measurements after one nicotine-free e-cigarette vaping session. MRI-protocol measured peripheral vascular reactivity in response to cuff-induced ischemia, quantifying femoral artery luminal flow mediated dilation ( $FMD_L$ ), blood flow velocity, venous saturation ( $SvO_2$ ).  $FMD_L$  decreased by 33% acutely after vaping, consistent with 20% NOx reduction and elevated inflammation (C-reactive protein increased by 95%). Reactive hyperemia was blunted as a chronic effect of both smoking and vaping, paired with anomalous biomarkers.

## Oral

### Multimodal fMRI - Multimodal Imaging of Brain Function

Thursday Parallel 4 Live Q&A

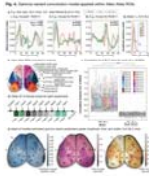
Thursday 15:50 - 16:35 UTC

Moderators: Karen Mullinger

1339

#### Simultaneous fMRI and mesoscopic Ca<sup>2+</sup> imaging indicates spontaneous excitatory neural activity accounts for 1/3rd of the variance in BOLD signal

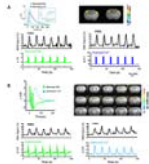
Evelyn MR Lake<sup>1</sup>, Xinxin Ge<sup>2</sup>, Xilin Shen<sup>1</sup>, Peter Herman<sup>1</sup>, Fahmeed Hyder<sup>1</sup>, Jessica A Cardin<sup>3</sup>, Michael J Higley<sup>3</sup>, Dustin Scheinost<sup>1</sup>, Xenophon Papademetris<sup>1</sup>, Michael C Crair<sup>2</sup>, and R Todd Constable<sup>1</sup>



<sup>1</sup>Radiology and Biomedical Imaging, Yale University, New Haven, CT, United States, <sup>2</sup>Department of Neurobiology, Yale University, New Haven, CT, United States, <sup>3</sup>Department of Neuroscience, Yale University, New Haven, CT, United States

We demonstrate longitudinal simultaneous whole-cortex Ca<sup>2+</sup> imaging and fMRI in mice expressing GCaMP in one of five different cell types (excitatory, inhibitory, two interneuron subtypes, and astrocytes). The high SNR of our dual-imaging approach is shown by the indistinguishable Ca<sup>2+</sup> responses to hind-paw or visual stimulation measured inside and outside the scanner. We optimize a spatially variable, three-parameter gamma-variant to investigate the transfer function between the BOLD and Ca<sup>2+</sup> signals throughout the cortex. This approach is applied in functionally and anatomically defined ROIs. Results show that 1/3<sup>rd</sup> of the variance in BOLD is accounted for from spontaneous excitatory Ca<sup>2+</sup> activity.

1340



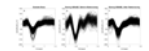
Deciphering the contribution of extracellular glutamate and intracellular calcium signaling to the BOLD fMRI signal

Yuanyuan Jiang<sup>1</sup>, Xuming Chen<sup>2</sup>, Patricia Pais Roldán<sup>2</sup>, Bruce Rosen<sup>1</sup>, and Xin Yu<sup>1,2</sup>

<sup>1</sup>Athinoula A. Martinos Center for Biomedical Imaging, Massachusetts General Hospital, Cambridge, MA, United States, <sup>2</sup>Max Planck Institute for Biological Cybernetics, Tuebingen, Germany

We established a multi-modal fMRI platform with two-channel fiber optic recording based on a genetically encoded fluorescent reporter, iGluSnFR, for extracellular glutamate (Glu) sensing and intracellular calcium indicator, GCaMP6f. Different from the intracellular neuronal and astrocytic calcium transients, the Glu signal, peak responses of spikes and baseline drift, show unique correlation features to the BOLD fMRI signal. Here, we applied the multi-modal fMRI platform to decipher the cellular and molecular interaction underlying the BOLD fMRI signal through the neuro-glio-vascular network in animal brains.

1341



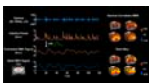
Adaptive Virtual Referencing Enables Recording of Extracellular Action Potentials in a 16.4 Tesla Animal Research MRI Scanner

Corey Cruttenden<sup>1</sup>, Wei Zhu<sup>2</sup>, Yi Zhang<sup>2</sup>, Rajesh Rajamani<sup>1</sup>, Xiao-Hong Zhu<sup>2</sup>, and Wei Chen<sup>2</sup>

<sup>1</sup>Mechanical Engineering, University of Minnesota, Minneapolis, MN, United States, <sup>2</sup>Center for Magnetic Resonance Research, University of Minnesota, Minneapolis, MN, United States

Recording neural signals such as extracellular action potentials during functional magnetic resonance imaging (fMRI) will improve our understanding of neurovascular coupling, which is responsible for the fMRI blood oxygen level dependent (BOLD) signal. Recording electrical neural signals during fMRI is challenging due to interactions between the recording hardware and electromagnetic (EM) fields involved in MRI that introduce noise and artifacts. We developed an adaptive virtual referencing technique to improve the action potential signal quality recorded in the bore of a 16.4T animal scanner during GRASE fMRI. This technique will enable us to further study neurovascular coupling at 16.4T.

1342



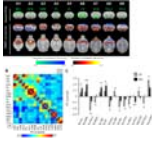
Simultaneous whole brain resting state fMRI and full-spectrum electrophysiology in rodents

Wenyu Tu<sup>1</sup>, Yuncong Ma<sup>2</sup>, Thomas Neuberger<sup>2</sup>, and Nanyin Zhang<sup>2</sup>

<sup>1</sup>The Huck Institutes of the Life Sciences, Penn State University, University Park, PA, United States, <sup>2</sup>Biomedical Engineering, Penn State University, University Park, PA, United States

To elucidate the neural basis of resting state functional network, it is important to continuously record neural activity during rsfMRI. In this study, we developed a platform including animal setup and a signal denoising pipeline to achieve continuous measurement of local field potential (LFP) and neuronal spikes with simultaneous whole-brain rsfMRI in rats.

1343

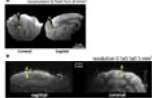


Diffusion functional MRI characterizes dynamical brain function in a neuropsychiatric disease model mouse  
Yoshifumi Abe<sup>1</sup>

<sup>1</sup>Keio University School of Medicine, Tokyo, Japan

We propose an analytical framework to characterize dynamic brain function in neuropsychiatric conditions by taking advantage of the technical aspects of diffusion functional MRI (DfMRI). The pipeline consists of local activity analysis with apparent diffusion coefficient (ADC) data, functional connectivity (FC) analysis with diffusion-weighted data ( $S_{b1800}$ ), and ignition-driven mean integration (IDMI) analysis combining both. We illustrated its utility by analyzing model mice with an obsessive-compulsive disorder (OCD)-related behavior. The framework was successful in detecting hyperactivation and biased connectivity across the cortico-striato-thalamic circuitry. The IDMI analysis found unseen local activity-initiated propagation to the global network.

1344



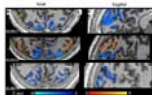
Evaluation of an improved microelectrode array for MR-compatibility and MR-simultaneous recording performance in 7T research system

Xiao Yu<sup>1,2</sup>, Bo-Wei Chen<sup>3</sup>, Xiaojun Tan<sup>1,4</sup>, Boyi Qu<sup>1,4</sup>, Tingting He<sup>1,2</sup>, Ching-Fu Wang<sup>3</sup>, Yu-Hao Lan<sup>3</sup>, You-Yin Chen<sup>3</sup>, and Hsin-Yi Lai<sup>1,2</sup>

<sup>1</sup>Interdisciplinary Institute of Neuroscience and Technology, School of Medicine, Zhejiang University, Hangzhou, China, <sup>2</sup>Department of Neurology of the Second Affiliated Hospital, Zhejiang University School of Medicine, Zhejiang University, Hangzhou, China, <sup>3</sup>Department of Biomedical Engineering, National Yang Ming University, Taipei, Taiwan, <sup>4</sup>College of Biomedical Engineering and Instrument Science, Zhejiang University, Hangzhou, China

Simultaneous recording of electrophysiological signals with functional magnetic resonance imaging (fMRI) can provide a solution for investigation of neurovascular coupling. However, this technique is challenged by 2 aspects, image artifact from electrode and electrophysiological noise from magnetic field. We improved our previous lab-designed microelectrode array and developed a de-noise method for use of its electrophysiological recording in 7T MRI. The results showed better structural image quality and stable acquisition of spike signals and local field potential. The proposed tool and method has the potential to facilitate simultaneous spike-recording during MR scanning in 7T MRI and further study the neurovascular coupling.

1345



Assessing the origin of human alpha oscillations using laminar layer 7T fMRI-EEG

Daniel C. Marsh<sup>1</sup>, Rodika Sokoliuk<sup>2</sup>, Kevin M. Aquino<sup>1,3</sup>, Daisie O. Pakenham<sup>1</sup>, Ross Wilson<sup>2</sup>, Rosa Sanchez Panchuelo<sup>1</sup>, Matthew J Brookes<sup>1</sup>, Simon Hanslmayr<sup>2</sup>, Stephen D. Mayhew<sup>2</sup>, Susan T Francis<sup>1</sup>, and Karen J Mullinger<sup>1,2</sup>

<sup>1</sup>Sir Peter Mansfield Imaging Centre, School of Physics and Astronomy, University of Nottingham, Nottingham, United Kingdom, <sup>2</sup>Centre for Human Brain Health, School of Psychology, University of Birmingham, Birmingham, United Kingdom, <sup>3</sup>Turner Institute for Brain and Mental Health, Monash University, Melbourne, Australia

EEG alpha (8-13Hz) oscillations occur throughout the cortex but the generating mechanisms are poorly understood. Opinion is divided between alpha being driven by bottom-up, top-down or both these processes. Here we use simultaneous 7T-fMRI-EEG during periods of eyes open/closed to assess the generator of alpha by determining the strongest BOLD-alpha negative layer correlations. We show the feasibility of using high spatial resolution 7T-fMRI with EEG to understand the origin of oscillations. Preliminary analysis shows BOLD-alpha correlations peak in middle layers of V1 (but not in V2/V3) providing suggestion that the alpha oscillations investigated are driven by bottom-up processing.

1346



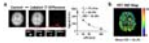
Simultaneous fMRI/fMRE reveals BOLD and viscoelastic changes in the cerebellum during motor planning

Patricia S. Lan<sup>1</sup>, Kevin J. Glaser<sup>2</sup>, Richard L. Ehman<sup>2</sup>, and Gary H. Glover<sup>3</sup>

<sup>1</sup>Bioengineering, Stanford University, Stanford, CA, United States, <sup>2</sup>Radiology, Mayo Clinic, Rochester, MN, United States, <sup>3</sup>Radiology, Stanford University, Stanford, CA, United States

In this work, we demonstrate the first fMRE (functional MR elastography) activation in the cerebellum using a motor planning task. A block paradigm of 24s ON (auditory-cued button pressing) and 24s OFF (rest) was used and images were acquired with a single-shot spin-echo EPI MRE sequence. Our results show that tissue stiffness within the cerebellum increases with motor planning. Furthermore, the stiffness and BOLD activation colocalize in the cerebellum but do not match exactly, suggesting that the two modalities may reveal different aspects of the mechanisms for neural activation.

1347



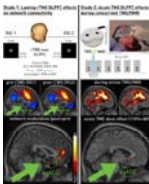
### Validation of MRI-based Oxygen Extraction Fraction (OEF) Measurement with <sup>15</sup>O Positron Emission Tomography

Dengrong Jiang<sup>1</sup>, Shengwen Deng<sup>2</sup>, Crystal G. Franklin<sup>2</sup>, Michael O'Boyle<sup>2</sup>, Wei Zhang<sup>2</sup>, Betty L. Heyl<sup>2</sup>, Li Pan<sup>3</sup>, Paul A. Jerabek<sup>2</sup>, Peter T. Fox<sup>2</sup>, and Hanzhang Lu<sup>1</sup>

<sup>1</sup>Department of Radiology, Johns Hopkins University School of Medicine, Baltimore, MD, United States, <sup>2</sup>Research Imaging Institute, University of Texas Health Science Center at San Antonio, San Antonio, TX, United States, <sup>3</sup>Siemens Healthineers, Baltimore, MD, United States

Cerebral oxygen extraction fraction (OEF) is a potential biomarker in various diseases. The current gold standard to measure OEF is <sup>15</sup>O-PET, but its clinical applications are impeded by inherent limitations. To facilitate broader clinical applications of OEF as a disease biomarker, in this work, we compared the whole-brain OEF measurement of a non-invasive MRI technique, T<sub>2</sub>-relaxation-under-spin-tagging (TRUST), with the gold standard PET measurement, and demonstrated a strong linear correlation and no systematic difference between the two methods.

1348



### Advanced methods for concurrent TMS/fMRI explain target engagement in 10Hz rTMS treatment

Martin Tik<sup>1</sup>, Michael Woletz<sup>1</sup>, Anna-Lisa Schuler<sup>1</sup>, Matic Prinic<sup>1</sup>, Allan Hummer<sup>1</sup>, and Christian Windischberger<sup>1</sup>

<sup>1</sup>Medical University of Vienna, Vienna, Austria

We have established and validated a concurrent TMS/fMRI setup to study target engagement of TMS-treatment during stimulation. The proposed marker for target engagement is a change in anti-correlation of the sgACC to the DLPFC. The direct sgACC effect due to DLPFC stimulation can only be observed by concurrent fMRI. We could show that TMS treatment over the left DLPFC leads to lasting effects in RS connectivity and importantly overlap with acute BOLD response during stimulation. We conclude that concurrent TMS/fMRI can be used to investigate efficacy of treatment and thereby propose a translation into clinical medicine.

## Oral

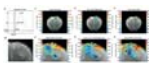
### Multimodal fMRI - fMRI in Animal Models

Thursday Parallel 4 Live Q&A

Thursday 15:50 - 16:35 UTC

Moderators: Shella Keilholz

1349



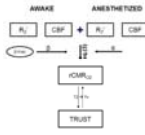
### Ultrafast functional MRI signals reflect activation sequence in the mouse visual pathway

Rita Gil<sup>1</sup>, Francisca F. Fernandes<sup>1</sup>, and Noam Shemesh<sup>1</sup>

<sup>1</sup>Champalimaud Neuroscience Programme, Champalimaud Centre for the Unknown, Lisbon, Portugal

We investigated BOLD response profiles along the entire mouse visual pathway (with monocular stimulation) using an ultrafast fMRI acquisition with 50 ms temporal resolution and quantified onset, half-maximum and peak times. To achieve the spatial coverage with this temporal resolution, an oblique slice covering the entire visual pathway was tailored. The quantified onset times were the only parameter correlating with the visual pathway neural input order. Our findings highlight a potential importance for onset time quantification – requiring ultrafast fMRI acquisitions – as a signature capable of mapping the underlying activation sequence of events in distributed neural networks.

1350



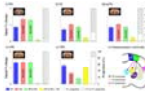
### M-Mapping Method for Calibrated fMRI in Awake Versus Anesthetized Mice

Binshi Bo<sup>1</sup>, Mengyang Xu<sup>2</sup>, Garth Thompson<sup>2</sup>, and Zhifeng Liang<sup>1</sup>

<sup>1</sup>Institute of Neuroscience, CAS Center for Excellence in Brain Sciences and Intelligence Technology, Key Laboratory of Primate Neurobiology, Chinese Academy of Sciences, Shanghai, China, <sup>2</sup>iHuman Institute, ShanghaiTech University, Shanghai, China

In functional brain imaging, the BOLD signal represents a mixture of CBF, CBV and the  $CMR_{O_2}$ . “Calibrated fMRI” methods aim to measure  $CMR_{O_2}$  through a metabolic model, but typically require administration of gases which is not possible in many clinical settings. Here, we developed a calibrated fMRI technique called “M-Mapping” which combines CBF and  $R2'$  maps together to calculate relative  $CMR_{O_2}$  and showed awake mice has a greater value than anesthetized mice in a region specific manner. This method may have a great potential to compare brain metabolic activity across different resting activity levels for further clinical study.

1351



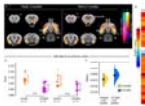
### Functional dissection of somatosensory processing pathways in mice

Won Beom Jung<sup>1,2</sup>, Hyun Seok Moon<sup>1,2</sup>, Taeyi You<sup>1,2</sup>, Jung Mi Lee<sup>1</sup>, and Seong-Gi Kim<sup>1,2</sup>

<sup>1</sup>Center for Neuroscience Imaging Research (CNIR), Institute for Basic Science (IBS), Suwon-si, Gyeonggi-do, Korea, Republic of, <sup>2</sup>Department of Biomedical Engineering, Sungkyunkwan University, Suwon-si, Gyeonggi-do, Korea, Republic of

Somatosensory system is communicated by feedforward and feedback projection each other during functional processing. Somatosensory fMRI response is attributed to these inter-regional reciprocal projections. Therefore, the separation of functional pathways in fMRI data is important to interpret fMRI data in circuit level. Here, to dissect somatosensory fMRI response, we compared CBV-weighted fMRI obtained at 15.2T under three conditions: excitation by sensory stimulation, silencing of somatosensory cortex by optogenetic stimulation, and combined excitation and silencing.

1352



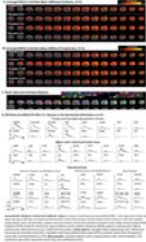
### Brain-wide functional mapping of the entorhinal cortex in young 3xTg mouse model for Alzheimer's disease

Francesca Mandino<sup>1,2</sup>, Ling Yun Yeow<sup>2</sup>, Chai Lean Teoh<sup>2</sup>, Chun-Yao Lee<sup>2</sup>, Renzhe Bi<sup>2</sup>, Hasan Mohammad<sup>2</sup>, Sejin Lee<sup>2</sup>, Han Gyu Bae<sup>2</sup>, Seung Hyun Baek<sup>2</sup>, Hanqing Jasinda Lee<sup>3</sup>, Kim Peng Mitchell Lai<sup>3</sup>, Sangyong Jung<sup>2</sup>, Fu Yu<sup>2</sup>, Malini Olivo<sup>2</sup>, John Gigg<sup>1</sup>, and Joanes Grandjean<sup>4</sup>

<sup>1</sup>Faculty of biology, medicine and health, University of Manchester, manchester, United Kingdom, <sup>2</sup>Singapore Bioimaging Consortium, A\*STAR, Singapore, Singapore, Singapore, <sup>3</sup>Department of Pharmacology, Yong Loo Lin School of Medicine, National University of Singapore, Singapore, Singapore, <sup>4</sup>Department of Radiology and Nuclear Medicine & Donders Institute for Brain, Cognition, and Behaviour, Donders Institute, Radboud University Medical Centre, Nijmegen, Netherlands

Alzheimer's disease (AD) is characterised by progressive memory loss, neurodegeneration and brain atrophy. Intra- and inter-regional connectivity across the brain is affected in AD, probably due to the aberrant accumulation of toxicity. The entorhinal cortex is a key region involved in the early stages of AD. We report synaptic connectivity increase in the 3xTg mouse model, by means of electrophysiological recordings in AD-susceptible brain regions, following stimulation of the entorhinal cortex, in vivo. Further, we demonstrate loss of functional connectivity with resting-state fMRI in AD-vulnerable brain regions, which converts into increased response during optogenetics photostimulation of the entorhinal cortex.

1353



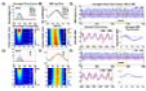
### Functional MRI investigation of Optogenetically-evoked Spindle-like Neural Activity and Memory Consolidation

Xunda Wang<sup>1,2</sup>, Alex T. L. Leong<sup>1,2</sup>, Shawn Zheng kai Tan<sup>3</sup>, Teng Ma<sup>1,2</sup>, Pek-Lan Khong<sup>4</sup>, Lee-Wei Lim<sup>3</sup>, and Ed Xuekui Wu<sup>1,2,3,4</sup>

<sup>1</sup>Laboratory of Biomedical Imaging and Signal Processing, The University of Hong Kong, Hong Kong, Hong Kong, <sup>2</sup>Department of Electrical and Electronic Engineering, The University of Hong Kong, Hong Kong, Hong Kong, <sup>3</sup>School of Biomedical Sciences, Li Ka Shing Faculty of Medicine, The University of Hong Kong, Hong Kong, Hong Kong, <sup>4</sup>Department of Diagnostic Radiology, Li Ka Shing Faculty of Medicine, The University of Hong Kong, Hong Kong, Hong Kong

Spindle is one of the most critical brain oscillatory activities that has been shown to mediate sensory transmission and memory consolidation. However, where and how spindle-related activities are distributed at the systems level and their brain-wide propagation targets remain elusive. In this study, we demonstrate the first integrative view of the causal recruitment of brain-wide networks by thalamo-cortically initiated spindle-related activities in a temporal-frequency specific manner and verified its role in facilitating memory consolidation.

1354



### Distinguish hemodynamic responses at the white matter tract from the laminar-specific gray matter fMRI signal with line-scanning fMRI

Sangcheon Choi<sup>1,2</sup>, Hang Zeng<sup>1,2</sup>, Bharat Biswal<sup>3</sup>, Bruce R. Rosen<sup>4</sup>, and Xin Yu<sup>1,4</sup>

<sup>1</sup>Max Planck Institute for Biological Cybernetics, Tuebingen, Germany, <sup>2</sup>Graduate Training Centre of Neuroscience, Tuebingen, Germany, <sup>3</sup>Department of Biomedical Engineering, NJIT, Newark, NJ, United States, <sup>4</sup>MGH/MIT/HMS Athinoula A. Martinos Center for Biomedical Imaging, Department of Radiology, Harvard Medical School, Massachusetts General Hospital, Charlestown, MA, United States

We applied line-scanning fMRI to investigate evoked hemodynamic responses in both laminar-specific gray matter (GM) and white matter (WM) in rats. Based on the WM-specific cross-correlation lag time to the laminar-specific fMRI signal, distinct WM hemodynamic responses were characterized across animals, showing a biphasic HRF with earlier lag times and a monophasic HRF with later lag times. Also, the lag-time dependent HRFs were detected in the subcortical area under the WM. Elucidating neurovascular coupling characteristics of distinct WM hemodynamic responses may help understand the progression of WM-related diseases, e.g. multiple sclerosis (MS) or small vessel disease (SVD).

1355



### Layer-specific optogenetic stimulation of motor cortex activates distinct brain-wide networks

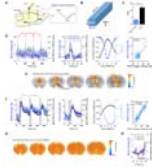
Russell W Chan<sup>1</sup>, Mazen Asaad<sup>2</sup>, Bradley J Edelman<sup>1</sup>, Hyun Joo Lee<sup>1</sup>, Hillel Adesnik<sup>3</sup>, David Feinberg<sup>3</sup>, and Jin Hyung Lee<sup>1,4,5,6</sup>

<sup>1</sup>Neurology and Neurological Sciences, Stanford University, Stanford, CA, United States, <sup>2</sup>Molecular and Cellular Physiology, Stanford University, Stanford, CA, United States, <sup>3</sup>Helen Wills Neuroscience Institute, University of California, Berkeley, CA, United States, <sup>4</sup>Bioengineering, Stanford University, Stanford, CA, United States, <sup>5</sup>Neurosurgery, Stanford University, Stanford, CA, United States, <sup>6</sup>Electrical Engineering, Stanford University, Stanford, CA, United States



The primary motor cortex (M1) consists of a stack of interconnected but distinct layers. However, knowledge of brain-wide circuit function of M1 layer-specific pathways is lacking. Here, we combined layer-specific Cre-driver mice, optogenetics, and fMRI with subsequent electrophysiological recordings to reveal distinct M1 layer-specific networks. All L2/3, L4, L5 and L6 stimulations evoked M1 fMRI responses, while only L5 and L6 evoked robust caudate putamen and ventrolateral thalamic nucleus responses. Subsequent LFP and spike recordings were in line with these fMRI results. Overall, our techniques and results could help investigate brain-wide layer-specific cortical circuit functions in development, aging and diseases.

1356



#### In Vivo Voltammetric Detection of Local Dopamine and Oxygen during Simultaneous BOLD fMRI

Lindsay Walton<sup>1,2,3</sup>, Matthew Verber<sup>4</sup>, Tzu-Hao Chao<sup>1,2,3</sup>, R. Mark Wightman<sup>4</sup>, and Yen-Yu Ian Shih<sup>1,2,3</sup>

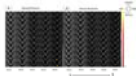
<sup>1</sup>Center for Animal MRI, University of North Carolina at Chapel Hill, Chapel Hill, NC, United States,

<sup>2</sup>Biomedical Research Imaging Center, University of North Carolina at Chapel Hill, Chapel Hill, NC, United States, <sup>3</sup>Department of Neurology, University of North Carolina at Chapel Hill, Chapel Hill, NC, United States,

<sup>4</sup>Department of Chemistry, University of North Carolina at Chapel Hill, Chapel Hill, NC, United States

fMRI interpretations based on traditional neurovascular coupling ignore the possible impact of vasoactive neurotransmitters released during brain activity. The striatum has atypical neurovascular coupling, and the highest concentrations of vasoactive dopamine. We evoked dopamine release in ventral striatum, and used simultaneous BOLD-fMRI and fast-scan cyclic voltammetry (FSCV) to observe global hemodynamics and quantify local dopamine and oxygen changes, respectively. Voltammetric oxygen correlated highly with BOLD, and increased linearly with local dopamine release, such that dopamine hemodynamic response functions could be derived. This multimodality explores hemodynamics at multiple spatiotemporal scales with the additional context of neurotransmission, which will improve fMRI interpretation.

1357



#### Intrinsic functional connectivity of spinal cord can be used to differentiate injured monkeys from normal using machine learning

Anirban Sengupta<sup>1</sup>, Arabinda Mishra<sup>1,2</sup>, Feng Wang<sup>1,2</sup>, Li Min Chen<sup>1,2,3</sup>, and John C Gore<sup>1,2,4,5,6</sup>

<sup>1</sup>Institute of Imaging Science, Vanderbilt University Medical Center, Nashville, TN, United States, <sup>2</sup>Radiology and Radiological Sciences, Vanderbilt University Medical Center, Nashville, TN, United States, <sup>3</sup>Psychology, Vanderbilt University Medical Center, Nashville, TN, United States, <sup>4</sup>Physics and Astronomy, Vanderbilt University Medical Center, Nashville, TN, United States, <sup>5</sup>Molecular Physiology and Biophysics, Vanderbilt University Medical Center, Nashville, TN, United States, <sup>6</sup>Biomedical Engineering, Vanderbilt University Medical Center, Nashville, TN, United States

The objective of this study was to investigate the presence of robust intrinsic networks inside the spinal cord of squirrel monkey and whether connectivity measures of these networks can detect injury in spinal cord. We used Independent Component Analysis of resting state fMRI data to obtain dorsal and ventral networks within the gray-matter of spinal cord. Within Horn Connectivity and Between Horn Connectivity measures were calculated based on the time course of Independent Components. A Support-Vector-Machine classifier could differentiate a spinal cord injured monkey from a control monkey using these connectivity measures with a low classification error of 6.67 %.

## Oral

### Multimodal fMRI - Mechanisms of Resting-State fMRI

Thursday Parallel 4 Live Q&A

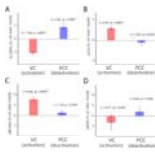
Thursday 15:50 - 16:35 UTC

Moderators: Robert Barry & Patricia Figueiredo

1358

#### Metabolic basis of activated and deactivated brain network nodes in fMRI paradigms

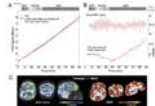
Yury Koush<sup>1</sup>, Robin A. de Graaf<sup>1</sup>, Ron Kupers<sup>2</sup>, Laurence Dricot<sup>3</sup>, Maurice Ptito<sup>4</sup>, Kevin Behar<sup>1</sup>, Douglas L. Rothman<sup>1</sup>, and Fahmeed Hyder<sup>1</sup>



<sup>1</sup>Yale University, New Haven, CT, United States, <sup>2</sup>University of Copenhagen, Copenhagen, Denmark, <sup>3</sup>University of Louvain, Louvain, Belgium, <sup>4</sup>School of Optometry, Montreal, QC, Canada

Functional MRI using blood oxygenation level dependent (BOLD) contrast identifies brain regions for task-induced (de)activation paradigms. We investigated the metabolic basis of these paradigms in activated (visual cortex, VC) and deactivated (posterior cingulate cortex, PCC) network nodes using concurrent acquisitions of J-edited lactate/GABA( $\gamma$ -aminobutyric acid)/Glx(pooled glutamate and glutamine) and diffusion-weighted BOLD signal. In VC, we detected increased BOLD/lactate/glutamate, and decreased GABA, whereas in PCC BOLD decreased, GABA increased but lactate/glutamate did not change. These results suggest that BOLD responses in (de)activated areas is regulated by relatively rapid GABAergic inhibition, whereas aerobic glycolysis and glutamatergic activity dominate in activated nodes.

1359



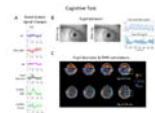
Employing simultaneous functional PET/MRI to map neuronal and vascular dynamics accompanying brain arousal fluctuations

Jingyuan E Chen<sup>1,2</sup>, Nina E Fultz<sup>1</sup>, Jonathan R Polimeni<sup>1,2</sup>, Ciprian Catana<sup>1,2</sup>, Bruce R Rosen<sup>1,2</sup>, Laura D Lewis<sup>3</sup>, and Christin Y Sander<sup>1,2</sup>

<sup>1</sup>Athinoula A. Martinos Center for Biomedical Imaging, Massachusetts General Hospital, Boston, MA, United States, <sup>2</sup>Radiology, Harvard Medical School, Boston, MA, United States, <sup>3</sup>Biomedical Engineering, Boston University, Boston, MA, United States

In this study, we investigated the feasibility of integrating simultaneous fMRI and functional PET to uncover metabolic and hemodynamic changes linked with arousal. Our findings suggested that this multi-modal toolset can reliably detect brain-wide hemodynamic and metabolic changes spanning “alert”, “drowsy” and “sleep” conditions, therefore holding great promise in disentangling arousal-induced neuronal and vascular dynamics in future investigations.

1360



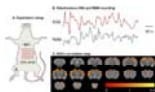
Variations in the sympathetic tone and fMRI signal during alert conditions

Pinar S Ozbay<sup>1</sup>, Catie Chang<sup>2</sup>, Jacco A de Zwart<sup>1</sup>, Peter van Gelderen<sup>1</sup>, and Jeff Duyn<sup>1</sup>

<sup>1</sup>NINDS, NIH, Bethesda, MD, United States, <sup>2</sup>Vanderbilt University, Nashville, TN, United States

During light-sleep, strong correlations were observed between fMRI and peripheral signals. This can be inferred from the fingertip pulse-oximeter signal as a proxy for sympathetic activity. Sympathetic activity may also affect fMRI during wake. In this work, we analyzed data collected during cognitive tasks and deep breathing, showed strong spatio-temporal relations between pupil behavior, skin vascular tone, and fMRI signal. We demonstrate that sympathetic activity can be elicited by a variety of stimuli, that those additional measures might be useful for physiological regression and to better distinguish neuronal and autonomic contributions, which are mostly observed as anti-correlation patterns in fMRI.

1361

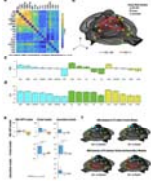


The Stomach and the Brain are Synchronized Intrinsically in Rats

Jiayue Cao<sup>1</sup>, Xiaokai Wang<sup>1</sup>, Kun-Han Lu<sup>2</sup>, Zhenjun Tan<sup>3</sup>, Robert Phillips<sup>3</sup>, Deborah Jaffey<sup>3</sup>, Terry Powley<sup>3</sup>, and Zhongming Liu<sup>1,2</sup>

<sup>1</sup>Biomedical Engineering, Purdue University, West Lafayette, IN, United States, <sup>2</sup>Electrical and Computer Engineering, Purdue University, West Lafayette, IN, United States, <sup>3</sup>Psychological Science, Purdue University, West Lafayette, IN, United States

The origins of fMRI in the resting state has been widely explored but yielded incomplete knowledge. Here, we hypothesize that gastric activity contributes to intrinsic brain activity observed with fMRI. We explored the gut-brain synchrony in rats by recording the electrogastrogram together with fMRI. We found that brain activity is intrinsically synchronized with gastric activity at a specific resting state network in which the BOLD activity is time-locked to gastric activity with varying time delays.



**Locus Coeruleus derived norepinephrine alters intrinsic functional connectivity at the Default-Mode Network**  
 Li-Ming Hsu<sup>1,2,3,4</sup>, Esteban Oyarzabal<sup>1,3,4</sup>, Manasmita Das<sup>1,3,4</sup>, Tzu-Hao Harry Chao<sup>1,3,4</sup>, Sheng Song<sup>1,3,4</sup>, Yu-Wei Chen<sup>5</sup>, Dinggang Shen<sup>2</sup>, Sungho Lee<sup>1,3,4</sup>, Patricia Jensen<sup>6</sup>, and Yen-Yu Ian Shih<sup>1,3,4</sup>

<sup>1</sup>Neurology, University of North Carolina at Chapel Hill, Chapel Hill, NC, United States, <sup>2</sup>Radiology, University of North Carolina at Chapel Hill, Chapel Hill, NC, United States, <sup>3</sup>Biomedical Imaging Center, University of North Carolina at Chapel Hill, Chapel Hill, NC, United States, <sup>4</sup>Center for Animal MRI, University of North Carolina at Chapel Hill, Chapel Hill, NC, United States, <sup>5</sup>Developmental Neurobiology, NIEHS/NIH, RDU, NC, United States, <sup>6</sup>Developmental Neurobiology, NIH/NIEHS, RDU, NC, United States

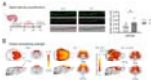
Norepinephrine (NE) is suspected to rapidly modulate strength and structure of intrinsic functional connectivity (FC). We used chemogenetic fMRI to selectively isolate the role of NE Locus Coeruleus (LC) neurons, compared to NE A1/A2/A4 neurons, on FC modulation. Among 19 parcellated FC modules, NE-LC neurons significantly enhanced ReHo, ALFF and DC within the anterior Default-Mode, Motor and Somatosensory modules and enhanced FC strength within and between Default-Mode modules. Dynamic FC analysis found Default-Mode differences were attributed to two co-activation patterns (CAPs) associated with Default-Mode suppression that explains the ability of NE to focus wandering minds into sensory attention.

**Exploring the neurovascular nature of spontaneous cerebral BOLD fluctuations in 1730 individuals – The Maastricht Study**

Laura W.M. Vergoossen<sup>1,2</sup>, Jacobus F.A. Jansen<sup>1,2,3</sup>, Daan Huybrechs<sup>4</sup>, Miranda T. Schram<sup>2,5,6</sup>, Walter H. Backes<sup>1,2</sup>, and on behalf of The Maastricht Study<sup>5</sup>

<sup>1</sup>Radiology and Nuclear Medicine, Maastricht University Medical Center, Maastricht, Netherlands, <sup>2</sup>Mental Health and Neuroscience, Maastricht University, Maastricht, Netherlands, <sup>3</sup>Electrical Engineering, Eindhoven University of Technology, Eindhoven, Netherlands, <sup>4</sup>Computer Science, KU Leuven, Leuven, Belgium, <sup>5</sup>Internal Medicine, Maastricht University Medical Center, Maastricht, Netherlands, <sup>6</sup>School for Cardiovascular Disease, Maastricht University, Maastricht, Netherlands

In addition to spatial patterns, also temporal patterns can be identified in brain signal as non-stationary components. Fourier-transform provides only information about characteristic frequency components in dynamic brain signals and assumes that these are of stationary nature. However, brain signals are non-stationary and discrete wavelet transformation can be used to separate the signal into both frequency subbands and time-scales. In The Maastricht Study (n=1730), we found that wavelet analysis is a suitable method to demonstrate that physiological measures are associated with specific frequency subbands of the BOLD signal, and to separate the neurovascular signal into subbands representing different physiological measures.



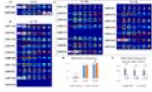
**A cross-species link between deficient synaptic pruning and functional hyper-connectivity in autism**

Marco Pagani<sup>1</sup>, Alice Bertero<sup>1,2</sup>, Alessia De Felice<sup>1</sup>, Andrea Locarno<sup>3</sup>, Ieva Miseviciute<sup>3</sup>, Stavros Trakoshis<sup>4,5</sup>, Carola Canella<sup>1,6</sup>, Elizabeth de Guzman<sup>1</sup>, Kaushtub Supekar<sup>7</sup>, Vinod Menon<sup>7</sup>, Alberto Galbusera<sup>1</sup>, Raffaella Tonini<sup>3</sup>, Michael V. Lombardo<sup>5</sup>, Massimo Pasqualetti<sup>2</sup>, and Alessandro Gozzi<sup>1</sup>

<sup>1</sup>Functional Neuroimaging Laboratory, Istituto Italiano di Tecnologia, Rovereto, Italy, <sup>2</sup>Biology Department, University of Pisa, Pisa, Italy, <sup>3</sup>Neuromodulation of Cortical and Subcortical Circuits Laboratory, Istituto Italiano di Tecnologia, Genova, Italy, <sup>4</sup>Department of Psychology, University of Cyprus, Nicosia, Cyprus, <sup>5</sup>Laboratory for Autism and Neurodevelopmental Disorders, Istituto Italiano di Tecnologia, Rovereto, Italy, <sup>6</sup>Center for Mind and Brain Sciences, University of Trento, Rovereto, Italy, <sup>7</sup>Stanford University, Stanford, CA, United States

Altered brain functional connectivity is a hallmark finding in autism but the neural basis of this phenomenon remains unclear. We show that a mouse line reconstituting synaptic pruning deficits observed in postmortem autistic brains exhibits widespread functional hyper-connectivity, and that pharmacological normalization of synaptic aberrancies completely rescues behavioral and functional connectivity deficits. We also show that a similar connectivity fingerprint can be isolated in human rsfMRI scans of people with autism, and linked to overexpression of genes related to this dysfunctional pathway. Our results reveal a possible mechanistic link between deficient synaptic pruning and functional hyper-connectivity in autism.

1365



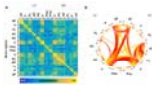
### Transition Frequencies across the Brain States under Stress Differentiate Depression Vulnerability

Xue Zhang<sup>1,2</sup>, Hua Guo<sup>1</sup>, and Lihong Wang<sup>3</sup>

<sup>1</sup>Center for Biomedical Imaging Research, Department of Biomedical Engineering, School of Medicine, Tsinghua University, Beijing, China, <sup>2</sup>Radiological Sciences Laboratory, Department of Radiology, Stanford University, Palo Alto, CA, United States, <sup>3</sup>Department of Psychiatry, University of Connecticut School of Medicine, Farmington, CT, United States

Brain state transitions during resting-state reflect the variation of the baseline homeostasis, it is still unclear how the state interactions are modulated under stress. In the current study, the stress-induced change of the co-activation pattern transitions was examined in two independent cohorts by scanning resting-state fMRI pre- and post- a math task, its association with depression vulnerability was also explored. The post- versus pre-stress resting-state comparison showed an increased state transition frequency under stress, and those with higher depression scores shifted more post-stress in both cohorts, indicating the disturbed brain homeostasis under stress and lower recovery ability from stress.

1366



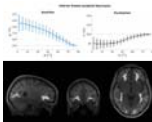
### Cross-cortical Depth-dependent Interactions in the Human Brain using EPIK

Patricia Pais-Roldán<sup>1</sup>, Seong Dae Yun<sup>1</sup>, Michael Schwerter<sup>1</sup>, and Jon N Shah<sup>1,2,3,4</sup>

<sup>1</sup>Forschungszentrum Jülich - INM-4, Jülich, Germany, <sup>2</sup>Forschungszentrum Jülich - INM-11, Jülich, Germany, <sup>3</sup>JARA-BRAIN, Aachen, Germany, <sup>4</sup>RWTH Aachen University, Aachen, Germany

Cross-cortical interactions in the human brain remain poorly understood and are often over-simplified as a 2-dimensional cortical model in fMRI studies. To date, high-resolution fMRI has been limited to relatively small brain slabs that cover particular areas of interest, providing fine mapping of local circuits but precluding macroscale analysis. Here, an EPIK sequence was used to measure the GE-BOLD signal from individual cortical layers through most of the brain. The combination of high resolution (0.63 mm isotropic) and large coverage fMRI enabled identification of long-distance neuronal interactions that take place between particular cortical depths during resting-state.

1367



### White matter resting-state BOLD signals depend on the orientation of the local diffusion tensor axis relative to the B<sub>0</sub>-field

Olivia Viessmann<sup>1</sup>, Qiyuan Tian<sup>1</sup>, Michaël Bernier<sup>1</sup>, David H Salat<sup>1,2</sup>, and Jonathan Rizzo Polimeni<sup>1,3</sup>

<sup>1</sup>Athinoula A. Martinos Center for Biomedical Imaging, Massachusetts General Hospital, Harvard Medical School, Charlestown, MA, United States, <sup>2</sup>VA Boston Healthcare System, Boston, MA, United States, <sup>3</sup>Division of Health Sciences and Technology, Massachusetts Institute of Technology, Cambridge, MA, United States

We aimed to test whether the amplitudes of resting-state BOLD signals within the white matter depend on the orientation of the local diffusion tensor relative to the  $B_0$ -field. This was assessed using resting-state BOLD and diffusion data provided by the HCP. Baseline BOLD signals were about 11% higher in voxels where primary DTI directions were parallel to  $B_0$  compared to perpendicular. Because myelinated fibres will change local tissue  $T_2^*$ , which will also impact the BOLD signal, we tested whether the observed BOLD orientation effect was driven by static effects on the baseline or dynamic effects from changes in blood oxygenation.

---

---

## Corporate Symposium

### Gold Corporate Symposium: Canon medical Systems Corporation/Olea Medical

Plenary Hall (Grand Ballroom)

Thursday 19:00 - 20:00 UTC

---

---

Friday, 14 August 2020

## Member-Initiated Symposium

### "The Captain of the Ship" in MRI: Does the Doctrine Apply?

Organizers: Claire Mulcahy, Martin Sherriff, Thao Tran

Friday 12:00 - 12:30 UTC

Moderators: Anne Dorte Blankholm & Chris Kokkinos

Ethical & Professional Considerations from a Radiographer's / Technologist's Perspective

Rhys Slough<sup>1</sup>

<sup>1</sup>Cambridge University Hospital, United Kingdom

---

Ethical Considerations From a Research Perspective

Bradford Moffat<sup>1</sup>

<sup>1</sup>University of Melbourne, Australia

---

Patient Care & Ethical Considerations From a Clinical Perspective

Pia Maly Sundgren<sup>1</sup>

<sup>1</sup>Lund University, Sweden

---

---

## Member-Initiated Symposium

### New Innovations & Alternatives to Conventional Contrast Agents

Organizers: Niviv Nyström, Or Perlman, Paula Ramos Delgado

Friday 12:00 - 12:30 UTC

Moderators: Niviv Nyström & Or Perlman

Expert talk: Inorganic Nanofluorides as Tunable Small-Sized Nanotracers for 19F-MRI

Amnon Bar-Shir

---

Trainee talk: 19F-MR Imaging of Inflammation in the Heart After Myocardial Infarction

Mariah R.R. Daal

---

Expert talk: Fluorine MRI: En Route to Clinical Imaging

Ruud B van Heeswijk<sup>1</sup>

*<sup>1</sup>Radiology, Lausanne University Hospital (CHUV) and University of Lausanne (UNIL), Lausanne, Switzerland*

---

Trainee talk: Iopamidol CEST pH Imaging for Noninvasive Monitoring of Kidney Disease & Injury  
KowsalyaDevi Pavuluri

---

Expert talk: Iron-Based MRI Contrast Agents: From Nanoparticles to Small Responsive Iron Complexes  
Veronica Clavijo Jordan <sup>1</sup>

*<sup>1</sup>Martinos Center for Biomedical Imaging, Massachusetts General Hospital/Harvard Medical School, Charlestown, MA, United States*

---

Trainee talk: Manganese-Enhanced MRI: An Early Imaging Biomarker of Cell Viability & Its Application in Acute Myocardial Infarction  
Nur Hayati Jasmin

---

Expert talk: Overview for Manganese-Enhanced MRI & Its Nanoparticle Applications  
Ichio Aoki<sup>1</sup>

*<sup>1</sup>Department of Molecular Imaging and Theranostics, Japan*

---

Trainee talk: Radiolabeled Iron Oxide/Aluminum Hydroxide Nanoparticles as PET/MRI Contrast Agents for Stem Cell Tracking  
Sarah Belderbos<sup>1</sup>

*<sup>1</sup>KU Leuven, Belgium*

---

---

## Member-Initiated Symposium

### A Window Through the Ages: Advanced Mapping of Brain Development from Neonate to Adolescence

Organizers: Sila Genc, Catherine Lebel, Marc Seal

Friday 12:30 - 13:00 UTC

Moderators: Sila Genc & Catherine Lebel

Linking Neonatal Cortical Morphology With Gene Expression in the Fetal Brain  
Gareth Ball

---

Characterising Axonal & Myelin Microstructure to Predict Behavioural Phenotypes in Childhood  
Jess E Reynolds<sup>1</sup>

*<sup>1</sup>Radiology, University of Calgary, Calgary, AB, Canada*

---

Unravelling the Influence of Age & Puberty in the Development of Amygdala Subnuclei  
Megan Herting

---

Combining Big Data & Machine Learning to Predict Clinical Depression in Childhood  
Akhil Kottaram

---

Disentangling Molecular Alterations From Water-Content Changes in the Developing Human Brain Using Quantitative MRI

Aviv Mezer

---

---

**Member-Initiated Symposium**

**Sustainable MRI: Pathways to a Carbon-Neutral Research Society**

Organizers: Ruth Oliver, Rajiv Ramasawmy, Simon Walker-Samuel

Friday 12:30 - 13:00 UTC

Moderators: Esther Warnert

Climate Change for MRI Scientists

Lesley Hughes

---

Sustainable MRI: An Academic Perspective

Simon Walker-Samuel

---

Panel Discussion

---

---

**Member-Initiated Symposium**

**How Open Should Our Science Be?**

Organizers: Maria Eugenia Caligiuri, Nikola Stikov, Martin Uecker

Friday 13:00 - 13:30 UTC

Moderators: Maria Eugenia Caligiuri & Florian Knoll

A Journal Editor's Perspective on Open Science

Peter Jezzard<sup>1</sup>

<sup>1</sup>FMRIB Centre, University of Oxford, United Kingdom

---

ISMRM Raw Data Format

Adrienne E Campbell-Washburn<sup>1</sup>

<sup>1</sup>National Institutes of Health, Bethesda, MD, United States

---

Standards in Quantitative MRI

Kathryn Keenan<sup>1</sup>

<sup>1</sup>NIST, United States

---

Software Tools for Reproducible Research

---

---

**Member-Initiated Symposium**

**Artificial Intelligence Enabling Cardiovascular Magnetic Resonance Imaging**

Organizers: René Botnar, Sonia Nielles-Vallespin, David Sosnovik

Friday 13:00 - 13:30 UTC

Moderators: René Botnar

AI Enabled CMR

Peter Kellman<sup>1</sup>

*<sup>1</sup>NIH, United States*

---

[AI in Flow & Other CMR Applications](#)

Ava Suinesiaputra

---

[Democratizing Cardiac MRI Using AI-Enabled Low Field MRI](#)

Adrienne E Campbell-Washburn<sup>1</sup>

*<sup>1</sup>National Institutes of Health, Bethesda, MD, United States*

---

[Fast & Efficient Multiparametric & Multi-Contrast MRI: All in One](#)

Claudia Prieto<sup>1</sup>

*<sup>1</sup>Kings College London, United Kingdom*

---

[Quantitative Perfusion Imaging: Technical Developments & Clinical Impact](#)

Michael Salerno<sup>1</sup>

*<sup>1</sup>UVA School of Medicine, United States*

---

---

**Weekday Course**

**Managing Motion and Artifacts - Artifacts Game Show**

*Organizers:* Eric Stinson, Jose Marques, Adrienne Campbell-Washburn, Avery Berman

Tuesday Parallel 4 Live Q&A

Friday 13:45 - 14:30 UTC

*Moderators:* Avery Berman & Adrienne Campbell-Washburn

[Artifact Game Show II](#)

Adrienne Campbell-Washburn<sup>1</sup>, Avery Berman<sup>2</sup>, and Eric Stinson<sup>3</sup>

*<sup>1</sup>National Institutes of Health, United States, <sup>2</sup>Massachusetts General Hospital, United States, <sup>3</sup>Siemens Healthcare, United States*

Come participate in the ISMRM Artifact Game Show! Learn about common MR artifacts and how to avoid them in a light-hearted game show setting. Contestants will participate in a variety of games to learn about artifacts, and then experts will provide more information. If you're in the room, you have the chance to play! Come for the artifacts, stay for the fun and prizes!

---

---

---